VOLUME 26 / NUMBER 21
NOVEMBER 8, 1988
ACC. NOS. N88-27147 TO N88-28000

STAR

AN ABSTRACT JOURNAL

Scientific and Technical Aerospace Reports

PRODUCED BY THE
SCIENTIFIC AND TECHNICAL
INFORMATION
DIVISION

NASA

NATIONAL AERONAUTICS AND SPACE ADMINISTRATION

WHAT YOU CAN DO FOR *STAR*

All users of this abstract service are urged to forward reports to be considered for announcement in *STAR*. This will aid NASA in its efforts to provide the fullest possible coverage of all scientific and technical publications that might support aeronautics and space research and development. If you have prepared relevant reports (other than those that you will transmit to NASA, DoD, or DOE through the usual contract- or grant-reporting channels), please send them for consideration to the NASA Scientific and Technical Information Facility, P.O. Box 8757, B.W.I. Airport, Maryland 21240.

Reprints of journal articles, book chapters, and conference papers are also welcome. These will be considered for announcement in *STAR*'s companion journal, *International Aerospace Abstracts*.

You may specify a particular source to be included in a report announcement if you wish; otherwise the report will be placed on public sale at the National Technical Information Service. Copyrighted publications will be announced but not distributed or sold.

PURCHASE OF *STAR*

The semimonthly issues are available for sale by the Superintendent of Documents, U.S. Government Printing Office, Washington, D.C. 20402.

PUBLISHED BY:

UNITED STATES GOVERNMENT
NATIONAL AERONAUTICS AND SPACE ADMINISTRATION
SCIENTIFIC AND TECHNICAL INFORMATION DIVISION
Scientific and Technical Aerospace Reports, Volume 26, is prepared by the NASA Scientific and Technical Information Facility operated for the National Aeronautics and Space Administration by RMS Associates.

The Administrator of the National Aeronautics and Space Administration has determined that the publication of this periodical is necessary in the transaction of the public business required by law of this Agency. Use of funds for printing this periodical has been approved by the Director of the Office of Management and Budget through March 22, 1989.

US ISSN 0036-8741

INTRODUCTION

Scientific and Technical Aerospace Reports (STAR) is a major component of a comprehensive National Aeronautics and Space Administration information system covering aeronautics, space, and supporting disciplines. *STAR* is issued on the 8th and 23rd of each month and announces current publications of the following types:

- NASA, NASA contractor, and NASA grantee reports
- Reports issued by other U.S. Government Agencies, domestic and foreign institutions, universities, and private firms
- Translations in report form
- NASA-owned patents and patent applications
- Dissertations and theses

Journal, book, and conference literature, cover-to-cover journal translations, and certain foreign dissertations are announced in a companion journal, *International Aerospace Abstracts (IAA)*, available on subscription from the American Institute of Aeronautics and Astronautics, Technical Information Service, 555 West 57th Street, 12th Floor, New York, New York 10019.

SUBJECT SCOPE

Subject scope of *STAR*, and *IAA* includes all aspects of aeronautics and space research and development, supporting basic and applied research, and applications. Aerospace aspects of earth resources, energy development, conservation, oceanography, environmental protection, urban transportation, and other topics of high national priority are also covered.

OTHER NASA PUBLICATIONS

Other NASA publications and information services are described in the publication, *The NASA Scientific and Technical Information System ... and How to Use It*, available without charge from the NASA Scientific and Technical Information Facility, P.O. Box 8757, B.W.I. Airport, Maryland 21240.

HOW TO USE *STAR* SUBJECT CATEGORIES

STAR is categorized by 10 major subject divisions divided into 76 specific subject categories and one general category/division. The major subject divisions are listed in the Table of Contents, together with a note for each that defines its scope and provides any cross-references. For example:

AERONAUTICS

Includes aeronautics (general); aerodynamics; air transportation and safety; aircraft communications and navigation; aircraft design, testing and performance; aircraft instrumentation; aircraft propulsion and power; aircraft stability and control; and research and support facilities (air).

For related information see also *Astronautics*.

Each major division is further divided into as many as nine specific categories, which are identified by category numbers.

Abstracts in *STAR* are grouped by specific category, the categories appearing in sequential order. Category breaks in the abstract section are identified by the category number and title, and a scope note. Cross-references to other categories are provided as appropriate. For example:

02 AERODYNAMICS

Includes aerodynamics of bodies, combinations, wings, rotors, and control surfaces; and internal flow in ducts and turbomachinery.

For related information see also *34 Fluid Mechanics and Heat Transfer.*

CROSS-REFERENCES

Individual *STAR* abstracts are not ordinarily cross-referenced, except for certain conference reports or book translations that have had separate abstracts written for their component papers or chapters. Citations and abstracts of the components follow immediately after those of the parent document. When the subject content of a component differs sufficiently from the general content of the parent, a cross-reference citation also is printed at the end of the category to which it normally would have been assigned if it were independent.

DOCUMENTS ON MICROFICHE

Documents on microfiche[1] are designated by a pound sign (#) following the accession number. The pound sign is used without regard to the source or quality of the microfiche.

AVAILABILITIES

One or more sources from which a document announced in *STAR* is available to the public is given in each citation. The most commonly indicated sources and their acronyms or abbreviations are listed below. If the publication is available from a source other than those listed, the publisher and his address will be displayed on the availability line or in combination with the corporate source line.

Avail: NTIS. Sold by the National Technical Information Service. Prices for hard copy (HC) and microfiche (MF) are indicated by a price code following the letters HC or MF in the *STAR* citation. Current values for the price codes are given in the tables on page vii.

Initially distributed microfiche under the NTIS SRIM (Selected Research in Microfiche) is available at greatly reduced unit prices. For this service and for information concerning subscription to NASA printed reports, consult the NTIS Subscription Section, Springfield, Va. 22161.

NOTE ON ORDERING DOCUMENTS: When ordering NASA publications (those followed by the * symbol), use the N accession number. NASA patent applications (only the specifications are offered) should be ordered by the US-Patent-Appl-SN number. Non-NASA publications (no asterisk) should be ordered by the AD, PB, or other *report number* shown on the last line of the citation, not by the N accession number. It is also advisable to cite the title and other bibliographic identification.

Avail: SOD (or GPO). Sold by the Superintendent of Documents, U.S. Government Printing Office, in hard copy. The current price and order number are given following the availability line. (NTIS will fill microfiche requests, as indicated above, for those documents identified by a # symbol.)

(1) A microfiche is a transparent sheet of film, 105 by 148 mm in size, containing as many as 60 to 98 pages of information reduced to micro images (not to exceed 26:1 reduction).

Avail: BLL (formerly NLL): British Library Lending Division, Boston Spa, Wetherby, Yorkshire, England. Photocopies available from this organization at the price shown. (If none is given, inquiry should be addressed to the BLL.)

Avail: DOE Depository Libraries. Organizations in U.S. cities and abroad that maintain collections of Department of Energy reports, usually in microfiche form, are listed in *Energy Research Abstracts*. Services available from the DOE and its depositories are described in a booklet, *DOE Technical Information Center - Its Functions and Services* (TID-4660), which may be obtained without charge from the DOE Technical Information Center.

Avail: ESDU. Pricing information on specific data, computer programs, and details on ESDU topic categories can be obtained from ESDU International Ltd. Requesters in North America should use the Virginia address while all other requesters should use the London address, both of which are on page vi.

Avail: Fachinformationszentrum, Karlsruhe. Sold by the Fachinformationszentrum Energie, Physik, Mathematik GMBH, Eggenstein Leopoldshafen, Federal Republic of Germany, at the price shown in deutschmarks (DM).

Avail: HMSO. Publications of Her Majesty's Stationery Office are sold in the U.S. by Pendragon House, Inc. (PHI), Redwood City, California. The U.S. price (including a service and mailing charge) is given, or a conversion table may be obtained from PHI.

Avail: NASA Public Document Rooms. Documents so indicated may be examined at or purchased from the National Aeronautics and Space Administration, Public Documents Room (Room 126), 600 Independence Ave., S.W., Washington, D.C. 20546, or public document rooms located at each of the NASA research centers, the NASA Space Technology Laboratories, and the NASA Pasadena Office at the Jet Propulsion Laboratory.

Avail: Univ. Microfilms. Documents so indicated are dissertations selected from *Dissertation Abstracts* and are sold by University Microfilms as xerographic copy (HC) and microfilm. All requests should cite the author and the Order Number as they appear in the citation.

Avail: US Patent and Trademark Office. Sold by Commissioner of Patents and Trademarks, U.S. Patent and Trademark Office, at the standard price of $1.50 each, postage free. (See discussion of NASA patents and patent applications below.)

Avail: (US Sales Only). These foreign documents are available to users within the United States from the National Technical Information Service (NTIS). They are available to users outside the United States through the International Nuclear Information Service (INIS) representative in their country, or by applying directly to the issuing organization.

Avail: USGS. Originals of many reports from the U.S. Geological Survey, which may contain color illustrations, or otherwise may not have the quality of illustrations preserved in the microfiche or facsimile reproduction, may be examined by the public at the libraries of the USGS field offices whose addresses are listed in this Introduction. The libraries may be queried concerning the availability of specific documents and the possible utilization of local copying services, such as color reproduction.

Avail: Issuing Activity, or Corporate Author, or no indication of availability. Inquiries as to the availability of these documents should be addressed to the organization shown in the citation as the corporate author of the document.

NASA PATENTS AND PATENT APPLICATIONS

Patents and patent applications owned by NASA are announced in *STAR* under appropriate subject categories and are referenced in the *STAR* indexes. In the Report/Accession Number Index, patents are indexed by the NASA Case Number (which appears in lieu of the report number in other indexes), the U.S. Patent Number, the U.S. Patent Application Serial Number, and the U.S. Patent Class. Patent applications for which patents have not yet been issued are indexed by the NASA Case Number and the U.S. Patent Application Serial Number.

NASA *patent application specifications* are sold in paper copy by the National Technical Information Service at price code A02. Microfiche are sold at price code A01. The US-Patent-Appl-SN- number should be used in ordering either paper copy or microfiche from NTIS. Printed copies of *patents* (which are not microfiched) are available for purchase at $1.50 per copy from:

Commissioner of Patents and Trademarks
U.S. Patent and Trademark Office
Washington, D.C. 20231

When ordering patents, the U.S. Patent Number should be used, and payment must be remitted in advance, preferably by money order or check payable to the Commissioner of Patents and Trademarks. Prepaid purchase coupons for ordering are also available from the Patent and Trademark Office. The patents and patent applications announced in *STAR* are owned by NASA and are available for royalty-free licensing. Requests for licensing terms and further information should be addressed to:

Associate General Counsel for Intellectual Property/Code GP
National Aeronautics and Space Administration
Washington, D.C. 20546

ELIGIBILITY AND REGISTRATION FOR NASA INFORMATION PRODUCTS AND SERVICES

A variety of services is available to organizations of the following types that have registered with NASA to receive specific services or products:

1. NASA offices, research centers, contractors, subcontractors, grantees, and consultants;
2. Other U.S. Government agencies and their contractors;
3. Libraries in the United States that have arrangements with NASA to maintain collections of NASA documents for public reference;
4. Other organizations in the United States having a need for NASA documents in work related to aeronautics and space research;
5. Organizations abroad that have established reciprocal document exchange arrangements with NASA.

Only the central service points or central points of document acquisition and control within qualified organizations are eligible to register for NASA products and services. Domestic organizations that may be eligible to receive various classes of NASA publications and services should address their requests for registration or for further information to:

NASA Scientific and Technical Information Facility
ATTN: Registration Activity
P.O. Box 8757
B.W.I. Airport, Maryland 21240

Organizations abroad should direct requests to the same address, but to the attention of: International Exchange Program.

AVAILABILITY OF *STAR* ABSTRACTS ON MICROFICHE

Microfiche of the abstract sections of this issue and other issues of *STAR* are available on annual subscription from NTIS as PB88-911300, Attn: Subscriptions, 5285 Port Royal Road, Springfield, Virginia 22161. Annual subscription rates are $70.00 North America; $140.00 foreign. Abstract sections for previous years retroactive to 1964 are available at the current rates. Microfiche for individual *STAR* issue abstract sections are not available.

PUBLIC COLLECTIONS OF NASA DOCUMENTS

DOMESTIC: NASA and NASA-sponsored documents and a large number of aerospace publications are available to the public for reference purposes at the library maintained by the American Institute of Aeronautics and Astronautics, Technical Information Service, 555 West 57th Street, 12th Floor, New York, New York 10019

EUROPEAN: An extensive collection of NASA and NASA-sponsored publications is maintained by the British Library Lending Division, Boston Spa, Wetherby, Yorkshire, England for public access. The British Library Lending Division also has available many of the non-NASA publications cited in *STAR*. European requesters may purchase facsimile copy or microfiche of NASA and NASA-sponsored documents, those identified by both the symbols # and * from ESA - Information Retrieval Service European Space Agency, 8-10 rue Mario-Nikis, 75738 Paris CEDEX 15, France.

FEDERAL DEPOSITORY LIBRARY PROGRAM

In order to provide the general public with greater access to U.S. Government publications, Congress established the Federal Depository Library Program under the Government Printing Office (GPO), with 50 regional depositories responsible for permanent retention of material, inter-library loan, and reference services. At least one copy of nearly every NASA and NASA-sponsored publication, either in printed or microfiche format, is received and retained by the 50 regional depositories. A list of the regional GPO libraries, arranged alphabetically by state, appears on the inside back cover. These libraries are *not* sales outlets. A local library can contact a Regional Depository to help locate specific reports, or direct contact may be made by an individual.

ADDRESSES OF ORGANIZATIONS

American Institute of Aeronautics and Astronautics
Technical Information Service
555 West 57th Street, 12th Floor
New York, New York 10019

British Library Lending Division,
Boston Spa, Wetherby, Yorkshire,
England

Commissioner of Patents and Trademarks
U.S. Patent and Trademark Office
Washington, D.C. 20231

Department of Energy
Technical Information Center
P.O. Box 62
Oak Ridge, Tennessee 37830

ESA-Information Retrieval Service
ESRIN
Via Galileo Galilei
00044 Frascati (Rome) Italy

ESDU International, Ltd.
1495 Chain Bridge Road
McLean, Virginia 22101

ESDU International, Ltd.
251-259 Regent Street
London, W1R 7AD, England

Fachinformationszentrum Energie, Physik, Mathematik GMBH
7514 Eggenstein Leopoldshafen
Federal Republic of Germany

Her Majesty's Stationery Office
P.O. Box 569, S.E. 1
London, England

NASA Scientific and Technical Information Facility
P.O. Box 8757
B.W.I. Airport, Maryland 21240

National Aeronautics and Space Administration
Scientific and Technical Information Division (NTT-1)
Washington, D.C. 20546

National Technical Information Service
5285 Port Royal Road
Springfield, Virginia 22161

Pendragon House, Inc.
899 Broadway Avenue
Redwood City, California 94063

Superintendent of Documents
U.S. Government Printing Office
Washington, D.C. 20402

University Microfilms
A Xerox Company
300 North Zeeb Road
Ann Arbor, Michigan 48106

University Microfilms, Ltd.
Tylers Green
London, England

U.S. Geological Survey Library
National Center - MS 950
12201 Sunrise Valley Drive
Reston, Virginia 22092

U.S. Geological Survey Library
2255 North Gemini Drive
Flagstaff, Arizona 86001

U.S. Geological Survey
345 Middlefield Road
Menlo Park, California 94025

U.S. Geological Survey Library
Box 25046
Denver Federal Center, MS914
Denver, Colorado 80225

NTIS PRICE SCHEDULES

(Effective January 1, 1988)

Schedule A
STANDARD PRICE DOCUMENTS AND MICROFICHE

PRICE CODE	NORTH AMERICAN PRICE	FOREIGN PRICE
A01	$ 6.95	$13.90
A02	9.95	19.90
A03	12.95	25.90
A04-A05	14.95	29.90
A06-A09	19.95	39.90
A10-A13	25.95	51.90
A14-A17	32.95	65.90
A18-A21	38.95	77.90
A22-A25	44.95	89.90
A99	*	*
NO1	49.50	89.90
NO2	48.00	80.00

Schedule E
EXCEPTION PRICE DOCUMENTS AND MICROFICHE

PRICE CODE	NORTH AMERICAN PRICE	FOREIGN PRICE
E01	$ 8.50	17.00
E02	11.00	22.00
E03	12.00	24.00
E04	14.50	29.00
E05	16.50	33.00
E06	19.00	38.00
E07	21.50	43.00
E08	24.00	48.00
E09	26.50	53.00
E10	29.00	58.00
E11	31.50	63.00
E12	34.00	68.00
E13	36.50	73.00
E14	39.50	79.00
E15	43.00	86.00
E16	47.00	94.00
E17	51.00	102.00
E18	55.00	110.00
E19	61.00	122.00
E20	71.00	142.00
E99	*	*

* Contact NTIS for price quote.

IMPORTANT NOTICE

NTIS Shipping and Handling Charges

U.S., Canada, Mexico — ADD $3.00 per TOTAL ORDER

All Other Countries — ADD $4.00 per TOTAL ORDER

Exceptions — Does NOT apply to:

ORDERS REQUESTING NTIS RUSH HANDLING

ORDERS FOR SUBSCRIPTION OR STANDING ORDER PRODUCTS *ONLY*

NOTE: Each additional delivery address on an order requires a separate shipping and handling charge.

VOLUME 26 NUMBER 21 / NOVEMBER 8, 1988

TABLE OF CONTENTS

AERONAUTICS

Includes aeronautics (general); aerodynamics; air transportation and safety; aircraft communications and navigation; aircraft design, testing and performance; aircraft instrumentation; aircraft propulsion and power; aircraft stability and control; and research and support facilities (air).

For related information see also *Astronautics.*

01 AERONAUTICS (GENERAL) 2889

02 AERODYNAMICS 2892

Includes aerodynamics of bodies, combinations, wings, rotors, and control surfaces; and internal flow in ducts and turbomachinery.

For related information see also *34 Fluid Mechanics and Heat Transfer*

03 AIR TRANSPORTATION AND SAFETY 2893

Includes passenger and cargo air transport operations; and aircraft accidents.

For related information see also *16 Space Transportation* and *85 Urban Technology and Transportation.*

04 AIRCRAFT COMMUNICATIONS AND NAVIGATION 2894

Includes digital and voice communication with aircraft; air navigation systems (satellite and ground based); and air traffic control.

For related information see also *17 Space Communications, Spacecraft Communications, Command and Tracking* and *32 Communications and Radar.*

05 AIRCRAFT DESIGN, TESTING AND PERFORMANCE 2895

Includes aircraft simulation technology.

For related information see also *18 Spacecraft Design, Testing and Performance* and *39 Structural Mechanics.* For land transportation vehicles see *85 Urban Technology and Transportation.*

06 AIRCRAFT INSTRUMENTATION 2896

Includes cockpit and cabin display devices; and flight instruments.

For related information see also *19 Spacecraft Instrumentation* and *35 Instrumentation and Photography.*

07 AIRCRAFT PROPULSION AND POWER 2897

Includes prime propulsion systems and systems components, e.g., gas turbine engines and compressors; and onboard auxiliary power plants for aircraft.

For related information see also *20 Spacecraft Propulsion and Power, 28 Propellants and Fuels,* and *44 Energy Production and Conversion.*

08 AIRCRAFT STABILITY AND CONTROL 2898

Includes aircraft handling qualities; piloting; flight controls; and autopilots.

For related information see also *05 Aircraft Design, Testing and Performance.*

09 RESEARCH AND SUPPORT FACILITIES (AIR) 2899

Includes airports, hangars and runways; aircraft repair and overhaul facilities; wind tunnels; shock tubes; and aircraft engine test stands.

For related information see also *14 Ground Support Systems and Facilities (Space).*

ASTRONAUTICS

Includes astronautics (general); astrodynamics; ground support systems and facilities (space); launch vehicles and space vehicles; space transportation; space communications, spacecraft communications, command and tracking; spacecraft design, testing and performance; spacecraft instrumentation; and spacecraft propulsion and power.

For related information see also *Aeronautics*

12 ASTRONAUTICS (GENERAL) 2900

For extraterrestrial exploration see *91 Lunar and Planetary Exploration.*

13 ASTRODYNAMICS 2901

Includes powered and free-flight trajectories; and orbital and launching dynamics.

14 GROUND SUPPORT SYSTEMS AND FACILITIES (SPACE) 2901

Includes launch complexes, research and production facilities; ground support equipment, e.g., mobile transporters; and simulators.

For related information see also *09 Research and Support Facilities (Air).*

15 LAUNCH VEHICLES AND SPACE VEHICLES N.A.

Includes boosters; operating problems of launch/space vehicle systems; and reusable vehicles.

For related information see also *20 Spacecraft Propulsion and Power.*

16 SPACE TRANSPORTATION N.A.

Includes passenger and cargo space transportation, e.g., shuttle operations; and space rescue techniques.

For related information see also *03 Air Transportation and Safety* and *18 Spacecraft Design, Testing and Performance.* For space suits see *54 Man/System Technology and Life Support.*

17 SPACE COMMUNICATIONS, SPACECRAFT COMMUNICATIONS, COMMAND AND TRACKING 2902

Includes telemetry; space communications networks; astronavigation and guidance; and radio blackout.

For related information see also *04 Aircraft Communications and Navigation* and *32 Communications and Radar.*

18 SPACECRAFT DESIGN, TESTING AND PERFORMANCE 2902

Includes satellites; space platforms; space stations; spacecraft systems and components such as thermal and environmental controls; and attitude controls.

For life support systems see *54 Man/System Technology and Life Support.* For related information see also *05 Aircraft Design, Testing and Performance, 39 Structural Mechanics,* and *16 Space Transportation.*

19 SPACECRAFT INSTRUMENTATION N.A.

For related information see also *06 Aircraft Instrumentation* and *35 Instrumentation and Photography.*

20 SPACECRAFT PROPULSION AND POWER 2903

Includes main propulsion systems and components, e.g. rocket engines; and spacecraft auxiliary power sources.

For related information see also *07 Aircraft Propulsion and Power, 28 Propellants and Fuels, 44 Energy Production and Conversion,* and *15 Launch Vehicles and Space Vehicles.*

CHEMISTRY AND MATERIALS

Includes chemistry and materials (general); composite materials; inorganic and physical chemistry; metallic materials; nonmetallic materials; propellants and fuels; and materials processing.

23 CHEMISTRY AND MATERIALS (GENERAL) N.A.

24 COMPOSITE MATERIALS 2904

Includes physical, chemical, and mechanical properties of laminates and other composite materials.

For ceramic materials see *27 Nonmetallic Materials.*

25 INORGANIC AND PHYSICAL CHEMISTRY 2908

Includes chemical analysis, e.g., chromatography; combustion theory; electrochemistry; and photochemistry.

For related information see also *77 Thermodynamics and Statistical Physics.*

26 METALLIC MATERIALS 2912

Includes physical, chemical, and mechanical properties of metals, e.g., corrosion; and metallurgy.

27 NONMETALLIC MATERIALS 2917

Includes physical, chemical, and mechanical properties of plastics, elastomers, lubricants, polymers, textiles, adhesives, and ceramic materials.

For composite materials see *24 Composite Materials.*

28 PROPELLANTS AND FUELS 2922

Includes rocket propellants, igniters and oxidizers; their storage and handling procedures; and aircraft fuels.

For related information see also *07 Aircraft Propulsion and Power, 20 Spacecraft Propulsion and Power,* and *44 Energy Production and Conversion.*

29 MATERIALS PROCESSING 2924

Includes space-based development of products and processes for commercial application.

For biological materials see *55 Space Biology.*

ENGINEERING

Includes engineering (general); communications and radar; electronics and electrical engineering; fluid mechanics and heat transfer; instrumentation and photography; lasers and masers; mechanical engineering; quality assurance and reliability; and structural mechanics.

For related information see also *Physics.*

31 ENGINEERING (GENERAL) 2924

Includes vacuum technology; control engineering; display engineering; cryogenics; and fire prevention.

32 COMMUNICATIONS AND RADAR 2931

Includes radar; land and global communications; communications theory; and optical communications.

For related information see also *04 Aircraft Communications and Navigation* and *17 Space Communications, Spacecraft Communications, Command and Tracking.* For search and rescue see *03 Air Transportation and Safety,* and *16 Space Transportation.*

33 ELECTRONICS AND ELECTRICAL ENGINEERING 2934

Includes test equipment and maintainability; components, e.g., tunnel diodes and transistors; microminiaturization; and integrated circuitry.

For related information see also *60 Computer Operations and Hardware* and *76 Solid-State Physics.*

34 FLUID MECHANICS AND HEAT TRANSFER 2941

Includes boundary layers; hydrodynamics; fluidics; mass transfer and ablation cooling.

For related information see also *02 Aerodynamics* and *77 Thermodynamics and Statistical Physics.*

35 INSTRUMENTATION AND PHOTOGRAPHY 2950

Includes remote sensors; measuring instruments and gages; detectors; cameras and photographic supplies; and holography.

For aerial photography see *43 Earth Resources and Remote Sensing.* For related information see also *06 Aircraft Instrumentation* and *19 Spacecraft Instrumentation.*

36 LASERS AND MASERS 2952

Includes parametric amplifiers.

For related information see also *76 Solid-State Physics.*

37 MECHANICAL ENGINEERING 2955

Includes auxiliary systems (nonpower); machine elements and processes; and mechanical equipment.

38 QUALITY ASSURANCE AND RELIABILITY 2959

Includes product sampling procedures and techniques; and quality control.

39 STRUCTURAL MECHANICS 2959

Includes structural element design and weight analysis; fatigue; and thermal stress.

For applications see *05 Aircraft Design, Testing and Performance* and *18 Spacecraft Design, Testing and Performance.*

GEOSCIENCES

Includes geosciences (general); earth resources and remote sensing; energy production and conversion; environment pollution; geophysics; meteorology and climatology; and oceanography.

For related information see also *Space Sciences.*

42 GEOSCIENCES (GENERAL) **N.A.**

43 EARTH RESOURCES AND REMOTE SENSING **2965**

Includes remote sensing of earth resources by aircraft and spacecraft; photogrammetry; and aerial photography.

For instrumentation see *35 Instrumentation and Photography.*

44 ENERGY PRODUCTION AND CONVERSION **2966**

Includes specific energy conversion systems, e.g., fuel cells; global sources of energy; geophysical conversion; and windpower.

For related information see also *07 Aircraft Propulsion and Power, 20 Spacecraft Propulsion and Power,* and *28 Propellants and Fuels.*

45 ENVIRONMENT POLLUTION **2970**

Includes atmospheric, noise, thermal, and water pollution.

46 GEOPHYSICS **2972**

Includes aeronomy; upper and lower atmosphere studies; ionospheric and magnetospheric physics; and geomagnetism.

For space radiation see *93 Space Radiation.*

47 METEOROLOGY AND CLIMATOLOGY **2974**

Includes weather forecasting and modification.

48 OCEANOGRAPHY **2976**

Includes biological, dynamic, and physical oceanography; and marine resources.

For related information see also *43 Earth Resources and Remote Sensing.*

LIFE SCIENCES

Includes life sciences (general); aerospace medicine; behavioral sciences; man/system technology and life support; and space biology.

51 LIFE SCIENCES (GENERAL) **2977**

52 AEROSPACE MEDICINE **2985**

Includes physiological factors; biological effects of radiation; and effects of weightlessness on man and animals.

53 BEHAVIORAL SCIENCES **2991**

Includes psychological factors; individual and group behavior; crew training and evaluation; and psychiatric research.

54 MAN/SYSTEM TECHNOLOGY AND LIFE SUPPORT **2993**

Includes human engineering; biotechnology; and space suits and protective clothing.

For related information see also *16 Space Transportation.*

55 SPACE BIOLOGY **N.A.**

Includes exobiology; planetary biology; and extraterrestrial life.

MATHEMATICAL AND COMPUTER SCIENCES

Includes mathematical and computer sciences (general); computer operations and hardware; computer programming and software; computer systems; cybernetics; numerical analysis; statistics and probability; systems analysis; and theoretical mathematics.

59 MATHEMATICAL AND COMPUTER SCIENCES (GENERAL) **N.A.**

60 COMPUTER OPERATIONS AND HARDWARE **2994**

Includes hardware for computer graphics, firmware, and data processing.

For components see *33 Electronics and Electrical Engineering.*

61 COMPUTER PROGRAMMING AND SOFTWARE **2995**

Includes computer programs, routines, algorithms, and specific applications, e.g., CAD/CAM.

62 COMPUTER SYSTEMS **3001**

Includes computer networks and special application computer systems.

63 CYBERNETICS **3002**

Includes feedback and control theory, artificial intelligence, robotics and expert systems.

For related information see also *54 Man/System Technology and Life Support.*

64 NUMERICAL ANALYSIS **3004**

Includes iteration, difference equations, and numerical approximation.

65 STATISTICS AND PROBABILITY **3008**

Includes data sampling and smoothing; Monte Carlo method; and stochastic processes.

66 SYSTEMS ANALYSIS **3010**

Includes mathematical modeling; network analysis; and operations research.

67 THEORETICAL MATHEMATICS **3011**

Includes topology and number theory.

PHYSICS

Includes physics (general); acoustics; atomic and molecular physics; nuclear and high-energy physics; optics; plasma physics; solid-state physics; and thermodynamics and statistical physics.

For related information see also *Engineering.*

70 PHYSICS (GENERAL) **3011**

For precision time and time interval (PTTI) see *35 Instrumentation and Photography;* for geophysics, astrophysics or solar physics see *46 Geophysics, 90 Astrophysics,* or *92 Solar Physics.*

71 ACOUSTICS 3012
Includes sound generation, transmission, and attenuation.
For noise pollution see *45 Environment Pollution.*

72 ATOMIC AND MOLECULAR PHYSICS 3013
Includes atomic structure, electron properties, and molecular spectra.

73 NUCLEAR AND HIGH-ENERGY PHYSICS 3015
Includes elementary and nuclear particles; and reactor theory.
For space radiation see *93 Space Radiation.*

74 OPTICS 3015
Includes light phenomena and optical devices.
For lasers see *36 Lasers and Masers.*

75 PLASMA PHYSICS 3016
Includes magnetohydrodynamics and plasma fusion.
For ionospheric plasmas see *46 Geophysics.* For space plasmas see *90 Astrophysics.*

76 SOLID-STATE PHYSICS 3019
Includes superconductivity.
For related information see also *33 Electronics and Electrical Engineering* and *36 Lasers and Masers.*

77 THERMODYNAMICS AND STATISTICAL PHYSICS 3026
Includes quantum mechanics; theoretical physics; and Bose and Fermi statistics.
For related information see also *25 Inorganic and Physical Chemistry* and *34 Fluid Mechanics and Heat Transfer.*

SOCIAL SCIENCES

Includes social sciences (general); administration and management; documentation and information science; economics and cost analysis; law, political science, and space policy; and urban technology and transportation.

80 SOCIAL SCIENCES (GENERAL) N.A.
Includes educational matters.

81 ADMINISTRATION AND MANAGEMENT 3027
Includes management planning and research.

82 DOCUMENTATION AND INFORMATION SCIENCE 3027
Includes information management; information storage and retrieval technology; technical writing; graphic arts; and micrography.
For computer documentation see *61 Computer Programming and Software.*

83 ECONOMICS AND COST ANALYSIS 3028
Includes cost effectiveness studies.

84 LAW, POLITICAL SCIENCE AND SPACE POLICY N.A.
Includes NASA appropriation hearings; aviation law; space law and policy; international law; international cooperation; and patent policy.

85 URBAN TECHNOLOGY AND TRANSPORTATION 3029
Includes applications of space technology to urban problems; technology transfer; technology assessment; and surface and mass transportation.
For related information see *03 Air Transportation and Safety, 16 Space Transportation,* and *44 Energy Production and Conversion.*

SPACE SCIENCES

Includes space sciences (general); astronomy; astrophysics; lunar and planetary exploration; solar physics; and space radiation.
For related information see also *Geosciences.*

88 SPACE SCIENCES (GENERAL) 3029

89 ASTRONOMY 3030
Includes radio, gamma-ray, and infrared astronomy; and astrometry.

90 ASTROPHYSICS 3030
Includes cosmology; celestial mechanics; space plasmas; and interstellar and interplanetary gases and dust.
For related information see also *75 Plasma Physics.*

91 LUNAR AND PLANETARY EXPLORATION 3031
Includes planetology; and manned and unmanned flights.
For spacecraft design or space stations see *18 Spacecraft Design, Testing and Performance.*

92 SOLAR PHYSICS 3031
Includes solar activity, solar flares, solar radiation and sunspots.
For related information see *93 Space Radiation.*

93 SPACE RADIATION 3032
Includes cosmic radiation; and inner and outer earth's radiation belts.
For biological effects of radiation see *52 Aerospace Medicine.* For theory see *73 Nuclear and High-Energy Physics.*

GENERAL

Includes aeronautical, astronautical, and space science related histories, biographies, and pertinent reports too broad for categorization; histories or broad overviews of NASA programs.

99 GENERAL 3032

Note: N.A. means that no abstracts were assigned to this category for this issue.

SUBJECT INDEX I-1
PERSONAL AUTHOR INDEX I-53
CORPORATE SOURCE INDEX I-61
CONTRACT NUMBER INDEX I-73
REPORT/ACCESSION NUMBER INDEX I-77

TYPICAL CITATION AND ABSTRACT

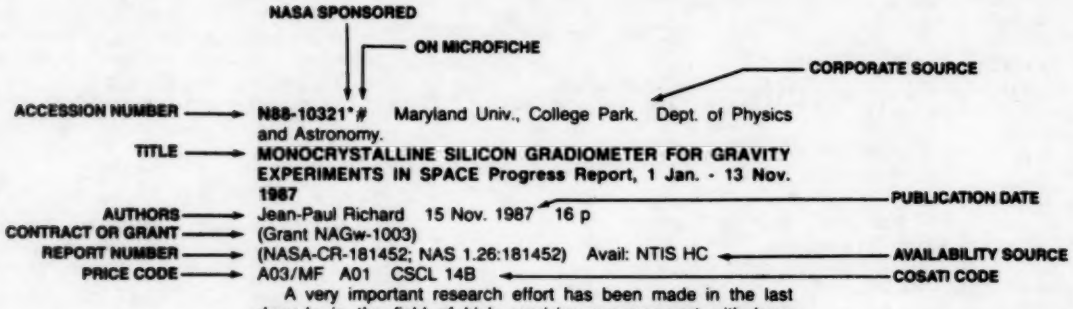
NASA SPONSORED
ON MICROFICHE
CORPORATE SOURCE
ACCESSION NUMBER
N88-10321*# Maryland Univ., College Park. Dept. of Physics and Astronomy.
TITLE
MONOCRYSTALLINE SILICON GRADIOMETER FOR GRAVITY EXPERIMENTS IN SPACE Progress Report, 1 Jan. - 13 Nov. 1987
PUBLICATION DATE
AUTHORS
Jean-Paul Richard 15 Nov. 1987 16 p
CONTRACT OR GRANT
(Grant NAGw-1003)
REPORT NUMBER
(NASA-CR-181452; NAS 1.26:181452) Avail: NTIS HC
AVAILABILITY SOURCE
PRICE CODE
A03/MF A01 CSCL 14B
COSATI CODE
A very important research effort has been made in the last decade in the field of high precision measurement with laser instrumentation. The development of a space borne gradiometer operating at a high sensitivity level using laser measurement of the distance between proof mass over a short base line of order one meter is discussed. Two aspects of laser technology make it a promising tool for gradiometry measurements: quantum limited accuracy and absolute distance measurements. The quantum limit associated with laser instrumentation was formulated. The relevant quantum and classical sources of errors in laser measurements were reviewed and corresponding laser performance requirements for gradient measurements were evaluated. Some mechanical quality factor measurements were made on simple resonant monocrystalline silicon suspensions. It was discovered that the use of zero derivative restoring forces to position the gradiometer test masses will dramatically reduce the gradiometer temperature control requirements. A laser beam side injection scheme was discovered which permits rejection of common mode accelerations. These concepts are briefly discussed. Author

VOLUME 26 NUMBER 21 / NOVEMBER 8, 1988

Scientific and Technical Aerospace Reports

A Semimonthly Publication of the National Aeronautics and Space Administration

01 AERONAUTICS (GENERAL)

N88-27147# Advisory Group for Aerospace Research and Development, Neuilly-Sur-Seine (France).
AEROSPACE APPLICATIONS STUDIES, 1971-1987
Jun. 1987 20 p
(AGARD-R-759) Copyright Avail: NTIS HC A03/MF A01

This volume provides the abstracts for systems related studies called Aerospace Applications Studies (AAS's) performed by AGARD under the supervision of the Aerospace Applications Studies Committee and the Military Committee Studies Division. These reports present the results of a one-year study effort performed by ad hoc teams made up of personnel from member nations and their military staffs. Included in the volume are the abstracts from AAS-1 published in 1972 through AAS-26 to be published in 1988. The Report was prepared by the Military Studies Committee of AGARD. Author

N88-27148*# National Aeronautics and Space Administration. Ames Research Center, Moffett Field, Calif.
INTEGRATED TECHNOLOGY ROTOR METHODOLOGY ASSESSMENT WORKSHOP
Michael J. McNulty, ed. and William G. Bousman, ed. Jun. 1988 381 p Workshop held in Moffett Field, Calif., 21-22 Jun. 1983; sponsored by NASA, Ames Research Center and the Army Prepared in cooperation with Army Aviation Systems Command, Moffett Field, Calif. Sponsored by NASA, Washington, D.C.
(NASA-CP-10007; A-86381; NAS 1.55:10007; USAAVSCOM-CP-88-A-001) Avail: NTIS HC A17/MF A01 CSCL 01B

The conference proceedings contains 14 formal papers and the results of two panel discussions. In addition, a transcript of discussion that followed the paper presentations and panels is included. The papers are of two kinds. The first seven papers were directed specifically to the correlation of industry and government mathematical models with data for rotorcraft stability from six experiments. The remaining 7 papers dealt with related topics in the prediction of rotor aeroelastic or aeromechanical stability. The first of the panels provided an evaluation of the correlation that was shown between the mathematical models and the experimental data. The second panel addressed the general problems of the validation of mathematical models. For individual titles, see N88-27149 through N88-27162.

N88-27149*# Army Aeromechanics Lab., Moffett Field, Calif.
A COMPARISON OF THE VARIOUS HELICOPTER MATHEMATICAL MODELS USED IN THE METHODOLOGY ASSESSMENT
Wendell B. Stephens *In* NASA, Ames Research Center, Integrated Technology Rotor Methodology Assessment Workshop Jun. 1988 p 1-6 (For primary document see N88-27148 21-01)
Avail: NTIS HC A17/MF A01 CSCL 01B

Various features of the computer codes used in the helicopter industry and by government agencies for rotorcraft aeroelastic stability analysis are compared. Mathematical rigor in modeling rotorcraft is given primarily to the rotor-system dynamic behavior; the aerodynamic modeling is still limited to strip theory and to uneven application of corrections for stall, reversed flow, yawed flow, radial flow, and unsteady aerodynamic effects. The forward-flight regime analysis is included in five of the 11 codes surveyed. However, only two of these codes are capable of a Floquet analysis for aeroelastic stability. For the hover regime, nine of the 11 codes use eigen-analysis approach. The remaining codes perform a harmonic analysis of the transient response of system. Author

N88-27150*# Army Aviation Systems Command, Moffett Field, Calif.
A COMPARISON OF THEORY AND EXPERIMENT FOR AEROELASTIC STABILITY OF A HINGELESS ROTOR MODEL IN HOVER **c08**
David L. Sharpe *In* NASA, Ames Research Center, Integrated Technology Rotor Methodology Assessment Workshop Jun. 1988 p 7-23 (For primary document see N88-27148 21-01)
Avail: NTIS HC A17/MF A01 CSCL 01B

Theoretical predictions of aeroelastic stability are compared with experimental, isolated, hingeless-rotor data. The six cases selected represent a torsionally soft rotor having either a stiff or soft pitch-control system in combination with zero precone and droop, 5 degree precone, or -5 degree droop. Analyses from Bell Helicopter Textron, Boeing Vertol, Hughes Helicopters, Sikorsky Aircraft, the National Aeronautics and Space Administration, and the U.S. Army Aeromechanics Laboratory were compared with the experimental data. The correlation ranged from poor to fair. Author

N88-27151*# Army Aviation Systems Command, Moffett Field, Calif.
A COMPARISON OF THEORY AND EXPERIMENT FOR COUPLED ROTOR-BODY STABILITY OF A HINGELESS ROTOR MODEL IN HOVER UNDER SIMULATED VACUUM CONDITIONS **c08**
William G. Bousman *In* NASA, Ames Research Center, Integrated Technology Rotor Methodology Assessment Workshop Jun. 1988 p 27-40 (For primary document see N88-27148 21-01)
Avail: NTIS HC A17/MF A01 CSCL 01B

Two cases were selected for correlation from an experiment that examined the aeromechanical stability of a small-scale model rotor that used tantalum rods instead of blades to simulate vacuum conditions. The first case involved body roll freedom only while the second case included body pitch and roll degrees of freedom together. Analyses from Hughes Helicopters and the U.S. Army Aeromechanics Laboratory were compared with the data and the correlations ranged from poor to good. Author

N88-27152*# Army Aviation Systems Command, Moffett Field, Calif.
A COMPARISON OF THEORY AND EXPERIMENT FOR COUPLED ROTOR-BODY STABILITY OF A HINGELESS ROTOR MODEL IN HOVER **c08**
William G. Bousman *In* NASA, Ames Research Center, Integrated Technology Rotor Methodology Assessment Workshop Jun. 1988 p 43-65 (For primary document see N88-27148 21-01)
Avail: NTIS HC A17/MF A01 CSCL 01B

Three cases were selected for correlation from an experiment that examined the aeromechanical stability of a small-scale model of a hingeless rotor and fuselage in hover. The first case examined the stability of a configuration with 0 degree blade pitch so that

coupling between dynamic modes was minimized. The second case was identical to the first except the blade pitch was set to 9 degrees which provides flap-lag coupling of the rotor modes. The third case had 9 degrees of blade pitch and also included negative pitch-lag coupling, and therefore was the most highly coupled configuration. Analytical calculations were made by Bell Helicopter Textron, Boeing Vertol, Hughes Helicopters, Sikorsky Aircraft, the U.S. Army Aeromechanics Laboratory, and NASA Ames Research Center and compared to some or all of the experimental cases. Overall, the correlation ranged from very poor-to-poor to good.
Author

N88-27153*# Army Aviation Systems Command, Moffett Field, Calif.
A COMPARISON OF THEORY AND EXPERIMENT FOR THE AEROELASTIC STABILITY OF A BEARINGLESS MODEL ROTOR IN HOVER **c08**
Seth Dawson *In* NASA, Ames Research Center, Integrated Technology Rotor Methodology Assessment Workshop Jun. 1988 p 67-80 (For primary document see N88-27148 21-01)
Avail: NTIS HC A17/MF A01 CSCL 01B

Three cases were selected for correlation from an experiment that examined the aeroelastic stability of a small-scale bearingless motor rotor in hover. The 1.8 m diameter model rotor included flap, lead-lag, and torsional degrees of freedom, but no body degrees of freedom. The first case looked at a configuration with a single pitch link on the leading edge, the second case examined a configuration with a single pitch link on the trailing edge, and the third case examined a configuration with pitch links on the leading and trailing edges to simulate a pitch link with shear restraint. Analyses from Bell Helicopter Textron, Boeing Vertol, Hughes Helicopters, Sikorsky Aircraft, and the U.S. Army Aeromechanics Laboratory were compared with the data, and the correlation ranged from poor to fair.
Author

N88-27154*# Army Aerostructures Directorate, Hampton, Va.
A COMPARISON OF THEORY AND EXPERIMENT FOR COUPLED ROTOR BODY STABILITY OF A BEARINGLESS ROTOR MODEL IN HOVER AND FORWARD FLIGHT **c08**
Paul H. Mirick *In* NASA, Ames Research Center, Integrated Technology Rotor Methodology Assessment Workshop Jun. 1988 p 87-101 (For primary document see N88-27148 21-01)
Avail: NTIS HC A17/MF A01 CSCL 01B

Seven cases were selected for correlation from a 1/5.86 Froude-scale experiment that examined several rotor designs which were being considered for full-scale flight testing as part of the Bearingless Main Rotor (BMR) program. The model rotor hub used in these tests consisted of back-to-back C-beams as flexbeam elements with a torque tube for pitch control. The first four cases selected from the experiment were hover tests which examined the effects on rotor stability of variations in hub-to-flexbeam coning, hub-to-flexbeam pitch, flexbeam-to-blade coning, and flexbeam-to-blade pitch. The final three cases were selected from the forward flight tests of optimum rotor configuration as defined during the hover test. The selected cases examined the effects of variations in forward speed, rotor speed, and shaft angle. Analytical results from Bell Helicopter Textron, Boeing Vertol, Sikorsky Aircraft, and the U.S. Army Aeromechanics Laboratory were compared with the data and the correlations ranged from poor-to-fair to fair-to-good.
Author

N88-27155*# Army Aerostructures Directorate, Hampton, Va.
A COMPARISON OF THEORY AND FLIGHT TEST OF THE BO 105/BMR IN HOVER AND FORWARD FLIGHT **c05**
Paul H. Mirick *In* NASA, Ames Research Center, Integrated Technology Rotor Methodology Assessment Workshop Jun. 1988 p 103-11 (For primary document see N88-27148 21-01)
Avail: NTIS HC A17/MF A01 CSCL 01C

Four cases were selected for comparison with theoretical predictions using stability data obtained during the flight test of the Bearingless Main Rotor (BMR) on a Messerschmidt-Boelkow-Blohm BO 105 helicopter. The four cases selected from the flight test included two ground resonance cases and two air resoncance cases. The BMR used four modified BO 105 blades attached to a bearingless hub. The hub consisted of dual fiberglass C-channel beams attached to the hub center at 0.0238R and attached to the blade root at 0.25R with blade pitch control provided by a torque tube. Analyses from Bell Helicopter Textron, Boeing Vertol, and Sikorsky Aircraft were compared with the data and the correlation ranged from very poor-to-poor to poor-to-fair.
Author

N88-27156*# Washington Univ., St. Louis, Mo. Dept. of Mechanical Engineering.
THE IMPORTANCE OF STEADY AND DYNAMIC INFLOW ON THE STABILITY OF ROTOR-BODY SYSTEMS **c08**
David A. Peters *In* NASA, Ames Research Center, Integrated Technology Rotor Methodology Assessment Workshop Jun. 1988 p 181-20 (For primary document see N88-27148 21-01)
Avail: NTIS HC A17/MF A01 CSCL 01C

The induced flow field of a rotor responds in a dynamic fashion to oscillations in rotor lift. This was long known to affect the stability and control derivatives of the rotor. More recently, however, it was also shown that this dynamic inflow also affects rotor and rotor-body aeroelastic stability. Thus, both the steady and unsteady inflow have pronounced effects on air resonance. Recent theoretical developments were made in the modeling of dynamic inflow, and these were verified experimentally. Thus, there is now a simple, verified dynamic inflow model for use in dynamic analyses.
Author

N88-27157*# Army Aeromechanics Lab., Moffett Field, Calif.
EFFECTS OF STATIC EQUILIBRIUM AND HIGHER-ORDER NONLINEARITIES ON ROTOR BLADE STABILITY IN HOVER **c08**
Marcelo R. M. CrespodaSilva and Dewey H. Hodges *In* NASA, Ames Research Center, Integrated Technology Rotor Methodology Assessment Workshop Jun. 1988 p 205-21 (For primary document see N88-27148 21-01)
Avail: NTIS HC A17/MF A01 CSCL 01C

The equilibrium and stability of the coupled elastic lead/lag, flap, and torsion motion of a cantilever rotor blade in hover are addressed, and the influence of several higher-order terms in the equations of motion of the blade is determined for a range of values of collective pitch. The blade is assumed to be untwisted and to have uniform properties along its span. In addition, chordwise offsets between its elastic, tension, mass, and aerodynamic centers are assumed to be negligible for simplicity. The aerodynamic forces acting on the blade are modeled using a quasi-steady, strip-theory approximation.
Author

N88-27158*# United Technologies Research Center, East Hartford, Conn.
AEROELASTIC MODELING OF ROTOR BLADES WITH SPANWISE VARIABLE ELASTIC AXIS OFFSET: CLASSIC ISSUES REVISITED AND NEW FORMULATIONS **c02**
Richard L. Bielawa *In* NASA, Ames Research Center, Integrated Technology Rotor Methodology Assessment Workshop Jun. 1988 p 217-22 (For primary document see N88-27148 21-01)
Avail: NTIS HC A17/MF A01 CSCL 01A

In response to a systematic methodology assessment program directed to the aeroelastic stability of hingeless helicopter rotor blades, improved basic aeroelastic reformulations and new formulations relating to structural sweep were achieved. Correlational results are presented showing the substantially improved performance of the G400 aeroelastic analysis incorporating these new formulations. The formulations pertain partly to sundry solutions to classic problem areas, relating to dynamic inflow with vortex-ring state operation and basic blade kinematics, but mostly to improved physical modeling of elastic axis offset (structural sweep) in the presence of nonlinear structural twist. Specific issues addressed are an alternate modeling of the delta EI torsional excitation due to compound bending using a force integration approach, and the detailed kinematic representation of an elastically deflected point mass of a beam with both structural sweep and nonlinear twist.
Author

N88-27159*# National Aeronautics and Space Administration. Ames Research Center, Moffett Field, Calif.
COMPARISON OF EXPERIMENTAL ROTOR DAMPING DATA-REDUCTION TECHNIQUES **c02**
William Warmbrodt *In its* Integrated Technology Rotor Methodology Assessment Workshop Jun. 1988 p 231-248 (For primary document see N88-27148 21-01)
Avail: NTIS HC A17/MF A01 CSCL 01A

The ability of existing data reduction techniques to determine frequency and damping from transient time-history records was evaluated. Analog data records representative of small-scale helicopter aeroelastic stability tests were analyzed. The data records were selected to provide information on the accuracy of reduced frequency and decay coefficients as a function of modal damping level, modal frequency, number of modes present in the time history record, proximity to other modes with different frequencies, steady offset in time history, and signal-to-noise ratio. The study utilized the results from each of the major U.S. helicopter manufacturers, the U.S. Army Aeroflightdynamics Directorate, and NASA Ames Research Center using their inhouse data reduction and analysis techniques. Consequently, the accuracy of different data analysis techniques and the manner in which they were implemented were also evaluated. It was found that modal frequencies can be accurately determined even in the presence of significant random and periodic noise. Identified decay coefficients do, however, show considerable variation, particularly for highly damped modes. The manner in which the data are reduced and the role of the data analyst was shown to be important. Although several different damping determination methods were used, no clear trends were evident for the observed differences between the individual analysis techniques. It is concluded that the data reduction of modal-damping characteristics from transient time histories results in a range of damping values. Author

N88-27160*# California Univ., Los Angeles. Dept. of Mechanics and Structures.
COMPARISON OF EXPERIMENTAL COUPLED HELICOPTER ROTOR/BODY STABILITY RESULTS WITH A SIMPLE ANALYTICAL MODEL **c08**
P. P. Friedmann and C. Venkatesan *In* NASA, Ames Research Center, Integrated Technology Rotor Methodology Assessment Workshop Jun. 1988 p 253-26 (For primary document see N88-27148 21-01)
Avail: NTIS HC A17/MF A01 CSCL 01C

The results of an analytical study aimed at predicting the aeromechanical stability of a helicopter in ground resonance, with the inclusion of aerodynamic forces are presented. The theoretical results are found to be in good agreement with the experimental results, available in literature, indicating that the coupled rotor/fuselage system can be represented by a reasonably simple mathematical model. Author

N88-27161*# Textron Bell Helicopter, Fort Worth, Tex.
AEROMECHANICAL STABILITY ANALYSIS OF COPTER **c08**
Sheng K. Yin and Jing G. Yen *In* NASA, Ames Research Center, Integrated Technology Rotor Methodology Assessment Workshop Jun. 1988 p 271-27 (For primary document see N88-27148 21-01)
Avail: NTIS HC A17/MF A01 CSCL 01C

A plan was formed for developing a comprehensive, second-generation system with analytical capabilities for predicting performance, loads and vibration, handling qualities, aeromechanical stability, and acoustics. This second-generation system named COPTER (COmprehensive Program for Theoretical Evaluation of Rotorcraft) is designed for operational efficiency, user friendliness, coding readability, maintainability, transportability, modularity, and expandability for future growth. The system is divided into an executive, a data deck validator, and a technology complex. At present a simple executive, the data deck validator, and the aeromechanical stability module of the technology complex were implemented. The system is described briefly, the implementation of the technology module is discussed, and correlation data presented. The correlation includes hingeless-rotor isolated stability, hingeless-rotor ground-resonance stability, and air-resonance stability of an advanced bearingless-rotor in forward flight. Author

N88-27162*# Hughes Helicopters, Culver City, Calif.
AEROELASTIC CHARACTERISTICS OF THE AH-64 BEARINGLESS TAIL ROTOR **c39**
D. Banerjee *In* NASA, Ames Research Center, Integrated Technology Rotor Methodology Assessment Workshop Jun. 1988 p 279-29 Previously announced in IAA as A85-20142 (For primary document see N88-27148 21-01)
Avail: NTIS HC A17/MF A01 CSCL 20K

The results of a wind tunnel test program to determine the performance loads and dynamic characteristics of the Composite Flexbeam Tail Rotor (CFTR) for the AH-64 Advanced Attack Helicopter are reported. The CFTR uses an elastomeric shear attachment of the flexbeam to the hub to provide soft-inplane S-mode and stiff-inplane C-mode configuration. The properties of the elastomer were selected for proper frequency placement and scale damping of the inplane S-mode. Kinematic pitch-lag coupling was introduced to provide the first cyclic inplane C-mode damping at high collective pitch. The CFTR was tested in a wind tunnel over the full slideslip envelop of the AH-64. It is found that the rotor was aeroelastically stable throughout the complete collective pitch range and up to rotor speeds of 1403 rpm. The dynamic characteristics of the rotor were found to be satisfactory at all pitch angles and rotor speeds of the tunnel tests. The design characteristics of the rotor which permit the high performance characteristics are discussed. Several schematic drawings and photographs of the rotor are provided. IAA

N88-27163* National Aeronautics and Space Administration, Washington, D.C.
AERONAUTICAL ENGINEERING: A CONTINUING BIBLIOGRAPHY WITH INDEXES
Aug. 1988 126 p
(NASA-SP-7037(229); NAS 1.21:7037(229)) Avail: NTIS HC A07 CSCL 01B

This bibliography lists 455 reports, articles, and other documents introduced into the NASA scientific and technical information system in July, 1988. Author

N88-27164*# Manchester Univ. (England). Dept. of Mathematics.
NONAXISYMMETRIC VISCOUS LOWER BRANCH MODES IN AXISYMMETRIC SUPERSONIC FLOWS Final Report
Peter W. Duck and Philip Hall (Exeter Univ., England) Jul. 1988 23 p Submitted for publication
(Contract NAS1-18107)
(NASA-CR-181687; ICASE-88-42; NAS 1.26:181687) Avail: NTIS HC A03/MF A01 CSCL 01B

In a previous paper, the weakly nonlinear interaction of a pair of axisymmetric lower branch Tollmien-Schlichting instabilities in cylindrical supersonic flows was considered. Here the possibility that nonaxisymmetric modes might also exist is investigated. In fact, it is found that such modes do exist and, on the basis of linear theory, it appears that these modes are the most important. The nonaxisymmetric modes are found to exist for flows around cylinders with nondimensional radius alpha less than some critical value alpha sub c. This critical value alpha sub c is found to increase monotonically with the azimuthal wavenumber nu of the disturbance and it is found that unstable modes always occur in pairs. It is also shown that, in general, instability in the form of lower branch Tollmien-Schlichting waves will occur first for nonaxisymmetric modes and that in the unstable regime the largest growth rates correspond to the latter modes. Author

02 AERODYNAMICS

Includes aerodynamics of bodies, combinations, wings, rotors, and control surfaces; and internal flow in ducts and turbomachinery.

For related information see also *34 Fluid Mechanics and Heat Transfer.*

N88-27165# Princeton Univ., N. J. Dept. of Mechanical and Aerospace Engineering.
VELOCITY MEASUREMENTS AND FLOW VISUALIZATION IN TURBULENT THREE-DIMENSIONAL SUPERSONIC FLOWS USING OXYGEN FLOW TAGGING Final Technical Report, 1 Nov. 1986 - 31 Oct. 1987
Richard B. Miles 17 Feb. 1988 4 p
(Grant AF AFOSR-0219-86)
(AD-A192551; AFOSR-88-0267TR) Avail: NTIS HC A02/MF A01 CSCL 20D

An axisymmetric jet flow facility with a laser fluorescence flow visualization system has been developed. Advanced techniques in nonlinear optics and spectroscopy are being used to track oxygen molecules for velocity measurements. Similar techniques are being used to determine the distribution of energy states of oxygen molecules for temperature measurements. Density can also be measured by observing the direct light scattering from both oxygen and nitrogen. The great advantage of these techniques is they are non-obtrusive, instantaneous, two-dimensional and require no seeding of the flow with foreign material. GRA

N88-27166# National Aeronautical Establishment, Ottawa (Ontario).
ANALYSIS OF EXPERIMENTAL DATA FOR CAST 10-2/DOA2 SUPERCRITICAL AIRFOIL AT HIGH REYNOLDS NUMBERS
Y. Y. Chan Jan. 1988 69 p
(AD-A192827; NAE-AN-49; NRC-28595) Avail: NTIS HC A04/MF A01 CSCL 20D

Experimental data obtained in the NAE Two Dimensional Test Facility for CAST 10-2/DOA2 supercritical airfoil have been analyzed for the effects of Reynolds number, transition fixing and Mach number. The data were obtained for Reynolds numbers from 6 to 30 million and Mach numbers from 0.3 to 0.8 with fixed and free transitions. The analysis indicates that the aerodynamic parameters of the airfoil depend strongly on Reynolds number and transition fixing. Above Reynolds number 10 million the trends of dependency on Reynolds number with free or fixed transition can be established. For lower Reynolds number, the long stretch of laminar boundary layer over the airfoil alters the flow characteristics significantly and the data do not follow the trends for high Reynolds numbers. GRA

N88-27167# Hokenson (Gustave J.), Los Angeles, Calif.
VARIABLE MACH NUMBER WALL JETS FOR CONTROL/PROPULSION ON HYPERVELOCITY PROJECTILES/INTERCEPTORS: TESTS WITH AN EXISTING MODEL Final Report, 22 Jul. 1987 - 21 Jan. 1988
Gustave J. Hokenson 1988 19 p
(Contract DASG60-87-C-0087)
(AD-A192845; THC-02GH88031A) Avail: NTIS HC A03/MF A01 CSCL 19A

Wind tunnel tests, utilizing a one-sixth scale model of a proposed interceptor configuration, were carried out to assess the feasibility of variable Mach number wall jets for propulsion and control applications at high altitude. The objective of this preliminary study was to assess the performance of such a thruster at high altitude where an enormous billowing of underexpanded exhaust plumes may cause a variety of problems. Included in these is sensor obscuration as a result of the upstream migration of low momentum nozzle boundary layer contaminants. The partially-bounded nature of the wall jet configuration, as well as its variable Mach number capabilities favorably impact this problem. In addition, the configuration admits a simple staging, wherein the nose may explosively separate from the afterbody prior to impact for damage enhancement. The tests indicated that no degradation in thrust is inherent to the configuration. Additional flowfield visualizations are required to quantify the obscuration problem at highly underexpanded conditions. Subsequent tests shall also assess the generation of control sideforces with an asymmetric nozzle throat. GRA

N88-27168*# West Virginia Univ., Morgantown. Dept. of Mechanical and Aerospace Engineering.
THEORETICAL-NUMERICAL STUDY OF FEASIBILITY OF USE OF WINGLETS ON LOW ASPECT RATION WINGS AT SUBSONIC AND TRANSONIC MACH NUMBERS AT REDUCE DRAG Contractor Report, Jan. 1986 - Aug. 1987
John M. Kuhlman, Paul Liaw, and Michael J. Cerney Washington NASA Aug. 1988 87 p
(Grant NAG1-625)
(NASA-CR-4174; NAS 1.26:4174) Avail: NTIS HC A05/MF A01 CSCL 01A

A numerical design study was conducted to assess the drag reduction potential of winglets installed on a series of low aspect ratio wings at a design point of M=0.8, C sub L=0.3. Wing-winglet and wing-alone design geometries were obtained for wings of aspect ratios between 1.75 and 2.67, having leading edge sweep angles between 45 and 60 deg. Winglet length was fixed at 15% of wing semispan. To assess the relative performance between wing-winglet and wing-alone configurations, the PPW nonlinear extended small disturbance potential flow code was utilized. This model has proven to yield plausible transonic flow field simulations for the series of low aspect ratio configurations selected. Predicted decreases in pressure drag coefficient for the wing-winglet configurations relative to the corresponding wing-alone planform are about 15% at the design point. Predicted decreases in wing-winglet total drag coefficient are about 12%, relative to the corresponding wing-alone design. Longer winglets (25% of the wing semispan) yielded decreases in the pressure drag of up to 22% and total drag of up to 16.4%. These predicted drag coefficient reductions are comparable to reductions already demonstrated by actual winglet designs installed on higher aspect ratio transport type aircraft. Author

N88-27169# Institut Franco-Allemand de Recherches, St. Louis (France).
THEORETICAL AND EXPERIMENTAL INVESTIGATIONS OF A VORTEX DRAG BEHIND A WING PROFILE WITH SPOILER [THEORETISCHE UND EXPERIMENTELLE UNTERSUCHUNG DER WIRBELSTRASSE HINTER EINEM TRAGFLUEGELPROFIL MIT SPOILER]
Wolfgang Czichowsky, Bernard-Charles Jaeggy, Germain Koerber, and Paul Meyer 1987 48 p In GEORGIAN
(ISL-PU-309/87; ETN-88-92736) Avail: NTIS HC A03/MF A01

A flow model behind a wing profile was studied in a subsonic wind tunnel. Laser anemometry and smoke are used for velocity components measurements and visualization of the vortex zone for two or three interference surfaces. Two analytical methods developed for the investigation of the vortex behavior are described. Numerical solutions for multivortex equations of motion and for Navier-Stokes equations are presented. ESA

N88-27170# Office National d'Etudes et de Recherches Aerospatiales, Paris (France). Direction de l'Aerodynamique.
FLOW AROUND A DELTA WING WITH OR WITHOUT A CANARD CONTROL SURFACE (phi BA = 60 DEG). PART 1: HYDRODYNAMIC VISUALIZATION IN PERMANENT REGIME [ECOULEMENT AUTOUR D'UNE AILE DELTA SANS OU AVEC PLAN CANARD (PHI BA=60 DEG). VISUALISATIONS HYDRODYNAMIQUES EN REGIME PERMANENT]
H. Werle Nov. 1987 31 p In FRENCH
(ONERA-RT-10/2891-AN-101-A-Pt-1; ETN-88-92749) Avail: NTIS HC A03/MF A01

The flow visualizations obtained in the hydrodynamics tunnel for a 60 deg wing and the same wing in canard configuration with a forebody control surface are presented. The results are a complement of data presented for 75 deg delta wings. The start

of vortices in a steady flow condition is considerably reduced when using the canard configuration. ESA

N88-27171# Deutsche Forschungs- und Versuchsanstalt fuer Luft- und Raumfahrt, Cologne (West Germany). Hauptabteilung Windkanaele.
WIND TUNNEL TESTS OF THE INFLUENCE OF AIRFOIL-THICKNESS ON NORMAL FORCE AND PITCHING MOMENT OF TWO SLENDER WINGS AT TRANSONIC AND SUPERSONIC MACH NUMBERS
Helmut Esch Nov. 1987 168 p In GERMAN; ENGLISH summary
(DFVLR-FB-88-17; ISSN-0171-1342; ETN-88-92935) Avail: NTIS HC A08/MF A01; DFVLR, VB-PL-DO, 90 60 58, 5000 Cologne, Federal Republic of Germany, 67.50 deutsche marks

Force measurements at subsonic, transonic, and supersonic Mach numbers were conducted to determine the infuence of airfoil thickness and shape on normal force and pitching moment of slender wings. Both wings, a rectangular and a clipped delta wing, had hexagonal wing sections. In addition to the variation of wing thickness, different angles of the wedge-like edges and rounded edges were investigated. The tests were performed in the trisonic wind tunnel at Mach numbers between 0.5 and 4. In supersonic flow the angle of attack varied from -10 to 90 deg, but was often limited to a lower value because of model blockage. ESA

N88-27172*# Chrysler Corp., New Orleans, La. Military Public Electronic Systems.
SPACE SHUTTLE PHASE B WIND TUNNEL MODEL AND TEST INFORMATION. VOLUME 2: ORBITER CONFIGURATION
J. L. Glynn and D. E. Poucher Jul. 1988 601 p
(Contract NAS1-18276)
(NASA-CR-178415-Vol-2-Pt-2; NAS 1.26:178415-Vol-2-Pt-2; DMS-DB-02-Vol-2) Avail: NTIS HC A99/MF A01 CSCL 01A

Archived wind tunnel test data are available for flyback booster or other alternative recoverable configurations as well as reusable orbiters studied during initial development (Phase B) of the Space Shuttle. Considerable wind tunnel data was acquired by the competing contractors and the NASA centers for an extensive variety of configurations with an array of wing and body planforms. All contractor and NASA wind tunnel test data acquired in the Phase B development have been compiled into a data base and are available for applying to current winged flyback or recoverable booster aerodynamic studies. The Space Shuttle Phase B Wind Tunnel Data Base is structured by vehicle component and configuration type. Basic components include the booster, the orbiter, and the launch vehicle. Booster configuration types include straight and delta wings, canard, cylindrical, retro-glide and twin body. Orbiter configuration types include straight and delta wings, lifting body, drop tanks, and double delta wings. Launch configuration types include booster and orbiter components in various stacked and tandem combinations. Author

N88-27173*# Ohio State Univ., Columbus. Aeronautical and Astronautical Research Lab.
AN EXPERIMENTAL STUDY OF THE EFFECT OF PITCH RATE ON DELTA WING AERODYNAMICS AND STABILITY Final Report, 1 Apr. 1986 - 30 Jun. 1988
M. B. Bragg Aug. 1988 55 p
(Grant NAG1-641)
(NASA-CR-183159; NAS 1.26:183159) Avail: NTIS HC A04/MF A01 CSCL 01A

The final report for the research conducted under this grant (NAG1-641) are contained in the two documents attached as Apendices A and B. The first is the presentation made to NASA Langley personnel on 10 December, 1987, which gave a brief analysis of the experiments. The second is a copy of an AIAA paper given in June 1988, which describes in detail the test setup, data acquisition and reduction, and results obtained. Author

N88-27174*# National Aeronautics and Space Administration. Lewis Research Center, Cleveland, Ohio.
A COMPUTATIONAL ANALYSIS OF UNDER-EXPANDED JETS IN THE HYPERSONIC REGIME
Andrew T. Hsu (Sverdrup Technology, Inc., Cleveland, Ohio.) and Meng-Sing Liou 1988 8 p Presented at the Atmospheric Flight Mechanics Conference, Minneapolis, Minn., 15-17 Aug. 1988; sponsored by AIAA
(NASA-TM-101319; E-4317; NAS 1.15:101319) Avail: NTIS HC A02/MF A01 CSCL 01A

Underexpanded axisymmetric jets are studied numerically using a full Navier-Stokes solver. Emphasis has been given to supersonic and hypersonic jets in supersonic and hypersonic ambient flows, a phenomenon previously overlooked. It is demonstrated that the shear layers and shock patterns in a jet plume can be captured without complicated viscous/inviscid and subsonic/supersonic coupling schemes. In addition, a supersonic pressure relief effect has been identified for underexpanded jets in supersonic ambient flows. While it is well known that an underexpanded jet in a quiescent ambience (or subsonic ambience) contains multiple shock cells, the present study shows that because of the supersonic pressure relief effect, an underexpanded jet in a supersonic or hypersonic ambience contains only one major shock cell. Author

N88-27158*# United Technologies Research Center, East Hartford, Conn.
AEROELASTIC MODELING OF ROTOR BLADES WITH SPANWISE VARIABLE ELASTIC AXIS OFFSET: CLASSIC ISSUES REVISITED AND NEW FORMULATIONS
Richard L. Bielawa *In* NASA, Ames Research Center, Integrated Technology Rotor Methodology Assessment Workshop Jun. 1988 p 217-22 (For primary document see N88-27148 21-01)
Avail: NTIS HC A17/MF A01 CSCL 01A

N88-27159*# National Aeronautics and Space Administration. Ames Research Center, Moffett Field, Calif.
COMPARISON OF EXPERIMENTAL ROTOR DAMPING DATA-REDUCTION TECHNIQUES
William Warmbrodt *In its* Integrated Technology Rotor Methodology Assessment Workshop Jun. 1988 p 231-248 (For primary document see N88-27148 21-01)
Avail: NTIS HC A17/MF A01 CSCL 01A

N88-27366# Colorado Univ., Boulder. Dept. of Aerospace.
CONTROL AND USE OF UNSTEADY FLOWS: INSECT USE OF VARIOUS WING KINEMATICS AND RELATED PRESSURE MEASUREMENTS USING A PITCHING AIRFOIL Final Report
Mark Andre Reavis *In* Universal Energy Systems, Inc., United States Air Force Graduate Student Summer Support Program, Volume 2 Dec. 1987 20 p (For primary document see N88-27355 21-31)
Avail: NTIS HC A99/MF E03 CSCL 01B

03 AIR TRANSPORTATION AND SAFETY

Includes passenger and cargo air transport operations; and aircraft accidents.

For related information see also *16 Space Transportation* and *85 Urban Technology and Transportation.*

N88-27175# Air Command and Staff Coll., Maxwell AFB, Ala.
EJECTION SITUATIONS IN THE U-2/TR-1: AN ANALYSIS OF EMOTIONS AND EVENTS
David J. Bonsi Apr. 1988 30 p
(AD-A192872; ACSC-88-0330) Avail: NTIS HC A03/MF A01 CSCL 01B

Although the Air Force continually attempts to make the flying profession a safer business, its primary focus has been the why-the reason for the mishap, be it mechanical failure, weather, pilot error, etc. In contrast, this study focuses on what the crewmember sees and feels. The author analyzes nine U-2/TR-1 potential or

actual ejection situations. The analysis includes discussion of the ejection decision process, emotional reactions, and subsequent chain of events initiated by these situations. The findings conclude that pilots who have ejected have significantly different perceptions of events and emotional reactions from their potential-ejection counterparts. GRA

N88-27176# Kernforschungsanlage, Juelich (West Germany). Inst. fuer Nukleare Sicherheitsforschung.
IMPROVED PROCEDURE FOR IMPACT PROBABILITY COMPUTATION OF AIRCRAFT CRASH BASED ON BALFANZ MODEL [VERBESSERTE VERFAHREN ZUR BERECHNUNG DER TREFFERWAHRSCHEINLICHKEIT DURCH ABSTUERZENDE FLUGZEUGE NACH DEM BALFANZ-MODELL]
Wilfried Hennings Jan. 1988 26 p In GERMAN
(JUEL-Spez-425; ISSN-0343-7639; ETN-88-92961) Avail: NTIS HC A03/MF A01

A mathematical model for impact probability of military aircraft crash accident is improved by Balfanz-model considering the crash angle statistical evaluation. The model is extended for cylindrical and parallelepiped buildings in dependance of shadow surface. ESA

04 AIRCRAFT COMMUNICATIONS AND NAVIGATION

Includes digital and voice communication with aircraft; air navigation systems (satellite and ground based); and air traffic control.

For related information see also *17 Space Communications, Spacecraft Communications, Command and Tracking* and *Communications and Radar.*

N88-27177# Naval Postgraduate School, Monterey, Calif.
A FEASIBILITY STUDY IN PATH PLANNING USING OPTIMIZATION TECHNIQUES M.S. Thesis
David W. Sanders Dec. 1987 91 p
(AD-A193030) Avail: NTIS HC A05/MF A01 CSCL 17G

Path Planning is an intricate part of the navigation function of any vehicle traveling between two points in space. In an autonomous underwater vehicle, a trajectory may be planned between two points using the optimization techniques of ADS (Advanced Design Synthesis) coupled to a motion analysis routine, DSL (Dynamic Simulation Language). The problem is posed as a two-point-boundary-value problem with initial states and desired final states known, as well as a final time specified. The objective function is minimized in the form of a quadratic regulator for the purpose of conserving the vehicles energy supply. An obstacle in the dive plane (X-Z plane) is introduced and successfully avoided using the constrained optimization technique. The use of optimization is proven as a feasible method for successfully planning the trajectories of underwater vehicles. GRA

N88-27178# Air Force Inst. of Tech., Wright-Patterson AFB, Ohio. School of Engineering.
THREE-DIMENSIONAL SCENE ANALYSIS USING STERO BASED IMAGING M.S. Thesis
Richard E. Roberts 9 Dec. 1987 127 p
(AD-A193120; AFIT/GE/ENG/87D-54) Avail: NTIS HC A07/MF A01 CSCL 17G

This thesis presents a new method for using passive binocular vision to create a map of the top-view of a robot's environment. While numerous autonomous robot navigation systems exist, most attempt to match objects in each image by following edges or locating significant groups of edge pixels. The method described in this paper uses two cameras (aligned in parallel) to generate stereo images. Low level image features were extracted using a new non-linear production rule system, rather than a conventional filter design. The features are registered by matching correspondingly shaped regions of constant brightness levels in both images and the offset are then computed. The use of heuristics to relieve the computational burden associated with low level image processing is unique; both in processing the images and in locating matching regions in the images. The feature extraction algorithm; the intermediate symbolic representations, and the application of these results to hierarchical structures common to context queuing systems are presented. GRA

N88-27179# Defence Research Establishment, Ottawa. (Ontario).
AUTOMATIC OMEGA STATION AND LOP (LINE OF POSITION) SELECTION
J. C. McMillan Sep. 1987 132 p
(AD-A193302; DREO-976) Avail: NTIS HC A07/MF A01 CSCL 17G

Omega is a worldwide navigation system based on 8 VLF transmitting stations dispersed widely around the globe. The phase difference between the signals of any two Omega stations can provide a line of position (LOP) on the earth's surface. Two such LOPs intersect to provide a position fix. Generally several LOPs are selected to improve the accuracy and reliability of the fix either by using a least squares technique or as in MINS (Marine Integrated Navigation System) a more sophisticated Kalman filter technique. The resulting position accuracy and reliability depends on many factors such as geometry and signal strength. This report describes these factors and a set of algorithms used by MINS to automatically select a best choice of 5 Omega stations and 4 LOPs. This includes a modal interference predictor and a multi-LOP geometric dilution of precision calculation. GRA

N88-27180*# Axiomatix, Los Angeles, Calif.
SPACECRAFT APPLICATIONS OF ADVANCED GLOBAL POSITIONING SYSTEM TECHNOLOGY Final Report
Gaylord Huth, James Dodds, Sergei Udalov, Richard Austin, Peter Loomis, and I. Newton Duboraw, III (Motorola, Inc., Chicago, Ill.)
31 May 1988 147 p
(Contract NAS9-17681)
(NASA-CR-172055; NAS 1.26:172055; R8805-5) Avail: NTIS HC A07/MF A01 CSCL 17G

The purpose of this study was to evaluate potential uses of Global Positioning System (GPS) in spacecraft applications in the following areas: attitude control and tracking; structural control; traffic control; and time base definition (synchronization). Each of these functions are addressed. Also addressed are the hardware related issues concerning the application of GPS technology and comparisons are provided with alternative instrumentation methods for specific functions required for an advanced low earth orbit spacecraft. B.G.

N88-27181*# National Aeronautics and Space Administration. Marshall Space Flight Center, Huntsville, Ala.
IPS GUIDESTAR SELECTION FOR STELLAR MODE (ASTRO)
Larry Mullins and Lewis Wooten Jun. 1988 134 p
(NASA-TM-100336; NAS 1.15:100336) Avail: NTIS HC A07/MF A01 CSCL 17G

This report describes how guide stars are selected for the Optical Sensor Package (OSP) for the Instrument Pointing System (IPS) when it is operating in the stellar mode on the ASTRO missions. It also describes how the objective loads are written and how the various roll angles are related; i.e., the celestial roll or position angle, the objective load roll angles, and the IPS gimbal angles. There is a brief description of how the IPS operates and its various modes of operation; i.e., IDOP, IDIN, and OSPCAL. Author

05 AIRCRAFT DESIGN, TESTING AND PERFORMANCE

Includes aircraft simulation technology.

For related information see also *18 Spacecraft Design, Testing and Performance* and *39 Structural Mechanics*. For land transportation vehicles see *85 Urban Technology and Transportation*.

N88-27182*# National Aeronautics and Space Administration. Langley Research Center, Hampton, Va.
CONCEPT DEVELOPMENT OF A MACH 3.0 HIGH-SPEED CIVIL TRANSPORT
A. Warner Robins, Samuel M. Dollyhigh, Fred L. Beissner, Jr., Karl Geiselhart, Glenn L. Martin, E. W. Shields, E. E. Swanson (PRC Kentron, Inc., Hampton, Va.), Peter G. Coen, and Shelby J. Morris, Jr. [1988] 50 p
(NASA-TM-4058; L-16445; NAS 1.15:4058) Avail: NTIS HC A03/MF A01 CSCL 01C

A baseline concept for a Mach 3.0 high-speed civil transport concept was developed as part of a national program with the goal that concepts and technologies be developed which will enable an effective long-range high-speed civil transport system. The Mach 3.0 concept reported represents an aggressive application of advanced technology to achieve the design goals. The level of technology is generally considered to be that which could have a demonstrated availability date of 1995 to 2000. The results indicate that aircraft are technically feasible that could carry 250 passengers at Mach 3.0 cruise for a 6500 nautical mile range at a size, weight and performance level that allows it to fit into the existing world airport structure. The details of the configuration development, aerodynamic design, propulsion system design and integration, mass properties, mission performance, and sizing are presented. Author

N88-27183# California Univ., Berkeley. Electronics Research Lab.
NUMERICAL OPTIMIZATION, SYSTEM THEORETIC AND SOFTWARE TOOLS FOR THE INTEGRATED DESIGN OF FLEXIBLE STRUCTURES AND THEIR CONTROL SYSTEMS
Annual Technical Report, 30 Sep. 1986 - 29 Sep. 1987
E. Polak 11 Apr. 1988 6 p
(Grant AF-AFOSR-86-0116)
(AD-A192927; AFOSR-88-0405TR) Avail: NTIS HC A02/MF A01 CSCL 01C

This research was motivated by a growing consensus that design specifications for projected controlled flexible aerospace structures, which are becoming larger and more flexible while performance requirements are becoming more stringent, can only be satisfied through an integrated design approach in which one determines simultaneously both structural and control system parameters. The work dealt with nonsmooth optimization techniques for the integrated design of flexible structures and their control systems. Nonsmooth optimization is an ideal tool for integrated design because it allows dynamic constraints and imposes no distinction between control system and structural variables. Major accomplishment include the development and testing of an optimal control algorithm which can be used to solve both free and fixed time optimal control problems, such as the problem of moving a flexible structure, modeled by a partial differential equation, from an in initial to a final position in minimum time, while guaranteeing upper bounds on the controls and deformations of the structure over the entire maneuver; and laying the ground-work for the frequency domain design of finite dimensional feedback controllers for flexible structures, without resorting to modal truncation and suffering the resulting spillover effects. GRA

N88-27184# Air Command and Staff Coll., Maxwell AFB, Ala.
PILOT REPORT: AFTI (ADVANCED FIGHTER TECHNOLOGY INTEGRATION) F-111
Scott E. Parks Apr. 1988 23 p
(AD-A192937; ACSC-88-2050) Avail: NTIS HC A03/MF A01 CSCL 01C

The Advanced Fighter Technology Integration (AFTI) F-111 research program is designed to evaluate a new wing design called the Mission Adaptive Wing (MAW). The MAW has the ability to continuously change it's shape in flight. This article provides a non-technical overview of the program with emphasis on the flight test and future uses of the wing on bomber, transport, and fighter aircraft. GRA

N88-27185# Advisory Group for Aerospace Research and Development, Neuilly-Sur-Seine (France).
DESIGN MANUAL FOR IMPACT DAMAGE TOLERANT AIRCRAFT STRUCTURE, ADDENDUM
M. J. Jacobson (Northrop Corp., Hawthorne, Calif.) Mar. 1988 36 p
(AGARD-AG-238-Add; ISBN-92-835-0443-7) Copyright Avail: NTIS HC A03/MF A01

In 1981 the Structures and Materials Panel of AGARD published a design manual for Impact Damage Tolerant Aircraft Structures (AG 238). Since that date, there have been significant advances in design to resist impact damage. The Panel has therefore considered it appropriate to record this information in an addendum to the AGARDograph. This Addendum has been prepared at the request of the USAF for presentation to the Structures and Materials Panel of AGARD. Author

N88-27186# Lear Siegler, Inc., Grand Rapids, Mich.
ELECTRICAL LOAD AND POWER SOURCE CAPACITY REPORT FOR THE C-130 AIRCRAFT SELF CONTAINED NAVIGATION SYSTEM (SCNS): LSI MODEL 6216A, 6216B, 6216C, REVISION
James M. Schieffer 28 Aug. 1987 20 p
(Contract F09603-85-C-1224)
(AD-A193079; GRR-6216-011-Rev) Avail: NTIS HC A03/MF A01 CSCL 17G

This report presents the electrical load analysis for the installation of the Self Contained Navigation System (SCNS) Class V Modification into the C-130 aircraft. It contains the delta load requirements by incorporation of the SCNS equipment, the load requirements of the SCNS equipment and the load requirements of removed aircraft equipment. GRA

N88-27187# Defence Research Establishment Suffield, Ralston (Alberta).
IN-FLIGHT LOAD MEASUREMENTS OF THE ROBOT-X CANARDS
S. G. Penzes Feb. 1988 41 p
(AD-A193428; DRES-SM-1191) Avail: NTIS HC A03/MF A01 CSCL 01A

The strain gauge system implemented in one of the Robot-X canards is described. The system is designed to measure lift, drag and torque. The description includes design considerations, calibration procedures and data reduction techniques. Data are presented from an early Robot-X flight test. GRA

N88-27188# Sandia National Labs., Albuquerque, N. Mex.
AIRBORNE REMOTE OPERATED DEVICE
H. D. Arlowe 1988 14 p Presented at the 15th AUVS Annual Technical Symposium, San Diego, Calif., 6 Jun. 1988
(Contract DE-AC04-76DP-00789)
(DE88-010324; SAND-88-0519C; CONF-880689-2) Avail: NTIS HC A03/MF A01

Sandia National Laboratories has recently delivered ten ducted fan airborne reconnaissance vehicles to the U.S. Marine Corps for training and evaluation. This Airborne Remote Operated Device (AROD) concept centers on a ducted fan lifting technique that uses on-board attitude sensors and a stabilization computer to minimize the operator training requirements. These vehicles have been flown under a variety of conditions for over twelve hours. Video tapes of various flights and on-board camera views will be shown. This paper will cover the design, construction, testing, and operator training. Component reliability will be discussed as well

as payload options., performance, and possible future program directors such as size, weight, communications, navigation, and operator aids. The paper will conclude that the concept of the AROD vehicle has been well demonstrated and is ready for use in solving problems of noise, communications, navigation, and integration into military tactical structures. DOE

N88-27189# Sandia National Labs., Albuquerque, N. Mex.
A METHOD FOR REDUCING THE CONING OF A SPINNING VEHICLE
T. M. Criel, J. K. Cole, and F. V. Wyatt May 1988 24 p
(Contract DE-AC04-76DP-00789)
(DE88-010971; SAND-87-2276) Avail: NTIS HC A03/MF A01

A technique for deconing a vehicle is described that involves only a single accelerometer or rate gyro, a thruster, and an electronic control unit. The testing of this technique is reviewed, and variations of the technique that can reduce the propellant required to decone are considered. A brief discussion of the dynamics of vehicles that are coning in space is also included to introduce the concept of deconing. DOE

N88-27190# Stuttgart Univ. (West Germany). Inst. fuer Mechanik.
CONTRIBUTION TO THE NUMERICAL SOLUTION OF AIRPLANE SPIN MOTION Ph.D. Thesis [BEITRAG ZUR NUMERISCHEN SIMULATION DER TRUDELBEWEGUNG VON FLUGZEUGEN]
Manfred Bubeck 1987 159 p In GERMAN
(ETN-88-92368) Avail: NTIS HC A08/MF A01

Procedures for the numerical modeling of airplane spin phenomena with related aerodynamic considerations are presented. All six degrees of freedom are conserved during the motion and modeling of flow is performed by a computational procedure for 2D wakes. Spinning tests on light airplanes show that the pressure for a given domain and moment is constant. Wake pressure is a function of the general structure of the airplane and is submitted to the reaction of the single airplane components. ESA

N88-27191# Institut Franco-Allemand de Recherches, St. Louis (France).
A NUMERICAL SIMULATION OF SIDE FORCE EFFECTS BY AERODYNAMIC FLIGHT TRAJECTORY CORRECTION [NUMERISCHE SIMULATION DES EINFLUSSES VON SEITENKRAEFTEN BEI AERODYNAMISCHER FLUGBAHNKORREKTUR]
Th. Merkel and V. Fleck 30 Jun. 1987 27 p In GERMAN Presented at the Seminar Aussenballistik an der Bundesakademie fuer Wehrverwaltung und Wehrtechnik, Mannheim, Fed. Republic of Germany, 26 May 1987
(ISL-CO-211/87; ETN-88-92738) Avail: NTIS HC A03/MF A01

Flight trajectory correction is performed by numerical simulation by a computer program for nonrotational symmetry projectiles with six degrees of freedom. Results indicate that several small corrections are more favorable than a large one. Transversal or side forces effects perpendicular to the correction surface are the most important disturbance factors. ESA

N88-27192# Societe Nationale Industrielle Aerospatiale, Toulouse (France). Div. Avions.
SUPERSONIC TRANSPORT/HYPERSONIC TRANSPORT (SST/HST) DEVELOPMENT
D. Collard and P. Picq 12 Feb. 1988 53 p Presented at the IAAAC Meeting, Stockholm, Sweden, Sep. 1987
(SNIAS-881-111-101; ETN-88-92842) Avail: NTIS HC A04/MF A01

The development of the Concorde is reviewed, and the advantages and pitfalls associated with the introduction of a radically new type of transportation such as hypersonic aircraft are discussed. The design of the year 2000 aircraft is outlined. Commercial and technical feasibility are analyzed. ESA

N88-27193# Advisory Group for Aerospace Research and Development, Neuilly-Sur-Seine (France).
AGARD STANDARD AEROELASTIC CONFIGURATIONS FOR DYNAMIC RESPONSE. 1: WING 445.6
E. Carson Yates, Jr. (National Aeronautics and Space Administration. Langley Research Center, Hampton, Va.) Jul. 1988 82 p Presented at the 61st Meeting of the Structures and Materials Panel at Oberammergau, Fed. Republic of Germany, 8-13 Sep. 1985
(AGARD-R-765; ISBN-92-835-0463-1) Copyright Avail: NTIS HC A05/MF A01 CSCL 01C

This report contains experimental flutter data for the AGARD 3-D swept tapered standard configuration Wing 445.6, along with related descriptive data of the model properties required for comparative flutter calculations. As part of a cooperative AGARD-SMP program, guided by the Sub-Committee on Aeroelasticity, this standard configuration may serve as a common basis for comparison of calculated and measured aeroelastic behavior. These comparisons will promote a better understanding of the assumptions, approximations and limitations underlying the various aerodynamic methods applied, thus pointing the way to further improvements. Author

N88-27155*# Army Aerostructures Directorate, Hampton, Va.
A COMPARISON OF THEORY AND FLIGHT TEST OF THE BO 105/BMR IN HOVER AND FORWARD FLIGHT
Paul H. Mirick *In* NASA, Ames Research Center, Integrated Technology Rotor Methodology Assessment Workshop Jun. 1988 p 103-11 (For primary document see N88-27148 21-01)
Avail: NTIS HC A17/MF A01 CSCL 01C

06 AIRCRAFT INSTRUMENTATION

Includes cockpit and cabin display devices; and flight instruments.

For related information see also *19 Spacecraft Instrumentation* and *35 Instrumentation and Photography.*

N88-27194# Air Force Wright Aeronautical Labs., Wright-Patterson AFB, Ohio.
AIR FORCE TECHNICAL OBJECTIVE DOCUMENT, FY89
Apr. 1988 42 p
(AD-A193110; AFWAL-TR-88-1000) Avail: NTIS HC A03/MF A01 CSCL 01C

Technical Objective Documents (TODs) are prepared to provide industry with Air Force objectives critical to maintaining aerospace superiority. This TOD, prepared by the AFWAL Avionics Lab., Plans Office, describes the technology required to meet future avionics operational needs. The Avionics Laboratory Investment Strategy is described. The technology program is described in terms of four technical areas which correspond to the groupings of the eight Laboratory Technology Planning Objectives (TPOs). The technology approaches are discussed together with related applications to Air Force needs and requirements. Information from the FY87 Technical Investment Plans is included. Points of contact in the laboratory are identified for each Laboratory TPO. If areas of interest are discovered, industry or academic organizations are encouraged to discuss the objectives further with the Laboratory contact identified to maximize contributions to military technology. Areas of interest/technologies include: Navigation; Surveillance; Reconnaissance; Electromagnetic warfare; Fire control; Weapon delivery; Communications; System architecture; Information processing and control; Subsystem integration; Artificial intelligence; Electronic/Electromagnetic device R&D; Radar; Electro-optical technology; Microelectronics; Integrated communications, Navigation, Identification; System integration; Software; Electronic warfare; Digital avionics; Airborne electronics and support electronics. GRA

N88-27195# Air Force Logistics Command, Wright-Patterson AFB, Ohio.
COMPUTATION OF ECM (ELECTRONIC COUNTER-MEASURES) WAR RESERVE MATERIEL SPARE REQUIREMENTS
Timothy J. Sakulich and George Zeck Nov. 1987 66 p
(AD-A193301) Avail: NTIS HC A04/MF A01 CSCL 15E

In this study we address the problem of how to convert sortie and operating hour failure data into factors compatible with the AFLC requirements system in order to improve the computation of Electronic Counter Measures (ECM) War Reserve Materiel (WRM) requirements. The current system estimates wartime spares requirements using flying hour demand rates and programs. Peacetime flying hour demand rates are transformed into wartime rates using estimated ratios of wartime-to-peacetime ECM usage per flying hour (ECM Factors). This methodology assumes that wartime ECM requirements are best predicted using flying hour programs and that wartime ECM demands are a linear multiple of peacetime demands. Using the results of a recent ECM exercise as evidence, Hq SAC/LGS demonstrated two related shortcomings of the current system. First, Hq SAC/LGS showed that wartime ECM requirements are not necessarily a linear multiple of peacetime demands. To solve this shortcomings, they proposed that future ECM wartime demand rates be developed directly from data collected during annual war exercises. GRA

N88-27196*# Lockheed Aeronautical Systems Co., Marietta, Ga.
AN EVALUATION OF FLIGHT PATH FORMATS HEAD-UP AND HEAD-DOWN Final Report
George A. Sexton, Laura E. Moody, JoAnne Evans, and Kenneth E. Williams Washington NASA [1988] 123 p
(Contract NAS1-18029)
(NASA-CR-4176; LG87ER0154; NAS 1.26:4176) Avail: NTIS HC A06/MF A01 CSCL 01D

Flight path primary flight display formats were incorporated on head-up and head-down electronic displays and integrated into an Advanced Concepts Flight Simulator. Objective and subjective data were collected while ten airline pilots evaluated the formats by flying an approach and landing task under various ceiling, visibility and wind conditions. Deviations from referenced/-commanded airspeed, horizontal track, vertical track and touchdown point were smaller using the head-up display (HUD) format than the head-down display (HDD) format, but not significantly smaller. Subjectively, the pilots overwhelmingly preferred (1) flight path formats over attitude formats used in current aircraft, and (2) the head-up presentation over the head-down, primarily because it eliminated the head-down to head-up transition during low visibility landing approaches. This report describes the simulator, the flight displays, the format evaluation, and the results of the objective and subjective data. Author

07 AIRCRAFT PROPULSION AND POWER

Includes prime propulsion systems and systems components, e.g., gas turbine engines and compressors; and onboard auxilliary power plants for aircraft.

For related information see also *20 Spacecraft Propulsion and Power, 28 Propellants and Fuels,* and *44 Energy Production and Conversion.*

N88-27197# Avco Lycoming Engine Group, Stratford, Conn.
T55-L-714 ENGINE DEVELOPMENT AND QUALIFICATION. ENGINE M11 LOW CYCLE FATIGUE TEST REPORT. (0213-005-87)
J. Kozub, Jr. Dec. 1987 113 p
(Contract DAAJ09-87-C-A043)
(AD-A192765; LYC-87-14) Avail: NTIS HC A06/MF A01 CSCL 21E

T55-L-713 engine M-11C, which had previously completed 1000 cycles (250 hours) of Low Cycle Fatigue (LCF) testing, was subjected to an additional 1000 cycles of LCF testing. Testing ended when there was a failure in the power turbine section of the engine. The results of investigations completed up to the publication of this report indicate a third turbine blade failure. Prior to the failure, the engine had satisfactorily completed 746 cycles (161.6 hours) of the scheduled second 1000 cycles. Thermodynamic deterioration was consistent with the number of cycles completed and there had been no significant mechanical or performance problems. The average actual gas producer speed (NI), shaft horsepower (SHP), and power turbine inlet temperature are listed. Except for secondary damage suffered in the failure, the T55-L-713 gas producer turbine components were in good condition and showed relatively little thermal distress. GRA

N88-27198# Avco Lycoming Engine Group, Stratford, Conn.
T55-L-714 ENGINE DEVELOPMENT AND QUALIFICATION. ENGINE M11 LOW CYCLE FATIGUE TEST REPORT. (0213-005-87), VOLUME 2, PART 1
J. Kozub, Jr. Dec. 1987 405 p
(Contract DAAJ09-87-C-A043)
(AD-A192766; LYC-87-14-Vol-2-Pt-1) Avail: NTIS HC A18/MF A01 CSCL 21E

Volume 2 - Part 1 contains the following for the first 1000 cycles. Section 1 - Engine Test Log Sheets: These sheets are an account of daily engine activity and test events. Section 2 - Engine Test Cycle Sheets: These sheets contain actual engine mechanical and performance data recorded during cycling. Section 3 - Engine Test Data Sheets: These sheets contain actual mechanical data and performance data (corrected to sea level standard conditions) recorded during engine checkout and calibrations. GRA

N88-27199# Institut National des Sciences Appliquees, Lyon (France). Lab. de Mecanique des Structures.
PREDICTION OF THE AEROELASTIC BEHAVIOR OF TUNED BLADES. APPLICATION TO AIRCRAFT ENGINES Ph.D. Thesis [PREVISION DU COMPORTEMENT AEROELASTIQUE DES AUBAGES ACCORDES. APPLICATION AUX MOTEURS D'AVIONS]
Benoit Vincent 1987 155 p In FRENCH Sponsored by SNECMA, France and the Ministere de la Recherche et de la Technologie, Paris, France
(ISAL-87-0046; ETN-88-92757) Avail: NTIS HC A08/MF A01

A method of analysis based on the study of the behavior of the tuned engine blades after investigation of resonant frequencies and dumping in the presence of fluid is proposed. The model presented, in Lagrange coordinates, allows the calculation of complex coefficient differential equation systems. The solution leads to the stability diagnostic. The results obtained in the two described examples show the predominant role played by the fluid. Mechanical and aerodynamic coupling analysis must be done over the whole length of the structure. ESA

N88-27200*# National Aeronautics and Space Administration. Lewis Research Center, Cleveland, Ohio.
EXPERIMENTAL DETERMINATION OF AERODYNAMIC DAMPING IN A THREE-STAGE TRANSONIC AXIAL-FLOW COMPRESSOR M.S. Thesis - Case Western Reserve Univ.
Frederick A. Newman Aug. 1988 113 p
(NASA-TM-100953; E-4267; NAS 1.15:100953) Avail: NTIS HC A06/MF A01 CSCL 21E

Rotor blade aerodynamic damping is experimentally determined in a three-stage transonic axial flow compressor having design aerodynamic performance goals of 4.5:1 pressure ratio and 65.5 lbm/sec weight flow. The combined damping associated with each mode is determined by a least squares fit of a single degree of freedom system transfer function to the nonsynchronous portion of the rotor blade strain gauge output power spectra. The combined damping consists of aerodynamic and structural and mechanical damping. The aerodynamic damping varies linearly with the inlet total pressure for a given equivalent speed, equivalent mass flow, and pressure ratio while structural and mechanical damping are assumed to be constant. The combined damping is determined at three inlet total pressure levels to obtain the aerodynamic damping.

The third stage rotor blade aerodynamic damping is presented and discussed for 70, 80, 90, and 100 percent design equivalent speed. The compressor overall performance and experimental Campbell diagrams for the third stage rotor blade row are also presented. Author

N88-27201*# National Aeronautics and Space Administration. Lewis Research Center, Cleveland, Ohio.
DOCUMENTATION OF THE BENSON DIESEL ENGINE SIMULATION PROGRAM
Jon VanGerpen Aug. 1988 136 p Prepared in cooperation with Army Aviation Research and Technical Command, Cleveland, Ohio
(DA Proj. 1L1-61102-AH-45)
(NASA-TM-100940; E-4221; NAS 1.15:100940; AVSCOM-TR-88-C-025) Avail: NTIS HC A07/MF A01 CSCL 21E

This report documents the Benson Diesel Engine Simulation Program and explains how it can be used to predict the performance of diesel engines. The program was obtained from the Garrett Turbine Engine Company but has been extensively modified since. The program is a thermodynamic simulation of the diesel engine cycle which uses a single zone combustion model. It can be used to predict the effect of changes in engine design and operating parameters such as valve timing, speed and boost pressure. The most significan change made to this program is the addition of a more detailed heat transfer model to predict metal part temperatures. This report contains a description of the sub-models used in the Benson program, a description of the input parameters and sample program runs. Author

08 AIRCRAFT STABILITY AND CONTROL

Includes aircraft handling qualities; piloting; flight controls; and autopilots.

For related information see also *05 Aircraft Design, Testing and Performance.*

N88-27202# Institut Franco-Allemand de Recherches, St. Louis (France).
INVESTIGATIONS OF AIRCRAFT CONTROL WITH JET SPOILERS [VERSUCHE ZUR STEUERUNG MIT STRAHLSPOILERN: UNTERHALB DES TITELS IST HINZUZUFUEGEN]
G. Patz 15 Apr. 1987 27 p In GERMAN
(Contract BMVg-T/R-760/G-0002/G-1702)
(ISL-R-112/87; ETN-88-92733) Avail: NTIS HC A03/MF A01

Aerodynamic effectiveness of jet spoilers for high speed aircraft control in comparison with flaperons is studied. An increased effect is obtained by energy addition in the recirculation zone of the jet spoiler. Tests are carried out in a square section shock tube for Mach number 2 to study vaporization and possible reactions of the mixture air/helium jet and of the combustion of air/ethanol mixture. ESA

N88-27203# Deutsche Forschungs- und Versuchsanstalt fuer Luft- und Raumfahrt, Brunswick (West Germany). Abteilung Drehfluegelflugzeuge.
ROBUST DIGITAL MODEL FOLLOWING CONTROLLER FOR HELICOPTERS Ph.D. Thesis - Technische Univ.
Gerhard Bouwer Jan. 1988 157 p In GERMAN; ENGLISH summary Report will also be announced as translation (ESA-TT-1041)
(DFVLR-FB-88-07; ISSN-0171-1342; ETN-88-92925) Avail: NTIS HC A08/MF A01; DFVLR, VB-PL-DO, 90 60 58, 5000 Cologne, Federal Republic of Germany, 60.50 deutsche marks

The digital model following controller for multivariable systems consists of a linear P-I-controller, nonlinear control laws, and a controller output optimization. To meet the physical limits of the helicopter, especially the rotor speed, a special actuator simulation is developed. A low order model and a helicopter simulation model are used for the investigations. The effectiveness of the control system in model following as well as in disturbance rejection is tested in numerical simulations. Limits of the model following control system are shown by model parameter variation. The influence of a decoupled model on the handling qualities of a helicopter are investigated in piloted simulations. Selected flight test results show the performance of the control system in model following and flying a helicopter in gusty environment. The simulation of two different helicopters in flight demonstrates the possibilities of in-flight simulation. ESA

N88-27204# Bodenseewerk Geraetetechnik G.m.b.H., Ueberlingen (West Germany). Geschaeftsbereich Regelung und Navigation.
COMPUTER SYSTEM FOR THE PRIMARY FLY-BY-WIRE CONTROL OF CIVIL TRANSPORT AIRCRAFT (EXPERIMENTAL SYSTEM) Final Report, 31 Dec. 1987
Franz Boos, Hans-Juergen Maier, and Rudolf Scharpf 30 Apr. 1988 200 p In GERMAN; ENGLISH summary
(Contract BMFT-FE-LFL-8560-1)
(FBW-TB-2086/88; ETN-88-92963) Avail: NTIS HC A09/MF A01

For fly-by-wire control of civil transport aircraft, a fault tolerant computer system was specified, designed, and an experimental prototype produced. The system consists of four identical FBW-computers assembled from avionic computer building blocks. It is characterized by: multi-processor operation within an FBW-computer to guarantee the required real time data throughput, and fault tolerant behavior defined by the software implemented redundancy management of the concurrent operation of the four computers. For proving functions (signal-processing, redundancy management) an extensive test system was designed and built. Its major features are: computer supported stimulation and analysis for real-time open-loop tests with dynamic data sets, and computer supported hardware fault stimulation to test the redundancy management. ESA

N88-27205*# Advanced Rotorcraft Technology, Inc., Mountain View, Calif.
DYNAMIC MODELLING AND ESTIMATION OF THE ERROR DUE TO ASYNCHRONISM IN A REDUNDANT ASYNCHRONOUS MULTIPROCESSOR SYSTEM
Loc C. Huynh and R. W. DuVal May 1986 36 p
(NASA Order A-30146-C)
(NASA-CR-177427; NAS 1.26:177427) Avail: NTIS HC A03/MF A01 CSCL 01C

The use of Redundant Asynchronous Multiprocessor System to achieve ultrareliable Fault Tolerant Control Systems shows great promise. The development has been hampered by the inability to determine whether differences in the outputs of redundant CPU's are due to failures or to accrued error built up by slight differences in CPU clock intervals. This study derives an analytical dynamic model of the difference between redundant CPU's due to differences in their clock intervals and uses this model with on-line parameter identification to idenitify the differences in the clock intervals. The ability of this methodology to accurately track errors due to asynchronisity generate an error signal with the effect of asynchronisity removed and this signal may be used to detect and isolate actual system failures. Author

N88-27150*# Army Aviation Systems Command, Moffett Field, Calif.
A COMPARISON OF THEORY AND EXPERIMENT FOR AEROELASTIC STABILITY OF A HINGELESS ROTOR MODEL IN HOVER
David L. Sharpe *In* NASA, Ames Research Center, Integrated Technology Rotor Methodology Assessment Workshop Jun. 1988 p 7-23 (For primary document see N88-27148 21-01)
Avail: NTIS HC A17/MF A01 CSCL 01B

N88-27151*# Army Aviation Systems Command, Moffett Field, Calif.
A COMPARISON OF THEORY AND EXPERIMENT FOR COUPLED ROTOR-BODY STABILITY OF A HINGELESS ROTOR MODEL IN HOVER UNDER SIMULATED VACUUM CONDITIONS
William G. Bousman *In* NASA, Ames Research Center, Integrated Technology Rotor Methodology Assessment Workshop Jun. 1988 p 27-40 (For primary document see N88-27148 21-01)
Avail: NTIS HC A17/MF A01 CSCL 01B

N88-27152*# Army Aviation Systems Command, Moffett Field, Calif.
A COMPARISON OF THEORY AND EXPERIMENT FOR COUPLED ROTOR-BODY STABILITY OF A HINGELESS ROTOR MODEL IN HOVER
William G. Bousman *In* NASA, Ames Research Center, Integrated Technology Rotor Methodology Assessment Workshop Jun. 1988 p 43-65 (For primary document see N88-27148 21-01)
Avail: NTIS HC A17/MF A01 CSCL 01B

N88-27153*# Army Aviation Systems Command, Moffett Field, Calif.
A COMPARISON OF THEORY AND EXPERIMENT FOR THE AEROELASTIC STABILITY OF A BEARINGLESS MODEL ROTOR IN HOVER
Seth Dawson *In* NASA, Ames Research Center, Integrated Technology Rotor Methodology Assessment Workshop Jun. 1988 p 67-80 (For primary document see N88-27148 21-01)
Avail: NTIS HC A17/MF A01 CSCL 01B

N88-27154*# Army Aerostructures Directorate, Hampton, Va.
A COMPARISON OF THEORY AND EXPERIMENT FOR COUPLED ROTOR BODY STABILITY OF A BEARINGLESS ROTOR MODEL IN HOVER AND FORWARD FLIGHT
Paul H. Mirick *In* NASA, Ames Research Center, Integrated Technology Rotor Methodology Assessment Workshop Jun. 1988 p 87-101 (For primary document see N88-27148 21-01)
Avail: NTIS HC A17/MF A01 CSCL 01B

N88-27156*# Washington Univ., St. Louis, Mo. Dept. of Mechanical Engineering.
THE IMPORTANCE OF STEADY AND DYNAMIC INFLOW ON THE STABILITY OF ROTOR-BODY SYSTEMS
David A. Peters *In* NASA, Ames Research Center, Integrated Technology Rotor Methodology Assessment Workshop Jun. 1988 p 181-20 (For primary document see N88-27148 21-01)
Avail: NTIS HC A17/MF A01 CSCL 01C

N88-27157*# Army Aeromechanics Lab., Moffett Field, Calif.
EFFECTS OF STATIC EQUILIBRIUM AND HIGHER-ORDER NONLINEARITIES ON ROTOR BLADE STABILITY IN HOVER
Marcelo R. M. CrespodaSilva and Dewey H. Hodges *In* NASA, Ames Research Center, Integrated Technology Rotor Methodology Assessment Workshop Jun. 1988 p 205-21 (For primary document see N88-27148 21-01)
Avail: NTIS HC A17/MF A01 CSCL 01C

N88-27160*# California Univ., Los Angeles. Dept. of Mechanics and Structures.
COMPARISON OF EXPERIMENTAL COUPLED HELICOPTER ROTOR/BODY STABILITY RESULTS WITH A SIMPLE ANALYTICAL MODEL
P. P. Friedmann and C. Venkatesan *In* NASA, Ames Research Center, Integrated Technology Rotor Methodology Assessment Workshop Jun. 1988 p 253-26 (For primary document see N88-27148 21-01)
Avail: NTIS HC A17/MF A01 CSCL 01C

N88-27161*# Textron Bell Helicopter, Fort Worth, Tex.
AEROMECHANICAL STABILITY ANALYSIS OF COPTER
Sheng K. Yin and Jing G. Yen *In* NASA, Ames Research Center, Integrated Technology Rotor Methodology Assessment Workshop Jun. 1988 p 271-27 (For primary document see N88-27148 21-01)
Avail: NTIS HC A17/MF A01 CSCL 01C

N88-27373# Iowa Univ., Iowa City. Dept. of Mechanical Engineering.
OPTIMAL CONTROL OF THE WING ROCK PHENOMENON Final Report
Christopher D. Sierra *In* Universal Energy Systems, Inc., United States Air Force Graduate Student Summer Support Program, Volume 2 Dec. 1987 16 p (For primary document see N88-27355 21-31)
Avail: NTIS HC A99/MF E03 CSCL 01C

09 RESEARCH AND SUPPORT FACILITIES (AIR)

Includes airports, hangars and runways; aircraft repair and overhaul facilities; wind tunnels; shock tubes; and aircraft engine test stands.

For related information see also *14 Ground Support Systems and Facilities (Space).*

N88-27206# Dundee Univ. (Scotland). Dept. of Civil Engineering.
ALTERNATE/MODIFIED BINDERS FOR AIRFIELD PAVEMENTS Periodic Report Nos. 1-3, Aug. 1986 - Jan. 1988
A. F. Stock Jan. 1988 52 p
(Contract DAJA45-86-C-0043)
(AD-A192781; R/D-5499-EN-01) Avail: NTIS HC A04/MF A01 CSCL 11A

The report contains fact sheet data on the following modifiers:- Sealgum, Polybilt, Escorene, Eva, Trinidad natural asphalt, Cariflex, Neolastic, Neoflex and Novophalt. A procedure for successfully screening modifiers is proposed. The report identifies and classifies all the additives for asphalt which have been identified to date. It also includes a note of the suppliers,and where data is available, and costs. GRA

N88-27207# Oak Ridge National Lab., Tenn. Energy Div.
VIBRATIONAL IMPACTS OF HUSH HOUSE OPERATION
A. J. Witten 1988 13 p Presented at the Joint CSCE-ASCE Conference on Environmental Engineering, Vancouver, British Columbia, 13 Jul. 1988
(Contract DE-AC05-84OR-21400)
(DE88-006983; CONF-880741-2) Avail: NTIS HC A03/MF A01

United States Air Force (USAF) facilities are required to test turboprop and turbojet engines before or after maintenance or repair and prior to installation on aircraft to ensure that no problems were introduced or remain uncorrected. This requirement prevents the installation of engines in aircraft which require further maintenance. There are a number of facilities in use by USAF for conducting engine diagnostic tests. The most modern of these facilities is the hush house which is a hangar-like structure designed to isolate the noise associated with extended engine operations from the surrounding environment. One type of hush house, the T-10, is of particular concern because of vibrational impacts to surrounding structures induced by subaudible sound (infrasound) emitted during operation. While these facilities fulfill the design requirement of reducing audible noise, serious sitting problems were reported at several installations because of infrasound-induced vibrations. The worst of these include the abandonment of an avionics laboratory because induced vibrations interfered with this facilities function and structural damage to a concrete block maintenance facility. This paper describes a predictive method for assessing vibration-driven structural impacts. DOE

N88-27208# Office National d'Etudes et de Recherches Aerospatiales, Paris (France). Directions des Grands Moyens d'Essais.
EUROPEAN TRANSONIC WIND TUNNEL PROJECT: ASSISTANCE TO THE DESIGN GROUP Final Report [ETUDE DE LA SOUFFLERIE TRANSSONIQUE EUROPEENE. ASSISTANCE AU GROUPE DE PROJET]
Gilbert Francois Feb. 1988 6 p In FRENCH
(Contract DRET-87-820)
(ONERA-RSF-11/0694-GY-010-G; ETN-88-92746) Avail: NTIS HC A02/MF A01

The assistance provided to the European transonic wind tunnel design group by personnel from the Test Facilities Direction of ONERA in 1987 is reported. Names, type of meeting, and purpose of meeting are detailed. ESA

N88-27209# Office National d'Etudes et de Recherches Aerospatiales, Paris (France). Grands Moyens d'Essais.
STUDIES CONCERNING THE EUROPEAN TRANSONIC WIND TUNNEL Final Report [ETUDES DE LA SOUFFLERIE TRANSSONIQUE EUROPENNE]
X. Bouis Feb. 1988 15 p In FRENCH
(Contract DRET-87-820)
(ONERA-RSF-10/0694-GY-010-G; ETN-88-92748) Avail: NTIS HC A03/MF A01

Activities of a design group participating in the PG-ETW transonic wind tunnel project are described. The phase 2.2 of the project includes the conceptual design, the distribution of tasks between national partners, the estimation of the investment and cost, and the definition of a legal status are presented. ESA

N88-27210# Deutsche Forschungs- und Versuchsanstalt fuer Luft- und Raumfahrt, Cologne (West Germany). Hauptabteilung Windkanaele.
CRYOGENIC FREE JETS
Knud Kindler Jun. 1987 62 p In GERMAN; ENGLISH summary
(DFVLR-FB-88-16; ISSN-0171-1342; ETN-88-92934) Avail: NTIS HC A04/MF A01; DFVLR, VB-PL-DO, 90 60 58, 5000 Cologne, Federal Republic of Germany, 25.50 deutsche marks

Differences in the development of subsonic axisymmetric free jets are investigated experimentally at cryogenic and ambient temperatures. The velocity distribution is found nearly independent of temperature level. That is not true for the temperature distribution. The decrease of entrainment rate at cryogenic conditions due to higher density level relative to the ambient conditions is compensated partly by the effect of energy exchange. ESA

N88-27211# Deutsche Forschungs- und Versuchsanstalt fuer Luft- und Raumfahrt, Goettingen (West Germany). Abteilung Hochgeschwindigkeitsstroemungen.
HYBRID PROCEDURE FOR DYNAMIC MEASUREMENTS IN TRANSONIC WIND TUNNELS: DEMONSTRATED BY PITCH OSCILLATION Ph.D. Thesis - Technische Univ.
Detlef Kuczka Apr. 1988 95 p In GERMAN; ENGLISH summary
(DFVLR-FB-88-19; ISSN-0171-1342; ETN-88-92936) Avail: NTIS HC A05/MF A01; DFVLR, VB-PL-DO, 90 60 58, 5000 Cologne, Federal Republic of Germany, 29 deutsche marks

For dynamic measurements in transonic wind tunnels a hybrid procedure is presented to obtain quasi interference-free results. Therefore, residual dynamic interferences are calculated, when first the stationary wall interferences are eliminated by wall adaptation for the stationary case. Using the Standard Dynamics Model, dynamic measurements were performed in the adaptive wall test section of the high-speed tunnel to validate the proposed procedure. The model was subjected to forced pitch oscillations. Measurements of stationary force coefficients, the dynamic derivatives, the stationary wall pressure distribution and significant dynamic wall pressures were taken as well in the straight walled test section, as in the test section adapted for the stationary case. Results are compared to those acquired in the 1 x 1 m transonic facility 4 x 4 ft tunnel and 0.9 x 0.9 m tunnel. Methods for the correction of dynamic derivatives are discussed to determine their range of validity. ESA

N88-27212# Deutsche Forschungs- und Versuchsanstalt fuer Luft- und Raumfahrt, Brunswick (West Germany). Hauptabteilung Windkanaele.
EQUIPMENT FOR MASS FLOW MEASUREMENTS IN THE LOW-SPEED WIND TUNNEL AT DFVLR IN BRUNSWICK, WEST GERMANY
Reinhard Friedrichs Dec. 1987 54 p In GERMAN; ENGLISH summary Report will also be announced as translation (ESA-TT-1125)
(DFVLR-Mitt-88-02; ISSN-0176-7739; ETN-88-92937) Avail: NTIS HC A04/MF A01; DFVLR, VB-PL-DO, 90 60 58, 5000 Cologne, Federal Republic of Germany, 22.50 deutsche marks

A mass flow measurement device inserted in the low speed wind tunnel determines air intake mass flow as a function of intake parameters. The device consists of a tank with ISA-1932 standard nozzles coupled to the existing vacuum pump and situated in the cellar beneath the wind tunnel. Nozzles are calibrated with choked nozzles for the test range 0.5 to 2.5 kg/sec and accuracy obtained is 0.3 percent. Tests results are compared with an air intake mass flow model and correction factors are derived. ESA

N88-27367# , Dayton Univ., Ohio. Dept. of Electrical Engineering.
AIRCRAFT REFUELING DEMONSTRATOR USING A MICROBOT ALPHA 2 ROBOT Final Report
Bryan P. Riddiford *In* Universal Energy Systems, Inc., United States Air Force Graduate Student Summer Support Program, Volume 2 Dec. 1987 18 p (For primary document see N88-27355 21-31)
Avail: NTIS HC A99/MF E03 CSCL 14B

N88-27370# Puerto Rico Univ., Mayaguez. Dept. of Mechanical Engineering.
DESIGN OF A MECHANISM TO CONTROL WIND TUNNEL TURBULENCE Final Report
Filiberto Santiago *In* Universal Energy Systems, Inc., United States Air Force Graduate Student Summer Support Program, Volume 2 Dec. 1987 33 p (For primary document see N88-27355 21-31)
Avail: NTIS HC A99/MF E03 CSCL 14B

12 ASTRONAUTICS (GENERAL)

For extraterrestrial exploration see *91 Lunar and Planetary Exploration.*

N88-27213# Los Alamos National Lab., N. Mex.
STEPS TOWARD LUNAR SETTLEMENT
E. M. Jones 1988 12 p Presented at the 100th Meeting of the Australia and New Zealand Association for the Advancement of Science, Sydney, Australia, 17 May 1988
(Contract W-7405-eng-36)
(DE88-009141; LA-UR-88-1192; CONF-880594-1) Avail: NTIS HC A03/MF A01

The costs of transporting people and material to low-earth-orbit (LEO), and hence to the lunar surface, will constrain the pace and pattern of lunar development. Beginning as a Spartan base camp completely supplied from Earth, a lunar science-and-resource-development facility could grow in size, amenities, and capability to the point that passenger transport becomes a major expense. At such a stage, some employees of the facility might be given the opportunity to become permanent residents; and at that point, lunar settlement will have begun. We assume growth rates of facilities and staff constrained by the annual delivery of 900 tons to LEO. During the base camp era, about 100 tons would be delivered annually to the lunar surface. Within six years, the facility could grow to a collection of 25 modules, housing a staff of about 16 with each member of the

staff serving a six-month tour on a staggered schedule. At the end of this first phase, oxygen produced from lunar ilmenite and delivered to lunar orbit for use as propellant would allow annual lunar-bound cargos of about 200 tons. Production from lunar materials of heat shields for aerobraking would enable economical delivery of lunar oxygen to LEO and, therefore, could raise lunar-bound cargoes to about 450 tons. DOE

N88-27214* National Aeronautics and Space Administration, Washington, D.C.
TECHNOLOGY FOR LARGE SPACE SYSTEMS: A BIBLIOGRAPHY WITH INDEXES (SUPPLEMENT 18)
Jun. 1988 162 p
(NASA-SP-7046(18); NAS 1.21:7046(18)) Avail: NTIS HC A07 CSCL 22B

This bibliography lists 569 reports, articles, and other documents introduced into the NASA scientific and technical information system between July 1,1987 and December 31, 1987. Its purpose is to provide helpful information to the researcher, manager, and designer in technology development and mission design according to system, interactive analysis and design, structural and thermal analysis and design, structural concepts and control systems, electronics, advanced materials, assembly concepts, propulsion, and solar power satellite systems. Author

N88-27215# Kienbaum Unternehmensberatung, Gummersbach (West Germany).
ECONOMIC IMPACT OF SPACE FLIGHT ACTIVITIES IN WEST GERMANY. INFLUENCE OF ALLOCATIONS OF BUNDESMINISTERIUM FUER FORSCHUNG UND TECHNOLOGIE Final Report [WIRTSCHAFTLICHE AUSWIRKUNGEN VON RAUMFAHRTAKTIVITAETEN IN DER BUNDESREPUBLIK DEUTSCHLAND, EINFLUSS DER FOERDERMITTEL DES BMFT (MITTELFLUSSANALYSE)]
1988 354 p In GERMAN Sponsored by DFVLR, Cologne, Fed. Republic of Germany
(ETN-88-92106) Avail: NTIS HC A16/MF A01

Analysis of economic impact of space activities in West Germany is performed using theoretical, practical, and empirical methods. Budget income and prejudices for the government and the industrial partners are indicated for the period 1976 to 1985. Contractors and industrial suppliers involved in space activities are questioned directly and indirectly about their financial contribution in space related research programs in six main equipment industries. Criteria for decision making about make or buy relative to costs and quality factors are presented. ESA

13 ASTRODYNAMICS

Includes powered and free-flight trajectories; and orbital and launching dynamics.

N88-27216# Bonn Univ. (West Germany). Inst. fuer Geodaesie.
FORTRAN PROGRAMS FOR COMPUTATION OF TIME DEPENDENT SEA LEVELS AND TRAJECTORY ERRORS FROM SATELLITE ALTIMETER DATA [FORTRAN-PROGRAMME FUER DIE BERECHNUNG VON ZEITVARIABLEN MEERESHOEHEN UND BAHNFEHLERN AUS SATILLITEN-ALTIMETERDATEN]
Peter Arnold 1987 142 p In GERMAN
(Contract BMFT-01-QS-233-1)
(Bonn-Mitt-73; ISSN-0723-4325; ETN-88-92968) Avail: NTIS HC A07/MF A01

The seven FORTRAN programs described are practical transpositions of ARNOLD proposed models for the determination of nonstationary sea levels and trajectory errors from satellite altimeter data, and the elimination of the attached noise effects. The programs are useful for oceanic circulation analysis, sea level topography, and geoid determination. ESA

14 GROUND SUPPORT SYSTEMS AND FACILITIES (SPACE)

Includes launch complexes, research and production facilities; ground support equipment, e.g., mobile transporters; and simulators.

For related information see also *09 Research and Support Facilities (Air).*

N88-27217# Ballistic Research Labs., Aberdeen Proving Ground, Md.
AN INTERFEROMETRIC MEASUREMENT TECHNIQUE FOR RAILGUN STRUCTURES
Alex Zielinski, Jeffrey Kezerian, and Joseph Beno Jan. 1988 29 p
(AD-A192851; BRL-MR-5646) Avail: NTIS HC A03/MF A01 CSCL 19F

A technique to measure the expansion of a railgun under conditions of high magnetic stress has been developed. Bore deflections are detected by a Michelson interferometer arrangement during the application of a current pulse which produced repulsive forces similar to those in an actual projectile launch. This technique has been successfully used with two different barrel set-ups whose rails were electrically connected outside the bore at the muzzle. The method should prove valuable for testing a wide variety of electromagnetic launcher structures owing to the small loading of the optics on the structure itself. GRA

N88-27218# Sandia National Labs., Albuquerque, N. Mex.
AN INVESTIGATION OF SOFT LAUNCH AND INSTABILITY BREAKUP WITH A TWO-STAGE LIGHT GAS GUN
D. E. Grady and R. L. Moody May 1988 31 p
(Contract DE-AC04-76DP-00789)
(DE88-010371; SAND-88-0260) Avail: NTIS HC A03/MF A01

Exploratory research has been performed in the use of a two-stage light gas gun facility to investigate the soft acceleration and breakup physics of rapidly launched thin plates. A flash radiograph system was joined with the gun facility to provide the principal diagnostic. In the study, radiographs of thin-plate acceleration and breakup were obtained. DOE

N88-27219# Societe Nationale Industrielle Aerospatiale, Cannes (France). Cryogenic Lab.
CYROGENIC TEST FACILITIES FOR AN OPTICAL CRYOMECHANISM QUALIFICATION
Serge Taride 1 Oct. 1987 5 p
(SNIAS-881-440-116; ETN-88-92879) Avail: NTIS HC A02/MF A01

The cryogenic test facilities available for qualification of infrared optical devices are described, including a gaseous thermal cycling cryostat, a cold shaking cryostat, a sophisticated shaking helium cryostat, and a general purpose helium cryostat. The facilities are to test ISOCAM cooled mechanisms onboard the infrared observation ISO satellite. ESA

N88-27385# Illinois Univ., Urbana. Dept. of Astronautical Engineering.
SLEW-INDUCED DEFORMATIONS IN A SPACE-BASED ELECTROMAGNETIC RAIL GUN Final Report
James W. Wade *In* Universal Energy Systems, Inc., United States Air Force Graduate Student Summer Support Program, Volume 2 Dec. 1987 21 p (For primary document see N88-27355 21-31)
Avail: NTIS HC A99/MF E03 CSCL 22D

15 LAUNCH VEHICLES AND SPACE VEHICLES

Includes boosters; operating problems of launch/space vehicle systems; and reusable vehicles.

For related information see also *20 Spacecraft Propulsion and Power.*

No abstracts in this category.

16 SPACE TRANSPORTATION

Includes passenger and cargo space transportation, e.g., shuttle operations; and space rescue techniques.

For related information see also *03 Air Transportation and Safety* and *18 Spacecraft Design, Testing and Performance.* For space suits see *54 Man/System Technology and Life Support.*

No abstracts in this category.

17 SPACE COMM., SPACECRAFT COMM., COMMAND & TRACKING

Includes telemetry; space communications networks; astronavigation and guidance; and radio blackout.

For related information see also *04 Aircraft Communications and Navigation* and *32 Communications and Radar.*

N88-27220*# National Aeronautics and Space Administration. Pasadena Office, Calif.

A VLSI SINGLE-CHIP (225,223) REED-SOLOMON ENCODER WITH INTERLEAVER Patent Application

In-Shek Hsu, inventor (to NASA), Leslie J. Deutsch, inventor (to NASA), Trieu-Kie Truong, inventor (to NASA), and Irving S. Reed, inventor (to NASA) (Jet Propulsion Lab., California Inst. of Tech., Pasadena.) 29 Apr. 1988 30 p

(Contract NAS7-918)

(NASA-Case-NPO-17280-1-CU; NAS 1.71:NPO-17280-1-CU; US-Patent-Appl-SN-195226) Avail: NTIS HC A03/MF A01 CSCL 09F

The invention relates to a concatenated Reed-Solomon/convolutional encoding system consisting of a Reed-Solomon outer code and a convolutional inner code for downlink telemetry in space missions, and more particularly to a Reed-Solomon encoder with programmable interleaving of the information symbols and code correction symbols to combat error bursts in the Viterbi decoder. NASA

18 SPACECRAFT DESIGN, TESTING AND PERFORMANCE

Includes satellites; space platforms; space stations; spacecraft systems and components such as thermal and environmental controls; and attitude controls.

For life support systems see *54 Man/System Technology and Life Support.* For related information see also *05 Aircraft Design, Testing and Performance, 39 Structural Mechanics,* and *16 Space Transportation.*

N88-27221# Lockheed Missiles and Space Co., Palo Alto, Calif. Space Sciences Lab.

MAXIE-1 (MAGNETOSPHERIC ATMOSPHERIC X-RAY IMAGING EXPERIMENT) Progress Report, 1 Jan. - 31 Mar. 1988

William L. Imhof, Henry D. Voss, and Victor Chinn 23 Mar. 1988 6 p

(Contract N00014-87-C-0050)

(AD-A192846; LMSC/F247006) Avail: NTIS HC A02/MF A01 CSCL 22B

The satellite flight of the MAXIE-1 (Magnetospheric Atmospheric X-ray Imaging Experiment) instrument is being implemented under ONR (the Office of Naval Research) sponsorship. The MAXIE-1 instrument is being developed as a joint activity of Lockheed, the Aerospace Corporation, and the University of Bergen; much of the Lockheed development has been done under the Independent Research Program. Under ONR sponsorship that institution is responsible for managing the program, for providing spacecraft interface requirements, for providing interface electronics for conditioning sensor signals, for developing test software and for conducting environmental tests needed for flight. This report describes some of the interface activities undertaken in the last three months including the Interface Critical Design Review. Interactions have continued with co-investigators at the Aerospace Corp. and at the University of Bergen. A common board has been designed to condition spacecraft signals so as to make them compatible with the MAXIE instrument and vice-versa for the MAXIE signals. A breadboard of this common board has been fabricated and tested. GRA

N88-27222# Sandia National Labs., Albuquerque, N. Mex.

IN-FLIGHT MOTOR TORQUE ESTIMATES FOR THE SECOND-STAGE STRYPI 9 LAUNCH VEHICLE

R. S. Edmunds 1988 8 p Presented at the 24th AIAA/ASME/SAE/ASEE Joint Propulsion Conference, Boston, Mass., 11 Jul. 1988

(Contract DE-AC04-76DP-00789)

(DE88-010833; SAND-87-2755C; CONF-880764-1) Avail: NTIS HC A02

This paper documents the results of a study to determine the character of body fixed torques generated by the Anteres 2A motor, during second-stage burn of the Strypi 9 launch vehicle. The Strypi 9 is a two-stage spin-stabilized solid-propellant launch vehicle designed to boost a variety of payloads to reentry environment conditions. The torque estimates were determined from postflight analysis of Euler angle telemetry data. Principal axis misalignments, and thrust misalignments were also estimated. Data was analyzed from two separate launches; a Precursor and a Prime flight. DOE

N88-27223# Societe Nationale Industrielle Aerospatiale, Cannes (France).

EXSAT: EXPERT SYSTEM TO CONFIGURE TELECOMMUNICATION SATELLITES [EXSAT: SYSTEME EXPERT CONFIGURATEUR DE SATELLITES DE TELECOMMUNICATIONS]

Brigitte Trousse 31 Mar. 1988 17 p In FRENCH; ENGLISH summary

(SNIAS-881-440-101; ETN-88-92871) Avail: NTIS HC A03/MF A01

Artificial intelligence concepts were developed and applied to spacecraft design. Background of the EXSAT system is given and

the scope of the problem as well as the knowledge base are discussed. The base was tested using real cases such as Arabsat and Eutelsat. The example developed shows satellite configurations obtained from given specifications ESA

19 SPACECRAFT INSTRUMENTATION

For related information see also *06 Aircraft Instrumentation* and *35 Instrumentation and Photography.*

No abstracts in this category.

20 SPACECRAFT PROPULSION AND POWER

Includes main propulsion systems and components, e.g., rocket engines; and spacecraft auxiliary power sources.

For related information see also *07 Aircraft Propulsion and Power, 28 Propellants and Fuels, 44 Energy Production and Conversion,* and *15 Launch Vehicles and Space Vehicles.*

N88-27224*# Tennessee Univ., Knoxville.
EVALUATION AND IMPROVEMENT OF LIQUID PROPELLANT ROCKET CHUGGING ANALYSIS TECHNIQUES. PART 1: A ONE-DIMENSIONAL ANALYSIS OF LOW FREQUENCY COMBUSTION INSTABILITY IN THE FUEL PREBURNER OF THE SPACE SHUTTLE MAIN ENGINE Final Report M.S. Thesis - Aug. 1986
Kair Chuan Lim 4 Aug. 1988 125 p
(Grant NAG8-542)
(NASA-CR-183106; NAS 1.26:183106) Avail: NTIS HC A06/MF A01 CSCL 21H

Low frequency combustion instability, known as chugging, is consistently experienced during shutdown in the fuel and oxidizer preburners of the Space Shuttle Main Engines. Such problems always occur during the helium purge of the residual oxidizer from the preburner manifolds during the shutdown sequence. Possible causes and triggering mechanisms are analyzed and details in modeling the fuel preburner chug are presented. A linearized chugging model, based on the foundation of previous models, capable of predicting the chug occurrence is discussed and the predicted results are presented and compared to experimental work performed by NASA. Sensitivity parameters such as chamber pressure, fuel and oxidizer temperatures, and the effective bulk modulus of the liquid oxidizer are considered in analyzing the fuel preburner chug. The computer program CHUGTEST is utilized to generate the stability boundary for each sensitivity study and the region for stable operation is identified. Author

N88-27225*# Tennessee Univ., Knoxville.
EVALUATION AND IMPROVEMENT OF LIQUID PROPELLANT ROCKET CHUGGING ANALYSIS TECHNIQUES. PART 2: A STUDY OF LOW FREQUENCY COMBUSTION INSTABILITY IN ROCKET ENGINE PREBURNERS USING A HETEROGENEOUS STIRRED TANK REACTOR MODEL Final Report M.S. Thesis - Aug. 1987
Timothy A. Bartrand 4 Aug. 1988 229 p
(Grant NAG8-542)
(NASA-CR-182724; NAS 1.26:182724) Avail: NTIS HC A11/MF A01 CSCL 21H

During the shutdown of the space shuttle main engine, oxygen flow is shut off from the fuel preburner and helium is used to push the residual oxygen into the combustion chamber. During this process a low frequency combustion instability, or chug, occurs. This chug has resulted in damage to the engine's augmented spark igniter due to backflow of the contents of the preburner combustion chamber into the oxidizer feed system. To determine possible causes and fixes for the chug, the fuel preburner was modeled as a heterogeneous stirred tank combustion chamber, a variable mass flow rate oxidizer feed system, a constant mass flow rate fuel feed system and an exit turbine. Within the combustion chamber gases were assumed perfectly mixed. To account for liquid in the combustion chamber, a uniform droplet distribution was assumed to exist in the chamber, with mean droplet diameter determined from an empirical relation. A computer program was written to integrate the resulting differential equations. Because chamber contents were assumed perfectly mixed, the fuel preburner model erroneously predicted that combustion would not take place during shutdown. The combustion rate model was modified to assume that all liquid oxygen that vaporized instantaneously combusted with fuel. Using this combustion model, the effect of engine parameters on chamber pressure oscillations during the SSME shutdown was calculated. Author

N88-27226*# Morton Thiokol, Brigham City, Utah. Aerospace Group.
ASSEMBLY TEST ARTICLE (ATA) Final Test Report, Feb. 1988
Glen A. Ricks 22 Feb. 1988 176 p
(Contract NAS8-30490)
(NASA-CR-179361; NAS 1.26:179361; TWR-16829;
WBS-HQ301-10-03) Avail: NTIS HC A09/MF A01 CSCL 21H

The assembly test article (ATA) consisted of two live loaded redesigned solid rocket motor (RSRM) segments which were assembled and disassembled to simulate the actual flight segment stacking process. The test assembly joint was flight RSRM design, which included the J-joint insulation design and metal capture feature. The ATA test was performed mid-November through 24 December 1987, at Kennedy Space Center (KSC), Florida. The purpose of the test was: certification that vertical RSRM segment mating and separation could be accomplished without any damage; verification and modification of the procedures in the segment stacking/destacking documents; and certification of various GSE to be used for flight assembly and inspection. The RSRM vertical segment assembly/disassembly is possible without any damage to the insulation, metal parts, or seals. The insulation J-joint contact area was very close to the predicted values. Numerous deviations and changes to the planning documents were made to ensure the flight segments are effectively and correctly stacked. Various GSE were also certified for use on flight segments, and are discussed in detail. Author

N88-27227# Stuttgart Univ. (West Germany). Inst. fuer Raumfahrtsysteme.
PROPULSION ANALYSIS AND APPLICATION POTENTIAL OF AIR BREATHING COMBINED PROPULSION FOR BALLISTIC SPACE TRANSPORTER Ph.D. Thesis [ANALYSE DES ANTRIEBS- UND EINSATZPOTENTIALS LUFTATMENDER KOMBINATIONSANTRIEBE FUER BALLISTISCHE RAUMTRANSPORTER]
Peter Kramer 1987 307 p In GERMAN
(ETN-88-92369) Avail: NTIS HC A14/MF A01

Space transportation systems with vertical start and ballistic elevation are presented. A numerical computer program for the evaluation of chemical and thermal jet propulsions is developed. Individual analysis of these propulsion systems and their combination for space transporters is performed and applied to specific aircraft performance analysis. Turborockets/ramjet systems and pure ramjet systems show advantageous transport potential. Propellant economy is 60 percent and hydrogen is the most suitable. ESA

N88-27228# Societe Nationale Industrielle Aerospatiale, Saint-Medard-en-Jalles (France). Programmes Structures Bobinees.
DESIGN OF BOOSTER WOUND STRUCTURES [CONCEPTION DES STRUCTURES DE PROPULSEUR BOBINEES]
J. P. Denost 1988 23 p In FRENCH
(SNIAS-881-430-102; ETN-88-92850) Avail: NTIS HC A03/MF A01

The theory of load distribution and mechanical stress in a filament wound structure is developed. Design principles and conditions are derived. The manufacturing procedures are described. It is shown that these structures have positive advantages over metallic structures. The fast evolution of this technology is demonstrated. ESA

23 CHEMISTRY AND MATERIALS (GENERAL)

No abstracts in this category.

24 COMPOSITE MATERIALS

Includes physical, chemical, and mechanical properties of laminates and other composite materials.

For ceramic materials see *27 Nonmetallic Materials*.

N88-27229 Kansas Univ., Lawrence.
BOUNDARY LAYER SOLUTIONS FOR THE FREE-EDGE PROBLEM IN COMPOSITE LAMINATES Ph.D. Thesis
Sergio Frascino Muel deAlmeida [1987] 282 p
Avail: Univ. Microfilms Order No. DA8727587

The use of boundary layer methods to solve the free-edge problem of a rectangular composite laminate under uniaxial extension is investigated. The boundary layer equations are derived and two original methods are presented to compute the stress field in the boundary layer region close to the free-edge. The first method is based on an assumed stress formulation and Rayleigh-Ritz method. The second procedure, uses a displacement formulation combined with the extended Galerkin method. Both methods are used to evaluate the stress field in angle-ply, cross-ply, and quasi-isotropic laminates. The presented methods yield stress distributions with accuracy comparable to the finite element solution with slightly less computational effort. Also, it is shown that the proposed methods present reasonably good convergence characteristics despite the fact that stress singularities are not incorporated into the formulations. It is concluded that the proposed methods represent viable alternatives to the finite element method for the computation of interlaminar stresses in composite materials. Dissert. Abstr.

N88-27230*# Washington Univ., Seattle. Dept. of Aeronautics and Astronautics.
THERMO-VISCOELASTIC ANALYSIS OF COMPOSITE MATERIALS, VOLUME 1 Final Report
K. Y. Lin and I. H. Hwang Jun. 1988 74 p
(Grant NAG1-621)
(NASA-CR-183048-Vol-1; NAS 1.26:183048-Vol-1) Avail: NTIS HC A04/MF A01 CSCL 11D

Advanced composite materials, especially graphite/epoxy, are being applied to aircraft structures in order to improve performance and save weight. An important consideration in composite design is the residual strength of a structure containing holes, delaminations, or interlaminar damage when subjected to compressive loads. Recent studies have revealed the importance of viscoelastic effects in polymer-based composites. The viscoelastic effect is particularly significant at elevated temperature/moisture conditions since the matrix material is strongly affected by the environment. The solution of viscoelastic problems in composites was limited to special cases which can be solved by classical lamination theory. A finite element procedure is presented for calculating time-dependent stresses and strains in composite structures with general configurations and complicated boundary conditions. Using this procedure the in-plane and interlaminar stress distributions and histories in notched and unnotched composites were obtained for mechanical and thermal loads. Both two-dimensional and three-dimensional viscoelastic problems are analyzed. The effects of layup orientation and load spectrum on creep response and stress relaxation were also studied. Author

N88-27231# Aerospace Corp., El Segundo, Calif. Lab. Operations.
THE TWO ISOTROPIC ASYMPTOTES OF FIBER COMPOSITES
Ernest Y. Robinson 1 Mar. 1988 23 p
(Contract F04701-85-C-0086)
(AD-A192305; TR-0088(3533-01)-1; SD-TR-88-43) Avail: NTIS HC A03/MF A01 CSCL 11D

In conventional laminate analysis of fiber reinforced materials, the in-plane directional stiffness of constituent plies is summed to determine the entire laminate's characteristics. Conventional laminate analysis indicates that in-plane elastic isotropy accompanies certain ply pattern combinations and in general all laminates with three or more plies and orientation uniformly distributed from 0 to 180 deg. A corresponding analog for this quasi isotropic stiffness also exists for in-plane compliance in which compliance values are serial, and overall in-plane material property is determined by compliance summation. The two isotropic asymptotes are analogous to the Voigt and Reuss models of summed stiffness and compliance. The compliance quasi isotropic asymptote, which has evidently not been discussed in the literature, is presented here with some useful applications. The compliance computation is cast in the compact multiple-angle form, in analogy with the form used by many authors for laminate stiffness. GRA

N88-27232# Naval Postgraduate School, Monterey, Calif.
PROBABILISTIC ANISOTROPIC FAILURE CRITERIA FOR COMPOSITE MATERIALS M.S. Thesis
Kenneth J. Nelson Dec. 1987 92 p
(AD-A193046) Avail: NTIS HC A05/MF A01 CSCL 11D

A most important structural design objective today is the reliable applications of composite materials. Reliability is associated with the probability of success or failure of a particular structure and/or composite material. For this study, the reliability associated with strength was investigated. The objective was to develop a probabilistic anisotropic failure criterion and an analytical model which would account for the inherent strength scatter and enhance the structural reliability phase of composite design. This study analytically described the failure criterion and probabilistic failure states of a anisotropic composite in a combined stress state. Strength sensitivity and the failure mechanism within the domain of the combined stress space was based on a numerical simulation of a theoretical mathematical model. GRA

N88-27233# Martin Co., Denver, Colo. Astronautics Group.
DAMPING CHARACTERISTICS OF METAL MATRIX COMPOSITES Quarterly Letter Progress Report No. 7, 11 Aug. - 9 Dec. 1987
Mohan S. Misra 9 Dec. 1987 7 p
(Contract N00014-85-C-0857)
(AD-A193144; MCR-85-721) Avail: NTIS HC A02/MF A01 CSCL 11D

Objectives of Present Research: Metal Matrix Composites (MMC) with enhanced material damping can be potential structural materials to improve significantly the stability, control and reliability of space structures. Objectives of this investigation are: - Identify the mechanisms and sources of damping in continuous fiber reinforced MMC (Gr/Al and Gr/Mg) using in situ characterization techniques. - Determine the role of microstructural parameters (fiber volume, fiber orientation, interfiber spacing, grain size, precipitate morphology) in damping. - Define the role of the fiber matrix interface in damping. - Develop high damping structural materials for space applications. GRA

N88-27234# Aerospace Corp., El Segundo, Calif. Materials Sciences Lab.
ANALYSIS OF TRANSVERSE STRENGTH OF COMPOSITES USING PERCOLATION THEORY

Leslie A. Feldman, Thomas B. Bhader, and Gary F. Hawkins 15 Feb. 1988 19 p
(Contract F04701-85-C-0086)
(AD-A193204; TR-0086(6935-08)-1; SD-TR-88-11) Avail: NTIS HC A03/MF A01 CSCL 11D

As the fiber content is increased in order to increase the tensile strength of a unidirectional metal matrix composite, the transverse strength decreases rapidly. This is caused by a combination of low transverse fiber strength and weak fiber/matrix bond strength. Percolation theory, which has been used to describe phenomena that involve phase transitions and that can be modeled as a number of particles interacting with a random medium, has been used here to show that low transverse fracture strengths may be expected as the fiber content of a unidirectional composite is increased. This increase results in connected chains of fibers, weakly bonded to each other and to the matrix. The expected strength is lower in this case than is predicted by a simple regular array of holes model. GRA

N88-27235# California Univ., Los Angeles. Dept. of Materials Science and Engineering.
EFFECT OF THE MATRIX ON THE CREEP-BEHAVIOR OF CARBON-CARBON COMPOSITE
George H. Sines, Zheng Yang, and Brian D. Vickers Nov. 1987 39 p
(Contract N00014-85-K-0667)
(AD-A193211; UCLA-ENG-87-44) Avail: NTIS HC A03/MF A01 CSCL 11D

Creep specimens and experiments were designed to determine the properties of carbon carbon composites at high temperatures (over 2310 C) and at high stress levels (over 770 MPa). During the course of these experiments it was observed that the carbon matrix greatly increases the creep resistance of carbon fibers in properly impregnated, uniaxial composites. Results show how a composite specimen creeped 3.6 percent after 5.9 hrs. of testing while a matrix-free specimen, at the same test conditions, ruptured with 138 percent strain after only 0.39 hrs. This improvement is attributed to the alignment of the mesophase layers of the carbon matrix, which distribute tensile loads more evenly amongst the filaments and which may also alter the filaments' stress state by restricting transverse strains. Also of interest was the large primary creep response associated with the composite specimens at these high stress and temperature levels. Because it was such a large percentage of the entire response, this initial, transient creep should become the main design parameter of any attempt to relax bundle stresses in the fabrication of carbon carbon billets. GRA

N88-27236# Pittsburgh Univ., Pa.
FAR- AND MID-INFRARED PROPERTIES OF METAL-INSULATOR COMPOSITE MATERIALS Annual Letter Report, 1 Jan. - 31 Dec. 1987
Robert P. Devaty 1987 18 p
(Contract N00014-85-K-0808)
(AD-A193227) Avail: NTIS HC A03/MF A01 CSCL 11D

Construction of the far infrared Fourier transform spectrometer was completed so that attention could now be focussed on experiments. Among the highlights are: *SPECAC Interferometer-Design and construction of mylar beamsplitters, which can be used in place of the supplied free-standing wire grids to extend the high frequency cutoff of the instrument from 200/cm to at least 350/cm; Design and construction of an output focussing mirror to replace the supplied TPX lens. Use of the mirror increases the throughput of the interferometer, especially at high frequencies; Design and construction of an optical chopper to modulate the Hg arc source for use with lock-in detection. The chopper can be used rather than phase modulation (vibrating the fixed mirror of the interferometer). Both methods have advantages and drawbacks, so it is desirable to have both. GRA

N88-27237# University Coll. of North Wales, Bangor. School of Electronic Engineering Science.
POLYMER-CERAMIC COMPOSITES Interim Report No. 3
D. K. Das-Gupta Jun. 1987 13 p
(Contract DAJA45-86-C-0034)
(AD-A193244) Avail: NTIS HC A03/MF A01 CSCL 20C

The first and second reports (combined) showed that the composite films of PZT/PVDF, prepared in our laboratories, may have a permittivity in excess of 100 for a 75 percent volume fraction of PZT powder introduced in the matrix of PVDF host polymer. The relative permittivity of the ceramic polymer composites were measured in the frequency range of 10Hz-65kHz and compared with the respective permittivity values of PZT and PVDF. It was also observed that the dielectric relaxation of this PZT/PVDF composite conforms with that of the polymer (PVDF). The present work investigates the dielectric loss behaviour of the composite. GRA

N88-27238# General Atomic Co., San Diego, Calif.
STUDIES IN SUPPORT OF OXIDATION-RESISTANT COMPOSITE MATERIALS Final Report, Nov. 1985 - Dec. 1987
J. L. Kaae, M. Dresselhaus, J. MacKenzie, B. McQuillan, and R. Price 1 Feb. 1988 134 p
(Contract F49620-86-C-0011)
(AD-A193320; GA-A19195; AFOSR-88-0284TR) Avail: NTIS HC A07/MF A01 CSCL 11D

Studies on elements required for oxidation resistant composite materials have been carried out in four areas: (1) investigations of moisture resistant sealant glasses for carbon-carbon composite materials and their interactions with oxidation barrier coatings; (2) investigations of the effects of electrochemical modification of carbon surfaces on the wetability of these surfaces by sealant glasses; (3) investigations of alkoxides sol-gel precursors of ceramic materials; and (4) investigations of the formation of ceramic fibers through the oxidation of inter-calculated carbon fibers. GRA

N88-27239# Japan Atomic Energy Research Inst., Tokyo. Dept. of Development.
EFFECTS OF ELECTRON BEAM IRRADIATION ON MECHANICAL PROPERTIES AT LOW AND HIGH TEMPERATURE OF FIBER REINFORCED COMPOSITES USING PEEK AS MATRIX MATERIAL
Tsuneo Sasuga, Tadao Seguchi, Hideo Sakai, Toshikazu Odajima, Toshiyuki Nakakura, and Masahiro Masutani Nov. 1987 22 p In JAPANESE; ENGLISH summary
(DE88-753134; JAERI-M-87-197) Avail: NTIS (US Sales Only) HC A03/MF A01

Carbon fiber reinforced composite (PEEK-CF) using polyarylether-ether-ketone (PEEK) as a matrix material was prepared and the electron beam radiation effects on the mechanical properties at low and high temperature and the effects of annealing after irradiation were studied. Cooling down to 77 K, the flexural strength of PEEK-CF increased to about 20 percent than that at room temperature. The data of flexural strength for the irradiated specimens showed some scattering, but the strength and modulus at 77 K were changed scarcely up to 120 MGy. The flexural strength and modulus in the unirradiated specimen decreased with an increasing of measurement temperature, and the strength at 140 C, which is the just below temperature of the glass transition of PEEK, was to 70 percent of the value at room temperature. For the irradiated specimens, the strength and modulus increased with dose and the values at 140 C for the specimen irradiated with 120 MGy were nearly the same with the unirradiated specimens measured at room temperature. The improvement of mechanical properties at high temperature by irradiation was supported by a viscoelastic measurement in which the glass transition shifted to the higher temperature by the radiation-induced crosslinking. DOE

N88-27240 Texas A&M Univ., College Station.
TECHNIQUES FOR CHARACTERIZING DAMAGE ZONES IN COMPOSITE MATERIALS Ph.D. Thesis
Richard Dale Tonda 1987 170 p
Avail: Univ. Microfilms Order No. DA8802148

Experimental methods for determining the existence of a work potential, useful in characterizing material response even in the

presence of significant damage, are developed and described. The underlying fracture theory and motivation for the development is briefly discussed. The theory involving the work potential and the existence and use of a damage parameter is reviewed, as is the basic composite laminate theory and underlying constitutive formulation. An experimental program which addresses these factors through the biaxial loading of composite tubes is presented. The results are analyzed incorporating viscoelasticity theory for power law time dependence of the matrix material, and it is demonstrated that the theory provides a less complicated presentation of the data by eliminating the superimposed effects of time dependent behavior. Dissert. Abstr.

N88-27241# Oak Ridge National Lab., Tenn.
THEORETICAL AND EXPERIMENTAL ANALYSIS OF THE TOUGHENING BEHAVIOR OF WHISKER REINFORCEMENT IN CERAMIC MATRIX COMPOSITES
P. F. Becher, C. H. Hsueh, P. Angelini, and T. N. Tiegs 1988 4 p Presented at the Symposium on Interfacial Phenomena in Composites, Newport, R.I., 1 Jun. 1988
(Contract DE-AC05-84OR-21400)
(DE88-011841; CONF-8806155-1) Avail: NTIS HC A02/MF A01

Analytical solutions are presented describing the experimentally verified toughening of whisker reinforced ceramics. Clear insights are provided into the interrelationships of whiskers, matrices, and interfaces in the case of strong interfaces with minimized whisker pullout. DOE

N88-27242*# Purdue Univ., West Lafayette, Ind.
CHARACTERIZATION OF ELASTIC-PLASTIC PROPERTIES OF AS4/APC-2 THERMOPLASTIC COMPOSITE
C. T. Sun and K. J. Yoon Aug. 1988 53 p
(Grant NAG1-825)
(NASA-CR-183145; NAS 1.26:183145; CML-88-3) Avail: NTIS HC A04/MF A01 CSCL 11D

Elastic and inelastic properties of AS4/APC-2 composites were characterized with respect to temperature variation by using a one-parameter orthotropic plasticity model and a one parameter failure criterion. Simple uniaxial off-axis tension tests were performed on coupon specimens of unidirectional AS4/APC-2 thermoplastic composite at various temperatures. To avoid the complication caused by the extension-shear coupling effect in off-axis testing, new tabs were designed and used on the test specimens. The experimental results showed that the nonlinear behavior of constitutive relations and the failure strengths can be characterized quite well using the one parameter plasticity model and the failure criterion, respectively. Author

N88-27243# Technische Hochschule, Aachen (West Germany). Fakultaet fuer Bergbau, Huettenwesen und Geowissenschaften.
CONTRIBUTION TO THE DEVELOPMENT OF COATED FIBER CERAMIC INSULATION MATERIAL Ph.D. Thesis [BEITRAG ZUR ENTWICKLUNG BESCHICHTETER FASERKERAMISCHER WAERMEDAEMMATERIALIEN]
Ines Maiwald 1987 124 p In GERMAN
(ETN-88-92361) Avail: NTIS HC A06/MF A01

Coated fiber ceramic insulation material temperature resistant up to 1250 C for gas turbine lining is developed. Aluminum oxide fiber with 5 percent SiO2 is processed and studied concerning the physical properties, i.e., resistance, elasticity modulus, thermal conductivity, and thermal cycling resistance in relation with material microstructure, distribution of fibers, and size of pores. Various coating materials and processes like enamels, alumines, and sprayed oxides are analyzed where coating bonding procedure on ceramic matrix is of great importance. ESA

N88-27244# Kaiserslautern Univ. (West Germany). Fachbereich Maschinenwesen.
FABRICATION OF SIC FIBER REINFORCED GLASS MATRIX BY EXTRUSION PROCESS AND INVESTIGATION OF ITS MECHANICAL PROPERTIES Ph.D. Thesis [HERSTELLUNG SIC-FASERVERSTAERKTER GLASVERBUNDKOERPER DURCH DAS STRANGPRESSVERFAHREN UND UNTERSUCHUNG IHRER CHARAKTERISTISCHEN MECHANISCHEN EIGENSCHAFTEN]
Wolfgang Semar 1986 160 p In GERMAN
(ETN-88-92367) Avail: NTIS HC A08/MF A01

By combination of extrusion and drawing processes, square diameter borosilicate glass bars and SiC fiber reinforced cores are manufactured at 796 C and 280 bar. Mechanical properties, i.e., elongation, residual stress, and strength are tested on the finished material. Composite material with 10 percent fiber developed an improved flexural strength, flexural impact strength, and tensile strength. With 33 percent fiber these properties can be improved by 200 percent to 700 percent. Experimental results for thermal elongation and axial residual stress obtained by differential dilatometer and polarization microscopy are presented. ESA

N88-27245# Research Inst. of National Defence, Stockholm (Sweden).
ROCKET MOTOR CASE MATERIALS. AN EVALUATION OF NEW FIBERS FOR COMPOSITES
Jan Erikson, Fritz Larsson, and Mikael Tibbing Feb. 1988 26 p In SWEDISH; ENGLISH summary
(FOA-C-20696-2.1; ISSN-0347-3694; ETN-88-92702) Avail: NTIS HC A03/MF A01

Fibers for filament winding of rocket engine cases were fabricated and pressurized to failure in a hydraulic test bench. The greatest weight gain was obtained with carbon fibers and with polyethylene fibers. Differences in stiffness, brittleness, machinability, heat resistance, and thermal expansion of composites reinforced with the two fibers are discussed. Composites reinforced with aramid fibers are definitely inferior in specific strength and stiffness. ESA

N88-27246# Construcciones Aeronauticas S.A., Madrid (Spain). Div. de Proyectos.
DETERMINATION OF THE GLASS TRANSITION TEMPERATURE OF CURED COMPOSITE MATERIALS [DETERMINACION DE TEMPERATURAS DE TRANSICION VITREA DE MATERIALES COMPUESTOS CURADOS]
A. Lavia and J. Sanchez 20 Jun. 1987 11 p In SPANISH Sponsored by Investigacion y Desarrollo de Technologia y Materiales
(DT-87/62-R; ETN-88-92712) Avail: NTIS HC A03/MF A01

The second order transition of composite materials was investigated using differential scanning calorimetry, dynamical modulus measurement, and expansion coefficient determination techniques. The rheometric results are consistently higher than the extensometric values. Dependence on the heating cycle and other post-curing phenomena is observed. ESA

N88-27247# Construcciones Aeronauticas S.A., Madrid (Spain). Div. de Proyectos.
DESIGN AND IMPLEMENTATION OF CONTACT ULTRASONIC SENSORS TO ASSESS INTERNAL DAMAGE [DESARROLLO Y PUESTA A PUNTO DE PALPADORES ULTRASONICOS FIJOS PARA EL SEGUIMIENTO DE DANOS INACCESIBLES]
9 Apr. 1987 13 p In SPANISH Sponsored by the Investigacion y Desarrollo de Tecnologia y Materiales
(I-177/87; ETN-88-92713) Avail: NTIS HC A03/MF A01

A sensor was developed to assess inner damage in fatigue tests of the carbon fiber-epoxy composite horizontal stabilizer of the A-320 aircraft. The sensor is implemented with a modified lead titanate crystal, a copper mesh acting as impedance adapter, plastic bodies, and aluminum case. The sensor is adhesive bonded to the surface of the element to be checked. The procedure works

correctly when the damage region is well identified. It does not measure the real size of the defect. ESA

N88-27248# Construcciones Aeronauticas S.A., Madrid (Spain). Div. de Proyectos.
FACTORS AFFECTING STRENGTH IN COMPOSITE MATERIALS USED FOR AIRCRAFT [FACTORES QUE AFECTAN LA TENACIDAD EN MATERIALES COMPUESTOS DE USO AERONAUTICO]
Leonardo Enriquez and Jose Sanchez 1 Nov. 1987 58 p In SPANISH Sponsored by the Investigacion y Desarrollo de Tecnologia y Materiales
(DT-212/87; ETN-88-92715) Avail: NTIS HC A04/MF A01

In the framework of aircraft construction, the characteristics and applications of composite materials are reviewed and compared with those of metallic materials. Surface treatments, epoxy and polyimide resins, carbon and aramid fibers, layer orientation, packing density, curing cycles, chemical resistance, fatigue resistance, and defect detection are discussed. ESA

N88-27249# Societe Nationale Industrielle Aerospatiale, Suresnes (France). Direction Centrale de la Qualite.
RELATION BETWEEN THE MECHANICAL CHARACTERISTICS OF CARBON-RESIN COMPOSITES AND THEIR IMPACT STRENGTH Final Report [RELATIONS ENTRE LES CARACTERISTIQUES MECANIQUES DES MATERIAUX COMPOSITES CARBONE-RESINE ET LEUR TENUE A L'IMPACT. PROCES-VERBAL 48-284/F]
J. Odorico and B. Soulezelle 4 Aug. 1987 181 p In FRENCH
(Contract DRET-85-34-489)
(Rept-48-284/F; ETN-88-92742) Avail: NTIS HC A09/MF A01

A correlation was established between the composite low velocity impact characteristics and mechanical properties and crack propagation properties. The tested materials included three type of resins and three types of fibers. The results show that the ductility of the resin has a large influence on the first damage impact characteristics, while the strength of the fiber determines the maximum strength. ESA

N88-27250# Societe Nationale Industrielle Aerospatiale, Saint-Medard-en-Jalles (France).
BALANCE OF X-RAY RADIOSCOPY APPLICATION TO NONDESTRUCTIVE TESTS OF COMPOSITE MATERIALS [BILAN D'UTILISATION DE LA RADIOSCOPIE A RAYONS X APPLIQUEE AU C.N.D. DES MATERIAUX COMPOSITES]
Daniel Loubet 1988 10 p In FRENCH
(SNIAS-881-430-110; ETN-88-92858) Avail: NTIS HC A02/MF A01

The results obtained using X ray radioscopy nondestructive control equipment are discussed. Examples refering to composite materials are described. The limitations are discussed. The resolution and the noise problems limit the performance in delamination control, although the application of digital techniques improves results. Remote video radioscopy is very useful for the nondestructive control of filament wound and woven composites, since the real time control of man-operation interactions is of great importance for this kind of product. ESA

N88-27251# Societe Nationale Industrielle Aerospatiale, Saint-Medard-en-Jalles (France).
PROGRAMS FOR PRELIMINARY DESIGN OF COMPOSITE MATERIALS WHICH WERE DEVELOPED BY THE DESIGN GROUP OF AEROSPATIALE AQUITAINE [PROGRAMMES DE PREDIMENSIONNEMENT DE STRUCTURES EN MATERIAUX COMPOSITES DEVELOPPES AU BUREAU D'ETUDES DE L'AEROSPATIALE AQUITAINE]
Lamalle 1988 5 p In FRENCH
(SNIAS-881-430-112; ETN-88-92860) Avail: NTIS HC A02/MF A01

A computer program named Compos is described. It works on VAX 11/780 and is designed to predict the behavior of a unidirectional composite for which the properties and percentages of components (fibers and matrix) are known. It is based on micromechanical computation allowing for the random distribution of fiber in the matrix. The program is used as a computer aid to the design of structures either to reduce the characterization tests of materials in preliminary design or as finite element computation for final design. ESA

N88-27252# Societe Nationale Industrielle Aerospatiale, Saint-Medard-en-Jalles (France).
ON THE ELECTRICAL PROPERTIES OF CARBON/CARBON COMPOSITES DENSIFIED BY CHEMICAL DEPOSIT IN VAPOR PHASE [SUR LES PROPRIETES ELECTRIQUES DE COMPOSITES CARBONE/CARBONE DENSIFIES PAR DEPOT CHIMIQUE EN PHASE VAPEUR]
P. Delhaes, M. Trinquecoste (Bordeaux 1 Univ., Talence, France), D. Beziers, and B. Capdepuy 1988 23 p In FRENCH
(SNIAS-881-430-117; ETN-88-92865) Avail: NTIS HC A03/MF A01

Densification is studied in order to optimize electrical conductivity in unidirectional specimens of carbon/carbon composites. The parameters studied include the pyrocarbon matrix microstructure, fiber percentage, type of fiber, and the highest temperature of later treatment (usually 2500 C for 90 min). It is shown that two opposite strategies are possible: a low initial fiber content (40 percent) with intensive carbon deposit, or a maximum (70 percent) fiber content choosing conductive fibers, finished with a slight carbon deposit used as a fiber binding agent only. ESA

N88-27253# Technische Univ., Brunswick (West Germany). Inst. fuer Flugzeugbau und Leichtbau.
SIMULATION OF MOISTURE DIFFUSION OF FIBER REINFORCED COMPONENTS OF AIRCRAFT FOR GENERAL AIR TRANSPORTATION [SIMULATION DER FEUCHTEVERTEILUNG IN BAUTEILEN AUS FASERVERBUNDWERKSTOFFEN FUER FLUGZEUGE DER ALLGEMEINEN LUFTFAHRT]
Peter Wetjen Sep. 1987 85 p In GERMAN
(Contract BMFT-LFF-8432/9)
(IFL-IB-87-05; ETN-88-92964) Avail: NTIS HC A05/MF A01

Investigation and comparison of diffusion properties of cold and hot cured fiber reinforced epoxy resins are performed. Diffusion models are developed by finite difference method and a simulation program is established for the prediction of water absorption by reinforced epoxy resins aircraft parts. Results indicate no difference in diffusion behavior between both types of epoxy resins. ESA

N88-27364# University of Southern Illinois, Carbondale. Dept. of Civil Engineering and Mechanics.
DETERMINATION OF LUMPED-MASS THERMAL PROPERTIES ASSOCIATED WITH AUTOCLAVE CURING OF GRAPHITE/EPOXY COMPOSITES Final Report
Charles W. Norfleet *In* Universal Energy Systems, Inc., United States Air Force Graduate Student Summer Support Program, Volume 2 Dec. 1987 15 p (For primary document see N88-27355 21-31)
Avail: NTIS HC A99/MF E03 CSCL 11D

N88-27383# Prairie View Agricultural and Mechanical Coll., Tex. Dept. of Chemical Engineering.
COMPUTER MODELING FOR SURFACE PROPERTIES OF CARBON FIBERS Final Report
Pretta L. VanDible *In* Universal Energy Systems, Inc., United States Air Force Graduate Student Summer Support Program, Volume 2 Dec. 1987 25 p (For primary document see N88-27355 21-31)
Avail: NTIS HC A99/MF E03 CSCL 11D

25 INORGANIC AND PHYSICAL CHEMISTRY

Includes chemical analysis, e.g., chromatography; combustion theory; electrochemistry; and photochemistry.

For related information see also *77 Thermodynamics and Statistical Physics.*.

N88-27254*# Aerojet TechSystems Co., Sacramento, Calif.
CARBON DEPOSITION MODEL FOR OXYGEN-HYDROCARBON COMBUSTION, VOLUME 1 Interim Final Report
R. Hernandez, J. I. Ito, and K. Y. Niiya Sep. 1987 252 p
(Contract NAS8-34715)
(NASA-CR-179375; NAS 1.26:179375; Rept-2427-IFR-Vol-1; RPT/AA0631-a/087-Vol-1) Avail: NTIS HC A12/MF A01 CSCL 21B

Presented are details of the design, fabrication, and testing of subscale hardware used in the evaluation of carbon deposition characteristics of liquid oxygen and three hydrocarbon fuels for both main chamber and preburner/gas generator operating conditions. In main chamber conditions, the deposition of carbon on the combustion chamber wall was investigated at mixture ratios of 2.0 to 4.0 and at pressures of 1000 to 1500 psia. No carbon deposition on the chamber walls was detected at these main chamber mixture ratios. In preburner/gas generator operating conditions, the deposition of carbon on the turbine simulator tubes was evaluated at mixture ratios of 0.20 to 0.60 and at chamber pressures of 720 to 1650 psia. The results of the tests showed carbon deposition rate to be a strong function of mixture ratio and a weak function of chamber pressure. Further analyses evaluated the operational consequences of carbon deposition on preburner/gas generator performance. The report is in two volumes, of which this is Volume 1 covering the main body of the report plus Appendixes A through D. Author

N88-27255*# Aerojet TechSystems Co., Sacramento, Calif.
CARBON DEPOSITION MODEL FOR OXYGEN-HYDROCARBON COMBUSTION, VOLUME 2 Interim Final Report
R. Hernandez, J. I. Ito, and K. Y. Niiya Sep. 1987 635 p
(Contract NAS8-34715)
(NASA-CR-179376; NAS 1.26:179376; Rept-2427-IFR-Vol-2; RPT/AA0631/087-Vol-2) Avail: NTIS HC A99/MF A01 CSCL 21B

Presented are details of the design, fabrication, and testing of subscale hardware used in the evaluation of carbon deposition characteristics of liquid oxygen and three hydrocarbon fuels for both main chamber and preburner/gas generator operating conditions. In main chamber conditions, the deposition of carbon on the combustion chamber wall was investigated at mixture ratios of 2.0 to 4.0 and at chamber pressures of 1000 to 1500 psia. No carbon deposition on chamber walls was detected at these main chamber mixture ratios. In preburner/gas generator operating conditions, the deposition of carbon on the turbine simulator tubes was evaluated at mixture ratios of 0.20 to 0.60 and at chamber pressures of 720 to 1650 psia. The results of the tests showed carbon deposition rate to be a strong function of mixture ratio and a weak function of chamber pressure. Further analyses evaluated the operational consequences of carbon deposition on preburner/gas generator performance. This is Volume 2 of the report, which contains data plots of all the test programs. Author

N88-27256# Tokyo Univ. (Japan). Inst. of Space and Astronautical Science.
PRECISE ULTRAVIOLET ABSORBANCE STUDY OF THE INTERACTION OF AMINO ACIDS AND MONONUCLEOSIDES IN AQUEOUS SOLUTION
Mikio Shimizu Jan. 1987 19 p
(ISAS-RN-356) Avail: NTIS HC A03/MF A01

Affinity coefficients of various amino acids or their derivatives (methyl esters, amides, etc.) with mononucleosides in aqueous solutions have been measured by using a precise ultraviolet difference absorbance photometry. The results are in general agreement with those of previous solubility experiments. The superiority of this ultraviolet absorbance experiments to the solubility experiments is that this method can discriminate stacking and hydrogen bonding interactions by using the hypochromicity and hyperchromicity of the absorbance, respectively. It is also confirmed that the hydrogen bonding interactions of the side chains of the amino acids with the nucleic acid bases observed in nonaqueous hydrophobic solutions by the nuclear magnetic resonance method clearly functions in aqueous solutions. New types of specific interactions of some amino acids with nucleic acid bases by using a peptydic carboxyl radical and another radical in their side chains have been found in this experiment. Author

N88-27257 Oklahoma Univ., Norman.
THE STRUCTURE AND STABILITY OF NONPREMIXED GAS JET FLAMES Ph.D. Thesis
Rong-Fung Huang 1987 232 p
Avail: Univ. Microfilms Order No. DA8729874

Experimental and computational studies of nonpremixed gas jet flames are described. The general behavior, the structure, and the burner-rim stability of both laminar and turbulent vertical jet flames and turbulent jet flames in cross flow are presented. Dissert. Abstr.

N88-27258 California Univ., Los Angeles.
A STUDY OF THE INTERACTION OF DIFFUSION FLAMES WITH A VORTEX PAIR FLOWFIELD Ph.D. Thesis
Bose V. S. Manda 1987 157 p
Avail: Univ. Microfilms Order No. DA8728703

The deformation of diffusion flames by a vortex pair flowfield is examined analytically, with emphasis in the reaction process due to the fluid mechanical straining of the flames. Two types of initial geometry are considered: a diffusion flame bounding a simi-infinite fuel strip distorted by the vortex pair, and two infinite diffusion flames bounding an infinite fuel strip interacting with the flowfield. The chemical reaction is diffusion controlled. The procedure for calculating flame deformation, reactant consumption, and the distribution of products about the flame surface accounts for the motion of the flame due to the stoichiometry of the reactions as well as the flowfield. Author

N88-27259# Institut Franco-Allemand de Recherches, St. Louis (France).
SOME PROPERTIES OF IGNITION GASES. REVIEW OF MEASURING RESULTS IN THE YEARS 1981-1986) [EINIGE EIGENSCHAFTEN VON ANZUENDSCHWADEN. ZUSAMMENFASSUNG VON MESSERGEBNISSEN AUS DEN JAHREN 1981-1986]
H. Mach, U. Werner, and H. Masur 1 Dec. 1986 36 p In GERMAN; FRENCH summary
(PB88-106968; ISL-R-130/86) Avail: NTIS HC E04/MF E04; copy not available from STI Facility CSCL 21B

The essential results of a number of measurements on ignition gases are summarized using four types of propellant igniters. Measurements were made on the gas flow during passage into the free space (speed, particle size distribution, particle concentration, particle mass and energy flow), as well as the corresponding measurements on the gas flow during penetration into an inert powder granulate with damming. Author

N88-27260# Pakistan Inst. of Nuclear Science and Technology, Rawalpindi.
COMPILATION OF TEMPERATURE FACTORS OF CUBIC ELEMENTS
N. M. Butt, B. T. M. Willis, G. Heger, and J. Bashir Dec. 1986 34 p Sponsored by International Union of Crystallography
(PB88-108170; PINSTECH/NPD-120) Avail: NTIS HC E03/MF A01; copy not available from STI Facility CSCL 07D

A compilation is presented of the temperature factors of twenty cubic elements. This represents the first stage of a Temperature

Factor project sponsored by the Neutron Diffraction Commission of the International Union of Crystallography. Author

N88-27261# Akron Univ., Ohio. Inst. of Polymer Science.
AN IETS (INELASTIC ELECTRON TUNNELING SPECTROSCOPY) STUDY OF SURFACE REACTIONS APPLICABLE TO ADHESION
P. N. Henriksen, A. N. Gent, R. D. Ramsier, and J. D. Alexander Mar. 1988 30 p
(Contract N00014-85-K-0222)
(AD-A192274; TR-12) Avail: NTIS HC A03/MF A01 CSCL 07C

Inelastic electron tunneling spectroscopy (IETS) has been used to study two classes of adhesion promoting compounds adsorbed on alumina: trialkoxysilanes and phosphonic acids. It has been shown that both types of compounds can condense directly with hydroxyl groups on the surface. Condensation is through the alkoxy groups in the case of the silanes and through the hydroxyl groups in case of the acids. The silanes can further condense to form surface siloxanes. The absence of bands characteristic of the phosphoryl group in the spectra of the acids is indicative of resonance bond formation followed by ionic bonding to the surface. GRA

N88-27262# Clarkson Univ., Potsdam, N.Y. Dept. of Chemistry.
CATALYTIC ACTIVATION OF CARBON DIOXIDE BY METAL COMPLEXES
L. Vaska 15 Mar. 1988 17 p
(Contract N00014-84-K-0658)
(AD-A192310; AD-E801594; TR-3) Avail: NTIS HC A03/MF A01 CSCL 07D

This paper summarizes some past and recent work from the author's laboratory on the reactions of carbon dioxide with metal complexes with the objective of suggesting the relevance of this research to some related biological systems. First, the various CO2-metal complex interactions in vivo and in vitro are briefly cited, followed by a description of the reversible activation of carbon dioxide by model rhodium and iridium compounds. Finally, recent results are presented on homogeneous catalytic hydrogenation/reduction of CO2 mediated by metal complexes, including a platinum cluster complex which catalyzes the carbon dioxde conversion at mild conditions. GRA

N88-27263# Maryland Univ., College Park. Dept. of Physics and Astronomy.
SCANNING TUNNELING MICROSCOPY AS A SURFACE CHEMICAL PROBE Final Report, 1 Aug. 1986 - 31 Jan. 1988
Ellen D. Williams 31 Mar. 1988 3 p
(Grant AF AFOSR-0235-86)
(AD-A192710; AFOSR-88-0427TR) Avail: NTIS HC A02/MF A01 CSCL 07D

This grant sponsored purchase of surface characterization spectrometers, data acquisition hardware, and sample manipulation for an ultrahigh vacuum chamber equipped with scanning tunneling microscope. This apparatus is designed to map atomic-scale surface morphology of well-controlled samples, particularly for absorbate-covered metal surfaces. The equipment assembly has been completed and experiments are underway. GRA

N88-27264# Columbia Univ., New York, N.Y. Center for Strategic Materials.
A FUNDAMENTAL UNDERSTANDING OF THE INTERFACIAL COMPATIBILITY IN HYBRID MATERIAL SYSTEMS Annual Technical Report, 1 Sep. 1986 - 31 Oct. 1987
John K. Tien 7 Mar. 1988 20 p
(Grant AF-AFOSR-0312-86)
(AD-A192921; AFOSR-88-0325TR) Avail: NTIS HC A03/MF A01 CSCL 07B

Among the problems associated with long-term high temperature service of hybrid material systems is interdiffusional compatibility of the system's component materials. Efforts in this program have focussed on several areas of this problem. One of the areas being examined is that of alkali metal and alkali earth metal diffusion barriers. These barriers are being applied by two different methods: ion implantation and a sol suspension slurry technique. For both methods, the system being utilized as a model is the tungsten/nickel system. Preliminary results of barrier effectiveness are given. Also being studied are the interdiffusional kinetics of metal/intermetallic and intermetallic/intermetallic ternary systems. Hybrids being examined include W/Ni3Al and TiAl/Ni3Al. GRA

N88-27265# Pennsylvania State Univ., University Park. Dept. of Mechanical Engineering.
PREMIXED TURBULENT FLAME PROPAGATION Annual Report, 1 Nov. 1986 - 31 Oct. 1987
D. A. Santavicca 8 Jan. 1988 15 p
(Grant AF-AFOSR-0097-87)
(AD-A192955; AFOSR-88-0298TR) Avail: NTIS HC A03/MF A01 CSCL 21B

Results are presented from an experimental study of premixed turbulent flame propagation under atmospheric pressure in unconfined conditions. Stoichiometric propane air flames at two turbulence conditions were studied. LDV was used to obtain ensemble averaged measurements of velocity, turbulence intensity and integral time scale through the propagating flame. The integral length scale ahead of the flame was obtained both directly from a two-point spatial correlation measurement and indirectly using Taylor's hypothesis. In addition, laser planar imaging was used to obtain two-dimensional flame structure measurements which were processed with a fractal analysis. Both the mean velocity and the turbulence were observed to change immediately ahead of the propagating flame. The mean velocity was found to decrease due to the unconfined nature of the flame and the turbulence intensity was found to increase due to the turbulence-flame interactions. Sudden increases in both the mean velocity and the turbulence intensity across the flame were observed, where the absolute increase in turbulence conditions. Similar results have been reported by other researchers. The integral time scale was observed to decrease ahead of the propagating flame but the changes behind the flame were inconsistent. GRA

N88-27266# Southwest Research Inst., San Antonio, Tex. Fuels and Lubricants Research Facility.
EFFECTS OF CERAMIC SURFACES ON AUTOIGNITION IN A CONSTANT VOLUME COMBUSTION APPARATUS Interim Report, Oct. 1984 - Dec. 1987
Thomas W. Ryan, III, Mike D. Kanakia, and Karen B. Kohl Dec. 1987 25 p
(Contracts DAAK70-85-C-0007; DAAK70-82-C-0001; DA Proj. 1L2-63104-D-150)
(AD-A193055; BFLRF-246) Avail: NTIS HC A03/MF A01 CSCL 21B

A constant volume combustion apparatus was used to determine the effects of ceramic-coated surfaces on the ignition of fuel sprays from a diesel injection nozzle. The goal was to determine if the ceramic surfaces could enhance ignition through catalytic effects on the surfaces. Statistical analysis of the data indicated that an aluminosilicate coating had no effect, while a partially stabilized zirconia increased the delay times. It appears, however, that the aluminosilicate coating could actually enhance the ignition, producing shorter ignition delay times, if the results of the appropriate baselines are considered. GRA

N88-27267*# National Aeronautics and Space Administration. Lewis Research Center, Cleveland, Ohio.
ALKALINE FUEL CELL PERFORMANCE INVESTIGATION
R. E. Martin (International Fuel Cells Corp., South Windsor, Conn.) and M. A. Manzo 5 Aug. 1988 10 p Presented at the 23rd Intersociety Energy Conversion Engineering Conference, Denver, Colo., 31 Jul. - 5 Aug. 1988; sponsored in part by ASME, AIAA, ANS, SAE, IEEE, ACS, and AIChE
(NASA-TM-100937; E-4217; NAS 1.15:100937) Avail: NTIS HC A02/MF A01 CSCL 07D

An exploratory experimental fuel cell test program was conducted to investigate the performance characteristics of alkaline

laboratory research electrodes. The objective of this work was to establish the effect of temperature, pressure, and concentration upon performance and evaluate candidate cathode configurations having the potential for improved performance. The performance characterization tests provided data to empirically establish the effect of temperature, pressure, and concentration upon performance for cell temperatures up to 300 F and reactant pressures up to 200 psia. Evaluation of five gold alloy cathode catalysts revealed that three doped gold alloys had more that two times the surface areas of reference cathodes and therefore offered the best potential for improved performance. Author

N88-27268# General Motors Research Labs., Warren, Mich.
MECHANISM OF THE NITRIC OXIDE-CARBON MONOXIDE-OXYGEN REACTION OVER A SINGLE CRYSTAL RHODIUM CATALYST
G. B. Fisher, Se H. Oh, C. L. DiMaggio, S. J. Schmieg, D. W. Goodman, and C. H. F. Peden 1988 16 p Presented at the 9th International Catalysis Congress, Calgary, Alberta, 26 Jun. 1988 Prepared in cooperation with Sandia National Labs., Albuquerque, N. Mex.
(Contract DE-AC04-76DP-00789)
(DE88-006274; SAND-87-1526C; CONF-880602-4) Avail: NTIS HC A03/MF A01

As part of a study of reactions important in automative exhaust catalysis, the absolute rates of the CO-O2 reaction over Rh(111) in the presence of NO have been measured and compared with the kinetics of the CO-NO and CO-O2 reactions over Rh(111) at partial pressures relevent to automative exhaust (8 Torr approx. equals 0.01 atm). At 550 K, as sequentially larger amounts of NO are added to equimolar mixtures of CO and O2 (P(CO) equals P(O2) equals 8 Torr), we find that inhibition of the CO-O2 reaction by NO is significant only when the NO pressure exceeds about one tenth of the equimolar pressures of CO and O2. For a 1:1:1 NO:CO:O2 mixture at 550 K, the CO2 formation rate has dropped two orders of magnitude from the CO-O2 rate without NO and, furthermore, has the same rate as the equimolar CO-NO mixture alone. Ultrahigh vacuum measurements of the low oxygen sticking coefficients on N atom-covered Rh single crystals suggest that the mechanism of NO inhibition of CO oxidation on Rh(111) is inhibition of oxygen adsorption by high nitrogen atom coverages. DOE

N88-27269# Sandia National Labs., Albuquerque, N. Mex.
SUMMARY OF DISCUSSIONS AT THE TENTH MEETING OF THE SANDIA COOPERATIVE GROUP ON THE AEROTHERMOCHEMISTRY OF TURBULENT COMBUSTION
R. W. Dibble and R. P. Lucht Mar. 1988 26 p Meeting held in Warren, Mich., 12 Oct. 1987
(Contract DE-AC04-76DR-00789)
(DE88-008467; SAND-88-8217; CONF-8710304-Summ) Avail: NTIS HC A03/MF A01

A turbulent reacting flow working group has been established through the sponsorship of the Department of Energy, Office of Basic Energy Sciences, Division of Chemical Sciences. The purpose of this group is to establish and maintain a strong interaction and active dialogue between workers currently involved in modeling turbulent reacting flows and those involved in related experiments. One objective of this collaboration is to develop an increased understanding of the fundamental interaction between the chemical and fluid dynamical processes occurring in chemically reacting flows and to utilize this understanding to improve predictive capabilities for turbulent combustion. Regular members, who represent academia, private industry, and national laboratories, and guests participate in the meetings. Several guests are invited to each meeting to provide an influx of different ideas and opinions to the discussions. This document is a summary of the discussions that took place during the tenth meeting, which was held at General Motors Research Laboratories, Warren, Michigan, October 12 to 13, 1987. DOE

N88-27270# California Univ., Berkeley. Lawrence Berkeley Lab.
A METHOD FOR DETERMINING THE SOLUBILITY OF HYDROGEN IN MOLTEN ALUMINUM-LITHIUM ALLOYS Ph.D. Thesis
T. Verma Aug. 1988 60 p
(Contract DE-AC03-76SF-00098)
(DE88-009807; LBL-24512) Avail: NTIS HC A04/MF A01

A constant volume technique, involving the measurement of differential pressure generated between a control volume subjected to an inert gas and an active volume subjected to hydrogen, has been used to determine the solubility of hydrogen in molten 2090 aluminum lithium alloys. The solubility of hydrogen in 2090 aluminum lithium alloys obeys Sievert's law and lies between 1 to 6 ppM for pressures varying from 250 to 950 mm Hg in the temperature range 650 to 750 C. The heat of dissolution of hydrogen is of the order of 135 kJ/mol this alloy. DOE

N88-27271# SRI International Corp., Menlo Park, Calif.
LASER PROBES OF NATURAL GAS IGNITION CHEMISTRY Annual Report, Jan. - Dec. 1987
D. R. Crosley, G. P. Smith, and D. M. Golden Jan. 1988 139 p
(Contract GRI-5087-260-1444)
(PB88-212568; SRI-MP-88-044; GRI-88/0095) Avail: NTIS HC A07/MF A01 CSCL 21B

The research described is aimed at developing and using laser induced fluorescence of various hydrocarbon species as probes in natural gas combustion research, and at developing an understanding of the mechanisms of ignition, catalytic combustion, and flame chemiluminescent emission of natural gas. LIF measurements were made of O atoms, OH radicals and temperatures above a catalytically augmented gas phase combustor, showing the influence of catalytic surfaces at various mixing ratios. Low pressure burner measurements show that, for OH and CH chemiluminescence, simple pressure scaling is inadequate and multiple mechanisms are probably present. Transition state/RRKM theory calculations to codify parameters for extrapolation of rate constants with temperature and pressure were systematically begun for abstraction, decomposition, and activation reactions important in natural gas combustion. Author

N88-27272# Oak Ridge National Lab., Tenn.
DIRECT DETERMINATION OF PART-PER-BILLION LEVELS OF VOLATILE ORGANICS IN WATER AND SOIL SAMPLES USING GLOW DISCHARGE MASS SPECTROMETRY
M. B. Wise and M. R. Guerin 1988 20 p Presented at the 4th Annual Waste Testing and Quality Assurance Symposium, Washington, D.C., 11 Jul. 1988
(Contract DE-AC05-84OR-21400)
(DE88-011389; CONF-880768-1) Avail: NTIS HC A03/MF A01

A low pressure glow discharge ion source has been constructed in our laboratory and interfaced with a quadrupole mass spectrometer for the direct monitoring of trace organic vapors in air. Important features of this ion source include a simple design, low cost, low maintenance, and the ability to sample air directly without the need for membranes, splitters, or capillary restrictors. Although the flow rate of air into the source is approximately 2 standard ml per second, the pressure within the ionization region is maintained at 200 mTorr which reduces interferences caused by the formation of water cluster ions. Furthermore, the high flow rate of air into the ion source provides a simple and convenient means of purging volatile organics from water or soil samples directly into the mass spectrometer without additional apparatus or extensive sample preparation. Early studies with this system indicate that low part-per-billion levels of volatile organics such as benzene or tri-chloroethylene can be quantitatively determined in water and soil samples either by monitoring headspace above a sample or by direct purging. Analysis time of 2 to 5 minutes provides a high throughput of 10 or more samples per hour. DOE

N88-27273# Lawrence Livermore National Lab., Calif.
PRECISE ROTATIONAL ALIGNMENT OF X-RAY TRANSMISSION DIFFRACTION GRATINGS
S. L. Hill 28 Mar. 1988 20 p
(Contract W-7405-eng-48)
(DE88-010599; UCID-21386) Avail: NTIS HC A03/MF A01

Gold transmission diffraction gratings used for X-ray spectroscopy must sometimes be rotationally aligned to the axis of a diagnostic instrument to within sub-milliradian accuracy. We have fabricated transmission diffraction gratings with high line-densities (grating period of 200 and 300 nm) using UV holographic and X-ray lithography. Since the submicron features of the gratings are not optically visible, precision alignment is time consuming and difficult to verify in situ. We have developed a technique to write an optically visible alignment pattern onto these gratings using a scanning electron microscope (SEM). At high magnification (15000 X) several submicron lines of the grating are observable in the SEM, making it possible to write an alignment pattern parallel to the grating lines in an electron-beam-sensitive coating that overlays the grating. We create an alignment pattern by following a 1 cm-long grating line using the SEM's joystick-controlled translation stage. By following the same grating line we are assured the traveled direction of the SEM electron beam is parallel to the grating. The pattern can be used to accurately align the grating to the axis of a diagnostic instrument. More importantly, the alignment of the grating can be quickly verified in situ. DOE

N88-27274# Sandia National Labs., Albuquerque, N. Mex.
GASEOUS TRACER TECHNIQUES FOR PORE STRUCTURE CHARACTERIZATION OF GRANULAR MATERIALS
K. L. Erickson 1988 15 p Presented at the 13th International Pyrotechnics Seminar, Grand Junction, Colo., 11 Jul. 1988
(Contract DE-AC04-76DP-00789)
(DE88-011542; SAND-88-0068C; CONF-880750-7) Avail: NTIS HC A03/MF A01

The pore structure of granular materials influences several physical and chemical phenomena, including: (1) heat and mass transfer rates, (2) fluid dynamics, (3) mechanical response, and (4) heterogeneous chemical reaction rates. In many systems, these phenomena are coupled, and accurate pore structure characterization is important to developing reliable predictive models. Gaseous tracer techniques show promise as a rapid nondestructive method for characterizing pore structures. To provide a basis for developing a theoretical and experimental approach involving multiple tracer techniques, five characteristic parameters were defined to describe the major features of a macroscopically uniform pore structure. Those parameters are the following: (1) the portion of the total pore space that forms flow paths (flow porosity), (2) the fraction that forms relatively stagnant paths (stagnant porosity), (3) the tortuosity of the flow porosity, (4) the specific surface area of the pore space, and (5) the fraction of the specific surface area that is associated with the flow porosity. Initial experiments with samples having simple, known pore structures were conducted to evaluate the theory and experimental techniques. Agreement between known and experimentally determined parameter values was good. Furthermore, it appears that the tracer techniques can have broad application as nondestructive diagnostic tools for examining granular materials. DOE

N88-27275# Sandia National Labs., Albuquerque, N. Mex.
LASER PROBES AND NUMERICAL MODELING AS PROCESS DIAGNOSTICS IN CHEMICAL VAPOR DEPOSITION
W. G. Breiland, P. Ho, M. E. Coltrin, R. J. Kee, and G. H. Evans 1988 12 p Presented at the Spring Meeting of the Materials Research Society, Reno, Nev., 4 Apr. 1988
(Contract DE-AC04-76DP-00789)
(DE88-011622; SAND-88-1313C; CONF-880408-26) Avail: NTIS HC A03/MF A01

The chemical vapor deposition process consists of a chemically reacting flow in which the fluid mechanics and chemical kinetics are strongly coupled. Laser probes such as Raman spectroscopy and laser induced fluorescence can be used to measure gas temperature fields and chemical species concentrations, but often the interpretation of such data is difficult because several interacting chemical and physical phenomena are occurring simultaneously. Detailed numerical modeling of the experimental system under study provides valuable insights into these interactions and allows one to make useful comparisons between experiment and the model to gain a fundamental understanding of the CVD process. Examples of this approach are given for silicon deposition from silane and fluid mechanics diagnostics in a rotating disk CVD reactor. DOE

N88-27276# Sandia National Labs., Albuquerque, N. Mex.
DEVELOPMENT OF AN EXPERIMENTAL SYSTEM FOR STUDYING FAST TRANSIENT IGNITION PHENOMENA
R. D. Skocypec and K. L. Erickson 1988 12 p Presented at the 13th International Pyrotechnics Seminar, Grand Junction, Colo., 11 Jul. 1988
(Contract DE-AC04-76DP-00789)
(DE88-011917; SAND-88-0553C; CONF-880750-11) Avail: NTIS HC A03/MF A01

This paper describes work in progress to develop an experimental system for studying fast transient ignition phenomena. The system integrates several diagnostic techniques to study the fast transient reaction kinetics (approx. 10 microsec temporal resolution) governing the thermal ignition of pyrotechnics and explosives. The principal components of the system include: (1) a time-of-flight (TOF) mass spectrometer and a quadrupole mass spectrometer, (2) a photo-elastic modulator (PEM) ellipsometer, (3) a pulsed dye laser and a continuous wave Nd:YAG laser, (4) an infrared detector array, (5) ultra-high vacuum systems, and (6) a high-speed, computer-based data acquisition system. The basic experimental concept is to react samples having a simple, known geometry for which complex heat and mass transfer effects are minimized so that reaction mechanisms and rates can be examined directly. DOE

N88-27277# Oak Ridge National Lab., Tenn.
SURVEY OF THE LITERATURE ON FRACTALS WITH POSSIBLE APPLICATIONS TO PHASE CHANGE PROCESSES
L. A. Renker and D. G. Wilson Jun. 1988 20 p
(Contract DE-AC05-84OR-21400)
(DE88-012240; ORNL/TM-10778) Avail: NTIS HC A03/MF A01

This paper is a partial collection of the literature on fractals and how they apply to phase change processes, specifically solidification. Fractals can be used to model the dendrites that are formed at the interface between a liquid and a solid with restrictions because either dendrites or non-dendritic fractals may be formed by diffusion limited solidification, depending on the presence of crystalline anisotropy. This anisotropy causes the tips of the structure being formed to remain stable, leading to the formation of a dendrite, rather than splitting to form a non-dendritic fractal. An additional type of structure is found when electrodeposition is used to model solidification. The formation of this dense radial structure depends on the level of the voltage and the electrolyte concentration. These structures are formed at intermediate values where the crossover from non-dendritic fractals to dendrites occur. Non-dendritic fractals are formed at the lower values and dendrites are formed at the higher values. A comprehensive bibliography is included with this paper. DOE

N88-27278# Institut National des Sciences Appliquees, Lyon (France). Lab. de Genie Electrique.
MANUFACTURING OF A BARIUM TITANATE WITH HIGH DIELECTRIC COEFFICIENT BY DECOMPOSITION OF PRECIPITATES OF DOUBLE OXALATES Ph.D. Thesis [ELABORATION D'UN TITANATE DE BARYUM DE HAUTE CONSTANTE DIELECTRIQUE PAR DECOMPOSITION D'OXALATES DOUBLES COPRECIPITES]
Serge Rimlinger 1988 127 p In FRENCH
(ISAL-IDI1-88-02; ETN-88-92756) Avail: NTIS HC A07/MF A01

A manufacturing procedure was developed in order to optimize the parameters controling the dielectric coefficient of the barium titanate used in multilayer condensers (X7R norm). The double titanyl and barium oxalate was obtained as a precipitate and later decomposed. Grain size was studied as a parameter of the resulting dielectric coefficient. It is shown that the ratio Ba/Ti and the grain size are effective controling parameters. A large sample of material with the best properties (1 kg, dielectric constant over 4000) was used to manufacture actual condensers. ESA

N88-27371# Iowa Univ., Iowa City. Dept. of Mechanical Engineering.
EXPERIMENTAL RESEARCH OF COMBUSTION SYSTEMS Final Report
James P. Seaba *In* Universal Energy Systems, Inc., United States Air Force Graduate Student Summer Support Program, Volume 2 Dec. 1987 10 p (For primary document see N88-27355 21-31)
Avail: NTIS HC A99/MF E03 CSCL 21B

N88-27397# Mitsubishi Electric Corp., Tokyo (Japan). LSI Development Lab.
POLARIZATION SELECTIVE RAMAN MICROSPECTROSCOPY
Yasuo Inoue, Tadashi Nishimura, and Yoichi Akasaka *In its* Mitsubishi Electric Advance (R and D Edition), Volume 41 Dec. 1987 7 p (For primary document see N88-27388 21-31)
Avail: NTIS HC A03/MF A01 CSCL 07D

26 METALLIC MATERIALS

Includes physical, chemical, and mechanical properties of metals, e.g., corrosion; and metallurgy.

N88-27279# Oak Ridge National Lab., Tenn.
MAGNETIC EXCITATIONS IN TRANSITION METAL SYSTEMS
J. F. Cooke and J. A. Blackman May 1988 11 p Presented at the International Conference on Magnetism, Paris, France, 25 Jul. 1988 Prepared in cooperation with Reading Univ., United Kingdom
(Contract DE-AC05-84OR-21400)
(DE88-011022; CONF-880705-1; CONF-880705) Avail: NTIS HC A03/MF A01

An expression for the neutron scattering cross section based on itinerant electron theory within RPA has been derived which incorporates the most general form of the exchange matrix consistent with crystal symmetry. Numerical results indicate a wider range of spin-wave behavior than found previously. DOE

N88-27280# Army Armament Research and Development Command, Watervliet, N. Y.
ULTRASONIC STUDIES OF STRESSES AND PLASTIC DEFORMATION IN STEEL DURING TENSION AND COMPRESSION Final Report
J. Frankel and W. Scholz Feb. 1988 23 p
(AD-A192308; AD-E801594; ARCCB-TR-88005) Avail: NTIS HC A03/MF A01 CSCL 11F

A steel bar subjected to four-point bending was instrumented so that various strains and sound velocities could be measured during elastic and plastic deformation on both the tension and compression side of the bar. During plastic deformation, the load was reduced several times before it was increased again. We present the acoustoelastic constants and the corresponding third-order elastic constants 1, m, and n in both tension and compression in the as-treated specimen and after various amounts of plastic deformation. GRA

N88-27281# Naval Postgraduate School, Monterey, Calif.
THERMOMECHANICAL PROCESSING OF Al ALLOY 2090 FOR GRAIN REFINEMENT AND SUPERPLASTICITY M.S. Thesis
Procopios T. Spiropoulos Dec. 1987 86 p
(AD-A192333; AD-E801594) Avail: NTIS HC A05/MF A01 CSCL 11F

An aluminum copper lithium zirconium alloy, recently registered as 2090, with 7 percent lower density and 10 percent higher elastic modulus, has been introduced as a replacement for the 7075-T6 alloy. The purpose of this research is to investigate the applicability of thermomechanical processing methods developed at NPS for materials including Al-Mg and Al-Mg-Li alloys, to the 2090 alloy. The material is hot worked, cold worked, aged and warm rolled to a total true strain of about 2.4. Tensile tests were conducted at different temperatures and strain rates allowing a determination of the effect of the processing on microstructural evolution and the superplastic behavior of this material. GRA

N88-27282# Naval Postgraduate School, Monterey, Calif.
DETERMINATION OF TAFEL CONSTANTS IN NONLINEAR POLARIZATION CURVES M.S. Thesis
Thomas E. OLoughlin Dec. 1987 140 p
(AD-A192335; AD-E801594) Avail: NTIS HC A07/MF A01 CSCL 11F

The presence of non-linear behavior in potentiodynamic polarization plots has resulted in difficulty in determining the Tafel constants from such plots. A FORTRAN based program involving numerical differentiation techniques was used to determine the existence of the Tafel regions. Various alloys polarized in synthetic seawater and a 3.5 percent NaCl solution were analyzed. Although severe concentration polarization often dominated the cathodic branches the techniques employed did allow for the selection of regions which approached linear behavior. The effects of concentration polarization in hindering the determination of Tafel constants were exemplified by the uncovering of a cathodic branch containing a small region where only activation polarization dominated followed by the onset and total domination of concentration polarization. A method of determining where the anodic and cathodic currents begin to dominate the potentiodynamic polarization curve is introduced. GRA

N88-27283# Naval Postgraduate School, Monterey, Calif.
ANALYSIS OF GRAIN REFINEMENT AND SUPERPLASTICITY IN ALUMINUM-MAGNESIUM ALLOYS Ph.D. Thesis
Ahmed A. Abou-Salama Dec. 1987 167 p
(AD-A193029) Avail: NTIS HC A08/MF A01 CSCL 11F

Previous research had demonstrated superplastic behavior in aluminum-magnesium alloys of high magnesium content to result from deformation processing to an initially non-recrystallized condition. Analysis here of those data has demonstrated that such a result may be understood in terms of constitutive equations developed for fine-grained materials and that the constitutive equations are applicable to materials achieving grain boundary misorientations in the range of only 2 to 7 by a process of continuous recrystallization. The constitutive equations provide a basis for analysis of anomalous temperature dependence of the strength and of the activation energy for plastic deformation seen as well in this work. A study of the separate effects of processing variables has lead to a model for continuous recrystallization during deformation processing. This model considers recovery of dislocations to sub-boundaries to be the critical step in this process. Application of this model to development of advanced aluminum alloys for air frame structural applications will result in increased weight savings by such processing methods. GRA

N88-27284# Virginia Univ., Charlottesville. Dept. of Materials Science.
PROCESSING AND PROPERTIES OF ADVANCED ALUMINUM ALLOYS Annual Report, 1 Jan. - 31 Dec. 1987
John A. Wert and Edgar A. Starke, Jr. Feb. 1988 97 p
(Grant AF AFOSR-0082-87)
(AD-A193224; UVA/525670/MS88/101; AFOSR-88-0285TR)
Avail: NTIS HC A05/MF A01 CSCL 11F

This project has as its focus microstructure control and fracture of advanced aluminum alloys. The progress report is divided into two major parts: Part 1 which is concerned with the effect of microstructure on the deformation and fracture of advanced aluminum alloys, and Part 2 which is concerned with the recovery and recrystallization mechanisms that operate during processing of advanced aluminum alloys. Age hardenable aluminum alloys

may undergo relatively brittle intergranular fracture at strains from 2 to 10 times smaller than the strain to fracture for pure aluminum. This phenomenon can be explained in broad terms as follows. Within a grain, an advancing dislocation either bypasses the coherent particles it encounters or cuts through them; cutting reduces the effective size of the obstacle, while bypassing the obstacle effectively enlarges it. If the obstacles are cut, the weakened plane will continue to slip and deformation will be localized. As a result, dislocations pile up at the grain boundaries at isolated points; the large associated tensions across the grain boundaries open intergranular cracks which propagate without absorbing much energy. GRA

N88-27285# Army Construction Engineering Research Lab., Champaign, Ill.

EVALUATION OF EXPLOSIVE BONDING FOR PATCHING ALUMINUM WITH ALUMINUM Final Report

Robert A. Weber and Vonne Linsey Mar. 1988 23 p
(AD-A193303; CERL-TR-M-88/09) Avail: NTIS HC A03/MF A01 CSCL 11F

The U.S. Army Corps of Engineers maintains many waterborne vehicles and floating devices that are made of aluminum. Repair of these items usually involves gas metal arc welding a patch over the damaged area. However, the arc welding process is difficult to learn and is not well suited to use in the field. For these reasons, the U.S. Army Construction Engineering Research Laboratory (USA-CERL) has explored an alternative repair method explosive bond welding. Weld techniques using explosives are fairly well established, although most work in this area has involved the bonding of dissimilar metals. USA-CERL investigated the feasibility of welding aluminum to aluminum using explosive bonding. Prerequisites for such a welding system are: must provide a single repair material compatible with both 5456 and 6061 aluminum alloys commonly used in the items; must be safe and portable for use in the field; must require a minimum amount of explosives; the explosives(s) must already be in the Army inventory (and thus meet safety standards); and must include internal support or backups required for the wall thicknesses to be repaired. GRA

N88-27286# Vanderbilt Univ., Nashville, Tenn. Dept. of Mechanical and Materials Engineering.

ANALYSIS OF CRACK ARREST TOUGHNESS Final Report

G. T. Hahn and C. A. Rubin 15 Jan. 1988 157 p
(Contract N00014-80-C-0521)
(AD-A193340) Avail: NTIS HC A08/MF A01 CSCL 11F

The objective of the research was to provide theoretical and experimental backing for three concepts that will facilitate the design of structures capable of arresting cracks. The first concept is that the conventional static toughness measures, Jlc or the JR curve, are bona fide measures of the fracture arrest capability of tough ductile steels. The second is that the J-values represent the crack driving force when a crack arrests in a tough material, provided the bulk of the propagation just prior to arrest occurs in a relatively brittle material. The work includes (1) Verification of J-integral evaluation of arrest properties: (a) Analysis of the crack velocity dependence of toughness for the fibrous mode of crack extension; (b) A new test method for studying fast fracture and arrest in tough steels; (c) Measurements of fast fracture and crack arrest; (d) Fractographic studies; (2) Application of J-resistance curve concept to crack arrest: (a) Development of a finite element model for analysis of a rapidly loaded stationary crack of a compact specimen of a tough, rate dependent steel; (b) Development of a general method for quantifying temperature and rate-sensitive constitutive relations for steel; (c) Development of crack extension capability using local control in the finite element program; (d) Finite element modeling of rapid crack extension in ductile viscoplastic materials. GRA

N88-27287# Air Force Wright Aeronautical Labs., Wright-Patterson AFB, Ohio.

CONSTANT AMPLITUDE FATIGUE LIFE DATA FOR NOTCHED AND UNNOTCHED ANNEALED Ti-6Al-4V SHEET Final Report, Jan. 1983 - Sep. 1986

Torsten M. Rhode and Patrick W. Ertel Jan. 1988 38 p
(AD-A193420; AFWAL-TR-88-4081) Avail: NTIS HC A03/MF A01 CSCL 11F

Three lots of annealed Ti-6A1-4v sheet material in thicknesses of 0.063 inch, 0.070 inch, and 0.078 inch, supplied by two manufacturers, were tested to develop fatigue life curves for MIL-HDBK-5. Notched (Kt=3.0) and unnotched configurations of longitudinal and transverse specimens were tested at R-ratios of +0.5, +0.1, and -0.5. Fatigue life data are presented in both tabular and graphical forms. Results were forwarded to the Battelle Memorial Institute, Columbus, Ohio, for analysis, reduction, and inclusion in MIL-HDBK-5. GRA

N88-27288# Lawrence Livermore National Lab., Calif.

ON THE SYSTEMATICS OF PHASE TRANSFORMATION IN METALLIC ALLOYS

L. E. Tanner 12 Feb. 1988 10 p Presented at the Conference on Competing Interactions and Microstructures, Statics and Dynamics, Los Alamos, N. Mex., 5 May 1988
(Contract W-7405-eng-48)
(DE88-008041; UCRL-98232; CONF-880586-1) Avail: NTIS HC A03/MF A01

Phase transformations in metallic alloys proceed by diffusional replacive or diffusionless displacive mechanisms. These are generally viewed as independent processes without significant interactive coupling. However, new studies of displacive transformations, particularly regarding pretransformation phenomena, suggest that such coupling may indeed occur. If so, it should have a significant effect on the mode, morphology and mechanisms of the replacive transformations. In this paper we examine these possibilities in light of the most recent observations and thinking in this field. DOE

N88-27289# Sandia National Labs., Albuquerque, N. Mex.

OPTICAL DIAGNOSTICS FOR METALLURGICAL PROCESSES

R. L. Williamson, H. C. Peebles, W. A. Hareland, and F. J. Zanner 1988 13 p Presented at the MRS Symposia on Process Diagnostics, Reno, Nev., 4 Apr. 1988
(Contract DE-AC04-76DP-00789)
(DE88-009255; SAND-87-2460C; CONF-8804121-1) Avail: NTIS HC A03/MF A01

Many industrially important metallurgical processes are accompanied by the emission of light, the analysis of which often supplies useful information concerning the current state of the process while also providing insight into the details of specific process mechanisms. Optical diagnostic techniques are finding an increasingly wide range of application throughout the metallurgical community. This paper discusses the application of emission spectroscopy and imaging techniques to the analysis of such diverse processes as vacuum arc remelting, laser welding, and arc welding. A discussion of these techniques is presented, addressing such subjects as instrumentation, data analysis, the kind of information available and its potential impact on the selection of process parameters. Special attention is given to discussing the difficulties encountered in applying these diagnostic technologies to real life processes in non-laboratory environments. DOE

N88-27290# California Univ., Berkeley. Lawrence Berkeley Lab.

DEVELOPMENT OF HIGH STRENGTH AND TOUGHNESS MICROCOMPOSITE HSLA Fe/Cr/Mn/C STEEL WITH AND WITHOUT Nb

G. Thomas, J. K. Kim, D. Manojlovic, and R. Milovic Dec. 1987 27 p Presented at the International Conference on HSLA Steels, Pittsburgh, Pa., 3 Nov. 1987
(Contract DE-AC03-76SF-00098)
(DE88-009813; LBL-23968; CONF-8711180-1) Avail: NTIS HC A03/MF A01

Microcomposite steels have been designed to consist of fine packet martensite and interlath austenite films in order to attain mechanical and corrosion properties with superior combinations of strength, fracture toughness, and formability in certain conditions.

In an effort to improve these properties for on-line production in a hot mill for rounds and plates, modifications with niobium have been investigated and the CCT diagrams determined. The addition of niobium has achieved grain refinement without destroying the microcomposite morphology of packet martensite and austenite. Comparisons of properties, structure and processing are presented. DOE

N88-27291# California Univ., Berkeley. Dept. of Materials Science and Mineral Engineering.
THEORETICAL PREDICTIONS OF PRECIPITATE SHAPES IN CUBIC ALLOYS Ph.D. Thesis
T. S. Edgecumbe May 1988 71 p Prepared in cooperation with California Univ., Berkeley, Lawrence Berkeley Lab.
(Contract DE-AC03-76SF-00098)
(DE88-010856; LBL-25260) Avail: NTIS HC A04/MF A01

The precipitate is spherical at small volumes, cuboidal at intermediate volumes, and eventually spreads into a plate of increasing aspect ratio beyond a certain critical volume. The volume at which these shape transitions occur depends on the surface tension, volume change, and elastic constants. These critical volumes were calculated and compared to volumes experimental for Ni-Al, Ni-Ti and Al-Li which form cubic Ni3Al (gamma'), Ni3Ti (gamma') and Al3Li (delta') precipitates. Good agreement was obtained for the sphere-to-cube transition. For Ni-Al and Ni-Ti, the gamma' sphere-to-cube shape transition is expected to occur at 110 A and 130 A. Spherical delta' precipitates were found to be stable until rather large volumes (30 cu microns) for the most part due to the low delta'-Al misfit. The stability of spherical delta' precipitates is also likely due to the relative isotropy of Al. Plate-like precipitates in the Ni-base alloys were found to be stable at volumes in excess of 130 - 200 cubic angstroms. The cube-to-plate shape transition of an isolated precipitate will occur at the volume predicted if the cuboidal shape is unstable with respect to the plate beyond the critical volume. If the cuboidal shape is metastable, however, the shape transition may not occur until much larger volumes. A plate-shaped precipitate may also be formed by the coalescence of an array of interacting cubes. The transition volumes in this case are most likely greater than the values predicted for the isolated inclusion. DOE

N88-27292# Foersvarets Forskingsanstalt, Stockholm (Sweden).
HOT ISOSTATIC PRESSING OF TUNGSTEN-NICKEL-IRON COMPOSITES
L. Ekbom, A. Eliasson, and S. Bogegard Feb. 1988 18 p
(PB88-203070; FOA-C-20698-2.1) Avail: NTIS HC A03/MF A01 CSCL 11F

Heavy metals or tungsten-nickel-iron alloys are usually produced from powders by liquid phase sintering. During this process a nickel iron tungsten melt is formed in which tungsten crystals are growing to a spherical shape. The resulting particle composite structure gives the material good mechanical properties. Studies were made to learn to what extent the liquid phase sintering could be replaced by HIP. For this purpose blends of different W, Ni and Fe powders were filled into steel containers, evacuated and sealed. The investigation shows that the microstructure after HIP is dependent on the powder grain size. To be able to improve the microstructure after HIP, the grain size of nickel and iron powders must be about one tenth of that of the tungsten powder. Author

N88-27293# Oak Ridge National Lab., Tenn.
CONTROLLING PHASE FORMATION AND STABILITY TO IMPROVE THE HIGH TEMPERATURE CREEP RESISTANCE OF AUSTENITIC STAINLESS STEELS
P. J. Maziasz 1988 9 p Presented at the Interfacial Structure, Properties and Designs in Solids, Reno, Nev., 5 Apr. 1988
(Contract DE-AC05-84OR-21400)
(DE88-011401; CONF-8804112-5) Avail: NTIS HC A02/MF A01

New Fe-14Cr-16Ni-2.5Mo-2Mn steels modified with carefully controlled additions of Ti, Nb, V, C, P and B have been developed which have outstanding creep rupture resistance at 700 C and 170 MPa, much better than comparable commercial steels. The minor alloying element levels and combinations were chosen a priori to produce specific microstructures of fine MC and FeTiP precipitates in the matrix and coarser carbides along grain boundaries before creep properties were ever measured. The precipitates directly produce the creep resistance observed in the new steels. The ideas that guided these modifications to tailor and control the precipitate microstructure stem from years of studying precipitation in aged and reactor irradiated steels by the use of analytical electron microscopy (AEM). DOE

N88-27294# Pittsburgh Univ., Pa. Dept. of Materials Science and Engineering.
MICROCHEMICAL ANALYSIS OF POLYCRYSTALLINE Ni3Al AND OTHER ORDERED ALLOYS USING THE FIELD-ION MICROSCOPE ATOM PROBE Technical Progress Report
S. S. Brenner 31 May 1988 15 p
(Contract DE-FG02-85ER-45213)
(DE88-011519; DOE/ER-45213/3) Avail: NTIS HC A03

We have used the field-ion microscope atom probe to detect chemical changes that occur at the grain-boundaries of nickel aluminide as a result of the boron additions. We have also examined the matrix of boron-doped hyperstoichiometric nickel aluminide to determine whether boron clustering could be responsible for the lack of response of these alloys to boron ductillization. Finally, we have measured the site occupation probability of hafnium and tantalum in nickel aluminide using the atom probe's atomic layer-by-layer analysis capability. The site occupation results are useful in understanding the solid solution strengthening effect in nickel aluminide. The results of our experimental program are briefly described. DOE

N88-27295# Japan Atomic Energy Research Inst., Tokyo. Dept. of High Temperature Engineering.
CREEP BEHAVIOR FOR HASTELLOY-XR
Yasushi Muto, Kazuhiko Hada, Yutaka Ogawa, and Sadao Ikeda Feb. 1988 54 p In JAPANESE; ENGLISH summary
(DE88-753428; JAERI-M-88-003) Avail: NTIS (US Sales Only) HC A04/MF A01

Creep-rupture tests for Hastelloy-XR, a Ni-base heat resistent alloy, were conducted in air at the temperature of 650 to 900 C. Times to rupture ranged from 1000 to 16000 h. As results of tests, creep curves were observed to vary depending on both temperature and stress, particularly on temperature. Namely, they showed typical classical shapes consisting of primary, secondary and tertiary creep at 650 to 700 C. The regions of primary and secondary creep decreased gradually as the temperature became higher and in one case of 900 C and high stress, only tertiary creep was observed. Metallurgical observation by optical microscope showed the similar inclination. Some differences were found concerning rupture morphology and void shape between temperatures below 750 C and above 850 C. DOE

N88-27296# International Centre for Theoretical Physics, Trieste (Italy).
DIFFUSION AND SOLUBILITY OF SOME INTERSTITIAL IMPURITIES IN DEFORMED METALS
Yu. S. Nechaev and B. Kidane Jun. 1987 32 p
(DE88-701859; IC-87/116) Avail: NTIS (US Sales Only) HC A03/MF A01

The problem of impurity diffusion accompanying segregation phase nucleation on dislocations has been studied using the approximation of the local equilibrium with respect to the impurity distribution between the volume solution and dislocation regions. It has been shown that the known experimental data on diffusion and solubility of some interstitial impurities in cold-worked body centered cubic and face centered cubic metals and alloys can be described in the framework of the dislocation trap model. The characteristics of the impurity segregation regions near dislocations have been obtained from the treatment of the diffusion and solubility data for the systems. On the basis of the crystallographic and thermodynamic considerations, the possibility of the existence of

such segregation phase regions along dislocations in the systems in question is shown. DOE

N88-27297# Joint Inst. for Nuclear Research, Dubna (USSR). Lab. of Nuclear Problems.
INVESTIGATION OF HYDROGEN ISOTOPE PENETRATION THROUGH STAINLESS STEELS Kh18N10T AND Kh3M2BFR
V. M. Bystritskij, V. P. Dzhelepov, and V. B. Granovskij 1987 8 p In RUSSIAN; ENGLISH summary
(DE88-702189; JINR-R-13-87-525) Avail: NTIS (US Sales Only) HC A02/MF A01

Compared are the parameters of hydrogen and deuterium penetration through austenitic (Kh18N10T) and ferritic-martensitic (Kh13M2BFR) steels measured at high saturation and at the gas pressure to 5000 atm in the temperature range 300 to 1050 K. The conclusion is made that the given steels can be applied as materials for pressure vessels only in the pressure range investigated. DOE

N88-27298# Lawrence Livermore National Lab., Calif.
FORMATION OF METASTABLE STRUCTURES AND AMORPHOUS PHASES IN Cu-W ALLOYS USING THE TRIOD SPUTTERING TECHNIQUE
H. F. Rizzo, L. E. Tanner, M. A. Wall, T. B. Massalski, and E. C. McClanahan Nov. 1987 13 p Presented at the Fall Meeting of the Materials Research Society, Boston, Mass., 30 Nov. 1987 Prepared in cooperation with Carnegie-Mellon Univ., Pittsburgh, Pa. and Pacific Northwest Lab., Richland, Wash.
(Contract W-7405-eng-48)
(DE88-009051; UCRL-96445; CONF-871124-100) Avail: NTIS HC A03/MF A01

The triode sputtering technique and a split-target arrangement were used to produce metastable crystalline and amorphous phases in the Cu-W system under essentially oxygen-free conditions. Large metastable extensions of solid solubility were observed both from the Cu (fcc) and W (bcc) sides of the phase diagram, and a wide range of metallic glass formation was observed, approximately between 30 and 65 at. percent W. The thickness of the amorphous Cu-W phase (40 to 160 microns) that can be deposited without the formation of the metastable bcc phase appears to be dependent on the Cu-W alloy composition. On heating, the crystallization temperature of the amorphous alloys was higher than 350 C. The behavior of the lattice parameter and near-neighbor distance has been studied with X-ray diffraction, showing small positive deviations from an assumed Vegard's Law. Hardness measurements indicate that the metastable crystalline phases are relatively harder than the amorphous phase. DOE

N88-27299# Sandia National Labs., Albuquerque, N. Mex.
PECVD OF AMORPHOUS NICKEL--PHOSPHORUS FILMS
A. K. Hays, G. C. Nelson, and C. H. Seager 1988 2 p Presented at the AT and T Task Group 5 Meeting, Albuquerque, N. Mex., 22 Mar. 1988
(Contract DE-AC04-76DP-00789)
(DE88-011088; SAND-88-0221C; CONF-880383-2) Avail: NTIS HC A02/MF A01

We have developed a plasma deposition technique capable of producing amorphous transition metal-metalloid coatings. The technique consists of decomposing gas mixtures containing transition metal carbonyls and metalloid hydrides in a radiofrequency discharge. Nickel-phosphorus was chosen as a proof-of-principle film for this work. The key to obtaining amorphous metals, as opposed to amorphous metal oxides, lies in the use of a hydrogen carrier gas to remove unwanted oxygen in the form of water as a gaseous by-product. In addition it was discovered that carbon could be completely removed from these films by heating the substrates slightly above room temperatures. DOE

N88-27300# Argonne National Lab., Ill.
OXIDATION-EROSION OF METALS AND ALLOYS: MODELS, VERIFICATION, AND PREDICTION
Yung Y. Liu and K. Natesan Jan. 1988 23 p Presented at the 15th International Conference on Metallurgical Coatings, San Diego, Calif., 11 Apr. 1988
(Contract W-31109-eng-38)
(DE88-010016; CONF-880488-4) Avail: NTIS HC A03/MF A01

Models have been developed for synergistic interaction of oxidation and erosion of metals and alloys. The models are based on an extension of earlier work on paralinear kinetics in which oxidation of metal is assumed to be diffusion controlled, and erosion is assumed to result in a uniform removal of materials. Predictions of oxidation-erosion behavior as a function of temperature and erosion conditions have been made for several chromia- and alumina-forming alloys, which included the construction of two master plots for these alloys that allow distinction of oxidation- or erosion-dominated regime as a function of the kinetic rate constants. The models have also provided reasonable explanations of the results obtained in the oxidation-erosion experiments on pure nickel and cobalt. DOE

N88-27301# Michigan Technological Univ., Houghton. Dept. of Metallurgical Engineering.
APPLICATION OF AUGER ELECTRON SPECTROSCOPY TO THE STUDY OF TRACE ELEMENT EFFECTS ON WELDABILITY
C. L. White, S. A. David, and M. W. Richey 1987 14 p Presented at the International Symposium on Welding Metallurgy of Structural Steels, Denver, Colo., 22 Feb. 1987 Prepared in cooperation with Oak Ridge National Lab., Tenn.; Oak Ridge Y-12 Plant, Tenn.
(Contract DE-AC05-84OR-21400)
(DE88-010457; CONF-8702142-1) Avail: NTIS HC A03/MF A01

In this paper, we briefly overview the application of AES (Auger Electron Spectroscopy) to the study of impurity segregation in weld cracking problems. Although these impurities have long been implicated in weld cracking, AES results thus far are not sufficiently extensive to demonstrate a clear correlation between their segregation, and the severity of weld cracking. DOE

N88-27302# Oak Ridge National Lab., Tenn.
THIN FILM AND NEAR-SURFACE CHARACTERIZATION USING A MECHANICAL PROPERTIES MICROPROBE
W. C. Oliver and C. J. McHargue 1988 6 p Presented at the Ion Implantation and Plasma Assisted Processes for Industrial Applications Conference, Atlanta, Ga., 21 May 1988
(Contract DE-AC05-84OR-21400)
(DE88-011399; CONF-8805134-3) Avail: NTIS HC A02/MF A01

Ion implantation of materials to improve their mechanical properties is a rapidly expanding industry. Such surface treatments result in very thin (less than 500 nm) surface films. These films can have extraordinary mechanical properties due to the tremendous variety of structures and compositions available via ion implantation. The mechanical properties microprobe (MPM) has been developed to determine the properties of such thin films. In this paper we will discuss the application of the MPM to several ion implanted material systems. DOE

N88-27303# Oak Ridge National Lab., Tenn.
INELASTIC ELECTRON SCATTERING AND ELECTRON-HOLE EXCITATIONS IN IRON AND NICKEL
J. A. Blackman and J. F. Cooke Jun. 1988 12 p Presented at the International Conference on Magnetism, Paris, France, 25 Jul. 1988
(Contract DE-AC05-84OR-21400)
(DE88-011843; CONF-880705-2) Avail: NTIS HC A03/MF A01

Spin-flip and non-spin-flip mechanisms have been proposed to explain polarization asymmetry in inelastic electron scattering from iron and nickel. A maximum in the asymmetry near 2eV in iron can occur by both mechanisms. The 300meV maximum in nickel is unlikely to occur by non-spin-flip transitions. DOE

N88-27304# Pennsylvania State Univ., University Park. Materials Research Lab.
TWIN BOUNDARIES AND HETEROPHASE INTERFACES IN FERROELASTIC MARTENSITES Annual Progress Report, 16 Jan. 1986 - 30 Jun. 1988
G. R. Barsch 1988 11 p
(Contract DE-FG02-85ER-45214)
(DE88-011894; DOE/ER-45214/T1; APR-3) Avail: NTIS HC A03/MF A01

A comprehensive theoretical study with concurrent supporting experimental investigations is being carried out on coherent and semicoherent interfaces in ferroelastic martensites, including twin boundaries and twin bands, heterophase parent/product interfaces and inclusions, and transformation precursors. This work is motivated by the need for a new theoretical basis for investigating the martensite nucleation mechanism and for establishing the conditions for nonclassical nucleation. Soliton-like solutions of a dynamic Ginzburg-Landau continuum theory for ferroelastic martensites are being studied in order to determine the strain distribution, strain energy and dynamical behavior for various geometric configurations as a function of the material parameters, temperature and boundary conditions. Model parameters of the theory consist of the second and higher order elastic constants and the harmonic strain gradient coefficients in the parent phase. X-ray measurements of the transformation strain versus temperature, and simultaneous ultrasonic velocity and attenuation measurements on biaxially stressed crystals in In(sub 1-x)Ti(sub x) alloys for determining the second and higher order elastic constants in the single domain tetragonal state and for studying the morphology and the dynamic behavior of the martensite interfaces and transformation precursors have been started or are in preparation, respectively. DOE

N88-27305# Argonne National Lab., Ill.
COMPUTER SIMULATION OF ELASTIC PROPERTIES OF GRAIN BOUNDARY MATERIALS
D. Wolf and J. F. Lutsko Apr. 1988 7 p Presented at the Adhesion in Solids, Reno, Nev., 5 Apr. 1988
(Contract W-31-109-eng-38)
(DE88-011965; CONF-8804117-3) Avail: NTIS HC A02/MF A01

Lattice statics and lattice dynamics computer simulation methods are applied to investigate the elastic properties of grain boundaries in f.c.c. metals. The elastic constants in the GB region are found to differ significantly from their bulk ideal-crystal values. Due to the broken symmetry in the GB region a pronounced anisotropy of the elastic properties is observed. Whereas Young's moduli are found to increase in the GB region, the shear modulus and Poisson's ratios generally decrease. The magnitude of these effects is shown to depend sensitively on the GB structure. DOE

N88-27306# Argonne National Lab., Ill.
THERMAL CONDUCTIVITY AND THERMAL EXPANSION OF STAINLESS STEELS D9 AND HT9
L. Leibowitz and R. A. Blomquist 1988 15 p Presented at the 10th Symposium on Thermophysical Properties, Gaithersburg, Md., 20 Jun. 1988
(Contract W-31-109-eng-38)
(DE88-011973; CONF-880606-3) Avail: NTIS HC A03/MF A01

Renewed interest in the use of metallic fuels in liquid-metal fast breeder reactors has prompted study of the thermodynamic and transport properties of its materials. Two stainless steels are of particular interest because of their good performance under irradiation. These are D9, an austenitic steel, and HT9, a ferritic steel. Thermal conductivity and thermal expansion data for these alloys are of particular interest in assessing in-reactor behavior. Because literature data were inadequate, measurements of these two properties for the two steels were performed and are reported to 1200 K. Of particular interest is the influence on these properties of a phase transition in HT9. DOE

N88-27307# Construcciones Aeronauticas S.A., Madrid (Spain). Div. de Proyectos.
STRESS CORROSION OF C RING SPECIMEN IN SALT SPRAY TESTS [ENSAYO DE TENSOCORROSION DE PROBETAS EN C (C-RING) REALIZADOS EN NIEBLA SALINA]
7 Jul. 1987 16 p In SPANISH Sponsored by the Investigacion y Desarrollo de Tecnologia y Meteriales
(I-186/87; ETN-88-92714) Avail: NTIS HC A03/MF A01

A metal component of the C-101 aircraft was tested including different thermal treatments and surface protections. The specimens were stressed to the maximum working load and sprayed with 5 percent ClNa solution at 37C till the first specimen fracture. A large corrosion strength difference due to the heat treatment is observed. The results confirm that failure in service is caused by stress corrosion and that a change in heat treatment is necessary. ESA

N88-27308# Societe Nationale Industrielle Aerospatiale, Suresnes (France).
STUDY OF SURFACE TREATMENTS BEFORE ADHESIVE BONDING OF LIGHT ALLOYS Final Report [ETUDE DES TRAITEMENTS DE SURFACE AVANT COLLAGE DES ALLIAGES LEGERS]
J. Odorico 1987 5 p In FRENCH
(Contract DRET-85-34-444)
(ETN-88-92743) Avail: NTIS HC A02/MF A01

Adhesion tests were carried out on 1.6 mm aluminum alloy plate specimens after surface treatment with sulfochromic scaling and chromic or phosphoric anodizing. Dry and wet exposures at variable lengths of time before bonding were also imposed. The results show that a hot wet (50 percent to 100 percent) exposure alters significantly the surface properties, especially in the case of phosphoric anodizing. ESA

N88-27309# Institut National des Sciences Appliquees, Lyon (France).
STUDY OF FEASIBILITY AND OPTIMIZATION CONDITIONS OF LASER TREATMENTS: APPLICATION OF THE LOCAL RECRYSTALLIZATION OF ALUMINUM Ph.D. Thesis [ETUDE DE LA FAISABILITE ET DES CONDITIONS D'OPTIMISATION DE TRAITEMENTS LASER: APPLICATION A LA RECRISTALLISATION LOCALISEE DE L'ALUMINIUM]
Jean Frederic Dietz 1987 259 p In FRENCH Sponsored by CNRS, France
(ISAL-87-0048; ETN-88-92759) Avail: NTIS HC A12/MF A01

Laser treatments are studied by a theoretical analysis of the pertinent parameters and the implementation of a model describing the interaction laser beam materials. The problem of aluminum recrystallization is examined. The results include the finding of a particular increase in the local temperature of the grain junctions, which has a consequence on the mobility of those joints and on the reactivity towards the atmosphere. The feasibility of industrial applications is suggested. ESA

N88-27310*# National Aeronautics and Space Administration. Lewis Research Center, Cleveland, Ohio.
REFRACTORY METAL ALLOYS AND COMPOSITES FOR SPACE POWER SYSTEMS
Joseph R. Stephens, Donald W. Petrasek, and Robert H. Titran 1988 31 p Presented at the Spring Meeting of the Materials Research Society, Reno, Nev., 4-9 Apr. 1988
(NASA-TM-100946; E-4237; NAS 1.15:100946) Avail: NTIS HC A03/MF A01 CSCL 11F

Space power requirements for future NASA and other U.S. missions will range from a few kilowatts to megawatts of electricity. Maximum efficiency is a key goal of any power system in order to minimize weight and size so that the space shuttle may be used a minimum number of times to put the power supply into orbit. Nuclear power has been identified as the primary source to meet these high levels of electrical demand. One way to achieve maximum efficiency is to operate the power supply, energy conversion system, and related components at relatively high temperatures. NASA Lewis Research Center has undertaken a

research program on advanced technology of refractory metal alloys and composites that will provide baseline information for space power systems in the 1900's and the 21st century. Basic research on the tensile and creep properties of fibers, matrices, and composites is discussed. Author

27 NONMETALLIC MATERIALS

Includes physical, chemical, and mechanical properties of plastics, elastomers, lubricants, polymers, textiles, adhesives, and ceramic materials.

For composite materials see *24 Composite Materials.*

N88-27311# Polytechnic Inst. of New York, Brooklyn. Polymer Research Inst.

IONIC CONDUCTIVE POLYMERS BASED ON CROSSLINKED ELASTIC SILOXANE-ETHYLENE OXIDE COPOLYMERS

H. L. Mei, Y. Okamoto, T. Skotheim, and C. S. Harris 1987 26 p Presented at the Symposium on Electroresponsive Polymers, Upton, N.Y., 4 Oct. 1987 Prepared in cooperation with Brookhaven National Lab., Upton, N.Y.

(Contract DE-AC02-76CH-00016)

(DE88-011243; BNL-41200; CONF-8710283-5) Avail: NTIS HC A03

Rubber-like elastic materials of poly(phenylsiloxane-ethylene oxide) crosslinked copolymers were synthesized and complexes with CF (sub 3)SO(sub 3)Li were made. The highest ionic conductivity was observed for the polymer/salt complex with the number of EO units n = 7 and OLi = 12. The room temperature conductivity is considerably higher than that of PEO-alkali metal salt complexes. Both Arrhenius (n = 23 and 34) and VTF (n = 3, 7, 9, and 14) type behavior for the temperature dependence of the conductivity were observed. These systems were found to be thermally stable in dry condition up to at least 225 C. DOE

N88-27312# Connecticut Univ., Storrs.

INTERFACIAL TENSION OF IMMISCIBLE POLYMER BLENDS: TEMPERATURE AND MOLECULAR WEIGHT DEPENDENCE

S. H. Anastasiadis, I. Gancarz, and J. T. Koberstein 2 Feb. 1988 41 p

(Contract DAAL03-86-K-0133)

(AD-A192463; ARO-24165.3-MS) Avail: NTIS HC A03/MF A01 CSCL 07F

Interfacial tensions between immiscible homopolymers are measured using an automated pendant drop apparatus, which utilizes Video Digital Image Processing techniques. A recently developed robust shape analysis algorithm is used to analyze the experimental drop profiles. The data show the effect of temperature and number average molecular weight (Mn) on the interfacial tension for the immiscible blends polystyrene-poly(methyl methacrylate), polybutadiene-poly(dimethyl siloxane) and polystyrene-hydrogenated 1,2 polybutadiene. Interfacial tension decreases linearly with temperature and increases with molecular weight. The data for all three systems can be approximated by an empirical relationship. The interfacial tension data for the latter blend system are compared with thermodynamic theories of polymeric interfaces. A square gradient theory approach, in conjunction with the Flory-Huggins expressions for the free energy of mixing, predicts a magnitude and temperature dependence of interfacial tension which are in reasonable agreement with experimental data, and does predict a molecular weight dependence which roughly follows the empirical relationship. GRA

N88-27313# Connecticut Univ., Storrs.

RUBBER-MODIFIED EPOXIES: INTERFACIAL TENSION AND MORPHOLOGY

J. E. Sohn, J. E. Emerson, P. A. Thompson, and J. T. Koberstein 2 Feb. 1988 20 p

(Contract DAAL03-86-K-0133)

(AD-A192464; ARO-24165.2-MS) Avail: NTIS HC A03/MF A01 CSCL 07F

The interfacial tension between carbomethoxy terminated butadiene acrylonitrile copolymers and an epoxy resin as a function of temperature and copolymer composition is investigated. Using a digital image processing technique, the shape of a pendant drop of the epoxy in the copolymer is determined. Analysis of the drop shape is performed by profile discrimination and subsequent robust shape analysis. The data are used to examine the relationship between interfacial tension and particle size of the dispersed copolymer phase in rubber-modified epoxy resins. The value of the apparent Flory-Huggins interaction parameter is estimated from the data. GRA

N88-27314# Massachusetts Univ., Amherst. Dept. of Chemistry.

SOLUBLE METAL CHELATE POLYMERS OF COORDINATION NUMBERS SIX, SEVEN AND EIGHT

Ronald D. Archer, Bing Wang, John Valentino, Annabel Y. Lee, and Ven Ochaya 1 Oct. 1987 11 p

(Contract N00014-86-K-0345)

(AD-A192485; TR-10) Avail: NTIS HC A03/MF A01 CSCL 07B

Metals coordination polymer syntheses are often plagued by insolubility, which prevents oligomers growing into polymers; however, four 6-coordinate cobalt(3) chelate polymers with acetylacetonato and leucinato ligands, a sizable number of 7-coordinate dioxouranium(6) dicarboxylate polymers, and two 8-coordinate zirconium(4) polymers with Schiff-base ligands can be prepared with degrees of polymerization which are only limited by reagent stochiometry. Chain growth of the inert cobalt(3) center is provided through ligand-centered condensation reactions of the acetylacetonato ligands with a sulfur or thionyl chloride. The problem of low ligand solubility of aromatic Schiff-bases has been side stepped by ligand synthesis during the polymerization reaction. Characterization has been accomplished primarily through infrared spectroscopy, nuclear magnetic resonance spectroscopy (both solution and solid state) and gel permeation chromatography. GRA

N88-27315# California Univ., Los Angeles. Dept. of Materials Science and Engineering.

PREPARATION AND PROPERTIES OF NEW INORGANIC GLASSES AND GEL-DERIVED SOLIDS Final Report, 1 Oct. 1983 - 30 Sep. 1987

J. D. Mackenzie Mar. 1988 31 p

(Grant AF-AFOSR-0022-84)

(AD-A192922; AFOSR-88-0409TR) Avail: NTIS HC A03/MF A01 CSCL 11B

Research has been carried out on two families of solids. This first one involves solids made by the sol-gel process and includes composites. The second one involves non-oxide glasses based on fluorides, chalcogenides and chalcohalides. The structures of oxide gels were studied by X-ray photoelectron spectroscopy, and the gelation of gels investigated as a function of temperature and catalyst. A new theory was developed on gel transformations. A number of new composites made by the sol-gel route were examined including the use of SiC and diamond powder as fillers and some triphasic solids. The viscosity and viscoelasticity of fluorozirconate glasses and glass fibers have been studied. New chalcohalide glasses were prepared and their optical properties evaluated. Structural information was derived from Raman spectra. GRA

N88-27316# Illinois Univ., Urbana. Dept. of Materials Science and Engineering.

PROCESSING AND ADDITIVE EFFECTS OF ZrO2 ON MICROSTRUCTURE AND DIELECTRIC PORPERTIES OF BaTiO3 CERAMICS Final Report No. 14, 1 Oct. 1986 - 1 Oct. 1987

T. R. Armstrong, L. M. Morgens, A. K. Maurice, and R. C. Buchanan 28 Dec. 1987 35 p

(Contract N00014-87-K-0452)

(AD-A193126) Avail: NTIS HC A03/MF A01 CSCL 20C

Dielectric properties and structure of BaTiO3 ceramics have

been shown to be significantly influenced by small additions of ZrO2. Scanning Electron Microscopy(SEM) and Transmission Electron Microscopy(TEM) observations revealed enhanced microstructural uniformity and retarded grain growth with ZrO2 addition, depending on sintering temperature (T sub S). For T sub S is less than 1320 C, TEM analysis showed ZrO2 at the grain boundaries as discrete particles in a bandwidth of + or - 50 A. Above 1320 C, diffusion of ZrO2 from the grain boundary region was observed, resulting in increased grain size and a tetragonal structure. X-ray diffraction analysis revealed a pseudo-cubic structure below 1320 C with both twinning and domain structure also suppressed. Ceramics with the pseudo-cubic structures showed a flattened dielectric constant response with temperature and significantly lower dielectric loss. GRA

N88-27317# Illinois Univ., Urbana. Dept. of Materials Science and Engineering.
PREPARATION AND PROPERTIES OF HIGH Q MICROWAVE DIELECTRICS IN THE (CA, SR, BA) ZIRCONATE SYSTEM Final Report No. 15, 1 Oct. 1986 - 1 Oct. 1987
B. P. Borglum and R. C. Buchanan 28 Dec. 1987 26 p
(Contract N00014-87-K-0452)
(AD-A193127) Avail: NTIS HC A03/MF A01 CSCL 07B

Effects of powder synthesis and processing parameters on non-stoichiometric CaZrO3 with added SrO and BaO were studied in order to optimize microstructure and microwave dielectric properties. Nitrate precursors of constituent oxides were in aqueous solutions to give the desired composition. The effect of solution pH (1-10) on powder characteristics and gel formation in the system were examined. Optimally high surface areas (31.4 sq.m./g), small particle size (0.05 microns), and uniform, dense microstructure were obtained only for the acidic (ph approx. 1) powders. Ceramic parts with uniform microstructures, high dielectric constants epsilon r = 30 - 35, and high Q (greater than 4000) were prepared from these powders. GRA

N88-27318# Purdue Univ., West Lafayette, Ind. Dept. of Physics.
CALCULATION OF FAR INFRARED ABSORPTION IN B POLY(dA).POLY(dT) Technical Report, Apr. 1981 - Mar. 1988
L. Young and Earl W. Prohofsky 10 Mar. 1988 28 p
(Contract N00014-86-K-0252)
(AD-A193128) Avail: NTIS HC A03/MF A01 CSCL 06B

We calculate the far infrared absorption of B conformation poly(dA) poly(dT), using eigenvectors from a lattice dynamical model refined with the latest inelastic neutron scattering data. Our various calculations include the isolated helix, the addition of counterions, and the addition of a 'spine of hydration' in the minor groove. We find agreement with experimental infrared data except for one mode. We then attempt to model a coupling between two helices and show some evidence that this mode is interhelical. Since our initial prediction of vibrational modes in deoxyribonucleic acid DNA in the 1-100 reciprocal centimeters frequency range, several experimental groups have used Brillouin, low frequency Raman, and infrared absorption measurements to study this region of the spectrum. Resonant rather than dissipative modes have been observed and in one case the lifetime of such a mode has been determined. In addition to this new Raman and infrared data, inelastic neutron scattering data is also now available. This neutron data is of particular interest to us as it has allowed refinement of our model of the long range nonbonded interactions in DNA. GRA

N88-27319# Naval Research Lab., Washington, D.C.
RADIATIVE HEAT TRANSFER AND SELECTIVE EMISSION IN PLANAR SLAB COATINGS ON HOT EMISSIVE SUBSTRATES Final Report, Oct. 1985 - Mar. 1987
John A. LaFemina and Harold D. Ladouceur 31 Dec. 1987 24 p
(AD-A193133; NRL-9073) Avail: NTIS HC A03/MF A01 CSCL 11C

The spectral radiance of infrared radiation emitted from a smooth planar coating in thermal contact with a hot substrate is analyzed by radiative transport theory. The solution of the radiative transfer equation, which governs the spectral radiance within the coating, is used to determine whether selective (nonblackbody) emitter coatings in infrared banded regions can be obtained in the limiting cases of optically thin or thick regimes. For the reader not interested in the mathematical details of this report, the key conclusions are given following Eq. (22). The results are presented in a summary that shows how varying the optical thickness of the coating, the coating material, and the substrate parameters affect the emitted radiation. GRA

N88-27320# Royal Institution of Great Britain, London.
ENERGY MIGRATION, MOTION AND ORDER IN SYNTHETIC POLYMERS Periodic Report No. 2, Jun. - Dec. 1987
David Phillips Dec. 1987 13 p
(Contract DAJA45-87-C-0031)
(AD-A193334) Avail: NTIS HC A03/MF A01 CSCL 07C

The initial phase of this work has been concerned exclusively with the luminescence of poly(diacetylenes), so-called one-dimensional polymers. The chemical structures of some commonly met conjugated polymers are given in Table 1. Of these, PDA's are virtually unique in that they are obtainable as single crystals, and have been selected for study here. The materials studied are the BCMU family, of structure indicated in Table 2. In discussing the chromism of Poly Diacetylenes PDA's it is important first to note there are fewer fluorescing forms than absorbing ones. This is because the R form consists of lone sections of continuously conjugated backbone - be it LCS, wormlike or rigid rods (Figure 4). These forms, as in infinitely conjugated crystals, have a very efficient non-radiative pathway which reduces the quantum yield on transition from Y to R forms. In 4BCMU the red-shifted forms do fluoresce although the quantum yield decreases with decreasing Xc. The presence of an isosbestic point is an important feature of PDA chromism which indicates a phase transition of the polymer without formation of stable, optically detectable, intermediates. GRA

N88-27321# Massachusetts Inst. of Tech., Cambridge. Dept. of Chemical Engineering.
SPATIAL ORGANIZATION OF HOMOPOLYMER CHAINS INSIDE SPHERICAL POLYBUTADIENE DOMAINS OF SB DIBLOCK COPOLYMERS
P. Cheng, C. V. Berney, and R. E. Cohen 16 Mar. 1988 29 p
(Contract N00014-87-K-0517)
(AD-A193390; TR-3) Avail: NTIS HC A03/MF A01 CSCL 07F

Blends of perdeuterated polybutadiene homopolymer and a polystyrene-polybutadiene diblock copolymer were prepared by solution casting techniques. Small angle neutron scattering and transmission electron microscopy experiments on blends containing homopolymer with chain length smaller than the corresponding block sequence showed that homopolymer chains are solubilized by the spherical microdomains up to a homopolymer content of about 15 mole percent. The solubilized homopolymer is distributed in a spatially uniform manner throughout the domain volume and the homopolymer radius of gyration is only slightly larger than that of an unperturbed chain in bulk. At about 18 mole percent pools, of homopolymer appear outside the microdomains; the change in scattering intensities indicate that pool formation is a kinetic phenomenon rather than a thermodynamically controlled event. Experiments on blends containing longer homopolymer chains revealed a lower concentration, between 3 and 6 mole percent, for the onset of homopolymer pool formation. GRA

N88-27322# IIT Research Inst., Bartlesville, Okla. National Inst. for Petroleum and Energy Research.
OPTIMAL RHEOLOGICAL CHARACTERISTICS IN DYNAMIC STABILITY OF POLYMER FLOW THROUGH POROUS MEDIA
H. W. Gao and T. R. French Apr. 1988 28 p
(Contract DE-FC22-83FE-60149)
(DE88-001225; NIPER-303) Avail: NTIS HC A03/MF A01

To identify the optimal rheological characteristics for maintaining the dynamic stability of polymer solutions flowing

through porous media, displacement tests with a Newtonian fluid and a non-Newtonian fluid were performed in a 4-ft Berea sandstone core. A solution of 63 wt pct gylcerin in 53 meg/1 NaCl and a solution of 1500 ppM Pusher 500 in 53 meq/1 NaCl were used as the Newtonian fluid and non-Newtonian fluid, respectively. Two flow rates, one in the purely viscous regime and one in the viscoelastic flow regime of Pusher 500 in Berea sandstone, were used in the displacement tests. The effluents collected were analyzed to determine polymer and tracer concentrations. The viscosities of the effluents were also measured with a Contraves viscometer. By comparing the concentration profiles obtained in tests with Pusher 500 and in those with gylcerin, the effects of flow rate, mobility ratio, and rheological characteristics on the dynamic stability of polymer flow in porous media were determined. At both leading and trailing edges of the polymer slug, stability increases with decreasing mobility ratio. At both high and low flow rates, a Newtonian fluid gives a more stable displacement at the fluid front than does a non-Newtonian fluid. DOE

N88-27323# Oak Ridge National Lab., Tenn.
CERAMIC TECHNOLOGY FOR ADVANCED HEAT ENGINES PROJECT Semiannual Progress Report, Apr. - Sep. 1987
Mar. 1988 443 p
(Contract DE-AC05-84OR-21400)
(DE88-008945; ORNL/TM-10705) Avail: NTIS HC A19/MF A01

Significant accomplishments in fabricating ceramic components for DOE, NASA, and DOD advanced heat engine programs have provided evidence that the operation of ceramic parts in high-temperature engine environments is feasible. However, these programs have also demonstrated that additional research is needed in materials and processing development, design methodology, and data base and life prediction before industry will have a sufficient technology base from which to produce reliable cost-effective ceramic engine components commercially. An assessment of needs was completed, and a 5-year project plan was developed with extensive input from private industry. The objective is to develop the industrial technology base required for reliable ceramics for application in advanced automotive heat engines. The project approach includes determining the mechanisms controlling reliability, improving processes for fabricating existing ceramics, developing new materials with increased reliability, and testing these materials in simulated engine environments to confirm reliability. Although this is a generic materials project, the focus is on the structural ceramics for advanced gas turbine and diesel engines, ceramic bearings and attachments, and ceramic coatings for thermal barrier and wear applications in these engines. This advanced materials technology is being developed in parallel and close coordination with the ongoing DOE and industry proof-of-concept engine development programs. DOE

N88-27324# Battelle Columbus Labs., Ohio.
STUDIES OF DYNAMIC CONTACT OF CERAMICS AND ALLOYS FOR ADVANCED HEAT ENGINES Final Report
K. F. Dufrane, W. A. Glaeser, and A. R. Rosenfield Mar. 1988 95 p
(Contract DE-AC05-84OR-21400)
(DE88-008996; ORNL/Sub-84-00216/1) Avail: NTIS HC A06/MF A01

In support of the efforts to apply ceramics in advanced heat engines, a study was made of the sliding performance of ceramics at the ring/cylinder interface of low heat rejection engines. The objective was to understand the basic mechanisms controlling the wear of candidate ceramics and thereby identify means for applying these ceramics effectively. Attempts to operate three different zirconias, silicon carbide, silicon nitride, and several plasma-sprayed ceramic coatings without lubrication were unsuccessful because of high friction and high wear rates. Experiments using a polyalphaolefin lubricant at temperatures to 260 C identified several combinations having wear rates in the general range likely to be acceptable for engines. Plasma-sprayed coatings of chromium oxide and hypersonic powder flame sprayed coatings of cobalt-bonded tungsten carbide performed particularly well as ring coatings. Similar performance was obtained with these ring coatings operating against silicon carbide, silicon nitride, silicon carbide whisker-reinforced alumina, and chromium oxide coatings. Zirconia experience high wear rates because of thermal-shock induced surface cracking. Low thermal conductivity of zirconia allows local areas to heat excessively from friction. Periodic heating induces thermal shock cracking and subsequent spalling. The study demonstrated the importance of lubrication to successful sliding of ceramics and the need for lubricants capable of operating at temperatures in the range of 250 to 650 C. DOE

N88-27325# California Univ., Berkeley. Lawrence Berkeley Lab.
EFFECTS OF NEAR INTERFACIAL MICROSTRUCTURE ON TOUGHNESS AND SUBCRITICAL CRACK GROWTH IN CERAMIC/METAL SYSTEMS
T. S. Oh, R. M. Cannon, J. Rodel, A. M. Glaeser, and R. O. Ritchie Feb. 1988 17 p Presented at the International Conference on Composite Interfaces, Cleveland, Ohio, 13 Jun. 1988
(Contract DE-AC03-76SF-00098)
(DE88-009842; LBL-24799; CONF-880671-2) Avail: NTIS HC A03/MF A01

Methods to toughen ceramic/metal interfaces that employ prescribed arrays of non-coplanar microcrack-like-voids and inclined interface steps are assessed. These features, developed in glasscopper samples made using photolithographic, metal deposition and diffusion bonding processes, promote crack-tip shielding principally from crack bridging by ligaments generated by plastic void growth within the copper. The ensuing plastic stretching, and sometimes tearing, of the Cu film ligaments yield the major energy dissipation. Crack deflection can also provide a smaller toughening contribution. Resistance-curve (R-curve) behavior obtains from the bridging, with fracture energies rising to an asymptote that varies from 9 to 160 J/sq m, compared with inherent toughness values of approximately 2 J/sq m for specific glass/Cu interfaces used. The arrays retard subcritical crack-growth rates, which are higher in moist atmospheres, by orders of magnitude compared to rates for plain interfaces. The behavior is contrasted with that gained by using better interface chemistry to increase the inherent fracture toughness of glass/Cu bonds. DOE

N88-27326# California Univ., Berkeley. Lawrence Berkeley Lab.
APPLICATION OF CONTROLLED INTERFACIAL PORE STRUCTURES TO KINETIC STUDIES IN ALUMINA
J. Roedel and A. M. Glaeser Apr. 1988 8 p Presented at the Interfacial Structure, Properties and Designs in Solids, Reno, Nev., 5 Apr. 1988
(Contract DE-AC03-76SF-00098)
(DE88-010884; LBL-25010; CONF-8804112-4; CONF-8804112) Avail: NTIS HC A02/MF A01

The application of controlled-geometry interfacial pore structures to fundamental kinetic studies in alumina is described. Results from studies of the morphological stability of high aspect ratio pore channels, crack healing, pore coarsening and pore elimination in sapphire are presented. DOE

N88-27327# Sandia National Labs., Albuquerque, N. Mex.
REFRACTORY FILMS FROM SPIN-CAST CARBON
C. L. Renschler and A. P. Sylwester 1988 10 p Presented at the International Conference on Science and Technology of Synthetic Metals, Santa Fe, N. Mex., 26 Jun. 1988
(Contract DE-AC04-76DP-00789)
(DE88-011251; SAND-88-1453C; CONF-880669-1) Avail: NTIS HC A02/MF A01

A method is described to produce thin films of carbon by the pyrolysis of spin-cast polyacrylonitrile. UV, IR, and Raman spectroscopies were employed to investigate the chemical structure of the films during pyrolysis. The electrical conductivity of films

made in this way can be varied over several decades by changing the final temperature of carbonization. These films can also be photolithographically patterned and manipulated by wet and dry transfer techniques. As such, these films may have utility in microelectronic and hybrid microcircuit applications. DOE

N88-27328# Sandia National Labs., Albuquerque, N. Mex.
PRECURSOR CHEMISTRY AND THE STRUCTURE OF SILICA AEROGELS
D. W. Schaefer, C. J. Brinker, J. P. Wilcoxon, D. Q. Wu, J. Phillips, and B. Chu 1988 5 p Presented at the Spring Meeting of the Materials Research Society, Reno, Nev., 4 Apr. 1988 Prepared in cooperation with State Univ. of New York, Stony Brook
(Contract DE-AC04-76DP-00789)
(DE88-011253; SAND-88-1213C; CONF-880408-25) Avail: NTIS HC A02/MF A01

Small-angle X-ray scattering is used to characterize the structure of aerogels prepared by two-stage polymerization processes. Second-stage catalysis controls the resistance to collapse during drying with the base-catalyzed system being most resistant. We find the origin of this resistance in the solution precursor chemistry. Base catalysis in the second stage leads to compaction of the polymer network on short length scales. This short-scale rigidity makes the networks sufficiently robust to withstand the surface tension forces present during drying. Aging in solution also improves aerogel quality. In this case, a dissolution-repolymerization process leads to short length scale circuits and improved rigidity. DOE

N88-27329# Japan Atomic Energy Research Inst., Tokyo.
DATA COMPILATION FOR RADIATION DAMAGE ON CERAMIC INSULATORS. REVISED WITH UPDATED DATA AND REVIEWS
Koji Fukuya, Mititaka Terasawa, and Kunio Ozawa Jan. 1988 181 p
(DE88-753426; JAERI-M-87-217) Avail: NTIS (US Sales Only) HC A09/MF A01

Data of radiation effects on ceramic insulators were compiled from the literatures and summarized from the viewpoint of fast neutron irradiation effects. The data were classified according to the properties of ceramics. The properties are dimensional stability, mechanical property, thermal property and electrical and dielectric properties. The data sheets for each table or graph in the literatures were made. The characteristic feature of the data base was briefly described. As to swelling, the data were complied according to the dose dependence and the temperature dependence for each ceramic and reviewed briefly. DOE

N88-27330# Minas Gerais Univ., Belo Horizonte (Brazil). Escola de Engenharia.
KINETIC OF OXIDATION TO AIR OF A Fe-Al-Mn ALLOY SYSTEM AT 600-800(SUP 0)C TEMPERATURE RANGE M.S. Thesis
V. F. C. Lins 1987 106 p In PORTUGUESE; ENGLISH summary
(DE88-702309; INIS-BR-1045) Avail: NTIS (US Sales Only) HC A06/MF A01

The Fe-Mn-Al-Si alloy, with 0.6 percent carbon content, was studied under oxidation to air conditions, at 600 to 800 C temperature range. The results of the continuous thermogravimetric tests indicate that, at 600 C, the oxidation can be described by logarithmic kinetics. For temperatures from 650 to 800 C, a parabolic kinetic behavior was obtained for the Fe-Mn-Al alloy. Using X-ray diffraction, austenite was initially observed and after oxidation, besides austenite, the presence of ferrite was detected, which is the only evidence of a possible decomposition of the matrix phase. The (Mn,Fe)2 O3 oxide was found as one of the components of the oxidized layer, using X-ray diffraction. Regions rich in aluminum, manganese and silicon in the oxide film, were observed by scanning electron microscopy. A good resistance to oxidation was obtained at 600 to 700 C temperature range. DOE

N88-27331# Mississippi Univ., University. Dept. of Mechanical Engineering.
DETERMINATION OF RADIATIVE PROPERTIES OF FIBERGLASS AND FOAM INSULATIONS
S. Yajnik and J. A. Roux Dec. 1987 179 p
(Contract DE-AC05-84OR-21400)
(DE88-007845; ORNL/Sub-86-55930/1) Avail: NTIS HC A09/MF A01

The spectral radiative properties of 1450(b) high density fiberglass, 1451 low density fiberglass, and expanded polystyrene were inverted from monochromatic directional-hemispherical reflectance and hemispherical-directional reflectance data coupled with an analytical model in the wavelength range of 4 to 40 microns. A set of ten samples were prepared for each of the three insulation materials. The Willey 318S Fourier transform spectrometer (DTS) was utilized to measure the directional-hemispherical reflectance data in the wavelength range of 2-20 microns for the three sample sets. The hemispherical, directional reflectance data for the two fiberglass samples sets were obtained with a hemiellipsoidal reflectometer in the wavelength range of 4-40 microns. From the directional, hemispherical reflectance data, the spectral absorption and scattering coefficients were inverted for the three test insulations using the non-linear least squares approach coupled with Chandrasekhar's discrete ordinates solution of the radiative transport equation. These radiative properties together with the true thermal conductivity values for fiberglass and foam insulations were used to compute typical heat transfer results which were then compared to experimental data where available. An optimization analysis was conducted for the fiberglass insulations to determine the bulk density at which the steady-state heat transfer through the fiberglass layer insulation was a minimum. DOE

N88-27332# California Univ., Berkeley. Lawrence Berkeley Lab.
IMPROVED ADHESION FOR SiO2 PARTICLES IN SILICA SUBSTRATES USING HELIUM-ION IRRADIATION
R. G. Musket and I. M. Thomas Mar. 1988 6 p Presented at the Spring Meeting of the Materials Research Society, Reno, Nev., 4 Apr. 1988
(Contract W-7405-eng-48)
(DE88-008915; UCRL-97598; CONF-880408-14) Avail: NTIS HC A02/MF A01

The effects of irradiation with 200-keV helium ions on the adhesion and optical transmission properties of 220 nm thick antireflective, optical coatings consisting of layers of spherical, 20 nm diameter silica particles have been examined. In the as-deposited state these sol-gel coatings have very low adhesion to the fused silica subtrates. Results for adhesion and optical transmission have been obtained for doses of 10 to the 13th to 10 to the 17thHe/sq cm. Significant improvement in adhesion was found for doses exceeding about 2 x 10 to the 14th He/sq cm. Optical transmission measurements for wavelengths of 200 to 1200 nm showed increasing absorption with dose. We have evidence that the helium ions decompose various contaminants in the coating into two types of degradation products. One is volatile and the other remains in the coating as optically absorbing species. UV/oxidative-gas treatment effectively removes the absorbing species. DOE

N88-27333# Sandia National Labs., Albuquerque, N. Mex.
ADHESION OF HYDRATED SILICATE FILMS
T. A. Michalske and K. D. Keefer 1988 11 p Presented at the Spring Meeting of the Materials Research Society, Reno, Nev., 4 Apr. 1988
(Contract DE-AC04-76DP-00789)
(DE88-011250; SAND-88-1131C; CONF-880408-24) Avail: NTIS HC A03/MF A01

We used fracture mechanics test techniques to measure the adhesive bond energy formed between hydrated silica glass surfaces and silicate species deposited from solution. In the case of silicate surfaces hydrated in room temperature water vapor, intermolecular bonding between hydrated surfaces can be attributed to either hydrogen bonding interactions between adsorbed water

molecules (0.15 J sq m) or electrostatic bonds formed between adsorbed cations and anionic-nonbridging surface oxygen groups (2.0 J sq m). The bonding interaction observed at room temperature depends upon the glass surface composition and the degree of surface hydration. When hydrated silicate solution species are added to the interface and heat treated, adhesion energies as large as the cohesive energy of silica glass can be obtained with heat treatments as low as 200 C. The adhesion of the silicate interfacial film produced by the addition of solution species is greatest for silicate precursors showing a low degree of molecular crosslinking. In addition, the presence of alkali in the silicate solution greatly enhances interface adhesion for heat treatments below 200 C. DOE

N88-27334# Sandia National Labs., Albuquerque, N. Mex.
PLASMA TREATMENT OF POLYMERS FOR IMPROVED ADHESION
J. A. Kelber 1988 12 p Presented at the Spring Meeting of the Materials Research Society, Reno, Nev., 4 Apr. 1988
(Contract DE-AC04-76DP-00789)
(DE88-011623; SAND-87-2508C; CONF-880408-27) Avail: NTIS HC A03/MF A01

A variety of plasma treatments of polymer surfaces for improved adhesion are reviewed: noble and reactive gas treatment of fluoropolymers; noble and reactive treatment of polyolefins, and plasma-induced amination of polymer fibers. The plasma induced surface chemical and morphological changes are discussed, as are the mechanisms of adhesion to polymeric adhesives, particularly epoxy. Noble gas plasma etching of flouropolymers produces a partially defluorinated, textured surface. The mechanical interlocking of this textured surface is the primary cause of improved adhesion to epoxy. Reactive gas plasmas also induce defluorination, but oxygen containing gases cause continual ablation of the fluoropolymer surface. Noble and reactive gas (except for hydrogen) etching of polyolefins results in surface oxidation and improved adhesion via hydrogen bonding of these oxygen containing groups across the interface. The introduction of amine groups to a polymer surface by amonia or amine plasma treatment generally results in improved adhesion to epoxy. However, amine-epoxy ring interactions can be severely effected by steric factors due to chemical groups surrounding the amine. DOE

N88-27335# Sandia National Labs., Albuquerque, N. Mex.
ELLIPSOMETRIC IMAGING OF DRYING SOL-GEL FILMS
A. J. Hurd and C. J. Brinker 1988 13 p Presented at the Spring Meeting of the Materials Research Society, Reno, Nev., 4 Apr. 1988
(Contract DE-AC04-76DP-00789)
(DE88-011785; SAND-88-1330C; CONF-880408-28) Avail: NTIS HC A03/MF A01

Although controlled dip-coating is an established way to apply high quality uniform coatings, the details of the coating and drying process have not been deeply studied. Depending on the physical and chemical state of the sol and the parameters of dipping (dipping angle and speed), a variety of thicknesses and porosities can be achieved. For optical coatings, the refractive index and optical thickness can thereby be controlled. The authors have developed a method to view the drying front of a dip-coated film using broad beam ellipsometry, or ellipsometric imaging. In dip-coated films we take full advantage of the fact that a steady state is quickly reached where the drying line velocity matches the withdrawal velocity; however, the technique might also be used in unsteady situations such as spin coating. Imaging ellipsometry makes it possible to measure the refractive index and thickness profiles of both wet and dry films point-by-point in an entire image at once. These profiles provide important clues as to the relative importance of gravity, evaporation and other phenomena. DOE

N88-27336*# National Aeronautics and Space Administration, Washington, D.C.
UNIFIED METHODS OF ACCELERATED LABORATORY TESTS OF THE PREPARATIONS FOR TEMPORARY PROTECTION OF CARS
Jerzy Iwanow and Olga Wojcieszek Jun. 1988 23 p Transl. into ENGLISH from Zunifikowana Metodyka Przyspieszonich Adan Laboratoryjnych Srodkow Ochrony Czasowej Samochodow, Ochronne (Poland), v. 14, no. 5, 1986 p 19-27 Transl. by SCITRAN, Inc., Santa Barbara, Calif.
(Contract NASw-4307)
(NASA-TT-20298; NAS 1.77:20298) Avail: NTIS HC A03/MF A01

The effectiveness of the anticorrosion protection of cars depends to a large degree on the quality of the preliminary protection preparations (SOC) applied for this purpose. In the period 1979 to 1985, the Institute of Precision Mechanics, within the cooperative CMEA framework, initiated and elaborated the project, Unified methods of accelerated laboratory tests of SOC used for cars. The outcome is a collection of basic requirements pertaining to anticorrosion properties and technological features of SOC intended for protection of enclosed components of the car body and of the underside of the chassis. Particular requirements are based on methods described in CMEA standards and RS (Recommended Standards), and also in other standardization documents (ISO, FIAT standards, etc.). CMEA experts, participating in these studies, consider these standards to be optimal for the evaluation of specific properties. Author

N88-27337# Ecole Superieure de Physique et de Chimie Industrielles, Paris (France). Lab. de Physiochimie Structurale et Macromoleculaire.
STUDY OF CROSSLINKING AND NONELASTIC MECHANICAL PROPERTIES OF EPOXY AND PSP NETWORKS Final Report [ETUDE DE LA RETICULATION ET DES PROPRIETES MECANIQUES NON ELASTIQUES DE QUELQUES RESEAUX EPOXY ET PSP]
L. Monnerie, F. Laupretre, and B. Jasse 1988 80 p In FRENCH
(Contract DRET-84-168)
(ETN-88-92740) Avail: NTIS HC A05/MF A01

Crosslinking kinetics is studied using infrared spectroscopy/Fourier transformation and solid state high resolution C13 nuclear magnetic resonance. The choice of catalyst leads to shorter or longer chains and high or low density of crosslinking in PSP resins. No secondary reactions are observed in the polymerization of epoxies with mono and diamines. The kinetics of the gel time is governed by the diamine, while the vitrification is controlled by the monoamine are discussed. ESA

N88-27338# Paris VI Univ. (France). Lab. de Spectrochimie du Solide.
APPLICATION OF SOL-GEL PROCEDURES TO CERAMIC COMPOSITES [APPLICATIONS DES PROCEDES SOL-GEL AUX COMPOSITES CERAMIQUES]
Laure Coury Oct. 1987 68 p In FRENCH
(Contract DRET-85-112)
(ETN-88-92741) Avail: NTIS HC A04/MF A01

Colloidal solutions were synthesized and characterized in order to contribute to the development of ceramics based on aluminum phosphate, lithium silico-aluminate, and magnesium silico-aluminate. The surface deposits on carbon-carbon and carbon-SiC composites were also investigated. The study of the solid phases was carried out with the help of thermal differential analysis, X-ray diffraction, scanning electron microscopy, and infrared techniques. In the case of aluminum phosphate, water solutions give the best results to obtain a single phase system at 950 C. The best deposits on composites are obtained from organic solutions. Magnesium silico-aluminates are possible at 1000 C in an impure form. ESA

N88-27339# Societe Nationale Industrielle Aerospatiale, Suresnes (France). Direction Centrale de la Qualite.
REFRACTORY FIBERS SURFACE TREATMENT Final Report [TRAITEMENT DE SURFACE DE FIBRES REFRACTAIRES. PROCES-VERBAL 47-803/F]
J. Odorico and P. Renard 9 Oct. 1987 55 p In FRENCH
(Contract DRET-84-34-584-00-470-75-01)
(Rept-47-803/F; ETN-88-92744) Avail: NTIS HC A04/MF A01

Surface deposits on refractory fibers were obtained by magnetron RF cathodic spraying. The coatings included Al2O3, Y2O3, ZrO2 stabilized with CaO, Nb2O5 and Nb. A device to coat continuously a line of fibers 10 m long was developed. A preliminary encouraging test is the effective coating of a carbon fiber of 10,000 filaments 10 m long with a 5000 A Nb2O5 coat. ESA

N88-27340# Ecole Nationale Superieure des Mines, Sainte-Etienne (France). Dept. Materiaux.
PREPARATION AND CHARACTERIZATION OF CERAMIC MATERIALS BASED ON Al2O3 REINFORCED WITH A ZrO2 DISPERSION Ph.D. Thesis - Inst. Nationale des Sciences Appliquees [PREPARATION ET CARACTERISATION DE MATERIAUX CERAMIQUES A BASE D'ALUMINE RENFORCES PAR UNE DISPERSION DE ZIRCONE]
Pierre Homerin 1987 187 p In FRENCH
(ISAL-87-0041; ETN-88-92758) Avail: NTIS HC A09/MF A01

The manufacturing parameters of ceramics prepared with the inclusion of ZrO2 dispersion were studied in order to optimize the resulting mechanical properties. A theoretical analysis of the reinforcement due to the ZrO2 is included. The experimental manufacturing procedures are described. Special attention is payed to optimizing the microstructure. Ceramic materials with outstanding thermomechanical properties are obtained, crack propagation characteristics in particular. Manufacturing methods including solutions of organic Zr compounds were also explored. ESA

N88-27341# Societe Nationale Industrielle Aerospatiale, Saint-Medard-en-Jalles (France). Div. Systemes Strategiques et Spatiaux.
REINFORCED PLASTICS: WINDING AND WEAVING TECHNOLOGIES FOR SPACE PRODUCTS
J. Bouvard 1988 12 p In FRENCH
(SNIAS-881-430-103; ETN-88-92851) Avail: NTIS HC A03/MF A01

Multidirectional weaving and filament winding techniques are described and application examples to space structures are presented, including the Ariane 5 booster model, sandwich structures for several spacecraft, solar panel structures, helium containers, pipes, and inserts. It is shown that the space applications of these techniques are growing very fast due to definite weight saving advantages. ESA

N88-27342# Societe Nationale Industrielle Aerospatiale, Saint-Medard-en-Jalles (France).
COMPARISON OF SOL-GEL PROCEDURES FOR ZIRCON AND ALUMINA [COMPARAISON ENTRE LES PROCEDES SOL-GEL DE LA ZIRCONE ET DE L'ALUMINE]
A. C. Pierre 1988 9 p In FRENCH
(SNIAS-881-430-108; ETN-88-92856) Avail: NTIS HC A02/MF A01

Zirconium and aluminum oxide sol-gel procedures are reviewed. Published results are presented, including both the physical and chemical aspects of the procedures. The differences in zircon and alumina behavior are explained. It is concluded that for both, the gelification mechanisms are well understood. ESA

N88-27343# Societe Nationale Industrielle Aerospatiale, Saint-Medard-en-Jalles (France).
MICROWAVE POLYMERIZATION OF COMPOSITE STRUCTURES [POLYMERISATION DE STRUCTURES COMPOSITES PAR MICRO-ONDES]
J. L. Miane, B. Prache, and D. Beziers 1988 8 p In FRENCH
Presented at the Journee d'Etudes: Applications Energetiques des Micro-Ondes, Paris, France, 19-22 Oct. 1987
(SNIAS-881-430-116; ETN-88-92864) Avail: NTIS HC A02/MF A01

The microwave energy absorption of epoxy resin/glass fiber or epoxy resin/carbon fiber systems was studied using an experimental volume limited by metallic walls and excited by an antenna waveguide including up to 10 antennas spaced at half wavelength. It is shown that to maintain optimum coupling during the polymerization, the coupling to the microwave system must be adjusted in consequence. The modification of the field distribution inside the volume is also discussed. ESA

N88-27344# Societe Nationale Industrielle Aerospatiale, Saint-Medard-en-Jalles (France). Lab. Materiaux et Procedes Nouveaux.
INJECTION COMPRESSION FOR SHORT FIBER REINFORCED PLASTICS [INJECTION COMPRESSION DES THERMOPLASTIQUES ARMES]
Jean Marc SainteLuceBanchelin 1988 9 p In FRENCH; In FRENCH; ENGLISH summary
(SNIAS-881-430-118; ETN-88-92866) Avail: NTIS HC A02/MF A01

The use of cut pre-impregnated roving and the injection compression traditionally used for thermoset moldings (bulk molding compound) is discussed. The interest of this process is the reduction of the injection pressure and the preservation of fiber length. The fiber weight ratios obtained are up to 50 percent. ESA

N88-27345# Deutsche Forschungs- und Versuchsanstalt fuer Luft- und Raumfahrt, Brunswick (West Germany). Abteilung Verbundstrukturen.
AGING OF CFRP DUE TO LONGTERM STORAGE IN HEATED AIR
Harald Twardy Dec. 1987 31 p In GERMAN; ENGLISH summary Report will also be announced as translation (ESA-TT-1124)
(DFVLR-FB-88-05; ISSN-0171-1342; ETN-88-92923) Avail: NTIS HC A03/MF A01; DFVLR, VB-PL-DO, 90 60 58, 5000 Cologne, Federal Republic of Germany, 15.50 deutsche marks

Thermal degradation of seven carbon fiber reinforced plastic (CFRP) materials exposed to heated air between 100 and 150 C for many years was studied. Continuous measurement of weight loss gave a criterion of the degree of irreversible degradation. Measurement of strength loss gave an impression how much this is influenced by a long-term aging process. ESA

28 PROPELLANTS AND FUELS

Includes rocket propellants, igniters, and oxidizers; their storage and handling procedures; and aircraft fuels.

For related information see also *07 Aircraft Propulsion and Power, 20 Spacecraft Propulsion and Power,* and *44 Energy Production and Conversion.*

N88-27346# Battelle Columbus Labs., Ohio.
HYDROCARBON FUEL SPILL DISPERSION ON WATER: LITERATURE REVIEW Interim Report, May - Sep. 1986
S. A. Edgerton and R. W. Coutant Dec. 1987 96 p
(Contract F08635-85-C-0122)
(AD-A192486; AFESC/ESL-TR-86-64) Avail: NTIS HC A05/MF A01 CSCL 21D

The literature concerning the fate of light hydrocarbon fuel spills on water is reviewed. The review focuses on jet fuels and contains some discussion of gasoline, diesel, marine, and kerosene fuel spills. The two major fates of light hydrocarbon spill on water are evaporation and dissolution, although biodegradation, photooxidation, and adsorption onto suspended sediments can also be of some importance. GRA

N88-27347# Southwest Research Inst., San Antonio, Tex. Fuels and Lubricants Research Facility.
A STUDY RELATING TO THE FOG OIL REPLACEMENT PROGRAM Interim Report
William W. Wimer, Bernard R. Wright, and Mike D. Kanakia Dec. 1987 41 p
(Contracts DAAK70-87-C-0043; DAAK70-85-C-0007; DA Proj. 1L7-62733-AH-20)
(AD-A192536; BFLRF-241) Avail: NTIS HC A03/MF A01 CSCL 21D

The U.S. Army has made a commitment to replace smoke generator fog oil with diesel fuel and/or JP-8. This report discusses the work done to help solve this existing fog oil substitution problem. Areas of research included: (1) modification of diesel fuel and JP-8 by removal of their lower boiling fractions; (2) design, construction, and development of a bench test for measuring obscuration; (3) running a computer-simulation program to assist in evaluating the engineering feasibility of designing, developing, and constructing a compact unit capable of fractionating diesel fuel and/or JP-8 should this be desired; (4) conducting a literature search to identify methods and/or compact equipment capable of fractionating diesel fuel and JP-8 to higher average molecular weight fractions. (5) production of test samples; and (6) chemical analyses and obscurant evaluations. GRA

N88-27348# Cambridge Univ. (England).
DEFORMATION, FRACTURE AND EXPLOSIVE PROPERTIES OF REACTIVE MATERIALS Interim Report, 1 Nov. 1985 - 31 May 1987
J. E. Field 31 May 1987 18 p
(Contract DAJA45-85-C-0052)
(AD-A193080) Avail: NTIS HC A03/MF A01 CSCL 19A

A range of techniques has been developed over the years for studies of the behavior of explosives when impacted and for recording their strength, failure and ignition properties. They include a drop-weight facility with transparent anvils, an instrumented drop-weight machine, a miniaturized Hopkinson bar system for high rate of strain property measurement, laser speckle for studies of deformation and fracture of PBXs, an automated system for analyzing speckle and moire records, and a heat sensitive film technique for recording the positions and temperatures of hot spots. With HMX, studies were made with samples of five different particle sizes. The coarser material gave a more violent response (i.e. had a greater explosiveness). Two important factors which influence this are: (1) the compacted structure of the impacted samples which, with the coarser material, leaves more channels (porosity) for deflagration; and (2) the greater thermal conductivity (by a factor of 2x) of compacted coarse grain material. A paper is in preparation. GRA

N88-27349# Sandia National Labs., Albuquerque, N. Mex.
A CONCEPT FOR AN ELECTRO-OPTIC EXPLOSIVE DEVICE
D. A. Benson and B. H. Rose 1988 20 p Presented at the 13th International Pyrotechnics Seminar, Grand Junction, Colo., 11 Jul. 1988
(Contract DE-AC04-76DP-00789)
(DE88-009696; SAND-87-3069C; CONF-880750-6) Avail: NTIS HC A03/MF A01

Enhancement of the safety and security of explosive devices by solely using fiber optic links to the device has been a development objective in both commercial and military applications. Much effort has centered on the direct ignition of explosive materials by light from an optical fiber. While such devices are beginning to emerge, the need to use high optical power levels and sensitive explosives has limited the approach. We have explored an indirect, but simple approach to operating an optically coupled detonator/igniter. This method is made possible by recent developments in low voltage explosive igniters combined with microcircuit series-connected photovoltaic arrays. They allow one to convert light from an optical fiber to electrical energy stored in a small capacitor and to trigger its discharge, all locally within the device to produce a precisely timed explosive ignition and subsequent detonation. This produces a component of about the same size as existing devices, which is highly resistant to electromagnetic disturbances and driven by a diode laser through an optical fiber. The method functions with a wide range of insensitive secondary explosives and pyrotechnics. DOE

N88-27350# Mound Lab., Miamisburg, Ohio.
RELATIVE FLOW RATES OF EXPLOSIVE POWDERS
V. P. Willson 31 May 1988 14 p
(Contract DE-AC04-76DP-00053)
(DE88-010767; MLM-3505) Avail: NTIS HC A03/MF A01

A study was performed to determine the relative flow rates of various explosive powders and evaluate their adaptability for use in automated dispensing systems. Results showed that PBX 9407, LX-15, RX-26-BH, and HNAB are potential candidates for use in these systems. It was also shown that powders with graphite and stearate additives generated the least amount of static and were the easiest to handle. DOE

N88-27351# Lawrence Livermore National Lab., Calif.
SHOCK INITIATION STUDIES ON HETEROGENEOUS EXPLOSIVES
R. L. Simpson, F. H. Helm, P. C. Crawford, and J. W. Kury 29 Mar. 1988 11 p Presented at the 19th International ICT Conference on Combustion and Detonation, Karlsruhe, Fed. Republic of Germany, 29 Jun. 1988
(Contract W-7405-eng-48)
(DE88-008681; UCRL-97787; CONF-880693-2) Avail: NTIS HC A03/MF A01

A set of laboratory experiments and a modeling analysis to determine and characterize the shock initiation behavior of high explosives are described. The experimental techniques include modified wedge tests, in situ magnanin pressure gauge measurements, and multichannel visible radiometry on explosive samples shock loaded with an electric gun. A description of the experimental methodologies and limitations is made examining the effect of particle size in the shock initiation of HMX/water mixtures. The theoretical analysis is based on reactive flow hydrodynamic calculations using a three term ignition and growth model. Author

N88-27352# Sandia National Labs., Albuquerque, N. Mex.
DIODE LASER IGNITION OF HIGH EXPLOSIVES AND PYROTECHNICS
Stephanie C. Kunz and F. Jim Salas 1988 19 p Presented at the 13th International Pyrotechnics Seminar, Grand Junction, Colo., 11 Jul. 1988
(Contract DE-AC04-76DP-00789)
(DE88-008771; SAND-87-3032C; CONF-880750-4) Avail: NTIS HC A03/MF A01

Thermal ignition of the explosive CP (2-(5-cyanotetrazolato)pentaamine cobalt (III) perchlorate) and of the pyrotechnic Ti/KClO4 has been achieved using a (GaAl)As diode laser that emitted 1 watt of optical power from the end of a 100 microns core fiber optic to which it was coupled. The wavelength of the emitted light was near 820 nm. Approximate ignition thresholds were obtained for pulse widths of between 2 and 10 ms. For a 10 ms pulse width, pure CP required approx. 6.7 mJ of e nergy for ignition whereas pure Ti/KClO4 required only approx. 3 mJ. Dopants such as carbon black, graphite and a laser dye were added in small concentrations to enhance light absorption and thereby reduce the ignition theshold. Their effects as well as those of powder density, particle size and spot size of the incident light on ignition threshold are described. DOE

29 MATERIALS PROCESSING

Includes space-based development of products and processes for commercial applications.
For biological materials see *55 Space Biology*.

N88-27353# Technische Univ., Clausthal-Zellerfeld (West Germany). Inst. fuer Nichtmetallische Werkstoffe.
HOMOGENEITY OF GLASSES: EXPERIMENT WL-IHF-05 IN D1 MISSION [HOMOGENITAET VON GLAESERN EXPERIMENT WL-IHF-05 IN DER D1-MISSION]
G. H. Frischat and V. Braetsch 31 Dec. 1986 52 p In GERMAN
(Contract BMFT-01-QV-4832)
(ETN-88-92339) Avail: NTIS HC A04/MF A01

Different compositions of the glass forming systems Li2O-SiO2 and Na2O-B2O3-SiO2 with and without platinum as a nucleation agent were melted at 1300 C and cooled with 2 dissimilar rates during Spacelab mission D1. The flight samples turned out to be much more homogeneous than the corresponding 1g reference samples. The reason is that under normal gravity conditions heterogeneous nuclei, formed in the contact zone container wall-melt, are transported into the bulk of the melt by buoyancy convection, there leading to crystalline or phase-separated regions during cooling. Platinum addition led to a much more fine-grained microstructure for the flight samples. The homogeneity measurements were done by electron-microprobe analysis and by the Christiansen-Shelybskii method. ESA

N88-27354# Societe Nationale Industrielle Aerospatiale, Saint-Medard-en-Jalles (France). Programmes Spatiaux.
EXPERIMENTS IN MICROGRAVITY ENVIRONMENT: PROTEIN CRYSTALLIZATION [EXPERIMENTATION EN MICROGRAVITE: CRISTALLISATION DE PROTEINES]
J. Bouvard 1988 14 p In FRENCH
(SNIAS-881-430-101; ETN-88-92849) Avail: NTIS HC A03/MF A01

The goal and the methodology of protein crystallization in space environments are discussed. The reasons why the microgravity condition could help to obtain protein crystals are detailed. ESA

31 ENGINEERING (GENERAL)

Includes vacuum technology; control engineering; display engineering; cryogenics; and fire prevention.

N88-27355# Universal Energy Systems, Inc., Dayton, Ohio.
UNITED STATES AIR FORCE GRADUATE STUDENT SUMMER SUPPORT PROGRAM, VOLUME 2 Program Technical Report, 1987
Rodney C. Darrah and Susan K. Espy Dec. 1987 730 p Program held in 1987; sponsored by AFOSR, AFSC, and USAF
(Contract F49620-85-C-0013; AF Proj. 3396)
(AD-A191122; AFOSR-88-0210TR-Vol-2) Avail: NTIS HC A99/MF E03 CSCL 13B

This program was conducted under the U.S. Air Force Summer Faculty Research Program. The program provided funds for selected graduate students to work at an appropriate A.F. facility with a supervising professor who holds a concurrent Summer Faculty Research Program appointment or with a supervising A.F. engineer. This is accomplished by the students being selected on a nationally advertised competitive basis for a 10 week assignment to perform research at A.F. labs or centers. Each assignment is in a subject area and at an A.F. facility mutually agreed upon by the students and the A.F. Continuing professional association among the scholars and their professional peers in the A.F. is stimulated. The research objectives of the A.F. are furthered. And the research productivity and capabilities of the graduate students, as they relate to the A.F. technical interest, are enhanced. Reports from these endeavors are presented. For individual titles, see N88-27356 through N88-27387.

N88-27356# Florida Univ., Gainesville. Dept. of Psychology.
PHYSIOLOGICAL MONITORING METHODOLOGY IN THE USAFSAM CENTRIFUGE Final Report **c51**
Jennifer B. McGovern *In* Universal Energy Systems, Inc., United States Air Force Graduate Student Summer Support Program, Volume 2 Dec. 1987 11 p (For primary document see N88-27355 21-31)
Avail: NTIS HC A99/MF E03 CSCL 06P

Loss of consciousness due to +Gz (G-LOC) was identified as a cause of many mishaps and loss of aircrews and aircraft. Previous studies have suggested that physiological measures, especially the EEG, would be useful to monitor pilot consciousness. Appropriate methodologies (including electrode placement and choice of electrode) are defined for use in a USAFSAM Centrifuge study of deliberate G-LOC. Physiological signals to be monitored included EEG, EMG, EOG, ear oximetry, and respiratory sounds. Author

N88-27357# Brown Univ., Providence, R. I. Div. of Biology and Medicine.
METHODS OF QUANTIFYING AND ENHANCING REACTIVE OXYGEN SPECIES PRODUCTION Final Report **c51**
Roland A. Medellin *In* Universal Energy Systems, Inc., United States Air Force Graduate Student Summer Support Program, Volume 2 Dec. 1987 20 p (For primary document see N88-27355 21-31)
Avail: NTIS HC A99/MF E03 CSCL 06P

Bioassays were run employing a reaction summarized by a given equation. Glucose oxidase, Horseradish peroxidase, Luminol, and Bovine serum albumin were immobilized on 7 mm filter paper disks. These disks when assayed by adding glucose demonstrated consistent, predictable enzyme kinetics, even when various inhibitors were added. A 150-fold greater chemiluminescence peaks were observed in disks to which glucose was added compared to controls. When Catalase was added, only 4.4 percent of this chemiluminescence was observed, while 15 percent of the chemiluminescence for glucose was seen when Bovine serum albumin was added. Virus sized nanoparticles (Glucose oxidase and Horseradish peroxidase) were produced along with a 1300-fold greater chemiluminescence over controls when a mixture of glucose and luminol was added. These nanoparticles were able to penetrate a 0.2 micron filter, and they retained their enzymatic activity for weeks. They produced 20-fold greater chemiluminescence over controls when immobilized on gel disks. Author

N88-27358# California Univ., Santa Cruz. Dept. of Mathematics.
APPLICATIONS OF DIFFERENTIAL GEOMETRY TO THE SHAPE ANALYSIS OF GRAY-VALUE IMAGES Final Report **c64**
Otto Michael Melko *In* Universal Energy Systems, Inc., United States Air Force Graduate Student Summer Support Program, Volume 2 Dec. 1987 20 p (For primary document see N88-27355 21-31)
Avail: NTIS HC A99/MF E03 CSCL 12P

A gray value image can be viewed as a discrete analog of a smooth surface in Euclidean space. The shape of a smooth surface can be described by the gauss curvature and mean curvature of that surface. It is therefore reasonable to expect that the discrete analogs of these curvature functions would be useful in the shape analysis of digitals (gray value) images. Two methods for discreting these curvature functions are discussed. These methods are then used to write algorithms for shape analysis of gray value images. Special attention is paid to the value of these algorithms for the identification of objects (such as tanks) in low resolution infrared images. Author

N88-27359# Wright State Univ., Dayton, Ohio. Dept. of Computer Engineering.
INVESTIGATION OF THE POTENTIAL IMPACT OF NEW PHOTONIC MATERIALS ON OPTICAL PROCESSING SYSTEMS Final Report **c74**
Frank W. Moore *In* Universal Energy Systems, Inc., United

States Air Force Graduate Student Summer Support Program, Volume 2 Dec. 1987 20 p (For primary document see N88-27355 21-31)
Avail: NTIS HC A99/MF E03 CSCL 20F

Claims for the speed and dynamic range properties of new photonic materials suggest that these materials could permit the development of competitive optical processors. The high resolution claimed for these materials may make them suitable for numerous information processing tasks. Non-cascadable Boolean operations were demonstrated. Analog addition of two dimensional images appear to be possible. Qualitative experiments suggesting uses of new photonic materials in optical systems were performed, general properties of these materials were determined, and future quantitative tests required for precise material characterization are proposed. Several multiplication schemes, aimed at performance which would be competitive with state-of-the-art electronic multipliers, are also proposed. Author

N88-27360# Montclair State Coll., Upper Montclair, N.J. Dept. of Psychology.
A REVIEW OF WORKLOAD MEASUREMENT IN RELATION TO VERBAL COMPREHENSION Final Report **c53**
Stephen T. Morgan *In* Universal Energy Systems, Inc., United States Air Force Graduate Student Summer Support Program, Volume 2 Dec. 1987 20 p (For primary document see N88-27355 21-31)
Avail: NTIS HC A99/MF E03 CSCL 05I

In a command and control environment, many individuals are called upon to engage in two activities simultaneously. Communication with others is often one of these tasks. It is crucial that there be no decrement in performance on either task, especially in crises situations where heavy loading on the cognitive system is apt to be present. In order to optimize an individual's performance, processing strategies need to be analyzed and the most efficient ones incorporated into appropriate training programs. The literature is reviewed regarding workload measurement techniques. The purpose is to investigate the most efficacious method of assessing processing load during verbal comprehension. Dual task paradigms are found to be valid indices of mental workload. Problems associated with this technique are evaluated and a possible assessment method is offered. Author

N88-27361# Kansas State Univ., Manhattan. Dept. of Psychology.
A HUMAN FACTORS EVALUATION OF THE ADVANCED VISUAL TECHNOLOGY SYSTEM (AVTS) EYE TRACKING OCULOMETER Final Report **c52**
Jerome I. Nadel *In* Universal Energy Systems, Inc., United States Air Force Graduate Student Summer Support Program, Volume 2 Dec. 1987 19 p (For primary document see N88-27355 21-31)
Avail: NTIS HC A99/MF E03 CSCL 06N

A human factors evaluation of the Honeywell helmet mounted eye tracking oculometer system was conducted. Experimental tests were directed at identifying the physical and anthropometric factors that lead to both successful and unsuccessful oculometer operability. Pupil size of the user was found to be the most significant factor affecting system performance. Other factors affecting system performance were interpupillary distance and helmet fit. It was recommended that the electronic pupillary signal from the system IR camera be amplified. This, in combination with a lower system pupil threshold, should ensure measurement accuracy for at least 80 percent of the user population. Author

N88-27362# Northwestern Univ., Evanston, Ill. Dept. of Psychology.
THE EFFECTS OF INCREASED COGNITIVE DEMANDS ON AUTONOMIC SELF-REGULATION: AN INDICATOR OF PARALLEL PROCESSING IN THE BRAIN Final Report **c53**
Victoria Tepe Nasman *In* Universal Energy Systems, Inc., United States Air Force Graduate Student Summer Support Program, Volume 2 Dec. 1987 13 p (For primary document see N88-27355 21-31)
Avail: NTIS HC A99/MF E03 CSCL 05I

A parallel processing scheme is proposed. Schemes were tested through a single subject experimental design in which subjects performed several tasks. Ongoing electroencephalographic signals were recorded over left and right occipital cortex, and compared between tasks within session. As expected, while performing various meditation and biofeedback tasks, subjects demonstrated characteristic dominant frequencies of 7 to 13 Hz (alpha). When performing such a task concomitant with another highly associative cognitive task, however, subjects produced results more like those obtained in the performance of the cognition task alone. These results support the notion that, while engaged in tasks which would require parallel brain processing, processes which would otherwise rely upon serial processing are uncoupled. A scheme is proposed upon which this interpretation is based. Although performance data on the cognitive task have not yet been analyzed, the preliminary interpretation of the data is that evidence was obtained to support a view of cognitive processing in which the flexibility to process either serially or in parallel exists, and in which the type of processing that is invoked will coincide with the demands of the task/tasks. Author

N88-27363# Meharry Medical Coll., Nashville, Tenn. School of Medicine.
MICROESOTROPIA PATIENTS PERFORMA WELL AS MILITARY JET PILOTS Final Report **c52**
Bernadette P. T. Njoku *In* Universal Energy Systems, Inc., United States Air Force Graduate Student Summer Support Program, Volume 2 Dec. 1987 10 p (For primary document see N88-27355 21-31)
Avail: NTIS HC A99/MF E03 CSCL 06N

A computer listing of patients examined with the diagnosis of microesotropia (microstrabismus, monofixation syndrome) was obtained. Key terms, especially used to determine patients not clearly defined as microesotropics include: failed depth perception, anisometropia, esotropia/esophoria, strabismus, microexotropia, hyperopia/hypermetropia, suppression/amblyopia, monofixation syndrome, diplopia, heterotropia/strabismus, and failed red lens test. The patients charts, mainly pilots and navigators, were studied and specific data gathered, then transferred to individual microstrabismus data sheets. From this, 6 straightforward graphs are constructed: refraction spherical equivalent vs patient no., refraction cylinder astigmatism vs patient no., Verhoeff vs patient no., Howard-Dolman vs patient no., alignment vs patient no., and stereo arc/sec vs patient no. These data and graphs allow primarily for at-a-glance obtaining of quantified information and comparisons from patient to patient; and thus, subsequent in-depth judgement and theories. Author

N88-27364# University of Southern Illinois, Carbondale. Dept. of Civil Engineering and Mechanics.
DETERMINATION OF LUMPED-MASS THERMAL PROPERTIES ASSOCIATED WITH AUTOCLAVE CURING OF GRAPHITE/EPOXY COMPOSITES Final Report **c24**
Charles W. Norfleet *In* Universal Energy Systems, Inc., United States Air Force Graduate Student Summer Support Program, Volume 2 Dec. 1987 15 p (For primary document see N88-27355 21-31)
Avail: NTIS HC A99/MF E03 CSCL 11D

Determination of the parameters affecting the thermal response of a graphite/epoxy composite was performed. A governing equation was developed for the process based on lumped-mass heat transfer principles. Numerical values of the thermal properties included in the energy balance equation were determined by a Newton-Raphson root solving method. The results of this method indicated that the bagging material surrounding the laminate during the cure process has significant thermal mass which created a slow response during the initial heating of the laminate. This observation led to the development of energy balance equations for both the bagging material and the laminate. Author

N88-27365# Missouri Univ., Rolla. Dept. of Computer Science.
INVESTIGATION OF EXPERT SYSTEM DESIGN APPROACHES FOR ELECTRONIC DESIGN ENVIRONMENTS Final Report **c33**

Susan A. Poppens *In* Universal Energy Systems, Inc., United States Air Force Graduate Student Summer Support Program, Volume 2 Dec. 1987 12 p (For primary document see N88-27355 21-31)
Avail: NTIS HC A99/MF E03 CSCL 10C

Various schemes were investigated that are available for the design effort of electronic systems. The information is to be incorporated into a knowledge base to determine approaches for a particular design. Various design methodologies are to be investigated for their appropriateness and application in the aforesaid design environment. The second phase is to focus on the knowledge base gathered in the design effort for electronic design. This knowledge base is to be incorporated into a rule based expert system which can be utilized by the design engineer in the design/development of functional specifications. Author

N88-27366# Colorado Univ., Boulder. Dept. of Aerospace.
CONTROL AND USE OF UNSTEADY FLOWS: INSECT USE OF VARIOUS WING KINEMATICS AND RELATED PRESSURE MEASUREMENTS USING A PITCHING AIRFOIL Final Report **c02**

Mark Andre Reavis *In* Universal Energy Systems, Inc., United States Air Force Graduate Student Summer Support Program, Volume 2 Dec. 1987 20 p (For primary document see N88-27355 21-31)
Avail: NTIS HC A99/MF E03 CSCL 01B

Based on a detailed analysis of insect flight kinematics, pressure measurements were made from a NACA 0015 airfoil undergoing a constant pitch motion carried to high angles of attack. Previous work revealed the important contribution that high pitch rates and high angles of attack play in dragonfly flight kinematics. Changes in the angle of attack, pitch displacement angle, pitch amplitude and non-dimensional pitch rate altered the integrated values of coefficient of lift and coefficient of drag in a reproducible and predictable manner. Pitching profiles were varied to provide different initial conditions for vorticity accumulation: (1) starting at 0 deg and pitching at constant rates to different maximum angles, (2) varying alpha initial and pitching to an alpha final of 60 deg, and (3) varying alpha initial but holding the displacement angle constant. All of the above tests were conducted at alpha plus values of 0.1 and 0.5. These results suggest that dynamic pitch motions of an airfoil can enhance lift even if the pitch motion is initiated beyond normal static stall angles. Also, an optimal maximum pitch angle exists which enhances the unsteady life potential while minimizing drag. Author

N88-27367# Dayton Univ., Ohio. Dept. of Electrical Engineering.
AIRCRAFT REFUELING DEMONSTRATOR USING A MICROBOT ALPHA 2 ROBOT Final Report **c09**

Bryan P. Riddiford *In* Universal Energy Systems, Inc., United States Air Force Graduate Student Summer Support Program, Volume 2 Dec. 1987 18 p (For primary document see N88-27355 21-31)
Avail: NTIS HC A99/MF E03 CSCL 14B

A demonstration was set up using a Microbot Alpha 2 robot to study the feasibility of robotic ground based aircraft refueling for use in chemically and biologically hazardous environments. An overhead gantry with the robot hanging beneath was designed to provide the easiest access to the aircraft midair refueling port. A 1/12 scale model of an F-16 was underneath and acted as the receiving aircraft. The midair refueling port was used so little or no modification was needed to accommodate existing aircraft. The robot was controlled by a Zenith 100 computer. Author

N88-27368# Nebraska Univ., Lincoln. Dept. of Electrical Engineering.
INFLUENCE OF MOVING VISUAL ENVIRONMENT ON SACCADIC EYE MOVEMENTS AND FIXATION Final Report **c52**

Keith A. Riese *In* Universal Energy Systems, Inc., United States Air Force Graduate Student Summer Support Program, Volume 2 Dec. 1987 15 p (For primary document see N88-27355 21-31)
Avail: NTIS HC A99/MF E03 CSCL 06N

Saccade parameters of amplitude, peak velocity, duration, and latency were compared for a stationary visual background environment versus a moving visual background environment to determine environmental effects. For visual stimuli, latency differences were significant while all other parameter variations were not. Mean saccade latency for a stationary visual background was 161.7 msec while for a moving visual background the mean latency was 175.3 msec. Saccades made in the same direction as the moving background showed minor variation as compared with those made in the opposite direction. No significant differences in saccade parameters were found when audio stimuli were used. Also, no parameter significance was found between target fixation and pseudo target fixation. Author

N88-27369# Alabama Univ., Scottsboro. Dept. of Health, Physical Education and Recreation.
THERMAL STRESS AND ITS EFFECTS ON FINE MOTOR SKILL AND DECODING TASKS **c52**

M. Carolyn Robinson *In* Universal Energy Systems, Inc., United States Air Force Graduate Student Summer Support Program, Volume 2 Dec. 1987 17 p (For primary document see N88-27355 21-31)
Avail: NTIS HC A99/MF E03 CSCL 06N

The current thermal research has focused on work productivity as measured by the amount of time a subject is engaged in gross motor movement. To help determine if thermal stress has an effect on fine motor and cognitive skills, two tasks were utilized to measure any change in these skills. The fine motor skill task was a hand-eye steadiness task; the cognitive task was a decoding task. An examination of the data indicated that under the thermal stress induced by a work-rest protocol resulting in a cyclic body core temperature (Tre): (1) there appears to be a trend between Tre and fine motor performance; (2) there does not appear to be a trend between Tre and decoding performance. An examination of the data indicates that personnel experiencing a cyclic variation in Tre may preserve cognition functioning, but may suffer a decrement of steadiness performance. The results of the decoding task may be an indication that the task utilized is not sensitive to Tre. Author

N88-27370# Puerto Rico Univ., Mayaguez. Dept. of Mechanical Engineering.
DESIGN OF A MECHANISM TO CONTROL WIND TUNNEL TURBULENCE Final Report **c09**

Filiberto Santiago *In* Universal Energy Systems, Inc., United States Air Force Graduate Student Summer Support Program, Volume 2 Dec. 1987 33 p (For primary document see N88-27355 21-31)
Avail: NTIS HC A99/MF E03 CSCL 14B

An intense literature survey was done covering the fundamental aspects of the turbulence phenomena. Turbulence of the air stream is generally recognized as a variable of considerable importance in many aerodynamics phenomena, especially those observed in wind tunnels. In the Acoustic Research Wind Tunnel, turbulence was generated in the stilling chamber using two devices. First, a grid, 20.5 by 20.5 in. with 1/2 in. diameter rods. This grid was used in two ways, one, the grid by itself, and the other, the grid with small tags attached to the horizontal center line and to the vertical center line. Second, a manifold with fourteen jets producing a flow of air perpendicular to its main stream flow in the wind tunnel. The turbulence level of the tunnel empty is approx. 3 percent. The turbulence level of the wind tunnel with the two devices is also given and a discussion of the results is presented. Author

N88-27371# Iowa Univ., Iowa City. Dept. of Mechanical Engineering.
EXPERIMENTAL RESEARCH OF COMBUSTION SYSTEMS Final Report **c25**
James P. Seaba *In* Universal Energy Systems, Inc., United States Air Force Graduate Student Summer Support Program, Volume 2 Dec. 1987 10 p (For primary document see N88-27355 21-31)
Avail: NTIS HC A99/MF E03 CSCL 21B

Several small experiments regarding different combustion phenomena were explored. A new diagnostic tool known as the phase Doppler anenometer was used in a spray environment, it measures droplet size and velocity. Diffusion flame work was completed from last summers work. Other experiments include a multiple jet flame, and multicomponent evaporation of a droplet. Author

N88-27372# Houston Univ., Tex. Dept. of Mechanical Engineering.
THE INTEGRATION OF DECISION SUPPORT PROBLEMS INTO FEATURE MODELING BASED DESIGN Final Report **c81**
Jon A. Shupe *In* Universal Energy Systems, Inc., United States Air Force Graduate Student Summer Support Program, Volume 2 Dec. 1987 20 p (For primary document see N88-27355 21-31)
Avail: NTIS HC A99/MF E03 CSCL 05A

Components of the design environment are consolidated and reported. Design is discussed as being composed of decisions of various types and activities. These design types and activities are set forth and described. Further, Feature Modeling as posed by the Materials Lab. is discussed, as well as the relationship of decision making to Feature Modeling. Finally, it is posed that an appropriate and useful design environment will utilize a balance of knowledge based techniques and numerical decision making algorithms, such as the Decision Support Problem technique for solving design problems. Several scenarios where this blend would be useful are discussed. Author

N88-27373# Iowa Univ., Iowa City. Dept. of Mechanical Engineering.
OPTIMAL CONTROL OF THE WING ROCK PHENOMENON Final Report **c08**
Christopher D. Sierra *In* Universal Energy Systems, Inc., United States Air Force Graduate Student Summer Support Program, Volume 2 Dec. 1987 16 p (For primary document see N88-27355 21-31)
Avail: NTIS HC A99/MF E03 CSCL 01C

The nonlinear phenomenon of the wing rock of a slender delta wing about the midspan axis was chosen for study. Time histories of the roll angle and the roll angle velocity were obtained and used to verify the results of the phase plane analysis of Nayfeh, Firbela and Mook. A simulation of the pilot changing the angle of shock of the wing was implemented in order to observe the effect the maneuver has on the behavior of the uncontrolled system. The time history of the build up of wing rock was developed. The need for a method of controlling this phenomena was observed. A control was then obtained using optimum systems control. The optimal control was also found for the system experiencing an unexpected pulse. The time histories of the roll angle for both cases were obtained. A Sub-Optimal Control Algorithm was also used to obtain a control for this wing rock phenomena. These results were presented so that a comparison between the two optimal control techniques could then be made. Author

N88-27374# Wyoming Univ., Laramie. Dept. of Physics and Astronomy.
CALIBRATION AND DATA REDUCTION TECHNIQUES FOR THE AFGL INFRARED ARRAY SPECTROMETER Final Report **c74**
Gregory Sloan *In* Universal Energy Systems, Inc., United States Air Force Graduate Student Summer Support Program, Volume 2 Dec. 1987 18 p (For primary document see N88-27355 21-31)
Avail: NTIS HC A99/MF E03 CSCL 20F

AFGL's Infrared Array Spectrometer has now taken data at the Wyoming Infrared Observatory on three occasions. This data was used to calibrate the array and to test data reduction schemes. The results of this effort are presented: a calibration and data reduction algorithm for future use with the instrument. Author

N88-27375# Pennsylvania Univ., Philadelphia. Dept. of Electrical Engineering.
THERMAL CONDUCTIVITY OF ISOTOPICALLY PURE SEMICONDUCTORS, SUPERLATTICES, SEMICONDUCTOR ALLOYS AND SEMICONDUCTORS AS A FUNCTION OF TEMPERATURE; CONTROL OF THE SEGREGATION COEFFICIENT IN LEC CRYSTAL GROWTH; AND PHOTO-HALL MEASUREMENTS OF GaAs Final Report **c76**
Elisabeth Smela *In* Universal Energy Systems, Inc., United States Air Force Graduate Student Summer Support Program, Volume 2 Dec. 1987 19 p (For primary document see N88-27355 21-31)
Avail: NTIS HC A99/MF E03 CSCL 20L

A table of isotopes was prepared. Literature searches on the effects of isotopes on thermal conductivity, the thermal conductivity of superlattices, the control of the segregation coefficient in LEC crystal growth, and on the relationship between in doping of GaAs and both CRSS and thermal conductivity were completed. Computer programs were written to evaluate the phonon mean free path and the thermal conductivity as a function of alloy composition. Finally, photo-Hall effect measurements were done on several GaAs samples. Author

N88-27376# New Mexico Univ., Albuquerque. Dept. of Mechanical Engineering.
PREDICTING OPTICAL DEGRADATION OF A LASER BEAM THROUGH A TURBULENT SHEAR LAYER Final Report **c76**
Rita Rex Smith *In* Universal Energy Systems, Inc., United States Air Force Graduate Student Summer Support Program, Volume 2 Dec. 1987 20 p (For primary document see N88-27355 21-31)
Avail: NTIS HC A99/MF E03 CSCL 20L

The degradation in optical quality of a coherent laser beam passing through a turbulent shear layer was predicted by relating the phase error of the coherent beam to the time-mean index of refraction profile across the shear layer. The prediction of the optical degradation is, therefore, dependent on the accuracy of the model used to analyze the turbulent shear layer. The turbulence model in the ALFA shear layer code was investigated. A code was developed to calculate the index of refraction profile, phase error, and Strehl ratio using the results of the turbulence analysis from ALFA and plot the significant turbulence parameters. This method employs a mixing length assumption. A better approach would be to predict optical degradation by relating the phase error to index of refraction fluctuations, eliminating the need to make a mixing length assumption. The scalar fluctuation equation in the ALFA code and perturbation of the Gladstone-Dale relation were examined for this purpose. Author

N88-27377# University of South Florida, Tampa. Dept. of Computer Science and Engineering.
AN ASPECT GRAPH-BASED CONTROL STRATEGY FOR 3-D OBJECT RECOGNITION Final Report **c74**
Louise Stark *In* Universal Energy Systems, Inc., United States Air Force Graduate Student Summer Support Program, Volume 2 Dec. 1987 19 p (For primary document see N88-27355 21-31)
Avail: NTIS HC A99/MF E03 CSCL 20F

Several researchers have described methodologies for three dimensional object recognition which use nonlinear optimization as a control strategy for matching features of a three dimensional object model to features found in an image. A problem with this type of system is how to efficiently choose a set of starting parameter estimates so as to avoid recognition errors due to local minima. A new methodology is presented for applying nonlinear optimization in three dimensional object recognition. The method enumerates a complete set of relevant starting points for each object model by choosing one starting point for each viewing cell defined by the aspect graph of the object. Constrained nonlinear

optimization is used to find a minimum within each viewing cell. Examples are given to illustrate how recognition errors can occur due to local minimum found from poor starting parameter estimates, and how the methodology based on the aspect graph object models eliminates this problem. Author

N88-27378# Johns Hopkins Univ., Baltimore, Md. Dept. of Mathematical Sciences.
LINEAR PROGRAMMING FOR AIR FORCE DECISION AIDING Final Report **c61**
Steven J. Steinsaltz *In* Universal Energy Systems, Inc., United States Air Force Graduate Student Summer Support Program, Volume 2 Dec. 1987 21 p (For primary document see N88-27355 21-31)
Avail: NTIS HC A99/MF E03 CSCL 09B

The program Enemy Sortie Capability Measurement Aid was examined to determine what was required of a linear program solver so that it could replace the commercial package being used. A program was written in PASCAL, using the upper bound form of the revised simplex method, and various problems with memory had to be overcome. The completed program took 23 minutes to solve, compared to 3 minutes for the commercial package. The program was rewritten in C, and when debugged, ran in 10 minutes. This was improved upon by changing the program so that, instead of using the revised simplex method, which saves memory (a problem not faced in C), the regular simplex method was used. This improved the running time to 7 minutes, within the bounds desired. Author

N88-27379# University of South Florida, St. Petersburg. Dept. of Computer Science and Engineering.
CREATING ASPECT GRAPHS FOR USE IN OBJECT RECOGNITION Final Report **c61**
John H. Stewman *In* Universal Energy Systems, Inc., United States Air Force Graduate Student Summer Support Program, Volume 2 Dec. 1987 21 p (For primary document see N88-27355 21-31)
Avail: NTIS HC A99/MF E03 CSCL 09B

The creation of aspect graphs for use as object models in a 3-D object recognition system is studied. A method is presented which directly creates the aspect graph of a convex planar face object from its boundary surface representation. The aspect graph created by this process is an undirected graph. Each node in the graph has attributes describing one aspect of the object and the cell of space from which that aspect can be viewed. Each arc in the graph indicates an adjacency between two aspects and is attributed with the plane separating the two associated cells. This representation is consistent with that originally proposed by Koen. There are two significant differences between this approach and others extant. First, determination of the structure of the aspect graph is done in a direct manner based on the geometry of the object. The resulting aspect and cell descriptions are exact rather than approximate. Second, the cell associated with each aspect is a true 3-D volume of space rather than a surface patch on a viewing sphere. Author

N88-27380# Rochester Univ., N. Y. Dept. of Physics and Astronomy.
ANALYSIS OF EMISSION FEATURES IN IRAS LRS SPECTRA Final Report **c74**
Tod Strohmayer *In* Universal Energy Systems, Inc., United States Air Force Graduate Student Summer Support Program, Volume 2 Dec. 1987 20 p (For primary document see N88-27355 21-31)
Avail: NTIS HC A99/MF E03 CSCL 20F

A study was made of IRAS low resolution spectra (LRS) of variable M stars. The 1n class of LRS was analyzed in order to study the various types of emission features seen in these spectra. Although originally classified as featureless, it was found that approx. 30 percent of the spectra have emission features in the 9 to 15 micron region. The average excess emission above the local continuum is about 7 percent and ranges from 2 to 20 percent. Emission due to silicates at about 10 to 18 microns is seen as well as emission due to silicon carbide at 11.6 microns. A large number of objects show a broad feature between 9 and 15 microns usually centered between 11 and 12 microns. It is not clear yet whether the feature is due to carbon rich or oxygen rich dust, and may possibly be evidence for evolution from spectral type M to C. A computer program was written and modified which graphically analyzes the LRS data. Programming was implemented that allows the fitting of the local continuum using two models. The first allows the user to co-add 2 blackbody distributions, and the second employs a simple dust shell model to estimate the continuum. The color corrections is calculated by another program. Author

N88-27381# Cincinnati Univ., Ohio. Dept. of Electrical and Computer Engineering.
OPTICAL INTERCONNECTIONS FOR DIGITAL IMAGE CODING Final Report **c74**
Tien N. Tran *In* Universal Energy Systems, Inc., United States Air Force Graduate Student Summer Support Program, Volume 2 Dec. 1987 13 p (For primary document see N88-27355 21-31)
Avail: NTIS HC A99/MF E03 CSCL 20F

To achieve a very high compression rate, Digital Image Coding algorithms are becoming more complicated than ever. Combining this with the high speed nature of image processing, transmission, parallel and pipeline processing have to be involved with the help of multiple processing units type of architecture. Because of the large number of cells or chips involved, communications between cells or chips pose many problems. Optical interconnections seems to offer a hope for a solution. Author

N88-27382# Louisiana State Dept. of Conservation, Baton Rouge. Dept. of Engineering Sciences.
AN INVESTIGATION OF PERFORMANCE IMPROVEMENT IN KNOWLEDGE-BASED CONTROL SYSTEMS Final Report **c61**
John M. Usher *In* Universal Energy Systems, Inc., United States Air Force Graduate Student Summer Support Program, Volume 2 Dec. 1987 17 p (For primary document see N88-27355 21-31)
Avail: NTIS HC A99/MF E03 CSCL 09B

The use of knowledge based systems in real time process control is a relatively new application. Even though there is much interest in this area, developers and users are reluctant to utilize the full potential that the knowledge based system can offer. This restraint is due to the problem of resolving conflicts in the control actions prescribed by the system. In most cases, a human operator is made an integral part of the control system by requiring him to select the action to implement from among the alternatives offered by the system. A new method is proposed for resolution of conflicts which uses deterministic process knowledge in addition to heuristics and statistics. It is hoped that such a system will encourage removal of the operator and use of the system in a fully automatic mode of operation. To further enhance the system, an idea is presented for the incorporation of a learning system to allow for on-line automatic editing of the process knowledge contained in the knowledge base. This configuration results in a coupled system which uses dynamic deterministic and heuristic knowledge to resolve process conflicts which arise. Author

N88-27383# Prairie View Agricultural and Mechanical Coll., Tex. Dept. of Chemical Engineering.
COMPUTER MODELING FOR SURFACE PROPERTIES OF CARBON FIBERS Final Report **c24**
Pretta L. VanDible *In* Universal Energy Systems, Inc., United States Air Force Graduate Student Summer Support Program, Volume 2 Dec. 1987 25 p (For primary document see N88-27355 21-31)
Avail: NTIS HC A99/MF E03 CSCL 11D

Defining the structure of carbonaceous materials required extensive computer solutions of several mathematical models. Pressure vs volume experimental data was displayed graphically to observe the shape of the curve. The external surface area as well as the internal surface areas of macropores and mesopores was defined by the BET method. The solutions of the Dubinin-Polanyi and Dubinin-Astakhov equations gave the

micropore surface area. The estimation of the shape of the pores was determined by solving a series of mathematical equations. The numerical solutions yielded average pore radius, Kelvin radius, adsorbed volume and surface area of the pore walls. Author

N88-27384# Kent State Univ., Ohio. Dept. of Physics.
NUMERICAL CALCULATIONS OF DOPENT DIFFUSION INVOLVING FLASHLAMP HEATING OF SILICON Final Report **c76**
Joseph C. Varga *In* Universal Energy Systems, Inc., United States Air Force Graduate Student Summer Support Program, Volume 2 Dec. 1987 10 p (For primary document see N88-27355 21-31)
Avail: NTIS HC A99/MF E03 CSCL 20L

Work was begun on finding a solution to the flashlamp heating of a doped semiconductor. A Blackbody spectrum was assumed to follow a Lorentzian lineshape. Finite difference techniques were used. The diffusion of dopant through a semiconductor was calculated. A comparison was made between an analytical solution and numerical calculation. The results agreed to within 0.002 percent. Author

N88-27385# . Illinois Univ., Urbana. Dept. of Astronautical Engineering.
SLEW-INDUCED DEFORMATIONS IN A SPACE-BASED ELECTROMAGNETIC RAIL GUN Final Report **c14**
James W. Wade *In* Universal Energy Systems, Inc., United States Air Force Graduate Student Summer Support Program, Volume 2 Dec. 1987 21 p (For primary document see N88-27355 21-31)
Avail: NTIS HC A99/MF E03 CSCL 22D

A space based rail gun has many possible uses, one of which is a component of a space based defense network. Stringent pointing requirements are placed on a rail gun to be used for this purpose. Disturbances to the rail gun may significantly affect pointing accuracy. Possible sources of disturbances identified include: onboard equipment, rail vibrations, environmental torques, and slew induced deformations. Slewing deformations are studied by including the coupling of the slew dynamics with the Bernoulli-Euler beam model. The slewing disturbances are modeled, with control methods suggested to overcome the resulting pointing errors. Author

N88-27386# University of Eastern Washington, Cheney. Dept. of Mathematics.
HOLE DIAMETERS IN PLATES IMPACTED BY PROJECTILES Final Report **c37**
Randall F. Westhoff *In* Universal Energy Systems, Inc., United States Air Force Graduate Student Summer Support Program, Volume 2 Dec. 1987 15 p (For primary document see N88-27355 21-31)
Avail: NTIS HC A99/MF E03 CSCL 13I

The hole diameter and rod loss models of SPADE, a program designed to calculate the damage to an array of spaced plates impacted by projectile, was evaluated. Comparison with actual test data showed that the hole diameter model was only accurate under certain impact conditions. Using experimental data and curve fitting techniques, the hole diameter model was modified to achieve greater fidelity over a broad range of test conditions. The only available data on rod loss was from the original report which suggested the rod loss model currently used by SPADE. The accuracy of that model is verified. Author

N88-27387# Wright State Univ., Dayton, Ohio. School of Medicine.
HUMAN RESPONSE TO PROLONGED MOTIONLESS SUSPENSION IN FOUR TYPES OF FULL BODY HARNESSES Final Report **c52**
Terri Wilkerson *In* Universal Energy Systems, Inc., United States Air Force Graduate Student Summer Support Program, Volume 2 Dec. 1987 20 p (For primary document see N88-27355 21-31)
Avail: NTIS HC A99/MF E03 CSCL 06N

The ability to withstand prolonged suspension while being restrained by fall protection harnesses is of vital interest to occupational safety. A fallen worker may be suspended in a fall protection harness for an indefinite period waiting for rescue. The relative capabilities of four types of full body harnesses (FBH) were evaluated to provide occupant body support and restraint during post fall suspension. A series of 42 randomized tests were conducted to evaluate the physiological effects and subjective responses to prolonged, motionless suspension in four different designs of FBH. Measured physiological parameters included blood pressure, heart rate, and respiratory rate. Author

N88-27388# Mitsubishi Electric Corp., Tokyo (Japan).
MITSUBISHI ELECTRIC ADVANCE (R AND D EDITION), VOLUME 41
Dec. 1987 39 p
(PB88-194162) Avail: NTIS HC A03/MF A01 CSCL 14B

Issues addressed are: new technologies for a new society; basic research on optical neural computers; computer-aided engineering (CAE) for engineering design; high-speed, precision processing using an electron beam; superconducting oxides with high critical temperatures; a 1/2-inch high-definition baseband VCR; thermal-sensation control (a new method of controlling cooled/heated environments; the MELCOM PSI II AI workshop; the MELMUX MX-7100 series high-speed digital multiplexers; and polarization selective Raman microspectroscopy. For individual titles, see N88-27389 through N88-27397.

N88-27389# Mitsubishi Electric Corp., Tokyo (Japan). Central Research Lab.
BASIC RESEARCH ON OPTICAL NEURAL COMPUTERS **c74**
Kazuo Kyuma and Satoru Shiono *In its* Mitsubishi Electric Advance (R and D Edition), Volume 41 Dec. 1987 4 p (For primary document see N88-27388 21-31)
Avail: NTIS HC A03/MF A01 CSCL 20F

Biological information processing mechanisms were investigated. The mathematical models for these mechanisms are expected to provide significant advantages for computer engineering. The final objective is to implement these results in optical computers. Progress in this field is introduced and the results of recent research are summarized. Author

N88-27390# Mitsubishi Electric Corp., Tokyo (Japan). Central Research Lab.
COMPUTER-AIDED ENGINEERING (CAE) FOR ENGINEERING DESIGN **c61**
Akemi Futakawa *In its* Mitsubishi Electric Advance (R and D Edition), Volume 41 Dec. 1987 3 p (For primary document see N88-27388 21-31)
Avail: NTIS HC A03/MF A01 CSCL 09B

During the 1980s, systemization of the accumulated technical-data processing software, and integration with existing artificial intelligence technology, has enabled all the routine information processing of the design process to be performed by computer. The end result is a computer-aided engineering (CAE) expert system that supports designing for product development and improvement. The computer's role is evolving from one of an expert system for analysis to that of a designer's assistant, resulting in significant changes in electrical and electronic product design methods, enhanced product development and improvement, and cost reductions. The development work on this CAE design expert system is described, including the development goals, an overview of the system itself, suggestions for design-process innovation, and topics for future work. Author

N88-27391# Mitsubishi Electric Corp., Tokyo (Japan). Product Development Lab.
HIGH-SPEED, PRECISION PROCESSING USING AN ELECTRON BEAM **c37**
Seiji Yasunaga and Megumi Ohmine *In its* Mitsubishi Electric Advance (R and D Edition), Volume 41 Dec. 1987 4 p (For primary document see N88-27388 21-31)
Avail: NTIS HC A03/MF A01 CSCL 13H

Achievements in developing powerful electron beam technology and the new possibilities unveiled by electron-beam processing techniques are presented. B.G.

N88-27392# Mitsubishi Electric Corp., Tokyo (Japan). Materials Engineering Lab.
SUPERCONDUCTING OXIDES WITH HIGH CRITICAL TEMPERATURES **c76**
Kiyoshi Yoshizaki *In its* Mitsubishi Electric Advance (R and D Edition), Volume 31 Dec. 1987 2 p (For primary document see N88-27388 21-31)
Avail: NTIS HC A03/MF A01 CSCL 20L

The main superconducting materials in commercial production are the NbTi alloy and Nb3Sn compound. Owing to their low critical temperatures, both of these materials require a costly and complex refrigeration system employing liquid helium, leading many researchers to search for materials that exhibit superconductivity at higher temperatures. In 1986, J.D. Bednorz and K.A. Muller discovered an La-Ba-Cu oxide that exhibited superconductivity at 35 K, spurring research and development at laboratories around the world. In 1987, a Y-Ba-Cu oxide was found that becomes superconducting at 90 K, the first ovserved instance of superconductivity at a temperature above the boiling point of liquid nitrogen (77 K). Mitsubishi Electric's research on superconducting Y-Ba-Cu oxides is examined. Author

N88-27393# Mitsubishi Electric Corp., Tokyo (Japan). Consumer Electronics Development Lab.
A 1/2-INCH HIGH-DEFINITION BASEBAND VCR **c33**
Michiyasu Ishibashi and Toshifumi Fujii *In its* Mitsubishi Electric Advance (R and D Edition), Volume 41 Dec. 1987 4 p (For primary document see N88-27388 21-31)
Avail: NTIS HC A03/MF A01 CSCL 09A

The prototype of the 1/2-inch High Definition (HD) baseband VCR is described. Its basic specifications and video characteristics are examined. B.G.

N88-27394# Mitsubishi Electric Corp., Tokyo (Japan). Consumer Products Research Lab.
THERMAL-SENSATION CONTROL: A NEW METHOD OF CONTROLLING COOLED/HEATED ENVIRONMENTS
Sakuo Sugawara and Masanori Hara *In its* Mitsubishi Electric Advance (R and D Edition), Volume 41 Dec. 1987 3 p (For primary document see N88-27388 21-31)
Avail: NTIS HC A03/MF A01 CSCL 13I

Historically, the principle behind the design of equipment for residential room cooling and heating was simply to cool or warm the room. Recent developments in room cooling and heating however, focus on controlling the comfort level (that is, maintaining a comfortable indoor living or working environment) and reducing energy consumption. Focusing on the techniques of controlling cooled and heated environments, Mitsubishi Electric has produced a more sophisticated method of environmental control. Called thermal-sensation control (TSC), this method differs significantly from existing airflow control systems, which regulated the environment by attempting to maintain an even temperature distribution in the room. Consideration of the interface between systems and their users has lead to major improvements in the operability and human comfort levels achievable by TSC. The main features of the new method, development of the TSCs thermal-environment sensor, and the software needed for control, with examples of how it is implemented, are described. Author

N88-27395# Mitsubishi Electric Corp., Tokyo (Japan). Information Systems and Electronics Development Lab.
THE MELCOM PSI 2 AI WORKSTATION **c63**
Takasumi Ueda and Hiroshi Nakashima *In its* Mitsubishi Electric Advance (R and D Edition), Volume 41 Dec. 1987 3 p (For primary document see N88-27388 21-31)
Avail: NTIS HC A03/MF A01 CSCL 09B

The MELCOM PSI 2 is a dedicated AI workstation that offers powerful artificial-intelligence language and program-development tools, sophisticated interactive operation, and a high inference speed. The system is suited for efficient development and execution of expert systems, natural-language processing programs, and similar artificial-intelligence applications. The PSI 2 was developed using the results of the Japanese-government sponsored the Fifth Generation Computer Program. It features extended self-contained Prolog (ESP), also a result of the project, as a programming language. Author

N88-27396# Mitsubishi Electric Corp., Tokyo (Japan). Information and Communication Systems Engineering Center.
THE MELMUX MX-7100 SERIES HIGH-SPEED DIGITAL MULTIPLEXERS **c60**
Kazuyoshi Oshima and Kazuhiko Sekikawa *In its* Mitsubishi Electric Advance (R and D Edition), Volume 41 Dec. 1987 3 p (For primary document see N88-27388 21-31)
Avail: NTIS HC A03/MF A01 CSCL 09B

Features of the MELMUX MX-7100 series high-speed digital multiplexer are described. B.G.

N88-27397# Mitsubishi Electric Corp., Tokyo (Japan). LSI Development Lab.
POLARIZATION SELECTIVE RAMAN MICROSPECTROSCOPY **c25**
Yasuo Inoue, Tadashi Nishimura, and Yoichi Akasaka *In its* Mitsubishi Electric Advance (R and D Edition), Volume 41 Dec. 1987 7 p (For primary document see N88-27388 21-31)
Avail: NTIS HC A03/MF A01 CSCL 07D

Microanalysis based on Raman microspectroscopy differs significantly from evaluation techniques such as observation by optical and scanning electron microscopes and elemental analyses by second ion mass spectroscopy and auger electron microscopes. Raman microspectroscopy, new technology, applications in technology development, and technique comparison are examined. B.G.

N88-27398# New Mexico Univ., Albuquerque. Engineering Research Inst.
EXTINGUISHING AGENT FOR MAGNESIUM FIRE, PHASES 5 AND 6 Final Report, Dec. 1985 - Sep. 1986
H. D. Beeson, R. E. Tapscott, and B. E. Mason Jul. 1987 98 p
(Contract F29601-84-C-0080)
(AD-A192436; NMERI-WA3-34(3.07); AFESC/ESL-TR-86-65)
Avail: NTIS HC A05/MF A01 CSCL 13L

This report documents the validation testing of the extinguishing system for metal fires developed as part of Phases 1 to 4. The results of this validation testing form the basis of information from which draft military specifications necessary to procure the agent and the agent delivery system may be developed. The developed system was tested against a variety of large-scale metal fire scenarios and the capabilities of the system were assessed. In addition the response of the system to storage and to changes in ambient conditions was tested. Results of this testing revealed that the developed system represented a reliable metal fire extinguishing system that could control and extinguish very large metal fires. The specifications developed for the agent and for the delivery system are discussed in detail. GRA

N88-27399# Naval Postgraduate School, Monterey, Calif.
A CONCEPTUAL DESIGN STUDY OF A HOVERING SYSTEM CONTROLLER FOR AN AUTONOMOUS UNDERWATER VEHICLE M.S. Thesis
Chris A. Thompson Dec. 1987 73 p
(AD-A193423) Avail: NTIS HC A04/MF A01 CSCL 13J

An Autonomous Underwater Vehicle (AUV) will have many operational scenarios that will include a transition from cruise to hover over a fixed position in the ocean. While hovering, the AUV must be able to balance the current induced forces, a difficult task to accomplish automatically. The magnitude of these forces induced on an example AUV have been estimated for currents from 4 m/s to 1 m/s with the incident current varying from 0 deg to 360 deg. Using the estimated forces, different configurations of thrusters were investigated and the power required for different

thruster configurations compared. Three thrusters (two longitudinal, one lateral) can balance the forces exactly and a unique solution was evaluated. With redundant thrusters, more economical schemes can developed using force allocation logic with minimum norm solutions. System horsepower requirements have been estimated and a conceptual model based controller methodology has been proposed. The force allocation logic proposed will now allow for a smooth transition from cruise to hover mode positions. GRA

N88-27400# Aerospace Corp., El Segundo, Calif. Materials Sciences Lab.
ANALYSIS OF DEBRIS FROM ACCELERATED LIFE TEST OF THE HUGHES FIVE-YEAR VUILLEUMIER CRYOCOOLER
D. C. Cranmer and E. J. Watts 29 May 1987 23 p
(Contract F04701-85-C-0086)
(AD-A193101; TOR-0086A(2057)-1) Avail: NTIS HC A03/MF A01 CSCL 13B

Unit S3 of the Hughes Vuilleumier (VM) Cryocooler Program has undergone accelerated life testing at twice the service speed expected in a normal unit. Debris samples were obtained from all areas of the cooler; samples of the regenerator balls were collected from the second and third stages only. The debris has been identified by an investigative analysis using the analytical techniques of X-ray diffraction, IMMA, and SEM/EDXS. Most of the particulates contain a combination of Fe, Cr, and Ni or Mo-Nb compounds. Author

N88-27401# Ecole Nationale Superieure des Telecommunications, Paris (France). Dept. Communications.
[ACTIVITIES REPORT OF THE COMMUNICATIONS DEPARTMENT] Annual Report, 1987 [RAPPORT D'ACTIVITE 1987 DU DEPARTEMENT COMMUNICATIONS]
Feb. 1988 46 p In FRENCH
(ENST-88D003; ISSN-0751-1345; ETN-88-92760) Avail: NTIS HC A03/MF A01

Research activities in telecommunication components, optoelectronics, microwave devices, theory of numerical communication, laser tuning, fast frequency modulation of semiconductor lasers, and microwave and numerical communication networks are described. ESA

32 COMMUNICATIONS AND RADAR

Includes radar; land and global communications; communications theory; and optical communications.

For related information see also *04 Aircraft Communications and Navigation* and *17 Space Communications, Spacecraft Communications, Command and Tracking.* For search and rescue see *03 Air Transportation and Safety,* and *16 Space Transportation.*

N88-27402# Newcastle-upon-Tyne Univ. (England). Computing Lab.
MODEL FOR DYNAMICALLY STRUCTURED COMMUNICATING SYSTEMS
R. P. Hopkins and M. Koutny 1987 44 p
(PB88-105283; TR-SER-239) Copyright Avail: NTIS HC E04/MF E04; copy not available from STI Facility CSCL 17B

A model is developed of structure and communication within systems of concurrently executing components connected by asynchronous communication links, and a definition of observational equivalence between systems is formulated. The most important aspect of the model is that it accommodates the dynamic system connectively required to model open and continuously operating systems, by allowing an end point of a communication link to be communicated as part of a message, with the recipient thus dynamically acquiring the ability to communicate on that link. For the model, a novel definition was formulated of observational equivalence in terms of equivalent operational behaviors of possible observing systems. Author

N88-27403# Naval Environmental Prediction Research Facility, Monterey, Calif.
AN EVALUATION OF TWO MILLIMETER WAVE PROPAGATION MODELS FOR HORIZONTAL ATMOSPHERIC ATTENUATION AT 70-115 GHZ Final Report, May - Aug. 1987
Gerard N. Vogel Feb. 1988 84 p
(AD-A192699; NEPRF-TR-88-02) Avail: NTIS HC A05/MF A01 CSCL 20N

An evaluation is performed for two millimeter wave propagation models: the LIEBE model, developed at the Institute for Telecommunications, Boulder, CO, under the guidance of Dr. H. Liebe; and the EOSAEL model, developed at the U. S. Army Atmospheric Laboratory at White Sands Missile Range, NM. This evaluation is conducted for horizontal attenuation due to both clear atmosphere and hydrometer effects under typical surface meteorological conditions, and within the frequency range 70-115 GHz. Intercomparisons of model theories and predictions show slight differences for molecular oxygen and fog attenuations, but significant differences for water vapor and rain attenuations. Results indicate that, while the qualitative agreement between either the EOSAEL or LIEBE model predictions, and measurements, for horizontal attenuation due to oxygen, water vapor, fog and rain is certainly satisfactory, there is a definite need for improvement. Overall, no clear preference for either the EOSAEL or LIEBE model for operational use is ascertained. Data comparisons suggest that, for several attenuation types, model preference is dependent on either the frequency or meteorological conditions. GRA

N88-27404# Advanced Decision Systems, Mountain View, Calif.
LINEAR FEATURE EXTRACTION FROM RADAR IMAGERY. PHASE 2: BASE CONTRACT REPORT Technical Report, 16 Jun. 1986 - 15 Jan. 1987
Gary D. Conner, Daryl T. Lawton, Christopher C. McConnell, and David L. Milgram Jul. 1987 40 p
(Contract DACW72-86-C-0004)
(AD-A192828; AI/DS-TR-3139-01; ETL-0649) Avail: NTIS HC A03/MF A01 CSCL 17I

The goal of this effort is to develop and demonstrate prototype processing capabilities for a knowledge based system to automatically extract and analyze linear features from synthetic aperture radar (SAR) imagery. This effort constitutes Phase 2 funding through the Defense Small Business Innovative Research (SBIR) Program. Previous work examined the feasibility of and technology issues involved in the development of an automated linear feature extraction system. The current effort continues this examination and is developing the technologies involved in automating this image understanding task. GRA

N88-27405# Rome Air Development Center, Griffiss AFB, N.Y.
AIRBORNE MEASUREMENT OF LOW FREQUENCY ATMOSPHERIC NOISE ALFAN 1
John P. Turtle and Wayne I. Klemetti Oct. 1987 24 p
(AD-A193056; RADC-TR-87-170) Avail: NTIS HC A03/MF A01 CSCL 20N

Essential airborne very low frequency/low frequency (VLF/LF) communication systems use long-wire transmitting antennas trailed behind high-flying aircraft. Radio frequency (RF) energy with a transverse magnetic polarization radiated by these antennas has been used in long-range communications. Recently, airborne systems have been upgraded and can receive transverse electric polarized waves. The range and connectivity of these communication systems are based on predictions from computer codes. Levels of atmospheric noise at aircraft altitude that are predicted from models of lightning indicate the possibility that airborne noise level predictions may need to be revised. The Airborne Low Frequency Atmospheric Noise (ALFAN) project was devised to measure atmospheric noise from a balloon-borne antenna/receiver system. In this report, the system and first flight are described. Initial results are presented and discussed in terms of their possible implications for communication systems. GRA

N88-27406# Advisory Group for Aerospace Research and Development, Neuilly-Sur-Seine (France).
AIR-TO-AIR RADAR FLIGHT TESTING
Randall E. Scott (Test Group, 6520th, Edwards AFB, Calif.) Jun. 1988 117 p
(AGARD-AG-300-Vol-7; ISBN-92-835-0460-7) Copyright Avail: NTIS HC A06/MF A01

This volume in the AGARD Flight Test Techniques Series describes flight test techniques, flight test instrumentation, ground simulation, data reduction and analysis methods used to determine the performance characteristics of a modern air-to-air (a/a) radar system. Following a general coverage of specification requirements, test plans, support requirements, development and operational testing, and management information systems, the report goes into more detailed flight test techniques covering a/a radar capabilities of: detection, manual acquisition, automatic acquisition, tracking a single target, and detection and tracking of multiple targets. There follows a section on additional flight test considerations such as electromagnetic compatibility, electronic countermeasures, displays and controls, degraded and backup modes, radome effects, environmental considerations, and use of testbeds. Other sections cover ground simulation, flight test instrumentation, and data reduction and analysis. The final sections deal with reporting and a discussion of considerations for the future and how they may affect radar flight testing. Author

N88-27407# Massachusetts Inst. of Tech., Lexington. Lincoln Lab.
TDWR (TERMINAL DOPPLER WEATHER RADAR) PRF (PULSE REPETITION FREQUENCY) SELECTION CRITERIA
S. C. Crocker 15 Mar. 1988 44 p
(Contract DTFA01-80-Y-10546)
(AD-A193089; DOT/FAA/PM-87-25) Avail: NTIS HC A03/MF A01 CSCL 17I

The Terminal Doppler Weather Radar (TDWR) system shall provide high quality Doppler radar data on weather phenomena near high traffic airports. These data shall be used in real time by automated TDWR algorithms to detect weather situations which may be hazardous to the safe operation of aircraft within the vicinity of the airport. One of the major factors which could cause the degradation of the quality of these TDWR data is obscuration by distant storm cells. This obscuration is caused by storms located beyond the range interval being sampled by the radar, yet whose radar echo ambiguously folds within the range interval of interest. These range aliased echoes could trigger false detections by the algorithms, and/or cause actual hazardous situations near the airport to remain undetected. By carefully selecting the pulse repetition frequency (PRF) of the radar, range obscuration from distant storms can be minimized over specified airport regions. This document describes techniques for predicting the obscuration as a function of PRF, and details the criteria which shall be used by the TDWR system to automatically and adaptively select an optimal PRF in order to minimize these obscuration effects. GRA

N88-27408# Naval Ocean Systems Center, San Diego, Calif.
SURFACE-WAVE MODEL UNCERTAINTY ASSESSMENT Final Report, Sep. 1986 - Oct. 1987
T. N. Roy, D. B. Sailors, and W. K. Moision Nov. 1987 72 p
(AD-A193094; NOSC-TR-1199) Avail: NTIS HC A04/MF A01 CSCL 20N

The GROUNDWAVE model is compared to 84 surface-wave measurements made at frequencies of 20, 50, and 101.5 MHz for mountainous, hilly, and flat terrain. Surface wave transmission loss error is evaluated as a function of distance, frequency, terrain and receiving antenna height. The overall average measured transmission loss is 144 dB with an average interdecile range of 11 dB. The overall average calculated transmission loss is 141 dB, well within the interdecile range. When the model was tested as a function of terrain type, a trend toward understanding the transmission loss as the terrain became more irregular was apparent. GROUNDWAVE model error is evaluated as a function of input effective ground conductivity and effective ground relative dielectric constant also. By using constant values for these ground frequency, as is the usual practice, the possibility exists for substantial error in transmission loss calculations as a function of frequency. In the frequency range 2 to 20 MHz, results how the GROUNDWAVE model to underestimate transmission loss by an average of 13.1 dB for desert, mountainous, and hilly terrain. For the rich agricultural and marsh terrain, the GROUNDWAVE model overestimated the transmission loss by an average of only 1.9 dB. When the GROUNDWAVE model predicted transmission losses were compared to measured over-ocean data, it was found that the model severely over-predicted at frequencies greater than 18 MHz. GRA

N88-27409# Naval Research Lab., Washington, D.C.
SIDELOBE LEVEL OF AN ADAPTIVE ARRAY USING THE SMI (SAMPLED MATRIX INVERSION) ALGORITHM Interim Report
Karl Gerlach 26 Feb. 1988 23 p
(AD-A193131; NRL-9079) Avail: NTIS HC A03/MF A01 CSCL 25B

The transient sidelobe level of an adaptive array is a function of the external noise environment, the number of adaptive antenna elements, the adaptive algorithm employed, auxiliary antenna gain margins, and the number of samples used to calculate the adaptive weights. In this report, an analytical result for the adaptive sidelobe level is formulated for when the adaptive algorithm is the open-loop Sampled Matrix Inversion (SMI) algorithm. This result is independent of whether the SMI algorithm is implemented using concurrent or nonconcurrent data processing. It is shown that the transient sidelobe level is eigenvalue dependent and increases proportionally to the gain margin of the auxiliary antenna elements with respect to the quiescent main antenna sidelobe level. Techniques that reduce this transient sidelobe level are discussed, and it is theoretically shown (as other researchers have discovered) that injecting independent noise into the auxiliary channels significantly reduces the transient sidelobe level. Also it is demonstrated that using this same technique reduces the SMI noise power residue settling time. GRA

N88-27410# Naval Research Lab., Washington, D.C.
A NUMERICALLY EFFICIENT DIGITAL MATCHED FILTER FOR PERIODIC AND WINDOWED PERIODIC RADAR WAVEFORMS Interim Report
Karl Gerlach 26 Feb. 1988 14 p
(AD-A193132; NRL-9055) Avail: NTIS HC A03/MF A01 CSCL 17I

An algorithm is presented for implementing a digital matched filter for periodic and windowed periodic radar waveforms. The algorithm is based on circular convolutional techniques. For moderate to high duty cycles d (radar on time to pulse repetition interval (PRI) ratio), the circular convolutional algorithm uses 50 percent fewer complex multiply operations (CMOPs) than does a fast convolution implementation. In fact, if BPRI is the radar waveform bandwidth-PRI product, then the circular convolutional technique is numerically more efficient if d is greater than 1/sq. rt(8(BPRI)). Furthermore, the circular convolution technique is numerically more efficient when the pulse compression ratio p is greater than sq. rt. (BPRI/8). GRA

N88-27411# Naval Research Lab., Washington, D.C.
SARLAC: A RELATIVISTIC ELECTRON BEAM CODE
Glenn Joyce, Richard Hubbard, Martin Lampe, and Steven Slinker 10 Feb. 1988 25 p
(ARPA Order 4395)
(AD-A193134; NRL-MR-6140) Avail: NTIS HC A03/MF A01 CSCL 20G

SARLAC is a particle simulation code for studying the propagation of ultrarelativistic electron beams. It is used to study the nonlinear evolution of the resistive hose instability. We have developed a fast, semi-implicit, iterative field solver which allows us to include a large number of Fourier modes in the azimuthal direction. The solver iterates about a solution of the field equations dominated by the axisymmetric (m = 0) conductivity. This technique has proved to be quite successful. We compare some results of

the code with those obtained from a linearized hose simulation code, and show differences when the hose oscillations reach large amplitude. GRA

N88-27412# Naval Research Lab., Washington, D.C.
DEFINITION OF LONG OCEAN WAVE SLOPE FOR RADAR APPLICATIONS
Dennis B. Trizna and Lee U. Martin 4 Mar. 1988 42 p
(AD-A193198; NRL-MR-6096) Avail: NTIS HC A03/MF A01 CSCL 17I

Consideration is given to the definition of open ocean long wave slope, as a parameter for correlation with radar section (RCS). In preparation for studies of dependence of short pulse radar statistics on long wave features, we have re-examined the long time averaged RCS data previously reported by Keller, Plant and Weissman (KPW), and its dependence on in-situ measurements of long wave slope. Comparisons of RCS are made with the significant slope defined by Huang and Long, using ocean wave spectrum features; the radar slope defined a KPW, using wave spectral features inferred from radar Doppler measure of orbital wave motions; and a variety of slope definitions from zero-crossing analysis of surface variance time series measured by a wave gauge. It appears that the in-situ measurements correlate with RCS better than the radar slope. Possible reasons for this are discussed. GRA

N88-27413# Naval Postgraduate School, Monterey, Calif.
PERFORMANCE STUDY OF A UNIPOLE ANTENNA WITH CONVENTIONAL AND ELEVATED RADIAL WIRE GROUND SCREENS M.S. Thesis
Dimitris A. Koutsouras Dec. 1987 105 p
(AD-A193283; NPS-62-88-007) Avail: NTIS HC A06/MF A01 CSCL 09A

The advantages of using elevated radial wire ground screens with vertical monopole antennas for medium frequency and high frequency broadcast have recently been reported. This study extends the concept to the folded unipole antenna and compares the performance of a folded unipole with elevated radials to that of monopoles operating with both elevated and conventional buried radial wire ground screens. The unipole's performance with 2,3 and 4 elevated radials, is within 2 percent of that for a standard monopole using 120 buried radial wires. GRA

N88-27414# IIT Research Inst., Chicago, Ill.
A NOTCH FILTER INSTRUMENT FOR MEASURING ELF (EXTREMELY LOW FREQUENCY) MSK (MINIMUM SHIFT KEYING) SIGNALS
R. G. Drexler and J. R. Gauger Jan. 1988 101 p
(Contract N00039-84-C-0070)
(AD-A193324; IITRI-E06549-34) Avail: NTIS HC A06/MF A01 CSCL 20C

This report presents a notch filter technique for measuring extremely low frequency (ELF) signals in the presence of other higher-level, low frequency voltages, specifically 60 Hz and harmonics, on public utility systems. The report also describes the design, development, and operation of a special-purpose notch filter instrument that allows the practical realization of this measurement technique. The instrument, called the Notch Box III, is compact (2.75 x 10 x 9 in.), lightweight (less than 4 lb), and battery operated for complete electrical isolation and portability of its electronic circuitry. It features input buffering and selectable attenuation, input overload warning, a narrow-band 60 Hz notch filter with greater than 80 dB of attenuation, a Chebyshev low-pass filter providing sharp roll-off above 100 Hz, output signal buffering, and battery charge status indication. The Notch Box III can operate 150 hours on a single battery charge. GRA

N88-27415# Naval Research Lab., Washington, D.C.
RADAR INFORMATION FROM THE PARTIAL DERIVATIVES OF THE ECHO SIGNAL PHASE FROM A POINT SCATTERER
Merrill I. Skolnik 17 Feb. 1988 54 p
(AD-A193402; NRL-MR-6148) Avail: NTIS HC A04/MF A01 CSCL 17I

This report is concerned with the target information from a point scatterer as obtained from the partial derivatives of the echo-signal phase as a function of frequency, time, and spatial position. These partial derivates provide the three basic radar measurements of range, range rate, and angle. The angle rate found from the spatial doppler-frequency shift (due to a scatterer with a component of velocity perpendicular to the radar line of sight) is suggested as a fourth basic radar measurement. The direct measurement of angle-rate from the spatial doppler frequency is illustrated by the example of a scanning interferometer radar with a cosine radiation pattern. The relationship between the partial phase-derivative measurements and the more conventional radar measurements is shown. GRA

N88-27416# Foerenade Fabriksverken, Linkoeping (Sweden).
ELECTROMAGNETIC CHARACTERIZATION AND ACCEPTANCE TEST OF THE EMP SIMULATOR SPERANS
Sven Garmland Jan. 1988 74 p
(PB88-203781; FOA-C-30476-4.2; EMP-Memo-805) Avail: NTIS HC A04/MF A01 CSCL 20N

An extensive mapping of the electromagnetic characteristics of the EMP simulator, SPERANS, is presented. The requirements according to the simulator specifications are verified. A large number of waveforms representing the electromagnetic fields in the different test areas are presented. It was shown that all the simulator specifications were fulfilled. The characteristics of the pulse generator and the measurement system is also detailed. Author

N88-27417# Joint Inst. for Nuclear Research, Dubna (USSR). Lab. of Computing Techniques and Automation.
CALCULATIONS OF HIGH-FREQUENCY PARAMETERS OF DISC-LOADED WAVEGUIDES
M. S. Kaschiev, V. N. Mamonov, Yu. L. Obukhov, K. A. Reshetnikova, and S. B. Rubin 1987 11 p In RUSSIAN; ENGLISH summary
(DE88-702178; JINR-R-9-87-268) Avail: NTIS (US Sales Only) HC A03/MF A01

Radio-technical parameters of a disc-loaded waveguide suitable for modeling two-beam acceleration are designed. Two series of calculations using the finite element method (MULTIMODE program) and restricted region method (ALF program) lead to coinciding resonance frequencies for rectangular-disc waveguide. The MULTIMODE program package is also used for the numerical simulation of the rounded-edge-disc waveguide, the field distribution picture and several energy parameters of the designed system. DOE

N88-27418# Academy of Sciences of the Ukrainian SSR, Kharkov.
EXPERIMENTAL INVESTIGATION OF SIMPLEST INHOMOGENEITIES IN CYLINDRICAL SLIT LINE
A. G. Kovalenko and V. P. Shestopalov 1986 35 p In RUSSIAN; ENGLISH summary
(DE88-702388; INIS-SU-27) Avail: NTIS (US Sales Only) HC A03/MF A01

The cylindrical slit line is a perspective SHF transmission line. The results of experimental investigations of inhomogeneities which can appear in a series of sections of the cylindrical slit line, i.e., different discontinuities, fractures in all planes, slit width changes, angle connection errors, slit overlap and others are given. For all inhomogeneities under investigation approximation dependences are obtained describing the maximum losses in the operating frequency band. It is shown that some inhomogeneities can find practical use in designing basic elements of the cylindrical slit line. DOE

N88-27419# Sandia National Labs., Albuquerque, N. Mex.
DEPENDENCE EFFECTS IN UNIQUE SIGNAL TRANSMISSION
J. A. Cooper Apr. 1988 27 p
(Contract DE-AC04-76DP-00789)
(DE88-010331; SAND-88-0394) Avail: NTIS HC A03/MF A01

Unique Signals are communicated from a source to a strong

link safety device in a weapon by means of one or more digital communication channels. The probability that the expected unique signal pattern could be generated accidentally (e.g., due to an abnormal environment) would be an important measure. A probabilistic assessment of this likelihood is deceptive, because it depends on characteristics of the other traffic on the communication channel. One such characteristic that is frequently neglected in analysis is dependence. This report gives a mathematical model for dependence; cites some of the ways in which dependence can increase the likelihood of inadvertent unique signal pattern generation; and suggests that communicating each unique signal event at the highest level of protocol in the communication system minimizes dependence effects. DOE

N88-27420# Lawrence Livermore National Lab., Calif.
NONLINEAR DYNAMICS OF THE ELECTRON SELF-FIELD INTERACTION
B. Ritchie and A. Steiger 18 Apr. 1988 9 p
(Contract W-7405-eng-48)
(DE88-010597; UCID-21394) Avail: NTIS HC A02/MF A01

There has been recent interest in the formulation of a nonperturbative theory of quantum electrodynamics (QED). In this report we critically discuss a recent theory of nonperturbative QED. We point out a difficulty with this theory and outline a theory which is free of this difficulty. Finally, computational schemes for implementing the theory are briefly discussed. DOE

N88-27421 City Univ. of New York, N.Y.
A STUDY OF A METEOR BURST COMMUNICATION SYSTEM Ph.D. Thesis
Eliphaz Hibshoosh 1987 158 p
Avail: Univ. Microfilms Order No. DA8801719

This study discusses the use of the meteor burst channel (MBC) in communication systems and has three main themes: (1) The development and enhancement of an accurate and reliable channel model based on recently available empirical data. Analysis of this model results in analytical expressions for communication parameters such as channel duration and throughput to be used as design and analysis tools; (2) The optimization of throughput for fixed transmission rate under the constraint of a given maximum error rate. This will demonstrate the room for improvement in existing systems using constant transmission rate; and (3) The feasibility of efficiently communicating over the MBC using variable bit rate and employing a feedback protocol to monitor the channel. This approach will improve throughput in comparison with constant transmission rate systems. Dissert. Abstr.

N88-27422# Lawrence Livermore National Lab., Calif.
A METHOD FOR ESTIMATING THE SUSCEPTIBILITY OF ELECTRONIC SYSTEMS TO HPM (HIGH POWER MICROWAVE)
R. W. Mensing, R. J. King, and H. S. Cabayan May 1988 69 p
(Contract W-7405-eng-48)
(DE88-012246; UCID-21430) Avail: NTIS HC A04/MF A01

In this report, a method for estimating the susceptibility of electronic systems to High Power Microwave (HPM) is advanced. This method is being incorporated into an overall DOD assessment methodology that is being prepared by a tri-service working group headed by the Air Force. In the next two years, the methodology will be applied to assess several military systems and modified as necessary to establish a nationally-approved standard methodology. The objective of the effort is to establish a standardized assessment methodology to guide all ongoing U.S. HPM system effects assessment activities. The work will involve development of a detailed, integrated assessment plan that includes system functional analyses (i.e., system analyses and including all analytical modeling of HPM coupling and subsystem/component susceptibility), low power characterization test, (i.e., coupling/subsystem component tests and system functional response tests), HPM effects tests, and post-test analyses combining system functional analyses, low power characterization test, and methods for extrapolating test results to possible threat parameter regimes not readily simulated. DOE

N88-27423# Fondazione Ugo Bordoni, Rome (Italy).
UTILIZATION OF A SATELLITE COMMUNICATION SYSTEM TO PROTECT THE NATIONAL COMMUNICATION NETWORK [IMPIEGO DI UN SISTEMA VIA SATELLITE PER LA PROTEZIONE DELLA RETE NAZIONALE DI COLLEGAMENTO]
U. Mocci and G. Ravaioli Dec. 1986 45 p In ITALIAN
(FUB-33-1986; ETN-88-92646) Avail: NTIS HC A03/MF A01

The expansion of the Italian national communication network is discussed. The requirements up to the year 2000 are examined. Decisions already adopted are described, including the utilization of the Italsat satellite and the installation of an optical fiber network. Study of the necessity to expand the individual links over the limits already planned is carried out. It is found that an expansion is desirable for specific geographical areas. ESA

N88-27424*# National Aeronautics and Space Administration. Lewis Research Center, Cleveland, Ohio.
ANALYTICAL APPROXIMATION OF A DISTORTED REFLECTOR SURFACE DEFINED BY A DISCRETE SET OF POINTS
Roberto J. Acosta and Afroz A. Zaman 1988 15 p Presented at the Antenna Applications Symposium, Monticello, Ill., 21-23 Sep. 1988; sponsored by Illinois Univ. and RADC
(NASA-TM-101323; E-4327; NAS 1.15:101323) Avail: NTIS HC A03/MF A01 CSCL 20N

Reflector antennas on Earth orbiting spacecrafts generally cannot be described analytically. The reflector surface is subjected to a large temperature fluctuation and gradients, and is thus warped from its true geometrical shape. Aside from distortion by thermal stresses, reflector surfaces are often purposely shaped to minimize phase aberrations and scanning losses. To analyze distorted reflector antennas defined by discrete surface points, a numerical technique must be applied to compute an interpolatory surface passing through a grid of discrete points. In this paper, the distorted reflector surface points are approximated by two analytical components: an undistorted surface component and a surface error component. The undistorted surface component is a best fit paraboloid polynomial for the given set of points and the surface error component is a Fourier series expansion of the deviation of the actual surface points, from the best fit paraboloid. By applying the numerical technique to approximate the surface normals of the distorted reflector surface, the induced surface current can be obtained using physical optics technique. These surface currents are integrated to find the far field radiation pattern. Author

33 ELECTRONICS AND ELECTRICAL ENGINEERING

Includes test equipment and maintainability; components, e.g., tunnel diodes and transistors; microminiaturization; and integrated circuitry.

For related information see also *60 Computer Operations and Hardware* and *76 Solid-State Physics.*

N88-27425# Aerospace Corp., El Segundo, Calif. Lab. Operations.
NDP (NEUTRON DEPTH PROFILING) EVALUATIONS OF BORON-IMPLANTED COMPOUND SEMICONDUCTORS
Robert C. Bowman, Jr., John F. Knudsen, and R. G. Downing 4 Mar. 1988 93 p
(Contract F04701-85-C-0086)
(AD-A192306; TR-0086A(2945-07)-3; SD-TR-88-44) Avail: NTIS HC A05/MF A01 CSCL 09A

This report describes recent neutron depth profiling (NDP) experiments on the distribution of implanted boron in several semiconductors. The objectives are to compare the boron profiles for different materials that had been simultaneously implanted and to assess the effects of annealing treatments that were used to remove implant damage and electrically activate the boron. GRA

N88-27426# Pennsylvania State Univ., University Park. Communications and Space Sciences Lab.
MULTIFILTER SPECTROMETER (FEB) FOR MICROWAVE ATMOSPHERIC SOUNDER Final Report
Charles L. Croskey Feb. 1988 6 p
(Contract N00014-86-K-0236)
(AD-A192312; AD-E801594) Avail: NTIS HC A02/MF A01 CSCL 20E

The purpose of the research was to develop the multifilter electronics box (FEB) which is part of the Millimeter Atmospheric Sounder, MAS. The MAS observes the Earth's atmosphere at five microwave/millimeter-wave frequencies to measure water vapor, ozone, and chlorine-monoxide. The FEB provides the detailed spectral analysis of the receiver outputs through the use of 240 separate filters and detectors, whose digitized outputs are passed on to the experiment computer. GRA

N88-27427# Pennsylvania State Univ., University Park. Communications and Space Sciences Lab.
FEB (MULTIFILTER ELECTRONICS BOX) LIFTING DEVICE ANALYSIS, REVISION A
Charles L. Croskey 10 Feb. 1988 9 p
(Contract N00014-86-K-0236)
(AD-A192313; AD-E801594; TN-2036-9180-NR/01-Rev-A) Avail: NTIS HC A02/MF A01 CSCL 13D

This document is to determine the mechanical loads produced when the FEB is either lifted manually with handles or by a sling and overhead hoist. 2. Relevant Documents 2.1 JA418 2.2 ES-MAS-DS-003 MAS Ground Support Equipment Specification 2.3 An Introduction to the Design and Behavior of Bolted Joints John H. Bickford, MARCEL DEKKER, New York 3. Lifting Apparatus 3.1 For the lifting of FEB by either handles or a sling from an overhead hoist, four eyebolts are attached to the top mounting edge, through the top cover and into the top flange of the sidewalls. When the FEB is to be lifted manually without mechanical assistance, two long stainless steel rods are inserted lengthwise through the upright eyebolts. A small collar is then slipped over the rod so that the rod cannot shift lengthwise. The rod ends which extend beyond the eyebolt positions serve as handles for two people to lift the FEB. When an overhead hoist is to be used, the rods are not used. Instead a wire-rope sling is attached to each eyebolt. The four sling arms meet at a center jump ring which is lifted by the hook of the overhead crane. A spreader frame is used just above the eye-bolt attachments so that the load transfered to the bolts is strictly vertical. GRA

N88-27428# Aerospace Corp., El Segundo, Calif. Chemistry and Physics Lab.
PICOSECOND OPTOELECTRONIC SAMPLING OF ELECTRICAL WAVEFORMS PRODUCED BY AN OPTICALLY EXCITED FIELD EFFECT TRANSISTOR
Steven C. Moss 30 Dec. 1987 8 p
(Contract F04701-85-C-0086)
(AD-A192384; TR-0086(6945-06)-5; SD-TR-87-63) Avail: NTIS HC A02/MF A01 CSCL 09A

Picosecond optoelectronic techniques were used to measure the electrical response of a submicron gate GaAs field effect transistors to optical excitation by picosecond laser pulses. Results indicated that carrier transport in these devices is strongly affected by screening of the applied electrical bias at high optical excitation levels. The use of these devices as ultrafast photodetectors and as generators of ultrafast transient electrical waveforms on GaAs integrated circuits was discussed. GRA

N88-27429# Pinnacle Research Inst., Cupertino, Calif.
HIGH POWER PULSE ENERGY SYSTEM CONCEPT Final Report, 1 Sep. 1987 - 28 Feb. 1988
Ho-Lun Lee, G. Mason, and K. Kern 28 Feb. 1988 52 p
(Contract N00014-87-C-0705)
(AD-A192440) Avail: NTIS HC A04/MF A01 CSCL 10C

New advances in capacitor technology create exciting opportunities in size and weight reduction for high-power, pulse energy systems having a broad range of applications. Characteristics of a proposed high power pulse energy system, formed by combining recently developed, high-energy outputs. Parametric relationships between most key design variables, such as average pulse power, system output voltages, load impedance, pulse width, pulse frequency, duty cycle and battery's voltage and current limits, were established. Projections of the system's weights in large scale applications suggested that the lithium/SO2 battery considered might be too heavy when high duty cycles were required. However, significant weight reductions could be foreseen with proper selection of the battery and further advances in the capacitor technology. GRA

N88-27430# Utah Univ., Salt Lake City. Dept. of Electrical Engineering.
AN INVESTIGATION OF THE USES OF TIME DOMAIN CAPABLE VECTOR NETWORK ANALYZERS AS A DIAGNOSTIC FOR HELIX TRAVELING-WAVE CIRCUITS Final Report, Sep. 1984 - Sep. 1987
James V. Davis, II Mar. 1988 63 p
(Contract F30602-84-C-0153)
(AD-A192460; UTEC-MD-87-038; RADC-TR-88-34) Avail: NTIS HC A04/MF A01 CSCL 09A

The purpose of this project is to investigate the uses of time domain capable vector network analyzers as diagnostics for the design and test of helix Traveling-Wave Tubes (TWT's). The uses of the Time Domain (TD) investigated included tracking the location of a bead in the circuit, determining the phase velocity versus frequency using the gating methods available in the time domain, and locating faults and discontinuities along the helix circuit. Good agreement with expected results were obtained for the phase velocity versus frequency in a 2-8 GHz circuit, except at the band edges, and uses for fault location were demonstrated. Another method was devised using the complex nature of the data without going into the time domain to measure phase velocity versus frequency data. This method proved to be more accurate overall than the time domain method. GRA

N88-27431# Pennsylvania State Univ., University Park. Dept. of Materials Science and Engineering.
A CRITICAL REVIEW OF IR DROPS AND ELECTRODE POTENTIALS WITHIN PITS, CREVICES AND CRACKS Annual Report
Howard W. Pickering Jan. 1988 39 p
(Contract N00014-84-K-0201)
(AD-A192481) Avail: NTIS HC A03/MF A01 CSCL 07D

The experimental data showing variations in electrode potential in actively growing pits, crevices and cracks are reviewed. Direct potential measurement, proton discharge within the local cell when thermodynamically unfavorable at the outer passive surface, faceting of the pit and crevice walls, and the presence of an active/passive boundary conclusively prove that pitting and crevicing of iron occurs when the electrode potential within the cell is below (less noble than) the Flade or passivation potential of the crevice solution. Low pH and Cl and other aggressive ions, are proposed to increase both the stability and rate of localized corrosion by increasing the size of the active loop and/or magnitude of the passive current of the cavity solution. GRA

N88-27432# Pennsylvania State Univ., University Park. Dept. of Materials Science and Engineering.
SIGNIFICANCE OF THE LOCAL ELECTRODE POTENTIAL WITHIN PITS, CREVICES AND CRACKS
Howard W. Pickering Feb. 1988 36 p
(Contract N00014-84-K-0201)
(AD-A192482) Avail: NTIS HC A03/MF A01 CSCL 07D

This paper begins with a review of the experimental measurements of the electrode potential within pits, crevices and cracks for several commercially important alloy systems. Then, recent results for crevicing are reviewed. They give further insight into the relationship of the important parameters within the cavity: IR drop, Flade or passivation potential and solution composition, namely that stable crevice corrosion occurs when the electrode potential in the crevice is less oxidizing than the Flade potential

of the crevice solution. This result fully supports and contributes to a more detailed understanding of the potential shift mechanism, as originally outlined for pitting in iron, and more recently applied widely to pitting, crevicing, stress corrosion and corrosion fatigue in different alloy systems. GRA

N88-27433# Johannes Kepler Univ., Linz (Austria). Microelectronics Inst.
A PLANAR IC-COMPATIBLE TRANSFERRED ELECTRON DEVICE FOR MILLIMETER-WAVE OPERATION Interim Report No. 4, 1 Sep. 1987 - 29 Feb. 1988
Hartwig W. Thim 23 Mar. 1988 8 p
(Contract DAJA45-86-C-0039)
(AD-A192692; R/D-5302-EE) Avail: NTIS HC A02/MF A01 CSCL 09A

Devices with 0.5-micrometer-long gates have been fabricated using E beam lithography. Since no improvement in efficiency has been obtained it is recommended to use 1 to 1.5-micrometer-long gates which are easy to fabricate. It was also found that finger gate devices exhibit ten times smaller efficiencies (0.1 percent) than overlapping gate devices do. In order to produce gain at a desired frequency (lambda/2 + delta)-lines terminated by radial stubs must be connected to both gate and source. Maximum gain occurs at that frequency at which the capacitive reactances of the lines with 0 less than delta less than lambda/4 compensate for lead and other parasitic inductances. The device breaks into oscillations when a dielectric resonator with its resonance frequency near the maximum gain frequency is placed near both drain and gate bonding pads. The oscillator frequency can be tuned over a few hundred megahertz by varying the gate voltage by approximately 10 percent . An unexpectedly steep (12db/octave) fall off of efficiency with frequency has been observed whose origin has not yet been identified. It is speculated that the low field region near the drain contact might cause this steep fall off. Future devices, therefore, will be made with reduced gate drain distance. That might perhaps enhance efficiency in general. GRA

N88-27434# Aerospace Corp., El Segundo, Calif. Chemistry and Physics Lab.
RESULTS FROM LIFE TEST IN PROGRESS ON EAGLE-PICHER NICKEL CADMIUM CELLS
Charles C. Badcock, Samuel W. Donley, Warren G. Hwang, James H. Matsumoto, and Talmadge M. Poston 1 Apr. 1988 23 p
(Contract F04701-85-C-0086)
(AD-A192816; TR-0086A(2945-01)-7; SD-TR-88-52) Avail: NTIS HC A03/MF A01 CSCL 10C

This report summarizes the results from low-earth-orbit life testing on Eagle Picher nickel cadmium cells of nominal 50 Ah capacity that have been undergoing testing since 1983. As these cells have limited ability to withstand overcharge, a V-T charging scheme was adopted at the outset after careful determination of safe peak charge voltages at the two operating temperatures of 0 and 20 C. Of the original 30 cells put on life cycling under a complex load profile (10 cells each of 0 C/25 percent maximum depth-of-discharging (DOD), O C/40 percent maximum DOD, and 20 C/25 percent maximum DOD), both cell packs at 0 C were discontinued after less than 5000 pack at 20 C has exceeded 15,000 cycles (in May 1987), with no evidence of voltage spreading or other serious decline in performance. The original V-T level selected for this pack has not required adjustment. GRA

N88-27435# State Univ. of New York, Stony Brook. Dept. of Physics.
EQUIPMENT FOR AN ADVANCED ELECTRON BEAM LITHOGRAPHY SYSTEM Final Report, 13 Jul. 1986 - 14 Jul. 1987
James Lukens 14 Jul. 1987 4 p
(Grant AF-AFOSR-0253-86)
(AD-A192956; AFOSR-88-0306TR) Avail: NTIS HC A02/MF A01 CSCL 14E

Equipment has been purchased under this grant to develop and build a research electron beam lithography (EBL) system at Stony Brook for the support of research projects on superconducting electronics. The system is based on an array scanning electron microscope (SEM) which has been modified to accept a laser interferometer to monitor stage position. High precision nonmagnetic stages have been added, and interface electronics have been designed and built to permit control of the beam position and beam blanking by an external computer. The completed system is designed to write over a four inch wafer with a resolution of 30nm and a positional accuracy of 100nm. GRA

N88-27436# Wisconsin Univ., Madison. Dept. of Electrical and Computer Engineering.
EQUIPMENT FOR BUILDING AND TESTING SUPERCONDUCTIVE FLUX FLOW ELECTRONIC DEVICES Final Report, 1 Nov. 1986 - 30 Nov. 1987
James E. Nordman and James B. Beyer 30 Nov. 1987 4 p
(Grant AF-AFOSR-0061-87)
(AD-A192959; AFOSR-88-0303TR) Avail: NTIS HC A02/MF A01 CSCL 09A

The equipment authorized by the grant is a thin film vacuum deposition system containing provisions for ion beam and magnetron sputter deposition and for ion beam etching. GRA

N88-27437# Texas Univ., Austin. Dept. of Electrical and Computer Engineering.
GUIDED WAVE INTERACTIONS IN MILLIMETER-WAVE INTEGRATED CIRCUITS Final Report, 1 Sep. 1984 - 15 Jan. 1988
Tatsuo Itoh 15 Jan. 1988 65 p
(Contract DAAG29-84-K-0076)
(AD-A193017; ARO-21438.41-EL) Avail: NTIS HC A04/MF A01 CSCL 09A

This report on guided wave interactions in millimeter-wave integrated circuits discusses the following: Planar Transmission Lines; Quasi-Optical Structures; Device Modeling and Characterizations; Slow Wave Structures; Broadband Planar Optical Modulator; Reprints: Comparative Study of Mode-Matching Formulations for Microstrip Discontinuity Problems; Generalized Scattering Matrix Method for Analysis of Cascaded and Offset Microstrip Step Discontinuities; Microstrip-Fed Planar Frequency-Multiplying Space Combiner; and Crosstie Overlay Slow-Wave Structure for Broadband Traveling-Wave Type Electro-Optical Modulators. GRA

N88-27438# Sandia National Labs., Albuquerque, N. Mex. Electronic Ceramics Div.
THE FIRST SYNTHESIS OF CHEM-PREP VARISTOR LAC (LIGHTNING ARRESTOR CONNECTOR) GRANULES
B. A. Tuttle, J. A. Voigt, and L. A. Andrews Mar. 1988 25 p
(Contract DE-AC04-76DP-00789)
(DE88-008005; SAND-87-3112) Avail: NTIS HC A03/MF A01

ZnO varistor granules are the active media for many lightning arrestor connectors (LACs). The 150 to 200 micron diameter granules provide a controlled electrical breakdown in the 400 micron gap between the electrically conductive pin and web of the connector. For the first time, varistor granules were synthesized from chemically prepared powders. These chem-prep varistor powders are more homogeneous and much finer than the mixed oxide powders: the mean particle size of the chem-prep powders is approximately 0.06 microns. LAC granules were formed from chemically prepared powders by traditional ceramic processing techniques. Although the chem-prep granules were not as spherical as the mixed oxide granules, the chem-prep granules did meet present LAC component requirements for fast rise breakdown voltage and insulation resistance. Author

N88-27439# Massachusetts Inst. of Tech., Cambridge. Research Lab. of Electronics.
FOCUSED ION BEAM FABRICATION OF GRADED CHANNEL FETs IN GaAs AND Si SemiAnnual Report, 1 Jul. - 31 Dec. 1987
John Melngailis 3 Feb. 1988 8 p

(Contract MDA903-85-C-0215)
(AD-A193098) Avail: NTIS HC A02/MF A01 CSCL 07B

The goal of this research is to exploit the novel capability of the focused ion beam to implant dopants whose density is a function of the lateral position. Thus, Field Effect Transistors in Gallium Arsenide and Silicon can be fabricated with a gradient of doping from source to drain. We have fabricated and tested such graded FET's in GaAs and have fabricated Si devices up to the point of focused ion beam implantation. In addition, programs for modeling the devices on the computer have been written. Recently, we have conceived and fabricated a new device: a tunable Gunn oscillator which makes use of doping gradients. To carry out these implantations, we have further developed the performance of our focused ion beam machine. GRA

N88-27440# Stanford Univ., Calif. Dept. of Applied Physics.
SUPERCONDUCTING THIN FILMS, COMPOSITES AND JUNCTIONS Final Report, 1 May 1987 - 31 Oct. 1987
T. H. Geballe 25 Nov. 1987 9 p
(Contract F49620-82-C-0014)
(AD-A193123; AFOSR-88-0307TR) Avail: NTIS HC A02/MF A01 CSCL 20C

The successful synthesis of high-Tc YBa2Cu3O7 films by means of electron beam codeposition has been accomplished. Several important growth parameters have been surveyed in a preliminary way. The substrates investigated include Al2O3, ZrO2, MgO and SrTiO3. The films were characterized by resistivity measurements, X-ray diffraction, microprobe, and Rutherford backscattering analysis. Some TEM and critical current density studies were also carried out. The best results to date have been obtained on SrTiO3 substrates with which polycrystalline epitaxial growth has been achieved. Resistive superconducting transitions with zero resistance at 89.5K and a 2K width have been observed in these films. GRA

N88-27441# EIC, Inc., Norwood, Mass.
PREPARATION AND DEVELOPMENT OF ADVANCED BATTERY CATALYSTS Interim Report, Aug. 1986 - Feb. 1987
W. P. Kilroy, K. M. Abraham, and M. Alamgir 1 Oct. 1987 61 p
(Contract N60921-86-C-0209)
(AD-A193208; C-868; NSWC-TR-87-104) Avail: NTIS HC A04/MF A01 CSCL 10C

New catalysts which improve the discharge performance of Li/SOCl2 cells have been identified. These catalysts were obtained by thermal treatment of acetylene black carbon doped with the precursors, Co(NO3)2, manganese phthalocyanine (MnPc) or vanadium phthalocyanine oxide (VOPc). The latter two materials appear to be superior to many catalysts presently available for use in Li/SOCl2 cells. Compared with uncatalyzed cells, MnPc-containing cells showed a 60 percent increase in cell capacity and a 10 percent increase in cell voltage at room temperature. VOPc-containing cathodes increased the cell capacity by 50 percent and cell voltage by 10 percent under the same conditions. The use of VOPc also resulted in significant improvements in cell performance at low temperature, e.g., at -30 C. GRA

N88-27442# Office of the Under Secretary of Defense (Acquisitions), Washington, D.C. VHSIC Program Office.
VERY HIGH SPEED INTEGRATED CIRCUITS (VHSIC) Annual Report
31 Dec. 1987 163 p
(AD-A193225) Avail: NTIS HC A08/MF A01 CSCL 09A

The contents of this report on very high speed integrated circuits are as follows: Summary; Technology insertion; Phase 1; Phase 2: Submicron Technology; Phase 3 and Other Supporting Technologies; Information Sources; Policy; and Appendices: Policy Documents, References, VHSIC Points of Contact - Government, VHSIC Contracts - Points of Contact, Exhibitors at VHSIC Conferences, Glossary. GRA

N88-27443# Army Lab. Command, Fort Monmouth, N.J. Electronics Technology and Devices Lab.
QUARTZ CRYSTAL RESONATORS AND OSCILLATORS FOR FREQUENCY CONTROL AND TIMING APPLICATIONS
John R. Vig Jan. 1988 197 p
(AD-A193310; SLCET-TR-88-1) Avail: NTIS HC A09/MF A01 CSCL 14B

The goal of this document is to assist with presenting to the non-specialist the most frequently encountered concepts in frequency control and timing. The document originated as a set of hard-copies of presentation visuals (i.e., VU-graphs). Subjects covered include: applications, types of oscillators; quartz resonator properties; quartz growth, sweeping, and material characteristics; Q and its significance; resonator and oscillator stability, including aging, short term instability, frequency vs. temperature characteristics, oscillator circuit caused instabilities, frequency vs. temperature characteristics, oscillator circuit caused instabilities, frequency vs. drive level effects, acceleration effects, the effect of shock, and radiation effects; emerging technologies; atomic frequency standards; comparison of the major oscillator types; time and timekeeping; clock errors; relativistic time; time transfer; time and frequency subsystem; and other applications of quartz resonators. GRA

N88-27444# Massachusetts Inst. of Tech., Lexington. Lincoln Lab.
FORCED-CONVECTION, LIQUID-COOLED, MICROCHANNEL HEAT SINKS
Richard J. Phillips 7 Jan. 1988 286 p
(Contract F19628-85-C-0002)
(AD-A193337; TR-787; ESD-TR-87-023) Avail: NTIS HC A13/MF A01 CSCL 09A

Water-cooled, microchannel heat sinks have been developed that can dissipate heat loads in excess of 1000 W/sq. cm with maximum surface temperatures of less than 120 C. A theorectical model of microchannel heat sink thermal and fluid performance is presented. The model applies to small-, moderate-, and large-aspect-ratio channels, with fully developed and developing flow in the laminar and turbulent regimes. The channel surfaces may be smooth or roughened with repeated-ribs. Variable property effects have been included for the heat-sink material and the liquid coolant (compressibility effects have not been included). A new computer program has been written to compute the thermal and fluid performance for a large variety of coolant-flow-rate constraints and heat-sink designs. (A complete listing of this MICROHEX computer program is provided in this technical report). Thermal spreading at the perimeter of a surface heat source (e.g., an integrated circuit) is taken into account using simplified one-dimensional models. A novel concept of a Compensation Heater is presented that can enhance the temperature uniformity across IC heat sources. Procedures for fabricating microchannels in indium phosphide are presented. Indium phosphide microchannel heat sinks have been tested that have total thermal resistance as low as 0.072 C/(W/sq. cm) for a 0.25-cm square resistor heat source. GRA

N88-27445# Rensselaer Polytechnic Inst., Troy, N.Y. Dept. of Electrical Computer and Systems Engineering.
SILICON-ON-INSULATOR PIN DIODES Final Technical Report, Mar. 1986 - Jul. 1987
Edward W. Maby, Ronald J. Gutmann, Ted Letavic, and Stephen Wu Dec. 1987 107 p
(Contract F19628-85-K-0038)
(AD-A193359; RADC-TR-87-262) Avail: NTIS HC A06/MF A01 CSCL 09A

Microwave monolithic integrated circuit (MMMIC) technology using recrystallized silicon-on-insulator substrates would permit PIN diode phase shifters to be fabricated with higher power-handling capability and lower insertion loss than conventional MMIC control circuits using GaAs MESFETs. Moreover, at frequencies below 10 GHz, where substrate area requirements can be extensive, the silicon-on-insulator substrate technology can be less expensive. The research program stresses recrystallization of

silicon-on-alumina films, followed by growth of silicon epitaxial layers and fabrication of surface-oriented PIN diodes. In the second year of the program, we have accomplished the following: (1) Recrystallization of silicon-on-alumina with various encapsulation and stress-relief layers, using both an electron-beam system and a graphite strip heater; (2) Evaluation of the effect of stress on film quality, which indicates directions for improved device-quality films; (3) Design and initial fabrication of surface-oriented PIN diodes on single crystal silicon to demonstrate device design concept; (4) Evaluation of future directions for the research program. This report covers the second-year results. Particularly noteworthy is the first recrystallization of silicon-on-alumina films and the first fabrication of surface-oriented PIN diodes with doped polysilicon handles for P+ and N+ injecting contacts. GRA

N88-27446# Scientific Research Associates, Inc., Glastonbury, Conn.
STUDYING THE PHYSICS AND OPERATION OF MULTI-TERMINAL NEAR-MICRON AND SUB-MICRON LENGTH, HOT ELECTRON SEMICONDUCTOR DEVICES Final Report, Jun. 1981 - May 1986
H. L. Grubin, J. P. Kreskovsky, M. Meyyappan, and B. J. Morrison 15 Feb. 1988 494 p
(Contract N00014-81-C-0452)
(AD-A193380; SRA-R88-920010-F) Avail: NTIS HC A21/MF A01 CSCL 09A

The study encompasses a broad examination of transport in submicron and near-micron semiconductor devices through implementation of the moments of the Boltzmann transport equation and the semiconductor drift and diffusion equation. The study utilized advanced algorithms developed at Scientific Research Associates, and recommends development of a network of user based algorithms for closely combined theoretical/experimental interactions. GRA

N88-27447*# National Aeronautics and Space Administration. Langley Research Center, Hampton, Va.
FTMP DATA ACQUISITION ENVIRONMENT
Peter A. Padilla Jul. 1988 38 p
(NASA-TM-100636; NAS 1.15:100636) Avail: NTIS HC A03/MF A01 CSCL 09C

The Fault-Tolerant Multi-Processing (FTMP) test-bed data acquisition environment is described. The performance of two data acquisition devices available in the test environment are estimated and compared. These estimated data rates are used as measures of the devices' capabilities. A new data acquisition device was developed and added to the FTMP environment. This path increases the data rate available by approximately a factor of 8, to 379 KW/S, while simplifying the experiment development process. Author

N88-27448# Sandia National Labs., Albuquerque, N. Mex.
FAILURE ANALYSIS OF CHLORIDE SILENT POWER, LTD. PB CELLS
E. K. Beauchamp 1988 13 p Presented at the 7th DOE/EPRI Beta Battery Workshop, Toronto, Ontario, 1 Jun. 1988
(Contract DE-AC04-76DP-00789)
(DE88-010567; SAND-88-1129C; CONF-8806127-4; CONF-8806127) Avail: NTIS HC A03/MF A01

Two beta double prime alumina electrolyte tubes from Chloride Silent Power, Ltd. PB cells which failed in testing at Sandia National Laboratories, showed extensive cracking. The cracks initiated at the interior surface under localized stress apparently resulting from nonuniform ionic currents. The nonuniform currents apparently were a result of nonuniform wetting of the interior surface of the electrolyte. Failure of the sodium electrode seal, which introduced contaminants to the electrolyte surface, may have been reponsible for the nonuniform wetting. In one of the electrolytes, large grains, produced by overfiring, contributed to the failure. DOE

N88-27449# Sandia National Labs., Albuquerque, N. Mex.
COMPONENT STRESS DURING FREEZE/THAW CYCLING
J. W. Braithwaite, S. R. Subia, C. M. Stone, and W. F. Hammetter 23 May 1988 21 p Presented at the 7th DOE/EPRI Beta Battery Workshop, Toronto, Ontario, 1 Jun. 1988
(Contract DE-AC04-76DP-00789)
(DE88-011204; SAND-88-1321C; CONF-8806127-3) Avail: NTIS HC A03/MF A01

During the past year, the feasibility and usefulness of mathematically modeling the processes occurring in Na/S cells during freeze/thaw (F/T) cycling has been demonstrated with the identification of potential stress producing phenomena. The first strain measurements on functioning cells have been completed that have shown the variable nature of the positive-electrode materials, a factor that may account for the randomness of actual F/T induced failures. Physical property measurements have quantified the important effect the presence of the graphite felt can have on Young's modulus for sulfur. With the completion of the physical-property and strain measurements in the coming year, final modification will be made to the material models contained in the thermo-mechanical code. The strain data will be used to validate the accuracy of the component stress calculations. Once validated, this code can be used to identify and simulate important aspects of various design options and to determine the feasibility of proposed failure mechanisms. DOE

N88-27450# Sandia National Labs., Albuquerque, N. Mex.
FRICTION, WEAR AND ELECTRICAL CONTACT RESISTANCE OF PRECIOUS METAL ALLOYS
L. E. Pope, D. E. Peebles, and B. M. Barton 1988 29 p Presented at the ASM Symposium on Engineered Materials for Advanced Friction and Applications, Gaithersburg, Md., 1 Mar. 1988 Prepared in cooperation with Mound Lab., Miamisburg, Ohio
(Contract DE-AC04-76DP-00789)
(DE88-011244; SAND-87-2541C; CONF-880317-1) Avail: NTIS HC A03/MF A01

The preferred selection of precious metal electrical contact materials depends on the contact geometry, contact stress, test ambient values of electrical contact resistance and whether friction and/or wear must be controlled. Wiper-type contact couples that operate in dry hydrocarbon-free atmospheres, particularly if low and steady friction coefficients and minimal wear are required, are typically that of a palladium alloy pin (ASTM B540) sliding on a gold alloy plate (ASTM B541). These materials have a contact resistance of approximately ten milliohms and a friction coefficient less than 0.5 for the most common operational environments. Segregation of sulfur up to a few atomic percent to wear tracks formed on the gold alloy is not detrimental. The accumulation of larger concentrations of sulfur can form surface films of cuprous sulfide which increases the contact resistance to a few tens of milliohms. Large electrical contact resistances (greater than one ohm) are measured only when rider wear becomes dominant and ridges of Pd-containing material are formed in wear tracks. Ion implantation of carbon into the Au alloy decreases the friction coefficient without increasing the electrical contact resistance. DOE

N88-27451# Sandia National Labs., Albuquerque, N. Mex.
SODIUM/SULFUR CELL EVALUATION RESULTS
J. M. Freese and P. C. Butler 1988 19 p Presented at the 7th DOE/EPRI Beta Battery Workshop, Toronto, Ontario, 1 Jun. 1988
(Contract DE-AC04-76DP-00789)
(DE88-011488; SAND-88-1421C; CONF-8806127-5) Avail: NTIS HC A03/MF A01

Sandia National Laboratories has been evaluating the performance of various sodium/sulfur cells since 1985. The objectives of these evaluations were to characterize the performance of these cells, determine their longevity, identify performance or life limiting design problems, and conduct post-test analyses to determine the cause of failure. These results were communicated to each developer with recommendations for design improvements or other suggestions to resolve problem areas. DOE

N88-27452# Pennsylvania State Univ., University Park. Dept. of Mineral Engineering.
SOME EQUIVALENT CIRCUIT MODELS FOR AC IMPEDANCE ANALYSIS OF PYRITE/SOLUTION INTERFACE
S. Chander, J. Pang, and A. Briceno 1988 17 p Presented at the Symposium on Electrochemistry in Mineral and Metal Processing, Atlanta, Ga., 15 May 1988
(Contract DE-FG22-85PC-80523)
(DE88-010574; CONF-8805139-1) Avail: NTIS HC A03/MF A01

Several equivalent circuit models are considered for analysis of the AC impedance spectra of pyrite/solution interface. These models take into account the presence of coating layers and the contributions from surface roughness and diffusion. An optimization procedure is described to estimate the parameters of the equivalent circuit, namely, the value of various resistors and capacitors. The procedure can also be used to identify the equivalent circuit which best describes the measured impedance spectra. The impedance results of a pyrite electrode in sodium carbonate and borate solutions are analyzed in terms of the parameters of an equivalent circuit. Such an analysis can be used to distinguish the type of processes which control reactions at the electrode. DOE

N88-27453# Sandia National Labs., Albuquerque, N. Mex.
THERMAL CYCLING TESTS ON SURFACE-MOUNT ASSEMBLIES
C. W. Jennings Mar. 1988 22 p
(Contract DE-AC04-76DP-00789)
(DE88-007695; SAND-87-0873) Avail: NTIS HC A03/MF A01

The capability of surface-mount (SM) solder joints to withstand various thermal cycle stresses was evaluated through electrical circuit resistance changes of a test pattern and by visual examination for cracks in the solder after exposure to thermal cycling. The joints connected different electrical components, primarily leadless-chip carriers (LCCs), and printed wiring-board (PWB) pads on different laminate substrates. Laminate compositions were epoxy-glass and polyimide-glass with and without copper/Invar/copper (CIC) inner layers, polyimide-quartz, epoxy-Kevlar, and polyimide-Kevlar. The most resistant joints were between small LCCs (24 and 48 pins) and polyimide-glass laminate with CIC inner layers. Processing in joint formation was found to be an important part of joint resistant. Thermal cycling was varied with respect to both time and temperature. A few resistors, capacitors, and inductors showed opens after 500 30-min cycles between -65 C and 125 C. Appreciable moisture contents were measured for laminate materials, especially those of polyimide-Kevlar after equilibration in 100 percent relative humidity at room temperature. If not removed or reduced, moisture can cause delamination in vapor-phase soldering. DOE

N88-27454# Sandia National Labs., Albuquerque, N. Mex.
THE KINETICS OF CHARGE-TRANSFER REACTIONS ON PASSIVE LITHIUM ELECTRODES
Frank M. Delnick 1988 19 p Presented at the 4th International Meeting on Lithium Batteries, Vancouver, British Columbia, 23 May 1988
(Contract DE-AC04-76DP-00789)
(DE88-009256; SAND-87-2082C; CONF-880598-1) Avail: NTIS HC A03/MF A01

Lithium anodes are covered by LiCl passive films in SOCl2 solutions. At open-circuit, film growth is controlled by electronic processes within the film. Under discharge, solid-state ionic processes control the kinetic behavior of the electrode. These processes are not independent of one another. In this report, the interaction of electronic and ionic processes in LiCl passive films is reviewed. Special attention is directed to the role of lattice imperfections in establishing and controlling the mechanisms of electronic and ionic charge transport. DOE

N88-27455# Sandia National Labs., Albuquerque, N. Mex. Storage Batteries Div.
EFFECT OF THERMAL CYCLING ON CSPL (CHLORIDE SILENT POWER LTD.) SODIUM/SULFUR CELLS
J. W. Braithwaite, F. M. Stackpool, S. R. Subia, and C. M. Stone 23 May 1988 20 p Presented at the 7th DOE/EPRI Beta Battery Workshop, Toronto, Ontario, 1 Jun. 1988 Prepared in cooperation with Chloride Silent Power Ltd., Runcorn, United Kingdom
(Contract DE-AC04-76DP-00789)
(DE88-011205; SAND-88-1322C; CONF-8806127-2) Avail: NTIS HC A03/MF A01

The initial phase of a task being performed to improve the freeze/thaw (F/T) durability of CSPL cells has been completed. Extensive experimental testing along with preliminary thermomechanical modeling results show that intrinsic F/T durability of the CSPL-PB cell design is excellent. Additionally, the thermomechanical modeling calculations demonstrated that the PB design may be more tolerant to undesirable conditions than conventional, higher capacity cells with larger L/D ratios. However, the results following thermal cycling of the initial battery modules fabricated at CSPL were not as encouraging. F/T failure increased significantly over that observed in individual cell tests. This situation may have been caused by other factors (e.g., cell production rate scale-up, poor temperature uniformity) and may not represent the inherent durability of the modules. Future activity includes characterizing cell performance in modules, completing the detailed evaluation of cell behavior, and refining the thero-mechanical model. DOE

N88-27456# Johnson Controls, Inc., Milwaukee, Wis.
RECENT DEVELOPMENTS IN NICKEL HYDROGEN TECHNOLOGY
R. L. Beauchamp and J. D. Dunlop 1988 9 p Presented at the 33rd International Power Source Symposium, Cherry Hill, N.J., 13 Jun. 1988 Prepared in cooperation with Communications Satellite Corp., Clarksburg, Md.
(Contract DE-AC04-76DP-00789)
(DE88-011248; SAND-88-7093C; CONF-880665-2) Avail: NTIS HC A02/MF A01

A program to design and develop a multikilowatt-hour nickel hydrogen battery for storing electricity from photovoltaic or other power sources is continuing under a cost sharing contract with Sandia National Laboratories. The challenge has been to dramatically reduce the first cost of the battery to make it economically competitive, on a life-cycle cost basis, with other energy storage batteries used in terrestrial applications. The advantages offered by nickel hydrogen batteries are: (1) long cycle life, (2) no maintenance, and (3) a high tolerance to abuse. The last being the most important, implying that there is no need for a charge controller between the solar array and the battery. This would have a beneficial effect on the installation's long term reliability and cost. It also means that one can take full advantage of the maximum output of the solar array, in contrast to systems where the controller isolates the battery during times of maximum insolation. Couple this to the battery's excellent energy efficiency and there can be a significant reduction in the size of the array. In addition, since the state-of-charge is directly related to pressure, the battery can be used as a load management system. DOE

N88-27457# Lawrence Livermore National Lab., Calif.
A GaAs SOLID STATE DEVICE MODEL FOR HIGH POWER APPLICATIONS
W. J. Orvis, G. H. Khanaka, and J. H. Yee May 1988 11 p Presented at the 4th National High Power Microwave Conference, Monterey, Calif., 9 May 1988
(Contract W-7405-eng-48)
(DE88-011320; UCRL-97765; CONF-8805132-3) Avail: NTIS HC A03/MF A01

Due to their speed and radiation tolerance, gallium arsenide solid state devices are becoming more and more prevalent in consumer and defense electronics. Because of this increase in use, we have modeled gallium arsenide device operation in the high power, short pulse regime. This modeling includes avalanche generation, heat generation and flow, and inter-valley transfer of electrons. DOE

N88-27458# Sandia National Labs., Albuquerque, N. Mex.
LONG-PULSE, HIGH-POWER VIRCATOR EXPERIMENTS
P. D. Coleman and J. F. Aurand 1988 11 p Presented at the 4th National High Power Microwave Conference, Monterey, Calif., 9 May 1988
(Contract DE-AC04-76DP-00789)
(DE88-011787; SAND-87-3007C; CONF-8805132-6) Avail: NTIS HC A03/MF A01

An experiment designed to achieve long pulse virtual cathode oscillator (VCO) operation at approx. 700 MHz is described. Low frequency operation allowed operating at large A-K gaps and low current densities which facilitated the 800 ns pulsewidth operation. The VCO was configured in a 91 cm diameter drift tube and consisted of a 76 cm diameter planar cathode separated from an anode screen by an A-K gap that was varied from 5 to 10 cm. The diode was directly driven by a Marx generator with a resultant A-K voltage of 350 kV. Power was extracted axially from the cylindrical waveguide through a Lexan window. Application of a transverse magnetic field downstream of the virtual cathode swept the beam into the wall. This method of dumping the beam avoided plasma formation at the window and a resultant shortening of the radiated pulse. The frequency was observed to chirp from 600 to 800 MHz. The radiation pattern was measured by a seven element B-dot array located 2.4 m from the exit window. Comparison of these patterns to computer code predictions indicated a mix of TM sub 01 and TM sub 02 modes. DOE

N88-27459# Pacific Northwest Labs., Richland, Wash.
METAL-AIR BATTERY ASSESSMENT
R. K. Sen, S. L. VanVoorhees, and T. Ferrel May 1988 84 p
(Contract DE-AC06-76RL-01830)
(DE88-011361; PNL-6475) Avail: NTIS HC A05/MF A01

The objective of this report is to evaluate the present technical status of the zinc-air, aluminum/air and iron/air batteries and assess their potential for use in an electric vehicle. In addition, this report will outline proposed research and development priorities for the successful development of metal-air batteries for electric vehicle application. DOE

N88-27460# California Univ., Berkeley. Lawrence Berkeley Lab.
ESTIMATION OF POWER-ENERGY PLOTS FOR SECONDARY BATTERIES
F. R. McLarnon, E. J. Cairns, and A. R. Landgrebe May 1988 12 p Presented at the 33rd International Power Source Symposium, Cherry Hill, N.J., 13 Jun. 1988 Prepared in cooperation with DOE, Washington, D.C.
(Contract DE-AC03-76SF-00098)
(DE88-011922; LBL-25253; CONF-880665-3) Avail: NTIS HC A03/MF A01

A fast convenient method for estimating power plots for galvanic cells is discussed. Comparisons between various electrochemical couples can be made with this method, along with the evaluation of different cell designs, and parameters, such as sustained peak power, can be estimated. DOE

N88-27461# Argonne National Lab., Ill.
POST-TEST OBSERVATIONS ON CSPL (CHLORIDE SILENT POWER LIMITED) CELLS
J. A. Smaga and J. J. Marr 1988 10 p Presented at the 7th DOE/EPRI Beta Battery Workshop, Toronto, Ontario, 1 Jun. 1988
(Contract W-31-109-eng-38)
(DE88-011975; CONF-8806127-7) Avail: NTIS HC A02/MF A01

The sulfur electrode from Chloride Silent Power Limited (CSPL) sodium/sulfur cells has been extensively studied as one part of our post-test analysis program at Argonne National Laboratory (ANL). The sulfur in electrodes from charged cells tended to settle in the base of the electrode, but this tendency was dependent on the density of graphite fibers in the cylindrical section of the electrode. Analysis by energy dispersive spectroscopy was used to measure polarization-induced compositional gradients for rapidly cooled discharged cells. Quantitative determinations were also made of the gases within the sulfur electrode, and the composition of these gases was found to change with cycling. DOE

N88-27462# Lawrence Livermore National Lab., Calif.
THE DESIGN OF A DIGITAL EPROM OSCILLATOR FOR ELECTRICAL IMPEDANCE TOMOGRAPHY
M. Pihlman Apr. 1988 13 p
(Contract W-7405-eng-48)
(DE88-012243; UCID-21376) Avail: NTIS HC A03/MF A01

This paper presents the design and operation of an Eprom logic oscillator for an Electrical Impedance Tomography (EIT) imaging tool currently being used to image biological subjects at Lawrence Livermore National Laboratory (LLNL). Due to very low injection signal levels and relatively high noise present in biological subjects, it is very important that an EIT imaging device (also known as an Impedance Camera) be designed to recover amplitude (and phase) information from a noisy received signal and that the noise generated by the system be minimized. The ability to detect small received signals masked by noise requires a comparison of the transmitted signal to the noisy received signal and precise timing to synchronize these two signals. System noise can be reduced by synchronizing the application of the sinewave (to the subject) to the zero volt crossings of the transmitted sinewave. To address these demands, an Eprom oscillator was designed that not only generates an accurate 10 kHz to 50 kHz transmit sinewave, but, also, controls the switching of the sinewave (to coincide with its zero crossings), and generates accurately timed, adjustable, in-phase and quadrature, signals to assist in demodulating the noisy received signal. DOE

N88-27463# Sandia National Labs., Albuquerque, N. Mex.
STAR: SANDIA TIMING ANALYZER ROUTINE
B. L. Donham Mar. 1988 25 p
(Contract DE-AC04-76DP-00789)
(DE88-012412; SAND-88-0905) Avail: NTIS HC A03/MF A01

Existing tools for circuit simulation have proven to be inadequate to accommodate the continuing increase in complexity and size of integrated circuits. Such a deficiency in simulation capability exists due to the limitations of both logic simulators and circuit simulators. Logic simulators, which functionally verify circuit operation, are unable to verify timing with the accuracy required to produce reliable parts. Circuit simulators, which, in the past, have been used to provide accurate timing verification, cannot simulate entire circuits due to design size and speed bounds. This report introduces STAR, a computer aided design (CAD) tool which addresses the simulation problem for complex integrated circuits, and enables a system to be simulated on a logic simulator with the accuracy of a circuit simulator. DOE

N88-27464# Technische Univ., Munich (West Germany). Lehrstuhl fuer Fuegetechnik.
CONDUCTIVITY MECHANISM AND OPERATING BEHAVIOR OF ELECTRICALLY CONDUCTIVE ADHESIVES ON THE EXAMPLE OF A POWER TRANSISTOR Ph.D. Thesis [LEITUNGSMECHANISMUS UND FUNKTIONSVERHALTEN ELEKTRISCH LEITENDER KLEBUNGEN AM BEISPIEL EINES LEISTUNGSTRANSISTORS]
Heinz Brunner 1987 182 p In GERMAN
(ETN-88-92355) Avail: NTIS HC A09/MF A01

Electrical properties and operating parameters of epoxy adhesive bonding of transistor chips are compared with the same characteristics for soldering. Bonding procedure is optimized by technical and environmental evaluation of each method. Thermal cycling, moisture deposits, electrical conductivity and resistance, thermal resistance, tensile strength and stress, and bubble formation in the bonding layer are the main parameters examined. ESA

N88-27465# Stuttgart Univ. (West Germany). Fakultaet fuer Elektrotechnik.
INTEGRATED MAGNETIC FIELD SENSOR USING HIGH MAGNETOTRANSISTORS Ph.D. Thesis [INTEGRIERTE MAGNETFELDSENSOREN AUF DER BASIS DES LATERALEN MAGNETOTRANSISTORS]
Joachim Burghartz 1986 137 p In GERMAN
(ETN-88-92356) Avail: NTIS HC A07/MF A01

Galvanomagnetic effects in lateral magnetotransistors (LMT) with emphasis on Hall field and Hall motion, effects of geometric dimensions, and effects of injection are investigated. Magnetic field sensors with integrated signal processing are presented in the case of analog output signals and frequency analog output signals. Two applications of measurement by LMT concern a position sensor and a magnetic induction measurement. ESA

N88-27466# Technische Univ., Brunswick (West Germany). Naturwissenschaftlichen Fakultaet.
DETERMINATION OF QUANTUM CORRECTIONS FOR ELECTRICAL CONDUCTIVITY MECHANISM OF THREE DIMENSIONAL, PERTURBED COPPER COATINGS. WEAK LOCALIZATION AND ELECTRON-ELECTRON INTERACTION Ph.D. Thesis [BESTIMMUNG DER QUANTENKORREKTUREN ZUM ELEKTRISCHEN LEITUNGSMECHANISMUS DREIDIMENSIONALER, GESTOERTER KUPFERLEGIERUNGEN: SCHWACHE LOKALISIERUNG UND ELEKTRON-ELEKTRON-WECHSELWIRKUNG]
Peter Warnecke 1986 184 p In GERMAN
(ETN-88-92378) Avail: NTIS HC A09/MF A01

The abnormal behavior of the electrical resistance of a perturbed metallic conductor is experimentally studied. At low temperature, electrical resistance depends on temperature and magnetic field and is explained by quantum correction terms, electron-electron interactions, weak localization, and supraconductive oscillations. Experimental verification of quantum correction theory is performed in the case of a 3-dimensional system of cube coatings between 0.2 and 76K and a magnetic field less than 7.5T. ESA

N88-27365# Missouri Univ., Rolla. Dept. of Computer Science.
INVESTIGATION OF EXPERT SYSTEM DESIGN APPROACHES FOR ELECTRONIC DESIGN ENVIRONMENTS Final Report
Susan A. Poppens *In* Universal Energy Systems, Inc., United States Air Force Graduate Student Summer Support Program, Volume 2 Dec. 1987 12 p (For primary document see N88-27355 21-31)
Avail: NTIS HC A99/MF E03 CSCL 10C

N88-27393# Mitsubishi Electric Corp., Tokyo (Japan). Consumer Electronics Development Lab.
A 1/2-INCH HIGH-DEFINITION BASEBAND VCR
Michiyasu Ishibashi and Toshifumi Fujii *In its* Mitsubishi Electric Advance (R and D Edition), Volume 41 Dec. 1987 4 p (For primary document see N88-27388 21-31)
Avail: NTIS HC A03/MF A01 CSCL 09A

34 FLUID MECHANICS AND HEAT TRANSFER

Includes boundary layers; hydrodynamics; fluidics; mass transfer; and ablation cooling.

For related information see also *02 Aerodynamics* and *77 Thermodynamics and Statistical Physics.*

N88-27467 Texas Univ., Austin.
AN h-p ADAPTIVE FINITE ELEMENT METHOD FOR STEADY COMPRESSIBLE FLOW Ph.D. Thesis
Philippe Remy Bernar Devloo 1987 197 p
Avail: Univ. Microfilms Order No. DA8728540

An h-p adaptive finite element method is derived for the numerical simulation of the compressible Navier-Stokes equations. Several numerical algorithms have been compared for the simulation of one- and two-dimensional convection problems. An adaptive procedure has been developed for simultaneously refining the finite element grid and increasing the degree of the polynomial approximation. Adaptive strategies have been developed for both steady state and time dependent problems. Finally, convergence acceleration techniques such as a block Jacobi method, a multigrid acceleration technique for adaptively refined meshes and an element elimination technique have been developed and implemented. Representative 2-D problems in compressible viscous flow are solved. Dissert. Abstr.

N88-27468 Northwestern Univ., Evanston, Ill.
A STUDY OF FLUID-STRUCTURE PROBLEMS Ph.D. Thesis
Dennis Kang-por Lam [1987] 170 p
Avail: Univ. Microfilms Order No. DA8729010

The stability of structures with and without fluid load is investigated. A method is developed for determining the fluid load in terms of added structural mass. Finite element methods are employed to study the buckling of a cylindrical shell under axial compression and liquid storage tanks under hydrodynamic load. Both linear and nonlinear analyses are performed. Diamond modes are found to be the possible postbuckling shapes of the cylindrical shell. Local buckling including elephant-foot buckle and diamond buckle are found for the liquid storage tank models. Comparison between the linear and nonlinear results indicates a substantial difference in buckling mode shapes, though the buckling loads are close to each other. The method for determining the hydrodynamic mass is applied to the impeller stage of a centrifugal pump. The method is based on a linear perturbation technique which assumes that the disturbance in the flow boundaries and velocities caused by the motion of the structure is small. A potential method is used to estimate the velocity flow field. The hydrodynamic mass is then obtained by calculating the total force which results from the pressure induced by a perturbation of the structure. Dissert. Abstr.

N88-27469# Yale Univ., New Haven, Conn. Dept. of Computer Science.
COMPUTATIONAL FLUID DYNAMICS ON PARALLEL PROCESSORS
William D. Gropp and Edward B. Smith Dec. 1987 26 p Prepared in cooperation with United Technologies Research Center, East Hartford, Conn.
(Grant AF AFOSR-0098-86)
(AD-A192397; YALEU/DCS/RR-570) Avail: NTIS HC A03/MF A01 CSCL 20D

Greater computational power is needed for solving Computational Fluid Dynamics (CFD) problems of interest in engineering design. Parallel architecture computers offer the promise of providing orders of magnitude greater computational power. In this paper we quantify that promise by considering an explicit CFD method and analyze the potential parallelism for three different parallel computer architectures. The use of an explicit method gives us a best case analysis from the point of view of parallelism, and allows us to uncover potential problems in exploiting significant parallelism. The analysis is validated against experiments on three representative parallel computers. The results allow us to predict the performance of different parallel architectures. In particular, our results show that distributed memory parallel processors offer greater potential speedup. We discuss the import of our model for the development of parallel CFD algorithms and parallel computers. We also discuss our experiences in converting our model code to run on the three different parallel computers. GRA

N88-27470# Naval Research Lab., Washington, D.C.
NUMERICAL SIMULATION OF FUEL DROPLET INTERACTIONS AND BREAKUP Final Report, 1 Oct. 1984 - 30 Sep. 1987
Julian Tishkoff 17 Dec. 1987 92 p
(Contract MIPR-87-0003; AF Proj. 2308)
(AD-A192431; AFOSR-88-0247TR) Avail: NTIS HC A05/MF A01 CSCL 21B

Langrangian methods on triangular grids are developed and applied to the calculation of life history and dynamics of fuel droplets. With respect to numerical technology, the two-dimensional code SPLISH was converted to a VAX and then to a CRAY computer. New graphics systems were developed. Further testing of the basic SPLISH hydrodynamic algorithms as well as the surface tension algorithm were performed on internal gravity and capillary waves. A reorganization of the computer code will make the code user-friendly and portable. Now it should be much easier to use, and therefore useable on many new kinds of problems. First previously calculated flows of the distortion and breakup of a droplet due to differences in flow velocities between the droplet and the external media were recomputed to verify the conversion. Then a number of calculation of droplet distortion and breakup due to shear flows were made. Qualitative comparisons to experimental results were made for the case when the droplet density and external fluid density were nearly equal. Calculation and experiments showed small droplets torn off the large drop by the forces in the shear flow. GRA

N88-27471# Yale Univ., New Haven, Conn. Dept. of Computer Science.
IMPLICIT FINITE-DIFFERENCE SIMULATION OF AN INTERNAL FLOW ON A HYPERCUBE
Pierre Porta Jan. 1988 21 p
(Contract N00014-86-K-0310)
(AD-A192474; YALEU/DCS/RR-594) Avail: NTIS HC A03/MF A01 CSCL 20D

The purpose of this work is to study the solution of a 2-D compressible viscous fluid flow in a nozzle on a Hypercube. The analysis of the physical problem on a serial computer and an outline of its parallelization on the hypercube were previously detailed. This paper will detail all the steps of the parallelization and our results: speedups, efficiencies and communication time versus arithmetic time. GRA

N88-27472# Yale Univ., New Haven, Conn. Dept. of Computer Science.
IMPLICIT FINITE-DIFFERENCE SIMULATION OF AN INTERNAL FLOW IN A NOZZLE: AN EXAMPLE OF A PHYSICAL APPLICATION ON A HYPERCUBE
Pierre Porta Aug. 1987 23 p
(Contract N00014-86-K-0310)
(AD-A192475; YALEU/DCS/RR-553) Avail: NTIS HC A03/MF A01 CSCL 20D

We are studying here the numerical simulation of high Reynolds number internal, 2-D flow in a convergent-divergent nozzle, for a compressible, viscous fluid. An implicit finite-difference scheme is used to solve the parabolic approximation of the Navier-Stokes equations, so that the time steps are not severely limited by the small grid sizes needed for the computation of the viscous effects. After the resolution of this problem on a serial computer, we describe the first steps of the parallelization of this problem on a Hypercube parallel version of the ADI method. GRA

N88-27473# Cornell Univ., Ithaca, N.Y.
NUMERICAL EXPERIMENTS ON TURBULENT MIXING Final Report, Dec. 1984 - Dec. 1987
Stephen B. Pope 2 Feb. 1988 7 p
(Grant AF AFOSR-0083-85)
(AD-A192572; AFOSR-88-0256TR) Avail: NTIS HC A02/MF A01 CSCL 20D

Mixing in simple turbulent flows has been investigating using 64 cubed and 128 cubed Direct Numerical Simulations. In turbulent combustion, mixing by molecular transport is an essential process that is not well understood. Because mixing occurs on the smallest length and time scales it is difficult to study experimentally. Instead, we have employed direct numerical simulation of turbulence, initially for a conserved passive scalar in homogeneous isotropic turbulence. The Eulerian velocity and scalar fields are calculated from the exact evolution equations, and both Eulerian and Lagrangian statistics are deduced from the computed fields. A particle-tracking scheme, needed to extract Lagrangian information, has been implemented. The testing of a number of such particle tracking schemes has been completed with good results: accurate Lagrangian information can be extracted at a modest computational cost. In order to study processes in stationary turbulence, a forcing algorithm has been implemented. Tests on this scheme are complete, again with good results: the small scales are unaffected by the details of the forcing. Studies have been performed of: the mixing of a passive scalar; Lagrangian velocity, Acceleration and dissipation statistics; and mixing and combustion problems viewed in terms of surfaces. GRA

N88-27474# Naval Postgraduate School, Monterey, Calif.
THE DIFFUSION OF VORTICITY FROM A PLANE BOUNDARY Final Report, Dec. 1986 - Sep. 1987
A. V. Hershey 1988 27 p
(AD-A192706; NPS012-87-006) Avail: NTIS HC A03/MF A01 CSCL 20D

Any discontinuity in flow at a plane boundary is dispersed by the diffusion of vorticity into a boundary layer and wake. Experimental measurements in the past have been correlated with empirical formulations. A generalization gives both the horizontal component and the vertical component of the mean velocity. In the laminar sublayer the velocity is a solution of the diffusion equation. In the turbulent boundary layer the velocity can be expressed by a Fourier integral. In the free stream there is a vertical persistence of velocity. The computation of velocity is provided by subroutines. GRA

N88-27475# Air Force Avionics Lab., Wright-Patterson AFB, Ohio.
NOZZLE LIP EFFECTS ON GAS EXPANSION INTO THE PLUME BACKFLOW REGION Final Report, Sep. 1986 - Dec. 1987
D. P. Weaver and D. H. Campbell Feb. 1988 23 p
(AD-A192806; AFAL-TR-88-018) Avail: NTIS HC A03/MF A01 CSCL 20D

The Direct Simulation Monte Carlo technique has been used to investigate the detailed flow structure in the region near the lip of a nozzle flowing to vacuum. The results for a range of nozzle lip thicknesses and shapes for argon are presented. GRA

N88-27476# Illinois Inst. of Tech., Chicago. Fluid Dynamics Center.
COUPLED EXPERIMENTAL AND THEORETICAL INVESTIGATIONS OF INSTABILITY, CHAOS AND TURBULENCE IN AN AXISYMMETRIC JET FLOW Final Technical Report, 15 Apr. 1986 - 15 Oct. 1987
Thomas C. Corke, Hassan M. Nagib, and Simon Rosenblat 22 Jan. 1988 9 p
(Grant AF-AFOSR-0165-86)
(AD-A192943; AFOSR-88-0293TR) Avail: NTIS HC A02/MF A01 CSCL 20D

The theoretical and experimental investigations on the instability, routes to chaos and transition to turbulence of an anisymmetric jet flow has been investigated. The first general task has involved the search for evidence of strange attractors in the unsteady dynamics of naturally (stochastically) and periodically excited jets. A special case of the periodically excited jets were ones having enhanced acoustic feedback. As part of this effort, substantial computer software was developed to analyze velocity time-series to determine attractor dimensions, Lyapunov exponents and topological entropy. Under conditions with strong feedback and without forcing, long highly sampled time-series were analyzed. Using independent measures of attractor dimension by a modified Grassberger-Procaccia algorithm and the singular decomposition method of Broomhead and King, the low-dimensional nature of the dynamics of the initial shear layer up to the point of pairing were confirmed. On the theoretical front, the first part of the work, now completed, dealt with the instability of thin inviscid circular shear layers. GRA

N88-27477# Virginia Polytechnic Inst. and State Univ., Blacksburg. Dept. of Aerospace and Ocean Engineering.
EXPERIMENTAL STUDY OF UNSTEADY SEPARATING TURBULENT BOUNDARY LAYERS Final Technical Report
N. K. Agarwal and R. L. Simpson Feb. 1988 189 p
(Grant AF-AFOSR-0134-24)
(AD-A192997; AFOSR-88-0271TR) Avail: NTIS HC A09/MF A01 CSCL 20D

A detailed experimental study of two large amplitude unsteady freestream flows and a third unsteady flow produced by an oscillating roof damper is reported. Detailed ensemble-averaged velocity and turbulence measurements were made using hot-wire and laser anemometers. While the primary function of this report is to present and document these data, some discussion of the results and a number of data plots are presented. The reduced data are available on computer diskettes. Upstream of detachment at the phases with no flow reversal, the flows are quasi-steady. For the large amplitude flows, at low velocity phases some flow reversal occurs upstream of detachment, which was not observed in the moderate amplitude flow studied by Simpson et al. (1983). After the beginning of detachment, large amplitude and phase variations develop through each flow. Huge backflow velocities, as large as free-stream, were measured. GRA

N88-27478# Washington Univ., Seattle. Dept. of Aeronautics and Astronautics.
TURBULENCE STRUCTURE OF MIXING SWIRLING FLOWS Annual Report, Oct. 1986 - 30 Sep. 1987
Frederick B. Gessner 18 Dec. 1987 7 p
(Grant AF AFOSR-0273-85)
(AD-A193063; AFOSR-88-0488TR) Avail: NTIS HC A02/MF A01 CSCL 20D

Modifications to the swirling jet flow facility and mean flow data taken in the initial mixing region are described. Measurements are made at six streamwise locations downstream of the nozzle exit for three different initial mass flow rate ratios. The data were analyzed in order to calculate static pressure profiles, total and component velocity profiles, and local wall shear stress values. The results show that an axially-directed outer stream inhibits the spreading rate of the swirling inner stream and the decay of the swirl within that stream. The results also show that near-wall similarity exists in flow near the centerbody, so that the two dimensional form of the law-of-the-wall, when applied to the total velocity, can serve as a valid wall function for prediction. GRA

N88-27479# Stanford Univ., Calif. Dept. of Mechanical Engineering.
THE HEAT TRANSFER AND FLUID DYNAMICS OF CONCAVE SURFACE CURVATURE Annual Report, 1 Jan. - 31 Dec. 1987
J. P. Johnston and R. J. Moffat 10 Mar. 1988 12 p
(Grant AF AFOSR-0073-86)
(AD-A193064; AFOSR-88-0503TR) Avail: NTIS HC A03/MF A01 CSCL 20M

The overall goal of this project is study convective heat transfer and fluid-mechanics in a concavely curved turbulent boundary layer. The objective is to identify the mechanisms whereby concavity increases surface heat transfer. Progress during the past year has centered on the recently added goal of studying the combined effects of moderate levels of grid-generated turbulence and concave curvature. Overall results from the fluid-mechanics section of the project are that grid-generated turbulence increases the skin friction, but does not alter the near-wall mean velocity scaling or the near-wall levels of the velocity fluctuations. The heat transfer measurements are showing that the Stanton number is increased by the grid-generated turbulence with the combined effects of curvature and the additional turbulence producing the largest increase. GRA

N88-27480# Advisory Group for Aerospace Research and Development, Neuilly-Sur-Seine (France).
AERODYNAMICS OF HYPERSONIC LIFTING VEHICLES: FLUID DYNAMICS PANEL AGARD SYMPOSIUM
S. M. Bogdonoff, H. Hornung, ed., and R. E. Whitehead, ed. (Office of Naval Research, Arlington, Va.) Apr. 1988 20 p Symposium held in Bristol, United Kingdom, 6-9 Apr. 1987
(AGARD-AR-246; ISBN-92-835-0453-4) Copyright Avail: NTIS HC A03/MF A01

This report reviews and evaluates the Fluid Dynamics Panel AGARD Symposium entitled, Aerodynamics of Hypersonic Lifting Vehicles, held 6 to 9 June 1987 in Bristol, UK. The purpose of the Symposium was to assess the technology status in the field of hypersonics after a comparative lull in the past decade. The author addresses each of the papers separately and makes general comments on the 5 major topic sessions. The limitations of test facilities for experimental studies at high Mach numbers were clearly evident. New developments in computational fluid dynamics provide possibilities that did not exist in the past. The reviewer stressed the areas that need special emphasis in the future. The papers presented at the Symposium are published in AGARD Conference Proceedings CP-429 and are listed in an Appendix to this report. Author

N88-27481# Naval Underwater Systems Center, Newport, R.I.
CHARACTERIZATION OF ACCELERATING PIPE FLOW Final Report
Paul J. Lefebvre 1 Mar. 1988 240 p
(AD-A193065; NUSC-TD-6666) Avail: NTIS HC A11/MF A01 CSCL 20D

A unique series of experiments was conducted to determine the effects of constant acceleration on the flow in a 5-cm-diameter pipe. These experiments, which differed substantially from those of previous researchers, investigated such phenomena as transition to turbulence and the general physics of the effect acceleration has on various flow parameters such as wall shear stress, velocity profile, and turbulence intensity profile. The experiments were conducted in the Naval Underwater Systems Center Flow Loop Facility, which was designed and built for this study. This facility provided the capability of programmed acceleration via a control system that uses the position of a downstream control valve for transient flow control. Based on the data collected during the experiments along with a linear momentum analysis, it was determined that hot-film wall shear stress sensors can be accurately used in transient flows up to at least 1 g acceleration. GRA

N88-27482# Ben Gurion Univ. of the Negev, Beersheva (Israel).
EXPERIMENTAL INVESTIGATION OF THE REFLECTION OF A PLANAR SHOCK WAVE OVER A DOUBLE WEDGE Periodic Report No. 1, 1 Oct. - 30 Nov. 1987
G. Ben-Dor 30 Nov. 1987 2 p
(Contract DAJA45-87-C-0042)
(AD-A193078; R/D-5838-PH-01) Avail: NTIS HC A02/MF A01 CSCL 20D

Work completed during the reported period: Experiments of the reflection of a planar shock wave over various double wedge combinations have been conducted; The experiments were conducted with M sub i = 1.3 and a variety of theta 1 sub w - theta 2 sub w combinations; and the experiments were recorded using schlieren photography, shadowgraphs and high speed photography. GRA

N88-27483# Scientific Research Associates, Inc., Glastonbury, Conn.
A NAVIER-STOKES STUDY OF CASCADE FLOW FIELDS INCLUDING INLET DISTORTION AND ROTATING STALL Final Report, Sep. 1984 - Aug. 1987
F. Davoudzadeh, N. S. Liu, S. J. Shamroth, and S. J. Thoren Dec. 1987 158 p
(Contract F33615-84-C-2479)
(AD-A193109; AFWAL-TR-87-2077) Avail: NTIS HC A08/MF A01 CSCL 20D

A two-dimensional, unsteady, Navier-Stokes computer code has been developed and applied to general cascade problems including inlet distortion and rotating stall. The code allows an arbitrary number of passages with periodicity conditions applied below the first and above the last passage, thus allowing flows in the computational domain to differ on a passage-by-passage basis.

Calculations were performed for both C-grid and H-grid coordinate systems for single passage steady flows, multiple passage flows with steady and time-dependent inlet distortions and for multiple passage flows with a disturbance first imposed and then removed. This latter set of calculations demonstrated the ability of the procedure to simulate rotating stall flow fields. Calculations for conditions of incipient rotating stall showed good agreement with data for a J-79 stator set. GRA

N88-27484# Texas Univ., Austin. Dept. of Aerospace Engineering and Engineering Mechanics.
PHYSICAL MECHANISMS IN SHOCK-INDUCED TURBULENT SEPARATED FLOW Annual Report, 1 Mar. 1986 - 30 Nov. 1987
D. S. Dolling 15 Dec. 1987 45 p
(Grant AF AFOSR-0112-86)
(AD-A193165; AFOSR-88-0292TR) Avail: NTIS HC A03/MF A01 CSCL 20D

It has been demonstrated that the flow downstream of the moving shock is separated and that the foot of the shock is effectively the instantaneous separation point. The shock induced turbulent separation is an intermittant process and the separation line indicated by surface tracer methods, such as kerosene-lampblack, is a downstream boundary of a region of intermittent separation. GRA

N88-27485# Cornell Univ., Ithaca, N.Y. Mathematical Sciences Inst.
EFFECTS OF NUMERICAL DISSIPATION ON FINITE-VOLUME SOLUTIONS OF COMPRESSIBLE FLOW PROBLEMS
D. A. Caughey and E. Turkel 7 Mar. 1988 13 p
(Contract DAAG29-85-C-0018)
(AD-A193173; ARO-23306.156-MA) Avail: NTIS HC A03/MF A01 CSCL 20D

The finite-volume scheme has been used widely to approximate the equations of compressible fluid flow. The evaluation of the fluxes in such schemes is equivalent to that provided by a centered difference scheme, and is second-order accurate if the mesh is sufficiently smooth. In order to prevent odd/even decoupling of the solution and to capture shock waves it is necessary to add some from of numerical dissipation, which normally is done using an adaptive blend of second and fourth differences of the solution. The present paper will focus upon the effects of various forms of the dissipative terms upon solution accuracy especially when the mesh is not smooth. Results for transonic flows past airfoils are used as test cases to evaluate the effect of the dissipative terms. The spatial discretization used in the present work is based upon the finite-volume scheme of Jameson, Schmidt, and Turkel (1) (see also Jameson (2), and the resulting difference equations are solved using either the explicit, Runge-Kutta time stepping scheme of that work, or the Diagonalized Alternating Direction Implicit (DADI) scheme of Caughey (3), Both schemes are developed with the framework of the multigrid algorithm, the formulation of which follows that of Jameson (4.). In the following section, the elements of the finite-volume method will be described, focusing on those aspects relevant to the incorporation of the numerical dissipation. GRA

N88-27486# SRI International Corp., Menlo Park, Calif.
USER'S MANUAL FOR C-HEMP: A TWO-DIMENSIONAL WAVE PROPAGATION CODE. VOLUME 1: DESCRIPTION AND DERIVATIONS OF THE CODE Contract Report, Sep. 1983 - Oct. 1985
L. Seaman, T. Cooper, and D. Erlich Oct. 1987 281 p
(Contract DAAK11-83-R-0105)
(AD-A193197; BRL-CR-587) Avail: NTIS HC A13/MF A01 CSCL 20D

C-HEMP is a two-dimensional finite-difference computer program for treating stress waves propagation, in either planar or axisymmetric flow, caused by impacts or explosive detonation. It was designed, implemented, and tested at SRI International under a three-year contract for the U.S. Army Ballistic Research Laboratory to develop a computational model for armor penetration. The manual for the C-HEMP stress wave propagation code consists of two volumes. This first volume contains the descriptions and derivations of the code. GRA

N88-27487# Wisconsin Univ., Madison. Center for Mathematical Sciences.
COMPUTATIONAL BOUNDARY CONDITIONS FOR THE INCOMPRESSIBLE NAVIER-STOKES EQUATIONS IN CHANNELS AND PIPES Technical Summary Report
Gerardo A. Ache Oct. 1987 38 p
(Contract DAAL03-87-K-0028)
(AD-A193356; CMS-TSR-88-12) Avail: NTIS HC A03/MF A01 CSCL 20D

This document derives inflow and outflow boundary conditions for the incompressible Navier-Stokes equations in cylindrical geometries. The purpose of these boundary conditions is to allow computations in a finite domain, which model flow in an unbounded domain, in a way that the accuracy of the finite difference solution is retained, making the computation more efficient. An approach previously used presents the solution asymptotically, far downstream and upstream, as a series expansion which involves eigenvalues and eigenfunctions. These eigensolutions satisfy certain systems of ordinary differential equations. The boundary conditions are represented by a family of differential operators in a way similar to what was done by Bayliss, Gunzberger and Turkel. To demonstrate the effectiveness of these boundary conditions we applied them in numerical computations of the incompressible Navier-Stokes equations in a channel with a step and in a pipe with a sudden enlargement of the cross section. To numerically solve the Navier-stokes equations we used a second order accurate finite difference scheme, also the boundary operators were approximated using second order accurate finite difference formulas. The numerical results show the effectiveness and the increase accuracy obtained by using the higher-order boundary conditions. GRA

N88-27488# Wisconsin Univ., Madison. Center for Mathematical Sciences.
NUMERICAL TREATMENT OF THE PRESSURE SINGULARITY AT A RE-ENTRANT CORNER Technical Summary Report
Gerardo A. Ache Oct. 1987 20 p
(Contract DAAL03-87-K-0028)
(AD-A193357; CMS-TSR-88-11) Avail: NTIS HC A03/MF A01 CSCL 20D

At re-entrant corners the pressure has a singularity for incompressible viscous flow. In fluid flow computations there are geometries that have re-entrant corners, and for which it is needed to provide an appropriate value for the pressure at such a corner when a finite difference method dealing with the primitive formulation is used. In this paper we address the problem of finding an efficient strategy for computing pressure values at a re-entrant corner which applied to Strikwerda's second-order numerical method for solving the Stokes and Navier-Stokes equations. The pressure at the corner is regarded as a double valued function. Also we examine Moffatt's solution for the Stokes's problem near a step where the pressure becomes unbounded as the re-entrant corner is approached. We show that this strategy models very well the pressure singularity making the computation more amenable and efficient. GRA

N88-27489# Los Alamos National Lab., N. Mex.
INVESTIGATION OF THE QUASI-STEADY APPROACH USED IN TRANSIENT TWO-PHASE FLOW ANALYSIS
K. D. Pasamehmetoglu and R. A. Nelson 1988 24 p Presented at the 25th American Society of Mechanical Engineers/American Inst. of Chemical Engineers/American Nuclear Society National Heat Transfer Conference, Houston, Tex., 24 Jul. 1988
(Contract W-7405-eng-36)
(DE88-004303; LA-UR-87-4161; CONF-880724-3) Avail: NTIS HC A03/MF A01

Implications of the quasi-steady approach to numerical solutions of two-phase flow problems are addressed by the application of basic principles. First, a simple criterion to determine the limitations

of the quasi-steady approach is discussed. This criterion is used to determine the minimum time-step size required during the quasi-steady solution. Using this same concept, a method for making truly transient problems artificially quasi-steady is developed. Finally, these concepts are applied to a simple interfacial heat-transfer problem. The numerical instability that results from the quasi-steady approach during the explicit solution of this problem is investigated. DOE

N88-27490*# Old Dominion Univ., Norfolk, Va. Institute for Computational and Applied Mechanics.
INVESTIGATION OF VISCOUS/INVISCID INTERACTION IN TRANSONIC FLOW OVER AIRFOILS WITH SUCTION
C. S. Vemuru and S. N. Tiwari Apr. 1988 124 p
(Grant NAG1-363)
(NASA-CR-183112; NAS 1.26:183112; ODU/ICAM-88-101)
Avail: NTIS HC A06/MF A01 CSCL 20D

The viscous/inviscid interaction over transonic airfoils with and without suction is studied. The streamline angle at the edge of the boundary layer is used to couple the viscous and inviscid flows. The potential flow equations are solved for the inviscid flow field. In the shock region, the Euler equations are solved using the method of integral relations. For this, the potential flow solution is used as the initial and boundary conditions. An integral method is used to solve the laminar boundary-layer equations. Since both methods are integral methods, a continuous interaction is allowed between the outer inviscid flow region and the inner viscous flow region. To avoid the Goldstein singularity near the separation point the laminar boundary-layer equations are derived in an inverse form to obtain solution for the flows with small separations. The displacement thickness distribution is specified instead of the usual pressure distribution to solve the boundry-layer equations. The Euler equations are solved for the inviscid flow using the finite volume technique and the coupling is achieved by a surface transpiration model. A method is developed to apply a minimum amount of suction that is required to have an attached flow on the airfoil. The turbulent boundary layer equations are derived using the bi-logarithmic wall law for mass transfer. The results are found to be in good agreement with available experimental data and with the results of other computational methods. Author

N88-27491# Sandia National Labs., Albuquerque, N. Mex.
FORCES AND MOMENTS ON A SLENDER, CAVITATING BODY
C. E. Hailey, E. L. Clark, and R. J. Buffington 1988 5 p Presented at the Cavitation and Multiphase Forum, Cincinnati, Ohio, 24 Jul. 1988
(Contract DE-AC04-76DP-00789)
(DE88-007208; SAND-88-0067C; CONF-880740-3) Avail: NTIS HC A02

Recently a numerical code has been developed at Sandia National Laboratories to predict the pitching moment, normal force, and axial force of a slender, supercavitating shape. The potential flow about the body and cavity is calculated using an axial distribution of source/sink elements. The cavity surface is assumed to be a constant pressure streamline, extending beyond the base of the model. Slender body approximation is used to model the crossflow for small angles of attack. A significant extension of previous work in cavitation flow is the inclusion of laminar and turbulent boundary layer solutions on the body. Predictions with this code, for axial force at zero angle of attack, show good agreement with experiments. An experiment was designed to measure forces and moments on a supercavitation shape. The primary reason for the test was to obtain much needed data to benchmark the hydrodynamic force and moment predictions. Since the numerical prediction is for super cavitating shapes at very small cavitation numbers, the experiment was designed to be a ventilated cavity test. This paper describes the experimental procedure used to measure the pitching moment, axial and normal forces, and base pressure on a slender body with a ventilated cavity. DOE

N88-27492# Purdue Univ., West Lafayette, Ind. Boiling and Two-Phase Flow Lab.
EFFECTS OF SURFACE TENSION AND CONTACT ANGLE ON SENSIBLE HEATING AND BOILING INCIPIENCE IN DIELECTRIC FALLING FILMS
W. J. Marsh and I. Mudawwar 1988 9 p Presented at the Session on Boiling Phenomena in Electronic Equipment, Houston, Tex., 1 Jul. 1988
(Contract DE-FG02-85ER-13398)
(DE88-007057; DOE/ER-13398/9; CONF-880744-1) Avail: NTIS HC A02

Predicting the point of incipient boiling is of paramount importance for reliable operation of liquid-cooled microelectronic heat sources during power transients. This study focuses on heat transfer from a simulated multichip module to a falling film. Experiments have been performed to develop an understanding of the influence of surface tension and wetting characteristics in sensible heat transfer and boiling incipience in free-falling dielectric (FC-72) liquid films. A correlation for the space-average heat transfer coefficient is presented which shows clear departure of FC-72 data from correlations obtained for fluids with higher surface tension. The boiling results reveal that the vanishingly small contact angle of FC-72 precluded the application of correlations currently employed to predict incipience. Also, the temperature overshoot commonly encountered upon boiling incipience in wetting fluids was nonexistent in all the experimental runs. DOE

N88-27493# Gosudarstvennyi Komitet po Ispolzovaniyu Atomnoi Energii, Obninsk (USSR). Fiziko-Ehnergeticheskij Inst.
HEAT AND MASS TRANSFER IN A TRANSPORT CHANNEL
S. A. Matyushina and A. N. Opanasenko 1987 7 p In RUSSIAN
(DE88-701968; FEI-1828) Avail: NTIS (US Sales Only) HC A02/MF A01

Heat and mass transfer in transport channels of a fast reactor charging complex is investigated. Results of studying mass transfer and temperature conditions in a model channel 430 mm in diameter and with relative length of 9.3 connecting heated gas (argon) cavity and environment are presented. A mathematical model for calculating fields of temperature and gas velocities with provision for diffusion based on solution of the Navier-Stokes equations in the Helmholtz form is considerd. The data obtained show that at similar conditions mass transfer is characterized with instability; it is proportional in value to a temperature difference between gas cavities. Mounting of a cooling heat exchanger in the upper channel section along its 1/3 length leads to a static gaseous lock abruptly decreasing mass transfer. DOE

N88-27494# Universidade do Estado do Rio de Janeiro (Brazil). Coordenacao dos Programas de Pos-Graduacao de Engenharia.
STREAM FUNCTION-VORTICITY FINITE ELEMENTS AND THE RESOLUTION OF THE NAVIER-STOKES EQUATIONS M.S. Thesis
R. C. C. deAlmeida Jul. 1987 121 p In PORTUGUESE; ENGLISH summary
(DE88-702318; INIS-BR-1054) Avail: NTIS (US Sales Only) HC A06/MF A01

A stream function-vorticity finite element formulation for the solution of the Navier-Stokes equations is proposed. The present work shows a procedure to solve the problem posed by the no-slip conditions on solid frontiers which can also be applied to flow problems in a multi-connected domain. Moreover, a methodology to solve the pressure is developed using the stream function-vorticity approximate solution. Numerical experiments were conducted for some steady and unsteady problems and the performance of the proposed methods is discussed. DOE

N88-27495# Joint Inst. for Nuclear Research, Dubna (USSR). Dept. of New Acceleration Methods.
MASS FLOW RATE INFLUENCE ON VOID FRACTION OF TWO-PHASE HELIUM FLOW
Gym Sek Ko, I. S. Mamedov, and Yu. P. Filippov 1987 14 p

In RUSSIAN; ENGLISH summary
(DE88-702456; JINR-R-8-87-505) Avail: NTIS (US Sales Only) HC A03/MF A01

Based on the minimum entropy production principle an analysis of mass flow rate influence on void fraction of two-phase adiabatic flows is made. The friction factor role and fraction of liquid entrained into vapor steam ones are demonstrated. The results of helium two-phase flow calculations as well as the comparison with analogous reference data are presented. The engineering calculation technique for void fraction of helium two-phase flows is suggested. DOE

N88-27496# Sandia National Labs., Albuquerque, N. Mex.
PREDICTION OF VELOCITY AND TEMPERATURE PROFILES IN THERMALLY DRIVEN GRAVITY CURRENTS APPLIED TO STRATIFIED THERMAL STORAGE TANKS
J. T. Nakos and M. W. Wildin 1988 27 p Presented at the 1st National Fluid Dynamics Congress, Cincinnati, Ohio, 24 Jul. 1988 Prepared in cooperation with New Mexico Univ., Albuquerque
(Contract DE-AC04-76DP-00789)
(DE88-004452; SAND-87-3061C; CONF-880716-2) Avail: NTIS HC A03/MF A01

It has been demonstrated that one way of producing thin thermoclines in a chilled water thermal storage tank is by introducing the fluid in the form of a gravity current. Early in the flow the gravity current is controlled mainly by inertia and buoyancy forces, producing what is called the inertia-buoyancy (I-B) regime. Subsequently, the viscous force dominates inertia, and the flow is governed by viscous and buoyancy forces, resulting in the viscous-buoyancy (V-B) regime. In the work to be reported, vertical profiles of velocity and temperature in two-dimensional, thermally driven, constant inflow gravity currents were studied. This was done to provide a basis for understanding the initial stages of the formation of a thermocline. The gravity current was modelled with three regions, the head, the main body and the mixed region. In this analysis, the head was ignored and a laminar flow model was used to predict velocity and temperature profiles in the main body near the floor and in the mixed region above the main body and behind the head. Analytical and numerical models were developed for both regimes. DOE

N88-27497# Sandia National Labs., Albuquerque, N. Mex.
CAVITATION INCEPTION IN A TURBULENT SHEAR FLOW
T. J. OHern 1988 34 p Presented at the 1st National Fluid Dynamics Congress, Cincinnati, Ohio, 24 Jul. 1988
(Contract DE-AC04-76DP-00789)
(DE88-011486; SAND-88-1110C; CONF-880716-5) Avail: NTIS HC A03/MF A01

Experimental investigations were made into the inception processes in a large turbulent free shear layer generated by a sharp edged plate in a water tunnel at Reynolds numbers up to 2 x 1000000. Optical techniques were used to study the relation of cavitation inception to flow characteristics, in particular to the coherent vortices of the free shear layer turbulent structure. Two distinct types of vortex motion were evident, primary spanwise and secondary longitudinal vortices. Cavitation inception consistently occurs in the secondary shear layer vortices and more fully developed cavitation is visible in both structures, with the streamwise cavities typically confined to the braid regions between adjacent spanwise vortices. Measurements of fluctuating pressures in the turbulent shear layer were made by holographically monitoring the size of air bubbles injected into the non-cavitating flow, showing that pressure fluctuations were much stronger than previously reported, with positive and negative pressure peaks as high as 3 times the freestream dynamic pressure, sufficient to explain the occurrence of cavitation inception at high values of the inception index. The occurrence of inception in the secondary vortices of the shear layer, and previous reports of velocity dependence of these cores, may provide the key to explaining the commonly observed Reynolds number scaling of the inception index in shear flows. DOE

N88-27498# Lawrence Livermore National Lab., Calif.
A FAST VORTEX CODE FOR COMPUTING 2-D FLOW IN A BOX
S. B. Baden and E. G. Puckett 29 Jun. 1988 21 p Presented at the 1st National Fluid Dynamics Congress, Cincinnati, Ohio, 24 Jul. 1988
(Contracts W-7405-eng-48; DE-AC03-76SF-00098)
(DE88-011732; UCRL-98638; CONF-880716-6) Avail: NTIS HC A03/MF A01

We present a fast, accurate hybrid vortex method for computing incompressible, viscous flow at large Reynolds numbers in a two-dimensional bounded domain. The random vortex method is used to model the flow away from the boundary and the vortex sheet method is used to model the flow near boundary. Our implementation of these methods exploits the localized nature of interactions among vortex elements in each of the respective regions of the domain. A local corrections approximation is used to accelerate the velocity computation in the interior. It is substantially faster than other methods of comparable accuracy and can economically handle tens of thousands of vortex elements. We evaluate the method on the flow in a box due to a central stationary vortex. The running time for this problem is roughly linear in the number of vortex elements and results are in good qualitiative agreement with other numerical solutions of the same problem. DOE

N88-27499 Cornell Univ., Ithaca, N.Y.
KINETIC THEORY FOR PLANE FLOWS OF ROUGH, INELASTIC, CIRCULAR DISKS Ph.D. Thesis
Masami Nakagawa 1988 113 p
Avail: Univ. Microfilms Order No. DA8804633

The behavior of a rapidly deforming granular assembly composed of rough, inelastic circular disks is considered. The classical kinetic theory is extended in order to account for the difference between a collision of point masses and that of grains of finite size. The collision dynamics used in determining the collisional changes of particle properties takes into account the inelastic and frictional nature of the disks. A general transport equation for means of particle properties is formulated and the balance laws of interest are derived from it. The balance laws are compared with those obtained from the continuum description. There, the classical notion of continuous matter is also extended so that the flow behavior of an aggregate of discrete particles can be described. Particular attention is focused on the relationship between the internal creation of spin and the antisymmetric part of the stress. In analyzing a simple shear flow, the statistical averaging scheme is improved by introducing the collison angle gamma. This incorporates the geometrical dependence of a collision into the statistics. Finally, the inadequacy of the Maxwellian velocity distribution function for a system with significant energy dissipation is recalled and an anisotropic Maxwellian velocity distribution is introduced in order to deal with plane flows of rough, inelastic, circular disks. A comparison is made with the results obtained by computer simulations. Dissert. Abstr.

N88-27500# Kentucky Univ., Lexington.
DETERMINATION OF THE LOCAL HEAT-TRANSFER CHARACTERISTICS ON GLAZE ICE ACCRETIONS ON A CYLINDER AND A NACA 0012 AIRFOIL Ph.D. Thesis
Martin Rabindra Pais 1987 172 p
Avail: Univ. Microfilms Order No. DA8802030

Laboratory scale experiments conducted in the subsonic wind tunnel facility at the University of Kentucky are discussed. Experimental convective local heat transfer coefficients were obtained for a simulated, full scale, selected set of 2, 5, 15 minute glaze ice models on a cylinder, and 0, 5 minute glaze ice models on a NACA 0012 airfoil. A steady state heat flux method was employed. The results show very good quantitative and qualitative agreement. The local heat transfer rate increases with increasing Reynolds number and as the ice grows shows a decreasing trend within the cup-like region formed in the forward zone. An attempt was made to define surface roughness by applying two-dimensional Fourier analysis to surface profiles of a 15 minute glaze ice

accretion on a cylinder. When results of smooth glaze ice models are compared to those of rough models increases of up to 115 percent in the local heat-transfer rate are observed to occur primarily at the tips of the horns. This increase is partially attributed to the increase in area subtended by the roughness elements to the flow. A numerical formulation of a two-dimensional, unsteady, compressible Navier-Stokes code is introduced. Numerical tests are performed on the NACA 0012 profile and compared with experimental results. Dissert. Abstr.

N88-27501 Cornell Univ., Ithaca, N.Y.
RETRIEVAL OF TEMPERATURE AND CONCENTRATION PROFILES FROM A LIMITED NUMBER OF ABSORPTION MEASUREMENTS Ph.D. Thesis
M. Ravichandran 1988 119 p
Avail: Univ. Microfilms Order No. DA8804589

The underlying reconstruction problems in the retrieval of temperature and concentration profiles from absorption measurements for spatially inhomogeneous flows were identified. Established methods for obtaining the inverse of the applicable integral equations, viz., Abel's equation for axisymmetric cases and the Radon transform for asymmetric ones, are not well-suited for limited data problems. For axisymmetric problems involving the Abel integral equations, a nonlinear inversion method bases on functional representation by cubic splines was developed with a view to minimize the number of measurements required. Factors affecting this number were studied, and the efficacy of the proposed inversion method was demonstrated using absorption data synthetically generated from typical experimentally observed temperature concentrated profiles. For the more general case on non-axisymmetric problems involving the Radon transform, two reconstruction methods that recognize smoothness to be a priori information and use numerically space-limited basis functions were developed. The first method is a modification of the well-known convolution backprojection method. The second method, termed the Finite Domain Direct Inversions, is a continuous ART that employs consistent basis functions for the projections as well as the distribution, and makes use in a rigorous way of their a priori information such as the constraint on the domain as well as the range of distribution. Dissert. Abstr.

N88-27502 Arizona State Univ., Tempe.
HEAT AND MASS TRANSFER IN LAMINAR WAVY FILM ABSORPTION WITH THE PRESENCE OF NON-ABSORBABLE GASES Ph.D. Thesis
Ru Yang 1987 280 p
Avail: Univ. Microfilms Order No. DA8802800

Experimental measurement for the heat and mass transfer in laminar wavy film absorption with the presence of nonabsorbables are presented. Water vapor was absorbed into a falling film of aqueous gas phase acting as the nonabsorbable whose concentration was accurately detected by a mass spectrometer gas analyzer. Although the depressing effect of the air on the absorption rate was much more significant in the low air concentration range, the absorption reduction rate with increasing air concentration was found to be lower than that reported previously. The reduction was found to be continuous even up to 30 percent of air content. Besides the nonabsorbables, the effects of other operational parameters such as solution flow rate, inlet solution temperature, inlet solution concentration, absorber wall temperature, absorber water vapor pressure, and effective contact length on the absorption rate were also tested. These effects were shown to follow trends similar to those predicted by a numerical solution for smooth film absorption. The heat and mass transfer coefficients were correlated by using Reynolds number, Prandtl number, Schmidt number, capillary-buoyancy coefficient and air concentration. Dissert. Abstr.

N88-27503 Cornell Univ., Ithaca, N.Y.
SIMULATION AND ANALYSIS OF WAVE PROPAGATION THROUGH RANDOM MEDIA Ph.D. Thesis
Alexander Pidwerbetsky 1988 289 p
Avail: Univ. Microfilms Order No. DA8804596

Various observable quantities related to wave propagation through random media are generated by computer simulation and analyzed. The results are related to the nature of the medium and the source. The random medium is represented by stochastic single and multiple phase screens. Thus the medium is characterized by the number of phase screens and their wavenumber spectra. The medium is assumed to be a plasma so that the frequency dependence is given by the plasma dispersion relation. The wave is propagated from a source plane, through the phase screens, to an observation plane by a FFT implementation of the Huygens-Fresnel integral. Ray tracings are also calculated. The observables generated by computer simulation include: dynamic spectra, intensity time series, dynamic and instantaneous images. The dynamic spectra are analyzed to provide gain, modulation indices, band slope of features drifting in frequency, decorrelation time, and decorrelation bandwidth. Comparison of the simulations with theoretical calculations were made where possible. The variations of the observables were separated into diffractive and refractive. The refractive modulation of the observables was treated theoretically and confirmed by simulations. An extended medium represented by multiple phase screens was treated. Analysis of the simulation ray and wave beam paths in the extended medium shows Kolmogorov entropy in agreement with theoretical prediction. Dissert. Abstr.

N88-27504 State Univ. of New York, Buffalo.
COHERENT STRUCTURES IN THE AXISYMMETRIC TURBULENT JET MIXING LAYER Ph.D. Thesis
Mark Nelson Glauser 1987 145 p
Avail: Univ. Microfilms Order No. DA8727702

An extensive experimental effort to obtain the necessary data to apply the orthogonal decomposition to the axisymmetric jet mixing layer is presented. Phase 1 of these experiments has generated cross-spectral data at seven radial positions across the jet mixing layer. The results show clearly how the existence of a large scale structure in the mixing layer contains 40 percent of the turbulent energy. The second and third order structures contain another 25 and 15 percent respectively of the energy. Phase 2 consists of a repeat of phase 1 with 13 radial positions instead of 7. Phases 3 and 4 involve adding the azimuthal variation to the problem of phase 1. These results show the existence of an azimuthal coherent ring-like structure, dominated by the axisymmetric mode near the potential core both with the fourth, fifth, and sixth modes dominating from the center of the mixing layer and outward toward the low-speed side of the mixing layer. A life-like cycle is proposed for the evolution of coherent structures in the jet mixing layer which begins with inception of rings of concentrated vorticity form an instability of the mean flow, than a vortex-ring type instability arising from the interaction of two different rings, and finally a cascade of energy to small scales by vortex breakup and stretching. Dissert. Abstr.

N88-27505# California Univ., Berkeley. Lawrence Berkeley Lab.
HIGHER ORDER VORTEX METHODS WITH REZONING Ph.D. Thesis
H. O. Nordmark May 1988 86 p
(Contract DE-AC03-76SF-00098)
(DE88-010777; LBL-25259) Avail: NTIS HC A05/MF A01

The vortex method is a numerical method for approximating the flow of an incompressible, inviscid fluid. We consider the two-dimensional case. The accuracy depends on the choice of the cutoff function which approximates the delta function, on the cutoff parameter delta and on the smoothness of the initial data. We derive a class of infinite-order cutoff functions with arbitrarily high rates of decay at infinity. We also derive an eighth order cutoff function with compact support. We test two versions of rezoning. Version 1 has been suggested and tested by Beale and Majda, while version 2 is new. Using rezoning, we test the eighth order cutoff function and one infinite-order cutoff function on three test problems for which the solution of Euler's equation is known analytically. The accuracies of the two methods are comparable. We also compute the evolution of two circular vorticity patches

and the evolution of one square vorticity patch over long time intervals. Finally, we make a comparison between the direct method of velocity evaluation and the Rokhlin-Greengard algorithm. The numerical experiments indicate that for smooth flows, high-order cutoffs combined with rezoning give high accuracy for long time integrations. DOE

N88-27506# Lawrence Livermore National Lab., Calif.
GRANULAR FLOW: PARTICLE-DYNAMICS SIMULATIONS OF STEADY FLOW
O. R. Walton and R. L. Braun 1987 14 p Presented at the AR and TD Solids Transport Contractors Review Meeting, Pittsburgh, Pa., 17 Sep. 1987
(Contract W-7405-eng-48)
(DE88-011342; UCRL-97505; CONF-8709155-2) Avail: NTIS HC A03/MF A01

New research tools in the form of two- and three-dimensional discrete-particle computer models that calculate the motion of each individual grain in assemblies of hundreds of particles in steady shearing flows with either periodic or real boundaries have been developed and are being utilized to study granular flow behavior. The particle interaction models reproduce experimentally measured recoil trajectories for colliding frictional particles, including rotation effects. The steady shearing flow models agree with laboratory measurements where such data are available and they agree with theories when comparable approximations are made in the model (such as assuming frictionless and nearly elastic particles). Calculational studies with these models have shown that stresses generally vary as the square of the shear rate and the square of the particle radii and depend strongly on inelasticity and void volume and less strongly, but still significantly, on friction coefficient. Less sensitive are dependences on particle stiffness, shear-to-normal stiffness ratio and details of the transition to full sliding during frictional collisions. Plans for extensions of the model capabilities, new boundaries, parameter studies and evaluation of new approaches for including the effects of interstitial fluids are discussed. DOE

N88-27507*# National Aeronautics and Space Administration. Ames Research Center, Moffett Field, Calif.
TEMPERATURE RISE IN SUPERFLUID HELIUM PUMPS
Peter Kittel Jul. 1988 8 p
(NASA-TM-100997; A-88172; NAS 1.15:100997) Avail: NTIS HC A02/MF A01 CSCL 20D

The temperature rise of a fountain effect pump (FEP) and of a centrifugal pump (CP) are compared. Calculations and estimates presented here show that under the operating conditions expected during the resupply of superfluid helium in space, a centrifugal pump will produce a smaller temperature rise than will a fountain effect pump. The temperature rise for the FEP is calculated assuming an ideal pump, while the temperature rise of the CP is estimated from the measured performance of a prototype pump. As a result of this smaller temperature rise and of the different operating characteristics of the two types of pumps, transfers will be more effective using a centrifugal pump. Author

N88-27508*# Old Dominion Univ., Norfolk, Va. Dept. of Mechanical Engineering and Mechanics.
NUMERICAL METHODS FOR INCOMPRESSIBLE VISCOUS FLOWS WITH ENGINEERING APPLICATIONS Final Report, period ending 16 Apr. 1986
M. E. Rose and R. L. Ash Aug. 1988 25 p
(Contract NAS1-17993)
(NASA-CR-183143; NAS 1.26:183143) Avail: NTIS HC A03/MF A01 CSCL 20D

A numerical scheme has been developed to solve the incompressible, 3-D Navier-Stokes equations using velocity-vorticity variables. This report summarizes the development of the numerical approximation schemes for the divergence and curl of the velocity vector fields and the development of compact schemes for handling boundary and initial boundary value problems. Author

N88-27509# Kiel Univ. (West Germany). Mathematisch-Naturwissenschaftlichen Fakultaet.
DISTRIBUTIVE ITERATION FOR INDEFINITE SYSTEMS AS SMOOTHING METHOD IN MULTIGRID PROCESS ON EXAMPLE OF STOKES AND NAVIER-STOKES EQUATIONS WITH EMPHASIS ON INCOMPLETE DECOMPOSITIONS Ph.D. Thesis [DISTRIBUTIVE ITERATIONEN FUER INDEFINITE SYSTEME ALS GLAETTER IN MEHRGITTERVERFAHREN AM BEISPIEL DER STOKES- UND NAVIER-STOKES-GLEICHUNGEN MIT SCHWERPUNKT AUF UNVOLLSTAENDIGEN ZERLEGUNGEN]
Gabriel Wittum 1986 193 p In GERMAN
(ETN-88-92127) Avail: NTIS HC A09/MF A01

An iterative procedure for the solution of large linear equation systems is presented. As distributive process, a generalization of quadratic methods associated with distributive Gauss-Seidel procedures are investigated. This method constitutes an efficient solution for smoothing of multigrid methods applied to Stokes equations and steady state and incompressible Navier-Stokes equations. ESA

N88-27510# Gesamthochschule, Siegen (West Germany). Lehrstuhl fuer Stroemungstechnik.
LASER-DOPPLER MEASUREMENTS OF TURBULENCE STRUCTURES IN FREE STREAMS BEHIND FLAT AND ROTATION SYMMETRICAL PROFILES [LDA MESSUNGEN VON TURBULENZSTRUKTUREN IN ABGELOESTEN STROEMUNGEN HINTER EBENEN UND ROTATIONSSYMMETRISCHEN KOERPERN]
D. Geropp and A. Leder Mar. 1986 18 p In GERMAN
(Contract DFG-Ge-317/4-4)
(ETN-88-92336) Avail: NTIS HC A03/MF A01

Experimental results of laser-Doppler measurements behind a perpendicular flat surface in a large diameter (1m x 1m) wind tunnel are discussed. Visualization of flow behavior and mixing process is performed in a smoke tunnel for rotation symmetrical models in free streams with emphasis on wake pressure variation behind the cylinder. ESA

N88-27511# Technische Hochschule, Aachen (West Germany). Fakultaet fuer Maschinenwesen.
NUMERICAL COMPUTATION OF THREE-DIMENSIONAL TURBULENT FLOW IN TIGHTLY CURVED DUCTS AND SPIRAL TURBINE CASINGS Ph.D. Thesis [NUMERISCHE BERECHNUNG DER DREIDIMENSIONALEN TURBULENTEN STROEMUNG IN STARK GEKRUEMMTEN KANAELEN UND IN SPIRAL-TURBINENGEHAEUSEN]
Kwang-Ho Kim 1987 103 p In GERMAN Sponsored by the Korea Science and Engineering Foundation, Seoul
(ETN-88-92362) Avail: NTIS HC A06/MF A01

Three-dimensional computation of turbulent flow in curved ducts and spiral turbine casings is performed. Mathematical models are described by basic equations resolved by a developed numerical partial parabolic computation procedure. Effect of turbulent oscillations on friction force is analyzed by Prandtl mixing length flow theory. Computational procedure is tested on a 90 deg curved channel. Main flow characteristics, secondary flow, double vortex formation, retroaction, and outlet boundary conditions are considered. Mathematical and experimental results are concordant. ESA

N88-27512# Technische Hochschule, Aachen (West Germany). Fakultaet fuer Maschinenwesen.
ROTATION SYMMETRIC VORTEX IN AXIPARALLEL FLOW Ph.D. Thesis [ROTATIONSSYMMETRISCHE WIRBEL IN ACHSPARALLELER STROEMUNG]
Stefan Menne 1986 136 p In GERMAN
(ETN-88-92364) Avail: NTIS HC A07/MF A01

Navier-Stokes equations are resolved for axisymmetric vortices to study the breakdown process. Approximation performed for thin vortices is extended to incompressible and compressible fluids in friction or frictionless flow. Axisymmetric vortex breakdown at small Reynolds numbers is computed by Poisson equations for flow

function and difference equations for circulation and vortex components. Boundary conditions are formulated and discussed. ESA

N88-27513# Technische Hochschule, Aachen (West Germany). Fakultaet fuer Maschinenwesen.
NUMERICAL INTEGRATION OF NAVIER-STOKES EQUATIONS BY APPLICATION OF MULTIGRID CONCEPT Ph.D. Thesis [NUMERISCHE INTEGRATION DER NAVIER-STOKES GLEICHUNGEN UNTER VERWENDUNG DES MEHRGITTERKONZEPTS]
Wolfgang Schroeder 1987 180 p In GERMAN
(ETN-88-92365) Avail: NTIS HC A09/MF A01

Direct and indirect parabolic multigrid methods are presented. A multigrid relaxation procedure for the resolution of Navier-Stokes equations in 2D-compressible flows in spherical coordinates is examined. Convection and pressure quantities are approximated by a high resolution scheme in relation with flux-vector splitting. Effective relaxation methods are obtained by numerical stability investigations for model equations and for Navier-Stokes equations. Calculus performed on examples shows an excellent convergence rate for the multigrid relaxation procedure. ESA

N88-27514# Technische Hochschule, Aachen (West Germany). Fakultaet fuer Maschinewesen.
COMPUTATION OF FLOW AND DIFFUSION PROCESS IN GAS CENTRIFUGES Ph.D. Thesis [BERECHNUNG VON STROEMUNGS- UND DIFFUSIONSVORGAENGEN IN GASZENTRIFUGEN]
Alfons Merten 1986 129 p In GERMAN
(ETN-88-92366) Avail: NTIS HC A07/MF A01

Numerical solutions of rotational symmetric behavior equations of flow and diffusion process in high speed gas centrifuges are presented. Numerical methods concern discretization of field equations, approximation of boundary conditions, consistency, and stability of differential equations. Time dependent rotational flows are examined for low, medium, and high Reynolds numbers. Application for flow and diffusion computation in gas centrifuges is developed. ESA

N88-27515# Technische Univ., Brunswick (West Germany). Naturwissenschaftlichen Fakultaet.
INVESTIGATIONS ON DRAG REDUCTION IN TURBULENT PIPE FLOWS BY ADDITION OF IONIC AND NONIONIC HIGH POLYMERS Ph.D. Thesis [UNTERSUCHUNGEN ZUR WIDERSTANDSVERMINDERUNG IN TURBULENTEN ROHRSTROEMUNGEN UNTER ANWENDUNG VON IONISCHEN UND NICHT - IONISCHEN HOCHPOLYMEREN]
Helmut Graeger 1987 142 p In GERMAN Sponsored in part by the Deutsche Forschungsgemeinschaft, Bonn, Fed. Republic of Germany
(ETN-88-92380) Avail: NTIS HC A07/MF A01

Drag reduction in turbulent pipe flow is obtained by addition of polymeric flow accelerator. Turbulent flow pattern is described on the basis of existing theories and reduction of loss of pressure heads is discussed. A turbulence rheometer is developed permitting the measurement of friction reduction for Reynolds numbers 1100 to 90,000. Effectiveness of water soluble polymer systems like polyacrylamide and coacrylate is studied in dependence of concentration, chemical composition, product aging and polymer chain deformation. ESA

N88-27516# Deutsche Forschungs- und Versuchsanstalt fuer Luft- und Raumfahrt, Oberpfaffenhofen (West Germany). Inst. fuer Physik der Atmosphaere.
DIRECT SIMULATION OF STABLE STRATIFIED HOMOGENEOUS TURBULENT SHEAR FLOWS Ph.D. Thesis - Ludwig-Maximilians Univ.
Thomas Gerz Jan. 1988 119 p In GERMAN; ENGLISH summary
(DFVLR-FB-88-04; ISSN-0171-1342; ETN-88-92922) Avail: NTIS HC A06/MF A01; DFVLR, VB-PL-DO, 90 60 58, 5000 Cologne, Federal Republic of Germany, 37.50 deutsche marks

The method of the direct numerical simulation is used to integrate the exact time-dependent three-dimensional Navier-Stokes and temperature equations for a homogeneous turbulent flow with moderate Reynolds numbers possessing uniform gradients of the mean velocity and of the mean temperature. Hot ascending and cold descending eddies occur in the stably stratified high Prandtl number flow at positions with large positive or negative temperature fluctuations. These eddies create a mean counter-gradient vertical heat-flux. Growing gravity waves force these eddies into a two-dimensional horizontal form where they degenerate to fossil turbulence. The validation of existing models of the correlations of the pressure-strain and the pressure-temperature gradients is investigated for flows with strongly stable stratification. It is shown that the dissipative time-scale ratio is inversely proportional to the molecular Prandtl number of the fluid and reacts very sensitively on influences of shear and buoyancy forces. Coherent vortex structures break into small scale, weakly inclined vortices when the shear flow is strongly-stable stratified. ESA

N88-27517# Deutsche Forschungs- und Versuchsanstalt fuer Luft- und Raumfahrt, Lampoldshausen (West Germany). Inst. fuer Chemische Antriebe und Verfahrenstechnik.
INVESTIGATION OF ANNULAR FLOW AT HIGH EVAPORATION RATES IN VIEW OF LIQUID FILM COOLING Ph.D. Thesis - Kaiserlautern Univ.
Juergen Nahstoll Jan. 1988 123 p In GERMAN; ENGLISH summary
(DFVLR-FB-88-08; ISSN-0171-1342; ETN-88-92926) Avail: NTIS HC A06/MF A01; DFVLR, VB-PL-DO, 90 60 58 5000 Cologne, Federal Republic of Germany, 45.50 deutsche marks

The process of liquid film cooling of combustion chamber walls which are subjected to extremely high heat rates was investigated. A theoretical model was developed for a reliable prediction of the film cooling length. The mass transfer at the liquid-gas interface results from evaporated liquid and entrained liquid droplets. The film cooling length analysis, which includes the physical effects in detail, is separated into two regions: heating the liquid and evaporating the liquid. The theoretical results were experimentally verified at high pressures and temperatures using a modified H2/O2-rocket motor. There is a good agreement between the theoretical and the experimental results over the experimental range. ESA

N88-27518# Deutsche Forschungs- und Versuchsanstalt fuer Luft- und Raumfahrt, Goettingen (West Germany). Inst. fuer Theoretische Stroemungsmechanik.
NUMERICAL SIMULATION AND STABILITY ANALYSIS OF THE ABSOLUTELY AND CONVECTIVELY UNSTABLE WAKE Ph.D. Thesis - Karlsruhe Univ.
Klaus Hannemann Oct. 1987 101 p In GERMAN; ENGLISH summary Report will also be announced as translation (ESA-TT-1122)
(DFVLR-FB-88-09; ISSN-0171-1342; ETN-88-92927) Avail: NTIS HC A06/MF A01; DFVLR, VP-PL-DO, 90 60 58, 5000 Cologne, Federal Republic of Germany, 34 deutsche marks

The wake behind a flat plate, held parallel to the free-stream, is simulated numerically using a finite difference Galerkin method for the solution of the time-dependent, incompressible Navier-Stokes equations. The temporal amplification process of perturbations at supercritical Reynolds numbers, leading finally to the saturation state, is studied. The Orr-Sommerfeld stability of the quasi-steady state, occurring during the wake development, reveals that the flow can be divided into a locally absolutely unstable and a locally convectively unstable region. The influence of these stability properties on the wake, as well as their changes with Reynolds number and base bleed, is discussed based on the numerical simulaton and the linear, local stability analysis. ESA

N88-27519*# National Aeronautics and Space Administration. Ames Research Center, Moffett Field, Calif.
A DOCUMENTATION OF TWO- AND THREE-DIMENSIONAL SHOCK-SEPARATED TURBULENT BOUNDARY LAYERS

J. D. Brown, J. L. Brown, and M. I. Kussoy Jul. 1988 105 p
(NASA-TM-101008; A-88211; NAS 1.15:101008) Avail: NTIS HC A06/MF A01 CSCL 20D

A shock-related separation of a turbulent boundary layer has been studied and documented. The flow was that of an axisymmetric turbulent boundary layer over a 5.02-cm-diam cylinder that was aligned with the wind tunnel axis. The boundary layer was compressed by a 30 deg half-angle conical flare, with the cone axis inclined at an angle alpha to the cylinder axis. Nominal test conditions were P sub tau equals 1.7 atm and M sub infinity equals 2.85. Measurements were confined to the upper-symmetry, phi equals 0 deg, plane. Data are presented for the cases of alpha equal to 0. 5. and 10 deg and include mean surface pressures, streamwise and normal mean velocities, kinematic turbulent stresses and kinetic energies, as well as reverse-flow intermittencies. All data are given in tabular form; pressures, streamwise velocities, turbulent shear stresses, and kinetic energies are also presented graphically. Author

N88-27520*# Sverdrup Technology, Inc., Cleveland, Ohio.
THREE-DIMENSIONAL ADAPTIVE GRID GENERATION FOR BODY-FITTED COORDINATE SYSTEM Final Contractor Report
S. C. Chen Aug. 1988 12 p Proposed for presentation at the 2nd International Conference on Numerical Grid Generation in Computational Fluid Dynamics, Miami Beach, Fla., 5-8 Dec. 1988; sponsored by NASA and AFOSR
(Contract NAS3-24105)
(NASA-CR-182192; E-4331; NAS 1.26:182192) Avail: NTIS HC A03/MF A01 CSCL 20D

This report describes a numerical method for generating 3-D grids for general configurations. The basic method involves the solution of a set of quasi-linear elliptic partial differential equations via pointwise relaxation with a local relaxation factor. It allows specification of the grid spacing off the boundary surfaces and the grid orthogonality at the boundary surfaces. It includes adaptive mechanisms to improve smoothness, orthogonality, and flow resolution in the grid interior. Author

35 INSTRUMENTATION AND PHOTOGRAPHY

Includes remote sensors; measuring instruments and gages; detectors; cameras and photographic supplies; and holography.

For aerial photography see *43 Earth Resources and Remote Sensing*. For related information see also *06 Aircraft Instrumentation*, and *19 Spacecraft Instrumentation*.

N88-27521 Michigan Univ., Ann Arbor.
TURBULENT FLOW FIELD VISUALIZATION WITH INTEGRAL INTERFEROMETRIC IMAGING AND COMPUTED TOMOGRAPHY Ph.D. Thesis
David Wilson Watt 1987 142 p
Avail: Univ. Microfilms Order DA8801441

Digital holographic interferometry and computer tomography for studying turbulent flows are developed. Digital holographic interferometry, a hybrid optical-digital technique for measuring interferometric phase, is developed for studying fluid flow. By measuring the two-dimensional distribution of the optical path integrals through a flow field, the technique forms integral projection images of the flow's refractive index field. Computed tomography uses an invertible integral transform relation between a field and its projections to recover a field's cross-sectional distribution. From a phase object's interferometric integral projections, its refractive index distribution can be obtained. A visualization study with integral imaging and computed tomography of a round helium jet under both laminar and turbulent conditions is presented. The integral image data demonstrates the various flow regimes of a laminar buoyant jet and illuminates large scale motions within the turbulent flows. The tomographic images of the turbulent flow demonstrate unmixed ambient fluid within the jet, a two-level concentration field structure, and stream-wise vorticity in the jet. The image artifacts in the reconstructions and the potential of interferometric tomographic measurements in turbulent flows are discussed. Dissert. Abstr.

N88-27522# Johns Hopkins Univ., Baltimore, Md. Dept. of Mechanical Engineering.
ATTACHABLE INTERFEROMETRIC STRAIN GAGES Final Report, 1 Oct. 1985 - 30 Sep. 1987
William N. Sharpe, Jr. and K. C. Wang Feb. 1988 27 p
(Contract N00014-85-K-0686)
(AD-A192390) Avail: NTIS HC A03/MF A01 CSCL 14B

Laser based interferometry from tiny reflective indentations can be used to measure in-plane strain/displacement over a very short gage length (on the order of 100 um). If the specimen material is not reflective, then some other means of generating the interference patterns must be found. This report describes two kinds of attachable gages: plated acetate replicas of indentations and reflective foils that are indented after application. In either case, the gage is applied with the techniques used for foil resistance gages and the gage itself is very small. The manufacturing procedures are described. GRA

N88-27523# Michigan Univ., Ann Arbor. Dept. of Chemical Engineering.
NUCLEAR MAGNETIC RESONANCE SPECTROMETER Final Report, 15 Jul. 1986 - 15 Jul. 1987
Francis M. Donahue 1987 2 p
(Grant AF-AFOSR-0231-86)
(AD-A192928; AFOSR-88-0573TR) Avail: NTIS HC A02/MF A01 CSCL 14B

The major purpose of the spectrometer was to support research on low temperature molten salts. Specifically, the spectrometer was to be used in the determination of the composition of the salt solutions (1H and 13C) and as a probe in the determination of the nature of complexation of metal complexes. In the case of the latter, the instrument was used to probe the nature of octahedral cationic complexes of aluminum and gallium in the melts (the first such observations). Some of the aluminum work has been in support of our work at the University of Michigan and some of the aluminum and all of the gallium work is collaboration with the F. J. Seiler Research Laboratory (AFSC) at the Air Force Academy. GRA

N88-27524# Air Force Wright Aeronautical Labs., Wright-Patterson AFB, Ohio.
CALIBRATION OF THE PORTABLE WEAR METAL ANALYZER Final Report, Mar. 1985 - Dec. 1986
Michael J. Quinn Dec. 1987 63 p
(AD-A192971; AFWAL-TR-87-2061) Avail: NTIS HC A04/MF A01 CSCL 11H

The Portable Wear Metal Analyzer (PWMA), a graphite furnace atomic absorption (AA) spectrometer, developed under a contract for this laboratory, was evaluated using powdered metal particles suspended in oil. The PWMA is a microprocessor controlled automatic sequential multielement AA spectrometer designed to support the deployed aircraft requirement for spectrometric oil analysis. The PWMA will analyze for nine elements (Ni, Fe, Cu, Cr, Ag, Mg, Si, Ti, Al) at a rate of 4 min per sample. The graphite tube and modified sample introduction system increase the detection of particles in oil when compared to the currently used techniques of flame AA or spark atomic emission (AE) spectroscopy. The PWMA shows good-to-excellent response for particles in sizes of 0 to 5 and 5 to 10 micrometers and fair response to particles of 10 to 20 and 20 to 30 micrometers. All trends in statistical variations are easily explained by system considerations. Correction factors to the calibration curves are necessary to correlate the analytical capability of the PWMA to the performance of existing spectrometric oil analysis (SOA) instruments. GRA

N88-27525# Advisory Group for Aerospace Research and Development, Neuilly-Sur-Seine (France).
FLIGHT TESTING UNDER EXTREME ENVIRONMENTAL CONDITIONS
Clendon L. Hendrickson (Air Force Flight Test Center, Edwards AFB, Calif.) Jun. 1988 73 p
(AGARD-AG-300-Vol-8; ISBN-92-835-0459-3) Copyright Avail: NTIS HC A04/MF A01

The major objective of Flight Testing under extreme environmental conditions is to determine to what extent a weapon system, including its essential support equipment and attendant crews can accomplish the design mission in the required climatic extremes, using Techical Order procedures. Such testing has historically often revealed design deficiencies that impact the operational capabilities of the air vehicle involved. This volume in the AGARD Flight Test Techniques Series discusses the philosophy, purpose and methods for conducting ground and flight tests of weapon systems in extreme environment conditions. The areas considered include testing in a controlled artificial environment, as well as cold arctic, hot desert, tropic, and adverse-weather conditions. Also included are the technical and safety aspects of planning, instrumentation, and data acquisition requirements, types of tests conducted and reporting requirements. Author

N88-27526# Sandia National Labs., Albuquerque, N. Mex.
THE P DELTA V FUNDAMENTAL GAS LEAK CALIBRATION SYSTEM QUALIFICATION REPORT
M. S. Benner Apr. 1988 44 p
(Contract DE-AC04-76DP-00789)
(DE88-008964; SAND-88-0503) Avail: NTIS HC A03/MF A01

Modifications, qualification testing, and recommendations for improvements to a fundamental gas leak calibration system (commonly called P delta V or PV) are presented. As a result of extensive modification, the system's measurement performance has been evaluated. Test results indicate that the PV system is still capable of calibrating leaks within its uncertainty limit of plus or minus three percent over the working range of leak rates from 1.5 E-10 to 4.5 E-8 moles/s. DOE

N88-27527# Sandia National Labs., Albuquerque, N. Mex.
LIQUID CRYSTALS FOR UNSTEADY SURFACE SHEAR STRESS VISUALIZATION
D. C. Reda 1988 15 p Presented at the 1st National Fluid Dynamics Congress, Cincinnati, Ohio, 24 Jul. 1988
(Contract DE-AC04-76DP-00789)
(DE88-010570; SAND-88-1360C; CONF-880716-3) Avail: NTIS HC A03/MF A01

Oscillating airfoil experiments were conducted to test the frequency response of thermochromic liquid crystal coatings to unsteady surface shear stresses under isothermal-flow conditions. The model was an NACA-0015 airfoil, exposed to an incompressible flow at a freestream Reynolds number (based on chord) of 1.14 x 1000000. Angle-of-attack forcing functions were sine waves of amplitude + or - 10 deg about each of three mean angles of attack: 0 deg 10 deg, and 20 deg. Frequencies of oscillation were 0.2, 0.6 and 1.2 hertz, corresponding to reduced frequencies of 0.0055, 0.0164 and 0.0328. Data acquisition was accomplished by video recording. Observations showed the liquid crystal technique capable of visualizing high surface sheer stress zones over the stated dynamic range in a continuous and reversible manner. DOE

N88-27528# Oak Ridge Y-12 Plant, Tenn.
ACOUSTIC EMISSION CALIBRATION INSTRUMENTATION
M. G. Duncan and J. W. Whittaker 13 Nov. 1987 34 p Presented at the IEEE Instrumentation and Measurement Technology Conference, San Diego, Calif., 20 Apr. 1988
(Contract DE-AC05-84OS-21400)
(DE88-010817; Y/DW-781; CONF-880425-1) Avail: NTIS HC A03/MF A01

An automatic calibration instrument was developed to improve calibration accuracy of acoustic emission (AE) transducers by one order-of-magnitude over commercially available equipment. The instrument facilitates calibration by automatically displaying the maximum value of the stress used to produce AE calibration pulses and the AE pulse. Low-noise amplifiers and filters were also developed to improve the sensitivity of AE measurements by more than one order-of-magnitude over commercially available instruments; thus smaller signals may be detected in parts. DOE

N88-27529# Sandia National Labs., Albuquerque, N. Mex.
FIBER-OPTICS USED TO RECORD HIGH-SPEED PHOTOGRAPHS INSIDE A PRESSURIZED TANK DURING LETHALITY TESTING
J. E. Grant Apr. 1988 32 p
(Contract DE-AC04-76DR-00789)
(DE88-011283; SAND-88-8205) Avail: NTIS HC A03/MF A01

Sandia National Laboratories has a program underway to determine the survivability and lethality of potential targets subjected to high order impulse loads. This effort is associated with the Strategic Defense Initiative's (SDI) Directed Energy Weapons (DEW) program and is managed by the Defense Nuclear Agency (DNA). The energy from this class of weapons, impact the target surface simultaneously and produce an impulse that varies as the cosine of the angle of incidence. The goals of the program are to determine the relevant failure mechanisms, assess the validity of our numerical codes in modeling target behavior, provide a series of benchmark tests that can be used to improve our numerical capability, and provide the SDI community with estimates of survivability and lethality levels for various generic targets. The experiment described in this report is one in a series of similar experiments designed to model target behavior in the absence of material degradation and spall. DOE

N88-27530# General Electric Co., Largo, Fla. Neutron Devices Dept.
COUPLING OF A SPARK SOURCE MASS SPECTROGRAPH AND A ND-YAG LASER
R. W. Bonham and J. C. Quattlebaum 15 Jun. 1988 15 p
(Contract DE-AC04-76DP-00656)
(DE88-012116; GEPP-TIS-1083) Avail: NTIS HC A03/MF A01

Spark source mass spectrograph (SSMS) has been used for many years for routine semi-quantitative analysis of metals to the ppB level. GR Neutron Devices (GEND) has added a laser to their spark source instrument, and a variety of both standard and unknown metals and insulators were analyzed to demonstrate the applicability and validity of the technique. The modifications made to the standard instrument, the necessary changes made in the operating technique, and the advantages which resulted are discussed in this report. The ability to simultaneously analyze all elements, from lithium through uranium, from 100 percent to the ppB range in any insulating matrix does not affect the ability of the instrument to function in the spark mode. This modification should prove useful to those interested in the analysis of insulators down to the trace level without a solution step or pretreatment. Data are given for materials ranging from National Bureau of Standards (NBS) glass standards to samples in which both the matrix and the impurities are unknown. Gold, aluminum, copper, titanium, and erbium metal, as well as several different types of glasses, silica, alumina, boron nitride, and diamond, have been analyzed. DOE

N88-27531# Technische Univ., Brunswick (West Germany). Fakultaet fuer Maschinenbau und Elektrotechnik.
STABILITY OF UNCAPSULATED WEIGHT CELLS WITH THIN FILM ELONGATION MEASUREMENT BANDS UNDER INFLUENCE OF HUMIDITY, TEMPERATURE AND OPERATION VOLTAGE Ph.D. Thesis [STABILITAET UNGEKAPSELTER WAEGEZELLEN MIT DUENNFILM-DEHNUNGSMESSSTREIFEN UNTER DEM EINFLUSS VON FEUCHTE, TEMPERATUR UND BETRIEBSSPANNUNG]
Heinrich Paul 1987 120 p In GERMAN
(ETN-88-92383) Avail: NTIS HC A06/MF A01

Weight cells for commercial scales up to 5 kg are investigated for their moisture resistance, temperature, and operation voltage

qualifications. Transformation of mechanical quantities into electric signal is performed by CuBe or FeNi foils with silicon film coating. Various silicon spray coatings are studied concerning the main operational parameters: zero signal stability, moisture test, elasticity modulus, electrolytic corrosion, temperature and humidity effects on measurement stability. ESA

N88-27532# Physics and Electronics Lab. TNO, The Hague (Netherlands).
THE FEL CCD-CAMERA: EXPERIMENTAL SYSTEM FOR CAMERA AND IMAGE PROCESSING RESEARCH
T. Bakker, H. G. M. Bennis, J. A. Boden, M. G. Disselen, A. J. Leutscher, J. A. v.d.Pol, W. T. M. Roussel, and F. P. P. deVries May 1987 60 p In DUTCH; ENGLISH summary
(Contract A80/KL/040)
(FEL-1987-34; ETN-88-92569) Avail: NTIS HC A04/MF A01

A camera system, based upon a matrix of photo-elements with a charge coupled device read-out is described. The main aspects of subsystems such as the camera, pattern generator, the search-memory, the record-memory, and computer with the relevant software are dealt with. Detailed information about the construction is given. The results with this system together with processed images of a gray-wedge pattern are analyzed. The processed images show at present a dynamic range of approximately 1000 in this experimental phase; conclusions and important fields for further research are given. ESA

N88-27533# Deutsche Forschungs- und Versuchsanstalt fuer Luft- und Raumfahrt, Brunswick (West Germany). Abteilung Systemtechnik und Navigation.
APPLICATION OF THE SINGLE-AXIS RATE TABLE (SAT) OF THE DFVLR FOR THE EVALUATION OF STATIONARY AND DYNAMIC GYRO PROPERTIES
Egmar Luebeck Feb. 1988 49 p In GERMAN; ENGLISH summary Report will also be announced as translation (ESA-TT-1119)
(DFVLR-Mitt-88-09; ISSN-0176-7739; ETN-88-92943) Avail: NTIS HC A03/MF A01; DFVLR. VB-PL-DO, 90 60 58, 5000 Cologne, Federal Republic of Germany, 22 deutsche marks

The Single-Axis-Rate-table (SAT) with additional temperature or magnetic fields facilities is described. To measure the frequency response of gyros, the accuracy of the angular velocity readout of the oscillating table is improved by mixing the signals of inductosyn, tachometer, and an accelerometer. Measures concerning the realization of the greatest possible bandwidth of SAT are considered. The necessary fast data acquisition (1000 Hz) is considered. ESA

36 LASERS AND MASERS

Includes parametric amplifiers.
For related information see also *76 Solid-State Physics.*

N88-27534# Maryland Univ., College Park. Lab. for Plasma and Fusion Energy Studies.
OPTICAL GUIDING IN THE SEPARABLE BEAM LIMIT
T. M. Antonsen, Jr. and B. Levush Sep. 1987 12 p
(Contract N00014-86-K-2005)
(AD-A192452; UMLPF-88-011) Avail: NTIS HC A03/MF A01 CSCL 09C

The nonlinear theory of optical guiding in a Free Electron Laser Amplifier is developed for the case in which the spatial dependence of the current source term in the wave equation can be separated into the product of a function of radius and a function of axial distance. Such a separation can be motivated if either the betatron wavelength is shorter than other lengths of interest (synchrotron wavelength, vacuum Rayleigh length) or if the radiation waist exceeds the beam radius. In this limit with the choice of a Gaussian profile for the electron beam density the wave equation can be solved exactly and the radiation field felt by the particles can be expressed as a 1-D convolution of the current source. With the given expression for the radiation field, the equations of motion can be solved in the trapped particle regime. Requiring consistency between the particle motion and the fields yields expressions describing nonlinear guided states. The adiabatic evolution of these guided states in the presence of a tapered wiggler is determined by conservation of the electrons action and total (field + electron beam) energy. Using these relations the growth of the radiation waist as the beam is decelerated can be calculated. GRA

N88-27535# Oklahoma State Univ., Stillwater. Dept. of Physics.
LASER SPECTROSCOPY INVESTIGATIONS OF MATERIALS FOR SOLID STATE LASER SYSTEMS Final Report, 16 Jan. 1985 - 15 Jan. 1988
Richard C. Powell Feb. 1988 155 p
(Contract DAAG29-85-K-0056)
(AD-A192514; ARO-22279.25-PH) Avail: NTIS HC A08/MF A01 CSCL 09C

Some of the results of major importance from this work are: (1) The development of a method for producing laser-induced grating optical devices in glasses; (2) The elucidation of the effects of Mg on inhibiting the photorefractive response of lithium niobate; (3) The demonstration of tunable single pass gain from a closed shell ion in the visible spectral region; (4) A demonstration of the decrease in fluorescence quenching in fiber crystals; (5) A demonstration of the effects of thermal annealing on the infrared absorption and visible emission in Ti-sapphire laser crystals; and (6) A measurement of the pump band to metastable state relaxation rate in alexandrite laser crystals. GRA

N88-27536# Maryland Univ., College Park. Lab. for Plasma and Fusion Energy Studies.
EFFICIENCY OPTIMIZATION FOR FEL OSCILLATORS
A. Serbeto, B. Levush, and T. M. Antonsen, Jr. Dec. 1987 24 p
(Contract N00014-86-K-2005)
(AD-A192541; UMLPF-88-031) Avail: NTIS HC A03/MF A01 CSCL 09C

Using a normalized set of nonlinear equations, which describe a Free Electron Laser oscillator, the efficiency of energy extraction from the electron beam to the radiation can be optimized. The optimum values of this efficiency are presented for an (1) untapered and for a (2) tapered wiggler FEL oscillator. GRA

N88-27537# Hampton Inst., Va. Dept. of Physics.
A PLASMA ULTRAVIOLET SOURCE FOR SHORT WAVELENGTH LASERS Final Report, 15 Jan. 1986 - 29 Feb. 1988
K. S. Han 15 Apr. 1988 31 p
(Contract DAAL03-86-G-0003)
(AD-A192844; ARO-23496.5-PH-H) Avail: NTIS HC A03/MF A01 CSCL 09C

A dense plasma focus (DPF) device was evaluated for the feasibility of blue-green and near ultraviolet laser pumping. As the result of optimizing the operating conditions of DPF and laser system, the maximum untuned laser output exceeded 4.0mJ corresponding to the energy density 8.3J/liter which is much higher than the typical flashlamp dye laser. The spectral irradiance of DPF at the absorption bands for LD390 and LD490 were 5.5W/sq cm-nm, 0.3W/sq cm-nm, respectively. Due to the lower pump power of DPF at 355nm than the threshold of LD390, the laser pumping of LD390 dye was not achieved. A hard core flashlamp (HCF) which has a coaxial geometry and array of inverse pinches was also evaluated for blue-green and near UV laser excitation. The short pulse (greater than 0.5us) surface discharges were produced across the core insulator of alumina. The spectral irradiance of the HCF depends on argon fill gas pressure and the core insulating material. The maximum radiative output of the HCF lies in the region of 340 to 400nm (absorption band of LD490). A LD490 dye laser pumped by a HCF prototype device had an output of 0.9mJ with a pulse of 0.5 microsec (full width at half maximum). GRA

N88-27538# National Bureau of Standards, Gaithersburg, Md.
RESEARCH OPPORTUNITIES BELOW 300 nm AT THE NBS FREE-ELECTRON LASER FACILITY
Philip H. Debenham and B. C. Johnson 1987 6 p
(Contract N00014-87-F-0066)
(AD-A193100) Avail: NTIS HC A02/MF A01 CSCL 14B

A free-electron laser (FEL) which will be driven by the cw racetrack microtron (RTM), will be operated as an oscillator with the fundamental wavelength variable from approximately 200 nm to 10 micrometers. The presence of harmonics should allow for operation in the VUV and EUV spectral regions. The cw RTM consists of a 5 MeV injector section and a 12 MeV, cw, rf linear accelerator (linac). The linac is placed between two uniform-field end magnets that recirculate the beam on successive orbits through the linac. The beam can be deflected out of the RTM after completing up to and including 15 passes through the linac, so that the final beam energy is 17 MeV to 185 MeV. As a FEL driver, the unique features of the RTM are the cw nature of the beam, excellent energy stability, small values of the transverse emittance and energy spread, and high average power. GRA

N88-27539# University Coll., London (England). Dept. of Physics and Astronomy.
COMPONENTS OF AN ATMOSPHERIC LIDAR SYSTEM Final Report, 1 Oct. 1986 - 30 Sep. 1987
David Rees 30 Nov. 1987 16 p
(Grant AF-AFOSR-0198-85)
(AD-A193366; CJT4; AFGL-TR-88-0031) Avail: NTIS HC A03/MF A01 CSCL 17E

A wavelength meter and a Doppler interferometric detector were developed to use with a lidar for measurements of atmospheric temperature and wind. These high spectral resolution instruments are used to measure the laser output line width and the backscatter wavelength shift. The sodium resonance lines are used to measure atmospheric structure properties in the 80 to 110 km altitude range. In this region, meteoric debris enters the Earth's upper atmosphere and forms a layer of dust with many species in atomic form. Sodium resonance line components can be used to find the temperature from line broadening and the Doppler velocity can be measured to determine wind velocity. The instruments which have been prepared are to assist in that research development. GRA

N88-27540# Lawrence Livermore National Lab., Calif.
INITIAL ELECTRON DISTRIBUTIONS FOR FREE-ELECTRON LASERS GENERATED BY INJECTOR AND ACCELERATOR SIMULATIONS
J. K. Boyd, W. B. Colson, and E. T. Scharlemann 16 Sep. 1987 17 p Presented at the 9th International Free-Electron Laser Conference, Williamsburg, Va., 14 Sep. 1987 Prepared in cooperation with Berkeley Research Associates, Inc., Calif.
(Contract W-7405-eng-48)
(DE88-007022; UCRL-96767; CONF-8709110-21) Avail: NTIS HC A03/MF A01

Early free-electron laser (FEL) development was guided by simple performance criteria based on the number of undulator periods, electron beam quality, and current. The beam quality (emittance and energy spread) was used to characterize the initial distribution of axial electron velocities along the undulator axis. While the emittance and energy spread determine the overall width of the distribution, its detailed shape is also important. As new accelerators are designed specifically for FEL applications, it becomes important to obtain distribution shape information from simulations that include the electron gun, accelerator, and beam transport in addition to the usual electron/optical interaction in the undulator. The distribution at the entrance to the undulator can be calculated from numerical simulations of the cathode emission, acceleration, and transport of an electron beam. We have modeled the beam generation, from cathode emission up to the energy of the accelerator injector, using an axisymmetric, cylindrical geometry particle simulation (DPC). This code solves the relativistic force equation with fields obtained from Maxwell's equations in the Darwin model. The DPC calculation is run repeatedly varying parameters such as accelerating stress, electrode configuration, and axial magnetic field profile until a good match is obtained for the accelerator. The beam exiting from the injector can be accelerated and transported using the transfer matrix technique with a simple model for accelerating gaps and magnets. Alternatively, acceleration and transport can be simulated with a particle code that solves for the axisymmetric evolution of a slice of an electron beam including possible emittance growth. The phase space obtained from the accelerator can be evaluated for performance using either the simple FEL integral equation method or the more complete FRED simulation code. DOE

N88-27541# Los Alamos National Lab., N. Mex.
DEVELOPMENT OF A FREE-ELECTRON LASER USER FACILITY FOR THE EXTREME ULTRAVIOLET
B. E. Newnam 1987 22 p Presented at Lasers '87, Lake Tahoe, Nev., 7 Dec. 1987
(Contract W-7405-eng-36)
(DE88-007892; LA-UR-88-837; CONF-871254-10; CONF-871254) Avail: NTIS HC A03/MF A01

A free-electron laser user facility for scientific experimentation in the extreme ultraviolet is being developed at Los Alamos. A series of laser oscillators and amplifiers, driven by a single, RF linear accelerator, will generate broadly tunable, picosecond-pulse, coherent radiation from 1 nm to 400 nm. The design and output parameters of this facility are described, comparison with synchrotron radiation sources is made, and recent progress in developing the three primary components (electron beam, undulator, and resonator mirrors) is reviewed, and various categories of scientific applications are indicated. DOE

N88-27542# Lawrence Livermore National Lab., Calif.
CHEMICAL VAPOR DEPOSITION OF TiO2 THIN FILMS AT ROOM TEMPERATURE
J. Wilder and I. Thomas 10 Feb. 1988 8 p Presented at the Boulder Damage Symposium, Boulder, Colo., 3 Nov. 1986
(Contract W-7405-eng-48)
(DE88-008892; UCRL-95282; CONF-8611154-3) Avail: NTIS HC A02/MF A01

Titania coatings were prepared using a chemical vapor deposition (CVD) apparatus at room temperature. Coatings were deposited by the reaction of gaseous TiCl4 and H2O at the substrate surface. High refractive indices were obtained with damage thresholds to 12.9 J/sq cm, at 1.06 microns, 1 ns. DOE

N88-27543# Allied-Signal Corp., Morristown, N.J.
A NEW NEAR-INFRARED TUNABLE-ROOM TEMPERATURE SOLID STATE LASER La3Ga5SiO14:Cr(3+)
S. T. Lai, B. H.T. Chai, M. Long, and M. D. Shinn 1987 2 p Presented at the Topical Meeting on Tunable Solid State Lasers, Williamsburg, Va., 26 Oct. 1987 Prepared in cooperation with Lawrence Livermore National Lab., Calif.
(Contract W-7405-eng-48)
(DE88-011341; UCRL-97575; CONF-871060-3) Avail: NTIS HC A02/MF A01

Laser action at room temperature has been achieved in La3Ga5SiO14:Cr(3+). The laser free running wavelength is 968 nm. The fluorescence quantum yield is 42 percent at room temperature. A large single crystal boule has been grown by the Czochralski method. DOE

N88-27544# Rochester Univ., N. Y. Lab. for Laser Energetics.
RADIAL COMPRESSION OF PICOSECOND ELECTRICAL PULSES
C. Bamber, W. Donaldson, T. Juhasz, L. Kingsley, and A. C. Melissinos Nov. 1987 19 p
(Contract DE-FC08-85DP-40200)
(DE88-008440; DOE/DP-40200/55) Avail: NTIS HC A03/MF A01

We used 1 ps, 1 mJ pulses from a Nd:glass laser system to produce kilovolt electrical pulses with rise time of the order of 15 ps. The pulses propagated radially between two circular discs resulting in a voltage gain of 2 at the center of the discs as

compared to the circumference in qualitative agreement with calculation. Such structures can be used to produce very high gradient accelerating fields. DOE

N88-27545# Sandia National Labs., Albuquerque, N. Mex.
PHASE COMPARATOR FOR RANGE IMAGING LASER RADAR
Kurt O. Wessendorf, Marion W. Scott, and Mark A. Grohman 1988 6 p Presented at the 10th Annual Ideas in Science and Electronics Exposition, Albuquerque, N. Mex., 10 May 1988
(Contract DE-AC04-76DP-00789)
(DE88-008109; SAND-87-3017C; CONF-880579-2) Avail: NTIS HC A02/MF A01

A range imaging laser radar using gallium arsenide (GaAs) laser technology has been developed. An image is constructed by scanning the beam in two dimensions over the scene. Our development system transmits an intensity modulated laser beam and determines range by measuring the phase difference of the local oscillator to that of the return signal. Since a 1GHz clock is used to measure this phase difference a theoretical maximum of 1 nsec., or six inches, of range change can be resolved. An amplifier is required to convert the received signal, of wide dynamic range, into a digital waveform for the counter circuit. To obtain the highest possible system resolution this amplifier must impart a minimum amount of phase shift over the dynamic range of the received signal. To maintain a high signal to noise ratio the amplifier must have a narrow bandwidth. Three approaches to the design of an appropriate signal amplifier were explored. A diode clamping amplifier, an automatic gain control circuit, and a cascaded differential amplifier were fabricated and tested. The differential amplifier circuit provided the best fit to the design goals and demonstrated a phase shift of + or - 3ns over a dynamic range of 70dB. This amplifier has been used in a radar to obtain range images of scale models of targets in the laboratory. DOE

N88-27546# Pacific Northwest Labs., Richland, Wash.
DIRECT MEASUREMENT OF SOLIDS: HIGH TEMPERATURE SENSING. EXPERIMENTAL DEVELOPMENT AND TESTING OF HIGH TEMPERATURE PULSED EMATs Final Report
D. M. Boyd, G. E. Spanner, and P. D. Sperline Apr. 1988 60 p
(Contract DE-AC06-76RL-01830)
(DE88-009859; PNL-6537) Avail: NTIS HC A04/MF A01

A pulsed laser/pulsed EMAT (electromagnetic acoustic transducer) receiver system has been demonstrated for measuring the time of flight of acoustic signals in hot steel samples. Attenuation and signal-to-noise ratio are important parameters to be monitored. A continuous contact EMAT application was not achieved; thermal analysis found that contact times of 5 seconds with cooling times of 45 seconds are required at 1300 C. The equipment requires field hardening and improved packaging before system reliability can be assessed. DOE

N88-27547# Sandia National Labs., Albuquerque, N. Mex.
TARGET DESIGNS FOR PLASMA-IMPLOSION-DRIVEN, PHOTOIONIZATION-PUMPED SOFT X-RAY LASERS
T. W. Hussey, M. K. Matzen, E. J. McGuire, and H. E. Dalhed May 1988 46 p Prepared in cooperation with Lawrence Livermore National Lab., Calif.
(Contract DE-AC04-76DP-00789)
(DE88-011278; SAND-88-0764) Avail: NTIS HC A03/MF A01

Designs are proposed for layered, hollow cylindrical targets to be placed on the axis of an imploding, hollow Z-pinch plasma that can create the approximate plasma conditions, as well as radiation spectrum, for a photoionization pumped, Ne-like recombination laser. The lasant must research the Ne-like state and be at the appropriate density concurrent with the photoionizing pump radiation. This places severe constraints on designs for such targets with the vertical vacuum feed diode on Proto 2. Target designs are further constrained by the fact that the 3s--2p resonance line, which depopulates the lower lasing state, must not be highly trapped and by the fact that the upper lasing state must not be collisionally depopulated. We find that hollow, cylindrical targets consisting of a few micron CH strongback, coated on the inside with a thin layer of Ni lasant and on the outside with an Al converter layer, can be optimized to achieve appropriate conditions for lasing. We note that a trade-off exists between larger targets, which better isolate the target from the shock of stagnation, and smaller targets, which deliver a higher intensity pump flux. We also find that trapping, together with uncertainties in the inward expansion of the lasant layer, are significant, and may limit optium available gain. DOE

N88-27548# Lawrence Livermore National Lab., Calif.
WAVE EQUATIONS FOR PULSE PROPAGATION
B. W. Shore 24 Jun. 1987 31 p
(Contract W-7405-eng-48)
(DE88-011760; UCID-20972) Avail: NTIS HC A03/MF A01

Theoretical discussions of the propagation of pulses of laser radiation through atomic or molecular vapor rely on a number of traditional approximations for idealizing the radiation and the molecules, and for quantifying their mutual interaction by various equations of propagation (for the radiation) and excitation (for the molecules). In treating short-pulse phenomena it is essential to consider coherent excitation phenomena of the sort that is manifest in Rabi oscillations of atomic or molecular populations. Such processes are not adequately treated by rate equations for excitation nor by rate equations for radiation. As part of a more comprehensive treatment of the coupled equations that describe propagation of short pulses, this memo presents background discussion of the equations that describe the field. This memo discusses the origin, in Maxwell's equations, of the wave equation used in the description of pulse propagation. It notes the separation into lamellar and solenoidal (or longitudinal and transverse) and positive and negative frequency parts. It mentions the possibility of separating the polarization field into linear and nonlinear parts, in order to define a susceptibility or index of refraction and, from these, a phase and group velocity. DOE

N88-27549# Lawrence Livermore National Lab., Calif.
TRANSVERSE RESISTIVE WALL INSTABILITY IN A HIGH-POWER, SHORT-WAVELENGTH FREE-ELECTRON LASER
V. K. Neil and D. H. Whittum 1987 24 p Presented at the 9th International Free-Electron Laser Conference, Williamsburg, Va., 14 Sep. 1987 Prepared in cooperation with Lawrence Berkeley Lab., Calif.
(Contract W-7405-eng-48)
(DE88-011730; UCRL-96712; CONF-8709110-24) Avail: NTIS HC A03/MF A01

The finite resistivity in walls surrounding a beam of charged particles can lead to unstable, coherent, transverse motion of the beam. For a beam pipe of circular cross section and radius b, the amplitude of the transverse motion grows exponentially with an e-folding length inversely proportional to the beam current and directly proportional to b(sup 2) or b(sup 3) depending on the parameter regime. In conventional accelerators and beam transport systems, b is at least a few centimeters, and the growth length is quite long. In a free-electron laser (FEL) wiggler magnet, we must have b less than lambda(sub w)/2, with lambda(sub w) the wiggler wavelength, so that b may be only a few millimeters. We treat a 20-m-long wiggler of an FEL amplifier driven by an induction linac. Results indicate the instability is of no consequence for the oscillator but does impose lower limits on the pipe radius for the amplifier. DOE

N88-27550# Technische Hochschule, Aachen (West Germany). Fakultaet fuer Maschinewesen.
INVESTIGATIONS ON BEAM QUALITY OF HIGH FREQUENCY EXCITED CO2 HIGH PERFORMANCE LASERS Ph.D. Thesis [UNTERSUCHUNGEN ZUR STRAHLQUALITAET VON HOCHEREQUENZANGEREGTEN CO2-HOCHLEISTUNGSLASERN]
Helmut Schuelke 1987 139 p In GERMAN
(ETN-88-92363) Avail: NTIS HC A07/MF A01

Experimental and theoretical investigations on a resonator design with transverse high frequency gas discharges are presented for laser system size reduction. Components dimensioning, high

frequency excitation, laser gas discharges, and laser kinetics are studied for resonator beam stability determination. Time constant and emission behavior of CO2-lasers are examined. Frequency modulation is 200 kHz for power density = 100 W/cc, rated pressure p = 100 to 200 mbar, gas mixture He,N2,Co2 = 8,1,1 ESA

N88-27551# Deutsche Forschungs- und Versuchsanstalt fuer Luft- und Raumfahrt, Goettingen (West Germany). Abteilung Turbulenzforschung.
MEASUREMENT OF PRESSURE FLUCTUATIONS IN A RESONANT CHAMBER WITH LASER-INDUCED IODINE FLUORESCENCE Final Report
Bernhard Stahl and Ulf Michel Dec. 1987 79 p In GERMAN; ENGLISH summary Report will also be announced as translation (ESA-TT-1123)
(Contracts DFG-Mi-149/2-1; DFG-149/2-2)
(DFVLR-FB-87-53; ISSN-0171-1342; ETN-88-92919) Avail: NTIS HC A05/MF A01; DFVLR, VB-PL-DO, 90 60 58, 5000 Cologne, Federal Republic of Germany, 23 deutsche marks

The feasibility of measuring pressure fluctuations with laser-induced iodine fluorescence was tested in a resonance chamber containing a gas mixture of iodine and nitrogen. The intensity of fluorescence light is a function of the thermodynamic condition of the gas mixture, the laser-light power, and the laser frequency. Experimental investigations show that the noninvasive measurement of pressure fluctuations is possible under restricted conditions. ESA

N88-27552# Deutsche Forschungs- und Versuchsanstalt fuer Luft- und Raumfahrt, Stuttgart (West Germany). Inst. fuer Technische Physik.
ON THE SMALL SIGNAL GAIN OF FREE ELECTRON LASERS IN THE LOW-CURRENT REGIME
Gerhard Spindler Feb. 1988 39 p In GERMAN; ENGLISH summary Report will also be announced as translation (ESA-TT-1120)
(DFVLR-FB-88-10; ISSN-0171-1342; ETN-88-92928) Avail: NTIS HC A03/MF A01; DFVLR, VB-PL-DO, 90 60 58, 5000 Cologne, Federal Republic of Germany, 15 deutsche marks

A physically transparent method for calculating the small-signal gain of a free-electron laser (FEL) in the low-current regime is presented. The approach, performed within the framework of the single-particle model, makes explicit use of the modulation of the electron distribution function (bunching). In comparison with the usual method (expansion of the energy perturbation to second order by the amplitude of the signal wave; averaging over a homogeneous initial distribution) a gain formula with a factor twice as high in case of the FEL with a helical periodic wiggler is obtained. This is in best agreement with the Stanford-Experiment (1975). For the wiggler-free FEL (gyration in a homogeneous longitudinal magnetic field in combination with relativistic longitudinal motion) there are significant deviations of the gain formula with respect to published results. ESA

N88-27553*# National Aeronautics and Space Administration. Langley Research Center, Hampton, Va.
OVERVIEW AND FUTURE DIRECTION FOR BLACKBODY SOLAR-PUMPED LASERS
R. J. DeYoung Aug. 1988 23 p
(NASA-TM-100621; NAS 1.15:100621) Avail: NTIS HC A03/MF A01 CSCL 20E

A review of solar-pumped blackbody lasers is given which addresses their present status and suggests future research directions. The blackbody laser concept is one system proposed to scale to muitimegawatt power levels for space-to-space power transmissions for such applications as onboard spacecraft electrical or propulsion needs. Among the critical technical issues are the scalability to high powers and the laser wavelength which impacts the transmission optics size as well as the laser-to-electric converter at the receiver. Because present blackbody solar-pumped lasers will have laser wavelengths longer than 4 microns, simple photovoltaic converters cannot be used, and transmission optics will be large. Thus, future blackbody laser systems should emphasize near visible laser wavelengths. Author

37 MECHANICAL ENGINEERING

Includes auxiliary systems (nonpower); machine elements and processes; and mechanical equipment.

N88-27554# Oak Ridge National Lab., Tenn.
MOTOR-RESPONSE LEARNING AT A PROCESS CONTROL PANEL BY AN AUTONOMOUS ROBOT
P. F. Spelt, G. deSaussure, E. Lyness, F. G. Pin, and C. R. Weisbin 1988 31 p Presented at the 5th International Conference on Machine Learning, Ann Arbor, Mich., 12 Jun. 1988
(Contract DE-AC05-84OR-21400)
(DE88-005055; CONF-880657-1) Avail: NTIS HC A03/MF A01

The Center for Engineering Systems Advanced Research (CESAR) was founded at Oak Ridge National Laboratory (ORNL) by the Department of Energy's Office of Energy Research/Division of Engineering and Geoscience (DOE-OER/DEG) to conduct basic research in the area of intelligent machines. Therefore, researchers at the CESAR Laboratory are engaged in a variety of research activities in the field of machine learning. In this paper, we describe our approach to a class of machine learning which involves motor response acquisition using feedback from trial-and-error learning. Our formulation is being experimentally validated using an autonomous robot, learning tasks of control panel monitoring and manipulation for effect process control. The CLIPS Expert System and the associated knowledge base used by the robot in the learning process, which reside in a hypercube computer aboard the robot, are described in detail. Benchmark testing of the learning process on a robot/control panel simulation system consisting of two intercommunicating computers is presented, along with results of sample problems used to train and test the expert system. These data illustrate machine learning and the resulting performance improvement in the robot for problems similar to, but not identical with, those on which the robot was trained. Conclusions are drawn concerning the learning problems, and implications for future work on machine learning for autonomous robots are discussed. DOE

N88-27555# Central Electricity Generating Board, Southampton (England). Technology Planning and Research Div.
DISTRIBUTION OF WELD QUALITY IN THIN SECTION STAINLESS STEEL TUBE ATTACHMENT WELDS
P. J. Alberry, R. R. L. Brunnstrom, and R. N. Wharmby 1987 23 p
(PB88-109632; TPRD/M/1622/R87) Avail: NTIS HC E04/MF E04; copy not available from STI Facility CSCL 13H

A statistical analysis of the geometrical variability of manual, thin section, stainless steel tube attachment weld was carried out on a number of samples taken during commercial production. The distribution of weld quality was determined. In addition, the variability between different manual welders was calculated and related to the overall variability in the welded population. The implications for the control of weld quality in large welded populations are discussed. Author

N88-27556# Duke Univ., Durham, N. C. Dept. of Civil and Environmental Engineering.
COMPLIANT ROBOTIC STRUCTURES, PART 3 Final Report, 1 Jun. 1986 - 31 Aug. 1987
James F. Wilson Nov. 1987 144 p
(Contract MDA903-84-C-0243; ARPA Order 5092)
(AD-A192426; DUKE-CE-001-87-3) Avail: NTIS HC A07/MF A01 CSCL 12I

This is the third and final report of a three-year study on complaint robotic structures. Such structures are designed of continuously flexible elastomeric tubes that either extend as bellows, or bend transversely, or twist about the longitudinal axis when subjected to internal pressure. The motion of such a tube

under controlled internal pressure depends on its directional stiffness, achieved through the orientation of both the wall corrugations and reinforcing fibers. Tube elements in series, or end-to-end, make up a robotic limb. A single limb may be employed as a manipulator arm. Several limbs acting in parallel may be used as a compliant gripping device that conforms to the object being manipulated; and multiple limbs in parallel may be used as legs for walking machines. The present report, concentrates on the analysis, the design, and the experimental evaluation of the above mentioned elements. These studies, the conceptual designs with a knowledge of muscle structure in selected animals. A computer-aided control scheme is applied to a demonstration project: a manipulator arm made up of bending elements in series. This 50 cm arm successfully manages smooth, open-loop, pick-and-place manipulations with cycle times as small as 4.2 seconds and with placement reproducibility within 5 percent of the target point. GRA

N88-27557# Air Force Inst. of Tech., Wright-Patterson AFB, Ohio. School of Engineering.
DEVELOPMENT OF A HYBRID SIMULATOR FOR ROBOTIC MANIPULATORS M.S. Thesis
Peter M. VanWirt Dec. 1987 123 p
(AD-A193119; AFIT/GE/ENG/87D-68) Avail: NTIS HC A06/MF A01 CSCL 12E

A real-time robot manipulator simulation capability has been developed. By programming the robot dynamics in the analog section of a SIMSTAR Hybrid Computer, the computational burden of digital integration techniques is avoided, and due to the analog nature of the model, the simulation can be run in real time without sacrificing accuracy. The ability to test analog and hybrid control schemes is also achieved through the development of an analog manipulator model on the SIMSTAR and because the SIMSTAR is both a digital and an analog computer. A hybrid controller contains an analog feedback portion to provide needed loop stiffness, and a digital feedforward portion to compensate for the changing dynamics of a robotic manipulator. The model is developed through a combination of previous research and experimental evaluation. Once programmed, the SIMSTAR model is validated using known trajectory/error data obtained from the AFIT PUMA 560. GRA

N88-27558# Army Tank-Automotive Command, Warren, Mich.
THE 210-HP DIESEL ENGINE ENDURANCE AND PERFORMANCE TESTING WITH FIRE RESISTANT DIESEL FUEL Final Technical Report, 11 Aug. 1986 - 29 Jul. 1987
Milad H. Mekari Oct. 1987 261 p
(AD-A193153; TACOM-TR-13322) Avail: NTIS HC A12/MF A01 CSCL 21G

The test program and report were conducted and prepared by the U.S. Army Tank-Automotive Command Propulsion Systems Division and laboratory. The report details performance and durability tests using Fire Resistant Diesel Fuel (FRDF). The objective of the FRDF program is to develop a future fuel that will reduce the vulnerability of military vehicles to fire, decrease the number of vehicles lost and repair costs, and increase crew survivability. The objective of this project is to evaluate the performance and endurance of a medium-sized, unmodified commercial production diesel engine of 200-hp range tested with FRDF. The FRDF contains tap water of 10.2 to 13.2 percent volume. Another objective of this project is to inspect the fuel-wetted parts of the fuel injection system and engine, and determine the effect of the water in the fuel on these parts. GRA

N88-27559# Southwest Research Inst., San Antonio, Tex.
ANALYTICAL AND EXPERIMENTAL INVESTIGATION OF RINGLESS PISTON CONCEPT Final Report, Sep. 1986 - Nov. 1987
Daniel W. Dickey and Charles D. Wood Mar. 1988 56 p
(Contracts DAAJ02-86-C-0030; DAAK70-85-C-0007; DA Proj. 1L1-62209-AH-76)
(AD-A193213; SWRI-1362; USAAVSCOM-TR-88-D-2) Avail: NTIS HC A04/MF A01 CSCL 21G

The purpose of this project was to analytically and experimentally investigate the concept of a ringless piston internal combustion engine. A joint objective was to design, build, and test a ringless piston to improve ringless piston engine performance. A computer model was developed to predict ringed and ringless piston engine performance. Experimental performance data were then collected by operating a small, liquid-cooled, two-stroke gasoline engine with and without the piston ring on the stock aluminum and Southwest Research Institute prototype steel piston. The experimental performance data were then compared with the results of the computer model. The results showed that a piston engine can operate without piston rings. Ringless piston engine power and efficiency were found to be defined by the expression C/NBS, where C = piston-to-bore diametrical clearance, N = engine speed in rpm, B = engine bore, and S = engine stroke. There was good agreement between predicted and measured performance results. The results of the prototype steel piston test showed that ringless piston engine performance can be improved by using piston and liner materials that have similar coefficients of thermal expansion. GRA

N88-27560# Aerospace Corp., El Segundo, Calif. Chemistry and Physics Lab.
PERFLUOROPOLYALKYLETHER LUBRICANTS UNDER BOUNDARY CONDITIONS: IRON CATALYSIS OF LUBRICANT DEGRADATION
David J. Carre 1 Mar. 1988 25 p
(Contract F04701-85-C-0086)
(AD-A193241; TR-0086A(2945-03)-6; SD-TR-88-27) Avail: NTIS HC A03/MF A01 CSCL 11H

Perfluoropolyalkylether (PFPE) oils and oil-based greases exhibit significant degradation under boundary lubrication conditions. In the absence of significant concentrations of oxygen, as in the case of spacecraft orbital environments, the degradation mechanism consists of two steps: (1) the initial reaction of the PFPE molecules with freshly exposed iron to form the Lewis acid, FeF3, followed by (2) the reaction of the FeF3 with unreacted PFPE molecules, which results in the cleavage of the etherate linkages. The result is an autocatalytic degradation that takes place at temperatures below the onset of thermal decomposition. This mechanistic hypothesis is supported by the following experimental results: (1) The reaction of PFPE with FeF3 has been shown to give rise to fluorinated-ketone and acid fluoride ether-cleavage products that are more reactive than the parent PFPE molecules and have lower molecular weights and thus poorer lubricating ability. (2) FeFX compounds are formed in the wear tracks of wear-test components under boundary lubrication conditions. GRA

N88-27561# Cambridge Univ. (England).
BASIC MECHANISMS OF DIESEL LUBRICATION CORRELATION OF BENCH AND ENGINE TESTS Annual Report No. 1
A. F. Alliston-Greiner and J. A. Greenwood Aug. 1987 80 p
(Contract DAJA45-86-C-0007)
(AD-A193360) Avail: NTIS HC A05/MF A01 CSCL 11H

A newly designed reciprocating ball-on-flat apparatus is described. Reaction film formation by commercially available ZDDP additives were observed and their thicknesses measured by capacitance during the rubbing process. The film behaviour is related to its composition and the thermal stability and reactivity of the additives. Preliminary observation is made of the running-in process with cast-iron cylinder liners. The programme of work proposed for the coming year is detailed in the Appendix. GRA

N88-27562*# Stanford Univ., Calif. Aerospace Robotics Lab.
CONTROL OF FREE-FLYING SPACE ROBOT MANIPULATOR SYSTEMS Semiannual Report No. 5, Mar. - Aug. 1987
Robert H. Cannon, Jr. 10 Aug. 1977 55 p
(Contract NCC2-333)
(NASA-CR-183017; NAS 1.26:183017) Avail: NTIS HC A04/MF A01 CSCL 13I

To accelerate the development of multi-armed, free-flying satellite manipulators, a fixed-base cooperative manipulation facility is being developed. The work performed on multiple arm cooperation on a free-flying robot is summarized. Research is also summarized on global navigation and control of free-flying space robots. The Locomotion Enhancement via Arm Pushoff (LEAP) approach is described and progress to date is presented. B.G.

N88-27563*# Stanford Univ., Calif. Aerospace Robotics Lab.
CONTROL OF FREE-FLYING SPACE ROBOT MANIPULATOR SYSTEMS Semiannual Report No. 6, Sep. 1987 - Feb. 1988
Robert H. Cannon, Jr. 10 Aug. 1988 31 p
(Contract NCC2-333)
(NASA-CR-183104; NAS 1.26:183104) Avail: NTIS HC A03/MF A01 CSCL 13I

The focus of the work is to develop and perform a set of research projects using laboratory models of satellite robots. These devices use air cushion technology to simulate in two dimensions the drag-free, zero-g conditions of space. Five research areas are examined: cooperative manipulation on a fixed base; cooperative manipulation on a free-floating base; global navigation and control of a free-floating robot; an alternative transport mode call Locomotion Enhancement via Arm Push-Off (LEAP), and adaptive control of LEAP. Author

N88-27564# Sandia National Labs., Albuquerque, N. Mex.
PROCESS CONTROL IMPROVEMENTS IN PULSED Nd:YAG LASER CLOSURE WELDING OF ELECTROMECHANICAL RELAYS
P. W. Fuerschbach May 1988 9 p Presented at the ASW/EWI Power Beam Conference, San Diego, Calif., 1 May 1988
(Contract DE-AC04-76DP-00789)
(DE88-006275; SAND-87-1574C; CONF-880547-2) Avail: NTIS HC A02/MF A01

The pulsed Nd:YAG laser welding process is often chosen today for closure welding of small hermetically sealed electrical devices. This is because it is a high power density welding process that can minimize total heat input and therefore is less likely to damage heat sensitive components. The effect of the pulsed Nd:YAG laser welding parameters on the incidence of glass-to-metal seal cracking and on the weld fusion zone dimensional parameters for an electromechanical relay has been determined. Fluctuations in weld penetration in production relays have been attributed to variability in sharp focus positioning. A large increase in blowholes and porosity in the fusion zone has been traced to the inadvertent substitution of 304 stainless steel for 304L stainless steel header material. The blowholes and porosity are thought to result from a carbon-oxygen gas reaction in the weld pool due to the presence of a 4 percent oxygen atmosphere and the increased carbon content of the 304 stainless steel. A technique using diamond apertures to measure laser spot size has been developed and has proved useful in determining the effect of the process control parameters on the actual workpiece irradiance. DOE

N88-27565# Southern Univ., Baton Rouge, La. Dept. of Mechanical Engineering.
EXPERIMENTAL VALIDATION OF A ZERO-DIMENSIONAL COMPUTER MODEL FOR SPARK-IGNITION ENGINES
Progress Report
R. L. Scott, Jr. 25 Apr. 1988 30 p
(Contract DE-AS04-86AL-38221)
(DE88-009034; DOE/AL-38221/T3) Avail: NTIS HC A03

This is a progress report on the subject contract. It contains a discussion of progress made to date on the engine design, and the computer code used for analysis. It also contains a statement on progress expected during the next reporting period. DOE

N88-27566# Oak Ridge National Lab., Tenn.
THE 000 STAGE EQUIPMENT BEARING PERFORMANCE WITH A LOWER VISCOSITY LUBRICANT
D. C. Lannom May 1988 34 p
(Contract DE-AC05-84OT-21400)
(DE88-011827; K/QT-198) Avail: NTIS HC A03/MF A01

One of the Gaseous Diffusion Ultimate Potential (GDUP) projects involves a study of methods to reduce process equipment bearing power losses. In support of this effort, an analytical study has been completed which assesses the performance and expected benefits of operating the 000 stage equipment with a lower viscosity lubricant. Fluid film bearing analysis codes were employed to study 000 stage compressor and motor bearings. Correlations depicting bearing minimum film thickness and power loss with variable lubricant inlet temperature are presented for two lubricants: (1) code BG oil (310 SSU at. 100 F) and code BE oil (150 SSU at. 100 F). DOE

N88-27567# Japan Atomic Energy Research Inst., Tokyo. Dept. of Reactor Engineering.
GENERAL EXPRESSION OF MANIPULATOR KINEMATICS
Shinobu Sasaki Feb. 1988 21 p In JAPANESE; ENGLISH summary
(DE88-753430; JAERI-M-88-018) Avail: NTIS (US Sales Only) HC A03/MF A01

In this paper, a general description for kinematic modelling of all types of manipulators is presented by expanding the concept of the homogeneous transformation (A sub i-matrix) based on Denavit-Hartenberg notation. Unlike the previous matrix method, the expression of recursive relationships which is suitable for computer-aided design makes it possible to derive automatically the position and orientation of manipulator hand. Two algorithms which take into consideration of the order of operation result in identical relations with respect to the kinematics between the reference system and the final link, which was proved by an application to a six-link manipulator. DOE

N88-27568# Sandia National Labs., Albuquerque, N. Mex.
A DEMONSTRATION OF RETRO-TRAVERSE USING A SEMI-AUTONOMOUS LAND VEHICLE
D. E. McGovern, P. R. Klarer, and D. P. Jones 1988 13 p Presented at the Conference on Space and Military Applications of Automation and Robotics, Huntsville, Ala., 13 Jun. 1988
(Contract DE-AC04-76DP-00789)
(DE88-009851; SAND-88-1222C; CONF-8806118-1) Avail: NTIS HC A03/MF A01

A Jeep Cherokee has been modified by Sandia National Laboratories to allow remote control either by teleoperation or through computer generated commands (autonomy). This vehicle has been used for development of hardware and software and in the demonstration of concepts for computer augmentation of remote controlled vehicles. As part of this activity, a system has been configured which allows an operator to teleoperate the vehicle from one location (home base) to another (destination). At the completion of teleoperation, the operator can instruct the vehicle to return to the starting position. The vehicle then autonomously performs a retro-tranverse, reversing the path by which it reached its destination. During teleoperation, operator commands are given through an operator control interface consisting of a steering wheel, brake and throttle pedals, and a video display. Commands are transmitted to the vehicle and video returned from the vehicle over RF communication links. Periodic way points are automatically recorded for later use by the vehicle system. Navigation during retro-traverse utilizes dead-reckoning inputs from an odometer, compass and steering angle potentiometer. Way points (previously identified during teleoperation of the vehicle) are linked by short, straight line segments. Along each path segment, the control system generates the steering and speed commands necessary to direct the vehicle towards the next way point. Retro-traverse has been demonstrated over open terrain at Sandia National Laboratories. Path following accuracy and final positional control is a function of dead-reckoning system limitations and control system design. These limitations are discussed, and an improved system is proposed. DOE

N88-27569# Technical Research Centre of Finland, Espoo.
ETHANOL AS A FUEL OF A LORRY. USE EXPERIENCE FROM A DIESEL ENGINE MODIFIED TO AN OTTO ENGINE
N.-O. Nylund and T. Eklund Oct. 1987 66 p In FINNISH; ENGLISH summary
(DE88-752870; VTT-TIED-772) Avail: NTIS (US Sales Only) HC A04/MF A01

When using alcohol for diesel fuel, either the engine or the fuel must be converted due to the poor ignition of alcohols. A direct injection diesel engine is usually easy to convert into an otto engine. The otto version is technically simple, although its efficiency is lower than that the diesel. The limit values of performance and the driveability characteristics of a simple otto engine version were determined in the test. This otto engine version could be of significance in a crisis provided that alcohol fuels are available. There is also a rising interest in alcohol-fueled spark-ignition versions in developing countries. A Finnish-made Valmet 611 turbo diesel engine was chosen for conversion. No special parts were used. The engine was first driven in an engine dynamometer. The maximum power of the free-respiration ethanol version was about 85 percent of that of a turbo diesel and the peak thermal efficiency was 34 percent. For the evaluation of driveability, the converted engine was installed in a Karhu-Sisu truck. The truck was driven about 8500 km with E90 fuel. The performance values of the truck were an average 15 percent lower than for the ethanlo-fueled engine than for the original diesel. The average fuel consumption was 52 1/100 km during the test, corresponding to about 30 1/100 km for a diesel engine. Hence, the energy consumption was about 20 percent higher than that of a diesel engine. The tests indicated that it is relatively easy to convert a diesel engine to a spark-ignition one and to achieve a satisfactory level of performance. The performance and availability of the alcohol engine is by far superior to a producer (wood) gas engine. DOE

N88-27570# Technical Research Centre of Finland, Espoo.
HYDRAULIC PUMPS AND HYDRAULIC EQUIPMENT AT LOW TEMPERATURES
R. Soudunsaari and A. Lehto Oct. 1987 76 p In FINNISH; ENGLISH summary
(DE88-752871; VTT-TIED-774) Avail: NTIS (US Sales Only) HC A05/MF A01

The ambient temperature may be -40 to -60 C in arctic conditions. This causes hardening and shrinkage of seals, deterioration of the suction ability of hydraulic pumps, brittleness in metals and increases viscosity in hydraulic fluids. This may result in oil leakages and component damage. The suction ability of a piston pump, a vane pump and a gear pump was measured at low temperatures. Mineral oil based hydraulic fluid and synthetic fluid were used. The viscosities of the oils during the tests were above the maximum values recommended by the pump manufacturers. The suction ability of each pump was good. The housing of the vane pump broke in a test carried out at -40 deg C. The cooling of the oil in the tank during the night can be decreased by at least 10 to 12 deg C by insulation. Use of a rotating heater is recommended to heat the oil in different parts of the tank. Assemblies composed of hydraulic tubes and hydraulic tube fittings are tight also at low temperatures if they have been carefully mounted and they are under no external strain. The operation of liquid level switches was good at low temperatures. The connecting pressure of pressure switches normally increased when the temperature decreased and the test pressure increased rapidly. DOE

N88-27571 Wisconsin Univ., Madison.
DYNAMIC STABILITY OF ELASTIC ROTOR-BEARING SYSTEMS VIA LIAPUNOV'S DIRECT METHOD Ph.D. Thesis
Abd Alla M. ElMarhomy 1987 218 p
Avail: Univ. Microfilms Order No. DA8727231

The effects of the various end support parameters coupled with the shaft stiffness parameters on the whirling stability of rotor-bearing systems are examined. The analysis is based on an appropriate model of a continuous elastic rotating shaft mounted on two dissimilar bearings having anisotropic and cross coupling stiffness and damping coefficients. The method of analysis utilizes Liapunov's direct method applied to the nonlinear equations of motion with modal expansions used for the spatial description of rotor elastic deflections. A general set of closed form sufficient conditions for whirling stability in terms of the various system parameters is formulated which functionally shows the effect of including additional modal terms on the accuracy of the stability boundaries of this elastic system. Thus, questions relating to the effect of truncation error on the stability of the system can be readily studied by this method. The results show that the use of a single modal term gives a very satisfactory approximation to the exact stability boundaries. Stability boundaries are presented in graphical form as functions of system parameters.
Dissert. Abstr.

N88-27572 Stanford Univ., Calif.
DEXTEROUS HANDS: OPTIMIZING GRASP BY DESIGN AND PLANNING Ph.D. Thesis
Zhiming Ji 1987 159 p
Avail: Univ. Microfilms Order No. DA8800959

Four issues related to dexterous hands are explored: hand design optimization and kinematic structure analysis; determining proper finger motions corresponding to desired grasp and manipulation of an object; developing efficient algorithms for directly optimizing the grasp force; and planning optimal grasp configurations. Most examples use a hand with three four-joint fingers, however, the analysis presented is applicable to any three-fingered hand, and can be extended to hands with more fingers. The kinematic structure analysis is based on a surface contact model. The dexterity requirements associated with this contact model and other factors suggest the use of three four-revolute-joint fingers for a dexterous hand, each finger has three distal joints parallel to each other, the proximal joint is parallel to them. It is shown how to obtain the inverse kinematics for moving fingers so as to make the desired contact with an object. Different ways to formulate pure rolling conditions are presented, and for sliding manipulation, the use of the direction and rate of contact point sliding in planning is discussed. Applying the right grasping forces is essential for a robust grasp and successful manipulation. An algorithm is presented to optimize the grasping force efficiently. Two measures of a grasp configuration: the form closure ability and the internal force ability are studied for the purposes of grasp planning. Dissert. Abstr.

N88-27573# Technische Univ., Brunswick (West Germany). Fakultaet fuer Maschinenbau und Elektrotechnik.
OPTIMIZATION OF PLANETARY GEARS Ph.D. Thesis [OPTIMIERUNG VON PLANETENGETRIEBEN]
Gerhard Grueschow 1987 132 p In GERMAN
(ETN-88-92375) Avail: NTIS HC A07/MF A01

Multiparametric optimization and elaboration of a computer program for planetary gear design is described. Basic considerations on computational procedures, operational behavior, DIN-normalization features, and optimization procedure are examined for simple, coupled, and reduced planetary gears. Computer program library is in FORTRAN 77. Optimization procedures are compared for their performance, optima quality, computing, and data storage characteristics. ESA

N88-27574 Illinois Univ., Urbana-Champaign.
A LUBRICATION STUDY OF ENGINE BEARINGS Ph.D. Thesis
Hoang-shen Lin 1987 179 p
Avail: Univ. Microfilms Order No. DA8803117

An algorithm based on the two dimensional Reynolds equation is developed for predicting the performance of dynamically loaded journal bearings. Using finite difference methods and a circular bearing geometry, the results obtained with full-Sommerfeld, Reynolds, and zero gradient boundary conditions are compared. In addition, the effects of temperature distribution on the bearing geometry are analytically investigated by using finite element programs. The temperature boundary conditions used for the thermal analysis are obtained experimentally with a test machine

which produces fluctuating loads. The computed journal center orbits are also qualitatively compared to the measurements obtained with the inductive proximity sensors installed on the test bearings. Furthermore, the algorithm is expanded to study the effects of an elliptical bearing clearance on the minimum oil film thickness. Dissert. Abstr.

N88-27386# University of Eastern Washington, Cheney. Dept. of Mathematics.
HOLE DIAMETERS IN PLATES IMPACTED BY PROJECTILES Final Report
Randall F. Westhoff *In* Universal Energy Systems, Inc., United States Air Force Graduate Student Summer Support Program, Volume 2 Dec. 1987 15 p (For primary document see N88-27355 21-31)
Avail: NTIS HC A99/MF E03 CSCL 13I

N88-27391# Mitsubishi Electric Corp., Tokyo (Japan). Product Development Lab.
HIGH-SPEED, PRECISION PROCESSING USING AN ELECTRON BEAM
Seiji Yasunaga and Megumi Ohmine *In its* Mitsubishi Electric Advance (R and D Edition), Volume 41 Dec. 1987 4 p (For primary document see N88-27388 21-31)
Avail: NTIS HC A03/MF A01 CSCL 13H

38 QUALITY ASSURANCE AND RELIABILITY

Includes product sampling procedures and techniques; and quality control.

N88-27575# Oak Ridge Y-12 Plant, Tenn.
NDE PERFORMANCE IN PREDICTING FAILURE STRENGTH OF SPHERICAL COMPOSITE SPECIMENS WITH IMPLANTED FLAWS
W. D. Brosey, M. T. Calfee, J. W. Whittaker, E. G. Henneke, D. Post, K. L. Reifsnider, and R. A. Blake Feb. 1988 21 p Presented at the American Society of Nondestructive Testing (ASNT) Spring Conference, Orlando, Fla., 11 Apr. 1988 Prepared in cooperation with Virginia Polytechnic Inst. and State Univ., Blacksburg and Delaware Univ., Newark
(Contract DE-AC05-84OR-21400)
(DE88-008223; Y/DW-741; CONF-880487-1) Avail: NTIS HC A03/MF A01

The results of a program to evaluate nondestructive inspection techniques on spherical composite specimens are presented. Seventy Kevlar-epoxy filament wound specimens were made such that ten of the specimens contained one of seven defect conditions which simulated manufacturing or handling defects. These defect conditions were a standard no-defect condition, Teflon-shim simulated delamination, ceramic bead simulated voids, 10 percent low-fiber alternate winding pattern, low-modulus alternate fiber type, variable tension, and dry (low-matrix) fiber. Some specimens were impact damaged by dropping them from various heights to a hard surface. Each specimen was inspected using a variety of nondestructive techniques to determine which methods were useful for detecting the defect conditions in the specimens. The specimens were subsequently pressurized to failure to determine any detrimental effect the implanted flaw types might have on enclosed geometry structures. One important finding in the study was that nominal defects introduced during the manufacturing or handling process do not significantly reduce the ultimate burst strength of the composite material in this geometry when creep and fatigue mechanisms are insignificant. DOE

N88-27576# Bordeaux 1 Univ., Talence (France).
USE OF MICROWAVE MEASURING SYSTEMS FOR THE NONDESTRUCTIVE CONTROL OF RESINS AND COMPOSITES [UTILISATION DE SYSTEMES DE MESURE MICRO-ONDE POUR LE CONTROLE NON DESTRUCTIF DE RESINES ET COMPOSITES]
Jean Louis Miane and Jean Francois Lacombe 1988 10 p In FRENCH Presented at the Journee Specialisee Trimestrielle Controle Non Destructif et Materiaux Composites, 7 Apr. 1987
(SNIAS-881-430-123; ETN-88-92870) Avail: NTIS HC A02/MF A01

Microwave circuits are used to measure the rate of resin deposited on kevlar or carbon fibers and to measure the physical chemical characteristics of resin systems. A resonant cavity coupled with a waveguide is used. These controls are being installed as standard process control procedures. ESA

N88-27577# Societe Nationale Industrielle Aerospatiale, Suresnes (France). Direction de la Qualite.
INTERFACE CONTROL USING LOW FREQUENCY (3 TO 20 MHz) ACOUSTIC MICROSCOPY Final Report [CONTROLE D'INTERFACES PAR MICROSCOPIE ACOUSTIQUE BASSE FREQUENCE (3-20 MHZ). PROCES-VERBAL 48-411/F]
J. Odorico and J. L. Arnaud 2 Jul. 1987 37 p In FRENCH
(Contract DRET-85-34-443)
(Rept-48-411/F; ETN-88-92882) Avail: NTIS HC A03/MF A01

A nondestructive test based on low frequency acoustic microscopy is described. The mechanical assembly is simpler than classical acoustical microscopy, but the resolution is better. The tested interfaces include bonded surfaces, delaminated composites, diffusion welding, and brazing. The technique is easy to employ and especially suited for controling thin materials (0.1 to 0.3 mm of metal) ESA

39 STRUCTURAL MECHANICS

Includes structural element design and weight analysis; fatigue; and thermal stress.

For applications see *05 Aircraft Design, Testing and Performance* and *18 Spacecraft Design, Testing and Performance*.

N88-27578 Purdue Univ., West Lafayette, Ind.
FAILURE ANALYSIS OF LAMINATED COMPOSITE ANGLES Ph.D. Thesis
Scott Roger Kelly 1987 140 p
Avail: Univ. Microfilms Order No. DA8729751

Laminated angles were studied to determine the failure mechanics. Analysis was performed using the finite element method. Additionally, several alternative analysis techniques were developed based on a strength of materials approach. Tests were conducted to obtain failure data for several different angle laminate stacking sequences. Specimens were fabricated using both graphite/epoxy and fiberglass/epoxy material systems. Two different failure modes, in-plane failur and out-of-plane, or delamination, failure, were found to occur in the angle laminate. Failure analysis was conducted using the Hill criterion, the Hill-Tsai criterion and the maximum radian stress criterion. The Hill-Tsai and maximum radial stress criteria were used together to predict in-plane and out-of-plane failures respectively. The Hill criterion was used to predict failure by either failure mode. Fracture mechanics analysis was utilized to study the relationship between in-plane and out-of-plane failure. It was determined that fracture mechanics could be used to predict the onset of delamination based on the branching of in-plane bending cracks. Finally, adhesive plies were studied as a means of preventing delamination in the curved laminate. Dissert. Abstr.

N88-27579 Michigan Univ., Ann Arbor.
OPTIMAL DESIGN OF VISCOELASTIC STRUCTURES Ph.D. Thesis
Tong Ching Lin 1987 144 p
Avail: Univ. Microfilms Order No. DA8801362

Damping layers for beams are used in two basic configurations, unconstrained and constrained. In the unconstrained configuration, damping material is bonded to the beam surface. In the constrained layers, an additional metallic facing is attached to the viscoelastic

coating. A key question addressed is, for a given volume of damping material, how much the peak displacement can be reduced over the uniform distribution case, if the profile of the damping layer is optimized. Alternations in fatigue life times are monitored as additional performance measures. The base beam and face sheets are treated as Euler-Bernoulli beams and the viscoelastic coatings are taken to be Timoshenko beams. A finite element approach is used in which rod and beam element interpolation functions are used for the longitudinal and tranverse displacement, respectively. Displacement response is obtained using both modal analysis and a direct method. Neuber's rule is used to calculate fatigue lifetimes. Optimization is approached using mathematical programming techniques, the method chosen being a sequential, unconstrained minimization technique. The finite element modeling was validated by comparing natural frequencies and loss factors for a three layer beam with published values. Results on optimum profiles, displacement performance measures and fatigue lifetime changes are given, for both unconstrained and constrained damping layers. Dissert. Abstr.

N88-27580# Technische Hogeschool, Delft (Netherlands). Engineering Mechanics Lab.
NONLINEAR INTERACTION BETWEEN OVERALL AND LOCAL BUCKLING OF STIFFENED PANELS WITH SYMMETRIC CROSS-SECTIONS
Q. S. Fan Jan. 1987 54 p
(PB88-104054; WHTD-183; Rept-843) Avail: NTIS HC E04/MF A01; copy not available from STI Facility CSCL 20K

This paper deals with the nonlinear interaction between overall buckling and local buckling of stiffened panels with symmetric cross sections. It is argued that the restriction to a single local mode should be adequate whenever the reduction in flexural rigidity is comparable to the reduction in compressive stiffness. The argument does not apply to a symmetric cross section in which significant deflections in the primary local mode occur on both sides of the neutral axis. In such cases the analysis should be improved by taking into account a second local mode. In the present paper, the interactions between overall and two local buckling modes (primary and secondary mode) are considered for both the perfect and imperfect panel. Application of the present analysis to a square tube gives some important results. Dissert. Abstr.

N88-27581# Purdue Univ., West Lafayette, Ind. School of Aeronautics and Astronautics.
THREE-DIMENSIONAL ASPECTS OF FATIGUE CRACK CLOSURE Final Report
A. F. Grandt, J. E. Pope, and S. K. Ray Feb. 1988 205 p
(Grant AF-AFOSR-0106-85)
(AD-A192296; AAE-88-1; AFOSR-88-0266TR) Avail: NTIS HC A10/MF A01 CSCL 20K

This final report summarizes progress on a basic research effort to determine three-dimensional aspects of the relationship between applied load and fatigue crack face separation. The research was motivated by the well known crack closure phenomenon, which indicates that naturally occurring fatigue cracks are physical held shut (or propped open) at zero load, so that crack surfaces do not separate in a linear elastic manner. Although prediction of fatigue crack opening behavior is of fundamental importance to many aspects of crack growth, relatively little is known about the three-dimensional character of closure. The research employed experimental and numerical procedures to develop predictive techniques for this important aspect of crack closure. Optical interference was used to measure crack opening in transparent polymer specimens, along with conventional crack opening and back face strain techniques for measuring crack closure. A numerical algorithm was developed to predict opening loads in surface flawed plates, and was compared with the experimental results. GRA

N88-27582# San Diego Aircraft Engineering, Inc., Calif.
PLASTIC YIELDING AT CRACK TIPS Final Report
S. B. Altan and A. C. Eringen Mar. 1988 48 p
(Contract DAAL03-86-K-0019)
(AD-A192549; ARO-22967.4-EG) Avail: NTIS HC A03/MF A01 CSCL 20K

Small scale plastic yielding at crack tips is studied by means of nonlocal elasticity. Plastic lines along the crack line of Mode 3 cracks are modelled by an array of dislocations. It is shown that plastic yield begins after a definite value of load, as a consequence of nonlocality. The length of plastic zone and the dislocation distribution are determined as functions of the applied load. Results are in good agreement with experimental observations. GRA

N88-27583# SRI International Corp., Menlo Park, Calif.
INFLUENCE OF MICROSTRUCTURE AND MICRODAMAGE PROCESSES ON FRACTURE AT HIGH LOADING RATES Annual Report, 1 Feb. 1987 - 31 Jan. 1988
J. H. Giovanola and D. A. Shockey 3 Mar. 1988 20 p
(Contract F49620-86-K-0010)
(AD-A192957; AFOSR-88-0291TR) Avail: NTIS HC A03/MF A01 CSCL 11F

The optimal use of advanced beta and near-beta titanium alloys in situations involving dynamic or shock loading requires an understanding of the influence of microstructure and loading rate on fracture behavior. To address this need, SRI is performing dynamic crack initiation and propagation experiments on Ti-10V-2Fe-3Al in three microstructural conditions, varying the loading rate to establish the rate-dependence of the fracture toughness. A new experimental method developed in a previous Air Force Office of Scientific Research program (the one point bend impact test) and numerical simulations of the experiments are used to determine dynamic initiation and propagation toughness. Further, the fracture surface topography analysis (FRASTA) technique is applied to the fractured specimens to elucidate the microstructural failure mechanisms controlling fracture in each of the investigated microstructures. GRA

N88-27584# Naval Research Lab., Washington, D.C.
CRITICAL ISSUES AND DIRECTIONS FOR FRACTURE MECHANICS AND STRUCTURAL INTEGRITY
M. I. Jolles, P. Matic, G. C. Kirby, III, V. M. Gensheimer, and D. P. Harvey, II 13 May 1988 22 p
(AD-A193050; NRL-MR-6035) Avail: NTIS HC A03/MF A01 CSCL 20K

The development of concepts and methods suitable for the correct analysis of nonlinear inelastic material deformation and fracture is essential for applications of nonlinear fracture mechanics to questions of structural integrity and design. Recent results by the authors have addressed the integration of constitutive behavior and continuum damage concepts in the development of a consistent and versatile fracture mechanics methodology; formulation and solution of a constitutive representation; application of these ideas to analyses of initiation of defect propagation in complex material-structural systems subjected to monotonically increasing loads. The definition and application of a continuum stress-strain relation and a local continuum toughness results in the ability to scale from test specimen to structure. The formative concepts are reviewed and their application to relevant problems are investigated. Computational analyses coupled to experimental data from material test specimens are used to determine the continuum material properties. Practical applications of the methodology are presented. The results indicate the concepts employed can provide a general approach for the analysis of relevant nonlinear fracture mechanics problems. GRA

N88-27585# Northwestern Univ., Evanston, Ill. Dept. of Civil Engineering.
ADAPTIVE FINITE ELEMENT METHODS FOR SHELLS Final Report, 1 Sep. 1985 - 31 Dec. 1987
Ted Belytschko, Wing K. Liu, and Hsiu-Guo Chang 30 Jan. 1988 127 p
(Contract F49620-85-C-0128)
(AD-A193221; AFOSR-88-0277TR) Avail: NTIS HC A07/MF A01 CSCL 13B

An adaptive finite element procedure is developed for the

transient analysis of nonlinear shells. The scheme is an h-method which employs fission and fusion. Criteria based on incremental work and deviation of the bilinear finite element approximation to the shell from a Kirchhoff-Love surface are used as criteria for adaptivity. The example problems show that the adaptive schemes are capable of achieving substantial improvements in accuracy for a given computational effort. They include both material and geometric nonlinearities and local and global buckling. In order to formulate an r-adaptive method, the conservation laws, the constitutive equations, and the equation of state for path-dependent materials are formulated for an arbitrary Lagrangian-Eulerian description. Both geometrical and material nonlinearities are included in this setting. GRA

N88-27586# New Mexico Univ., Albuquerque. Dept. of Mechanical Engineering.
THERMO-MECHANICAL CRACKING IN COATED MEDIA WITH A CAVITY BY A MOVING ASPERITY FRICTION
Frederick D. Ju and Tsu-Yen Chen Mar. 1988 192 p
(Contract N00014-84-K-0252)
(AD-A193311; ME-144(88)ONR-233-3) Avail: NTIS HC A09/MF A01 CSCL 20K

The research deals with the problem of asperity excited thermomechanical fields in a medium with a surface layer and a near surface void defect. The thermomechanical field governs the mode of cracking, which leads to failure in the wear surface. The presence and location of the void defect is most critical. This investigation obtained the solutions for the temperature distribution and the stress state in a layered medium with a rectangular cavity. This temperature distribution and stress state result when the solid medium is subjected to Coulomb frictional loading from an asperity moving at a moderately high speed (of approximately 10-15 m/s). In the analysis, the coated medium was represented by a solid half space, with a thin top surface-layer of solid wear material. The cavity defect required a mathematical model in terms of the material coordinates. The corresponding governing differential equations were time-explicit and transient. A general finite difference formulation was developed to calculate both the temperature and the stress fields. The energy balance method was applied at the corners of the rectangular cavity to resolve the problem of singularities in the temperature field. GRA

N88-27587# European Nuclear Energy Agency, Paris (France).
VIBRATION CONTROL OF LARGE STRUCTURES Final Report, 1 Jan. 1986 - 31 Dec. 1987
Walter D. Pilkev 1 Mar. 1988 46 p
(Contract F49620-86-K-0009)
(AD-A193317; UVA/525673/MAE88/103; AFOSR-88-0369TR)
Avail: NTIS HC A03/MF A01 CSCL 13M

This is a study of some fundamental aspects of the structural dynamics and vibration control of large structures. One focus is the development of a limiting performance formulation with minimum settling time which can accept multiple design objectives efficiently. This new formulation is intended to meet the need of rather comprehensive design objectives for the control of large space structures. Another objective of the study is to develop a systematic way of designing a control system based on the limiting performance characteristics. An indirect synthesis method is proposed. It is shown that closed loop control laws can be based on the optimal response trajectories in the time domain. The method is successfully applied to the control of proof-mass actuators. GRA

N88-27588# Naval Research Lab., Washington, D.C.
THE INFLUENCE OF WELD METAL PROPERTIES, WELD GEOMETRY AND APPLIED LOAD ON WELD SYSTEM PERFORMANCE
Peter Matic and Mitchell I. Jolles 25 Feb. 1988 31 p
(AD-A193403; NRL-MR-5987) Avail: NTIS HC A03/MF A01 CSCL 11F

Alloy development programs have significantly increased the ductility of steels available for ship structures. Design decisions regarding the optimum use of these alloys often reflect limitations imposed by weld performance considerations and available analytical methods. In this investigation, a sufficiently general analytical methodology, based on the distribution of strain energy density, is applied to the computational prediction of weld performance and fracture. Fracture at a material point coincides with a critical strain energy density value associated with the continuum fracture toughness of the material. The critical strain energy density value for each component of the weld metal, heat affected zone and base metal system are obtained from uniaxial tension test data. The role of weld crown, weld metal strength and applied load to butt welded panel performance are examined parametrically. The results suggest that particular combinations of these parameters may offer significant advantages in weld performance. GRA

N88-27589# Texas Technological Univ., Lubbock. Dept. of Mechanical Engineering.
NONLINEAR STOCHASTIC INTERACTION IN AEROELASTIC STRUCTURES Final Report, 1 Nov. 1984 - 31 Dec. 1987
Raouf A. Ibrahim 29 Jan. 1988 117 p
(Grant AF AFOSR-0008-85)
(AD-A193427; AFOSR-88-0368TR) Avail: NTIS HC A06/MF A01 CSCL 20D

The linear and nonlinear modal interactions in aeroelastic structures under wide band random excitation are examined analytically and experimentally. The analytical investigation deals with the random response characteristics of two- and three-degree-of-freedom nonlinear models in the neighborhood of internal resonance conditions. These conditions take the form of linear relationships between the normal mode frequencies and are established from the linear model analysis of each model. The Fokker-Planck equation approach is used to derive a general differential equation is found to constitute a set of infinite coupled first order differential equations. These equations are closed by using two different truncation schemes which are based on the properties of response joint cumulants. These two schemes are known as Gaussian and non-Gaussian closures. The analytical manipulations are performed by using the computer algebraic software MACSYMA, while the response statistical moments are determined by numerical integration by using the IMSL software DVERK. The Gaussian closure solution gives a quasi-stationary response in the form of fluctuations between two limits. However, the non-Gaussian closure results in a strict stationary response. The general trend of the nonlinear interaction takes the form of energy exchange between the interacted modes when the system is internally tuned. GRA

N88-27590# Sandia National Labs., Albuquerque, N. Mex.
STRESS RELAXATION OF A TITANIUM (Ti-6Al-4V) THREADED JOINT
J. J. Stephens and J. W. Munford May 1988 24 p
(Contract DE-AC04-76DP-00789)
(DE88-010102; SAND-87-1818) Avail: NTIS HC A03/MF A01

The amount of load relaxation which can be expected in the W88 Titanium Mounting Ring is summarized. We have performed analytical estimates of the amount of stress relaxation under uniaxial loading conditions, using room temperature creep data for Ti-6Al-4V alloy which was generated in support of previous Sandia programs. In addition, we performed load-relaxation experiments up to 1000 hours duration on torque-loaded model components in order to evaluate experimentally the amount of load relaxation under loading conditions which are identical to those experienced by the mounting ring. Results of both approaches indicate that the amount of load relaxation during a thirty-year component life will not be enough for concern. DOE

N88-27591# Sandia National Labs., Albuquerque, N. Mex.
TEMPERATURE, MOISTURE AND STRAIN RATE EFFECTS ON THE COMPRESSIVE MECHANICAL BEHAVIOR OF NYLON 6/6
Wendell A. Kawahara, Stephen L. Brandon, and John S. Korellis Apr. 1988 35 p
(Contract DE-AC04-76DP-00789)
(DE88-010734; SAND-88-8219) Avail: NTIS HC A03

Material test results are presented for the mechanical behavior of Nylon 6/6 in compression. Static compression modes include direct compression, stress relaxation and creep. Dynamic direct compression results are included. Tests are performed at atmospheric pressure; strain rates range from 0.0004 to 100 sec; temperatures are 20, 65, 110, 150 and 200 C; moisture levels are 0 percent (dry), 2 and 6 percent (saturated); true strains to -0.25 are imposed. Our empirical Temperature-Moisture equivalence of 14 C per 1 percent moisture is discussed with respect to the free volume concept. DOE

N88-27592# Sandia National Labs., Albuquerque, N. Mex.
DEVELOPMENT OF A BIAXIAL TEST SYSTEM FOR THIN-WALLED METAL TUBES USING TENSILE-COMPRESSIVE AXIAL LOAD AND INTERNAL-EXTERNAL PRESSURE
D. T. Schmale and R. J. Bourcier May 1988 48 p
(Contract DE-AC04-76DP-00789)
(DE88-011279; SAND-88-0825) Avail: NTIS HC A03/MF A01

A biaxial deformation test system has been developed to perform tensile-compressive axial loading and internal-external pressurization of thin-walled metal tubes. The system has been added to an existing MTS 490 kN load frame with a PDP 11/34 based computer control system. It consists of: (1) specimen grips, (2) high pressure chamber, (3) a hydraulic intensifier and controller, and (4) associated valving and switching. Software has been written in the MTS MultiUser-BASIC language to perform simple multiaxial cyclic deformation of a tubular specimen. The design of the mechanical test system and software are described and preliminary test results for the deformation of 316 stainless steel tubing under various proportional loading paths are presented. DOE

N88-27593*# Clemson Univ., S.C. Dept. of Mechanical Engineering.
AN EXPERIMENTAL AND ANALYTICAL EVALUATION OF A BIAXIAL TEST FOR DETERMINING SHEAR PROPERTIES OF COMPOSITE MATERIALS
John M. Kennedy and Terry R. Barnett Jul. 1988 75 p
(Contract NCC1-93)
(NASA-CR-182928; NAS 1.26:182928) Avail: NTIS HC A04/MF A01 CSCL 20K

The results of an experimental and analytical investigation of a biaxial tension/compression test for determining shear properties of composite materials are reported. Using finite element models of isotropic and orthotropic laminates, a specimen geometry was optimized. A kinematic fixture was designed to introduce an equal and opposite pair of forces into a specimen with a one inch square test section. Aluminum and several composite laminates with the optimized geometry and a configuration with large stress gradients were tested in the fixture. The specimens were instrumented with strain gages in the center of the test section for shear stiffness measurements. Pure shear strain was measured. The results from the experiments correlated well with finite element results. Failure of the specimens occurred through the center of the test section and appeared to have initiated at the high stress points. The results lead to the conclusion that the optimized specimen is suitable for determining shear modulus for composite materials. Further revisions to the specimen geometry are necessary if the method is to give shear strength data. Author

N88-27594# Oak Ridge National Lab., Tenn.
VERIFICATION OF THE ADINA FINITE ELEMENT CODE FOR CREEP ANALYSIS: PROBLEMS FROM THE OPEN LITERATURE
S. V. McGrath, M. A. Faulkner, B. R. Bass, and W. G. Johnson Mar. 1988 30 p
(Contract DE-AC05-84OT-21400)
(DE88-011826; K/ETAC-57) Avail: NTIS HC A03/MF A01

This report presents the ADINA finite element analysis of several sample creep problems taken from the open literature. In addition to creep, the nonlinearities of plasticity and geometric stiffness are addressed. DOE

N88-27595# Stanford Univ., Calif. Dept. of Civil Engineering.
DIFFUSION MODELS OF CRACK GROWTH DUE TO RANDOM OVERLOADS
S. R. Winterstein and P. S. Veers 1988 5 p Presented at the ASCE Specialty Conference on Probabilistic Mechanics and Structural Safety, Blacksburg, Va., 25 May 1988 Prepared in cooperation with Sandia National Labs., Albuquerque, N. Mex.
(Contract DE-AC04-76DP-00789)
(DE88-008811; SAND-87-2791C; CONF-880587-1) Avail: NTIS HC A02/MF A01

For certain random vibration loads, crack growth may be adequately estimated with random load models that ignore sequence effects. America Society for Testing and Materials (ASTM) test results have been accurately predicted from narrow-band (Rayleigh) load models; analytical results may also include bandwidth effects and racetrack cycle-counting (Veers, 1987) and non-Gaussian loads (Winterstein, to appear). Systematic tensile overloads may produce greater load sequence effects. These are predicted from simple diffusion models, which estimate the crack-opening stress from plastic zone considerations. The reset stress has been fixed during retarded growth; more generally, a steady-state reset stress distribution can be estimated from diffusion theory (Veers, 1987). In general as overload variability increases, overload-affected regions overlap more often and net retardation is less. Therefore, the assumption of regular overloads, common in fatigue block-load testing, may generally be unconservative. DOE

N88-27596# Sandia National Labs., Albuquerque, N. Mex.
A COMPARISON OF ANALYTICAL TECHNIQUES FOR MODELING THE RAYLEIGH-TAYLOR RESPONSE OF ELASTIC-PLASTIC SOLIDS
A. C. Robinson Apr. 1988 34 p
(Contract DE-AC04-76DP-00789)
(DE88-010372; SAND-88-0108) Avail: NTIS HC A03/MF A01

The Rayleigh-Taylor instability response of elastic-plastic solids can be modeled by approximate means. However, neither the linear elastic response equation nor the so-called minimum amplitude instability criterion derived from rigid plastic analyses is sufficient to describe overall stability characteristics at very large driving pressures. We compare several versions of the modal or one-degree-of-freedom approximation technique and indicate the common features which must be included to obtain the qualitative response seen in numerical experiments. DOE

N88-27597# Foreign Applied Sciences Assessment Center, La Jolla, Calif.
SOVIET DYNAMIC FRACTURE MECHANICS RESEARCH
W. G. Knauss, J. P. Dempsey, L. B. Freund, H. T. Hahn, A. S. Kobayashi, J. F. Mescall, and W. A. Nash (Massachusetts Univ., Amherst.) Feb. 1988 204 p Sponsored by US Government
(FASAC-TAR-3140) Avail: NTIS HC A10/MF A01

Soviet publications concerned with processes governing damage and failure in high speed impact are reviewed. The intent is to assess the state of science in the Soviet Union and compare it with that in the United States and other Western countries. The large number of publications surveyed, however limited a picture of the whole field it may present, seems to indicate that the Soviet effort is somewhat behind in adopting many of the more refined analytical and experimental methods commonplace in the West. However, taking into account that publications on some topics may be considered sensitive defense information, the Soviets may be more advanced in some areas than revealed in this study. There appears to be no significant experimental work in progress in the Soviet Union relating to dynamic fracture, a field in which study in the West has been under way for a decade. Moreover, it appears that Soviet researchers have a more difficult time in accessing large computation facilities, from which their work must suffer since computer capability is an essential part of high-speed impact research. However, Soviet researchers are capable, contribute significantly to the subject, keep up with the field, and could quickly adapt. Author

N88-27598 Washington Univ., Seattle.
NONLINEAR VIBRATIONS OF PERIODICALLY STIFFENED PLATES Ph.D. Thesis
Ronald N. Miles 1987 200 p
Avail: Univ. Microfilms Order No. DA8802301

A study is presented of the vibration and sound radiation of airplane fuselage structures when they are excited by intense driving fields. The fuselage structure is idealized as a section of a shell which is supported on a grid of periodically spaced stiffeners. An analytical method is presented for including nonlinear effects in the analysis of the vibrations of periodically stiffened plate structures. The approach consists of first determining the mode shapes and natural frequencies of a finite periodic structure when nonlinearities are neglected. These mode shapes are then used as approximate shape functions in a nonlinear model of the structure. The result is a coupled system of nonlinear ordinary differential equations which are solved numerically. Dissert. Abstr.

N88-27599 Arizona State Univ., Tempe.
PERIODIC OSCILLATIONS IN NONLINEAR MECHANICAL SYSTEMS Ph.D. Thesis
Chandrasekhar Nataraj 1987 175 p
Avail: Univ. Microfilms Order No. DA8802793

A new quantitative method of estimating steady state periodic behavior in nonlinear systems, based on the trigonometric collocation method (TCM), is outlined. A procedure is developed to analyze large mechanical systems with nonlinear components by the use of the above method in conjunction with Component Mode Synthesis. The algorithm discussed is seen to reduce the original problem to solving nonlinear algebraic equations in terms of only the coordinates associated with the nonlinear subsystems and is a big improvement over commonly used integration methods. Based on the above procedure, a computer code is written with specific application to rotor dynamic systems. Also outlined are two stability algorithms that can be used to investigate the existence of the periodic solutions obtained by TCM. Several examples are worked out using the procedure developed. Parametric studies are made for the problem of a journal on a hydrodynamic bearing. The effect of Coulomb friction in a coupling connecting two rigid rotors is analyzed using the TCM as well as analytical approximation method. A simple model of a squeeze film damper is considered and parametric studies carried out to compare centered and eccentric operations. Dissert. Abstr.

N88-27600 Union for Experimenting Coll. and Univ., Yellow Springs, Ohio.
AN INVESTIGATION OF TECHNIQUES FOR DETERMINATION OF OPTIMUM/SELF-OPTIMIZING SYSTEMS Ph.D. Thesis
Michael Emanuel Croslin 1987 170 p
Avail: Univ. Microfilms Order No. DA8801985

Mathematical optimization techniques typically are not applied to most structural engineering problems because the large number of calculations required to complete an optimization require a hefty amount of computer power. Though optimization algorithms are well-developed, they are considered too complex to be applied in general purpose finite-element codes. Availability of relatively low-cost, high-power computers is making optimization feasible for a large number of engineering problems. Also, developments in approximation techniques and geometric modeling are contributions to greater use of the method Computer optimization techniques attempt to locate the nearest minimum of an object, or merit function. This function is a single variable that characterizes the design, and it can be almost any combination of performance, or cost. Generally, certain constraints are placed on the optimization problem, and the design variables are manipulated to produce the optimum design within the constraints. Depending on the technique used, the number of variables allow hundreds of variables, to be considered, while other methods might limit the user to less than 50 geometric parameters. Dissert. Abstr.

N88-27601 Wisconsin Univ., Madison.
COUPLED THERMAL VIBRATIONS OF BEAMS WITH TEMPERATURE-DEPENDENT PROPERTIES Ph.D. Thesis
Abulkhair Mohammad Masoom 1987 105 p
Avail: Univ. Microfilms Order No. DA8727247

Intense thermal loadings applied for a short time period may produce mechanical vibrations of thin structural components. For many usual engineering problems the uncoupled solution procedure is quite valid. But in areas where characteristic times of structural and thermal disturbances are of comparable magnitude, coupled theories of thermoelasticity should be used for accuracy. For materials used at elevated temperatures such as graphite and silicon carbide, the thermal conductivity and modulus of elasticity of materials are functions of temperature. Thus for the accurate design of components operating in a high temperature range, it is necessary to account for the effects of the temperature dependent properties. An analysis is made of beams using the coupled theory of thermoelasticity in which temperature dependent conductivity and elasticity are considered. The equations are coupled in the sense that the energy equation contains the strain terms and temperature dependent coefficients are used in the equations of motion. Temperature and stress histories throughout the beams are obtained by the finite difference method. Dissert. Abstr.

N88-27602 Utah Univ., Salt Lake City.
THE THREE-DIMENSIONAL STRESS FIELD AROUND A CYLINDRICAL INCLUSION IN A PLATE OF ARBITRARY THICKNESS Ph.D. Thesis
Federico Ernesto Penado 1987 105 p
Avail: Univ. Microfilms Order No. DA8803560

The three-dimensional Navier's equations are solved analytically for the case of a cylindrical inclusion of radius, a, which is embedded in a plate of arbitary thickness, 2h. Both the plate and the inclusion are assumed to be of homogeneous and isotropic materials with different material properties. At the interface, perfect bonding is assumed to prevail. As to loading, a uniform tension is applied at the boundary of the plate at points remote from the inclusion. The analysis shows all stresses including the octahecral shear stress to be sensitive to the radium to half thickness ratio (a/h) as well as the material properties. Dissert. Abstr.

N88-27603# Oak Ridge National Lab., Tenn.
EVALUATION OF FRACTURE MODELS THROUGH PRESSURIZED-THERMAL-SHOCK TESTING
C. E. Pugh, R. H. Bryan, B. R. Bass, and R. K. Nanstad 1988 25 p Presented at the IAEA Specialists' Meeting on Fracture Mechanics Verification by Large-Scale Testing, Stuttgart, Federal Republic of Germany, 25 May 1988
(Contract DE-AC05-84OR-21400)
(DE88-011834; CONF-8805141-1) Avail: NTIS HC A03/MF A01

Two multiple-transient pressurized-thermal-shock experiments (PTSEs) have been conducted under the NRC-sponsored Heavy-Section Steel Technology (HSST) program. The first test (PTSE-1) employed an SA-508 class 2 steel with high Charpy upper-shelf energy level and a relatively high brittle-to-ductile transition temperature. The second test (PTSE-2) used a 2 1/4 Cr-1 Mo steel (SA-387 grade 22) that had been given a special heat treatment to yield a low Charpy upper-shelf energy level and attendant low tearing resistance. Each experiment included two combined thermal and pressure transients that give rise to propagation and arrest of an initial long flaw that extended about 10 percent through the thick wall of the test cylinder. Both materials exhibited the ability to inhibit crack propagation by warm prestressing, high initiation toughness values and high crack-arrest toughness values. Cleavage initiation and arrest are modeled well by available fracture theories. However, calculations of ductile tearing based on resistance curves did not consistently predict the observed tearing. DOE

N88-27604# Lawrence Livermore National Lab., Calif.
DYNA3D (NONLINEAR DYNAMIC ANALYSIS OF STRUCTURES IN THREE DIMENSIONS) USER'S MANUAL

J. O. Hallquist Apr. 1988 199 p
(Contract W-7405-eng-48)
(DE88-012242; UCID-19592-Rev-4) Avail: NTIS HC A10/MF A01

This report provides an updated user's manual for DYNA3D, an explicit three-dimensional finite element code for analyzing the large deformation dynamic response of inelastic solids and structures. A contact-impact algorithm permits gaps and sliding along material interfaces with friction. By a specialization of this algorithm, such interfaces can be rigidly tied to admit variable zoning without the need of transition regions. Spatial discretization is achieved by the use of 8-node solid elements, 2-node beam elements, 4-node shell elements, 8-node solid shell elements, and rigid bodies. The equations-of-motion are integrated in time by the central difference method. DYNA3D contains twenty-eight material models and eleven equations of state to cover a wide range of material behavior. DOE

N88-27605# Lehigh Univ., Bethlehem, Pa. Dept. of Mechanical Engineering and Mechanics.
CORROSION FATIGUE OF SMALL CRACKS: MECHANICS AND CHEMISTRY Final Technical Report, 1 Jul. 1984 - 31 Oct. 1987
R. P. Wei Mar. 1988 10 p
(Contract DE-FG02-84ER-45138)
(DE88-012121; DOE/ER-45138/T3) Avail: NTIS HC A02/MF A01

The proposed research was designed to address certain fundamental issues relating to the growth of small cracks in corrosion fatigue, and utilized the unique approach and capabilities developed at Lehigh University. Electro-chemical reaction control of corrosion fatigue crack growth in ferrous alloys was demonstrated. The controlling reactions are those involving equilibration of the crack-tip bare surfaces with its neighboring filmed or oxidized surfaces. Electrolyte within the crack serves as a high resistance path that separates the crack tip region from the bulk (external) environment. Because of this high resistance, the crack tip region is effectively shielded and the reactions are affected little by the externally imposed conditions, with the crack-tip potential tending to remain very near the free corrosion potential. With increases in test temperature, it becomes increasingly difficult to displace the crack-tip potential away from the free corrosion potential. DOE

N88-27606*# Old Dominion Univ., Norfolk, Va. Dept. of Mechanical Engineering and Mechanics.
FINITE ELEMENT METHODOLOGY FOR INTEGRATED FLOW-THERMAL-STRUCTURAL ANALYSIS Progress Report, for period ended 29 Feb. 1988
Earl A. Thornton, R. Ramakrishnan, and G. R. Vemaganti Aug. 1988 22 p
(Grant NsG-1321)
(NASA-CR-183144; NAS 1.26:183144) Avail: NTIS HC A03/MF A01 CSCL 20K

Papers entitled, An Adaptive Finite Element Procedure for Compressible Flows and Strong Viscous-Inviscid Interactions, and An Adaptive Remeshing Method for Finite Element Thermal Analysis, were presented at the June 27 to 29, 1988, meeting of the AIAA Thermophysics, Plasma Dynamics and Lasers Conference, San Antonio, Texas. The papers describe research work supported under NASA/Langley Research Grant NsG-1321, and are submitted in fulfillment of the progress report requirement on the grant for the period ending February 29, 1988. Author

N88-27607# Karlsruhe Univ. (West Germany). Fakultaet fuer Maschinenbau.
COMPUTATION OF FAILURE PROBABILITY OF FATIGUE LOADED CRACKED STRUCTURES Ph.D. Thesis [BERECHNUNG DER AUSFALLWAHRSCHEINLICHKEIT RISSBEHAFTETER STRUKTUREN UNTER ERMUEDUNGSBEANSPRUCHUNG]
Jannis Theodoropoulos 1987 155 p In GERMAN
(ETN-88-92360) Avail: NTIS HC A08/MF A01

Failure probability of components with fatigue crack propagation is analyzed by computer program PARIS and a reliability analysis is described for a U-bend pipe of SNR-300 fast nuclear reactor. The deterministic model considers fatigue crack growth, stress intensity factors, and failure mechanism. The statistical model examines size and distribution of cracks, distribution of parameter C for crack growth, and distribution of axis conditions for the computation of failure probability. A parametric study investigates the effects of operational parameters on failure probability. ESA

N88-27608 Georgia Inst. of Tech., Atlanta.
AN ANISOTROPIC CONTINUUM DAMAGE MODEL FOR CREEP-DOMINATED, MULTIAXIAL LOADING HISTORIES Ph.D. Thesis
Kwang-Il Ho 1987 111 p
Avail: Univ. Microfilms Order No. DA8803701

The development of an anisotropic creep damage theory couched within the framework of continuum damage mechanics, applicable to creep dominated cyclic loading histories is examined. A damage distribution with even symmetry is introduced on the unit sphere; this distribution is expressed in rate form as a symmetric tensor of rank necessary to match physically measured damage distributions. Various damage theories are reviewed and their deficiencies are presented. A theoretical model which expresses general anisotropic creep is proposed. The coupling of damage with a bounding surface cyclic viscoplasticity theory is also accomplished. Comparisons with experimental results are made for both weakly and strongly anisotropically damaging materials, type 304 stainless steel at 593 C and pure copper at 250 C, respectively. Good correlation of rupture time, secondary creep, and tertiary creep was obtained for proportional and nonproportional, isothermal, constant isochronous nominal stress loading histories. A modification of the isochronous stress for compressive hydrostatic stress state is offered. Approaches for inclusion of aging effects and several cavity growth mechanisms are suggested. Dissert. Abstr.

N88-27609 Carnegie-Mellon Univ., Pittsburgh, Pa.
SIZE EFFECTS IN LINEAR ELASTIC FRACTURE MECHANICS Ph.D. Thesis
Robert Victor Pieri 1987 101 p
Avail: Univ. Microfilms Order No. DA8802940

An appraisal is made of the predictive ability of Linear Elastic Fracture Mechanics (LEFM) with respect to size scalings. The basic tenants of LEFM are described and what they would predict for three specific scaling problems. These problems are in-plane and out-of-plane scaling of a brittle material, each in a monotonic loading situation. Then the current literature is reviewed for experimental data applicable to these problems. These findings are presented in tabular and graph form and discussed. Next, three series of experiments are described, which are undertaken to augment the literature. Two of the series fracture common steel specimens in liquid nitrogen baths to obtain brittle response. The remaining experiments use aluminum alloy specimens to study cyclic loading with constant stress cycles. The study concludes by summarizing the ability of LEFM to deal with the problems, the resulting implications, and possible actions to overcome them. Dissert. Abstr.

N88-27610# Technical Research Centre of Finland, Espoo.
COLD WORKED REINFORCING BARS IN TENSILE TEST UNDER HIGH LOADING RATE AND LOW TEMPERATURES
T. Hyvoenen Sep. 1987 61 p In FINNISH; ENGLISH summary
(DE88-752993; VTT-TIED-752) Avail: NTIS (US Sales Only) HC A04/MF A01

The behavior of reinforcing steels in rapid loadings, e.g., in piling, explosions, impact, must be known for proper design analysis. There are no studies of such properties of reinforced steels in Finland. This report presents the behavior of reinforcing steels in rapid tensile tests carried out at temperatures of 20, -20, and -60 C. The steels are tested with a pendulum which swings around a bearing on the one end, fixed to the roof and the other

end catches the test bar and pulls until it breaks. The tensile-time curve is recorded electrically and elongation is measured from experiments. The results show that strength values are about 1.5 x values in ordinary tensile tests at room temperature. Strengths increase a little with decreasing test temperature. Thus the elongation values are higher at temperatures of 20 deg C , and at -20 and -60 C elongation decreases under the reference value by ordinary test. DOE

N88-27611*# Illinois Univ., Urbana-Champaign. Dept. of Mechanical and Industrial Engineering.
THE RELATIONSHIP BETWEEN OBSERVED FATIGUE DAMAGE AND LIFE ESTIMATION MODELS Final Contractor Report
Peter Kurath and Darrell F. Socie Aug. 1988 43 p
(Grant NAG3-465)
(NASA-CR-182191; NAS 1.26:182191) Avail: NTIS HC A03/MF A01 CSCL 20K

Observations of the surface of laboratory specimens subjected to axial and torsional fatigue loadings has resulted in the identification of three damage fatigue phenomena: crack nucleation, shear crack growth, and tensile crack growth. Material, microstructure, state of stress/strain, and loading amplitude all influence which of the three types of fatigue damage occurs during a dominant fatigue life fraction. Fatigue damage maps are employed to summarize the experimental observations. Appropriate bulk stress/strain damage parameters are suggested to model fatigue damage for the dominant fatigue life fraction. Extension of the damage map concept to more complex loadings is presented. Author

N88-27162*# Hughes Helicopters, Culver City, Calif.
AEROELASTIC CHARACTERISTICS OF THE AH-64 BEARINGLESS TAIL ROTOR
D. Banerjee *In* NASA, Ames Research Center, Integrated Technology Rotor Methodology Assessment Workshop Jun. 1988 p 279-29 Previously announced in IAA as A85-20142
(For primary document see N88-27148 21-01)
Avail: NTIS HC A17/MF A01 CSCL 20K

42 GEOSCIENCES (GENERAL)

No abstracts in this category.

43 EARTH RESOURCES AND REMOTE SENSING

Includes remote sensing of earth resources by aircraft and spacecraft; photogrammetry; and aerial photography.

For instrumentation see *35 Instrumentation and Photography.*

N88-27612# Army Engineer Topographic Labs., Fort Belvoir, Va.
METHODS OF DETERMINING PLAYA SURFACE CONDITIONS USING REMOTE SENSING
J. P. Henley 8 Oct. 1987 11 p
(AD-A192663; ETL-R-135) Avail: NTIS HC A03/MF A01 CSCL 08F

Playas (dried lakes) commonly found in arid regions are geomorphic surfaces of importance for military and civilian use as aircraft landing sites, areas of easy or difficult vehicular movement, sources of dust produced by vehicles or munitions, and as a source of chemical and mineral deposits. The ability to remotely detect and determine the surface character of playas is of concern to the modern Army in preparing terrain intelligence for desert operations. To this end, 20 Mojave Desert playas were sampled and classified as to surface type, ranging from hard and dry to wet and soft. Spectral reflectance measurements were collected using a Geophysical Environmental Research IRIS MkIV spectroradiometer over the 400 to 2500 nm spectral range. This range includes the non-thermal bands of LANDSAT TM and all the bands of the Airborne Imaging Spectrometer (AIS). Physical and chemical analyses of the surfaces were compared to the spectral curves and to the surface character of the playas. Air photo pattern analysis was also used to determine special patterns associated with the surface types. The results show limited success in assessing the mineralogy important to surface hardness. The relative moisture conditions could be detected using reflectance spectra in the short wave infrared region and gypsum surfaces could be determined. The use of the spectral data in conjunction with air photo pattern analysis gave the best results for determining surface conditions. GRA

N88-27613# Army Engineer Topographic Labs., Fort Belvoir, Va.
ARMY SPACE SYSTEMS FOR TERRESTRIAL APPLICATIONS
Ronald L. Dickerman and Richard B. Gomez 14 Jan. 1988 4 p
(AD-A192735; ETL-R-129) Avail: NTIS HC A02/MF A01 CSCL 17G

Army combat forces involved in global military operations require knowledge of the terrain and accurate positioning and navigation capability to effectively perform their missions. Combat critical data from satellite-based systems to augment ground and airborne data collection, processing, and dissemination systems are crucial for the delivery and use of the needed information and intelligence in near-real time. The Army is developing ground-based testbed systems to utilize terrain and weather data collected from space-based platforms to enhance Army commanders; battlefield capabilities, and is researching new applications for the NAVSAT Global Positioning System and the Defense Advanced Research Projects Agency-sponsored (DARPA) LIGHTSAT program that are unique to the Army. In addition, the Army is designing experiments to be conducted on the Space Shuttle. GRA

N88-27614# Army Engineer Topographic Labs., Fort Belvoir, Va.
ANALYSIS OF REMOTELY SENSED IMAGERY USING DIGITAL MORPHOLOGY
Frederick W. Rohde 8 Oct. 1987 10 p
(AD-A192738; ETL-R-136) Avail: NTIS HC A02/MF A01 CSCL 17I

An approach to the automated extraction of cultural terrain features from remotely sensed imagery is the development of structuring elements that are based on the concepts of digital morphology. The image structures of cultural terrain features show a great deal of regularity and can be represented by models. Operators that measure and analyze image structures provide effective tools for the automated feature extraction process. Morphological operations that belong to the class of hit-or-miss transforms are discussed in some detail. The operations of dilation and erosion are explained and demonstrated on radar imagery. An operation that combines gray-tone differencing and thresholding is used for extracting a road segment from an image. The future applications of digital morphology for analyzing and measuring image primitives, attributes, descriptors and descriptor sets of terrain features in support of automated feature extraction are briefly discussed. GRA

N88-27615# Forschungsinstitut fuer Informationsverarbeitung, Ettlingen (West Germany).
AUTOMATIC LINE NETWORK EXTRACTION FROM AERIAL IMAGERY OF URBAN AREAS THROUGH KNOWLEDGE BASED IMAGE ANALYSIS Interim Report No. 2
H. Kazmierczak 20 May 1987 7 p
(Contract DAJA45-86-C-0049)
(AD-A193067) Avail: NTIS HC A02/MF A01 CSCL 08B

During the past 4 months work has been concentrated on

three topics, namely application of road extraction methods to multiresolution test images, application of general segmentation methods to multiresolution test images, and design of a common data bases for all intermediate results. These activities are explained to some detail in this paper. GRA

N88-27616# Army Engineer Waterways Experiment Station, Vicksburg, Miss.
IEMIS (INTEGRATED EMERGENCY MANAGEMENT INFORMATION SYSTEM) FLOODPLAIN MAPPING BASED ON A LIDAR DERIVED DATA SET Final Report
Jack K. Stoll, Dale A. Lehman, and Daniel M. Cotter 5 Feb. 1988 22 p
(AD-A193071) Avail: NTIS HC A03/MF A01 CSCL 08B

The LIDAR demonstration project has shown that ground elevation data required by FIA for FISs can be collected digitally, and rapidly, through the application of laser ranging technology. LIDAR technology offers some clear advantages in flexibility, speed, and data quantity over conventional surveying. Laser ranging technology is mature and precise; however, the ability to maintain aircraft position control at all times within accuracy limits that allow LIDAR data to be applied to FISs remains a challenge. The analysis of the test data indicates that, with due care and planning, this objective can be achieved. IEMIS, with GIS, modeling, and networking capabilities, can be used to automate the revision, update, and analysis of flood hazard maps produced by FIA. The major constraint to the development of digital floodplain analyses is the lack of digital topographic data. Through application of FAST software, WES has demonstrated that digital LIDAR can make the automation of flood hazard analysis and mapping, and the exploitation of IEMIS for NFIP applications, feasible. GRA

N88-27617# Massachusetts Inst. of Tech., Cambridge. Research Lab. of Electronics.
ACTIVE AND PASSIVE REMOTE SENSING OF ICE Semiannual Progress Report, 1 Aug. 1987 - 31 Jan. 1988
Jin A. Kong 31 Jan. 1988 13 p
(Contract N00014-83-K-0258)
(AD-A193307) Avail: NTIS HC A03/MF A01 CSCL 20N

Volume scattering effects of snow-covered sea ice are studied with a three-layer random medium model for microwave remote sensing. The strong fluctuation theory and the bilocal approximation are applied to calculate the effective permittivities for snow and sea ice. Remote sensing of sea ice is studied with the two-layer random medium model where a correlation function is used to characterize the randomly fluctuating part of the permittivity. A systematic approach for the identification of terrain media is developed using the optimum polarimetric classifier. The covariance matrices for various terrain cover are computed from theoretical models of random medium by evaluating the full polarimetric scattering matrix elements. The Mueller matrix and polarization covariance matrix are described for polarimetric radar systems. The clutter is modelled by a layer of random permittivity, described by a three-dimensional correlation function, with variance, and horizontal and vertical correlation lengths. Electromagnetic waves scattering from a randomly perturbed periodic surface is solved using the Extended Boundary Condition method. We have also derived a general mixing formula for discrete scatterers immersed in a host medium. GRA

N88-27618# Du Pont de Nemours (E. I.) and Co., Aiken, S.C.
REMOTE SENSING OF WETLANDS: APPLICATIONS OVERVIEW
H. E. Mackey, Jr. and J. R. Jensen 1988 3 p Presented at the 1st Special Workshop on Videography, Terre Haute, Ind., 19 May 1988 Prepared in cooperation with South Carolina Univ., Columbia
(Contract DE-AC09-76SR-00001)
(DE88-010895; DP-MS-88-87; CONF-8805118-1) Avail: NTIS HC A02/MF A01

Wetlands, unlike many upland plant community types, present various challenges to effective evaluation and quantification. Wetlands cover a wide range from small tributary streams to shrub/scrub and marsh communities to open water lacustrine environment. Thus, the heterogeneity of species composition and spacial distribution of wetlands can present a formidable challenge for evalaution with remote sensing techniques. In addition, wetlands can change dramatically seasonally, especially with the development of non-persistent species. Various types of remote sensing data have been used to map and characterize wetlands. Regionally LANDSAT MSS and TM satellite data have been used for wetland mapping by various government agencies and private organizations, such as Ducks Unlimited. In addition, multispectral SPOT data are becoming available and provide opportunities for increased spatial resolution and frequency of coverage. DOE

44 ENERGY PRODUCTION AND CONVERSION

Includes specific energy conversion systems, e.g., fuel cells; global sources of energy; geophysical conversion; and windpower.

For related information see also *07 Aircraft Propulsion and Power, 20 Spacecraft Propulsion and Power,* and *28 Propellants and Fuels.*

N88-27619# Keuring van Electrotechnische Materialen N.V., Arnhem (Netherlands).
STORAGE OF THERMAL ENERGY BY MEANS OF AN ABSORPTION CYCLE
J. P. Ruiter 1987 114 p Submitted for publication
(PB88-190814; ISBN-90-353-0054-8) Avail: NTIS HC A06/MF A01 CSCL 10C

The possibilities for storing thermal energy by means of an absorption cycle are described. In such a cycle two components of a mixture are separated by the supply of energy (heat or mechanical energy). The components can be stored at ambient temperature; consequently there is no heat loss during storage. At the moment of heat demand, both components are recombined to produce heat of absorption. This heat consists of the heat of mixing and the heat of condensation, provided that one of the component is gaseous. The required heat of evaporation is extracted from the environment. The energetic efficiency of such a cycle, related to the net heat production and the supplied primary energy, can theoretically be over 100 percent. The absorption cycle was investigated for three different storage alternative. In the first alternative the components are separated by heat supply. In the second storage alternative the heat of desorption is supplied by a heat pump that uses the heat of condensation as a heat source. In the third alternative the heat of condensation is produced at such a high temperature that this heat can be used directly for desorption. To achieve this higher temperature, the gaseous component is condensed at a higher pressure. A compressor is applied for this purpose. GRA

N88-27620# Aerospace Corp., El Segundo, Calif. Chemistry and Physics Lab.
SOLAR CELL MODELING AND SIMULATION
D. C. Marvin 5 Feb. 1988 30 p
(Contract F04701-85-C-0086)
(AD-A193249; TR-0086A(2945-01)-6; SD-TR-88-20) Avail: NTIS HC A03/MF A01 CSCL 10B

An important aspect of solar cell design and analysis is the ability to model the wide variety of structures presently under study. This document reports on the application of the Poisson and Continuity Solver (PISCES) semiconductor modeling code to solar cell studies. The original program supplied by Stanford University has been modified to include optical generation processes as required and to correct a number of significant programming errors. In its present form, nearly all solar cell structures proposed can be simulated by PISCES, as well as a variety of other opto-electronic devices and processes. The material parameters which may be adjusted include, but are not restricted to, doping profiles, bulk, interface and surface recombination characteristics, and contact properties such as ohmic, Schottky or

insulating. The major model selections available include Boltzmann or Fermi-Dirac carrier statistics, voltage or current boundary conditions, and steady state or time-dependent analyses. The program capabilities are demonstrated by analysis of several state-of-the-art solar cell designs in which the important design parameters are varied and their effect on the cell output parameters shown. GRA

N88-27621*# Purdue Univ., West Lafayette, Ind. School of Electrical Engineering.
SOLAR ENERGY CONVERSION THROUGH THE INTERACTION OF PLASMONS WITH TUNNEL JUNCTIONS. PART A: SOLAR CELL ANALYSIS. PART B: PHOTOCONDUCTOR ANALYSIS Final Report
P. E. Welsh and R. J. Schwartz Jul. 1988 145 p
(Grant NAG3-433)
(NASA-CR-183044; NAS 1.26:183044; TR-EE-88-37) Avail: NTIS HC A07/MF A01 CSCL 10A

A solar cell utilizing guided optical waves and tunnel junctions was analyzed to determine its feasibility. From this analysis, it appears that the limits imposed upon conventional multiple cell systems also limit this solar cell. Due to this limitation, it appears that the relative simplicity of the conventional multiple cell systems over the solar cell make the conventional multiple cell systems the more promising candidate for improvement. It was discovered that some superlattice structures studied could be incorporated into an infrared photodetector. This photoconductor appears to be promising as a high speed, sensitive (high D sup star sub BLIP) detector in the wavelength range from 15 to over 100 micrometers. Author

N88-27622# Colorado State Univ., Fort Collins. Dept. of Physics.
DEVICE PHYSICS RELATED TO THE GRANULAR NATURE OF CuInSe2 SOLAR CELLS Annual Subcontract Report, 1 Apr. 1986 - 31 Mar. 1987
J. R. Sites Feb. 1988 25 p
(Contract DE-AC02-83CH-10093)
(DE88-001159; SERI/STR-211-3215) Avail: NTIS HC A03/MF A01

Several aspects of the impact of CuInSe2 polycrystallinity on solar cell performance were investigated. Reflection measurements on a variety of CuInSe2 layers and completed cells show large variations in both the magnitude and angular distribution of scattered light. Localized illumination reveals spatial variations in photovoltaic response which imply collection losses as high as 10 percent. Capacitance studies allow extraction of the density of extraneous electronic states at the diode junction. These decrease in reverse bias but increase under illumination and, hence, forward bias. A physical model of polycrystalline CuInSe2 is presented, and finally the status of CuInSe2 cells is analyzed in terms of the extent to which various factors are limiting performance. DOE

N88-27623# Midwest Research Inst., Golden, Colo.
LASER-HEATED CVD PROCESS FOR DEPOSITING THIN FILMS FOR LOW-COST SOLAR-CELL APPLICATIONS Final Subcontract Report, 1 Feb. 1984 - 28 Feb. 1987
D. Adler and J. S. Haggerty Feb. 1988 205 p
(Contract DE-AC02-83CH-10093)
(DE88-001162; SERI/STR-211-3235) Avail: NTIS HC A10/MF A01

Experimental and theoretical investigations of the growth and properties of doped hydrogenated amorphous silicon (a-Si:H) materials were performed. Controlled doping of laser-induced chemical-vapor-deposited (LICVD) a-Si:H, both n-type and p-type, was achieved, and the resulting films were characterized by a variety of techniques. Representative-quality films were produced at high growth rates. The doped layers were then used in fabricating the first LICVD photovoltaic cells. A detailed analysis of the sweep-out experiment was performed. This experiment can serve as a new spectroscopy of the electronic density of states in doped semiconductors. Based on the analysis, several previously unknown features in the electronic density of states of n-type and p-type glow-discharge-produced a-Si:H were postulated. DOE

N88-27624*# National Aeronautics and Space Administration. Lewis Research Center, Cleveland, Ohio.
A COMPARISON OF THE RADIATION TOLERANCE CHARACTERISTICS OF MULTIJUNCTION SOLAR CELLS WITH SERIES AND VOLTAGE-MATCHED CONFIGURATIONS
J. M Gee (Sandia National Labs., Albuquerque, N. Mex.) and H. B. Curtis 1988 7 p Presented at the 9th Space Photovoltaic Research and Technology Conference, Cleveland, Ohio, 19 Apr. 1988
(Contract DE-AC04-76DP-00789)
(NASA-TM-101177; NAS 1.15:101177; DE88-009468; SAND-88-0865C; CONF-8804122-1) Avail: NTIS HC A02/MF A01 CSCL 10A

The effect of series and voltage-matched configurations on the performance of multijunction solar cells in a radiation environment was investigated. It was found that the configuration of the multijunction solar cell can have a significant impact on its radiation tolerence characteristics. DOE

N88-27625# Oak Ridge National Lab., Tenn.
THERMAL ENERGY STORAGE Technical Progress Report, Apr. 1986 - Mar. 1987
J. J. Tomlinson and M. J. Taylor Feb. 1988 58 p
(Contract DE-AC05-84OR-21400)
(DE88-010753; ORNL/TM-10715) Avail: NTIS HC A04/MF A01

Progress in the development of Thermal Energy Storage (TES) technology under the Oak Ridge National Laboratory TES Program for the period April 1986-March 1987 is reported. Program goals and project structure are presented. Each of the projects active during this report period is discussed, and the interrelation of specific projects toward major technology transfer activities is described. DOE

N88-27626# National Academy of Sciences - National Research Council, Washington, D. C.
GEOTHERMAL ENERGY TECHNOLOGY: ISSUES, R AND D (RESEARCH AND DEVELOPMENT) AND COOPERATIVE ARRANGEMENTS Final Report
Dec. 1987 108 p
(Contract DE-FG01-86CE-31010)
(PB88-193107) Avail: NTIS HC A06/MF A01 CSCL 10B

Major issues are addressed in geothermal energy technology, recommendations are made for research and development, and cooperative arrangements are considered among government, industry, and universities to facilitate research and development under current budget constraints. Four types of geothermal energy are considered: hydrothermal, geopressed, hot dry rock, and magma systems. Author

N88-27627# Electrotechnical Lab., Sakura (Japan).
EXPERIMENTAL FABRICATION OF THIN FILM SINGLE CRYSTALLINE SOLAR CELLS
Y. Hayashi, K. Nagai, K. Ishii, and H. Yoshihara 1987 3 p In JAPANESE Submitted for publication
(PB88-131958) Copyright Avail: NTIS HC E05 as PB88-131933; copy not available from STI Facility CSCL 10A

Experimental thin film single crystalline solar cells with various cell thickness were fabricated. The thin films were made by etching single crystalline silicon wafers in KOH etchant. The cell structure was n(+)p junction type with front and back surface passivation by thermal SiO2 and back surface field by a high concentration boron doped layer at the back surface. Conversion efficiency of the cell depended on the thickness and showed maximum value of 17 percent (AM 1.5 100mW/sq cm) at the thickness around diffusion length of minority carriers (about 36 microns in this case). This dependency coincides well with a theoretical calculation. The thin film crystalline solar cell was proved to be one of the best approaches to realize low cost and high efficiency. GRA

N88-27628# Electrotechnical Lab., Sakura (Japan).
AMORPHOUS SILICON SOLAR CELLS USING A METAL SUBSTRATE
M. Yamanaka, Y. Hayashi, and H. Karasawa 1987 8 p In JAPANESE Submitted for publication
(PB88-131941) Copyright Avail: NTIS HC E05 as PB88-131933; copy not available from STI Facility CSCL 10A

The electrical contact characteristics of alpha-Si:H films on metal substrates were studied. Good ohmic contacts between alpha-Si:H films and the metal substrates was obtained by the hydrogen plasma treatment of the metal substrates prior to alpha-Si:H film deposition. Then, fabrication conditions to avoid micro-void formation in the surface of alpha-Si:H p-i-n- solar cells on the metal substrates were investigated. The micro-void formation was avoidable by the selection of p-layer growth conditions (substrate temperature, concentration of B2H6, and thickness of p-layer). Finally, the alpha-Si:H solar cell was experimentally fabricated to put the above developed technology to practical use. A conversion efficiency of 7.8 percent was obtained by optimizing growth conditions of alpha-Si:H solar cells. The highest efficiency among the alpha-Si:H solar cells was for that without an alpha-Si:H or a crystalline p-layer. GRA

N88-27629# Midwest Research Inst., Golden, Colo.
PERFORMANCE SENSITIVITIES FOR POINT-FOCUS DISH SYSTEMS WITH SECONDARY CONCENTRATORS
A. Lewandowski and J. OGallagher Apr. 1988 7 p Presented at Solar '88: American Solar Energy Society Annual Meeting and 13th National Passive Solar Conference, Cambridge, Mass., 18 Jun. 1988 Prepared in cooperation with Chicago Univ., Ill.
(Contract DE-AC02-83CH-10093)
(DE88-001152; SERI/TP-253-3324; CONF-880615-1) Avail: NTIS HC A02

This paper describes an analytical study of several performance--related benefits of using a secondary concentrator in point-focus dish designs. Previous research efforts have shown that design-point performance of dishes can be improved with secondary concentrators, especially for dishes with higher optical errors or at higher receiver operating temperatures. This work addresses the sensitivity to changes in design-point parameter values corresponding to both tracking and optical errors. An analytical model and a ray-trace model were used in analyzing these sensitivities. Results indicate that properly designed secondaries can significantly increase the tolerance to tracking errors and decrease the sensitivity to changes in optical errors from design-point values. Two approaches are recommended on which to base the design of the secondary. DOE

N88-27630# Midwest Research Inst., Golden, Colo.
SPECULAR STEEL SURFACES FOR SOLAR MIRROR SUBSTRATES
C. E. Tracy and G. E. Gross Apr. 1988 45 p
(Contract DE-AC02-83CH-10093)
(DE88-001153; SERI/TR-255-3242) Avail: NTIS HC A03/MF A01

The long-range objective is to develop a process for making a silvered stainless steel mirror that has the optical performance and service life of a mirror coupled with the mechanical durability, structural strength, and flexibility of sheet steel. Such reflectors are expected to minimize the cost handling, shipping, and fabrication into concentrators. Applications for helistats are assumed to require a lifetime average reflectance of 90 percent in a full-cone aperture angle of 8 mrad. Specifically, this work is designed to produce thin metal membranes with sufficiently fine surface finishes to serve as substrates for direct silver deposition or indirectly for silvered polymer films or silvered sol-gel coatings in heliostat, parabolic trough, and dish applications. Our focus is on the effect of the sheet metal finish on specularity and the ways to obtain the optimum surface finish by conventional manufacturing processes. This report addresses the relationship of optical quality to surface finish and the results of a cooperative research venture with a commercial sheet manufacturer to produce specular stainless steel surfaces by cold-rolling with highly polished rollers. DOE

N88-27631# Sandia National Labs., Albuquerque, N. Mex.
REFLUX HEAT-PIPE SOLAR RECEIVERS FOR DISH-ELECTRIC SYSTEMS
Charles E. Andraka and Richard B. Diver 1988 14 p Presented at the 23rd Intersociety Energy Conversion Engineering Conference, Denver, Colo., 31 Jul. 1988
(Contract DE-AC04-76DP-00789)
(DE88-008671; SAND-87-2976C; CONF-880702-1) Avail: NTIS HC A03

The feasibility of competitive, modular bulk electric power from the sun may be greatly enhanced by the use of a reflux heat pipe receiver to combine a heat engine with a paraboloidal dish concentrator. This combination represents a potential improvement over previous successful demonstrations of dish-electric technology in terms of enhanced performance, lower cost, longer life, and greater flexibility in engine design. In the reflux (i.e., gravity assisted) heat pipe receiver, concentrated solar radiation causes liquid metal (sodium, potassium, or NaK) to evaporate. The vapor flows to the engine interface heat exchanger, where it condenses and releases the latent heat. The condensate is returned to the receiver absorber by gravity (refluxing), and distributed over the surface by gravity and/or capillary forces in a wick lining the receiver. It is essentially an adaptation of heat pipe technology to the peculiar requirements of concentrated solar flux, and provides many advantages over conventional heated tub receiver technology. This overview paper describes the current status and future plans for the U.S. Solar Thermal Program reflux receiver development program at Sandia National Laboratories. Current work includes conventional mesh wick receivers, sintered metal wicks, and pool boiler receivers. The relative design merits and concerns of the different approaches and technology development test plans are discussed. DOE

N88-27632# Sandia National Labs., Albuquerque, N. Mex.
MODAL TESTING IN THE DESIGN EVALUATION OF WIND TURBINES
J. P. Lauffer, T. G. Carne, and T. D. Ashwill Apr. 1988 25 p
(Contract DE-AC04-76DP-00789)
(DE88-010374; SAND-87-2461) Avail: NTIS HC A03/MF A01

This report reviews several techniques of low-frequency excitation used successfully to measure modal parameters for wind turbines, including impact, wind, step-relaxation, and human input. As one application of these techniques, a prototype turbine was tested and two modal frequencies were found to be close to integral multiples of the operating speed, which caused a resonant condition. The design was modified to shift these frequencies, and the turbine was retested to confirm expected changes in modal frequencies. DOE

N88-27633# Midwest Research Inst., Golden, Colo. Solar Energy Research Inst.
PHOTOVOLTAIC MEASUREMENTS AND PERFORMANCE BRANCH Annual Report, FY 1987
R. J. Matson, ed. Jan. 1988 110 p
(Contract DE-AC02-83CH-10093)
(DE88-001142; SERI/PR-213-3291) Avail: NTIS HC A06/MF A01

The Photovoltaic (PV) Measurements and Performance Branch of the Solar Energy Research Institute (SERI) provides extensive PV materials, device, and component characterization, measurement, fabrication, and modeling research and support for the international PV research community in the context of the U.S. Department of Energy's PV Research Program goals. This report summarizes the branch's progress from 1 October 1986 through 1 October 1987. The five technical sections present a succinct overview of the capabilities and accomplishments of the various research groups in the branch, namely, surface and interface analysis, materials characterization, devices and modeling, cell performance and electro-optical characterization, and advanced module testing and performance. The report highlights the main research projects completed in FY87, including more than 7000

measurements and tests of PV materials, cells, submodules, and modules, which resulted in more than 100 branch-originated journal and conference publications, in collaboration with or in support of about 130 university, industrial, government, and in-house research groups. DOE

N88-27634# Department of Energy, Oak Ridge, Tenn. Office of Scientific and Technical Information.
PHOTOVOLTAIC ENERGY. ELECTRICITY FROM SUNLIGHT: A CURRENT AWARENESS BULLETIN
L. E. Williams, ed. Jan. 1988 47 p
(DE88-008289; DOE/PHV-88-1) Avail: NTIS HC A03/MF A01

Photovoltaic Energy: Electricity from Sunlight (PHV) announces on a bi-monthly basis the current worldwide information available on all aspects of photovoltaic amorphous technology, polycrystalline thin films, gallium arsenide, crystalline silicon, concentrator technology, and systems research. This publication contains the abstracts of DOE reports, journal articles, conference papers, patents, theses, and monographs added to the Energy Data Base (EDB) during the past two months. Also included are U.S. information obtained through acquisition programs or interagency agreements and international information obtained through the International Energy Agency's Energy Technology Data Exchange or government-to-government agreements. DOE

N88-27635# Purdue Univ., West Lafayette, Ind. School of Electrical Engineering.
REDUCED ORDER MODELING OF GRID-CONNECTED PHOTOVOLTAIC INVERTER SYSTEMS
O. Wasynczuk, P. C. Krause, and N. A. Anwah Apr. 1988 117 p
(Contract DE-AC04-76DP-00789)
(DE88-010603; SAND-87-7017) Avail: NTIS HC A06/MF A01

This report summarizes the development of reduced order models of three-phase, line- and self-commutated inverter systems. This work was performed as part of the National Photovoltaics Program within the United States Department of Energy and was supervised by Sandia National Laboratories. The overall objective of the national program is to promote the development of low cost, reliable terrestrial photovoltaic systems for widespread use in residential, commercial and utility applications. The purpose of the effort reported herein is to provide reduced order models of three-phase, line- and self-commutated PV systems suitable for implementation into transient stability programs, which are commonly used to predict the stability characteristics of large-scale power systems. The accuracy of the reduced models is verified by comparing the response characteristics predicted therefrom with the response established using highly detailed PV system models in which the inverter switching is represented in detail. DOE

N88-27636# Sandia National Labs., Albuquerque, N. Mex.
PERFORMANCE EVALUATION OF LARGE-AREA GLASS-MIRROR HELIOSTATS
D. J. Alpert and R. M. Houser 1988 11 p Presented at the 4th International Symposium on Research, Development and Applications of Solar Thermal Technology, Santa Fe, N. Mex., 13 Jun. 1988
(Contract DE-AC04-76DP-00789)
(DE88-011883; SAND-87-2910C; CONF-880655-3) Avail: NTIS HC A03/MF A01

Heliostats using glass-mirror reflectors have been built in sizes up to 200 square meters. These large-area heliostats are over three times bigger than second-generation heliostats and represent the culmination of DOE's second-generation heliostat development program. Using larger heliostats provides economies of scale resulting in lower costs per unit area. There is, however, a penalty in optical performance with using large-area heliostats. In addition, because of their size, large heliostats are more difficult to clean and could be more prone to damage by wind loading. To address these concerns, Sandia National Laboratories purchased two large-area heliostats, one from Advanced Thermal Systems (ATS) and the other from Solar Power Engineering Co. (SPECO), with reflective areas of 150 and 200 square meters, respectively. Both incorporate design improvements that were suggested but not employed during previous development programs. The heliostats were installed at the Central Receiver Test Facility (CRTF) for Sandia to test and evaluate. Tests were designed to provide a basis for comparing the performance of the heliostats against Sandia's specifications for optical performance and structural integrity. Specific issues addressed included: (1) quality of the reflective beam, (2) performance of the tracking and heliostat control system, (3) quality and pointing accuracy of the beam under wind loads, (4) efficacy of alternative methods for cleaning the mirrors, and (5) long-term durability of the mirror, drives, and support structure. DOE

N88-27637# Sandia National Labs., Albuquerque, N. Mex.
OPTICAL EVALUATION OF PROTOTYPE STRETCHED-MEMBRANE MIRROR MODULES FOR SOLAR CENTRAL RECEIVERS
D. J. Alpert and R. M. Houser 1988 11 p Presented at the 4th International Symposium on Research, Development, and Applications of Solar Thermal Technology, Santa Fe, N. Mex. 13 Jun 1988
(Contract DE-AC04-76DP-00789)
(DE88-011884; SAND-87-2886C; CONF-880655-4) Avail: NTIS HC A03/MF A01

Under contract to Sandia National Laboratories, two independent studies were performed to develop a commercial-scale heliostat design and to assess the fabrication and costs of stretched-membrane heliostats. The studies, performed by Solar Kinetics, Inc., and Science Applications International Corp., concluded that stretched-membrane heliostats would cost between 15 and 20 percent less than comparable glass-mirror designs. Fifty-sq m prototype mirror modules were built and tested at Sandia. Major issues addressed included the optical performance of the stretched-membrane mirror, the performance of the mirror's focus-control system in windy conditions, the performance of the defocus system, and the durability of the reflective film. The results indicate that the optical performance of SKI's first-of-a-kind mirror module is at least as good as that of current glass-mirror designs. In calm conditions, the mirror can be defocused to a convex focal length of -200 m in 7 sec. The optical performance on windy days is within Sandia's heliostat specifications. After 2 years of exposure, the reflective surface was generally in good condition, having a clean reflectivity of nearly 90 percent. DOE

N88-27638# Argonne National Lab., Ill.
MONOLITHIC FUEL CELLS
C. C. McPheeters, U. Balachandran, D. W. Dees, S. E. Dorris, J. J. Heiberger, F. C. Mrazek, K. M. Myles, J. J. Picciolo, and R. B. Poeppel 1988 7 p Presented at the 33rd International Power Source Symposium, Cherry Hill, N.J., 13 Jun. 1988
(Contract W-31-109-eng-38)
(DE88-012004; CONF-880665-4) Avail: NTIS HC A02/MF A01

Recent work on the MSOFC (Monolithic Solid Oxide Fuel Cell) has resulted in the following accomplishments: (1) the feasibility of the MSOFC concept has been proven, (2) the fabrication processes have advanced to the point of production of near defect-free fuel cell stacks, (3) the electrode characteristics have been significantly improved to enhance MSOFC performance, (4) single-cell performance has been demonstrated at very high current densities, and (5) multi-cell stack performance has improved significantly in terms of both higher open-circuit potential and lower cell resistance. The objectives of further development are to scale up the MSOFC in terms of power level, active area, and stack height. Scale-up to significant power levels (above 1 kw) will involve development in several areas including manifolding, insulation, gas handling and control, electrical contacts, and power control. DOE

N88-27639# Argonne National Lab., Ill.
MAGNETIC HEAT PUMPS
J. R. Hull and K. L. Uherka 1988 28 p Presented at the 23rd Intersociety Energy Conversion Engineering Conference, Denver, Colo., 31 Jul. 1988

(Contract W-31-109-eng-38)
(DE88-012058; CONF-880702-13) Avail: NTIS HC A03/MF A01

Magnetic heat pumps and refrigerators are potential replacements for vapor-compression devices that use chlorofluorocarbon refrigerants. Several room-temperature designs, using low-temperature superconducting magnets, have reached the experimental device stage. High-temperature superconducting materials may significantly increase the viability of the technology, both by enhancing existing design concepts and by enabling new major design types such as field switching of the superconducting magnets. DOE

N88-27640# Societe Nationale Industrielle Aerospatiale, Cannes (France).
SPACE PHOTOVOLTAIC GENERATORS. STATE OF THE ART, TRENDS [PHOTOVOLTAIQUE SPATIAL. ETAT DE'LART, TENDANCES]
M. Zilani and L. Pelenc 6 Apr. 1987 13 p In FRENCH Presented at the Agence Francaise pour la Maitrisede l'Energie Seminaire d'Evaluation des Conventions et Contrats de Recherche Conversion Photovoltaique, Nov. 1986
(SNIAS-881-440-106; ETN-88-92875) Avail: NTIS HC A03/MF A01

Different aspects of space photovoltaic generators are discussed, including useful range of power, specifications, life, manufacturing procedures, and limitations. It is shown that they are the choice generators for geosynchronous satellites requiring few kilowatts generated. It is thought that AsGa devices will expand the space applications due to longer life and powers going up to hundreds of kW. ESA

45 ENVIRONMENT POLLUTION

Includes atmospheric, noise, thermal, and water pollution.

N88-27641# Unisearch Associates, Inc., Concord (Ontario).
INITIAL TESTING OF THE TUNABLE DIODE LASER ABSORPTION SPECTROMETER FOR MEASURING HNO3 IN DIESEL ENGINE EXHAUST, STAGE 2
G. W. Harris, G. I. Mackay, L. K. Mayne, and H. I. Schiff 29 Oct. 1987 36 p Sponsored by Coordinating Research Council, Inc., Atlanta, Ga.
(PB88-193073; CRC-APRAC-CAPE-30-81-04A) Avail: NTIS HC A03/MF A01 CSCL 13B

Unisearch's tunable diode laser absorption spectrometer designed for tropospheric air monitoring (TAMS-2B) was used at the Ontario Research Founation Diesel Dynamometer test facility to investigate the effect of the dilution tunnel and sampling system on HNO3 to assess the ability of the TAMS-2B to make real time measurements of this species in diesel engine exhaust. Nitric acid and HCHO were measured in the range of 40 to 800 ppbv and 3.5 to 5.5 ppmv, respectively. The mixing ratio of HNO3 was found to decrease as engine load was increased, while the reverse was found for HCHO. The HNO3 levels exhibited slow respnse (1 to 30 min) for changes in engine operating condition. Similar response times were observed when controlled spikes of HNO3 were added to the diluted exhaust gas flow but the reponse time of the instrument itself to added HNO3 was more rapid. In marked contrast, the response to HCHO was immediate. Results also indicated that the observed HNO3 is present in the exhaust stream immediately after dilution and is not produced by subsequent reactions of NOx. GRA

N88-27642# Georgia Inst. of Tech., Atlanta. School of Geophysical Sciences.
ATMOSPHERIC NITROGEN OXIDES: THEIR DETECTION AND CHEMISTRY Annual Report No. 3
D. Davis, J. Bradshaw, M. Rodgers, S. Sandholm, and S. Dorris 1987 129 p Sponsored by Coordinating Research Council, Inc., Atlantic, Ga. Prepared in cooperation with Colorado Coll., Colorado Springs
(PB88-193057; CRC-APRAC-AP-11) Avail: NTIS HC A07/MF A01 CSCL 13B

Instrument development activity during the third year study was focused on the detection of NO2, HNO2, and NO2. A third-generation NO2/NO sensor, capable of measuring NO and NO2 simultaneously, was developed and fully tested both for ground-based and airborne field-sampling operations. An in-situ photofragmentaion LIF HNO2 was also successfully developed and was used to collect the first NHO3 data for urban Atlanta. Significant progress was also achieved in the development of a long-path differential absorption (LPDA) NO3 system. Three major field studies and one major laboratory investigation were also completed: additional nighttime NO measurements at a filed station outside Atlanta; field measurements of HNO2 in urban Atlanta; airborne measurements of NO/NO2 over marine and continental terrain at both high altitudes and within the boundary layer; and laboratory measurements to establish the potential importance of corona discharge in the generation of NOx within electrified clouds. GRA

N88-27643# Oak Ridge National Lab., Tenn.
REVIEW OF GEOGRAPHIC PROCESSING TECHNIQUES APPLICABLE TO REGIONAL ANALYSIS
R. C. Durfee Feb. 1988 131 p
(Contract DE-AC05-84OR-21400)
(DE88-010759; ORNL/CSD/TM-226) Avail: NTIS HC A07/MF A01

Since the early 1970s regional environmental studies have been carried out at the Oak Ridge National Laboratory using computer-assisted techniques. Presented is an overview of some of these past experiences and the capabilities developed at the Laboratory for processing, analyzing, and displaying geographic data. A variety of technologies has resulted such as computer cartography, image processing, spatial modeling, computer graphics, data base management, and geographic information systems. These tools have been used in a wide range of spatial applications involving facility siting, transportation routing, coal resource analysis, environmental impacts, terrain modeling, inventory development, demographic studies, water resource analyses, etc. The report discusses a number of topics dealing with geographic data bases and structures, software and processing techniques, hardware systems, models and analysis tools, data acquisition techniques, and graphical display methods. Numerous results from many different applications are shown to aid the reader interested in using geographic information systems for environmental analyses. DOE

N88-27644# National Oceanic and Atmospheric Administration, Silver Spring, Md. Air Resources Lab.
ECC (ELECTROCHEMICAL CONCENTRATION CELL) OZONESONDE OBSERVATIONS AT SOUTH POLE, ANTARCTICA DURING 1987
W. D. Komhyr, P. R. Franchois, S. E. Kuester, P. J. Reitelback, and M. L. Fanning Mar. 1988 326 p Prepared in cooperation with Colorado Univ., Boulder
(PB88-202015; NOAA-DR-ERL-ARL-15) Avail: NTIS HC A15/MF A01 CSCL 13B

Atmospheric ozone verticle distributions, air temperatures, and wind speed and wind direction data are presented for 76 balloon electrochemical concentration cell ozonesonde soundings made at the South Pole, Antarctica, in 1987. Author

N88-27645# Radian Corp., Austin, Tex.
NATIONAL AIR TOXICS INFORMATION CLEARINGHOUSE: NATICH DATA BASE USERS GUIDE FOR DATA VIEWING, FEBRUARY 1988
S. A. Smith 27 Jan. 1988 111 p
(Contract EPA-68-02-4330)
(PB88-197470; EPA-450/5-88-002) Avail: NTIS HC A06/MF A01 CSCL 13B

The national air toxics information clearinghouse (The clearinghouse, The NATICH data base, Data collection, Obtaining

information from NATICH, Using this guide) is detailed. Access to the NATICH data base (Hardware and software requirements, Authorization to logon, Logon procedures, Logoff procedures) is also detailed. An overview is presented of the interactive data viewing system. Selected report programs are also presented.
Author

N88-27646# Nero and Associates, Inc., Portland, Oreg.
NATIONAL AMBIENT VOLATILE ORGANIC COMPOUNDS (VOCs) DATA BASE UPDATE, DOCUMENTATION Final Report
J. J. Shah and E. K. Heyerdahl Mar. 1988 131 p
(Contract EPA-68-02-4190)
(PB88-195631; EPA-600/3-88-010A; EPA/DF/DK-88/043A)
Avail: NTIS HC A07/MF A01 CSCL 13B

Data on the observed concentrations of 320 volatile organic compounds were compiled, critically evaluated, and assembled into a relational data base. Ambient measurements, indoor data, and data collected with personal monitors are included. The data are primarily from the period 1970 to 1987 and for locations within the U.S. The total data base contains more than 175,000 concentration records. Summaries of the data distributions are tabulated. Averages, medians and quartile values are given for each chemical measured in both the ambient and indoor site categories. The ambient site types are: remote, rural, suburban, urban, and source dominated. The indoor category of site types include residential indoor, workplace, and personal monitors. A complete description is given of the data base files along with a guide describing the use of a prepared program for searching and maintaining the data base.
Author

N88-27647# Environmental Protection Agency, Research Triangle Park, N.C. Atmospheric Sciences Research Lab.
PHOTOCHEMICAL OXIDANT FORMATION: OVERVIEW OF CURRENT KNOWLEDGE AND EMERGING ISSUES
B. Dimitriades Apr. 1988 13 p
(PB88-195235; EPA-600/D-88-064) Avail: NTIS HC A03/MF A01 CSCL 13B

Despite 1 and 1/2 decades of control efforts, the photochemical ozone problem continues to plague human society and ecology in the U.S. One reason alleged for the difficulty in achieving the established ozone air quality standard is that current understanding of the science underlying the problem is still insufficient. Scrutiny of existing empirical and theoretical/experimental evidence revealed imperfections in ozone air quality models and model application procedures. Latest chemical mechanism developments established the Carbon Bond Mechanism (CBM) and Carter Atkinson Lurmann Lloyd (CALL) mechanisms as superior to other but still lacking in some respects. Precursor related uncertainties are of consequence both for models requiring emission rate input and for models requiring ambient concentration input. Other factors affecting model predictions are the composition of volatile organic compound emissions and the amount and makeup of pollutants transported into the modeled atmosphere. Regional ozone air quality models are now available and procedures are being developed for use of such models in formulating regional ozone control strategies. The role of hydrocarbons and nitrogen oxides differ in ozone formation.
Author

N88-27648# Oak Ridge National Lab., Tenn.
FOLIAR NITRATE REDUCTASE: A MARKER FOR ASSIMILATION OF ATMOSPHERIC NITROGEN OXIDES
R. J. Norby 1988 12 p Presented at the National Research Council Workshop on Biological Markers of Air Pollution Exposure in Trees, Little Switzerland, N.C., 25 Apr. 1988
(Contract DE-AC05-84OR-21400)
(DE88-010453; CONF-8804140-1; CONF-8804140) Avail: NTIS HC A03/MF A01

Atmospheric deposition of nitrates to forest canopies has been implicated as predisposing trees to environmental stresses. A first step in the evaluation of this hypothesis is the determination of whether atmospheric nitrates are absorbed and metabolized by tree foliage. The enzyme nitrate reductase (NR) is an appropriate marker for nitrate metabolism because it is the rate-limiting step in the assimilation of nitrate into organic compounds and it is substrate-inducible. In laboratory studies, NR was not induced in red spruce foliage exposed to NO3(-) in acid mist, but NR activity increased dramatically in spruce seedlings exposed to NO2 or HNO3 vapor, suggesting that gaseous nitrogen oxides can be assimilated by spruce foliage. Nitrate reductase activity also can be measured in the field and may be a useful marker for trees that are impacted by nitrogen pollution, but extensive characterization of diurnal and seasonal variation in foliar NR activity is an important prerequisite.
DOE

N88-27649 Utah Univ., Salt Lake City.
PREDICTION OF REGIONAL POLLUTANT DISPERSION USING A NESTED-GRID, THREE-DIMENSIONAL NUMERICAL MODEL Ph.D. Thesis
Kung-Wei Yeh 1987 197 p
Avail: Univ. Microfilms Order No. DA8803561

A 3-D numerical model has been developed to predict the meso- or subsynoptic-scale transport of pollutants in the atmosphere below 500 mb with the use of the numerical predicted wind, temperature, and precipitation fields from a limited area dynamic model. The dispersion model takes into account all possible sink mechanisms in the atmosphere, including the chemical conversion from sulfur dioxide to sulfate, and dry and wet deposition. First-order kinetics are considered. A nested grid system is designed according to the direction of the prevailing wind in the emission source area. Combining this grid system with a sophisticated second-order upwind differencing scheme for advection terms the model is able to overcome the difficulties in the regional numerical simulation experiment. The negative concentrations near the source grid points, which usually appear in diffusion model results, are eliminated. The model also has the capability to accommodate multiple sources simultaneously by applying the control grid system concept. The results obtained in the present model are in good agreement with available observational data.
Dissert. Abstr.

N88-27650*# National Aeronautics and Space Administration. Goddard Space Flight Center, Greenbelt, Md.
THE DETECTION AND INTERPRETATION OF LONG-TERM CHANGES IN OZONE FROM SPACE
John E. Frederick, Xufeng Niu (Chicago Univ., Ill.), and Ernest Hilsenrath 1988 10 p
(Grant NAG5-873)
(NASA-TM-101135; NAS 1.15:101135) Avail: NTIS HC A02/MF A01 CSCL 13B

Long-term measurements of backscattered ultraviolet radiances, now being acquired by orbiting monochromators, will provide the basis for seeking trends in atmospheric ozone. The unambiguous detection of ozone trends on decadal time scales demands a data set that is essentially free of instrument drifts. Periodic flights of an ultraviolet monochromator on the space shuttle will provide an independent means of evaluating the long-term stability of identical instruments operating on free-flying satellites. A successful calibration of the free-flying sensors using the shuttle instrument places strict demands on calibration repeatability from one flight to the next. In addition, spatial and temporal variability in cloud cover could pose further complications in carrying out these in-flight calibrations.
Author

N88-27651# Societe Nationale Industrielle Aerospatiale, Saint-Medard-en-Jalles (France).
WASTE DESTRUCTION BY PLASMA [DESTRUCTION DE DECHETS PAR PLASMA]
M. D. Pineau 1988 8 p In FRENCH
(SNIAS-881-430-113; ETN-88-92861) Avail: NTIS HC A02/MF A01

The utilization of high power plasma torches to destroy dangerous industrial wastes is discussed. The operational status of plasma torches of up to 10 MW power allows its application to treat chemical waste at temperatures of up to 10,000 C, to make sure of the destruction of dangerous chemical species such as

dioxines. The technique is applicable to special waste, since ordinary waste is conveniently processed by conventional means. ESA

46 GEOPHYSICS

Includes aeronomy; upper and lower atmosphere studies; ionospheric and magnetospheric physics; and geomagnetism.

For space radiation see *93 Space Radiation*.

N88-27652# Air Force Weapons Lab., Kirtland AFB, N. Mex.
STOCHASTIC GEOLOGIC EFFECTS ON NEAR-FIELD GROUND MOTIONS IN ALLUVIUM Final Report, 1 Jan. 1984 - 30 Jun. 1986
R. E. Reinke and B. W. Stump Nov. 1987 50 p
(AD-A192315; AD-E801594; AFWL-TR-86-133) Avail: NTIS HC A03/MF A01 CSCL 08K

Analysis of accelerograms recorded at the 20-m range from a buried 5-lb detonation in alluvium revealed wide (as large as 20 dB in the amplitude modulus of the Fourier transform) variations in response for frequencies above 35 Hz. Additional experiments were performed which ruled out source asymmetry or instrumental irregularity as the cause of these variations. The observations suggest that scattering by geologic inhomogeneity is responsible for the frequency-dependent spatial variability in ground motion. A thorough understanding of the physical processes responsible for this variability requires that a quantitative relationship be established between the subsurface material property information and the observed ground motion characteristics. An attempt was made to do this using available standard penetration test (SPT) data from the test-bed where the initial experiment was detonated. Autocorrelations of the blow count data from the SPT test were computed and compared with theoretical exponential and Gaussian distributions. The exponential distribution with a scale length between 2.0 and 3.0 m best matched the data. Assuming the Born approximation, a scale length of 2.0 to 3.0 m implies that significant scattering should occur above 10 Hz. GRA

N88-27653# Aerospace Corp., El Segundo, Calif. Space Sciences Lab.
FIELD-ALIGNED STRUCTURE OF THE STORM TIME PC 5 WAVE OF NOVEMBER 14-15, 1979
K. Takahashi, P. R. Higbie, J. F. Fennell, and E. Amata 1 Feb. 1988 42 p Previously announced in IAA as A87-43737
(Contract F04701-85-C-0086)
(AD-A193022; TR-0086A(2940-05)-3; SD-TR-88-05) Avail: NTIS HC A03/MF A01 CSCL 04A

Magnetic field data from the four satellites--SCATHA (P78-2), GOES 2, GOES 3, and GEOS 2--have been analyzed to examine the magnetic-field-aligned structure of a storm time Pc 5 wave which occurred on November 14-15, 1979. The wave had both transverse and compressional components. At a given instance, the compressional and the radial components oscillated in phase or 180 deg out of phase, and the compressional and the azimuthal components oscillated +90 deg or -90 deg out of phase. In addition, each component changed its amplitude with magnetic latitude: the compressional component had a minimum at the magnetic equator, whereas the transverse components had a maximum at the equator and minima several degrees off the equator. At 180 deg relative phase switching among the components occurred across the latitudes of amplitude minima. From these observations, the field-line displacement of the wave is confirmed to have an antisymmetric standing structure about the magnetic equator with a parallel wave length of a few earth radii. We aslo observed other intriguing properties of the wave, such as different parallel wavelengths of different field components and small-amplitude second harmonics near the nodes. A dielectric tensor appropriate for the ring current plasma is found to give an explanation for the relation between the polarization and the propagation of the wave. However, plasma data available from SCATHA do not support either the drift-mirror instability of Hasegawa or tht coupling between a drift mirror wave and a shear Alfven wave, as discussed by Walker et al. GRA

N88-27654# Naval Research Lab., Washington, D.C.
APPROXIMATE ANALYTICAL FORMULAE FOR ELECTRON DENSITY AND COLLISION FREQUENCY IN THE NATURAL AND NUCLEAR-DISTURBED IONOSPHERE AND INNER MAGNETOSPHERE
M. J. Keskinen and J. A. Fedder 22 Feb. 1988 27 p
(AD-A193129; NRL-MR-6134) Avail: NTIS HC A03/MF A01 CSCL 04A

The phenomenological models of global electron density for the natural ionosphere of Ching and Chiu (1973) and Chiu (1975) have been extended to both lower (60 km) and higher (36,000 km) altitudes. Computer simulations of a high altitude nuclear explosion are analyzed to develop a phenomenological model of electron density. Approximate analytical formulae for electron density and associated electron collision frequency in both the natural and nuclear-distributed near earth space plasma environment are derived. GRA

N88-27655# Imperial Coll. of Science and Technology, London (England).
PHOTON LIMITED IMAGE PROCESSING IN THE SPACE-TIME DOMAIN Final Technical Report, 1985 - 1987
J. C. Dainty Jan. 1988 159 p
(Contract DAJA45-85-C-0028; DA Proj. 1L1-61102-BH-57)
(AD-A193142) Avail: NTIS HC A08/MF A01 CSCL 14D

This report is principally concerned with the use of the triple correlation function and its Fourier transform, the bispectrum, for the imaging of randomly translating objects or objects viewed through atmospheric turbulence. The triple correlation has significant advantages over the second order correlation, although it does involve additional computational complexity. Specific consideration is given to algorithms for computing the triple correlation, the use of a moving time window and centroiding procedures. GRA

N88-27656# Aerospace Corp., El Segundo, Calif. Space Sciences Lab.
THE LOW-LATITUDE AURORAL BOUNDARY: STEADY-STATE AND TIME-DEPENDENT REPRESENTATIONS
D. J. Gorney and D. S. Evans 25 Mar. 1988 32 p
(Contract F04701-85-C-0086)
(AD-A193200; TR-0086(2940-06)-3; SD-TR-88-47) Avail: NTIS HC A03/MF A01 CSCL 04A

Recently, extensive data sets have been acquired from charged-particle detectors on low-altitude satellites pertinent to the study of the low-latitude boundary of the aurora, including both case studies and statistical treatments. The low latitude auroral boundary can be thought of as the low-altitude manifestation of convection boundaries for magnetospheric particles of moderate energy, although the detailed shape of the boundary might be modified locally by spatial variations or temporal modulation of precipitation rates. Several attempts have been made to compare observed equatorial and low-altitude boundaries with theoretical representations, with varying degrees of success. Here, the results of statistical analysis and case studies of the auroral boundary using precipitating particle data acquired by the NOAA spacecraft are presented. The ability of standard convection models to account for the observed boundary characteristics is discussed, with emphasis on the roles of convection strength and time dependence. It is demonstrated that, within reasonable parameter limits, steady-state convection patterns for moderate energy electrons generally fail to account for certain observed characteristics of boundary shapes. GRA

N88-27657# Northeastern Univ., Boston, Mass.
ON THE DYNAMICS OF THE AURORAL IONOSPHERE DURING THE BREAKUP OF A SUBSTORM Final Report, 28 Jan. 1983 - 31 Aug. 1986
Michael B. Silevitch 1 Mar. 1988 38 p

(Contract F19628-83-K-0014)
(AD-A193368; AFGL-TR-88-0020) Avail: NTIS HC A03/MF A01 CSCL 04A

The research investigation described here concentrated on several dynamic features of substorm evolution during its breakup phase. More specifically, we focussed upon the development of a model for the propagation of the Westward Travelling Surge (WTS) as seen from the viewpoint of an active ionosphere. We also considered a mechanism for the generation of pi2 pulsations. An important feature of our approach is the natural coupling which exists between the WTS motion and the frequency spectrum of the Pi2 modes. Thus, our theory predicts the correlation of Pi2 waveforms to substorm onsets. This correlation seems to be a reasonable one in light of recent observations of substorm morphology. GRA

N88-27658# Utah Univ., Salt Lake City. Dept. of Meteorology.
DEVELOPMENT OF RADIATION AND CLOUD PARAMETERIZATION PROGRAMS FOR AFGL (AIR FORCE GEOPHYSICS LABORATORY) GLOBAL MODELS Final Report, 1 Aug. 1984 - 31 Oct. 1987
Szu-Chen Ou and Kuo-Nan Liou 6 Jan. 1988 94 p
(Contract F19628-83-K-0040)
(AD-A193369; AFGL-TR-88-0018) Avail: NTIS HC A05/MF A01 CSCL 04A

A computationally economic and accurate radiation program has been devised for incorporation in the global models developed at the A.F. Geophysics Laboratory. The program was specifically developed for applications to atmospheres containing high, middle, and low clouds and combinations of these clouds. In addition, we have also developed cloud formation schemes for general circulation models in connection with the radiation program. The present radiation and cloud parameterization program has been successfully incorporated in the AFGL 12-layer global model. Simulations have been performed for cloud and radiation budget distributions using the initial humidity and temperature fields from 12Z, 17 June 1979. Zonally averaged global distributions of cloud cover and radiation budgets at the top of the atmosphere are in general agreement with available cloud and radiation budget climatologies. We also discuss the importance of clouds in the generation of global atmospheric cooling using the results from the AFGL 12-layer model. GRA

N88-27659# Air Force Geophysics Lab., Hanscom AFB, Mass.
SCALING LAWS FOR GEOMAGNETIC TAIL CURRENT SHEET ACCELERATION
Christopher Sherman 22 Jul. 1987 12 p
(AD-A193379; AFGL-TR-87-0235; AFGL-ERP-981) Avail: NTIS HC A03/MF A01 CSCL 04A

Solutions of the equation describing proton acceleration in the electric field of the Earth's geomagnetic tail often require lengthy numerical calculations and parametric exploration can be difficult. Here, considerations are presented of a scaling nature and shown that these considerations may be used to extend, correlate, organize, and verify groups of solutions with regard to parametric variation. GRA

N88-27660# Pacific Northwest Labs., Richland, Wash.
LARGE-EDDY SIMULATIONS OF CONCENTRATION FLUCTUATIONS
D. C. Bader and T. W. Horst Feb. 1988 4 p Presented at the 8th Symposium on Turbulence and Diffusion of the American Meteorological Society, San Diego, Calif., 1 Apr. 1988
(Contract DE-AC06-76RL-01830)
(DE88-009480; PNL-SA-15687; CONF-880463-3) Avail: NTIS HC A02/MF A01

Described is an initial effort to develop a model for numerical simulation of atmospheric diffusion that has spatial and temporal resolution adequate for the estimation of concentration fluctuation statistics. The intention is to develop a research model whose output has the realism necessary for development and testing of simpler models and parameterizations of concentration fluctuation statistics, which can in turn be used to solve applied problems. This model is built on a large-eddy simulation (LES) model of the turbulent flow field and a time-dependent solution of a passive tracer conservation equation, with a turbulence closure that parallels the LES closure of the Navier-Stokes equations. The model is used to simulate the neutral boundary layer wind-tunnel experiments of Fackrell and Robbins (1982) and the results are evaluated against their measurements. It is believed that once the model can faithfully reproduce observed data, it can then be used as an experimental tool to produce realistic simulations of new and currently unobserved cases. DOE

N88-27661 Princeton Univ., N. J.
AIR-SEA INTERACTION IN THE VICINITY OF A LAND-SEA BOUNDARY IN THE PRESENCE OF UPWELLING Ph.D. Thesis
Borivoj Rajkovic 1987 122 p
Avail: Univ. Microfilms Order No. DA8727391

In order to examine the nature of sea-air interactions in the vicinity of the western slope of continents, successive integrations of a 2-D atmospheric model and oceanic model were performed. The atmospheric model had prescribed sea surface temperature that was independent of time and prescribed, time dependent land surface temperature. Both modals are for a hydrostatic and Boussinesq fluid with a sigma coordinate system. Seaward boundary conditions for the ocean model and later boundary conditions for the atmospheric model were of the radiation type. The diurnal cycle for the atmosphere model was implemented through the specification of the land surface temperature while night time cooling was modeled with a Newtonian forcing. A change from coastal sea surface temperature that correponds to the state of coastal upwelling affects cross-shore significantly. In the case of constant sea surface temperature, the wind-stress distribution was fairly constant in the cross-shore direction except in the vicinity of the coast line. The model ocean, forced with the wind stress obtained from the atmosphere run that had homogeneous sea surface temperature, developed a strong upwelling zone and a strong equatorward current with an embedded jet near the coast. Forced with the wind stress from the atmospheric run with nonhomogeneous sea surface temperature, the ocean run had a much weaker upwelling and a double structured alongshore current with poleward flow in the vicinity of the coast line and equatorward flow in the region away from the coast. Dissert. Abstr.

N88-27662*# Ohio State Univ., Columbus. Dept. of Geodetic Science and Surveying.
BASIC RESEARCH FOR THE GEODYNAMICS PROGRAM Semiannual Status Report
Ivan I. Mueller Jul. 1988 114 p
(Grant NsG-5265)
(NASA-CR-183149; NAS 1.26:183149; SASR-19; SASR-20)
Avail: NTIS HC A06/MF A01 CSCL 08G

Additional results are presented concerning a study that considers improvements over present Earth Rotation Parameter (ERP) determination methods by directly combining observations from various space geodetic systems in one adjustment. Earlier results are extended, showing that in addition to slight improvements in accuracy, substantial (a factor of three or more) improvements in precision and significant reductions in correlations between various parameters can be obtained (by combining Lunar Laser Ranging - LLR, Satellite Laser Ranging - SLR to Lageos, and Very Long Baseline Interferometry - VLBI data in one adjustment) as compared to results from individual systems. Smaller improvements are also seen over the weighted means of the individual system results. Although data transmission would not be significantly reduced, negligible additional computer time would be required if (standardized) normal equations were available from individual solutions. Suggestions for future work and implications for the New Earth Rotation Service (IERS) are also presented. Author

N88-27663# Cologne Univ. (West Germany). Inst. fuer Geophysik und Meteorologie.
TIME-DEPENDENT THERMAL CONVECTION OF EARTH MANTLE AND DOUBLE DIFFUSIVE CONVECTION IN MAGMA CHAMBERS [ZUR ZEITABHAENGIGKEIT DER THERMISCHEN KONVEKTION IM ERDMANTEL UND DER DOPPELT-DIFFUSIVEN KONVEKTION IN MAGMAKAMMERN]
Ulrich Hansen, A. Ebel, ed., F. M. Neubauer, ed., E. Raschke, ed., and P. Speth, ed. 1987 160 p In GERMAN; ENGLISH summary
(Contract DFG-Eb-56/11-1)
(Mitt-52; ISSN-0069-5882; ETN-88-92345) Avail: NTIS HC A08/MF A01

Thermal convection in the Earth's mantle and double-diffusive convection in magma-chambers are investigated by a finite-element-scheme. In both cases a Boussinesq-fluid at infinite Prandtl-number in a two-dimensional domain was assumed. Time dependent convection can exist at moderate Rayleigh-numbers in stress-free, base-heated configurations, provided the aspect ratio is significantly larger than unity. With increasing Ra the route to more complex forms of time dependence is interrupted by laminar windows in which a steady state displaying an elongated flow pattern exists. The investigation of double-diffusive convection shows that in the diffusive regime stationary convection rolls can exist at sufficiently high Lewis-number even under strongly subcritical conditions. By means of time dependent simulations it is shown that for initial conditions of geophysical importance, transient layering may occur. ESA

47 METEOROLOGY AND CLIMATOLOGY

Includes weather forecasting and modification.

N88-27664# Wisconsin Univ., Madison. Space Science and Engineering Center.
VALIDATE ALGORITHMS FOR THE DETERMINATION OF RAINFALL RATES FROM SSM/I MICROWAVE SATELLITE IMAGERY Progress Report, Dec. 1987 - Jan. 1988
John P. Roberts 22 Feb. 1988 8 p
(Contract N00014-86-K-2001)
(AD-A192299) Avail: NTIS HC A02/MF A01 CSCL 04A

During the past two months, our research activities have included: (1) updating our catalog of rain cases observed by the SSM/I coincident with radar coverage from our primary or secondary sites, (2) ordering SSM/I, radar, and raingage data for the aforementioned cases, (3) processing the gage-calibrated United Kingdom radar data and merging this data with SSM/I observations to create statistics files, (4) developing software for deriving gage calibration coefficients to be used with uncalibrated radars, (5) writing routines for applying BMDP scatterplot and step-wise multiple linear regression software to the SSM/I-ground truth statistics files, and (6) adapting the NCAR SCD plotting package for the contouring of data fields and the production of other high-quality graphics. In addition, software for creating vertical integrals of volume-scan radar data has been nearly completed. Codes are also under development (with the cooperation of Dr. Gene Poe of NRL) for constructing antenna pattern-matching filters. We are continuing our collaboration with Dr. Chris Kummerow and his colleagues at the Severe Storms Branch of NASA/Goddard Space FLight Center. By this cooperative effort we hope to expedite the radiative transfer modeling necessary for the analysis of SSM/I-ground truth data sets and improve the current rain rate algorithm. GRA

N88-27665# Army Engineer Topographic Labs., Fort Belvoir, Va.
AN EMPIRICAL SURFACE TEMPERATURE MODEL
A. E. Krusinger 8 Oct. 1987 8 p
(AD-A192737; ETL-R-132) Avail: NTIS HC A02/MF A01 CSCL 17E

To help fill a critical gap in Assisted Target Recognition (ATR) capabilities, an empirical surface temperature model is developed with a few simple inputs, and based upon long term radiometric and meteorological measurements in several climates. It is based upon analogous climates and type days of similar weather conditions. GRA

N88-27666# Missouri Univ., Rolla. Graduate Center for Cloud Physics Research.
CLOUD SIMULATION WARM CLOUD EXPERIMENTS: DROPLET GROWTH AND AEROSOL SCAVENGING Final Technical Report
D. R. White, D. E. Hagen, and J. C. Carstens 2 Mar. 1988 142 p
(Grant AF-AFOSR-0071-85)
(AD-A192944; AFOSR-88-0317TR) Avail: NTIS HC A07/MF A01 CSCL 04B

During the research period starting January 1, 1985 and ending December 31, 1987 the following research objectives were achieved: (1) the Proto II facility is operating according to original specifications, including its capability of reaching temperatures sufficiently low (approximately -36 C) to homogeneously nucleate ice from supercooled water drops; (2) the warm cloud experiments, designed to measure the condensation coefficient of water, have been completed as well as the analysis. It has been found that the condensation coefficient tends to decrease from a value near unity to a significantly low value, approximately .01, as the drop grows from submicron size range to several microns, radius; (3) the problem of chamber humidification, the resolution of which became a major research objective during the course of these investigations, has been solved and we are now able to determine initial relative humidities to required accuracy; (4) the larger Romulus chamber is now producing cloud. The scavenging experiment has not been completed, although considerable progress has been made in its design and implementation. We should be producing results on scavenging by summer 1988. GRA

N88-27667# Wisconsin Univ., Madison. Science and Engineering Center.
THE COLLECTION OF STATISTICS ON THE FREQUENCY OF CLOUD COVER OVER NORTH AMERICA Final Report, 1 Jul. 1985 - 30 Sep. 1987
Edwin W. Eloranta and Donald P. Wylie Feb. 1988 115 p
(Contract N00014-85-K-0581)
(AD-A193093) Avail: NTIS HC A06/MF A01 CSCL 04B

Statistics were collected on cloud cover and atmospheric obstructions to LIDAR propagation. The GOES/VAS satellite was used for data acquisition. It was determined with the GOES/VAS system what percentage of the cloud cover is partially transmissive. One and three quarter years of data were collected, which is being studied for geographic, seasonal and temporal variations in cloud cover, both those that are transmissive and those which are opaque to terrestrial radiation. The satellite data is being calibrated with LIDAR data. E.R.

N88-27668# National Center for Atmospheric Research, Boulder, Colo.
INTERCOMPARISON OF NMC (NATIONAL METEOROLOGICAL CENTER) AND ECMWF (EUROPEAN CENTRE FOR MEDIUM RANGE WEATHER FORECASTS) GLOBAL ANALYSES: 1980-1986
K. E. Trenberth and J. G. Olson Mar. 1988 89 p
(Grant NSF ATM-87-09659)
(PB88-196548; NCAR/TN-310/STR) Avail: NTIS HC A05/MF A01 CSCL 04B

Global analyses from the U.S. National Meteorological Center and the European Centre for Medium Range Weather Forecasting are intercompared. The main results presented are monthly mean and root mean square differences between the analyses which have been zonally averaged and plotted as time series from 1980 to 1986 at single levels and as cross sections, and they have also been mapped geographically for each month. At the surface, separate fields are presented for the oceans as a whole, and for each ocean separately. Results show fairly widespread agreement

between the analyses from the centers over the Northern Hemispheres extratropics. However, the uncertainty in the analyses is much greater in the tropics and Southern Hemisphere. This is reflected in much greater differences in wind fields south of 20 deg N, with RMS differences in both components often exceeding 5/ms above approx. 500 mb throughout most of this region.
Author

N88-27669# Advisory Group for Aerospace Research and Development, Neuilly-Sur-Seine (France).
ATMOSPHERIC TURBULENCE RESEARCH AT DFVLR
Anne M. Jochum (Deutsche Forschungs- und Versuchsanstalt fuer Luft- und Raumfahrt, Wesseling, West Germany) Jul. 1988 19 p
(AGARD-R-752; ISBN-92-835-0462-3) Copyright Avail: NTIS HC A03/MF A01

A brief overview is given of work on atmospheric turbulence at DFVLR (German Aerospace Research Establishment), and describes the research tools, which include instrumented aircraft and numerical models. Some results of research on turbulence characteristics are given; these are mostly in the convective boundary layer. The report discusses their application to the study of aircraft response and airframe loadings. Author

N88-27670# Los Alamos National Lab., N. Mex.
UPDATE ON THE MESO-MICROSCALE METEOROLOGICAL HIERARCHY
M. D. Williams 1987 19 p Presented at the Workshop on Mesoscale Modelling, Turbulence and Diffusion, Riso, Denmark, 12 May 1987
(Contract W-7405-eng-36)
(DE88-009133; LA-UR-88-1238; CONF-8705282-1) Avail: NTIS HC A03

SIGTRA is designed to define the height of the material layer and provide interpolated mass and energy fluxes to VARYME. It also provides interpolated winds, temperatures, and potential densities at levels within the material layer. VARTRA uses similarity theory surface energy budget considerations, and the VARYME solutions to perturb the SIGMET profiles. It is the principal vehicle for converting the VARYME solutions into wind and temperature profiles and for incorporating the effects of local heating into the SIGMET solutions. VARTRA also is used to provide input to HRWHER. A number of shortcomings were identified after the early simulations of project WIND measurements in the Sacramento Valley of California. In particular, the surface temperatures were quite different from the measurements and the VARYME solutions were playing a very limited role in the perturbation of the SIGMET solutions. This note describes some of the efforts to cure these problems and the new simulations. The specific case represents the period June 27 to 28, 1985. The simulations began at 1pm Pacific Standard Time. Results are presented for 3pm on the 27th and 1am and 9am on the 28th. DOE

N88-27671# Sandia National Labs., Albuquerque, N. Mex.
THREE-DIMENSIONAL WIND SIMULATION
P. S. Veers Mar. 1988 40 p
(Contract DE-AC04-76DP-00789)
(DE88-009793; SAND-88-0152) Avail: NTIS HC A03/MF A01

A method for numerically simulating a three-dimensional field of turbulent windspeed (the Sandia method) for use in the aerodynamic and structural analyses of wind turbines is presented. The required inputs are single point power spectral densities (PSDs) and the coherence function. Suggestions for appropriate inputs and an example calculation are included. The simulation method is used to obtain rotationally sampled PSDs, which are compared with measurements obtained by Pacific Northwest Laboratories. The results show that the Sandia method is capable of producing simulations that agree with the measurements, especially when the coherence function is augmented from the usual form to include the ratio of spatial separation over height raised to the 0.25 power. The method is specialized for horizontal axis wind turbine analysis by phase lagging the simulations at each point in space so that wind speeds are simulated only when the turbine blade passes the point, reducing storage requirements and computation time by about an order of magnitude. For vertical axis applications, where interpolation will be required, the error induced by the interpolation is estimated and eliminated by the addition of white noise. DOE

N88-27672# Pacific Northwest Labs., Richland, Wash.
THE HANFORD METEOROLOGICAL DATA COLLECTION SYSTEM AND DATA BASE
G. L. Andrews Apr. 1988 42 p
(Contract DE-AC06-76RL-01830)
(DE88-008632; PNL-6509) Avail: NTIS HC A03

The Hanford Meterological Station (HMS) provides meteorological and climatological services to the Department of Energy in Richland and its contractors. On a 24-hour basis, the HMS measures, records, and archives meteorological data collected hourly throughout the year. The current data base consists of five components: wind telemetry stations, doppler acoustic sounders (SODAR), 200-ft towers, 410-ft tower at the HMS, and surface weather observations at the HMS. The wind telemetry station data, 410-ft tower data, and surface weather observation data are archived into yearly ACSII files, and the remaining components are permanently archived in binary form on magnetic tape. The future data base will consist of the same five components, but all components will be permanently archived into yearly ASCII files. Quality assurance computer programs will be written to validate the current data base, and data archival program will be written to improve the archival method that is currently used.
DOE

N88-27673# Atmospheric and Environmental Research, Inc., Cambridge, Mass.
SURFACE ENERGY BALANCE OF THREE GENERAL CIRCULATION MODELS: CURRENT CLIMATE AND RESPONSE TO INCREASING ATMOSPHERIC CO2
W. J. Gutowski, D. S. Gutzler, D. Portman, and W. C. Wang May 1988 119 p
(Contract DE-FG02-86ER-60422)
(DE88-010967; DOE/ER-60422/H1; TR-042) Avail: NTIS HC A06/MF A01

The surface energy balance simulated by state-of-the-art general circulation models at GFDL, GISS, and NCAR is examined for climates with current levels of atmospheric CO2 concentration (control climate) and with twice the current levels. The work is part of an effort sponsored by DOE to assess climate simulations produced by these models. The surface energy balance enables us to diagnose differences between models in surface temperature climatology and sensitivity to doubling CO2 in terms of the processes that control surface temperature. The analysis compares the simulated balances by averaging the fields of interest over a hierarchy of spatial domains ranging from the entire globe down to regions a few hundred kilometers across. DOE

N88-27674# Pacific Northwest Labs., Richland, Wash.
COMPUTER SIMULATION PROCEDURE FOR DESIGNING AIRBORNE AEROMETRIC MONITORING PROGRAMS
J. M. Hales and W. T. Pennell Mar. 1988 3 p Presented at the Conference on Lower Troposphere Profiling: Needs and Technologies, Boulder, Colo., 31 May 1988
(Contract DE-AC06-76RL-01830)
(DE88-011896; PNL-SA-15768; CONF-8805101-2) Avail: NTIS HC A02/MF A01

With the growing cost and sophistication of modern meteorological and air pollution field experiments, it is becoming increasingly necessary to improve the quality of the design phase of these programs. Experiment designers are faced with the difficult task of choosing, from an ever-expanding assortment of choices, the optimum mix of fixed and mobile, in situ- and remote-sensing devices needed to meet the measurement objectives of their programs. Choosing this optimum mix also requires the designer to determine how these sensing devices should be deployed - given some hypothesis about the spatial and temporal structure of the fields to be observed. The demands of this design process suggest the need for objective analysis tools that allow a designer

to examine quantitatively the operational behavior of various measurements techniques and measurements platforms and to assess the effectiveness of alternative sampling strategies. DOE

N88-27675# GKSS-Forschungszentrum Geesthacht (West Germany).
INVESTIGATIONS ON MIE AND RAYLEIGH SCATTERING AS BASIS FOR THE DEVELOPMENT OF RAYLEIGH TEMPERATURE LIDARS WITH AID OF MICHELSON INTERFEROMETRY Thesis - Hamburg Univ.
[UNTERSUCHUNGEN ZUR MIE- UND RAYLEIGHSTREUUNG ALS GRUNDLAGE FUER DIE ENTWICKLUNG EINES RAYLEIGH-TEMPERATUR-LIDARS AUF DER BASIS DER MICHELSON-INTERFEROMETRIE]
W. Schmidt 1988 165 p In GERMAN; ENGLISH summary
(GKSS-87/E/62; ISSN-0344-9629; ETN-88-92962) Avail: NTIS HC A08/MF A01

Theoretical and experimental studies of atmospheric temperature measurement possibilities by Michelson interferometry are presented. A procedure with real interferometer is developed permitting temperature remote measuring in the presence of aerosol diffusion. Error and sensitivity considerations are outlined, and their influence on temperature determination is analyzed. Design and test of Michelson interferometer with high contrast and wide angle for high spectral resolution is described. ESA

N88-27676*# Computer Sciences Corp., Huntsville, Ala. Applied Technology Div.
SPACE SHUTTLE NATURAL ENVIRONMENT ANALYSIS Final Report, 22 Jun. 1984 - 30 Apr. 1988
Wade Batts 2 May 1988 5 p
(Contract NAS8-35975)
(NASA-CR-179337; NAS 1.26:179337) Avail: NTIS HC A02/MF A01 CSCL 04B

Five major tasks are briefly outlined: development of detailed wind profile measurements for Kennedy Space Center (KSC) and Vandenberg Air Force Base (VAFB): development of software to construct meteorological data tapes for use in the STS Post Ascent Analysis; development of storage, access, and utilization codes for Global Cloud Cover data; development of software and meteorological data bases to establish launch delay risks at KSC and VAFB; and development of the meteorological tower 301 climatological data base at VAFB. Author

N88-27677*# National Aeronautics and Space Administration. Langley Research Center, Hampton, Va.
ANGULAR RADIATION MODELS FOR EARTH-ATMOSPHERE SYSTEM. VOLUME 1: SHORTWAVE RADIATION
J. T. Suttles, R. N. Green, P. Minnis, G. L. Smith, W. F. Staylor, B. A. Wielicki, I. J. Walker, D. F. Young, V. R. Taylor, and L. L. Stowe (National Oceanic and Atmospheric Administration, Washington, D. C.) Jul. 1988 148 p
(NASA-RP-1184; L-16414; NAS 1.61:1184) Avail: NTIS HC A07/MF A01 CSCL 04B

Presented are shortwave angular radiation models which are required for analysis of satellite measurements of Earth radiation, such as those fro the Earth Radiation Budget Experiment (ERBE). The models consist of both bidirectional and directional parameters. The bidirectional parameters are anisotropic function, standard deviation of mean radiance, and shortwave-longwave radiance correlation coefficient. The directional parameters are mean albedo as a function of Sun zenith angle and mean albedo normalized to overhead Sun. Derivation of these models from the Nimbus 7 ERB (Earth Radiation Budget) and Geostationary Operational Environmental Satellite (GOES) data sets is described. Tabulated values and computer-generated plots are included for the bidirectional and directional modes. Author

48 OCEANOGRAPHY

Includes biological, dynamic, and physical oceanography; and marine resources.

For related information see also *43 Earth Resources and Remote Sensing.*

N88-27678# Naval Postgraduate School, Monterey, Calif.
AN ANALYSIS OF HORIZONTAL TEMPERATURE GRADIENTS AND HEAT CONTENT IN THE MIXED LAYER AND THE SURFACE FORCING DURING PATCHEX M.S. Thesis
John J. Murray Dec. 1987 81 p
(AD-A192330; AD-E801594) Avail: NTIS HC A05/MF A01 CSCL 08C

This study is an analysis of high resolution measurements taken during the PATCHEX experiment. PATCHEX was designed to study shear related mixing in the upper thermocline. As a participant in the study, the R/V POINT SUR's contribution was to survey an 8 kilometer square area centered on the R/P FLIP which was moored at 34 N127 W. The survey which was conducted from 4 to 16 November 1986, gathered high resolution CTD, microconductivity and current velocity data to allow a detailed analysis of the small scale dynamics and thermohaline structure of the site. This thesis examined a subset of the R/V POINT SUR structure, surface fluxes and heat content of the upper 120 meters at the PATCHEX site. GRA

N88-27679# Naval Ocean Systems Center, San Diego, Calif.
MIZPAC (MARGINAL ICE ZONE PACIFIC) 84-86 CTD (CONDUCTIVITY, TEMPERATURE, DEPTH) DATA REPORT Final Technical Document, Sep. 1984 - Oct. 1986
R. R. Judd Jan. 1988 427 p
(AD-A192478; NUSC/TD-1188) Avail: NTIS HC A19/MF A01 CSCL 08C

Temperature, salinity, density, sound speed, and depth measurements obtained in the Beaufort Sea during the summer and fall of 1984, 1985, and 1986 are reported. GRA

N88-27680# Berkeley Research Associates, Inc., Calif.
RESEARCH ON OCEAN FORECASTING AND NONLINEAR WAVE PROPAGATION AND NUMERICAL HYDRODYNAMICS IN THE OCEAN Final Report
Jan. 1988 174 p
(Contract N00014-85-C-0680)
(AD-A193363; BRA-88-W016R) Avail: NTIS HC A08/MF A01 CSCL 08C

During this reporting period we carried out research which would improve the accuracy of the NPE (Nonlinear Progressive-Wave Equation), TOPS (Thermodynamic Ocean Prediction System) and Hibler Sea Ice models and would reduce the discrepancies between the models and actual experimental observations. To simulate a greater variety of ocean environments, the NPE computer code was modified to include a damping region. The inclusion of these enhancements has provided a means to better understand real oceans. We also examined the ability of statistical techniques to forecast upper ocean deviations from climatology on 1 to 7 day time scales. Sea surface temperature deviations in the 2.5 to 62.5 meter region in depth were predicted using available information on surface conditions and recent deviations at the same location. We used a hydrodynamic and/or thermodynamic sea ice model to predict sea ice concentration, thickness and drift. The operational model, the Polar Ice Prediction System is based on the Hibler (1979) model only with the addition of thermodynamics similar to that used by Semtner(1976). It is driven by atmospheric forcing from the Navy Operational Global Atmospheric Prediction System (NOGAPS) model, as well as monthly mean climatological ocean currents and oceanic heat fluxes. GRA

N88-27681# National Oceanic and Atmospheric Administration, Seattle, Wash. Marine Environmental Lab.
BEAUFORT SEA MESOSCALE CIRCULATION STUDY: HYDROGRAPHY HELICOPTER OPERATIONS, APRIL 1987

K. Aagaard, S. Salo, and K. Krogslund Mar. 1988 30 p (PB88-203658; NOAA-DR-ERL-PMEL-22; CONTRIB-1029) Avail: NTIS HC A03/MF A01 CSCL 08F

Data is presented from 28 hydrographic stations occupied in April 1987 over the Beaufort Sea continental shelf and slope, as part of the Beaufort Sea Mesoscale Circulation Study. The casts which were made along 4 transects, each roughly perpendicular to the coast, repeat most of the stations sampled in October 1986 from the USCGC Polar Star. Author

N88-27682# Woods Hole Oceanographic Institution, Mass.
THE DISTRIBUTION OF SOME CHEMICAL ELEMENTS BETWEEN DISSOLVED AND PARTICULATE PHASES IN THE OCEAN Progress Report, 1 Apr. 1987 - 31 Mar. 1988
D. W. Spencer, M. P. Bacon, P. L. Sachs, A. P. Fleer, D. K. Shafer, R. A. Belastock, and T. R. Hammar 1988 38 p (Contract DE-AC02-76EV-03566)
(DE88-010181; DOE/EV-03566/54) Avail: NTIS HC A03/MF A01

The long-range goal of our research under this contract is an understanding of the processes that control the distribution and fate of chemical species in the ocean, with a particular emphasis on species which are reactive with respect to uptake by marine particulate matter. Such an understanding is essential in predicting the fate of reactive pollutants, such as heavy metals and radionuclides, that are released to the environment as a consequence of energy-producing activities. In pursuit of this goal we have, during the present contract period, been devoting all of our effort to participation in the Shelf-Edge Exchange Processes (SEEP) program. DOE

51 LIFE SCIENCES (GENERAL)

N88-27683# Advisory Group for Aerospace Research and Development, Neuilly-Sur-Seine (France). Aerospace Medical Panel.
ELECTRIC AND MAGNETIC ACTIVITY OF THE CENTRAL NERVOUS SYSTEM: RESEARCH AND CLINICAL APPLICATIONS IN AEROSPACE MEDICINE
Feb. 1988 404 p In ENGLISH and FRENCH Symposium held in Trondheim, Norway, 25-29 May 1987 Original contains color illustrations
(AGARD-CP-432; ISBN-92-835-0447-X) Copyright Avail: NTIS HC A18/MF A01

The physical and mental demands imposed on aircrew operating high performance combat aircraft will be severe. The heavy loads of information received from the aircraft sensors must be assimilated and managed in a timely and efficient manner. Severe physiological stresses will be imposed by the environment of rapid onset, high sustained G-acceleration. The purpose of this symposium was to explore the feasibility of using electrical potentials and magnetic fields of the central nervous system as objective measures of the human condition. Topics addressed include: the computer-aided imaging of background and evoked brain electrical activity; magnetoencephalography; the functional significance of P300, contingent negative variation (CNV), and electroencephalogram (EEG) events as indices of behavior; the use of physiological measures for indexing in-flight and simulator mission effectiveness; and the effects of acceleration, drugs, and diseases on CNS For individual titles, see N88-276

N88-27684# New York Univ., New York. Dept. of Psychology.
STUDIES OF THE INTACT HUMAN BRAIN: IMPLICATIONS FOR PERFORMANCE c52
Lloyd Kaufman *In* AGARD, Electric and Magnetic Activity of the Central Nervous System: Research and Clinical Applications in Aerospace Medicine Feb. 1988 17 p (For primary document see N88-27683 21-51)
Copyright Avail: NTIS HC A18/MF A01

The development and testing of multi-channel neuromagnetometers are discussed in relationship to providing information needed concerning brain activity. Also discussed is the relationship between the number of sensing channels and the background noise. A brief account of some of the analytical methods applied to neuromagnetic data is provided. B.G.

N88-27685# New York Medical Coll., N.Y. Div. of Biological Psychiatry.
CEEG DYNAMIC BRAIN MAPPING: A NEW METHOD TO EVALUATE BRAIN FUNCTION IN DIFFERENT PSYCHOLOGICAL AND DRUG CONDITIONS c52
Turan M. Itil, Kurt Z. Itil, Emin Eralp, A. Akman (HZI Research Center, Tarrytown, N.Y.), and A. Manco *In* AGARD, Electric and Magnetic Activity of the Central Nervous System: Research and Clinical Applications in Aerospace Medicine Feb. 1988 16 p (For primary document see N88-27683 21-51)
Copyright Avail: NTIS HC A18/MF A01

The electroencephalogram (EEG), discovered more than half a century ago, is still the only non-invasive, simple and objective method to continuously and repetitively study brain function, and has recently gained new significance since quantification by microprocessors was developed. Quantification of single-lead EEG proved to be of significant value in psychotropic drug development. Discoveries of the psychotropic properties of drugs and the determination of bioavailability of CNS-active compounds validated this method. It was demonstrated that the brain's bioelectrical activity, even recorded in only one area of the brain, can represent brain function and is closely associated with human behavior. A newly-developed brain function monitoring system using multi-lead, broad frequency spectrum Computer-analyzed Electroencephalogram (CEEG) with Dynamic Brain Mapping seems to be a very promising methodology to study human behavior and to monitor its changes due to external and internal factors. Author

N88-27686# EEG Systems Lab., San Francisco, Calif.
FOURTH GENERATION NEUROCOGNITIVE PATTERN ANALYSIS SYSTEM c52
A. S. Gevins, N. H. Morgan, S. L. Bressler, D. S. Greer, B. Costales, K. Smith, and R. Faucette *In* AGARD, Electric and Magnetic Activity of the Central Nervous System: Research and Clinical Applications in Aerospace Medicine Feb. 1988 13 p Original contains color illustrations (For primary document see N88-27683 21-51)
Copyright Avail: NTIS HC A18/MF A01

The generic term neurocognitive pattern (NCP) analysis is used to refer to procedures being developed to extract spatiotemporal neurocognitive patterns from the unrelated neuroelectric noise of the brain. Recordings with up to 64 scalp channels during highly controlled tasks are now routine in the laboratory, as is the extended signal processing sequence required to extract minute neurocognitive singals from gigabyte sets of single-trial data. More robust measures of the degree of functional interdependency between electrodes were developed and applied to several prior neuropsychological models of the rapidly shifting cortical network accompanying expectancy, stimulus registration and feature extraction, response preparation and execution, and updating to feedback about response accuracy. These results suggest that it is possible to characterize functional interdependencies of event-related processing between local neural areas by measuring the wave congruence and lag time of appropriately preprocessed low-frequency brain waves. Determining the distributed functional network of specialized areas of the brain producing the observed patterns is a formidable problem which is being attacked on a number of fronts. Author

N88-27687# New York Univ. Medical Center. Brain Research Labs.
NORMATIVE DEVELOPMENTAL EQUATIONS FOR THE EEG AND THEIR SENSITIVITY TO NEUROLOGICAL AND PSYCHIATRIC DISORDERS c52
E. R. John and L. S. Prichep *In* AGARD, Electric and Magnetic Activity of the Central Nervous System: Research and Clinical

Applications in Aerospace Medicine Feb. 1988 7 p Prepared in cooperation with Kline (Nathan S.) Inst. for Psychiatric Research, Orangeburg, N.Y. Original contains color illustrations (For primary document see N88-27683 21-51)
Copyright Avail: NTIS HC A18/MF A01

Although the electroencephalogram (EEG) is altered by many brain dysfunctions, its clinical utility is severely limited by reliance upon visual pattern recognition and subjective interpretation. The goal was to not only replace subjective judgments by objective quantification, but to extend the utility of electrophysiological examinations beyond their traditional role in the detection of neurological disorders to the assessment of cognitive impairments and the evaluation of psychiatric patients. The initial studies were focussed on the problem of learning disabilities in children. As the techniques evolves, they were applied successfully to the assessment of pediatric neurological patients, to adult patients with mild head injury, cerebrovascular disease including transient ischemic attacks, alcoholism, cognitve impairment due to senile dementia, affective disorders, and psychoses. The method which was developed for these purposes, called neurometrics, is based upon the computerized extraction of a wide variety of objective indices of brain function as reflected in electrophysiological activity, the multivariate statistical evaluation of these quantitive measures, and the display of diagnostically significant findings in color coded topographic maps easily interpretable by the clinician without extensive specialized training. Author

N88-27688# Royal Air Force Inst. of Aviation Medicine, Farnborough (England).
THE APPLICATION OF NON-STATIONARY DATA ANALYSIS TECHNIQUES IN THE IDENTIFICATION OF CHANGES IN THE ELECTROENCEPHALOGRAM ASSOCIATED WITH THE ONSET OF DROWSINESS **c52**
Nicola A. Wright, R. G. Borland, and Amanda McGown *In* AGARD, Electric and Magnetic Activity of the Central Nervous System: Research and Clinical Applications in Aerospace Medicine Feb. 1988 5 p (For primary document see N88-27683 21-51)
Copyright Avail: NTIS HC A18/MF A01

The electrical activity of the brain was analyzed using techniques to detect the occurrence of non-stationarities associated with transitional states between alert wakefulness and sleep. Eight minutes of resting eyes closed data were used in the analysis. A visual inspection was performed to classify the record into epochs of varying lengths according to the different states of arousal. Three states were defined: alert wakefulness, drowsy sleep, and a transitional state. Nonstationary data analysis techniques were used to identify these changes automatically. The techniques used were autoregressive modeling, in which the prediction error was used as a criterion to detect change, and evolutionary power spectrum analysis, where a spectral ratio was defined to detect differences between short epochs of the signal. In addition, the autocorrelation function was calculated for a limited number of lags, and changes in the function with reference to previous epochs used to identify the onset of change. These techniques were compared with methods of analysis based on a pre-defined epoch length, to determine the most efficient method of detecting changes associated with the transition between alertness and drowsiness. A discriminant function was calculated for each of the three visually classified states to define a classification rule, which was then used to allocate the segments produced by each of the automatic analysis techniques to one of the three states of alertness. Finally, the performance of each technique was assessed in terms of its ability to correctly classify segments of data. Author

N88-27689# National Hospital, Oslo (Norway). Lab. for Clinical Neurophysiology.
A STATISTICAL PROCEDURE FOR THE EVALUATION OF PRESENCE/NON-PRESENCE OF STIMULUS-RELATED EEG ACTIVITY **c52**
Nils Irgens Bachen *In* AGARD, Electric and Magnetic Activity of the Central Nervous System: Research and Clinical Applications in Aerospace Medicine Feb. 1988 9 p (For primary document see N88-27683 21-51)
Copyright Avail: NTIS HC A18/MF A01

Averaging of a sufficient number of stimulus-related sample functions is a commonly applied method for the demonstration of evoked activity in the electroencephalogram (EEG). However, problems may arise in the visual evaluation of averaged waveforms when the signal-to-noise ratio is low, such as for instance in certain cerebral disease conditions, or when the intensity of the stimuli is low. In such situations the question of presence or not of evoked activity may be of material importance. Even experienced observers will find it difficult to give a reliable answer if their judgment has to depend only on visual assessment of the averaged waveforms obtained. A statistical test for the presence of evoked activity may be a guide to the correct decision in such cases. A statistical procedure based on phase value measurements of Fourier component in the post stimulus sample functions is presented. The distribution of these phase values is uniform in the interval 0 to 360 degree when the EEG sample functions contain no evoked activity. On the other hand, an aggregation of phase values in a certain angular region and hence a nonuniform distribution is to be expected if evoked activity is present. A statistical procedure testing a null hypothesis assumption of uniformity may thus be applied in the evaluation of presence/nonpresence of stimulus-related activity in the critical situations. A test of the Kolmogorov-Smirnov type, Kuiper's V(sub n) test, was applied with satisfactory results. Author

N88-27690# Dalhousie Univ., Halifax (Nova Scotia). Dept. of Ophthalmology.
DISSECTING THE VISUAL AND AUDITORY PATHWAYS BY MEANS OF THE TWO-INPUT TECHNIQUE **c52**
D. Regan and M. P. Regan *In* AGARD, Electric and Magnetic Activity of the Central Nervous System: Research and Clinical Applications in Aerospace Medicine Feb. 1988 9 p Sponsored by the National Sciences and Engineering Research Council, Canada, MRC, Canada and AFOSR, Washington, D.C. (For primary document see N88-27683 21-51)
Copyright Avail: NTIS HC A18/MF A01

An evoked potential for identifying the nonlinear characteristics of specialized sensory neural mechanisms in the human brain is described. For example, subjects viewed a grating pattern modulated at F(sub 1) Hz superimposed on a second grating modulated at F(sub 2) Hz. The VEP consisted of about 20 discrete frequency components, each of less than 0.004 Hz bandwidth. Most would be destroyed by conventional averaging, but could be measured by zoom-FTT technique that gives 25,000 resolvable bins over DC-100 Hz. A mathematical treatment was developed such that the pattern of behavior among these VEP components fingerprints the nonlinear processing. Orientation tuning bandwidths (20 deg) and the spatial frequency tuning of a phase-independent visual mechanism; strong interactions between response to orthogonal orientations; and a possible EP means of investigating the auditory hair cell transducer characteristic are reported.
Author

N88-27691# Consiglio Nazionale delle Ricerche, Rome (Italy). Istituto de Elettronica dello Stato Solido.
SQUID INSTRUMENTATION FOR NEUROMAGNETIC STUDY OF COMPLEX BRAIN ACTIVITY **c52**
Gian Luca Romani *In* AGARD, Electric and Magnetic Activity of the Central Nervous System: Research and Clinical Applications in Aerospace Medicine Feb. 1988 7 p (For primary document see N88-27683 21-51)
Copyright Avail: NTIS HC A18/MF A01

The impressive results obtained during the last few years by applying the neuromagnetic method to the investigation of brain physiology and pathology have given an extraordinary impulse to the development of large multi-sensor systems, which should permit, in a relatively near future, to simultaneously detect the distribution of the magnetic field over a large area of the scalp and to achieve a real time functional localization of active cerebral sources. An outline of the main instrumental problems in the choice of an optimal sensor configuration (for large mutlichannel systems)

is presented, with particular emphasis on the capability featured by different kinds of superconducting gradiometers to identify complex cerebral sources, and on the need for more sophisticated model sources. Author

N88-27692# Consiglio Nazionale delle Ricerche, Rome (Italy). Istituto di Elettronica dello Stato Solido.
ELECTRIC AND MAGNETIC BRAIN ACTIVITY RELATED TO COGNITIVE PERFORMANCE **c52**
Robert M. Chapman, Ivo Modena, Livio Marici, Vittorio Pizzella, Gian Luca Romani, Carlo Salustri, John W. McCrary, and Susan Garnsey (Rochester Univ., N. Y.) *In* AGARD, Electric and Magnetic Activity of the Central Nervous System: Research and Clinical Applications in Aerospace Medicine Feb. 1988 8 p (For primary document see N88-27683 21-51)
(Contracts MH40703; HD22271; EY01319)
Copyright Avail: NTIS HC A18/MF A01

Cognitive performance and brain activity; memory storage component in evoked potentials; connotative meaning; and syntactic differences in words and linguistic processing were examined. B.G.

N88-27693# Muenster Univ. (West Germany). Inst. of Experimental Audiology.
NEUROMAGNETIC EVIDENCE OF PLACE MECHANISMS FOR FREQUENCY AND INTENSITY CODING IN THE HUMAN AUDITORY CORTEX **c52**
M. Hoke, C. Pantew, K. Lehnertz, and B. Luetkenhoener *In* AGARD, Electric and Magnetic Activity of the Central Nervous System: Research and Clinical Applications in Aerospace Medicine Feb. 1988 12 p Sponsored by Deutsche Forschungsgemeinschaft, West Germany and Heinrich-Hertz-Stiftung, West Germany (For primary document see N88-27683 21-51)
Copyright Avail: NTIS HC A18/MF A01

The influence of two decisive parameters of the acoustic stimulus (frequency and intensity) on the auditory evoked magnetic field in response to tone-burst stimulation was investigated in four normal-hearing subjects. The influence was quantified in terms of changes of the parameters of an equivalent current dipole (spatial coordinates, direction, and strength). The frequency dependence was investigated by varying the carrier frequency of the tone-burst between 250 and 4000 Hz in octave steps with the intensity kept constant at 60 dB HL, while the intensity dependence was investigated by varying the intensity of a 1000 Hz tone-burst between 30 and 80 dB HL in 10 dB steps. The parameters of an equivanlent current dipole (ECD) were determined such that a maximum correspondence between observed and calculated field distribution (semi-infinite volume model) was obtained. The main results are as follows: the location of the ECD changes significantly as a function of test frequency and intensity. Especially the depth increases with the logarithm of test frequency which proves that also in humans the tonotopic organization of the cochlea is maintained in the auditory cortex. The decrease in depth of the ECD with increasing stimulus intensity supports the hypothesis that place mechanisms also play a role for intensity coding. Author

N88-27694# Simon Fraser Univ., Burnaby (British Columbia). Brain Behaviour Lab.
THE INTERACTION OF THALAMO-CORTICAL SYSTEMS IN THE 40 Hz FOLLOWING RESPONSE **c52**
H. Weinberg, D. Cheyne, P. Brickett, R. Gordon, and R. Harrop *In* AGARD, Electric and Magnetic Activity of the Central Nervous System: Research and Clinical Applications in Aerospace Medicine Feb. 1988 6 p (For primary document see N88-27683 21-51)
Copyright Avail: NTIS HC A18/MF A01

The study reported is an extension of the initial auditory experiments to include the study of 40 Hz vibration of glaborous skin receptors and examination of the interaction of simultaneous (in phase) auditory and tactile simulation. The data presented suggest that different systems are active in response to 40 Hz tactile vibration and auditory stimulation, although the EEG response at the vertex remains quite similar. B.G.

N88-27695# Simon Fraser Univ., Burnaby (British Columbia). Brain Behaviour Lab.
A STUDY OF SOURCES IN THE HUMAN BRAIN ASSOCIATED WITH STEREOPSIS **c52**
H. Weinberg, P. Brickett, A. Robertson, D. Crisp, D. Cheyne, and R. Harrop *In* AGARD, Electric and Magnetic Activity of the Central Nervous System: Research and Clinical Applications in Aerospace Medicine Feb. 1988 6 p Sponsored by the Defence and Civil Inst. of Environmental Medicine, Canada (For primary document see N88-27683 21-51)
Copyright Avail: NTIS HC A18/MF A01

The purpose of the initial stage of the research was to confirm with myoelectrography (MEG) the evidence for multiple stages of processing binocular information, establish what these stages are, and estimate location of generators. Initial experiments are designed to compare the magnetic fields evoked by dynamic random-dot stereograms (DRDSs) and dynamic RDCs in the same subject to see if the DRDC evoked field is similar to the early component of the response to the DRDS. The continuation of these experiments is concerned with the later component of the evoked field and the nature and location of the estimated sources. Author

N88-27696*# Illinois Univ., Champaign. Dept. of Psychology.
EVENT-RELATED BRAIN POTENTIALS AS INDICES OF MENTAL WORKLOAD AND ATTENTIONAL ALLOCATION **c52**
Arthur F. Kramer, Emanuel Donchin, and Christopher D. Wickens *In* AGARD, Electric and Magnetic Activity of the Central Nervous System: Research and Clinical Applications in Aerospace Medicine Feb. 1988 15 p Sponsored by NASA, Ames Research Center, Moffett Field, Calif. (For primary document see N88-27683 21-51)
(Contract F49620-79-C-0233)
Copyright Avail: NTIS HC A18/MF A01 CSCL 06P

Over the past decade considerable strides were made in explicating the antecedant conditions necessary for the elicitation, and the modulation of the amplitude and latency, of a number of components of the event-related brain potential (ERP). The focus of this report is on P300. The degree to which the psychophysiological measures contribute to issues in two real-world domains (communication devices for the motor impaired and the assessment of mental workload of aircraft pilots) are examined. Author

N88-27697# York Univ., Downsview (Ontario). Dept. of Physical Education.
THE EFFECTS OF HYPOXIA ON P300 AND REACTION TIME **c52**
B. Fowler, B. Kelso, J. P. Landolt, and G. Porlier (Defence and Civil Inst. of Environmental Medicine, Downsview, Ontario) *In* AGARD, Electric and Magnetic Activity of the Central Nervous System: Research and Clinical Applications in Aerospace Medicine Feb. 1988 7 p (For primary document see N88-27683 21-51)
(Contract DCIEM-W7711-6-9019)
(DCIEM-87-RR-12) Copyright Avail: NTIS HC A18/MF A01

This experiment investigated the effects of three levels of arterial oxyhemoglobin saturation (SaO2 of 75, 70, and 65 percent) on reaction time (RT) and P300 latency and amplitude. Ten subjects responded to visually presented male or female names in an oddball paradigm with accuracy controlled at a high level. Hypoxia increased both RT and P300 latency in a dose-related manner and these variables were strongly correlated. Hypoxia did not influence P300 amplitude. The increase in P300 latency is interpreted as further evidence that hypoxia allows stimulus evaluation processes and that, under the right circumstances, P300 could be used to index the effects of hypoxia on performance. Author

N88-27698# Organisatie voor Toegepast Natuurwetenschappelijk Onderzoek, Soesterberg (Netherlands). Human Performance Group.

USING ERPS TO STUDY HUMAN INFORMATION PROCESSING **c53**

A. W. K. Gaillard *In* AGARD, Electric and Magnetic Activity of the Central Nervous System: Research and Clinical Applications in Aerospace Medicine Feb. 1988 6 p (For primary document see N88-27683 21-51)

Copyright Avail: NTIS HC A18/MF A01

The event-related brain potential (ERP) technique may provide an inobtrusive measure of the processing of psychological information during task performance. Some investigators regard ERPs even as a direct manifestation of the ongoing psychological processes. Before such a strong claim can be made several methodological problems have still to be solved. The definition and identification of the various components in the ERP, the separation of exogenous and endogenous components, and the differenct ways in which inferences can be made about psychological processes on the basis of ERP components, is the low comparability of ERP measures across paradigms are discussed. Author

N88-27699# Washington Univ., St. Louis, Mo. Behavior Research Lab.

COGNITIVE TASK DEMANDS AS REFLECTED IN PHYSIOLOGICAL MEASURES **c52**

John A. Stern and Lance O. Bauer (Oklahoma Univ., Oklahoma City.) *In* AGARD, Electric and Magnetic Activity of the Central Nervous System: Research and Clinical Applications in Aerospace Medicine Feb. 1988 11 p (For primary document see N88-27683 21-51)

(Contract F49620-83-C-0059)

Copyright Avail: NTIS HC A18/MF A01

Three experiments are described in which cognitive demands were manipulated. The task was a modified Sternberg paradigm comprised of three task stimuli: the cue, providing information about the memory set, the memory set itself, and a test stimulus, a member of the memory set on half the trials. Among variables investigated were set size and nature of the stimulus material. Physiological measures included EEG event-related potentials (ERP) to the three stimuli (task-RSPs), ERPs to probe stimuli (probe-ERPs), and flashes irrelevant to performance. Three measures derived from the eye blink and one heart rate measure were used. Results demonstrated ERP changes related to task difficulty. Some involved the ERP to the memory stimulus and some, the prove ERP. Heart rate changes, some related to expectancy, others to task demands, were also obtained. Blink probability, duration and timing, all reflected stimulus expectancy and difficulty. These results suggest that work load, as well as attention, can be evaluated using physiological measures.

Author

N88-27700# Royal Army Medical Coll., London (England).

CAN CNV AMPLITUDE PREDICT ABILITY TO ACCOMPLISH A DEMANDING TASK? **c54**

Peter Abraham *In* AGARD, Electric and Magnetic Activity of the Central Nervous System: Research and Clinical Applications in Aerospace Medicine Feb. 1988 2 p (For primary document see N88-27683 21-51)

Copyright Avail: NTIS HC A18/MF A01

Increased Contingent Negative Variation (CNV) was related to attention, effort, and quick response to stimuli, while decreased CNV amplitude was related to distraction, delayed reaction times, and disorder of mental or emotional functioning. These observations suggest that CNV amplitude measured in the laboratory might be a useful predictor of an individual's ability to accomplish a demanding sensorimotor task under operational conditions. One such task is the operation of a surface-to-air missile known as Blowpipe. Firing this weapon requires rapid responses to that information, under stressful conditions. It also requires auditory stimuli emanating from the weapon. Thus firing operation is not unlike a CNV-generating situation. The Blowpipe training program afforded an opportunity to test the usefulness of CNV measurement for predicting operational performance as assessed during the firing of real missiles on a testing range. It was hypothesized that low laboratory CNV amplitude would predict unsuccessful Blowpipe firing and vice versa. The CNV amplitude was measured in 75 soldiers engaged in training as missile operators. Sixty-nine subjects completed the qualifying course and fired real missiles. Those who showed poor firing performance had CNV amplitudes at the extremes of the range. Selection strategies are discussed.

Author

N88-27701# Defence and Civil Inst. of Environmental Medicine, Downsview (Ontario).

THE EFFECT OF ENDOGENOUS ALPHA ON HEMISPHERIC ASYMMETRIES AND THE RELATIONSHIP OF FRONTAL THETA TO SUSTAINED ATTENTION **c53**

R. Pigeau, R. Hoffmann, S. Purcell, and A. Moffitt (Carleton Univ., Ottawa, Ontario) *In* AGARD, Electric and Magnetic Activity of the Central Nervous System: Research and Clinical Applications in Aerospace Medicine Feb. 1988 16 p (For primary document see N88-27683 21-51)

Copyright Avail: NTIS HC A18/MF A01

Data are represented which suggest that the degree of hemispheric alpha asymmetry is related to resting eyes closed endogeneous alpha activity. Also, it is demonstrated that frontal theta activity varies with the difficulty level of an additional tasks. Both results share a common emphasis on electrophysiological individual difference. The electroencephalogram (EEG) recordings from 54 right-handed subjects performing 5 cognitive tasks were collected and quantified using period analysis. The subjects were rank ordered on the basis of their hemispherically averaged alpha activity during an eyes closed baseline condition. A similar procedure was performed for frontal theta to distinguish theta generators. Utilizing a L-R/L+R asymmetry index the results indicate that high and middle alpha generators displayed the hypothesized and asymmetry relationship whereas the low alpha generators did not. This implies that low alpha generating subjects may negatively affect EEG laterality studies. Results from the addition task indicate that hemispherically averaged theta activity varies curvelinearily as a function of increaseing task difficulty. Subjects displaying higher performance scores on the additional task also demonstrate higher frontal theta values, suggesting theta is associated with sustained focused attention of higher order cognitive processes. Author

N88-27702# Defence and Civil Inst. of Environmental Medicine, Downsview (Ontario).

PSYCHOPHYSIOLOGICAL MEASURES OF DROWSINESS AS ESTIMATORS OF MENTAL FATIGUE AND PERFORMANCE DEGRADATION DURING SLEEP DEPRIVATION **c52**

R. A. Pigeau, R. J. Heslegrave, and R. G. Angus *In* AGARD, Electric and Magnetic Activity of the Central Nervous System: Research and Clinical Applications in Aerospace Medicine Feb. 1988 16 p (For primary document see N88-27683 21-51)

Copyright Avail: NTIS HC A18/MF A01

A methodology developed to measure drowsiness electrophysiologically as an index of chronic fatigue experienced during periods of sleep loss is described. Nine volunteers performed a continuous cognitive workload schedule with 15 minute breaks occurring every 2 hours throughout a 64 hour sleep deprivation experiment. To measure fatigue a 4 minute eyes closed relaxation period was embedded once every hour within a battery of cognitive tasks. The subjects were instructed to relax with their eyes closed but remain awake and alert. The EEG signals collected during these periods were both visually scored and computer quantified. Two raters visually scored the signals for: time of first stage 1 sleep onset, number of stage 1 sleep onsets, shortest and longest time in stage 1, and total amount of state 1 sleep (or deepest). Period analysis was performed on the digitized data and a drowsiness scale was developed by subtracting the amount of theta and delta from alpha while controlling for individual differences by dividing the results by alpha minus theta minus delta activity present in the baseline. The results indicate that for individual

subjects drowsiness onset latencies, performance, subjective scales, and the drowsiness index are all intercorrelated. It is suggested that these EEG techniques, as well as the methodology of embedding eyes close relaxation periods, yield sensitive measures for detecting differential levels of drowsiness during sleep deprivation. Author

N88-27703# EEG Systems Lab., San Francisco, Calif.
NEUROPHYSIOLOGICAL PATTERNS OF OPERATIONAL FATIGUE: PRELIMINARY RESULTS **c52**
A. S. Gevins, B. A. Cutillo, R. M. Fowler-White, J. Illes, S. L. Bressler, and J. C. Miller (Test Group, 6520th, Edwards AFB, Calif.) *In* AGARD, Electric and Magnetic Activity of the Central Nervous System: Research and Clinical Applications in Aerospace Medicine Feb. 1988 9 p Sponsored by AFOSR, Washington, D.C., School of Aerospace Medicine, Brooks, AFB, Tex., National Inst. of Neurological and Communicative Diseases and Strokes, Washington, D.C. and NSF, Washington, D.C. Original contains color illustrations (For primary document see N88-27683 21-51)
Copyright Avail: NTIS HC A18/MF A01

Impaired behavior consequent to prolonged mental work is commonly attributed to the effects of fatigue on higher cognitive functions rather than to changes in rote perceptuomotor or motor functions. A deeper understanding of these effects awaits better knowledge of the underlying neurophysiological mechanisms. Here a modes contribution is made toward this end with a study of event-related, spatiotemporal neuroelectric patterns of five U.S. Air Force test pilots performing a high-load visuomotor monitoring task while alert, becoming fatigued, and fully fatigued. The preliminary results suggest that although neural systems responsible for primary visual stimulus processing remain relatively unaffected, cortical associative areas implicated in task-specific response inhibition are affected even during early stages of fatigue. With further research, it may be possible to design on-line devices for predicting transient cognitive lapses and performance decrements resulting from operational fatigue. Author

N88-27704# Aerospace Medical Research Labs., Wright-Patterson AFB, Ohio. Human Engineering Div.
FIGHTER PILOT PERFORMANCE DURING AIRBORNE AND SIMULATOR MISSIONS: PHYSIOLOGICAL COMPARISONS **c54**
June J. Skelly, Bradley Purvis, and Glenn Wilson *In* AGARD, Electric and Magnetic Activity of the Central Nervous System: Research and Clinical Applications in Aerospace Medicine Feb. 1988 16 p (For primary document see N88-27683 21-51)
Copyright Avail: NTIS HC A18/MF A01

The growing importance of simulators for training, research, and certification focuses attention on how little is known about whether the behavioral outcomes obtained in a simulator really represent the operational situation. The research addresses this issue, and proposes that use of physiological measures to examine the correspondence between pilot responses during actual missions and comparable simulated missions. Physiological measures of electrical brain activity, heart rate, and eye movements were taken while pilots flow tactical training missions in both the A-7 aircraft and simulator. These measures did discriminate between: flight position (wing vs lead); actual and simulated flight; type of mission event (e.g., takeoff, maneuvers, weapons delivery), and individual pilots. Author

N88-27705# Burden Neurological Inst., Bristol (England).
EVENT-RELATED AND STEADY POTENTIAL CHANGES IN THE BRAIN RELATED TO WORKLOAD DURING TRACKING **c52**
W. C. McCallum, R. Cooper, and P. V. Pocock *In* AGARD, Electric and Magnetic Activity of the Central Nervous System: Research and Clinical Applications in Aerospace Medicine Feb. 1988 10 p Sponsored by British Aerospace, United Kingdom and the Ministry of Defence, United Kingdom (For primary document see N88-27683 21-51)
Copyright Avail: NTIS HC A18/MF A01

In two experiments event-related potentials (ERPs) and slow potential changes were recorded from normal subjects performing a visual tracking in which the level of difficulty was systematically varied. In the second experiment a secondary discrimination task was added to increase the level of operator load and to probe the allocation of cerebral processing resources. The most notable feature to emerge was a protracted slow potential shift, associated with the primary task. The amplitude of this shift proved to be sensitive to the difficulty manipulations such that increased difficulty resulted in increased negativity. However, a memory task introduced in the early part of each trial tended progressively to decrease the amplitude of the shift as the memory demand increased. The ERPs to the individual points of decision and response during the course of a trial were also found to be sensitive to the level of task loading. The introduction of the secondary task resulted in a possible further increase in the negative shift to tracking, but in reductions in the amplitude of late cognition components of the secondary task ERPs compared with their levels when this task was presented on its own. Author

N88-27706# EEG Systems Lab., San Francisco, Calif.
NEUROPHYSIOLOGICAL PRECURSORS OF ACCURATE VISUOMOTOR PERFORMANCE **c52**
A. S. Gevins, B. A. Cutillo, S. L. Bressler, N. H. Morgan, R. M. Fowler-White, D. S. Greer, J. Illes, J. C. Doyle, R. S. Tannehill, and G. M. Zeitlin *In* AGARD, Electric and Magnetic Activity of the Central Nervous System: Research and Clinical Applications in Aerospace Medicine Feb. 1988 11 p Sponsored by AFOSR, Washington, D.C., School of Aerospace Medicine, Brooks, AFB, Tex., NSF, Washington, D.C., National Inst. of Neurological Diseases and Strokes, Washington, D.C. and ONR, Washington, D.C. Original contains color illustrations (For primary document see N88-27683 21-51)
Copyright Avail: NTIS HC A18/MF A01

Using advanced, signal processing techniques, the rapidly changing, spatial mass neuroelectric patterns associated with preparation and execution of precise right- and left-hand finger pressures in response to visual numeric stimuli in seven healthy right-handed adult male subjects were measured. Previously unseen pre-stimulus differences between patterns associated with subsequently accurate and inaccurate performance were revealed. A spatially specific, multi-component neural preparatory set, composed of invariant left frontal and midline precentral components and hand-specific central and posterior parietal components, appear to be essential for accurate performance of certain types of difficult visuomotor tasks. When this preparatory set is weakened, or inappropriate, subsequent performance is likely to be inaccurate. Author

N88-27707# Naval Aerospace Medical Research Lab., Pensacola, Fla.
THE NEUROELECTRIC SELECTION OF NAVAL AVIATION PERSONNEL: AN EVALUATION **c53**
R. R. Stanny, D. L. Reeves, M. R. Blackburn, and G. R. Banta (Naval Medical Research and Development Command, Bethesda, Md.) *In* AGARD, Electric and Magnetic Activity of the Central Nervous System: Research and Clinical Applications in Aerospace Medicine Feb. 1988 8 p (For primary document see N88-27683 21-51)
Copyright Avail: NTIS HC A18/MF A01

The value of using event-related potentials to predict success in naval aviation is examined. The background of the project, some methodological considerations, and the approach to the problem are discussed. Some early results have become available and are encouraging. Author

N88-27708# Naval Biodynamics Lab., New Orleans, La. Impact Sciences Dept.
EVOKED POTENTIAL ANALYSIS OF IMPACT ACCELERATION EXPERIMENTS **c52**
David L. Matson and Marc S. Weiss *In* AGARD, Electric and Magnetic Activity of the Central Nervous System: Research and Clinical Applications in Aerospace Medicine Feb. 1988 13 p

(For primary document see N88-27683 21-51)
Copyright Avail: NTIS HC A18/MF A01

The use of somatosensory evoked potentials (SEPs) as an assessment tool for transient injury in rhesus macaques undergoing impact acceleration in the -Gx direction is examined. Adult male rhesus macaques, seated on a sled and restrained (except for the head and neck), were accelerated at peak sled accelerations ranging from 95.5 to 1039.6 m/sec squared. The sled was decelerated by friction forces ranging from 0.7 to 3.0 m/sec squared. Somatosensory stimuli were delivered prior to, during, and after impact. Amplified SEP activity was telemetered and recorded on magnetic tape. The raw SEP data were digitized and analyzed off-line. Results for cortical SEPs are consistent with and extend previous analyses, suggesting a threshold for transitory changes in cervical SEP latencies in macaques at peak -Gx sled accelerations below 550 m/sec squared. This threshold is below the threshold for single impact -Gx neuropathological injury in macaques (800 m/sec squared), and suggests a role for cortical SEPs in establishing injury critieria for humans. Author

N88-27709# School of Aerospace Medicine, Brooks AFB, Tex.
EEG INDICES OF G-INDUCED LOSS OF CONSCIOUSNESS (G-LOC) **c52**
Nita L. Lewis, Jennifer B. McGovern, James C. Miller, Douglas R. Eddy, and Estrella M. Forster (Rothe Development, San Antonio, Tex.) *In* AGARD, Electric and Magnetic Activity of the Central Nervous System: Research and Clinical Applications in Aerospace Medicine Feb. 1988 12 p (For primary document see N88-27683 21-51)
Copyright Avail: NTIS HC A18/MF A01

To investigate the utility of the electroencephalogram (EEG) as an indicator of state of consciousness, human brain activity was recorded during exposure to rapid onset (6 G/sec) centrifugation (+7G). Eight healthy volunteers were given at least two sessions of sustained acceleration on the USAFSAM human centrifuge. The sessions were conducted without G-suits and subjects were instructed to relax and not attempt anti-G straining maneuvers. Six subjects each experienced two episodes of G-induced loss of consciousness (G-LOC) while one subject lost consciousness once and experienced visual blackout once. One subject remained conscious but experienced visual grayout in both sessions. The EEG signals were recorded with EEG Grass gold-cup electrodes which were held in place by using gauze and collodion. Data were digitized at 256 samples per second and transferred to a DEC PDP-11/55 computer for analysis. Results demonstrated a shift from beta to delta activity with pronounced absence of beta activity during unconsciousness. These results are in keeping with findings in the anesthesia and aerospace medicine literature. The EEG can be useful in detecting unconsciousness during acceleration. Author

N88-27710# Naval Air Development Center, Warminster, Pa.
DETECTION OF ACCELERATION (+Gz) INDUCED BLACKOUT BY MATCHED-FILTERING OF VISUAL EVOKED POTENTIALS **c52**
John G. Nelson, Joseph P. Cammarota, and Leonid Hrebien *In* AGARD, Electric and Magnetic Activity of the Central Nervous System: Research and Clinical Applications in Aerospace Medicine Feb. 1988 13 p (For primary document see N88-27683 21-51)
Copyright Avail: NTIS HC A18/MF A01

In air-combat-maneuvering and on human centrifuges, moderate levels of positive acceleration (+Gz), coupled with moderate rates of onset, produce visual symptoms which are ordinarily progressive: decreasing visual sensitivity, dimming of visual field, peripheral light-loss, and central light-loss of consciousness, subjective visual symptoms are the most commonly used tolerance end point in acceleration research. In order to provide an objective indication of the integrity of the visual system, a method for real-time monitoring of the steady-state visual evoked potential (VEP) was developed. Using the Fast Fourier Transform (FFT), a method for maximizing the signal-to-noise ratios was developed: a digital, frequency domain, non-white-noise matched filter, with evaluation only at the expected response peak. Experiments on the U.S. Naval Development Center's Human Centrifuge demonstrated that the response does progressively decrease, disappearing at black-out. Improved computer facilities have permitted evaluation of alternative methods of processing, and the effectiveness of such processing. Data from a static experiment using four stimulus repetition rates and two electrode positions showed that windowing of the time record prior to FFT does not necessarily improve detection. Author

N88-27711# Veterans Administration Hospital, Sepulveda, Calif. Neuropsychology Research Dept.
ELECTROENCEPHALOGRAPHIC CORRELATES OF PILOT PERFORMANCE: SIMULATION AND IN-FLIGHT STUDIES **c53**
M. B. Sterman, G. J. Schummer, T. W. Dushenko, and J. C. Smith *In* AGARD, Electric and Magnetic Activity of the Central Nervous System: Research and Clinical Applications in Aerospace Medicine Feb. 1988 16 p (For primary document see N88-27683 21-51)
(Grants AF-AFOSR-0231-83; AF-AFOSR-0335-82)
Copyright Avail: NTIS HC A18/MF A01

Both laboratory and in-flight studies were performed in order to evaluate the utility and feasibility of EEG monitoring as a means of identifying central nervous system correlates of performance and G-force effects during military flight operations. Four studies were conducted, two with controlled laboratory simulation, and two in actural flight during military training missions. Data analysis focused on EEG power-spectral density characteristics and their temporal modulation, specifically in sensorimotor and visual cortical areas. Several consistent findings emerged. During competent performance, a highly unique discrepancy appeared between the left and right hemispheres in central 8 to 15 Hz activity. This pattern disappeared as performance degraded. The temporal modulation of this activity also reflected these changes. During high G-force situations, power at frequencies below 8 Hz was progressively and non-specifically enhanced. Continued competent performance, however, was still reflected by the pattern described. These findings are discussed in terms of their neurophysiological implications. Author

N88-27712# Aerospace Medical Research Labs., Wright-Patterson AFB, Ohio.
MOTION EVOKED VESTIBULAR POTENTIALS **c52**
G. Wilson, R. Luciani, and D. Ratino (Air Force Human Resources Lab., Williams AFB, Ariz.) *In* AGARD, Electric and Magnetic Activity of the Central Nervous System: Research and Clinical Applications in Aerospace Medicine Feb. 1988 5 p (For primary document see N88-27683 21-51)
Copyright Avail: NTIS HC A18/MF A01

Motion evoked potentials (MER) were collected from subjects while they were rotated from side to side in a seated position. The MERs were biphasic with major component mean latencies of 278 and 388 msec. It is concluded that the MERs are of brain origin and not due to artifacts from the recording environment. The latencies of the waveform components of the MER suggests that the MER results from the onset of the rotation stimulus. Differences between the MERs reported and those of other published reports may be due to the added involvement of the saccule/utricle apparatus and the more rapid onset of the stimulus. Author

N88-27713# Defence and Civil Inst. of Environmental Medicine, Downsview (Ontario).
THE EFFECT OF MILD HYPOXIA ON THE VESTIBULAR EVOKED RESPONSE **c52**
W. D. Fraser, N. Black, D. E. Eastman, and J. P. Landolt *In* AGARD, Electric and Magnetic Activity of the Central Nervous System: Research and Clinical Applications in Aerospace Medicine Feb. 1988 10 p (For primary document see N88-27683 21-51)
Copyright Avail: NTIS HC A18/MF A01

The effect of hypoxia on the long-term vestibular evoked response was examined in eight sitting subjects on a small target light that rotated with the subject. Evoked responses were recorded during 10 minutes of rotational stimulation after breathing each

gas mixture for a minimum of 25 minutes. For intermittent clockwise (CW) rotation in the horizontal plane, a reproducible negative potential developed at electrode sites located between the vertex and the linked ears during air breathing conditions. It peaked close to the point of maximum velocity of the sinusoidal stimulus. The results indicate that the cortical processing of vestibular sensations may be affected even under very mildly phyoxic conditions. Animal studies have indicated that the levels of hypoxia used in this study can significantly alter neurotransmitter metabolism in brain tissue. Modification in neurotransmitter synthesis and concentration by the hypoxic conditions may explain the susceptibility of cortical processing of sensory information to very mild hypoxia. Compensatory changes in cerebral blood flow and neurotransmitter synthesis may be responsible for the reduced effect under the more severe hypoxic conditions. Author

N88-27714# Hordt Research, Development and Therapy, Rodgau (West Germany).

MEASUREMENT AND CLASSIFICATION OF THE MODE OF ACTION OF ANTIDEPRESSANT DRUGS c52

Albrecht Frauendorf, David Johnson, and Lothar Demisch (Johann-Wolfgang-Goethe-Univ., Frankfurt am Main, West Germany) *In* AGARD, Electric and Magnetic Activity of the Central Nervous System: Research and Clinical Applications in Aerospace Medicine Feb. 1988 9 p (For primary document see N88-27683 21-51)

Copyright Avail: NTIS HC A18/MF A01

In a comparison of the chronic effects on the central nervous system of five new generation antidepresssant, a dose-response study was performed with 5 to 7 healthy subjects per substance. Following standard medical screening, intraindividual comparisons after one week at each of the three dosages. Two MAO-inhibitors, a NA-reuptake inhibitor, a serotonine-reuptake inhibitor, and an alpha 1/alpha 2 adrenergic receptor, and serotonine S sub 2 (receptor-antagonist). The visual evoked potentials were recorded from electrode position O sub z between O sub 1 and O sub 2. The brightness, contract, and color channels of the visual system were stimulated using on-off, checkerboard, and color changes respectively. After digitizing, the evoked potentials were subjected to Fourier filtering and analyzed in the standard EEG frequency ranges delta, theta, alpha, and beta. This improved stability and precision of measurement without phase shifts. The latency changes of all components were measured and used to form attenuation and activation coefficients in each range. With the help of factor analysis, an activity profile of the effects of each of these drugs in the CNS was plotted in three-dimensions. Both activation and attenuation coefficients were used to classify the effects of the antidepressants at the cortical level. Author

N88-27715# Johann-Wolfgang-Goethe-Univ., Frankfurt am Main (West Germany).

MEASUREMENT OF ELECTRICAL ACTIVITY IN THE CNS WITH CORTICAL EVOKED POTENTIALS AND EEG: EFFICACY PROFILES OF DRUGS USING FACTOR ANALYSIS c52

David Johnson, Albrecht Frauendorf (Hordt Research, Development and Therapy, Rodgau, West Germany), and Kurt Offenloch *In* AGARD, Electric and Magnetic Activity of the Central Nervous System: Research and Clinical Applications in Aerospace Medicine Feb. 1988 8 p (For primary document see N88-27683 21-51)

Copyright Avail: NTIS HC A18/MF A01

In a series of experiments with 20 healthy, subjects per substance, the influences of a new nootropic drug and three cardiovascular agents on the CNS were measured and placebo controlled. The EEG and visual cortical evoked potentials were recorded from electrode position O sub z between O sub 1 and O sub 2 according to the 10 to 20 system. Three channels of the visual system were selectively stimulated (contrast, brightness, and color using checkerboard, flash, and color change). Acute and chronic studies were reported. Each VEP was filtered into the standard EEG-frequency range. Latency changes of the EP were evaluated in each range and analyzed with the Fourier technique. The cardiovascular substances caused a significant latency increase of beta-components with apparent latencies of 80 to 100 ms. This attenuation was shown in the contrast and even stronger in the color channel of the visual system. For the nootropic substance, a significant latency decrease was found for three components of the visual evoked potential in the theta-range. Their latencies are from 170 to 360 ms. The results of the EEG analysis are compared to the EP results. Generalized changes for groups of substances and highly specific profiles of activity for individual substances may be measured using this set of stimulus and analysis techniques. Activation and attenuation of activity for one and the same substances also were measured indicating multiple modes of actions. This may reflect cognitive processes and sensomotor activity. Author

N88-27716# Centre d'Etudes et de Recherches de Medecine Aerospatiale, Paris (France). Div. de Neurophysiologie Appliquee.

AN APPROACH TO STUDYING THE EFFECTS OF PSYCHOSTIMULANTS ON CEREBRAL ELECTRICAL ACTIVITY IN THE NON-HUMAN PRIMATE [UNE APPROCHE DES EFFETS DE PSYCHOSTIMULANTS SUR L'ACTIVITE ELECTRIQUE CEREBRALE CHEZ LE PRIMATE NON HUMAIN] c52

D. Lagarde and C. Milhaud *In* AGARD, Electric and Magnetic Activity of the Central Nervous System: Research and Clinical Applications in Aerospace Medicine Feb. 1988 11 p In FRENCH (For primary document see N88-27683 21-51)

Copyright Avail: NTIS HC A18/MF A01

The effects of three psychostimulant substances on brain electrical activity in the rhesus monkey were studied. The prime objective of these experiments was to obtain a data base of EEG properties and the changes caused by well-known psychostimulants at different dosages, and compare them to the EEG modifications induced by experimental psychotropic drugs. The power spectral density was used to analyze EEG data into different frequency bands for caffeine, d-amphetamine sulfate, and the experimental drug CRL 40476. In general, the results showed that caffeine caused a significant increase in delta activity, some decrease in the theta and alpha bands, and variable decreases in the beta band. Amphetamine produced an increase in delta and alpha activities, relative stability with signs towards an increase in theta activity, and a clear decrease in beta activity. The CRL 40476 caused important increases in delta activity, no changes in theta and alpha activity, and some decrease in the level of beta activity. Author

N88-27717# Italian Air Force Aerospace Medical Center, Rome. Neuropsychophysiology Group.

SPONTANEOUS CEREBRAL ELECTRICAL ACTIVITY DURING PROLONGED HYPOGLYCEMIA: A QUANTITATIVE STUDY IN HUMANS c52

Silvio Porcu, Roberto Berti, and Alberto Lala *In* AGARD, Electric and Magnetic Activity of the Central Nervous System: Research and Clinical Applications in Aerospace Medicine Feb. 1988 12 p (For primary document see N88-27683 21-51)

Copyright Avail: NTIS HC A18/MF A01

The importance of neuroglycopenia secondary to hypoglycemia as a possible cause or contributing factor in aircraft accidents was stressed. The study was designed to investigate the neurophysiological correlations of neuroglycopenia. The generation of spontaneous cerebral electrical activity in healthy young adults is quantified in a computer-assisted study, with subjects placed under fixed hypoglycemic conditions. Author

N88-27718# Dalhousie Univ., Halifax (Nova Scotia). Dept. of Ophthalmology.

RELATION BETWEEN VEP AND VISUAL FUNCTION IN LESIONS OF THE OPTIC NERVE AND VISUAL PATHWAY c52

D. Regan and D. Neims *In* AGARD, Electric and Magnetic Activity of the Central Nervous System: Research and Clinical Applications in Aerospace Medicine Feb. 1988 8 p Sponsored in part by Medical Research Council of Canada, Multiple Sclerosis Society of Canada, Baker Trust of Canada and NIH, Bethesda,

Md. (For primary document see N88-27683 21-51)
Copyright Avail: NTIS HC A18/MF A01

Several authors have claimed that visual evoked potential (VEP) abnormality is not closely related to sensory visual loss in patients with multiple sclerosis. However, all of the studies assessed sensory visual loss entirely in terms of Snellen visual acuity. Recent findings indicate the possibility that this lack of correlation between VEPs and sensory data might be due, at least in part, to the inability of Snellen's test to detect the full range of visual losses associated with visual pathway dysfunction. Before discussing abnormalities of pattern VEPs in patients with demyelinating diseases, the reasons why the Snellen acuity provides only an incomplete test of visual function loss are explained. Author

N88-27719# Hellenic Air Force General Hospital, Athens (Greece). Neurological Clinic.
CORRELATION BETWEEN EEG ABNORMAL ACTIVITY AND AIRCRAFT ACCIDENTS: A LONG TERM OBSERVATION c53
A. Stavropoulos *In* AGARD, Electric and Magnetic Activity of the Central Nervous System: Research and Clinical Applications in Aerospace Medicine Feb. 1988 5 p (For primary document see N88-27683 21-51)
Copyright Avail: NTIS HC A18/MF A01

During 1975 to 1976, 64 student pilots of the Hellenic Air Force Air Academy were studied with electroencephalographic protocol including activation procedures. In 13 of them, abnormal encephalographic activity was observed. During their 10-year flying career as fighter pilots, six pilots with abnormal EEGs were involved in 10 aircraft accidents due to pilot error, while only 3 pilots of the 51 with normal EEGs were involved in 4 accidents due to pilot errors. Author

N88-27720# Royal Air Force, Wroughton (England). Neurology Dept.
DETECTION OF LATENT EPILEPSY IN AIRCREW CANDIDATES c52
R. T. G. Merry *In* AGARD, Electric and Magnetic Activity of the Central Nervous System: Research and Clinical Applications in Aerospace Medicine Feb. 1988 3 p (For primary document see N88-27683 21-51)
Copyright Avail: NTIS HC A18/MF A01

Epilepsy is a common medical disorder, with a prevalence of 0.5 to 0.8 percent, and is the commonest cause of accidents due to medical incapacity in drivers. Although imperfect, the electroencephalogram (EEG) is useful in the detection of a latent predisposition to epilepsy, and is recommended as an obligatory part of the initial medical examination of candidates for military aircrew. Author

N88-27721# Oficinas Gerais de Material Aeronautico, Alverca (Portugal).
THE AUDITORY EVOKED RESPONSE IN MILITARY PILOTS c52
Nuno A. A. CasteloBranco, Jose H. Marvao, M. Salome CasteloBranco, and Antonio J. Entrudo (Portugal Air Force Hospital.) *In* AGARD, Electric and Magnetic Activity of the Central Nervous System: Research and Clinical Applications in Aerospace Medicine Feb. 1988 8 p (For primary document see N88-27683 21-51)
Copyright Avail: NTIS HC A18/MF A01

This study relates to the effect of G forces, through an aerobatic flight profile without G suit protection, upon twenty military pilots with varying flight experience. The auditory evoked response during rest showed significant differences in wave 5 and in the 1 to 5 interval. Immediately following the flight, differences were observed in wave 3. These results suggest the importance which this electrophysiological method may have on measuring accumulated fatigue. Immediate fatigue implies complex mathematical problems presently under study. Simultaneously, hemorrheologic, hormonal and biochemical studies were conducted for a better understanding of the physiological effects of fatigue. Though it is recognized that the test population is relatively small (20 pilots), an expanded study is underway in order to compile more conclusive data. Author

N88-27722# Jackson Lab., Bar Harbor, Maine.
GENETIC EFFECTS OF LOW LEVEL MICROWAVE RADIATION Annual Report, Mar. 1987 - Mar. 1988
Jeffery D. Saffer 1 Mar. 1988 5 p
(Contract N00014-87-K-0145; S40-0021)
(AD-A192687) Avail: NTIS HC A02/MF A01 CSCL 06G

We have developed a biological model system for examining the effects of electromagnetic radiation at the cellular level. This system features(1) a simple bacterial model with plasmid DNA which can be manipulated at the molecular level,(2) an assay which includes biological amplification for detecting subtle alterations, and(3) low variability usually inherent in biological assays. This system will now be used to study the effects of nondestructive free electron laser (FEL) radiation on biological processes in whole cells. We have tested the model system using microwave radiation and have been able to detect subtle changes in the plasmid-encoded Beta-galactosidase activity. The effect observed is not duplicated by bulk heating of the bacterial culture and there is no effect on purified Beta-galactosidase. GRA

N88-27723# Midwest Research Inst., Golden, Colo.
AN OUTDOOR TEST FACILITY FOR THE LARGE-SCALE PRODUCTION OF MICROALGAE
D. A. Johnson, J. Weissman, and R. Goebel Mar. 1988 12 p Presented at the Energy From Biomass and Wastes, New Orleans, La., 15 Feb. 1988 Prepared in cooperation with Microbial Products, Inc., Fairfield, Calif.
(Contract DE-AC02-83CH-10093)
(DE88-001146; SERI/TP-231-3325; CONF-880215-4) Avail: NTIS HC A03/MF A01

The goal of the U.S. Department of Energy Solar Energy Research Institute's Aquatic Species Program is to develop the technology base to produce liquid fuels from microalgae. This technology is being initially developed for the desert Southwest. As part of this program an outdoor test facility was designed and constructed in Roswell, New Mexico. The site has a large existing infrastructure, a suitable climate, and abundant saline groundwater. This facility will be used to evaluate productivity of microalgae strains and conduct large-scale experiments to increase biomass productivity while decreasing production costs. Six 3-sq m fiberglass raceways were constructed. Several microalgae strains were screened for growth, one of which had a short-term productivity rate of greater than 50 g dry wt/sqm/d. Two large-scale, 0.1-ha raceways were also built. These are being used to evaluate the performance trade-offs between low-cost earthen liners and higher cost plastic liners. A series of hydraulic measurements is also being carried out to evaluate future improved pond designs. Future plans include a 0.5-ha pond. This facility will be available to other researchers and industry for studies on microalgae productivity. DOE

N88-27724# Pennsylvania Univ., Philadelphia. Dept. of Biochemistry and Biophysics.
FACTORS GOVERNING LIGHT DRIVEN ELECTRON AND PROTON TRANSLOCATION IN PROTEINS ACROSS MEMBRANES
P. L. Dutton 1988 25 p
(Contract DE-AC02-80ER-10590)
(DE88-011120; DOE/ER-10590/2) Avail: NTIS HC A03

A series of preliminary studies showed that both the direct electrical and the Q(sub A) replacement avenues of approach were feasible. That the reaction centers could be incorporated in planar bilayer membranes to a density of approximately 10 to the 9th power sq cm was determined and with metal electrodes on either side of the supporting membranes flash activated voltages and transient currents could be monitored. The reaction centers were deposited in a 50:50 mix of vectorially opposing populations. By this approach, simple optical studies cannot easily be performed on the film either alone or simultaneous with electrical assay. The successful construction of reaction center mono (and multi) layers

formed in a Langmuir Blodgett trough and deposited on planar solid supports was demonstrated. A simple spectrophotometric analysis was done on the dry film. Direct transmission assay of the optical properties of single monolayers supported the finding of approximately 5 x 10 to the 12th power reaction centers/sq cm; linear dichroism showed that the orientation of the reaction center chromophores were as found in vivo. The reaction centers responded to flash activation. DOE

N88-27725# California Univ., Berkeley. Lawrence Berkeley Lab.
STRUCTURE AND FUNCTION OF THE MANGANESE COMPLEX INVOLVED IN PHOTOSYNTHETIC OXYGEN EVOLUTION DETERMINED BY X-RAY ADSORPTION SPECTROSCOPY AND ELECTRON PARAMAGNETIC RESONANCE SPECTROSCOPY Ph.D. Thesis
R. D. Guiles Apr. 1988 274 p
(Contract DE-AC03-76SF-00098)
(DE88-010360; LBL-25186) Avail: NTIS HC A12/MF A01

Water is the terminal electron donor in the linear light-driven electron transport chain used by higher plants, cyanobacteria and green algae to fix carbon dioxide. The involvement of a membrane-bound manganese-containing protein complex has been demonstrated at the site of water oxidation within the photosystem II (PSII) reaction center. The photosynthetic oxidation of water to molecular oxygen is believed to involve intermediate S-states (S sub 0 to S sub 4), of the oxygen evolving complex (OEC). The use of multiline EPR signal associated with Mn and assigned to the S sub 2 state has greatly facilitated structural characterization of the OEC. This thesis contains a description of methods used to cryogenically stabilize PSII preparations suitable for X-ray absorption spectroscopy in the S sub 1, S sub 2 and S sub 3 states as well as a state induced by hydroxylamine resembling the S sub 0 state of the OEC. Studies of the Mn K-edges of PSII preparations indicate that a light-induced oxidation of Mn occurring during the S sub 1 yield S sub 2 state transition corresponds to a formal valence change from Mn(III) to Mn(IV). An analysis of the extended X-ray absorption fine structure (EXAFS) of the Mn complex within PSII preparations poised in the S sub 1, S sub 2, S sub 3 and hydroxylamine-induced S sub 0 states indicates that the four manganese present are organized as two di-mu-oxo bridged binuclear managanese complexes. An essential component of the analysis of the EXAFS was a parallel analysis of a set of crystallographically characterized multinuclear mu-oxo bridged manganese complexes. Based on conclusions drawn from the analysis of the Mn K-edge and EXAFS of PSII preparations cryogenically stabilized in the S-states described above, a model for the mechanism of photosynthetic water oxidation is presented. DOE

N88-27356# Florida Univ., Gainesville. Dept. of Psychology.
PHYSIOLOGICAL MONITORING METHODOLOGY IN THE USAFSAM CENTRIFUGE Final Report
Jennifer B. McGovern *In* Universal Energy Systems, Inc., United States Air Force Graduate Student Summer Support Program, Volume 2 Dec. 1987 11 p (For primary document see N88-27355 21-31)
Avail: NTIS HC A99/MF E03 CSCL 06P

N88-27357# Brown Univ., Providence, R. I. Div. of Biology and Medicine.
METHODS OF QUANTIFYING AND ENHANCING REACTIVE OXYGEN SPECIES PRODUCTION Final Report
Roland A. Medellin *In* Universal Energy Systems, Inc., United States Air Force Graduate Student Summer Support Program, Volume 2 Dec. 1987 20 p (For primary document see N88-27355 21-31)
Avail: NTIS HC A99/MF E03 CSCL 06P

52 AEROSPACE MEDICINE

Includes physiological factors; biological effects of radiation; and effects of weightlessness on man and animals.

N88-27726# National Inst. of Health, Bethesda, Md. National Eye Inst.
VISION RESEARCH. A NATIONAL PLAN: 1983-1987, 1987 EVALUATION AND UPDATE Final Report, Oct. 1984 - Dec. 1986
1987 334 p
(PB88-192604; NIH/Pub-87-2755) Avail: NTIS HC A15/MF A01 CSCL 06P

The evaluation project examined the current level and distribution of effort in all the scientific research areas addressed by Vision Research-A National Plant: 1983-1987, the National Advisory eye Council's most resecent planning and evaluation document. It recognized and encouraged activity in important new ares that had developed since the Plan was prepared. It identified recommendations that were not sufficiently specific or those that were prematrue or too narrow in focus and might have benefitted from consolidation with other recommendations. A computerized system was developed and used to track grant applications wherin every grant application, whether funded or not, was coded according to the relevance to one of the Plan's recommendations. The report produced by this effort was used by the National Advisory Eye Council and the staff of the NEI to determine long-range and day-to-day management decisions, by scientists in the vision research community as a guide to most important needs and opportunity as a guide to the most important needs and opportunities in the field; and by organizations, foundations, all those interested in recent problems and challenges in ophthalmology, optometry, and vision science, including current activites and plans for continued success in the prevention, treatment, and control of blinding disease. GRA

N88-27727# Army Research Inst. of Environmental Medicine, Natick, Mass.
HYPOTHALAMIC-PITUITARY-ADRENAL RESPONSES TO SHORT DURATION HIGH INTENSITY CYCLE EXERCISE
William J. Kraemer, John F. Patton, Howard G. Knuttgen, Louis J. Marchitelli, and Charles Cruthirds Jan. 1988 32 p
(AD-A192597; USARIEM-M-16/88) Avail: NTIS HC A03/MF A01 CSCL 06A

Beta-endorphin (B-EP), adrenocorticotropin (ACTH) and cortisol plasma concentrations were examined before and after maximal exercise at four intensities (36, 55, 73 and 100 percent of Maximal Leg Power (MLP) utilizing a computerized cycle ergometer. All intensities were greater than those eliciting peak oxygen uptake for the individual subjects. Blood samples were collected at rest, immediately following exercise (IP) and at 5 and 15 min post-exercise. Significant (p less than 0.05) increases were observed at 36 percent MLP for B-EP and ACTH at IP, 5 and 15 min post-exercise. Plasma cortisol increased at 36 percent MLP at 15 min post exercise. Blood lactate significantly increased at all post-exercise collection points for exercise intensities of 36, 55 and 73 percent MLP and at 5 min post exercise for 100 percent MLP. B-EP concentrations at 36 percent MLP were significantly correlated (r=0.75) with capillary density (mm-2) and cortisol concentrations at 36 percent MLP were significantly correlated (r=0.89) with percent type 2 muscle fibers. No other significant relationships were observed. GRA

N88-27728# Army Research Inst. of Environmental Medicine, Natick, Mass.
METABOLIC AND CARDIORESPIRATORY PARAMETERS DURING THREE CONSECUTIVE DAYS OF EXHAUSTIVE RUNNING Report, Feb. - Mar. 1982
Joseph Knapik, James Wright, Michael Welch, Marilyn Sharp, and Robert Mello Nov. 1987 22 p
(AD-A192598; USARIEM-M-10/88) Avail: NTIS HC A03/MF A01 CSCL 06D

Serum metabolites, cardiorespiratory parameters and creatine kinase were examined during running on 3 consecutive days.

Thirteen trained marathon runners exercised to exhaustion on a treadmill at 85 plus or minus 3 percent VO2 max on each day. Expired gases and blood samples were obtained at rest, after 10 and 30 min of exercise and at exhaustion. There were no significant differences over days for glucose, insulin, lactate, free fatty acids, creatine kinase, oxygen uptake, minute ventilation, heart rate, rating of perceived exertion, respiratory exchange ratio or run times. Serum glycerol was elevated (p .05) both at rest and during exercise on each successive day. The findings suggested that except for serum glycerol, acute metabolic and cardiorespiratory responses to exhaustive aerobic exercise are not altered by daily repetition at least up to 3 days. GRA

N88-27729# Army Research Inst. of Environmental Medicine, Natick, Mass.

VALIDATION OF A MODIFIED ONE-STEP REBREATHING TECHNIQUE FOR MEASURING EXERCISE CARDIAC OUTPUT Final Report, Jan. - Dec. 1987

Patricia C. Szlyk, Karleyton C. Evans, and Ingrid V. Sils 19 Jan. 1988 22 p

(AD-A192600; USARIEM-M-19/88) Avail: NTIS HC A03/MF A01 CSCL 05H

A modification of the Farhi one-step rebreathing technique is described for determining submaximal exercise cardiac output (Q). Factors critical in the estimation of Q are initial rebreathing bag volume and constant bag volume during the maneuver. By substituting a high flow rate analyzer for the recommended low flow rate mass spectrometer, adding a recirculation circuit from the outlet of the analyzer to an inlet at the base of the rebreathing bag and reducing the length of sample tubing to the analyzer, we were able to recirculate the subject's expired gas and achieve no loss of bag volume. No statistically significant differences in estimate of cardiac output were noted between the mass spectrometer and LB-2 analyzer with recirculation circuit during submaximal cycling. Heart rate and oxygen uptake were highly correlated with cardiac output and agreed well with the literature, irrespective of the CO2 analyzer system used. A unique feature of our method is that the subject's tidal volume is measured prior to the maneuver and then used as the initial rebreathing bag volume. Varying the bag volume by + or - 0.2L from the tidal volume had no significant effect on the estimate of cardiac output during exercise. Now quick, reliable and noninvasive measurements of cardiac output are feasible in subjects not only in the laboratory but also in the field where a mass spectrometer is not readily portable. GRA

N88-27730# Army Research Inst. of Environmental Medicine, Natick, Mass.

A RESISTIVE-FILM BASED FORCE TRANSDUCER FOR THE STUDY OF EXERCISE

Peter N. Frykman, Everett A. Harman, Richard M. Rosenstein, and Stephen P. Mullen Jan. 1988 208 p

(AD-A192601; USARIEM-M-17/88) Avail: NTIS HC A10/MF A01 CSCL 14B

A new pressure sensitive resistive film was used to construct a pair of force sensing pedals designed to fit a Universal leg press machine. The sensors were calibrated by recording their output voltages on a microcomputer via an A/D converter sampling at 100 Hz as weight was placed on each pedal's top surface. Third order polynomial equations were fit to the data and resulted in correlation coefficients between actual and predicted force of .9965 for the right pedal and .9918 for the left. Within day reliability coefficients were .9997 and .9994 for the right and left pedals respectively, while across day reliability coefficients were .9989 and .9877. The upper limit of accurate force transduction is over 5000 N per pedal. The pedal transducer is reliable, valid, inexpensive, and relatively easy to work with. The resistance film requires considerably less engineering than do strain gages in the construction of transducers to measure forces applied to a flat surface. GRA

N88-27731# Army Research Inst. of Environmental Medicine, Natick, Mass.

HYPERTHERMIA: NEW THOUGHTS ON AN OLD PROBLEM

Roger W. Hubbard and Lawrence E. Armstrong Dec. 1987 18 p

(AD-A192602; USARIEM-M-13/88) Avail: NTIS HC A03/MF A01 CSCL 06E

In this article, the common heat illnesses (heat syncope, salt-and water depletion-heat exhaustion and exertion-induced heatstroke) are briefly reviewed from the perspective of their underlying physiological disturbances, which provide a rational basis for therapy. Due to an apparent paradox between the current clinical dogma and laboratory data, however, the evaluation of the consequences of hyperthermia is extended beyond the usual systematic approach. What translates heat stress into heat strain and whether the mechanism is identifiable is studied. A new hypothesis, based upon experimental research, is offered which suggests that a series of factors operate in exercise-induced hyperthermia to increase the permeability of the cell membrane, primarily to sodium ions. This stimulates sodium-potassium ATPase (the Sodium Pump) and results in an inefficient energy drain upon the cell (the Energy Depletion Model). This concept takes the form of a vicious circle leading to increased heat production and storage, reduced exercise-heat tolerance and significant morbidity and mortality. This model predicts that cellular/metabolic processes and deficits operate for some time after hyperthermia has subsided with cooling. GRA

N88-27732# Army Research Inst. of Environmental Medicine, Natick, Mass.

PHYSIOLOGICAL RESPONSES TO ACUTE EXERCISE-HEAT STRESS

Michael N. Sawka and C. B. Wenger Jan. 1988 103 p

(AD-A192606; USARIEM-M-14/88) Avail: NTIS HC A06/MF A01 CSCL 06J

Human body temperature is regulated by a proportionate control system. It is unclear however, which internal body temperature is regulated by the control of the thermoregulatory effector responses of skin blood flow and sweating. The core temperature increases during exercise as a result of a load error and not a change in the regulated set-point temperature. During exercise the magnitude of core temperature elevation at steady-state is proportional to the metabolic rate and is largely independent of the environmental condition. However, dependent upon the environmental conditions the relative contributions of sensible (radiative and convective) and insensible (evaporative) heat exchange to the total heat loss will vary. The hotter the environment the greater the dependence on insensible heat loss. During exercise in the heat, the primary problem is to simultaneously provide the cardiovascular support to maintain the metabolism for skeletal muscle contraction and to dissipate the associated heat release. In hot environments, the core to skin temperature gradient is reduced to skin blood flow needs to be relatively high (compared to cooler environments) to achieve heat transfer sufficient for thermal balance. In addition, sweat secretion can result in a reduced plasma (by dehydration) and thus blood volume. Both high skin blood flow and reduced plasma volume can reduce cardiac filling and perhaps cardiac output during exercise in the heat. As a result syncope or reduced exercise preformance will occur. GRA

N88-27733# Naval Health Research Center, San Diego, Calif.

BEHAVIORAL, PSYCHOLOGICAL AND DEMOGRAPHIC PREDICTORS OF PHYSICAL FITNESS Interim Report

Terry L. Conway 14 Dec. 1987 21 p

(AD-A192697; NHRC-87-37) Avail: NTIS HC A03/MF A01 CSCL 06J

Achieving higher levels of physical fitness has become a goal of many Americans both for personal reasons (e.g., improved health, appearance, and perceived well-being) and for organizational reasons (e.g., corporate cost savings with healthy employees; operational readiness for the military services). Understanding the factors which relate to physical fitness could help people improve their fitness levels. This study examined 1,357

Navy men to determine the associations between a variety of behavioral, psychological, and background factors and four components of physical fitness: (1) cardiorespiratory endurance (1.5-mile run), (2) muscular endurance (sit-ups), (3) flexibility (sit-and-reach test), and (4) body composition (estimated percent body fat). After controlling for exercise activities, physical fitness was positively associated with wellness behaviors, believing in the importance of physical fitness, expecting to reach/maintain ideal weight, being athletic as a youth, and years of schooling; fitness was negatively associated with tobacco use, preventive/avoidance behaviors, age, and ever being overweight. Identifying such factors may help to structure better fitness programs tailored to the individual. GRA

N88-27734# Boston Univ., Mass. Center for Adaptive Systems.
THE VITE MODEL: A NEUTRAL COMMAND CIRCUIT FOR A GENERATING ARM AND ARTICULATOR TRAJECTORIES
Stephen Grossberg and Daniel Bullock Mar. 1988 23 p
(Contract F49620-86-C-0037; Grant NSF IRI-84-17756)
(AD-A192715; AFOSR-88-0384TR) Avail: NTIS HC A03/MF A01 CSCL 12I

A major issue in research on the neural basis of motor control is the nature of movement planning in systems with many degrees of freedom; for example, an arm with many controlling muscles acting at several joints or a speech system with many articulators. All solutions to the planning problem depend upon assumptions about both the mechanics of the effectors and the sensory and computational resources. For example, if an arm has few mechanical degrees of freedom, than the serial preplanning required to work around the arm's inherent constraints becomes a salient issue. Alternatively, if the arm has many degrees of freedom, the computational load imposed by the need for simultaneous coordination becomes a salient issue. If the arm is part of a body that grows, or if a robotic arm must remain in service without external maintenance despite unpredictable changes in its mechanical parameters, then yet another issue comes into view; autonomous recalibration. GRA

N88-27735# Army Research Inst. of Environmental Medicine, Natick, Mass.
VALIDATION OF A MODIFIED ONE-STEP REBREATHING TECHNIQUE FOR NON-INVASIVE MEASUREMENT OF SUBMAXIMAL CARDIAC OUTPUT Final Report, Jan. - Nov. 1987
Patricia C. Szlyk, Karleyton C. Evans, and Ingrid V. Sils Jan. 1988 47 p
(AD-A192852; USARIEM-T8-88) Avail: NTIS HC A03/MF A01 CSCL 06E

The primary objectives of this study were to modify the Farhi one-step carbon dioxide (CO_2) rebreathing technique for measuring cardiac output during rest and submaximal exercise, and then to validate our modifications. The novelty of Farhi's technique is that it (1) requires only one-step to acquire all data necessary for computations, (2) is noninvasive, (3) takes less than 30 seconds for each rebreathing maneuver, (4) can be repeated at rapid intervals (1 to 2 minutes), and (5) is accurate and highly reproducible. Because a low flow rate analyzer (mass spectrometer) that Farhi specified as being essential for monitoring CO_2 at the mouth during rebreathing was available to us only on a limited basis and is not readily field portable, we modified both available equipment and technique. GRA

N88-27736# Maryland Univ., College Park. Dept. of Electrical Engineering.
EFFECTS OF PULSED AND CW (CONTINUOUS WAVE) 2450 MHz RADIATION ON TRANSFORMATION AND CHROMOSOMES OF HUMAN LYMPHOCYTES IN VITRO Progress Report, 1 Oct. 1986 - 1 Oct. 1987
Christopher C. Davis 16 Feb. 1988 47 p
(Contract N00014-86-K-0716)
(AD-A193104) Avail: NTIS HC A03/MF A01 CSCL 06J

The main objective of this project is to determine conditions of exposure of human lymphocytes in vitro to continuous wave (CW) or pulsed wave (PW) 2450 MHz microwaves, which: affect the course of spontaneous or phytohemagglutin in (PHA)-induced lymphoblastoid transformation, and may induce numerical and/or structural aberrations in chromosomes of cells undergoing division following transformation. In order to provide reliable quantitative data on exposure, a system will automated dosimetry was developed, and tested for biocompatibility with lymphocyte cultures in vitro for periods of up to 120 hrs. (5 days). A method for quantitation of lymphocyte transformation based on image analysis was developed and tested. Experiments on effects of exposure on spontaneous transformation were carried out. For convenience and clarity the work performed is described under two separate headings: (1) exposure system and dosimetry, and (2) studies on lymphocyte cultures. GRA

N88-27737# Washington Univ., St. Louis, Mo. Dept. of Otolaryngology.
ASSESSMENT OF COCHLEAR DAMAGE AFTER MICROWAVE IRRADIATION Final Report, 30 Sep. 1985 - 17 Feb. 1988
Barbara A. Bohne, Mary M. Gruner, and Howard I. Bassen Feb. 1988 35 p
(Contract DAMD17-85-C-5321)
(AD-A193237; OTO-1-88) Avail: NTIS HC A03/MF A01 CSCL 06G

The objective of this project was to determine if excessive exposure to microwaves results in permanent damage to the inner ear. A group of 15 chinchillas was exposed for one hour to pulsed microwaves (1250 MHz) of 20 microsec duration and 0.1-Hz repetition rate and an average power of 1 Watt. The specific absorption rate of various measurement sites in the head ranged from 2 to 8 Wkg. The exposures were done at the WRAIR Microwave Laboratory, Washington, D.C. Seven animals were sham-exposed for one hour using the same apparatus and sedation. For the sham exposures, the microwave equipment was powered but no radiation was delivered. The cochleas from 20 control chinchillas of the same age range as the animals in the present study were available for comparison purposes. The controls had spent their entire lives in sound-treated animal quarters at Washington University in St. Louis, MO. The cochleas from all animals were processed for histological evaluation as plastic-embedded flat preparations. Some animals were processed less than 24 hour after their exposures; the rest were processed after a month or more of recovery. In each cochlea, the following quantitative data were obtained: the extent and pattern of degeneration in the sensory cell populations; the number of missing pillar cells; the extent and location of degeneration of the stria vascularis and of the myelinated nerve fibers in the osseous spiral lamina. GRA

N88-27738# School of Aerospace Medicine, Brooks AFB, Tex.
BEHAVIORAL EFFECTS OF EXPOSURE TO THE TEMPO HIGH-POWER MICROWAVE SYSTEM Interim Report, Jan. - Jun. 1987
B. J. Klauenberg, James H. Merritt, and David N. Erwin Mar. 1988 20 p
(AD-A193305; USAFSAM-TR-87-35) Avail: NTIS HC A03/MF A01 CSCL 06G

Safety standard for exposure to radiofrequency radiation must be based upon biologic consequences of exposure to such environments. Behavioral based measures are considered to be the most sensitive indices of biological effects. Current safety guidelines are based upon average power density and may not be relevant to the high peak power, short pulse width microwave radiation produced by newly developed high peak power microwave sources. The effects of exposure to high peak power radiation on reflexive responding and motor function in Fischer 344/N rats were assessed by measuring startle and general activity, and disruption of on-going performance of a rotarod task respectively. The emitter used was the TEMPO repeat pulse axially extracted vircator. Exposure to single pulses resulted in significant startle responses. Exposure to 1 pps for 10 s produced significant alterations in baseline activity and marked disruption of performance of the rotarod task. The apparently greater effect observed in the

rotarod task is discussed in relation to the greater workload that task requires. Experiments are currently being conducted to identify the limits of detection and the quality of the sensory/perceptual experience of exposure to the TEMPO radiation. GRA

N88-27739# Army Aeromedical Research Lab., Fort Rucker, Ala.
SIMULATOR SICKNESS IN THE AH-64 APACHE COMBAT MISSION SIMULATOR Final Report
Daniel W. Gower, Jr., Michael G. Lilienthal, Robert S. Kennedy, Jennifer E. Fowlkes, and Dennis R. Baltzley Nov. 1987 51 p
(DA Proj. 3E1-62777-A8-79)
(AD-A193419; USAARL-88-1) Avail: NTIS HC A04/MF A01 CSCL 06J

As technology has been developed to provide improved visual and motion systems in operational flight trainers and weapons tactics trainers, there have been increasing reports of the occurrence of simulator sickness. Simulator sickness here refers to one or more symptoms which can occur while in a simulator, immediately postexposure, or at some later time following exposure. Some pilots have reported while driving following postexposure, they had to pull off the road and wait for symptoms to subside. Instructor-operators have reported experiencing the room spinning when they went to bed. More critical is the potential for in-flight problems due to prolonged physiological effects. The U.S. Army Aeromedical Research Laboratory at Fort Rucker, Alabama, conducted a field survey to document the extent of the simulator sickness problems at operational AH-64 simulator sites. The simulator sickness incidence rates and the relative frequency of specific symptoms are presented and correlational factors such as flight experience, simulator experience, and flight mode also are presented. The study reinforces the need for continued research related to system design, training methods, and crew rest guidelines between simulator and actual flight. GRA

N88-27740# Kansas Univ., Lawrence.
DEMODULATION PROCESSES IN AUDITORY PERCEPTION Annual Report, 1 Dec. 1986 - 30 Nov. 1987
Lawrence L. Feth 1 Mar. 1988 5 p
(Grant AF AFOSR-0091-87)
(AD-A193421; AFOSR-88-0376TR) Avail: NTIS HC A02/MF A01 CSCL 06D

The attached interim report covers the first 12 month period of the project. A signal-processing computer model of human auditory perception of complex, time-varying sounds has been revised to incorporate the ability to follow a frequency that changes over time. Such frequency changes are thought to convey the information important for the perception of speech, music and other important sounds. Testing of the revised model is underway using a two alternative forced choice discrimination task. Listeners are required to distinguish between a sound with a smooth linear frequency glide and another covering the same trajectory in a series of discrete steps. We expect to determine the temporal parameters for the revised model from these discrimination experiments. GRA

N88-27741# Naval Health Research Center, San Diego, Calif.
THE HUMAN ELEMENT IN SPACE: LESSONS FROM ANTARCTICA Final Report
Lawrence A. Palinkas 10 Feb. 1988 23 p
(AD-A193440; NHRC-88-8) Avail: NTIS HC A03/MF A01 CSCL 05H

The ability of humans to adapt and perform in an extreme environment during periods of prolonged isolation is influenced by a number of social, cultural, and psychological parameters. These parameters must be taken into consideration in the design, construction, and operation of space facilities and off-world bases. This paper describes the human experience in the Antarctic and examines its relevance to the design and operation of manned space facilities and off-world communities. The author concludes that the human element in space may be enhanced by altering the environment or developing programs to strengthen the processes of adaptation and adjustment to this environment. GRA

N88-27742* National Aeronautics and Space Administration, Washington, D.C.
AEROSPACE MEDICINE AND BIOLOGY: A CONTINUING BIBLIOGRAPHY WITH INDEXES (SUPPLEMENT 314)
Sep. 1988 55 p
(NASA-SP-7011(314); NAS 1.21:7011(314)) Avail: NTIS HC A04 CSCL 06E

This bibliography lists 139 reports, articles, and other documents introduced into the NASA scientific and technical information system in August, 1988. Author

N88-27361# Kansas State Univ., Manhattan. Dept. of Psychology.
A HUMAN FACTORS EVALUATION OF THE ADVANCED VISUAL TECHNOLOGY SYSTEM (AVTS) EYE TRACKING OCULOMETER Final Report
Jerome I. Nadel *In* Universal Energy Systems, Inc., United States Air Force Graduate Student Summer Support Program, Volume 2 Dec. 1987 19 p (For primary document see N88-27355 21-31)
Avail: NTIS HC A99/MF E03 CSCL 06N

N88-27363# Meharry Medical Coll., Nashville, Tenn. School of Medicine.
MICROESOTROPIA PATIENTS PERFORMA WELL AS MILITARY JET PILOTS Final Report
Bernadette P. T. Njoku *In* Universal Energy Systems, Inc., United States Air Force Graduate Student Summer Support Program, Volume 2 Dec. 1987 10 p (For primary document see N88-27355 21-31)
Avail: NTIS HC A99/MF E03 CSCL 06N

N88-27368# Nebraska Univ., Lincoln. Dept. of Electrical Engineering.
INFLUENCE OF MOVING VISUAL ENVIRONMENT ON SACCADIC EYE MOVEMENTS AND FIXATION Final Report
Keith A. Riese *In* Universal Energy Systems, Inc., United States Air Force Graduate Student Summer Support Program, Volume 2 Dec. 1987 15 p (For primary document see N88-27355 21-31)
Avail: NTIS HC A99/MF E03 CSCL 06N

N88-27369# Alabama Univ., Scottsboro. Dept. of Health, Physical Education and Recreation.
THERMAL STRESS AND ITS EFFECTS ON FINE MOTOR SKILL AND DECODING TASKS
M. Carolyn Robinson *In* Universal Energy Systems, Inc., United States Air Force Graduate Student Summer Support Program, Volume 2 Dec. 1987 17 p (For primary document see N88-27355 21-31)
Avail: NTIS HC A99/MF E03 CSCL 06N

N88-27387# Wright State Univ., Dayton, Ohio. School of Medicine.
HUMAN RESPONSE TO PROLONGED MOTIONLESS SUSPENSION IN FOUR TYPES OF FULL BODY HARNESSES Final Report
Terri Wilkerson *In* Universal Energy Systems, Inc., United States Air Force Graduate Student Summer Support Program, Volume 2 Dec. 1987 20 p (For primary document see N88-27355 21-31)
Avail: NTIS HC A99/MF E03 CSCL 06N

N88-27684# New York Univ., New York. Dept. of Psychology.
STUDIES OF THE INTACT HUMAN BRAIN: IMPLICATIONS FOR PERFORMANCE
Lloyd Kaufman *In* AGARD, Electric and Magnetic Activity of the Central Nervous System: Research and Clinical Applications in Aerospace Medicine Feb. 1988 17 p (For primary document see N88-27683 21-51)
Copyright Avail: NTIS HC A18/MF A01

N88-27685# New York Medical Coll., N.Y. Div. of Biological Psychiatry.
CEEG DYNAMIC BRAIN MAPPING: A NEW METHOD TO EVALUATE BRAIN FUNCTION IN DIFFERENT PSYCHOLOGICAL AND DRUG CONDITIONS
Turan M. Itil, Kurt Z. Itil, Emin Eralp, A. Akman (HZI Research Center, Tarrytown, N.Y.), and A. Manco *In* AGARD, Electric and Magnetic Activity of the Central Nervous System: Research and Clinical Applications in Aerospace Medicine Feb. 1988 16 p (For primary document see N88-27683 21-51)
Copyright Avail: NTIS HC A18/MF A01

N88-27686# EEG Systems Lab., San Francisco, Calif.
FOURTH GENERATION NEUROCOGNITIVE PATTERN ANALYSIS SYSTEM
A. S. Gevins, N. H. Morgan, S. L. Bressler, D. S. Greer, B. Costales, K. Smith, and R. Faucette *In* AGARD, Electric and Magnetic Activity of the Central Nervous System: Research and Clinical Applications in Aerospace Medicine Feb. 1988 13 p Original contains color illustrations (For primary document see N88-27683 21-51)
Copyright Avail: NTIS HC A18/MF A01

N88-27687# New York Univ. Medical Center. Brain Research Labs.
NORMATIVE DEVELOPMENTAL EQUATIONS FOR THE EEG AND THEIR SENSITIVITY TO NEUROLOGICAL AND PSYCHIATRIC DISORDERS
E. R. John and L. S. Prichep *In* AGARD, Electric and Magnetic Activity of the Central Nervous System: Research and Clinical Applications in Aerospace Medicine Feb. 1988 7 p Prepared in cooperation with Kline (Nathan S.) Inst. for Psychiatric Research, Orangeburg, N.Y. Original contains color illustrations (For primary document see N88-27683 21-51)
Copyright Avail: NTIS HC A18/MF A01

N88-27688# Royal Air Force Inst. of Aviation Medicine, Farnborough (England).
THE APPLICATION OF NON-STATIONARY DATA ANALYSIS TECHNIQUES IN THE IDENTIFICATION OF CHANGES IN THE ELECTROENCEPHALOGRAM ASSOCIATED WITH THE ONSET OF DROWSINESS
Nicola A. Wright, R. G. Borland, and Amanda McGown *In* AGARD, Electric and Magnetic Activity of the Central Nervous System: Research and Clinical Applications in Aerospace Medicine Feb. 1988 5 p (For primary document see N88-27683 21-51)
Copyright Avail: NTIS HC A18/MF A01

N88-27689# National Hospital, Oslo (Norway). Lab. for Clinical Neurophysiology.
A STATISTICAL PROCEDURE FOR THE EVALUATION OF PRESENCE/NON-PRESENCE OF STIMULUS-RELATED EEG ACTIVITY
Nils Irgens Bachen *In* AGARD, Electric and Magnetic Activity of the Central Nervous System: Research and Clinical Applications in Aerospace Medicine Feb. 1988 9 p (For primary document see N88-27683 21-51)
Copyright Avail: NTIS HC A18/MF A01

N88-27690# Dalhousie Univ., Halifax (Nova Scotia). Dept. of Ophthalmology.
DISSECTING THE VISUAL AND AUDITORY PATHWAYS BY MEANS OF THE TWO-INPUT TECHNIQUE
D. Regan and M. P. Regan *In* AGARD, Electric and Magnetic Activity of the Central Nervous System: Research and Clinical Applications in Aerospace Medicine Feb. 1988 9 p Sponsored by the National Sciences and Engineering Research Council, Canada, MRC, Canada and AFOSR, Washington, D.C. (For primary document see N88-27683 21-51)
Copyright Avail: NTIS HC A18/MF A01

N88-27691# Consiglio Nazionale delle Ricerche, Rome (Italy). Istituto de Elettronica dello Stato Solido.
SQUID INSTRUMENTATION FOR NEUROMAGNETIC STUDY OF COMPLEX BRAIN ACTIVITY
Gian Luca Romani *In* AGARD, Electric and Magnetic Activity of the Central Nervous System: Research and Clinical Applications in Aerospace Medicine Feb. 1988 7 p (For primary document see N88-27683 21-51)
Copyright Avail: NTIS HC A18/MF A01

N88-27692# Consiglio Nazionale delle Ricerche, Rome (Italy). Istituto di Elettronica dello Stato Solido.
ELECTRIC AND MAGNETIC BRAIN ACTIVITY RELATED TO COGNITIVE PERFORMANCE
Robert M. Chapman, Ivo Modena, Livio Marici, Vittorio Pizzella, Gian Luca Romani, Carlo Salustri, John W. McCrary, and Susan Garnsey (Rochester Univ., N. Y.) *In* AGARD, Electric and Magnetic Activity of the Central Nervous System: Research and Clinical Applications in Aerospace Medicine Feb. 1988 8 p (For primary document see N88-27683 21-51)
(Contracts MH40703; HD22271; EY01319)
Copyright Avail: NTIS HC A18/MF A01

N88-27693# Muenster Univ. (West Germany). Inst. of Experimental Audiology.
NEUROMAGNETIC EVIDENCE OF PLACE MECHANISMS FOR FREQUENCY AND INTENSITY CODING IN THE HUMAN AUDITORY CORTEX
M. Hoke, C. Pantew, K. Lehnertz, and B. Luetkenhoener *In* AGARD, Electric and Magnetic Activity of the Central Nervous System: Research and Clinical Applications in Aerospace Medicine Feb. 1988 12 p Sponsored by Deutsche Forschungsgemeinschaft, West Germany and Heinrich-Hertz-Stiftung, West Germany (For primary document see N88-27683 21-51)
Copyright Avail: NTIS HC A18/MF A01

N88-27694# Simon Fraser Univ., Burnaby (British Columbia). Brain Behaviour Lab.
THE INTERACTION OF THALAMO-CORTICAL SYSTEMS IN THE 40 Hz FOLLOWING RESPONSE
H. Weinberg, D. Cheyne, P. Brickett, R. Gordon, and R. Harrop *In* AGARD, Electric and Magnetic Activity of the Central Nervous System: Research and Clinical Applications in Aerospace Medicine Feb. 1988 6 p (For primary document see N88-27683 21-51)
Copyright Avail: NTIS HC A18/MF A01

N88-27695# Simon Fraser Univ., Burnaby (British Columbia). Brain Behaviour Lab.
A STUDY OF SOURCES IN THE HUMAN BRAIN ASSOCIATED WITH STEREOPSIS
H. Weinberg, P. Brickett, A. Robertson, D. Crisp, D. Cheyne, and R. Harrop *In* AGARD, Electric and Magnetic Activity of the Central Nervous System: Research and Clinical Applications in Aerospace Medicine Feb. 1988 6 p Sponsored by the Defence and Civil Inst. of Environmental Medicine, Canada (For primary document see N88-27683 21-51)
Copyright Avail: NTIS HC A18/MF A01

N88-27696*# Illinois Univ., Champaign. Dept. of Psychology.
EVENT-RELATED BRAIN POTENTIALS AS INDICES OF MENTAL WORKLOAD AND ATTENTIONAL ALLOCATION
Arthur F. Kramer, Emanuel Donchin, and Christopher D. Wickens *In* AGARD, Electric and Magnetic Activity of the Central Nervous System: Research and Clinical Applications in Aerospace Medicine Feb. 1988 15 p Sponsored by NASA, Ames Research Center, Moffett Field, Calif. (For primary document see N88-27683 21-51)
(Contract F49620-79-C-0233)
Copyright Avail: NTIS HC A18/MF A01 CSCL 06P

N88-27697# York Univ., Downsview (Ontario). Dept. of Physical Education.
THE EFFECTS OF HYPOXIA ON P300 AND REACTION TIME

B. Fowler, B. Kelso, J. P. Landolt, and G. Porlier (Defence and Civil Inst. of Environmental Medicine, Downsview, Ontario) *In* AGARD, Electric and Magnetic Activity of the Central Nervous System: Research and Clinical Applications in Aerospace Medicine Feb. 1988 7 p (For primary document see N88-27683 21-51)
(Contract DCIEM-W7711-6-9019)
(DCIEM-87-RR-12) Copyright Avail: NTIS HC A18/MF A01

N88-27699# Washington Univ., St. Louis, Mo. Behavior Research Lab.
COGNITIVE TASK DEMANDS AS REFLECTED IN PHYSIOLOGICAL MEASURES
John A. Stern and Lance O. Bauer (Oklahoma Univ., Oklahoma City.) *In* AGARD, Electric and Magnetic Activity of the Central Nervous System: Research and Clinical Applications in Aerospace Medicine Feb. 1988 11 p (For primary document see N88-27683 21-51)
(Contract F49620-83-C-0059)
Copyright Avail: NTIS HC A18/MF A01

N88-27702# Defence and Civil Inst. of Environmental Medicine, Downsview (Ontario).
PSYCHOPHYSIOLOGICAL MEASURES OF DROWSINESS AS ESTIMATORS OF MENTAL FATIGUE AND PERFORMANCE DEGRADATION DURING SLEEP DEPRIVATION
R. A. Pigeau, R. J. Heslegrave, and R. G. Angus *In* AGARD, Electric and Magnetic Activity of the Central Nervous System: Research and Clinical Applications in Aerospace Medicine Feb. 1988 16 p (For primary document see N88-27683 21-51)
Copyright Avail: NTIS HC A18/MF A01

N88-27703# EEG Systems Lab., San Francisco, Calif.
NEUROPHYSIOLOGICAL PATTERNS OF OPERATIONAL FATIGUE: PRELIMINARY RESULTS
A. S. Gevins, B. A. Cutillo, R. M. Fowler-White, J. Illes, S. L. Bressler, and J. C. Miller (Test Group, 6520th, Edwards AFB, Calif) *In* AGARD, Electric and Magnetic Activity of the Central Nervous System: Research and Clinical Applications in Aerospace Medicine Feb. 1988 9 p Sponsored by AFOSR, Washington, D.C., School of Aerospace Medicine, Brooks, AFB, Tex., National Inst. of Neurological and Communicative Diseases and Strokes, Washington, D.C. and NSF, Washington, D.C. Original contains color illustrations (For primary document see N88-27683 21-51)
Copyright Avail: NTIS HC A18/MF A01

N88-27705# Burden Neurological Inst., Bristol (England).
EVENT-RELATED AND STEADY POTENTIAL CHANGES IN THE BRAIN RELATED TO WORKLOAD DURING TRACKING
W. C. McCallum, R. Cooper, and P. V. Pocock *In* AGARD, Electric and Magnetic Activity of the Central Nervous System: Research and Clinical Applications in Aerospace Medicine Feb. 1988 10 p Sponsored by British Aerospace, United Kingdom and the Ministry of Defence, United Kingdom (For primary document see N88-27683 21-51)
Copyright Avail: NTIS HC A18/MF A01

N88-27706# EEG Systems Lab., San Francisco, Calif.
NEUROPHYSIOLOGICAL PRECURSORS OF ACCURATE VISUOMOTOR PERFORMANCE
A. S. Gevins, B. A. Cutillo, S. L. Bressler, N. H. Morgan, R. M. Fowler-White, D. S. Greer, J. Illes, J. C. Doyle, R. S. Tannehill, and G. M. Zeitlin *In* AGARD, Electric and Magnetic Activity of the Central Nervous System: Research and Clinical Applications in Aerospace Medicine Feb. 1988 11 p Sponsored by AFOSR, Washington, D.C., School of Aerospace Medicine, Brooks, AFB, Tex., NSF, Washington, D.C., National Inst. of Neurological Diseases and Strokes, Washington, D.C. and ONR, Washington, D.C. Original contains color illustrations (For primary document see N88-27683 21-51)
Copyright Avail: NTIS HC A18/MF A01

N88-27708# Naval Biodynamics Lab., New Orleans, La. Impact Sciences Dept.
EVOKED POTENTIAL ANALYSIS OF IMPACT ACCELERATION EXPERIMENTS
David L. Matson and Marc S. Weiss *In* AGARD, Electric and Magnetic Activity of the Central Nervous System: Research and Clinical Applications in Aerospace Medicine Feb. 1988 13 p (For primary document see N88-27683 21-51)
Copyright Avail: NTIS HC A18/MF A01

N88-27709# School of Aerospace Medicine, Brooks AFB, Tex.
EEG INDICES OF G-INDUCED LOSS OF CONSCIOUSNESS (G-LOC)
Nita L. Lewis, Jennifer B. McGovern, James C. Miller, Douglas R. Eddy, and Estrella M. Forster (Rothe Development, San Antonio, Tex.) *In* AGARD, Electric and Magnetic Activity of the Central Nervous System: Research and Clinical Applications in Aerospace Medicine Feb. 1988 12 p (For primary document see N88-27683 21-51)
Copyright Avail: NTIS HC A18/MF A01

N88-27710# Naval Air Development Center, Warminster, Pa.
DETECTION OF ACCELERATION (+Gz) INDUCED BLACKOUT BY MATCHED-FILTERING OF VISUAL EVOKED POTENTIALS
John G. Nelson, Joseph P. Cammarota, and Leonid Hrebien *In* AGARD, Electric and Magnetic Activity of the Central Nervous System: Research and Clinical Applications in Aerospace Medicine Feb. 1988 13 p (For primary document see N88-27683 21-51)
Copyright Avail: NTIS HC A18/MF A01

N88-27712# Aerospace Medical Research Labs., Wright-Patterson AFB, Ohio.
MOTION EVOKED VESTIBULAR POTENTIALS
G. Wilson, R. Luciani, and D. Ratino (Air Force Human Resources Lab., Williams AFB, Ariz.) *In* AGARD, Electric and Magnetic Activity of the Central Nervous System: Research and Clinical Applications in Aerospace Medicine Feb. 1988 5 p (For primary document see N88-27683 21-51)
Copyright Avail: NTIS HC A18/MF A01

N88-27713# Defence and Civil Inst. of Environmental Medicine, Downsview (Ontario).
THE EFFECT OF MILD HYPOXIA ON THE VESTIBULAR EVOKED RESPONSE
W. D. Fraser, N. Black, D. E. Eastman, and J. P. Landolt *In* AGARD, Electric and Magnetic Activity of the Central Nervous System: Research and Clinical Applications in Aerospace Medicine Feb. 1988 10 p (For primary document see N88-27683 21-51)
Copyright Avail: NTIS HC A18/MF A01

N88-27714# Hordt Research, Development and Therapy, Rodgau (West Germany).
MEASUREMENT AND CLASSIFICATION OF THE MODE OF ACTION OF ANTIDEPRESSANT DRUGS
Albrecht Frauendorf, David Johnson, and Lothar Demisch (Johann-Wolfgang-Goethe-Univ., Frankfurt am Main, West Germany) *In* AGARD, Electric and Magnetic Activity of the Central Nervous System: Research and Clinical Applications in Aerospace Medicine Feb. 1988 9 p (For primary document see N88-27683 21-51)
Copyright Avail: NTIS HC A18/MF A01

N88-27715# Johann-Wolfgang-Goethe-Univ., Frankfurt am Main (West Germany).
MEASUREMENT OF ELECTRICAL ACTIVITY IN THE CNS WITH CORTICAL EVOKED POTENTIALS AND EEG: EFFICACY PROFILES OF DRUGS USING FACTOR ANALYSIS
David Johnson, Albrecht Frauendorf (Hordt Research, Development and Therapy, Rodgau, West Germany), and Kurt Offenloch *In* AGARD, Electric and Magnetic Activity of the Central Nervous System: Research and Clinical Applications in Aerospace Medicine Feb. 1988 8 p (For primary document see N88-27683 21-51)
Copyright Avail: NTIS HC A18/MF A01

N88-27716# Centre d'Etudes et de Recherches de Medecine Aerospatiale, Paris (France). Div. de Neurophysiologie Appliquee.
AN APPROACH TO STUDYING THE EFFECTS OF PSYCHOSTIMULANTS ON CEREBRAL ELECTRICAL ACTIVITY IN THE NON-HUMAN PRIMATE [UNE APPROCHE DES EFFETS DE PSYCHOSTIMULANTS SUR L'ACTIVITE ELECTRIQUE CEREBRALE CHEZ LE PRIMATE NON HUMAIN]
D. Lagarde and C. Milhaud *In* AGARD, Electric and Magnetic Activity of the Central Nervous System: Research and Clinical Applications in Aerospace Medicine Feb. 1988 11 p In FRENCH (For primary document see N88-27683 21-51)
Copyright Avail: NTIS HC A18/MF A01

N88-27717# Italian Air Force Aerospace Medical Center, Rome. Neuropsychophysiology Group.
SPONTANEOUS CEREBRAL ELECTRICAL ACTIVITY DURING PROLONGED HYPOGLYCEMIA: A QUANTITATIVE STUDY IN HUMANS
Silvio Porcu, Roberto Berti, and Alberto Lala *In* AGARD, Electric and Magnetic Activity of the Central Nervous System: Research and Clinical Applications in Aerospace Medicine Feb. 1988 12 p (For primary document see N88-27683 21-51)
Copyright Avail: NTIS HC A18/MF A01

N88-27718# Dalhousie Univ., Halifax (Nova Scotia). Dept. of Ophthalmology.
RELATION BETWEEN VEP AND VISUAL FUNCTION IN LESIONS OF THE OPTIC NERVE AND VISUAL PATHWAY
D. Regan and D. Neims *In* AGARD, Electric and Magnetic Activity of the Central Nervous System: Research and Clinical Applications in Aerospace Medicine Feb. 1988 8 p Sponsored in part by Medical Research Council of Canada, Multiple Sclerosis Society of Canada, Baker Trust of Canada and NIH, Bethesda, Md. (For primary document see N88-27683 21-51)
Copyright Avail: NTIS HC A18/MF A01

N88-27720# Royal Air Force, Wroughton (England). Neurology Dept.
DETECTION OF LATENT EPILEPSY IN AIRCREW CANDIDATES
R. T. G. Merry *In* AGARD, Electric and Magnetic Activity of the Central Nervous System: Research and Clinical Applications in Aerospace Medicine Feb. 1988 3 p (For primary document see N88-27683 21-51)
Copyright Avail: NTIS HC A18/MF A01

N88-27721# Oficinas Gerais de Material Aeronautico, Alverca (Portugal).
THE AUDITORY EVOKED RESPONSE IN MILITARY PILOTS
Nuno A. A. CasteloBranco, Jose H. Marvao, M. Salome CasteloBranco, and Antonio J. Entrudo (Portugal Air Force Hospital.) *In* AGARD, Electric and Magnetic Activity of the Central Nervous System: Research and Clinical Applications in Aerospace Medicine Feb. 1988 8 p (For primary document see N88-27683 21-51)
Copyright Avail: NTIS HC A18/MF A01

53 BEHAVIORAL SCIENCES

Includes psychological factors; individual and group behavior; crew training and evaluation; and psychiatric research.

N88-27743# Johns Hopkins Univ., Baltimore, Md. Dept. of Psychology.
ASSESSING AND ENHANCING HUMAN PERFORMANCE: UTILITY OF A WORKSTATION NETWORK Final Report, 1 Oct. 1986 - 1 Oct. 1987
Bert F. Green, Jr., Steven J. Breckler, Howard E. Egeth, and Neal J. Cohen 20 Mar. 1988 10 p
(Grant AF-AFOSR-0068-87)
(AD-A192840; JHU-RR-88-100; AFOSR-88-0440TR) Avail: NTIS HC A02/MF A01 CSCL 05I

An articulated state of the art network of computer based workstations has been installed and is being used for behavioral and personnel research. This report describes the network configuration, discusses the current experience in using the equipment, and identifies current research projects that are using the equipment. GRA

N88-27744# Northeastern Univ., Boston, Mass.
A MODEL FOR VISUAL ATTENTION Technical Report, Mar. 1987 - Mar. 1988
Adam Reeves 1 Apr. 1988 8 p
(Grant AF AFOSR-0172-87)
(AD-A193061; AFOSR-88-0485TR) Avail: NTIS HC A02/MF A01 CSCL 06D

Research has been undertaken on visual attention and short term visual memory (VSTM). One set of experiments has concerned the role that depth information might play in retrieval from VSTM, using an iconic memory paradigm. Another set concerns development of the attention gating model, using the attention shift RSVP paradigm. Finally, we are studying some effects of attention and visual imagery on visual acuity. GRA

N88-27745# Northwestern Univ., Evanston, Ill. Neuroscience Lab.
PERCEPTION OF MOTION IN STATISTICALLY-DEFINED DISPLAYS Annual Scientific Report, 1 Oct. 1986 - 30 Sep. 1987
Robert Sekuler 15 Feb. 1988 102 p
(Grant AF AFOSR-0370-85)
(AD-A193076; AFOSR-88-0288TR) Avail: NTIS HC A06/MF A01 CSCL 05H

Though motion perception does depend upon spatially local processes, under certain circumstances global processes make an important contribution. For example, the human visual system can integrate different, spatially-intermingled motion vectors into a global percept of motion in a single direction. Such integrated percepts may offer important clues to the mechanisms of motion perception. To exploit such clues we have followed the tradition of using discrimination performance to probe underlying psychophysical mechanisms. Specifically, we were interested in how easily observers could discriminate between two different global motions when each had resulted from the integration of many different motion vectors. Our stimuli were random dot cinematograms in which each dot took an independent two-dimensional random walk with steps of constant size. The direction any dot moved, from one display frame to the next, was independent of the dot's previous movements as well as the movements of other dots. All dots chose their directions of movement from the same probability distribution. GRA

N88-27746# Air Force Human Resources Lab., Brooks AFB, Tex.
PERSONALITY, ATTITUDES, AND PILOT TRAINING PERFORMANCE: PRELIMINARY ANALYSIS Interim Report, Jan. 1983 - Jan. 1987
Frederick M. Siem, Thomas R. Carretta, and Theresa A. Mercatante May 1988 20 p
(AD-A193102; AFHRL-TP-87-62) Avail: NTIS HC A03/MF A01 CSCL 05I

Developments in research concerning personality characteristics have led to a renewed interest in applications of individual measures for selection of pilot candidates. Recent research efforts have focused on selecting for positive characteristics, rather than screening out pathological traits. Another development is the use of tests in which the dimension of interest is not readily apparent to the examinee. In the present study, five personality and attitude measures were administered to 883 USAF pilot candidates as part of an experimental test battery under consideration for operational use in pilot selection and classification. These tests were designed to assess decisiveness, risk-taking, self-confidence, survival attitudes, and field dependence/independence. Scores from these tests were examined for their utility in predicting training outcome (graduation

or elimination) and advanced training recommendation (fighter or non-fighter aircraft). Results indicated that as a group, the tests demonstrated weak relationships with the performance criteria. No test manifested a consistent pattern of validity for both performance measures. Only the test of self-confidence appeared to contribute to predicting completion of training. Future research efforts are discussed with regard to refining the current test of self-confidence and establishing its construct validity. GRA

N88-27747# New York Univ., New York.
COGNITIVE AND NEURAL BASES OF SKILLED PERFORMANCE Annual Technical Report, Sep. 1986 - Sep. 1987
Lloyd Kaufman 4 Oct. 1987 179 p
(Contract F49620-86-C-0131)
(AD-A193392; AFOSR-87-1710TR) Avail: NTIS HC A09/MF A01 CSCL 05H

Research in seven interrelated areas has been carried out during this first year. A major advance in the capability of neuromagnetic monitoring of higher levels of brain function was achieved with the installation of a large magnetically shielded room for the sensing system. This together with a computer-controlled adaptive filter dramatically improved sensitivity to slowly-varying brain signals. A new analysis technique based on a multidimensional signal space has also been developed to characterize the neural configurations that give rise to differing field patterns, without restricting consideration to only the simplest that can be attributed to an equivalent current dipole. Successful application of these concepts to studies of the alpha rhythm also demonstrated a major advantage in using elements of the covariance matrix across sensors to reduce interference from extraneous neural sources, thereby improving the signal-to-noise ratio by an order of magnitude. In preparing for a series of collaborative studies, various methods for producing visual displays in the shielded room were evaluated, and one based on a single-lens TV projection system was chosen. The system can be controlled by a computer peripheral to the HP9000/550 used to record and analyze neuromagnetic data. Software was successfully developed so that either an IBM/PC-compatible or Amega computer can be used for this purpose. An Adage 3000 frame buffer was obtained for psychophysical studies, and programs were developed to present a display where only color or only luminance changes are produced. GRA

N88-27748# Deutsche Forschungs- und Versuchsanstalt fuer Luft- und Raumfahrt, Hamburg (West Germany). Abteilung Luft- und Raumfahrtpsychologie.
DETERMINANTS OF DUAL-TASK INTERFERENCE AND RESOURCE THEORIES IN COGNITIVE PSYCHOLOGY Ph.D. Thesis - Kiel Univ.
Dietrich Manzey Feb. 1988 234 p In GERMAN; ENGLISH summary
(DFVLR-FB-88-14; ISSN-0171-1342; ETN-88-92932) Avail: NTIS HC A11/MF A01; DFVLR, VB-PI-DO, 90 60 58, 5000 Cologne, Federal Republic of Germany, 64 deutsche marks

In two experiments (22 subjects) the determinants of interference effects are investigated by an analysis of performance-operating characteristics for several different task-combinations. It can be shown that the degree of task-interference in dual-task situations depends mainly on the similarity of both tasks with regard to their perceptual-cognitive and response-related demands, and that task difficulty is of minor importance for dual-task interference effects. The results are interpreted as a proof for the prognostic value of a certain model of human timesharing: the theory of multiple resources. ESA

N88-27360# Montclair State Coll., Upper Montclair, N.J. Dept. of Psychology.
A REVIEW OF WORKLOAD MEASUREMENT IN RELATION TO VERBAL COMPREHENSION Final Report
Stephen T. Morgan *In* Universal Energy Systems, Inc., United States Air Force Graduate Student Summer Support Program, Volume 2 Dec. 1987 20 p (For primary document see N88-27355 21-31)
Avail: NTIS HC A99/MF E03 CSCL 05I

N88-27362# Northwestern Univ., Evanston, Ill. Dept. of Psychology.
THE EFFECTS OF INCREASED COGNITIVE DEMANDS ON AUTONOMIC SELF-REGULATION: AN INDICATOR OF PARALLEL PROCESSING IN THE BRAIN Final Report
Victoria Tepe Nasman *In* Universal Energy Systems, Inc., United States Air Force Graduate Student Summer Support Program, Volume 2 Dec. 1987 13 p (For primary document see N88-27355 21-31)
Avail: NTIS HC A99/MF E03 CSCL 05I

N88-27698# Organisatie voor Toegepast Natuurwetenschappelijk Onderzoek, Soesterberg (Netherlands). Human Performance Group.
USING ERPS TO STUDY HUMAN INFORMATION PROCESSING
A. W. K. Gaillard *In* AGARD, Electric and Magnetic Activity of the Central Nervous System: Research and Clinical Applications in Aerospace Medicine Feb. 1988 6 p (For primary document see N88-27683 21-51)
Copyright Avail: NTIS HC A18/MF A01

N88-27701# Defence and Civil Inst. of Environmental Medicine, Downsview (Ontario).
THE EFFECT OF ENDOGENOUS ALPHA ON HEMISPHERIC ASYMMETRIES AND THE RELATIONSHIP OF FRONTAL THETA TO SUSTAINED ATTENTION
R. Pigeau, R. Hoffmann, S. Purcell, and A. Moffitt (Carleton Univ., Ottawa, Ontario) *In* AGARD, Electric and Magnetic Activity of the Central Nervous System: Research and Clinical Applications in Aerospace Medicine Feb. 1988 16 p (For primary document see N88-27683 21-51)
Copyright Avail: NTIS HC A18/MF A01

N88-27707# Naval Aerospace Medical Research Lab., Pensacola, Fla.
THE NEUROELECTRIC SELECTION OF NAVAL AVIATION PERSONNEL: AN EVALUATION
R. R. Stanny, D. L. Reeves, M. R. Blackburn, and G. R. Banta (Naval Medical Research and Development Command, Bethesda, Md.) *In* AGARD, Electric and Magnetic Activity of the Central Nervous System: Research and Clinical Applications in Aerospace Medicine Feb. 1988 8 p (For primary document see N88-27683 21-51)
Copyright Avail: NTIS HC A18/MF A01

N88-27711# Veterans Administration Hospital, Sepulveda, Calif. Neuropsychology Research Dept.
ELECTROENCEPHALOGRAPHIC CORRELATES OF PILOT PERFORMANCE: SIMULATION AND IN-FLIGHT STUDIES
M. B. Sterman, G. J. Schummer, T. W. Dushenko, and J. C. Smith *In* AGARD, Electric and Magnetic Activity of the Central Nervous System: Research and Clinical Applications in Aerospace Medicine Feb. 1988 16 p (For primary document see N88-27683 21-51)
(Grants AF-AFOSR-0231-83; AF-AFOSR-0335-82)
Copyright Avail: NTIS HC A18/MF A01

N88-27719# Hellenic Air Force General Hospital, Athens (Greece). Neurological Clinic.
CORRELATION BETWEEN EEG ABNORMAL ACTIVITY AND AIRCRAFT ACCIDENTS: A LONG TERM OBSERVATION
A. Stavropoulos *In* AGARD, Electric and Magnetic Activity of the Central Nervous System: Research and Clinical Applications in Aerospace Medicine Feb. 1988 5 p (For primary document see N88-27683 21-51)
Copyright Avail: NTIS HC A18/MF A01

54 MAN/SYSTEM TECHNOLOGY AND LIFE SUPPORT

Includes human engineering; biotechnology; and space suits and protective clothing.

For related information see also *16 Space Transportation.*

N88-27749# Aerospace Medical Research Labs., Wright-Patterson AFB, Ohio. Human Engineering Div.
ENGINEERING DATA COMPENDIUM. HUMAN PERCEPTION AND PERFORMANCE. USER'S GUIDE
Kenneth R. Boff, ed. and Janet E. Lincoln, ed. (Dayton Univ., Ohio.) 1988 142 p
(LC-87-19560) Avail: NTIS HC A07/MF A01 CSCL 05H

The concept underlying the Engineering Data Compendium was the product of a research and development program (Integrated Perceptual Information for Designers project) aimed at facilitating the application of basic research findings in human performance to the design and military crew systems. The principal objective was to develop a workable strategy for: (1) identifying and distilling information of potential value to system design from the existing research literature, and (2) presenting this technical information in a way that would aid its accessibility, interpretability, and applicability by systems designers. The present four volumes of the Engineering Data Compendium represent the first implementation of this strategy. This is the first volume, the User's Guide, containing a description of the program and instructions for its use. F.M.R.

N88-27750# Lawrence Livermore National Lab., Calif.
THE ASSESSMENT OF HUMAN/COMPUTER PERFORMANCE USING HUMAN PRODUCTIVITY MEASURES: MIPS AND BIPS ARE MEGAFLOPS
W. W. Banks, E. B. Schultz, E. Crane, and M. Riley 23 Jul. 1987 17 p Presented at the Computer Human Interaction Conference, Washington, D.C., 15 May 1988 Prepared in cooperation with Air Force Logistics Command, Wright-Patterson AFB, Ohio
(Contract W-7405-eng-48)
(DE87-013491; UCRL-97113; CONF-880516-1) Avail: NTIS HC A03/MF A01

Multiple logistics processing systems were evaluated using human productivity measures. Comparisons were made to determine which system produced; greater savings in task execution time/errors; minimal task steps; and provided users with the greatest degree of connectivity and error feed back. Multiple assessment methods including interviews, deterministic analysis, and statistical inferential testing were used. Results indicated the superiority of gateway processors and the multiple methods approach. Traditional hardware bench-marking assessments topically omit the user, leaving ambiguous results and severe predictive validity limits. Benefits derived from including the human component, include greater levels of predictive validity and causality determinates. DOE

N88-27751# Naval Ocean Systems Center, San Diego, Calif.
ASSESSMENTS OF MANEUVERABILITY WITH THE TELEOPERATED VEHICLE (TOV)
Edward H. Spain Jan. 1988 32 p Presented at the AUVS Symposium, Washington, D.C., 19-21 Jul. 1987
(AD-A191584) Avail: NTIS HC A03/MF A01 CSCL 05H

The Naval Ocean Systems Center's Hawaii Laboratory is undertaking a program to develop airborne remotely operated devices (ARODs) and teleoperated land vehicles (TOVs) that will be delivered to the U.S. Marine Crops for field assessments of the applicability and effectiveness of such vehicles for reconnaissance and combat in tactical environments. An essential component of both remotely operated systems is a visual sensor suite and helmet operated display that allows an operator to view the remote scene in a familiar, natural fashion well enough to drive the TOV safely and reliably across unfamiliar terrain. In order to facilitate the development of this mobility sensor system, a field testing program was established in which alternate mobility viewing system options are being objectively compared with regard to their impact on maneuverability. The procedures and specific tasks used in making comparisons of maneuverability across the various viewing system options tested are described. Specific results in the terms of times through courses, steering, and braking accuracy are reported. Author

N88-27752# Transportation Systems Center, Cambridge, Mass.
COCKPIT AND CABIN CREW COORDINATION Final Report, Oct. - Nov. 1985
Kim M. Cardosi and M. S. Huntley, Jr. Feb. 1988 72 p
(AD-A192445; DOT-TSC-FAA-87-4; FAA-FS-88/1) Avail: NTIS HC A04/MF A01 CSCL 05H

Cockpit and cabin crew coordination is crucial not only in emergencies, but also during normal operations. The purposes of this study were to determine the status of crew coordination in the industry and to identify the implications for flight safety. This examination of crew coordination included: an examination of accidents and incidents in which cockpit and cabin crew coordination was a factor, an analysis of the results of surveys of pilot and flight attendant safety representatives, a survey of manuals and training programs for flight attendants and pilots, interviews with training administrators from seven Part 121 carriers, and interviews with Principal Operations Inspectors and their managers. Problem areas identified in this study included: inadequate crew communication in emergencies, confusion over the sterile cockpit (FAR 121.542) concept, inadequate instruction on the duties of the other crew in training, failure to properly secure the cabin for takeoff and landing, and inadequate support for and staffing of the FAA inspector workforce. Recommendations for improving the status of cockpit and cabin crew coordination include changes in training and operational procedures. GRA

N88-27753# Midwest Systems Research, Inc., Dayton, Ohio.
A COCKPIT NATURAL LANGUAGE STUDY: VOCABULARY AND GRAMMAR ANALYSES Final Report, Oct. 1986 - Sep. 1987
Michael P. Munger, Ronald L. Small, and David T. Williamson Feb. 1988 69 p
(Contract F33615-85-C-3623)
(AD-A193289; AFWAL-TR-87-3108) Avail: NTIS HC A04/MF A01 CSCL 05G

This report describes recent work which was conducted to facilitate research and development efforts in the use of voice interaction in fighter cockpits. Definitions of an operational vocabulary and grammar are starting points for studying the use of voice interaction in fighter cockpits. This report provides an initial definition of a vocabulary, based on a Pilot's Associate equipped fighter. It also provides software tools for vocabulary, and grammar analysis. Researchers in this area need such tools to adapt quickly to changing technologies as they are applied to cockpits, with consequent changes to vocabulary and grammars. These software tools (1) assist in processing a vocabulary into a lexicon for use by parsers, (2) assist in developing grammars for parsers, and (3) assist in determining semantics from parsers steps. GRA

N88-27754*# Life Systems, Inc., Cleveland, Ohio.
ADVANCED EMU ELECTROCHEMICALLY REGENERABLE CO2 AND MOISTURE ABSORBER MODULE BREADBOARD Final Report
M. C. Lee, M. Sudar, and B. J. Chang Feb. 1988 124 p
(Contract NAS9-17307)
(NASA-CR-172054; NAS 1.26:172054; LSI-TR-769-4) Avail: NTIS HC A06/MF A01 CSCL 06K

The applicability of the Electrochemically Regenerable Carbon Dioxide and Moisture Absorption Technology to the advanced extravehicular mobility unit was demonstrated by designing, fabricating, and testing a breadboard Absorber Module and an Electrochemical Regenerator. Test results indicated that the absorber module meets or exceeds the carbon dioxide removal requirements specified for the design and can meet the moisture

removal requirement when proper cooling is provided. CO2 concentration in the vent gas stream was reduced from 0.52 to 0.027 kPa (3.9 to 0.20 mm Hg) for the full five hour test period. Vent gas dew point was reduced from inlet values of 294 K (69 F) to 278 K (41 F) at the outlet. The regeneration of expended absorbent was achieved by the electrochemical method employed in the testing. An absorbent bed using microporous hydrophobic membrane sheets with circulating absorbent is shown to be the best approach to the design of an Absorber Module based on sizing and performance. Absorber Module safety design, comparison of various absorbents and their characteristics, moisture absorption and cooling study and subsystem design and operation time-lining study were also performed. Author

N88-27755*# Life Systems, Inc., Cleveland, Ohio.
VAPOR COMPRESSION DISTILLATION SUBSYSTEM (VCDS) COMPONENT ENHANCEMENT, TESTING AND EXPERT FAULT DIAGNOSTICS DEVELOPMENT, VOLUME 2 Final Report
E. S. Mallinak Dec. 1987 75 p
(Contract NAS9-16374)
(NASA-CR-172076; NAS 1.26:172076; LSI-TR-471-26-Vol-2)
Avail: NTIS HC A04/MF A01 CSCL 06K

A wide variety of Space Station functions will be managed via computerized controls. Many of these functions are at the same time very complex and very critical to the operation of the Space Station. The Environmental Control and Life Support System is one group of very complex and critical subsystems which directly affects the ability of the crew to perform their mission. Failure of the Environmental Control and Life Support Subsystems are to be avoided and, in the event of failure, repair must be effected as rapidly as possible. Due to the complex and diverse nature of the subsystems, it is not possible to train the Space Station crew to be experts in the operation of all of the subsystems. By applying the concepts of computer-based expert systems, it may be possible to provide the necessary expertise for these subsystems in dedicated controllers. In this way, an expert system could avoid failures and extend the operating time of the subsystems even in the event of failure of some components, and could reduce the time to repair by being able to pinpoint the cause of a failure when one cannot be avoided. Author

N88-27700# Royal Army Medical Coll., London (England).
CAN CNV AMPLITUDE PREDICT ABILITY TO ACCOMPLISH A DEMANDING TASK?
Peter Abraham *In* AGARD, Electric and Magnetic Activity of the Central Nervous System: Research and Clinical Applications in Aerospace Medicine Feb. 1988 2 p (For primary document see N88-27683 21-51)
Copyright Avail: NTIS HC A18/MF A01

N88-27704# Aerospace Medical Research Labs., Wright-Patterson AFB, Ohio. Human Engineering Div.
FIGHTER PILOT PERFORMANCE DURING AIRBORNE AND SIMULATOR MISSIONS: PHYSIOLOGICAL COMPARISONS
June J. Skelly, Bradley Purvis, and Glenn Wilson *In* AGARD, Electric and Magnetic Activity of the Central Nervous System: Research and Clinical Applications in Aerospace Medicine Feb. 1988 16 p (For primary document see N88-27683 21-51)
Copyright Avail: NTIS HC A18/MF A01

55 SPACE BIOLOGY

Includes exobiology; planetary biology; and extraterrestrial life.

No abstracts in this category.

59 MATHEMATICAL AND COMPUTER SCIENCES (GENERAL)

No abstracts in this category.

60 COMPUTER OPERATIONS AND HARDWARE

Includes hardware for computer graphics, firmware, and data processing.

For components see *33 Electronics and Electrical Engineering.*

N88-27756# Office of Science and Technology, Washington, D.C.
FEDERAL COUNCIL ON SCIENCE, ENGINEERING AND TECHNOLOGY: COMMITTEE ON COMPUTER RESEARCH AND APPLICATIONS, SUBCOMMITTEE ON SCIENCE AND ENGINEERING COMPUTING: THE US SUPERCOMPUTER INDUSTRY
Dec. 1987 180 p
(DE88-011262; DOE/ER-0362) Avail: NTIS HC A09

The Federal Coordinating Council on Science, Engineering, and Technology (FCCSET) Committee on Supercomputing was chartered by the Director of the Office of Science and Technology Policy in 1982 to examine the status of supercomputing in the United States and to recommend a role for the Federal Government in the development of this technology. In this study, the FCCSET Committee (now called the Subcommittee on Science and Engineering Computing of the FCCSET Committee on Computer Research and Applications) reports on the status of the supercomputer industry and addresses changes that have occurred since issuance of the 1983 and 1985 reports. The review based on periodic meetings with and site visits to supercomputer manufacturers and consultation with experts in high performance scientific computing. White papers have been contributed to this report by industry leaders and supercomputer experts. DOE

N88-27757# Sandia National Labs., Albuquerque, N. Mex.
MINIAC: A SMALL EMBEDDED COMPUTER
G. S. Davidosn and V. G. Grafe Jan. 1988 17 p
(Contract DE-AC04-76DP-00789)
(DE88-008142; SAND-86-2855) Avail: NTIS HC A03/MF A01

The new generation of processor chips and denser memories, all operating at higher clock rates, has made possible a new class of computer. These small, single processor computers are suitable for applications that until recently required several slower processors. The MINIAC computer exploits these new components and takes further advantage of new fabrication and packaging techniques to produce a miniature computer. The result is a 3.1 MIPS machine in approximately 11 cu. in. that is less expensive to produce than earlier multiprocessors with equivalent performance. Significant for embedded applications, its power consumption is under 5 watts when active. During inactive, standby operation, only 4 milliwatts are required to maintain the contents of the memory chips. As a result, an embedded system with MINIAC only needs small batteries, which further reduces the volume and weight resources allocated to computer functions. Author

N88-27758# Oak Ridge National Lab., Tenn.
IMPLEMENTATION OF AN OPS5 DERIVATIVE ON THE NOVIX RISC PROCESSOR
L. C. Williams 1988 5 p Presented at the Rochester Fourth Conference, Rochester, N.Y., 14 Jun. 1988
(Contract DE-AC05-84OR-21400)
(DE88-011392; CONF-8806149-1) Avail: NTIS HC A02/MF A01

The recent popularity of rule-based programming and reduced instruction set computer (RISC) architectures has made the marriage of these two technologies an almost inevitable alternative for applying artificial intelligence (AI) techniques to real-time computing tasks. This paper presents an overview of the software development environment for a rule-based expert-system language based on OPS5 that was written specifically for the Novix NC4016 CPU. DOE

N88-27759# Joint Inst. for Nuclear Research, Dubna (USSR). Lab. of High Energy.
SUPERCOMPUTER FOR PARALLEL DATA ANALYSIS
I. F. Kolpakov, A. E. Senner, and V. A. Smirnov 1987 11 p
(DE88-702148; JINR-E-10-87-378) Avail: NTIS (US Sales Only) HC A03/MF A01

The project of a powerful multiprocessor system is proposed. The main purpose of the project is to develop a low cost computer system with a processing rate of a few tens of millions of operations per second. The system solves many problems of data analysis from high-energy physics spectrometers. It includes about 70 MOTOROLA-68020 based powerful slave microprocessor boards liaisoned through the VME crates to a host VAX micro computer. Each single microprocessor board performs the same algorithm requiring large computing time. The host computer distributes data over the microprocessor board, collects and combines obtained results. The architecture of the system easily allows one to use it in the real time mode. DOE

N88-27396# Mitsubishi Electric Corp., Tokyo (Japan). Information and Communication Systems Engineering Center.
THE MELMUX MX-7100 SERIES HIGH-SPEED DIGITAL MULTIPLEXERS
Kazuyoshi Oshima and Kazuhiko Sekikawa *In its* Mitsubishi Electric Advance (R and D Edition), Volume 41 Dec. 1987 3 p (For primary document see N88-27388 21-31)
Avail: NTIS HC A03/MF A01 CSCL 09B

61 COMPUTER PROGRAMMING AND SOFTWARE

Includes computer programs, routines, alogorithms, and specific applications, e.g., CAD/CAM.

N88-27760*# TRW Defense and Space Systems Group, Redondo Beach, Calif.
BLOCK ORIENTED SIMULATION SYSTEM (BOSS)
Jaimie Ratcliffe [1988] 45 p Submitted for publication
(Contract NAS9-17677)
(NASA-CR-182947; NAS 1.26:182947) Avail: NTIS HC A03/MF A01 CSCL 09B

Computer simulation is assuming greater importance as a flexible and expedient approach to modeling system and subsystem behavior. Simulation has played a key role in the growth of complex, multiple access space communications such as those used by the space shuttle and the TRW-built Tracking and Data Relay Satellites (TDRS). A powerful new simulator for use in designing and modeling the communication system of NASA's planned Space Station is being developed. Progress to date on the Block (Diagram) Oriented Simulation System (BOSS) is described. B.G.

N88-27761# Science Research Council, Chilton (England).
LINGUISTIC SEMANTICS FOR PARALLEL COMPUTATION
M. Bertran-Salvans Apr. 1987 30 p
(PB88-105960; RAL-87-023) Avail: NTIS HC E04/MF E04; copy not available from STI Facility CSCL 09B

A model and a semantics for an extended grammar notation is given. The sentences of the language defined by the grammar correspond to a certain type of parallel composition of linear strings of values. They are referred to as Data streams or simply Streams. The notation can be used as a programming language involving procedures, parallelism and multiple input-output but no communication; in a design stage where the internal communication among subsystems is of no concern. A version of it was used in the development of a computerized power network telecontrol system. Properties and laws of the semantic and syntactic domains are introduced, and some of them are informally proved. A set of transformation laws proved to be confluent with the help of a computerized equational reasoning system. Formal proofs of the properties of the model will be developed in the future with the help of the system. Author

N88-27762# Yale Univ., New Haven, Conn. Dept. of Computer Science.
A PROGRAMMABLE SYSTOLIC ARRAY FOR FACTORIAL ANALYSIS. PART 2: THE SYMMETRIC EIGENVALUE PROBLEM
Tiba Porta Jun. 1987 22 p
(Grant AF AFOSR-0098-86)
(AD-A192396; YALEU/DCS/RR-543-Pt-2) Avail: NTIS HC A03/MF A01 CSCL 12A

Several systolic algorithms were previously presented for Factorial Data Analysis all running on the same triangular systolic array with orthogonal connections: SARDA (Systolic Array for Data Analysis). The study was restricted to matrix computations. This paper will now turn to the symmetric eigenvalue problem on SARDA and study especially tridiagonalization followed by multisection for the eigenvalues and inverse iteration method for the associated eigenvectors. GRA

N88-27763# Virginia Univ., Charlottesville.
FULL ANALYSIS OF A POWERFUL WINDOW RANDOM ACCESS ALGORITHM
P. P. Kazakos and M. Paterakis Mar. 1988 36 p
(Contract N00014-86-K-0742)
(AD-A192437; UVA/525415/EE88/112) Avail: NTIS HC A03/MF A01 CSCL 12F

A simple full sensing window random access algorithm is analyzed in the presence of the limit Poisson user model. The throughput of the algorithm is 0.43, and its delay and resistance to channel errors characteristics are superior to those induced by the Capetanakis window algorithm. In addition, the simple operations of the algorithm, in conjunction with its regenerative properties, allow for the computation and evaluation of the output traffic interdeparture distribution. The latter is needed in the evaluation of interacting systems which use the algorithm for their internal transmissions. GRA

N88-27764# Stanford Univ., Calif. Dept. of Operations Research.
SIMULATION METHODOLOGY Final Report, 1 Mar. 1984 - 31 Dec. 1987
Peter W. Glynn and Donald L. Iglehart 10 Mar. 1988 11 p
(Contract DAAG29-84-K-0030)
(AD-A192548; ARO-20927.22-MA) Avail: NTIS HC A03/MF A01 CSCL 12E

The main thrust of our research has been in developing new methods for analyzing the output from computer simulations. The technical work can be divided into three areas: simulation output analysis, variance reduction, and stochastic optimization. GRA

N88-27765# Army Research Inst. of Environmental Medicine, Natick, Mass.
USING IMSL MATHEMATICAL AND STATISTICAL COMPUTER SUBROUTINES IN PHYSIOLOGICAL AND BIOMECHANICAL RESEARCH Technical Report, May 1978 - Sep. 1987
Everett Harman Oct. 1987 59 p
(AD-A192594; USARIEM-T-5/88) Avail: NTIS HC A0 '/MF A01 CSCL 12E

IMSL Corporation sells a widely used and respected package of mathematical and statistical computer subroutines written in the FORTRAN language. While engineers, mathematicians and others who work regularly with computation are familiar with the usefulness of the subroutines most medical researchers are neither aware of how the package could be useful to them nor

knowledgeable enough in FORTRAN to be able to write programs to call the routines. This report gives examples which illustrate the applicability of IMSL subroutines to research in physiology and biomechanics, and shows how to write simple FORTRAN programs to define variables, read data from a file, call the IMSL subroutines, and store or display results. Increased usage of IMSL software by medical researchers can lead to more sophisticated and quantitative treatment of data, and improve the overall quality of research. GRA

N88-27766# Massachusetts Inst. of Tech., Cambridge. Lab. for Computer Science.
BISIMULATION CAN'T BE TRACED
Bard Bloom, Sorin Istrail, and Albert R. Meyer Nov. 1987 24 p
(Contract N00014-83-K-0125; Grant NSF DCR-85-11190)
(AD-A192725; MIT/LCS/TM-345) Avail: NTIS HC A03/MF A01 CSCL 12E

Bisimulation is the primitive notion of equivalence between concurrent processes in Milner's Calculus of Communicating Systems (CCS); there is a nontrivial game-like protocol for distinguishing nonbisimular processes. In contrast, process distinguishability in Hoare's theory of Communicating Sequential Processes (CSP) is determined soley on the basis of traces of visible actions. We examine what additional operations are needed to explain bisimulation similarly-specifically in the case of finitely branching processes without silent moves. We formulate a general notion of Structured Operational Semantics for processes with Guarded recursion (GSOS), and demonstrate that bisimulation does not agree with trace congruence with respect to any set of GSOS-definable contexts. In justifying the generality and significance of GSOS's, we work out some of the basic proof theoretic facts which justify the SOS discipline. GRA

N88-27767# Massachusetts Inst. of Tech., Cambridge. Artificial Intelligence Lab.
INSPECTION METHODS IN PROGRAMMING: CLICHES AND PLANS
Charles Rich Dec. 1987 94 p
(Contract N00014-85-K-0124; Grant NSF IRI-86-16644)
(AD-A192782; AI-M-1005) Avail: NTIS HC A05/MF A01 CSCL 12E

Inspection methods are a kind of engineering problem solving based on the recognition and use of standard forms or cliches. Examples are given of program analysis, program synthesis and program validation by inspection. A formalism, called the Plan Calculus, is defined and used to represent programming cliches in a convenient, canonical, and programming-language independent fashion. GRA

N88-27768# Massachusetts Inst. of Tech., Cambridge. Artificial Intelligence Lab.
SYNCHRONIZABLE SERIES EXPRESSIONS. PART 2: OVERVIEW OF THE THEORY AND IMPLEMENTATION
Richard C. Waters Nov. 1987 49 p
(Contract N00014-85-K-0124; Grant NSF IRI-86-16644)
(AD-A192783; AI-M-959-Pt-2) Avail: NTIS HC A03/MF A01 CSCL 12E

The benefits of programming in a functional style are well known. In particular, algorithms that are expressed as compositions of functions operating on series/vectors/streams of data elements are much easier to understand and modify than equivalent algorithms expressed as loops. Unfortunately, many programmers hesitate to use series expressions, because the are typically implemented very inefficiently-the prime source of inefficiency being the creation of intermediate series objects. A restricted class of series expressions, obviously synchronizable series expressions, is defined which can be evaluated very efficiently. At the cost of introducing restrictions which place modest limits on the series expressions which can be written, the restrictions guarantee that the creation of intermediate series objects is never necessary. This makes it possible to automatically convert obviously synchronizable series expressions into highly efficient loops using straightforward algorithms. GRA

N88-27769# Massachusetts Inst. of Tech., Cambridge. Artificial Intelligence Lab.
THE PROGRAMMER'S APPRENTICE PROJECT: A RESEARCH OVERVIEW
Charles Rich and Richard C. Waters Nov. 1987 32 p
(Contract N00014-85-K-0124; Grant NSF IRI-86-16644)
(AD-A192784; AI-M-1004) Avail: NTIS HC A03/MF A01 CSCL 12E

The goal of the Programmer's Apprentice project is to develop a theory of how expert programmers analyze, synthesize, modify, explain, specify, verify and document programs. This research goal overlaps both artificial intelligence and software engineering. From the viewpoint of artificial intelligence, we have chosen programming as a domain in which to study fundamental issues of knowledge representation and reasoning. From the viewpoint of software engineering, we seek to automate the programming process by applying techniques from artificial intelligence. GRA

N88-27770# Battelle Memorial Inst., Columbus, Ohio.
DEVELOPMENT OF AUTOMATIC NAMES PLACEMENT SOFTWARE Technical Report, Jul. 1986 - Sep. 1987
Herbert Freeman Dec. 1987 29 p
(Contract DAAG29-81-D-0100)
(AD-A192786; ETL-0484) Avail: NTIS HC A03/MF A01 CSCL 12E

This report describes the development of a software system intended to demonstrate the capability of automatically placing geographic names on maps. The system, which is based on the previously developed AUTOCOR and AUTONAP name placement routines, is designed to label area, line, and point features in 1:24,000 scale United States Geological Survey (USGS) Digital Line Graph (DLG) maps using names extracted from corresponding USGS Geographic Names Information System (GNIS) files. The system performs its task well provided the data in the DLG and GNIS files is of high quality. As is to be expected, the system fails in its task where the correlation between DLG features and GNIS names is unclear, ambiguous, or erroneous. The system was developed for the DEC VAX family computers running under the VMS operating system. GRA

N88-27771# Illinois Univ., Urbana. Coordinated Science Lab.
TEXTURE PERCEPTION AND SHAPE FROM TEXTURE Final Report, 1 Dec. 1986 - 30 Nov. 1987
Narendra Ahuja 1 Mar. 1988 3 p
(Grant AF-AFOSR-0100-87)
(AD-A192923; AFOSR-88-0561TR) Avail: NTIS HC A02/MF A01 CSCL 12E

This report describes the progress of research in texture perception. The goal of the research included perceptual grouping in dot textures, where the goal was to segment a given dot pattern into its perceptual components, and developing a computational theory for an integrated representation of texture. GRA

N88-27772# Texas Instruments, Inc., Dallas.
THE EFFECT OF INPUT DEVICE ON USER PERFORMANCE WITH A MENU-BASED NATURAL LANGUAGE INTERFACE Final Report, Jul. 1985 - Dec. 1987
J. J. Hendrickson and R. D. Williams Jan. 1988 69 p
(Contract N66001-87-C-0187)
(AD-A193095; NOSC-TD-1224) Avail: NTIS HC A04/MF A01 CSCL 12F

Menu-Based Natural Language (MBNL) provides a form of constrained natural language dialogue for human-computer interaction where natural language words and phrases are displayed on the screen as menu items. Previous research on cursor devices has provided mixed results concerning the best cursor device and no firm recommendations were available for use with MBNL interfaces. This study was developed to determine the best input device for MBNL interfaces to Naval command and control databases. Results showed that search keys were slower than cursor keys and trackball. No-scrolling was faster than scrolling. Trackball was preferred, and was more quickly learned than cursor keys. GRA

N88-27773# Scientific Systems, Inc., Cambridge, Mass.
DISTRIBUTED ALGORITHMS FOR PROBABILISTIC SOLUTION OF COMPUTATIONAL VISION PROBLEMS Final Report, Aug. 1987 - Jan. 1988
Donald E. Gustafson and Sanjoy K. Mitter 1 Mar. 1988 44 p
(Contract N00014-87-C-0763)
(AD-A193150) Avail: NTIS HC A03/MF A01 CSCL 09E

A new approach is developed for solving the moving target detection and tracking problem using highly cluttered images. The unknown target is assumed to be moving over a cluttered background in the presence of foreground noise. Using a Markov random field model for the target and a probabilistic description of the noise, the posterior distribution of the target is a Gibbs distribution. The maximum aposteriori target image is found by a randomized search process. Both batch and recursive formulations are developed, with the recursive approach yielding superior results. Numerical results indicate that this approach can successfully detect and track small targets in environments where the target is essentially made invisible by noise. The algorithms are almost completely parallelizable: for n pixels a total of n/4 processors may be used, with the result that solutions would require on the order of 2 seconds on current machines for the examples presented. GRA

N88-27774# Information Systems and Technology Center, Wright-Patterson AFB, Ohio. Ada Validation Facility.
ADA (TRADE NAME) COMPILER VALIDATION SUMMARY REPORT: VERDIX CORPORATION VADA-010-03315, VERSION 5.5 MICROVAX 2 HOST ISBC 386/20P INTEL TARGET Report, 19 Jun. 1987 - 19 Jun. 1988
19 Jun. 1987 36 p
(AD-A193226) Avail: NTIS HC A03/MF A01 CSCL 12E

This Validation Summary Report (VSR) describes the extent to which a specific Ada compiler conforms to the Ada Standard, ANSI/MIL-STD-1815A. This report explains all technical terms used within it and thoroughly reports the results of testing this compiler using the Ada Compiler Validation Capability (ACVC). An Ada compiler must be implemented according to the Ada Standard, and any implementation-dependent features must conform to the requirements of the Ada Standard. The Ada Standard must be implemented in its entirety, and nothing can be implemented that is not in the Standard. Even though all validated Ada compilers conform to the Ada Standard, it must be understood that some differences do exist between implementation. The Ada Standard permits some implementation dependencies-for example, the maximum length of identifiers or the maximum values of integer types. Other differences between compilers result from characteristics of particular operating systems, hardware, or implementation strategies. All of the dependencies observed during the process of testing this compiler are given in this report. The information in this report is derived from the test results produced during validation testing. The validation process includes submitting a suite of standardized tests, the ACVC, as inputs to an Ada compiler and evaluating the results. GRA

N88-27775# Naval Postgraduate School, Monterey, Calif.
COMPUTER AIDED DESIGN FOR LINEAR CONTROL STATE VARIABLE SYSTEM (SVS) M.S. Thesis
Ismail Unlu Dec. 1987 164 p
(AD-A193282) Avail: NTIS HC A08/MF A01 CSCL 12I

The theory, detailed outline of operating and algorithm procedures of a continuous, time-invariant, linear control state variable systems design and analysis computer program is presented. The program, SVS, which is based on Melsa's LINCON, was modified to demonstrate Controllability, Observability, Bode Plot, Root locus plot, Nyquist plot, pole placement, Luenberger observer design, optimal control design, time response plot and some basic matrix manipulations. Worked examples with the program output are included. Some options give only numeric data output; others give both numeric data and high-resolution graphs. The software, which is fully interactive, menu-driven and user friendly is written in Turbo Pascal to be run on the IBM-PC microcomputers. All options are presented via option menus and the user will be prompted for all input parameters. GRA

N88-27776# Michigan Univ., Ann Arbor.
RESEARCH INTO THE ARCHITECTURE OF CAD BASED ROBOT VISION SYSTEMS Final Report, May 1984 - 31 Oct. 1987
T. N. Mudge and R. A. Volz 9 Feb. 1988 8 p
(Contract DAAG29-84-K-0070)
(AD-A193330; ARO-20244.10-EL) Avail: NTIS HC A02/MF A01 CSCL 12E

The research conducted under this grant has been to investigate techniques for recognizing objects that are partially hidden or occluded. It was assumed that geometrical data about the objects was available either as a by-product of the CAD process used to design the object or as the output of a training phase. There were three aspects to this work. First, recognition techniques were developed that used only a single view gray-level image. Second, complementary techniques were developed that used range images. Third, computation times for both of these techniques were studied with the intent of reducing them through the use of parallel processing. The work on gray-level images resulted in a number of new techniques to speedup recognition. These included the concept of saliency and critical point neighborhood, and a fast matching algorithm based on k-d trees. Techniques for recognizing occluded objects that can be at varying distances from the viewer were also developed. The work with range data was aimed at the recognition and pose estimation of three-dimensional industrial parts. The major subproblems addressed were: (1) segmentation and surface parameter extraction, (2) grouping regions into a set (a Convex Region Set), and (3) Convex Region Set matching. The work to develop fast parallel versions of our recognition algorithms made extensive use of a 64 processor NCUBE hypercube multiprocessor. Speedups of 30:1 over VAX 11/780 implementations were obtained for some low-level image processing algorithms. GRA

N88-27777# Information Systems and Technology Center, Wright-Patterson AFB, Ohio. Ada Validation Facility.
ADA (TRADE NAME) COMPILER VALIDATION SUMMARY REPORT: VERDIX CORPORATION VADA-010-13125, VERSION 5.41 SUN MICROSYSTEMS SUN-3/160 HOST MICROBAR GPC68020 TARGET
17 Jun. 1987 39 p
(AD-A193415; AVF-VSR-90.0987; AVF-87-04-09-VRX) Avail: NTIS HC A03/MF A01 CSCL 12E

This Validation Summary Report describes the extent to which a specific Ada compiler conforms to the Ada Standard, ANSI/MIL-STD-1815A. This report explains all technical terms used within it and thoroughly reports the results of testing this compiler using the Ada Compiler Validation Capability (ACVC). An Ada compiler must be implemented according to the Ada Standard, and any implementation-dependent features must conform to the requirements of the Ada Standard. The Ada Standard must be implemented in its entirety, and nothing can be implemented that is not in the Standard. Even though all validated Ada compilers conform to the Ada Standard, it must be understood that some differences do exist between implementations. The Ada Standard permits some implementation dependencies--for example, the maximum length of identifiers or the maximum values of integer types. Other differences between compilers result from characteristics of particular operating systems, hardware, or implementation strategies. All of the dependencies observed during the process of testing this compiler are given in this report. The information in this report is derived from the test results produced during validation testing. GRA

N88-27778# Washington Univ., Seattle. Dept. of Psychology.
SIMULATION OF REAL TIME PROBLEM SOLVING Final Report, 1 Jan. 1985 - 30 Sep. 1987
Earl Hunt 30 Nov. 1987 17 p
(Contract N00014-84-K-5553)
(AD-A193436) Avail: NTIS HC A03/MF A01 CSCL 12E

Hybrid computer simulations of problem solving can be constructed by combining the production system architecture with a semantic activation process for selecting productions. This technique has been used to construct simulations of problem solving done under time pressure, and in the presence of interruptions. The power of the simulations is limited by the pattern recognition capacity of the semantic networks. This has been analyzed and some mathematical limits obtained. Whether these (or analogous) limits apply to connectionist networks is to base pattern recognition on case-based memory models, which store specific experiences rather than statistical associations between features of experiences. A study is presented showing that case based models may be an alternative to semantic networks. GRA

N88-27779# Sandia National Labs., Albuquerque, N. Mex.
VERIFICATION OF FLIGHT SOFTWARE WRITTEN IN C USING ACSL
R. C. Edmunds 1988 11 p Presented at the Summer Computer Simulation Conference, Seattle, Wash., 25 Jul. 1988
(Contract DE-AC04-76DP-00789)
(DE88-006100; SAND-87-2565C; CONF-880733-1) Avail: NTIS HC A03/MF A01

This paper documents a technique that has been used to interface the ACSL simulation package to C modules on a VAX computer. Using the technique documented in this memo, it should be possible to verify major portions of flight software (e.g., guidance and control algorithms) in a dynamic simulation environment. This verification can be accomplished fairly early in the development cycle, and if the flight software algorithms are written in C to begin with, then the time and effort required to convert them from FORTRAN (or ACSL code) to C can be avoided entirely. Also, when the C code is moved to the target flight computer, the debug time should be greatly reduced. DOE

N88-27780# Sandia National Labs., Albuquerque, N. Mex.
AN OPTICAL 2-DIMENSIONAL CORRELATOR FOR PATTERN RECOGNITION IN EMBEDDED COMPUTING
P. A. Molley and K. T. Stalker 1988 9 p Presented at the Military Computing Conference, Anaheim, Calif., 3 May 1988
(Contract DE-AC04-76DP-00789)
(DE88-007198; SAND-88-0578C; CONF-880577-1) Avail: NTIS HC A02/MF A01

Optical processing technology can be applied to a variety of problems in embedded computing. It is particularly well suited for problems involving large two-dimensional arrays of data, for example in correlation based pattern recognition. For large kernel correlations, the parallelism of optics offers the high throughput necessary to perform the desired correlation or convolution operations in real time. In addition, the latest generation of optical hardware provides the opportunity to construct processors ideally suited to the embedded computer environment because of their potential size, weight, and power consumption advantages over alternative technologies. Using currently available optical devices, one such architecture was constructed which demonstrated the ability to do real-time pattern recognition. The optical processor was able to perform a 2-D correlation of a 64 x 44 pixel reference object with a 256 x 232 pixel input image at standard video rates. This represents an equivalent computation rate of over 10 billion operations per second. Results of the optical processor as well as a discussion of the potential of this technology in the embedded computer environment. DOE

N88-27781# Lawrence Livermore National Lab., Calif.
A MENU-DRIVEN MENU EDITOR AND ASSOCIATED MENU SYSTEM
G. G. Preckshot and D. N. Butner 18 Feb. 1988 17 p Presented at the 7th Topical Conference on High Temperature Plasma Diagnostics, Napa, Calif., 13 Mar. 1988
(Contract W-7405-eng-48)
(DE88-008026; UCRL-97872; CONF-880364-16) Avail: NTIS HC A03/MF A01

A menu-style user interface has been developed at Lawrence Livermore National Laboratory (LLNL) for distributed control, data acquisition and data processing. A graphical menu editor, which is itself the first application of the menu system, is used to construct or modify menu hierarchies. Unlike many menu systems, no code need be written to demonstrate a set of menus because there are no subroutine calls to make menus; developers need only write the code which performs the actions indicated by user menu picks. In addition to this rapid prototyping feature, the menu system is integrated with operating system asynchronous traps (in Unix, signals and selects) so that it supports real-time user interfaces for control in a distributed computer system. DOE

N88-27782# California Univ., Davis. Dept. of Electrical and Computer Engineering.
ENHANCEMENT OF MODELING AND IMAGE GENERATION TECHNIQUES FOR HIGH-RESOLUTION 3-DIMENSIONAL IMAGERY
K. I. Joy Mar. 1988 37 p Prepared in cooperation with Lawrence Livermore National Lab., Calif.
(Contract W-7405-eng-48)
(DE88-008923; UCRL-21033) Avail: NTIS HC A03/MF A01

The document consists of three parts: (1) It presents the data formats for the modeling system developed at the UC Davis Computer Graphics Laboratory. These files convey modeling information to the research systems currently being developed at the laboratory. All files contain keyword and numerical data information to describe polygons, patches, spheres, light parameters, textures and camera descriptions. The files are in ascii format for ease of transfer between machines and so that they can be edited in order to tweak the data. (2) A dissection is given for the Fujimoto algorithm. In 1985, Akira Fujimoto first published his algorithm for speeding up the ray tracing operation. This algorithm works on a unique principle that trades off the substantial ray/surface intersection calculations with a search, along the ray, through a set of cuboid cells. The principal speedup in the algorithm is twofold: a routine based upon integer arithmetic is used to quickly identify the cells that lie in the path of the ray, and only those objects that intersect the chosen cells must be tested for intersection against the ray. Presented is a thorough analysis of Fujimoto's algorithm, specifically concentrating on the integer calculations. (3) A description is given for modeling and image generation techniques for high-resolution 3-dimensional imagery. DOE

N88-27783# University Coll., London (England). Dept. of Computer Science.
ISSUES IN COMPUTER-ASSISTED INTERPRETATION OF GRAPHS AND QUANTITATIVE INFORMATION
J. A. Campbell and S. P. Ross May 1987 13 p
(PB88-116280; UCL-CS-TR-131) Avail: NTIS HC E04/MF E04; copy not available from STI Facility CSCL 09B

Although there are many sources of information from experimental psychology on the subjective human factors that enter into interpretation of graphs and quantitative displays, these have not yet been exploited for the purpose of specifying software that can reproduce the characteristics of human judgement and therefore act as a human user's assistant, e.g., when the volumes of information are too large or complex for unaided examination. The paper outlines some of the methods and issues that are relevant in the specification of appropriate software and the improved presentation of graphical information. Examples include support for reasoning about qualitative similarities between curves, effective graphical use of non-ordinal identifiers, interpretation of scatterplots, gestalt rules, scaling and labelling effects. GRA

N88-27784# Bettis Atomic Power Lab., West Mifflin, Pa.
TRANSL: A PATRAN TRANSLATOR SUBROUTINE LIBRARY
K. M. Butler, ed. and C. S. Caldwell, ed. May 1988 54 p
(Contract DE-AC11-76PN-00014)
(DE88-010976; WAPD-TM-1619) Avail: NTIS HC A04/MF A01

The TRANSL subroutine library enables a programmer to easily interface and translate engineering models developed using PATRAN interactive graphics software to engineering analysis computer programs, typically executed on large mainframe

computers. PATRAN is a powerful program which greatly simplifies the tasks of generating 2- or 3-D geometry models, creating finite element grids, and applying boundary conditions. In order to use a model created in PATRAN in any analysis program, a translator must be written to convert the model from the PATRAN neutral file format into an input format specific to the analysis program. TRANSL is a versatile FORTRAN-77 subroutine library implemented on VAX computers which performs activities common to any interactive PATRAN translator. Its capabilities include reading specified PATRAN neutral file data into memory, sorting neutral file data and general arrays, searching for a specific piece of information, communicating with the user, and file handling. A session file for automatic submission of input in a later translator session and a print file containing all communication with the user may be automatically generated. The driver for the TRANSL subroutine library is a program which reads all data from the neutral file into memory and writes it out again in the same format. This program demonstrates the use of TRANSL subroutines for developing a PATRAN translator and provides a means for testing the TRANSL subroutines. DOE

N88-27785# Lawrence Livermore National Lab., Calif.
THE SUB-IMPLICIT METHOD: NEW MULTIPROCESSOR ALGORITHMS FOR OLD IMPLICIT CODES
P. G. Eltgroth and M. K. Seager Jul. 1987 12 p Presented at the Vector and Parallel Processing in Computational Science, Liverpool, United Kingdom, 25 Aug. 1987
(Contract W-7405-eng-48)
(DE88-011345; UCRL-96744; CONF-8708148-4) Avail: NTIS HC A03/MF A01

This paper presents a new approach to the parallel solution of an implicit system of difference equations. The sub-implicit method operates on sub-regions of the data which are evaluated at spatial points and synchronous time. Each sub-region has a border node which is shared with an adjacent sub-region (in one dimension). Values for this shared node are computed independently by the two solution processes for two adjacent sub-regions. Nodes outside the sub-region are treated as having fixed values during the solution. At the finish of the two sub-region solutions, the two sub-regions are blocked against further changes (a pairwise synchronization) and the two different values for the shared node are reconciled. This can be done in such a way that energy conservation is exact. Results for test problems for heat diffusion in one dimension are given and compared against standard methods and analytic results. Implementation of the method into a demonstration two-dimensional hydrodynamics code SIMPLE is described. The best speedups observed for parallel execution of this version of SIMPLE on a twelve CPU Sequent multiprocessor were 9.6 for a 50 by 50 grid and 10.4 for a 95 by 95 grid. Some generalizations of this approach are discussed. DOE

N88-27786# Sandia National Labs., Albuquerque, N. Mex.
FACTORIZATION OF LARGE INTEGERS ON A MASSIVELY PARALLEL COMPUTER
J. A. Davis and D. B. Holdridge 1988 9 p Presented at Eurocrypt '88, Davos, Switzerland, 25 May 1988
(Contract DE-AC04-76DP-00789)
(DE88-011625; SAND-88-0262C; CONF-8805114-2) Avail: NTIS HC A02/MF A01

Our interest in integer factorization at Sandia National Laboratories is motivated by cryptographic applications and in particular the security of the RSA encryption-decryption algorithm. We have implemented our version of the quadratic sieve procedure on the NCUBE computer with 1024 processors (nodes). The new code is significantly different in all important aspects from the program used to factor number of order 10 to the 70th power on a single processor CRAY computer. Capabilities of parallel processing and limitation of small local memory necessitated this entirely new implementation. This effort involved several restarts as realizations of program structures that seemed appealing bogged down due to inter-processor communications. We are presently working with integers of magnitude about 10 to the 70th power in tuning this code to the novel hardware. DOE

N88-27787# Sandia National Labs., Albuquerque, N. Mex.
MAXIMUM ENTROPY SIGNAL RESTORATION WITH LINEAR PROGRAMMING
G. A. Mastin and R. J. Hanson May 1988 34 p
(Contract DE-AC04-76DP-00789)
(DE88-011740; SAND-88-0451) Avail: NTIS HC A03/MF A01

Dantzig's bounded-variable method is used to express the maximum entropy restoration problem as a linear programming problem. This is done by approximating the nonlinear objective function with piecewise linear segments, then bounding the variables as a function of the number of segments used. The use of a linear programming approach allows equality constraints found in the traditional Lagrange multiplier method to be relaxed. A robust revised simplex algorithm is used to implement the restoration. Experimental results from 128- and 512-point signal restorations are presented. DOE

N88-27788 California Univ., Los Angeles.
THE ROBUST TRACKING CONTROL OF NONLINEAR SYSTEMS WITH UNCERTAIN DYNAMICS Ph.D. Thesis
Dauchung Wang 1987 165 p
Avail: Univ. Microfilms Order No. DA8802515

A robust tracking control algorithm based mainly on the theory of variable structure systems and Lyapunov's direct method is developed to treat the tracking control problem of the nonlinear time-varying system with uncertain dynamics. A nominal model is used instead of an exact one, together with a description of the bounds of plant uncertainty, and the objective is to design a control law that will drive all plants lying within the specified band of uncertainty to reach the goal. The modeling error, time-varying system dynamics, and disturbances are all treated as system uncertainties. This algorithm will much ease the difficulties in the need of a precise model of a physical system for control purposes and to handle the nonlinear time-varying system with uncertainties. The nonlinear time-varying system is first linearized to a linear time-varying system, with time-varying coefficients completely defined, via the method of variable structure systems. Then the control method is switched to Lyapunov's direct method to complete the tracking of the nonlinear time-varying system and to eliminate the control chattering problem caused by the method of variable structure systems. The tracking control of a simple two-link manipulator system is used as an example for the application of this robust tracking control algorithm. Dissert. Abstr.

N88-27789# Technische Univ., Berlin (West Germany). Fachbereich Informatik.
CONTRIBUTION TO ALMOST REALISTIC PICTURE PROCESSING BY A COMPUTER GRAPHICS PROCEDURE Ph.D. Thesis [EIN BEITRAG ZUR REALITAETSNAHEN BILDGENERIERUNG MITTELS VERFAHREN DER COMPUTER GRAPHICS]
Bernd J. Knobloch 1988 195 p In GERMAN
(ETN-88-92372) Avail: NTIS HC A09/MF A01

Methods of object geometry representation and visualization procedures are presented for realistic picture processing. Physical conditions of light scattering in the environment, surface macro-structures and textures, transparence, and mirroring are considered. Object geometry is processed by polygonal representation and parametric surface descriptions. Lagrange, Hermite, Bezier and B-Spline surfaces are examined. Visualization is obtained by ray tracing and bounding volumes techniques. Grid tree and grid array hierachical data structures are used. Surface structures are investigated by two part mapping and solid texturing. ESA

N88-27790# Fondazione Ugo Bordoni, Rome (Italy).
APPROXIMATION PROBLEMS OF THE HILBERT TRANSFORM TO IDENTIFY MINIMUM PHASE LINEAR SYSTEMS [PROBLEMI DI APPROSSIMAZIONE DELLA TRASFORMATA DI HILBERT PER L'IDENTIFICAZIONE DEI SISTEMI LINEARI A FASE MINIMA]
Odoardo Brugia and Salvatore Improta Dec. 1986 18 p In

ITALIAN
(FUB-42-1986; ETN-88-92647) Avail: NTIS HC A03/MF A01

A fast and robust method to evaluate the Hilbert transform is presented. So-called minimum phase linear systems are characterized by the relationship of the phase to the attenuation. The procedure includes interpolation of the measured points using an approximation function to obtain a function that may be integrated numerically. The algorithm is tested with a transfer function including two zeros and three poles. The error of the computed phases is less than quantization error is presented.
ESA

N88-27791# Societe Nationale Industrielle Aerospatiale, Cannes (France).
BENEFITS OF AN OBJECT APPROACH IN A COMPUTER AIDED DESIGN ENVIRONMENT [BENEFICES D'UNE APPROCHE ORIENTEE OBJET POUR UN ENVIRONNEMENT DE CAO]
Brigitte Trousse 31 Mar. 1988 15 p In FRENCH; ENGLISH summary
(SNIAS-881-440-102; ETN-88-92872) Avail: NTIS HC A03/MF A01

The limitations of commercial computer aided design tools such as object modeling are discussed. The analysis includes multirepresentation of an object, relations between several objects, and top-down and bottom-up methodology. A way to solve these problems is presented in the form of a virtual computer aided design object-oriented tool called XCAD linked to an expert system shell and coupled to a solid modeller.
ESA

N88-27792# Deutsche Forschungs- und Versuchsanstalt fuer Luft- und Raumfahrt, Oberpfaffenhofen (West Germany). Abteilung HF-Physik.
A HIDDEN-SURFACE REMOVAL ALGORITHM FOR STRUCTURES DEFINED BY TRIANGULAR AND RECTANGULAR SURFACE PATCHES
Rolf Schwemmer Jan. 1988 93 p In GERMAN; ENGLISH summary
(DFVLR-Mitt-88-03; ISSN-0176-7739; ETN-88-92938) Avail: NTIS HC A05/MF A01; DFVLR VB-PL-DO, 90 60 58, 5000 Cologne, Federal Republic of Germany, 31.50 deutsche marks

An algorithm for visualization of three-dimensional structures described by plane surface patches is presented. Instead of producing two-dimensional output-data for graphical use, this algorithm renders a three-dimensional solution. The algorithm compares the surface patches with each other, if their topside does not show away from the observer, who is located on the z-axis at infinity. In order to reduce the number of patches that have to be compared with each other, a stack-management had to be implemented.
ESA

N88-27793# Deutsche Forschungs- und Versuchsanstalt fuer Luft- und Raumfahrt, Oberpfaffenhofen (West Germany). Abteilung Regelung.
SOFTWARE ENGINEERING GUIDELINES FOR RASP AND ANDECS: REQUIREMENTS AND ARCHITECTURAL DESIGN
Johann Bals, Hans-Dieter Joos, and Martin Otter Feb. 1988 67 p In GERMAN; ENGLISH summary
(DFVLR-Mitt-88-07; ISSN-0176-7739; ETN-88-92941) Avail: NTIS HC A04/MF A01; DFVLR, VB-PL-DO, 90 60 58 5000 Cologne, Federal Republic of Germany, 23 deutsche marks

The guidelines for the requirements and architectural design phase in the software life cycle of the engineering-software projects RASP and ANDECS are described. In the design phase a combination of a functional and an object-oriented approach is used. Abstract datatype modules play and important role. The specification is performed by means of standardized documents are presented.
ESA

N88-27794# Deutsche Forschungs- und Versuchsanstalt fuer Luft- und Raumfahrt, Oberpfaffenhofen (West Germany). Abteilung Regelung.
FORTRAN 77 IMPLEMENTATION OF ABSTRACT DATATYPE MODELS
Reinhard Finsterwalder and Martin Otter Feb. 1988 122 p Partly in ENGLISH and GERMAN
(DFVLR-Mitt-88-08; ISSN-0176-7739; ETN-88-92942) Avail: NTIS HC A06/MF A01; DFVLR, VB-PL-DO, 90 60 58, 5000 Cologne, Federal Republic of Germany, 40.50 deutsche marks

Abstract datatype programming is developed for software engineering and for enhancing the visual subroutine methodology. Powerful abstract datatype modules can be easily programmed in FORTRAN 77 as well, provided (non-trivial) auxiliary tools are available. As an example for such a programming procedure the auxiliary subroutines for the software project ANDECS are explained.
ESA

N88-27795# Deutsche Forschungs- und Versuchsanstalt fuer Luft- und Raumfahrt, Oberpfaffenhofen (West Germany). Abteilung Regelung.
A PRELUDE (ANALYSIS AND DESIGN OF CONTROL SYSTEMS-PRELIMINARY UTILITIES DEPOSITORY). A DATA-BASED INTERACTIVE SYSTEM OF CONTROL SOFTWARE, USER'S GUID E
Hans-Dieter Joos Mar. 1988 106 p In GERMAN; ENGLISH summary
(DFVLR-Mitt-88-12; ISSN-0176-7739; ETN-88-92945) Avail: NTIS HC A06/MF A01; DFVLR, VB-PL-DO, 90 60 58, 5000 Cologne, Federal Republic of Germany, 38 deutsche marks

A PRELUDE supplies the user with a database system and an interactive environment for control analysis and design procedures. It is an open software system in the sense that user-defined applications can be added easily. The computer science basis of A PRELUDE is RSYST, a data and method base system for technical and scientific applications. The system theory and control methods in A PRELUDE are those of the control engineering software library RASP (Regulator Analysis and Synthesis Programs). The procedures in A PRELUDE use predefined composed control-oriented data structures. This avoids user problems with data interfaces between different procedures.
ESA

N88-27796*# National Aeronautics and Space Administration. Lewis Research Center, Cleveland, Ohio.
IMPLEMENTING DIRECT, SPATIALLY ISOLATED PROBLEMS ON TRANSPUTER NETWORKS
Graham K. Ellis Aug. 1988 57 p
(NASA-TM-101297; ICOMP-88-14; E-4278; NAS 1.15:101297) Avail: NTIS HC A04/MF A01 CSCL 09B

Parametric studies were performed on transputer networks of up to 40 processors to determine how to implement and maximize the performance of the solution of problems where no processor-to-processor data transfer is required for the problem solution (spatially isolated). Two types of problems are investigated a computationally intensive problem where the solution required the transmission of 160 bytes of data through the parallel network, and a communication intensive example that required the transmission of 3 Mbytes of data through the network. This data consists of solutions being sent back to the host processor and not intermediate results for another processor to work on. Studies were performed on both integer and floating-point transputers. The latter features an on-chip floating-point math unit and offers approximately an order of magnitude performance increase over the integer transputer on real valued computations. The results indicate that a minimum amount of work is required on each node per communication to achieve high network speedups (efficiencies). The floating-point processor requires approximately an order of magnitude more work per communication than the integer processor because of the floating-point unit's increased computing capacity.
Author

N88-27797# Lawrence Livermore National Lab., Calif.
HYPERVELOCITY IMPACT ANALYSIS WITH SUPERCOMPUTERS
G. W. Pomykal 31 Mar. 1988 7 p Presented at the Military Computing Conference, Anaheim, Calif., 3 May 1988
(Contract W-7405-eng-48)
(DE88-008907; UCRL-98364; CONF-880577-5) Avail: NTIS HC A02/MF A01

With numerical codes designed and developed for the extensive computational capability of Cray X-MP supercomputers, 2- and 3-D modeling of hypervelocity impacts has been conducted. This modeling provides the only means of understanding complex shock-wave interaction in such experiments. It also permits us to simulate complex and hazardous tests that otherwise would be difficult or impossible to run, thus making the experiments more productive and less costly. Examples are given of hypervelocity-impact models, together with a description of the codes used, calculational results with available experimental results are compared. DOE

N88-27798*# Eloret Corp., Sunnyvale, Calif.
SYNOPSIS OF A COMPUTER PROGRAM DESIGNED TO INTERFACE A PERSONAL COMPUTER WITH THE FAST DATA ACQUISITION SYSTEM OF A TIME-OF-FLIGHT MASS SPECTROMETER
R. D. Bechtel, M. A. Mateos, and K. A. Lincoln Mar. 1988 51 p
(Contract NCC2-462)
(NASA-CR-177474; NAS 1.26:177474) Avail: NTIS HC A04/MF A01 CSCL 09B

Briefly described are the essential features of a computer program designed to interface a personal computer with the fast, digital data acquisition system of a time-of-flight mass spectrometer. The instrumentation was developed to provide a time-resolved analysis of individual vapor pulses produced by the incidence of a pulsed laser beam on an ablative material. The high repetition rate spectrometer coupled to a fast transient recorder captures complete mass spectra every 20 to 35 microsecs, thereby providing the time resolution needed for the study of this sort of transient event. The program enables the computer to record the large amount of data generated by the system in short time intervals, and it provides the operator the immediate option of presenting the spectral data in several different formats. Furthermore, the system does this with a high degree of automation, including the tasks of mass labeling the spectra and logging pertinent instrumental parameters. Author

N88-27799*# National Aeronautics and Space Administration. Lewis Research Center, Cleveland, Ohio.
USER'S MANUAL FOR THE TWO-DIMENSIONAL TRANSPUTER GRAPHICS TOOLKIT
Graham K. Ellis Aug. 1988 105 p
(NASA Order C-99066-G)
(NASA-TM-100974; ICOMP-88-13; E-4266; NAS 1.15:100974)
Avail: NTIS HC A06/MF A01 CSCL 09B

The user manual for the 2-D graphics toolkit for a transputer based parallel processor is presented. The toolkit consists of a package of 2-D display routines that can be used for the simulation visualizations. It supports multiple windows, double buffered screens for animations, and simple graphics transformations such as translation, rotation, and scaling. The display routines are written in occam to take advantage of the multiprocessing features available on transputers. The package is designed to run on a transputer separate from the graphics board. Author

N88-27378# Johns Hopkins Univ., Baltimore, Md. Dept. of Mathematical Sciences.
LINEAR PROGRAMMING FOR AIR FORCE DECISION AIDING Final Report
Steven J. Steinsaltz *In* Universal Energy Systems, Inc., United States Air Force Graduate Student Summer Support Program, Volume 2 Dec. 1987 21 p (For primary document see N88-27355 21-31)
Avail: NTIS HC A99/MF E03 CSCL 09B

N88-27379# University of South Florida, St. Petersburg. Dept. of Computer Science and Engineering.
CREATING ASPECT GRAPHS FOR USE IN OBJECT RECOGNITION Final Report
John H. Stewman *In* Universal Energy Systems, Inc., United States Air Force Graduate Student Summer Support Program, Volume 2 Dec. 1987 21 p (For primary document see N88-27355 21-31)
Avail: NTIS HC A99/MF E03 CSCL 09B

N88-27382# Louisiana State Dept. of Conservation, Baton Rouge. Dept. of Engineering Sciences.
AN INVESTIGATION OF PERFORMANCE IMPROVEMENT IN KNOWLEDGE-BASED CONTROL SYSTEMS Final Report
John M. Usher *In* Universal Energy Systems, Inc., United States Air Force Graduate Student Summer Support Program, Volume 2 Dec. 1987 17 p (For primary document see N88-27355 21-31)
Avail: NTIS HC A99/MF E03 CSCL 09B

N88-27390# Mitsubishi Electric Corp., Tokyo (Japan). Central Research Lab.
COMPUTER-AIDED ENGINEERING (CAE) FOR ENGINEERING DESIGN
Akemi Futakawa *In its* Mitsubishi Electric Advance (R and D Edition), Volume 41 Dec. 1987 3 p (For primary document see N88-27388 21-31)
Avail: NTIS HC A03/MF A01 CSCL 09B

62 COMPUTER SYSTEMS

Includes computer networks and special application computer systems.

N88-27800# Yale Univ., New Haven, Conn. Dept. of Computer Science.
PERFORMABILITY ANALYSIS: MEASURES, AN ALGORITHM AND A CASE STUDY
R. M. Smith, K. S. Trivedi, and A. V. Ramesh Jan. 1988 29 p
(Contracts DAAG29-84-K-0045; DAAL03-87-G-0066)
(AD-A192477; YALEU/DCS/TR-600) Avail: NTIS HC A03/MF A01 CSCL 12F

Multiple-processor systems can provide higher performance and higher reliability/availability than single-processor systems. To properly assess the effectiveness of multi-processor systems, measures that combine performance and reliability are needed. The behavior of the multi-processor system is described as a continuous time Markov chain and associate a reward rate (performance measure) with each state. The distribution of performability for analytical models of a multi-processor system is evaluated using a recently improved polynomial-time algorithm that obtains the distribution of performability for non-repairable as well as repairable systems with heterogeneous components with a substantial speedup over earlier work. The system analyzed with several Markov reward models is the (C.mmp) multi-processor system developed at Carnegie Mellon University. The example indicates that distributions of cumulative performance measures over finite intervals reveal behavior of multi-processor systems not indicated by either steady-state or mean values alone. GRA

N88-27801# Massachusetts Inst. of Tech., Cambridge. Lab. for Computer Science.
CONSTRUCTING A HIGHLY-AVAILABLE LOCATION SERVICE FOR A DISTRIBUTED ENVIRONMENT
Deborah J. Hwang Jan. 1988 89 p
(Contract N00014-83-K-0125; Grant NSF DCR-85-03662)
(AD-A192723; MIT/LCS/TR-410) Avail: NTIS HC A05/MF A01 CSCL 12G

One possible advantage a distributed system has over a centralized system is the ability to move objects from one node to another. For example, we may want to move an object if the

node where it resides is overloaded. This thesis proposes to use a location service to aid in finding objects that move. The service is highly available; it will tolerate system failures like node crashes and network partitions without shutting down completely. The service is also efficient; the response time of the service is reasonable, and it does not increase the number and sizes of messages excessively. We achieve high availability and efficiency by replicating the service state. The replication technique we have chosen is a new method, the multipart timestamp technique that is based on multipart timestamps and gossip messages. This technique provides us with higher availability and efficiency than traditional replication techniques without sacrificing consistency. We also extend this technique to allow reconfiguration. GRA

N88-27802# Massachusetts Inst. of Tech., Cambridge. Lab. for Computer Science.
A MODULAR PROOF OF CORRECTNESS FOR A NETWORK SYNCHRONIZER
A. Fekete, N. Lynch, and L. Shira Sep. 1987 75 p
(Contracts N00014-85-K-0168; N00014-83-K-0125)
(AD-A192726; MIT/LCS/TM-341) Avail: NTIS HC A04/MF A01 CSCL 12F

In this paper we offer a formal, rigorous proof of the correctness of Awerbuch's algorithm for network synchronization. We specify both the algorithm and the correctness condition using the I/O automation model, which has previously been used to describe and verify algorithms for concurrency control and resource allocation. We show that the model is also a powerful tool for reasoning about distributed graph algorithms. Our proof of correctness follows closely the intuitive arguments made by the design techniques as stepwise refinement and modularity. In particular, since the algorithm uses simpler algorithms for synchronization within and between clusters of nodes, our proof can import as lemmas the correctness of these simpler algorithms. GRA

N88-27803# Air Force Inst. of Tech., Wright-Patterson AFB, Ohio. School of Engineering.
IMAGE PROCESSING USING A PARALLEL ARCHITECTURE M.S. Thesis
Billy R. Hodges Dec. 1987 119 p
(AD-A192833; AFIT/GE/ENG/87D-25) Avail: NTIS HC A06/MF A01 CSCL 12I

This study developed a set of low level image processing on a parallel computer that allows concurrent processing of images in order to support development of systems that use multiple images to gather information. The parallel computer used is a collection of powerful processors connected in a hypercube topology. The software developed simplifies the interface between the parallel computer and the applications developer by providing a library of functions in the C programming language. These functions are used to control image processor programs that run independently in the parallel computer and perform the image processing operations. The complexities of the parallel processor are hidden and replaced with a flexible structure specifically designed for image processing. This structure provides a simplified interface, but also acts as a framework to which additional image processing operations can be added. GRA

N88-27804# Naval Research Lab., Washington, D.C.
BASIC DATABASE OPERATIONS ON THE BUTTERFLY PARALLEL PROCESSOR: EXPERIMENT RESULTS Memorandum Report, Jan. - Dec. 1987
Todd J. Rosenau and Sushil Jajodia 4 Mar. 1988 63 p
(AD-A193199; NRL-MR-6173) Avail: NTIS HC A04/MF A01 CSCL 12G

The next phase in speeding up database queries will be through the use of highly parallel computers. This paper will discuss the basic database operations (select, project, natural join, and scaler aggregates) on a shared-memory multiple instruction stream, multiple data stream (MIMD) computer and the problems associated with implementing them. Some problems associated with getting maximum parallelization are improper data division and hot spots. Improper data division results when the number of tasks does not divide evenly among the processors. Hot spots or contentions occur due to locking if accesses are made to the same segment of a RAMFile and also if attempts are made to get data from the same remote processor at the same time. These algorithms have been implemented on the Butterfly Parallel Processor, and the results of our experiments are described in detail. GRA

N88-27805# Lawrence Livermore National Lab., Calif.
NOTES ON OPERATING SYSTEM REQUIREMENTS FOR THE NEXT MILLENNIUM
R. W. Watson 13 May 1988 7 p Presented at the Cray Users Group Meeting, Minneapolis, Minn., 26 Apr. 1988
(Contract W-7405-eng-48)
(DE88-010712; UCRL-98751; CONF-8804136-1) Avail: NTIS HC A02/MF A01

The central characteristic of the operating system architectures of the future will be their focus on communication, modularity, explicit tasking based concurrency, and transparency of naming, protection, and error control. We believe these characteristics will be increasingly important to their user communities because they will allow support for easy addition of new services and accommodate new computing and communication architectures and capabilities. This paper discusses these operating systems. DOE

N88-27806# Technische Univ., Munich (West Germany). Inst. fuer Informatik.
MODELING AND APPROXIMATE PERFORMANCE ANALYSIS OF MULTIUSER COMPUTER SYSTEMS Ph.D. Thesis [ZUR MODELLIERUNG UND APPROXIMATIVEN LEISTUNGSANALYSE VON VIELTEILNEHMER-RECHENSYSTEMEN]
Peter Chylla 1986 148 p In GERMAN
(ETN-88-92137) Avail: NTIS HC A07/MF A01

Approximate modeling of multiuser computer systems as queueing model is performed. Modeling language SLANG, its syntax, and properties are described and an approximate decomposition procedure is used for performance evaluation of SLANG models. Various approximations are tested and empirically compared with simulation results. ESA

63 CYBERNETICS

Includes feedback and control theory, artificial intelligence, robotics and expert systems.

For related information see also *54 Man/System Technology and Life Support.*

N88-27807# Boston Univ., Mass. Center for Adaptive Systems.
CONTENT-ADDRESSABLE MEMORY STORAGE BY NEURAL NETWORKS: A GENERAL MODEL AND GLOBAL LIAPUNOV METHOD
Stephen Grossberg Mar. 1988 24 p
(Contracts F49620-86-C-0037; F49620-86-C-0018)
(AD-A192716; AFOSR-88-0431TR) Avail: NTIS HC A03/MF A01 CSCL 12I

Many neural network models capable of content-addressable memory are shown to be special cases of the general model and global Liapunov function. These include examples of the additive, brain-state-in-a-box, McCulloch-Pitts, Boltzmann machine, shunting, masking field, bidirectional associative memory, Volterra-Lotka, Gilpin-Ayala, and Eigen-Schuster models. The Cohen-Grossberg model thus defines a general principle for the design of content addressable memory, that is shared by all model exemplars of such a general design constitutes a computational invariant. Such a general model and analytic method defines a computational framework within which specialized model exemplars may be compared to discover which models are best able to explain particular parametric data about brain and behavior, or to solve particular technological problems. GRA

N88-27806# Boston Univ., Mass. Center for Adaptive Systems.
NEURAL NETWORK RESEARCH: A PERSONAL PERSPECTIVE
Stephen Grossberg Mar. 1988 16 p
(Contracts F49620-86-C-0037; F49620-86-C-0018)
(AD-A192717; AFOSR-88-0432TR) Avail: NTIS HC A03/MF A01 CSCL 12I

These vision preprocessor and ART autonomous classifier examples are just two of the many neural network architectures now being developed by engineers and scientists worldwide. Some of them provide a fertile ground for gaining a new understanding of biological intelligence. Others suggest novel computational theories with natural realizations as real-time adaptive neural network architectures with promising properties for tackling some of the outstanding problems in computer science and technology today. Still others do both. Whatever the focus, here is a field ready to challenge and reward the sustained efforts of a wide variety of gifted people. GRA

N88-27809# Auburn Univ., Ala. Dept. of Computer Science and Engineering.
IMPROVING THE PERFORMANCE OF AI ALGORITHMS Final Report, May 1985 - Apr. 1987
Cherri M. Pancake Sep. 1987 116 p
(Contract F30602-81-C-0193)
(AD-A192848; SCEE-PDP/85-48; RADC-TR-87-131) Avail: NTIS HC A06/MF A01 CSCL 12I

The feasibility of improving the efficiency of AI(Artificial Intelligence) software using available systems and methodologies is addressed. By modeling program behavior as a series of concurrent problem solution systems, it is possible to isolate the inefficiencies inherent in the implementation scheme for those due to conceptual difficulties or inadequacies in the underlying physical system. The processing environment selected for the implementation of AI software effectively establishes a computational paradigm which shapes the development and ultimate performance of any program executing within it. Sequential environments view the underlying architecture as von Neuman and approach a problem in terms of the Turing Model of Computation, while applicative environments exemplify the recursion theory approach. Established optimization techniques are intimately tied to the computational model and cannot be transported from one environment to the other with ease or efficiency. Since some AI tasks are inherently sequential and others inherently recursive, no single processing system can facilitate uniformly optimum performance. The concept of environment spanning is suggested as a means of maximizing program optimizability by allowing the assignment of subproblems individually to whatever processing system offers the best chance for automatic improvement. Three mechanisms for implementing spanned environments are presented: parallel environments, multitasked environments, and intersequenced subenvironment modules. GRA

N88-27810# Brown Univ., Providence, R. I. Center for Dynamical Systems.
FEEDBACK CONTROL OF A HYPERBOLIC PARTIAL-DIFFERENTIAL EQUATION WITH VISCOELASTIC DAMPING
J. A. Burns and R. H. Fabiano 15 Apr. 1988 56 p
(Contracts F49620-87-C-0110; F49620-87-C-0088)
(AD-A192896; LCDS/CCS-88-5; AFOSR-88-0575TR) Avail: NTIS HC A04/MF A01 CSCL 12A

In this paper we consider an approximation scheme for an optimal control problem described by a hyperbolic partial-functional differential equation used to model the elastic motion of a viscoelastic body of Boltzmann type. The method is based on combined finite element/averaging approximations. We present theoretical and numerical results for a problem with quadratic cost functional. GRA

N88-27811# Drexel Univ., Philadelphia, Pa. Dept. of Electrical and Computer Engineering.
INTELLIGENT MOBILE AUTONOMOUS SYSTEM (IMAS)
A. M. Meystel 1987 96 p
(AD-A193181) Avail: NTIS HC A05/MF A01 CSCL 12I

This report concludes the research initiated in 1983 with the objective to contribute to fundamentals of the new emerging area of autonomous robotics. The goal of this research is to develop a theory of design and functioning of Intelligent Mobile Autonomous Systems (IMAS) to be utilized for solving various problems of combat engineering. It was the initiative of the research team to combine the fundamental research with the experimental analysis of the IMAS testbed. This work has premises different from those determined in the corresponding DARPA research. It started before the DARPA program (in January 1983), and is based upon the scientific principles, that at the time of the beginning of the research, were pioneering in this area. This research resulted in creation of a theory of nested hierarchical systems and in particular, of the structure of a multiresolutional nonhomogeneous system of representation interacting with a similarly built planning/control system (PLANNER-NAVIGATOR-PILOT-CONTROLLER). The hierarchical nested structure, together with the unique structure of knowledge-representation, as well as capabilities of minimum-time dynamic navigation, and the knowledge-based controller, are promising for IMAS, and are expected to be expanded into the domain of multilink manipulators as well. Testing has confirmed the viability of scientific premises, and has clarified the program of subsequent analysis and scientific research. GRA

N88-27812# Colorado Univ., Boulder. Dept. of Computer Science.
PARALLEL QUASI-NEWTON METHODS FOR UNCONSTRAINED OPTIMIZATION Final Report, 1 Aug. 1984 - 31 Dec. 1987
Richard H. Byrd, Robert B. Schnabel, and Gerald A. Shultz 1 Apr. 1988 46 p
(Contract DAAG29-84-K-0140; Grant NSF CCR-87-02403)
(AD-A193250; CU-CS-396-88; ARO-21453.12-MA) Avail: NTIS HC A03/MF A01 CSCL 12C

This document discusses methods for solving the unconstrained optimization problem on parallel computers, when the number of variables is sufficiently small that quasi-Newton methods can be used. The authors concentrate mainly, but not exclusively, on problems where function evaluation is expensive. First they discuss ways to parallelize both the function evaluation costs and the linear algebra calculations in the standard sequential secant method, the BFGS method. Then described are new methods that are appropriate when there are enough processors to evaluate the function, gradient, and part but not all of the Hessian at each iteration. Developed are new algorithms that utilize this information and analyze their convergence properties. The authors present computational experiments showing that they are superior to parallelization of either the BFGS method or Newton's method under our assumptions on the number of processors and cost of function evaluation. Finally they discuss ways to effectively utilize the gradient values at unsuccessful trial points that are available in our parallel methods and also in some sequential software packages. GRA

N88-27813# Iowa Univ., Iowa City. Optimal Design Lab.
DATABASE DESIGN AND MANAGEMENT IN ENGINEERING OPTIMIZATION Final Technical Report, Oct. 1982 - Feb. 1988
Jasbir S. Arora Feb. 1988 151 p
(Grant AF AFOSR-0322-82)
(AD-A193325; ODL-88.2; AFOSR-88-0366TR) Avail: NTIS HC A08/MF A01 CSCL 12G

In this report, the research completed under the project in the area of database management in engineering design and optimization is described. Database management concepts used in business applications were studied and concepts suitable for engineering applications were developed. Data structures that need to be managed were identified. Database design methodologies were studied and a suitable methodology for engineering designs and optimization applications was developed. Several prototype database management systems (DBMS) were designed, developed

and evaluated. Several prototype application programs utilizing a database management were developed to evaluate performance of DBMS. Based on these implementations and studies, the usual relational data model was generalized to handle engineering data types. Specifications for an integrated DBMS capable of handling relations, vectors and matrices (of different types) were developed. A system based on the specifications, called MIDAS/GR was implemented and evaluated. MIDAS/GR stands for Management of Information for Design and Analysis of Systems/Generalized Relational Model. GRA

N88-27814# Societe Nationale Industrielle Aerospatiale, Paris (France). Div. Engins Tactiques.
INTRODUCTION TO ARTIFICIAL INTELLIGENCE AND EXPERT SYSTEMS [INTRODUCTION A L'INTELLIGENCE ARTIFICIELLE ET AUX SYSTEMES EXPERTS]
S. L. Dupuy 10 Aug. 1987 28 p In FRENCH
(SNIAS-881-320-101; Note-E/ES4-20-126; ETN-88-92843)
Copyright Avail: NTIS HC A03/MF A01

The history and characteristics of artificial intelligence and its expert systems branch are reviewed. The applications to logistics are examined. The difficulties and the very large development effort are discussed. ESA

N88-27815# Societe Nationale Industrielle Aerospatiale, Paris (France). Div. Engins Tactiques.
EXPERT SYSTEM CONTRIBUTION TO LOGISTICS IMPROVEMENT [CONTRIBUTION DES SYSTEMES EXPERTS A L'AMELIORATION DE LA LOGISTIQUE]
S. L. Dupuy 7 Aug. 1987 20 p In FRENCH
(SNIAS-881-320-102; Note-E/ES4-20-120; ETN-88-92844)
Copyright Avail: NTIS HC A03/MF A01

The main characteristics of expert systems are reviewed, and the applications of expert systems to logistics are examined. It is shown that most logistics problems can take advantage of expert systems. An expert system is described in detail. It was developed for the maintenance of the A-30 laser missile battery. ESA

N88-27395# Mitsubishi Electric Corp., Tokyo (Japan). Information Systems and Electronics Development Lab.
THE MELCOM PSI 2 AI WORKSTATION
Takasumi Ueda and Hiroshi Nakashima *In its* Mitsubishi Electric Advance (R and D Edition), Volume 41 Dec. 1987 3 p (For primary document see N88-27388 21-31)
Avail: NTIS HC A03/MF A01 CSCL 09B

64 NUMERICAL ANALYSIS

Includes iteration, difference equations, and numerical approximation.

N88-27816# Oak Ridge National Lab., Tenn.
A ZOOMABLE AND ADAPTABLE HIDDEN FINE-MESH APPROACH TO SOLVING ADVECTION-DISPERSION EQUATIONS
G. T. Yeh 1988 6 p Presented at the 7th International Conference on Computation Methods in Water Resources, Cambridge, Mass., 13 Jun. 1988
(Contract DE-AC05-84OR-21400)
(DE88-006174; CONF-880672-2) Avail: NTIS HC A02/MF A01

A zoomable and adaptable hidden fine-mesh approach (ZAHFMA), that can be used with either finite element or finite difference methods, is proposed to solve the advection-dispersion equation. The approach is based on automatic adaptation of zooming a hidden fine-mesh in the place where the sharp front locates. Preliminary results indicate that ZAHFMA used with finite element methods can handle the advection-dispersion problems with Peclet number ranging from 0 to infinity. DOE

N88-27817# Illinois Univ., Urbana. Dept. of Computer Science.
A TAXONOMY FOR CONJUGATE GRADIENT METHODS
S. F. Ashby, T. A. Manteuffel, and P. E. Saylor Mar. 1988 45 p
(Contracts DE-FG02-87ER25026; W-7405-eng-48)
(DE88-008574; DOE/ER-25026/19; UIUCDCS-R-88-1414; UILU-ENG-88-1719) Avail: NTIS HC A03/MF A01

The conjugate method of Hestenes and Stiefel is an effective method to solve large, sparse hermitian positive definite (hpd) systems of linear equations, Ax equals b. Generalizations to non-hpd matrices have long been sought. The recent theory of Faber and Manteuffle gives necessary and sufficient conditions for the existence of the CG method. This paper uses these conditions to develop and organize such methods. We show that any CG method for Ax equals b is characterized by an hpd inner product matrix B and a left preconditioning matrix C. At each step the method minimizes the B-norm of the error over a Krylov space. This characterization is then used to classify known and new methods. Finally, it is shown how eigenvalue estimates may be obtained from the iteration parameters, generalizing the well known connection between CG and Lanczos. Such estimates allow implementation of a stopping criterion based more nearly on the true error. DOE

N88-27818# Commission of the European Communities (Luxembourg).
CONTROL, STABILITY AND FILTER FOR A DISCRETE LINEAR STOCHASTIC SYSTEM WITH CORRELATED NOISE
O. Lessi 1986 18 p
(PB88-109525; EUR-10632-EN) Copyright Avail: NTIS HC E03/MF E03; copy not available from STI Facility CSCL 12A

For a discrete stationary stochastic linear system with correlated noise, the existence is shown of a linear control which leads to an equivalent model with uncorrelated noise without modifying the stability of the system. Under the hypothesis of correlated noise, the gain of the Kalman filter and the solution of the Riccati equation are determined. Author

N88-27819# Massachusetts Inst. of Tech., Cambridge. Artificial Intelligence Lab.
PARALLEL SOLUTIONS TO GEOMETRIC PROBLEMS ON THE SCAN MODEL OF COMPUTATION Memorandum Report
Guy E. Blelloch and James J. Little Feb. 1988 34 p
(Contracts DACA76-85-C-0010; N00014-85-K-0124)
(AD-A192321; AD-E801594; AI-M-952) Avail: NTIS HC A03/MF A01 CSCL 12B

This paper describes several parallel algorithms that solve geometric problems. The algorithms are based on a vector model of computation - the scan-model. The purpose of this paper is both to show how the model can be used and to show a set of interesting algorithms. A k-D tree algorithm is described that, for n points, requires 0(1g n) calls to the primitives, a closets-pair algorithm that requires 0(1g n) calls to the primitives, a line-drawing algorithm that requires 0(1) calls to the primitives, a line-of-sight algorithm that requires 0(1) calls to the primitives, and finally three different convex-hull algorithms. All these algorithms should be noted for their simplicity rather than complexity; many of them are parallel versions of known serial algorithms. Most of the algorithms discussed in this paper have been implemented on the Connection Machine, a highly parallel single instruction multiple data (SIMD) computer. GRA

N88-27820# California Inst. of Tech., Pasadena. Dept. of Applied Mathematics.
RESEARCH IN APPLIED MATHEMATICS Final Report
G. B. Whitham 14 Mar. 1988 5 p
(Contract N00014-85-K-0403)
(AD-A192385; Rept-57) Avail: NTIS HC A02/MF A01 CSCL 20A

Most of the work has been on shock dynamics, a term we use of problems of the focusing of curved shocks, the diffraction of shocks by bodies or density layers, the propagation of shocks down curved tubes and channels, and the stability of converging shocks. Our earlier theoretical work is described in the book Linear and Nonlinear by G.B. Whitham, and references given there. This theoretical work on shock dynamics had been found by experiments to be extremely useful in practical situations. However, the analytic

results had been limited to fairly simple situations. The numerical scheme originally proposed was again limited and could not hope to handle some of the interesting practical situations. GRA

N88-27821# Yale Univ., New Haven, Conn. Dept. of Computer Science.
A NUMERICAL TREATMENT OF THE FLUID/ELASTIC INTERFACE UNDER RANGE-DEPENDENT ENVIRONMENTS
E. C. Shang and Ding Lee Jan. 1988 44 p
(Contract N00014-87-WX-24234)
(AD-A192476; YALEU/DCS/RR-558) Avail: NTIS HC A03/MF A01 CSCL 08K

The technique introduced by McDaniel-Lee for the handling of the fluid/fluid interface boundary under range-dependent environments is extended to handle the horizontal fluid/elastic interface boundary. Representative wave equations of the parabolic type are considered in both fluid and elastic media. The required interface conditions, (1) continuity of vertical components of displacement, (2) continuity of vertical components of stress, and (3) horizontal components of stress vanish on the interface, are satisfied with this numerical treatment. A complete theoretical development is presented along with a test example to demonstrate its validity. GRA

N88-27822# Brown Univ., Providence, R. I. Center for Dynamical Systems.
A WONG-ZAKAI TYPE THEOREM FOR CERTAIN DISCONTINUOUS SEMIMARTINGALES
Guillermo Ferreyra Jan. 1988 17 p
(Contract DAAG29-84-K-0082; Grant AF AFOSR-0315-85)
(AD-A192713; LCDS/CCS-88-1; AFOSR-88-0388TR) Avail: NTIS HC A03/MF A01 CSCL 12A

Solutions of stochastic differential equations having differentials of bounded variation processes on the right hand side can be defined by means of Lebesgue Stieltjes integrals or by continuous extension of Stieltjes integrals. Both solutions are compared here and formulas that extend the Wong-Zakai theorem are obtained. GRA

N88-27823# Brown Univ., Providence, R. I. Center for Dynamical Systems.
APPROXIMATIONS OF STOCHASTIC EQUATIONS DRIVEN BY PREDICTABLE PROCESSES
Guillermo Ferreyra Dec. 1987 13 p
(Contract DAAG29-84-K-0082; Grant AF AFOSR-0315-85)
(AD-A192714; LCDS/CCS-87-39; AFOSR-88-0387TR) Avail: NTIS HC A03/MF A01 CSCL 12A

A theory of stochastic integral equations driven by predictable processes in Stratonovich sense is developed. These driving processes include a large class of discontinuous semimartingales. The theory of stochastic differential equations driven by continuous semimartingales in Stratonovich sense is extended without involving Lebesgue-Stieltjes integrals as done by Meyer. Moreover, a change of variables formula without extra terms involving the jumps of the processes holds for this theory. Results on approximation of driving processes are preserved. GRA

N88-27824# Massachusetts Inst. of Tech., Cambridge. Lab. for Computer Science.
FINDING MINIMUM-COST CIRCULATIONS BY SUCCESSIVE APPROXIMATION
Andrew V. Goldberg and Robert E. Tarjan Jul. 1987 57 p
(Contract N00014-80-C-0622)
(AD-A192724; MIT/LCS/TM-333) Avail: NTIS HC A04/MF A01 CSCL 12D

We develop a new approach to solving minimum cost circulation problems. Our approach combines methods for solving the maximum flow problems with successive approximation techniques based on cost scaling. We measure the accuracy of a solution by the amount that the complementary slackness conditions are violated. We propose a simple minimum cost circulation algorithm, one version of which runs in O(n3log(nC)) time on an n-vertex network with integer arc costs of absolute value at most C. By incorporating sophisticated data structures into the algorithm, we obtain a time bound of O(nmlog(n2/m)log(nC)) on a network with m arcs. A slightly different use of our approach shows that a minimum cost circulation can be computed by solving a sequence of O(nlog(nC)) blocking flow problems. A corollary of this result is an O(n2(logn)log(nC)-time, n-processor parallel minimum cost circulation algorithm. Our approach also yields strongly polynomial minimum cost circulation algorithms. Our results provide evidence that the minimum cost circulation problem is not much harder than the maximum flow problem. We believe that a suitable implementation of our method will perform extremely well in practice. GRA

N88-27825# Massachusetts Inst. of Tech., Cambridge. Lab. for Computer Science.
FINDING MINIMUM-COST CIRCULATIONS BY CANCELING NEGATIVE CYCLES
Andrew V. Goldberg and Robert E. Tarjan Jul. 1987 20 p
(Contracts N00014-80-C-0622; N00014-87-K-0467)
(AD-A192727; MIT/LCS/TM-334) Avail: NTIS HC A03/MF A01 CSCL 12D

A classical algorithm for finding a minimum cost circulation consists of repeatedly finding a residual cycle of negative cost and canceling it by pushing enough flow around the cycle to saturate an arc. We show that a judicious choice of cycles for canceling leads to a polynomial bound on the number of iterations in this algorithm. This gives a very simple strongly polynomial algorithm that uses no scaling. A variant of the algorithm that uses dynamic trees runs in 0(nm(log n)min(log(nC), mlog n)) time on a network of n vertices, m arcs, and arc costs of maximum absolute value C. This bound is comparable to those of the fastest previously known algorithms. GRA

N88-27826# North Carolina Univ., Chapel Hill. Center for Stochastic Processes.
COMPUTATION OF FILTERS BY SAMPLING AND QUANTIZATION Report, Sep. 1987 - Aug. 1988
A. H. Korezlioglu Sep. 1987 31 p
(Contract F49620-85-C-0144)
(AD-A192839; TR-208; AFOSR-88-0356TR) Avail: NTIS HC A03/MF A01 CSCL 12C

Various approximation procedures of filters by sampling and quantization are considered for effective computation. The corresponding approximation degrees are estimated without the boundedness condition on the modulated signal. GRA

N88-27827# Rome Univ. (Italy). Dept. of Mathematics.
NUMERICAL OPTIMIZATION Periodic Report, 1-4, Jul. 1986 - Jan. 1988
Francesco Zirilli Jan. 1988 82 p
(Contract DAJA45-86-C-0028)
(AD-A193032) Avail: NTIS HC A05/MF A01 CSCL 12A

The first objective the authors pursued was to build some test problems in the area of linear and nonlinear complementarity problems in order to be able to verify the practical value of our algorithms before submitting them to a detailed mathematical analysis. A large variety of problems of different difficulty belongs to the area of linear and nonlinear complementarity; to start our investigation we have considered three problems that come from the discretization of variational inequalities of mathematical physics. The first two problems are linear complementarity problems; the third one is a nonlinear complementarity problem. The corresponding continuous problems involve ordinary or partial differential operators so that when discretized a large number (up to a few thousand) independent variables can be considered. A FORTRAN computer code implementing these three complementarity problems has been written. The complementarity problems considered above have been translated into a system of nonlinear equations. On the resulting systems of nonlinear equations, the algorithm DAFNE based on the use of ordinary differential equations and the algorithm SIGMA based on the use of stochastic differential equations have been used. GRA

N88-27828# Pittsburgh Univ., Pa. Center for Multivariate Analysis.
ON SOLVABILITY OF AN EQUATION ARISING IN THE THEORY OF M-ESTIMATES
Z. D. Bai, X. R. Chen, B. Q. Miao, and Y. H. Wu Nov. 1987 18 p
(Contracts N00014-85-K-0292; F49620-85-C-0008)
(AD-A193059; TR-87-46; AFOSR-88-0400TR) Avail: NTIS HC A03/MF A01 CSCL 12C

This article, by obtaining the limit of probability that some equation arising in a case of M-estimate possesses at least one solution, establishes the fact that even in the simplest case, when the function rho is not differentiable at least at one point, it is not legitimate to convert a minimization problem defining the M-estimate to the solution of equations. GRA

N88-27829# Pittsburgh Univ., Pa. Center for Multivariate Analysis.
A UNIFIED APPROACH TO ESTIMATION IN LINEAR MODELS WITH FIXED AND MIXED EFFECTS
C. R. Rao Nov. 1987 19 p
(Contracts N00014-85-K-0292; F49620-85-C-0008)
(AD-A193060; TR-87-44; AFOSR-88-0399TR) Avail: NTIS HC A03/MF A01 CSCL 12C

A unified approach is developed for the estimation of unknown fixed parameters and prediction of random effects in a mixed Gauss-Markoff linear model. It is shown that both the estimators and their mean square errors can be expressed in terms of the elements of a g-inverse of a partitioned matrix which can be set up in terms of the matrices used in expressing the model. No assumptions are made on the ranks of the matrices involved. The method is parallel to the one developed by the author in the case of the fixed effects Gauss-Markoff model using a g-inverse of a partitioned matrix. A new concept of generalized normal equations is introduced for the simultaneous estimation of fixed parameters, random effects and random error. All the results are deduced from a general lemma on an optimization problem. This paper is self contained as all the algebraic results used are stated and proved. The unified theory developed in an earlier paper (Rao, 1988) is somewhat simplified. GRA

N88-27830# Hatfield Polytechnic (England). Numerical Optimisation Centre.
A REVIEW OF PARALLEL METHODS FOR SOLVING SETS OF LINEAR EQUATIONS AND THEIR APPLICATION WITHIN OPTIMISATION ALGORITHMS Interim Report No. 1
L. C. Dixon Nov. 1987 22 p
(Contract DAJA45-87-C-0038)
(AD-A193137; TR-188) Avail: NTIS HC A03/MF A01 CSCL 12E

When solving optimization problems on a parallel computing system, the first consideration must be to utilize the parallelism to speed up the 95 percent of the time typically spent in function and gradient evaluations or the division of each function evaluation into a number of parallel tasks. Assuming this prime task has been undertaken effectively then for efficiency the other 5 percent of the computation must also utilize the parallelism available on the system. The dominant remaining calculation is usually the solution of a set of linear equations. In this paper the implication of parallel processing on the solution method for solving linear equations will be reviewed. GRA

N88-27831# California Univ., Riverside.
MEASURING DISPERSION EFFECTS OF FACTORS IN FACTORIAL EXPERIMENTS
Subir Ghosh and Eric S. Lagergren Jan. 1988 29 p
(Grant AF AFOSR-0048-87)
(AD-A193216; TR-159; AFOSR-88-0493TR) Avail: NTIS HC A03/MF A01 CSCL 12D

This paper is an attempt to understand and measure dispersion effects of factors in factorial experiments. The simplest setting is considered in order to develop better comprehension and insight. The properties of the proposed descriptive measures are examined. A method of adjusting residuals and its use in measuring dispersion effects are discussed. Illustrative examples are also given. The problem considered in this paper arises in quality control studies and the methodologies are applicable to industrial experiments. GRA

N88-27832# Wisconsin Univ., Madison. Center for Mathematical Sciences.
A SIMPLE EXPLANATION OF THE STOKES PHENOMENON Technical Summary Report
Richard E. Meyer Nov. 1987 24 p
(Grants AF AFOSR-0194-87; NSF DMS-85-21687)
(AD-A193253; CMS-TSR-88-18) Avail: NTIS HC A03/MF A01 CSCL 12A

The Stokes Phenomenon is known to be a pervasive feature of asymptotics, but its explanation in the literature is obscured by intricate and lengthy technicalities. This article presents a simpler approach to its understanding and treatment as a natural aspect of a well-motivated characterization of functions by approximants of different multivaluedness. GRA

N88-27833# Virginia Univ., Charlottesville. Dept. of Electrical Engineering.
ROBUST PREDICTION FOR STATIONARY PROCESSES: 2D ENRICHED VERSION Report, 1 Jul. 1987 - 30 Jun. 1988
P. Papantoni-Kazakos and Kailash Birmiwal 24 Nov. 1987 75 p
(Grant AF AFOSR-0224-87)
(AD-A193318; UVA/525682/EE88/103; AFOSR-88-0361TR)
Avail: NTIS HC A04/MF A01 CSCL 12C

Predictions are considered for stationary processes in environments where data outliers may be present. Two sequences are developed for outlier resistant prediction operations, which are uniformly qualitatively robust. The asymptotic mean-squared performance of the developed operations are studied in the absence of data outliers. Important performance characteristics studied include the breakdown point and the influence function. Included are numerical results, for some autoregressive nominal processes. GRA

N88-27834# Pittsburgh Univ., Pa. Center for Multivariate Analysis.
FURTHER EXTENSIONS OF THE CHOQUET-DENY AND DENY THEOREMS WITH APPLICATIONS IN CHARACTERIZATION THEORY Technical Report, period ending Aug. 1987
C. R. Rao and D. N. Shanbhag Aug. 1987 30 p
(Contract F49620-85-C-0008)
(AD-A193358; TR-87-26; AFOSR-88-0204TR) Avail: NTIS HC A03/MF A01 CSCL 12A

This paper aims at extending the Davies-Shanbhag (1987) result to situations covering the problems considered by Schimizu (1978, 1980), Gu and Lau (1984) and Ramachandran et al (1987). Section 2 gives the results when H is bounded and micron is replaced by a certain bounded signed measure subsuming the specialized versions of the results given earlier by Shimizu (1978) and Ramchandran et al (1987); these turn out to be also extended versions of the Choquet-Deny theorem. Section 3 considers an extension of the Davies-Shanbhag result for the case of two simultaneous equations yielding the results of Ramachandran et al (1987) and those arrived at by some of the authors as special cases. Section 4 obtains extended versions of the results involving error terms given earlier by Shimizu (1980) and Gu and Lau (1984), and finally in Section 5, we discuss some applications. GRA

N88-27835# Pittsburgh Univ., Pa. Center for Multivariate Analysis.
ASYMPTOTIC NORMALITY OF MINIMUM L1-NORM ESTIMATES IN LINEAR MODELS
Z. D. Bai, X. R. Chen, Y. Wu, and L. C. Zhao Sep. 1987 36 p
(Contracts N00014-85-K-0292; F49620-85-C-0008)
(AD-A193399; TR-87-35; AFOSR-88-0202TR) Avail: NTIS HC A03/MF A01 CSCL 12C

This document considers a standard linear regression model

with assumed known p-vectors, unknown p-vectors of regression coefficients, and an independent random error sequence each having a median zero. GRA

N88-27836# California Univ., Davis.
MATRIX SUBSTRUCTURING, DOMAIN DECOMPOSITION AND PARTICLE METHODS: CURRENT TRENDS FOR SOLVING PDEs IN PARALLEL
Bracy Elton, A. Louise Perkins, and Garry Rodrigue 21 Apr. 1988 28 p Presented at the IEE Workshop on Design and Application of Parallel Digital Processors, Lisbon, Portugal, 11 Apr. 1988 Prepared in cooperation with Lawrence Livermore National Lab., Calif.
(Contract W-7405-eng-48)
(DE88-009826; UCRL-98663; CONF-8804118-1) Avail: NTIS HC A03/MF A01

This paper discusses some of the directions being taken in the development of numerical algorithms that can be efficiently executed on vector and parallel computers. Heretofore, most of the research has been on developing parallel algorithms for solving a linear system of equations. Realizing that the brief description does not do justice to many of the algorithms so devised, an extensive reference list is given. Two approaches are discussed that will have an important impact on the development of parallel algorithms. Each is motivated from the assumption that the most effective way for obtaining parallelism is to approach the scientific problem differently. A technique that has been labeled domain decomposition is studied. The basic idea is that the scientific problem is not modeled by a single mathematical model but rather as a collection of mathematical models coupled to one another through the spatial domain of influence of the global physical problem. New directions in particle methods are studied. The idea of viewing the physical world as particles instead of continuum is resurrected, and new particle methods developed for use on parallel computers are discussed. DOE

N88-27837# Joint Inst. for Nuclear Research, Dubna (USSR). Lab. of Theoretical Physics.
STRUCTURE OF BOUND STATES IN POLYNOMIAL POTENTIALS
M. Znojil 1987 9 p
(DE88-702437; JINR-E-5-87-481) Avail: NTIS (US Sales Only) HC A02/MF A01

For an arbitrary polynomial potential, a rigorous construction of the corresponding difference Schroedinger equation and its non-variational asymptotical physical boundary conditions is given. The two alternative solution methods are also described. If applicable, the method of Hill determinants may be recovered as the simple special case. DOE

N88-27838# Lawrence Livermore National Lab., Calif.
STAGGERED-GRID FINITE ELEMENT SOLUTION TECHNIQUE FOR THE MAXWELL'S EQUATIONS IN THE TIME DOMAIN
R. L. Lee and N. K. Madsen May 1988 8 p Presented at the 1st Woodward Conference on Wave Phenomena Theoretical, Computational and Practical Aspects, San Jose, Calif., 2 Jun. 1988
(Contract W-7405-eng-48)
(DE88-011731; UCRL-98822; CONF-8806147-1) Avail: NTIS HC A02/MF A01

In this paper, the authors present a two-dimensional Galerkin finite element formulation of the Maxwell's equations in the time domain. The Galerkin element integrals are computed analytically and an explicit forward-backward time integration scheme is employed for advancing the resulting set of ordinary differential equations in time. The authors will compare two formulations of the simple 4-node bilinear element: (1) an equal-order interpolation element in which both the electric field and the magnetic field are approximated by bilinear basis functions; and (2) a mixed-interpolation element in which the electric field is approximated as piecewise constant and the magnetic field as piecewise bilinear functions. The mixed formulation may be viewed as a finite element analog to certain staggered finite difference representations. Numerical examples will be presented to evaluate the accuracy of these two elements. DOE

N88-27839# Oak Ridge National Lab., Tenn.
PARALLEL IMPLEMENTATION OF THE BOUNDARY ELEMENT METHOD
J. Drake and L. J. Gray 1988 15 p Presented at the 2nd International Conference on Vector and Parallel Computing: Issues in Applied Research and Development, Tromso, Norway, 6 Jun. 1988
(Contract DE-AC05-84OR-21400)
(DE88-011846; CONF-8806154-1) Avail: NTIS HC A03/MF A01

The issues associated with the parallel implementation of the boundary element method (BEM) on a hypercube are addressed. The program for solving the three-dimensional Laplace equation is specifically adapted for electro-plating simulations; this application involves nonlinear boundary conditions and a time step iteration to follow the development of the plated surface. As a consequence, the coefficient matrices of the potential and normal derivative values are formed separately and stored. A step of the algorithm is thus required to combine and rearrange the system of equations into the standard form $AX = B$. The matrix A is dense and non-symmetric and recent advances in the solution of such systems on a hypercube are employed. Estimates of the arithmetic complexity at each step of the algorithm and a model for the communication costs are used to study the parallel performance of the BEM; timing results are presented for an implementation on an Intel iPSC2/d6 hypercube. The authors conclude that the BEM is particularly well suited for parallel solution and can be implemented efficiently on a hypercube. DOE

N88-27840# Illinois Univ., Urbana. Dept. of Computer Science.
UNIFIED MULTILEVEL ADAPTIVE FINITE ELEMENT METHODS FOR ELLIPTIC PROBLEMS Ph.D. Thesis
W. F. Mitchell May 1988 111 p
(Contract DE-FG02-87ER-25026)
(DE88-011938; DOE/ER-25026/21; UIUCDCS-R-88-1436; UILU-ENG-88-1741) Avail: NTIS HC A06/MF A01

Many elliptic partial differential equations can be solved numerically with near optimal efficiency through the uses of adaptive refinement and multigrid solution techniques. It is our goal to develop a more unified approach to the combined process of adaptive refinement and multigrid solution which can be with high order finite elements. The basic step of the refinement process is the bisection of a pair of triangles, which corresponds to the addition of one or more basis functions to the approximation space. An approximation of the resulting change in the solution is used as an error indicator to determine which triangles to divide. The multigrid iteration uses a red-black Gauss--Seidel relaxation in which the black relaxations are used only locally. The grid transfers use the change between the nodal and hierarchical bases. This multigrid iteration requires only O(N) operations, even for highly nonuniform grids, and is defined for any finite element space. The full multigrid method is an optimal blending of the processes of adaptive refinement and multigrid iteration. So as to minimize the number of operations required, the duration of the refinement phase is based on increasing the dimension of the approximation space by some fixed factor which is determined to be the largest possible for the given error-reducing power of the multigrid iteration. The result is an algorithm which: (1) uses only O(N) operations with a reasonable constant of proportionality, (2) solves the discrete system to the accuracy of the discretization error, and (3) is able to achieve the optimal order of convergence of the discretization error in the presence of singularities. Numerical experiments confirm this for linear, quadratic and cubic elements. It is believed that the method can also be applied to more practical problems involving systems of PDE'S, time dependence, and three spatial dimensions. DOE

N88-27841# Lawrence Livermore National Lab., Calif.
KRYSI, AN ODE SOLVER COMBINING A SEMI-IMPLICIT RUNGE-KUTTA METHOD AND A PRECONDITIONED KRYLOV METHOD
A. C. Hindmarsh and S. P. Noersett May 1988 31 p Prepared in cooperation with Trondheim Univ., Norway
(Contract W-7405-eng-48)
(DE88-012245; UCID-21422) Avail: NTIS HC A03/MF A01

This report describes KRYSI, a solver for ordinary differential equation (ODE) initial value problems that uses a combination of two powerful techniques in the case of stiff systems. KRYSI is based on the SIMPLE solver, and (like SIMPLE) uses a 3-stage 3rd order SDIRK method. When solving the implicit stage equations in the stiff case, both use some form of Newton iteration. But there, KRYSI (unlike SIMPLE) uses a Krylov subspace iteration method, called SPIGMR: scaled Preconditioned Incomplete Generalized Minimum Residual method. The SPIGMR algorithm is outlined in the SDIRK context. No explicit Jacobian storage is required, except where used in preconditioning. The KRYSI package and its usage are described briefly. One test (demonstration) problem is given, along with a description of two preconditioners that are natural for its solution by KRYSI. The KRYSI solution results are given, and compared with those of LSODPK, a solver that combines a BDF method with the same SPIGMR algorithm. DOE

N88-27842# Technische Univ., Berlin (West Germany). Inst. fuer Luft- und Raumfahrt.
FINITE ELEMENT METHOD FOR PLATE STRUCTURES WITH INCLINED ANGLES [EIN FINITE-ELEMENT-VERFAHREN ZUR BERECHNUNG VON SCHIEFWINKLIGEN PLATTENSTRUKTUREN]
Martin Wiedemann 1987 55 p In GERMAN
(ILR-Mitt-182; ETN-88-92109) Avail: NTIS HC A04/MF A01

Finite element theory is presented on the example of square plates and extrapolated for the analysis of inclined angle plate structures and other parallelogram shaped plates. Finite element stiffness matrix, element load vectors, inhomogeneous boundary conditions, and knots load in system load vector are included in the computer program. ESA

N88-27843# Technische Univ., Brunswick (West Germany). Naturwissenschaftlichen Fakultaet.
ASYMPTOTIC OF PEANOKERNS OF FINITE FIXED ORDER Ph.D. Thesis [ASYMPTOTIK VON PEANOKERNEN BELIEBIGER FESTER ORDNUNG]
Knut Petras 1987 117 p In GERMAN
(ETN-88-92381) Avail: NTIS HC A06/MF A01

Functional relations between Peanokern and Bernouilli polynomials are studied for the determination of asymptotic of Peanokern norms. Quadrature procedure and norm approximation for the first Peanokerns are described. Numerical results are presented in tables for higher order Peanokerns. ESA

N88-27844# Technische Univ., Brunswick (West Germany). Naturwissenschaftlichen Fakultaet.
FLEXIBLE VALUED ALGEBRAS OF FOUR-DIMENSIONS Ph.D. Thesis [FLEXIBLE BEWERTETE ALGEBREN DER DIMENSION 4]
Uwe Kuehne 1987 57 p In GERMAN
(ETN-88-92382) Avail: NTIS HC A04/MF A01

Structure of flexible valued algebras is studied for 1-, 2-, 4-, and 8-dimensions. Properties, conjugators, and K-roots are outlined emphasizing the structure of 4-dimension algebras. ESA

N88-27358# California Univ., Santa Cruz. Dept. of Mathematics.
APPLICATIONS OF DIFFERENTIAL GEOMETRY TO THE SHAPE ANALYSIS OF GRAY-VALUE IMAGES Final Report
Otto Michael Melko *In* Universal Energy Systems, Inc., United States Air Force Graduate Student Summer Support Program, Volume 2 Dec. 1987 20 p (For primary document see N88-27355 21-31)
Avail: NTIS HC A99/MF E03 CSCL 12P

65 STATISTICS AND PROBABILITY

Includes data sampling and smoothing; Monte Carlo method; and stochastic processes.

N88-27845# Pittsburgh Univ., Pa. Inst. for Computational Mathematics and Applications.
GENERALIZED JORDAN CHAINS AND TWO BIFURCATION THEOREMS OF KRASNOSELSKII
Patrick J. Rabier 2 Jan. 1988 60 p
(Grant AF AFOSR-0131-84)
(AD-A192353; ICMA-88-115; AFOSR-88-0246TR) Avail: NTIS HC A04/MF A01 CSCL 12B

Given two Banach spaces X and Y over K = R or C and a parameterized family A (mu) an element of L(X, Y) with mu an element of K, partial and algebraic multiplicities of any value mu sub 0 an element of K such that A (mu sub 0) if Fredholm with index zero are defined by the means of generalized Jordan chains. These notions are developed in close connection with bifurcation problems and we show that partial and algebraic multiplicities are not affected by Lyapunov-Schmidt reduction. Properties of invariance under equivalence are also established. These general results are used to give a proof of Magnus' generalization of the classical bifurcation theorem by Krasnoselskii through a somewhat more natural approach than his. But the convincing evidence of the usefulness of the notions developed here has to be found in a new and wide extension of the Boehme-Marino-Rabinowitz theorem on bifurcation for gradient operators, the ancestor of which is also due to Krasnoselskii. GRA

N88-27846# Florida State Univ., Tallahassee. Dept. of Statistics.
FREE BOUNDARY CONTROL OF THE MARKOV PROCESS Final Report, 15 Jul. - 15 Dec. 1987
Michael Taksar 4 Jan. 1988 5 p
(Grant AF AFOSR-0278-87)
(AD-A192401; AFOSR-88-0047TR) Avail: NTIS HC A02/MF A01 CSCL 12C

The investigator made progress extending the theory of free boundary control (or singular control) to the multidimensional case. Two papers were submitted for publication: Optimal corrections problem of a multidimensional stochastic system and Deterministic equivalents for a continuous linear-convex stochastic control problem. GRA

N88-27847# Brown Univ., Providence, R. I. Center for Dynamical Systems.
APPROXIMATIONS AND OPTIMAL CONTROL FOR THE PATHWISE AVERAGE COST PER UNIT TIME AND DISCOUNTED PROBLEMS FOR WIDEBAND NOISE DRIVEN SYSTEMS
Harold J. Kushner Jan. 1988 35 p
(Contract DAAL03-86-K-0171; Grant AF AFOSR-0315-85)
(AD-A192712; LCDS/CCS-88-3; AFOSR-88-0394TR) Avail: NTIS HC A03/MF A01 CSCL 09A

Average cost per unit time (over an infinite time horizon) optimal control problems for diffusion and other Markov models have been dealt with in various ways. We treat such a problem for wideband noise driven and related systems, which are close to a diffusion, and when the average is in the pathwise but not necessarily in the mean value sense. The general method works for many other classes of processes which are suitable approximated by an appropriate controlled Markov process. The results have applications to many other problems where pathwise averages are important, and the noises are wideband. GRA

N88-27848# North Carolina Univ., Chapel Hill. Center for Stochastic Processes.
ON THE EXCEEDANCE RANDOM MEASURES FOR STATIONARY PROCESSES Report, Sep. 1987 - Aug. 1988
M. R. Leadbetter Nov. 1987 27 p
(Contract F49620-85-C-0144)
(AD-A192838; TR-215; AFOSR-88-0350TR) Avail: NTIS HC A03/MF A01 CSCL 12C

Two common approaches to extremal theory for stationary processes involve: (1) consideration of point processes of upcrossings of high levels, and (2) use of the total exceedance time above such levels. The approach (1) yields a greater variety of interesting results regarding the global and local maxima, but requires more by way of regularity conditions on the sample paths, than does the approach (2). This work combines both approaches by consideration of the exceedance random measure thereby obtaining general results under weak conditions on the sample functions. These include previously known results in the case where more sample function regularity is assumed. GRA

N88-27849# North Carolina Univ., Chapel Hill. Center for Stochastic Processes.
A NOTE ON VECTOR BIMEASURES Report, Sep. 1987 - Aug. 1988
Christian Houdre Nov. 1987 8 p
(Contract F49620-85-C-0144)
(AD-A192841; TR-214; AFOSR-88-0349TR) Avail: NTIS HC A02/MF A01 CSCL 12C

A Fubini type theorem is obtained for vector bimeasure integrals. GRA

N88-27850# North Carolina Univ., Chapel Hill. Center for Stochastic Processes.
A STUDY ON LEBESGUE DECOMPOSITION OF MEASURES INDUCED BY STABLE PROCESSES Technical Report, Sep. 1987 - Aug. 1988
Mauro Sergio DeFreitasMarques Nov. 1987 85 p
(Contract F49620-85-C-0144)
(AD-A192893; TR-216; AFOSR-88-0360TR) Avail: NTIS HC A05/MF A01 CSCL 12C

The Lebesgue decomposition of measures induced by symmetric stable process is considered. An upper bound for the set of admissible translates of a general pth order process is presented, which is a partial analog of the reproducing kernel Hilbert space of a second order process. For invertible processes a dichotomy is established: each translate is either admissible or singular, and the admissible translates are characterized. As a consequence, most continuous time moving averages and all harmonizable processes with nonatomic spectral measure have no admissible translate. Necessary and sufficient conditions for equivalence and singularity of certain product measures are given and applied to the problem of distinguishing a sequence of random vectors from affine transformations of itself; in particular sequences of stable random variables are considered and the singularity of sequences with different indexes of stability is proved. Sufficient conditions for singularity and necessary conditions for absolute continuity are given for the pth order processes. Finally the dichotomy two processes are either equivalent or singular, is shown to hold for certain stable processes such as independently scattered random measures and harmonizable processes. GRA

N88-27851# North Carolina Univ., Chapel Hill. Center for Stochastic Processes.
MULTIPLE INTEGRATION WITH RESPECT TO POISSON AND LEVY PROCESSES Report, Sep. 1987 - Aug. 1988
Olav Kallenberg and Jerzy Szulga Feb. 1988 48 p
(Contract F49620-85-C-0144; Grants NSF DMS-87-03804; NSF DMS-87-13103)
(AD-A192895; TR-224; AFOSR-88-0420TR) Avail: NTIS HC A03/MF A01 CSCL 12C

Necessary and sufficient conditions are given for the existence of a multiple stochastic integral of the form (integral over) fdx1...dXd, where X1,...,Xd are components of a positive or symmetric pure jump type Levy process in R to the dth power. Conditions are also given for a sequence of integrals of this type to converge in probability to zero or infinity, or to be tight. All arguments proceed via reduction to the special case of Poisson integrals. GRA

N88-27852# Massachusetts Inst. of Tech., Cambridge.
STATISTICAL DESCRIPTION OF STOCHASTIC DYNAMICS Final Report, 1 Jun. 1987 - 31 May 1988
Alexander B. Rechester 15 May 1988 5 p
(Grant AF-AFOSR-0254-87)
(AD-A192924; AFOSR-88-0407TR) Avail: NTIS HC A02/MF A01 CSCL 12C

The main result of our research is the establishment of a general relationship for fluctuation of the spectral density of the chaotic motion which is similar to the Einstein fluctuation formula in statistical mechanics. A Gibbs-type partition of the chaotic motion is introduced. The distribution function of the spectral density defined on such partition is Gaussian. The variance of this distribution is the Fourier transform of the correlation function. This is demonstrated by direct numerical computations for the simple models of chaos. These results are the consequence of translational invariance and should be valid for the general case of chaotic motion described by differential equations. GRA

N88-27853# Pittsburgh Univ., Pa. Center for Multivariate Analysis.
STATISTICAL ANALYSIS OF DYADIC STATIONARY PROCESSES
M. Taniguchi, L. C. Zhao, P. R. Krishnaiah, and Z. D. Bai Sep. 1987 32 p
(Contracts N00014-85-K-0292; F49620-85-C-0008)
(AD-A193057; TR-87-40; AFOSR-88-0398TR) Avail: NTIS HC A03/MF A01 CSCL 12C

There has been much discussion of Walsh spectral analysis for dyadic stationary processes. Morettin investigated some asymptotic properties of the finite Walsh transforms of dyadic stationary processes. Nagai gave the spectral respresentations for dyadic stationary processes. If we consider finite dyadic linear models then the greatest differences between dyadic stationary processes and ordinary stationary ones appear. Nagai and Nagai and Taniguchi established that a dyadic autoregressive and moving average process of finite order and also as a dyadic moving average process of finite order. Nagai and Taniguchi discussed the principal component analysis of a multiple dyadic process, and also the canonical correlation analysis. Morettin gave a convenient survey for Walsh spectral analysis. This paper considers a multiple dyadic stationary process with a Walsh spectral density matrix. GRA

N88-27854# Stanford Univ., Calif. Dept. of Statistics.
ON THE ESTIMATION OF A VARIANCE RATIO
Alan E. Gelfand and Dipak K. Dey 6 Apr. 1988 19 p
(Contract N00014-86-K-0156)
(AD-A193190; TR-403) Avail: NTIS HC A03/MF A01 CSCL 12C

The estimation of the ratio of two independent normal variances is considered under scale invariant squared error loss function, when the means are unknown. The best invariant estimator is shown to be inadmissible. Two new classes of improved estimators are obtained, one by extending Stein (1964) and the other by extending Brown (1968). Numerical studies are presented to indicate the percent improvements in risk. GRA

N88-27855# North Carolina Univ., Chapel Hill. Dept. of Statistics.
THE COMPUTATION OF STATIONARY DISTRIBUTIONS ON MARKOV CHAINS THROUGH PERTURBATIONS Technical Report, Sep. 1987 - Aug. 1988
Jeffrey J. Hunter Mar. 1988 23 p
(Contract F49620-85-C-0144)
(AD-A193191; TR-227; AFOSR-88-0396TR) Avail: NTIS HC A03/MF A01 CSCL 12C

An algorithmic procedure, for the determination of the stationary distribution of a finite, m-state, irreducible Markov chain, that does

not require the use of methods for solving systems of linear equations, is presented. The technique is based upon a succession of m, rank one, perturbations of the trivial doubly stochastic matrix whose known steady state vector is updated at each stage to yield the required stationary probability vector. GRA

N88-27856# Pittsburgh Univ., Pa. Center for Multivariate Analysis.
JOINT ASYMPTOTIC DISTRIBUTION OF MARGINAL QUANTILES AND QUANTILE FUNCTIONS IN SAMPLES FROM A MULTIVARIATE POPULATION
C. J. Babu and C. R. Rao Oct. 1987 16 p
(Contract F49620-85-C-0008)
(AD-A193385; TR-87-42; AFOSR-88-0199TR) Avail: NTIS HC A03/MF A01 CSCL 12C

The joint asymptotic distributions of the marginal quantiles and quantile functions in samples from a p-variate population are derived. Of particular interest is the joint asymptotic distribution of the marginal sample medians, on the basis of which tests of significance for population medians are developed. Methods of estimating unknown nuisance parameters are discussed. The approach is completely nonparametric. GRA

N88-27857# Sandia National Labs., Albuquerque, N. Mex.
THE SAS SYSTEM BY FORMS: PUTTING STATISTICAL POWER INTO THE HANDS OF AN END-USER
J. W. Lee Apr. 1988 16 p
(Contract DE-AC04-76DP-00789)
(DE88-010512; SAND-87-2356) Avail: NTIS HC A03/MF A01

A major step in speed and flexibility in statistical calculations was achieved with fourth-generation languages like base SAS software. Programming is reduced to a few lines of commands and options. However, because of the proliferation of options, proper training is required to learn which lines of code (with proper syntax) will achieve the desired purpose. Since most end-users lack this training, fourth-generation languages have fallen short of their potential. Canned SAS programs written for applications that reference a limited and static database are a possible solution. These programs, however, are not effective in a dynamic environment where multiple datasets are individually defined and are unstable, i.e., they change in time. With a database of several hundred different datasets, producing a single application for each dataset would be difficult, let alone providing the flexible functionality that is desired. In this report, we hope to demonstrate how the full power of the SAS System can be integrated so that end-users with limited training can perform their own analyses in this environment. Specifically, we will describe how SAS software is integrated into a menu-driven, interactive retrieval and analysis system (MIRACLE). DOE

N88-27858# Oak Ridge National Lab., Tenn.
COMPARISON OF RESULTS BASED ON A DETERMINISTIC VERSUS A STATISTICAL UNCERTAINTY ANALYSIS
R. E. Maerker May 1988 78 p
(Contract DE-AC05-84OR-21400)
(DE88-010751; ORNL/TM-10773) Avail: NTIS HC A05/MF A01

A deterministic method for performing an uncertainty analysis is applied to the results of a system of three codes previously analyzed by purely statistical means. This new method propagates joint probabilities through computer models to obtain the distributions of model results by linear extrapolation from a pool of several gradient-enhanced reference runs. Results employing various options in the method are tested against those from the earlier statistical treatment. Both point-by-point and cumulative distribution comparisons were generally performed. The effort leads to the conclusion that in the present application 15 gradient enhanced runs provide virtually as much uncertainty information as 200 statistical executions of the code system, and this feature of the analysis is expected to remain generally valid for most types of problems. The advantage of significant reduction in the number if reference runs required by the deterministic method is partially offset by the longer execution times of the enhanced versions of the codes, however. Thus efficient derivative-taking algorithms will be necessary to insure cost efectiveness. DOE

N88-27859# Sandia National Labs., Albuquerque, N. Mex.
A COMPARISON OF GENERATORS FOR PSEUDO-RANDOM NORMAL DEVIATES
J. M. DeLaurentis and B. A. Boughton Apr. 1988 12 p
(Contract DE-AC04-76DP-00789)
(DE88-011711; SAND-88-0952) Avail: NTIS HC A03/MF A01

Stochastic models of physical systems often require the generation of a large number of normally distributed random numbers. This investigation studies three different algorithms for generating pseudo-random normal deviates: a method based on the Central Limit Theorem, the polar method and the ratio method. These techniques were chosen because they provide portable generators that are easily implemented in any higher-level programming language. This report shows that all three methods produce reliable statistics, but that the polar method is considerably faster. DOE

66 SYSTEMS ANALYSIS

Includes mathematical modeling; network analysis; and operations research.

N88-27860# Army War Coll., Carlisle Barracks, Pa.
FUTURE SDI (STRATEGIC DEFENSE INITIATIVE) DECISION MAKING
Barry W. Holman 29 Mar. 1988 36 p
(AD-A192794) Avail: NTIS HC A03/MF A01 CSCL 05D

Nearly five years have lapsed since President Reagan made his now famous speech launching his Strategic Defense Initiative. Yet, polarized debate continues over the program's feasibility, desirability, affordability, goals, and direction. Some claim the program's goals have changed over time, and that today the primary goal is for an enhanced deterrence rather than providing a population defense as originally envisioned. Although the Congress has provided continuing and expanded funding for SDI, a consensus does not exist between the Congress and the Administration over the program's direction and goals. Some concerns exist within the Congress that the Administration is rushing too quickly to reach a decision on initial system development. Others would like to see initial development of a more limited defensive capability than that envisioned by the SDI program. This paper examines the evolution of SDI from a policy standpoint and addresses a series of questions that taken together may suggest parameters for future decision making. GRA

N88-27861# Los Alamos National Lab., N. Mex.
OVERVIEW OF THE SDI (STRATEGIC DEFENSE INITIATIVE) PROGRAM IN SHORT WAVELENGTH CHEMICAL LASERS
C. R. Jones 1988 19 p Presented at the Society of Photo-Optical Instrumentation Engineers Meeting, Los Angeles, Calif., 1 Nov. 1987
(Contract W-7405-eng-36)
(DE88-007912; LA-UR-88-640; CONF-8711172-1) Avail: NTIS HC A03/MF A01

Advanced chemical lasers promise to be effective space-based weapons against responsive threats. In this program, both CW and pulsed concepts are developed to achieve this goal. Certain approaches may also be appropriate as ground-based weapons and fusion drivers. DOE

67 THEORETICAL MATHEMATICS

Includes topology and number theory.

N88-27862# International Centre for Theoretical Physics, Trieste (Italy).
SUPERALGEBRAS WITH GRASSMANN ALGEBRA-VALUED STRUCTURE CONSTANTS FROM SUPERFIELDS
J. A. deAzcarraga and J. Lukierski May 1987 17 p
(DE88-702239; IC-87/68) Avail: NTIS (US Sales Only) HC A03/MF A01

We introduce generalized Lie algebras and superalgebras with generators and structure constants taking values in a Grassmann algebra. Such algebraic structures describe the equal time algebras in the superfield formalism. As an example we consider the equal time commutators and anticommutators among bilinears made out of the D=1 quantum superfields describing the supersymmetric harmonic oscillator. DOE

N88-27863# Gosudarstvennyi Komitet po Ispolzovaniyu Atomnoi Energii, Moscow (USSR). Inst. Teoreticheskoj i Ehksperimental'noj Fiziki.
GEOMETRY OF SUPERCONFORMAL MANIFOLDS, PART 1
A. A. Roslyi, A. S. Schwarz, and A. A. Voronov 1987 22 p
(DE88-702405; ITEP-107(1987)-Pt-1) Avail: NTIS (US Sales Only) HC A03/MF A01

The main facts about complex curves are generalized to superconformal manifolds. The results thus obtained are relevant to the dermion string theory and, in particular, they are useful for computation of determinants of superlaplacians which enter the string partition function. DOE

N88-27864# Gosudarstvennyi Komitet po Ispolzovaniyu Atomnoi Energii, Moscow (USSR). Inst. Teoreticheskoj i Ehksperimental'noj Fiziki.
GEOMETRY OF SUPERCONFORMAL MANIFOLDS, PART 2
A. A. Roslyi, A. S. Schwarz, and A. A. Voronov 1987 23 p
(DE88-702406; ITEP-115(1987)-Pt-2) Avail: NTIS (US Sales Only) HC A03/MF A01

The study of superconfirmal manifolds is continued. The cohomologies of such manifolds with coefficients in a holomorphic line bundle are investigated. DOE

N88-27865# Joint Inst. for Nuclear Research, Dubna (USSR). Lab. of Computing Techniques and Automation.
EVALUATION OF QUANTUM MECHANICS PATH INTEGRALS BY THE APPROXIMATIONS EXACT ON A CLASS OF POLYNOMIAL FUNCTIONALS
Yu. Yu. Lobanov and E. P. Shidkov 1987 12 p
(DE88-702434; JINR-E-2-87-507) Avail: NTIS (US Sales Only) HC A03/MF A01

The method for numerical evaluation of path integrals in Euclidean quantum mechanics without lattice discretization is elaborated. The method is based on the representation of these integrals in the form of functional integrals with respect to the conditional Wiener measure and on the use of the derived approximate exact on a class of polynomial functionals of a given degree. By the computations of non-perturbative characteristics, concerned the topological structure of vacuum, the advantages of this method versus lattice Monte-Carlo calculations are demonstrated. DOE

N88-27866# Joint Inst. for Nuclear Research, Dubna (USSR). Lab. of Theoretical Physics.
PERTURBATION EXPANSIONS GENERATED BY AN APPROXIMATE PROPAGATOR
M. Znojil 1987 11 p
(DE88-702435; JINR-E-4-87-667) Avail: NTIS (US Sales Only) HC A03/MF A01

Starting from a knowledge of an approximate propagator R at some trial energy guess E sub 0 , a new perturbative prescription for p-plet of bound states and of their energies is proposed. It generalizes the Rayleigh-Schroedinger (RS) degenerate perturbation theory to the nondiagonal operators R (eliminates a RS need of their diagnalization) and defines an approximate Hamiltonian T by mere inversion. The deviation V of T from the exact Hamiltonian H is assumed small only after a subtraction of a further auxiliary Hartree-Fock-like separable selfconsistent potential U of rank p. The convergence is illustrated numerically on the anharmonic oscillator example. DOE

N88-27867# Joint Inst. for Nuclear Research, Dubna (USSR). Lab. of Computing Techniques and Automation.
CAUCHY PROBLEM FOR THE NONLINEAR SCHROEDINGER EQUATION
P. E. Zhidkov 1987 13 p In RUSSIAN; ENGLISH summary
(DE88-702454; JINR-R-5-87-373) Avail: NTIS (US Sales Only) HC A03/MF A01

The theorems of existence, uniqueness and continuous dependence upon the initial condition for the Cauchy problem are proved for the nonlinear Schroedinger equation. There is not a proposition that the solution tends to zero as the space variable tends to infinity in contrast to other papers. Only the continuity and boundedness of initial data and belonging of initial data derivatives to L(sub 2)(R) are proposed. DOE

70 PHYSICS (GENERAL)

For precision time and time interval (PTTI) see *35 Instrumentation and Photography;* for geophysics, astrophysics or solar physics see *46 Geophysics, 90 Astrophysics,* or *92 Solar Physics.*

N88-27868# Aerospace Corp., El Segundo, Calif. Chemistry and Physics Lab.
A THREE-DIMENSIONAL MODEL OF THE GAS-CELL ATOMIC FREQUENCY STANDARD
James C. Camparo and Robert P. Frueholz 25 Feb. 1988 27 p
(Contract F04701-85-C-0086)
(AD-A193218; TR-0086A(2945-05)-2; SD-TR-88-41) Avail: NTIS HC A03/MF A01 CSCL 20C

Preliminary calculations from a three-dimensional clock model are discussed. In particular, a recent conclusion that short-term stability might be improved by varying the microwave power is considered. Results support the general conclusion, but show that the degree of sensitivity is less than predicted by a one-dimensional model. The difference in the results of the two models is a manifestation of the more accurate treatment of the position-shift effect in the three-dimensional model. This more accurate treatment is highlighted by the three-dimensional model's determination of isoefficiency contours (contours showing spatial regions in the clock cavity that have equal efficiency for producing clock signal), and noting their spatial dependence upon microwave power. GRA

N88-27869# Massachusetts Inst. of Tech., Cambridge. Research Lab. of Electronics
RLE PROGRESS REPORT, JANUARY 1 TO DECEMBER 31, 1987
Jonathan Allen and Daniel Kleppner Jul. 1988 316 p
(RLE-PR-130) Avail: NTIS HC A14/MF A01

The Research Laboratory of Electronics (RLE) of the Massachusetts Institute of Technology was established in 1946. Originally organized under the joint sponsorship of the Departments of Physics and Electrical Engineering, RLE has broadened its interests to cover a wide range of research. The RLE environment provides both the freedom of action essential in an academic institution and the availability of large-scale laboratory facilities and services required by researchers. Progress Report 130 describes research programs at RLE for the period January 1 through December 31, 1987. The report contains both a statement of research objectives and a summary of research efforts. Chapter 30 is a bibliography of RLE publications and papers presented during 1987. Chapter 31 is a roster of current RLE staff. In addition, indexes of project personnel and sponsored research projects are located at the end of the report. Research topics include the

following: submicron structures, thin film electronic materials, optics, quantun electronics, ultralow temperature measurement, custom integrated circuits, molecular physics. quantum optics, plasma dynamics, digital signal processing, and radio astronomy. Author

71 ACOUSTICS

Includes sound generation, transmission and attenuation. For noise pollution see *45 Environmental Pollution*.

N88-27870# South Bank Polytechnic, London (England). Inst. of Environmental Engineering.
REFLECTION OF SOUND IN OPEN ENDED DUCTS
D. M. Fairhall Feb. 1987 13 p
(PB88-103478; RM-101) Avail: NTIS HC E04/MF E04; copy not available from STI Facility CSCL 20A

Tables of attenuation due to end reflection effects at duct terminations frequently appear in design guides used by the building services engineer to aid calculation of sound power levels at air duct exits. Recent investigations indicate that the process of reflection differs according to whether the opening is at the end, or on the side, of the duct; results for the open ended duct agreeing with currently accepted theory, but those for a side opening showing that such theory has no validity in this application. Results are presented of recent work and the implications of these results for the building services engineer are discussed. Author

N88-27871# Lowell Univ., Mass. Dept. of Mathematics.
ROBUST METHODS FOR ARRAY SIGNAL PROCESSING Final Report, 15 May - 30 Sep. 1987
Charles M. Byrne 28 Dec. 1987 44 p
(Contract N00014-87-K-0394)
(AD-A192854) Avail: NTIS HC A03/MF A01 CSCL 17A

Research was ongoing in several areas: stable array processing; two-dimensional reconstruction algorithms; extensions of the concept of cross-entropy distance measures; and the beginning of new work on array processing in more complicated acoustic environments. GRA

N88-27872# Scripps Institution of Oceanography, La Jolla, Calif. Marine Physical Lab.
VERTICAL DIRECTIONALITY OF AMBIENT NOISE AT 32 DEG N AS A FUNCTION OF LONGITUDE: TAPE NUMBER 86180
W. S. Hodgkiss and F. H. Fisher Jan. 1988 123 p
(Contracts N00014-84-K-0097; N00014-87-C-0127)
(AD-A193228; MPL-TM-387-E; MPL-U-32/86) Avail: NTIS HC A06/MF A01 CSCL 20A

Measurements have been made of the ambient noise field between 25 and 300 Hz with vertical arrays at 32 N (124 W, 136 W, and 150 W). This technical report contains the complete analysis results for the MPL 27-element vertical array Tape No. 86180. The tape was recorded at 32 N, 150 W (approximately 1700 nmi due west of San Diego) on 5 May 1986 beginning at 10:09 PDT. At that time, the wind speed was 10 kts. GRA

N88-27873# Naval Postgraduate School, Monterey, Calif.
PASSIVE MULTIPATH TARGET TRACKING IN AN INHOMOGENEOUS ACOUSTIC MEDIUM Ph.D. Thesis
Amnon Shefi Dec. 1987 238 p
(AD-A193284) Avail: NTIS HC A11/MF A01 CSCL 17K

Tracking a maneuvering acoustic source using multipath (MP) arrivals in an inhomogeneous (IH) ocean medium is investigated. Errors introduced by a horizontally stratified sound speed profile are quantitatively evaluated. A new method of converting MP time difference of arrivals to depth and range which accounts for the IH effect is developed and evaluated. A 3-D target tracker previously used in MP tracking is modified in order to remove estimation biases and improve computational efficiency. Tracking performance is demonstrated using extensive simulation and shown to be greatly improved. GRA

N88-27874# Virginia Univ., Charlottesville. Dept. of Materials Science.
OUTLINER RESISTANT FILTERING AND SMOOTHING: 2D VERSION Technical Report, 2 Jul. 1987 - 30 Jun. 1988
P. Papantoni-Kazakos and Haralampos Tsaknakis 4 Feb. 1988 51 p
(Grant AF AFOSR-0224-87)
(AD-A193319; UVA/525682/EE88/104; AFOSR-88-0362TR)
Avail: NTIS HC A04/MF A01 CSCL 09F

Consider a stationary Gaussian information process transmitted through an additive noise channel. The noise and information processes are mutually independent, and the noise process modeled as nominally Gaussian with additive outliers. For the above system model a theory is developed for outliers resistant filtering and smoothing operations. Then specific are designed such nonlinear operations. The performance criteria are the asymptotic mean squared error at the Gaussian nominal model, the breakdown point, and the influence function. The proposed operations combine excellent performance at the nominal model with strong resistance to outliers. GRA

N88-27875# Bolt, Beranek, and Newman, Inc., Cambridge, Mass.
THEORY OF SOUND PRODUCTION BY VORTEX-AIRFOIL INTERACTION
M. S. Howe Jan. 1988 53 p
(Contract N00167-87-C-0021)
(AD-A193386; BBN-6710) Avail: NTIS HC A04/MF A01 CSCL 20A

An analysis is made of the sound produced when a field of vorticity is cut by an airfoil in low Mach number flow. A general formula is given for the acoustic pressure when the airfoil is rigid and the chord is acoustically compact. This expresses the radiation in terms of an integral over the region occupied by the vorticity; the integrand contains factors describing the influence of the thickness, twist and camber of the airfoil. Explicit analytical results are derived for the case of a rectilinear vortex, having small core diameter and finite axial velocity defect, which is chopped by an airfoil of large aspect ratio. The acoustic signature generally comprises two components associated respectively with the axial and azimuthal vorticity, the latter being determined by the velocity defect distribution within the core. Sound is generated predominantly when the core is in the neighborhoods of the leading and trailing edges. The contribution from the trailing edge is usually small, however, because of destructive interference between sound produced by edge-diffraction of near field energy of the vortex and that produced by vorticity shed into the wake of the airfoil in order to satisfy the unsteady Kutta condition that the pressure and velocity should be bounded at the edge. GRA

N88-27876# Bolt, Beranek, and Newman, Inc., Cambridge, Mass.
THE INFLUENCE OF SURFACE ROUNDING ON TRAILING EDGE NOISE
M. S. Howe Jan. 1988 48 p
(Contract N00167-87-C-0021)
(AD-A193387; BBN-6715) Avail: NTIS HC A03/MF A01 CSCL 20A

An analysis is made of the sound produced by low Mach number turbulent flow over an asymmetrically rounded trailing edge of an airfoil. Such airfoils are used in experimental studies of trailing edge noise and vortex shedding phenomena, and have a flat pressure side and a rounded, or 'beveled', suction surface at the trailing edge, so that in the immediate vicinity of the edge the airfoil has a wedge shaped profile. There are two principal interaction noise sources: a lift dipole associated with the unsteady transverse forces exerted on the airfoil, and a thickness dipole which radiates preferentially in the plane of the airfoil. The latter is usually negligible except possibly at low frequencies, and at large included angles of the trailing edge wedge. Detailed results are given for included angles of 90 deg and less. It is concluded that, for given turbulence intensity, surface beveling has a significant

effect on the radiation only at sufficiently high frequencies that the trailing edge may be regarded as a straight-sided wedge over distances of the order of the turbulence length scale. GRA

N88-27877*# Virginia Polytechnic Inst. and State Univ., Blacksburg.
APPLICATION OF PATTERN RECOGNITION TECHNIQUES TO THE IDENTIFICATION OF AEROSPACE ACOUSTIC SOURCES Annual Report No. 1
Chris R. Fuller, Walter F. OBrien, and Randolph H. Cabell Jun. 1988 11 p
(Grant NAG1-762)
(NASA-CR-183116; NAS 1.26:183116) Avail: NTIS HC A03/MF A01 CSCL 20A

A pattern recognition system was developed that successfully recognizes simulated spectra of five different types of transportation noise sources. The system generates hyperplanes during a training stage to separate the classes and correctly classify unknown patterns in classification mode. A feature selector in the system reduces a large number of features to a smaller optimal set, maximizing performance and minimizing computation. Author

N88-27878# Institut Franco-Allemand de Recherches, St. Louis (France).
ACOUSTIC PROPAGATION IN THE LOWER ATMOSPHERE Ph.D. Thesis - Univ. de Haute Alsace [LA PROPAGATION ACOUSTIQUE DANS LA BASSE ATMOSPHERE]
Jacques Vermorel 19 Nov. 1987 359 p In FRENCH
(Contract DRET-85/053)
(ISL-R-126/87; ETN-88-92735) Avail: NTIS HC A16/MF A01

Modeling of the influence of aerologic parameters on the acoustic wave; a simplified representation of ground relief; the introduction of experimental absorption values; and the comparison between theory and experiment are summarized. The models developed include Euler and a Lagrange type models; algorithms and computation procedures were implemented for both modeling principles. The measurements verify the influence of wind profiles and temperature distribution of the propagation and the formation of focus points and pressure time fluctuations. It is concluded that the two development principles (Euler/Lagrange) are complementary. ESA

N88-27879# Deutsche Forschungs- und Versuchsanstalt fuer Luft- und Raumfahrt, Brunswick (West Germany). Abteilung Technische Akustik.
AEROACOUSTIC INVESTIGATION ON THE NOISE FROM ULTRALIGHT AIRCRAFT
Helmut Dahlen, Werner Dobrzynski, and Hanno Heller Aug. 1987 275 p In GERMAN; ENGLISH summary
(DFVLR-FB-88-03; ISSN-0171-1342; ETN-88-92921) Avail: NTIS HC A12/MF A01; DFVLR, VB-PL-DO, 90 60 58, 5000 Cologne, Federal Republic of Germany, 76.50 deutsche marks

Flyover and ground/static noise measurements as well as wind tunnel tests on individual propellers of ultralight aircraft led to the identification of the essential noise sources and to recommendations for noise reduction. For undisturbed inflow conditions (tractor propellers) and blade tip Mach numbers below 0.5 the resulting propeller noise is of broadband nature, while above that limit discrete-frequency rotational-noise sources dominate. Additional sources occur with pusher-propeller configurations as a consequence of the disturbed inflow. It is demonstrated that ground/static noise measurements are not suitable for certification testing. ESA

N88-27880# Deutsche Forschungs- und Versuchsanstalt fuer Luft- und Raumfahrt, Goettingen (West Germany). Abteilung Instationaere Aerodynamik.
PROPAGATION OF ACOUSTIC DISTURBANCES IN TRANSONIC FLOW FIELDS OF LIFTING WINGS Ph.D. Thesis - Goettingen Univ.
Ralph Voss Feb. 1988 151 p In GERMAN; ENGLISH summary
(DFVLR-FB-88-13; ISSN-0171-1342; ETN-88-92931) Avail: NTIS HC A08/MF A01; DFVLR, VB-PL-DO, 90 60 58, 5000 Cologne, Federal Republic of Germany, 53.50 deutsche marks

The propagation of small disturbances in the vicinity of transonic flutter surfaces with mixed sub-/supersonic regions is investigated based on the approximation of geometrical acoustics. Waves, rays, and the spatial density distribution of the dissipated disturbance energy are numericaly calculated using a system of 18 differential equations. The effects of various two and three-dimensional fields, of the source locus, and of reflections on the wing surface are investigated. The results of the acoustic theory are used to derive a general influence function for sources of disturbance in arbitrary transonic fields. This function represents a step toward a surface panel method to calculate unsteady transonic flows. The acoustic results are compared with measured unsteady pressure distributions on oscillating transonic wings and with results of a numerical field panel method. ESA

N88-27881*# National Aeronautics and Space Administration. Langley Research Center, Hampton, Va.
PUBLICATIONS ON ACOUSTICS RESEARCH AT THE LANGLEY RESEARCH CENTER DURING 1980-1986
Linda W. Sutherland, comp. Jul. 1988 67 p
(NASA-TM-100590; NAS 1.15:100590) Avail: NTIS HC A04/MF A01 CSCL 20A

This report is a compilation of publications from acoustics research at the Langley Research Center. The reports are listed in chronological order and summarize the written output of the Acoustics Division and its predecessor, The Acoustics and Noise Reduction Division, for the period 1980 through 1986. The information assembled has been extracted from the 1980 through 1986 issues for the Technical Memorandum entitled, Scientific and Technical Information Output of the Langley Research Center for the Calendar Year. Author

72 ATOMIC AND MOLECULAR PHYSICS

Includes atomic structure, electron properties, and molecular spectra.

N88-27882# Massachusetts Univ., Amherst. Dept. of Chemistry.
THEORY OF THE DISSOCIATION DYNAMICS OF SMALL MOLECULES ON METAL SURFACES: FINITE TEMPERATURE STUDIES Progress Report
B. E. Jackson 1988 3 p
(Contract DE-FG02-87ER-13744)
(DE88-007763; DOE/ER-13744/T1) Avail: NTIS HC A02/MF A01

Progress is reported on three approaches: quantum mechanics of dissociative adsorption of H sub 2 on metals; same at finite surface temperatures; and multi-dimensional models for dissociative adsorption. DOE

N88-27883# Tokyo Univ. (Japan). Inst. of Space and Astronautical Science.
A THEORETICAL DETERMINATION OF THE DENSITY AT A TRAVELING SOURCE THAT EMITTS PARTICLES
Osamu Ashihara Aug. 1986 28 p
(ISAS-RN-351) Avail: NTIS HC A03/MF A01

Different from the so far known methods of calculating the Lyman alpha intensity of a comet, which were treated in the rest frame of the comet, a new formulation is attempted to well incorporate the differential nature of the force field working on particles in the coma. The formulation is based on the so-called Lambert problem in the theory of orbit determination and carried out in an inertial frame of coordinates centered at the Sun. An expression of the density at an arbitrary point of time and place is derived as an integral over time (or, equivalently, over the trajectory of a moving source). Particularly for the inverse square force field, a term representing the expansion of the flux tube of particles is estimated by using the power series method. An

extension of the present result to the non-point-like sources is also attempted. Lastly, relating to the Lyman alpha intensity calculation of Comet Halley, the orbital property of the hydrogen atoms in the coma is examined and behavior of the Lambert solution vector (initial velocity vector of the ejected hydrogen atom) on time is discussed. Author

N88-27884# Brookhaven National Lab., Upton, N. Y. Dept. of Chemistry.
MULTIPHOTON IONIZATION OF ALKALINE EARTH ATOMS IN AN INTENSE LASER FIELD
D. Kim and L. F. DiMauro 1988 5 p Presented at the 4th International Symposium on Resonance Ionization Spectroscopy and its Applications, Gaithersburg, Md., 10 Apr. 1988
(Contract DE-AC02-76CH-00016)
(DE88-008078; BNL-41103; CONF-880435-1) Avail: NTIS HC A02/MF A01

We have studied the single and double nonresonant multiphoton ionization of calcium atom using both 532-nm and 1.06 micron radiation. These studies were conducted in the intensity regime of 10(10 to 13) W sq cm. We use mass and angularly resolved electron energy analysis in an attempt to gain insight into the dominant mechanisms responsible for ionization. DOE

N88-27885# Clemson Univ., S.C. Dept. of Physics and Astronomy.
SELF-ENERGIES AND THE INTERACTIONS OF PARTICLES WITH SURFACES
J. R. Manson, R. H. Ritchie, P. M. Echenique, and A. Gras-Marti (Alicante Univ., Spain) 1987 12 p Presented at the 10th Werner Brandt Workshop on Penetration Phenomena: Dynamic Actions of Energetic Probes with Condensed Matter, Alicante, Spain, 7 Jan. 1987 Prepared in cooperation with Oak Ridge National Lab., Tenn; Universidad del Pais Vasco, San Sebastian (Spain) Dept. de Fisica; Alicante Univ. (Spain) Dept. de Fisica
(Contract DE-AC05-84OR-21400)
(DE88-010451; CONF-870155-9; CONF-870155) Avail: NTIS HC A03/MF A01

The method of treating many-body problems by means of an effective interaction self-energy is reviewed. An alternatvie approach to the self-energy has been developed which is simpler and more straight-forward than standard methods, and its use illustrated with two examples of a charge interacting with a metal surface. In each case the self-energy produces the classical image potential together with corrections due to quantum mechanical effects. This method has also been successfully applied to the problem of an atom interacting with a surface. Corrections to the Van der Waals dispersion force are obtained, and via the non-conservative imaginary parts to Summation(sub i) (z) we discuss transition rates and energy exchange. DOE

N88-27886# Harvard Univ., Cambridge, Mass.
STUDY OF ENERGY LEVELS AND DECAY MECHANISMS FOR SINGLET RYDBERG STATES OF MOLECULAR NITROGEN Final Report, for 1 Oct. 1983 - 1 Aug. 1987
F. M. Pipkin 15 Sep. 1987 52 p
(Contract F19628-84-K-0015)
(AD-A192505; AFGL-TR-87-0274) Avail: NTIS HC A04/MF A01 CSCL 07B

This report summarizes a series of investigations of the singlet Rydberg States of molecular nitrogen. The objective of the research was to use laser excitation out of a metastable singlet state in N2 to study the energy levels and decay mechanisms for the high lying singlet Rydberg and valence states. The first section summarizes the current knowledge of these states. The second section describes the initial attempts to produce a beam of molecules in the a'(0)1 epsilon +g state and use laser excitation to gain access to higher lying singlet states. GRA

N88-27887# Naval Research Lab., Washington, D.C.
PROPAGATION OF CHARGED PARTICLE BEAMS IN THE ATMOSPHERE
Martin Lampe 4 Mar. 1988 34 p
(AD-A193185; NRL-MR-6159) Avail: NTIS HC A03/MF A01 CSCL 20H

The basic physical processes is reviewed involved in charge particle beam propagation, in a self-pinched mode, in the atmosphere or other dense neutral gases. These processes include single-particle collisional and radiative energy losses, collective energy loss, radial expansion due to scattering, and instabilities. Each of these imposes requirements and limitations on beam propagation. Highly relativistic electron beams are the main subject. Ion beam physics is similar but more complex (because ultra-relativistic approximations are inappropriate), and has been less studied. GRA

N88-27888# Centro Brasileiro de Pesquisas Fisicas, Rio de Janeiro.
DISCRETE VARIATIONAL METHODS AND THEIR APPLICATION TO ELECTRONIC STRUCTURES
D. E. Ellis and D. Guenzburger 1987 37 p
(DE88-702215; CBPF-MO-004/87) Avail: NTIS (US Sales Only) HC A03/MF A01

Some general concepts concerning discrete variational methods are developed and applied to problems of determination of electronic spectra, charge densities and bonding of free molecules, surface-chemisorbed species and bulk solids. DOE

N88-27889# Lawrence Livermore National Lab., Calif.
STEADY-STATE APPROXIMATIONS IN RAMAN EXCITATION EQUATIONS
B. W. Shore 20 Dec. 1987 17 p
(Contract W-7405-eng-48)
(DE88-011759; UCID-21077) Avail: NTIS HC A03/MF A01

This memo presents equations describing propagation of beams of nearly monochromatic radiation through a Raman-active molecular vapor, under conditions of steady excitation of quantum-mechanical molecules by classical radiation (i.e., radiation that comprises a large number of photons per mode). Such conditions apply in the continuous-wave experiments that are conducted to measure such properties as Raman gain or Raman scattering cross sections. Under those circumstances the propagation is described by rate equations for molecular excitation and rate equations for photon numbers. Although these conditions do not apply for short-pulse transient excitation, both types of processes are parameterized by the same molecular polarizability matrix elements. This memo discusses those parameters, as extracted from steady state observations. DOE

N88-27890# Technische Univ., Brunswick (West Germany). Naturwissenschaftlichen Fakultaet.
MEASUREMENT OF BETA-DECAY ENERGIES OF SHORT-LIVED NEUTRON-RICH NUCLEI IN THE VICINITY OF MASS NUMBER BETWEEN 101 AND 106, AND A = 109 Ph.D. Thesis [MESSUNG VON BETA-ZERFALLSENERGIEN KURZLEBIGER, NEUTRONENREICHER ATOMKERNE IM MASSENBEREICH 101 LESS THAN OR EQUAL TO A LESS THAN OR EQUAL TO 106 UND A=109]
Helmut Weikard 1986 139 p In GERMAN
(ETN-88-92376) Avail: NTIS HC A07/MF A01

The recoil separator LOHENGRIN was used for Beta-decay energies measurement of 18 nuclei, negative ions (Zr, Nb, Mo, Tc, Rv, Rh) for the determination of Q beta-values. Beta-gamma coincidence is considered. The Beta detector is a plastic scintillation telescope. From Q-values of fission products, atomic weights are determined with an accuracy of 1 percent. ESA

N88-27891# Rome Univ. (Italy). Dipt. di Fisica.
QUARK NUCLEAR MODEL: CLASSIFICATION GROUPS AND TWO AND THREE BODY CORRELATIONS [MODELLO NUCLEARE A QUARKS: GRUPPI DI CLASSIFICAZIONE E ANALISI DELLE CORRELAZIONI A DUE E TRE CORPI]
P. Camiz and F. Cavanna 9 Oct. 1987 85 p In ITALIAN
(Nota-Interna-896; ETN-88-92624) Avail: NTIS HC A05/MF A01

Within a shell model for quarks, the configurations (n, l, j) exp k are studied using group theory. Analysis of the case I = 0 leads to a complete classification of the second state of a group chain. The energy of the two body interaction is deduced. The study of the three body correlations leads to a measurement of the tensor characteristics of the nucleon. ESA

N88-27892# Rome Univ. (Italy). Dipt. di Fisica.
STUDY OF THE PRODUCTION OF Ko MESONS IN PROTON ANTIPROTON INTERACTIONS AT 630 GeV [STUDIO DELLA PRODUZIONE DI MESONI KO IN INTERAZIONI PROTONE ANTIPROTONE A 630 GEV]
A. Nisati 7 Mar. 1988 24 p In ITALIAN Presented at the 73rd National Congress of the Societa Italiana di Fisica, Naples, Italy, 12-17 Oct. 1987
(Nota-Interna-908; ETN-88-92628) Avail: NTIS HC A03/MF A01

Data were obtained with a proton-antiproton collider facility. The collision cross-section results are particularly interesting. The Feynman scaling law is violated and the value of cross-section limit grows logarithmically instead of remaining constant. The finding confirms identical conclusions obtained during the emission of charged particles. ESA

N88-27893# Max-Planck-Inst. fuer Physik und Astrophysik, Garching (West Germany). Inst. fuer Physik.
[ACTIVITIES REPORT OF THE WERNER-HEISENBERG INSTITUTE OF PHYSICS] Annual Report, 1987 [JAHRESBERICHT 1987]
Dec. 1987 138 p In GERMAN Original contains color illustrations
(ETN-88-92946) Avail: NTIS HC A07/MF A01

Theoretical and experimental studies on elementary particles and their interactions especially strong interactions, standard models, cosmology, quantum mechanics and nonlinear multiparticle physics are summarized. Experiments in CERN on neutrino and antineutrino interactions, and on lepton, nucleon, and hadron scattering; on FERMILAB'S Teratron accelerator, and on PETRA and HERA storage rings are described. Investigation of particles with charm properties, and development of semiconductor detectors and of calorimeters are discussed. ESA

73 NUCLEAR AND HIGH-ENERGY PHYSICS

Includes elementary and nuclear particles; and reactor theory.
For space radiation see *93 Space Radiation.*

N88-27894# Sandia National Labs., Albuquerque, N. Mex.
HYPERSONIC FLIGHT TESTING
W. Williamson 1987 48 p Presented at the Joint US/Europe Short Course on Hypersonics, Paris, France, 7 Dec. 1987
(Contract DE-AC04-76DP-00789)
(DE88-001655; SAND-87-2570C; CONF-871227-1; CONF-8704229-1) Avail: NTIS HC A03/MF A01

This presentation is developed for people attending the University of Texas week-long short course in hypersonics. The presentation will be late in the program after the audience has been exposed to computational techniques and ground test methods. It will attempt to show why we flight test, flight test options, what we learn from flight tests and how we use this information to improve out knowledge of hypersonics. It presupposes that our primary interest is in developing vehicles which will fly in the hypersonic flight region and not in simply developing technology for technology's sake. The material is presented in annotated vugraph form so that the author's comments on each vugraph are on the back of the preceding page. It is hoped that the comments will help reinforce the message on the vugraph. Author

N88-27895# Westinghouse Hanford Co., Richland, Wash.
SP-100 GROUND ENGINEERING SYSTEMS: TEST FACILITY CONTROL SYSTEMS
W. F. Carlson, J. B. Henshall, and K. L. Hampsten Jan. 1988 14 p Presented at the 5th Symposium on Space Nuclear Power Systems, Albuquerque, N. Mex., 11 Jan. 1988
(Contract DE-AC06-87RL-10930)
(DE88-009195; WHC-SA-0025-FP; CONF-880122-11) Avail: NTIS HC A03/MF A01

One of the major objectives of the current phase of the SP-100 program is to demonstrate the performance of a full-scale, prototypic nuclear subsystem of a 100 kWe space nuclear power supply. Such a test is planned at the SP-100 Test Site located at U.S. Department of Energy facilities near Richland, Washington. Considerations involved in selecting a design for the central, integrated facility control system which will control and monitor the performance of the nuclear subsystem and supporting facility systems are discussed. These considerations have been translated into the design of a modern, commercially available, microprocessor based control and monitoring system, using color graphics techniques for the operator interface. DOE

N88-27896# National Lab. for High Energy Physics, Ibaraki (Japan).
DISTORTION FUNCTIONS
King-Yuen Ng Sep. 1987 18 p
(DE88-752634; KEK-87-11) Avail: NTIS (US Sales Only) HC A03/MF A01

This report deals with the analytic computation of the distortions of beam shapes in the horizontal and vertical phase spaces due to the introduction of nonlinear multipoles. Unfortunately, no machine is perfectly linear. There are systematic sextupole components in dipole fields from steel saturation, remanent fields, persistent currents, eddy currents, and random sextupole components due to field errors. Of course, there are also sextupoles placed around the ring on purpose to counteract the above and to modify chromaticity. Perturbation theory can be used away from resonances. A set of distortion functions has been proposed for each order of the perturbation. These functions are closed, i.e., periodic. They are independent of the beam amplitude and are very similar to the beta-functions and alpha-functions of the linear theory. Though the projections of the beam profile onto the transverse phase planes are the only thing that can be examined, these distortion functions can give the exact projections. This report previews these distortion functions, the formulae for their computation, and how they can be used in computing the phase-space projections of the beam and the tuneshifts. All these formulae are derived from a Hamiltonian theory. Some applications are also discussed. DOE

74 OPTICS

Includes light phenomena; and optical devices.
For lasers see *36 Lasers and Masers.*

N88-27897# Japan Atomic Energy Research Inst., Tokyo. Dept. of Thermonuclear Fusion Research.
MULTI-MODE OPTICAL FIBERS FOR SIMULTANEOUS 13-POSITION MEASUREMENTS THOMSON SCATTERING APPARATUS IN THE JFT-2M TOKAMAK
Toshihiko Yamauchi, Ichiro Nakazawa, Tohru Matoba, and Yoshiaki Ogura Nov. 1987 22 p
(DE88-753133; JAERI-M-87-196) Avail: NTIS (US Sales Only) HC A03/MF A01

The characteristics of fiber bundles for Thomson scattering optics are studied. The fibers are made of multi-mode optical fibers. The variety of output patterns were observed by weighting on the fiber as well as by bending it after passing a He-Ne laser through a fiber bundle. This variety influenced the matching loss considerably. Then, the effect of former is larger than the latter, which is caused by the micro bending. And also, the spread of

pulse width by weighting is connected with the spread of output pattern. The spread of pulse width was about 3 ns at the most in a 2.3 m length of fiber bundle. DOE

N88-27898# Rochester Univ., N. Y. Lab. for Laser Energetics.
MEASUREMENT OF THE THERMAL CONDUCTIVITY OF DIELECTRIC THIN SOLID FILMS WITH A THERMAL COMPARATOR
C. A. Amsden, S. E. Gilman, S. D. Jacobs, and J. S. Torok Apr. 1988 5 p Presented at the 4th Topical Meeting on Optical Interference Coatings, Tucson, Ariz., 12 Apr. 1988
(Contract DE-FC08-85DP-40200)
(DE88-008468; DOE/DP-40200/70; CONF-880434-1) Avail: NTIS HC A02/MF A01

Low thermal conductivity has important implications for electric and optical applications, where heat deposited in a thin layer must be dissipated to prevent damage. Models which account for thermal transport in thin film structures may have no predictive value if they employ bulk conductivity data. Most techniques utilized to measure the thermal conductivity of thin solid films are difficult and time consuming. The method we have developed is relatively rapid, nondestructive, and is capable of evaluating the samples in a conventional film on substrate geometry. Our thermal conductivity apparatus consists of a control and readout module, signal processing equipment, and an environmentally isolated sample chamber enclosing a sample stage. The commercial unit was converted into a high precision device by temperature controlling both the samples and the sample stage, and by performing averaging of the output signal. The thermal conductivity values obtained are below those of bulk solids. In addition, the conductivities seem to increase with increasing film thickness. Titania seems to have a higher thermal conductivity when deposited by ion-beam sputtering rather than electron-beam evaporation. Some of the electron-beam films were crazed, indicating high levels of stress. The effect of stress and crazing on thermal conductivity is not readily apparent. DOE

N88-27899# Sandia National Labs., Albuquerque, N. Mex.
A FIBER OPTIC SYNCHRONOUS DETECTOR USING SAMPLE-AND-HOLD CIRCUITS
K. B. Pfeifer May 1988 22 p
(Contract DE-AC04-76DP-00789)
(DE88-010973; SAND-88-0389) Avail: NTIS HC A03/MF A01

A design for a synchronous driver and detector for single-ended optical fiber sensing applications is presented. The circuit is discussed in detail. A derivation of the equations relating the input to the output for the sampler is given. A brief discussion of the operation of the prototype is given. Finally, the paper concludes with an example of an application of the device. DOE

N88-27900# Technische Univ., Brunswick (West Germany). Fakultaet fuer Maschinenbau und Elektrotechnik.
PHOTODIODES FOR OPTICAL COMMUNICATION IN THE NEAR INFRARED Ph.D. Thesis [PHOTODIODEN FUER DIE OPTISCHE NACHRICHTENTECHNIK IM NAHEN INFRAROT]
Sungur Aytac 1986 204 p In GERMAN
(ETN-88-92379) Avail: NTIS HC A10/MF A01

Fabrication and analysis of photodiode detectors in InGaAsP/InP is described with emphasis on acceptor-diffusion in InP and InGaAs. Diffusion coefficients of Zn and Cd in InP and InGaAs are measured for a large domain of temperature and activation energy is determined by Arrhenius diagrams. Schottky diodes are manufactured and charge carrier concentration and defects are analyzed. The developed technology allows the reproducible fabrication of P-N junctions of good quality. ESA

N88-27359# Wright State Univ., Dayton, Ohio. Dept. of Computer Engineering.
INVESTIGATION OF THE POTENTIAL IMPACT OF NEW PHOTONIC MATERIALS ON OPTICAL PROCESSING SYSTEMS Final Report
Frank W. Moore *In* Universal Energy Systems, Inc., United States Air Force Graduate Student Summer Support Program, Volume 2 Dec. 1987 20 p (For primary document see N88-27355 21-31)
Avail: NTIS HC A99/MF E03 CSCL 20F

N88-27374# Wyoming Univ., Laramie. Dept. of Physics and Astronomy.
CALIBRATION AND DATA REDUCTION TECHNIQUES FOR THE AFGL INFRARED ARRAY SPECTROMETER Final Report
Gregory Sloan *In* Universal Energy Systems, Inc., United States Air Force Graduate Student Summer Support Program, Volume 2 Dec. 1987 18 p (For primary document see N88-27355 21-31)
Avail: NTIS HC A99/MF E03 CSCL 20F

N88-27377# University of South Florida, Tampa. Dept. of Computer Science and Engineering.
AN ASPECT GRAPH-BASED CONTROL STRATEGY FOR 3-D OBJECT RECOGNITION Final Report
Louise Stark *In* Universal Energy Systems, Inc., United States Air Force Graduate Student Summer Support Program, Volume 2 Dec. 1987 19 p (For primary document see N88-27355 21-31)
Avail: NTIS HC A99/MF E03 CSCL 20F

N88-27380# Rochester Univ., N. Y. Dept. of Physics and Astronomy.
ANALYSIS OF EMISSION FEATURES IN IRAS LRS SPECTRA Final Report
Tod Strohmayer *In* Universal Energy Systems, Inc., United States Air Force Graduate Student Summer Support Program, Volume 2 Dec. 1987 20 p (For primary document see N88-27355 21-31)
Avail: NTIS HC A99/MF E03 CSCL 20F

N88-27381# Cincinnati Univ., Ohio. Dept. of Electrical and Computer Engineering.
OPTICAL INTERCONNECTIONS FOR DIGITAL IMAGE CODING Final Report
Tien N. Tran *In* Universal Energy Systems, Inc., United States Air Force Graduate Student Summer Support Program, Volume 2 Dec. 1987 13 p (For primary document see N88-27355 21-31)
Avail: NTIS HC A99/MF E03 CSCL 20F

N88-27389# Mitsubishi Electric Corp., Tokyo (Japan). Central Research Lab.
BASIC RESEARCH ON OPTICAL NEURAL COMPUTERS
Kazuo Kyuma and Satoru Shiono *In its* Mitsubishi Electric Advance (R and D Edition), Volume 41 Dec. 1987 4 p (For primary document see N88-27388 21-31)
Avail: NTIS HC A03/MF A01 CSCL 20F

75 PLASMA PHYSICS

Includes magnetohydrodynamics and plasma fusion.

For ionospheric plasmas see *46 Geophysics*. For space plasmas see *90 Astrophysics*.

N88-27901# Wisconsin Univ., Madison. Dept. of Physics.
MOMENT APPROACH TO NEOCLASSICAL FLOWS, CURRENTS AND TRANSPORT IN AUXILIARY HEATED TOKAMAKS
Yil Bong Kim Feb. 1988 66 p
(Contract DE-FG02-86ER-53218)
(DE88-008024; UWPR-88-2) Avail: NTIS HC A04/MF A01

The moment approach is utilized to derive the full complement of neoclassical transport processes in auxiliary heated tokamaks. The effects of auxiliary heating (neutral beam injection (NBI) and ion cyclotron resonance heating (ICRH)) considered arise from the collisional interaction between the background plasma species and the fast-ion-tail species. From a known fast ion distribution function we evaluate the parallel (to the magnetic field) momentum and heat flow inputs to the background plasma. Then, through the momentum and heat flow balance equations, we can determine the induced parallel flows (and current) and radial transport fluxes in equilibrium (on the time scale much longer than the collisional

relaxation time, i.e., t much greater than upsilon sub ii). In addition to the fast-ion-induced current, the total neoclassical current includes the bootstrap current, which is driven by the pressure and temperature gradients, the Pfirsch-Schlueter current which is required for charge neutrality, and the neoclassical (including trapped particle effects) Spitzer current due to the parallel electric field. The radial transport fluxes also include off-diagonal compnents in the transport matrix which correspond to the Ware (neoclassical) pinch due to the inductive applied electric field and the fast-ion-induced radial fluxes, in addition to the usual pressure- and temperature-gradient-driven fluxes (particle diffusion and heat conduction). Once the tranport coefficient are completely determined, the radial fluxes and the heat fluxes can be substituted into the density and energy evolution equations to provide a complete description of equilibrium (delta/delta t much less than upsilon sub ii) neoclassical transport processes in a plasma. DOE

N88-27902# Gosudarstvennyi Komitet po Ispolzovaniyu Atomnoi Energii, Moscow (USSR). Inst. Atomnoj Ehnergii.
DYNAMICS OF A PLASMA PRODUCED UNDER EFFECT OF THE XeCl-LASER RADIATION ON METALLIC SURFACE
R. V. Arutyunyan, V. Yu. Baranov, and L. A. Bolshov et al. 1987 11 p In RUSSIAN
(DE88-701983; IAE-4443/7) Avail: NTIS (US Sales Only) HC A03/MF A01

The results of preliminary experiments and theoretical analysis permitting clarification of the main parameters of interaction of excimeric radiation with a metal surface at intensities of the order of 10 to the 9th power Watts/sq cm are presented. Dynamics of plasma production, heating and expansion of near-surface breakdown at the presence of atmosphere counterpressure is investigated. Spectroscopic study of luminosity of different plasma compounds of metal vapors and its probing by different wave lengths permit the qualitative determination of the pressure, temperature and concentration of plasma. DOE

N88-27903 California Univ., Los Angeles.
ION BERNSTEIN MODES IN CURRENT-CARRYING PLASMAS Ph.D. Thesis
Jose Luis Milovich 1987 343 p
Avail: Univ. Microfilms Order No. DA8800612

Two aspects of ion Bernstein wave (IBW) propagation in current-carrying plasmas are studied. The first is the inclusion of an electron tail in addition to the Maxwellian background. The second is the modifications introduced by a shearless poloidal magnetic field. The former is studied in the electrostatic and electromagnetic cases. The presence of a poloidal field is studied by considering a bounded homogeneous cylindrical plasma in the electrostatic limit. Dissert. Abstr.

N88-27904# Wisconsin Univ., Madison. Dept. of Physics.
TOKAMAK MAGNETIC TURBULENCE OVER THE SAFETY FACTOR RANGE 0.6 LESS THAN q LESS THAN 3
D. E. Graessle, S. C. Prager, and R. N. Dexter Mar. 1988 17 p
(Contract DE-FG02-86ER-53227)
(DE88-008421; DOE/ER-53227/119) Avail: NTIS HC A03/MF A01

Magnetic turbulence (V less than 400kHz) has been measured both internally and externally to a tokamak plasma as the edge q is varied from 0.6 to 3. The radial and poloidal spatial dependence of the coherence is investigated. The spatial and frequency dependence of the fluctuations are similar over the wide range of q. DOE

N88-27905# California Univ., Los Angeles. Center for Plasma Physics and Fusion Engineering.
HEATING EFFICIENCY OF BEAT WAVE EXCITATION IN A DENSITY GRADIENT
G. J. Morales and J. E. Maggs Feb. 1988 12 p
(Contract N00014-84-K-0583)
(AD-A193066; PPG-1130) Avail: NTIS HC A03/MF A01 CSCL 20I

A simple model is presented which yields analytical expressions for the heating efficiency of beat-wave excitation in a plasma with a linear density profile. The effect of self-consistent Landau damping by tail electrons is included without recourse to WKB approximations. GRA

N88-27906# Naval Postgraduate School, Monterey, Calif.
THE INFLUENCE OF IONIZATION WITHIN A PLASMA OPENING SWITCH M.S. Thesis
Wenzel G. Evans, Jr. Dec. 1987 49 p
(AD-A193147) Avail: NTIS HC A03/MF A01 CSCL 09A

An alternate description of the Plasma Opening Switch (POS) is presented. In addition, a preliminary study was conducted into the ionization of desorbed carbon particles from the cathode surface in the switch region. The formation of a locally dense plasma layer surrounding the cathode is shown to influence the electric field and the Debye screening distance. This effect influences the emission of electrons from the cathode as well as providing a mechanism for opening the switch. GRA

N88-27907# Naval Research Lab., Washington, D.C.
SPECTRAL LINE SHAPES FROM HIGHLY IONIZED SODIUM PLASMAS Interim Report, Oct. 1987 - Oct. 1988
G. Mehlman, P. G. Burkhalter, and D. A. Newman 8 Mar. 1988 14 p
(AD-A193401; NRL-MR-6186) Avail: NTIS HC A03/MF A01 CSCL 20I

Line widths have been measured on spectra from implosions with the Gamble II generator. The K-shell transitions from sodium ions were observed with a curved crystal x-ray spectrograph and imaged with a pinhole camera. The various contributions to spectral line broadening were analyzed. The conclusion is that the line widths were comprised essentially of a source broadening due to the finite plasma size and a plasma broadening due to the ion motion during the implosion final stage. Despite the comparable contribution from both effects, under our conditions of observation, it is possible to derive an upper limit for the ion velocity to account for the large line widths observed. GRA

N88-27908# California Univ., Berkeley. Coll. of Engineering.
EFFECTS OF LOW REFLECTION ON THE COLLECTOR AND SOURCE SHEATHS OF A FINITE ION TEMPERATURE PLASMA
L. A. Schwager 13 Apr. 1988 62 p
(Contract DE-FG03-86ER-53220)
(DE88-008929; UCB/ERL-M-88/25) Avail: NTIS HC A04/MF A01

The region between a Maxwellian plasma source and an absorbing surface which reflects a fraction of the incident ions is modeled numerically with dynamic, electrostatic particle simulation and theoretically with a static, kinetic plasma-sheath model. The fraction zeta of ions reflected is varied from 0 to 0.6 which generally increases both the potential drop from the source to the collector and the energy transported to the collector surface. Results from both models agree well when the fraction reflected is less than 0.4 for full energy transfer to reflected ions. With larger fractions and with slightly less than full reflected energy, simulations show an ion-ion two-streaming interaction which slightly reduces the collector potential drop and decreases the ion energy deposited on the collector surface relative to predictions from the static theory. According to theory, for a deuterium-tritium plasma, a collector material causing the reflected ion fraction to be zeta = 0.2 with full reflected energy increases the magnitude of collector potential by 12 percent and the ion energy deposited by 6 percent over those predicted when zeta = 0. DOE

N88-27909# Lawrence Livermore National Lab., Calif.
PLASMA BEHAVIOR IN THE BOUNDARY LAYER NEAR A RAILGUN SURFACE
Sang-Wook Kang and R. E. McCallen Mar. 1988 3 p Presented at the 4th Symposium on Electromagnetic Launch Technology,

Austin, Tex., 12 Apr. 1988
(Contract W-7405-eng-48)
(DE88-008889; UCRL-97431; CONF-880478-12) Avail: NTIS HC A02/MF A01

Viscous flow and thermal characteristics are theoretically analyzed for the plasma behind a moving projectile inside a railgun. When only convective effects are included in the turbulent boundary layer analysis, the results suggest a temperature maximum in the wall region for very high velocity flows. The case of radiative as well as convective transport has also been investigated for an optically thick boundary layer flow by application of an approximate method. Results show a sizable effect of radiation on the flow characteristics, especially on the heat transfer rate to the railgun surface. Author

N88-27910# Lawrence Livermore National Lab., Calif.
OPTICAL IMAGING DIAGNOSTICS FOR FUSION PLASMAS
S. L. Allen 1 Apr. 1988 12 p Presented at the Spring Meeting of the Materials Research Society, Reno, Nev., 4 Apr. 1988
(DE88-997572; UCRL-97661; CONF-880408-10) Avail: NTIS HC A03/MF A01

Imaging diagnostics are used for spatially and temporally resolved quantitative measurements of plasma properties such as the ionization particle source, particle energy loss, and impurity radiation in magnetically confined fusion plasmas. Diagnostics equipped with multielement solid state detectors are well suited to the environment of large fusion machines with high magnetic field and X-ray neutron fluxes. Both conventional and highspeed video cameras are used to measure neutral deuterium H sub alpha emissions from fusion plasmas. Continuous high speed measurements are made with video cameras operating at 0.1 to 0.5 ms frame; gated cameras provide snapshots of 10 to 100 ms during each 16 ms video frame. Digital data acquisition and absolute intensity calibrations of the cameras enable detailed quantitative source measurements; these are extremely important in determining the particle balance of the plasma. In a liner confinement device, radial transport can be determined from the total particle balance. In a toroidal confinement device, the details of particle recycling can be determined. Author

N88-27911# Wisconsin Univ., Madison. Dept. of Physics.
REMINIMIZATION OF ENERGY INTEGRAL AND STABILITY LIMIT FOR NON-IDEAL MHD (MAGNETOHYDRODYNAMIC) PLASMA
Y. Kondoh Mar. 1988 24 p
(Contract DE-FG02-85ER-53212)
(DE88-008422; DOE/ER-53212/121) Avail: NTIS HC A03/MF A01

The stability condition of relaxed states is derived from the energy principle for the non-ideal MHD plasma. An Euler equation for the reminimization of energy integral is derived and shown to give the marginal stable, non-singular perturbations for the stability condition. An extended stability limit for the beta = 0 relaxed states is derived from the stability condition, with use of the eigenvalue analysis for the Euler equation. By using the perturbation method, the extended stability limit is solved in the 1st order approximation to explain the deviation of the experimental stability limit from the idealized stability limit by Taylor. A procedure to get overall stability limit against both the non-singular and the singular perturbations is discussed. DOE

N88-27912# Oak Ridge National Lab., Tenn.
ITER PLASMA EQUILIBRIUM AND POLOIDAL FIELD SYSTEM DESIGN
D. J. Strickler, J. D. Galambos, and Y. K. M. Peng 1988 14 p Presented at the PF Systems Workshop, Garching, Fed. Republic of Germany, 5 May 1988
(Contract DE-AC05-84OR-21400)
(DE88-011005; CONF-8805126-1; CONF-8805126) Avail: NTIS HC A03/MF A01

Several poloidal field coil design issues are identified when assessing the benefits of high plasma elongation in an ITER device. Among these are the sensitivity of PF ampere-turns and coil energy to specific constraints on the plasma shape and profiles and the optimal placement of PF coils subject to assumed operating scenarios. Two versions of free boundary equilibrium codes presently under development at the Oak Ridge National Laboratory (ORNL), HEQ and VEQ, are used to solve several PF design problems related to these issues. Recent efforts have been directed toward problems in the analysis of highly elongated, magnetically-limited plasmas, such as X-point and divertor strike-point placement and control. In this report, we describe the capabilities of HEQ and discuss the major options available to the user. Applications of HEQ and VEQ in the area of plasma elongation tradeoff studies are presented. DOE

N88-27913# Hiroshima Univ. (Japan). Inst. for Fusion Theory.
GLOBAL AND LOCAL MAGNETOHYDRODYNAMIC RELAXATIONS
Tetsuya Sato, Ritoku Horiuchi, and Kanya Kusano Jun. 1987 23 p
(DE88-752602; HIFT-137) Avail: NTIS (US Sales Only) HC A03/MF A01

Based on theoretical and computational considerations, magnetic reconnection driven nonlinearly by an kink instability is confirmed to play the key role in the magnetohydrodynamic relaxation. An important finding is that the relaxation takes either global relaxation or local relaxation, depending on whether the involved reconnection is total or partial. DOE

N88-27914# Japan Atomic Energy Research Inst., Tokyo.
DESIGN OF DIVERTOR PLATE AND MEASUREMENTS OF DOUBLE-NULL OPEN DIVERTOR PLASMA IN THE JFT-2M TOKAMAK
Ichiro Yanagisawa, Teruaki Shoji, Masahiro Mori, Kazuo Odajima, Hideo Ohtsuka, Norio Suzuki, Mitsuru Hasegawa, Kanji Ohta, Masayoshi Sugihara, and Yoshihiko Uesugi et al. Oct. 1987 24 p In JAPANESE; ENGLISH summary
(DE88-753130; JAERI-M-87-192) Avail: NTIS (US Sales Only) HC A03/MF A01

The Design of the divertor plate, the results of the computational simulation and the experimental results on the compact diverter of the JFT-2 tokamak are described. Graphite divertor plates have showed a good performance as divertor target materials through divertor discharges. The H-mode plasma and low temperature, high density divertor plasma are obtained. From computational results, this is in the intermediate region between low and high recycling region. DOE

N88-27915# Japan Atomic Energy Research Inst., Tokyo. Dept. of Large Tokamak Research.
ANALYSIS OF LOWER HYBRID CURRENT DRIVE AND RAMPUP EXPERIMENTS ON THE JT-60 TOKAMAK
Yuichi Takase, Masao Honda, Yoshitaka Ikeda, Tsuyoshi Imai, Keishi Sakamoto, Shunji Tsuji, Kazuya Uehara, and Kenkichi Ushigusa Dec. 1987 15 p
(DE88-753136; JAERI-M-87-200) Avail: NTIS (US Sales Only) HC A03/MF A01

Lower hybrid current drive and current rampup data obtained on JT-60 are analyzed. Both the current drive efficiency and the current rampup efficiency are similar to those obtained in smaller tokamaks. The stored energy and the pressure anisotropy of the current-carrying superthermal electrons are obtained from magnetic measurements. The distribution function of the superthermal electrons is modelled by a three-temperature Maxwellian with a flat tail extending to the accessibility energy in the forward direction, a perpendicular temperature of 150 keV, a backward parallel temperature of 250 keV, and a backward-to-forward ratio of 2. These results are consistent with expectations based on a detailed numerical modelling and the model distribution functions inferred previously on smaller tokamaks. DOE

N88-27916# Academy of Sciences of the Ukrainian SSR, Kiev.
EQUILIBRIUM DISTRIBUTION FUNCTIONS FOR LIMITED PLASMA-MOLECULAR SYSTEMS

A. G. Zagorodnij, A. S. Usenko, and I. P. Yakimenko 1986 49 p In RUSSIAN; ENGLISH summary
(DE88-702412; ITF-86-161) Avail: NTIS (US Sales Only) HC A03/MF A01

The equilibrium distribution of charged and neutral particles in limited plasma-molecular systems with an arbitrary configuration of boundaries are calculated with all multiple expansion terms taken into account. The distributions of free and bound particles in the case of semi-limited systems that have harmonic oscillators or rigidly coupled pairs of charged particles as a molecular subsystem are also studied. DOE

N88-27917# Academy of Sciences of the Ukrainian SSR, Kiev.
ELECTROMAGNETIC WAVE INCOHERENT REFLECTION BY A HALF-SPACE OF WEAKLY-IONIZED PLASMA WITH AN ABSORBING BOUNDARY
A. G. Zagorodnij, A. S. Usenko, and I. P. Yakimenko 1987 33 p In RUSSIAN; ENGLISH summary
(DE88-702413; ITF-87-18) Avail: NTIS (US Sales Only) HC A03/MF A01

The spectra of incoherent electromagnetic waves reflected by a half-space of weakly ionized plasmas taking into account the charged particle absorptions by a boundary are calculated using the diffusion approximation. The effect of the boundary absorption properties on frequency and angular distributions of the incoherent reflection differential coefficients is studied in detail. DOE

N88-27918# Academy of Sciences of the Ukrainian SSR, Kiev.
ON PLASMA STABILITY UNDER ANISOTROPIC RANDOM ELECTRIC FIELD INFLUENCE
L. N. Rabich and P. P. Sosenko 1987 9 p
(DE88-702422; ITP-87-12) Avail: NTIS (US Sales Only) HC A02/MF A01

The influence of anisotropic random field on plasma stability is studied. The thresholds and instability increments are obtained. The stabilizing influence of frequency missmatch and external magnetic field is pointed out. DOE

N88-27919 Michigan State Univ., East Lansing.
ENERGY DISTRIBUTION AND TRANSFER IN FLOWING HYDROGEN MICROWAVE PLASMAS Ph.D. Thesis
Randall A. Chapman 1987 226 p
Avail: Univ. Microfilms Order No. DA8801797

The physical and chemical properties of a hydrogen discharge in a flowing microwave plasma system were investigated. The plasma system is the mechanism utilized in an electrothermal propulsion concept to convert electromagnetic energy into the kinetic energy of flowing hydrogen gas. The physical and chemical properties were examined for absorbed powers of 20 to 100 W, pressures of 0.5 to 1.0 torr, and flow rates of 0 to 10,000 micromoles/sec. A calorimetry system enclosing the plasma system to accurately measure the energy inputs and outputs was developed. The rate of energy that was transferred to the hydrogen gas as it flowed through the plasma system was determined as a function of absorbed power, pressure, and flow rate. The percentage of power that is transferred to the gas is found to increase with increasing flowrate, decrease with increasing pressure, and to be independent of absorbed power. An optical spectroscopy system to measure the line intensities and widths of the plasma emission was developed. The electron density, plasma frequency, percent ionization, atomic electronic temperature, and molecular rotational and vibrational temperatures of the plasma are determined as functions of absorbed power, pressure, and flow rate. A simplistic heat transfer model that characterizes the energy transfer of the plasma-wall interactions utilizing the calorimetry and spectroscopy results was developed to lend some insight to the dominant processes involved. Dissert. Abstr.

N88-27920# Institut Franco-Allemand de Recherches, St. Louis (France).
PRODUCTION OF INTENSIVE ELECTRON BEAM IMPULSIONS BY SETUP OF PSEUDOGLARE DISCHARGES [ERZEUGUNG INTENSIVER ELEKTRONENSTRAHLPULSE MIT GETRIGGERTEN PSEUDOFUNKEN-ENTLADUNGEN]
K. Stockwald and M. Schwertl 29 Apr. 1987 20 p In GERMAN Presented at the DPG-Fruehjahrstagung, Goettingen, Fed. Republic of Germany, 1987
(ISL-CO-210/87; ETN-88-92737) Avail: NTIS HC A03/MF A01

Electron beam impulsions at a maximum intensity of 500 to 700 A and duration of 20 to 60 nsec generated by pseudoglare discharges are described. The system is composed of a pseudoglare chamber with several electrodes coupled to a high voltage pulse generator of 30 to 80 kV. A preionization device allows the discharge momentum regulation and the subsequent electron beam emission through anodes opening. Electric and geometric electron beam characteristics are determined by Faraday cylinder measurements and by material destruction effects. ESA

76 SOLID-STATE PHYSICS

Includes superconductivity.

For related information, see also *33 Electronics and Electrical Engineering* and *36 Lasers and Masers.*

N88-27921# Naval Research Lab., Washington, D.C.
COMPILATION OF NRL PUBLICATIONS ON HIGH TEMPERATURE SUPERCONDUCTIVITY Report, 1 Jan. - 1 Jul. 1987
Donald U. Gubser 1987 250 p
(AD-A189137) Avail: NTIS HC A11/MF A01 CSCL 20C

Some areas of study include: Superconducting Phase Transitions in the La-M-Cu-O Layered Perovskite system, M = La, Ba Sr, and Pb; Temperature Dependent X-Ray Studies of the High T sub c Superconductor La(1.9)Ba(0.1)CuO4; X-Ray Identification of the Superconducting High T sub c Phase in the Y-Ba-Cu-O System; Processing and Properties of the High T sub c Superconducting Oxide Ceramic YBasub2Cu3O7; Phonon Density of States and Structure of the Superconductor YBasub2Cu3O7; Magnetic Field Studies of the La(2-x)MxCuO4 and Ba2Y1Cu3O7 High T sub c Superconductors; Preparation, Structure, and Magnetic Field Studies of High T sub c Superconductors; Electronic Structure, Bonding and Electron-Phonon Interaction in La-Ba-Cu-O Superconductors; Band Theory Analysis Of Anisotropic Transport in La2CuO4-Based Superconductors; Prediction of Anisotrophic Thermopower of La(2-x)MxCuO4; Character of States Near the Fermi Level in YBa2Cu3O7; Complex Hamiltonians: Common Features of Mechanisms of High-T sub c and Slow Relaxation; Plasma Sprayed Superconducting Oxide Coatings; Resonant Photoemission Study of Superconducting Y-Ba-Cu-O; Observed Trends in the X-Ray Photoelectron and Auger Spectra of High Temperature Superconductors; and Impact of High-Temperature Superconductors on High Power, Millimeter Wave Source Technology. GRA

N88-27922# Academy of Sciences of the Ukrainian SSR, Kharkov. Fiziko-Tekhnicheskij Inst.
EFFECT OF HIGH-AMPLITUDE HIGH-FREQUENCY CURRENT ON NON-ISOTHERMAL EQUILIBRIUM OF NS-BOUNDARY IN INHOMOGENEOUS SUPERCONDUCTOR
A. I. Bezuglyj and V. A. Shklovskij 1987 24 p In RUSSIAN
(DE88-701682; KFTI-87-21) Avail: NTIS (US Sales Only) HC A03/MF A01

Effect of high-amplitude high-frequency current and the arbitrary shape on averaged in oscillations non-isothermal equilibrium of the vibrating interphase boundary in a long superconductor has been theoretically investigated using the phenomenological approach based on the equation of a thermal balance and dependence of the superconductor critical temperature on the current value. The averaged self-consistent temperature field of

fast-oscillating non-isothermal NS-boundary (thermal kink) allowing to go out beyond the limits of the known conception of mean-square heating and to take into account the effect of a current oscillation shape. It is established that in case of current oscillations, being alternate pulses of the reversed polarity, NS-boundary, being originally in equilibrium, will drift to N-phase, if their shape becomes stronger when the pulse amplitude being fixed. Stronger pulses lead to motion of the interphase boundary in the S-phase region when current efficiency being fixed (i.e. heat release in the normal region). In case of current pulses of a sufficiently plane shape it is established that the width of the kink oscillation region has an order of the known heat length. Classifications of experiments on high-power SHF radiation effect on volt-ampere characteristics (VAC) of superconducting films is carried out in the paper; VAC families for inhomogeneous superconductors, where current runs with high-frequency component of a large amplitude, are constructed. It is shown that nonlinear VAC stages are related to the presence in the film a local domain near inhomogeneity, which length changes with the high-frequency current component amplitude change. Series of VAC has hystheresis of thermal nature. DOE

N88-27923# Electrotechnical Lab., Sakura (Japan).
MOLECULAR BEAM EPITAXY OF GaP FILMS ON Si SUBSTRATES Abstract Only
H. Kawanami, S. Ishihara, K. Nagai, K. Ishii, and Y. Hayashi 1987 13 p In JAPANESE Submitted for publication
(PB88-131974) Avail: NTIS HC E05 as PB88-131933; copy not available from STI Facility CSCL 20L

Molecular beam epitaxy (MBE) of GaP films on Si substrates was developed because this structure has possibilities to realize GaP/Si based high efficiency (about 36 percent) tandem solar cell and also GaP/Si based optoelectronic ICs. A low temperature Si surface celaning method at a temperature as low as 800 C was established. Single-crystalline GaP films were successfully grown on Si(001) substrates in a wide growth temperature range from 300 to 600 C. During the film growth, Sn and Si were doped for n-type dopants and Be was doped for p-types. Also Zn-O complexes which act as radiative recombination centers were successfully doped during the growth of GaP films. Process compatibility of Si device process and GaP device process was shown by a fabrication of optoelectronic ICs which integrate GaP LEDs and Si MOSFETs. GRA

N88-27924# Joint Inst. for Nuclear Research, Dubna (USSR). Lab. of Theoretical Physics.
ANHARMONIC MODEL FOR HIGH-Tc SUPERCONDUCTORS
N. M. Plakida, V. L. Aksenov, and Sh. L. Dreksler 1987 11 p In RUSSIAN
(DE88-702196; JINR-R-17-87-498) Avail: NTIS (US Sales Only) HC A03/MF A01

A considerable ehancement of the superconducting transition temperature T(sub C) in perovskite-type oxides is explained in the framework of the anharmonic model for superconductors with structurally unstable lattices. It is shown that interaction of electrons with highly anharmonic oxygen-ion vibrations of a rotational type results in a sufficiently large coupling constant lambda. The obtained estimation for T(sub C) is in agreement with experimental data for La(Y)BaCuO systems. DOE

N88-27925# International Centre for Theoretical Physics, Trieste (Italy).
HIGH-TEMPERATURE SUPERCONDUCTIVITY: AN OVERVIEW
V. L. Ginzburg Jul. 1987 31 p Presented at the Adriatico Conference on High Temperature Superconductors, Triests, Italy, 6 Jul. 1987
(DE88-702051; IC-87/164; CONF-8707109) Avail: NTIS (US Sales Only) HC A03/MF A01

After a short account of the history of experimental studies on superconductivity, the microscopic theory of superconductivity, the calculation of the control temperature and its possible maximum value are presented. An explanation of the mechanism of superconductivity in recently discovered superconducting metal oxide ceramics and the perspectives for the realization of new high-temperature superconducting materials are discussed. DOE

N88-27926# Sandia National Labs., Albuquerque, N. Mex.
DOSE-ENHANCEMENT EFFECTS IN TaSi/Al- AND Al-GATE MOS DEVICES
D. M. Fleetwood, D. E. Beutler, B. L. Draper, D. Knott, D. B. Brown, and H. Rosenstock 1988 5 p Presented at the 25th Annual Conference on Nuclear and Space Radiation Effects, Portland, Ore., 12 Jul. 1988 Prepared in cooperation with Naval Research Lab., Washington, D.C.
(Contract DE-AC04-76DP-00789)
(DE88-005483; SAND-88-0249C; CONF-880730-2) Avail: NTIS HC A02

The response of MOS capacitors with TaSi/Al and Al electrodes to medium- and low-energy X-irradiation is investigated. Experimentally measured dose-enhancement effects are compared with computer simulations for these structures. DOE

N88-27927# International Centre for Theoretical Physics, Trieste (Italy).
SELF ENERGY CORRECTIONS TO THE AB INITIO BAND STRUCTURES: CHROMIUM
N. I. Kulikov, M. V. Magnitskaya, M. Alouani, and M. A. Khan May 1987 31 p
(DE88-701825; IC-86/251) Avail: NTIS (US Sales Only) HC A03/MF A01

We describe the effect of many particle corrections to improve the electronic energy spectrum calculated in the framework of the Density Functional Formalism (DFF). We show that it is possible to consider an n particle diagram like a correction to the DFF results for electronic structure, if we take into account the electron-electron interaction with non-zero transmitted momentum q or energy epsilon. The model is proposed for calculating the leading term of the self-energy expansion as a power series in interactions, i.e., the second order term under the conditions q equals O and epsilon not equals O. This model is illustrated by calculating the electronic band structure and optical properties of anti ferromagnetic chromium. The self-energy correction leads to a better agreement between the theoretical calculations and experimental measurements of electronic properties. DOE

N88-27928# Rockwell International Corp., Thousand Oaks, Calif. Science Center.
ATOMIC LAYER EPITAXY OF ZnS AND ZnSe Final Report, 8 May 1986 - 18 Jun. 1987
J. G. Nelson Feb. 1988 40 p
(Contract DAAB07-86-C-F013; DA Proj. IL1-62709-DH-95)
(AD-A192307; SC5461.FR; AMSEL-NV-1-21) Avail: NTIS HC A03/MF A01 CSCL 07B

The objective of this program was to determine the feasibility of using Atomic Layer Epitaxy (ALE) as a deposition technique for fabricating IR rugate structures. Theoretical activities under the contract consisted of designing and modeling rugate structures containing ZnS and ZnSe or ZnSe and ZnTe. The experimental work resulted in the growth of high-quality epitaxial films of ZnS, ZnSe and ZnTe on (001)-oriented GaAs substrates. Multi-layer structures (quarter-wave stacks and rugate filters) of ZnSe and ZnTe were deposited, but although certain aspects of these ALE structures were successful, the devices did not show the optical performance that was expected. This has been understood as resulting from differences in film nucleation and growth rates between the two candidate materials which were chosen for this program. Our conclusions are that, although ALE is capable of producing high-quality epitaxial and chalcogenide thin films, it is not a practical technique for fabricating IR rugate filters. GRA

N88-27929# Massachusetts Inst. of Tech., Lexington. Lincoln Lab.
SOLID STATE RESEARCH Quarterly Technical Report, 1 May - 31 Jul. 1987
Alan L. McWhorter 15 Aug. 1987 94 p

(Contract F49620-85-C-0002)
(AD-A192837; Rept-1987; Rept-3; ESD-TR-87-073) Avail: NTIS HC A05/MF A01 CSCL 20L

The topics covered are solid state device research, quantum electronics, materials research, microelectronics, and analog device technology. GRA

N88-27930# Brown Univ., Providence, R. I. Dept. of Chemistry.
GROWTH AND CHARACTERIZATION OF CuGaS2, CuAlS2 AND CuGa0.9Al0.1S2 SINGLE CRYSTALS
X-C. He, H-S. Shen, P. Wu, K. Dwight, and A. Wold 15 Mar. 1988 21 p
(Contract N00014-85-K-0177)
(AD-A192963; TR-7) Avail: NTIS HC A03/MF A01 CSCL 20B

In the search for suitable chalcogenides which may be used as infrared windows at 10 micrometers, several chalcogenides of copper, gallium and aluminum have been investigated. Single crystals of CuGaS2, CuAlS2 and CuGa0.9Al0.1S2 have been grown by chemical vapor transport using iodine as the transport agent. They all crystalline with the chalcopyrite structure. The energy gap, infrared transmission, stability in oxygen and microhardness have been measured for these compounds. CuAlS2 has higher thermal stability and hardness than CuGaS2, but its IR transmission range is smaller. The IR transmission range of the 10 percent solid solution lies between those of the two end members; its thermal stability and optical band gap are lower than those of both end members. GRA

N88-27931# Aerospace Corp., El Segundo, Calif. Chemistry and Physics Lab.
SCHOTTKY-BARRIER FORMATION ON A COVALENT SEMICONDUCTOR WITHOUT FERMI-LEVEL PINNING: THE METAL-MoS2(0001) INTERFACE
Jeffrey R. Lince, David J. Carre, and Paul D. Fleischauer 15 Apr. 1988 35 p
(Contract F04701-82-C-0083)
(AD-A193044; TR-0086A(2945-03)-1; SD-TR-88-19) Avail: NTIS HC A03/MF A01 CSCL 07B

Chemical interaction and Schottky-barrier formation at the metal-MoS2 interface were studied by evaporating metals (Ag, Al, Au, Co, Fe, In, Mn, Pd, Rh, Ti, and V) onto the (0001) basalplane surface of cleaved molybdenite, and then analyzing the interface with x-ray photoelectron spectroscopy (XPS). Except for Mn, negligible changes were revealed in the Mo(3d(5/2) and S(2p(3/2) peak shapes, or widths, after deposition. The shifts in the binding energies did not correlate with the electron configuration of the metal but rather with the metal electronegativity, and are interpreted in terms of band bending at the metal-semiconductor interface, rather than chemical reaction. Plot of both Mo and S binding energies versus metal electronegativity yield approximately linear curves with nonzero (positive) slopes, which provide an average index of interface behavior of $S' = 1.28 + \text{or} - 0.22$. This value is considerably higher than for other covalent semiconductors, which exhibit $S' < 0.3$ due to Fermi-level pinning. The anomalous behavior of MoS2 results from the extreme inertness of the basal-plane surface and the stability of the layered crystal lattice of MoS2. The absence of chemical interaction at the interface causes the formation of a Schottky barrier exhibiting behavior that may approach the Schottky limit. This behavior for MoS2(0001) is compared with that of other semiconductors, and is discussed in terms of their ionicity, reactivity, and dielectric response. GRA

N88-27932# North Carolina Univ., Chapel Hill. Dept. of Chemistry.
SILICON OXIDATION STUDIES: A REVIEW OF RECENT STUDIES ON THIN FILM SILICON DIOXIDE FORMATION IN THE PHYSICS AND CHEMISTRY OF SiO2 AND THE Si-SiO2 INTERFACE Interim Technical Report
E. A. Irene 25 Mar. 1988 16 p
(Contract N00014-86-K-0305)
(AD-A193176; TR-20) Avail: NTIS HC A03/MF A01 CSCL 07D

The formation of the thin silicon dioxide (SiO2) films via thermal oxidation on single crystal silicon substrates has been found to depend on the method of Si cleaning, impurities on the Si surface, the Si crystal orientation, film stress, and the availability of electrons at the Si surface. Recent studies on these topics are recounted along with a framework for understanding. No fully acceptable model for thin Si02 formation yet exists, but recent studies lead in new directions towards this goal. GRA

N88-27933# Aerospace Corp., El Segundo, Calif. Chemistry and Physics Lab.
PICOSECOND TRANSIENT REFLECTIVITY OF UNPINNED GALLIUM ARSENIDE (100) SURFACES
Steven M. Beck and John E. Wessel 1 Feb. 1988 18 p
(Contract F04701-85-C-0086)
(AD-A193242; TR-0086(6945-06)-4; SD-TR-87-62) Avail: NTIS HC A03/MF A01 CSCL 20L

Surface recombination was measured for photowashed and unwashed gallium arsenide using picosecond transient photoreflectance methods. The results for the washed surfaces clearly demonstrate slow surface recombination that is accurately described by an ambipolar diffusion model. The fast decay observed for unwashed samples implies rapid surface recombination involving a more complex mechanism. GRA

N88-27934# Aerospace Corp., El Segundo, Calif. Chemistry and Physics Lab.
PARAMAGNETIC POINT DEFECTS IN BORON-IMPLANTED HgO.7CdO.3Te
Robert C. Bowman, Jr., E. L. Venturini, and S. N. Witt 1 Feb. 1988 22 p Prepared in cooperation with Sandia National Laboratories, Albuquerque, N. Mex. and California Inst. of Tech., Pasadena
(Contract F04701-85-C-0086)
(AD-A193276; TR-0086(6945-07)-4; SD-TR-88-03) Avail: NTIS HC A03/MF A01 CSCL 07B

The initial observations of Electron Paramagnetic Resonance (EPR) spectra from Hg0.7Cd0.3Te and CdTe after implantation with boron ions are described in this report. Sharp and nearly isotropic EPR signals with the free electron g-values were easily detected at low temperatures (= or > 78 K) when the boron ion implant dose was 1 x 10 to the 16th power ions/sq cm or larger. For identical implant conditions, more intense signals and narrower peaks were obtained from Hg0.78Cd0.3Te samples than from CdTe samples. However, the g-factors for all implanted Hg(1-x)Cd(x)Te samples appear to be equivalent and are similar to the values reported for the dangling-bond defects in other ion-implanted semiconductors. The EPR spectra produced by the boron implants do not correspond to either the degenerate conduction electron bands that form in ion-implanted Hg(1-x)Cd(x)Te or to the shallow donor states previously found in chemically doped CdTe. When implanted crystals are cooled below 4 K, partially resolved, two-component lineshapes are observed at some orientations. Increasing the temperature causes these two-component lines to collapse into nearly Lorentzian lineshapes with temperature dependent widths. This behavior is consistent with a thermally activated process by which the paramagnetic spins hop between different locations. GRA

N88-27935# Washington Univ., Seattle. Dept. of Materials Science and Engineering.
MIGRATION AND STABILITY OF HgCdTe LATTICE DEFECTS Final Report, 24 Jun. 1985 - 30 Dec. 1987
Ryoichi Kikuchi 29 Feb. 1988 32 p
(Contracts DAAG29-85-K-0167; DAAG29-84-K-0203)
(AD-A193293; ARO-23187.3-PH) Avail: NTIS HC A03/MF A01 CSCL 20B

Continuing from our previous work on equilibrium phase diagrams of Hg-Cd-Te systems, diffusion of Hg and Cd in HgCdTe has been studied in this project. The Path Probability Method (PPM) of irreversible statistical mechanics is used with a point as the basic cluster. Basic formulation of diffusion: A gradient of atomic density is applied to the system and the responding atomic

flux is formulated. It is noteworthy to see that chemical potential gradient appears quite naturally as the driving force, as the Onsager theory requires, rather than the atomic density gradient. Hg fast diffusion consists of two branches. In the vacancy mechanism branch, diffusion decreases with Hg vapor pressure, P(Hg), while it increases in the interstitial mechanism branch. Equations are derived to show these branches and curves for the diffusion coefficient are plotted. Experimentally observed activation energy is given atomic interpretation. GRA

N88-27936# City Coll. of the City Univ. of New York. Inst. for Ultrafast Spectroscopy and Lasers.
ULTRAFAST PHYSICS IN SEMICONDUCTOR MICROSTRUCTURES Annual Progress Report, 1 Dec. 1986 - 30 Nov. 1987
Robert Alfano 19 Feb. 1988 108 p
(Grant AF AFOSR-0031-86)
(AD-A193300; RF-447230; AFOSR-88-0301TR) Avail: NTIS HC A06/MF A01 CSCL 09A

Analyzed is picosecond photoluminescence data obtained from quasi-two- and quasi-zero-dimensional electron systems in GaAs/AlGaAs multiple quantum wells and CdSSe/glass spherical quantum wells. Important results are: (1) nonequilibrium phonons produced in the energy relaxation process of quasi-two-dimensional carriers in a vicinity of phonon wave number q sub e could behave like coherent Bosons within a short time period. The effects of nonequilibrium phonons for photogenerated carriers in undoped GaAs quantum wells are to slow the energy relaxation and to shorten the recombination lifetime. (2) Electron-hole recombination dynamics in quasi-OD was interpreted based on the carrier confinement model. Ultrafast expansion of carriers in asymmetric GaAs quantum wells as observed under picosecond excitation. Dynamical changes in the band structure of GaAs and GaSe were measured under shock waves. GRA

N88-27937# Strathclyde Univ., Glasgow (Scotland).
LASER SPECTROSCOPY OF QUANTUM WELL AND SUPERLATTICE STRUCTURES Interim Report No. 1, 3 Dec. 1987 - 2 Feb. 1988
B. Henderson 15 Feb. 1988 15 p
(Contract DAJA45-88-C-0006)
(AD-A193336) Avail: NTIS HC A03/MF A01 CSCL 07D

The research described in this report aims to understand the effects of disorder on the lineshapes of exciton luminescence in quantum well (QW) materials. The low temperature photoluminescence (PL) and photoluminescence excitation (PLE) spectra of the excitonic transition in QW material are a sensitive test of interfacial quality. Contributions to the linewidth arise from homogeneous (lifetime) and inhomogeneous (disorder) effects. In a typical 50 A well in GaAs, a linewidth at low temperatures of a few meV compares to a typical linewidth about one hundred times smaller in bulk material. GRA

N88-27938# State Univ. of New York, Buffalo. Dept. of Chemistry.
COUPLED EVEN-PARITY SUPERCONDUCTING STATES: SQUARE LATTICE
A. Langner, D. Sahu, and Thomas F. George Apr. 1988 12 p
(Contract N00014-86-K-0043)
(AD-A193432; UBUFFALO/DC/88/TR-67) Avail: NTIS HC A03/MF A01 CSCL 20C

The Ginzburg-Landau free energy density for the coupling of s-wave and d-wave superconducting states in square planar symmetry is considered. Four single-order parameter states and a mixed state are enumerated along with analytical relations for their thermodynamic critical fields, Hc, and critical temperatures. The differential Ginzburg-Landau equations are derived and applied to the calculation of the upper and lower critical fields, Hc2 and Hcl. The relevance of the analysis to superconductivity in the Cu-O planes of the high-Tc materials is discussed. GRA

N88-27939# Lawrence Livermore National Lab., Calif.
PROBING THE ELECTRONIC AND DEFECT STRUCTURE OF PEROVSKITE SUPERCONDUCTORS
M. J. Fluss, A. L. Wachs, P. E. A. Turchi, R. H. Howell, Y. C. Jean, J. Kyle, H. Nakanishi, C. W. Chu, R. L. Meng, and H. P. Hor et al. Feb. 1988 9 p Presented at the 1st World Congress on Superconductivity, Houston, Tex., 22 Feb. 1988 Prepared in cooperation with Missouri Univ., Kansas City and Houston Univ., Tex.
(Contract W-7405-eng-48)
(DE88-008349; UCRL-98070; CONF-880210-1) Avail: NTIS HC A02/MF A01

Positrons, either localized or delocalized, in the perovskite superconductors are sensitive to changes in electron density accompanying the normal-to-superconducting transition. We have been using this probe in our laboratory to study the nature of this new phenomena. Our work to date, which is briefly reviewed here, has consisted of a series of lifetime studies on La(sub 1.85)Sr(sub 0.15)CuO4 and YBa2Cu3O(sub 7-d) superconducting samples, the determination of the positron wave function in the perfect crystal, and a direct measurement of the electron momentum density in single crystal La2CuO4. Several important observations have resulted from this early work: the similar response of the positron annihilation lifetime to superconductivity in both La(sub 1.85)Sr(sub 0.15)CuO4 and YBa2Cu3O7, and a quantitative description of the electronic structure for La(sub 1.85)Sr(sub 0.15)CuO4 in terms of a linear combination of atomic orbital-molecular orbital (LCAO-MO) model. DOE

N88-27940# California Univ., Berkeley. Lawrence Berkeley Lab.
THERMODYNAMICS OF OXYGEN-VACANCY ORDERING IN YBa2Cu3O(SUB z)
A. Berea, L. T. Wille, and D. deFontaine Mar. 1988 4 p Presented at the International Conference on High Temperature Superconductors and Materials and Mechanisms of Superconductivity, Interlaken, Switzerland, 29 Feb. 1988
(Contract DE-AC03-76SF-00098)
(DE88-009816; LBL-24936; CONF-880206-8; CONF-880206) Avail: NTIS HC A02/MF A01

The ordering in the Cu-O basal plane of YBa2Cu3O(sub z) is investigated as a function of oxygen content and temperature. Several phase diagrams are calculated by means of the Cluster Variation Method applied to asymmetric two-dimensional Ising models. The interaction parameters selected guarantee the stability of the orthorhombic structures near $z = 7$, and for certain choices, also include a double-cell phase around $z = 6.5$. O-Cu-O correlations are investigated as function of temperature and concentrations. Calculated orthorhombic to tetragonal transition temperatures and concentrations for various oxygen partial pressures are in excellent agreement with recent experimental data. DOE

N88-27941# Michigan Univ., Ann Arbor. Dept. of Electrical Engineering and Computer Science.
INVESTIGATIONS ON THE MBE (MOLECULAR BEAM EPITAXY) GROWTH AND PROPERTIES OF Al(SUB y)Ga(SUB y)In(SUB 1-x-y)AsInP AND InGaAs-InAlAs SUPERLATTICES Progress Report, 1 Feb. 1987 - 31 Dec. 1987
P. K. Bhattacharya and R. Gibala 1987 46 p
(Contract DE-FG02-86ER-45250)
(DE88-009105; DOE/ER-45250/1) Avail: NTIS HC A03/MF A01

Focus of the work was to grow wide-bandgap ternary and quaternary semiconductors InAlAs and InGaAlAs by molecular beam epitaxy and to investigate their electronic, optical and structural characteristics. Techniques being used are X-ray, TEM, photoluminescence and absorption, DLTS, Hall transport, and Raman Spectroscopy. Experiments included both lattice matched and strained layers. We have grown a series of InGaAlAs quaternary alloys lattice matched to InP, covering the bandgap range from 0.75 to 1.45 eV. Low-temperature photoluminescence measurements indicate that the layers are possibly the best ever

grown. The excitonic linewidths are extremely narrow and indicate minimal amounts of clustering. The hole lifetimes in the alloys are comparable to those in high-purity GaAs. Deep levels in these alloys are being investigated and several dominant trap centers have been identified. Studies are under way to establish their physico-chemical origin. Preliminary Raman Spectroscopy measurements have been done on the same samples and the data are being analyzed. Intention is to establish the GaAs, AlAs and InAs-like phonon spectra as a function of composition. We have realized the narrowest PL excitonic linewidths in InGaAs/GaAs MQWs. The linewidths (approximately) 1 to 2 meV are almost a factor of 3 better than anything ever reported previously. A proper understanding of strained layer epitaxy by non-equilibrium growth techniques such as MBE is emerging for the first time. DOE

N88-27942# Oak Ridge National Lab., Tenn.
USE OF MOESSBAUER SPECTROSCOPY TO STUDY IMPLANTED SURFACES
C. J. McHargue 1988 7 p Presented at the Ion Implantation and Plasma Assisted Processes for Industrial Applications Conference, Atlanta, Ga., 21 May 1988
(Contract DE-AC05-84OR-21400)
(DE88-010452; CONF-8805134-2) Avail: NTIS HC A02/MF A01

The technique of Moessbauer spectroscopy in which the conversion electrons emitted during the decay of an excited nucleus are measured in the backscattered geometry is particularly useful for the study of ion implanted materials. The technique is nondestructive and probes a depth comparable to the ion range for most implantation conditions. The hyperfine structure of the Moessbauer spectra gives three important parameters: the isomer shift, the quadrupole splitting, and the magnetic hyperfine splitting. The analysis of these parameters provides information on the electronic structure and local symmetry of the implanted ion. Examples will be given for the use of conversion electron Moessbauer spectroscopy (CEMS) to study implanted metals and ceramics. DOE

N88-27943# Centro Brasileiro de Pesquisas Fisicas, Rio de Janeiro.
MEANING OF ENERGY DIAGRAMS USED TO DESCRIBE HETERO-STRUCTURES
J. S. Helman 1987 10 p In PORTUGUESE; ENGLISH summary
(DE88-702219; CBPF-NF-055/87) Avail: NTIS (US Sales Only) HC A02/MF A01

Energy diagrams used to describe superlattices built by alternate doping are based on electrostatics, while those for heterostructures use potential barriers to simulate the effect of interferences produced by periodic potentials limited in space. DOE

N88-27944# Delaware Univ., Newark. Inst. of Energy Conversion.
LOW-BAND-GAP, AMORPHOUS-SILICON-BASED ALLOYS BY PHOTOCHEMICAL VAPOR DEPOSITION Final Report, 1 Oct. 1985 - 30 Nov. 1986
B. N. Baron, S. S. Hegedus, and S. C. Jackson Feb. 1988 28 p
(Contract DE-AC02-83CH-10093)
(DE88-001165; SERI/STR-211-3214) Avail: NTIS HC A03/MF A01

Thin films of hydrogenated amorphous silicon-germanium alloys were deposited by mercury-sensitized photochemical vapor deposition using a novel photo-CVD reactor. Thin films of a-Si(sub 1-x)Ge(sub x):H with 0 less than or equal to x less than or equal to 1 and 1.0 less than E sub g less than 1.8 eV were deposited from mixtures of silane and disilane with germane and inert gas diluents at substrate temperatures from 160 to 200 C. Alloy films were characterized by measurements of photo- and dark conductivity, electron mobility-lifetime product, sub-bandgap absorption, and density of states. Dilution with hydrogen increased the photoconductivity to 10 to the -5 S/cm and mobility-lifetime product to 6 x 10 to the -8 sq cm/V for alloys having a band gap of 1.4 eV. DOE

N88-27945 Arizona State Univ., Tempe.
PREDICTION OF DEEP LEVELS AND EQUILIBRIUM CONCENTRATIONS OF DEFECTS IN SEMICONDUCTORS Ph.D. Thesis
Robert Werner Jansen 1987 285 p
Avail: Univ. Microfilms Order No. DA8802785

Electronic structure and total energy calculations are performed on a number of defect systems in semiconductors. Predictions are made for deep levels and total energies associated with point defects and defect complexes, using both empirical and first-principles approaches. First, a study is made of the trends in the deep levels associated with chalcogen complexes of from one to five impurities in Si. It is found that the deep level moves upward toward the conduction band edge with increasing complex size. The results are compared to experimental observations on unidentified deep levels associated with chalcogen impurities in Si. An ab-initio pseudoatomic orbital method to calculate the deep levels and total energies for vacancies, interstitials and substitutional point defects for a large variety of compounds is developed. The trends in the deep levels associated with interstitial impurities are calculated from first principles and appear much the same as those expected through the tight binding technique. Finally, predictions are made for native and extrinsic equilibrium defect concentrations of vacancies, interstitials and substitutional point defects in III-IV and II-VI materials. Dissert. Abstr.

N88-27946 Cornell Univ., Ithaca, N.Y.
A STUDY OF TUNNELING PHENOMENA IN GALLIUM ARSENIDE-ALUMINUM GALLIUM ARSENIDE HETEROSTRUCTURES Ph.D. Thesis
John Andrew Lebens 1988 197 p
Avail: Univ. Microfilms Order No. DA8804519

The tunneling of electrons from a quantum well is investigated. The sample is a tunnel capacitor structure in which a GaAs well, containing a two dimensional electron gas, is separated by an AlGaAs tunnel barrier from the bottom n(+) electrode and by a much thicker AlGaAs barrier from the top n(+) electrode. Application of a dc bias across the structure allows control of the density of electrons in the well. Three experiments are presented. The device allow experimental testing of how well the transverse wave vector conservation law holds in the presence of scattering. In a regime where the transverse wave vector cannot be conserved in the absence of scattering, a model is presented that includes scattering effects and shows that it agrees with the experimental data. Some conclusions are drawn about the efficiency of spacer layers to reduce these scattering effects. The effect of a magnetic field on the tunneling process is examined. The application of a magnetic field perpendicular to the growth layer caused additional confinement of the electrons in the quantum well. An experiment which allow the measurement of the resulting density of states reflecting the induced Landau level structure via two different models is described. The fabrication steps taken to develop lateral confinement of the quantum well in the sample is discussed. This electrostatic confinement technique creates dots of electrons of a small enough size scale that total quantization of electrons can be achieved. Dissert. Abstr.

N88-27947 Cornell Univ., Ithaca, N.Y.
TOPICS IN QUASICRYSTALLOGRAPHY Ph.D. Thesis
Daniel Soleyman Rokhsar 1987 149 p
Avail: Univ. Microfilms Order No. DA8725769

Quasicrystals are materials with diffraction patterns consisting of sharp peaks, but with crystallographically forbidden symmetry. A complete classification of two-dimensional quasicrystalline structures for rotational symmetry less than 46-fold is presented. The same methods developed here can also be applied to the classification of three-dimensional quasicrystals; the first step in this classification is presented in a determination of the possible three-dimensional reciprocal lattices with rotational symmetry less than 23-fold. The focus was on the properties of quasicrystals in

Fourier space, where the most straightforward generalization of the classical crystallographic concepts is possible. The classification problem divides into two parts: determining the allowed sets of wave-vectors in the Fourier space (the reciprocal lattices) and enumerating the allowed Fourier amplitudes at these wave-vectors (the space groups). The restriction to cases with 46- and 23-fold symmetry arises from the connection between the lattice problem and a much-studied problem in the algebraic number theory, related to Fermat's last theorem. The lattice problem becomes rapidly more complicated as the rotational order increases above 47. Unlike crystallographic lattices, quasicrystallographic lattices can be invariant under a non-trivial scale change. The systematics of these scale invariances and their ramifications for quasicrystallographic space groups are discussed. Dissert. Abstr.

N88-27948# California Univ., Berkeley. Lawrence Berkeley Lab.
DEEP LEVEL DEFECTS IN SEMICONDUCTORS: STRESS AND PRESSURE STUDIES Ph.D. Thesis
D. D. Nolte May 1988 195 p
(Contract DE-AC03-76SF-00098)
(DE88-010855; LBL-25242) Avail: NTIS HC A09/MF A01

Deep-level defects in semiconductors have strongly localized wavefunctions, which sample near-neighbor potentials around the defect center. These defects therefore can couple strongly to the local lattice, leading to many interesting phenomena, including large lattice relaxation. One method to probe the defect-lattice coupling is by applying stress or pressure. The application of stress or pressure to a semiconductor sample containing deep-level defects alters the lattice spacings around the defects and consequently alters their energy position in the bandgap. The magnitude of the energy shift under stress, as well as the dependence of the energy shift on uniaxial stress direction, can provide information concerning the structure of the deep level and its symmetry. Uniaxial stress applied in conjunction with deep level transient spectroscopy is a relatively new technique for probing the symmetry of deep-level defects. Uniaxial stress lowers the symmetry of the crystal and can break the degeneracy of defects, leading to energy splitting. The effect of these splittings on the thermal emission of carriers from defects is discussed in detail. The limit of energy resolution for this thermal ionization technique is also investigated. DOE

N88-27949# Los Alamos National Lab., N. Mex.
SUPERCONDUCTOR CONSOLIDATION
K. P. Staudhammer 1988 7 p Presented at the 1st Industrial Applications of Shock Processing Powders, Socorro, N. Mex., 1 Jun. 1988
(Contract W-7405-eng-36)
(DE88-010938; LA-UR-88-1588; CONF-8806131-1) Avail: NTIS HC A02/MF A01

A program to develop explosively shock consolidated monoliths of YBa2Cu3O(sub 7-x) ceramic superconductors has been ongoing at Los Alamos National Laboratory since last year. Shock consolidation can produce a near 100 percent theoretical density, bulk superconductor that does not require a post anneal in oxygen. Shock compaction is also an excellent means of creating a good electrical contact weld between the ceramic superconductor and a metal such as copper. Elimination of the post anneal and low temperature shock welding of the cladding metal are unique advantages stemming from the shock compaction processing. Successful shock compaction processing will enable production of a wide variety of complex ceramic superconductor forms tailored for specific defense application requirements. Shock compaction can be developed into industrial manufacturing processes. Shock compacted superconductor billets can be used in applications where a solid superconductor form is required (e.g., magnetic bearings, bus bar for a niobium-tin FEL SMES, motor rotors, etc.) or they can be post processed by extrusion and other swaging processes to produce textured wires and tapes for electrical current carrying applications. DOE

N88-27950# Oak Ridge National Lab., Tenn.
STUDY OF THE FRICTION AND WEAR-RELATED PROPERTIES OF CERAMIC SUPERCONDUCTORS
P. J. Blau and C. E. DeVore 1988 12 p Presented at the ASM Symposium on Engineered Materials for Advanced Friction and Applications, Gaithersburg, Md., 1 Mar. 1988
(Contract DE-AC05-84OR-21400)
(DE88-011844; CONF-880317-2) Avail: NTIS HC A03/MF A01

The recent interest in high critical temperature (T sub c) superconductors has created a need to examine the tribological properties of these materials for defining potential applications and handling characteristics. This paper discusses preliminary information about the reciprocating sliding friction coefficients (self-mated and on gold), scratch resistance, microindentation hardness, and surface damage mechanisms in Y-Ba-Cu-O compounds. These compounds are fabricated in several ways including traditional powder compaction and solution-growing of single crystals. As expected, the materials are quite brittle, but Knoop microindentation hardness numbers for single crystals can exceed 4.41 GPa (450 kg/sq mm). Scratch resistance using a diamond-stylus test decreases with increasing load because intergranular and transgranular cracking increases with load. Friction coefficients on gold range from 0.12 to 1.0, depending on test duration, and those for self-mated sliding range between 0.15 and 1.1, also depending on test duration. Results suggest that the materials are brittle in their monolithic form, but that they show some ability to resist abrasion and sliding wear in a controlled environment. DOE

N88-27951# California Univ., Berkeley. Lawrence Berkeley Lab.
PROPERTIES OF NEW LOW DIMENSIONAL MATERIALS AND MECHANISMS OF HIGH T(SUB c) SUPERCONDUCTIVITY
V. Z. Kresin Jul. 1987 25 p Presented at the International Conference on High Temperature Superconductivity, Philadelphia, Pa., 29 Jul. 1987
(Contract DE-AC03-76SF-00098)
(DE88-012026; LBL-24111; CONF-870766-1) Avail: NTIS HC A03/MF A01

The new low dimensional high T(sub c) superconductors are characterized by unusual values of normal and superconducting parameters, by the peculiar behavior of the thermal conductivity. It is possible to observe a multigap structure. High T(sub c) is due to the coexistence of the phonon and plasmon mechanisms. Proximity systems containing high T(sub c) superconductors are promising from the point of view of building a three-terminal device and obtaining a high critical current. DOE

N88-27952# Argonne National Lab., Ill. Materials and Components Technology Div.
SUPERCONDUCTING PROPERTIES OF LaBa2Cu3O(SUB x) AND YBa2Cu3O(SUB y)
U. Balachandran, K. C. Goretta, D. Shi, R. B. Poeppel, and N. G. Eror Apr. 1988 7 p Presented at the 90th Annual Meeting of American Ceramic Society, Cincinnati, Ohio, 1 May 1988 Prepared in cooperation with Oregon Graduate Center, Beaverton.
(Contract W-31-109-eng-38)
(DE88-012038; CONF-880504-3) Avail: NTIS HC A02/MF A01

The liquid-mix technique has been used to synthesize powders of LaBa2Cu3O(sub x) and YBa2Cu3O(sub y). The powders were then pressed into pellets and sintered. After annealing in oxygen, specimens from both materials exhibited sharp drops in resistivity at 90 K. The Y-based material reached zero resistivity at about 86 K, regardless of the cooling rate from the sintering temperature. The La-based material required rapid cooling and relatively short anneals to achieve onset of superconducting at 90 K, but zero resistivity was not obtained above 77 K. DOE

N88-27953# Argonne National Lab., Ill.
CERAMIC FABRICATION TECHNOLOGY FOR HIGH-T(SUB)c MATERIALS
M. T. Lanagan, K. C. Goretta, J. P. Singh, G. T. Goudey, J. T. Dusek, D. I. DosSantos, and R. B. Poeppel Apr. 1988 10 p

Presented at the Conference on Superconductivity and Applications, Buffalo, N.Y., 18 Apr. 1988
(Contract W-31-109-eng-38)
(DE88-012060; CONF-880466-7) Avail: NTIS HC A02/MF A01

Three basic processes are discussed for the fabrication of high T(sub c) superconductors. Superconducting wires of YBa2Cu3O(sub 7-x) are fabricated by extrusion. Tape casting and thick film technology are utilized for the manufacture of YBa2Cu3O(sub 7-x) and silver composite structures. Grain orientation is observed for extruded and tape cast specimens, which is attributed to high shear stresses during plastic forming. DOE

N88-27954# Department of Energy, Washington, D. C.
X-RAY STUDIES OF STRAIN, INTERFACE AND IMPURITIES IN SEMICONDUCTORS Technical Progress Report, 1 Jul. 1987 - 30 Jun. 1988
Y. H. Kao 1988 10 p
(Contract DE-FG02-87ER-45283)
(DE88-012460; DOE/ER-45283/2) Avail: NTIS HC A02/MF A01

X-rays from synchrotron radiation are used to investigate various structural effects in semiconductors and high-Tc superconductors. Several different material systems were studied. These experiments include: probing the microstructure, optical constants, and interfacial roughness in ZnSe/GaAs, AlGaAs/GaAs, CoSi2/Si(111), InAs/GaAs heterojunctions; studies of X-ray fluorescence from layer-structure materials (heterojunctions and superlattices) both as a physical phenomenon and as an experimental tool; studies of total electron yield due to X-ray excitation; investigation of high-Tc superconducting materials by atomic substitution and by X-ray absorption studies; and measurements of lattice strain in As-implanted Si using double crystal topography. DOE

N88-27955# Bundesministerium fuer Forschung und Technologie, Bonn (West Germany).
MATERIALS RESEARCH, SUPERCONDUCTOR AND THIN LAYER TECHNOLOGY [MATERIALFORSCHUNG, SUPRALEITER- UND DUENNSCHICHTTECHNOLOGIEN]
19 Nov. 1987 26 p In GERMAN
(Rept-50/87; ETN-88-92333) Avail: NTIS HC A03/MF A01

Materials research into polymer electric conductors, organic and inorganic polymer microspheres for chromatography, electronic gas sensor corrosion protection of historic glass windows, soldering of ceramics and metals, fiber reinforced automobile parts, superconductors, and thin layer technology is summarized. ESA

N88-27956# Technische Univ., Munich (West Germany). Inst. fuer Anorganische-Chemie.
CHARACTERIZATION OF CRYSTALLINE SILICON BY ELECTROCHEMICAL AND RAMAN SPECTROSCOPY AT THE FRONTIER SEMICONDUCTOR/ELECTROLYTE Ph.D. Thesis [CHARAKTERISIERUNG VON KRISTALLINEM SILICIUM DURCH ELEKTROCHEMISCHE UND RAMAN-SPEKTROSKOPISCHE UNTERSUCHUNGEN AN DER HALBLEITER/ELEKTROLYT-GRENZFLAECHE]
Thomas Salbert 1987 157 p In GERMAN
(ETN-88-92354) Avail: NTIS HC A08/MF A01

A fully automatic electrochemical diffusion length analyzer for crystalline silicon material properties characterization is developed. Determination of minority carrier diffusion length and spectral sensitivity of crystalline solar silicon is described. Silicon/electrolyte frontier surface is examined by surface Raman spectroscopy. Pure and metal coated silicon surfaces for r and p silicon structures are treated. This method is valid for crystal defects and semiconductor surface examination ESA

N88-27957# Technische Univ., Berlin (West Germany). Fachbereich Physik.
INVESTIGATION OF ELECTRONIC BAND STRUCTURE OF SEMICONDUCTORS BY PHOTOEMISSION Ph.D. Thesis [UNTERSUCHUNG DER ELEKTRONISCHEN BANDSTRUKTUR VON HALBLEITERN MITTELS PHOTOEMISSION]
Heinz-Udo Middelmann 1987 109 p In GERMAN
(ETN-88-92370) Avail: NTIS HC A06/MF A01

Development and operation of a 2-D electron energy analyzer similar to ellipsoid mirror analyzer filter principle and its application to angle integrated synchrotron beam apparatus are described. Band structures of InSb, InP, Sn semiconductors are examined by photoelectron emission perpendicular to the sample surface. By variation of the excitation energy the electron wave vectors of Brillouin zone are analyzed. ESA

N88-27958# Technische Univ., Brunswick (West Germany). Naturwissenschaftlichen Fakultaet.
INTERACTIONS BETWEEN SUPERCONDUCTIVITY AND KONDO-GRID PROPERTIES IN CeCu2Si2. MEASUREMENT RESULTS OF SPECIFIC HEAT UNDER HIGH PRESSURE Ph.D. Thesis [ZUSAMMENHAENGE ZWISCHEN SUPRALEITUNG UND KONDO-GITTER-EIGENSCHAFTEN IN CECU2SI2: ERGEBNISSE AUS MESSUNGEN DER SPEZIFISCHEN WAERME UNTER HOHEM DRUCK]
Axel Bleckwedel 1986 141 p In GERMAN Sponsored by the Deutsche Forschungsgemeinschaft, Bonn, Fed. Republic of Germany
(ETN-88-92377) Avail: NTIS HC A07/MF A01

Specific heat of the heavy Fermion superconductor CeCu2Si2 in the temperature range 0.3 to 2K by 9.3kbar pressure is determined. Low temperature properties of the superconductor are explained by Kondo effects. High pressure calorimetric measurements near the critical point are described; experimental and pratical difficulties for specific heat measurement are outlined. ESA

N88-27959# Ecole Centrale de Lyon (France). Lab. d'Electronique Automatique et Mesures Electriques.
TECHNIQUES AND INSTRUMENTATION FOR TRANSIENT CHARACTERIZATION OF METAL-INSULATOR-SEMICONDUCTOR DIODES. APPLICATIONS TO METAL-INSULATOR InP SYSTEM Ph.D. Thesis [INSTRUMENTATION ET TECHNIQUES DE CARACTERISATION TRANSITOIRE DE DIODES METAL-ISOLANT-SEMICONDUCTEUR. APPLICATIONS AU SYSTEME METAL-ISOLANT INP]
Nejat Zencirci 1987 434 p In FRENCH
(Contracts DAII-82-35-178-00-790-75-00-19; CNET-86-1B-156-00-780-92-45-PA)
(ECL-87-17; ETN-88-92840) Avail: NTIS HC A19/MF A01

The theory of interactions of carriers with the defects found at the interface of the insulator-semiconductor system is reviewed and a characterization method is presented. The general principles of the electrical determination of doping profiles are examined and applied to the determination of transient charges. A computer program was developed for the numerical analysis of the resulting signals. Experimental observations are presented, including phenomena such as the existence of an interface state peak just below the conduction band, the fast disappearing of the charges responsible for the positive polarization, and the plasticity of the interface states under polarization. ESA

N88-27375# Pennsylvania Univ., Philadelphia. Dept. of Electrical Engineering.
THERMAL CONDUCTIVITY OF ISOTOPICALLY PURE SEMICONDUCTORS, SUPERLATTICES, SEMICONDUCTOR ALLOYS AND SEMICONDUCTORS AS A FUNCTION OF TEMPERATURE; CONTROL OF THE SEGREGATION COEFFICIENT IN LEC CRYSTAL GROWTH; AND PHOTO-HALL MEASUREMENTS OF GaAs Final Report
Elisabeth Smela *In* Universal Energy Systems, Inc., United States Air Force Graduate Student Summer Support Program, Volume 2 Dec. 1987 19 p (For primary document see N88-27355 21-31)
Avail: NTIS HC A99/MF E03 CSCL 20L

N88-27376# New Mexico Univ., Albuquerque. Dept. of Mechanical Engineering.
PREDICTING OPTICAL DEGRADATION OF A LASER BEAM THROUGH A TURBULENT SHEAR LAYER Final Report
Rita Rex Smith *In* Universal Energy Systems, Inc., United States Air Force Graduate Student Summer Support Program, Volume 2 Dec. 1987 20 p (For primary document see N88-27355 21-31)
Avail: NTIS HC A99/MF E03 CSCL 20L

N88-27384# Kent State Univ., Ohio. Dept. of Physics.
NUMERICAL CALCULATIONS OF DOPENT DIFFUSION INVOLVING FLASHLAMP HEATING OF SILICON Final Report
Joseph C. Varga *In* Universal Energy Systems, Inc., United States Air Force Graduate Student Summer Support Program, Volume 2 Dec. 1987 10 p (For primary document see N88-27355 21-31)
Avail: NTIS HC A99/MF E03 CSCL 20L

N88-27392# Mitsubishi Electric Corp., Tokyo (Japan). Materials Engineering Lab.
SUPERCONDUCTING OXIDES WITH HIGH CRITICAL TEMPERATURES
Kiyoshi Yoshizaki *In its* Mitsubishi Electric Advance (R and D Edition), Volume 31 Dec. 1987 2 p (For primary document see N88-27388 21-31)
Avail: NTIS HC A03/MF A01 CSCL 20L

77 THERMODYNAMICS AND STATISTICAL PHYSICS

Includes quantum mechanics; theoretical physics; and Bose and Fermi statistics.

For related information see also *25 Inorganic and Physical Chemistry* and *34 Fluid Mechanics and Heat Transfer.*

N88-27960# International Centre for Theoretical Physics, Trieste (Italy).
CLOSED STRING FIELDS AS PARAMETERS OF EXTRA GAUGE SYMMETRY OF OPEN STRING FIELD THEORY
I. Ya. Arefeva and L. O. Chekhov May 1987 29 p
(DE88-702046; IC-87/62) Avail: NTIS (US Sales Only) HC A03/MF A01

A gauge invariant action for mixed system of closed and open bosonic strings is considered. We notice that in the open string sector a gauge group parametrized by closed string states does act. In the description of mixed system the open-to-closed transition operator plays a crucial role. We show that this transition operator is an intertwining operator between BRST charges for closed and open string. The closed-open-open analog of Caneschi-Schwimmer-Veneziano amplitude is presented and the triple application of the transition operator to all the tree legs of the open CVS vertex is also discussed. DOE

N88-27961# Gosudarstvennyi Komitet po Ispolzovaniyu Atomnoi Energii, Moscow (USSR). Inst. Teoreticheskoj i Ehksperimental'noj Fiziki.
VORTICES ON THE WORLD SHEET AND STRING'S CRITICAL DYNAMICS
Ya. I. Kogan 1987 15 p
(DE88-702116; ITEP-110(1987)) Avail: NTIS (US Sales Only) HC A03/MF A01

Non-perturbative effects in the first quantized string propagating in non-simply connected space are considered. These effects are due to vortices on the string world sheet, which have to appear in properly regularized two-dimensional field theory describing the world sheet's dynamics. The strings on the lattices are discussed and the dynamical reasons for self dual lattices are suggested. It is shown that non-positively definite lattices, such as a hyperbolic, can be described as an antiferromagnetics in the formalism of functional integral. The critical dynamics on non-simply connected orbifolds and Calabi-Yau manifolds are shortly considered. The two new issues are: the field condensate mechanism different from the Hosotani one, and the open question about the real dimension of compact manifold. DOE

N88-27962# International Centre for Theoretical Physics, Trieste (Italy).
INITIAL BOUNDARY VALUE PROBLEMS OF NONLINEAR WAVE EQUATIONS IN AN EXTERIOR DOMAIN
Yunmei Chen Jun. 1987 19 p
(DE88-701883; IC-87/141) Avail: NTIS (US Sales Only) HC A03/MF A01

In this paper, we investigate the existence and uniqueness of the global solutions to the initial boundary value problems of nonlinear wave equations in an exterior domain. When the space dimension n greater than equals 3, the unique global solution of the above problem is obtained for small initial data, even if the nonlinear term is fully nonlinear and contains the unknown function itself. DOE

N88-27963# Tri-Univ. Meson Facility, Vancouver (British Columbia).
AN OVERVIEW OF LATTICE QCD
R. M. Woloshyn Mar. 1988 16 p Presented at the 3rd Lake Louise Winter Inst. on Quantum Chromodynamics: Theory and Experiment, Lake Louise, Alberta, 6 Mar. 1988
(DE88-010867; TRI-PP-88-9; CONF-880331-3) Avail: NTIS (US Sales Only) HC A03/MF A01

The basic concepts of the Lagrangian formulation of lattice field theory are discussed. The Wilson and staggered schemes for dealing with fermions on the lattice are described. Some recent results for hadron masses and vector and axial vector current matrix elements in lattice quantum chromodynamics (QCD) are reviewed. DOE

N88-27964# Joint Inst. for Nuclear Research, Dubna (USSR). Lab. of Theoretical Physics.
SYMMETRY PROBLEM OF ENERGY-MOMENTUM TENSOR AND THE CREATION OF GRAVITATIONAL FIELD
M. Dubets 1987 10 p In RUSSIAN; ENGLISH summary
(DE88-702442; JINR-R-2-87-331) Avail: NTIS (US Sales Only) HC A02/MF A01

The problem of the symmetry of the energy-momentum tensor (EMT) of an electromagnetic field in a medium is considered as a general problem of Lagrange formalism with external fields. It is shown that the asymmetrical Minkowski EMT correctly describes the system of field and medium, being the result of symmetrization of canonical EMT. But a symmetrical, conserving source of a gravitational field is needed, while the symmetrical Hilbert EMT, which should be used in this role, is not conserved. So a formal method of obtaining such a source is proposed. DOE

N88-27965# Oak Ridge National Lab., Tenn.
CALCULATION OF THE SPECIFIC AND VOLUMETRIC ENTHALPIES OF Ge-Si ALLOYS
V. Alexiades and R. P. Wichner Apr. 1988 35 p
(Contract DE-AC05-84OR-21400)
(DE88-008949; ORNL/TM-10548) Avail: NTIS HC A03/MF A01

A procedure is developed for the calculation of specific and volumetric enthalpies of Ge-Si alloys as an initial step in the evaluation of these materials for heat storage in solar dynamic power systems. The calculation is based on the thermodynamics of non-ideal solutions and the reported regular nature of liquid and solid Ge-Si solutions. With only minor modifications, all of the other thermodynamic properties of this alloy system may additionally be evaluated. Use of Ge-Si alloys for heat storage purposes in solar receivers entails both negative and positive aspects. The negative aspects relate largely to the non-congruent nature of the phase change process which precludes isothermal heat delivery. However, on the positive side are high thermal conductance, low volume change on melting, and the availability of a range of heat delivery temperatures by modification of only the alloy composition. DOE

N88-27966 Cornell Univ., Ithaca, N.Y.
SOME STABILITY CRITERIA IN FLUID AND SOLID MECHANICS Ph.D. Thesis
Jong Chul Song 1988 115 p
Avail: Univ. Microfilms Order No. DA8804628

In modeling a problem in continuum mechanics numerous errors are made which may or may not greatly affect the solution itself, i.e., errors in data, errors in time and/or spatial geometry, errors in modeling the governing equations, etc. Explicit continuous dependence results (appropriate to a number of these different types of possible errors) are derived for a class of initial and boundary value problems for the Navier-Stokes equations, for the equations of linear thermoelasticity, and for a coupled system of equations modeling the double diffusion in thawing subsea permafrost. Dissert. Abstr.

80 SOCIAL SCIENCES (GENERAL)

Includes educational matters.

No abstracts in this category.

81 ADMINISTRATION AND MANAGEMENT

Includes management planning and research.

N88-27967# Engineering Research Associates, Inc., Vienna, Va.
RULES, SCHEMA AND DECISION MAKING Interim Report
David Noble, Carla Grosz, and Deborah Boehm-Davis Sep. 1987 91 p
(Contract N00014-84-C-0484)
(AD-A193389; R-125-87) Avail: NTIS HC A05/MF A01 CSCL 05H

The development and use of schemata in decision making is examined. Subjects are trained to evaluate alternatives by calculating expected outcomes. In subsequent tests, subjects are required to select the best alternative without being given enough time to compute outcomes. Under these conditions subjects adopted a hybrid decision strategy employing both schemata and approximations to outcome calculation. The schemata were organized around a prototype. They specify a judgement associated with the prototype and also contain feature oriented data useful for accommodating differences between observed situations and the situation prototype. There was no evidence for other memory reference structures examined. These included indicator/counterindicator features and wholistic schemata that could entirely replace the learned outcome calculation procedure. There was also no support for memory structures that define discriminator boundaries between different types of judgements or decisons. GRA

N88-27372# Houston Univ., Tex. Dept. of Mechanical Engineering.
THE INTEGRATION OF DECISION SUPPORT PROBLEMS INTO FEATURE MODELING BASED DESIGN Final Report
Jon A. Shupe *In* Universal Energy Systems, Inc., United States Air Force Graduate Student Summer Support Program, Volume 2 Dec. 1987 20 p (For primary document see N88-27355 21-31)
Avail: NTIS HC A99/MF E03 CSCL 05A

82 DOCUMENTATION AND INFORMATION SCIENCE

Includes information management; information storage and retrieval technology; technical writing; graphic arts; and micrography.

For computer documentation see *61 Computer Programming and Software.*

N88-27968 Northwestern Univ., Evanston, Ill.
EFFECTIVE BUFFERING SCHEMES FOR PERFORMING MATRIX OPERATIONS FOR NUMERICAL DATABASES Ph.D. Thesis
Changho Kim 1987 175 p
Avail: Univ. Microfilms Order No. DA8729004

For efficient management of numerical databases for large sparse matrices, it is essential to obtain right storage schemes and effective algorithms to perform matrix operations. A number of storage schemes are identified suitable for databases for large sparse matrices. Based on the storage schemes, algorithms are presented which exploit locality of reference to minimize the number of page accesses involved in performing matrix operations on numerical databases. An important component of the algorithms is the allocation of pages of the main memory buffer among the differnet partitions of the matrices. Using these algorithms, the storage schemes are evaluated by computing the number of page accesses and CPU time. These performance measures are used to develop a tool which aids the database designer to find right storage schemes. Furthermore, performance measures are compared with those from implementation results obtained by running the selected algorithms on synthetically generated data. Dissert. Abstr.

N88-27969# Air Command and Staff Coll., Maxwell AFB, Ala.
USE OF OPTICAL DISK TECHNOLOGY AT THE AIR COMMAND AND STAFF COLLEGE
Curtis H. Arrington, III Apr. 1988 30 p
(AD-A192424; ACSC-88-0130) Avail: NTIS HC A03/MF A01 CSCL 12F

Optical disk technology, the use of lasers to store and retrieve information, is a growing technology for use in audio, video, computer storage and multi-media applications. This technology has a great potential in educational applications. After reviewing the history of information capture and storage, this paper examines how optical disk technology works, its capabilities and limitations. The paper reviews current and potential educational applications, and matches ACSC technology requirements against the potential of optical disk. The paper concludes that optical disk is a viable technology to meet several ACSC requirements and recommends the acquisition of optical disk systems for use in specific applications. GRA

N88-27970# Princeton Univ., N. J. Cognitive Science Lab.
WORDNET: AN ELECTRONIC LEXICAL REFERENCE SYSTEM BASED ON THEORIES OF LEXICAL MEMORY
George A. Miller, Christiane Fellbaum, Judy Kegl, and Katherine Miller Jan. 1988 32 p
(Contract N00014-86-K-0492; RM3-3-M-20)
(AD-A193086; CSL-11) Avail: NTIS HC A03/MF A01 CSCL 05G

This paper describes WORDNET, an online lexical reference system whose design is based on psycholinquistic theories of human lexical organization and memory. English nouns, verbs, and adjectives are organized into synonym sets, each representing one underlying lexical concept. Synonym sets are then related via three principal conceptual relations: hyponymy, meronymy and antonymy. Verbs are additionally specified for presupposition relations that hold among them, and for their most common semantic/syntactic frames. By attempting to mirror the organization of the mental lexicon, WORDNET strives to serve the linquistically unsophisticated user. GRA

N88-27971# Logistics Management Inst., Bethesda, Md.
CAPITALIZING ON EXPERIENCE WITH INTELLIGENCE GATEWAY SOFTWARE Final Report
Cynthia W. Shockley Jan. 1988 139 p
(Contract MDA903-85-C-0139)
(AD-A193362; LMI-DL604R1; DTIC-TR-88/7) Avail: NTIS HC A07/MF A01 CSCL 12E

The Defense Technical Information Center (DTIC) and National Library of Medicine (NLM) both developed gateway software to help users search, retrieve, and analyze information from different data systems, even when hardware and software incompatibilities exist. DTIC has two gateways: Defense Gateway Information System (DGIS) and Search Menu-Aided Easy Searching Through Relevant Options (Search MAESTRO). NLM also has two: Micro-Chemical Substances Information Network (Micro-CSIN) and Grateful MED. Each has strengths and weaknesses; DTIC and NLM experience with them, along with commercial and academic developments, reveal opportunities for improvements. We recommend that: (1) DTIC enhance DGIS to enable all users structure search strategies and select suitable databases, and adapt DGIS so that search terms used for one database can be used in several. Such improvements should enable DTIC to use DGIS to meet all user needs; (2) NLM improve the user-friendliness of Micro-CSIN with online and window prompting techniques and modify Micro-CSIN to incorporate controlled vocabulary terms and names into a search strategy. NLM should decide how to incorporate Micro-CSIN and Grateful MED into ABIDE; (3) DTIC and NLM adopt developments from the commercial and academic sectors such as an object-oriented gateway environment, develop expert systems to aid in creating more effective search strategies, and consider cooperative funding arrangements for future gateway development. GRA

N88-27972# Sandia National Labs., Albuquerque, N. Mex.
DEVELOPING A CONNECTOR SELECTION DBMS (DATABASE MANAGEMENT SYSTEM) USING NIAM (NIJSSEN'S INFORMATION ANALYSIS METHODOLOGY)
N. E. Sevier 1988 29 p Presented at the ASME International Computers in Engineering Conference and Exhibition, San Francisco, Calif., 31 Jul. 1988
(Contract DE-AC04-76DP-00789)
(DE88-008110; SAND-88-0272C; CONF-880719-5) Avail: NTIS HC A03

At Sandia there exist over 1200 qualified electrical connectors that an engineer can choose from for a given application. Currently, engineers select a connector from a small group of familiar connectors. This technique may not select the connector which is best suited for the application. To assist engineers in selecting the most suitable connector from those available, a user friendly, menu driven database was required. Nijssen's Information Analysis Methodology (NIAM), a conceptual information modeling technique, was used to characterize the connector data requirements. NIAM gives the designer techniques for gathering, modeling, and analyzing information. The major benefit of the NIAM was the ability to gain acceptance and approval of the conceptual model from management and users. The conceptual model may then be implemented in any specified database management system. This paper will discuss the development of the connector selection database at Sandia using NIAM. DOE

N88-27973# Electrotechnical Lab., Sakura (Japan).
PATTERN INFORMATION PROCESSING AND MULTIMEDIA DATABASE SYSTEM: CURRENT RESEARCH ON MULTIMEDIA INFORMATION SYSTEM
T. Kato and K. Fujimura 1987 19 p In JAPANESE Submitted for publication
(PB88-131917) Copyright Avail: NTIS HC E04 as PB88-131909; copy not available from STI Facility CSCL 05B

A multimedia database requires the integration of methodologies for pattern information processing, artificial intelligence, and conventional database technology. The framework of multimedia database is proposed from the viewpoint of open-ended architecture for pattern information processing facilities. These requirements are as follows: data abstraction, extended abstracted data types for data and process, and extended interoperability with media independence and database access method. Several classical database models, semantic data models and recent approaches in artificial intelligence are summarized and evaluated with the proposed framework. The object-oriented approach and the logic programming approach are expected to provide a well formed interface for pattern information processings on control mechanism and on media independence. Author

N88-27974 Case Western Reserve Univ., Cleveland, Ohio.
AN ASSESSMENT OF INDEX TERM RANKING Ph.D. Thesis
Carole Agatha Chauncey 1987 252 p
Avail: Univ. Microfilms Order No. DA8802457

The enhancement of document retrieval is dependent on the use of index terms which convey adequate information. It has been postulated that index terms are not equally content-bearing and therefore cannot promote the retrieval of relevant documents with the same degree of dependability. This investigation assesses how several indexers rank the selected index terms, as well as how the agreement/consistency patterns among indexers vary within the titles and the abstract. Author

N88-27975# Midwest Research Inst., Golden, Colo. Solar Energy Research Inst.
SERI STANDARD BROADBAND FORMAT: A SOLAR AND METEOROLOGICAL DATA ARCHIVAL FORMAT
Apr. 1988 53 p
(Contract DE-AC02-83CH-10093)
(DE88-001145; SERI/SP-320-3305) Avail: NTIS HC A04/MF A01

This manual describes a tape archival format appropriate for use with research-level solar radiation data. It serves both as a reference for users reading data recorded in SERI Broadband Format (SBF) and as a guide to archiving solar, meteorological, and weather data in SBF. The manual's intended audience includes solar researchers, engineers, and climatologists as well as data processing professionals. A comprehensive list of solar, meteorological, and weather parameters is included in the format. In addition, the format's flexibility allows the user to add parameters and otherwise tailor the format to meet individual needs. SBF is particularly well suited to handling broadband solar radiation data. Also, instrument orientations (viewing angles), of special interest in solar applications, are given complete, unambiguous coverage in the header for each parameter. Standardized block lengths and detailed header information make it easy to read the data. A researcher recording in this format should be able to include all the basic information a user would require to interpret the data. Blanks and nulls are interspersed in the header and between data elements to make tape dumps readable. DOE

83 ECONOMICS AND COST ANALYSIS

Includes cost effectiveness studies.

N88-27976# Army Aviation Systems Command, St. Louis, Mo.
SOURCES AND NATURE OF COST ANALYSIS DATA BASE REFERENCE MANUAL Interim Report
Douglas Horacek and Robert Pavlovici Jan. 1988 168 p
(AD-A193099; USAAVSCOM-TM-88-F-1) Avail: NTIS HC A08/MF A01 CSCL 05C

Citing specific examples, the report examines, evaluates, analyzes and portrays the sources and nature of the Cost Analysis data base emphasizing important interrelationships between process (gathering, normalization, evaluation), professional skill requirements, the planning of future report revisions, and the development of new data sources. For analysis, the main body of the report employs an expanded 13-step format. Entries on the format were obtained from personal interviews. The report is organized to permit future changes and to facilitate cross-referencing. GRA

84 LAW, POLITICAL SCIENCE AND SPACE POLICY

Includes NASA appropriation hearings; aviation law; space law and policy; international law; international cooperation; and patent policy.

No abstracts in this category.

85 URBAN TECHNOLOGY AND TRANSPORTATION

Includes applications of space technology to urban problems; technology transfer; technology assessment; and surface and mass transportation.

For related information see also *03 Air Transportation and Safety, 16 Space Transportation,* and *44 Energy Production and Conversion.*

N88-27977# Oak Ridge National Lab., Tenn.
TECHNOLOGY TRANSFER FOR DOE'S OFFICE OF TRANSPORTATION SYSTEMS: ASSESSMENT AND STRATEGIES
S. A. Snell, M. A. Brown, and A. M. Zerega Apr. 1988 105 p
(Contract DE-AC05-84OR-21400)
(DE88-010760; ORNL/CON-244) Avail: NTIS HC A06/MF A01

This report reviews and assesses the technology transfer effort of the DOE's Office of Transportation Systems (OTS) and offers recommendations for future technology transfer activities. The OTS technology transfer strategy calls for maximum industry involvement in both the identification and solution of R and D problems. This strategy is supported not only by utilizing industry as the research contractor, but also through a variety of other technology transfer activities. After reviewing the technical accomplishments of the Office, the report describes some of the barriers that inhibit commercialization of these accomplishments. Primary, secondary, and spin-off audiences for OTS R and D are then characterized. An inventory of recent OTS technology transfer activities follows and is supplemented by nine detailed case studies of technology transfer. These case studies represent five distinct approaches to technology transfer and a wide array of mechanisms including: contracting to industry, licensing, demonstration projects, user facilities, and financial incentives. The report ends with a list of recommended future technology transfer activities. DOE

N88-27978# Department of Energy, Washington, D. C.
TECHNOLOGY SECURITY, VOLUME 1
Mar. 1988 121 p
(DE88-008612; DOE/DP-8008612-Vol-1) Avail: NTIS HC A06/MF A01

This study defines the scope of DOE nuclear and nuclear-related technology transfer and security interests and explains their interrelationship, describes existing programs and activities which support these interests and assesses their impact on one another, and identifies pertinent factors that should be taken into consideration in devising measures that may enhance these programs. The focus is on those DOE nuclear and nuclear-related technologies which could make significant contributions to military programs in other countries. The study examines several mechanisms which are viewed as important avenues for technology transfer, (i.e., visits assignments, and foreign travel; public releases; international activities; and clandestine acquisition). The input of various DOE program offices and laboratories was elicited. This provided the benefits of each organization's expertise in technology controls. Moreover, the responsibilities and programs of other U.S. government agencies involved in technology controls were examined in conjunction with DOE's area of responsibilities. DOE

N88-27979# Deutsche Forschungs- und Versuchsanstalt fuer Luft- und Raumfahrt, Cologne (West Germany).
HIGH TECHNOLOGY SPACE FLIGHT ORIENTATION PROGRAM: OVERVIEW AND RECOMMENDATIONS [ORIENTIERUNGSRAHMEN. HOCHTECHNOLOGIE RAUMFART. GESAMTUEBERBLICK UND EMPFEHLUNGEN]
Apr. 1987 144 p In GERMAN
(ETN-88-92332) Avail: NTIS HC A07/MF A01

High technological considerations on space transport and associated techniques are given for decision makers involved in West German research program evaluation. Goals, strategic concepts, prospects for space flight in European and international programs, and long term scenarios are outlined. Guidelines for transport systems, orbital systems, aerothermodynamics, propulsion systems, materials and construction technologies, communication, automation, and robotics are reviewed. ESA

N88-27980*# National Aeronautics and Space Administration. Lewis Research Center, Cleveland, Ohio.
PHASE 1 RESULTS FROM THE STIRLING-POWERED VEHICLE PROJECT
Richard K. Shaltens 1988 17 p Proposed for presentation at the 4th International Conference on Stirling Engines, Tokyo, Japan, 7-10 Nov. 1988; sponsored by Japan Society of Mechanical Engineers
(NASA-TM-100978; DOE/NASA/50112-76; E-4270; NAS 1.15:100978) Avail: NTIS HC A03/MF A01 CSCL 10B

The NASA Technology Utilization (TU) Office is sponsoring a multiyear, multiphase demonstration program to assess the technology developed under the DOE/NASA automotive Stirling engine (ASE) program with engines installed in various Air Force vehicles while being evaluated by independent third parties under realistic conditions. This paper reviews the operational history of Phase 1 with a Mod 1 Stirling engine installed in an Air Force multistop van in a variety of missions. Ten months of operation were with Air Force personnel at Langley Air Force Base, Virginia, where over 1100 hr and 4000 mi were logged on the Langley flight line. The Stirling-powered van operated on unleaded gasoline, JP-4 aircraft fuel, and diesel fuel at Langley Air Force Base. Two months of operation were completed with Deere and Company personnel in the Moline, Illinois area where over 175 hr and 2650 mi were logged on a Deere mail delivery route. Author

88 SPACE SCIENCES (GENERAL)

N88-27981# Max-Planck-Inst. fuer Physik und Astrophysik, Garching (West Germany). Inst. fuer Extraterrestrische Physik.
[ACTIVITIES REPORT OF THE INSTITUTE FOR EXTRATERRESTRIAL PHYSICS] Annual Report, 1987 [INSTITUT FUER EXTRATERRISTRISCHE PHYSIK: TAETIGKEITSBERICHT 1987]
Jan. 1988 152 p In GERMAN Original contains color illustrations
(MPE-206; ISSN-0173-699X; ETN-88-92388) Copyright Avail: NTIS HC A08/MF A01

Research concerning near earth space and the solar system including plasmas physics; energetic ions and electrons in the magnetosphere and in interplanetary space; infrared astronomy; X-ray astronomy; and gamma ray astronomy is summarized. Astronomical observations, theoretical studies, and future projects are outlined. ESA

89 ASTRONOMY

Includes radio, gamma-ray, and infrared astronomy, and astrometry.

N88-27982# Gosudarstvennyi Komitet po Ispolzovaniyu Atomnoi Energii, Moscow (USSR). Inst. Teoreticheskoj i Ehksperimental'noj Fiziki.
TO THE OPPORTUNITIES OF CLUSTER ANALYSIS OF LIGHT CURVES OF SUPERNOVAE
O. S. Bartunov, D. Yu. Tsvetkov, and Yu. I. Morozov 1986 21 p In RUSSIAN; ENGLISH summary
(DE88-701642; ITEF-177(1986)) Avail: NTIS (US Sales Only) HC A03/MF A01

A new approach to analysis of empirical data about supernova (SN), based on a method of cluster analysis, is offered. One of the variants - a method of nearest neighbour, is briefly described. The effectiveness of this method, applied to a problem of classification of 44 light curves of SN in a B-filter, and 22 curves in a V-filter, are demonstrated. This area of opportunities of this approach is briefly outlined. DOE

N88-27983# Smithsonian Astrophysical Observatory, Cambridge, Mass.
APPLICATION OF TWO-DIMENSIONAL IMAGING TO VERY HIGH ENERGY GAMMA RAY ASTRONOMY Progress Report, 1987-1988
1988 22 p
(Contract DE-AC02-82ER-40063)
(DE88-010120; DOE/ER-40063/2) Avail: NTIS HC A03/MF A01

The major accomplishment of this project was the development of a gamma camera for detection of very weak flux from the Crab Nebula. In addition, the detection of a pulsed flux from Hercules X-1 and the installation of a new high resolution camera are reported. DOE

N88-27984# Gosudarstvennyi Komitet po Ispolzovaniyu Atomnoi Energii, Moscow (USSR). Inst. Teoreticheskoj i Ehksperimental'noj Fiziki.
STRANGE, QUARK AND METASTABLE NEUTRON STARS
M. I. Krivoruchenko 1987 13 p
(DE88-702404; ITEP-87(1987)) Avail: NTIS (US Sales Only) HC A03/MF A01

Observable consequences of the possible existence of strange, quark, and metastable neutron stars are discussed. Bose condensation of dibaryons in dense nuclear matter is taken into account. The data on glitches from a pulsar in Crab Nebula are used to obtain limits on binding energy of stable strange matter and on masses of dibaryon resonances. A scenario for two step collapse of supernova SN 1987 a is suggested. Masses of diagonal neutrinos are extracted from the data on a second neutrino burst observed from supernova SN 1987 a. DOE

N88-27985# Bonn Univ. (West Germany). Naturwissenschaftlichen Fakultaet.
SURFACE PHOTOMETRIC INVESTIGATIONS FOR SPIRAL GALAXIES OF LARGE DIMENSION STRUCTURES IN EDGE-ON GEMETRY Ph.D. Thesis
[FLAECHENPHOTOMETRISCHE UNTERSUCHUNGEN ZUR GROSSRAEUMIGEN STRUKTUR VON SPIRALGALAXIEN IN EDGE-ON-GEOMETRIE]
Ralf-Juergen Dettmar 1986 188 p In GERMAN
(ETN-88-92126) Avail: NTIS HC A09/MF A01

Photoelectric, photographic and CCD-photometry of 16 edge-on galaxies covering T between 0 and 9 is presented and analyzed with respect to the global structure of disk-galaxies. A photographic photometry, predominantly in BJ and RF, is used to study five prominent galaxies which have angular diameters larger than 20 arcmin: NGC 55, NGC 253, NGC 4594, NGC 4631, and NGC 4945. Photoelectric measurements supply the absolute scale and CCD imaging is used to check the linearity. Isophote maps with resolution of 6 to 20 arcsec are given. ESA

90 ASTROPHYSICS

Includes cosmology; celestial mechanics; space plasmas; and interstellar and interplanetary gases and dust.
For related information see also *75 Plasma Physics*.

N88-27986*# Stanford Univ., Calif. Center for Space Science and Astrophysics.
COSMOLOGICAL PARAMETERS AND EVOLUTION OF THE GALAXY LUMINOSITY FUNCTION
David Caditz and Vahe Petrosian [1988] 23 p
(Contract NCC2-322; Grant NGR-05-020-668)
(NASA-CR-183081; NAS 1.26:183081) Avail: NTIS HC A03/MF A01 CSCL 03B

The relationship between the observed distribution of discrete sources of a flux limited sample, the luminosity function of these sources, and the cosmological model is discussed. It is stressed that some assumptions about the form and evolution of the luminosity function must be made in order to determine the cosmological parameters from the observed distribution of sources. Presented is a method to test the validity of these assumptions using the observations. It is shown how, using higher moments of the observed distribution, one can determine, independently of the cosmological model, all parameters of the luminosity function except those describing evolution of the density and the luminosity of the luminosity function. These methods are applied to the sample of approximately 1000 galaxies recently used by Loh and Spillar to determine a value of the cosmological density parameter Omega approx = 1. It is shown that the assumptions made by Loh and Spillar about the luminosity function are inconsistent with the data, and that a self-consistent treatment of the data indicates a lower value of Omega approx = 0.2 and a flatter luminosity function. It should be noted, however, that incompleteness in the sample could cause a flattening of the luminosity function and lower the calculated value of Omega and that uncertainty in the values of these parameters due to random fluctuations is large. Author

N88-27987# Los Alamos National Lab., N. Mex.
THE CLASSICAL NOVA OUTBURST
S. G. Starrfield 11 Apr. 1988 30 p Presented at the Multiwavelength Astrophysics, Taos, N. Mex., 11 Aug. 1987
(Contract W-7405-eng-36)
(DE88-009138; LA-UR-88-1210; CONF-8708243-1) Avail: NTIS HC A03/MF A01

The classical nova outburst occurs on the white dwarf component in a close binary system. Nova systems are members of the general class of cataclysmic variables and other members of the class are the Dwarf Novae, AM Her variables, Intermediate Polars, Recurrent Novae, and some of the Symbiotic variables. Although multiwavelength observations have already provided important information about all of these systems, in this review I will concentrate on the outbursts of the classical and recurrent novae and refer to other members of the class only when necessary. DOE

N88-27988# Gosudarstvennyi Komitet po Ispolzovaniyu Atomnoi Energii, Moscow (USSR). Inst. Atomnoj Ehnergii.
IS THE 3C273 QUASAR MACH NEARER
G. A. Kotelnikov 1987 16 p In RUSSIAN
(DE88-702235; IAE-4405/1) Avail: NTIS (US Sales Only) HC A03/MF A01

The effect of superlight expansion of some quasars resulting from cosmologic interpretation of red shift is considered. The possibility of determining the distance to 3C273 quasar, taking account of its expansion angular velocity in frames of Doppler interpretation of quasar red shift value, is discussed. DOE

N88-27989# Lawrence Livermore National Lab., Calif.
DYNAMICAL EVOLUTION OF COSMIC STRINGS
F. R. Bouchet 11 May 1988 12 p Presented at the 8th Moriond Astrophysics Meeting on Dark Matter, Les Arcs, France, 6 Mar. 1988
(Contract W-7405-eng-48)

(DE88-011724; UCRL-98783; CONF-8803113-2) Avail: NTIS HC A03/MF A01

The dynamical evolution of a network of cosmic strings has been studied by means of numerical simulations, both in the radiation and matter era. The basic conclusion is that a scaling solution exists, i.e., the string energy density evolves as t sup -2. This means that the process by which long strings dump their energy into closed loops (which can gravitationally radiate away) is efficient enough to prevent the string domination over other forms of energy. This conclusion does not depend on the initial string energy density, nor on the various numerical parameters. On the other hand, the generated spectrum of loop sizes does depend on the value of our numerical lower cutoff (i.e., the minimum length of loop we allow to be chopped off the network). Furthermore, the network evolution is very different from what was assumed before), namely the creation of a few horizon sized loops per horizon volume and per hubble time, which subsequently fragment into about 10 smaller daughter loops. Rather, many tiny loops are directly cut from the network of infinite strings, and it appears that the only fundamental scale (the horizon) has been lost. This is probably because a fundamental ingredient has been overlooked, namely the kinks. These kinks are created in pairs at each intercommutation, and very rapidly, the long strings appear to be very kinky. Thus the number of long strings per horizon is still of the order of a few, but their total length is fairly large. Furthermore, a large number of kinks favors the formation of small loops, and their sizes might well be governed by the kink density along the long strings. DOE

91 LUNAR AND PLANETARY EXPLORATION

Includes planetology; and manned and unmanned flights.

For spacecraft design or space stations see *18 Spacecraft Design, Testing and Performance.*

N88-27990# Los Alamos National Lab., N. Mex.
USES OF LUNAR SULFUR
D. T. Vaniman, D. R. Pettit, and G. Heiken 1988 20 p Presented at the NASA Symposium on Lunar Bases and Space Activities of the 21st Century, Houston, Tex., 5 Apr. 1988
(Contract W-7405-eng-36)
(DE88-009119; LA-UR-88-1345; CONF-8804104-2) Avail: NTIS HC A03/MF A01

Sulfur and sulfur compounds have a wide range of applications for their fluid, electrical, chemical and biochemical properties. Although low in abundance on the Moon (approximately 0.1 percent in mare soils), sulfur is surface-correlated and relatively extractable. Co-production of sulfur during oxygen extraction from ilmenite-rich soils could yield sulfur in masses up to 10 percent of the mass of oxygen produced. Sulfur deserves serious consideration as a lunar resource. DOE

N88-27991# Academy of Sciences of the Ukrainian SSR, Kiev.
INTERPRETATION OF THE POLARIMETRIC OBSERVATIONS OF JUPITER
M. I. Mishchenko 1987 24 p In RUSSIAN; ENGLISH summary
(DE88-702414; ITF-87-22) Avail: NTIS (US Sales Only) HC A03/MF A01

The analysis of the ground based polarimetric observations of Jupiter is represented. Some properties of aerosol component of the upper cloud layer are established: the effective radius of the cloud particles is r(sub eff)= 0.385 plus or minus 0.030 microns, real part of the refractive index is n(sub r)= 1.386 plus or minus 0.005. The results are obtained by means of polarization calculations with multiple scattering taken into account. DOE

N88-27992# Academy of Sciences of the Ukrainian SSR, Kiev.
POLARIZATION OF LIGHT REFLECTED BY VERTICALLY INHOMOGENEOUS PLANETARY ATMOSPHERE
M. I. Mishchenko 1987 23 p In RUSSIAN; ENGLISH summary
(DE88-702416; ITF-87-27) Avail: NTIS (US Sales Only) HC A03/MF A01

The computational method is proposed for calculating the reflection matrix for a plane-parallel vertically inhomogeneous isotropic atmosphere. The method is based on the numerical solution of the initial value problem for the reflection matrix. DOE

92 SOLAR PHYSICS

Includes solar activity, solar flares, solar radiation and sunspots.

For related information see *93 Space Radiation.*

N88-27993# Cambridge Research and Instrumentation, Inc., Mass.
MEASUREMENT OF MACROSCOPIC ELECTRIC FIELDS IN SOLAR PLASMA STRUCTURES Final Technical Report, 27 May - 27 Nov. 1987
Peter Foukal 14 Dec. 1987 32 p
(Contract F19628-87-C-0110)
(AD-A193291; AFGL-TR-88-0012) Avail: NTIS HC A03/MF A01 CSCL 03B

The work performed in this effort has led to several important advances in our investigation of a new technique for remote sensing of plasma electric fields. The atomic physics underlying the technique is placed on a firmer basis and the polarization structure of the high Balmer and Paschen lines behaves as predicted by perturbation theory. Balmer- and Paschen-line observations of erupting prominences are obtained at Sacramento Peak Observatory and show that the marked increase in sensitivity of the technique expected with the Paschen lines can be realized. Understanding of the interpretation of the observed hydrogen-line broadening is improved, and shown that the sensitivity of the technique, when applied to structures emitting intense hydrogen lines, can exceed 10 volts/cm. This sensitivity is more than adequate to test predictions of transverse electric fields intensities and orientations, in models of flares and other active phenomena. The goal is to construct an instrument optimized for solar plasma electric field measurements, to be installed at the SPO Big Dome. Such an electrograph would make important advances toward understanding the mechanisms and prediction of solar eruptions such as flares and active filaments. GRA

N88-27994# Louisiana State Univ., Baton Rouge. Dept. of Physics and Astronomy.
SOLAR FLARES AND MAGNETOSPHERIC PARTICLES: INVESTIGATIONS BASED UPON THE ONR-602 AND ONR-604 EXPERIMENTS Annual Letter Report, period ending 30 Nov. 1987
John P. Wefel 10 Feb. 1988 22 p
(Contract N00014-83-K-0365)
(AD-A193396) Avail: NTIS HC A03/MF A01 CSCL 03B

Data from the ONR-602 experiment, obtained in a low altitude, polar orbit are being analyzed the investigate the composition, intensity levels and time variations of energetic charged particles both trapped within the Earth's magnetosphere and incident upon the magnetosphere from interplanetary space, particularly solar flare particles. The effort involves both data analysis/interpretation and detailed modeling of the near-Earth environment. The research focusses on the global zones of low energy particle precipitation, including the South Atlantic Anomaly region from which access to the radiation belts is obtained, and the solar particle events of May-Nov., 1982. In addition, scientific/technical support is being provided to the ONR-604 experiment to be launched on the CRRES mission. The results of these investigations will enhance our understanding of the geospace radiation environment and its effects on men, materials and electronic systems in space. The objectives of this research are to investigate the nature and origins of the particle populations in near Earth space by focusing on their spatial distributions, composition, energy spectra and temporal variations

and to look at couplings between interplanetary (solar flare generated) and magnetospheric populations. The goal is to understand the Geospace environment in which men and spacecraft must survive and function. GRA

N88-27995# Academy of Sciences of the Ukrainian SSR, Kiev.
MAGNETOHYDRODYNAMIC WAVE PROPAGATION IN THE SOLAR WIND
P. P. Malovichko 1986 12 p In RUSSIAN; ENGLISH summary
(DE88-702411; ITF-86-137) Avail: NTIS (US Sales Only) HC A03/MF A01

Magnetohydrodynamic wave propagation in the solar wind is investigated. The wave decrement and amplitude dependence on heliocentric distance is obtained. It is shown that wave damping has an essential influence on the index of the wave spectrum generated in the vicinity of the Sun. DOE

93 SPACE RADIATION

Includes cosmic radiation; and inner and outer earth's radiation belts.

For biological effects of radiation see *52 Aerospace Medicine*. For theory see *73 Nuclear and High-Energy Physics*.

N88-27996# Rockefeller Univ., New York.
ARE CENTAUROS DIFFRACTIVE
K. Goulianos 1987 10 p Presented at the 2nd International Conference on Elastic and Diffractive Scattering, New York, N.Y., 15 Oct. 1987
(Contract DE-AC02-87ER-40325)
(DE88-008767; DOE/ER-40325/7A; CONF-8710274-7) Avail: NTIS HC A02/MF A01

Some new experimental information is discussed, which supports the hypothesis that the Centauro events reported by cosmic ray experiments may indeed be produced diffractively as proposed by the author in 1986. DOE

N88-27997# Mission Research Corp., Alexandria, Va.
THEORY AND SIMULATION OF RELAXED PLASMOIDS Final Report, 1 Sep. 1986 - 31 Oct. 1987
John Brandenburg and Karna Wahlstrand Dec. 1987 27 p
(Contract F49620-86-C-0098)
(AD-A192884; MRC/WDC-R-148; AFOSR-88-0552TR) Avail: NTIS HC A03/MF A01 CSCL 03B

Plasmoids can be described as a group of electrons and ions that propagate as a unit through vacuum. In their present conception they consist of an expanding halo region, carrying return current and bearing a slight charge imbalance, and an equilibrium core region that propagates like a pinched charged particle beam. This model was first suggested by T. Lockner of Sandia. Since they are a type of charged particle beam, they can be generated with higher efficiency and deposit their energy over a deeper distance in matter than laser beams. This makes plasmoids attractive for defense applications; however, the structure, formation, and propagation of plasmoids in a space environment are not known at present. Theory and one-dimensional simulations aimed at finding the core structure of plasmoids by using variational principles have been successful. This report documents the progress made in this first phase of research. A proposed second phase of research will use similar techniques to model the three-dimensional formation and propagation of plasmoids in a space environment. GRA

N88-27998*# National Aeronautics and Space Administration. Goddard Space Flight Center, Greenbelt, Md.
CASCADE MODEL OF GAMMA-RAY BURSTS: POWER-LAW AND ANNIHILATION-LINE COMPONENTS
A. K. Harding, P. A. Sturrock, and J. K. Daugherty (North Carolina Univ., Asheville.) Aug. 1988 27 p Submitted for publication
(Grant NGR-05-020-668)
(NASA-TM-101176; NAS 1.15:101176; CSSA-ASTRO-88-13)
Avail: NTIS HC A03/MF A01 CSCL 03B

If, in a neutron star magnetosphere, an electron is accelerated to an energy of 10 to the 11th or 12th power eV by an electric field parallel to the magnetic field, motion of the electron along the curved field line leads to a cascade of gamma rays and electron-positron pairs. This process is believed to occur in radio pulsars and gamma ray burst sources. Results are presented from numerical simulations of the radiation and photon annihilation pair production processes, using a computer code previously developed for the study of radio pulsars. A range of values of initial energy of a primary electron was considered along with initial injection position, and magnetic dipole moment of the neutron star. The resulting spectra was found to exhibit complex forms that are typically power law over a substantial range of photon energy, and typically include a dip in the spectrum near the electron gyro-frequency at the injection point. The results of a number of models are compared with data for the 5 Mar., 1979 gamma ray burst. A good fit was found to the gamma ray part of the spectrum, including the equivalent width of the annihilation line. Author

N88-27999# Max-Planck-Inst. fuer Physik und Astrophysik, Garching (West Germany). Inst. fuer Extraterrestrische Physik.
GAMMA RADIATION FROM CENTER OF THE GALAXY OF THE ORDER OF MeV VALUES [GAMMA-STRAHLUNG VON GALAKTISCHEN ZENTRUM IN MEV-BEREICH]
Roland Diehl Mar. 1988 166 p In GERMAN
(MPE-207; ISSN-0178-0719; ETN-88-91453) Copyright Avail: NTIS HC A08/MF A01

Measurement results for gamma emission from our galaxy center are presented. Compton telescope data obtained in the Southern Hemisphere by a stratospheric balloon at 38 km heights are evaluated. Gamma rays of the Milky Way are measured with a sensitivity of 0.0001 photons/cc/sec, and a significant gamma energy signal at 1.8 MeV is determined. Model structure and nature of Al-26 sources are also investigated. ESA

99 GENERAL

N88-28000# Centre National d'Etudes Spatiales, Toulouse (France). Centre Spatial.
HISTORY OF MANNED SPACEFLIGHT [HISTORIQUE DES VOLS HABITES]
Philippe Lebocq Feb. 1988 60 p In FRENCH; ENGLISH summary
(CNES-NT-121; ETN-88-92762) Avail: NTIS HC A04/MF A01

A compilation of all Soviet and U.S. space missions since Gagarin's flight in 1961 is presented. Identity of crew members, flight dates, type of mission (U.S.S.R. or U.S.), type of vehicle and launcher, duration of flight, and extravehicular activity are shown. ESA

Typical Subject Index Listing

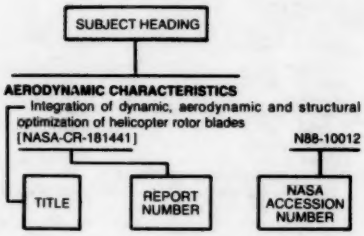

The subject heading is the key to the subject content of the document. Titles, report numbers, and accession numbers of pertinent documents are provided under each subject heading. When the title is insufficiently descriptive of the document content, a title extension has been added, separated from the title by three hyphens. The report number helps to indicate the type of document cited (e.g., NASA report, NASA translation, NASA contractor report). The NASA accession number is the number by which the document abstracts are arranged in this journal and by which the document is sold or requested. The titles, with title extensions if present, are arranged under each subject heading in ascending accession number order. The subject headings have been selected from the latest revision of the *NASA Thesaurus* (NASA SP-7053).

A

A-320 AIRCRAFT
Design and implementation of contact ultrasonic sensors to assess internal damage
[I-177/87] N88-27247

ABEL FUNCTION
Retrieval of temperature and concentration profiles from a limited number of absorption measurements
N88-27501

ABNORMALITIES
Correlation between EEG abnormal activity and aircraft accidents: A long term observation N88-27719
Detection of latent epilepsy in aircrew candidates
N88-27720

ABRASION RESISTANCE
Study of the friction and wear-related properties of ceramic superconductors
[DE88-011844] N88-27950

ABSORBERS (MATERIALS)
Heat and mass transfer in laminar wavy film absorption with the presence of non-absorbable gases N88-27502

ABSORPTIVITY
Storage of thermal energy by means of an absorption cycle
[PB88-190814] N88-27619
Atmospheric nitrogen oxides: Their detection and chemistry
[PB88-193057] N88-27642

ABSTRACTS
Aerospace applications studies, 1971-1987
[AGARD-R-759] N88-27147

ACCELERATED LIFE TESTS
Analysis of debris from accelerated life test of the Hughes five-year Vuilleumier cryocooler
[AD-A193101] N88-27400

ACCELERATION (PHYSICS)
An investigation of soft launch and instability breakup with a two-stage light gas gun
[DE88-010371] N88-27218
Characterization of accelerating pipe flow
[AD-A193065] N88-27481
Stochastic geologic effects on near-field ground motions in alluvium
[AD-A192315] N88-27652

ACCELERATION STRESSES (PHYSIOLOGY)
Evoked potential analysis of impact acceleration experiments N88-27708
EEG indices of G-induced Loss Of Consciousness (G-LOC) N88-27709

ACCELERATION TOLERANCE
Physiological monitoring methodology in the USAFSAM centrifuge N88-27356
Detection of acceleration (+Gz) induced blackout by matched-filtering of visual evoked potentials
N88-27710

ACCURACY
Basic research for the geodynamics program
[NASA-CR-183149] N88-27662

ACOUSTIC ATTENUATION
Reflection of sound in open ended ducts
[PB88-103478] N88-27870
Acoustic propagation in the lower atmosphere
[ISL-R-126/87] N88-27878

ACOUSTIC EMISSION
Acoustic emission calibration instrumentation
[DE88-010817] N88-27528
Application of pattern recognition techniques to the identification of aerospace acoustic sources
[NASA-CR-183116] N88-27877

ACOUSTIC INSTABILITY
Propagation of acoustic disturbances in transonic flow fields of lifting wings
[DFVLR-FB-88-13] N88-27880

ACOUSTIC MEASUREMENT
Acoustic propagation in the lower atmosphere
[ISL-R-126/87] N88-27878

ACOUSTIC MICROSCOPES
Interface control using low frequency (3 to 20 MHz) acoustic microscopy
[REPT-48-411/F] N88-27577

ACOUSTIC PROPAGATION
Acoustic propagation in the lower atmosphere
[ISL-R-126/87] N88-27878

ACOUSTIC VELOCITY
Ultrasonic studies of stresses and plastic deformation in steel during tension and compression
[AD-A192308] N88-27280

ACOUSTICS
Robust methods for array signal processing
[AD-A192854] N88-27871
Publications on acoustics research at the Langley Research Center during 1980-1986
[NASA-TM-100590] N88-27881

ACTIVATION
Determination of Tafel constants in nonlinear polarization curves
[AD-A192335] N88-27282

ADA (PROGRAMMING LANGUAGE)
Ada (trade name) compiler validation summary report: Verdix Corporation VAda-010-03315, version 5.5 MicroVAX 2 host ISBC 386/20P Intel target
[AD-A193226] N88-27774
Ada (trade name) compiler validation summary report: Verdix corporation VAda-010-13125, version 5.41 Sun Microsystems Sun-3/160 host microbar GPC68020 target
[AD-A193415] N88-27777

ADAPTATION
The human element in space: Lessons from Antarctica
[AD-A193440] N88-27741

ADAPTIVE CONTROL
An h-p adaptive finite element method for steady compressible flow N88-27467
Control of free-flying space robot manipulator systems
[NASA-CR-183104] N88-27563
Unified multilevel adaptive finite element methods for elliptic problems
[DE88-011938] N88-27840

ADAPTIVE FILTERS
Sidelobe level of an adaptive array using the SMI (Sampled Matrix Inversion) algorithm
[AD-A193131] N88-27409

ADDITIVES
Alternate/modified binders for airfield pavements
[AD-A192781] N88-27206
Processing and additive effects of ZrO2 on microstructure and dielectric porperties of BaTiO3 ceramics
[AD-A193126] N88-27316
Relative flow rates of explosive powders
[DE88-010767] N88-27350
Numerical calculations of dopent diffusion involving flashlamp heating of silicon N88-27384

ADHESION
An IETS (Inelastic Electron Tunneling Spectroscopy) study of surface reactions applicable to adhesion
[AD-A192274] N88-27261
Improved adhesion for SiO2 particles in silica substrates using helium-ion irradiation
[DE88-008915] N88-27332
Plasma treatment of polymers for improved adhesion
[DE88-011623] N88-27334

ADHESION TESTS
Study of surface treatments before adhesive bonding of light alloys — aircraft industry
[ETN-88-92743] N88-27308
Adhesion of hydrated silicate films
[DE88-011250] N88-27333

ADHESIVE BONDING
Study of surface treatments before adhesive bonding of light alloys — aircraft industry
[ETN-88-92743] N88-27308
Adhesion of hydrated silicate films
[DE88-011250] N88-27333

ADHESIVES
Conductivity mechanism and operating behavior of electrically conductive adhesives on the example of a power transistor
[ETN-88-92355] N88-27464

ADRENAL GLAND
Hypothalamic-pituitary-adrenal responses to short duration high intensity cycle exercise
[AD-A192597] N88-27727

ADSORPTION
Theory of the dissociation dynamics of small molecules on metal surfaces: Finite temperature studies
[DE88-007763] N88-27882

ADVECTION
A zoomable and adaptable hidden fine-mesh approach to solving advection-dispersion equations
[DE88-006174] N88-27816

AERIAL PHOTOGRAPHY
Automatic line network extraction from aerial imagery of urban areas through knowledge based image analysis
[AD-A193067] N88-27615

AERIAL RECONNAISSANCE
Air-to-air radar flight testing
[AGARD-AG-300-VOL-7] N88-27406

AEROACOUSTICS
The influence of surface rounding on trailing edge noise
[AD-A193387] N88-27876
Acoustic propagation in the lower atmosphere
[ISL-R-126/87] N88-27878

AERODYNAMIC CONFIGURATIONS
Wind tunnel tests of the influence of airfoil-thickness on normal force and pitching moment of two slender wings at transonic and supersonic Mach numbers
[DFVLR-FB-88-17] N88-27171
AGARD standard aeroelastic configurations for dynamic response. 1: Wing 445.6
[AGARD-R-765] N88-27193

AERODYNAMIC DRAG
Theoretical and experimental investigations of a vortex drag behind a wing profile with spoiler
[ISL-PU-309/87] N88-27169

AERODYNAMIC LOADS
In-flight load measurements of the Robot-X canards
[AD-A193428] N88-27187

AERODYNAMIC NOISE
Theory of sound production by vortex-airfoil interaction
[AD-A193386] N88-27875
The influence of surface rounding on trailing edge noise
[AD-A193387] N88-27876

AERODYNAMIC STABILITY
Integrated Technology Rotor Methodology Assessment Workshop
[NASA-CP-10007] N88-27148
A comparison of the various helicopter mathematical models used in the methodology assessment N88-27149
A comparison of theory and experiment for aeroelastic stability of a hingeless rotor model in hover N88-27150
A comparison of theory and experiment for coupled rotor-body stability of a hingeless rotor model in hover under simulated vacuum conditions N88-27151
A comparison of theory and experiment for coupled rotor-body stability of a hingeless rotor model in hover N88-27152
A comparison of theory and experiment for the aeroelastic stability of a bearingless model rotor in hover N88-27153
A comparison of theory and experiment for coupled rotor body stability of a bearingless rotor model in hover and forward flight N88-27154
The importance of steady and dynamic inflow on the stability of rotor-body systems N88-27156
Effects of static equilibrium and higher-order nonlinearities on rotor blade stability in hover N88-27157
Aeroelastic modeling of rotor blades with spanwise variable elastic axis offset: Classic issues revisited and new formulations N88-27158
Comparison of experimental rotor damping data-reduction techniques N88-27159
Comparison of experimental coupled helicopter rotor/body stability results with a simple analytical model N88-27160
Aeromechanical stability analysis of COPTER N88-27161

AERODYNAMICS
Aeronautical engineering: A continuing bibliography with indexes
[NASA-SP-7037(229)] N88-27163
Analysis of experimental data for cast 10-2/DOA2 supercritical airfoil at high Reynolds numbers
[AD-A192827] N88-27166
An experimental study of the effect of pitch rate on delta wing aerodynamics and stability
[NASA-CR-183159] N88-27173
Design of a mechanism to control wind tunnel turbulence N88-27370
Aerodynamics of Hypersonic Lifting Vehicles: Fluid Dynamics Panel AGARD Symposium
[AGARD-AR-246] N88-27480

AEROELASTICITY
Integrated Technology Rotor Methodology Assessment Workshop
[NASA-CP-10007] N88-27148
A comparison of theory and experiment for aeroelastic stability of a hingeless rotor model in hover N88-27150
A comparison of theory and experiment for coupled rotor-body stability of a hingeless rotor model in hover N88-27152
A comparison of theory and experiment for the aeroelastic stability of a bearingless model rotor in hover N88-27153
Effects of static equilibrium and higher-order nonlinearities on rotor blade stability in hover N88-27157
Aeroelastic modeling of rotor blades with spanwise variable elastic axis offset: Classic issues revisited and new formulations N88-27158
Comparison of experimental rotor damping data-reduction techniques N88-27159
Comparison of experimental coupled helicopter rotor/body stability results with a simple analytical model N88-27160
Aeromechanical stability analysis of COPTER N88-27161
Aeroelastic characteristics of the AH-64 bearingless tail rotor N88-27162
AGARD standard aeroelastic configurations for dynamic response. 1: Wing 445.6
[AGARD-R-765] N88-27193
Prediction of the aeroelastic behavior of tuned blades. Application to aircraft engines
[ISAL-87-0046] N88-27199
Nonlinear stochastic interaction in aeroelastic structures
[AD-A193427] N88-27589

AEROLOGY
Acoustic propagation in the lower atmosphere
[ISL-R-126/87] N88-27878

AERONAUTICAL ENGINEERING
Aeronautical engineering: A continuing bibliography with indexes
[NASA-SP-7037(229)] N88-27163

AERONOMY
Computer simulation procedure for designing airborne aerometric monitoring programs
[DE88-011896] N88-27674

AEROSOLS
Cloud simulation warm cloud experiments: Droplet growth and aerosol scavenging
[AD-A192944] N88-27666
Interpretation of the polarimetric observations of Jupiter
[DE88-702414] N88-27991

AEROSPACE ENGINEERING
Aerospace applications studies, 1971-1987
[AGARD-R-759] N88-27147
Damping characteristics of metal matrix composites
[AD-A193144] N88-27233

AEROSPACE INDUSTRY
Air Force technical objective document, FY89
[AD-A193110] N88-27194

AEROSPACE MEDICINE
Electric and Magnetic Activity of the Central Nervous System: Research and Clinical Applications in Aerospace Medicine
[AGARD-CP-432] N88-27683
Simulator sickness in the AH-64 Apache combat mission simulator
[AD-A193419] N88-27739
Aerospace Medicine and Biology: A continuing bibliography with indexes (supplement 314)
[NASA-SP-7011(314)] N88-27742

AEROSPACE SYSTEMS
Army space systems for terrestrial applications
[AD-A192735] N88-27613

AEROTHERMOCHEMISTRY
Summary of discussions at the Tenth Meeting of the Sandia Cooperative Group on the Aerothermochemistry of Turbulent Combustion
[DE88-008467] N88-27269

AFTERBODIES
Variable Mach number wall jets for control/propulsion on hypervelocity projectiles/interceptors: Tests with an existing model
[AD-A192845] N88-27167

AGING (MATERIALS)
Aging of CFRP due to longterm storage in heated air
[DFVLR-FB-88-05] N88-27345

AH-64 HELICOPTER
Aeroelastic characteristics of the AH-64 bearingless tail rotor N88-27162

AIR
Heat and mass transfer in laminar wavy film absorption with the presence of non-absorbable gases N88-27502

AIR DUCTS
Reflection of sound in open ended ducts
[PB88-103478] N88-27870

AIR INTAKES
Equipment for mass flow measurements in the low-speed wind tunnel at DFVLR in Brunswick, West Germany
[DFVLR-MITT-88-02] N88-27212

AIR NAVIGATION
Electrical load and power source capacity report for the C-130 aircraft Self Contained Navigation System (SCNS): LSI model 6216A, 6216B, 6216C, revision
[AD-A193079] N88-27186

AIR POLLUTION
National air toxics information clearinghouse: NATICH data base users guide for data viewing, February 1988
[PB88-197470] N88-27645
National ambient Volatile Organic Compounds (VOCs) data base update, documentation
[PB88-195631] N88-27646
Photochemical oxidant formation: Overview of current knowledge and emerging issues
[PB88-195235] N88-27647
Foliar nitrate reductase: A marker for assimilation of atmospheric nitrogen oxides
[DE88-010453] N88-27648

AIR START
Propulsion analysis and application potential of air breathing combined propulsion for ballistic space transporter
[ETN-88-92369] N88-27227

AIR TO AIR REFUELING
Aircraft refueling demonstrator using a microbot alpha 2 robot N88-27367

AIR WATER INTERACTIONS
Air-sea interaction in the vicinity of a land-sea boundary in the presence of upwelling N88-27661

AIRBORNE EQUIPMENT
Computer simulation procedure for designing airborne aerometric monitoring programs
[DE88-011896] N88-27674

AIRBORNE SURVEILLANCE RADAR
Air-to-air radar flight testing
[AGARD-AG-300-VOL-7] N88-27406

AIRBORNE/SPACEBORNE COMPUTERS
Airborne remote operated device
[DE88-010324] N88-27188

AIRCRAFT ACCIDENTS
Improved procedure for impact probability computation of aircraft crash based on Balfanz model
[JUEL-SPEZ-425] N88-27176
Correlation between EEG abnormal activity and aircraft accidents: A long term observation N88-27719

AIRCRAFT ANTENNAS
Airborne measurement of low frequency atmospheric noise ALFAN 1
[AD-A193056] N88-27405

AIRCRAFT COMMUNICATION
Airborne measurement of low frequency atmospheric noise ALFAN 1
[AD-A193056] N88-27405

AIRCRAFT CONSTRUCTION MATERIALS
Factors affecting strength in composite materials used for aircraft
[DT-212/87] N88-27248

AIRCRAFT CONTROL
Investigations of aircraft control with jet spoilers
[ISL-R-112/87] N88-27202
Computer system for the primary fly-by-wire control of civil transport aircraft (experimental system)
[FBW-TB-2086/88] N88-27204
Optimal control of the wing rock phenomenon N88-27373

AIRCRAFT DESIGN
Concept development of a Mach 3.0 high-speed civil transport
[NASA-TM-4058] N88-27182
Supersonic transport/hypersonic transport (SST/HST) development
[SNIAS-881-111-101] N88-27192

AIRCRAFT ENGINES
Prediction of the aeroelastic behavior of tuned blades. Application to aircraft engines
[ISAL-87-0046] N88-27199

AIRCRAFT EQUIPMENT
Electrical load and power source capacity report for the C-130 aircraft Self Contained Navigation System (SCNS): LSI model 6216A, 6216B, 6216C, revision
[AD-A193079] N88-27186

AIRCRAFT HAZARDS
Extinguishing agent for magnesium fire, phases 5 and 6
[AD-A192436] N88-27398
TDWR (Terminal Doppler Weather Radar) PRF (Pulse Repetition Frequency) selection criteria
[AD-A193089] N88-27407

AIRCRAFT NOISE
Application of pattern recognition techniques to the identification of aerospace acoustic sources
[NASA-CR-183116] N88-27877
Aeroacoustic investigation on the noise from ultralight aircraft
[DFVLR-FB-88-03] N88-27879

AIRCRAFT PARTS
Simulation of moisture diffusion of fiber reinforced components of aircraft for general air transportation
[IFL-IB-87-05] N88-27253
Stress corrosion of C ring specimen in salt spray tests
[I-186/87] N88-27307

AIRCRAFT PILOTS
Personality, attitudes, and pilot training performance: Preliminary analysis
[AD-A193102] N88-27746

AIRCRAFT SPIN
Contribution to the numerical solution of airplane spin motion
[ETN-88-92368] N88-27190

AIRCRAFT STRUCTURES
Design manual for impact damage tolerant aircraft structure, addendum
[AGARD-AG-238-ADD] N88-27185
Design and implementation of contact ultrasonic sensors to assess internal damage
[I-177/87] N88-27247
Nonlinear vibrations of periodically stiffened plates N88-27596

AIRCRAFT WAKES
Laser-Doppler measurements of turbulence structures in free streams behind flat and rotation symmetrical profiles
[ETN-88-92336] N88-27510

AIRFOIL OSCILLATIONS
Control and use of unsteady flows: Insect use of various wing kinematics and related pressure measurements using a pitching airfoil N88-27366
Liquid crystals for unsteady surface shear stress visualization
[DE88-010570] N88-27527
AIRFOIL PROFILES
Wind tunnel tests of the influence of airfoil-thickness on normal force and pitching moment of two slender wings at transonic and supersonic Mach numbers
[DFVLR-FB-88-17] N88-27171
Theory of sound production by vortex-airfoil interaction
[AD-A193386] N88-27875
The influence of surface rounding on trailing edge noise
[AD-A193387] N88-27876
AIRFOILS
Effects of numerical dissipation on finite-volume solutions of compressible flow problems
[AD-A193173] N88-27485
Investigation of viscous/inviscid interaction in transonic flow over airfoils with suction
[NASA-CR-183112] N88-27490
Determination of the local heat-transfer characteristics on glaze ice accretions on a cylinder and a NACA 0012 airfoil N88-27500
AIRFRAMES
Design manual for impact damage tolerant aircraft structure, addendum
[AGARD-AG-238-ADD] N88-27185
ALERTNESS
The application of non-stationary data analysis techniques in the identification of changes in the electroencephalogram associated with the onset of drowsiness N88-27688
ALGAE
An outdoor test facility for the large-scale production of microalgae
[DE88-001146] N88-27723
ALGEBRA
Flexible valued algebras of four-dimensions
[ETN-88-92382] N88-27844
ALGORITHMS
Three-dimensional scene analysis using stero based imaging
[AD-A193120] N88-27178
Automatic omega station and LOP (Line Of Position) selection
[AD-A193302] N88-27179
Numerical optimization, system theoretic and software tools for the integrated design of flexible structures and their control systems
[AD-A192927] N88-27183
The integration of decision support problems into feature modeling based design N88-27372
Optimal control of the wing rock phenomenon N88-27373
Calibration and data reduction techniques for the AFGL infrared array spectrometer N88-27374
Creating aspect graphs for use in object recognition N88-27379
Optical interconnections for digital image coding N88-27381
TDWR (Terminal Doppler Weather Radar) PRF (Pulse Repetition Frequency) selection criteria
[AD-A193089] N88-27407
Sidelobe level of an adaptive array using the SMI (Sampled Matrix Inversion) algorithm
[AD-A193131] N88-27409
A numerically efficient digital matched filter for periodic and windowed periodic radar waveforms
[AD-A193132] N88-27410
Effects of numerical dissipation on finite-volume solutions of compressible flow problems
[AD-A193173] N88-27485
Higher order vortex methods with rezoning
[DE88-010777] N88-27505
Dexterous hands: Optimizing grasp by design and planning N88-27572
A lubrication study of engine bearings N88-27574
Three-dimensional aspects of fatigue crack closure
[AD-A192296] N88-27581
Photon limited image processing in the space-time domain
[AD-A193142] N88-27655
Validate algorithms for the determination of rainfall rates from SSM/I microwave satellite imagery
[AD-A192299] N88-27664
Full analysis of a powerful window random access algorithm
[AD-A192437] N88-27763
Synchronizable series expressions. Part 2: Overview of the theory and implementation
[AD-A192783] N88-27768
Distributed algorithms for probabilistic solution of computational vision problems
[AD-A193150] N88-27773
Computer aided design for linear control State Variable System (SVS)
[AD-A193282] N88-27775
Verification of flight software written in C using ACSL
[DE88-006100] N88-27779
The sub-implicit method: New multiprocessor algorithms for old implicit codes
[DE88-011345] N88-27785
Maximum entropy signal restoration with linear programming
[DE88-011740] N88-27787
A hidden-surface removal algorithm for structures defined by triangular and rectangular surface patches
[DFVLR-MITT-88-03] N88-27792
Performability analysis: Measures, an algorithm and a case study
[AD-A192477] N88-27800
A modular proof of correctness for a network synchronizer
[AD-A192726] N88-27802
Improving the performance of AI algorithms
[AD-A192848] N88-27809
Parallel quasi-Newton methods for unconstrained optimization
[AD-A193250] N88-27812
Parallel solutions to geometric problems on the scan model of computation
[AD-A192321] N88-27819
Finding minimum-cost circulations by successive approximation
[AD-A192724] N88-27824
Finding minimum-cost circulations by canceling negative cycles
[AD-A192727] N88-27825
Numerical optimization
[AD-A193032] N88-27827
A review of parallel methods for solving sets of linear equations and their application within optimisation algorithms
[AD-A193137] N88-27830
The computation of stationary distributions on Markov chains through perturbations
[AD-A193191] N88-27855
A comparison of generators for pseudo-random normal deviates
[DE88-011711] N88-27859
Robust methods for array signal processing
[AD-A192854] N88-27871
ALIGNMENT
Precise rotational alignment of X-ray transmission diffraction gratings
[DE88-010599] N88-27273
ALKALI METALS
A fundamental understanding of the interfacial compatibility in hybrid material systems
[AD-A192921] N88-27264
ALKALINE BATTERIES
Alkaline fuel cell performance investigation
[NASA-TM-100937] N88-27267
ALKALINE EARTH METALS
Multiphoton ionization of alkaline earth atoms in an intense laser field
[DE88-008078] N88-27884
ALLOYS
On the systematics of phase transformation in metallic alloys
[DE88-008041] N88-27288
Theoretical predictions of precipitate shapes in cubic alloys
[DE88-010856] N88-27291
Oxidation-erosion of metals and alloys: Models, verification, and prediction
[DE88-010016] N88-27300
Refractory metal alloys and composites for space power systems
[NASA-TM-100946] N88-27310
Thermal conductivity of isotopically pure semiconductors, superlattices, semiconductor alloys and semiconductors as a function of temperature; control of the segregation coefficient in LEC crystal growth; and photo-Hall measurements of GaAs N88-27375
Significance of the local electrode potential within pits, crevices and cracks
[AD-A192482] N88-27432
ALLUVIUM
Stochastic geologic effects on near-field ground motions in alluvium
[AD-A192315] N88-27652
ALPHA PARTICLES
The distribution of some chemical elements between dissolved and particulate phases in the ocean
[DE88-010181] N88-27682
ALTERNATING CURRENT
Some equivalent circuit models for AC impedance analysis of pyrite/solution interface
[DE88-010574] N88-27452
ALUMINIDES
A fundamental understanding of the interfacial compatibility in hybrid material systems
[AD-A192921] N88-27264
ALUMINUM
Evaluation of explosive bonding for patching aluminum with aluminum
[AD-A193303] N88-27285
Nuclear magnetic resonance spectrometer
[AD-A192928] N88-27523
Growth and characterization of CuGaS2, CuAlS2 and CuGa0.9Al0.1S2 single crystals
[AD-A192963] N88-27930
ALUMINUM ALLOYS
A fundamental understanding of the interfacial compatibility in hybrid material systems
[AD-A192921] N88-27264
A method for determining the solubility of hydrogen in molten aluminum-lithium alloys
[DE88-009807] N88-27270
Thermomechanical processing of Al alloy 2090 for grain refinement and superplasticity
[AD-A192333] N88-27281
Analysis of grain refinement and superplasticity in aluminum-magnesium alloys
[AD-A193029] N88-27283
Processing and properties of advanced aluminum alloys
[AD-A193224] N88-27284
Constant amplitude fatigue life data for notched and unnotched annealed Ti-6Al-4V sheet
[AD-A193420] N88-27287
Study of surface treatments before adhesive bonding of light alloys — aircraft industry
[ETN-88-92743] N88-27308
Study of feasibility and optimization conditions of laser treatments: Application of the local recrystallization of aluminum
[ISAL-87-0048] N88-27309
Kinetic of oxidation to air of a Fe-Al-Mn alloy system at 600-800(sup 0)C temperature range
[DE88-702309] N88-27330
Influence of microstructure and microdamage processes on fracture at high loading rates
[AD-A192957] N88-27583
Stress relaxation of a titanium (Ti-6Al-4V) threaded joint
[DE88-010102] N88-27590
ALUMINUM ARSENIDES
Investigations on the MBE (Molecular Beam Epitaxy) growth and properties of Al(sub y)Ga(sub y)In(sub 1-x-y)AsinP and InGaAs-InAlAs superlattices
[DE88-009105] N88-27941
ALUMINUM COMPOUNDS
Application of sol-gel procedures to ceramic composites
[ETN-88-92741] N88-27338
ALUMINUM GALLIUM ARSENIDES
Ultrafast physics in semiconductor microstructures
[AD-A193300] N88-27936
ALUMINUM OXIDES
Application of controlled interfacial pore structures to kinetic studies in alumina
[DE88-010884] N88-27326
Preparation and characterization of ceramic materials based on Al2O3 reinforced with a ZrO2 dispersion
[ISAL-87-0041] N88-27340
Comparison of sol-gel procedures for zircon and alumina
[SNIAS-881-430-108] N88-27342
AMBIENCE
Vertical directionality of ambient noise at 32 deg N as a function of longitude: Tape number 86180
[AD-A193228] N88-27872
AMINO ACIDS
Precise ultraviolet absorbance study of the interaction of amino acids and mononucleosides in aqueous solution
[ISAS-RN-356] N88-27256
AMORPHOUS MATERIALS
Formation of metastable structures and amorphous phases in Cu-W alloys using the triod sputtering technique
[DE88-009051] N88-27298
PECVD of amorphous nickel–phosphorus films
[DE88-011088] N88-27299
AMORPHOUS SILICON
Amorphous silicon solar cells using a metal substrate
[PB88-131941] N88-27628

AMPLIFICATION
On the small signal gain of free electron lasers in the low-current regime
[DFVLR-FB-88-10] N88-27552
AMPLITUDES
Constant amplitude fatigue life data for notched and unnotched annealed Ti-6Al-4V sheet
[AD-A193420] N88-27287
ANALOG SIMULATION
Development of a hybrid simulator for robotic manipulators
[AD-A193119] N88-27557
ANALYZERS
An investigation of the uses of time domain capable vector network analyzers as a diagnostic for helix traveling-wave circuits
[AD-A192460] N88-27430
Calibration of the portable wear metal analyzer
[AD-A192971] N88-27524
ANGULAR DISTRIBUTION
Angular radiation models for Earth-atmosphere system. Volume 1: Shortwave radiation
[NASA-RP-1184] N88-27677
ANISOTROPY
Probabilistic anisotropic failure criteria for composite materials
[AD-A193046] N88-27232
An anisotropic continuum damage model for creep-dominated, multiaxial loading histories N88-27606
On plasma stability under anisotropic random electric field influence
[DE88-702422] N88-27918
ANNEALING
NDP (Neutron Depth Profiling) evaluations of boron-implanted compound semiconductors
[AD-A192306] N88-27425
ANNIHILATION REACTIONS
Study of the production of Ko mesons in proton antiproton interactions at 630 GeV
[NOTA-INTERNA-908] N88-27892
ANNULAR FLOW
Investigation of annular flow at high evaporation rates in view of liquid film cooling
[DFVLR-FB-88-08] N88-27517
ANTARCTIC REGIONS
ECC (Electrochemical Concentration Cell) ozonesonde observations at South Pole, Antarctica during 1987
[PB88-202015] N88-27644
ANTENNA COMPONENTS
Sidelobe level of an adaptive array using the SMI (Sampled Matrix Inversion) algorithm
[AD-A193131] N88-27409
ANTENNA RADIATION PATTERNS
Electromagnetic characterization and acceptance test of the EMP simulator SPERANS
[PB88-203781] N88-27416
Analytical approximation of a distorted reflector surface defined by a discrete set of points
[NASA-TM-101323] N88-27424
ANTIFERROMAGNETISM
Self energy corrections to the ab initio band structures: Chromium
[DE88-701825] N88-27927
ANTIMISSILE DEFENSE
Future SDI (Strategic Defense Initiative) decision making
[AD-A192794] N88-27860
ANTIREFLECTION COATINGS
Improved adhesion for SiO2 particles in silica substrates using helium-ion irradiation
[DE88-008915] N88-27332
APPLICATIONS PROGRAMS (COMPUTERS)
Determination of Tafel constants in nonlinear polarization curves
[AD-A192335] N88-27282
APPROXIMATION
Analytical approximation of a distorted reflector surface defined by a discrete set of points
[NASA-TM-101323] N88-27424
A fast vortex code for computing 2-D flow in a box
[DE88-011732] N88-27498
Approximation problems of the Hilbert transform to identify minimum phase linear systems
[FUB-42-1986] N88-27790
Modeling and approximate performance analysis of multiuser computer systems
[ETN-88-92137] N88-27806
Approximations of stochastic equations driven by predictable processes
[AD-A192714] N88-27823
Finding minimum-cost circulations by successive approximation
[AD-A192724] N88-27824
Asymptotic of Peanokerns of finite fixed order
[ETN-88-92361] N88-27843
Approximations and optimal control for the pathwise average cost per unit time and discounted problems for wideband noise driven systems
[AD-A192712] N88-27847
Evaluation of quantum mechanics path integrals by the approximations exact on a class of polynomial functionals
[DE88-702434] N88-27865
Perturbation expansions generated by an approximate propagator
[DE88-702435] N88-27866
Steady-state approximations in Raman excitation equations
[DE88-011759] N88-27889
AQUEOUS SOLUTIONS
Precise ultraviolet absorbance study of the interaction of amino acids and mononucleosides in aqueous solution
[ISAS-RN-356] N88-27256
ARCHITECTURE (COMPUTERS)
An investigation of performance improvement in knowledge-based control systems N88-27382
Computational fluid dynamics on parallel processors
[AD-A192397] N88-27469
A demonstration of retro-traverse using a semi-autonomous land vehicle
[DE88-009851] N88-27568
Assessing and enhancing human performance: Utility of a workstation network
[AD-A192840] N88-27743
MINIAC: A small embedded computer
[DE88-008142] N88-27757
Research into the architecture of CAD based robot vision systems
[AD-A193330] N88-27776
Software engineering guidelines for RASP and ANDECS: Requirements and architectural design
[DFVLR-MITT-88-07] N88-27793
FORTRAN 77 implementation of abstract datatype models
[DFVLR-MITT-88-08] N88-27794
Image processing using a parallel architecture
[AD-A192833] N88-27803
Notes on operating system requirements for the next millennium
[DE88-010712] N88-27805
Neural network research: A personal perspective
[AD-A192717] N88-27808
Parallel quasi-Newton methods for unconstrained optimization
[AD-A193250] N88-27812
AREA
Computer modeling for surface properties of carbon fibers N88-27383
ARMED FORCES (UNITED STATES)
Army space systems for terrestrial applications
[AD-A192735] N88-27613
ARTIFICIAL INTELLIGENCE
EXSAT: Expert system to configure telecommunication satellites
[SNIAS-881-440-101] N88-27223
Mitsubishi Electric Advance (R and D Edition), Volume 41
[PB88-194162] N88-27388
Computer-Aided Engineering (CAE) for engineering design N88-27390
The MELCOM PSI 2 AI workstation N88-27395
Motor-response learning at a process control panel by an autonomous robot
[DE88-005055] N88-27554
Block Oriented Simulation System (BOSS)
[NASA-CR-182947] N88-27760
Synchronizable series expressions. Part 2: Overview of the theory and implementation
[AD-A192783] N88-27768
The programmer's apprentice project: A research overview
[AD-A192784] N88-27769
Improving the performance of AI algorithms
[AD-A192848] N88-27809
ASCENT PROPULSION SYSTEMS
Propulsion analysis and application potential of air breathing combined propulsion for ballistic space transporter
[ETN-88-92369] N88-27227
ASSEMBLING
Assembly Test Article (ATA)
[NASA-CR-179361] N88-27226
ASSOCIATIVE PROCESSING (COMPUTERS)
Content-addressable memory storage by neural networks: A general model and global Liapunov method
[AD-A192716] N88-27807
ASTRO MISSIONS (STS)
IPS guidestar selection for stellar mode (ASTRO)
[NASA-TM-100336] N88-27181
ASTRONOMICAL MODELS
Gamma radiation from center of the galaxy of the order of MeV values
[MPE-207] N88-27999
ASTRONOMICAL PHOTOMETRY
Surface photometric investigations for spiral galaxies of large dimension structures in edge-on gemetry
[ETN-88-92126] N88-27985
ASTRONOMICAL SPECTROSCOPY
Analysis of emission features in IRAS LRS spectra N88-27380
ASTROPHYSICS
The classical nova outburst
[DE88-009138] N88-27987
ASYMPTOTES
The two isotropic asymptotes of fiber composites
[AD-A192305] N88-27231
ASYMPTOTIC METHODS
A simple explanation of the Stokes phenomenon
[AD-A193253] N88-27832
Asymptotic normality of minimum L1-norm estimates in linear models
[AD-A193399] N88-27835
ASYMPTOTIC SERIES
Asymptotic of Peanokerns of finite fixed order
[ETN-88-92361] N88-27843
Statistical analysis of dyadic stationary processes
[AD-A193057] N88-27853
Joint asymptotic distribution of marginal quantiles and quantile functions in samples from a multivariate population
[AD-A193365] N88-27856
ATMOSPHERIC ATTENUATION
An evaluation of two millimeter wave propagation models for horizontal atmospheric attenuation at 70-115 GHZ
[AD-A192699] N88-27403
ATMOSPHERIC CHEMISTRY
Atmospheric nitrogen oxides: Their detection and chemistry
[PB88-193057] N88-27642
Large-eddy simulations of concentration fluctuations
[DE88-009480] N88-27660
ATMOSPHERIC CIRCULATION
Photon limited image processing in the space-time domain
[AD-A193142] N88-27655
Intercomparison of NMC (National Meteorological Center) and ECMWF (European Centre for Medium Range Weather Forecasts) global analyses: 1980-1986
[PB88-196548] N88-27668
Surface energy balance of three general circulation models: Current climate and response to increasing atmospheric CO2
[DE88-010967] N88-27673
Beaufort sea mesoscale circulation study: Hydrography helicopter operations, April 1987
[PB88-203658] N88-27681
ATMOSPHERIC COMPOSITION
ECC (Electrochemical Concentration Cell) ozonesonde observations at South Pole, Antarctica during 1987
[PB88-202015] N88-27644
National air toxics information clearinghouse: NATICH data base users guide for data viewing, February 1988
[PB88-197470] N88-27645
National ambient Volatile Organic Compounds (VOCs) data base update, documentation
[PB88-195631] N88-27646
Photochemical oxidant formation: Overview of current knowledge and emerging issues
[PB88-195235] N88-27647
ATMOSPHERIC MODELS
Photochemical oxidant formation: Overview of current knowledge and emerging issues
[PB88-195235] N88-27647
Approximate analytical formulae for electron density and collision frequency in the natural and nuclear-disturbed ionosphere and inner magnetosphere
[AD-A193129] N88-27654
Development of radiation and cloud parameterization programs for AFGL (Air Force Geophysics Laboratory) global models
[AD-A193369] N88-27658
Air-sea interaction in the vicinity of a land-sea boundary in the presence of upwelling N88-27661
Surface energy balance of three general circulation models: Current climate and response to increasing atmospheric CO2
[DE88-010967] N88-27673
ATMOSPHERIC PRESSURE
Premixed turbulent flame propagation
[AD-A192955] N88-27265
ATMOSPHERIC SOUNDING
Components of an atmospheric lidar system
[AD-A193366] N88-27539

ECC (Electrochemical Concentration Cell) ozonesonde observations at South Pole, Antarctica during 1987
[PB88-202015] N88-27644

ATMOSPHERIC TEMPERATURE
Investigations on Mie and Rayleigh scattering as basis for the development of Rayleigh temperature lidars with aid of Michelson interferometry
[GKSS-87/E/62] N88-27675

ATMOSPHERIC TURBULENCE
Atmospheric turbulence research at DFVLR
[AGARD-R-752] N88-27669

ATOMIC CLOCKS
Quartz crystal resonators and oscillators for frequency control and timing applications
[AD-A193310] N88-27443
A three-dimensional model of the gas-cell atomic frequency standard
[AD-A193218] N88-27868

ATOMIC INTERACTIONS
Determination of quantum corrections for electrical conductivity mechanism of three dimensional, perturbed copper coatings. Weak localization and electron-electron interaction
[ETN-88-92378] N88-27466

ATOMIC STRUCTURE
Discrete variational methods and their application to electronic structures
[DE88-702215] N88-27888
Probing the electronic and defect structure of perovskite superconductors
[DE88-008349] N88-27939

ATOMIC WEIGHTS
Measurement of Beta-decay energies of short-lived neutron-rich nuclei in the vicinity of mass number between 101 and 106, and A = 109
[ETN-88-92376] N88-27890

ATOMS
Multiphoton ionization of alkaline earth atoms in an intense laser field
[DE88-008078] N88-27884

ATTENTION
A model for visual attention
[AD-A193061] N88-27744

ATTITUDE CONTROL
Spacecraft applications of advanced global positioning system technology
[NASA-CR-172055] N88-27180
Airborne remote operated device
[DE88-010324] N88-27188

AUDIO FREQUENCIES
Use of optical disk technology at the Air Command and Staff College
[AD-A192424] N88-27969

AUDITORY PERCEPTION
Demodulation processes in auditory perception
[AD-A193421] N88-27740

AUDITORY STIMULI
The interaction of thalamo-cortical systems in the 40 Hz following response N88-27694

AUGER SPECTROSCOPY
Application of Auger electron spectroscopy to the study of trace element effects on weldability
[DE88-010457] N88-27301

AUGMENTATION
Vapor Compression Distillation Subsystem (VCDS) component enhancement, testing and expert fault diagnostics development, volume 2
[NASA-CR-172076] N88-27755

AURORAS
The low-latitude auroral boundary: Steady-state and time-dependent representations
[AD-A193200] N88-27656
On the dynamics of the auroral ionosphere during the breakup of a substorm
[AD-A193368] N88-27657

AUSTENITE
Ultrasonic studies of stresses and plastic deformation in steel during tension and compression
[AD-A192308] N88-27280

AUSTENITIC STAINLESS STEELS
Controlling phase formation and stability to improve the high temperature creep resistance of austenitic stainless steels
[DE88-011401] N88-27293

AUTOCLAVING
Determination of lumped-mass thermal properties associated with autoclave curing of graphite/epoxy composites N88-27364

AUTOMOBILE ENGINES
Phase 1 results from the Stirling-powered vehicle project
[NASA-TM-100978] N88-27980

AUTOMOBILES
Unified methods of accelerated laboratory tests of the preparations for temporary protection of cars
[NASA-TT-20298] N88-27336
A demonstration of retro-traverse using a semi-autonomous land vehicle
[DE88-009851] N88-27568

AUTONOMOUS NAVIGATION
A feasibility study in path planning using optimization techniques
[AD-A193030] N88-27177
Three-dimensional scene analysis using stero based imaging
[AD-A193120] N88-27178
A demonstration of retro-traverse using a semi-autonomous land vehicle
[DE88-009851] N88-27568
Assessments of maneuverability with the TeleOperated Vehicle (TOV)
[AD-A191584] N88-27751

AUTONOMY
Intelligent Mobile Autonomous System (IMAS)
[AD-A193181] N88-27811

AVIONICS
Air Force technical objective document, FY89
[AD-A193110] N88-27194
Computation of ECM (Electronic Counter-Measures) war reserve materiel spare requirements
[AD-A193301] N88-27195

AXIAL LOADS
Forces and moments on a slender, cavitating body
[DE88-007208] N88-27491
Stress relaxation of a titanium (Ti-6Al-4V) threaded joint
[DE88-010102] N88-27590
Development of a biaxial test system for thin-walled metal tubes using tensile-compressive axial load and internal-external pressure
[DE88-011279] N88-27592
An experimental and analytical evaluation of a biaxial test for determining shear properties of composite materials
[NASA-CR-182928] N88-27593
An anisotropic continuum damage model for creep-dominated, multiaxial loading histories N88-27608

AXISYMMETRIC FLOW
Nonaxisymmetric viscous lower branch modes in axisymmetric supersonic flows
[NASA-CR-181687] N88-27164
Velocity measurements and flow visualization in turbulent three-dimensional supersonic flows using oxygen flow tagging
[AD-A192551] N88-27165
Coupled experimental and theoretical investigations of instability, chaos and turbulence in an axisymmetric jet flow
[AD-A192943] N88-27476

B

BACTERIA
Genetic effects of low level microwave radiation
[AD-A192687] N88-27722

BALANCE
Stability of uncapsulated weight cells with thin film elongation measurement bands under influence of humidity, temperature and operation voltage
[ETN-88-92383] N88-27531

BAND STRUCTURE OF SOLIDS
Self energy corrections to the ab initio band structures: Chromium
[DE88-701825] N88-27927

BANDSTOP FILTERS
A notch filter instrument for measuring ELF (Extremely Low Frequency) MSK (Minimum Shift Keying) signals
[AD-A193324] N88-27414

BARIUM COMPOUNDS
Anharmonic model for high-Tc superconductors
[DE88-702196] N88-27924
Superconducting properties of LaBa2Cu3O(sub x) and YBa2Cu3O(sub y)
[DE88-012038] N88-27952

BARIUM OXIDES
Compilation of NRL publications on high temperature superconductivity
[AD-A189137] N88-27921
Thermodynamics of oxygen-vacancy ordering in YBa2Cu3O(sub z)
[DE88-009816] N88-27940

BARIUM TITANATES
Manufacturing of a barium titanate with high dielectric coefficient by decomposition of precipitates of double oxalates
[ISAL-IDI1-88-02] N88-27278

BEAM SWITCHING
Investigations on beam quality of high frequency excited CO2 high performance lasers
[ETN-88-92363] N88-27550

BEAMS (RADIATION)
Distortion functions
[DE88-752634] N88-27896

BEAMS (SUPPORTS)
Optimal design of viscoelastic structures N88-27579
Coupled thermal vibrations of beams with temperature-dependent properties N88-27601

BEARINGLESS ROTORS
A comparison of theory and experiment for the aeroelastic stability of a bearingless model rotor in hover N88-27153
A comparison of theory and experiment for coupled rotor body stability of a bearingless rotor model in hover and forward flight N88-27154
A comparison of theory and flight test of the BO 105/BMR in hover and forward flight N88-27155
Aeromechanical stability analysis of COPTER N88-27161
Aeroelastic characteristics of the AH-64 bearingless tail rotor N88-27162

BEARINGS
The 000 stage equipment bearing performance with a lower viscosity lubricant
[DE88-011827] N88-27566

BEAT FREQUENCIES
Heating efficiency of beat wave excitation in a density gradient
[AD-A193066] N88-27905

BEAUFORT SEA (NORTH AMERICA)
MIZPAC (marginal ice zone Pacific) 84-86 CTD (Conductivity, Temperature, Depth) data report
[AD-A192478] N88-27679
Beaufort sea mesoscale circulation study: Hydrography helicopter operations, April 1987
[PB88-203658] N88-27681

BEHAVIOR
Behavioral, psychological and demographic predictors of physical fitness
[AD-A192697] N88-27733

BERNSTEIN ENERGY PRINCIPLE
Ion Bernstein modes in current-carrying plasmas N88-27903

BETA PARTICLES
Measurement of Beta-decay energies of short-lived neutron-rich nuclei in the vicinity of mass number between 101 and 106, and A = 109
[ETN-88-92376] N88-27890

BETATRONS
Optical guiding in the separable beam limit
[AD-A192452] N88-27534
Distortion functions
[DE88-752634] N88-27896

BIBLIOGRAPHIES
Aeronautical engineering: A continuing bibliography with indexes
[NASA-SP-7037(229)] N88-27163
Technology for large space systems: A bibliography with indexes (supplement 18)
[NASA-SP-7046(18)] N88-27214
Photovoltaic Energy. Electricity from Sunlight: A current awareness bulletin
[DE88-008289] N88-27634
Aerospace Medicine and Biology: A continuing bibliography with indexes (supplement 314)
[NASA-SP-7011(314)] N88-27742

BIDIRECTIONAL REFLECTANCE
Angular radiation models for Earth-atmosphere system. Volume 1: Shortwave radiation
[NASA-RP-1184] N88-27677

BINDERS (MATERIALS)
Alternate/modified binders for airfield pavements
[AD-A192781] N88-27206

BIOASSAY
Methods of quantifying and enhancing reactive oxygen species production N88-27357
Genetic effects of low level microwave radiation
[AD-A192687] N88-27722

BIOCHEMISTRY
Methods of quantifying and enhancing reactive oxygen species production N88-27357

BIODYNAMICS
Using IMSL mathematical and statistical computer subroutines in physiological and biomechanical research
[AD-A192594] N88-27765

BIOELECTRICITY
Studies of the intact human brain: Implications for performance N88-27684
CEEG dynamic brain mapping: A new method to evaluate brain function in different psychological and drug conditions N88-27685
Fourth generation neurocognitive pattern analysis system N88-27686
The application of non-stationary data analysis techniques in the identification of changes in the electroencephalogram associated with the onset of drowsiness N88-27688

Neurophysiological patterns of operational fatigue: Preliminary results N88-27703
Fighter pilot performance during airborne and simulator missions: Physiological comparisons N88-27704
Event-related and steady potential changes in the brain related to workload during tracking N88-27705
Neurophysiological precursors of accurate visuomotor performance N88-27706
The neuroelectric selection of Naval aviation personnel: An evaluation N88-27707
Evoked potential analysis of impact acceleration experiments N88-27708
EEG indices of G-induced Loss Of Consciousness (G-LOC) N88-27709
Detection of acceleration (+Gz) induced blackout by matched-filtering of visual evoked potentials N88-27710
Electroencephalographic correlates of pilot performance: Simulation and in-flight studies N88-27711
Motion evoked vestibular potentials N88-27712
Measurement and classification of the mode of action of antidepressant drugs N88-27714
Measurement of electrical activity in the CNS with cortical evoked potentials and EEG: Efficacy profiles of drugs using factor analysis N88-27715
An approach to studying the effects of psychostimulants on cerebral electrical activity in the non-human primate N88-27716
Spontaneous cerebral electrical activity during prolonged hypoglycemia: A quantitative study in humans N88-27717
Correlation between EEG abnormal activity and aircraft accidents: A long term observation N88-27719

BIOFEEDBACK
The effects of increased cognitive demands on autonomic self-regulation: An indicator of parallel processing in the brain N88-27362

BIOLOGICAL EFFECTS
Aerospace Medicine and Biology: A continuing bibliography with indexes (supplement 314) [NASA-SP-7011(314)] N88-27742

BIOMASS ENERGY PRODUCTION
An outdoor test facility for the large-scale production of microalgae [DE88-001146] N88-27723

BIOPOLYMERS
Calculation of far infrared absorption in B poly(dA).poly(dT) [AD-A193128] N88-27318

BLACK BODY RADIATION
Numerical calculations of dopent diffusion involving flashlamp heating of silicon N88-27384
Overview and future direction for blackbody solar-pumped lasers [NASA-TM-100621] N88-27553

BLACKOUT (PHYSIOLOGY)
Detection of acceleration (+Gz) induced blackout by matched-filtering of visual evoked potentials N88-27710

BLADE-VORTEX INTERACTION
Theory of sound production by vortex-airfoil interaction [AD-A193386] N88-27875

BLOOD VOLUME
Validation of a modified one-step rebreathing technique for non-invasive measurement of submaximal cardiac output [AD-A192852] N88-27735

BOILING
Effects of surface tension and contact angle on sensible heating and boiling incipience in dielectric falling films [DE88-007057] N88-27492

BOLTZMANN TRANSPORT EQUATION
Feedback control of a hyperbolic partial-differential equation with viscoelastic damping [AD-A192896] N88-27810

BOMBER AIRCRAFT
Pilot report: AFTI (Advanced Fighter Technology Integration) F-111 [AD-A192937] N88-27184

BONDING
Effect of the matrix on the creep-behavior of carbon-carbon composite [AD-A193211] N88-27235
An IETS (Inelastic Electron Tunneling Spectroscopy) study of surface reactions applicable to adhesion [AD-A192274] N88-27261

BOOLEAN FUNCTIONS
Investigation of the potential impact of new photonic materials on optical processing systems N88-27359

BORON
NDP (Neutron Depth Profiling) evaluations of boron-implanted compound semiconductors [AD-A192308] N88-27425
Paramagnetic point defects in boron-implanted HgO.7CdO.3Te [AD-A193276] N88-27934

BOROSILICATE GLASS
Homogeneity of glasses: Experiment WL-IHF-05 in D1 mission --- Spacelab [ETN-88-92339] N88-27353

BOUNDARIES
Physical mechanisms in shock-induced turbulent separated flow [AD-A193165] N88-27484
Computational boundary conditions for the incompressible Navier-Stokes equations in channels and pipes [AD-A193356] N88-27487
The low-latitude auroral boundary: Steady-state and time-dependent representations [AD-A193200] N88-27656

BOUNDARY ELEMENT METHOD
Parallel implementation of the boundary element method [DE88-011846] N88-27839

BOUNDARY LAYER EQUATIONS
Boundary layer solutions for the free-edge problem in composite laminates N88-27229

BOUNDARY LAYER FLOW
The heat transfer and fluid dynamics of concave surface curvature [AD-A193064] N88-27479

BOUNDARY LAYER PLASMAS
Plasma behavior in the boundary layer near a railgun surface [DE88-006889] N88-27909

BOUNDARY LAYER SEPARATION
Experimental study of unsteady separating turbulent boundary layers [AD-A192997] N88-27477
Physical mechanisms in shock-induced turbulent separated flow [AD-A193165] N88-27484

BOUNDARY LAYERS
The diffusion of vorticity from a plane boundary [AD-A192706] N88-27474

BOUNDARY LUBRICATION
Perfluoropolyalkylether lubricants under boundary conditions: Iron catalysis of lubricant degradation [AD-A193241] N88-27560

BOUNDARY VALUE PROBLEMS
Thermo-viscoelastic analysis of composite materials, volume 1 [NASA-CR-183048-VOL-1] N88-27230
Investigation of viscous/inviscid interaction in transonic flow over airfoils with suction [NASA-CR-183112] N88-27490
Initial boundary value problems of nonlinear wave equations in an exterior domain [DE88-701883] N88-27962

BOXES (CONTAINERS)
FEB (Multifilter Electronics Box) lifting device analysis, revision A [AD-A192313] N88-27427

BRAIN
Studies of the intact human brain: Implications for performance N88-27684
CEEG dynamic brain mapping: A new method to evaluate brain function in different psychological and drug conditions N88-27685
Fourth generation neurocognitive pattern analysis system N88-27686
Normative developmental equations for the EEG and their sensitivity to neurological and psychiatric disorders N88-27687
Squid instrumentation for neuromagnetic study of complex brain activity N88-27691
Electric and magnetic brain activity related to cognitive performance N88-27692
Neuromagnetic evidence of place mechanisms for frequency and intensity coding in the human auditory cortex N88-27693
A study of sources in the human brain associated with stereopsis N88-27695
Event-related brain potentials as indices of mental workload and attentional allocation N88-27696
Using ERPS to study human information processing N88-27698
Cognitive task demands as reflected in physiological measures N88-27699
The effect of endogenous alpha on hemispheric asymmetries and the relationship of frontal theta to sustained attention N88-27701
Fighter pilot performance during airborne and simulator missions: Physiological comparisons N88-27704
Event-related and steady potential changes in the brain related to workload during tracking N88-27705
EEG indices of G-induced Loss Of Consciousness (G-LOC) N88-27709
Motion evoked vestibular potentials N88-27712
The effect of mild hypoxia on the vestibular evoked response N88-27713
An approach to studying the effects of psychostimulants on cerebral electrical activity in the non-human primate N88-27716
Spontaneous cerebral electrical activity during prolonged hypoglycemia: A quantitative study in humans N88-27717
Correlation between EEG abnormal activity and aircraft accidents: A long term observation N88-27719
Cognitive and neural bases of skilled performance [AD-A193392] N88-27747
Content-addressable memory storage by neural networks: A general model and global Liapunov method [AD-A192716] N88-27807

BRANCHING (MATHEMATICS)
Generalized Jordan chains and two bifurcation theorems of Krasnoselskii [AD-A192353] N88-27845

BRILLOUIN ZONES
Calculation of far infrared absorption in B poly(dA).poly(dT) [AD-A193128] N88-27318

BRITTLE MATERIALS
Size effects in linear elastic fracture mechanics N88-27609

BROADBAND
Approximations and optimal control for the pathwise average cost per unit time and discounted problems for wideband noise driven systems [AD-A192712] N88-27847
SERI standard broadband format: A solar and meteorological data archival format [DE88-001145] N88-27975

BROADCASTING
Performance study of a unipole antenna with conventional and elevated radial wire ground screens [AD-A193283] N88-27413

BUCKLING
A study of fluid-structure problems N88-27468
Nonlinear interaction between overall and local buckling of stiffened panels with symmetric cross-sections [PB88-104054] N88-27580
Adaptive finite element methods for shells [AD-A193221] N88-27585

BUDGETING
Economic impact of space flight activities in West Germany. Influence of allocations of Bundesministerium fuer Forschung und Technologie [ETN-88-92106] N88-27215

BUFFER STORAGE
Effective buffering schemes for performing matrix operations for numerical databases N88-27968

C

C-130 AIRCRAFT
Electrical load and power source capacity report for the C-130 aircraft Self Contained Navigation System (SCNS): LSI model 6216A, 6216B, 6216C, revision [AD-A193079] N88-27186

CADMIUM SELENIDES
Ultrafast physics in semiconductor microstructures [AD-A193300] N88-27936

CALCULUS OF VARIATIONS
Discrete variational methods and their application to electronic structures [DE88-702215] N88-27888

CALIBRATING
Calibration and data reduction techniques for the AFGL infrared array spectrometer N88-27374
Calibration of the portable wear metal analyzer [AD-A192971] N88-27524
Acoustic emission calibration instrumentation [DE88-010817] N88-27528
Validate algorithms for the determination of rainfall rates from SSM/I microwave satellite imagery [AD-A192299] N88-27664

CAMERAS
The FEL CCD-camera: Experimental system for camera and image processing research [FEL-1987-34] N88-27532

CANARD CONFIGURATIONS
Flow around a delta wing with or without a canard control surface (phi BA = 60 deg). Part 1: Hydrodynamic visualization in permanent regime [ONERA-RT-10/2891-AN-101-A-PT-1] N88-27170
In-flight load measurements of the Robot-X canards [AD-A193428] N88-27187

CANOPIES (VEGETATION)
Foliar nitrate reductase: A marker for assimilation of atmospheric nitrogen oxides [DE88-010453] N88-27648

CAPACITORS
High power pulse energy system concept
[AD-A192440] N88-27429
CARBON
Carbon deposition model for oxygen-hydrocarbon combustion, volume 1
[NASA-CR-179375] N88-27254
Carbon deposition model for oxygen-hydrocarbon combustion, volume 2
[NASA-CR-179376] N88-27255
Refractory films from spin-cast carbon
[DE88-011251] N88-27327
CARBON DIOXIDE
Catalytic activation of carbon dioxide by metal complexes
[AD-A192310] N88-27262
Surface energy balance of three general circulation models: Current climate and response to increasing atmospheric CO2
[DE88-010967] N88-27673
Validation of a modified one-step rebreathing technique for non-invasive measurement of submaximal cardiac output
[AD-A192852] N88-27735
CARBON DIOXIDE LASERS
Investigations on beam quality of high frequency excited CO2 high performance lasers
[ETN-88-92363] N88-27550
CARBON DIOXIDE REMOVAL
Advanced EMU electrochemically regenerable CO2 and moisture absorber module breadboard
[NASA-CR-172054] N88-27754
CARBON FIBER REINFORCED PLASTICS
Rocket motor case materials. An evaluation of new fibers for composites
[FOA-C-20696-2.1] N88-27245
Determination of the glass transition temperature of cured composite materials
[DT-87/62-R] N88-27246
Design and implementation of contact ultrasonic sensors to assess internal damage
[I-177/87] N88-27247
Relation between the mechanical characteristics of carbon-resin composites and their impact strength
[REPT-48-284/F] N88-27249
Aging of CFRP due to longterm storage in heated air
[DFVLR-FB-88-05] N88-27345
Use of microwave measuring systems for the nondestructive control of resins and composites
[SNIAS-881-430-123] N88-27576
CARBON FIBERS
Effect of the matrix on the creep-behavior of carbon-carbon composite
[AD-A193211] N88-27235
Effects of electron beam irradiation on mechanical properties at low and high temperature of fiber reinforced composites using PEEK as matrix material
[DE88-753134] N88-27239
Fabrication of SiC fiber reinforced glass matrix by extrusion process and investigation of its mechanical properties
[ETN-88-92367] N88-27244
Refractory fibers surface treatment
[REPT-47-803/F] N88-27339
Computer modeling for surface properties of carbon fibers N88-27383
CARBON MONOXIDE
Mechanism of the nitric oxide-carbon monoxide-oxygen reaction over a single crystal rhodium catalyst
[DE88-006274] N88-27268
CARBON STEELS
Diffusion and solubility of some interstitial impurities in deformed metals
[DE88-701859] N88-27296
CARBON-CARBON COMPOSITES
Effect of the matrix on the creep-behavior of carbon-carbon composite
[AD-A193211] N88-27235
Studies in support of oxidation-resistant composite materials
[AD-A193320] N88-27238
On the electrical properties of carbon/carbon composites densified by chemical deposit in vapor phase
[SNIAS-881-430-117] N88-27252
CARGO
Steps toward lunar settlement
[DE88-009141] N88-27213
CASCADE FLOW
A Navier-Stokes study of cascade flow fields including inlet distortion and rotating stall
[AD-A193109] N88-27483
CASTING
Spatial organization of homopolymer chains inside spherical polybutadiene domains of SB diblock copolymers
[AD-A193390] N88-27321
CATALYSIS
Catalytic activation of carbon dioxide by metal complexes
[AD-A192310] N88-27262
Precursor chemistry and the structure of silica aerogels
[DE88-011253] N88-27328
Perfluoropolyalkylether lubricants under boundary conditions: Iron catalysis of lubricant degradation
[AD-A193241] N88-27560
CATALYSTS
Alkaline fuel cell performance investigation
[NASA-TM-100937] N88-27267
Preparation and development of advanced battery catalysts
[AD-A193208] N88-27441
CATHODES
Alkaline fuel cell performance investigation
[NASA-TM-100937] N88-27267
Long-pulse, high-power vircator experiments
[DE88-011787] N88-27458
CAUCHY PROBLEM
Further extensions of the choquet-deny and deny theorems with applications in characterization theory
[AD-A193358] N88-27834
Cauchy problem for the nonlinear Schroedinger equation
[DE88-702454] N88-27867
CAVITATION FLOW
Forces and moments on a slender, cavitating body
[DE88-007208] N88-27491
Cavitation inception in a turbulent shear flow
[DE88-011486] N88-27497
CAVITIES
A critical review of IR drops and electrode potentials within pits, crevices and cracks
[AD-A192481] N88-27431
Thermo-mechanical cracking in coated media with a cavity by a moving asperity friction
[AD-A193311] N88-27586
CELLS (BIOLOGY)
Genetic effects of low level microwave radiation
[AD-A192687] N88-27722
CENTRAL NERVOUS SYSTEM
Measurement and classification of the mode of action of antidepressant drugs N88-27714
Measurement of electrical activity in the CNS with cortical evoked potentials and EEG: Efficacy profiles of drugs using factor analysis N88-27715
CENTRIFUGES
Computation of flow and diffusion process in gas centrifuges
[ETN-88-92366] N88-27514
CERAMIC COATINGS
Effects of ceramic surfaces on autoignition in a constant volume combustion apparatus
[AD-A193055] N88-27266
CERAMIC FIBERS
Studies in support of oxidation-resistant composite materials
[AD-A193320] N88-27238
CERAMIC MATRIX COMPOSITES
Theoretical and experimental analysis of the toughening behavior of whisker reinforcement in ceramic matrix composites
[DE88-011841] N88-27241
Contribution to the development of coated fiber ceramic insolation material
[ETN-88-92361] N88-27243
CERAMICS
Polymer-ceramic composites
[AD-A193244] N88-27237
Studies in support of oxidation-resistant composite materials
[AD-A193320] N88-27238
Theoretical and experimental analysis of the toughening behavior of whisker reinforcement in ceramic matrix composites
[DE88-011841] N88-27241
Preparation and properties of new inorganic glasses and gel-derived solids
[AD-A192922] N88-27315
Processing and additive effects of ZrO2 on microstructure and dielectric porperties of BaTiO3 ceramics
[AD-A193126] N88-27316
Preparation and properties of high Q microwave dielectrics in the (CA, SR, BA) zirconate system
[AD-A193127] N88-27317
Ceramic technology for advanced heat engines project
[DE88-008945] N88-27323
Studies of dynamic contact of ceramics and alloys for advanced heat engines
[DE88-008996] N88-27324
Effects of near interfacial microstructure on toughness and subcritical crack growth in ceramic/metal systems
[DE88-009842] N88-27325
Data compilation for radiation damage on ceramic insulators. Revised with updated data and reviews
[DE88-753426] N88-27329
Application of sol-gel procedures to ceramic composites
[ETN-88-92741] N88-27338
Preparation and characterization of ceramic materials based on Al2O3 reinforced with a ZrO2 dispersion
[ISAL-87-0041] N88-27340
Study of the friction and wear-related properties of ceramic superconductors
[DE88-011844] N88-27950
Ceramic fabrication technology for high-T(sub)c materials
[DE88-012060] N88-27953
CHAINS
Spatial organization of homopolymer chains inside spherical polybutadiene domains of SB diblock copolymers
[AD-A193390] N88-27321
CHANNEL FLOW
Computational boundary conditions for the incompressible Navier-Stokes equations in channels and pipes
[AD-A193356] N88-27487
CHANNEL NOISE
Outliner resistant filtering and smoothing: 2D version
[AD-A193319] N88-27874
CHANNELS
A study of a meteor burst communication system N88-27421
CHAOS
Coupled experimental and theoretical investigations of instability, chaos and turbulence in an axisymmetric jet flow
[AD-A192943] N88-27476
Statistical description of stochastic dynamics
[AD-A192924] N88-27852
CHARACTERIZATION
Techniques for characterizing damage zones in composite materials N88-27240
Preparation and characterization of ceramic materials based on Al2O3 reinforced with a ZrO2 dispersion
[ISAL-87-0041] N88-27340
CHARGE CARRIERS
Picosecond optoelectronic sampling of electrical waveforms produced by an optically excited field effect transistor
[AD-A192384] N88-27428
CHARGE COUPLED DEVICES
The FEL CCD-camera: Experimental system for camera and image processing research
[FEL-1987-34] N88-27532
CHARGE EFFICIENCY
Results from life test in progress on eagle-picher nickel cadmium cells
[AD-A192816] N88-27434
CHARGE TRANSFER
The kinetics of charge-transfer reactions on passive lithium electrodes
[DE88-009256] N88-27454
CHARGED PARTICLES
Optical guiding in the separable beam limit
[AD-A192452] N88-27534
Self-energies and the interactions of particles with surfaces
[DE88-010451] N88-27885
Propagation of charged particle beams in the atmosphere
[AD-A193185] N88-27887
Solar flares and magnetospheric particles: Investigations based upon the ONR-602 and ONR-604 experiments
[AD-A193396] N88-27994
CHASSIS
Unified methods of accelerated laboratory tests of the preparations for temporary protection of cars
[NASA-TT-20298] N88-27336
CHELATES
Soluble metal chelate polymers of coordination numbers six, seven and eight
[AD-A192485] N88-27314
CHEMICAL ANALYSIS
Microchemical analysis of polycrystalline Ni3Al and other ordered alloys using the field-ion microscope atom probe
[DE88-011519] N88-27294

CHEMICAL BONDS
Structure of bound states in polynomial potentials
[DE88-702437] N88-27837
Discrete variational methods and their application to electronic structures
[DE88-702215] N88-27888
Deep level defects in semiconductors: Stress and pressure studies
[DE88-010855] N88-27948
CHEMICAL COMPOSITION
Initial testing of the tunable diode laser absorption spectrometer for measuring HNO3 in diesel engine exhaust, stage 2
[PB88-193073] N88-27641
The distribution of some chemical elements between dissolved and particulate phases in the ocean
[DE88-010181] N88-27682
Structure of bound states in polynomial potentials
[DE88-702437] N88-27837
CHEMICAL ELEMENTS
Compilation of temperature factors of cubic elements
[PB88-108170] N88-27260
CHEMICAL ENERGY
Prediction of deep levels and equilibrium concentrations of defects in semiconductors N88-27945
CHEMICAL EXPLOSIONS
Shock initiation studies on heterogeneous explosives
[DE88-006681] N88-27351
Diode laser ignition of high explosives and pyrotechnics
[DE88-008771] N88-27352
CHEMICAL LASERS
Overview of the SDI (Strategic Defense Initiative) Program in short wavelength chemical lasers
[DE88-007912] N88-27861
CHEMICAL PROPERTIES
Scanning tunneling microscopy as a surface chemical probe
[AD-A192710] N88-27263
Energy distribution and transfer in flowing hydrogen microwave plasmas N88-27919
Growth and characterization of CuGaS2, CuAlS2 and CuGa0.9Al0.1S2 single crystals
[AD-A192963] N88-27930
CHEMICAL REACTIONS
A study of the interaction of diffusion flames with a vortex pair flowfield N88-27258
Mechanism of the nitric oxide-carbon monoxide-oxygen reaction over a single crystal rhodium catalyst
[DE88-006274] N88-27268
CHEMILUMINESCENCE
Methods of quantifying and enhancing reactive oxygen species production N88-27357
CHIPS (MEMORY DEVICES)
MINIAC: A small embedded computer
[DE88-008142] N88-27757
CHLORIDES
Effect of thermal cycling on CSPL (Chloride Silent Power Ltd.) sodium/sulfur cells
[DE88-011205] N88-27455
Post-test observations on CSPL (Chloride Silent Power Limited) cells
[DE88-011975] N88-27461
CHROMIUM
Self energy corrections to the ab initio band structures: Chromium
[DE88-701825] N88-27927
CHROMOSOMES
Genetic effects of low level microwave radiation
[AD-A192887] N88-27722
Effects of pulsed and CW (Continuous Wave) 2450 MHz radiation on transformation and chromosomes of human lymphocytes in vitro
[AD-A193104] N88-27736
CIRCUITS
An investigation of the uses of time domain capable vector network analyzers as a diagnostic for helix traveling-wave circuits
[AD-A192460] N88-27430
A fiber optic synchronous detector using sample-and-hold circuits
[DE88-010973] N88-27899
CIRRUS CLOUDS
The collection of statistics on the frequency of cloud cover over North America
[AD-A193093] N88-27667
CLASSIFICATIONS
Topics in quasicrystallography N88-27947
CLIMATOLOGY
Development of radiation and cloud parameterization programs for AFGL (Air Force Geophysics Laboratory) global models
[AD-A193369] N88-27658
Air-sea interaction in the vicinity of a land-sea boundary in the presence of upwelling N88-27661
Intercomparison of NMC (National Meteorological Center) and ECMWF (European Centre for Medium Range Weather Forecasts) global analyses: 1960-1986
[PB88-196548] N88-27668
Surface energy balance of three general circulation models: Current climate and response to increasing atmospheric CO2
[DE88-010967] N88-27673
Space shuttle natural environment analysis
[NASA-CR-179337] N88-27676
CLOUD COVER
Development of radiation and cloud parameterization programs for AFGL (Air Force Geophysics Laboratory) global models
[AD-A193369] N88-27658
The collection of statistics on the frequency of cloud cover over North America
[AD-A193093] N88-27667
CLOUD PHYSICS
Cloud simulation warm cloud experiments: Droplet growth and aerosol scavenging
[AD-A192944] N88-27666
CLOUDS
Cloud simulation warm cloud experiments: Droplet growth and aerosol scavenging
[AD-A192944] N88-27666
CLUSTER ANALYSIS
To the opportunities of cluster analysis of light curves of supernovae
[DE88-701642] N88-27982
COATINGS
Contribution to the development of coated fiber ceramic insolation material
[ETN-88-92361] N88-27243
PECVD of amorphous nickel--phosphorus films
[DE88-011088] N88-27299
Radiative heat transfer and selective emission in planar slab coatings on hot emissive substrates
[AD-A193133] N88-27319
Thermo-mechanical cracking in coated media with a cavity by a moving asperity friction
[AD-A193311] N88-27586
COCHLEA
Assessment of cochlear damage after microwave irradiation
[AD-A193237] N88-27737
COCKPITS
Cockpit and cabin crew coordination
[AD-A192445] N88-27752
A cockpit natural language study: Vocabulary and grammar analyses
[AD-A193289] N88-27753
CODING
A VLSI single-chip (225,223) Reed-Solomon encoder with interleaver
[NASA-CASE-NPO-17280-1-CU] N88-27220
SARLAC: A relativistic electron beam code
[AD-A193134] N88-27411
COGNITION
The effects of increased cognitive demands on autonomic self-regulation: An indicator of parallel processing in the brain N88-27362
Electric and magnetic brain activity related to cognitive performance N88-27692
The effects of hypoxia on P300 and reaction time
[DCIEM-87-RR-12] N88-27697
Cognitive task demands as reflected in physiological measures N88-27699
Event-related and steady potential changes in the brain related to workload during tracking N88-27705
Cognitive and neural bases of skilled performance
[AD-A193392] N88-27747
COGNITIVE PSYCHOLOGY
Determinants of dual-task interference and resource theories in cognitive psychology
[DFVLR-FB-88-14] N88-27748
COLD WEATHER TESTS
Flight testing under extreme environmental conditions
[AGARD-AG-300-VOL-8] N88-27525
COLD WORKING
Cold worked reinforcing bars in tensile test under high loading rate and low temperatures
[DE88-752993] N88-27810
COLLECTION
The Hanford meteorological data collection system and data base
[DE88-008632] N88-27672
COLLISION PARAMETERS
Study of the production of Ko mesons in proton antiproton interactions at 630 GeV
[NOTA-INTERNA-908] N88-27892
COLLISION RATES
Approximate analytical formulae for electron density and collision frequency in the natural and nuclear-disturbed ionosphere and inner magnetosphere
[AD-A193129] N88-27654
COLLISIONS
Approximate analytical formulae for electron density and collision frequency in the natural and nuclear-disturbed ionosphere and inner magnetosphere
[AD-A193129] N88-27654
COMBAT
Computation of ECM (Electronic Counter-Measures) war reserve materiel spare requirements
[AD-A193301] N88-27195
COMBUSTIBLE FLOW
Experimental research of combustion systems N88-27371
COMBUSTION
Premixed turbulent flame propagation
[AD-A192955] N88-27265
Summary of discussions at the Tenth Meeting of the Sandia Cooperative Group on the Aerothermochemistry of Turbulent Combustion
[DE88-008467] N88-27269
COMBUSTION CHAMBERS
Effects of ceramic surfaces on autoignition in a constant volume combustion apparatus
[AD-A193055] N88-27266
Investigation of annular flow at high evaporation rates in view of liquid film cooling
[DFVLR-FB-88-08] N88-27517
Experimental validation of a zero-dimensional computer model for spark-ignition engines
[DE88-009034] N88-27565
COMBUSTION PRODUCTS
Carbon deposition model for oxygen-hydrocarbon combustion, volume 1
[NASA-CR-179375] N88-27254
Carbon deposition model for oxygen-hydrocarbon combustion, volume 2
[NASA-CR-179376] N88-27255
COMBUSTION STABILITY
Evaluation and improvement of liquid propellant rocket chugging analysis techniques. Part 1: A one-dimensional analysis of low frequency combustion instability in the fuel preburner of the space shuttle main engine
[NASA-CR-183106] N88-27224
Evaluation and improvement of liquid propellant rocket chugging analysis techniques. Part 2: A study of low frequency combustion instability in rocket engine preburners using a heterogeneous stirred tank reactor model
[NASA-CR-182724] N88-27225
COMMUNICATION
A study of a meteor burst communication system N88-27421
COMMUNICATION EQUIPMENT
Event-related brain potentials as indices of mental workload and attentional allocation N88-27696
COMMUNICATION NETWORKS
The MELMUX MX-7100 series high-speed digital multiplexers N88-27396
Activities report of the Communications Department
[ENST-88D003] N88-27401
Utilization of a satellite communication system to protect the national communication network
[FUB-33-1986] N88-27423
COMMUNICATION SATELLITES
EXSAT: Expert system to configure telecommunication satellites
[SNIAS-881-440-101] N88-27223
Utilization of a satellite communication system to protect the national communication network
[FUB-33-1986] N88-27423
COMMUTATION
Reduced order modeling of grid-connected photovoltaic inverter systems
[DE88-010603] N88-27635
COMPACTING
Superconductor consolidation
[DE88-010938] N88-27949
COMPARATORS
Measurement of the thermal conductivity of dielectric thin solid films with a thermal comparator
[DE88-008468] N88-27898
COMPARISON
A comparison of generators for pseudo-random normal deviates
[DE88-011711] N88-27859
COMPATIBILITY
A fundamental understanding of the interfacial compatibility in hybrid material systems
[AD-A192921] N88-27264
Capitalizing on experience with intelligence gateway software
[AD-A193362] N88-27971
COMPILERS
Ada (trade name) compiler validation summary report: Verdix Corporation VAda-010-03315, version 5.5 MicroVAX 2 host ISBC 386/20P Intel target
[AD-A193226] N88-27774

Ada (trade name) compiler validation summary report: Verdix corporation VAda-010-13125, version 5.41 Sun Microsystems Sun-3/160 host microbar GPC68020 target
[AD-A193415] N88-27777

COMPLEX COMPOUNDS
Catalytic activation of carbon dioxide by metal complexes
[AD-A192310] N88-27262
Structure and function of the manganese complex involved in photosynthetic oxygen evolution determined by X-ray adsorption spectroscopy and electron paramagnetic resonance spectroscopy
[DE88-010360] N88-27725

COMPONENTS
Vapor Compression Distillation Subsystem (VCDS) component enhancement, testing and expert fault diagnostics development, volume 2
[NASA-CR-172076] N88-27755

COMPOSITE MATERIALS
Boundary layer solutions for the free-edge problem in composite laminates N88-27229
Thermo-viscoelastic analysis of composite materials, volume 1
[NASA-CR-183048-VOL-1] N88-27230
Probabilistic anisotropic failure criteria for composite materials
[AD-A193046] N88-27232
Analysis of transverse strength of composites using percolation theory
[AD-A193204] N88-27234
Far- and mid-infrared properties of metal-insulator composite materials
[AD-A193227] N88-27236
Polymer-ceramic composites
[AD-A193244] N88-27237
Techniques for characterizing damage zones in composite materials N88-27240
Characterization of elastic-plastic properties of AS4/APC-2 thermoplastic composite
[NASA-CR-183145] N88-27242
Preparation and properties of new inorganic glasses and gel-derived solids
[AD-A192922] N88-27315
Application of sol-gel procedures to ceramic composites
[ETN-88-92741] N88-27338

COMPOSITE STRUCTURES
Balance of X-ray radioscopy application to nondestructive tests of composite materials
[SNIAS-881-430-110] N88-27250

COMPRESSIBILITY
Temperature, moisture and strain rate effects on the compressive mechanical behavior of Nylon 6/6
[DE88-010734] N88-27591

COMPRESSIBLE FLOW
An h-p adaptive finite element method for steady compressible flow N88-27467
Implicit finite-difference simulation of an internal flow on a hypercube
[AD-A192474] N88-27471

COMPRESSIBLE FLUIDS
Implicit finite-difference simulation of an internal flow in a nozzle: An example of a physical application on a hypercube
[AD-A192475] N88-27472

COMPRESSING
Ultrasonic studies of stresses and plastic deformation in steel during tension and compression
[AD-A192306] N88-27280

COMPRESSION TESTS
An experimental and analytical evaluation of a biaxial test for determining shear properties of composite materials
[NASA-CR-182928] N88-27593

COMPRESSIVE STRENGTH
Development of a biaxial test system for thin-walled metal tubes using tensile-compressive axial load and internal-external pressure
[DE88-011279] N88-27592

COMPUTATION
A computational analysis of under-expanded jets in the hypersonic regime
[NASA-TM-101319] N88-27174
Numerical simulation of fuel droplet interactions and breakup
[AD-A192431] N88-27470
Numerical experiments on turbulent mixing
[AD-A192572] N88-27473
Computational boundary conditions for the incompressible Navier-Stokes equations in channels and pipes
[AD-A193356] N88-27487
Numerical treatment of the pressure singularity at a re-entrant corner
[AD-A193357] N88-27488
Neural network research: A personal perspective
[AD-A192717] N88-27808
Parallel solutions to geometric problems on the scan model of computation
[AD-A192321] N88-27819

COMPUTATIONAL FLUID DYNAMICS
Hybrid procedure for dynamic measurements in transonic wind tunnels: Demonstrated by pitch oscillation
[DFVLR-FB-88-19] N88-27211
Computational fluid dynamics on parallel processors
[AD-A192397] N88-27469
Aerodynamics of Hypersonic Lifting Vehicles: Fluid Dynamics Panel AGARD Symposium
[AGARD-AR-246] N88-27480
A Navier-Stokes study of cascade flow fields including inlet distortion and rotating stall
[AD-A193109] N88-27483
Numerical computation of three-dimensional turbulent flow in tightly curved ducts and spiral turbine casings
[ETN-88-92362] N88-27511

COMPUTATIONAL GRIDS
Creating aspect graphs for use in object recognition N88-27379

COMPUTER AIDED DESIGN
Programs for preliminary design of composite materials which were developed by the design group of Aerospatiale Aquitaine
[SNIAS-881-430-112] N88-27251
Investigation of expert system design approaches for electronic design environments N88-27365
The integration of decision support problems into feature modeling based design N88-27372
Mitsubishi Electric Advance (R and D Edition), Volume 41
[PB88-194162] N88-27388
Computer-Aided Engineering (CAE) for engineering design N88-27390
STAR: Sandia Timing Analyzer Routine
[DE88-012412] N88-27463
Optimization of planetary gears
[ETN-88-92375] N88-27573
Computer aided design for linear control State Variable System (SVS)
[AD-A193282] N88-27775
Research into the architecture of CAD based robot vision systems
[AD-A193330] N88-27776
Benefits of an object approach in a computer aided design environment
[SNIAS-881-440-102] N88-27791
A PRELUDE (analysis and design of control systems-preliminary utilities depository). A data-based interactive system of control software, user's guid e
[DFVLR-MITT-88-12] N88-27795

COMPUTER AIDED MAPPING
Development of automatic names placement software
[AD-A192786] N88-27770

COMPUTER AIDED TOMOGRAPHY
Turbulent flow field visualization with integral interferometric imaging and computed tomography N88-27521

COMPUTER GRAPHICS
Three-dimensional scene analysis using stero based imaging
[AD-A193120] N88-27178
An aspect graph-based control strategy for 3-D object recognition N88-27377
Creating aspect graphs for use in object recognition N88-27379
The effect of input device on user performance with a menu-based natural language interface
[AD-A193095] N88-27772
A menu-driven menu editor and associated menu system
[DE88-008026] N88-27781
TRANSL: A PATRAN translator subroutine library
[DE88-010976] N88-27784
Contribution to almost realistic picture processing by a computer graphics procedure
[ETN-88-92372] N88-27789
A hidden-surface removal algorithm for structures defined by triangular and rectangular surface patches
[DFVLR-MITT-88-03] N88-27792
User's manual for the two-dimensional transputer graphics toolkit
[NASA-TM-100974] N88-27799

COMPUTER NETWORKS
Optical interconnections for digital image coding N88-27381
Implementing direct, spatially isolated problems on transputer networks
[NASA-TM-101297] N88-27796
A modular proof of correctness for a network synchronizer
[AD-A192726] N88-27802
Improving the performance of AI algorithms
[AD-A192848] N88-27809
Finding minimum-cost circulations by canceling negative cycles
[AD-A192727] N88-27825

COMPUTER PROGRAMMING
Linear programming for Air Force decision aiding N88-27376
A programmable systolic array for factorial analysis. Part 2: The symmetric eigenvalue problem
[AD-A192396] N88-27762
Inspection methods in programming: Cliches and plans
[AD-A192782] N88-27767
Synchronizable series expressions. Part 2: Overview of the theory and implementation
[AD-A192783] N88-27768
The programmer's apprentice project: A research overview
[AD-A192784] N88-27769
Contribution to almost realistic picture processing by a computer graphics procedure
[ETN-88-92372] N88-27789
FORTRAN 77 implementation of abstract datatype models
[DFVLR-MITT-88-08] N88-27794
Improving the performance of AI algorithms
[AD-A192848] N88-27809

COMPUTER PROGRAMS
A comparison of the various helicopter mathematical models used in the methodology assessment N88-27149
Aeromechanical stability analysis of COPTER N88-27161
FORTRAN programs for computation of time dependent sea levels and trajectory errors from satellite altimeter data
[BONN-MITT-73] N88-27216
Evaluation and improvement of liquid propellant rocket chugging analysis techniques. Part 1: A one-dimensional analysis of low frequency combustion instability in the fuel preburner of the space shuttle main engine
[NASA-CR-183106] N88-27224
Evaluation and improvement of liquid propellant rocket chugging analysis techniques. Part 2: A study of low frequency combustion instability in rocket engine preburners using a heterogeneous stirred tank reactor model
[NASA-CR-182724] N88-27225
Programs for preliminary design of composite materials which were developed by the design group of Aerospatiale Aquitaine
[SNIAS-881-430-112] N88-27251
Hole diameters in plates impacted by projectiles N88-27386
Control of free-flying space robot manipulator systems
[NASA-CR-183017] N88-27562
Development of a biaxial test system for thin-walled metal tubes using tensile-compressive axial load and internal-external pressure
[DE88-011279] N88-27592
IEMIS (Integrated Emergency Management Information System) floodplain mapping based on a LIDAR derived data set
[AD-A193071] N88-27616
Validate algorithms for the determination of rainfall rates from SSM/I microwave satellite imagery
[AD-A192299] N88-27664
Vision research. A national plan: 1983-1987, 1987 evaluation and update
[PB88-192604] N88-27726
A cockpit natural language study: Vocabulary and grammar analyses
[AD-A193289] N88-27753
Full analysis of a powerful window random access algorithm
[AD-A192437] N88-27763
Using IMSL mathematical and statistical computer subroutines in physiological and biomechanical research
[AD-A192594] N88-27765
Development of automatic names placement software
[AD-A192786] N88-27770
The effect of input device on user performance with a menu-based natural language interface
[AD-A193095] N88-27772
Computer aided design for linear control State Variable System (SVS)
[AD-A193282] N88-27775
Synopsis of a computer program designed to interface a personal computer with the fast data acquisition system of a time-of-flight mass spectrometer
[NASA-CR-177474] N88-27798
The SAS System by forms: Putting statistical power into the hands of an end-user
[DE88-010512] N88-27857

Comparison of results based on a deterministic versus a statistical uncertainty analysis
[DE88-010751] N88-27858
COMPUTER STORAGE DEVICES
Implementation of an OPS5 derivative on the Novix RISC processor
[DE88-011392] N88-27758
Content-addressable memory storage by neural networks: A general model and global Liapunov method
[AD-A192716] N88-27807
COMPUTER SYSTEMS DESIGN
Computer system for the primary fly-by-wire control of civil transport aircraft (experimental system)
[FBW-TB-2086/88] N88-27204
MINIAC: A small embedded computer
[DE88-008142] N88-27757
A menu-driven menu editor and associated menu system
[DE88-008026] N88-27781
Notes on operating system requirements for the next millennium
[DE88-010712] N88-27805
COMPUTER SYSTEMS PERFORMANCE
Aircraft refueling demonstrator using a microbot alpha 2 robot N88-27367
Constructing a highly-available location service for a distributed environment
[AD-A192723] N88-27801
Modeling and approximate performance analysis of multiuser computer systems
[ETN-88-92137] N88-27806
The SAS System by forms: Putting statistical power into the hands of an end-user
[DE88-010512] N88-27857
COMPUTER SYSTEMS PROGRAMS
Capitalizing on experience with intelligence gateway software
[AD-A193362] N88-27971
COMPUTER TECHNIQUES
United States Air Force Graduate Student Summer Support Program, volume 2
[AD-A191122] N88-27355
CEEG dynamic brain mapping: A new method to evaluate brain function in different psychological and drug conditions N88-27685
Fourth generation neurocognitive pattern analysis system N88-27686
A statistical procedure for the evaluation of presence/non-presence of stimulus-related EEG activity N88-27689
Assessing and enhancing human performance: Utility of a workstation network
[AD-A192840] N88-27743
Issues in computer-assisted interpretation of graphs and quantitative information
[PB88-116280] N88-27783
A review of parallel methods for solving sets of linear equations and their application within optimisation algorithms
[AD-A193137] N88-27830
COMPUTER VISION
Research into the architecture of CAD based robot vision systems
[AD-A193330] N88-27776
Neural network research: A personal perspective
[AD-A192717] N88-27808
COMPUTERIZED SIMULATION
A feasibility study in path planning using optimization techniques
[AD-A193030] N88-27177
Simulation of moisture diffusion of fiber reinforced components of aircraft for general air transportation
[IFL-IB-87-05] N88-27253
Computer simulation of elastic properties of grain boundary materials
[DE88-011965] N88-27305
SARLAC: A relativistic electron beam code
[AD-A193134] N88-27411
Calculations of high-frequency parameters of disc-loaded waveguides
[DE88-702178] N88-27417
STAR: Sandia Timing Analyzer Routine
[DE88-012412] N88-27463
Implicit finite-difference simulation of an internal flow on a hypercube
[AD-A192474] N88-27471
Simulation and analysis of wave propagation through random media N88-27503
Numerical simulation and stability analysis of the absolutely and convectively unstable wake
[DFVLR-FB-88-09] N88-27518
Initial electron distributions for free-electron lasers generated by injector and accelerator simulations
[DE88-007022] N88-27540
Development of a hybrid simulator for robotic manipulators
[AD-A193119] N88-27557
Control of free-flying space robot manipulator systems
[NASA-CR-183017] N88-27562
Experimental validation of a zero-dimensional computer model for spark-ignition engines
[DE88-009034] N88-27565
Solar cell modeling and simulation
[AD-A193249] N88-27620
Approximate analytical formulae for electron density and collision frequency in the natural and nuclear-disturbed ionosphere and inner magnetosphere
[AD-A193129] N88-27654
Large-eddy simulations of concentration fluctuations
[DE88-009480] N88-27660
Update on the meso-microscale meteorological hierarchy
[DE88-009133] N88-27670
Three-dimensional wind simulation
[DE88-009793] N88-27671
Computer simulation procedure for designing airborne aerometric monitoring programs
[DE88-011896] N88-27674
The VITE model: A neutral command circuit for a generating arm and articulator trajectories
[AD-A192715] N88-27734
Demodulation processes in auditory perception
[AD-A193421] N88-27740
Assessing and enhancing human performance: Utility of a workstation network
[AD-A192840] N88-27743
Block Oriented Simulation System (BOSS)
[NASA-CR-182947] N88-27760
Simulation methodology
[AD-A192548] N88-27764
Bisimulation can't be traced
[AD-A192725] N88-27766
Simulation of real time problem solving
[AD-A193436] N88-27778
Verification of flight software written in C using ACSL
[DE88-006100] N88-27779
Dose-enhancement effects in TaSi/Al- and Al-gate MOS devices
[DE88-005483] N88-27926
Dynamical evolution of cosmic strings
[DE88-011724] N88-27989
CONCAVITY
The heat transfer and fluid dynamics of concave surface curvature
[AD-A193064] N88-27479
CONCENTRATION (COMPOSITION)
Retrieval of temperature and concentration profiles from a limited number of absorption measurements N88-27501
National ambient Volatile Organic Compounds (VOCs) data base update, documentation
[PB88-195631] N88-27646
CONCENTRATORS
Performance sensitivities for point-focus dish systems with secondary concentrators
[DE88-001152] N88-27629
Photovoltaic Energy. Electricity from Sunlight: A current awareness bulletin
[DE88-008289] N88-27634
CONCORDE AIRCRAFT
Supersonic transport/hypersonic transport (SST/HST) development
[SNIAS-881-111-101] N88-27192
CONCURRENT PROCESSING
Computer system for the primary fly-by-wire control of civil transport aircraft (experimental system)
[FBW-TB-2086/88] N88-27204
Model for dynamically structured communicating systems
[PB88-105283] N88-27402
Bisimulation can't be traced
[AD-A192725] N88-27766
Image processing using a parallel architecture
[AD-A192833] N88-27803
CONDENSING
Storage of thermal energy by means of an absorption cycle
[PB88-190814] N88-27619
CONDUCTION BANDS
Investigation of electronic band structure of semiconductors by photoemission
[ETN-88-92370] N88-27957
CONDUCTIVE HEAT TRANSFER
Moment approach to neoclassical flows, currents and transport in auxiliary heated tokamaks
[DE88-008024] N88-27901
CONFERENCES
Integrated Technology Rotor Methodology Assessment Workshop
[NASA-CP-10007] N88-27148
Very High Speed Integrated Circuits (VHSIC)
[AD-A193225] N88-27442
Aerodynamics of Hypersonic Lifting Vehicles: Fluid Dynamics Panel AGARD Symposium
[AGARD-AR-246] N88-27480
Finite element methodology for integrated flow-thermal-structural analysis
[NASA-CR-183144] N88-27606
Photovoltaic Energy. Electricity from Sunlight: A current awareness bulletin
[DE88-008289] N88-27634
Electric and Magnetic Activity of the Central Nervous System: Research and Clinical Applications in Aerospace Medicine
[AGARD-CP-432] N88-27683
CONFORMAL MAPPING
Geometry of superconformal manifolds, part 1
[DE88-702405] N88-27863
Geometry of superconformal manifolds, part 2
[DE88-702406] N88-27864
CONJUGATE GRADIENT METHOD
A taxonomy for conjugate gradient methods
[DE88-008574] N88-27817
CONNECTORS
Developing a connector selection DBMS (database management system) using NIAM (Nijssen's Information Analysis Methodology)
[DE88-008110] N88-27972
CONSCIOUSNESS
Physiological monitoring methodology in the USAFSAM centrifuge N88-27356
CONSERVATION EQUATIONS
Adaptive finite element methods for shells
[AD-A193221] N88-27585
CONSISTENCY
Constant amplitude fatigue life data for notched and unnotched annealed Ti-6Al-4V sheet
[AD-A193420] N88-27287
CONSOLIDATION
Superconductor consolidation
[DE88-010938] N88-27949
CONTACT RESISTANCE
Friction, wear and electrical contact resistance of precious metal alloys
[DE88-011244] N88-27450
CONTAMINANTS
Analysis of debris from accelerated life test of the Hughes five-year Vuilleumier cryocooler
[AD-A193101] N88-27400
CONTAMINATION
A zoomable and adaptable hidden fine-mesh approach to solving advection-dispersion equations
[DE88-006174] N88-27816
CONTINUOUS RADIATION
Effects of pulsed and CW (Continuous Wave) 2450 MHz radiation on transformation and chromosomes of human lymphocytes in vitro
[AD-A193104] N88-27736
CONTINUUM MECHANICS
An anisotropic continuum damage model for creep-dominated, multiaxial loading histories N88-27608
Some stability criteria in fluid and solid mechanics N88-27966
CONTINUUM MODELING
An anisotropic continuum damage model for creep-dominated, multiaxial loading histories N88-27608
CONTROL SYSTEMS DESIGN
Numerical optimization, system theoretic and software tools for the integrated design of flexible structures and their control systems
[AD-A192927] N88-27183
Thermal-sensation control: A new method of controlling cooled/heated environments N88-27394
A conceptual design study of a hovering system controller for an autonomous underwater vehicle
[AD-A193423] N88-27399
The robust tracking control of nonlinear systems with uncertain dynamics N88-27788
A PRELUDE (analysis and design of control systems-preliminary utilities depository). A data-based interactive system of control software, user's guid e
[DFVLR-MITT-88-12] N88-27795
CONTROL UNITS (COMPUTERS)
An investigation of performance improvement in knowledge-based control systems N88-27382
CONTROL VALVES
Characterization of accelerating pipe flow
[AD-A193065] N88-27481
CONTROLLERS
SP-100 Ground Engineering Systems: Test facility control systems
[DE88-009195] N88-27895

CONVECTION
Time-dependent thermal convection of Earth mantle and double diffusive convection in magma chambers
[MITT-52] N88-27663
CONVECTIVE HEAT TRANSFER
The heat transfer and fluid dynamics of concave surface curvature
[AD-A193064] N88-27479
CONVERGENT-DIVERGENT NOZZLES
Implicit finite-difference simulation of an internal flow in a nozzle: An example of a physical application on a hypercube
[AD-A192475] N88-27472
CONVERSION
Ethanol as a fuel of a lorry. Use experience from a diesel engine modified to an otto engine
[DE88-752870] N88-27569
COOLING
Thermal-sensation control: A new method of controlling cooled/heated environments N88-27394
COORDINATES
Three-dimensional adaptive grid generation for body-fitted coordinate system
[NASA-CR-182192] N88-27520
COORDINATION
Soluble metal chelate polymers of coordination numbers six, seven and eight
[AD-A192485] N88-27314
Cockpit and cabin crew coordination
[AD-A192445] N88-27752
COPOLYMERS
Ionic conductive polymers based on crosslinked elastic siloxane-ethylene oxide copolymers
[DE88-011243] N88-27311
Spatial organization of homopolymer chains inside spherical polybutadiene domains of SB diblock copolymers
[AD-A193390] N88-27321
COPPER
Growth and characterization of CuGaS2, CuAlS2 and CuGa0.9Al0.1S2 single crystals
[AD-A192963] N88-27930
COPPER ALLOYS
Formation of metastable structures and amorphous phases in Cu-W alloys using the triod sputtering technique
[DE88-009051] N88-27298
COPPER COMPOUNDS
Compilation of NRL publications on high temperature superconductivity
[AD-A189137] N88-27921
COPPER OXIDES
Superconducting properties of LaBa2Cu3O(sub x) and YBa2Cu3O(sub y)
[DE88-012038] N88-27952
COPPER SELENIDES
Device physics related to the granular nature of CuInSe2 solar cells
[DE88-001159] N88-27622
CORE FLOW
Physiological responses to acute exercise-heat stress
[AD-A192606] N88-27732
CORNERS
Numerical treatment of the pressure singularity at a re-entrant corner
[AD-A193357] N88-27488
CORRECTION
A numerical simulation of side force effects by aerodynamic flight trajectory correction
[ISL-CO-211/87] N88-27191
CORRELATORS
An optical 2-dimensional correlator for pattern recognition in embedded computing
[DE88-007198] N88-27780
A fiber optic synchronous detector using sample-and-hold circuits
[DE88-010973] N88-27899
CORROSION
Determination of Tafel constants in nonlinear polarization curves
[AD-A192335] N88-27282
A critical review of IR drops and electrode potentials within pits, crevices and cracks
[AD-A192481] N88-27431
Significance of the local electrode potential within pits, crevices and cracks
[AD-A192482] N88-27432
Corrosion fatigue of small cracks: Mechanics and chemistry
[DE88-012121] N88-27605
CORROSION PREVENTION
Unified methods of accelerated laboratory tests of the preparations for temporary protection of cars
[NASA-TT-20298] N88-27336
COSMIC RAYS
Are Centauros diffractive
[DE88-008767] N88-27996
COSMOLOGY
Cosmological parameters and evolution of the galaxy luminosity function
[NASA-CR-183081] N88-27986
Dynamical evolution of cosmic strings
[DE88-011724] N88-27969
COSMONAUTS
History of manned spaceflight
[CNES-NT-121] N88-28000
COST ANALYSIS
Finding minimum-cost circulations by successive approximation
[AD-A192724] N88-27824
Approximations and optimal control for the pathwise average cost per unit time and discounted problems for wideband noise driven systems
[AD-A192712] N88-27847
Sources and nature of cost analysis data base reference manual
[AD-A193099] N88-27976
COUPLED MODES
Coupled even-parity superconducting states: Square lattice
[AD-A193432] N88-27938
COUPLING
Coupling of a spark source mass spectrograph and a ND-YAG laser
[DE88-012116] N88-27530
CRAB NEBULA
Application of two-dimensional imaging to very high energy gamma ray astronomy
[DE88-010120] N88-27983
CRACK ARREST
Analysis of crack arrest toughness
[AD-A193340] N88-27286
CRACK CLOSURE
Three-dimensional aspects of fatigue crack closure
[AD-A192296] N88-27581
CRACK INITIATION
Failure analysis of Chloride Silent Power, Ltd. PB cells
[DE88-010567] N88-27448
CRACK PROPAGATION
Analysis of crack arrest toughness
[AD-A193340] N88-27286
Three-dimensional aspects of fatigue crack closure
[AD-A192296] N88-27581
Diffusion models of crack growth due to random overloads
[DE88-008811] N88-27595
Corrosion fatigue of small cracks: Mechanics and chemistry
[DE88-012121] N88-27605
Computation of failure probability of fatigue loaded cracked structures
[ETN-88-92360] N88-27607
CRACK TIPS
Plastic yielding at crack tips
[AD-A192549] N88-27582
CRACKING (FRACTURING)
Influence of microstructure and microdamage processes on fracture at high loading rates
[AD-A192957] N88-27583
CRACKS
Application of controlled interfacial pore structures to kinetic studies in alumina
[DE88-010864] N88-27326
Significance of the local electrode potential within pits, crevices and cracks
[AD-A192482] N88-27432
Plastic yielding at crack tips
[AD-A192549] N88-27582
Thermo-mechanical cracking in coated media with a cavity by a moving asperity friction
[AD-A193311] N88-27586
CRASHES
Improved procedure for impact probability computation of aircraft crash based on Balfanz model
[JUEL-SPEZ-425] N88-27176
CREEP ANALYSIS
Verification of the ADINA finite element code for creep analysis: Problems from the open literature
[DE88-011826] N88-27594
CREEP PROPERTIES
Effect of the matrix on the creep-behavior of carbon-carbon composite
[AD-A193211] N88-27235
Controlling phase formation and stability to improve the high temperature creep resistance of austenitic stainless steels
[DE88-011401] N88-27293
Creep behavior for Hastelloy-XR
[DE88-753428] N88-27295
Verification of the ADINA finite element code for creep analysis: Problems from the open literature
[DE88-011826] N88-27594
An anisotropic continuum damage model for creep-dominated, multiaxial loading histories N88-27608
CREEP STRENGTH
Effect of the matrix on the creep-behavior of carbon-carbon composite
[AD-A193211] N88-27235
CROSS SECTIONS
Nonlinear interaction between overall and local buckling of stiffened panels with symmetric cross-sections
[PB88-104054] N88-27580
CROSSLINKING
Study of crosslinking and nonelastic mechanical properties of epoxy and PSP networks --- epoxy resins; polystyrylpyridine resins (psp)
[ETN-88-92740] N88-27337
CRYOGENIC COOLING
Analysis of debris from accelerated life test of the Hughes five-year Vuilleumier cryocooler
[AD-A193101] N88-27400
CRYOGENIC EQUIPMENT
Cyrogenic test facilities for an optical cryomechanism qualification
[SNIAS-881-440-116] N88-27219
Analysis of debris from accelerated life test of the Hughes five-year Vuilleumier cryocooler
[AD-A193101] N88-27400
CRYOGENIC TEMPERATURE
Cryogenic free jets
[DFVLR-FB-88-16] N88-27210
CRYSTAL DEFECTS
Migration and stability of HgCdTe lattice defects
[AD-A193293] N88-27935
Probing the electronic and defect structure of perovskite superconductors
[DE88-008349] N88-27939
Deep level defects in semiconductors: Stress and pressure studies
[DE88-010855] N88-27948
CRYSTAL DISLOCATIONS
Diffusion and solubility of some interstitial impurities in deformed metals
[DE88-701859] N88-27296
CRYSTAL GROWTH
Analysis of grain refinement and superplasticity in aluminum-magnesium alloys
[AD-A193029] N88-27283
Processing and additive effects of ZrO2 on microstructure and dielectric porperties of BaTiO3 ceramics
[AD-A193126] N88-27316
Growth and characterization of CuGaS2, CuAlS2 and CuGa0.9Al0.1S2 single crystals
[AD-A192963] N88-27930
CRYSTAL LATTICES
Picosecond transient reflectivity of unpinned gallium arsenide (100) surfaces
[AD-A193242] N88-27933
Topics in quasicrystallography N88-27947
Deep level defects in semiconductors: Stress and pressure studies
[DE88-010855] N88-27948
CRYSTAL OSCILLATORS
Quartz crystal resonators and oscillators for frequency control and timing applications
[AD-A193310] N88-27443
CRYSTAL STRUCTURE
Thermomechanical processing of Al alloy 2090 for grain refinement and superplasticity
[AD-A192333] N88-27281
Analysis of grain refinement and superplasticity in aluminum-magnesium alloys
[AD-A193029] N88-27283
Polarization selective Raman microspectroscopy N88-27397
Meaning of energy diagrams used to describe hetero-structures
[DE88-702219] N88-27943
Prediction of deep levels and equilibrium concentrations of defects in semiconductors N88-27945
X-ray studies of strain, interface and impurities in semiconductors
[DE88-012460] N88-27954
Characterization of crystalline silicon by electrochemical and Raman spectroscopy at the frontier semiconductor/electrolyte
[ETN-88-92354] N88-27956
CRYSTALLIZATION
Microchemical analysis of polycrystalline Ni3Al and other ordered alloys using the field-ion microscope atom probe
[DE88-011519] N88-27294

Formation of metastable structures and amorphous phases in Cu-W alloys using the triod sputtering technique
[DE88-009051] N88-27298
Homogeneity of glasses: Experiment WL-IHF-05 in D1 mission --- Spacelab
[ETN-88-92339] N88-27353
Experiments in microgravity environment: Protein crystallization
[SNIAS-881-430-101] N88-27354
CRYSTALLOGRAPHY
Topics in quasicrystallography N88-27947
Characterization of crystalline silicon by electrochemical and Raman spectroscopy at the frontier semiconductor/electrolyte
[ETN-88-92354] N88-27956
CUBIC LATTICES
Compilation of temperature factors of cubic elements
[PB88-108170] N88-27260
Theoretical predictions of precipitate shapes in cubic alloys
[DE88-010856] N88-27291
CULTURE TECHNIQUES
Effects of pulsed and CW (Continuous Wave) 2450 MHz radiation on transformation and chromosomes of human lymphocytes in vitro
[AD-A193104] N88-27736
CURING
Determination of the glass transition temperature of cured composite materials
[DT-87/62-R] N88-27246
Determination of lumped-mass thermal properties associated with autoclave curing of graphite/epoxy composites N88-27364
CURRENT SHEETS
Scaling laws for geomagnetic tail current sheet acceleration
[AD-A193379] N88-27659
CURVATURE
Applications of differential geometry to the shape analysis of gray-value images N88-27358
CYLINDRICAL BODIES
Experimental investigation of simplest inhomogeneities in cylindrical slit line
[DE88-702386] N88-27418
Determination of the local heat-transfer characteristics on glaze ice accretions on a cylinder and a NACA 0012 airfoil N88-27500
The three-dimensional stress field around a cylindrical inclusion in a plate of arbitrary thickness N88-27602
CYLINDRICAL SHELLS
A study of fluid-structure problems N88-27468

D

DAMAGE
Vibrational impacts of hush house operation
[DE88-006983] N88-27207
Fiber-optics used to record high-speed photographs inside a pressurized tank during lethality testing
[DE88-011283] N88-27529
Critical issues and directions for fracture mechanics and structural integrity
[AD-A193050] N88-27584
The relationship between observed fatigue damage and life estimation models
[NASA-CR-182191] N88-27611
DAMAGE ASSESSMENT
T55-L-714 engine development and qualification. Engine M11 low cycle fatigue test report. (0213-005-87)
[AD-A192765] N88-27197
T55-l-714 engine development and qualification. Engine M11 low cycle fatigue test report. (0213-005-87), volume 2, part 1
[AD-A192766] N88-27198
Techniques for characterizing damage zones in composite materials N88-27240
Design and implementation of contact ultrasonic sensors to assess internal damage
[I-177/87] N88-27247
An anisotropic continuum damage model for creep-dominated, multiaxial loading histories N88-27608
Assessment of cochlear damage after microwave irradiation
[AD-A193237] N88-27737
DAMPING
The importance of steady and dynamic inflow on the stability of rotor-body systems N88-27156
Comparison of experimental rotor damping data-reduction techniques N88-27159
Experimental determination of aerodynamic damping in a three-stage transonic axial-flow compressor
[NASA-TM-100953] N88-27200
Damping characteristics of metal matrix composites
[AD-A193144] N88-27233
DATA ACQUISITION
FTMP data acquisition environment
[NASA-TM-100636] N88-27447
Army space systems for terrestrial applications
[AD-A192735] N88-27613
The Hanford meteorological data collection system and data base
[DE88-008632] N88-27672
Synopsis of a computer program designed to interface a personal computer with the fast data acquisition system of a time-of-flight mass spectrometer
[NASA-CR-177474] N88-27798
SERI standard broadband format: A solar and meteorological data archival format
[DE88-001145] N88-27975
DATA BASE MANAGEMENT SYSTEMS
Space shuttle phase B wind tunnel model and test information. Volume 2: Orbiter configuration
[NASA-CR-178415-VOL-2-PT-2] N88-27172
Database design and management in engineering optimization
[AD-A193325] N88-27813
Developing a connector selection DBMS (database management system) using NIAM (Nijssen's Information Analysis Methodology)
[DE88-008110] N88-27972
Pattern information processing and multimedia database system: Current research on multimedia information system
[PB88-131917] N88-27973
Sources and nature of cost analysis data base reference manual
[AD-A193099] N88-27976
DATA BASES
Automatic line network extraction from aerial imagery of urban areas through knowledge based image analysis
[AD-A193067] N88-27615
National air toxics information clearinghouse: NATICH data base users guide for data viewing, February 1988
[PB88-197470] N88-27645
Space shuttle natural environment analysis
[NASA-CR-179337] N88-27676
A PRELUDE (analysis and design of control systems-preliminary utilities depository). A data-based interactive system of control software, user's guid e
[DFVLR-MITT-88-12] N88-27795
Basic database operations on the butterfly parallel processor: Experiment results
[AD-A193199] N88-27804
Capitalizing on experience with intelligence gateway software
[AD-A193362] N88-27971
DATA COMPRESSION
Optical interconnections for digital image coding N88-27381
DATA FLOW ANALYSIS
Finding minimum-cost circulations by canceling negative cycles
[AD-A192727] N88-27825
DATA LINKS
Model for dynamically structured communicating systems
[PB88-105283] N88-27402
DATA MANAGEMENT
A PRELUDE (analysis and design of control systems-preliminary utilities depository). A data-based interactive system of control software, user's guid e
[DFVLR-MITT-88-12] N88-27795
DATA PROCESSING
Supercomputer for parallel data analysis
[DE88-702148] N88-27759
A programmable systolic array for factorial analysis. Part 2: The symmetric eigenvalue problem
[AD-A192396] N88-27762
Issues in computer-assisted interpretation of graphs and quantitative information
[PB88-116280] N88-27783
Basic database operations on the butterfly parallel processor: Experiment results
[AD-A193199] N88-27804
Analysis of lower hybrid current drive and rampup experiments on the JT-60 tokamak
[DE88-753136] N88-27915
Pattern information processing and multimedia database system: Current research on multimedia information system
[PB88-131917] N88-27973
DATA REDUCTION
Comparison of experimental rotor damping data-reduction techniques N88-27159
Calibration and data reduction techniques for the AFGL infrared array spectrometer N88-27374
DATA RETRIEVAL
Retrieval of temperature and concentration profiles from a limited number of absorption measurements N88-27501
DATA STORAGE
Use of optical disk technology at the Air Command and Staff College
[AD-A192424] N88-27969
DATA TRANSMISSION
A VLSI single-chip (225,223) Reed-Solomon encoder with interleaver
[NASA-CASE-NPO-17280-1-CU] N88-27220
DEBRIS
Analysis of debris from accelerated life test of the Hughes five-year Vuilleumier cryocooler
[AD-A193101] N88-27400
DECAY
Study of energy levels and decay mechanisms for singlet Rydberg states of molecular nitrogen
[AD-A192505] N88-27886
DECISION MAKING
The integration of decision support problems into feature modeling based design N88-27372
Linear programming for Air Force decision aiding N88-27378
Future SDI (Strategic Defense Initiative) decision making
[AD-A192794] N88-27860
Rules, schema and decision making
[AD-A193389] N88-27967
DECOMPOSITION
Manufacturing of a barium titanate with high dielectric coefficient by decomposition of precipitates of double oxalates
[ISAL-IDI1-88-02] N88-27278
Coherent structures in the axisymmetric turbulent jet mixing layer N88-27504
A study on Lebesgue decomposition of measures induced by stable processes
[AD-A192893] N88-27850
DEFECTS
NDE performance in predicting failure strength of spherical composite specimens with implanted flaws
[DE88-008223] N88-27575
Critical issues and directions for fracture mechanics and structural integrity
[AD-A193050] N88-27584
Probing the electronic and defect structure of perovskite superconductors
[DE88-008349] N88-27939
DEFENSE PROGRAM
Overview of the SDI (Strategic Defense Initiative) Program in short wavelength chemical lasers
[DE88-007912] N88-27861
DEFLAGRATION
Deformation, fracture and explosive properties of reactive materials
[AD-A193080] N88-27348
DEFORMATION
Diffusion and solubility of some interstitial impurities in deformed metals
[DE88-701859] N88-27296
Slew-induced deformations in a space-based electromagnetic rail gun N88-27385
Development of a biaxial test system for thin-walled metal tubes using tensile-compressive axial load and internal-external pressure
[DE88-011279] N88-27592
DYNA3D (Nonlinear Dynamic Analysis of Structures in Three Dimensions) user's manual
[DE88-012242] N88-27604
DEGRADATION
Predicting optical degradation of a laser beam through a turbulent shear layer N88-27376
DEGREES OF FREEDOM
The VITE model: A neutral command circuit for a generating arm and articulator trajectories
[AD-A192715] N88-27734
DELAMINATING
Failure analysis of laminated composite angles N88-27578
DELTA WINGS
Flow around a delta wing with or without a canard control surface (phi BA = 60 deg). Part 1: Hydrodynamic visualization in permanent regime
[ONERA-RT-10/2891-AN-101-A-PT-1] N88-27170
An experimental study of the effect of pitch rate on delta wing aerodynamics and stability
[NASA-CR-183159] N88-27173
Optimal control of the wing rock phenomenon N88-27373
DEMODULATION
Demodulation processes in auditory perception
[AD-A193421] N88-27740

DEMOGRAPHY
Behavioral, psychological and demographic predictors of physical fitness
[AD-A192697] N88-27733
DENDRITIC CRYSTALS
Survey of the literature on fractals with possible applications to phase change processes
[DE88-012240] N88-27277
DENSE PLASMAS
The influence of ionization within a plasma opening switch
[AD-A193147] N88-27906
DENSITY (MASS/VOLUME)
Injection compression for short fiber reinforced plastics
[SNIAS-881-430-118] N88-27344
A theoretical determination of the density at a traveling source that emitts particles
[ISAS-RN-351] N88-27883
DEOXYRIBONUCLEIC ACID
Calculation of far infrared absorption in B poly(dA).poly(dT)
[AD-A193128] N88-27318
DEPENDENCE
Dependence effects in unique signal transmission
[DE88-010331] N88-27419
DEPOSITION
Carbon deposition model for oxygen-hydrocarbon combustion, volume 1
[NASA-CR-179375] N88-27254
Carbon deposition model for oxygen-hydrocarbon combustion, volume 2
[NASA-CR-179376] N88-27255
Amorphous silicon solar cells using a metal substrate
[PB88-131941] N88-27628
Foliar nitrate reductase: A marker for assimilation of atmospheric nitrogen oxides
[DE88-010453] N88-27648
Atomic layer epitaxy of ZnS and ZnSe
[AD-A192307] N88-27928
DEPTH
MIZPAC (marginal ice zone Pacific) 84-86 CTD (Conductivity, Temperature, Depth) data report
[AD-A192478] N88-27679
DESIGN ANALYSIS
Programs for preliminary design of composite materials which were developed by the design group of Aerospatiale Aquitaine
[SNIAS-881-430-112] N88-27251
Estimation of power-energy plots for secondary batteries
[DE88-011922] N88-27460
Optimization of planetary gears
[ETN-88-92375] N88-27573
Modal testing in the design evaluation of wind turbines
[DE88-010374] N88-27632
Magnetic heat pumps
[DE88-012058] N88-27639
Computer simulation procedure for designing airborne aeromeiric monitoring programs
[DE88-011896] N88-27674
DETECTION
The P delta V fundamental gas leak calibration system qualification report
[DE88-008964] N88-27526
The detection and interpretation of long-term changes in ozone from space
[NASA-TM-101135] N88-27650
DETONATION
A concept for an electro-optic explosive device
[DE88-009696] N88-27349
DETONATION WAVES
Shock initiation studies on heterogeneous explosives
[DE88-008681] N88-27351
DETONATORS
A concept for an electro-optic explosive device
[DE88-009696] N88-27349
DIAGNOSIS
Laser probes and numerical modeling as process diagnostics in chemical vapor deposition
[DE88-011622] N88-27275
DIAMETERS
Hole diameters in plates impacted by projectiles N88-27386
DIELECTRIC POLARIZATION
Field-aligned structure of the storm time Pc 5 wave of November 14-15, 1979
[AD-A193022] N88-27653
DIELECTRIC PROPERTIES
Manufacturing of a barium titanate with high dielectric coefficient by decomposition of precipitates of double oxalates
[ISAL-IDI1-88-02] N88-27278
Processing and additive effects of ZrO2 on microstructure and dielectric porperties of BaTiO3 ceramics
[AD-A193126] N88-27316
Surface-wave model uncertainty assessment
[AD-A193094] N88-27408
DIELECTRICS
Processing and additive effects of ZrO2 on microstructure and dielectric porperties of BaTiO3 ceramics
[AD-A193126] N88-27316
Preparation and properties of high Q microwave dielectrics in the (CA, SR, BA) zirconate system
[AD-A193127] N88-27317
Effects of surface tension and contact angle on sensible heating and boiling incipience in dielectric falling films
[DE88-007057] N88-27492
Measurement of the thermal conductivity of dielectric thin solid films with a thermal comparator
[DE88-008468] N88-27898
DIESEL ENGINES
Documentation of the Benson Diesel Engine Simulation Program
[NASA-TM-100940] N88-27201
Ceramic technology for advanced heat engines project
[DE88-008945] N88-27323
The 210-HP diesel engine endurance and performance testing with fire resistant diesel fuel
[AD-A193153] N88-27558
Basic mechanisms of diesel lubrication correlation of bench and engine tests
[AD-A193360] N88-27561
Ethanol as a fuel of a lorry. Use experience from a diesel engine modified to an otto engine
[DE88-752870] N88-27569
DIESEL FUELS
Effects of ceramic surfaces on autoignition in a constant volume combustion apparatus
[AD-A193055] N88-27266
A study relating to the fog oil replacement program
[AD-A192536] N88-27347
The 210-HP diesel engine endurance and performance testing with fire resistant diesel fuel
[AD-A193153] N88-27558
DIFFERENCE EQUATIONS
Effects of numerical dissipation on finite-volume solutions of compressible flow problems
[AD-A193173] N88-27485
DIFFERENTIAL EQUATIONS
A Wong-Zakai type theorem for certain discontinuous semimartingales
[AD-A192713] N88-27822
KRYSI, an ODE solver combining a semi-implicit Runge-Kutta method and a preconditioned Krylov method
[DE88-012245] N88-27841
DIFFERENTIAL GEOMETRY
Applications of differential geometry to the shape analysis of gray-value images N88-27358
DIFFRACTION
Are Centauros diffractive
[DE88-008767] N88-27996
DIFFUSION
Simulation of moisture diffusion of fiber reinforced components of aircraft for general air transportation
[IFL-IB-87-05] N88-27253
Diffusion and solubility of some interstitial impurities in deformed metals
[DE88-701859] N88-27296
The diffusion of vorticity from a plane boundary
[AD-A192706] N88-27474
Diffusion models of crack growth due to random overloads
[DE88-008811] N88-27595
Large-eddy simulations of concentration fluctuations
[DE88-009480] N88-27660
DIFFUSION FLAMES
The structure and stability of nonpremixed gas jet flames N88-27257
A study of the interaction of diffusion flames with a vortex pair flowfield N88-27258
Experimental research of combustion systems N88-27371
DIGITAL DATA
Space shuttle phase B wind tunnel model and test information. Volume 2: Orbiter configuration
[NASA-CR-178415-VOL-2-PT-2] N88-27172
Optical interconnections for digital image coding N88-27381
Analysis of remotely sensed imagery using digital morphology
[AD-A192738] N88-27614
DIGITAL FILTERS
A numerically efficient digital matched filter for periodic and windowed periodic radar waveforms
[AD-A193132] N88-27410
DIGITAL SIMULATION
Robust digital model following controller for helicopters
[DFVLR-FB-88-07] N88-27203
DIGITAL SYSTEMS
Development of a hybrid simulator for robotic manipulators
[AD-A193119] N88-27557
DIODES
Silicon-on-insulator pin diodes
[AD-A193359] N88-27445
Techniques and instrumentation for transient characterization of metal-insulator-semiconductor diodes. Applications to metal-insulator InP system
[ECL-87-17] N88-27959
DIRECTIONAL ANTENNAS
Sidelobe level of an adaptive array using the SMI (Sampled Matrix Inversion) algorithm
[AD-A193131] N88-27409
DIRECTIONAL CONTROL
Compliant robotic structures, part 3
[AD-A192426] N88-27556
DIRECTORIES
Federal Council on Science, Engineering and Technology: Committee on Computer Research and Applications, Subcommittee on Science and Engineering Computing: The US Supercomputer Industry
[DE88-011262] N88-27756
DISCONTINUITY
A Wong-Zakai type theorem for certain discontinuous semimartingales
[AD-A192713] N88-27822
DISCRIMINATORS
Rules, schema and decision making
[AD-A193389] N88-27967
DISKS
Kinetic theory for plane flows of rough, inelastic, circular disks N88-27499
DISORDERS
Normative developmental equations for the EEG and their sensitivity to neurological and psychiatric disorders N88-27687
DISPERSING
Prediction of regional pollutant dispersion using a nested-grid, three-dimensional numerical model N88-27649
Measuring dispersion effects of factors in factorial experiments
[AD-A193216] N88-27831
DISPERSION
A zoomable and adaptable hidden fine-mesh approach to solving advection-dispersion equations
[DE88-006174] N88-27816
DISPERSIONS
Preparation and characterization of ceramic materials based on Al2O3 reinforced with a ZrO2 dispersion
[ISAL-87-0041] N88-27340
DISPLAY DEVICES
An evaluation of flight path formats head-up and head-down
[NASA-CR-4176] N88-27196
The effect of input device on user performance with a menu-based natural language interface
[AD-A193095] N88-27772
DISSOCIATION
Theory of the dissociation dynamics of small molecules on metal surfaces: Finite temperature studies
[DE88-007763] N88-27882
DISTILLATION
Vapor Compression Distillation Subsystem (VCDS) component enhancement, testing and expert fault diagnostics development, volume 2
[NASA-CR-172076] N88-27755
DISTORTION
Analytical approximation of a distorted reflector surface defined by a discrete set of points
[NASA-TM-101323] N88-27424
A Navier-Stokes study of cascade flow fields including inlet distortion and rotating stall
[AD-A193109] N88-27483
Effects of pulsed and CW (Continuous Wave) 2450 MHz radiation on transformation and chromosomes of human lymphocytes in vitro
[AD-A193104] N88-27736
Distortion functions
[DE88-752634] N88-27896
DISTRIBUTED PROCESSING
Computational fluid dynamics on parallel processors
[AD-A192397] N88-27469
Distributed algorithms for probabilistic solution of computational vision problems
[AD-A193150] N88-27773

A menu-driven menu editor and associated menu system
[DE88-008026] N88-27781
Constructing a highly-available location service for a distributed environment
[AD-A192723] N88-27801
DISTRIBUTION FUNCTIONS
Moment approach to neoclassical flows, currents and transport in auxiliary heated tokamaks
[DE88-008024] N88-27901
Analysis of lower hybrid current drive and rampup experiments on the JT-60 tokamak
[DE88-753136] N88-27915
Equilibrium distribution functions for limited plasma-molecular systems
[DE88-702412] N88-27916
DIVERTERS
Design of divertor plate and measurements of double-null open divertor plasma in the JFT-2M tokamak
[DE88-753130] N88-27914
DOCUMENTATION
Documentation of the Benson Diesel Engine Simulation Program
[NASA-TM-100940] N88-27201
Engineering data compendium. Human perception and performance. User's guide
[LC-87-19560] N88-27749
DOCUMENTS
Publications on acoustics research at the Langley Research Center during 1980-1986
[NASA-TM-100590] N88-27881
DOMAINS
Spatial organization of homopolymer chains inside spherical polybutadiene domains of SB diblock copolymers
[AD-A193390] N88-27321
DOPES
Numerical calculations of dopent diffusion involving flashlamp heating of silicon N88-27384
DOPPLER EFFECT
Radar information from the partial derivatives of the echo signal phase from a point scatterer
[AD-A193402] N88-27415
Is the 3C273 quasar Mach nearer
[DE88-702235] N88-27988
DOPPLER RADAR
TDWR (Terminal Doppler Weather Radar) PRF (Pulse Repetition Frequency) selection criteria
[AD-A193089] N88-27407
Definition of long ocean wave slope for radar applications
[AD-A193198] N88-27412
DOWNLINKING
A VLSI single-chip (225,223) Reed-Solomon encoder with interleaver
[NASA-CASE-NPO-17280-1-CU] N88-27220
DRAG REDUCTION
Investigations on drag reduction in turbulent pipe flows by addition of ionic and nonionic high polymers
[ETN-88-92360] N88-27515
DROP SIZE
Experimental research of combustion systems N88-27371
Cloud simulation warm cloud experiments: Droplet growth and aerosol scavenging
[AD-A192944] N88-27666
DROPS (LIQUIDS)
Numerical simulation of fuel droplet interactions and breakup
[AD-A192431] N88-27470
DRUGS
Measurement and classification of the mode of action of antidepressant drugs N88-27714
Measurement of electrical activity in the CNS with cortical evoked potentials and EEG: Efficacy profiles of drugs using factor analysis N88-27715
An approach to studying the effects of psychostimulants on cerebral electrical activity in the non-human primate N88-27716
DRY HEAT
Geothermal energy technology: Issues, R and D (Research and Development) and cooperative arrangements
[PB88-193107] N88-27626
DRYING
Ellipsometric imaging of drying sol-gel films
[DE88-011785] N88-27335
DUCTED FANS
Airborne remote operated device
[DE88-010324] N88-27188
DUCTILITY
Microchemical analysis of polycrystalline Ni3Al and other ordered alloys using the field-ion microscope atom probe
[DE88-011519] N88-27294
Plastic yielding at crack tips
[AD-A192549] N88-27582
DYADICS
Statistical analysis of dyadic stationary processes
[AD-A193057] N88-27853
DYE LASERS
A plasma ultraviolet source for short wavelength lasers
[AD-A192844] N88-27537
DYNAMIC CHARACTERISTICS
Numerical simulation of fuel droplet interactions and breakup
[AD-A192431] N88-27470
Coupled experimental and theoretical investigations of instability, chaos and turbulence in an axisymmetric jet flow
[AD-A192943] N88-27476
An analysis of horizontal temperature gradients and heat content in the mixed layer and the surface forcing during PATCHEX
[AD-A192330] N88-27678
Research in applied mathematics
[AD-A192365] N88-27820
DYNAMIC CONTROL
A method for reducing the coning of a spinning vehicle
[DE88-010971] N88-27189
Development of a hybrid simulator for robotic manipulators
[AD-A193119] N88-27557
Vibration control of large structures
[AD-A193317] N88-27587
DYNAMIC LOADS
Diffusion models of crack growth due to random overloads
[DE88-006811] N88-27595
Modal testing in the design evaluation of wind turbines
[DE88-010374] N88-27632
DYNAMIC MODELS
Dynamic modelling and estimation of the error due to asynchronism in a redundant asynchronous multiprocessor system
[NASA-CR-177427] N88-27205
Control of free-flying space robot manipulator systems
[NASA-CR-183017] N88-27562
DYNAMIC RESPONSE
AGARD standard aeroelastic configurations for dynamic response. 1: Wing 445.6
[AGARD-R-765] N88-27193
The robust tracking control of nonlinear systems with uncertain dynamics N88-27788
Self-energies and the interactions of particles with surfaces
[DE88-010451] N88-27885
DYNAMIC STABILITY
Optimal rheological characteristics in dynamic stability of polymer flow through porous media
[DE88-001225] N88-27322
Application of the Single-Axis rate Table (SAT) of the DFVLR for the evaluation of stationary and dynamic gyro properties
[DFVLR-MITT-88-09] N88-27533
Dynamic stability of elastic rotor-bearing systems via Liapunov's direct method N88-27571
DYNAMIC STRUCTURAL ANALYSIS
Vibration control of large structures
[AD-A193317] N88-27587
DYNA3D (Nonlinear Dynamic Analysis of Structures in Three Dimensions) user's manual
[DE88-012242] N88-27604
DYNAMIC TESTS
Hybrid procedure for dynamic measurements in transonic wind tunnels: Demonstrated by pitch oscillation
[DFVLR-FB-88-19] N88-27211
Soviet dynamic fracture mechanics research
[FASAC-TAR-3140] N88-27597
DYNAMICAL SYSTEMS
Dynamical evolution of cosmic strings
[DE88-011724] N88-27989

E

EAR
Assessment of cochlear damage after microwave irradiation
[AD-A193237] N88-27737
EARTH ATMOSPHERE
Multifilter spectrometer (FEB) for microwave atmospheric sounder
[AD-A192312] N88-27426
Activities report of the Institute for Extraterrestrial Physics
[MPE-206] N88-27981
EARTH IONOSPHERE
On the dynamics of the auroral ionosphere during the breakup of a substorm
[AD-A193368] N88-27657
EARTH MAGNETOSPHERE
MAXIE-1 (Magnetospheric Atmospheric X-ray Imaging Experiment)
[AD-A192846] N88-27221
Field-aligned structure of the storm time Pc 5 wave of November 14-15, 1979
[AD-A193022] N88-27653
The low-latitude auroral boundary: Steady-state and time-dependent representations
[AD-A193200] N88-27656
Solar flares and magnetospheric particles: Investigations based upon the ONR-602 and ONR-604 experiments
[AD-A193396] N88-27994
EARTH MANTLE
Time-dependent thermal convection of Earth mantle and double diffusive convection in magma chambers
[MITT-52] N88-27663
EARTH MOVEMENTS
Stochastic geologic effects on near-field ground motions in alluvium
[AD-A192315] N88-27652
EARTH OBSERVATIONS (FROM SPACE)
The detection and interpretation of long-term changes in ozone from space
[NASA-TM-101135] N88-27850
EARTH ROTATION
Basic research for the geodynamics program
[NASA-CR-183149] N88-27662
ECHOES
Radar information from the partial derivatives of the echo signal phase from a point scatterer
[AD-A193402] N88-27415
ECONOMIC IMPACT
Economic impact of space flight activities in West Germany. Influence of allocations of Bundesministerium fuer Forschung und Technologie
[ETN-88-92106] N88-27215
EDGE LOADING
FEB (Multifilter Electronics Box) lifting device analysis, revision A
[AD-A192313] N88-27427
EDUCATION
United States Air Force Graduate Student Summer Support Program, volume 2
[AD-A191122] N88-27355
Can CNV amplitude predict ability to accomplish a demanding task? N88-27700
EFFICIENCY
Efficiency optimization for FEL oscillators
[AD-A192541] N88-27536
EJECTION
Ejection situations in the U-2/TR-1: An analysis of emotions and events
[AD-A192872] N88-27175
ELASTIC BENDING
Compliant robotic structures, part 3
[AD-A192426] N88-27556
ELASTIC BODIES
Dynamic stability of elastic rotor-bearing systems via Liapunov's direct method N88-27571
ELASTIC DEFORMATION
Critical issues and directions for fracture mechanics and structural integrity
[AD-A193050] N88-27584
ELASTIC MEDIA
A numerical treatment of the fluid/elastic interface under range-dependent environments
[AD-A192476] N88-27821
ELASTIC PROPERTIES
Characterization of elastic-plastic properties of AS4/APC-2 thermoplastic composite
[NASA-CR-183145] N88-27242
An IETS (Inelastic Electron Tunneling Spectroscopy) study of surface reactions applicable to adhesion
[AD-A192274] N88-27261
Computer simulation of elastic properties of grain boundary materials
[DE88-011965] N88-27305
Ionic conductive polymers based on crosslinked elastic siloxane-ethylene oxide copolymers
[DE88-011243] N88-27311
Three-dimensional aspects of fatigue crack closure
[AD-A192296] N88-27581
ELASTIC SCATTERING
Are Centauros diffractive
[DE88-008767] N88-27996
ELASTOPLASTICITY
A comparison of analytical techniques for modeling the Rayleigh-Taylor response of elastic-plastic solids
[DE88-010372] N88-27596
ELECTRIC AUTOMOBILES
Metal-air battery assessment
[DE88-011361] N88-27459
ELECTRIC BATTERIES
High power pulse energy system concept
[AD-A192440] N88-27429

Preparation and development of advanced battery catalysts
[AD-A193208] N88-27441
Estimation of power-energy plots for secondary batteries
[DE88-011922] N88-27460

ELECTRIC CHARGE
Results from life test in progress on eagle-picher nickel cadmium cells
[AD-A192816] N88-27434
Discrete variational methods and their application to electronic structures
[DE88-702215] N88-27888

ELECTRIC CONDUCTORS
Determination of quantum corrections for electrical conductivity mechanism of three dimensional, perturbed copper coatings. Weak localization and electron-electron interaction
[ETN-88-92378] N88-27466

ELECTRIC CONTACTS
Friction, wear and electrical contact resistance of precious metal alloys
[DE88-011244] N88-27450

ELECTRIC DISCHARGES
Failure analysis of Chloride Silent Power, Ltd. PB cells
[DE88-010567] N88-27448
Production of intensive electron beam impulsions by setup of pseudoglare discharges
[ISL-CO-210/87] N88-27920

ELECTRIC FIELDS
Electric and Magnetic Activity of the Central Nervous System: Research and Clinical Applications in Aerospace Medicine
[AGARD-CP-432] N88-27683
Electric and magnetic brain activity related to cognitive performance N88-27692
Staggered-grid finite element solution technique for the Maxwell's equations in the time domain
[DE88-011731] N88-27838
On plasma stability under anisotropic random electric field influence
[DE88-702422] N88-27918
Measurement of macroscopic electric fields in solar plasma structures
[AD-A193291] N88-27993

ELECTRIC NETWORKS
Some equivalent circuit models for AC impedance analysis of pyrite/solution interface
[DE88-010574] N88-27452

ELECTRIC POTENTIAL
A planar IC-compatible transferred electron device for millimeter-wave operation
[AD-A192692] N88-27433
Results from life test in progress on eagle-picher nickel cadmium cells
[AD-A192816] N88-27434
Studies of the intact human brain: Implications for performance N88-27684
Dissecting the visual and auditory pathways by means of the two-input technique N88-27690
Event-related brain potentials as indices of mental workload and attentional allocation N88-27696
Using ERPS to study human information processing N88-27698

ELECTRICAL PROPERTIES
Investigations on the MBE (Molecular Beam Epitaxy) growth and properties of Al(sub y)Ga(sub y)In(sub 1-x-y)AsInP and InGaAs-InAlAs superlattices
[DE88-009105] N88-27941

ELECTRICAL RESISTANCE
A critical review of IR drops and electrode potentials within pits, crevices and cracks
[AD-A192481] N88-27431
Friction, wear and electrical contact resistance of precious metal alloys
[DE88-011244] N88-27450
Conductivity mechanism and operating behavior of electrically conductive adhesives on the example of a power transistor
[ETN-88-92355] N88-27464

ELECTRICAL RESISTIVITY
On the electrical properties of carbon/carbon composites densified by chemical deposit in vapor phase
[SNIAS-881-430-117] N88-27252
Thermal cycling tests on surface-mount assemblies
[DE88-007695] N88-27453
Conductivity mechanism and operating behavior of electrically conductive adhesives on the example of a power transistor
[ETN-88-92355] N88-27464
Determination of quantum corrections for electrical conductivity mechanism of three dimensional, perturbed copper coatings. Weak localization and electron-electron interaction
[ETN-88-92378] N88-27466
MIZPAC (marginal ice zone Pacific) 84-86 CTD (Conductivity, Temperature, Depth) data report
[AD-A192478] N88-27679
A resistive-film based force transducer for the study of exercise
[AD-A192601] N88-27730

ELECTRO-OPTICS
A concept for an electro-optic explosive device
[DE88-009696] N88-27349
Picosecond optoelectronic sampling of electrical waveforms produced by an optically excited field effect transistor
[AD-A192384] N88-27428
Solar cell modeling and simulation
[AD-A193249] N88-27620
Molecular beam epitaxy of GaP films on Si substrates
[PB88-131974] N88-27923

ELECTROCHEMICAL CELLS
Preparation and development of advanced battery catalysts
[AD-A193208] N88-27441

ELECTROCHEMICAL OXIDATION
Studies in support of oxidation-resistant composite materials
[AD-A193320] N88-27238

ELECTROCHEMISTRY
High power pulse energy system concept
[AD-A192440] N88-27429
Corrosion fatigue of small cracks: Mechanics and chemistry
[DE88-012121] N88-27605
Advanced EMU electrochemically regenerable CO2 and moisture absorber module breadboard
[NASA-CR-172054] N88-27754

ELECTRODES
A critical review of IR drops and electrode potentials within pits, crevices and cracks
[AD-A192481] N88-27431
The kinetics of charge-transfer reactions on passive lithium electrodes
[DE88-009256] N88-27454
Metal-air battery assessment
[DE88-011361] N88-27459
Post-test observations on CSPL (Chloride Silent Power Limited) cells
[DE88-011975] N88-27461
Monolithic fuel cells
[DE88-012004] N88-27638

ELECTROENCEPHALOGRAPHY
Physiological monitoring methodology in the USAFSAM centrifuge N88-27356
Normative developmental equations for the EEG and their sensitivity to neurological and psychiatric disorders N88-27687
The application of non-stationary data analysis techniques in the identification of changes in the electroencephalogram associated with the onset of drowsiness N88-27688
A statistical procedure for the evaluation of presence/non-presence of stimulus-related EEG activity N88-27689
The effect of endogenous alpha on hemispheric asymmetries and the relationship of frontal theta to sustained attention N88-27701
Evoked potential analysis of impact acceleration experiments N88-27708
EEG indices of G-induced Loss Of Consciousness (G-LOC) N88-27709
Electroencephalographic correlates of pilot performance: Simulation and in-flight studies N88-27711
Measurement of electrical activity in the CNS with cortical evoked potentials and EEG: Efficacy profiles of drugs using factor analysis N88-27715
An approach to studying the effects of psychostimulants on cerebral electrical activity in the non-human primate N88-27716
Correlation between EEG abnormal activity and aircraft accidents: A long term observation N88-27719
Detection of latent epilepsy in aircrew candidates N88-27720

ELECTROLYTES
Characterization of crystalline silicon by electrochemical and Raman spectroscopy at the frontier semiconductor/electrolyte
[ETN-88-92354] N88-27956

ELECTROLYTIC CELLS
Preparation and development of advanced battery catalysts
[AD-A193208] N88-27441
Estimation of power-energy plots for secondary batteries
[DE88-011922] N88-27460

ELECTROMAGNETIC ABSORPTION
Diode laser ignition of high explosives and pyrotechnics
[DE88-008771] N88-27352

ELECTROMAGNETIC FIELDS
Electromagnetic characterization and acceptance test of the EMP simulator SPERANS
[PB88-203781] N88-27416

ELECTROMAGNETIC PROPERTIES
Preparation and properties of high Q microwave dielectrics in the (CA, SR, BA) zirconate system
[AD-A193127] N88-27317

ELECTROMAGNETIC PULSES
Electromagnetic characterization and acceptance test of the EMP simulator SPERANS
[PB88-203781] N88-27416
Picosecond optoelectronic sampling of electrical waveforms produced by an optically excited field effect transistor
[AD-A192384] N88-27428
A GaAs solid state device model for high power applications
[DE88-011320] N88-27457
Direct measurement of solids: High temperature sensing. Experimental development and testing of high temperature pulsed EMATs
[DE88-009859] N88-27546
Wave equations for pulse propagation
[DE88-011760] N88-27548

ELECTROMAGNETIC WAVE FILTERS
A notch filter instrument for measuring ELF (Extremely Low Frequency) MSK (Minimum Shift Keying) signals
[AD-A193324] N88-27414

ELECTROMAGNETIC WAVE TRANSMISSION
Airborne measurement of low frequency atmospheric noise ALFAN 1
[AD-A193056] N88-27405
SARLAC: A relativistic electron beam code
[AD-A193134] N88-27411
Staggered-grid finite element solution technique for the Maxwell's equations in the time domain
[DE88-011731] N88-27838
Propagation of charged particle beams in the atmosphere
[AD-A193185] N88-27887
Electromagnetic wave incoherent reflection by a half-space of weakly-ionized plasma with an absorbing boundary
[DE88-702413] N88-27917

ELECTRON BEAMS
High-speed, precision processing using an electron beam N88-27391
Equipment for an advanced electron beam lithography system
[AD-A192956] N88-27435
Optical guiding in the separable beam limit
[AD-A192452] N88-27534
Production of intensive electron beam impulsions by setup of pseudoglare discharges
[ISL-CO-210/87] N88-27920

ELECTRON DENSITY (CONCENTRATION)
Optical guiding in the separable beam limit
[AD-A192452] N88-27534
Approximate analytical formulae for electron density and collision frequency in the natural and nuclear-disturbed ionosphere and inner magnetosphere
[AD-A193129] N88-27654
A study of tunneling phenomena in gallium arsenide-aluminum gallium arsenide heterostructures N88-27946

ELECTRON DISTRIBUTION
Initial electron distributions for free-electron lasers generated by injector and accelerator simulations
[DE88-007022] N88-27540

ELECTRON ENERGY
Studying the physics and operation of multi-terminal near-micron and sub-micron length, hot electron semiconductor devices
[AD-A193380] N88-27446
A study of tunneling phenomena in gallium arsenide-aluminum gallium arsenide heterostructures N88-27946

ELECTRON MICROSCOPES
Equipment for an advanced electron beam lithography system
[AD-A192956] N88-27435

ELECTRON MOBILITY
A GaAs solid state device model for high power applications
[DE88-011320] N88-27457

ELECTRON PARAMAGNETIC RESONANCE
Structure and function of the manganese complex involved in photosynthetic oxygen evolution determined by X-ray adsorption spectroscopy and electron paramagnetic resonance spectroscopy
[DE88-010360] N88-27725

Paramagnetic point defects in boron-implanted HgO.7CdO.3Te
[AD-A193276] N88-27934
ELECTRON PHONON INTERACTIONS
Anharmonic model for high-Tc superconductors
[DE88-702196] N88-27924
ELECTRON PRECIPITATION
Investigation of the potential impact of new photonic materials on optical processing systems N88-27359
The low-latitude auroral boundary: Steady-state and time-dependent representations
[AD-A193200] N88-27656
ELECTRON SCATTERING
Inelastic electron scattering and electron-hole excitations in iron and nickel
[DE88-011843] N88-27303
Nonlinear dynamics of the electron self-field interaction
[DE88-010597] N88-27420
Self energy corrections to the ab initio band structures: Chromium
[DE88-701825] N88-27927
ELECTRON SOURCES
Optical guiding in the separable beam limit
[AD-A192452] N88-27534
ELECTRON SPECTROSCOPY
An IETS (Inelastic Electron Tunneling Spectroscopy) study of surface reactions applicable to adhesion
[AD-A192274] N88-27261
Application of Auger electron spectroscopy to the study of trace element effects on weldability
[DE88-010457] N88-27301
ELECTRON TRANSFER
Factors governing light driven electron and proton translocation in proteins across membranes
[DE88-011120] N88-27724
ELECTRON TUNNELING
An IETS (Inelastic Electron Tunneling Spectroscopy) study of surface reactions applicable to adhesion
[AD-A192274] N88-27261
Solar energy conversion through the interaction of plasmons with tunnel junctions. Part A: Solar cell analysis. Part B: Photoconductor analysis
[NASA-CR-183044] N88-27621
A study of tunneling phenomena in gallium arsenide-aluminum gallium arsenide heterostructures N88-27946
ELECTRONIC COUNTERMEASURES
Computation of ECM (Electronic Counter-Measures) war reserve materiel spare requirements
[AD-A193301] N88-27195
Sidelobe level of an adaptive array using the SMI (Sampled Matrix Inversion) algorithm
[AD-A193131] N88-27409
ELECTRONIC EQUIPMENT
Investigation of expert system design approaches for electronic design environments N88-27365
A method for estimating the susceptibility of electronic systems to HPM (High Power Microwave)
[DE88-012246] N88-27422
FEB (Multifilter Electronics Box) lifting device analysis, revision A
[AD-A192313] N88-27427
Equipment for an advanced electron beam lithography system
[AD-A192956] N88-27435
ELECTRONIC EQUIPMENT TESTS
RLE progress report, January 1 to December 31, 1987
[RLE-PR-130] N88-27869
ELECTRONS
Nonlinear dynamics of the electron self-field interaction
[DE88-010597] N88-27420
Theory and simulation of relaxed plasmoids
[AD-A192884] N88-27997
ELECTROPHOTOMETRY
Surface photometric investigations for spiral galaxies of large dimension structures in edge-on gametry
[ETN-88-92126] N88-27965
ELECTROPHYSIOLOGY
Electric and Magnetic Activity of the Central Nervous System: Research and Clinical Applications in Aerospace Medicine
[AGARD-CP-432] N88-27683
Normative developmental equations for the EEG and their sensitivity to neurological and psychiatric disorders N88-27687
The application of non-stationary data analysis techniques in the identification of changes in the electroencephalogram associated with the onset of drowsiness N88-27688
A statistical procedure for the evaluation of presence/non-presence of stimulus-related EEG activity N88-27689
Electric and magnetic brain activity related to cognitive performance N88-27692
Cognitive task demands as reflected in physiological measures N88-27699
The effect of endogenous alpha on hemispheric asymmetries and the relationship of frontal theta to sustained attention N88-27701
Psychophysiological measures of drowsiness as estimators of mental fatigue and performance degradation during sleep deprivation N88-27702
Fighter pilot performance during airborne and simulator missions: Physiological comparisons N88-27704
Event-related and steady potential changes in the brain related to workload during tracking N88-27705
The neuroelectric selection of Naval aviation personnel: An evaluation N88-27707
An approach to studying the effects of psychostimulants on cerebral electrical activity in the non-human primate N88-27716
Relation between VEP and visual function in lesions of the optic nerve and visual pathway N88-27718
The auditory evoked response in military pilots N88-27721
ELECTRORETINOGRAPHY
Microesotropia patients performa well as military jet pilots N88-27383
ELECTROSTATICS
Meaning of energy diagrams used to describe hetero-structures
[DE88-702219] N88-27943
ELEMENTARY PARTICLE INTERACTIONS
Activities report of the Werner-Heisenberg Institute of Physics
[ETN-88-92946] N88-27893
ELLIPSOMETERS
Ellipsometric imaging of drying sol-gel films
[DE88-011785] N88-27335
ELLIPTIC DIFFERENTIAL EQUATIONS
Unified multilevel adaptive finite element methods for elliptic problems
[DE88-011938] N88-27840
EMBEDDED COMPUTER SYSTEMS
MINIAC: A small embedded computer
[DE88-008142] N88-27757
An optical 2-dimensional correlator for pattern recognition in embedded computing
[DE88-007196] N88-27780
EMERGENCIES
IEMIS (Integrated Emergency Management Information System) floodplain mapping based on a LIDAR derived data set
[AD-A193071] N88-27616
Cockpit and cabin crew coordination
[AD-A192445] N88-27752
EMISSION
Radiative heat transfer and selective emission in planar slab coatings on hot emissive substrates
[AD-A193133] N88-27319
EMISSION SPECTRA
Analysis of emission features in IRAS LRS spectra N88-27380
Spectral line shapes from highly ionized sodium plasmas
[AD-A193401] N88-27907
EMOTIONAL FACTORS
Ejection situations in the U-2/TR-1: An analysis of emotions and events
[AD-A192872] N88-27175
ENAMELS
Contribution to the development of coated fiber ceramic insolation material
[ETN-88-92361] N88-27243
ENERGY BANDS
Self energy corrections to the ab initio band structures: Chromium
[DE88-701825] N88-27927
Investigation of electronic band structure of semiconductors by photoemission
[ETN-88-92370] N88-27957
ENERGY CONVERSION EFFICIENCY
Estimation of power-energy plots for secondary batteries
[DE88-011922] N88-27460
Solar energy conversion through the interaction of plasmons with tunnel junctions. Part A: Solar cell analysis. Part B: Photoconductor analysis
[NASA-CR-183044] N88-27621
ENERGY DISSIPATION
Propagation of charged particle beams in the atmosphere
[AD-A193185] N88-27887
ENERGY DISTRIBUTION
Energy distribution and transfer in flowing hydrogen microwave plasmas N88-27919
ENERGY GAPS (SOLID STATE)
Meaning of energy diagrams used to describe hetero-structures
[DE88-702219] N88-27943
Techniques and instrumentation for transient characterization of metal-insulator-semiconductor diodes. Applications to metal-insulator InP system
[ECL-87-17] N88-27959
ENERGY SPECTRA
Meaning of energy diagrams used to describe hetero-structures
[DE88-702219] N88-27943
Cascade model of gamma-ray bursts: Power-law and annihilation-line components
[NASA-TM-101176] N88-27998
ENERGY STORAGE
Recent developments in nickel hydrogen technology
[DE88-011248] N88-27456
Storage of thermal energy by means of an absorption cycle
[PB88-190814] N88-27619
Thermal energy storage
[DE88-010753] N88-27625
ENERGY TRANSFER
Energy migration, motion and order in synthetic polymers
[AD-A193334] N88-27320
Energy distribution and transfer in flowing hydrogen microwave plasmas N88-27919
ENGINE DESIGN
Documentation of the Benson Diesel Engine Simulation Program
[NASA-TM-100940] N88-27201
Analytical and experimental investigation of ringless piston concept
[AD-A193213] N88-27559
ENGINE PARTS
T55-l-714 engine development and qualification. Engine M11 low cycle fatigue test report. (0213-005-87), volume 2, part 1
[AD-A192786] N88-27198
Ceramic technology for advanced heat engines project
[DE88-008945] N88-27323
Studies of dynamic contact of ceramics and alloys for advanced heat engines
[DE88-008996] N88-27324
ENGINE TESTS
T55-L-714 engine development and qualification. Engine M11 low cycle fatigue test report. (0213-005-87)
[AD-A192765] N88-27197
T55-l-714 engine development and qualification. Engine M11 low cycle fatigue test report. (0213-005-87), volume 2, part 1
[AD-A192786] N88-27198
Documentation of the Benson Diesel Engine Simulation Program
[NASA-TM-100940] N88-27201
Ceramic technology for advanced heat engines project
[DE88-008945] N88-27323
The 210-HP diesel engine endurance and performance testing with fire resistant diesel fuel
[AD-A193153] N88-27558
Analytical and experimental investigation of ringless piston concept
[AD-A193213] N88-27559
Basic mechanisms of diesel lubrication correlation of bench and engine tests
[AD-A193360] N88-27561
Phase 1 results from the Stirling-powered vehicle project
[NASA-TM-100978] N88-27980
ENGINEERING MANAGEMENT
Numerical methods for incompressible viscous flows with engineering applications
[NASA-CR-183143] N88-27508
Engineering data compendium. Human perception and performance. User's guide
[LC-87-19560] N88-27749
TRANSL: A PATRAN translator subroutine library
[DE88-010976] N88-27784
ENGINES
Experimental validation of a zero-dimensional computer model for spark-ignition engines
[DE88-009034] N88-27565
A lubrication study of engine bearings N88-27574
ENTHALPY
Calculation of the specific and volumetric enthalpies of Ge-Si alloys
[DE88-008949] N88-27965
ENVIRONMENTAL MONITORING
Initial testing of the tunable diode laser absorption spectrometer for measuring HNO3 in diesel engine exhaust, stage 2
[PB88-193073] N88-27641
Computer simulation procedure for designing airborne aerometric monitoring programs
[DE88-011896] N88-27674

ENVIRONMENTAL TESTS
Flight testing under extreme environmental conditions
[AGARD-AG-300-VOL-8] N88-27525
ENZYME ACTIVITY
Methods of quantifying and enhancing reactive oxygen species production N88-27357
EPILEPSY
Detection of latent epilepsy in aircrew candidates N88-27720
EPITAXY
Superconducting thin films, composites and junctions
[AD-A193123] N88-27440
Atomic layer epitaxy of ZnS and ZnSe
[AD-A192307] N88-27928
EPOXY MATRIX COMPOSITES
Determination of the glass transition temperature of cured composite materials
[DT-87/62-R] N88-27246
EPOXY RESINS
Relation between the mechanical characteristics of carbon-resin composites and their impact strength
[REPT-48-284/F] N88-27249
Simulation of moisture diffusion of fiber reinforced components of aircraft for general air transportation
[IFL-IB-87-05] N88-27253
Rubber-modified epoxies: Interfacial tension and morphology
[AD-A192464] N88-27313
Study of crosslinking and nonelastic mechanical properties of epoxy and PSP networks --- epoxy resins; polystyrylpyridine resins (psp)
[ETN-88-92740] N88-27337
EQUATIONS OF MOTION
Effects of static equilibrium and higher-order nonlinearities on rotor blade stability in hover N88-27157
In-flight motor torque estimates for the second-stage Strypi 9 launch vehicle
[DE88-010833] N88-27222
EQUILIBRIUM
Equilibrium distribution functions for limited plasma-molecular systems
[DE88-702412] N88-27916
EQUIVALENT CIRCUITS
Some equivalent circuit models for AC impedance analysis of pyrite/solution interface
[DE88-010574] N88-27452
EROSION
Oxidation-erosion of metals and alloys: Models, verification, and prediction
[DE88-010016] N88-27300
ERROR ANALYSIS
Dynamic modelling and estimation of the error due to asynchronism in a redundant asynchronous multiprocessor system
[NASA-CR-177427] N88-27205
ERRORS
A VLSI single-chip (225,223) Reed-Solomon encoder with interleaver
[NASA-CASE-NPO-17280-1-CU] N88-27220
A unified approach to estimation in linear models with fixed and mixed effects
[AD-A193060] N88-27829
ESTIMATES
Dynamic modelling and estimation of the error due to asynchronism in a redundant asynchronous multiprocessor system
[NASA-CR-177427] N88-27205
Estimation of power-energy plots for secondary batteries
[DE88-011922] N88-27460
A unified approach to estimation in linear models with fixed and mixed effects
[AD-A193060] N88-27829
On the estimation of a variance ratio
[AD-A193190] N88-27854
ETCHING
Equipment for building and testing superconductive flux flow electronic devices
[AD-A192959] N88-27436
ETHYL ALCOHOL
Ethanol as a fuel of a lorry. Use experience from a diesel engine modified to an otto engine
[DE88-752870] N88-27569
ETHYLENE
Ionic conductive polymers based on crosslinked elastic siloxane-ethylene oxide copolymers
[DE88-011243] N88-27311
EUROPE
European transonic wind tunnel project: Assistance to the design group
[ONERA-RSF-11/0694-GY-010-G] N88-27208
Studies concerning the European transonic wind tunnel
[ONERA-RSF-10/0694-GY-010-G] N88-27209
EUROPEAN SPACE PROGRAMS
Economic impact of space flight activities in West Germany. Influence of allocations of Bundesministerium fuer Forschung und Technologie
[ETN-88-92106] N88-27215
Cyrogenic test facilities for an optical cryomechanism qualification
[SNIAS-881-440-116] N88-27219
EVALUATION
An evaluation of flight path formats head-up and head-down
[NASA-CR-4176] N88-27196
Evaluation of fracture models through pressurized-thermal-shock testing
[DE88-011834] N88-27603
Performance evaluation of large-area glass-mirror heliostats
[DE88-011883] N88-27636
EVAPORATION
Schottky-barrier formation on a covalent semiconductor without Fermi-level pinning: The Metal-MoS2(0001) interface
[AD-A193044] N88-27931
EVOKED RESPONSE (PSYCHOPHYSIOLOGY)
A statistical procedure for the evaluation of presence/non-presence of stimulus-related EEG activity N88-27689
Dissecting the visual and auditory pathways by means of the two-input technique N88-27690
Squid instrumentation for neuromagnetic study of complex brain activity N88-27691
Neuromagnetic evidence of place mechanisms for frequency and intensity coding in the human auditory cortex N88-27693
Neurophysiological precursors of accurate visuomotor performance N88-27706
The effect of mild hypoxia on the vestibular evoked response N88-27713
Measurement of electrical activity in the CNS with cortical evoked potentials and EEG: Efficacy profiles of drugs using factor analysis N88-27715
The auditory evoked response in military pilots N88-27721
EVOLUTION (DEVELOPMENT)
Dynamical evolution of cosmic strings
[DE88-011724] N88-27989
EXCITATION
Magnetic excitations in transition metal systems
[DE88-011022] N88-27279
Inelastic electron scattering and electron-hole excitations in iron and nickel
[DE88-011843] N88-27303
Picosecond optoelectronic sampling of electrical waveforms produced by an optically excited field effect transistor
[AD-A192384] N88-27428
Nonlinear stochastic interaction in aeroelastic structures
[AD-A193427] N88-27589
EXCITONS
Laser spectroscopy of quantum well and superlattice structures
[AD-A193336] N88-27937
EXHAUST EMISSION
Initial testing of the tunable diode laser absorption spectrometer for measuring HNO3 in diesel engine exhaust, stage 2
[PB88-193073] N88-27641
EXHAUST NOZZLES
Variable Mach number wall jets for control/propulsion on hypervelocity projectiles/interceptors: Tests with an existing model
[AD-A192845] N88-27167
EXHAUSTION
Metabolic and cardiorespiratory parameters during three consecutive days of exhaustive running
[AD-A192598] N88-27728
EXOBIOLOGY
Aerospace Medicine and Biology: A continuing bibliography with indexes (supplement 314)
[NASA-SP-7011(314)] N88-27742
EXPANSION
An interferometric measurement technique for railgun structures
[AD-A192851] N88-27217
Perturbation expansions generated by an approximate propagator
[DE88-702435] N88-27866
EXPERT SYSTEMS
EXSAT: Expert system to configure telecommunication satellites
[SNIAS-881-440-101] N88-27223
United States Air Force Graduate Student Summer Support Program, volume 2
[AD-A191122] N88-27355
Investigation of expert system design approaches for electronic design environments N88-27385
An investigation of performance improvement in knowledge-based control systems N88-27382
Computer-Aided Engineering (CAE) for engineering design N88-27390
The MELCOM PSI 2 AI workstation N88-27395
Motor-response learning at a process control panel by an autonomous robot
[DE88-005055] N88-27554
Vapor Compression Distillation Subsystem (VCDS) component enhancement, testing and expert fault diagnostics development, volume 2
[NASA-CR-172076] N88-27755
Implementation of an OPS5 derivative on the Novix RISC processor
[DE88-011392] N88-27758
Block Oriented Simulation System (BOSS)
[NASA-CR-182947] N88-27760
Benefits of an object approach in a computer aided design environment
[SNIAS-881-440-102] N88-27791
Intelligent Mobile Autonomous System (IMAS)
[AD-A193181] N88-27811
Introduction to artificial intelligence and expert systems
[SNIAS-881-320-101] N88-27814
Expert system contribution to logistics improvement
[SNIAS-881-320-102] N88-27815
EXPLOSIONS
Development of an experimental system for studying fast transient ignition phenomena
[DE88-011917] N88-27276
Stochastic geologic effects on near-field ground motions in alluvium
[AD-A192315] N88-27652
EXPLOSIVE FORMING
Superconductor consolidation
[DE88-010938] N88-27949
EXPLOSIVE WELDING
Evaluation of explosive bonding for patching aluminum with aluminum
[AD-A193303] N88-27285
EXPLOSIVES
Deformation, fracture and explosive properties of reactive materials
[AD-A193080] N88-27348
A concept for an electro-optic explosive device
[DE88-009696] N88-27349
Relative flow rates of explosive powders
[DE88-010767] N88-27350
Stochastic geologic effects on near-field ground motions in alluvium
[AD-A192315] N88-27652
EXPOSURE
Assessment of cochlear damage after microwave irradiation
[AD-A193237] N88-27737
EXTINGUISHING
Extinguishing agent for magnesium fire, phases 5 and 6
[AD-A192436] N88-27398
EXTRACTION
Automatic line network extraction from aerial imagery of urban areas through knowledge based image analysis
[AD-A193067] N88-27615
Uses of lunar sulfur
[DE88-009119] N88-27990
EXTRAPOLATION
Comparison of results based on a deterministic versus a statistical uncertainty analysis
[DE88-010751] N88-27858
EXTRAVEHICULAR MOBILITY UNITS
Advanced EMU electrochemically regenerable CO2 and moisture absorber module breadboard
[NASA-CR-172054] N88-27754
EXTREME ULTRAVIOLET RADIATION
Development of a free-electron laser user facility for the extreme ultraviolet
[DE88-007892] N88-27541
EXTREMELY HIGH FREQUENCIES
An evaluation of two millimeter wave propagation models for horizontal atmospheric attenuation at 70-115 GHZ
[AD-A192699] N88-27403
EYE MOVEMENTS
A human factors evaluation of the Advanced Visual Technology System (AVTS) eye tracking oculometer N88-27361
Fighter pilot performance during airborne and simulator missions: Physiological comparisons N88-27704

F

FABRICATION
Focused ion beam fabrication of graded channel FETs in GaAs and Si
[AD-A193098] N88-27439
Experimental fabrication of thin film single crystalline solar cells
[PB88-131958] N88-27627
Amorphous silicon solar cells using a metal substrate
[PB88-131941] N88-27628
Optical evaluation of prototype stretched-membrane mirror modules for solar central receivers
[DE88-011884] N88-27637
Ceramic fabrication technology for high-T(sub)c materials
[DE88-012060] N88-27953

FACTOR ANALYSIS
A programmable systolic array for factorial analysis. Part 2: The symmetric eigenvalue problem
[AD-A192396] N88-27762

FACTORIAL DESIGN
A programmable systolic array for factorial analysis. Part 2: The symmetric eigenvalue problem
[AD-A192396] N88-27762
Measuring dispersion effects of factors in factorial experiments
[AD-A193216] N88-27831

FACTORIZATION
Factorization of large integers on a massively parallel computer
[DE88-011625] N88-27786

FAILURE
Probabilistic anisotropic failure criteria for composite materials
[AD-A193046] N88-27232
NDE performance in predicting failure strength of spherical composite specimens with implanted flaws
[DE88-008223] N88-27575
Influence of microstructure and microdamage processes on fracture at high loading rates
[AD-A192957] N88-27583

FAILURE ANALYSIS
Failure analysis of Chloride Silent Power, Ltd. PB cells
[DE88-010567] N88-27448
Sodium/sulfur cell evaluation results
[DE88-011488] N88-27451
Failure analysis of laminated composite angles N88-27578
Computation of failure probability of fatigue loaded cracked structures
[ETN-88-92360] N88-27607
Vapor Compression Distillation Subsystem (VCDS) component enhancement, testing and expert fault diagnostics development, volume 2
[NASA-CR-172076] N88-27755

FAILURE MODES
Failure analysis of laminated composite angles N88-27578

FAR INFRARED RADIATION
Far- and mid-infrared properties of metal-insulator composite materials
[AD-A193227] N88-27236
Calculation of far infrared absorption in B poly(dA).poly(dT)
[AD-A193128] N88-27318

FAST FOURIER TRANSFORMATIONS
Simulation and analysis of wave propagation through random media N88-27503
Detection of acceleration (+Gz) induced blackout by matched-filtering of visual evoked potentials N88-27710

FAST NUCLEAR REACTORS
Heat and mass transfer in a transport channel
[DE88-701968] N88-27493

FATIGUE (BIOLOGY)
Psychophysiological measures of drowsiness as estimators of mental fatigue and performance degradation during sleep deprivation N88-27702
Neurophysiological patterns of operational fatigue: Preliminary results N88-27703

FATIGUE (MATERIALS)
Significance of the local electrode potential within pits, crevices and cracks
[AD-A192482] N88-27432
Three-dimensional aspects of fatigue crack closure
[AD-A192296] N88-27581

FATIGUE LIFE
Constant amplitude fatigue life data for notched and unnotched annealed Ti-6Al-4V sheet
[AD-A193420] N88-27287
Optimal design of viscoelastic structures N88-27579
The relationship between observed fatigue damage and life estimation models
[NASA-CR-182191] N88-27611

FATIGUE TESTS
T55-L-714 engine development and qualification. Engine M11 low cycle fatigue test report. (0213-005-87)
[AD-A192765] N88-27197
T55-l-714 engine development and qualification. Engine M11 low cycle fatigue test report. (0213-005-87), volume 2, part 1
[AD-A192766] N88-27198

FAULT TOLERANCE
FTMP data acquisition environment
[NASA-TM-100636] N88-27447

FEASIBILITY ANALYSIS
Theoretical-numerical study of feasibility of use of winglets on low aspect ration wings at subsonic and transonic Mach numbers at reduce drag
[NASA-CR-4174] N88-27168
Supersonic transport/hypersonic transport (SST/HST) development
[SNIAS-881-111-101] N88-27192
Experimental investigation of simplest inhomogeneities in cylindrical slit line
[DE88-702388] N88-27418

FEEDBACK CONTROL
Vibration control of large structures
[AD-A193317] N88-27587
Feedback control of a hyperbolic partial-differential equation with viscoelastic damping
[AD-A192896] N88-27810

FERMIONS
Geometry of superconformal manifolds, part 1
[DE88-702405] N88-27863
An overview of lattice QCD
[DE88-010867] N88-27963

FIBER COMPOSITES
The two isotropic asymptotes of fiber composites
[AD-A192305] N88-27231
Effects of electron beam irradiation on mechanical properties at low and high temperature of fiber reinforced composites using PEEK as matrix material
[DE88-753134] N88-27239
Fabrication of SiC fiber reinforced glass matrix by extrusion process and investigation of its mechanical properties
[ETN-88-92367] N88-27244
Programs for preliminary design of composite materials which were developed by the design group of Aerospatiale Aquitaine
[SNIAS-881-430-112] N88-27251
Simulation of moisture diffusion of fiber reinforced components of aircraft for general air transportation
[IFL-IB-87-05] N88-27253

FIBER OPTICS
A concept for an electro-optic explosive device
[DE88-009696] N88-27349
Fiber-optics used to record high-speed photographs inside a pressurized tank during lethality testing
[DE88-011283] N88-27529
A fiber optic synchronous detector using sample-and-hold circuits
[DE88-010973] N88-27899

FIBER STRENGTH
Relation between the mechanical characteristics of carbon-resin composites and their impact strength
[REPT-48-284/F] N88-27249

FIELD EFFECT TRANSISTORS
Picosecond optoelectronic sampling of electrical waveforms produced by an optically excited field effect transistor
[AD-A192384] N88-27428
Focused ion beam fabrication of graded channel FETs in GaAs and Si
[AD-A193098] N88-27439
Techniques and instrumentation for transient characterization of metal-insulator-semiconductor diodes. Applications to metal-insulator InP system
[ECL-87-17] N88-27959

FIELD OF VIEW
Assessments of maneuverability with the TeleOperated Vehicle (TOV)
[AD-A191584] N88-27751

FIELD STRENGTH
Measurement of macroscopic electric fields in solar plasma structures
[AD-A193291] N88-27993

FIELD THEORY (PHYSICS)
Superalgebras with Grassmann algebra-valued structure constants from superfields
[DE88-702239] N88-27862
Closed string fields as parameters of extra gauge symmetry of open string field theory
[DE88-702045] N88-27960

FIGHTER AIRCRAFT
Pilot report: AFTI (Advanced Fighter Technology Integration) F-111
[AD-A192937] N88-27184
A cockpit natural language study: Vocabulary and grammar analyses
[AD-A193289] N88-27753

FILAMENT WINDING
Design of booster wound structures --- spacecraft structures
[SNIAS-881-430-102] N88-27228
Reinforced plastics: Winding and weaving technologies for space products
[SNIAS-881-430-103] N88-27341
NDE performance in predicting failure strength of spherical composite specimens with implanted flaws
[DE88-008223] N88-27575

FILM BOILING
Effects of surface tension and contact angle on sensible heating and boiling incipience in dielectric falling films
[DE88-007057] N88-27492

FILM COOLING
Investigation of annular flow at high evaporation rates in view of liquid film cooling
[DFVLR-FB-88-08] N88-27517

FILM THICKNESS
Basic mechanisms of diesel lubrication correlation of bench and engine tests
[AD-A193360] N88-27561

FINITE DIFFERENCE THEORY
Implicit finite-difference simulation of an internal flow on a hypercube
[AD-A192474] N88-27471
Implicit finite-difference simulation of an internal flow in a nozzle: An example of a physical application on a hypercube
[AD-A192475] N88-27472
User's manual for C-HEMP: A two-dimensional wave propagation code. Volume 1: Description and derivations of the code
[AD-A193197] N88-27486

FINITE ELEMENT METHOD
Thermo-viscoelastic analysis of composite materials, volume 1
[NASA-CR-183048-VOL-1] N88-27230
An h-p adaptive finite element method for steady compressible flow N88-27467
A study of fluid-structure problems N88-27468
Stream function-vorticity finite elements and the resolution of the Navier-Stokes equations
[DE88-702318] N88-27494
Optimal design of viscoelastic structures N88-27579
Adaptive finite element methods for shells
[AD-A193221] N88-27585
Verification of the ADINA finite element code for creep analysis: Problems from the open literature
[DE88-011826] N88-27594
DYNA3D (Nonlinear Dynamic Analysis of Structures in Three Dimensions) user's manual
[DE88-012242] N88-27604
Finite element methodology for integrated flow-thermal-structural analysis
[NASA-CR-183144] N88-27606
Staggered-grid finite element solution technique for the Maxwell's equations in the time domain
[DE88-011731] N88-27838
Unified multilevel adaptive finite element methods for elliptic problems
[DE88-011938] N88-27840
Finite element method for plate structures with inclined angles
[ILR-MITT-182] N88-27842

FINITE VOLUME METHOD
Effects of numerical dissipation on finite-volume solutions of compressible flow problems
[AD-A193173] N88-27485
Investigation of viscous/inviscid interaction in transonic flow over airfoils with suction
[NASA-CR-183112] N88-27490

FIRE EXTINGUISHERS
Extinguishing agent for magnesium fire, phases 5 and 6
[AD-A192436] N88-27398

FIRES
Extinguishing agent for magnesium fire, phases 5 and 6
[AD-A192436] N88-27398
The 210-HP diesel engine endurance and performance testing with fire resistant diesel fuel
[AD-A193153] N88-27558

FITNESS
Three-dimensional adaptive grid generation for body-fitted coordinate system
[NASA-CR-182192] N88-27520

FLAME PROPAGATION
Premixed turbulent flame propagation
[AD-A192955] N88-27265

Summary of discussions at the Tenth Meeting of the Sandia Cooperative Group on the Aerothermochemistry of Turbulent Combustion
[DE88-008467] N88-27269

FLAME RETARDANTS
The 210-HP diesel engine endurance and performance testing with fire resistant diesel fuel
[AD-A193153] N88-27558

FLAMES
Summary of discussions at the Tenth Meeting of the Sandia Cooperative Group on the Aerothermochemistry of Turbulent Combustion
[DE88-008467] N88-27269

FLEXIBLE SPACECRAFT
Numerical optimization, system theoretic and software tools for the integrated design of flexible structures and their control systems
[AD-A192927] N88-27183

FLIGHT CHARACTERISTICS
Contribution to the numerical solution of airplane spin motion
[ETN-88-92368] N88-27190
A numerical simulation of side force effects by aerodynamic flight trajectory correction
[ISL-CO-211/87] N88-27191

FLIGHT CONTROL
Theoretical and experimental investigations of a vortex drag behind a wing profile with spoiler
[ISL-PU-309/87] N88-27169
Investigations of aircraft control with jet spoilers
[ISL-R-112/87] N88-27202
Robust digital model following controller for helicopters
[DFVLR-FB-88-07] N88-27203

FLIGHT CREWS
Detection of latent epilepsy in aircrew candidates N88-27720
Cockpit and cabin crew coordination
[AD-A192445] N88-27752

FLIGHT PATHS
An evaluation of flight path formats head-up and head-down
[NASA-CR-4176] N88-27196

FLIGHT SIMULATION
Robust digital model following controller for helicopters
[DFVLR-FB-88-07] N88-27203

FLIGHT SIMULATORS
An evaluation of flight path formats head-up and head-down
[NASA-CR-4176] N88-27196
Simulator sickness in the AH-64 Apache combat mission simulator
[AD-A193419] N88-27739

FLIGHT TESTS
A comparison of theory and flight test of the BO 105/BMR in hover and forward flight N88-27155
Pilot report: AFTI (Advanced Fighter Technology Integration) F-111
[AD-A192937] N88-27184
Air-to-air radar flight testing
[AGARD-AG-300-VOL-7] N88-27406
Flight testing under extreme environmental conditions
[AGARD-AG-300-VOL-8] N88-27525
Hypersonic flight testing
[DE88-001655] N88-27894

FLOOD PLAINS
IEMIS (Integrated Emergency Management Information System) floodplain mapping based on a LIDAR derived data set
[AD-A193071] N88-27616

FLOODS
IEMIS (Integrated Emergency Management Information System) floodplain mapping based on a LIDAR derived data set
[AD-A193071] N88-27616

FLOW DISTORTION
Numerical simulation of fuel droplet interactions and breakup
[AD-A192431] N88-27470

FLOW DISTRIBUTION
Flow around a delta wing with or without a canard control surface (phi BA = 60 deg). Part 1: Hydrodynamic visualization in permanent regime
[ONERA-RT-10/2891-AN-101-A-PT-1] N88-27170
Prediction of the aeroelastic behavior of tuned blades. Application to aircraft engines
[ISAL-87-0046] N88-27199
Gaseous tracer techniques for pore structure characterization of granular materials
[DE88-011542] N88-27274
Design of a mechanism to control wind tunnel turbulence N88-27370
A Navier-Stokes study of cascade flow fields including inlet distortion and rotating stall
[AD-A193109] N88-27483
Cavitation inception in a turbulent shear flow
[DE88-011486] N88-27497
Turbulent flow field visualization with integral interferometric imaging and computed tomography N88-27521

FLOW MEASUREMENT
Velocity measurements and flow visualization in turbulent three-dimensional supersonic flows using oxygen flow tagging
[AD-A192551] N88-27165
Investigation of the quasi-steady approach used in transient two-phase flow analysis
[DE88-004303] N88-27489
Laser-Doppler measurements of turbulence structures in free streams behind flat and rotation symmetrical profiles
[ETN-88-92336] N88-27510

FLOW STABILITY
Numerical simulation and stability analysis of the absolutely and convectively unstable wake
[DFVLR-FB-88-09] N88-27518

FLOW VELOCITY
Cryogenic free jets
[DFVLR-FB-88-16] N88-27210
Optimal rheological characteristics in dynamic stability of polymer flow through porous media
[DE88-001225] N88-27322
Relative flow rates of explosive powders
[DE88-010767] N88-27350
Heat and mass transfer in a transport channel
[DE88-701968] N88-27493
Energy distribution and transfer in flowing hydrogen microwave plasmas N88-27919

FLOW VISUALIZATION
Velocity measurements and flow visualization in turbulent three-dimensional supersonic flows using oxygen flow tagging
[AD-A192551] N88-27165
Flow around a delta wing with or without a canard control surface (phi BA = 60 deg). Part 1: Hydrodynamic visualization in permanent regime
[ONERA-RT-10/2891-AN-101-A-PT-1] N88-27170
The structure and stability of nonpremixed gas jet flames N88-27257
Experimental research of combustion systems N88-27371
Liquid crystals for unsteady surface shear stress visualization
[DE88-010570] N88-27527

FLUID BOUNDARIES
A numerical treatment of the fluid/elastic interface under range-dependent environments
[AD-A192476] N88-27821

FLUID DYNAMICS
The heat transfer and fluid dynamics of concave surface curvature
[AD-A193064] N88-27479

FLUID FLOW
Optimal rheological characteristics in dynamic stability of polymer flow through porous media
[DE88-001225] N88-27322
Characterization of accelerating pipe flow
[AD-A193065] N88-27481
Effects of numerical dissipation on finite-volume solutions of compressible flow problems
[AD-A193173] N88-27485
Numerical treatment of the pressure singularity at a re-entrant corner
[AD-A193357] N88-27488
Stream function-vorticity finite elements and the resolution of the Navier-Stokes equations
[DE88-702318] N88-27494

FLUID MECHANICS
Laser probes and numerical modeling as process diagnostics in chemical vapor deposition
[DE88-011622] N88-27275
Some stability criteria in fluid and solid mechanics N88-27966

FLUOROPOLYMERS
Polymer-ceramic composites
[AD-A193244] N88-27237
Plasma treatment of polymers for improved adhesion
[DE88-011623] N88-27334

FLY BY WIRE CONTROL
Computer system for the primary fly-by-wire control of civil transport aircraft (experimental system)
[FBW-TB-2086/88] N88-27204

FOAMS
Determination of radiative properties of fiberglass and foam insulations
[DE88-007845] N88-27331

FOKKER-PLANCK EQUATION
Nonlinear stochastic interaction in aeroelastic structures
[AD-A193427] N88-27589

FOLIAGE
Foliar nitrate reductase: A marker for assimilation of atmospheric nitrogen oxides
[DE88-010453] N88-27648

FORTRAN
FORTRAN 77 implementation of abstract datatype models
[DFVLR-MITT-88-08] N88-27794

FOURIER ANALYSIS
SARLAC: A relativistic electron beam code
[AD-A193134] N88-27411

FOURIER TRANSFORMATION
Photon limited image processing in the space-time domain
[AD-A193142] N88-27655

FRACTALS
Survey of the literature on fractals with possible applications to phase change processes
[DE88-012240] N88-27277

FRACTIONS
Mass flow rate influence on void fraction of two-phase helium flow
[DE88-702456] N88-27495

FRACTURE MECHANICS
An investigation of soft launch and instability breakup with a two-stage light gas gun
[DE88-010371] N88-27218
Processing and properties of advanced aluminum alloys
[AD-A193224] N88-27284
Analysis of crack arrest toughness
[AD-A193340] N88-27286
Adhesion of hydrated silicate films
[DE88-011250] N88-27333
Failure analysis of laminated composite angles N88-27578
Plastic yielding at crack tips
[AD-A192549] N88-27582
Influence of microstructure and microdamage processes on fracture at high loading rates
[AD-A192957] N88-27583
Critical issues and directions for fracture mechanics and structural integrity
[AD-A193050] N88-27584
Soviet dynamic fracture mechanics research
[FASAC-TAR-3140] N88-27597
Corrosion fatigue of small cracks: Mechanics and chemistry
[DE88-012121] N88-27605
Size effects in linear elastic fracture mechanics N88-27609

FRACTURE STRENGTH
Analysis of transverse strength of composites using percolation theory
[AD-A193204] N88-27234

FRACTURES (MATERIALS)
Deformation, fracture and explosive properties of reactive materials
[AD-A193080] N88-27348

FRACTURING
Influence of microstructure and microdamage processes on fracture at high loading rates
[AD-A192957] N88-27583
Evaluation of fracture models through pressurized-thermal-shock testing
[DE88-011834] N88-27603

FREDHOLM EQUATIONS
Generalized Jordan chains and two bifurcation theorems of Krasnoselskii
[AD-A192353] N88-27845

FREE BOUNDARIES
Free boundary control of the Markov process
[AD-A192401] N88-27846

FREE ELECTRON LASERS
Optical guiding in the separable beam limit
[AD-A192452] N88-27534
Efficiency optimization for FEL oscillators
[AD-A192541] N88-27536
Research opportunities below 300 nm at the NBS Free-Electron Laser Facility
[AD-A193100] N88-27538
Initial electron distributions for free-electron lasers generated by injector and accelerator simulations
[DE88-007022] N88-27540
Development of a free-electron laser user facility for the extreme ultraviolet
[DE88-007892] N88-27541
Transverse resistive wall instability in a high-power, short-wavelength free-electron laser
[DE88-011730] N88-27549
On the small signal gain of free electron lasers in the low-current regime
[DFVLR-FB-88-10] N88-27552
Genetic effects of low level microwave radiation
[AD-A192687] N88-27722

FREE FLOW
Experimental study of unsteady separating turbulent boundary layers
[AD-A192997] N88-27477
FREE JETS
Cryogenic free jets
[DFVLR-FB-88-16] N88-27210
FREEZING
Component stress during freeze/thaw cycling
[DE88-011204] N88-27449
Effect of thermal cycling on CSPL (Chloride Silent Power Ltd.) sodium/sulfur cells
[DE88-011205] N88-27455
FREQUENCY CONTROL
Quartz crystal resonators and oscillators for frequency control and timing applications
[AD-A193310] N88-27443
FREQUENCY MEASUREMENT
Airborne measurement of low frequency atmospheric noise ALFAN 1
[AD-A193056] N88-27405
A notch filter instrument for measuring ELF (Extremely Low Frequency) MSK (Minimum Shift Keying) signals
[AD-A193324] N88-27414
FREQUENCY SHIFT KEYING
A notch filter instrument for measuring ELF (Extremely Low Frequency) MSK (Minimum Shift Keying) signals
[AD-A193324] N88-27414
FREQUENCY STANDARDS
A three-dimensional model of the gas-cell atomic frequency standard
[AD-A193218] N88-27868
FRICTION
Friction, wear and electrical contact resistance of precious metal alloys
[DE88-011244] N88-27450
Granular flow: Particle-dynamics simulations of steady flow
[DE88-011342] N88-27506
Thermo-mechanical cracking in coated media with a cavity by a moving asperity friction
[AD-A193311] N88-27586
FUEL CELLS
Monolithic fuel cells
[DE88-012004] N88-27638
FUEL COMBUSTION
Effects of ceramic surfaces on autoignition in a constant volume combustion apparatus
[AD-A193055] N88-27266
FUEL INJECTION
The 210-HP diesel engine endurance and performance testing with fire resistant diesel fuel
[AD-A193153] N88-27558
FUEL PRODUCTION
The 210-HP diesel engine endurance and performance testing with fire resistant diesel fuel
[AD-A193153] N88-27558
FUEL SPRAYS
Effects of ceramic surfaces on autoignition in a constant volume combustion apparatus
[AD-A193055] N88-27266
FUELS
Ethanol as a fuel of a lorry. Use experience from a diesel engine modified to an otto engine
[DE88-752870] N88-27569
FUNCTIONAL ANALYSIS
Further extensions of the choquet-deny and deny theorems with applications in characterization theory
[AD-A193358] N88-27834
FUNCTIONAL DESIGN SPECIFICATIONS
Software engineering guidelines for RASP and ANDECS: Requirements and architectural design
[DFVLR-MITT-88-07] N88-27793
FUNCTIONALS
Evaluation of quantum mechanics path integrals by the approximations exact on a class of polynomial functionals
[DE88-702434] N88-27865
FUNCTIONS (MATHEMATICS)
A simple explanation of the Stokes phenomenon
[AD-A193253] N88-27832
An overview of lattice QCD
[DE88-010867] N88-27963
FUSION REACTORS
Optical imaging diagnostics for fusion plasmas
[DE88-997572] N88-27910

G

GALACTIC EVOLUTION
Cosmological parameters and evolution of the galaxy luminosity function
[NASA-CR-183081] N88-27986
GALACTIC RADIATION
Gamma radiation from center of the galaxy of the order of MeV values
[MPE-207] N88-27999
GALERKIN METHOD
Numerical simulation and stability analysis of the absolutely and convectively unstable wake
[DFVLR-FB-88-09] N88-27518
GALLIUM
Nuclear magnetic resonance spectrometer
[AD-A192928] N88-27523
Growth and characterization of CuGaS2, CuAlS2 and CuGa0.9Al0.1S2 single crystals
[AD-A192963] N88-27930
GALLIUM ARSENIDE LASERS
Diode laser ignition of high explosives and pyrotechnics
[DE88-008771] N88-27352
GALLIUM ARSENIDES
Thermal conductivity of isotopically pure semiconductors, superlattices, semiconductor alloys and semiconductors as a function of temperature; control of the segregation coefficient in LEC crystal growth; and photo-Hall measurements of GaAs N88-27375
Picosecond optoelectronic sampling of electrical waveforms produced by an optically excited field effect transistor
[AD-A192384] N88-27428
Studying the physics and operation of multi-terminal near-micron and sub-micron length, hot electron semiconductor devices
[AD-A193380] N88-27446
A GaAs solid state device model for high power applications
[DE88-011320] N88-27457
Phase comparator for range imaging laser radar
[DE86-008109] N88-27545
Photodiodes for optical communication in the near infrared
[ETN-88-92379] N88-27900
Picosecond transient reflectivity of unpinned gallium arsenide (100) surfaces
[AD-A193242] N88-27933
Investigations on the MBE (Molecular Beam Epitaxy) growth and properties of Al(sub y)Ga(sub y)In(sub 1-x-y)AsInP and InGaAs-InAlAs superlattices
[DE88-009105] N88-27941
GALLIUM PHOSPHIDES
Molecular beam epitaxy of GaP films on Si substrates
[PB88-131974] N88-27923
GALVANOMAGNETIC EFFECTS
Integrated magnetic field sensor using high magnetotransistors
[ETN-88-92356] N88-27485
GAMMA RAY ASTRONOMY
Application of two-dimensional imaging to very high energy gamma ray astronomy
[DE88-010120] N88-27983
Gamma radiation from center of the galaxy of the order of MeV values
[MPE-207] N88-27999
GAMMA RAY BURSTS
Cascade model of gamma-ray bursts: Power-law and annihilation-line components
[NASA-TM-101176] N88-27998
GAMMA RAYS
Gamma radiation from center of the galaxy of the order of MeV values
[MPE-207] N88-27999
GAS DISCHARGES
Investigations on beam quality of high frequency excited CO2 high performance lasers
[ETN-88-92363] N88-27550
GAS DYNAMICS
Nozzle lip effects on gas expansion into the plume backflow region
[AD-A192806] N88-27475
Investigations on beam quality of high frequency excited CO2 high performance lasers
[ETN-88-92363] N88-27550
GAS EXPANSION
Nozzle lip effects on gas expansion into the plume backflow region
[AD-A192806] N88-27475
GAS FLOW
Some properties of ignition gases. Review of measuring results in the years 1981-1986)
[PB88-106968] N88-27259
Gaseous tracer techniques for pore structure characterization of granular materials
[DE88-011542] N88-27274
Computation of flow and diffusion process in gas centrifuges
[ETN-88-92366] N88-27514
GASEOUS DIFFUSION
Computation of flow and diffusion process in gas centrifuges
[ETN-88-92366] N88-27514
GATES (CIRCUITS)
Picosecond optoelectronic sampling of electrical waveforms produced by an optically excited field effect transistor
[AD-A192384] N88-27428
GAUGE THEORY
Closed string fields as parameters of extra gauge symmetry of open string field theory
[DE88-702046] N88-27960
GAUSS-MARKOV THEOREM
A unified approach to estimation in linear models with fixed and mixed effects
[AD-A193060] N88-27829
GEARS
Optimization of planetary gears
[ETN-88-92375] N88-27573
GELS
Preparation and properties of new inorganic glasses and gel-derived solids
[AD-A192922] N88-27315
GENETICS
Genetic effects of low level microwave radiation
[AD-A192687] N88-27722
GEODETIC SURVEYS
Basic research for the geodynamics program
[NASA-CR-183149] N88-27682
GEOGRAPHIC INFORMATION SYSTEMS
Review of geographic processing techniques applicable to regional analysis
[DE88-010759] N88-27843
GEOMAGNETIC MICROPULSATIONS
Field-aligned structure of the storm time Pc 5 wave of November 14-15, 1979
[AD-A193022] N88-27853
GEOMAGNETIC TAIL
Scaling laws for geomagnetic tail current sheet acceleration
[AD-A193379] N88-27859
GEOMETRIC DILUTION OF PRECISION
Automatic omega station and LOP (Line Of Position) selection
[AD-A193302] N88-27179
GEOMETRICAL ACOUSTICS
Propagation of acoustic disturbances in transonic flow fields of lifting wings
[DFVLR-FB-88-13] N88-27880
GEOMETRY
The influence of weld metal properties, weld geometry and applied load on weld system performance
[AD-A193403] N88-27588
An investigation of techniques for determination of optimum/self-optimizing systems N88-27600
Automatic line network extraction from aerial imagery of urban areas through knowledge based image analysis
[AD-A193067] N88-27615
Parallel solutions to geometric problems on the scan model of computation
[AD-A192321] N88-27819
Geometry of superconformal manifolds, part 1
[DE88-702405] N88-27883
Geometry of superconformal manifolds, part 2
[DE88-702406] N88-27864
GEOPHYSICS
Development of radiation and cloud parameterization programs for AFGL (Air Force Geophysics Laboratory) global models
[AD-A193369] N88-27858
GEOPRESSURE
Geothermal energy technology: Issues, R and D (Research and Development) and cooperative arrangements
[PB88-193107] N88-27626
GEOTHERMAL TECHNOLOGY
Geothermal energy technology: Issues, R and D (Research and Development) and cooperative arrangements
[PB88-193107] N88-27626
GERMANIUM ALLOYS
Calculation of the specific and volumetric enthalpies of Ge-Si alloys
[DE88-008949] N88-27965
GLASS
Fabrication of SiC fiber reinforced glass matrix by extrusion process and investigation of its mechanical properties
[ETN-88-92367] N88-27244
Preparation and properties of new inorganic glasses and gel-derived solids
[AD-A192922] N88-27315
Performance evaluation of large-area glass-mirror heliostats
[DE88-011883] N88-27638

GLASS FIBER REINFORCED PLASTICS
Rocket motor case materials. An evaluation of new fibers for composites
[FOA-C-20696-2.1] N88-27245
GLASS FIBERS
Effects of electron beam irradiation on mechanical properties at low and high temperature of fiber reinforced composites using PEEK as matrix material
[DE88-753134] N88-27239
Contribution to the development of coated fiber ceramic insulation material
[ETN-88-92361] N88-27243
Determination of radiative properties of fiberglass and foam insulations
[DE88-007845] N88-27331
GLASS TRANSITION TEMPERATURE
Determination of the glass transition temperature of cured composite materials
[DT-87/62-R] N88-27246
GLOBAL POSITIONING SYSTEM
Spacecraft applications of advanced global positioning system technology
[NASA-CR-172055] N88-27180
GLOW DISCHARGES
Direct determination of part-per-billion levels of volatile organics in water and soil samples using glow discharge mass spectrometry
[DE88-011389] N88-27272
GLYCEROLS
Metabolic and cardiorespiratory parameters during three consecutive days of exhaustive running
[AD-A192598] N88-27728
GOALS
Computer-Aided Engineering (CAE) for engineering design N88-27390
GOVERNMENT/INDUSTRY RELATIONS
Economic impact of space flight activities in West Germany. Influence of allocations of Bundesministerium fuer Forschung und Technologie
[ETN-88-92106] N88-27215
GRAIN BOUNDARIES
Analysis of grain refinement and superplasticity in aluminum-magnesium alloys
[AD-A193029] N88-27283
Processing and properties of advanced aluminum alloys
[AD-A193224] N88-27284
Microchemical analysis of polycrystalline Ni3Al and other ordered alloys using the field-ion microscope atom probe
[DE88-011519] N88-27294
Computer simulation of elastic properties of grain boundary materials
[DE88-011965] N88-27305
Study of feasibility and optimization conditions of laser treatments: Application of the local recrystallization of aluminum
[ISAL-87-0048] N88-27309
GRAIN SIZE
Hot isostatic pressing of tungsten-nickel-iron composites
[PB88-203070] N88-27292
The first synthesis of chem-prep varistor LAC (Lightning Arrestor Connector) granules
[DE88-006005] N88-27438
GRAMMARS
A cockpit natural language study: Vocabulary and grammar analyses
[AD-A193289] N88-27753
Linguistic semantics for parallel computation
[PB88-105960] N88-27761
GRANULAR MATERIALS
Gaseous tracer techniques for pore structure characterization of granular materials
[DE88-011542] N88-27274
Granular flow: Particle-dynamics simulations of steady flow
[DE88-011342] N88-27506
Device physics related to the granular nature of CuInSe2 solar cells
[DE88-001159] N88-27622
GRAPHITE-EPOXY COMPOSITES
Determination of lumped-mass thermal properties associated with autoclave curing of graphite/epoxy composites N88-27364
Failure analysis of laminated composite angles N88-27578
GRAPHS (CHARTS)
Issues in computer-assisted interpretation of graphs and quantitative information
[PB88-116280] N88-27783
GRATINGS (SPECTRA)
Precise rotational alignment of X-ray transmission diffraction gratings
[DE88-010599] N88-27273
GRAVITATION
Prediction of velocity and temperature profiles in thermally driven gravity currents applied to stratified thermal storage tanks
[DE88-004452] N88-27496
GRAVITATIONAL EFFECTS
EEG indices of G-induced Loss Of Consciousness (G-LOC) N88-27709
The auditory evoked response in military pilots N88-27721
GRAVITATIONAL FIELDS
Symmetry problem of energy-momentum tensor and the creation of gravitational field
[DE88-702442] N88-27964
GRAY SCALE
Applications of differential geometry to the shape analysis of gray-value images N88-27358
GREENHOUSE EFFECT
Surface energy balance of three general circulation models: Current climate and response to increasing atmospheric CO2
[DE88-010967] N88-27673
GRID GENERATION (MATHEMATICS)
Three-dimensional adaptive grid generation for body-fitted coordinate system
[NASA-CR-182192] N88-27520
GROUND BASED CONTROL
SP-100 Ground Engineering Systems: Test facility control systems
[DE88-009195] N88-27895
GROUND EFFECT (COMMUNICATIONS)
Performance study of a unipole antenna with conventional and elevated radial wire ground screens
[AD-A193283] N88-27413
GROUND WATER
A zoomable and adaptable hidden fine-mesh approach to solving advection-dispersion equations
[DE88-006174] N88-27816
GROUND WAVE PROPAGATION
Surface-wave model uncertainty assessment
[AD-A193094] N88-27408
GROUP DYNAMICS
The human element in space: Lessons from Antarctica
[AD-A193440] N88-27741
GUNN DIODES
Focused ion beam fabrication of graded channel FETs in GaAs and Si
[AD-A193098] N88-27439
GUNS (ORDNANCE)
An interferometric measurement technique for railgun structures
[AD-A192851] N88-27217
GYROSCOPES
Application of the Single-Axis rate Table (SAT) of the DFVLR for the evaluation of stationary and dynamic gyro properties
[DFVLR-MITT-88-09] N88-27533
GYROSCOPIC STABILITY
Application of the Single-Axis rate Table (SAT) of the DFVLR for the evaluation of stationary and dynamic gyro properties
[DFVLR-MITT-88-09] N88-27533

H

HALL EFFECT
Thermal conductivity of isotopically pure semiconductors, superlattices, semiconductor alloys and semiconductors as a function of temperature; control of the segregation coefficient in LEC crystal growth; and photo-Hall measurements of GaAs N88-27375
HALLEY'S COMET
A theoretical determination of the density at a traveling source that emitts particles
[ISAS-RN-351] N88-27883
HARDNESS
Study of the friction and wear-related properties of ceramic superconductors
[DE88-011844] N88-27950
HARMONIC OSCILLATORS
Research opportunities below 300 nm at the NBS Free-Electron Laser Facility
[AD-A193100] N88-27538
HARNESSES
Human response to prolonged motionless suspension in four types of full body harnesses N88-27387
HASTELLOY (TRADEMARK)
Creep behavior for Hastelloy-XR
[DE88-753428] N88-27295
HEAD DOWN TILT
An evaluation of flight path formats head-up and head-down
[NASA-CR-4176] N88-27196
HEAD-UP DISPLAYS
An evaluation of flight path formats head-up and head-down
[NASA-CR-4176] N88-27196
HEARING
Dissecting the visual and auditory pathways by means of the two-input technique N88-27690
Neuromagnetic evidence of place mechanisms for frequency and intensity coding in the human auditory cortex N88-27693
HEART FUNCTION
Validation of a modified one-step rebreathing technique for measuring exercise cardiac output
[AD-A192600] N88-27729
HEART RATE
Fighter pilot performance during airborne and simulator missions: Physiological comparisons N88-27704
Metabolic and cardiorespiratory parameters during three consecutive days of exhaustive running
[AD-A192598] N88-27728
Validation of a modified one-step rebreathing technique for measuring exercise cardiac output
[AD-A192600] N88-27729
Validation of a modified one-step rebreathing technique for non-invasive measurement of submaximal cardiac output
[AD-A192852] N88-27735
HEAT FLUX
Optical imaging diagnostics for fusion plasmas
[DE88-997572] N88-27910
HEAT PIPES
Reflux heat-pipe solar receivers for dish-electric systems
[DE88-008671] N88-27631
HEAT PUMPS
Magnetic heat pumps
[DE88-012058] N88-27639
HEAT RESISTANT ALLOYS
A fundamental understanding of the interfacial compatibility in hybrid material systems
[AD-A192921] N88-27264
HEAT SINKS
Forced-convection, liquid-cooled, microchannel heat sinks
[AD-A193337] N88-27444
HEAT SOURCES
Storage of thermal energy by means of an absorption cycle
[PB88-190814] N88-27619
HEAT STORAGE
Prediction of velocity and temperature profiles in thermally driven gravity currents applied to stratified thermal storage tanks
[DE88-004452] N88-27496
HEAT TOLERANCE
Hyperthermia: New thoughts on an old problem
[AD-A192602] N88-27731
HEAT TRANSFER
Development of an experimental system for studying fast transient ignition phenomena
[DE88-011917] N88-27276
Ceramic technology for advanced heat engines project
[DE88-008945] N88-27323
Determination of lumped-mass thermal properties associated with autoclave curing of graphite/epoxy composites N88-27364
Heat and mass transfer in a transport channel
[DE88-701968] N88-27493
Determination of the local heat-transfer characteristics on glaze ice accretions on a cylinder and a NACA 0012 airfoil N88-27500
Heat and mass transfer in laminar wavy film absorption with the presence of non-absorbable gases N88-27502
Plasma behavior in the boundary layer near a railgun surface
[DE88-008889] N88-27909
HEAT TREATMENT
Stress corrosion of C ring specimen in salt spray tests
[I-186/87] N88-27307
High-speed, precision processing using an electron beam N88-27391
Preparation and development of advanced battery catalysts
[AD-A193208] N88-27441
HEATING
Numerical calculations of dopent diffusion involving flashlamp heating of silicon N88-27384
Thermal-sensation control: A new method of controlling cooled/heated environments N88-27394
Effects of surface tension and contact angle on sensible heating and boiling incipience in dielectric falling films
[DE88-007057] N88-27492
HELICOPTER DESIGN
Aeroelastic characteristics of the AH-64 bearingless tail rotor N88-27162

HELICOPTER PERFORMANCE
Robust digital model following controller for helicopters
[DFVLR-FB-88-07] N88-27203
HELICOPTERS
A comparison of the various helicopter mathematical models used in the methodology assessment N88-27149
A comparison of theory and experiment for aeroelastic stability of a hingeless rotor model in hover N88-27150
A comparison of theory and flight test of the BO 105/BMR in hover and forward flight N88-27155
Comparison of experimental coupled helicopter rotor/body stability results with a simple analytical model N88-27160
HELIOSTATS
Performance evaluation of large-area glass-mirror heliostats
[DE88-011883] N88-27636
Optical evaluation of prototype stretched-membrane mirror modules for solar central receivers
[DE88-011884] N88-27637
HELIUM
Improved adhesion for SiO2 particles in silica substrates using helium-ion irradiation
[DE88-006915] N88-27332
Mass flow rate influence on void fraction of two-phase helium flow
[DE88-702456] N88-27495
Temperature rise in superfluid helium pumps
[NASA-TM-100997] N88-27507
HELMET MOUNTED DISPLAYS
Assessments of maneuverability with the TeleOperated Vehicle (TOV)
[AD-A191584] N88-27751
HEMOGLOBIN
Effects of pulsed and CW (Continuous Wave) 2450 MHz radiation on transformation and chromosomes of human lymphocytes in vitro
[AD-A193104] N88-27736
HERMITIAN POLYNOMIAL
A taxonomy for conjugate gradient methods
[DE88-006574] N88-27817
HEURISTIC METHODS
Three-dimensional scene analysis using stereo based imaging
[AD-A193120] N88-27178
An investigation of performance improvement in knowledge-based control systems N88-27382
HIERARCHIES
Update on the meso-microscale meteorological hierarchy
[DE88-009133] N88-27670
HIGH ENERGY INTERACTIONS
Studying the physics and operation of multi-terminal near-micron and sub-micron length, hot electron semiconductor devices
[AD-A193380] N88-27446
HIGH FREQUENCIES
Performance study of a unipole antenna with conventional and elevated radial wire ground screens
[AD-A193283] N88-27413
Calculations of high-frequency parameters of disc-loaded waveguides
[DE88-702178] N88-27417
HIGH IMPULSE
Production of intensive electron beam impulsions by setup of pseudoglare discharges
[ISL-CO-210/87] N88-27920
HIGH POLYMERS
Investigations on drag reduction in turbulent pipe flows by addition of ionic and nonionic high polymers
[ETN-88-92360] N88-27515
HIGH PRESSURE
Investigation of hydrogen isotope penetration through stainless steels Kh18N10T and Kh3M2BFR
[DE88-702189] N88-27297
HIGH RESOLUTION
Enhancement of modeling and image generation techniques for high-resolution 3-dimensional imagery
[DE88-008923] N88-27782
HIGH REYNOLDS NUMBER
Analysis of experimental data for cast 10-2/DOA2 supercritical airfoil at high Reynolds numbers
[AD-A192827] N88-27166
HIGH SPEED
The MELMUX MX-7100 series high-speed digital multiplexers N88-27396
HIGH STRENGTH STEELS
Analysis of crack arrest toughness
[AD-A193340] N88-27286
Development of high strength and toughness microcomposite HSLA Fe/Cr/Mn/C steel with and without Nb
[DE88-009813] N88-27290
HIGH TEMPERATURE
Creep behavior for Hastelloy-XR
[DE88-753428] N88-27295
Investigation of hydrogen isotope penetration through stainless steels Kh18N10T and Kh3M2BFR
[DE88-702189] N88-27297
Kinetic of oxidation to air of a Fe-Al-Mn alloy system at 600-800(sup 0)C temperature range
[DE88-702309] N88-27330
Properties of new low dimensional materials and mechanisms of high T(sub c) superconductivity
[DE88-012026] N88-27951
HIGH TEMPERATURE SUPERCONDUCTORS
Compilation of NRL publications on high temperature superconductivity
[AD-A189137] N88-27921
Anharmonic model for high-Tc superconductors
[DE88-702196] N88-27924
HILBERT TRANSFORMATION
Approximation problems of the Hilbert transform to identify minimum phase linear systems
[FUB-42-1986] N88-27790
HISTORIES
High-temperature superconductivity: An overview
[DE88-702051] N88-27925
History of manned spaceflight
[CNES-NT-121] N88-28000
HOLES (ELECTRON DEFICIENCIES)
Inelastic electron scattering and electron-hole excitations in iron and nickel
[DE88-011843] N88-27303
HOLES (MECHANICS)
Hole diameters in plates impacted by projectiles N88-27386
HOLOGRAPHIC INTERFEROMETRY
Turbulent flow field visualization with integral interferometric imaging and computed tomography N88-27521
HOLOGRAPHY
Precise rotational alignment of X-ray transmission diffraction gratings
[DE88-010599] N88-27273
HOMOGENEITY
Homogeneity of glasses: Experiment WL-IHF-05 in D1 mission — Spacelab
[ETN-88-92339] N88-27353
HOT ELECTRONS
Studying the physics and operation of multi-terminal near-micron and sub-micron length, hot electron semiconductor devices
[AD-A193380] N88-27446
HOT ISOSTATIC PRESSING
Hot isostatic pressing of tungsten-nickel-iron composites
[PB88-203070] N88-27292
HOVERING
A comparison of theory and experiment for coupled rotor-body stability of a hingeless rotor model in hover N88-27152
A comparison of theory and experiment for coupled rotor body stability of a bearingless rotor model in hover and forward flight N88-27154
Effects of static equilibrium and higher-order nonlinearities on rotor blade stability in hover N88-27157
A conceptual design study of a hovering system controller for an autonomous underwater vehicle
[AD-A193423] N88-27399
HUBS
A comparison of theory and flight test of the BO 105/BMR in hover and forward flight N88-27155
HUMAN BEINGS
Effects of pulsed and CW (Continuous Wave) 2450 MHz radiation on transformation and chromosomes of human lymphocytes in vitro
[AD-A193104] N88-27736
Demodulation processes in auditory perception
[AD-A193421] N88-27740
HUMAN BODY
Behavioral, psychological and demographic predictors of physical fitness
[AD-A192697] N88-27733
HUMAN CENTRIFUGES
Physiological monitoring methodology in the USAFSAM centrifuge N88-27356
HUMAN FACTORS ENGINEERING
A human factors evaluation of the Advanced Visual Technology System (AVTS) eye tracking oculometer N88-27361
The human element in space: Lessons from Antarctica
[AD-A193440] N88-27741
The assessment of human/computer performance using human productivity measures: MIPS and BIPS are MEGAFLOPS
[DE87-013491] N88-27750
Issues in computer-assisted interpretation of graphs and quantitative information
[PB88-116280] N88-27783
HUMAN PERFORMANCE
Electric and Magnetic Activity of the Central Nervous System: Research and Clinical Applications in Aerospace Medicine
[AGARD-CP-432] N88-27683
Studies of the intact human brain: Implications for performance N88-27684
The effects of hypoxia on P300 and reaction time
[DCIEM-87-RR-12] N88-27697
Can CNV amplitude predict ability to accomplish a demanding task? N88-27700
Physiological responses to acute exercise-heat stress
[AD-A192606] N88-27732
Determinants of dual-task interference and resource theories in cognitive psychology
[DFVLR-FB-88-14] N88-27748
HUMAN TOLERANCES
Human response to prolonged motionless suspension in four types of full body harnesses N88-27387
HUMIDITY
Intercomparison of NMC (National Meteorological Center) and ECMWF (European Centre for Medium Range Weather Forecasts) global analyses: 1980-1986
[PB88-196548] N88-27668
HYBRID COMPUTERS
Simulation of real time problem solving
[AD-A193436] N88-27778
HYDRAULIC EQUIPMENT
Hydraulic pumps and hydraulic equipment at low temperatures
[DE88-752871] N88-27570
HYDRAULIC FLUIDS
Hydraulic pumps and hydraulic equipment at low temperatures
[DE88-752871] N88-27570
HYDROCARBON COMBUSTION
Laser probes of natural gas ignition chemistry
[PB88-212568] N88-27271
HYDROCARBON FUELS
Carbon deposition model for oxygen-hydrocarbon combustion, volume 1
[NASA-CR-179375] N88-27254
Carbon deposition model for oxygen-hydrocarbon combustion, volume 2
[NASA-CR-179376] N88-27255
Hydrocarbon fuel spill dispersion on water: Literature review
[AD-A192486] N88-27346
HYDRODYNAMICS
A study of fluid-structure problems N88-27468
Numerical simulation of fuel droplet interactions and breakup
[AD-A192431] N88-27470
Research on ocean forecasting and nonlinear wave propagation and numerical hydrodynamics in the ocean
[AD-A193363] N88-27680
HYDROGEN
A method for determining the solubility of hydrogen in molten aluminum-lithium alloys
[DE88-009807] N88-27270
Theory of the dissociation dynamics of small molecules on metal surfaces: Finite temperature studies
[DE88-007763] N88-27882
HYDROGEN ISOTOPES
Investigation of hydrogen isotope penetration through stainless steels Kh18N10T and Kh3M2BFR
[DE88-702189] N88-27297
HYDROGRAPHY
Beaufort sea mesoscale circulation study: Hydrography helicopter operations, April 1987
[PB88-203658] N88-27681
HYDROTHERMAL SYSTEMS
Geothermal energy technology: Issues, R and D (Research and Development) and cooperative arrangements
[PB88-193107] N88-27626
HYPERBOLIC DIFFERENTIAL EQUATIONS
Feedback control of a hyperbolic partial-differential equation with viscoelastic damping
[AD-A192896] N88-27810
HYPERCUBE MULTIPROCESSORS
Motor-response learning at a process control panel by an autonomous robot
[DE88-005055] N88-27554
Parallel implementation of the boundary element method
[DE88-011846] N88-27839
HYPERSONIC AIRCRAFT
Supersonic transport/hypersonic transport (SST/HST) development
[SNIAS-881-111-101] N88-27192

HYPERSONIC FLIGHT
Hypersonic flight testing
[DE88-001655] N88-27894
HYPERSONIC SPEED
A computational analysis of under-expanded jets in the hypersonic regime
[NASA-TM-101319] N88-27174
HYPERSONIC VEHICLES
Aerodynamics of Hypersonic Lifting Vehicles: Fluid Dynamics Panel AGARD Symposium
[AGARD-AR-246] N88-27480
HYPERTHERMIA
Hyperthermia: New thoughts on an old problem
[AD-A192602] N88-27731
HYPERVELOCITY IMPACT
Hypervelocity impact analysis with supercomputers
[DE88-008907] N88-27797
HYPERVELOCITY PROJECTILES
Variable Mach number wall jets for control/propulsion on hypervelocity projectiles/interceptors: Tests with an existing model
[AD-A192845] N88-27167
HYPOGLYCEMIA
Spontaneous cerebral electrical activity during prolonged hypoglycemia: A quantitative study in humans N88-27717
HYPOTHALAMUS
Hypothalamic-pituitary-adrenal responses to short duration high intensity cycle exercise
[AD-A192597] N88-27727
HYPOXIA
The effects of hypoxia on P300 and reaction time
[DCIEM-87-RR-12] N88-27697
The effect of mild hypoxia on the vestibular evoked response N88-27713

I

ICE
MIZPAC (marginal ice zone Pacific) 84-86 CTD (Conductivity, Temperature, Depth) data report
[AD-A192478] N88-27679
ICE FORMATION
Determination of the local heat-transfer characteristics on glaze ice accretions on a cylinder and a NACA 0012 airfoil N88-27500
IGNITERS
Some properties of ignition gases. Review of measuring results in the years 1981-1986)
[PB88-106968] N88-27259
IGNITION
Effects of ceramic surfaces on autoignition in a constant volume combustion apparatus
[AD-A193055] N88-27266
Laser probes of natural gas ignition chemistry
[PB88-212568] N88-27271
Development of an experimental system for studying fast transient ignition phenomena
[DE88-011917] N88-27276
Shock initiation studies on heterogeneous explosives
[DE88-008681] N88-27351
Diode laser ignition of high explosives and pyrotechnics
[DE88-008771] N88-27352
IMAGE ANALYSIS
Automatic line network extraction from aerial imagery of urban areas through knowledge based image analysis
[AD-A193067] N88-27615
Remote sensing of wetlands: Applications overview
[DE88-010895] N88-27618
IMAGE CONTRAST
The FEL CCD-camera: Experimental system for camera and image processing research
[FEL-1987-34] N88-27532
IMAGE ENHANCEMENT
Enhancement of modeling and image generation techniques for high-resolution 3-dimensional imagery
[DE88-008923] N88-27782
IMAGE PROCESSING
Three-dimensional scene analysis using stero based imaging
[AD-A193120] N88-27178
Applications of differential geometry to the shape analysis of gray-value images N88-27358
Optical interconnections for digital image coding N88-27381
Linear feature extraction from radar imagery. Phase 2: Base contract report
[AD-A192828] N88-27404
The design of a digital Eprom oscillator for electrical impedance tomography
[DE88-012243] N88-27462
The FEL CCD-camera: Experimental system for camera and image processing research
[FEL-1987-34] N88-27532
Phase comparator for range imaging laser radar
[DE88-008109] N88-27545
Interface control using low frequency (3 to 20 MHz) acoustic microscopy
[REPT-48-411/F] N88-27577
Automatic line network extraction from aerial imagery of urban areas through knowledge based image analysis
[AD-A193067] N88-27615
Review of geographic processing techniques applicable to regional analysis
[DE88-010759] N88-27643
Photon limited image processing in the space-time domain
[AD-A193142] N88-27655
Effects of pulsed and CW (Continuous Wave) 2450 MHz radiation on transformation and chromosomes of human lymphocytes in vitro
[AD-A193104] N88-27736
Texture perception and shape from texture
[AD-A192923] N88-27771
Research into the architecture of CAD based robot vision systems
[AD-A193330] N88-27776
Enhancement of modeling and image generation techniques for high-resolution 3-dimensional imagery
[DE88-008923] N88-27782
Maximum entropy signal restoration with linear programming
[DE88-011740] N88-27787
Contribution to almost realistic picture processing by a computer graphics procedure
[ETN-88-92372] N88-27789
Image processing using a parallel architecture
[AD-A192833] N88-27803
IMAGING RADAR
Phase comparator for range imaging laser radar
[DE88-008109] N88-27545
IMAGING TECHNIQUES
Optical diagnostics for metallurgical processes
[DE88-009255] N88-27289
Ellipsometric imaging of drying sol-gel films
[DE88-011785] N88-27335
Turbulent flow field visualization with integral interferometric imaging and computed tomography N88-27521
Optical imaging diagnostics for fusion plasmas
[DE88-997572] N88-27910
Application of two-dimensional imaging to very high energy gamma ray astronomy
[DE88-010120] N88-27983
IMMOBILIZATION
Human response to prolonged motionless suspension in four types of full body harnesses N88-27387
IMPACT DAMAGE
Design manual for impact damage tolerant aircraft structure, addendum
[AGARD-AG-238-ADD] N88-27185
Hole diameters in plates impacted by projectiles N88-27386
IMPACT RESISTANCE
Improved procedure for impact probability computation of aircraft crash based on Balfanz model
[JUEL-SPEZ-425] N88-27176
Deformation, fracture and explosive properties of reactive materials
[AD-A193080] N88-27348
IMPACT STRENGTH
Relation between the mechanical characteristics of carbon-resin composites and their impact strength
[REPT-48-284/F] N88-27249
IMPACT TESTS
Hypervelocity impact analysis with supercomputers
[DE88-008907] N88-27797
IMPACT TOLERANCES
Design manual for impact damage tolerant aircraft structure, addendum
[AGARD-AG-238-ADD] N88-27185
IMPEDANCE
Some equivalent circuit models for AC impedance analysis of pyrite/solution interface
[DE88-010574] N88-27452
IMPELLERS
A study of fluid-structure problems N88-27468
IMPLANTATION
NDP (Neutron Depth Profiling) evaluations of boron-implanted compound semiconductors
[AD-A192306] N88-27425
IMPULSES
Fiber-optics used to record high-speed photographs inside a pressurized tank during lethality testing
[DE88-011283] N88-27529
IMPURITIES
Diffusion and solubility of some interstitial impurities in deformed metals
[DE88-701659] N88-27296
Application of Auger electron spectroscopy to the study of trace element effects on weldability
[DE88-010457] N88-27301
Prediction of deep levels and equilibrium concentrations of defects in semiconductors N88-27945
X-ray studies of strain, interface and impurities in semiconductors
[DE88-012460] N88-27954
IN-FLIGHT MONITORING
In-flight load measurements of the Robot-X canards
[AD-A193428] N88-27187
Robust digital model following controller for helicopters
[DFVLR-FB-88-07] N88-27203
INCOMPRESSIBLE FLOW
Computational boundary conditions for the incompressible Navier-Stokes equations in channels and pipes
[AD-A193356] N88-27487
Numerical treatment of the pressure singularity at a re-entrant corner
[AD-A193357] N88-27488
A fast vortex code for computing 2-D flow in a box
[DE88-011732] N88-27498
Numerical methods for incompressible viscous flows with engineering applications
[NASA-CR-183143] N88-27508
INCOMPRESSIBLE FLUIDS
Higher order vortex methods with rezoning
[DE88-010777] N88-27505
Distributive iteration for indefinite systems as smoothing method in multigrid process on example of Stokes and Navier-Stokes equations with emphasis on incomplete decompositions
[ETN-88-92127] N88-27509
INDEPENDENT VARIABLES
Superconducting thin films, composites and junctions
[AD-A193123] N88-27440
INDEXES (DOCUMENTATION)
An assessment of index term ranking N88-27974
INDICATING INSTRUMENTS
The P delta V fundamental gas leak calibration system qualification report
[DE88-008964] N88-27526
INDIUM
Device physics related to the granular nature of CuInSe2 solar cells
[DE88-001159] N88-27622
INDIUM ARSENIDES
Photodiodes for optical communication in the near infrared
[ETN-88-92379] N88-27900
INDIUM PHOSPHIDES
Investigations on the MBE (Molecular Beam Epitaxy) growth and properties of Al(sub y)Ga(sub y)In(sub 1-x-y)AsInP and InGaAs-InAlAs superlattices
[DE88-009105] N88-27941
INDUSTRIAL WASTES
Waste destruction by plasma
[SNIAS-881-430-113] N88-27651
INDUSTRIES
Federal Council on Science, Engineering and Technology: Committee on Computer Research and Applications, Subcommittee on Science and Engineering Computing: The US Supercomputer Industry
[DE88-011262] N88-27756
INELASTIC SCATTERING
Inelastic electron scattering and electron-hole excitations in iron and nickel
[DE88-011843] N88-27303
INERTIAL PLATFORMS
Application of the Single-Axis rate Table (SAT) of the DFVLR for the evaluation of stationary and dynamic gyro properties
[DFVLR-MITT-88-09] N88-27533
INFORMATION MANAGEMENT
Developing a connector selection DBMS (database management system) using NIAM (Nijssen's Information Analysis Methodology)
[DE88-008110] N88-27972
Pattern information processing and multimedia database system: Current research on multimedia information system
[PB88-131917] N88-27973
INFORMATION PROCESSING (BIOLOGY)
A review of workload measurement in relation to verbal comprehension N88-27360
The effects of increased cognitive demands on autonomic self-regulation: An indicator of parallel processing in the brain N88-27362
Mitsubishi Electric Advance (R and D Edition), Volume 41
[PB88-194162] N88-27388
Basic research on optical neural computers N88-27389

Electric and Magnetic Activity of the Central Nervous System: Research and Clinical Applications in Aerospace Medicine
[AGARD-CP-432] N88-27683
Dissecting the visual and auditory pathways by means of the two-input technique N88-27690
Electric and magnetic brain activity related to cognitive performance N88-27692
Neuromagnetic evidence of place mechanisms for frequency and intensity coding in the human auditory cortex N88-27693
A study of sources in the human brain associated with stereopsis N88-27695
The effects of hypoxia on P300 and reaction time
[DCIEM-87-RR-12] N88-27697
Using ERPS to study human information processing N88-27698
The effect of mild hypoxia on the vestibular evoked response N88-27713

INFORMATION RETRIEVAL
Use of optical disk technology at the Air Command and Staff College
[AD-A192424] N88-27969
Capitalizing on experience with intelligence gateway software
[AD-A193382] N88-27971
An assessment of index term ranking N88-27974

INFORMATION SYSTEMS
Capitalizing on experience with intelligence gateway software
[AD-A193382] N88-27971

INFRARED ABSORPTION
Calculation of far infrared absorption in B poly(dA).poly(dT)
[AD-A193128] N88-27318

INFRARED DETECTORS
Photodiodes for optical communication in the near infrared
[ETN-88-92379] N88-27900

INFRARED IMAGERY
Cyrogenic test facilities for an optical cryomechanism qualification
[SNIAS-881-440-116] N88-27219

INFRARED RADIATION
Far- and mid-infrared properties of metal-insulator composite materials
[AD-A193227] N88-27236
Development of radiation and cloud parameterization programs for AFGL (Air Force Geophysics Laboratory) global models
[AD-A193369] N88-27658

INFRARED SPECTRA
Development of an experimental system for studying fast transient ignition phenomena
[DE88-011917] N88-27276

INFRARED SPECTROMETERS
Calibration and data reduction techniques for the AFGL infrared array spectrometer N88-27374

INFRARED WINDOWS
Growth and characterization of CuGaS2, CuAlS2 and CuGa0.9Al0.1S2 single crystals
[AD-A192963] N88-27930

INHOMOGENEITY
Experimental investigation of simplest inhomogeneities in cylindrical slit line
[DE88-702368] N88-27418

INITIATION
Shock initiation studies on heterogeneous explosives
[DE88-008681] N88-27351

INJECTION
Design of divertor plate and measurements of double-null open divertor plasma in the JFT-2M tokamak
[DE88-753130] N88-27914

INJECTORS
Initial electron distributions for free-electron lasers generated by injector and accelerator simulations
[DE88-007022] N88-27540

INNER RADIATION BELT
Approximate analytical formulae for electron density and collision frequency in the natural and nuclear-disturbed ionosphere and inner magnetosphere
[AD-A193129] N88-27654

INSPECTION
Inspection methods in programming: Cliches and plans
[AD-A192782] N88-27767
Use of Moessbauer spectroscopy to study implanted surfaces
[DE88-010452] N88-27942

INSULATION
Far- and mid-infrared properties of metal-insulator composite materials
[AD-A193227] N88-27236

INSULATORS
Data compilation for radiation damage on ceramic insulators. Revised with updated data and reviews
[DE88-753426] N88-27329

INTEGERS
Factorization of large integers on a massively parallel computer
[DE88-011625] N88-27786

INTEGRALS
Evaluation of quantum mechanics path integrals by the approximations exact on a class of polynomial functionals
[DE88-702434] N88-27865

INTEGRATED CIRCUITS
Picosecond optoelectronic sampling of electrical waveforms produced by an optically excited field effect transistor
[AD-A192384] N88-27428
A planar IC-compatible transferred electron device for millimeter-wave operation
[AD-A192692] N88-27433
Guided wave interactions in millimeter-wave integrated circuits
[AD-A193017] N88-27437
Very High Speed Integrated Circuits (VHSIC)
[AD-A193225] N88-27442
Silicon-on-insulator pin diodes
[AD-A193359] N88-27445
STAR: Sandia Timing Analyzer Routine
[DE88-012412] N88-27463
Molecular beam epitaxy of GaP films on Si substrates
[PB88-131974] N88-27923
Dose-enhancement effects in TaSi/Al- and Al-gate MOS devices
[DE88-005483] N88-27926

INTERACTIONAL AERODYNAMICS
Theory of sound production by vortex-airfoil interaction
[AD-A193386] N88-27875

INTERFACES
Twin boundaries and heterophase interfaces in ferroelastic martensites
[DE88-011894] N88-27304
Effects of near interfacial microstructure on toughness and subcritical crack growth in ceramic/metal systems
[DE88-009842] N88-27325
Application of controlled interfacial pore structures to kinetic studies in alumina
[DE88-010884] N88-27326
Some equivalent circuit models for AC impedance analysis of pyrite/solution interface
[DE88-010574] N88-27452
Synopsis of a computer program designed to interface a personal computer with the fast data acquisition system of a time-of-flight mass spectrometer
[NASA-CR-177474] N88-27798
X-ray studies of strain, interface and impurities in semiconductors
[DE88-012460] N88-27954
Capitalizing on experience with intelligence gateway software
[AD-A193382] N88-27971

INTERFACIAL ENERGY
Adhesion of hydrated silicate films
[DE88-011250] N88-27333

INTERFACIAL TENSION
Interfacial tension of immiscible polymer blends: Temperature and molecular weight dependence
[AD-A192483] N88-27312
Rubber-modified epoxies: Interfacial tension and morphology
[AD-A192484] N88-27313
Plasma treatment of polymers for improved adhesion
[DE88-011623] N88-27334
Effects of surface tension and contact angle on sensible heating and boiling incipience in dielectric falling films
[DE88-007057] N88-27492

INTERFEROMETERS
Equipment for an advanced electron beam lithography system
[AD-A192956] N88-27435

INTERFEROMETRY
Is the 3C273 quasar Mach nearer
[DE88-702235] N88-27988

INTERMEDIATE FREQUENCIES
Performance study of a unipole antenna with conventional and elevated radial wire ground screens
[AD-A193283] N88-27413

INTERMETALLICS
A fundamental understanding of the interfacial compatibility in hybrid material systems
[AD-A192921] N88-27264
Microchemical analysis of polycrystalline Ni3Al and other ordered alloys using the field-ion microscope atom probe
[DE88-011519] N88-27294

INTERNAL COMBUSTION ENGINES
Analytical and experimental investigation of ringless piston concept
[AD-A193213] N88-27559

INTERNATIONAL COOPERATION
European transonic wind tunnel project: Assistance to the design group
[ONERA-RSF-11/0694-GY-010-G] N88-27208
Studies concerning the European transonic wind tunnel
[ONERA-RSF-10/0694-GY-010-G] N88-27209

INTERPLANETARY SPACE
Activities report of the Institute for Extraterrestrial Physics
[MPE-206] N88-27981
Solar flares and magnetospheric particles: Investigations based upon the ONR-602 and ONR-604 experiments
[AD-A193396] N88-27994

INTERPROCESSOR COMMUNICATION
Constructing a highly-available location service for a distributed environment
[AD-A192723] N88-27801
A modular proof of correctness for a network synchronizer
[AD-A192726] N88-27802

INTERSTITIALS
Migration and stability of HgCdTe lattice defects
[AD-A193293] N88-27935

INVARIANCE
Generalized Jordan chains and two bifurcation theorems of Krasnoselskii
[AD-A192353] N88-27845
On the estimation of a variance ratio
[AD-A193190] N88-27854

INVARIANT IMBEDDINGS
Vortices on the world sheet and string's critical dynamics
[DE88-702116] N88-27961

INVERSIONS
Sidelobe level of an adaptive array using the SMI (Sampled Matrix Inversion) algorithm
[AD-A193131] N88-27409

INVERTERS
Reduced order modeling of grid-connected photovoltaic inverter systems
[DE88-010603] N88-27635

INVISCID FLOW
Higher order vortex methods with rezoning
[DE88-010777] N88-27505

IODINE
Measurement of pressure fluctuations in a resonant chamber with laser-induced iodine fluorescence
[DFVLR-FB-87-53] N88-27551
Growth and characterization of CuGaS2, CuAlS2 and CuGa0.9Al0.1S2 single crystals
[AD-A192963] N88-27930

ION BEAMS
Equipment for building and testing superconductive flux flow electronic devices
[AD-A192959] N88-27436
Propagation of charged particle beams in the atmosphere
[AD-A193195] N88-27887

ION DISTRIBUTION
Moment approach to neoclassical flows, currents and transport in auxiliary heated tokamaks
[DE88-008024] N88-27901

ION IMPLANTATION
A fundamental understanding of the interfacial compatibility in hybrid material systems
[AD-A192921] N88-27264
Thin film and near-surface characterization using a mechanical properties microprobe
[DE88-011399] N88-27302
Focused ion beam fabrication of graded channel FETs in GaAs and Si
[AD-A193098] N88-27439
Friction, wear and electrical contact resistance of precious metal alloys
[DE88-011244] N88-27450
Use of Moessbauer spectroscopy to study implanted surfaces
[DE88-010452] N88-27942

ION TEMPERATURE
Effects of low reflection on the collector and source sheaths of a finite ion temperature plasma
[DE88-008929] N88-27908

IONIZATION
Multiphoton ionization of alkaline earth atoms in an intense laser field
[DE88-008078] N88-27884
The influence of ionization within a plasma opening switch
[AD-A193147] N88-27906

IONOSPHERIC DISTURBANCES
Approximate analytical formulae for electron density and collision frequency in the natural and nuclear-disturbed ionosphere and inner magnetosphere
[AD-A193129] N88-27654
IONS
Ion Bernstein modes in current-carrying plasmas N88-27903
Theory and simulation of relaxed plasmoids
[AD-A192884] N88-27997
IRIDIUM
Catalytic activation of carbon dioxide by metal complexes
[AD-A192310] N88-27262
IRON
Inelastic electron scattering and electron-hole excitations in iron and nickel
[DE88-011843] N88-27303
Kinetic of oxidation to air of a Fe-Al-Mn alloy system at 600-800(sup 0)C temperature range
[DE88-702309] N88-27330
Perfluoropolyalkylether lubricants under boundary conditions: Iron catalysis of lubricant degradation
[AD-A193241] N88-27560
IRON ALLOYS
Hot isostatic pressing of tungsten-nickel-iron composites
[PB88-203070] N88-27292
IRRADIATION
Effects of electron beam irradiation on mechanical properties at low and high temperature of fiber reinforced composites using PEEK as matrix material
[DE88-753134] N88-27239
Improved adhesion for SiO2 particles in silica substrates using helium-ion irradiation
[DE88-008915] N88-27332
Assessment of cochlear damage after microwave irradiation
[AD-A193237] N88-27737
ISOLATION
The human element in space: Lessons from Antarctica
[AD-A193440] N88-27741
ISOTHERMAL FLOW
Liquid crystals for unsteady surface shear stress visualization
[DE88-010570] N88-27527
ISOTOPE EFFECT
Thermal conductivity of isotopically pure semiconductors, superlattices, semiconductor alloys and semiconductors as a function of temperature; control of the segregation coefficient in LEC crystal growth; and photo-Hall measurements of GaAs N88-27375
ISOTROPISM
The two isotropic asymptotes of fiber composites
[AD-A192305] N88-27231
ITALY
Utilization of a satellite communication system to protect the national communication network
[FUB-33-1986] N88-27423
ITERATION
SARLAC: A relativistic electron beam code
[AD-A193134] N88-27411
KRYSI, an ODE solver combining a semi-implicit Runge-Kutta method and a preconditioned Krylov method
[DE88-012245] N88-27841
ITERATIVE SOLUTION
Distributive iteration for indefinite systems as smoothing method in multigrid process on example of Stokes and Navier-Stokes equations with emphasis on incomplete decompositions
[ETN-88-92127] N88-27509

J

JET AIRCRAFT
Pilot report: AFTI (Advanced Fighter Technology Integration) F-111
[AD-A192937] N88-27184
JET CONTROL
Variable Mach number wall jets for control/propulsion on hypervelocity projectiles/interceptors: Tests with an existing model
[AD-A192845] N88-27167
JET ENGINE FUELS
A study relating to the fog oil replacement program
[AD-A192536] N88-27347
JET ENGINES
A fundamental understanding of the interfacial compatibility in hybrid material systems
[AD-A192921] N88-27264
JET FLAPS
Investigations of aircraft control with jet spoilers
[ISL-R-112/87] N88-27202
JET FLOW
A computational analysis of under-expanded jets in the hypersonic regime
[NASA-TM-101319] N88-27174
Coupled experimental and theoretical investigations of instability, chaos and turbulence in an axisymmetric jet flow
[AD-A192943] N88-27476
Turbulence structure of mixing swirling flows
[AD-A193063] N88-27478
JET PROPULSION
Variable Mach number wall jets for control/propulsion on hypervelocity projectiles/interceptors: Tests with an existing model
[AD-A192845] N88-27167
JOINTS (JUNCTIONS)
General expression of manipulator kinematics
[DE88-753430] N88-27567
JOURNAL BEARINGS
A lubrication study of engine bearings N88-27574
JUDGMENTS
Rules, schema and decision making
[AD-A193389] N88-27967
JUPITER (PLANET)
Interpretation of the polarimetric observations of Jupiter
[DE88-702414] N88-27991

K

KALMAN FILTERS
Control, stability and filter for a discrete linear stochastic system with correlated noise
[PB88-109525] N88-27818
KAONS
Study of the production of Ko mesons in proton antiproton interactions at 630 GeV
[NOTA-INTERNA-908] N88-27892
KEVLAR (TRADEMARK)
NDE performance in predicting failure strength of spherical composite specimens with implanted flaws
[DE88-008223] N88-27575
Use of microwave measuring systems for the nondestructive control of resins and composites
[SNIAS-881-430-123] N88-27576
KINEMATICS
Aeroelastic modeling of rotor blades with spanwise variable elastic axis offset: Classic issues revisited and new formulations N88-27158
Control and use of unsteady flows: Insect use of various wing kinematics and related pressure measurements using a pitching airfoil N88-27366
Control of free-flying space robot manipulator systems
[NASA-CR-183017] N88-27562
General expression of manipulator kinematics
[DE88-753430] N88-27567
Dexterous hands: Optimizing grasp by design and planning N88-27572
KINETIC THEORY
Kinetic theory for plane flows of rough, inelastic, circular disks N88-27499
KINETICS
Kinetic of oxidation to air of a Fe-Al-Mn alloy system at 600-800(sup 0)C temperature range
[DE88-702309] N88-27330
KONDO EFFECT
Interactions between superconductivity and Kondo-grid properties in CeCu2Si2. Measurement results of specific heat under high pressure
[ETN-88-92377] N88-27958

L

LABORATORIES
Development of radiation and cloud parameterization programs for AFGL (Air Force Geophysics Laboratory) global models
[AD-A193389] N88-27658
Activities report of the Werner-Heisenberg Institute of Physics
[ETN-88-92946] N88-27893
LAMINAR BOUNDARY LAYER
Analysis of experimental data for cast 10-2/DOA2 supercritical airfoil at high Reynolds numbers
[AD-A192827] N88-27166
LAMINAR FLOW
The structure and stability of nonpremixed gas jet flames N88-27257
Turbulent flow field visualization with integral interferometric imaging and computed tomography N88-27521
LAMINAR HEAT TRANSFER
Forced-convection, liquid-cooled, microchannel heat sinks
[AD-A193337] N88-27444
LAMINATES
The two isotropic asymptotes of fiber composites
[AD-A192305] N88-27231
An experimental and analytical evaluation of a biaxial test for determining shear properties of composite materials
[NASA-CR-182928] N88-27593
LANTHANUM COMPOUNDS
Compilation of NRL publications on high temperature superconductivity
[AD-A189137] N88-27921
Anharmonic model for high-Tc superconductors
[DE88-702196] N88-27924
LANTHANUM OXIDES
Superconducting properties of LaBa2Cu3O(sub x) and YBa2Cu3O(sub y)
[DE88-012038] N88-27952
LARGE SPACE STRUCTURES
Spacecraft applications of advanced global positioning system technology
[NASA-CR-172055] N88-27180
Technology for large space systems: A bibliography with indexes (supplement 18)
[NASA-SP-7046(18)] N88-27214
Vibration control of large structures
[AD-A193317] N88-27587
LASER ANNEALING
Laser spectroscopy investigations of materials for solid state laser systems
[AD-A192514] N88-27535
LASER APPLICATIONS
Study of feasibility and optimization conditions of laser treatments: Application of the local recrystallization of aluminum
[ISAL-87-0048] N88-27309
Attachable interferometric strain gages
[AD-A192390] N88-27522
Measurement of pressure fluctuations in a resonant chamber with laser-induced iodine fluorescence
[DFVLR-FB-87-53] N88-27551
LASER DOPPLER VELOCIMETERS
Laser-Doppler measurements of turbulence structures in free streams behind flat and rotation symmetrical profiles
[ETN-88-92336] N88-27510
LASER HEATING
Laser-heated CVD process for depositing thin films for low-cost solar-cell applications
[DE88-001162] N88-27623
LASER INDUCED FLUORESCENCE
Velocity measurements and flow visualization in turbulent three-dimensional supersonic flows using oxygen flow tagging
[AD-A192551] N88-27165
Laser probes of natural gas ignition chemistry
[PB88-212568] N88-27271
Measurement of pressure fluctuations in a resonant chamber with laser-induced iodine fluorescence
[DFVLR-FB-87-53] N88-27551
LASER INTERFEROMETRY
Attachable interferometric strain gages
[AD-A192390] N88-27522
LASER OUTPUTS
Predicting optical degradation of a laser beam through a turbulent shear layer N88-27376
Wave equations for pulse propagation
[DE88-011760] N88-27548
Multiphoton ionization of alkaline earth atoms in an intense laser field
[DE88-008078] N88-27884
Theory and simulation of relaxed plasmoids
[AD-A192884] N88-27997
LASER PLASMAS
Target designs for plasma-implosion-driven, photoionization-pumped soft X-ray lasers
[DE88-011278] N88-27547
LASER PUMPING
A plasma ultraviolet source for short wavelength lasers
[AD-A192844] N88-27537
Overview and future direction for blackbody solar-pumped lasers
[NASA-TM-100621] N88-27553
LASER RANGE FINDERS
Phase comparator for range imaging laser radar
[DE88-008109] N88-27545
IEMIS (Integrated Emergency Management Information System) floodplain mapping based on a LIDAR derived data set
[AD-A193071] N88-27616

LASER SPECTROSCOPY
Laser spectroscopy investigations of materials for solid state laser systems
[AD-A192514] N88-27535
Laser spectroscopy of quantum well and superlattice structures
[AD-A193336] N88-27937
LASER TARGETS
Target designs for plasma-implosion-driven, photoionization-pumped soft X-ray lasers
[DE88-011278] N88-27547
LASER WELDING
Process control improvements in pulsed Nd:YAG laser closure welding of electromechanical relays
[DE88-006275] N88-27564
LASERS
Direct measurement of solids: High temperature sensing. Experimental development and testing of high temperature pulsed EMATs
[DE88-009659] N88-27546
Finite element methodology for integrated flow-thermal-structural analysis
[NASA-CR-183144] N88-27606
Future SDI (Strategic Defense Initiative) decision making
[AD-A192794] N88-27660
LATTICE VIBRATIONS
Coupled even-parity superconducting states: Square lattice
[AD-A193432] N88-27938
LATTICES (MATHEMATICS)
An overview of lattice QCD
[DE88-010867] N88-27963
LAUNCH VEHICLES
In-flight motor torque estimates for the second-stage Strypi 9 launch vehicle
[DE88-010833] N88-27222
LAUNCHING BASES
Space shuttle natural environment analysis
[NASA-CR-179337] N88-27676
LAY-UP
Factors affecting strength in composite materials used for aircraft
[DT-212/87] N88-27248
LEAKAGE
The P delta V fundamental gas leak calibration system qualification report
[DE88-008964] N88-27526
LEARNING
Motor-response learning at a process control panel by an autonomous robot
[DE88-005055] N88-27554
LEBESGUE THEOREM
A study on Lebesgue decomposition of measures induced by stable processes
[AD-A192893] N88-27850
LESIONS
Relation between VEP and visual function in lesions of the optic nerve and visual pathway N88-27718
LETHALITY
Fiber-optics used to record high-speed photographs inside a pressurized tank during lethality testing
[DE88-011283] N88-27529
LIAPUNOV FUNCTIONS
Dynamic stability of elastic rotor-bearing systems via Liapunov's direct method N88-27571
Generalized Jordan chains and two bifurcation theorems of Krasnoselskii
[AD-A192353] N88-27845
LIE GROUPS
Superalgebras with Grassmann algebra-valued structure constants from superfields
[DE88-702239] N88-27862
LIFE (DURABILITY)
The relationship between observed fatigue damage and life estimation models
[NASA-CR-182191] N88-27611
LIFE SUPPORT SYSTEMS
Advanced EMU electrochemically regenerable CO2 and moisture absorber module breadboard
[NASA-CR-172054] N88-27754
LIFT
FEB (Multifilter Electronics Box) lifting device analysis, revision A
[AD-A192313] N88-27427
LIFT FANS
Airborne remote operated device
[DE88-010324] N88-27188
LIFTING BODIES
Aerodynamics of Hypersonic Lifting Vehicles: Fluid Dynamics Panel AGARD Symposium
[AGARD-AR-246] N88-27460
LIGHT AMPLIFIERS
Optical guiding in the separable beam limit
[AD-A192452] N88-27534
LIGHT CURVE
To the opportunities of cluster analysis of light curves of supernovae
[DE88-701642] N88-27982
LIGHT GAS GUNS
An investigation of soft launch and instability breakup with a two-stage light gas gun
[DE88-010371] N88-27218
LIGHTNING SUPPRESSION
The first synthesis of chem-prep varistor LAC (Lightning Arrestor Connector) granules
[DE88-008005] N88-27438
LIMITS (MATHEMATICS)
Computation of filters by sampling and quantization
[AD-A192839] N88-27826
LINE SPECTRA
Spectral line shapes from highly ionized sodium plasmas
[AD-A193401] N88-27907
Paramagnetic point defects in boron-implanted HgO.7CdO.3Te
[AD-A193276] N88-27934
LINEAR ACCELERATORS
Research opportunities below 300 nm at the NBS Free-Electron Laser Facility
[AD-A193100] N88-27538
LINEAR EQUATIONS
Parallel quasi-Newton methods for unconstrained optimization
[AD-A193250] N88-27812
A review of parallel methods for solving sets of linear equations and their application within optimisation algorithms
[AD-A193137] N88-27830
The computation of stationary distributions on Markov chains through perturbations
[AD-A193191] N88-27855
LINEAR PROGRAMMING
Linear programming for Air Force decision aiding N88-27378
Maximum entropy signal restoration with linear programming
[DE88-011740] N88-27787
LINEAR SYSTEMS
Characterization of accelerating pipe flow
[AD-A193065] N88-27481
Approximation problems of the Hilbert transform to identify minimum phase linear systems
[FUB-42-1986] N88-27790
LINEARITY
On solvability of an equation arising in the theory of M-estimates
[AD-A193059] N88-27828
LININGS
Basic mechanisms of diesel lubrication correlation of bench and engine tests
[AD-A193360] N88-27561
LIQUID COOLING
Forced-convection, liquid-cooled, microchannel heat sinks
[AD-A193337] N88-27444
LIQUID CRYSTALS
Liquid crystals for unsteady surface shear stress visualization
[DE88-010570] N88-27527
LIQUID FUELS
An outdoor test facility for the large-scale production of microalgae
[DE88-001146] N88-27723
LIQUID METAL FAST BREEDER REACTORS
Computation of failure probability of fatigue loaded cracked structures
[ETN-88-92360] N88-27607
LIQUID METALS
A method for determining the solubility of hydrogen in molten aluminum-lithium alloys
[DE88-009807] N88-27270
LIQUID OXYGEN
Carbon deposition model for oxygen-hydrocarbon combustion, volume 2
[NASA-CR-179376] N88-27255
LITHIUM ALLOYS
A method for determining the solubility of hydrogen in molten aluminum-lithium alloys
[DE88-009807] N88-27270
LITHIUM SULFUR BATTERIES
The kinetics of charge-transfer reactions on passive lithium electrodes
[DE88-009256] N88-27454
LITHOGRAPHY
Precise rotational alignment of X-ray transmission diffraction gratings
[DE88-010599] N88-27273
High-speed, precision processing using an electron beam N88-27391
Equipment for an advanced electron beam lithography system
[AD-A192956] N88-27435
LOAD TESTS
Development of a biaxial test system for thin-walled metal tubes using tensile-compressive axial load and internal-external pressure
[DE88-011279] N88-27592
Modal testing in the design evaluation of wind turbines
[DE88-010374] N88-27632
LOADING RATE
Cold worked reinforcing bars in tensile test under high loading rate and low temperatures
[DE88-752993] N88-27610
LOADS (FORCES)
A comparison of the various helicopter mathematical models used in the methodology assessment N88-27149
Wind tunnel tests of the influence of airfoil-thickness on normal force and pitching moment of two slender wings at transonic and supersonic Mach numbers
[DFVLR-FB-88-17] N88-27171
Thermo-viscoelastic analysis of composite materials, volume 1
[NASA-CR-183048-VOL-1] N88-27230
Analysis of crack arrest toughness
[AD-A193340] N88-27286
A study of fluid-structure problems N88-27468
The influence of weld metal properties, weld geometry and applied load on weld system performance
[AD-A193403] N88-27588
LOGIC CIRCUITS
The design of a digital Eprom oscillator for electrical impedance tomography
[DE88-012243] N88-27462
STAR: Sandia Timing Analyzer Routine
[DE88-012412] N88-27463
LOGISTICS
The assessment of human/computer performance using human productivity measures: MIPS and BIPS are MEGAFLOPS
[DE87-013491] N88-27750
Introduction to artificial intelligence and expert systems
[SNIAS-881-320-101] N88-27814
Expert system contribution to logistics improvement
[SNIAS-881-320-102] N88-27815
LOGISTICS MANAGEMENT
Introduction to artificial intelligence and expert systems
[SNIAS-881-320-101] N88-27814
Expert system contribution to logistics improvement
[SNIAS-881-320-102] N88-27815
LONG TERM EFFECTS
Aging of CFRP due to longterm storage in heated air
[DFVLR-FB-88-05] N88-27345
LONGITUDE
Vertical directionality of ambient noise at 32 deg N as a function of longitude: Tape number 86180
[AD-A193228] N88-27872
LOW ALTITUDE
The low-latitude auroral boundary: Steady-state and time-dependent representations
[AD-A193200] N88-27656
LOW ASPECT RATIO WINGS
Theoretical-numerical study of feasibility of use of winglets on low aspect ration wings at subsonic and transonic Mach numbers at reduce drag
[NASA-CR-4174] N88-27168
LOW COST
Laser-heated CVD process for depositing thin films for low-cost solar-cell applications
[DE88-001162] N88-27623
Finding minimum-cost circulations by successive approximation
[AD-A192724] N88-27824
Finding minimum-cost circulations by canceling negative cycles
[AD-A192727] N88-27825
LOW FREQUENCIES
Airborne measurement of low frequency atmospheric noise ALFAN 1
[AD-A193056] N88-27405
LOW PASS FILTERS
A notch filter instrument for measuring ELF (Extremely Low Frequency) MSK (Minimum Shift Keying) signals
[AD-A193324] N88-27414
LOW TEMPERATURE
Preparation and development of advanced battery catalysts
[AD-A193208] N88-27441
Cold worked reinforcing bars in tensile test under high loading rate and low temperatures
[DE88-752993] N88-27610

LOW TEMPERATURE ENVIRONMENTS
Hydraulic pumps and hydraulic equipment at low temperatures
[DE88-752871] N88-27570
LOW TEMPERATURE PHYSICS
Interactions between superconductivity and Kondo-grid properties in CeCu2Si2. Measurement results of specific heat under high pressure
[ETN-88-92377] N88-27958
LUBRICANTS
Studies of dynamic contact of ceramics and alloys for advanced heat engines
[DE88-008996] N88-27324
Perfluoropolyalkylether lubricants under boundary conditions: Iron catalysis of lubricant degradation
[AD-A193241] N88-27560
The 000 stage equipment bearing performance with a lower viscosity lubricant
[DE88-011827] N88-27566
LUBRICATING OILS
Calibration of the portable wear metal analyzer
[AD-A192971] N88-27524
LUBRICATION
Basic mechanisms of diesel lubrication correlation of bench and engine tests
[AD-A193360] N88-27561
The 000 stage equipment bearing performance with a lower viscosity lubricant
[DE88-011827] N88-27566
A lubrication study of engine bearings N88-27574
LUMINESCENCE
Laser spectroscopy of quantum well and superlattice structures
[AD-A193336] N88-27937
LUMINOSITY
Cosmological parameters and evolution of the galaxy luminosity function
[NASA-CR-183081] N88-27986
LUMPING
Determination of lumped-mass thermal properties associated with autoclave curing of graphite/epoxy composites N88-27364
LUNAR BASES
Steps toward lunar settlement
[DE88-009141] N88-27213
LUNAR SOIL
Uses of lunar sulfur
[DE88-009119] N88-27990
LYMAN ALPHA RADIATION
A theoretical determination of the density at a traveling source that emitts particles
[ISAS-RN-351] N88-27883
LYMPHOCYTES
Effects of pulsed and CW (Continuous Wave) 2450 MHz radiation on transformation and chromosomes of human lymphocytes in vitro
[AD-A193104] N88-27736

M

M STARS
Analysis of emission features in IRAS LRS spectra N88-27380
MACH NUMBER
Analysis of experimental data for cast 10-2/DOA2 supercritical airfoil at high Reynolds numbers
[AD-A192827] N88-27166
Theoretical-numerical study of feasibility of use of winglets on low aspect ration wings at subsonic and transonic Mach numbers at reduce drag
[NASA-CR-4174] N88-27168
MAGMA
Geothermal energy technology: Issues, R and D (Research and Development) and cooperative arrangements
[PB88-193107] N88-27626
Time-dependent thermal convection of Earth mantle and double diffusive convection in magma chambers
[MITT-52] N88-27663
MAGNESIUM ALLOYS
Analysis of grain refinement and superplasticity in aluminum-magnesium alloys
[AD-A193029] N88-27283
MAGNETIC DIPOLES
Far- and mid-infrared properties of metal-insulator composite materials
[AD-A193227] N88-27236
MAGNETIC FIELD CONFIGURATIONS
Global and local magnetohydrodynamic relaxations
[DE88-752602] N88-27913
MAGNETIC FIELDS
An interferometric measurement technique for railgun structures
[AD-A192851] N88-27217
Magnetic excitations in transition metal systems
[DE88-011022] N88-27279
Electric and Magnetic Activity of the Central Nervous System: Research and Clinical Applications in Aerospace Medicine
[AGARD-CP-432] N88-27683
Studies of the intact human brain: Implications for performance N88-27684
Squid instrumentation for neuromagnetic study of complex brain activity N88-27691
Electric and magnetic brain activity related to cognitive performance N88-27692
Neuromagnetic evidence of place mechanisms for frequency and intensity coding in the human auditory cortex N88-27693
Staggered-grid finite element solution technique for the Maxwell's equations in the time domain
[DE88-011731] N88-27838
Tokamak magnetic turbulence over the safety factor range 0.6 less than q less than 3
[DE88-008421] N88-27904
MAGNETIC INDUCTION
Integrated magnetic field sensor using high magnetotransistors
[ETN-88-92356] N88-27465
MAGNETIC MEASUREMENT
Tokamak magnetic turbulence over the safety factor range 0.6 less than q less than 3
[DE88-008421] N88-27904
MAGNETIC STORMS
Field-aligned structure of the storm time Pc 5 wave of November 14-15, 1979
[AD-A193022] N88-27653
On the dynamics of the auroral ionosphere during the breakup of a substorm
[AD-A193368] N88-27657
MAGNETOHYDRODYNAMIC STABILITY
Reminimization of energy integral and stability limit for non-ideal MHD (magnetohydrodynamic) plasma
[DE88-008422] N88-27911
On plasma stability under anisotropic random electric field influence
[DE88-702422] N88-27918
MAGNETOHYDRODYNAMIC WAVES
Magnetohydrodynamic wave propagation in the solar wind
[DE88-702411] N88-27995
MAGNETOHYDRODYNAMICS
Global and local magnetohydrodynamic relaxations
[DE88-752602] N88-27913
MAGNETOMETERS
Studies of the intact human brain: Implications for performance N88-27684
MAGNETOSPHERIC ELECTRON DENSITY
Approximate analytical formulae for electron density and collision frequency in the natural and nuclear-disturbed ionosphere and inner magnetosphere
[AD-A193129] N88-27654
MAGNETRON SPUTTERING
Equipment for building and testing superconductive flux flow electronic devices
[AD-A192959] N88-27436
MAINTAINABILITY
Behavioral, psychological and demographic predictors of physical fitness
[AD-A192697] N88-27733
MAINTENANCE
Evaluation of explosive bonding for patching aluminum with aluminum
[AD-A193303] N88-27285
MAN-COMPUTER INTERFACE
The assessment of human/computer performance using human productivity measures: MIPS and BIPS are MEGAFLOPS
[DE87-013491] N88-27750
The effect of input device on user performance with a menu-based natural language interface
[AD-A193095] N88-27772
Image processing using a parallel architecture
[AD-A192833] N88-27803
MANAGEMENT INFORMATION SYSTEMS
IEMIS (Integrated Emergency Management Information System) floodplain mapping based on a LIDAR derived data set
[AD-A193071] N88-27616
Database design and management in engineering optimization
[AD-A193325] N88-27813
Developing a connector selection DBMS (database management system) using NIAM (Nijssen's Information Analysis Methodology)
[DE88-008110] N88-27972
MANEUVERABILITY
Assessments of maneuverability with the TeleOperated Vehicle (TOV)
[AD-A191584] N88-27751
Passive multipath target tracking in an inhomogeneous acoustic medium
[AD-A193284] N88-27873
MANGANESE
Kinetic of oxidation to air of a Fe-Al-Mn alloy system at 600-800(sup 0)C temperature range
[DE88-702309] N88-27330
MANGANESE COMPOUNDS
Structure and function of the manganese complex involved in photosynthetic oxygen evolution determined by X-ray adsorption spectroscopy and electron paramagnetic resonance spectroscopy
[DE88-010360] N88-27725
MANIFOLDS (MATHEMATICS)
Geometry of superconformal manifolds, part 1
[DE88-702405] N88-27863
Geometry of superconformal manifolds, part 2
[DE88-702406] N88-27864
MANIPULATORS
Development of a hybrid simulator for robotic manipulators
[AD-A193119] N88-27557
Control of free-flying space robot manipulator systems
[NASA-CR-183017] N88-27562
Control of free-flying space robot manipulator systems
[NASA-CR-183104] N88-27563
General expression of manipulator kinematics
[DE88-753430] N88-27567
Dexterous hands: Optimizing grasp by design and planning N88-27572
The VITE model: A neutral command circuit for a generating arm and articulator trajectories
[AD-A192715] N88-27734
MANNED SPACE FLIGHT
History of manned spaceflight
[CNES-NT-121] N88-28000
MANNED SPACECRAFT
The human element in space: Lessons from Antarctica
[AD-A193440] N88-27741
MANUALS
Engineering data compendium. Human perception and performance. User's guide
[LC-87-19560] N88-27749
SERI standard broadband format: A solar and meteorological data archival format
[DE88-001145] N88-27975
MANUFACTURING
Application of sol-gel procedures to ceramic composites
[ETN-88-92741] N88-27338
MAPPING
IEMIS (Integrated Emergency Management Information System) floodplain mapping based on a LIDAR derived data set
[AD-A193071] N88-27616
Review of geographic processing techniques applicable to regional analysis
[DE88-010759] N88-27643
CEEG dynamic brain mapping: A new method to evaluate brain function in different psychological and drug conditions N88-27685
MARKING
Velocity measurements and flow visualization in turbulent three-dimensional supersonic flows using oxygen flow tagging
[AD-A192551] N88-27165
Development of automatic names placement software
[AD-A192786] N88-27770
MARKOV PROCESSES
Distributed algorithms for probabilistic solution of computational vision problems
[AD-A193150] N88-27773
Performability analysis: Measures, an algorithm and a case study
[AD-A192477] N88-27800
Free boundary control of the Markov process
[AD-A192401] N88-27846
The computation of stationary distributions on Markov chains through perturbations
[AD-A193191] N88-27855
MARTENSITE
Twin boundaries and heterophase interfaces in ferroelastic martensites
[DE88-011894] N88-27304
MARTINGALES
A Wong-Zakai type theorem for certain discontinuous semimartingales
[AD-A192713] N88-27822
MASS FLOW RATE
Equipment for mass flow measurements in the low-speed wind tunnel at DFVLR in Brunswick, West Germany
[DFVLR-MITT-88-02] N88-27212
Turbulence structure of mixing swirling flows
[AD-A193063] N88-27478

Mass flow rate influence on void fraction of two-phase helium flow
[DE88-702456] N88-27495
MASS SPECTROMETERS
Synopsis of a computer program designed to interface a personal computer with the fast data acquisition system of a time-of-flight mass spectrometer
[NASA-CR-177474] N88-27798
MASS SPECTROSCOPY
Measurement of Beta-decay energies of short-lived neutron-rich nuclei in the vicinity of mass number between 101 and 106, and A = 109
[ETN-88-92376] N88-27890
MASS TRANSFER
Development of an experimental system for studying fast transient ignition phenomena
[DE88-011917] N88-27276
Heat and mass transfer in a transport channel
[DE88-701968] N88-27493
Heat and mass transfer in laminar wavy film absorption with the presence of non-absorbable gases N88-27502
MATCHED FILTERS
A numerically efficient digital matched filter for periodic and windowed periodic radar waveforms
[AD-A193132] N88-27410
MATERIALS HANDLING
Aircraft refueling demonstrator using a microbot alpha 2 robot N88-27367
MATHEMATICAL LOGIC
Improving the performance of AI algorithms
[AD-A192848] N88-27809
MATHEMATICAL MODELS
Integrated Technology Rotor Methodology Assessment Workshop
[NASA-CP-10007] N88-27148
A comparison of the various helicopter mathematical models used in the methodology assessment N88-27149
A comparison of theory and experiment for coupled rotor-body stability of a hingeless rotor model in hover under simulated vacuum conditions N88-27151
A comparison of theory and experiment for coupled rotor-body stability of a hingeless rotor model in hover N88-27152
A comparison of theory and experiment for the aeroelastic stability of a bearingless model rotor in hover N88-27153
The importance of steady and dynamic inflow on the stability of rotor-body systems N88-27156
Effects of static equilibrium and higher-order nonlinearities on rotor blade stability in hover N88-27157
Aeroelastic modeling of rotor blades with spanwise variable elastic axis offset: Classic issues revisited and new formulations N88-27158
Comparison of experimental coupled helicopter rotor/body stability results with a simple analytical model N88-27160
Aeromechanical stability analysis of COPTER N88-27161
Improved procedure for impact probability computation of aircraft crash based on Baltanz model
[JUEL-SPEZ-425] N88-27176
Contribution to the numerical solution of airplane spin motion
[ETN-88-92368] N88-27190
In-flight motor torque estimates for the second-stage Strypi 9 launch vehicle
[DE88-010833] N88-27222
Evaluation and improvement of liquid propellant rocket chugging analysis techniques. Part 2: A study of low frequency combustion instability in rocket engine preburners using a heterogeneous stirred tank reactor model
[NASA-CR-182724] N88-27225
Probabilistic anisotropic failure criteria for composite materials
[AD-A193046] N88-27232
Analysis of transverse strength of composites using percolation theory
[AD-A193204] N88-27234
The structure and stability of nonpremixed gas jet flames N88-27257
Laser probes and numerical modeling as process diagnostics in chemical vapor deposition
[DE88-011622] N88-27275
Computer modeling for surface properties of carbon fibers N88-27383
Basic research on optical neural computers N88-27389
Model for dynamically structured communicating systems
[PB88-105283] N88-27402
Dependence effects in unique signal transmission
[DE88-010331] N88-27419
Numerical experiments on turbulent mixing
[AD-A192572] N88-27473
User's manual for C-HEMP: A two-dimensional wave propagation code. Volume 1: Description and derivations of the code
[AD-A193197] N88-27486
A comparison of analytical techniques for modeling the Rayleigh-Taylor response of elastic-plastic solids
[DE88-010372] N88-27596
Reduced order modeling of grid-connected photovoltaic inverter systems
[DE88-010603] N88-27635
Prediction of regional pollutant dispersion using a nested-grid, three-dimensional numerical model N88-27649
An empirical surface temperature model
[AD-A192737] N88-27665
Angular radiation models for Earth-atmosphere system. Volume 1: Shortwave radiation
[NASA-RP-1184] N88-27677
Dissecting the visual and auditory pathways by means of the two-input technique N88-27690
Contribution to almost realistic picture processing by a computer graphics procedure
[ETN-88-92372] N88-27789
Benefits of an object approach in a computer aided design environment
[SNIAS-881-440-102] N88-27791
Modeling and approximate performance analysis of multiuser computer systems
[ETN-88-92137] N88-27806
Feedback control of a hyperbolic partial-differential equation with viscoelastic damping
[AD-A192896] N88-27810
A zoomable and adaptable hidden fine-mesh approach to solving advection-dispersion equations
[DE88-006174] N88-27816
Parallel solutions to geometric problems on the scan model of computation
[AD-A192321] N88-27819
Measuring dispersion effects of factors in factorial experiments
[AD-A193216] N88-27831
Asymptotic normality of minimum L1-norm estimates in linear models
[AD-A193399] N88-27835
Matrix substructuring, domain decomposition and particle methods: Current trends for solving PDEs in parallel
[DE88-009826] N88-27836
Reminimization of energy integral and stability limit for non-ideal MHD (magnetohydrodynamic) plasma
[DE88-006422] N88-27911
Cascade model of gamma-ray bursts: Power-law and annihilation-line components
[NASA-TM-101176] N88-27998
MATHEMATICAL PROGRAMMING
Optimal design of viscoelastic structures N88-27579
MATRICES (MATHEMATICS)
Sidelobe level of an adaptive array using the SMI (Sampled Matrix Inversion) algorithm
[AD-A193131] N88-27409
A programmable systolic array for factorial analysis. Part 2: The symmetric eigenvalue problem
[AD-A192396] N88-27762
A unified approach to estimation in linear models with fixed and mixed effects
[AD-A193060] N88-27829
MATRIX MATERIALS
Effects of electron beam irradiation on mechanical properties at low and high temperature of fiber reinforced composites using PEEK as matrix material
[DE88-753134] N88-27239
Fabrication of SiC fiber reinforced glass matrix by extrusion process and investigation of its mechanical properties
[ETN-88-92367] N88-27244
Programs for preliminary design of composite materials which were developed by the design group of Aerospatiale Aquitaine
[SNIAS-881-430-112] N88-27251
MATRIX METHODS
Effective buffering schemes for performing matrix operations for numerical databases N88-27968
MAXIMUM ENTROPY METHOD
Maximum entropy signal restoration with linear programming
[DE88-011740] N88-27787
MAXWELL EQUATION
SARLAC: A relativistic electron beam code
[AD-A193134] N88-27411
Kinetic theory for plane flows of rough, inelastic, circular disks N88-27499
Wave equations for pulse propagation
[DE88-011760] N88-27548
Staggered-grid finite element solution technique for the Maxwell's equations in the time domain
[DE88-011731] N88-27838
MAXWELL-BOLTZMANN DENSITY FUNCTION
Effects of low reflection on the collector and source sheaths of a finite ion temperature plasma
[DE88-008929] N88-27908
MEASURING INSTRUMENTS
Acoustic emission calibration instrumentation
[DE88-010817] N88-27528
Components of an atmospheric lidar system
[AD-A193366] N88-27539
Direct measurement of solids: High temperature sensing. Experimental development and testing of high temperature pulsed EMATs
[DE88-009859] N88-27546
Atmospheric nitrogen oxides: Their detection and chemistry
[PB88-193057] N88-27642
MECHANICAL DRIVES
Optimization of planetary gears
[ETN-88-92375] N88-27573
MECHANICAL PROPERTIES
Analysis of transverse strength of composites using percolation theory
[AD-A193204] N88-27234
Fabrication of SiC fiber reinforced glass matrix by extrusion process and investigation of its mechanical properties
[ETN-88-92367] N88-27244
Rocket motor case materials. An evaluation of new fibers for composites
[FOA-C-20696-2.1] N88-27245
Factors affecting strength in composite materials used for aircraft
[DT-212/87] N88-27248
Development of high strength and toughness microcomposite HSLA Fe/Cr/Mn/C steel with and without Nb
[DE88-009813] N88-27290
Thin film and near-surface characterization using a mechanical properties microprobe
[DE88-011399] N88-27302
Superconducting oxides with high critical temperatures N88-27392
FEB (Multifilter Electronics Box) lifting device analysis, revision A
[AD-A192313] N88-27427
The influence of weld metal properties, weld geometry and applied load on weld system performance
[AD-A193403] N88-27588
Corrosion fatigue of small cracks: Mechanics and chemistry
[DE88-012121] N88-27605
MEDICAL SCIENCE
Using IMSL mathematical and statistical computer subroutines in physiological and biomechanical research
[AD-A192594] N88-27765
MELTING
Component stress during freeze/thaw cycling
[DE88-011204] N88-27449
Effect of thermal cycling on CSPL (Chloride Silent Power Ltd.) sodium/sulfur cells
[DE88-011205] N88-27455
MEMBRANES
Optical evaluation of prototype stretched-membrane mirror modules for solar central receivers
[DE88-011884] N88-27637
Factors governing light driven electron and proton translocation in proteins across membranes
[DE88-011120] N88-27724
Hyperthermia: New thoughts on an old problem
[AD-A192602] N88-27731
MEMORY
Cognitive and neural bases of skilled performance
[AD-A193392] N88-27747
MEMORY (COMPUTERS)
Content-addressable memory storage by neural networks: A general model and global Liapunov method
[AD-A192716] N88-27807
MENTAL PERFORMANCE
The effects of increased cognitive demands on autonomic self-regulation: An indicator of parallel processing in the brain N88-27362
Thermal stress and its effects on fine motor skill and decoding tasks N88-27369
Event-related brain potentials as indices of mental workload and attentional allocation N88-27696
Cognitive and neural bases of skilled performance
[AD-A193392] N88-27747
WORDNET: An electronic lexical reference system based on theories of lexical memory
[AD-A193086] N88-27970

MERCURY CADMIUM TELLURIDES
Paramagnetic point defects in boron-implanted HgO.7CdO.3Te
[AD-A193276] N88-27934
Migration and stability of HgCdTe lattice defects
[AD-A193293] N88-27935
MESOSCALE PHENOMENA
Beaufort sea mesoscale circulation study: Hydrography helicopter operations, April 1987
[PB88-203658] N88-27681
METABOLISM
Metabolic and cardiorespiratory parameters during three consecutive days of exhaustive running
[AD-A192598] N88-27728
METAL AIR BATTERIES
Metal-air battery assessment
[DE88-011361] N88-27459
METAL FILMS
PECVD of amorphous nickel--phosphorus films
[DE88-011088] N88-27299
METAL JOINTS
Stress relaxation of a titanium (Ti-6Al-4V) threaded joint
[DE88-010102] N88-27590
METAL MATRIX COMPOSITES
Damping characteristics of metal matrix composites
[AD-A193144] N88-27233
Analysis of transverse strength of composites using percolation theory
[AD-A193204] N88-27234
Refractory metal alloys and composites for space power systems
[NASA-TM-100946] N88-27310
METAL OXIDE SEMICONDUCTORS
Dose-enhancement effects in TaSi/Al- and Al-gate MOS devices
[DE88-005483] N88-27926
METAL PARTICLES
Far- and mid-infrared properties of metal-insulator composite materials
[AD-A193227] N88-27236
Calibration of the portable wear metal analyzer
[AD-A192971] N88-27524
METAL PLATES
Finite element method for plate structures with inclined angles
[ILR-MITT-182] N88-27842
METAL SHEETS
Constant amplitude fatigue life data for notched and unnotched annealed Ti-6Al-4V sheet
[AD-A193420] N88-27287
METAL SURFACES
Specular steel surfaces for solar mirror substrates
[DE88-001153] N88-27630
Theory of the dissociation dynamics of small molecules on metal surfaces: Finite temperature studies
[DE88-007763] N88-27882
Dynamics of a plasma produced under effect of the XeCl-laser radiation on metallic surface
[DE88-701983] N88-27902
METAL-METAL BONDING
Evaluation of explosive bonding for patching aluminum with aluminum
[AD-A193303] N88-27285
METALLIC PLASMAS
Spectral line shapes from highly ionized sodium plasmas
[AD-A193401] N88-27907
METALS
On the systematics of phase transformation in metallic alloys
[DE88-008041] N88-27288
Oxidation-erosion of metals and alloys: Models, verification, and prediction
[DE88-010016] N88-27300
Soluble metal chelate polymers of coordination numbers six, seven and eight
[AD-A192485] N88-27314
Effects of near interfacial microstructure on toughness and subcritical crack growth in ceramic/metal systems
[DE88-009842] N88-27325
The influence of weld metal properties, weld geometry and applied load on weld system performance
[AD-A193403] N88-27588
Amorphous silicon solar cells using a metal substrate
[PB88-131941] N88-27628
METASTABLE STATE
Formation of metastable structures and amorphous phases in Cu-W alloys using the triod sputtering technique
[DE88-009051] N88-27298
METEOROID SHOWERS
A study of a meteor burst communication system
N88-27421
METEOROLOGICAL CHARTS
Intercomparison of NMC (National Meteorological Center) and ECMWF (European Centre for Medium Range Weather Forecasts) global analyses: 1980-1986
[PB88-196548] N88-27668
METEOROLOGICAL PARAMETERS
Intercomparison of NMC (National Meteorological Center) and ECMWF (European Centre for Medium Range Weather Forecasts) global analyses: 1980-1986
[PB88-196548] N88-27668
The Hanford meteorological data collection system and data base
[DE88-008632] N88-27672
Space shuttle natural environment analysis
[NASA-CR-179337] N88-27676
SERI standard broadband format: A solar and meteorological data archival format
[DE88-001145] N88-27975
METEOROLOGICAL RADAR
TDWR (Terminal Doppler Weather Radar) PRF (Pulse Repetition Frequency) selection criteria
[AD-A193089] N88-27407
METEOROLOGY
An evaluation of two millimeter wave propagation models for horizontal atmospheric attenuation at 70-115 GHZ
[AD-A192699] N88-27403
Update on the meso-microscale meteorological hierarchy
[DE88-009133] N88-27670
MICHELSON INTERFEROMETERS
An interferometric measurement technique for railgun structures
[AD-A192851] N88-27217
Investigations on Mie and Rayleigh scattering as basis for the development of Rayleigh temperature lidars with aid of Michelson interferometry
[GKSS-87/E/62] N88-27675
MICROANALYSIS
Microchemical analysis of polycrystalline Ni3Al and other ordered alloys using the field-ion microscope atom probe
[DE88-011519] N88-27294
Thin film and near-surface characterization using a mechanical properties microprobe
[DE88-011399] N88-27302
Superconducting oxides with high critical temperatures
N88-27392
MICROCHANNELS
Forced-convection, liquid-cooled, microchannel heat sinks
[AD-A193337] N88-27444
MICROELECTRONICS
Solid state research
[AD-A192837] N88-27929
MICROORGANISMS
An outdoor test facility for the large-scale production of microalgae
[DE88-001146] N88-27723
MICROPROCESSORS
SP-100 Ground Engineering Systems: Test facility control systems
[DE88-009195] N88-27895
MICROSCOPY
Scanning tunneling microscopy as a surface chemical probe
[AD-A192710] N88-27263
MICROSTRUCTURE
Damping characteristics of metal matrix composites
[AD-A193144] N88-27233
Gaseous tracer techniques for pore structure characterization of granular materials
[DE88-011542] N88-27274
Thermomechanical processing of Al alloy 2090 for grain refinement and superplasticity
[AD-A192333] N88-27281
Processing and properties of advanced aluminum alloys
[AD-A193224] N88-27284
On the systematics of phase transformation in metallic alloys
[DE88-008041] N88-27288
Development of high strength and toughness microcomposite HSLA Fe/Cr/Mn/C steel with and without Nb
[DE88-009813] N88-27290
Hot isostatic pressing of tungsten-nickel-iron composites
[PB88-203070] N88-27292
Controlling phase formation and stability to improve the high temperature creep resistance of austenitic stainless steels
[DE88-011401] N88-27293
Processing and additive effects of ZrO2 on microstructure and dielectric porperties of BaTiO3 ceramics
[AD-A193126] N88-27316
Preparation and properties of high Q microwave dielectrics in the (CA, SR, BA) zirconate system
[AD-A193127] N88-27317
Effects of near interfacial microstructure on toughness and subcritical crack growth in ceramic/metal systems
[DE88-009842] N88-27325
Influence of microstructure and microdamage processes on fracture at high loading rates
[AD-A192957] N88-27583
Ultrafast physics in semiconductor microstructures
[AD-A193300] N88-27936
X-ray studies of strain, interface and impurities in semiconductors
[DE88-012460] N88-27954
MICROWAVE ATTENUATION
An evaluation of two millimeter wave propagation models for horizontal atmospheric attenuation at 70-115 GHZ
[AD-A192699] N88-27403
MICROWAVE CIRCUITS
Guided wave interactions in millimeter-wave integrated circuits
[AD-A193017] N88-27437
MICROWAVE COUPLING
Microwave polymerization of composite structures
[SNIAS-881-430-116] N88-27343
MICROWAVE EQUIPMENT
Microwave polymerization of composite structures
[SNIAS-881-430-116] N88-27343
Use of microwave measuring systems for the nondestructive control of resins and composites
[SNIAS-881-430-123] N88-27576
Solid state research
[AD-A192837] N88-27929
MICROWAVE IMAGERY
Validate algorithms for the determination of rainfall rates from SSM/I microwave satellite imagery
[AD-A192299] N88-27684
MICROWAVE SENSORS
Active and passive remote sensing of ice
[AD-A193307] N88-27617
MICROWAVE SOUNDING
Multifilter spectrometer (FEB) for microwave atmospheric sounder
[AD-A192312] N88-27426
MICROWAVES
Preparation and properties of high Q microwave dielectrics in the (CA, SR, BA) zirconate system
[AD-A193127] N88-27317
A method for estimating the susceptibility of electronic systems to HPM (High Power Microwave)
[DE88-012246] N88-27422
Genetic effects of low level microwave radiation
[AD-A192687] N88-27722
Effects of pulsed and CW (Continuous Wave) 2450 MHz radiation on transformation and chromosomes of human lymphocytes in vitro
[AD-A193104] N88-27736
Assessment of cochlear damage after microwave irradiation
[AD-A193237] N88-27737
Behavioral effects of exposure to the tempo high-power microwave system
[AD-A193305] N88-27738
MIE SCATTERING
Investigations on Mie and Rayleigh scattering as basis for the development of Rayleigh temperature lidars with aid of Michelson interferometry
[GKSS-87/E/62] N88-27675
MIGRATION
Energy migration, motion and order in synthetic polymers
[AD-A193334] N88-27320
Migration and stability of HgCdTe lattice defects
[AD-A193293] N88-27935
MILITARY OPERATIONS
Aerospace applications studies, 1971-1987
[AGARD-R-759] N88-27147
Army space systems for terrestrial applications
[AD-A192735] N88-27613
MILITARY TECHNOLOGY
Air Force technical objective document, FY89
[AD-A193110] N88-27194
Intelligent Mobile Autonomous System (IMAS)
[AD-A193181] N88-27811
MILKY WAY GALAXY
Gamma radiation from center of the galaxy of the order of MeV values
[MPE-207] N88-27999
MILLIMETER WAVES
An evaluation of two millimeter wave propagation models for horizontal atmospheric attenuation at 70-115 GHZ
[AD-A192699] N88-27403
Multifilter spectrometer (FEB) for microwave atmospheric sounder
[AD-A192312] N88-27426

A planar IC-compatible transferred electron device for millimeter-wave operation
[AD-A192692] N88-27433
Guided wave interactions in millimeter-wave integrated circuits
[AD-A193017] N88-27437
MIMD (COMPUTERS)
Basic database operations on the butterfly parallel processor: Experiment results
[AD-A193199] N88-27804
MINERAL OILS
A study relating to the fog oil replacement program
[AD-A192536] N88-27347
MIRRORS
Specular steel surfaces for solar mirror substrates
[DE88-001153] N88-27630
Performance evaluation of large-area glass-mirror heliostats
[DE88-011883] N88-27636
MISSILE LAUNCHERS
Expert system contribution to logistics improvement
[SNIAS-881-320-102] N88-27815
MIXING
Turbulence structure of mixing swirling flows
[AD-A193063] N88-27478
MODELS
Carbon deposition model for oxygen-hydrocarbon combustion, volume 1
[NASA-CR-179375] N88-27254
Carbon deposition model for oxygen-hydrocarbon combustion, volume 2
[NASA-CR-179376] N88-27255
Surface-wave model uncertainty assessment
[AD-A193094] N88-27408
Evaluation of fracture models through pressurized-thermal-shock testing
[DE88-011834] N88-27603
The relationship between observed fatigue damage and life estimation models
[NASA-CR-182191] N88-27611
Solar cell modeling and simulation
[AD-A193249] N88-27620
Enhancement of modeling and image generation techniques for high-resolution 3-dimensional imagery
[DE88-008923] N88-27782
Some stability criteria in fluid and solid mechanics N88-27966
MOISTURE
Temperature, moisture and strain rate effects on the compressive mechanical behavior of Nylon 6/6
[DE88-010734] N88-27591
MOISTURE CONTENT
Simulation of moisture diffusion of fiber reinforced components of aircraft for general air transportation
[IFL-IB-87-05] N88-27253
MOISTURE RESISTANCE
Stability of uncapsulated weight cells with thin film elongation measurement bands under influence of humidity, temperature and operation voltage
[ETN-88-92363] N88-27531
MOLDS
Injection compression for short fiber reinforced plastics
[SNIAS-881-430-118] N88-27344
MOLECULAR BEAM EPITAXY
Molecular beam epitaxy of GaP films on Si substrates
[PB88-131974] N88-27923
Investigations on the MBE (Molecular Beam Epitaxy) growth and properties of Al(sub y)Ga(sub y)In(sub 1-x-y)AsInP and InGaAs-InAlAs superlattices
[DE88-009105] N88-27941
MOLECULAR ENERGY LEVELS
Study of energy levels and decay mechanisms for singlet Rydberg states of molecular nitrogen
[AD-A192505] N88-27886
MOLECULAR EXCITATION
Steady-state approximations in Raman excitation equations
[DE88-011759] N88-27889
MOLECULAR INTERACTIONS
Precise ultraviolet absorbance study of the interaction of amino acids and mononucleosides in aqueous solution
[ISAS-RN-356] N88-27256
MOLECULAR STRUCTURE
Spatial organization of homopolymer chains inside spherical polybutadiene domains of SB diblock copolymers
[AD-A193390] N88-27321
Experiments in microgravity environment: Protein crystallization
[SNIAS-881-430-101] N88-27354
MOLECULAR WEIGHT
Interfacial tension of immiscible polymer blends: Temperature and molecular weight dependence
[AD-A192463] N88-27312
MOLECULES
Equilibrium distribution functions for limited plasma-molecular systems
[DE88-702412] N88-27916
MOLTEN SALTS
Nuclear magnetic resonance spectrometer
[AD-A192928] N88-27523
MOLYBDENUM SULFIDES
Schottky-barrier formation on a covalent semiconductor without Fermi-level pinning: The Metal-MoS2(0001) interface
[AD-A193044] N88-27931
MOMENTUM
Symmetry problem of energy-momentum tensor and the creation of gravitational field
[DE88-702442] N88-27964
MONKEYS
Evoked potential analysis of impact acceleration experiments N88-27708
MONOCHROMATORS
The detection and interpretation of long-term changes in ozone from space
[NASA-TM-101135] N88-27650
MONOPOLE ANTENNAS
Performance study of a unipole antenna with conventional and elevated radial wire ground screens
[AD-A193283] N88-27413
MOON
Steps toward lunar settlement
[DE88-009141] N88-27213
MORPHOLOGY
Damping characteristics of metal matrix composites
[AD-A193144] N88-27233
Rubber-modified epoxies: Interfacial tension and morphology
[AD-A192464] N88-27313
Plasma treatment of polymers for improved adhesion
[DE88-011623] N88-27334
Analysis of remotely sensed imagery using digital morphology
[AD-A192738] N88-27614
MOTION PERCEPTION
Influence of moving visual environment on saccadic eye movements and fixation N88-27368
Perception of motion in statistically-defined displays
[AD-A193076] N88-27745
MOTION SICKNESS
Simulator sickness in the AH-64 Apache combat mission simulator
[AD-A193419] N88-27739
MOTION SIMULATION
Motion evoked vestibular potentials N88-27712
MOVING TARGET INDICATORS
Passive multipath target tracking in an inhomogeneous acoustic medium
[AD-A193284] N88-27873
MULTIPATH TRANSMISSION
Passive multipath target tracking in an inhomogeneous acoustic medium
[AD-A193284] N88-27873
MULTIPLEXING
The MELMUX MX-7100 series high-speed digital multiplexers N88-27396
MULTIPROCESSING (COMPUTERS)
Dynamic modelling and estimation of the error due to asynchronism in a redundant asynchronous multiprocessor system
[NASA-CR-177427] N88-27205
FTMP data acquisition environment
[NASA-TM-100636] N88-27447
MINIAC: A small embedded computer
[DE88-008142] N88-27757
The sub-implicit method: New multiprocessor algorithms for old implicit codes
[DE88-011345] N88-27785
Performability analysis: Measures, an algorithm and a case study
[AD-A192477] N88-27800
Constructing a highly-available location service for a distributed environment
[AD-A192723] N88-27801
Modeling and approximate performance analysis of multiuser computer systems
[ETN-88-92137] N88-27806
MULTISPECTRAL PHOTOGRAPHY
Remote sensing of wetlands: Applications overview
[DE88-010895] N88-27618
MULTIVARIATE STATISTICAL ANALYSIS
On solvability of an equation arising in the theory of M-estimates
[AD-A193059] N88-27828
Further extensions of the choquet-deny and deny theorems with applications in characterization theory
[AD-A193358] N88-27834
Asymptotic normality of minimum L1-norm estimates in linear models
[AD-A193399] N88-27835
Joint asymptotic distribution of marginal quantiles and quantile functions in samples from a multivariate population
[AD-A193385] N88-27856
MUTAGENS
Genetic effects of low level microwave radiation
[AD-A192687] N88-27722

N

N-TYPE SEMICONDUCTORS
Growth and characterization of CuGaS2, CuAlS2 and CuGa0.9Al0.1S2 single crystals
[AD-A192963] N88-27930
NATURAL GAS
Laser probes of natural gas ignition chemistry
[PB88-212568] N88-27271
NATURAL LANGUAGE (COMPUTERS)
The effect of input device on user performance with a menu-based natural language interface
[AD-A193095] N88-27772
NAVIER-STOKES EQUATION
An h-p adaptive finite element method for steady compressible flow N88-27467
A Navier-Stokes study of cascade flow fields including inlet distortion and rotating stall
[AD-A193109] N88-27483
Computational boundary conditions for the incompressible Navier-Stokes equations in channels and pipes
[AD-A193356] N88-27487
Numerical treatment of the pressure singularity at a re-entrant corner
[AD-A193357] N88-27488
Stream function-vorticity finite elements and the resolution of the Navier-Stokes equations
[DE88-702318] N88-27494
Determination of the local heat-transfer characteristics on glaze ice accretions on a cylinder and a NACA 0012 airfoil N88-27500
Distributive iteration for indefinite systems as smoothing method in multigrid process on example of Stokes and Navier-Stokes equations with emphasis on incomplete decompositions
[ETN-88-92127] N88-27509
Numerical integration of Navier-Stokes equations by application of multigrid concept
[ETN-88-92365] N88-27513
The three-dimensional stress field around a cylindrical inclusion in a plate of arbitrary thickness N88-27602
NEAR INFRARED RADIATION
A new near-infrared tunable-room temperature solid state laser La3Ga5SiO14:Cr(3+)
[DE88-011341] N88-27543
NEODYMIUM LASERS
Coupling of a spark source mass spectrograph and a ND-YAG laser
[DE88-012116] N88-27530
Radial compression of picosecond electrical pulses
[DE88-008440] N88-27544
Process control improvements in pulsed Nd:YAG laser closure welding of electromechanical relays
[DE88-006275] N88-27564
NERVES
Relation between VEP and visual function in lesions of the optic nerve and visual pathway N88-27718
NETWORK ANALYSIS
Some equivalent circuit models for AC impedance analysis of pyrite/solution interface
[DE88-010574] N88-27452
Automatic line network extraction from aerial imagery of urban areas through knowledge based image analysis
[AD-A193067] N88-27615
NETWORK CONTROL
The MELMUX MX-7100 series high-speed digital multiplexers N88-27396
NEURAL NETS
Basic research on optical neural computers N88-27389
Content-addressable memory storage by neural networks: A general model and global Liapunov method
[AD-A192716] N88-27807
Neural network research: A personal perspective
[AD-A192717] N88-27808
NEUROLOGY
Normative developmental equations for the EEG and their sensitivity to neurological and psychiatric disorders N88-27687
NEUROMUSCULAR TRANSMISSION
The VITE model: A neutral command circuit for a generating arm and articulator trajectories
[AD-A192715] N88-27734

NEUROPHYSIOLOGY
Electric and Magnetic Activity of the Central Nervous System: Research and Clinical Applications in Aerospace Medicine
[AGARD-CP-432] N88-27683
Fourth generation neurocognitive pattern analysis system N88-27686
Neurophysiological patterns of operational fatigue: Preliminary results N88-27703
Neurophysiological precursors of accurate visuomotor performance N88-27706
The neuroelectric selection of Naval aviation personnel: An evaluation N88-27707
Electroencephalographic correlates of pilot performance: Simulation and in-flight studies N88-27711
Spontaneous cerebral electrical activity during prolonged hypoglycemia: A quantitative study in humans N88-27717
Relation between VEP and visual function in lesions of the optic nerve and visual pathway N88-27718

NEUTRINOS
Strange, quark and metastable neutron stars
[DE88-702404] N88-27984

NEUTRON DECAY
Measurement of Beta-decay energies of short-lived neutron-rich nuclei in the vicinity of mass number between 101 and 106, and A = 109
[ETN-88-92376] N88-27890

NEUTRON SCATTERING
Calculation of far infrared absorption in B poly(dA).poly(dT)
[AD-A193126] N88-27318

NEUTRON STARS
Strange, quark and metastable neutron stars
[DE88-702404] N88-27984

NEWTON METHODS
Parallel quasi-Newton methods for unconstrained optimization
[AD-A193250] N88-27812

NICKEL
A fundamental understanding of the interfacial compatibility in hybrid material systems
[AD-A192921] N88-27264
Inelastic electron scattering and electron-hole excitations in iron and nickel
[DE88-011843] N88-27303

NICKEL ALLOYS
Hot isostatic pressing of tungsten-nickel-iron composites
[PB88-203070] N88-27292
PECVD of amorphous nickel–phosphorus films
[DE88-011088] N88-27299

NICKEL CADMIUM BATTERIES
Results from life test in progress on eagle-picher nickel cadmium cells
[AD-A192616] N88-27434

NICKEL HYDROGEN BATTERIES
Recent developments in nickel hydrogen technology
[DE88-011248] N88-27456

NITRATES
Foliar nitrate reductase: A marker for assimilation of atmospheric nitrogen oxides
[DE88-010453] N88-27648

NITRIC ACID
Mechanism of the nitric oxide-carbon monoxide-oxygen reaction over a single crystal rhodium catalyst
[DE88-006274] N88-27268

NITROGEN
Study of energy levels and decay mechanisms for singlet Rydberg states of molecular nitrogen
[AD-A192505] N88-27886

NITROGEN OXIDES
Atmospheric nitrogen oxides: Their detection and chemistry
[PB88-193057] N88-27642

NOISE (SOUND)
Vertical directionality of ambient noise at 32 deg N as a function of longitude: Tape number 86180
[AD-A193228] N88-27872

NOISE MEASUREMENT
Aeroacoustic investigation on the noise from ultralight aircraft
[DFVLR-FB-88-03] N88-27879

NOISE SPECTRA
Application of pattern recognition techniques to the identification of aerospace acoustic sources
[NASA-CR-183116] N88-27877
Aeroacoustic investigation on the noise from ultralight aircraft
[DFVLR-FB-88-03] N88-27879

NONDESTRUCTIVE TESTS
Assembly Test Article (ATA)
[NASA-CR-179361] N88-27226
Design and implementation of contact ultrasonic sensors to assess internal damage
[I-177/87] N88-27247
Balance of X-ray radioscopy application to nondestructive tests of composite materials
[SNIAS-881-430-110] N88-27250
NDE performance in predicting failure strength of spherical composite specimens with implanted flaws
[DE88-008223] N88-27575
Interface control using low frequency (3 to 20 MHz) acoustic microscopy
[REPT-48-411/F] N88-27577
Genetic effects of low level microwave radiation
[AD-A192687] N88-27722

NONLINEAR EQUATIONS
Numerical optimization
[AD-A193032] N88-27827
Cauchy problem for the nonlinear Schroedinger equation
[DE88-702454] N88-27867
Initial boundary value problems of nonlinear wave equations in an exterior domain
[DE88-701883] N88-27962

NONLINEAR OPTICS
Solid state research
[AD-A192837] N88-27929

NONLINEAR SYSTEMS
Determination of Tafel constants in nonlinear polarization curves
[AD-A192335] N88-27282
Nonlinear vibrations of periodically stiffened plates N88-27596
Periodic oscillations in nonlinear mechanical systems N88-27599
The robust tracking control of nonlinear systems with uncertain dynamics N88-27788

NONLINEARITY
Effects of static equilibrium and higher-order nonlinearities on rotor blade stability in hover N88-27157
Nonlinear dynamics of the electron self-field interaction
[DE88-010597] N88-27420
Nonlinear interaction between overall and local buckling of stiffened panels with symmetric cross-sections
[PB88-104054] N88-27580

NONPARAMETRIC STATISTICS
Joint asymptotic distribution of marginal quantiles and quantile functions in samples from a multivariate population
[AD-A193385] N88-27856

NORMALITY
Asymptotic normality of minimum L1-norm estimates in linear models
[AD-A193399] N88-27835

NORMS
Asymptotic of Peanokerns of finite fixed order
[ETN-88-92381] N88-27843

NOVAE
The classical nova outburst
[DE88-009138] N88-27987

NOZZLE DESIGN
Variable Mach number wall jets for control/propulsion on hypervelocity projectiles/interceptors: Tests with an existing model
[AD-A192845] N88-27167

NOZZLE FLOW
Nozzle lip effects on gas expansion into the plume backflow region
[AD-A192806] N88-27475

NUCLEAR BINDING ENERGY
Schottky-barrier formation on a covalent semiconductor without Fermi-level pinning: The Metal-MoS2(0001) interface
[AD-A193044] N88-27931

NUCLEAR EXPLOSIONS
Approximate analytical formulae for electron density and collision frequency in the natural and nuclear-disturbed ionosphere and inner magnetosphere
[AD-A193129] N88-27654

NUCLEAR MAGNETIC RESONANCE
Nuclear magnetic resonance spectrometer
[AD-A192928] N88-27523

NUCLEAR RESEARCH
Technology security, volume 1
[DE88-008612] N88-27978

NUCLEAR WEAPONS
Technology security, volume 1
[DE88-008612] N88-27978

NUCLEATION
Cloud simulation warm cloud experiments: Droplet growth and aerosol scavenging
[AD-A192944] N88-27666
Atomic layer epitaxy of ZnS and ZnSe
[AD-A192307] N88-27928

NUCLEOSIDES
Precise ultraviolet absorbance study of the interaction of amino acids and mononucleosides in aqueous solution
[ISAS-RN-356] N88-27256

NUMERICAL ANALYSIS
A computational analysis of under-expanded jets in the hypersonic regime
[NASA-TM-101319] N88-27174
Evaluation and improvement of liquid propellant rocket chugging analysis techniques. Part 1: A one-dimensional analysis of low frequency combustion instability in the fuel preburner of the space shuttle main engine
[NASA-CR-183106] N88-27224
The structure and stability of nonpremixed gas jet flames N88-27257
Analytical approximation of a distorted reflector surface defined by a discrete set of points
[NASA-TM-101323] N88-27424
Numerical simulation of fuel droplet interactions and breakup
[AD-A192431] N88-27470
Numerical experiments on turbulent mixing
[AD-A192572] N88-27473
Effects of numerical dissipation on finite-volume solutions of compressible flow problems
[AD-A193173] N88-27485
Numerical treatment of the pressure singularity at a re-entrant corner
[AD-A193357] N88-27488
Numerical methods for incompressible viscous flows with engineering applications
[NASA-CR-183143] N88-27508
Three-dimensional aspects of fatigue crack closure
[AD-A192296] N88-27581
A zoomable and adaptable hidden fine-mesh approach to solving advection-dispersion equations
[DE88-006174] N88-27816
Research in applied mathematics
[AD-A192385] N88-27820
A numerical treatment of the fluid/elastic interface under range-dependent environments
[AD-A192476] N88-27821
Numerical optimization
[AD-A193032] N88-27827
On the estimation of a variance ratio
[AD-A193190] N88-27854

NUMERICAL CONTROL
Compliant robotic structures, part 3
[AD-A192426] N88-27556
IEMIS (Integrated Emergency Management Information System) floodplain mapping based on a LIDAR derived data set
[AD-A193071] N88-27616

NUMERICAL DATA BASES
Effective buffering schemes for performing matrix operations for numerical databases N88-27968

NUMERICAL INTEGRATION
Numerical integration of Navier-Stokes equations by application of multigrid concept
[ETN-88-92365] N88-27513
Multiple integration with respect to Poisson and Levy processes
[AD-A192895] N88-27851

NUMERICAL STABILITY
A study on Lebesgue decomposition of measures induced by stable processes
[AD-A192893] N88-27850

NYLON (TRADEMARK)
Temperature, moisture and strain rate effects on the compressive mechanical behavior of Nylon 6/6
[DE88-010734] N88-27591

O

OCCULTATION
A study relating to the fog oil replacement program
[AD-A192536] N88-27347

OCEAN MODELS
Air-sea interaction in the vicinity of a land-sea boundary in the presence of upwelling N88-27661
Research on ocean forecasting and nonlinear wave propagation and numerical hydrodynamics in the ocean
[AD-A193363] N88-27680

OCEAN SURFACE
Definition of long ocean wave slope for radar applications
[AD-A193198] N88-27412
Research on ocean forecasting and nonlinear wave propagation and numerical hydrodynamics in the ocean
[AD-A193363] N88-27680

OCEANOGRAPHIC PARAMETERS
MIZPAC (marginal ice zone Pacific) 84-86 CTD (Conductivity, Temperature, Depth) data report
[AD-A192478] N88-27679

OCEANOGRAPHY
An analysis of horizontal temperature gradients and heat content in the mixed layer and the surface forcing during PATCHEX
[AD-A192330] N88-27678
Beaufort sea mesoscale circulation study: Hydrography helicopter operations, April 1987
[PB88-203658] N88-27681
OCEANS
The distribution of some chemical elements between dissolved and particulate phases in the ocean
[DE88-010181] N88-27682
OCULOMETERS
A human factors evaluation of the Advanced Visual Technology System (AVTS) eye tracking oculometer N88-27361
OMEGA NAVIGATION SYSTEM
Automatic omega station and LOP (Line Of Position) selection
[AD-A193302] N88-27179
ON-LINE SYSTEMS
WORDNET: An electronic lexical reference system based on theories of lexical memory
[AD-A193086] N88-27970
OPERATING SYSTEMS (COMPUTERS)
The MELCOM PSI 2 AI workstation N88-27395
OPERATOR PERFORMANCE
Neurophysiological patterns of operational fatigue: Preliminary results N88-27703
OPHTHALMOLOGY
Microesotropia patients performs well as military jet pilots N88-27363
OPTICAL COMPUTERS
Mitsubishi Electric Advance (R and D Edition), Volume 41
[PB88-194162] N88-27388
Basic research on optical neural computers N88-27389
OPTICAL DATA PROCESSING
Investigation of the potential impact of new photonic materials on optical processing systems N88-27359
Optical interconnections for digital image coding N88-27381
An optical 2-dimensional correlator for pattern recognition in embedded computing
[DE88-007198] N88-27780
OPTICAL DISKS
Use of optical disk technology at the Air Command and Staff College
[AD-A192424] N88-27969
OPTICAL EQUIPMENT
An optical 2-dimensional correlator for pattern recognition in embedded computing
[DE88-007198] N88-27780
OPTICAL FIBERS
Multi-mode optical fibers for simultaneous 13-position measurements Thomson scattering apparatus in the JFT-2M tokamak
[DE88-753133] N88-27897
OPTICAL MEASURING INSTRUMENTS
IPS guidestar selection for stellar mode (ASTRO)
[NASA-TM-100336] N88-27181
OPTICAL PROPERTIES
Performance evaluation of large-area glass-mirror heliostats
[DE88-011883] N88-27636
The collection of statistics on the frequency of cloud cover over North America
[AD-A193093] N88-27667
Atomic layer epitaxy of ZnS and ZnSe
[AD-A192307] N88-27928
OPTICAL RADAR
Components of an atmospheric lidar system
[AD-A193366] N88-27539
IEMIS (Integrated Emergency Management Information System) floodplain mapping based on a LIDAR derived data set
[AD-A193071] N88-27616
Investigations on Mie and Rayleigh scattering as basis for the development of Rayleigh temperature lidars with aid of Michelson interferometry
[GKSS-87/E/62] N88-27675
OPTIMAL CONTROL
Optimal control of the wing rock phenomenon N88-27373
Computer aided design for linear control State Variable System (SVS)
[AD-A193282] N88-27775
Free boundary control of the Markov process
[AD-A192401] N88-27846
Approximations and optimal control for the pathwise average cost per unit time and discounted problems for wideband noise driven systems
[AD-A192712] N88-27847
OPTIMIZATION
A feasibility study in path planning using optimization techniques
[AD-A193030] N88-27177
Numerical optimization, system theoretic and software tools for the integrated design of flexible structures and their control systems
[AD-A192927] N88-27183
Optimal rheological characteristics in dynamic stability of polymer flow through porous media
[DE88-001225] N88-27322
An aspect graph-based control strategy for 3-D object recognition N88-27377
Efficiency optimization for FEL oscillators
[AD-A192541] N88-27536
Dexterous hands: Optimizing grasp by design and planning N88-27572
An investigation of techniques for determination of optimum/self-optimizing systems N88-27600
Parallel quasi-Newton methods for unconstrained optimization
[AD-A193250] N88-27812
Database design and management in engineering optimization
[AD-A193325] N88-27813
Finding minimum-cost circulations by successive approximation
[AD-A192724] N88-27824
Finding minimum-cost circulations by canceling negative cycles
[AD-A192727] N88-27825
Numerical optimization
[AD-A193032] N88-27827
ORBITAL SERVICING
Temperature rise in superfluid helium pumps
[NASA-TM-100997] N88-27507
ORBITS
Distortion functions
[DE88-752634] N88-27896
ORGANIC COMPOUNDS
Direct determination of part-per-billion levels of volatile organics in water and soil samples using glow discharge mass spectrometry
[DE88-011389] N88-27272
National ambient Volatile Organic Compounds (VOCs) data base update, documentation
[PB88-195631] N88-27646
ORTHOGONAL FUNCTIONS
Coherent structures in the axisymmetric turbulent jet mixing layer N88-27504
OSCILLATION DAMPERS
Experimental study of unsteady separating turbulent boundary layers
[AD-A192997] N88-27477
OSCILLATIONS
The importance of steady and dynamic inflow on the stability of rotor-body systems N88-27158
Periodic oscillations in nonlinear mechanical systems N88-27599
OSCILLATORS
Focused ion beam fabrication of graded channel FETs in GaAs and Si
[AD-A193098] N88-27439
Long-pulse, high-power vircator experiments
[DE88-011787] N88-27458
The design of a digital Eprom oscillator for electrical impedance tomography
[DE88-012243] N88-27462
Efficiency optimization for FEL oscillators
[AD-A192541] N88-27536
OUTLIERS (STATISTICS)
Outliner resistant filtering and smoothing: 2D version
[AD-A193319] N88-27874
OUTPUT
Simulation methodology
[AD-A192548] N88-27764
OXALATES
Manufacturing of a barium titanate with high dielectric coefficient by decomposition of precipitates of double oxalates
[ISAL-IDI1-88-02] N88-27278
OXIDATION
Oxidation-erosion of metals and alloys: Models, verification, and prediction
[DE88-010016] N88-27300
Kinetic of oxidation to air of a Fe-Al-Mn alloy system at 600-800(sup 0)C temperature range
[DE88-702309] N88-27330
Methods of quantifying and enhancing reactive oxygen species production N88-27357
Silicon oxidation studies: A review of recent studies on thin film silicon dioxide formation in the physics and chemistry of SiO2 and the Si-SiO2 interface
[AD-A193176] N88-27932
OXIDATION RESISTANCE
Studies in support of oxidation-resistant composite materials
[AD-A193320] N88-27238
OXIDES
Preparation and properties of new inorganic glasses and gel-derived solids
[AD-A192922] N88-27315
Monolithic fuel cells
[DE88-012004] N88-27638
OXYGEN
Carbon deposition model for oxygen-hydrocarbon combustion, volume 1
[NASA-CR-179375] N88-27254
Mechanism of the nitric oxide-carbon monoxide-oxygen reaction over a single crystal rhodium catalyst
[DE88-006274] N88-27268
OXYGEN CONSUMPTION
Hypothalamic-pituitary-adrenal responses to short duration high intensity cycle exercise
[AD-A192597] N88-27727
OZONE
ECC (Electrochemical Concentration Cell) ozonesonde observations at South Pole, Antarctica during 1987
[PB88-202015] N88-27644
Photochemical oxidant formation: Overview of current knowledge and emerging issues
[PB88-195235] N88-27647
The detection and interpretation of long-term changes in ozone from space
[NASA-TM-101135] N88-27650

P

P-I-N JUNCTIONS
Silicon-on-insulator pin diodes
[AD-A193359] N88-27445
PACIFIC OCEAN
MIZPAC (marginal ice zone Pacific) 84-86 CTD (Conductivity, Temperature, Depth) data report
[AD-A192478] N88-27679
PAIR PRODUCTION
Cascade model of gamma-ray bursts: Power-law and annihilation-line components
[NASA-TM-101176] N88-27998
PANELS
Nonlinear interaction between overall and local buckling of stiffened panels with symmetric cross-sections
[PB88-104054] N88-27580
PARABOLIC REFLECTORS
Reflux heat-pipe solar receivers for dish-electric systems
[DE88-008671] N88-27631
PARALLEL COMPUTERS
Factorization of large integers on a massively parallel computer
[DE88-011625] N88-27786
PARALLEL PROCESSING (COMPUTERS)
Computational fluid dynamics on parallel processors
[AD-A192397] N88-27469
Supercomputer for parallel data analysis
[DE88-702148] N88-27759
Linguistic semantics for parallel computation
[PB88-105960] N88-27761
Bisimulation can't be traced
[AD-A192725] N88-27766
Research into the architecture of CAD based robot vision systems
[AD-A193330] N88-27776
The sub-implicit method: New multiprocessor algorithms for old implicit codes
[DE88-011345] N88-27785
Implementing direct, spatially isolated problems on transputer networks
[NASA-TM-101297] N88-27796
User's manual for the two-dimensional transputer graphics toolkit
[NASA-TM-100974] N88-27799
Image processing using a parallel architecture
[AD-A192833] N88-27803
Basic database operations on the butterfly parallel processor: Experiment results
[AD-A193199] N88-27804
Parallel solutions to geometric problems on the scan model of computation
[AD-A192321] N88-27819
A review of parallel methods for solving sets of linear equations and their application within optimisation algorithms
[AD-A193137] N88-27830
Matrix substructuring, domain decomposition and particle methods: Current trends for solving PDEs in parallel
[DE88-009826] N88-27836

Parallel implementation of the boundary element method
[DE88-011846] N88-27839
PARAMAGNETIC RESONANCE
Paramagnetic point defects in boron-implanted HgO.7CdO.3Te
[AD-A193276] N88-27934
PARAMETERIZATION
An aspect graph-based control strategy for 3-D object recognition N88-27377
Development of radiation and cloud parameterization programs for AFGL (Air Force Geophysics Laboratory) global models
[AD-A193369] N88-27658
PARITY
Coupled even-parity superconducting states: Square lattice
[AD-A193432] N88-27938
PARSING ALGORITHMS
A cockpit natural language study: Vocabulary and grammar analyses
[AD-A193289] N88-27753
PARTIAL DIFFERENTIAL EQUATIONS
Feedback control of a hyperbolic partial-differential equation with viscoelastic damping
[AD-A192896] N88-27810
Numerical optimization
[AD-A193032] N88-27827
Unified multilevel adaptive finite element methods for elliptic problems
[DE88-011938] N88-27840
PARTICLE ACCELERATORS
Scaling laws for geomagnetic tail current sheet acceleration
[AD-A193379] N88-27659
Activities report of the Werner-Heisenberg Institute of Physics
[ETN-88-92946] N88-27893
PARTICLE BEAMS
Propagation of charged particle beams in the atmosphere
[AD-A193185] N88-27887
PARTICLE DENSITY (CONCENTRATION)
The influence of ionization within a plasma opening switch
[AD-A193147] N88-27906
PARTICLE EMISSION
A theoretical determination of the density at a traveling source that emitts particles
[ISAS-RN-351] N88-27883
PARTICLE ENERGY
The low-latitude auroral boundary: Steady-state and time-dependent representations
[AD-A193200] N88-27656
Solar flares and magnetospheric particles: Investigations based upon the ONR-602 and ONR-604 experiments
[AD-A193396] N88-27994
PARTICLE INTERACTIONS
Self-energies and the interactions of particles with surfaces
[DE88-010451] N88-27885
Quark nuclear model: Classification groups and two and three body correlations
[NOTA-INTERNA-896] N88-27891
Study of the production of Ko mesons in proton antiproton interactions at 630 GeV
[NOTA-INTERNA-908] N88-27892
PARTICLE MOTION
Optical guiding in the separable beam limit
[AD-A192452] N88-27534
PARTICLE PRECIPITATION
The low-latitude auroral boundary: Steady-state and time-dependent representations
[AD-A193200] N88-27656
Solar flares and magnetospheric particles: Investigations based upon the ONR-602 and ONR-604 experiments
[AD-A193396] N88-27994
PARTICLE SIZE DISTRIBUTION
Preparation and properties of high Q microwave dielectrics in the (CA, SR, BA) zirconate system
[AD-A193127] N88-27317
PARTICLE THEORY
Analysis of transverse strength of composites using percolation theory
[AD-A193204] N88-27234
Quark nuclear model: Classification groups and two and three body correlations
[NOTA-INTERNA-896] N88-27891
PARTICLES
Matrix substructuring, domain decomposition and particle methods: Current trends for solving PDEs in parallel
[DE88-009826] N88-27836
PARTICULATES
Analysis of debris from accelerated life test of the Hughes five-year Vuilleumier cryocooler
[AD-A193101] N88-27400
The distribution of some chemical elements between dissolved and particulate phases in the ocean
[DE88-010181] N88-27682
PATHOLOGY
Squid instrumentation for neuromagnetic study of complex brain activity N88-27691
PATTERN RECOGNITION
Applications of differential geometry to the shape analysis of gray-value images N88-27358
An aspect graph-based control strategy for 3-D object recognition N88-27377
Creating aspect graphs for use in object recognition N88-27379
Linear feature extraction from radar imagery. Phase 2: Base contract report
[AD-A192828] N88-27404
Analysis of remotely sensed imagery using digital morphology
[AD-A192738] N88-27614
Fourth generation neurocognitive pattern analysis system N88-27686
Texture perception and shape from texture
[AD-A192923] N88-27771
Simulation of real time problem solving
[AD-A193436] N88-27778
An optical 2-dimensional correlator for pattern recognition in embedded computing
[DE88-007198] N88-27780
Application of pattern recognition techniques to the identification of aerospace acoustic sources
[NASA-CR-183116] N88-27877
Pattern information processing and multimedia database system: Current research on multimedia information system
[PB88-131917] N88-27973
PENETRATION
Investigation of hydrogen isotope penetration through stainless steels Kh18N10T and Kh3M2BFR
[DE88-702189] N88-27297
PERCEPTION
Cognitive and neural bases of skilled performance
[AD-A193392] N88-27747
Texture perception and shape from texture
[AD-A192923] N88-27771
Issues in computer-assisted interpretation of graphs and quantitative information
[PB88-116280] N88-27783
PERCEPTUAL ERRORS
Ejection situations in the U-2/TR-1: An analysis of emotions and events
[AD-A192872] N88-27175
PERCOLATION
Analysis of transverse strength of composites using percolation theory
[AD-A193204] N88-27234
PERFORMANCE PREDICTION
A comparison of the various helicopter mathematical models used in the methodology assessment N88-27149
A comparison of theory and experiment for aeroelastic stability of a hingeless rotor model in hover N88-27150
A comparison of theory and flight test of the BO 105/BMR in hover and forward flight N88-27155
Failure analysis of laminated composite angles N88-27578
PERFORMANCE TESTS
A comparison of theory and experiment for aeroelastic stability of a hingeless rotor model in hover N88-27150
A comparison of theory and experiment for coupled rotor-body stability of a hingeless rotor model in hover under simulated vacuum conditions N88-27151
A comparison of theory and experiment for the aeroelastic stability of a bearingless model rotor in hover N88-27153
Assembly Test Article (ATA)
[NASA-CR-179361] N88-27226
Alkaline fuel cell performance investigation
[NASA-TM-100937] N88-27267
Thermomechanical processing of Al alloy 2090 for grain refinement and superplasticity
[AD-A192333] N88-27281
Sodium/sulfur cell evaluation results
[DE88-011488] N88-27451
Post-test observations on CSPL (Chloride Silent Power Limited) cells
[DE88-011975] N88-27461
The 210-HP diesel engine endurance and performance testing with fire resistant diesel fuel
[AD-A193153] N88-27558
Basic mechanisms of diesel lubrication correlation of bench and engine tests
[AD-A193360] N88-27561
Performance sensitivities for point-focus dish systems with secondary concentrators
[DE88-001152] N88-27629
Photovoltaic Measurements and Performance Branch
[DE88-001142] N88-27633
Performance evaluation of large-area glass-mirror heliostats
[DE88-011883] N88-27636
Vapor Compression Distillation Subsystem (VCDS) component enhancement, testing and expert fault diagnostics development, volume 2
[NASA-CR-172076] N88-27755
PERIODIC VARIATIONS
Nonlinear vibrations of periodically stiffened plates N88-27598
Periodic oscillations in nonlinear mechanical systems N88-27599
PERIPHERAL CIRCULATION
Physiological responses to acute exercise-heat stress
[AD-A192606] N88-27732
PERMEABILITY
Investigation of hydrogen isotope penetration through stainless steels Kh18N10T and Kh3M2BFR
[DE88-702189] N88-27297
Optimal rheological characteristics in dynamic stability of polymer flow through porous media
[DE88-001225] N88-27322
Hyperthermia: New thoughts on an old problem
[AD-A192602] N88-27731
PERMITTIVITY
Processing and additive effects of ZrO2 on microstructure and dielectric porperties of BaTiO3 ceramics
[AD-A193126] N88-27316
Active and passive remote sensing of ice
[AD-A193307] N88-27617
PEROVSKITES
Probing the electronic and defect structure of perovskite superconductors
[DE88-006349] N88-27939
PERSONAL COMPUTERS
Synopsis of a computer program designed to interface a personal computer with the fast data acquisition system of a time-of-flight mass spectrometer
[NASA-CR-177474] N88-27798
PERSPIRATION
Physiological responses to acute exercise-heat stress
[AD-A192606] N88-27732
PERTURBATION THEORY
Perturbation expansions generated by an approximate propagator
[DE88-702435] N88-27866
Reminimization of energy integral and stability limit for non-ideal MHD (magnetohydrodynamic) plasma
[DE88-008422] N88-27911
Self energy corrections to the ab initio band structures: Chromium
[DE88-701825] N88-27927
Vortices on the world sheet and string's critical dynamics
[DE88-702116] N88-27961
PHASE DIAGRAMS
Migration and stability of HgCdTe lattice defects
[AD-A193293] N88-27935
PHASE ERROR
Approximation problems of the Hilbert transform to identify minimum phase linear systems
[FUB-42-1986] N88-27760
PHASE SHIFT
Phase comparator for range imaging laser radar
[DE88-008109] N88-27545
PHASE TRANSFORMATIONS
Survey of the literature on fractals with possible applications to phase change processes
[DE88-012240] N88-27277
On the systematics of phase transformation in metallic alloys
[DE88-008041] N88-27288
Twin boundaries and heterophase interfaces in ferroelastic martensites
[DE88-011894] N88-27304
Energy migration, motion and order in synthetic polymers
[AD-A193334] N88-27320
Component stress during freeze/thaw cycling
[DE88-011204] N88-27449
PHOSPHORUS
PECVD of amorphous nickel–phosphorus films
[DE88-011088] N88-27299
PHOTOCHEMICAL REACTIONS
Photochemical oxidant formation: Overview of current knowledge and emerging issues
[PB88-195235] N88-27647
Low-band-gap, amorphous-silicon-based alloys by photochemical vapor deposition
[DE88-001165] N88-27944

PHOTODIODES
Photodiodes for optical communication in the near infrared
[ETN-88-92378] N88-27900
PHOTOELECTRIC CELLS
Space photovoltaic generators. State of the art, trends
[SNIAS-881-440-106] N88-27640
PHOTOELECTRIC EMISSION
Investigation of electronic band structure of semiconductors by photoemission
[ETN-88-92370] N88-27957
PHOTOINTERPRETATION
Methods of determining playa surface conditions using remote sensing
[AD-A192663] N88-27612
PHOTOIONIZATION
Target designs for plasma-implosion-driven, photoionization-pumped soft X-ray lasers
[DE88-011278] N88-27547
Multiphoton ionization of alkaline earth atoms in an intense laser field
[DE88-008078] N88-27884
PHOTOLUMINESCENCE
Picosecond transient reflectivity of unpinned gallium arsenide (100) surfaces
[AD-A193242] N88-27933
Ultrafast physics in semiconductor microstructures
[AD-A193300] N88-27936
PHOTOOXIDATION
Structure and function of the manganese complex involved in photosynthetic oxygen evolution determined by X-ray adsorption spectroscopy and electron paramagnetic resonance spectroscopy
[DE88-010360] N88-27725
PHOTOSYNTHESIS
Factors governing light driven electron and proton translocation in proteins across membranes
[DE88-011120] N88-27724
Structure and function of the manganese complex involved in photosynthetic oxygen evolution determined by X-ray adsorption spectroscopy and electron paramagnetic resonance spectroscopy
[DE88-010360] N88-27725
PHOTOVOLTAIC CELLS
Photovoltaic Energy. Electricity from Sunlight: A current awareness bulletin
[DE88-008289] N88-27634
Reduced order modeling of grid-connected photovoltaic inverter systems
[DE88-010803] N88-27635
PHOTOVOLTAIC CONVERSION
Photovoltaic Measurements and Performance Branch
[DE88-001142] N88-27633
PHYSICAL EXERCISE
Hypothalamic-pituitary-adrenal responses to short duration high intensity cycle exercise
[AD-A192597] N88-27727
Metabolic and cardiorespiratory parameters during three consecutive days of exhaustive running
[AD-A192598] N88-27728
Validation of a modified one-step rebreathing technique for measuring exercise cardiac output
[AD-A192600] N88-27729
A resistive-film based force transducer for the study of exercise
[AD-A192601] N88-27730
PHYSICAL FITNESS
Behavioral, psychological and demographic predictors of physical fitness
[AD-A192697] N88-27733
PHYSIOLOGICAL EFFECTS
Physiological monitoring methodology in the USAFSAM centrifuge N88-27356
Hyperthermia: New thoughts on an old problem
[AD-A192602] N88-27731
Simulator sickness in the AH-64 Apache combat mission simulator
[AD-A193419] N88-27739
PHYSIOLOGICAL RESPONSES
Human response to prolonged motionless suspension in four types of full body harnesses N88-27387
Electric and Magnetic Activity of the Central Nervous System: Research and Clinical Applications in Aerospace Medicine
[AGARD-CP-432] N88-27683
The interaction of thalamo-cortical systems in the 40 Hz following response N88-27694
A study of sources in the human brain associated with stereopsis N88-27695
Cognitive task demands as reflected in physiological measures N88-27699
Hypothalamic-pituitary-adrenal responses to short duration high intensity cycle exercise
[AD-A192597] N88-27727
Physiological responses to acute exercise-heat stress
[AD-A192606] N88-27732
Behavioral effects of exposure to the tempo high-power microwave system
[AD-A193305] N88-27738
PHYSIOLOGY
Squid instrumentation for neuromagnetic study of complex brain activity N88-27691
Using IMSL mathematical and statistical computer subroutines in physiological and biomechanical research
[AD-A192594] N88-27785
PICOSECOND PULSES
Radial compression of picosecond electrical pulses
[DE88-008440] N88-27544
PILOT PERFORMANCE
Microesotropia patients performa well as military jet pilots N88-27363
Event-related brain potentials as indices of mental workload and attentional allocation N88-27696
Fighter pilot performance during airborne and simulator missions: Physiological comparisons N88-27704
The neuroelectric selection of Naval aviation personnel: An evaluation N88-27707
Electroencephalographic correlates of pilot performance: Simulation and in-flight studies N88-27711
Correlation between EEG abnormal activity and aircraft accidents: A long term observation N88-27719
The auditory evoked response in military pilots N88-27721
Personality, attitudes, and pilot training performance: Preliminary analysis
[AD-A193102] N88-27746
PILOT PLANTS
An outdoor test facility for the large-scale production of microalgae
[DE88-001146] N88-27723
PILOT SELECTION
Personality, attitudes, and pilot training performance: Preliminary analysis
[AD-A193102] N88-27746
PILOT TRAINING
Personality, attitudes, and pilot training performance: Preliminary analysis
[AD-A193102] N88-27746
Cockpit and cabin crew coordination
[AD-A192445] N88-27752
PINNING
Schottky-barrier formation on a covalent semiconductor without Fermi-level pinning: The Metal-MoS2(0001) interface
[AD-A193044] N88-27931
Picosecond transient reflectivity of unpinned gallium arsenide (100) surfaces
[AD-A193242] N88-27933
PIPE FLOW
Characterization of accelerating pipe flow
[AD-A193065] N88-27481
Computational boundary conditions for the incompressible Navier-Stokes equations in channels and pipes
[AD-A193356] N88-27487
Numerical computation of three-dimensional turbulent flow in tightly curved ducts and spiral turbine casings
[ETN-88-92362] N88-27511
Investigations on drag reduction in turbulent pipe flows by addition of ionic and nonionic high polymers
[ETN-88-92360] N88-27515
PIPES (TUBES)
Characterization of accelerating pipe flow
[AD-A193065] N88-27481
Distribution of weld quality in thin section stainless steel tube attachment welds
[PB88-109632] N88-27555
Computation of failure probability of fatigue loaded cracked structures
[ETN-88-92360] N88-27607
PISTON ENGINES
Analytical and experimental investigation of ringless piston concept
[AD-A193213] N88-27559
PITCH (INCLINATION)
Hybrid procedure for dynamic measurements in transonic wind tunnels: Demonstrated by pitch oscillation
[DFVLR-FB-88-19] N88-27211
PITCHING MOMENTS
An experimental study of the effect of pitch rate on delta wing aerodynamics and stability
[NASA-CR-183159] N88-27173
Control and use of unsteady flows: Insect use of various wing kinematics and related pressure measurements using a pitching airfoil N88-27366
Forces and moments on a slender, cavitating body
[DE88-007208] N88-27491
PITTING
Significance of the local electrode potential within pits, crevices and cracks
[AD-A192482] N88-27432
PITUITARY GLAND
Hypothalamic-pituitary-adrenal responses to short duration high intensity cycle exercise
[AD-A192597] N88-27727
PLANAR STRUCTURES
Radiative heat transfer and selective emission in planar slab coatings on hot emissive substrates
[AD-A193133] N88-27319
Guided wave interactions in millimeter-wave integrated circuits
[AD-A193017] N88-27437
PLANE WAVES
Experimental investigation of the reflection of a planar shock wave over a double wedge
[AD-A193078] N88-27482
PLANETARY ATMOSPHERES
Interpretation of the polarimetric observations of Jupiter
[DE88-702414] N88-27991
Polarization of light reflected by vertically inhomogeneous planetary atmosphere
[DE88-702416] N88-27992
PLANNING
Vision research. A national plan: 1983-1987, 1987 evaluation and update
[PB88-192604] N88-27726
PLASMA CONTROL
Tokamak magnetic turbulence over the safety factor range 0.6 less than q less than 3
[DE88-008421] N88-27904
Optical imaging diagnostics for fusion plasmas
[DE88-997572] N88-27910
PLASMA DENSITY
A plasma ultraviolet source for short wavelength lasers
[AD-A192844] N88-27537
Heating efficiency of beat wave excitation in a density gradient
[AD-A193066] N88-27905
PLASMA DIAGNOSTICS
Dynamics of a plasma produced under effect of the XeCl-laser radiation on metallic surface
[DE88-701983] N88-27902
Optical imaging diagnostics for fusion plasmas
[DE88-997572] N88-27910
PLASMA DYNAMICS
Finite element methodology for integrated flow-thermal-structural analysis
[NASA-CR-183144] N88-27606
PLASMA EQUILIBRIUM
Moment approach to neoclassical flows, currents and transport in auxiliary heated tokamaks
[DE88-008024] N88-27901
ITER plasma equilibrium and poloidal field system design
[DE88-011005] N88-27912
Theory and simulation of relaxed plasmoids
[AD-A192884] N88-27997
PLASMA FOCUS
A plasma ultraviolet source for short wavelength lasers
[AD-A192844] N88-27537
PLASMA GUNS
Refractory fibers surface treatment
[REPT-47-803/F] N88-27339
PLASMA HEATING
Moment approach to neoclassical flows, currents and transport in auxiliary heated tokamaks
[DE88-008024] N88-27901
Heating efficiency of beat wave excitation in a density gradient
[AD-A193066] N88-27905
PLASMA LAYERS
The influence of ionization within a plasma opening switch
[AD-A193147] N88-27906
PLASMA PINCH
Theory and simulation of relaxed plasmoids
[AD-A192884] N88-27997
PLASMA PUMPING
A plasma ultraviolet source for short wavelength lasers
[AD-A192844] N88-27537
PLASMA RADIATION
Dynamics of a plasma produced under effect of the XeCl-laser radiation on metallic surface
[DE88-701983] N88-27902
PLASMA SHEATHS
The influence of ionization within a plasma opening switch
[AD-A193147] N88-27906
PLASMA TORCHES
Waste destruction by plasma
[SNIAS-881-430-113] N88-27651

PLASMA-PARTICLE INTERACTIONS
Equilibrium distribution functions for limited plasma-molecular systems
[DE88-702412] N88-27916
PLASMAS (PHYSICS)
Plasma treatment of polymers for improved adhesion
[DE88-011623] N88-27334
Ion Bernstein modes in current-carrying plasmas N88-27903
Tokamak magnetic turbulence over the safety factor range 0.6 less than q less than 3
[DE88-008421] N88-27904
The influence of ionization within a plasma opening switch
[AD-A193147] N88-27906
Effects of low reflection on the collector and source sheaths of a finite ion temperature plasma
[DE88-008929] N88-27908
Reminimization of energy integral and stability limit for non-ideal MHD (magnetohydrodynamic) plasma
[DE88-008422] N88-27911
Global and local magnetohydrodynamic relaxations
[DE88-752602] N88-27913
Design of divertor plate and measurements of double-null open divertor plasma in the JFT-2M tokamak
[DE88-753130] N88-27914
Design of divertor plate and measurements of double-null open divertor plasma in the JFT-2M tokamak
[DE88-753130] N88-27914
Analysis of lower hybrid current drive and rampup experiments on the JT-60 tokamak
[DE88-753136] N88-27915
Electromagnetic wave incoherent reflection by a half-space of weakly-ionized plasma with an absorbing boundary
[DE88-702413] N88-27917
Energy distribution and transfer in flowing hydrogen microwave plasmas N88-27919
Activities report of the Institute for Extraterrestrial Physics
[MPE-206] N88-27981
Measurement of macroscopic electric fields in solar plasma structures
[AD-A193291] N88-27993
Theory and simulation of relaxed plasmoids
[AD-A192884] N88-27997
PLASMASPHERE
Field-aligned structure of the storm time Pc 5 wave of November 14-15, 1979
[AD-A193022] N88-27653
PLASMONS
Solar energy conversion through the interaction of plasmons with tunnel junctions. Part A: Solar cell analysis. Part B: Photoconductor analysis
[NASA-CR-183044] N88-27621
PLASTIC DEFORMATION
Ultrasonic studies of stresses and plastic deformation in steel during tension and compression
[AD-A192308] N88-27280
Analysis of grain refinement and superplasticity in aluminum-magnesium alloys
[AD-A193029] N88-27283
Plastic yielding at crack tips
[AD-A192549] N88-27582
PLASTIC PROPERTIES
Characterization of elastic-plastic properties of AS4/APC-2 thermoplastic composite
[NASA-CR-183145] N88-27242
Thermomechanical processing of Al alloy 2090 for grain refinement and superplasticity
[AD-A192333] N88-27281
PLATES
Nonlinear vibrations of periodically stiffened plates N88-27598
PLATES (STRUCTURAL MEMBERS)
Hole diameters in plates impacted by projectiles N88-27386
PLAYAS
Methods of determining playa surface conditions using remote sensing
[AD-A192663] N88-27612
PLUMES
Variable Mach number wall jets for control/propulsion on hypervelocity projectiles/interceptors: Tests with an existing model
[AD-A192845] N88-27167
A computational analysis of under-expanded jets in the hypersonic regime
[NASA-TM-101319] N88-27174
Nozzle lip effects on gas expansion into the plume backflow region
[AD-A192806] N88-27475
POINT DEFECTS
Paramagnetic point defects in boron-implanted HgO.7CdO.3Te
[AD-A193276] N88-27934
Prediction of deep levels and equilibrium concentrations of defects in semiconductors N88-27945
POINTING CONTROL SYSTEMS
IPS guidestar selection for stellar mode (ASTRO)
[NASA-TM-100336] N88-27181
Slew-induced deformations in a space-based electromagnetic rail gun N88-27385
POISSON DENSITY FUNCTIONS
Full analysis of a powerful window random access algorithm
[AD-A192437] N88-27763
Multiple integration with respect to Poisson and Levy processes
[AD-A192895] N88-27851
POISSON EQUATION
Heating efficiency of beat wave excitation in a density gradient
[AD-A193066] N88-27905
POLARIMETRY
Interpretation of the polarimetric observations of Jupiter
[DE88-702414] N88-27991
POLARIZATION (CHARGE SEPARATION)
Determination of Tafel constants in nonlinear polarization curves
[AD-A192335] N88-27282
Techniques and instrumentation for transient characterization of metal-insulator-semiconductor diodes. Applications to metal-insulator InP system
[ECL-87-17] N88-27959
POLARIZED LIGHT
Polarization of light reflected by vertically inhomogeneous planetary atmosphere
[DE88-702416] N88-27992
POLLUTION TRANSPORT
Prediction of regional pollutant dispersion using a nested-grid, three-dimensional numerical model N88-27649
POLOIDAL FLUX
ITER plasma equilibrium and poloidal field system design
[DE88-011005] N88-27912
POLYBUTADIENE
Spatial organization of homopolymer chains inside spherical polybutadiene domains of SB diblock copolymers
[AD-A193390] N88-27321
POLYCRYSTALS
Microchemical analysis of polycrystalline Ni3Al and other ordered alloys using the field-ion microscope atom probe
[DE88-011519] N88-27294
Superconducting thin films, composites and junctions
[AD-A193123] N88-27440
POLYMER CHEMISTRY
Energy migration, motion and order in synthetic polymers
[AD-A193334] N88-27320
POLYMER MATRIX COMPOSITES
Microwave polymerization of composite structures
[SNIAS-881-430-116] N88-27343
POLYMERIC FILMS
Refractory films from spin-cast carbon
[DE88-011251] N88-27327
A resistive-film based force transducer for the study of exercise
[AD-A192601] N88-27730
POLYMERIZATION
Soluble metal chelate polymers of coordination numbers six, seven and eight
[AD-A192485] N88-27314
Precursor chemistry and the structure of silica aerogels
[DE88-011253] N88-27326
Study of crosslinking and nonelastic mechanical properties of epoxy and PSP networks — epoxy resins; polystyrylpyridine resins (psp)
[ETN-88-92740] N88-27337
Microwave polymerization of composite structures
[SNIAS-881-430-116] N88-27343
POLYNOMIALS
Finding minimum-cost circulations by canceling negative cycles
[AD-A192727] N88-27825
Structure of bound states in polynomial potentials
[DE88-702437] N88-27837
Evaluation of quantum mechanics path integrals by the approximations exact on a class of polynomial functionals
[DE88-702434] N88-27865
POROSITY
Gaseous tracer techniques for pore structure characterization of granular materials
[DE88-011542] N88-27274
Application of controlled interfacial pore structures to kinetic studies in alumina
[DE88-010884] N88-27326
Computer modeling for surface properties of carbon fibers N88-27383
POSITION (LOCATION)
Automatic omega station and LOP (Line Of Position) selection
[AD-A193302] N88-27179
Radar information from the partial derivatives of the echo signal phase from a point scatterer
[AD-A193402] N88-27415
Constructing a highly-available location service for a distributed environment
[AD-A192723] N88-27801
POSITRON ANNIHILATION
Cascade model of gamma-ray bursts: Power-law and annihilation-line components
[NASA-TM-101176] N88-27998
POSTFLIGHT ANALYSIS
Space shuttle natural environment analysis
[NASA-CR-179337] N88-27676
POWDER (PARTICLES)
Preparation and properties of high Q microwave dielectrics in the (CA, SR, BA) zirconate system
[AD-A193127] N88-27317
Relative flow rates of explosive powders
[DE88-010767] N88-27350
The first synthesis of chem-prep varistor LAC (Lightning Arrestor Connector) granules
[DE88-008005] N88-27438
POWER TRANSMISSION (LASERS)
Overview and future direction for blackbody solar-pumped lasers
[NASA-TM-100521] N88-27553
PREBURNERS
Evaluation and improvement of liquid propellant rocket chugging analysis techniques. Part 2: A study of low frequency combustion instability in rocket engine preburners using a heterogeneous stirred tank reactor model
[NASA-CR-182724] N88-27225
PRECIPITATES
Theoretical predictions of precipitate shapes in cubic alloys
[DE88-010856] N88-27291
PREDICTION ANALYSIS TECHNIQUES
Computation of ECM (Electronic Counter-Measures) war reserve materiel spare requirements
[AD-A193301] N88-27195
Approximations of stochastic equations driven by predictable processes
[AD-A192714] N88-27823
Robust prediction for stationary processes: 2D enriched version
[AD-A193318] N88-27833
PREDICTIONS
Oxidation-erosion of metals and alloys: Models, verification, and prediction
[DE88-010016] N88-27300
Prediction of velocity and temperature profiles in thermally driven gravity currents applied to stratified thermal storage tanks
[DE88-004452] N88-27496
NDE performance in predicting failure strength of spherical composite specimens with implanted flaws
[DE88-008223] N88-27575
Size effects in linear elastic fracture mechanics N88-27609
Behavioral, psychological and demographic predictors of physical fitness
[AD-A192697] N88-27733
PREMIXED FLAMES
Premixed turbulent flame propagation
[AD-A192955] N88-27265
PRESSURE DISTRIBUTION
Turbulence structure of mixing swirling flows
[AD-A193063] N88-27478
PRESSURE EFFECTS
Deep level defects in semiconductors: Stress and pressure studies
[DE88-010855] N88-27948
PRESSURE MEASUREMENT
Shock initiation studies on heterogeneous explosives
[DE88-008681] N88-27351
Control and use of unsteady flows: Insect use of various wing kinematics and related pressure measurements using a pitching airfoil N88-27366
Measurement of pressure fluctuations in a resonant chamber with laser-induced iodine fluorescence
[DFVLR-FB-87-53] N88-27551
A resistive-film based force transducer for the study of exercise
[AD-A192601] N88-27730
Energy distribution and transfer in flowing hydrogen microwave plasmas N88-27919

PRESSURE RECORDERS
A resistive-film based force transducer for the study of exercise
[AD-A192601] N88-27730
PRESSURE SENSORS
A resistive-film based force transducer for the study of exercise
[AD-A192601] N88-27730
PRESSURIZING
Evaluation of fracture models through pressurized-thermal-shock testing
[DE88-011834] N88-27603
PRIMARY BATTERIES
The kinetics of charge-transfer reactions on passive lithium electrodes
[DE88-009256] N88-27454
PRINTED CIRCUITS
Thermal cycling tests on surface-mount assemblies
[DE88-007696] N88-27453
PROBABILITY DISTRIBUTION FUNCTIONS
On solvability of an equation arising in the theory of M-estimates
[AD-A193059] N88-27828
PROBABILITY THEORY
Improved procedure for impact probability computation of aircraft crash based on Ballanz model
[JUEL-SPEZ-425] N88-27176
Probabilistic anisotropic failure criteria for composite materials
[AD-A193046] N88-27232
Computation of failure probability of fatigue loaded cracked structures
[ETN-88-92360] N88-27607
Distributed algorithms for probabilistic solution of computational vision problems
[AD-A193150] N88-27773
The computation of stationary distributions on Markov chains through perturbations
[AD-A193191] N88-27855
Comparison of results based on a deterministic versus a statistical uncertainty analysis
[DE88-010751] N88-27858
PROBLEM SOLVING
Boundary layer solutions for the free-edge problem in composite laminates N88-27229
The integration of decision support problems into feature modeling based design N88-27372
Effects of numerical dissipation on finite-volume solutions of compressible flow problems
[AD-A193173] N88-27485
An investigation of techniques for determination of optimum/self-optimizing systems N88-27600
Inspection methods in programming: Cliches and plans
[AD-A192782] N88-27767
Simulation of real time problem solving
[AD-A193436] N88-27778
Implementing direct, spatially isolated problems on transputer networks
[NASA-TM-101297] N88-27796
Intelligent Mobile Autonomous System (IMAS)
[AD-A193181] N88-27811
PROCEDURES
Benefits of an object approach in a computer aided design environment
[SNIAS-881-440-102] N88-27791
PROCESS CONTROL (INDUSTRY)
Processing and properties of advanced aluminum alloys
[AD-A193224] N88-27284
Optical diagnostics for metallurgical processes
[DE88-009255] N88-27289
Use of microwave measuring systems for the nondestructive control of resins and composites
[SNIAS-881-430-123] N88-27576
PRODUCT DEVELOPMENT
Investigation of expert system design approaches for electronic design environments N88-27365
PRODUCTIVITY
The assessment of human/computer performance using human productivity measures: MIPS and BIPS are MEGAFLOPS
[DE87-013491] N88-27750
PROGRAM VERIFICATION (COMPUTERS)
Inspection methods in programming: Cliches and plans
[AD-A192782] N88-27767
Verification of flight software written in C using ACSL
[DE88-006100] N88-27779
A modular proof of correctness for a network synchronizer
[AD-A192726] N88-27802
PROGRAMMERS
The programmer's apprentice project: A research overview
[AD-A192784] N88-27769
PROGRAMMING LANGUAGES
Implementation of an OPS5 derivative on the Novix RISC processor
[DE88-011392] N88-27758
Linguistic semantics for parallel computation
[PB88-105960] N88-27761
Bisimulation can't be traced
[AD-A192725] N88-27766
The SAS System by forms: Putting statistical power into the hands of an end-user
[DE88-010512] N88-27857
PROJECT PLANNING
European transonic wind tunnel project: Assistance to the design group
[ONERA-RSF-11/0694-GY-010-G] N88-27208
Studies concerning the European transonic wind tunnel
[ONERA-RSF-10/0694-GY-010-G] N88-27209
PROJECTILE CRATERING
Hole diameters in plates impacted by projectiles N88-27386
PROPAGATION
Perturbation expansions generated by an approximate propagator
[DE88-702435] N88-27866
PROPELLANT COMBUSTION
Some properties of ignition gases. Review of measuring results in the years 1981-1986)
[PB88-106968] N88-27259
PROPELLANT GRAINS
Some properties of ignition gases. Review of measuring results in the years 1981-1986)
[PB88-106968] N88-27259
PROPULSION SYSTEM CONFIGURATIONS
Variable Mach number wall jets for control/propulsion on hypervelocity projectiles/interceptors: Tests with an existing model
[AD-A192845] N88-27167
PROPULSION SYSTEM PERFORMANCE
Propulsion analysis and application potential of air breathing combined propulsion for ballistic space transporter
[ETN-88-92359] N88-27227
PROPULSIVE EFFICIENCY
Analytical and experimental investigation of ringless piston concept
[AD-A193213] N88-27559
PROTECTIVE COATINGS
Studies in support of oxidation-resistant composite materials
[AD-A193320] N88-27238
Refractory fibers surface treatment
[REPT-47-803/F] N88-27339
PROTEINS
Experiments in microgravity environment: Protein crystallization
[SNIAS-881-430-101] N88-27354
PROTOCOL (COMPUTERS)
A modular proof of correctness for a network synchronizer
[AD-A192726] N88-27802
PROTON ENERGY
Study of the production of Ko mesons in proton antiproton interactions at 630 GeV
[NOTA-INTERNA-908] N88-27892
PROTONS
Scaling laws for geomagnetic tail current sheet acceleration
[AD-A193379] N88-27659
PROTOTYPES
Optical evaluation of prototype stretched-membrane mirror modules for solar central receivers
[DE88-011884] N88-27637
SP-100 Ground Engineering Systems: Test facility control systems
[DE88-009195] N88-27895
PROVING
Oxidation-erosion of metals and alloys: Models, verification, and prediction
[DE88-010016] N88-27300
Ada (trade name) compiler validation summary report: Verdix Corporation VAda-010-03315, version 5.5 MicroVAX 2 host ISBC 386/20P Intel target
[AD-A193226] N88-27774
Ada (trade name) compiler validation summary report: Verdix corporation VAda-010-13125, version 5.41 Sun Microsystems Sun-3/160 host microbar GPC68020 target
[AD-A193415] N88-27777
PSEUDORANDOM SEQUENCES
A comparison of generators for pseudo-random normal deviates
[DE88-011711] N88-27859
PSYCHIATRY
Normative developmental equations for the EEG and their sensitivity to neurological and psychiatric disorders N88-27687
PSYCHOLOGICAL EFFECTS
Ejection situations in the U-2/TR-1: An analysis of emotions and events
[AD-A192872] N88-27175
CEEG dynamic brain mapping: A new method to evaluate brain function in different psychological and drug conditions N88-27685
Using ERPS to study human information processing N88-27698
Behavioral, psychological and demographic predictors of physical fitness
[AD-A192697] N88-27733
PSYCHOLOGICAL FACTORS
Rules, schema and decision making
[AD-A193389] N88-27967
PSYCHOMOTOR PERFORMANCE
Cognitive and neural bases of skilled performance
[AD-A193392] N88-27747
Determinants of dual-task interference and resource theories in cognitive psychology
[DFVLR-FB-88-14] N88-27748
PSYCHOPHYSICS
Perception of motion in statistically-defined displays
[AD-A193076] N88-27745
PSYCHOPHYSIOLOGY
Psychophysiological measures of drowsiness as estimators of mental fatigue and performance degradation during sleep deprivation N88-27702
PSYCHOTROPIC DRUGS
CEEG dynamic brain mapping: A new method to evaluate brain function in different psychological and drug conditions N88-27685
PULMONARY CIRCULATION
Validation of a modified one-step rebreathing technique for non-invasive measurement of submaximal cardiac output
[AD-A192852] N88-27735
PULSARS
Strange, quark and metastable neutron stars
[DE88-702404] N88-27984
Cascade model of gamma-ray bursts: Power-law and annihilation-line components
[NASA-TM-101176] N88-27998
PULSE GENERATORS
Radial compression of picosecond electrical pulses
[DE88-008440] N88-27544
Production of intensive electron beam impulsions by setup of pseudoglare discharges
[ISL-CO-210/87] N88-27920
PULSE RADAR
TDWR (Terminal Doppler Weather Radar) PRF (Pulse Repetition Frequency) selection criteria
[AD-A193089] N88-27407
PULSED LASERS
Process control improvements in pulsed Nd:YAG laser closure welding of electromechanical relays
[DE88-006275] N88-27564
PULSES
Long-pulse, high-power vircator experiments
[DE88-011787] N88-27458
PUMPS
Temperature rise in superfluid helium pumps
[NASA-TM-100997] N88-27507
Hydraulic pumps and hydraulic equipment at low temperatures
[DE88-752871] N88-27570
PUPIL SIZE
A human factors evaluation of the Advanced Visual Technology System (AVTS) eye tracking oculometer N88-27361
PURGING
Evaluation and improvement of liquid propellant rocket chugging analysis techniques. Part 1: A one-dimensional analysis of low frequency combustion instability in the fuel preburner of the space shuttle main engine
[NASA-CR-183106] N88-27224
PYRIDINES
Study of crosslinking and nonelastic mechanical properties of epoxy and PSP networks --- epoxy resins; polystyrylpyridine resins (psp)
[ETN-88-92740] N88-27337
PYRITES
Some equivalent circuit models for AC impedance analysis of pyrite/solution interface
[DE88-010574] N88-27452
PYROLYSIS
Refractory films from spin-cast carbon
[DE88-011251] N88-27327
PYROTECHNICS
Diode laser ignition of high explosives and pyrotechnics
[DE88-008771] N88-27352

Q

QUADRATIC EQUATIONS
A feasibility study in path planning using optimization techniques
[AD-A193030] N88-27177
QUADRATURES
Asymptotic of Peanokerns of finite fixed order
[ETN-88-92381] N88-27843
QUALITY CONTROL
Measuring dispersion effects of factors in factorial experiments
[AD-A193216] N88-27831
QUANTILES
Joint asymptotic distribution of marginal quantiles and quantile functions in samples from a multivariate population
[AD-A193385] N88-27856
QUANTITATIVE ANALYSIS
Direct determination of part-per-billion levels of volatile organics in water and soil samples using glow discharge mass spectrometry
[DE88-011389] N88-27272
QUANTUM CHROMODYNAMICS
An overview of lattice QCD
[DE88-010867] N88-27963
QUANTUM ELECTRODYNAMICS
Nonlinear dynamics of the electron self-field interaction
[DE88-010597] N88-27420
QUANTUM ELECTRONICS
Solid state research
[AD-A192837] N88-27929
QUANTUM MECHANICS
Determination of quantum corrections for electrical conductivity mechanism of three dimensional, perturbed copper coatings. Weak localization and electron-electron interaction
[ETN-88-92378] N88-27466
Evaluation of quantum mechanics path integrals by the approximations exact on a class of polynomial functionals
[DE88-702434] N88-27865
QUANTUM THEORY
Superalgebras with Grassmann algebra-valued structure constants from superfields
[DE88-702239] N88-27862
Quark nuclear model: Classification groups and two and three body correlations
[NOTA-INTERNA-896] N88-27891
QUANTUM WELLS
Solar energy conversion through the interaction of plasmons with tunnel junctions. Part A: Solar cell analysis. Part B: Photoconductor analysis
[NASA-CR-183044] N88-27621
Ultrafast physics in semiconductor microstructures
[AD-A193300] N88-27936
Laser spectroscopy of quantum well and superlattice structures
[AD-A193336] N88-27937
A study of tunneling phenomena in gallium arsenide-aluminum gallium arsenide heterostructures N88-27946
QUARK MODELS
Quark nuclear model: Classification groups and two and three body correlations
[NOTA-INTERNA-896] N88-27891
QUARKS
Strange, quark and metastable neutron stars
[DE88-702404] N88-27964
QUARTZ CRYSTALS
Quartz crystal resonators and oscillators for frequency control and timing applications
[AD-A193310] N88-27443
QUASARS
Is the 3C273 quasar Mach nearer
[DE88-702235] N88-27988
QUASI-STEADY STATES
Investigation of the quasi-steady approach used in transient two-phase flow analysis
[DE88-004303] N88-27489
QUEUEING THEORY
Three-dimensional scene analysis using stereo based imaging
[AD-A193120] N88-27178

R

RADAR CROSS SECTIONS
Definition of long ocean wave slope for radar applications
[AD-A193196] N88-27412
RADAR ECHOES
TDWR (Terminal Doppler Weather Radar) PRF (Pulse Repetition Frequency) selection criteria
[AD-A193089] N88-27407
Definition of long ocean wave slope for radar applications
[AD-A193196] N88-27412
Radar information from the partial derivatives of the echo signal phase from a point scatterer
[AD-A193402] N88-27415
RADAR IMAGERY
Linear feature extraction from radar imagery. Phase 2: Base contract report
[AD-A192828] N88-27404
RADAR RANGE
TDWR (Terminal Doppler Weather Radar) PRF (Pulse Repetition Frequency) selection criteria
[AD-A193089] N88-27407
RADAR SCANNING
Radar information from the partial derivatives of the echo signal phase from a point scatterer
[AD-A193402] N88-27415
RADIATION ABSORPTION
Assessment of cochlear damage after microwave irradiation
[AD-A193237] N88-27737
RADIATION BELTS
Solar flares and magnetospheric particles: Investigations based upon the ONR-602 and ONR-604 experiments
[AD-A193396] N88-27994
RADIATION DAMAGE
Data compilation for radiation damage on ceramic insulators. Revised with updated data and reviews
[DE88-753426] N88-27329
RADIATION DISTRIBUTION
Development of radiation and cloud parameterization programs for AFGL (Air Force Geophysics Laboratory) global models
[AD-A193369] N88-27658
RADIATION DOSAGE
Behavioral effects of exposure to the tempo high-power microwave system
[AD-A193305] N88-27738
RADIATION EFFECTS
A method for estimating the susceptibility of electronic systems to HPM (High Power Microwave)
[DE88-012246] N88-27422
Genetic effects of low level microwave radiation
[AD-A192687] N88-27722
Effects of pulsed and CW (Continuous Wave) 2450 MHz radiation on transformation and chromosomes of human lymphocytes in vitro
[AD-A193104] N88-27736
Assessment of cochlear damage after microwave irradiation
[AD-A193237] N88-27737
Behavioral effects of exposure to the tempo high-power microwave system
[AD-A193305] N88-27738
Dynamics of a plasma produced under effect of the XeCl-laser radiation on metallic surface
[DE88-701983] N88-27902
Dose-enhancement effects in TaSi/Al- and Al-gate MOS devices
[DE88-005483] N88-27926
RADIATION INJURIES
Assessment of cochlear damage after microwave irradiation
[AD-A193237] N88-27737
RADIATION MEASUREMENT
Angular radiation models for Earth-atmosphere system. Volume 1: Shortwave radiation
[NASA-RP-1184] N88-27677
RADIATION SHIELDING
A method for estimating the susceptibility of electronic systems to HPM (High Power Microwave)
[DE88-012246] N88-27422
RADIATION SOURCES
A plasma ultraviolet source for short wavelength lasers
[AD-A192844] N88-27537
RADIATION TOLERANCE
A comparison of the radiation tolerance characteristics of multijunction solar cells with series and voltage-matched configurations
[NASA-TM-101177] N88-27624
RADIATIVE HEAT TRANSFER
Radiative heat transfer and selective emission in planar slab coatings on hot emissive substrates
[AD-A193133] N88-27319
RADIATIVE TRANSFER
Validate algorithms for the determination of rainfall rates from SSM/I microwave satellite imagery
[AD-A192299] N88-27664
RADIO FREQUENCY INTERFERENCE
Airborne measurement of low frequency atmospheric noise ALFAN 1
[AD-A193056] N88-27405
A notch filter instrument for measuring ELF (Extremely Low Frequency) MSK (Minimum Shift Keying) signals
[AD-A193324] N88-27414
RADIO TRANSMISSION
An evaluation of two millimeter wave propagation models for horizontal atmospheric attenuation at 70-115 GHZ
[AD-A192699] N88-27403
RADIOACTIVE CONTAMINANTS
The distribution of some chemical elements between dissolved and particulate phases in the ocean
[DE88-010181] N88-27682
RADIOGENIC MATERIALS
The distribution of some chemical elements between dissolved and particulate phases in the ocean
[DE88-010181] N88-27682
RAILGUN ACCELERATORS
An interferometric measurement technique for railgun structures
[AD-A192851] N88-27217
Slew-induced deformations in a space-based electromagnetic rail gun N88-27385
Plasma behavior in the boundary layer near a railgun surface
[DE88-008889] N88-27909
RAINSTORMS
Validate algorithms for the determination of rainfall rates from SSM/I microwave satellite imagery
[AD-A192299] N88-27664
RAMAN SPECTRA
Refractory films from spin-cast carbon
[DE88-011251] N88-27327
RAMAN SPECTROSCOPY
Mitsubishi Electric Advance (R and D Edition), Volume 41
[PB88-194162] N88-27388
Polarization selective Raman microspectroscopy N88-27397
Steady-state approximations in Raman excitation equations
[DE88-011759] N88-27889
Characterization of crystalline silicon by electrochemical and Raman spectroscopy at the frontier semiconductor/electrolyte
[ETN-88-92354] N88-27956
RANDOM ACCESS
Full analysis of a powerful window random access algorithm
[AD-A192437] N88-27763
RANDOM NUMBERS
A comparison of generators for pseudo-random normal deviates
[DE88-011711] N88-27859
RANDOM PROCESSES
On the exceedance random measures for stationary processes
[AD-A192838] N88-27848
RANDOM VIBRATION
Diffusion models of crack growth due to random overloads
[DE88-008811] N88-27595
RANKING
An assessment of index term ranking N88-27974
RAREFIED GASES
Nozzle lip effects on gas expansion into the plume backflow region
[AD-A192806] N88-27475
RATIOS
On the estimation of a variance ratio
[AD-A193190] N88-27854
RAY TRACING
Simulation and analysis of wave propagation through random media N88-27503
RAYLEIGH SCATTERING
Investigations on Mie and Rayleigh scattering as basis for the development of Rayleigh temperature lidars with aid of Michelson interferometry
[GKSS-87/E/62] N88-27675
RAYLEIGH WAVES
A comparison of analytical techniques for modeling the Rayleigh-Taylor response of elastic-plastic solids
[DE88-010372] N88-27596
REACTION KINETICS
Laser probes of natural gas ignition chemistry
[PB88-212568] N88-27271
Laser probes and numerical modeling as process diagnostics in chemical vapor deposition
[DE88-011622] N88-27275
Study of crosslinking and nonelastic mechanical properties of epoxy and PSP networks — epoxy resins; polystyrylpyridine resins (psp)
[ETN-88-92740] N88-27337

Shock initiation studies on heterogeneous explosives
[DE88-008681] N88-27351
Methods of quantifying and enhancing reactive oxygen species production N88-27357
The kinetics of charge-transfer reactions on passive lithium electrodes
[DE88-009256] N88-27454

REACTION TIME
The effects of hypoxia on P300 and reaction time
[DCIEM-87-RR-12] N88-27697

REACTIVITY
Deformation, fracture and explosive properties of reactive materials
[AD-A193060] N88-27348

REACTOR MATERIALS
Creep behavior for Hastelloy-XR
[DE88-753428] N88-27295

REAL NUMBERS
Flexible valued algebras of four-dimensions
[ETN-88-92382] N88-27844

REAL TIME OPERATION
An investigation of performance improvement in knowledge-based control systems N88-27382
TDWR (Terminal Doppler Weather Radar) PRF (Pulse Repetition Frequency) selection criteria
[AD-A193069] N88-27407
FTMP data acquisition environment
[NASA-TM-100636] N88-27447
Development of a hybrid simulator for robotic manipulators
[AD-A193119] N88-27557
Army space systems for terrestrial applications
[AD-A192735] N88-27613
Implementation of an OPS5 derivative on the Novix RISC processor
[DE88-011392] N88-27758
Simulation of real time problem solving
[AD-A193436] N88-27778
Notes on operating system requirements for the next millennium
[DE88-010712] N88-27805

REBREATHING
Validation of a modified one-step rebreathing technique for measuring exercise cardiac output
[AD-A192600] N88-27729
Validation of a modified one-step rebreathing technique for non-invasive measurement of submaximal cardiac output
[AD-A192852] N88-27735

RECEIVERS
Airborne measurement of low frequency atmospheric noise ALFAN 1
[AD-A193056] N88-27405
Multifilter spectrometer (FEB) for microwave atmospheric sounder
[AD-A192312] N88-27426

RECOGNITION
Rules, schema and decision making
[AD-A193389] N88-27967

RECORDING
A 1/2-inch high-definition baseband VCR N88-27393

RECRYSTALLIZATION
Analysis of grain refinement and superplasticity in aluminum-magnesium alloys
[AD-A193029] N88-27283
Study of feasibility and optimization conditions of laser treatments: Application of the local recrystallization of aluminum
[ISAL-87-0048] N88-27309

RECTANGULAR WAVEGUIDES
Calculations of high-frequency parameters of disc-loaded waveguides
[DE88-702178] N88-27417

RECURSIVE FUNCTIONS
Parallel solutions to geometric problems on the scan model of computation
[AD-A192321] N88-27819

RED SHIFT
Is the 3C273 quasar Mach nearer
[DE88-702235] N88-27968

REDUCED GRAVITY
Experiments in microgravity environment: Protein crystallization
[SNIAS-881-430-101] N88-27354

REDUNDANCY
Dynamic modelling and estimation of the error due to asynchronism in a redundant asynchronous multiprocessor system
[NASA-CR-177427] N88-27205

REENTRY VEHICLES
In-flight motor torque estimates for the second-stage Strypi 9 launch vehicle
[DE88-010833] N88-27222

REFERENCE STARS
IPS guidestar selection for stellar mode (ASTRO)
[NASA-TM-100336] N88-27181

REFLECTANCE
Picosecond transient reflectivity of unpinned gallium arsenide (100) surfaces
[AD-A193242] N88-27933

REFLECTION
Experimental investigation of the reflection of a planar shock wave over a double wedge
[AD-A193078] N88-27482
Attachable interferometric strain gages
[AD-A192390] N88-27522
Effects of low reflection on the collector and source sheaths of a finite ion temperature plasma
[DE88-008929] N88-27908
Electromagnetic wave incoherent reflection by a half-space of weakly-ionized plasma with an absorbing boundary
[DE88-702413] N88-27917
Polarization of light reflected by vertically inhomogeneous planetary atmosphere
[DE88-702416] N88-27992

REFLECTOR ANTENNAS
Analytical approximation of a distorted reflector surface defined by a discrete set of points
[NASA-TM-101323] N88-27424

REFRACTIVITY
Predicting optical degradation of a laser beam through a turbulent shear layer N88-27376

REFRACTORY MATERIALS
Radiative heat transfer and selective emission in planar slab coatings on hot emissive substrates
[AD-A193133] N88-27319
Refractory fibers surface treatment
[REPT-47-803/F] N88-27339

REFRACTORY METALS
Refractory metal alloys and composites for space power systems
[NASA-TM-100946] N88-27310

REFRIGERATORS
Magnetic heat pumps
[DE88-012058] N88-27639

REFUELING
Temperature rise in superfluid helium pumps
[NASA-TM-100997] N88-27507

REGENERATION (ENGINEERING)
Full analysis of a powerful window random access algorithm
[AD-A192437] N88-27763

REGENERATORS
Advanced EMU electrochemically regenerable CO2 and moisture absorber module breadboard
[NASA-CR-172054] N88-27754

REGIONAL PLANNING
Utilization of a satellite communication system to protect the national communication network
[FUB-33-1986] N88-27423

REGRESSION ANALYSIS
Asymptotic normality of minimum L1-norm estimates in linear models
[AD-A193399] N88-27835

REGULATORS
A feasibility study in path planning using optimization techniques
[AD-A193030] N88-27177

REINFORCED PLASTICS
Injection compression for short fiber reinforced plastics
[SNIAS-881-430-118] N88-27344

REINFORCEMENT (STRUCTURES)
Cold worked reinforcing bars in tensile test under high loading rate and low temperatures
[DE88-752993] N88-27610

REINFORCING FIBERS
The two isotropic asymptotes of fiber composites
[AD-A192305] N88-27231
Theoretical and experimental analysis of the toughening behavior of whisker reinforcement in ceramic matrix composites
[DE88-011841] N88-27241

REINFORCING MATERIALS
The two isotropic asymptotes of fiber composites
[AD-A192305] N88-27231

RELATIVISTIC ELECTRON BEAMS
SARLAC: A relativistic electron beam code
[AD-A193134] N88-27411
Propagation of charged particle beams in the atmosphere
[AD-A193185] N88-27887

RELAXATION METHOD (MATHEMATICS)
Numerical integration of Navier-Stokes equations by application of multigrid concept
[ETN-88-92365] N88-27513

RELIABILITY
Probabilistic anisotropic failure criteria for composite materials
[AD-A193046] N88-27232

REMOTE CONTROL
Airborne remote operated device
[DE88-010324] N88-27188

REMOTE SENSING
Methods of determining playa surface conditions using remote sensing
[AD-A192663] N88-27612
Analysis of remotely sensed imagery using digital morphology
[AD-A192738] N88-27614
Active and passive remote sensing of ice
[AD-A193307] N88-27617
Remote sensing of wetlands: Applications overview
[DE88-010895] N88-27618
The detection and interpretation of long-term changes in ozone from space
[NASA-TM-101135] N88-27650
Computer simulation procedure for designing airborne aerometric monitoring programs
[DE88-011896] N88-27674

REMOTELY PILOTED VEHICLES
A demonstration of retro-traverse using a semi-autonomous land vehicle
[DE88-009851] N88-27568

REPORTS
RLE progress report, January 1 to December 31, 1987
[RLE-PR-130] N88-27869

REQUIREMENTS
Electrical load and power source capacity report for the C-130 aircraft Self Contained Navigation System (SCNS): LSI model 6216A, 6216B, 6216C, revision
[AD-A193079] N88-27186
Sources and nature of cost analysis data base reference manual
[AD-A193099] N88-27976

RESEARCH
Activities report of the Communications Department
[ENST-88D003] N88-27401

RESEARCH AND DEVELOPMENT
United States Air Force Graduate Student Summer Support Program, volume 2
[AD-A191122] N88-27355
Vision research. A national plan: 1983-1987, 1987 evaluation and update
[PB88-192604] N88-27726
Engineering data compendium. Human perception and performance. User's guide
[LC-87-19560] N88-27749
Materials research, superconductor and thin layer technology
[REPT-50/87] N88-27955
High technology space flight orientation program: Overview and recommendations
[ETN-88-92332] N88-27979

RESEARCH FACILITIES
Photovoltaic Measurements and Performance Branch
[DE88-001142] N88-27633
Publications on acoustics research at the Langley Research Center during 1980-1986
[NASA-TM-100590] N88-27881

RESEARCH MANAGEMENT
Aerospace applications studies, 1971-1987
[AGARD-R-759] N88-27147
Air Force technical objective document, FY89
[AD-A193110] N88-27194
Soviet dynamic fracture mechanics research
[FASAC-TAR-3140] N88-27597
Finite element methodology for integrated flow-thermal-structural analysis
[NASA-CR-183144] N88-27806
Atmospheric turbulence research at DFVLR
[AGARD-R-752] N88-27669
Federal Council on Science, Engineering and Technology: Committee on Computer Research and Applications, Subcommittee on Science and Engineering Computing: The US Supercomputer Industry
[DE88-011262] N88-27756
RLE progress report, January 1 to December 31, 1987
[RLE-PR-130] N88-27869
Publications on acoustics research at the Langley Research Center during 1980-1986
[NASA-TM-100590] N88-27881

RESIDUAL STRESS
Thermo-viscoelastic analysis of composite materials, volume 1
[NASA-CR-183048-VOL-1] N88-27230

RESONANCE
Aeromechanical stability analysis of COPTER N88-27161
Nonlinear stochastic interaction in aeroelastic structures
[AD-A193427] N88-27589

RESONANT FREQUENCIES
Prediction of the aeroelastic behavior of tuned blades. Application to aircraft engines
[ISAL-87-0046] N88-27199

RESONATORS
Quartz crystal resonators and oscillators for frequency control and timing applications
[AD-A193310] N88-27443
RESPIRATION
Metabolic and cardiorespiratory parameters during three consecutive days of exhaustive running
[AD-A192598] N88-27728
REYNOLDS STRESS
Coherent structures in the axisymmetric turbulent jet mixing layer N88-27504
RHEOLOGY
Optimal rheological characteristics in dynamic stability of polymer flow through porous media
[DE88-001225] N88-27322
RHODIUM
Mechanism of the nitric oxide-carbon monoxide-oxygen reaction over a single crystal rhodium catalyst
[DE88-006274] N88-27268
RHODIUM COMPOUNDS
Catalytic activation of carbon dioxide by metal complexes
[AD-A192310] N88-27262
RICCATI EQUATION
Control, stability and filter for a discrete linear stochastic system with correlated noise
[PB88-109525] N88-27818
RIEMANN MANIFOLD
Vortices on the world sheet and string's critical dynamics
[DE88-702116] N88-27961
RIGID ROTORS
A comparison of theory and experiment for coupled rotor-body stability of a hingeless rotor model in hover under simulated vacuum conditions N88-27151
A comparison of theory and experiment for coupled rotor-body stability of a hingeless rotor model in hover N88-27152
Aeroelastic modeling of rotor blades with spanwise variable elastic axis offset: Classic issues revisited and new formulations N88-27158
Aeromechanical stability analysis of COPTER N88-27161
ROBOTICS
Aircraft refueling demonstrator using a microbot alpha 2 robot N88-27367
Compliant robotic structures, part 3
[AD-A192426] N88-27556
Development of a hybrid simulator for robotic manipulators
[AD-A193119] N88-27557
Dexterous hands: Optimizing grasp by design and planning N88-27572
The VITE model: A neutral command circuit for a generating arm and articulator trajectories
[AD-A192715] N88-27734
The robust tracking control of nonlinear systems with uncertain dynamics N88-27788
Intelligent Mobile Autonomous System (IMAS)
[AD-A193181] N88-27811
ROBOTS
Three-dimensional scene analysis using stero based imaging
[AD-A193120] N88-27178
In-flight load measurements of the Robot-X canards
[AD-A193428] N88-27187
Aircraft refueling demonstrator using a microbot alpha 2 robot N88-27367
Motor-response learning at a process control panel by an autonomous robot
[DE88-005055] N88-27554
Compliant robotic structures, part 3
[AD-A192426] N88-27556
Development of a hybrid simulator for robotic manipulators
[AD-A193119] N88-27557
Control of free-flying space robot manipulator systems
[NASA-CR-183017] N88-27562
Control of free-flying space robot manipulator systems
[NASA-CR-183104] N88-27563
Research into the architecture of CAD based robot vision systems
[AD-A193330] N88-27776
ROBUSTNESS (MATHEMATICS)
The robust tracking control of nonlinear systems with uncertain dynamics N88-27788
Robust prediction for stationary processes: 2D enriched version
[AD-A193318] N88-27833
ROCKET ENGINE CASES
Rocket motor case materials. An evaluation of new fibers for composites
[FOA-C-20696-2.1] N88-27245
ROCKET EXHAUST
Variable Mach number wall jets for control/propulsion on hypervelocity projectiles/interceptors: Tests with an existing model
[AD-A192845] N88-27167
ROOM TEMPERATURE
Chemical vapor deposition of TiO2 thin films at room temperature
[DE88-008892] N88-27542
A new near-infrared tunable-room temperature solid state laser La3Ga5SiO14:Cr(3+)
[DE88-011341] N88-27543
ROTATING SHAFTS
Dynamic stability of elastic rotor-bearing systems via Liapunov's direct method N88-27571
ROTATING STALLS
A Navier-Stokes study of cascade flow fields including inlet distortion and rotating stall
[AD-A193109] N88-27483
ROTATION
Rotation symmetric vortex in axiparallel flow
[ETN-88-92364] N88-27512
ROTOR AERODYNAMICS
Integrated Technology Rotor Methodology Assessment Workshop
[NASA-CP-10007] N88-27148
Comparison of experimental rotor damping data-reduction techniques N88-27159
Comparison of experimental coupled helicopter rotor/body stability results with a simple analytical model N88-27160
ROTOR BLADES (TURBOMACHINERY)
Effects of static equilibrium and higher-order nonlinearities on rotor blade stability in hover N88-27157
ROTOR BODY INTERACTIONS
Integrated Technology Rotor Methodology Assessment Workshop
[NASA-CP-10007] N88-27148
A comparison of theory and experiment for coupled rotor-body stability of a hingeless rotor model in hover under simulated vacuum conditions N88-27151
A comparison of theory and experiment for coupled rotor-body stability of a hingeless rotor model in hover N88-27152
A comparison of theory and experiment for coupled rotor body stability of a bearingless rotor model in hover and forward flight N88-27154
The importance of steady and dynamic inflow on the stability of rotor-body systems N88-27156
Comparison of experimental coupled helicopter rotor/body stability results with a simple analytical model N88-27160
ROTORS
Dynamic stability of elastic rotor-bearing systems via Liapunov's direct method N88-27571
RUBBER
Rubber-modified epoxies: Interfacial tension and morphology
[AD-A192464] N88-27313
RULES
Rules, schema and decision making
[AD-A193389] N88-27967
RUN TIME (COMPUTERS)
Matrix substructuring, domain decomposition and particle methods: Current trends for solving PDEs in parallel
[DE88-009826] N88-27836
RUNGE-KUTTA METHOD
Effects of numerical dissipation on finite-volume solutions of compressible flow problems
[AD-A193173] N88-27485
KRYSI, an ODE solver combining a semi-implicit Runge-Kutta method and a preconditioned Krylov method
[DE88-012245] N88-27841
RUNNING
Metabolic and cardiorespiratory parameters during three consecutive days of exhaustive running
[AD-A192598] N88-27728
RUNWAYS
Alternate/modified binders for airfield pavements
[AD-A192781] N88-27206
RYDBERG SERIES
Study of energy levels and decay mechanisms for singlet Rydberg states of molecular nitrogen
[AD-A192505] N88-27886

S

S MATRIX THEORY
Polarization of light reflected by vertically inhomogeneous planetary atmosphere
[DE88-702416] N88-27992
SACCADIC EYE MOVEMENTS
Influence of moving visual environment on saccadic eye movements and fixation N88-27368
SALT SPRAY TESTS
Stress corrosion of C ring specimen in salt spray tests
[I-186/87] N88-27307
SAMPLING
Analysis of debris from accelerated life test of the Hughes five-year Vuilleumier cryocooler
[AD-A193101] N88-27400
SATELLITE ALTIMETRY
FORTRAN programs for computation of time dependent sea levels and trajectory errors from satellite altimeter data
[BONN-MITT-73] N88-27216
SATELLITE IMAGERY
Validate algorithms for the determination of rainfall rates from SSM/I microwave satellite imagery
[AD-A192299] N88-27664
SATELLITE OBSERVATION
Cyrogenic test facilities for an optical cryomechanism qualification
[SNIAS-881-440-116] N88-27219
SATELLITE SOUNDING
Field-aligned structure of the storm time Pc 5 wave of November 14-15, 1979
[AD-A193022] N88-27653
SATELLITE-BORNE INSTRUMENTS
Basic research for the geodynamics program
[NASA-CR-183149] N88-27662
SCALE EFFECT
Size effects in linear elastic fracture mechanics N88-27609
SCALING LAWS
Scaling laws for geomagnetic tail current sheet acceleration
[AD-A193379] N88-27659
SCANNERS
Equipment for an advanced electron beam lithography system
[AD-A192956] N88-27435
Parallel solutions to geometric problems on the scan model of computation
[AD-A192321] N88-27819
SCANNING
Scanning tunneling microscopy as a surface chemical probe
[AD-A192710] N88-27263
SCATTERING
Radar information from the partial derivatives of the echo signal phase from a point scatterer
[AD-A193402] N88-27415
SCENE ANALYSIS
Three-dimensional scene analysis using stero based imaging
[AD-A193120] N88-27178
SCHOTTKY DIODES
Schottky-barrier formation on a covalent semiconductor without Fermi-level pinning: The Metal-MoS2(0001) interface
[AD-A193044] N88-27931
SCHROEDINGER EQUATION
Cauchy problem for the nonlinear Schroedinger equation
[DE88-702454] N88-27867
SCIENTIFIC SATELLITES
MAXIE-1 (Magnetospheric Atmospheric X-ray Imaging Experiment)
[AD-A192848] N88-27221
SEA ICE
Active and passive remote sensing of ice
[AD-A193307] N88-27617
SEA LEVEL
FORTRAN programs for computation of time dependent sea levels and trajectory errors from satellite altimeter data
[BONN-MITT-73] N88-27216
SEA WATER
MIZPAC (marginal ice zone Pacific) 84-86 CTD (Conductivity, Temperature, Depth) data report
[AD-A192478] N88-27679
SECURITY
Technology security, volume 1
[DE88-008612] N88-27978
SEISMIC WAVES
Stochastic geologic effects on near-field ground motions in alluvium
[AD-A192315] N88-27652
SEISMOLOGY
Stochastic geologic effects on near-field ground motions in alluvium
[AD-A192315] N88-27652
SEMANTICS
A cockpit natural language study: Vocabulary and grammar analyses
[AD-A193289] N88-27753

Linguistic semantics for parallel computation
[PB88-105960] N88-27761

SEMICONDUCTING FILMS
Silicon-on-insulator pin diodes
[AD-A193359] N88-27445
Molecular beam epitaxy of GaP films on Si substrates
[PB88-131974] N88-27923

SEMICONDUCTOR DEVICES
Studying the physics and operation of multi-terminal near-micron and sub-micron length, hot electron semiconductor devices
[AD-A193380] N88-27446
Solid state research
[AD-A192837] N88-27929
Investigation of electronic band structure of semiconductors by photoemission
[ETN-88-92370] N88-27957

SEMICONDUCTOR DIODES
Diode laser ignition of high explosives and pyrotechnics
[DE88-008771] N88-27352
A GaAs solid state device model for high power applications
[DE88-011320] N88-27457
Photodiodes for optical communication in the near infrared
[ETN-88-92370] N88-27900

SEMICONDUCTOR JUNCTIONS
A comparison of the radiation tolerance characteristics of multijunction solar cells with series and voltage-matched configurations
[NASA-TM-101177] N88-27624

SEMICONDUCTORS (MATERIALS)
Numerical calculations of dopent diffusion involving flashlamp heating of silicon N88-27384
Polarization selective Raman microspectroscopy N88-27397
NDP (Neutron Depth Profiling) evaluations of boron-implanted compound semiconductors
[AD-A192306] N88-27425
Studying the physics and operation of multi-terminal near-micron and sub-micron length, hot electron semiconductor devices
[AD-A193380] N88-27446
Solid state research
[AD-A192837] N88-27929
Schottky-barrier formation on a covalent semiconductor without Fermi-level pinning: The Metal-MoS2(0001) interface
[AD-A193044] N88-27931
Ultrafast physics in semiconductor microstructures
[AD-A193300] N88-27936
Prediction of deep levels and equilibrium concentrations of defects in semiconductors N88-27945
Deep level defects in semiconductors: Stress and pressure studies
[DE88-010855] N88-27948
X-ray studies of strain, interface and impurities in semiconductors
[DE88-012460] N88-27954
Techniques and instrumentation for transient characterization of metal-insulator-semiconductor diodes. Applications to metal-insulator InP system
[ECL-87-17] N88-27959

SENSITIVITY
Performance sensitivities for point-focus dish systems with secondary concentrators
[DE88-001152] N88-27629

SENSORIMOTOR PERFORMANCE
Neurophysiological precursors of accurate visuomotor performance N88-27706

SENSORY PERCEPTION
Engineering data compendium. Human perception and performance. User's guide
[LC-87-19560] N88-27749

SEPARATED FLOW
Experimental study of unsteady separating turbulent boundary layers
[AD-A192997] N88-27477
Physical mechanisms in shock-induced turbulent separated flow
[AD-A193165] N88-27484
A documentation of two- and three-dimensional shock-separated turbulent boundary layers
[NASA-TM-101008] N88-27519

SEQUENCING
Spatial organization of homopolymer chains inside spherical polybutadiene domains of SB diblock copolymers
[AD-A193390] N88-27321
Robust prediction for stationary processes: 2D enriched version
[AD-A193318] N88-27833

SERVICE LIFE
Results from life test in progress on eagle-picher nickel cadmium cells
[AD-A192816] N88-27434
Sodium/sulfur cell evaluation results
[DE88-011488] N88-27451

SHAPES
Theoretical predictions of precipitate shapes in cubic alloys
[DE88-010856] N88-27291
Texture perception and shape from texture
[AD-A192923] N88-27771
Distortion functions
[DE88-752634] N88-27896

SHEAR FLOW
Cavitation inception in a turbulent shear flow
[DE88-011486] N88-27497
Granular flow: Particle-dynamics simulations of steady flow
[DE88-011342] N88-27506
Direct simulation of stable stratified homogeneous turbulent shear flows
[DFVLR-FB-88-04] N88-27516

SHEAR LAYERS
Predicting optical degradation of a laser beam through a turbulent shear layer N88-27376
An analysis of horizontal temperature gradients and heat content in the mixed layer and the surface forcing during PATCHEX
[AD-A192330] N88-27678

SHEAR PROPERTIES
An experimental and analytical evaluation of a biaxial test for determining shear properties of composite materials
[NASA-CR-182926] N88-27593

SHEAR STRESS
Characterization of accelerating pipe flow
[AD-A193065] N88-27481
Liquid crystals for unsteady surface shear stress visualization
[DE88-010570] N88-27527

SHEATHS
Effects of low reflection on the collector and source sheaths of a finite ion temperature plasma
[DE88-006929] N88-27908

SHELLS (STRUCTURAL FORMS)
Adaptive finite element methods for shells
[AD-A193221] N88-27585

SHOCK LAYERS
Research in applied mathematics
[AD-A192385] N88-27820

SHOCK WAVE INTERACTION
A documentation of two- and three-dimensional shock-separated turbulent boundary layers
[NASA-TM-101008] N88-27519

SHOCK WAVE PROPAGATION
Research in applied mathematics
[AD-A192385] N88-27820

SHOCK WAVES
Experimental investigation of the reflection of a planar shock wave over a double wedge
[AD-A193078] N88-27482
A documentation of two- and three-dimensional shock-separated turbulent boundary layers
[NASA-TM-101008] N88-27519

SHORT WAVE RADIATION
Angular radiation models for Earth-atmosphere system. Volume 1: Shortwave radiation
[NASA-RP-1184] N88-27677

SHUTDOWNS
Evaluation and improvement of liquid propellant rocket chugging analysis techniques. Part 1: A one-dimensional analysis of low frequency combustion instability in the fuel preburner of the space shuttle main engine
[NASA-CR-183106] N88-27224
Evaluation and improvement of liquid propellant rocket chugging analysis techniques. Part 2: A study of low frequency combustion instability in rocket engine preburners using a heterogeneous stirred tank reactor model
[NASA-CR-182724] N88-27225

SIDELOBES
Sidelobe level of an adaptive array using the SMI (Sampled Matrix Inversion) algorithm
[AD-A193131] N88-27409

SIGNAL MEASUREMENT
A notch filter instrument for measuring ELF (Extremely Low Frequency) MSK (Minimum Shift Keying) signals
[AD-A193324] N88-27414

SIGNAL PROCESSING
MAXIE-1 (Magnetospheric Atmospheric X-ray Imaging Experiment)
[AD-A192846] N88-27221
A numerically efficient digital matched filter for periodic and windowed periodic radar waveforms
[AD-A193132] N88-27410
Fourth generation neurocognitive pattern analysis system N88-27686
The application of non-stationary data analysis techniques in the identification of changes in the electroencephalogram associated with the onset of drowsiness N88-27688
A statistical procedure for the evaluation of presence/non-presence of stimulus-related EEG activity N88-27689
Demodulation processes in auditory perception
[AD-A193421] N88-27740
Robust methods for array signal processing
[AD-A192854] N88-27871
Solid state research
[AD-A192837] N88-27929

SIGNAL TO NOISE RATIOS
Detection of acceleration (+Gz) induced blackout by matched-filtering of visual evoked potentials N88-27710

SIGNAL TRANSMISSION
A 1/2-inch high-definition baseband VCR N88-27393
Dependence effects in unique signal transmission
[DE88-010331] N88-27419

SIGNS AND SYMPTOMS
Simulator sickness in the AH-64 Apache combat mission simulator
[AD-A193419] N88-27739

SILICA GEL
Precursor chemistry and the structure of silica aerogels
[DE88-011253] N88-27328

SILICA GLASS
Adhesion of hydrated silicate films
[DE88-011250] N88-27333

SILICATES
Adhesion of hydrated silicate films
[DE88-011250] N88-27333

SILICON
Kinetic of oxidation to air of a Fe-Al-Mn alloy system at 600-800(sup 0)C temperature range
[DE88-702309] N88-27330
Studying the physics and operation of multi-terminal near-micron and sub-micron length, hot electron semiconductor devices
[AD-A193380] N88-27446
Molecular beam epitaxy of GaP films on Si substrates
[PB88-131974] N88-27923

SILICON ALLOYS
Low-band-gap, amorphous-silicon-based alloys by photochemical vapor deposition
[DE88-001165] N88-27944
Calculation of the specific and volumetric enthalpies of Ge-Si alloys
[DE88-008949] N88-27965

SILICON DIOXIDE
Improved adhesion for SiO2 particles in silica substrates using helium-ion irradiation
[DE88-008915] N88-27332
Silicon oxidation studies: A review of recent studies on thin film silicon dioxide formation in the physics and chemistry of SiO2 and the Si-SiO2 interface
[AD-A193176] N88-27932

SILICON FILMS
Stability of uncapsulated weight cells with thin film elongation measurement bands under influence of humidity, temperature and operation voltage
[ETN-88-92383] N88-27531
Silicon oxidation studies: A review of recent studies on thin film silicon dioxide formation in the physics and chemistry of SiO2 and the Si-SiO2 interface
[AD-A193176] N88-27932

SILICON JUNCTIONS
Characterization of crystalline silicon by electrochemical and Raman spectroscopy at the frontier semiconductor/electrolyte
[ETN-88-92354] N88-27956

SILICON POLYMERS
Silicon-on-insulator pin diodes
[AD-A193359] N88-27445

SILICON TRANSISTORS
Integrated magnetic field sensor using high magnetotransistors
[ETN-88-92356] N88-27465

SILOXANES
Ionic conductive polymers based on crosslinked elastic siloxane-ethylene oxide copolymers
[DE88-011243] N88-27311

SIMPLEX METHOD
Linear programming for Air Force decision aiding N88-27378

SIMULATION
Documentation of the Benson Diesel Engine Simulation Program
[NASA-TM-100940] N88-27201

Implicit finite-difference simulation of an internal flow in a nozzle: An example of a physical application on a hypercube
[AD-A192475] N88-27472
Numerical experiments on turbulent mixing
[AD-A192572] N88-27473
Granular flow: Particle-dynamics simulations of steady flow
[DE88-011342] N88-27506
Direct simulation of stable stratified homogeneous turbulent shear flows
[DFVLR-FB-88-04] N88-27516
Cloud simulation warm cloud experiments: Droplet growth and aerosol scavenging
[AD-A192944] N88-27666
Electroencephalographic correlates of pilot performance: Simulation and in-flight studies
N88-27711
Analysis of lower hybrid current drive and rampup experiments on the JT-60 tokamak
[DE88-753136] N88-27915

SIMULATORS
Electromagnetic characterization and acceptance test of the EMP simulator SPERANS
[PB88-203781] N88-27416
Can CNV amplitude predict ability to accomplish a demanding task? N88-27700
Block Oriented Simulation System (BOSS)
[NASA-CR-182947] N88-27760

SINGLE CRYSTALS
Mechanism of the nitric oxide-carbon monoxide-oxygen reaction over a single crystal rhodium catalyst
[DE88-006274] N88-27268
Energy migration, motion and order in synthetic polymers
[AD-A193334] N88-27320
Silicon-on-insulator pin diodes
[AD-A193359] N88-27445
Experimental fabrication of thin film single crystalline solar cells
[PB88-131958] N88-27627
Growth and characterization of CuGaS2, CuAlS2 and CuGa0.9Al0.1S2 single crystals
[AD-A192963] N88-27930

SITE SELECTION
Review of geographic processing techniques applicable to regional analysis
[DE88-010759] N88-27643

SIZE (DIMENSIONS)
Size effects in linear elastic fracture mechanics
N88-27609

SKIN TEMPERATURE (BIOLOGY)
Physiological responses to acute exercise-heat stress
[AD-A192606] N88-27732

SLEEP
The application of non-stationary data analysis techniques in the identification of changes in the electroencephalogram associated with the onset of drowsiness N88-27688
Psychophysiological measures of drowsiness as estimators of mental fatigue and performance degradation during sleep deprivation N88-27702

SLEEP DEPRIVATION
Psychophysiological measures of drowsiness as estimators of mental fatigue and performance degradation during sleep deprivation N88-27702

SLENDER BODIES
Forces and moments on a slender, cavitating body
[DE88-007208] N88-27491

SLENDER WINGS
Optimal control of the wing rock phenomenon
N88-27373

SLEWING
Slew-induced deformations in a space-based electromagnetic rail gun N88-27385

SLIDING FRICTION
Studies of dynamic contact of ceramics and alloys for advanced heat engines
[DE88-008996] N88-27324

SLITS
Experimental investigation of simplest inhomogeneities in cylindrical slit line
[DE88-702388] N88-27418

SMOKE
A study relating to the fog oil replacement program
[AD-A192536] N88-27347

SMOOTHING
Distributive iteration for indefinite systems as smoothing method in multigrid process on example of Stokes and Navier-Stokes equations with emphasis on incomplete decompositions
[ETN-88-92127] N88-27509
Outliner resistant filtering and smoothing: 2D version
[AD-A193319] N88-27874

SNOW COVER
Active and passive remote sensing of ice
[AD-A193307] N88-27617

SODIUM
Spectral line shapes from highly ionized sodium plasmas
[AD-A193401] N88-27907

SODIUM CHLORIDES
Nuclear magnetic resonance spectrometer
[AD-A192928] N88-27523

SODIUM SULFUR BATTERIES
Failure analysis of Chloride Silent Power, Ltd. PB cells
[DE88-010567] N88-27448
Component stress during freeze/thaw cycling
[DE88-011204] N88-27449
Sodium/sulfur cell evaluation results
[DE88-011488] N88-27451
Effect of thermal cycling on CSPL (Chloride Silent Power Ltd.) sodium/sulfur cells
[DE88-011205] N88-27455
Post-test observations on CSPL (Chloride Silent Power Limited) cells
[DE88-011975] N88-27461

SOFTWARE ENGINEERING
Control of free-flying space robot manipulator systems
[NASA-CR-183104] N88-27563
Space shuttle natural environment analysis
[NASA-CR-179337] N88-27676
Block Oriented Simulation System (BOSS)
[NASA-CR-182947] N88-27760
The programmer's apprentice project: A research overview
[AD-A192784] N88-27769
Software engineering guidelines for RASP and ANDECS: Requirements and architectural design
[DFVLR-MITT-88-07] N88-27793
FORTRAN 77 implementation of abstract datatype models
[DFVLR-MITT-88-08] N88-27794
A PRELUDE (analysis and design of control systems-preliminary utilities depository). A data-based interactive system of control software, user's guid e
[DFVLR-MITT-88-12] N88-27795

SOFTWARE TOOLS
Numerical optimization, system theoretic and software tools for the integrated design of flexible structures and their control systems
[AD-A192927] N88-27183
User's manual for the two-dimensional transputer graphics toolkit
[NASA-TM-100974] N88-27799
Improving the performance of AI algorithms
[AD-A192848] N88-27809

SOI (SEMICONDUCTORS)
Silicon-on-insulator pin diodes
[AD-A193359] N88-27445

SOILS
Direct determination of part-per-billion levels of volatile organics in water and soil samples using glow discharge mass spectrometry
[DE88-011389] N88-27272

SOL-GEL PROCESSES
Preparation and properties of new inorganic glasses and gel-derived solids
[AD-A192922] N88-27315
Ellipsometric imaging of drying sol-gel films
[DE88-011785] N88-27335
Application of sol-gel procedures to ceramic composites
[ETN-88-92741] N88-27338
Comparison of sol-gel procedures for zircon and alumina
[SNIAS-881-430-108] N88-27342

SOLAR CELLS
Solar cell modeling and simulation
[AD-A193249] N88-27620
Solar energy conversion through the interaction of plasmons with tunnel junctions. Part A: Solar cell analysis. Part B: Photoconductor analysis
[NASA-CR-183044] N88-27621
Device physics related to the granular nature of CuInSe2 solar cells
[DE88-001159] N88-27622
Laser-heated CVD process for depositing thin films for low-cost solar-cell applications
[DE88-001162] N88-27623
A comparison of the radiation tolerance characteristics of multijunction solar cells with series and voltage-matched configurations
[NASA-TM-101177] N88-27624
Experimental fabrication of thin film single crystalline solar cells
[PB88-131958] N88-27627
Amorphous silicon solar cells using a metal substrate
[PB88-131941] N88-27628
Space photovoltaic generators. State of the art, trends
[SNIAS-881-440-106] N88-27640
Low-band-gap, amorphous-silicon-based alloys by photochemical vapor deposition
[DE88-001165] N88-27944

SOLAR COLLECTORS
Performance sensitivities for point-focus dish systems with secondary concentrators
[DE88-001152] N88-27629
Calculation of the specific and volumetric enthalpies of Ge-Si alloys
[DE88-008949] N88-27985

SOLAR COSMIC RAYS
Solar flares and magnetospheric particles: Investigations based upon the ONR-602 and ONR-604 experiments
[AD-A193396] N88-27994

SOLAR ENERGY
Photovoltaic Measurements and Performance Branch
[DE88-001142] N88-27633

SOLAR ENERGY CONVERSION
Performance sensitivities for point-focus dish systems with secondary concentrators
[DE88-001152] N88-27629
Reflux heat-pipe solar receivers for dish-electric systems
[DE88-008671] N88-27631

SOLAR FLARES
Measurement of macroscopic electric fields in solar plasma structures
[AD-A193291] N88-27993
Solar flares and magnetospheric particles: Investigations based upon the ONR-602 and ONR-604 experiments
[AD-A193396] N88-27994

SOLAR FLUX
Reflux heat-pipe solar receivers for dish-electric systems
[DE88-008671] N88-27631

SOLAR GENERATORS
Reflux heat-pipe solar receivers for dish-electric systems
[DE88-008671] N88-27631
Photovoltaic Energy. Electricity from Sunlight: A current awareness bulletin
[DE88-008289] N88-27634
Space photovoltaic generators. State of the art, trends
[SNIAS-881-440-106] N88-27640

SOLAR POWER SATELLITES
Technology for large space systems: A bibliography with indexes (supplement 18)
[NASA-SP-7046(18)] N88-27214

SOLAR PROMINENCES
Measurement of macroscopic electric fields in solar plasma structures
[AD-A193291] N88-27993

SOLAR RADIATION
Overview and future direction for blackbody solar-pumped lasers
[NASA-TM-100621] N88-27553
Development of radiation and cloud parameterization programs for AFGL (Air Force Geophysics Laboratory) global models
[AD-A193369] N88-27658
SERI standard broadband format: A solar and meteorological data archival format
[DE88-001145] N88-27975

SOLAR REFLECTORS
Specular steel surfaces for solar mirror substrates
[DE88-001153] N88-27630

SOLAR SPECTRA
Measurement of macroscopic electric fields in solar plasma structures
[AD-A193291] N88-27993

SOLAR SYSTEM
Activities report of the Institute for Extraterrestrial Physics
[MPE-206] N88-27981

SOLAR WIND
Magnetohydrodynamic wave propagation in the solar wind
[DE88-702411] N88-27995

SOLDERED JOINTS
Thermal cycling tests on surface-mount assemblies
[DE88-007695] N88-27453

SOLDERING
Conductivity mechanism and operating behavior of electrically conductive adhesives on the example of a power transistor
[ETN-88-92355] N88-27464

SOLID ELECTROLYTES
Failure analysis of Chloride Silent Power, Ltd. PB cells
[DE88-010567] N88-27448

SOLID MECHANICS
Finite element method for plate structures with inclined angles
[ILR-MITT-182] N88-27842

Some stability criteria in fluid and solid mechanics N88-27966

SOLID PROPELLANT IGNITION
Some properties of ignition gases. Review of measuring results in the years 1981-1986) [PB88-106968] N88-27259

SOLID STATE DEVICES
A GaAs solid state device model for high power applications [DE88-011320] N88-27457
Solid state research [AD-A192837] N88-27929

SOLID STATE LASERS
Laser spectroscopy investigations of materials for solid state laser systems [AD-A192514] N88-27535
A new near-infrared tunable-room temperature solid state laser La3Ga5SiO14:Cr(3+) [DE88-011341] N88-27543

SOLID-SOLID INTERFACES
Thermo-mechanical cracking in coated media with a cavity by a moving asperity friction [AD-A193311] N88-27586

SOLIDIFICATION
Survey of the literature on fractals with possible applications to phase change processes [DE88-012240] N88-27277

SOLIDS
A comparison of analytical techniques for modeling the Rayleigh-Taylor response of elastic-plastic solids [DE88-010372] N88-27596
Monolithic fuel cells [DE88-012004] N88-27638

SOLUBILITY
A method for determining the solubility of hydrogen in molten aluminum-lithium alloys [DE88-009807] N88-27270
Interfacial tension of immiscible polymer blends: Temperature and molecular weight dependence [AD-A192463] N88-27312
Soluble metal chelate polymers of coordination numbers six, seven and eight [AD-A192485] N88-27314

SOUND FIELDS
Vertical directionality of ambient noise at 32 deg N as a function of longitude: Tape number 86180 [AD-A193228] N88-27872

SOUND WAVES
Reflection of sound in open ended ducts [PB88-103478] N88-27870
Propagation of acoustic disturbances in transonic flow fields of lifting wings [DFVLR-FB-88-13] N88-27880

SPACE COLONIES
Steps toward lunar settlement [DE88-009141] N88-27213

SPACE INDUSTRIALIZATION
Economic impact of space flight activities in West Germany. Influence of allocations of Bundesministerium fuer Forschung und Technologie [ETN-88-92106] N88-27215

SPACE MANUFACTURING
Steps toward lunar settlement [DE88-009141] N88-27213
Homogeneity of glasses: Experiment WL-IHF-05 in D1 mission --- Spacelab [ETN-88-92339] N88-27353
Experiments in microgravity environment: Protein crystallization [SNIAS-881-430-101] N88-27354

SPACE PERCEPTION
A model for visual attention [AD-A193061] N88-27744

SPACE POWER REACTORS
SP-100 Ground Engineering Systems: Test facility control systems [DE88-009195] N88-27695

SPACE PROGRAMS
High technology space flight orientation program: Overview and recommendations [ETN-88-92332] N88-27979
History of manned spaceflight [CNES-NT-121] N88-28000

SPACE SHUTTLE BOOSTERS
Assembly Test Article (ATA) [NASA-CR-179361] N88-27226

SPACE SHUTTLE MAIN ENGINE
Evaluation and improvement of liquid propellant rocket chugging analysis techniques. Part 1: A one-dimensional analysis of low frequency combustion instability in the fuel preburner of the space shuttle main engine [NASA-CR-183106] N88-27224
Evaluation and improvement of liquid propellant rocket chugging analysis techniques. Part 2: A study of low frequency combustion instability in rocket engine preburners using a heterogeneous stirred tank reactor model [NASA-CR-182724] N88-27225

SPACE SHUTTLE PAYLOADS
The detection and interpretation of long-term changes in ozone from space [NASA-TM-101135] N88-27650

SPACE SHUTTLES
Space shuttle phase B wind tunnel model and test information. Volume 2: Orbiter configuration [NASA-CR-178415-VOL-2-PT-2] N88-27172
Space shuttle natural environment analysis [NASA-CR-179337] N88-27676

SPACE STATIONS
Vapor Compression Distillation Subsystem (VCDS) component enhancement, testing and expert fault diagnostics development, volume 2 [NASA-CR-172076] N88-27755
Block Oriented Simulation System (BOSS) [NASA-CR-182947] N88-27760

SPACE WEAPONS
Slew-induced deformations in a space-based electromagnetic rail gun N88-27385
Future SDI (Strategic Defense Initiative) decision making [AD-A192794] N88-27860
Overview of the SDI (Strategic Defense Initiative) Program in short wavelength chemical lasers [DE88-007912] N88-27861

SPACE-TIME FUNCTIONS
Photon limited image processing in the space-time domain [AD-A193142] N88-27655

SPACECRAFT CONFIGURATIONS
EXSAT: Expert system to configure telecommunication satellites [SNIAS-881-440-101] N88-27223

SPACECRAFT CONSTRUCTION MATERIALS
Reinforced plastics: Winding and weaving technologies for space products [SNIAS-881-430-103] N88-27341

SPACECRAFT DESIGN
EXSAT: Expert system to configure telecommunication satellites [SNIAS-881-440-101] N88-27223
Design of booster wound structures --- spacecraft structures [SNIAS-881-430-102] N88-27228

SPACECRAFT MOTION
Contribution to the numerical solution of airplane spin motion [ETN-88-92368] N88-27190

SPACECRAFT POWER SUPPLIES
Refractory metal alloys and composites for space power systems [NASA-TM-100948] N88-27310
Space photovoltaic generators. State of the art, trends [SNIAS-881-440-106] N88-27640

SPACECRAFT PROPULSION
Propulsion analysis and application potential of air breathing combined propulsion for ballistic space transporter [ETN-88-92369] N88-27227

SPACECRAFT STRUCTURES
Design of booster wound structures --- spacecraft structures [SNIAS-881-430-102] N88-27228
Reinforced plastics: Winding and weaving technologies for space products [SNIAS-881-430-103] N88-27341
Vibration control of large structures [AD-A193317] N88-27587

SPACECRAFT TRACKING
Spacecraft applications of advanced global positioning system technology [NASA-CR-172055] N88-27180

SPACECREWS
The human element in space: Lessons from Antarctica [AD-A193440] N88-27741
History of manned spaceflight [CNES-NT-121] N88-28000

SPACELAB PAYLOADS
Homogeneity of glasses: Experiment WL-IHF-05 in D1 mission --- Spacelab [ETN-88-92339] N88-27353

SPARE PARTS
Computation of ECM (Electronic Counter-Measures) war reserve materiel spare requirements [AD-A193301] N88-27195

SPARK IGNITION
Summary of discussions at the Tenth Meeting of the Sandia Cooperative Group on the Aerothermochemistry of Turbulent Combustion [DE88-008467] N88-27269
Experimental validation of a zero-dimensional computer model for spark-ignition engines [DE88-009034] N88-27565

SPARKS
Coupling of a spark source mass spectrograph and a ND-YAG laser [DE88-012116] N88-27530

SPATIAL DISTRIBUTION
Spatial organization of homopolymer chains inside spherical polybutadiene domains of SB diblock copolymers [AD-A193390] N88-27321
Radar information from the partial derivatives of the echo signal phase from a point scatterer [AD-A193402] N88-27415
A three-dimensional model of the gas-cell atomic frequency standard [AD-A193218] N88-27868

SPATIAL RESOLUTION
Investigation of the potential impact of new photonic materials on optical processing systems N88-27359
Perception of motion in statistically-defined displays [AD-A193076] N88-27745

SPECIFIC HEAT
Interactions between superconductivity and Kondo-grid properties in CeCu2Si2. Measurement results of specific heat under high pressure [ETN-88-92377] N88-27958

SPECIFICATIONS
Assembly Test Article (ATA) [NASA-CR-179361] N88-27226
The MELMUX MX-7100 series high-speed digital multiplexers N88-27396

SPECIMEN GEOMETRY
Stress corrosion of C ring specimen in salt spray tests [I-186/87] N88-27307
An experimental and analytical evaluation of a biaxial test for determining shear properties of composite materials [NASA-CR-182928] N88-27593

SPECTRAL ENERGY DISTRIBUTION
Statistical description of stochastic dynamics [AD-A192924] N88-27852

SPECTRAL LINE WIDTH
Spectral line shapes from highly ionized sodium plasmas [AD-A193401] N88-27907

SPECTRAL REFLECTANCE
Methods of determining playa surface conditions using remote sensing [AD-A192663] N88-27612

SPECTRAL RESOLUTION
The collection of statistics on the frequency of cloud cover over North America [AD-A193093] N88-27667

SPECTROGRAPHS
Coupling of a spark source mass spectrograph and a ND-YAG laser [DE88-012116] N88-27530

SPECTROMETERS
Scanning tunneling microscopy as a surface chemical probe [AD-A192710] N88-27263
Multifilter spectrometer (FEB) for microwave atmospheric sounder [AD-A192312] N88-27426
Nuclear magnetic resonance spectrometer [AD-A192928] N88-27523
Calibration of the portable wear metal analyzer [AD-A192971] N88-27524

SPECTROSCOPY
Velocity measurements and flow visualization in turbulent three-dimensional supersonic flows using oxygen flow tagging [AD-A192551] N88-27165
Optical diagnostics for metallurgical processes [DE88-009255] N88-27289
Calibration of the portable wear metal analyzer [AD-A192971] N88-27524
Use of Moessbauer spectroscopy to study implanted surfaces [DE88-010452] N88-27942

SPECTRUM ANALYSIS
Multifilter spectrometer (FEB) for microwave atmospheric sounder [AD-A192312] N88-27426
Statistical analysis of dyadic stationary processes [AD-A193057] N88-27853

SPECULAR REFLECTION
Deformation, fracture and explosive properties of reactive materials
[AD-A193080] N88-27348
SPEECH
A cockpit natural language study: Vocabulary and grammar analyses
[AD-A193289] N88-27753
SPEECH RECOGNITION
A review of workload measurement in relation to verbal comprehension N88-27360
Demodulation processes in auditory perception
[AD-A193421] N88-27740
SPHERES
Theoretical predictions of precipitate shapes in cubic alloys
[DE88-010856] N88-27291
SPILLING
Hydrocarbon fuel spill dispersion on water: Literature review
[AD-A192486] N88-27346
SPIN
Refractory films from spin-cast carbon
[DE88-011251] N88-27327
SPIN DYNAMICS
A method for reducing the coning of a spinning vehicle
[DE88-010971] N88-27189
Contribution to the numerical solution of airplane spin motion
[ETN-88-92368] N88-27190
SPIN STABILIZATION
A method for reducing the coning of a spinning vehicle
[DE88-010971] N88-27189
SPIRAL GALAXIES
Surface photometric investigations for spiral galaxies of large dimension structures in edge-on gemetry
[ETN-88-92126] N88-27985
SPOILERS
Theoretical and experimental investigations of a vortex drag behind a wing profile with spoiler
[ISL-PU-309/87] N88-27169
Investigations of aircraft control with jet spoilers
[ISL-R-112/87] N88-27202
SPRAY CHARACTERISTICS
Experimental research of combustion systems N88-27371
SPRAYED COATINGS
Stability of uncapsulated weight cells with thin film elongation measurement bands under influence of humidity, temperature and operation voltage
[ETN-88-92383] N88-27531
SPUTTERING
Formation of metastable structures and amorphous phases in Cu-W alloys using the triod sputtering technique
[DE88-009051] N88-27298
SQUID (DETECTORS)
Squid instrumentation for neuromagnetic study of complex brain activity N88-27691
STABILITY
An experimental study of the effect of pitch rate on delta wing aerodynamics and stability
[NASA-CR-183159] N88-27173
Research opportunities below 300 nm at the NBS Free-Electron Laser Facility
[AD-A193100] N88-27538
Transverse resistive wall instability in a high-power, short-wavelength free-electron laser
[DE88-011730] N88-27549
On plasma stability under anisotropic random electric field influence
[DE88-702422] N88-27918
Migration and stability of HgCdTe lattice defects
[AD-A193293] N88-27935
Some stability criteria in fluid and solid mechanics N88-27966
STAINLESS STEELS
Investigation of hydrogen isotope penetration through stainless steels Kh18N10T and Kh3M2BFR
[DE88-702189] N88-27297
Thermal conductivity and thermal expansion of stainless steels D9 and HT9
[DE88-011973] N88-27306
Distribution of weld quality in thin section stainless steel tube attachment welds
[PB88-109632] N88-27555
STANDARDS
Unified methods of accelerated laboratory tests of the preparations for temporary protection of cars
[NASA-TT-20298] N88-27336
A 1/2-inch high-definition baseband VCR N88-27393
Ada (trade name) compiler validation summary report: Verdix Corporation VAda-010-03315, version 5.5 MicroVAX 2 host ISBC 386/20P Intel target
[AD-A193226] N88-27774
Ada (trade name) compiler validation summary report: Verdix corporation VAda-010-13125, version 5.41 Sun Microsystems Sun-3/160 host microbar GPC68020 target
[AD-A193415] N88-27777
STATE ESTIMATION
Computer aided design for linear control State Variable System (SVS)
[AD-A193282] N88-27775
STATIC LOADS
Diffusion models of crack growth due to random overloads
[DE88-008811] N88-27595
STATISTICAL ANALYSIS
Kinetic theory for plane flows of rough, inelastic, circular disks N88-27499
The low-latitude auroral boundary: Steady-state and time-dependent representations
[AD-A193200] N88-27656
The collection of statistics on the frequency of cloud cover over North America
[AD-A193093] N88-27667
A statistical procedure for the evaluation of presence/non-presence of stimulus-related EEG activity N88-27689
Computation of filters by sampling and quantization
[AD-A192839] N88-27826
On the exceedance random measures for stationary processes
[AD-A192838] N88-27848
Statistical analysis of dyadic stationary processes
[AD-A193057] N88-27853
The SAS System by forms: Putting statistical power into the hands of an end-user
[DE88-010512] N88-27857
Comparison of results based on a deterministic versus a statistical uncertainty analysis
[DE88-010751] N88-27858
Analysis of lower hybrid current drive and rampup experiments on the JT-60 tokamak
[DE88-753136] N88-27915
STATISTICAL DISTRIBUTIONS
The computation of stationary distributions on Markov chains through perturbations
[AD-A193191] N88-27855
STATISTICAL MECHANICS
Statistical description of stochastic dynamics
[AD-A192924] N88-27852
STEADY FLOW
An h-p adaptive finite element method for steady compressible flow N88-27467
STEADY STATE
Periodic oscillations in nonlinear mechanical systems N88-27599
The low-latitude auroral boundary: Steady-state and time-dependent representations
[AD-A193200] N88-27656
Steady-state approximations in Raman excitation equations
[DE88-011759] N88-27889
STEELS
Ultrasonic studies of stresses and plastic deformation in steel during tension and compression
[AD-A192308] N88-27280
Cold worked reinforcing bars in tensile test under high loading rate and low temperatures
[DE88-752993] N88-27610
Specular steel surfaces for solar mirror substrates
[DE88-001153] N88-27630
STELLAR RADIATION
To the opportunities of cluster analysis of light curves of supernovae
[DE88-701642] N88-27982
STELLAR SPECTRA
Analysis of emission features in IRAS LRS spectra N88-27380
STELLAR STRUCTURE
Surface photometric investigations for spiral galaxies of large dimension structures in edge-on gemetry
[ETN-88-92126] N88-27985
STIFFENING
Nonlinear vibrations of periodically stiffened plates N88-27598
STIFFNESS
Nonlinear interaction between overall and local buckling of stiffened panels with symmetric cross-sections
[PB88-104054] N88-27580
STIMULI
Cognitive task demands as reflected in physiological measures N88-27699
STIRLING ENGINES
Phase 1 results from the Stirling-powered vehicle project
[NASA-TM-100978] N88-27980
STOCHASTIC PROCESSES
Simulation and analysis of wave propagation through random media N88-27503
Nonlinear stochastic interaction in aeroelastic structures
[AD-A193427] N88-27589
Stochastic geologic effects on near-field ground motions in alluvium
[AD-A192315] N88-27652
Simulation methodology
[AD-A192548] N88-27764
Control, stability and filter for a discrete linear stochastic system with correlated noise
[PB88-109525] N88-27818
A Wong-Zakai type theorem for certain discontinuous semimartingales
[AD-A192713] N88-27822
Approximations of stochastic equations driven by predictable processes
[AD-A192714] N88-27823
Computation of filters by sampling and quantization
[AD-A192839] N88-27826
On the exceedance random measures for stationary processes
[AD-A192838] N88-27848
A note on vector bimeasures
[AD-A192841] N88-27849
A study on Lebesgue decomposition of measures induced by stable processes
[AD-A192893] N88-27850
Multiple integration with respect to Poisson and Levy processes
[AD-A192895] N88-27851
Statistical description of stochastic dynamics
[AD-A192924] N88-27852
STOICHIOMETRY
A study of the interaction of diffusion flames with a vortex pair flowfield N88-27258
Premixed turbulent flame propagation
[AD-A192955] N88-27265
STOKES LAW (FLUID MECHANICS)
A simple explanation of the Stokes phenomenon
[AD-A193253] N88-27832
STORAGE RINGS (PARTICLE ACCELERATORS)
Activities report of the Werner-Heisenberg Institute of Physics
[ETN-88-92946] N88-27893
Distortion functions
[DE88-752634] N88-27896
STORAGE STABILITY
Aging of CFRP due to longterm storage in heated air
[DFVLR-FB-88-05] N88-27345
STORAGE TANKS
Prediction of velocity and temperature profiles in thermally driven gravity currents applied to stratified thermal storage tanks
[DE88-004452] N88-27496
STORMS
TDWR (Terminal Doppler Weather Radar) PRF (Pulse Repetition Frequency) selection criteria
[AD-A193089] N88-27407
STRAIN GAGES
In-flight load measurements of the Robot-X canards
[AD-A193428] N88-27187
Attachable interferometric strain gages
[AD-A192390] N88-27522
STRAIN MEASUREMENT
Component stress during freeze/thaw cycling
[DE88-011204] N88-27449
STRAIN RATE
Temperature, moisture and strain rate effects on the compressive mechanical behavior of Nylon 6/6
[DE88-010734] N88-27591
STRATEGY
Rules, schema and decision making
[AD-A193389] N88-27987
Technology transfer for DOE's Office of Transportation Systems: Assessment and strategies
[DE88-010760] N88-27977
STRATIFIED FLOW
Direct simulation of stable stratified homogeneous turbulent shear flows
[DFVLR-FB-88-04] N88-27516
STREAMS
Stream function-vorticity finite elements and the resolution of the Navier-Stokes equations
[DE88-702318] N88-27494
STRESS (PHYSIOLOGY)
Can CNV amplitude predict ability to accomplish a demanding task? N88-27700
Hyperthermia: New thoughts on an old problem
[AD-A192602] N88-27731

STRESS (PSYCHOLOGY)
Thermal stress and its effects on fine motor skill and decoding tasks N88-27369
STRESS ANALYSIS
Boundary layer solutions for the free-edge problem in composite laminates N88-27229
Thermal stress and its effects on fine motor skill and decoding tasks N88-27369
An experimental and analytical evaluation of a biaxial test for determining shear properties of composite materials
[NASA-CR-182928] N88-27593
Verification of the ADINA finite element code for creep analysis: Problems from the open literature
[DE88-011826] N88-27594
STRESS CORROSION
Stress corrosion of C ring specimen in salt spray tests
[I-186/87] N88-27307
STRESS DISTRIBUTION
Boundary layer solutions for the free-edge problem in composite laminates N88-27229
The three-dimensional stress field around a cylindrical inclusion in a plate of arbitrary thickness N88-27602
STRESS MEASUREMENT
In-flight load measurements of the Robot-X canards
[AD-A193428] N88-27187
Polarization selective Raman microspectroscopy N88-27397
STRESS PROPAGATION
User's manual for C-HEMP: A two-dimensional wave propagation code. Volume 1: Description and derivations of the code
[AD-A193197] N88-27486
STRESS RELAXATION
Stress relaxation of a titanium (Ti-6Al-4V) threaded joint
[DE88-010102] N88-27590
STRESSES
Ultrasonic studies of stresses and plastic deformation in steel during tension and compression
[AD-A192308] N88-27280
Granular flow: Particle-dynamics simulations of steady flow
[DE88-011342] N88-27506
Fiber-optics used to record high-speed photographs inside a pressurized tank during lethality testing
[DE88-011283] N88-27529
Deep level defects in semiconductors: Stress and pressure studies
[DE88-010855] N88-27948
STRETCHING
Optical evaluation of prototype stretched-membrane mirror modules for solar central receivers
[DE88-011884] N88-27637
STRING THEORY
Geometry of superconformal manifolds, part 1
[DE88-702405] N88-27863
Closed string fields as parameters of extra gauge symmetry of open string field theory
[DE88-702045] N88-27960
Vortices on the world sheet and string's critical dynamics
[DE88-702116] N88-27961
Dynamical evolution of cosmic strings
[DE88-011724] N88-27969
STRUCTURAL ANALYSIS
Vibrational impacts of hush house operation
[DE88-006983] N88-27207
Microchemical analysis of polycrystalline Ni3Al and other ordered alloys using the field-ion microscope atom probe
[DE88-011519] N88-27294
Finite element method for plate structures with inclined angles
[ILR-MITT-182] N88-27842
STRUCTURAL DESIGN
Computer-Aided Engineering (CAE) for engineering design N88-27390
Optimal design of viscoelastic structures N88-27579
A hidden-surface removal algorithm for structures defined by triangular and rectangular surface patches
[DFVLR-MITT-88-03] N88-27792
STRUCTURAL ENGINEERING
Probabilistic anisotropic failure criteria for composite materials
[AD-A193046] N88-27232
An investigation of techniques for determination of optimum/self-optimizing systems N88-27600
STRUCTURAL FAILURE
Critical issues and directions for fracture mechanics and structural integrity
[AD-A193050] N88-27584
STRUCTURAL MEMBERS
Critical issues and directions for fracture mechanics and structural integrity
[AD-A193050] N88-27584
STRUCTURAL PROPERTIES (GEOLOGY)
Stochastic geologic effects on near-field ground motions in alluvium
[AD-A192315] N88-27652
STRUCTURAL RELIABILITY
Critical issues and directions for fracture mechanics and structural integrity
[AD-A193050] N88-27584
Computation of failure probability of fatigue loaded cracked structures
[ETN-88-92360] N88-27607
STRUCTURAL VIBRATION
Vibration control of large structures
[AD-A193317] N88-27587
Coupled thermal vibrations of beams with temperature-dependent properties N88-27601
SUBROUTINE LIBRARIES (COMPUTERS)
TRANSL: A PATRAN translator subroutine library
[DE88-010976] N88-27784
SUBROUTINES
Using IMSL mathematical and statistical computer subroutines in physiological and biomechanical research
[AD-A192594] N88-27765
SUBSONIC SPEED
Theoretical-numerical study of feasibility of use of winglets on low aspect ration wings at subsonic and transonic Mach numbers at reduce drag
[NASA-CR-4174] N88-27168
SUBSTRATES
Improved adhesion for SiO2 particles in silica substrates using helium-ion irradiation
[DE88-008915] N88-27332
Amorphous silicon solar cells using a metal substrate
[PB88-131941] N88-27628
Specular steel surfaces for solar mirror substrates
[DE88-001153] N88-27630
SUCTION
Investigation of viscous/inviscid interaction in transonic flow over airfoils with suction
[NASA-CR-183112] N88-27490
SULFUR COMPOUNDS
Uses of lunar sulfur
[DE88-009119] N88-27990
SUMMER
MIZPAC (marginal ice zone Pacific) 84-86 CTD (Conductivity, Temperature, Depth) data report
[AD-A192478] N88-27679
SUPERCOMPUTERS
Federal Council on Science, Engineering and Technology: Committee on Computer Research and Applications, Subcommittee on Science and Engineering Computing: The US Supercomputer Industry
[DE88-011262] N88-27756
Supercomputer for parallel data analysis
[DE88-702148] N88-27759
Hypervelocity impact analysis with supercomputers
[DE88-006907] N88-27797
Notes on operating system requirements for the next millennium
[DE88-010712] N88-27805
SUPERCONDUCTING MAGNETS
Magnetic heat pumps
[DE88-012058] N88-27639
SUPERCONDUCTIVITY
Compilation of NRL publications on high temperature superconductivity
[AD-A189137] N88-27921
Effect of high-amplitude high-frequency current on non-isothermal equilibrium of NS-boundary in inhomogeneous superconductor
[DE88-701682] N88-27922
Anharmonic model for high-Tc superconductors
[DE88-702196] N88-27924
High-temperature superconductivity: An overview
[DE88-702051] N88-27925
Coupled even-parity superconducting states: Square lattice
[AD-A193432] N88-27938
Properties of new low dimensional materials and mechanisms of high T(sub c) superconductivity
[DE88-012026] N88-27951
Superconducting properties of LaBa2Cu3O(sub x) and YBa2Cu3O(sub y)
[DE88-012038] N88-27952
X-ray studies of strain, interface and impurities in semiconductors
[DE88-012460] N88-27954
SUPERCONDUCTORS
Mitsubishi Electric Advance (R and D Edition), Volume 41
[PB88-194162] N88-27388
Superconducting oxides with high critical temperatures N88-27392
Effect of high-amplitude high-frequency current on non-isothermal equilibrium of NS-boundary in inhomogeneous superconductor
[DE88-701682] N88-27922
Probing the electronic and defect structure of perovskite superconductors
[DE88-008349] N88-27939
Thermodynamics of oxygen-vacancy ordering in YBa2Cu3O(sub z)
[DE88-009816] N88-27940
Superconductor consolidation
[DE88-010938] N88-27949
Study of the friction and wear-related properties of ceramic superconductors
[DE88-011844] N88-27950
Ceramic fabrication technology for high-T(sub)c materials
[DE88-012060] N88-27953
Materials research, superconductor and thin layer technology
[REPT-50/87] N88-27955
Interactions between superconductivity and Kondo-grid properties in CeCu2Si2. Measurement results of specific heat under high pressure
[ETN-88-92377] N88-27958
SUPERCRITICAL WINGS
Analysis of experimental data for cast 10-2/DOA2 supercritical airfoil at high Reynolds numbers
[AD-A192827] N88-27166
SUPERFLUIDITY
Temperature rise in superfluid helium pumps
[NASA-TM-100997] N88-27507
SUPERLATTICES
Thermal conductivity of isotopically pure semiconductors, superlattices, semiconductor alloys and semiconductors as a function of temperature; control of the segregation coefficient in LEC crystal growth; and photo-Hall measurements of GaAs N88-27375
Solar energy conversion through the interaction of plasmons with tunnel junctions. Part A: Solar cell analysis. Part B: Photoconductor analysis
[NASA-CR-183044] N88-27621
Laser spectroscopy of quantum well and superlattice structures
[AD-A193336] N88-27937
Investigations on the MBE (Molecular Beam Epitaxy) growth and properties of Al(sub y)Ga(sub y)In(sub 1-x-y)AsInP and InGaAs-InAlAs superlattices
[DE88-009105] N88-27941
Meaning of energy diagrams used to describe hetero-structures
[DE88-702219] N88-27943
SUPERNOVAE
To the opportunities of cluster analysis of light curves of supernovae
[DE88-701642] N88-27982
Strange, quark and metastable neutron stars
[DE88-702404] N88-27984
SUPERPLASTICITY
Thermomechanical processing of Al alloy 2090 for grain refinement and superplasticity
[AD-A192333] N88-27281
Analysis of grain refinement and superplasticity in aluminum-magnesium alloys
[AD-A193029] N88-27283
SUPERSONIC AIRCRAFT
Supersonic transport/hypersonic transport (SST/HST) development
[SNIAS-881-111-101] N88-27192
SUPERSONIC CRUISE AIRCRAFT RESEARCH
Concept development of a Mach 3.0 high-speed civil transport
[NASA-TM-4058] N88-27182
SUPERSONIC FLOW
Nonaxisymmetric viscous lower branch modes in axisymmetric supersonic flows
[NASA-CR-181687] N88-27164
Velocity measurements and flow visualization in turbulent three-dimensional supersonic flows using oxygen flow tagging
[AD-A192551] N88-27165
Cryogenic free jets
[DFVLR-FB-88-16] N88-27210
SUPERSONIC JET FLOW
Velocity measurements and flow visualization in turbulent three-dimensional supersonic flows using oxygen flow tagging
[AD-A192551] N88-27165
SUPERSONIC TRANSPORTS
Concept development of a Mach 3.0 high-speed civil transport
[NASA-TM-4058] N88-27182
SUPERSYMMETRY
Superalgebras with Grassmann algebra-valued structure constants from superfields
[DE88-702239] N88-27862

SUPPLYING
Steps toward lunar settlement
[DE88-009141] N88-27213
SUPPORTS
FEB (Multifilter Electronics Box) lifting device analysis, revision A
[AD-A192313] N88-27427
SURFACE COOLING
Investigation of annular flow at high evaporation rates in view of liquid film cooling
[DFVLR-FB-88-08] N88-27517
SURFACE CRACKS
A critical review of IR drops and electrode potentials within pits, crevices and cracks
[AD-A192481] N88-27431
Thermo-mechanical cracking in coated media with a cavity by a moving asperity friction
[AD-A193311] N88-27586
SURFACE FINISHING
Study of surface treatments before adhesive bonding of light alloys --- aircraft industry
[ETN-88-92743] N88-27308
SURFACE LAYERS
Thermo-mechanical cracking in coated media with a cavity by a moving asperity friction
[AD-A193311] N88-27586
SURFACE NAVIGATION
Automatic omega station and LOP (Line Of Position) selection
[AD-A193302] N88-27179
SURFACE PROPERTIES
Computer modeling for surface properties of carbon fibers N88-27383
Analytical approximation of a distorted reflector surface defined by a discrete set of points
[NASA-TM-101323] N88-27424
Methods of determining playa surface conditions using remote sensing
[AD-A192663] N88-27612
Self-energies and the interactions of particles with surfaces
[DE88-010451] N88-27885
Characterization of crystalline silicon by electrochemical and Raman spectroscopy at the frontier semiconductor/electrolyte
[ETN-88-92354] N88-27956
Surface photometric investigations for spiral galaxies of large dimension structures in edge-on gemetry
[ETN-88-92126] N88-27985
SURFACE REACTIONS
An IETS (Inelastic Electron Tunneling Spectroscopy) study of surface reactions applicable to adhesion
[AD-A192274] N88-27261
Scanning tunneling microscopy as a surface chemical probe
[AD-A192710] N88-27263
Self-energies and the interactions of particles with surfaces
[DE88-010451] N88-27885
SURFACE TEMPERATURE
An empirical surface temperature model
[AD-A192737] N88-27665
Surface energy balance of three general circulation models: Current climate and response to increasing atmospheric CO2
[DE88-010967] N88-27673
SURFACE VEHICLES
Assessments of maneuverability with the TeleOperated Vehicle (TOV)
[AD-A191584] N88-27751
SURFACE WAVES
Surface-wave model uncertainty assessment
[AD-A193094] N88-27408
SURGES
Characterization of accelerating pipe flow
[AD-A193065] N88-27481
Investigation of the quasi-steady approach used in transient two-phase flow analysis
[DE88-004303] N88-27489
SUSPENDING (HANGING)
Human response to prolonged motionless suspension in four types of full body harnesses N88-27387
SWEPT WINGS
AGARD standard aeroelastic configurations for dynamic response. 1: Wing 445.6
[AGARD-R-765] N88-27193
SWIRLING
Turbulence structure of mixing swirling flows
[AD-A193063] N88-27478
SYMMETRY
Nonlinear interaction between overall and local buckling of stiffened panels with symmetric cross-sections
[PB88-104054] N88-27580
Closed string fields as parameters of extra gauge symmetry of open string field theory
[DE88-702046] N88-27960
Symmetry problem of energy-momentum tensor and the creation of gravitational field
[DE88-702442] N88-27964
SYNCHRONISM
A modular proof of correctness for a network synchronizer
[AD-A192726] N88-27802
Heating efficiency of beat wave excitation in a density gradient
[AD-A193066] N88-27905
SYNCHROTRONS
Optical guiding in the separable beam limit
[AD-A192452] N88-27534
SYNTAX
WORDNET: An electronic lexical reference system based on theories of lexical memory
[AD-A193086] N88-27970
SYNTHESIS (CHEMISTRY)
Ionic conductive polymers based on crosslinked elastic siloxane-ethylene oxide copolymers
[DE88-011243] N88-27311
Soluble metal chelate polymers of coordination numbers six, seven and eight
[AD-A192485] N88-27314
Preparation and properties of high Q microwave dielectrics in the (CA, SR, BA) zirconate system
[AD-A193127] N88-27317
Energy migration, motion and order in synthetic polymers
[AD-A193334] N88-27320
SYNTHETIC FUELS
An outdoor test facility for the large-scale production of microalgae
[DE88-001146] N88-27723
SYSTEMS ANALYSIS
The influence of weld metal properties, weld geometry and applied load on weld system performance
[AD-A193403] N88-27588
Performability analysis: Measures, an algorithm and a case study
[AD-A192477] N88-27800
Sources and nature of cost analysis data base reference manual
[AD-A193099] N88-27976
SYSTEMS ENGINEERING
Database design and management in engineering optimization
[AD-A193325] N88-27813
SYSTOLIC ARRAYS
A programmable systolic array for factorial analysis. Part 2: The symmetric eigenvalue problem
[AD-A192396] N88-27762

T

TAIL ROTORS
Aeroelastic characteristics of the AH-64 bearingless tail rotor N88-27162
TAPERING
AGARD standard aeroelastic configurations for dynamic response. 1: Wing 445.6
[AGARD-R-765] N88-27193
TARGET ACQUISITION
Air-to-air radar flight testing
[AGARD-AG-300-VOL-7] N88-27406
TARGET RECOGNITION
An empirical surface temperature model
[AD-A192737] N88-27665
Distributed algorithms for probabilistic solution of computational vision problems
[AD-A193150] N88-27773
TARGETS
Fiber-optics used to record high-speed photographs inside a pressurized tank during lethality testing
[DE88-011283] N88-27529
TAXONOMY
A taxonomy for conjugate gradient methods
[DE88-008574] N88-27817
TAYLOR INSTABILITY
A comparison of analytical techniques for modeling the Rayleigh-Taylor response of elastic-plastic solids
[DE88-010372] N88-27596
TECHNOLOGICAL FORECASTING
Air Force technical objective document, FY89
[AD-A193110] N88-27194
TECHNOLOGY ASSESSMENT
Design of booster wound structures --- spacecraft structures
[SNIAS-881-430-102] N88-27228
Recent developments in nickel hydrogen technology
[DE88-011248] N88-27456
Ceramic fabrication technology for high-T(sub)c materials
[DE88-012060] N88-27953
Technology transfer for DOE's Office of Transportation Systems: Assessment and strategies
[DE88-010760] N88-27977
Phase 1 results from the Stirling-powered vehicle project
[NASA-TM-100978] N88-27980
TECHNOLOGY TRANSFER
Thermal energy storage
[DE88-010753] N88-27625
Technology transfer for DOE's Office of Transportation Systems: Assessment and strategies
[DE88-010760] N88-27977
TECHNOLOGY UTILIZATION
High technology space flight orientation program: Overview and recommendations
[ETN-88-92332] N88-27979
TELECOMMUNICATION
Activities report of the Communications Department
[ENST-88D003] N88-27401
An evaluation of two millimeter wave propagation models for horizontal atmospheric attenuation at 70-115 GHZ
[AD-A192698] N88-27403
TELEMETRY
A VLSI single-chip (225,223) Reed-Solomon encoder with interleaver
[NASA-CASE-NPO-17280-1-CU] N88-27220
TELEOPERATORS
A demonstration of retro-traverse using a semi-autonomous land vehicle
[DE88-009851] N88-27568
Assessments of maneuverability with the TeleOperated Vehicle (TOV)
[AD-A191584] N88-27751
TELEVISION EQUIPMENT
A 1/2-inch high-definition baseband VCR N88-27393
TEMPERATURE
Interfacial tension of immiscible polymer blends: Temperature and molecular weight dependence
[AD-A192463] N88-27312
TEMPERATURE CONTROL
Thermal-sensation control: A new method of controlling cooled/heated environments N88-27394
TEMPERATURE DISTRIBUTION
Cryogenic free jets
[DFVLR-FB-88-16] N88-27210
A lubrication study of engine bearings N88-27574
Analysis of lower hybrid current drive and rampup experiments on the JT-60 tokamak
[DE88-753136] N88-27915
Effect of high-amplitude high-frequency current on non-isothermal equilibrium of NS-boundary in inhomogeneous superconductor
[DE88-701682] N88-27922
TEMPERATURE EFFECTS
Compilation of temperature factors of cubic elements
[PB88-108170] N88-27260
Determination of lumped-mass thermal properties associated with autoclave curing of graphite/epoxy composites N88-27364
Thermal stress and its effects on fine motor skill and decoding tasks N88-27369
Temperature, moisture and strain rate effects on the compressive mechanical behavior of Nylon 6/6
[DE88-010734] N88-27591
Photodiodes for optical communication in the near infrared
[ETN-88-92379] N88-27900
TEMPERATURE GRADIENTS
Prediction of velocity and temperature profiles in thermally driven gravity currents applied to stratified thermal storage tanks
[DE88-004452] N88-27496
An analysis of horizontal temperature gradients and heat content in the mixed layer and the surface forcing during PATCHEX
[AD-A192330] N88-27678
TEMPERATURE PROFILES
Prediction of velocity and temperature profiles in thermally driven gravity currents applied to stratified thermal storage tanks
[DE88-004452] N88-27496
Retrieval of temperature and concentration profiles from a limited number of absorption measurements N88-27501
TENSILE PROPERTIES
Thermomechanical processing of Al alloy 2090 for grain refinement and superplasticity
[AD-A192333] N88-27281
TENSILE STRENGTH
Development of a biaxial test system for thin-walled metal tubes using tensile-compressive axial load and internal-external pressure
[DE88-011279] N88-27592

TENSILE TESTS
Cold worked reinforcing bars in tensile test under high loading rate and low temperatures
[DE88-752993] N88-27610
TENSORS
Symmetry problem of energy-momentum tensor and the creation of gravitational field
[DE88-702442] N88-27964
TERMS
An assessment of index term ranking N88-27974
TERRAIN
Surface-wave model uncertainty assessment
[AD-A193094] N88-27408
Army space systems for terrestrial applications
[AD-A192735] N88-27613
Analysis of remotely sensed imagery using digital morphology
[AD-A192738] N88-27614
Active and passive remote sensing of ice
[AD-A193307] N88-27617
TERRAIN ANALYSIS
Linear feature extraction from radar imagery. Phase 2: Base contract report
[AD-A192828] N88-27404
Methods of determining playa surface conditions using remote sensing
[AD-A192663] N88-27612
TERRESTRIAL RADIATION
Angular radiation models for Earth-atmosphere system. Volume 1: Shortwave radiation
[NASA-RP-1184] N88-27677
TEST FACILITIES
Vibrational impacts of hush house operation
[DE88-006983] N88-27207
Development of a free-electron laser user facility for the extreme ultraviolet
[DE88-007892] N88-27541
Atmospheric turbulence research at DFVLR
[AGARD-R-752] N88-27669
An outdoor test facility for the large-scale production of microalgae
[DE88-001146] N88-27723
SP-100 Ground Engineering System: Test facility control systems
[DE88-009195] N88-27895
TEXTURES
Texture perception and shape from texture
[AD-A192923] N88-27771
THALAMUS
The interaction of thalamo-cortical systems in the 40 Hz following response N88-27694
THEMATIC MAPPING
Development of automatic names placement software
[AD-A192786] N88-27770
THEOREMS
A Wong-Zakai type theorem for certain discontinuous semimartingales
[AD-A192713] N88-27822
THERMAL CONDUCTIVITY
Thermal conductivity and thermal expansion of stainless steels D9 and HT9
[DE88-011973] N88-27306
Ceramic technology for advanced heat engines project
[DE88-008945] N88-27323
Studies of dynamic contact of ceramics and alloys for advanced heat engines
[DE88-008996] N88-27324
Data compilation for radiation damage on ceramic insulators. Revised with updated data and reviews
[DE88-753426] N88-27329
Determination of radiative properties of fiberglass and foam insulations
[DE88-007845] N88-27331
Deformation, fracture and explosive properties of reactive materials
[AD-A193080] N88-27348
Thermal conductivity of isotopically pure semiconductors, superlattices, semiconductor alloys and semiconductors as a function of temperature; control of the segregation coefficient in LEC crystal growth; and photo-Hall measurements of GaAs N88-27375
Coupled thermal vibrations of beams with temperature-dependent properties N88-27601
Measurement of the thermal conductivity of dielectric thin solid films with a thermal comparator
[DE88-008468] N88-27898
THERMAL CYCLING TESTS
A fundamental understanding of the interfacial compatibility in hybrid material systems
[AD-A192921] N88-27264
Thermal cycling tests on surface-mount assemblies
[DE88-007695] N88-27453
THERMAL DEGRADATION
T55-L-714 engine development and qualification. Engine M11 low cycle fatigue test report. (0213-005-87)
[AD-A192765] N88-27197
Aging of CFRP due to longterm storage in heated air
[DFVLR-FB-88-05] N88-27345
Perfluoropolyalkylether lubricants under boundary conditions: Iron catalysis of lubricant degradation
[AD-A193241] N88-27560
THERMAL DIFFUSION
Numerical calculations of dopent diffusion involving flashlamp heating of silicon N88-27384
Heat and mass transfer in a transport channel
[DE88-701968] N88-27493
Time-dependent thermal convection of Earth mantle and double diffusive convection in magma chambers
[MITT-52] N88-27663
THERMAL ENERGY
Storage of thermal energy by means of an absorption cycle
[PB88-190814] N88-27619
Thermal energy storage
[DE88-010753] N88-27625
THERMAL EXPANSION
Thermal conductivity and thermal expansion of stainless steels D9 and HT9
[DE88-011973] N88-27306
THERMAL INSULATION
Contribution to the development of coated fiber ceramic insolation material
[ETN-88-92361] N88-27243
Determination of radiative properties of fiberglass and foam insulations
[DE88-007845] N88-27331
THERMAL SHOCK
Studies of dynamic contact of ceramics and alloys for advanced heat engines
[DE88-008996] N88-27324
Evaluation of fracture models through pressurized-thermal-shock testing
[DE88-011834] N88-27603
THERMAL STRESSES
Thermal cycling tests on surface-mount assemblies
[DE88-007695] N88-27453
Coupled thermal vibrations of beams with temperature-dependent properties N88-27601
THERMOCHEMISTRY
Silicon oxidation studies: A review of recent studies on thin film silicon dioxide formation in the physics and chemistry of SiO2 and the Si-SiO2 interface
[AD-A193176] N88-27932
THERMOCLINES
An analysis of horizontal temperature gradients and heat content in the mixed layer and the surface forcing during PATCHEX
[AD-A192330] N88-27678
THERMODYNAMIC COUPLING
Coupled even-parity superconducting states: Square lattice
[AD-A193432] N88-27938
THERMODYNAMIC PROPERTIES
Radiative heat transfer and selective emission in planar slab coatings on hot emissive substrates
[AD-A193133] N88-27319
An analysis of horizontal temperature gradients and heat content in the mixed layer and the surface forcing during PATCHEX
[AD-A192330] N88-27678
THERMODYNAMICS
Thermomechanical processing of Al alloy 2090 for grain refinement and superplasticity
[AD-A192333] N88-27281
Finite element methodology for integrated flow-thermal-structural analysis
[NASA-CR-183144] N88-27606
Air-sea interaction in the vicinity of a land-sea boundary in the presence of upwelling N88-27661
A study of tunneling phenomena in gallium arsenide-aluminum gallium arsenide heterostructures N88-27946
THERMOELASTICITY
Coupled thermal vibrations of beams with temperature-dependent properties N88-27601
THERMONUCLEAR REACTIONS
The classical nova outburst
[DE88-009138] N88-27987
THERMOPLASTIC RESINS
Characterization of elastic-plastic properties of AS4/APC-2 thermoplastic composite
[NASA-CR-183145] N88-27242
THERMOREGULATION
Physiological responses to acute exercise-heat stress
[AD-A192606] N88-27732
THERMOSETTING RESINS
Injection compression for short fiber reinforced plastics
[SNIAS-881-430-118] N88-27344
THESAURI
WORDNET: An electronic lexical reference system based on theories of lexical memory
[AD-A193086] N88-27970
Capitalizing on experience with intelligence gateway software
[AD-A193362] N88-27971
THIN FILMS
Thin film and near-surface characterization using a mechanical properties microprobe
[DE88-011399] N88-27302
Equipment for building and testing superconductive flux flow electronic devices
[AD-A192959] N88-27436
Superconducting thin films, composites and junctions
[AD-A193123] N88-27440
Effects of surface tension and contact angle on sensible heating and boiling incipience in dielectric falling films
[DE88-007057] N88-27492
Chemical vapor deposition of TiO2 thin films at room temperature
[DE88-008892] N88-27542
Laser-heated CVD process for depositing thin films for low-cost solar-cell applications
[DE88-001162] N88-27623
Experimental fabrication of thin film single crystalline solar cells
[PB88-131958] N88-27627
Amorphous silicon solar cells using a metal substrate
[PB88-131941] N88-27628
Measurement of the thermal conductivity of dielectric thin solid films with a thermal comparator
[DE88-008468] N88-27898
Materials research, superconductor and thin layer technology
[REPT-50/87] N88-27955
THIN PLATES
An investigation of soft launch and instability breakup with a two-stage light gas gun
[DE88-010371] N88-27218
THOMSON SCATTERING
Multi-mode optical fibers for simultaneous 13-position measurements Thomson scattering apparatus in the JFT-2M tokamak
[DE88-753133] N88-27897
THREE DIMENSIONAL BODIES
An aspect graph-based control strategy for 3-D object recognition N88-27377
Creating aspect graphs for use in object recognition N88-27379
Enhancement of modeling and image generation techniques for high-resolution 3-dimensional imagery
[DE88-008923] N88-27782
THREE DIMENSIONAL BOUNDARY LAYER
A documentation of two- and three-dimensional shock-separated turbulent boundary layers
[NASA-TM-101008] N88-27519
THREE DIMENSIONAL FLOW
Velocity measurements and flow visualization in turbulent three-dimensional supersonic flows using oxygen flow tagging
[AD-A192551] N88-27165
Numerical methods for incompressible viscous flows with engineering applications
[NASA-CR-183143] N88-27508
THREE DIMENSIONAL MODELS
Three-dimensional adaptive grid generation for body-fitted coordinate system
[NASA-CR-182192] N88-27520
The three-dimensional stress field around a cylindrical inclusion in a plate of arbitrary thickness N88-27602
Prediction of regional pollutant dispersion using a nested-grid, three-dimensional numerical model N88-27649
A three-dimensional model of the gas-cell atomic frequency standard
[AD-A193218] N88-27868
TIME DEPENDENCE
The low-latitude auroral boundary: Steady-state and time-dependent representations
[AD-A193200] N88-27656
Time-dependent thermal convection of Earth mantle and double diffusive convection in magma chambers
[MITT-52] N88-27663
Staggered-grid finite element solution technique for the Maxwell's equations in the time domain
[DE88-011731] N88-27838
TIME MEASUREMENT
Quartz crystal resonators and oscillators for frequency control and timing applications
[AD-A193310] N88-27443

TIME OF FLIGHT SPECTROMETERS
Synopsis of a computer program designed to interface a personal computer with the fast data acquisition system of a time-of-flight mass spectrometer
[NASA-CR-177474] N88-27796
TIME OPTIMAL CONTROL
Approximations and optimal control for the pathwise average cost per unit time and discounted problems for wideband noise driven systems
[AD-A192712] N88-27847
TIME SERIES ANALYSIS
Comparison of experimental rotor damping data-reduction techniques N88-27159
Definition of long ocean wave slope for radar applications
[AD-A193198] N88-27412
TITANIUM ALLOYS
A fundamental understanding of the interfacial compatibility in hybrid material systems
[AD-A192921] N88-27264
Constant amplitude fatigue life data for notched and unnotched annealed Ti-6Al-4V sheet
[AD-A193420] N88-27287
Influence of microstructure and microdamage processes on fracture at high loading rates
[AD-A192957] N88-27583
Stress relaxation of a titanium (Ti-6Al-4V) threaded joint
[DE88-010102] N88-27590
TITANIUM OXIDES
Chemical vapor deposition of TiO2 thin films at room temperature
[DE88-008892] N88-27542
TOKAMAK DEVICES
Multi-mode optical fibers for simultaneous 13-position measurements Thomson scattering apparatus in the JFT-2M tokamak
[DE88-753133] N88-27897
Moment approach to neoclassical flows, currents and transport in auxiliary heated tokamaks
[DE88-008024] N88-27901
Tokamak magnetic turbulence over the safety factor range 0.6 less than q less than 3
[DE88-008421] N88-27904
ITER plasma equilibrium and poloidal field system design
[DE88-011005] N88-27912
Global and local magnetohydrodynamic relaxations
[DE88-752602] N88-27913
Design of divertor plate and measurements of double-null open divertor plasma in the JFT-2M tokamak
[DE88-753130] N88-27914
Analysis of lower hybrid current drive and rampup experiments on the JT-60 tokamak
[DE88-753136] N88-27915
TOLERANCES (PHYSIOLOGY)
Assessment of cochlear damage after microwave irradiation
[AD-A193237] N88-27737
TOMOGRAPHY
The design of a digital Eprom oscillator for electrical impedance tomography
[DE88-012243] N88-27462
TOPOGRAPHY
Influence of microstructure and microdamage processes on fracture at high loading rates
[AD-A192957] N88-27583
X-ray studies of strain, interface and impurities in semiconductors
[DE88-012460] N88-27954
TORQUE
In-flight motor torque estimates for the second-stage Strypi 9 launch vehicle
[DE88-010833] N88-27222
TOUCH
The interaction of thalamo-cortical systems in the 40 Hz following response N88-27694
TOUGHNESS
Theoretical and experimental analysis of the toughening behavior of whisker reinforcement in ceramic matrix composites
[DE88-011841] N88-27241
Development of high strength and toughness microcomposite HSLA Fe/Cr/Mn/C steel with and without Nb
[DE88-009813] N88-27290
Effects of near interfacial microstructure on toughness and subcritical crack growth in ceramic/metal systems
[DE88-009842] N88-27325
The influence of weld metal properties, weld geometry and applied load on weld system performance
[AD-A193403] N88-27588
TOXICITY
National air toxics information clearinghouse: NATICH data base users guide for data viewing, February 1988
[PB88-197470] N88-27645
TOXICITY AND SAFETY HAZARD
Waste destruction by plasma
[SNIAS-881-430-113] N88-27651
TRACE ELEMENTS
Application of Auger electron spectroscopy to the study of trace element effects on weldability
[DE88-010457] N88-27301
TRACKING (POSITION)
A human factors evaluation of the Advanced Visual Technology System (AVTS) eye tracking oculometer N88-27361
Passive multipath target tracking in an inhomogeneous acoustic medium
[AD-A193284] N88-27873
TRACKING NETWORKS
An investigation of the uses of time domain capable vector network analyzers as a diagnostic for helix traveling-wave circuits
[AD-A192460] N88-27430
TRACKING PROBLEM
The robust tracking control of nonlinear systems with uncertain dynamics N88-27788
TRAILING EDGES
The influence of surface rounding on trailing edge noise
[AD-A193387] N88-27876
TRAINING EVALUATION
Personality, attitudes, and pilot training performance: Preliminary analysis
[AD-A193102] N88-27746
TRAJECTORY ANALYSIS
A numerical simulation of side force effects by aerodynamic flight trajectory correction
[ISL-CO-211/87] N88-27191
FORTRAN programs for computation of time dependent sea levels and trajectory errors from satellite altimeter data
[BONN-MITT-73] N88-27216
A theoretical determination of the density at a traveling source that emitts particles
[ISAS-RN-351] N88-27883
TRAJECTORY CONTROL
A numerical simulation of side force effects by aerodynamic flight trajectory correction
[ISL-CO-211/87] N88-27191
The VITE model: A neutral command circuit for a generating arm and articulator trajectories
[AD-A192715] N88-27734
TRANSDUCERS
Acoustic emission calibration instrumentation
[DE88-010817] N88-27528
Direct measurement of solids: High temperature sensing. Experimental development and testing of high temperature pulsed EMATs
[DE88-009859] N88-27546
TRANSFERRED ELECTRON DEVICES
A planar IC-compatible transferred electron device for millimeter-wave operation
[AD-A192692] N88-27433
TRANSIENT RESPONSE
Techniques and instrumentation for transient characterization of metal-insulator-semiconductor diodes. Applications to metal-insulator InP system
[ECL-87-17] N88-27959
TRANSITION METALS
Magnetic excitations in transition metal systems
[DE88-011022] N88-27279
TRANSITION TEMPERATURE
High-temperature superconductivity: An overview
[DE88-702051] N88-27925
Thermodynamics of oxygen-vacancy ordering in YBa2Cu3O(sub z)
[DE88-009816] N88-27940
Properties of new low dimensional materials and mechanisms of high T(sub c) superconductivity
[DE88-012026] N88-27951
TRANSLATING
TRANSL: A PATRAN translator subroutine library
[DE88-010976] N88-27784
TRANSMISSION LINES
Experimental investigation of simplest inhomogeneities in cylindrical slit line
[DE88-702388] N88-27418
TRANSMISSION LOSS
Surface-wave model uncertainty assessment
[AD-A193094] N88-27408
TRANSMISSIONS (MACHINE ELEMENTS)
Optimization of planetary gears
[ETN-88-92375] N88-27573
TRANSONIC FLOW
Theoretical-numerical study of feasibility of use of winglets on low aspect ration wings at subsonic and transonic Mach numbers at reduce drag
[NASA-CR-4174] N88-27168
Experimental determination of aerodynamic damping in a three-stage transonic axial-flow compressor
[NASA-TM-100953] N88-27200
Investigation of viscous/inviscid interaction in transonic flow over airfoils with suction
[NASA-CR-183112] N88-27490
TRANSONIC FLUTTER
Propagation of acoustic disturbances in transonic flow fields of lifting wings
[DFVLR-FB-88-13] N88-27880
TRANSONIC WIND TUNNELS
European transonic wind tunnel project: Assistance to the design group
[ONERA-RSF-11/0694-GY-010-G] N88-27208
Studies concerning the European transonic wind tunnel
[ONERA-RSF-10/0694-GY-010-G] N88-27209
Hybrid procedure for dynamic measurements in transonic wind tunnels: Demonstrated by pitch oscillation
[DFVLR-FB-88-19] N88-27211
TRANSPORT AIRCRAFT
Concept development of a Mach 3.0 high-speed civil transport
[NASA-TM-4058] N88-27182
TRANSPORT THEORY
Kinetic theory for plane flows of rough, inelastic, circular disks N88-27499
TRANSPORTATION
Technology transfer for DOE's Office of Transportation Systems: Assessment and strategies
[DE88-010760] N88-27977
TRAPPED PARTICLES
Investigation of the potential impact of new photonic materials on optical processing systems N88-27359
TRAVELING IONOSPHERIC DISTURBANCES
On the dynamics of the auroral ionosphere during the breakup of a substorm
[AD-A193368] N88-27857
TRAVELING WAVE TUBES
An investigation of the uses of time domain capable vector network analyzers as a diagnostic for helix traveling-wave circuits
[AD-A192460] N88-27430
TRUCKS
Ethanol as a fuel of a lorry. Use experience from a diesel engine modified to an otto engine
[DE88-752870] N88-27589
TUNABLE LASERS
A new near-infrared tunable-room temperature solid state laser La3Ga5SiO14:Cr(3+)
[DE88-011341] N88-27543
Initial testing of the tunable diode laser absorption spectrometer for measuring HNO3 in diesel engine exhaust, stage 2
[PB88-193073] N88-27641
TUNGSTEN ALLOYS
Hot isostatic pressing of tungsten-nickel-iron composites
[PB88-203070] N88-27292
Formation of metastable structures and amorphous phases in Cu-W alloys using the triod sputtering technique
[DE88-009051] N88-27298
TUNING
Prediction of the aeroelastic behavior of tuned blades. Application to aircraft engines
[ISAL-87-0046] N88-27199
TURBINE BLADES
T55-L-714 engine development and qualification. Engine M11 low cycle fatigue test report. (0213-005-87)
[AD-A192765] N88-27197
Prediction of the aeroelastic behavior of tuned blades. Application to aircraft engines
[ISAL-87-0046] N88-27199
TURBINES
Numerical computation of three-dimensional turbulent flow in tightly curved ducts and spiral turbine casings
[ETN-88-92362] N88-27511
Calibration of the portable wear metal analyzer
[AD-A192971] N88-27524
TURBOCOMPRESSORS
Experimental determination of aerodynamic damping in a three-stage transonic axial-flow compressor
[NASA-TM-100953] N88-27200
TURBOJET ENGINES
Vibrational impacts of hush house operation
[DE88-006983] N88-27207
TURBULENCE
Summary of discussions at the Tenth Meeting of the Sandia Cooperative Group on the Aerothermochemistry of Turbulent Combustion
[DE88-008467] N88-27269
Coupled experimental and theoretical investigations of instability, chaos and turbulence in an axisymmetric jet flow
[AD-A192943] N88-27476

Characterization of accelerating pipe flow
[AD-A193065] N88-27481
Tokamak magnetic turbulence over the safety factor range 0.6 less than q less than 3
[DE88-008421] N88-27904

TURBULENCE EFFECTS
Design of a mechanism to control wind tunnel turbulence N88-27370

TURBULENT BOUNDARY LAYER
The diffusion of vorticity from a plane boundary
[AD-A192706] N88-27474
Experimental study of unsteady separating turbulent boundary layers
[AD-A192997] N88-27477
The heat transfer and fluid dynamics of concave surface curvature
[AD-A193064] N88-27479
A documentation of two- and three-dimensional shock-separated turbulent boundary layers
[NASA-TM-101008] N88-27519
Plasma behavior in the boundary layer near a railgun surface
[DE88-006889] N88-27909

TURBULENT FLOW
Velocity measurements and flow visualization in turbulent three-dimensional supersonic flows using oxygen flow tagging
[AD-A192551] N88-27185
The structure and stability of nonpremixed gas jet flames N88-27257
Premixed turbulent flame propagation
[AD-A192955] N88-27265
Summary of discussions at the Tenth Meeting of the Sandia Cooperative Group on the Aerothermochemistry of Turbulent Combustion
[DE88-008467] N88-27269
Design of a mechanism to control wind tunnel turbulence N88-27370
Predicting optical degradation of a laser beam through a turbulent shear layer N88-27376
Numerical experiments on turbulent mixing
[AD-A192572] N88-27473
Turbulence structure of mixing swirling flows
[AD-A193063] N88-27478
Physical mechanisms in shock-induced turbulent separated flow
[AD-A193165] N88-27484
Cavitation inception in a turbulent shear flow
[DE88-011486] N88-27497
Laser-Doppler measurements of turbulence structures in free streams behind flat and rotation symmetrical profiles
[ETN-88-92336] N88-27510
Numerical computation of three-dimensional turbulent flow in tightly curved ducts and spiral turbine casings
[ETN-88-92362] N88-27511
Investigations on drag reduction in turbulent pipe flows by addition of ionic and nonionic high polymers
[ETN-88-92380] N88-27515
Turbulent flow field visualization with integral interferometric imaging and computed tomography N88-27521
Photon limited image processing in the space-time domain
[AD-A193142] N88-27655
The influence of surface rounding on trailing edge noise
[AD-A193387] N88-27878

TURBULENT HEAT TRANSFER
The heat transfer and fluid dynamics of concave surface curvature
[AD-A193064] N88-27479

TURBULENT JETS
Coherent structures in the axisymmetric turbulent jet mixing layer N88-27504

TURBULENT MIXING
Numerical experiments on turbulent mixing
[AD-A192572] N88-27473
Coherent structures in the axisymmetric turbulent jet mixing layer N88-27504

TURBULENT WAKES
Numerical simulation and stability analysis of the absolutely and convectively unstable wake
[DFVLR-FB-88-09] N88-27516

TWO DIMENSIONAL FLOW
Implicit finite-difference simulation of an internal flow on a hypercube
[AD-A192474] N88-27471

TWO PHASE FLOW
Investigation of the quasi-steady approach used in transient two-phase flow analysis
[DE88-004303] N88-27489
Mass flow rate influence on void fraction of two-phase helium flow
[DE88-702456] N88-27495

U

U BENDS
Numerical computation of three-dimensional turbulent flow in tightly curved ducts and spiral turbine casings
[ETN-88-92362] N88-27511

U.S.S.R.
Soviet dynamic fracture mechanics research
[FASAC-TAR-3140] N88-27587
History of manned spaceflight
[CNES-NT-121] N88-28000

ULTRALIGHT AIRCRAFT
Aeroacoustic investigation on the noise from ultralight aircraft
[DFVLR-FB-88-03] N88-27879

ULTRASONIC FLAW DETECTION
Design and implementation of contact ultrasonic sensors to assess internal damage
[I-177/87] N88-27247
Interface control using low frequency (3 to 20 MHz) acoustic microscopy
[REPT-48-411/F] N88-27577

ULTRASONICS
Ultrasonic studies of stresses and plastic deformation in steel during tension and compression
[AD-A192306] N88-27280

ULTRAVIOLET ABSORPTION
Precise ultraviolet absorbance study of the interaction of amino acids and mononucleosides in aqueous solution
[ISAS-RN-356] N88-27256

ULTRAVIOLET LASERS
A plasma ultraviolet source for short wavelength lasers
[AD-A192844] N88-27537

ULTRAVIOLET RADIATION
A plasma ultraviolet source for short wavelength lasers
[AD-A192844] N88-27537

UNDERWATER ACOUSTICS
Robust methods for array signal processing
[AD-A192854] N88-27871
Vertical directionality of ambient noise at 32 deg N as a function of longitude: Tape number 86180
[AD-A193228] N88-27872

UNDERWATER TRAJECTORIES
A feasibility study in path planning using optimization techniques
[AD-A193030] N88-27177

UNDERWATER VEHICLES
A feasibility study in path planning using optimization techniques
[AD-A193030] N88-27177
A conceptual design study of a hovering system controller for an autonomous underwater vehicle
[AD-A193423] N88-27399

UNITED STATES
Federal Council on Science, Engineering and Technology: Committee on Computer Research and Applications, Subcommittee on Science and Engineering Computing: The US Supercomputer Industry
[DE88-011262] N88-27756

UNIVERSITIES
RLE progress report, January 1 to December 31, 1987
[RLE-PR-130] N88-27869

UNSTEADY AERODYNAMICS
Experimental determination of aerodynamic damping in a three-stage transonic axial-flow compressor
[NASA-TM-100953] N88-27200

UNSTEADY FLOW
Control and use of unsteady flows: Insect use of various wing kinematics and related pressure measurements using a pitching airfoil N88-27368
Coupled experimental and theoretical investigations of instability, chaos and turbulence in an axisymmetric jet flow
[AD-A192943] N88-27476
Experimental study of unsteady separating turbulent boundary layers
[AD-A192997] N88-27477

UPPER ATMOSPHERE
Components of an atmospheric lidar system
[AD-A193366] N88-27539

USER MANUALS (COMPUTER PROGRAMS)
User's manual for C-HEMP: A two-dimensional wave propagation code. Volume 1: Description and derivations of the code
[AD-A193197] N88-27486
DYNA3D (Nonlinear Dynamic Analysis of Structures in Three Dimensions) user's manual
[DE88-012242] N88-27604
National air toxics information clearinghouse: NATICH data base users guide for data viewing, February 1988
[PB88-197470] N88-27645
A PRELUDE (analysis and design of control systems-preliminary utilities depository). A data-based interactive system of control software, user's guid e
[DFVLR-MITT-88-12] N88-27795
User's manual for the two-dimensional transputer graphics toolkit
[NASA-TM-100974] N88-27799

USER REQUIREMENTS
Engineering data compendium. Human perception and performance. User's guide
[LC-87-19560] N88-27749
Software engineering guidelines for RASP and ANDECS: Requirements and architectural design
[DFVLR-MITT-88-07] N88-27793
Capitalizing on experience with intelligence gateway software
[AD-A193362] N88-27971

V

VACUUM
Theory and simulation of relaxed plasmoids
[AD-A192884] N88-27997

VACUUM ARC SWITCHES
The influence of ionization within a plasma opening switch
[AD-A193147] N88-27906

VACUUM DEPOSITION
Equipment for building and testing superconductive flux flow electronic devices
[AD-A192959] N88-27436

VANADIUM
Constant amplitude fatigue life data for notched and unnotched annealed Ti-6Al-4V sheet
[AD-A193420] N88-27287

VANADIUM ALLOYS
Stress relaxation of a titanium (Ti-6Al-4V) threaded joint
[DE88-010102] N88-27590

VAPOR DEPOSITION
On the electrical properties of carbon/carbon composites densified by chemical deposit in vapor phase
[SNIAS-881-430-117] N88-27252
Laser probes and numerical modeling as process diagnostics in chemical vapor deposition
[DE88-011622] N88-27275
PECVD of amorphous nickel--phosphorus films
[DE88-011088] N88-27299
Superconducting thin films, composites and junctions
[AD-A193123] N88-27440
Chemical vapor deposition of TiO2 thin films at room temperature
[DE88-008892] N88-27542
Laser-heated CVD process for depositing thin films for low-cost solar-cell applications
[DE88-001162] N88-27623
Low-band-gap, amorphous-silicon-based alloys by photochemical vapor deposition
[DE88-001165] N88-27944

VAPOR PHASES
On the electrical properties of carbon/carbon composites densified by chemical deposit in vapor phase
[SNIAS-881-430-117] N88-27252

VAPOR PRESSURE
Vapor Compression Distillation Subsystem (VCDS) component enhancement, testing and expert fault diagnostics development, volume 2
[NASA-CR-172076] N88-27755

VAPORIZING
Investigation of annular flow at high evaporation rates in view of liquid film cooling
[DFVLR-FB-88-08] N88-27517

VARIABLE STARS
Analysis of emission features in IRAS LRS spectra N88-27380

VARIABLE SWEEP WINGS
Pilot report: AFTI (Advanced Fighter Technology Integration) F-111
[AD-A192937] N88-27184

VARIANCE (STATISTICS)
Definition of long ocean wave slope for radar applications
[AD-A193198] N88-27412

VARIATIONAL PRINCIPLES
Theory and simulation of relaxed plasmoids
[AD-A192884] N88-27997

VARIATIONS
Large-eddy simulations of concentration fluctuations
[DE88-009480] N88-27660
On the estimation of a variance ratio
[AD-A193190] N88-27854

VARISTORS
The first synthesis of chem-prep varistor LAC (Lightning Arrestor Connector) granules
[DE88-008005] N88-27438
VECTOR ANALYSIS
An investigation of the uses of time domain capable vector network analyzers as a diagnostic for helix traveling-wave circuits
[AD-A192460] N88-27430
Parallel solutions to geometric problems on the scan model of computation
[AD-A192321] N88-27819
A note on vector bimeasures
[AD-A192841] N88-27849
VELOCITY
Prediction of velocity and temperature profiles in thermally driven gravity currents applied to stratified thermal storage tanks
[DE88-004452] N88-27496
VELOCITY DISTRIBUTION
Prediction of velocity and temperature profiles in thermally driven gravity currents applied to stratified thermal storage tanks
[DE88-004452] N88-27496
VELOCITY MEASUREMENT
Velocity measurements and flow visualization in turbulent three-dimensional supersonic flows using oxygen flow tagging
[AD-A192551] N88-27165
VERBAL COMMUNICATION
A review of workload measurement in relation to verbal comprehension N88-27360
VERTICAL ORIENTATION
Vertical directionality of ambient noise at 32 deg N as a function of longitude: Tape number 86180
[AD-A193228] N88-27872
VERY LOW FREQUENCIES
Airborne measurement of low frequency atmospheric noise ALFAN 1
[AD-A193056] N88-27405
VESTIBULAR TESTS
Motion evoked vestibular potentials N88-27712
VHSIC (CIRCUITS)
Very High Speed Integrated Circuits (VHSIC)
[AD-A193225] N88-27442
VIBRATION
Vibrational impacts of hush house operation
[DE88-006983] N88-27207
Nonlinear vibrations of periodically stiffened plates N88-27598
VIBRATION DAMPING
Vibration control of large structures
[AD-A193317] N88-27587
VIDEO DATA
Balance of X-ray radioscopy application to nondestructive tests of composite materials
[SNIAS-881-430-110] N88-27250
Use of optical disk technology at the Air Command and Staff College
[AD-A192424] N88-27969
VIDEO SIGNALS
A 1/2-inch high-definition baseband VCR N88-27393
VINYL POLYMERS
Polymer-ceramic composites
[AD-A193244] N88-27237
VIRTUAL PROPERTIES
Long-pulse, high-power vircator experiments
[DE88-011787] N88-27458
VISCOELASTIC DAMPING
Feedback control of a hyperbolic partial-differential equation with viscoelastic damping
[AD-A192896] N88-27810
VISCOELASTICITY
Thermo-viscoelastic analysis of composite materials, volume 1
[NASA-CR-183048-VOL-1] N88-27230
Optimal design of viscoelastic structures N88-27579
VISCOSITY
Optimal rheological characteristics in dynamic stability of polymer flow through porous media
[DE88-001225] N88-27322
VISCOUS FLOW
Nonaxisymmetric viscous lower branch modes in axisymmetric supersonic flows
[NASA-CR-181687] N88-27164
Prediction of velocity and temperature profiles in thermally driven gravity currents applied to stratified thermal storage tanks
[DE88-004452] N88-27496
A fast vortex code for computing 2-D flow in a box
[DE88-011732] N88-27498
Numerical methods for incompressible viscous flows with engineering applications
[NASA-CR-183143] N88-27508
Plasma behavior in the boundary layer near a railgun surface
[DE88-008889] N88-27909
VISCOUS FLUIDS
Implicit finite-difference simulation of an internal flow in a nozzle: An example of a physical application on a hypercube
[AD-A192475] N88-27472
VISION
Dissecting the visual and auditory pathways by means of the two-input technique N88-27690
A study of sources in the human brain associated with stereopsis N88-27695
Relation between VEP and visual function in lesions of the optic nerve and visual pathway N88-27718
Vision research. A national plan: 1983-1987, 1987 evaluation and update
[PB88-192604] N88-27726
A model for visual attention
[AD-A193061] N88-27744
Distributed algorithms for probabilistic solution of computational vision problems
[AD-A193150] N88-27773
VISUAL ACUITY
Microesotropia patients performa well as military jet pilots N88-27363
A model for visual attention
[AD-A193061] N88-27744
VISUAL DISCRIMINATION
Perception of motion in statistically-defined displays
[AD-A193076] N88-27745
VISUAL FIELDS
Influence of moving visual environment on saccadic eye movements and fixation N88-27368
VISUAL PERCEPTION
Three-dimensional scene analysis using stero based imaging
[AD-A193120] N88-27178
Microesotropia patients performa well as military jet pilots N88-27363
Assessments of maneuverability with the TeleOperated Vehicle (TOV)
[AD-A191584] N88-27751
VISUAL STIMULI
Influence of moving visual environment on saccadic eye movements and fixation N88-27368
Perception of motion in statistically-defined displays
[AD-A193076] N88-27745
VOICE COMMUNICATION
Cockpit and cabin crew coordination
[AD-A192445] N88-27752
A cockpit natural language study: Vocabulary and grammar analyses
[AD-A193289] N88-27753
VOIDS
Mass flow rate influence on void fraction of two-phase helium flow
[DE88-702456] N88-27495
VOLATILITY
National ambient Volatile Organic Compounds (VOCs) data base update, documentation
[PB88-195631] N88-27646
VORTEX BREAKDOWN
Rotation symmetric vortex in axiparallel flow
[ETN-88-92364] N88-27512
VORTEX SHEDDING
Theory of sound production by vortex-airfoil interaction
[AD-A193386] N88-27875
VORTEX SHEETS
Vortices on the world sheet and string's critical dynamics
[DE88-702116] N88-27961
VORTICES
Theoretical and experimental investigations of a vortex drag behind a wing profile with spoiler
[ISL-PU-309/87] N88-27169
A study of the interaction of diffusion flames with a vortex pair flowfield N88-27258
Stream function-vorticity finite elements and the resolution of the Navier-Stokes equations
[DE88-702318] N88-27494
A fast vortex code for computing 2-D flow in a box
[DE88-011732] N88-27498
Higher order vortex methods with rezoning
[DE88-010777] N88-27505
Rotation symmetric vortex in axiparallel flow
[ETN-88-92364] N88-27512
VORTICITY
The diffusion of vorticity from a plane boundary
[AD-A192706] N88-27474
Cavitation inception in a turbulent shear flow
[DE88-011486] N88-27497
Higher order vortex methods with rezoning
[DE88-010777] N88-27505
VULNERABILITY
Fiber-optics used to record high-speed photographs inside a pressurized tank during lethality testing
[DE88-011283] N88-27529

W

WAKES
The diffusion of vorticity from a plane boundary
[AD-A192706] N88-27474
WALKING MACHINES
Compliant robotic structures, part 3
[AD-A192426] N88-27556
WALL JETS
Variable Mach number wall jets for control/propulsion on hypervelocity projectiles/interceptors: Tests with an existing model
[AD-A192845] N88-27167
WALLS
Characterization of accelerating pipe flow
[AD-A193065] N88-27481
Transverse resistive wall instability in a high-power, short-wavelength free-electron laser
[DE88-011730] N88-27549
WARFARE
Computation of ECM (Electronic Counter-Measures) war reserve materiel spare requirements
[AD-A193301] N88-27195
WASTE DISPOSAL
Waste destruction by plasma
[SNIAS-881-430-113] N88-27651
WATER
Direct determination of part-per-billion levels of volatile organics in water and soil samples using glow discharge mass spectrometry
[DE88-011389] N88-27272
Structure and function of the manganese complex involved in photosynthetic oxygen evolution determined by X-ray adsorption spectroscopy and electron paramagnetic resonance spectroscopy
[DE88-010360] N88-27725
WATER CURRENTS
FORTRAN programs for computation of time dependent sea levels and trajectory errors from satellite altimeter data
[BONN-MITT-73] N88-27216
WATER POLLUTION
Hydrocarbon fuel spill dispersion on water: Literature review
[AD-A192486] N88-27346
WATER VAPOR
Heat and mass transfer in laminar wavy film absorption with the presence of non-absorbable gases N88-27502
WATER WAVES
Definition of long ocean wave slope for radar applications
[AD-A193198] N88-27412
Research on ocean forecasting and nonlinear wave propagation and numerical hydrodynamics in the ocean
[AD-A193363] N88-27680
WAVE EQUATIONS
Wave equations for pulse propagation
[DE88-011760] N88-27548
Research on ocean forecasting and nonlinear wave propagation and numerical hydrodynamics in the ocean
[AD-A193363] N88-27680
A numerical treatment of the fluid/elastic interface under range-dependent environments
[AD-A192476] N88-27821
Initial boundary value problems of nonlinear wave equations in an exterior domain
[DE88-701883] N88-27962
WAVE EXCITATION
Heating efficiency of beat wave excitation in a density gradient
[AD-A193066] N88-27905
WAVE INTERACTION
Guided wave interactions in millimeter-wave integrated circuits
[AD-A193017] N88-27437
WAVE PROPAGATION
An evaluation of two millimeter wave propagation models for horizontal atmospheric attenuation at 70-115 GHZ
[AD-A192699] N88-27403
User's manual for C-HEMP: A two-dimensional wave propagation code. Volume 1: Description and derivations of the code
[AD-A193197] N88-27486
Simulation and analysis of wave propagation through random media N88-27503
Wave equations for pulse propagation
[DE88-011760] N88-27548
On the small signal gain of free electron lasers in the low-current regime
[DFVLR-FB-88-10] N88-27552

Research on ocean forecasting and nonlinear wave propagation and numerical hydrodynamics in the ocean
[AD-A193363] N88-27680
Ion Bernstein modes in current-carrying plasmas
N88-27903
Magnetohydrodynamic wave propagation in the solar wind
[DE88-702411] N88-27995

WAVE REFLECTION
Reflection of sound in open ended ducts
[PB88-103478] N88-27870
Electromagnetic wave incoherent reflection by a half-space of weakly-ionized plasma with an absorbing boundary
[DE88-702413] N88-27917

WAVE SCATTERING
Staggered-grid finite element solution technique for the Maxwell's equations in the time domain
[DE88-011731] N88-27838
Electromagnetic wave incoherent reflection by a half-space of weakly-ionized plasma with an absorbing boundary
[DE88-702413] N88-27917

WAVEFORMS
A numerically efficient digital matched filter for periodic and windowed periodic radar waveforms
[AD-A193132] N88-27410
Picosecond optoelectronic sampling of electrical waveforms produced by an optically excited field effect transistor
[AD-A192384] N88-27428

WAVEGUIDES
Experimental investigation of simplest inhomogeneities in cylindrical slit line
[DE88-702388] N88-27418
Guided wave interactions in millimeter-wave integrated circuits
[AD-A193017] N88-27437

WEAPON SYSTEMS
Flight testing under extreme environmental conditions
[AGARD-AG-300-VOL-8] N88-27525
Can CNV amplitude predict ability to accomplish a demanding task? N88-27700

WEAPONS
Dependence effects in unique signal transmission
[DE88-010331] N88-27419
A method for estimating the susceptibility of electronic systems to HPM (High Power Microwave)
[DE88-012246] N88-27422
Fiber-optics used to record high-speed photographs inside a pressurized tank during lethality testing
[DE88-011263] N88-27529

WEAR
Ceramic technology for advanced heat engines project
[DE88-008945] N88-27323
Studies of dynamic contact of ceramics and alloys for advanced heat engines
[DE88-008996] N88-27324
Friction, wear and electrical contact resistance of precious metal alloys
[DE88-011244] N88-27450
Calibration of the portable wear metal analyzer
[AD-A192971] N88-27524

WEAR RESISTANCE
Basic mechanisms of diesel lubrication correlation of bench and engine tests
[AD-A193360] N88-27561

WEATHER
TDWR (Terminal Doppler Weather Radar) PRF (Pulse Repetition Frequency) selection criteria
[AD-A193089] N88-27407

WEATHER FORECASTING
Intercomparison of NMC (National Meteorological Center) and ECMWF (European Centre for Medium Range Weather Forecasts) global analyses: 1980-1986
[PB88-196548] N88-27668
The Hanford meteorological data collection system and data base
[DE88-008632] N88-27672

WEDGES
Wind tunnel tests of the influence of airfoil-thickness on normal force and pitching moment of two slender wings at transonic and supersonic Mach numbers
[DFVLR-FB-88-17] N88-27171
Experimental investigation of the reflection of a planar shock wave over a double wedge
[AD-A193078] N88-27482

WEIGHT MEASUREMENT
Stability of uncapsulated weight cells with thin film elongation measurement bands under influence of humidity, temperature and operation voltage
[ETN-88-92383] N88-27531

WEIGHT REDUCTION
High power pulse energy system concept
[AD-A192440] N88-27429

WELD STRENGTH
Distribution of weld quality in thin section stainless steel tube attachment welds
[PB88-109632] N88-27555
The influence of weld metal properties, weld geometry and applied load on weld system performance
[AD-A193403] N88-27588

WELD TESTS
Distribution of weld quality in thin section stainless steel tube attachment welds
[PB88-109632] N88-27555

WELDABILITY
Application of Auger electron spectroscopy to the study of trace element effects on weldability
[DE88-010457] N88-27301

WELDED JOINTS
Distribution of weld quality in thin section stainless steel tube attachment welds
[PB88-109632] N88-27555

WELDING
High-speed, precision processing using an electron beam N88-27391
The influence of weld metal properties, weld geometry and applied load on weld system performance
[AD-A193403] N88-27588

WEST GERMANY
Economic impact of space flight activities in West Germany. Influence of allocations of Bundesministerium fuer Forschung und Technologie
[ETN-88-92106] N88-27215
Atmospheric turbulence research at DFVLR
[AGARD-R-752] N88-27669

WETLANDS
Remote sensing of wetlands: Applications overview
[DE88-010895] N88-27618

WHISKER COMPOSITES
Theoretical and experimental analysis of the toughening behavior of whisker reinforcement in ceramic matrix composites
[DE88-011841] N88-27241

WIGGLER MAGNETS
On the small signal gain of free electron lasers in the low-current regime
[DFVLR-FB-88-10] N88-27552

WIND PROFILES
Three-dimensional wind simulation
[DE88-009793] N88-27671
Space shuttle natural environment analysis
[NASA-CR-179337] N88-27676

WIND TUNNEL APPARATUS
Equipment for mass flow measurements in the low-speed wind tunnel at DFVLR in Brunswick, West Germany
[DFVLR-MITT-88-02] N88-27212

WIND TUNNEL TESTS
Aeroelastic characteristics of the AH-64 bearingless tail rotor N88-27162
Theoretical and experimental investigations of a vortex drag behind a wing profile with spoiler
[ISL-PU-309/87] N88-27169
Wind tunnel tests of the influence of airfoil-thickness on normal force and pitching moment of two slender wings at transonic and supersonic Mach numbers
[DFVLR-FB-88-17] N88-27171
Space shuttle phase B wind tunnel model and test information. Volume 2: Orbiter configuration
[NASA-CR-178415-VOL-2-PT-2] N88-27172
Hybrid procedure for dynamic measurements in transonic wind tunnels: Demonstrated by pitch oscillation
[DFVLR-FB-88-19] N88-27211
Design of a mechanism to control wind tunnel turbulence N88-27370
Determination of the local heat-transfer characteristics on glaze ice accretions on a cylinder and a NACA 0012 airfoil N88-27500
Laser-Doppler measurements of turbulence structures in free streams behind flat and rotation symmetrical profiles
[ETN-88-92336] N88-27510
Hypersonic flight testing
[DE88-001655] N88-27894

WIND TURBINES
Modal testing in the design evaluation of wind turbines
[DE88-010374] N88-27632
Three-dimensional wind simulation
[DE88-009793] N88-27671

WIND VELOCITY
Three-dimensional wind simulation
[DE88-009793] N88-27671

WING OSCILLATIONS
Optimal control of the wing rock phenomenon
N88-27373

WING PROFILES
Theoretical and experimental investigations of a vortex drag behind a wing profile with spoiler
[ISL-PU-309/87] N88-27169

WINGLETS
Theoretical-numerical study of feasibility of use of winglets on low aspect ration wings at subsonic and transonic Mach numbers at reduce drag
[NASA-CR-4174] N88-27168

WIRE
Performance study of a unipole antenna with conventional and elevated radial wire ground screens
[AD-A193283] N88-27413

WORDS (LANGUAGE)
WORDNET: An electronic lexical reference system based on theories of lexical memory
[AD-A193086] N88-27970

WORK CAPACITY
A review of workload measurement in relation to verbal comprehension N88-27360
Thermal stress and its effects on fine motor skill and decoding tasks N88-27369

WORKING FLUIDS
The heat transfer and fluid dynamics of concave surface curvature
[AD-A193064] N88-27479

WORKLOADS (PSYCHOPHYSIOLOGY)
A review of workload measurement in relation to verbal comprehension N88-27360
Event-related brain potentials as indices of mental workload and attentional allocation N88-27696
Event-related and steady potential changes in the brain related to workload during tracking N88-27705
Behavioral effects of exposure to the tempo high-power microwave system
[AD-A193305] N88-27738
Determinants of dual-task interference and resource theories in cognitive psychology
[DFVLR-FB-88-14] N88-27748

WORKSTATIONS
The MELCOM PSI 2 AI workstation N88-27395
Assessing and enhancing human performance: Utility of a workstation network
[AD-A192840] N88-27743

X

X RAY ANALYSIS
X-ray studies of strain, interface and impurities in semiconductors
[DE88-012460] N88-27954

X RAY APPARATUS
MAXIE-1 (Magnetospheric Atmospheric X-ray Imaging Experiment)
[AD-A192846] N88-27221

X RAY DIFFRACTION
Precise rotational alignment of X-ray transmission diffraction gratings
[DE88-010599] N88-27273
Superconducting oxides with high critical temperatures
N88-27392

X RAY IMAGERY
MAXIE-1 (Magnetospheric Atmospheric X-ray Imaging Experiment)
[AD-A192846] N88-27221

X RAY INSPECTION
Balance of X-ray radioscopy application to nondestructive tests of composite materials
[SNIAS-881-430-110] N88-27250

X RAY LASERS
Target designs for plasma-implosion-driven, photoionization-pumped soft X-ray lasers
[DE88-011278] N88-27547

XENON CHLORIDE LASERS
Dynamics of a plasma produced under effect of the XeCl-laser radiation on metallic surface
[DE88-701983] N88-27902

Y

YAG LASERS
Process control improvements in pulsed Nd:YAG laser closure welding of electromechanical relays
[DE88-006275] N88-27564

YTTRIUM COMPOUNDS
Anharmonic model for high-Tc superconductors
[DE88-702196] N88-27924
Superconducting properties of LaBa2Cu3O(sub x) and YBa2Cu3O(sub y)
[DE88-012038] N88-27952

YTTRIUM OXIDES
Compilation of NRL publications on high temperature superconductivity
[AD-A189137] N88-27921
Thermodynamics of oxygen-vacancy ordering in YBa2Cu3O(sub z)
[DE88-009816] N88-27940

Z

ZINC OXIDES
The first synthesis of chem-prep varistor LAC (Lightning Arrestor Connector) granules
[DE88-008005] N88-27438
ZINC SELENIDES
Atomic layer epitaxy of ZnS and ZnSe
[AD-A192307] N88-27928
ZINC SULFIDES
Atomic layer epitaxy of ZnS and ZnSe
[AD-A192307] N88-27928
ZIRCONATES
Preparation and properties of high Q microwave dielectrics in the (CA, SR, BA) zirconate system
[AD-A193127] N88-27317
ZIRCONIUM OXIDES
Preparation and characterization of ceramic materials based on Al2O3 reinforced with a ZrO2 dispersion
[ISAL-87-0041] N88-27340
Comparison of sol-gel procedures for zircon and alumina
[SNIAS-881-430-108] N88-27342

Typical Personal Author Index Listing

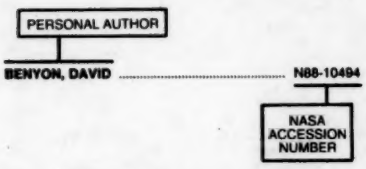

Listings in this index are arranged alphabetically by personal author. The NASA accession number denotes the number by which the citation is identified.

A

AAGAARD, K. N88-27681
ABOU-SALAMA, AHMED A. N88-27283
ABRAHAM, K. M. N88-27441
ABRAHAM, PETER N88-27700
ACHE, GERARDO A. N88-27487
N88-27488
ACOSTA, ROBERTO J. N88-27424
ADLER, D. N88-27623
AGARWAL, N. K. N88-27477
AHUJA, NARENDRA N88-27771
AKASAKA, YOICHI N88-27397
AKMAN, A. N88-27685
AKSENOV, V. L. N88-27924
ALAMGIR, M. N88-27441
ALBERRY, P. J. N88-27555
ALEXANDER, J. D. N88-27261
ALEXIADES, V. N88-27965
ALFANO, ROBERT N88-27936
ALLEN, JONATHAN N88-27869
ALLEN, S. L. N88-27910
ALLISTON-GREINER, A. F. N88-27561
ALOUANI, M. N88-27927
ALPERT, D. J. N88-27636
N88-27637
ALTAN, S. B. N88-27582
AMATA, E. N88-27653
AMSDEN, C. A. N88-27898
ANASTASIADIS, S. H. N88-27312
ANDRAKA, CHARLES E. N88-27631
ANDREWS, G. L. N88-27672
ANDREWS, L. A. N88-27438
ANGELINI, P. N88-27241
ANGUS, R. G. N88-27702
ANTONSEN, T. M., JR. N88-27534
N88-27536
ANWAH, N. A. N88-27635
ARCHER, RONALD D. N88-27314
AREFEVA, I. YA. N88-27960
ARLOWE, H. D. N88-27188
ARMSTRONG, LAWRENCE E. N88-27731
ARMSTRONG, T. R. N88-27316
ARNAUD, J. L. N88-27577
ARNOLD, PETER N88-27216
ARORA, JASBIR S. N88-27813
ARRINGTON, CURTIS H., III N88-27969
ARUTYUNYAN, R. V. N88-27902
ASH, R. L. N88-27508
ASHBY, S. F. N88-27817
ASHIHARA, OSAMU N88-27883
ASHWILL, T. D. N88-27632
AURAND, J. F. N88-27458
AUSTIN, RICHARD N88-27180
AYTAC, SUNGUR N88-27900

B

BABU, C. J. N88-27856
BACHEN, NILS IRGENS N88-27689
BACON, M. P. N88-27682
BADCOCK, CHARLES C. N88-27434
BADEN, S. B. N88-27498
BADER, D. C. N88-27660
BAI, Z. D. N88-27828
N88-27835
N88-27853
BAKKER, T. N88-27532
BALACHANDRAN, U. N88-27636
N88-27952
BALS, JOHANN N88-27793
BALTZLEY, DENNIS R. N88-27739
BAMBER, C. N88-27544
BANERJEE, D. N88-27162
BANKS, W. W. N88-27750
BANTA, G. R. N88-27707
BARANOV, V. YU. N88-27902
BARNETT, TERRY R. N88-27593
BARON, B. N. N88-27944
BARSCH, G. R. N88-27304
BARTON, B. M. N88-27450
BARTRAND, TIMOTHY A. N88-27225
BARTUNOV, O. S. N88-27982
BASHIR, J. N88-27260
BASS, B. R. N88-27594
N88-27603
BASSEN, HOWARD I. N88-27737
BATTS, WADE N88-27676
BAUER, LANCE O. N88-27699
BEAUCHAMP, E. K. N88-27448
BEAUCHAMP, R. L. N88-27456
BECHER, P. F. N88-27241
BECHTEL, R. D. N88-27798
BECK, STEVEN M. N88-27933
BEESON, H. D. N88-27398
BEISSNER, FRED L., JR. N88-27182
BELASTOCK, R. A. N88-27682
BELYTSCHKO, TED N88-27585
BEN-DOR, G. N88-27482
BENNER, M. S. N88-27526
BENNIS, H. G. M. N88-27532
BENO, JOSEPH N88-27217
BENSON, D. A. N88-27349
BEREA, A. N88-27940
BERNEY, C. V. N88-27321
BERTI, ROBERTO N88-27717
BERTRAN-SALVANS, M. N88-27761
BEUTLER, D. E. N88-27926
BEYER, JAMES B. N88-27436
BEZIERS, D. N88-27252
N88-27343
BEZUGLYJ, A. I. N88-27922
BHADER, THOMAS B. N88-27234
BHATTACHARYA, P. K. N88-27941
BIELAWA, RICHARD L. N88-27158
BIRMIWAL, KAILASH N88-27833
BLACK, N. N88-27713
BLACKBURN, M. R. N88-27707
BLACKMAN, J. A. N88-27279
N88-27303
BLAKE, R. A. N88-27575
BLAU, P. J. N88-27950
BLECKWEDEL, AXEL N88-27958
BLELLOCH, GUY E. N88-27819
BLOMQUIST, R. A. N88-27306
BLOOM, BARD N88-27766
BODEN, J. A. N88-27532
BOEHM-DAVIS, DEBORAH N88-27967
BOFF, KENNETH R. N88-27749
BOGDONOFF, S. M. N88-27480
BOGEGARD, S. N88-27292
BOHNE, BARBARA A. N88-27737
BOLSHOV, L. A. N88-27902
BONHAM, R. W. N88-27530
BONSI, DAVID J. N88-27175
BOOS, FRANZ N88-27204
BORGLUM, B. P. N88-27317
BORLAND, R. G. N88-27688
BOUCHET, F. R. N88-27989
BOUGHTON, B. A. N88-27859
BOUIS, X. N88-27209
BOURCIER, R. J. N88-27592
BOUSMAN, WILLIAM G. N88-27148
N88-27151
N88-27152
BOUVARD, J. N88-27341
N88-27354
BOUWER, GERHARD N88-27203
BOWMAN, ROBERT C., JR. N88-27425
N88-27934
BOYD, D. M. N88-27546
BOYD, J. K. N88-27540
BRADSHAW, J. N88-27642
BRAETSCH, V. N88-27353
BRAGG, M. B. N88-27173
BRAITHWAITE, J. W. N88-27449
N88-27455
BRANDENBURG, JOHN N88-27997
BRANDON, STEPHEN L. N88-27591
BRAUN, R. L. N88-27506
BRECKLER, STEVEN J. N88-27743
BREILAND, W. G. N88-27275
BRENNER, S. S. N88-27294
BRESSLER, S. L. N88-27688
N88-27703
N88-27706
BRICENO, A. N88-27452
BRICKETT, P. N88-27694
N88-27695
BRINKER, C. J. N88-27328
N88-27335
BROSEY, W. D. N88-27575
BROWN, D. B. N88-27926
BROWN, J. D. N88-27519
BROWN, J. L. N88-27519
BROWN, M. A. N88-27977
BRUGIA, ODOARDO N88-27790
BRUNNER, HEINZ N88-27464
BRUNNSTROM, R. R. L. N88-27555
BRYAN, R. H. N88-27603
BUBECK, MANFRED N88-27190
BUCHANAN, R. C. N88-27316
N88-27317
BUFFINGTON, R. J. N88-27491
BULLOCK, DANIEL N88-27734
BURGHARTZ, JOACHIM N88-27465
BURKHALTER, P. G. N88-27907
BURNS, J. A. N88-27810
BUTLER, K. M. N88-27784
BUTLER, P. C. N88-27451
BUTNER, D. N. N88-27781
BUTT, N. M. ..... N88-2726[illegible]
BYRD, RICHARD H. ..... N88-2781[illegible]
BYRNE, CHARLES M. N88-27871
BYSTRITSKIJ, V. M. N88-27297

C

CABAYAN, H. S. N88-27422
CABELL, RANDOLPH H. N88-27877
CADITZ, DAVID N88-27986
CAIRNS, E. J. N88-27460
CALDWELL, C. S. N88-27784
CALFEE, M. T. N88-27575
CAMIZ, P. N88-27891
CAMMAROTA, JOSEPH P. N88-27710
CAMPARO, JAMES C. N88-27868
CAMPBELL, D. H. N88-27475
CAMPBELL, J. A. N88-27783
CANNON, R. M. N88-27325
CANNON, ROBERT H., JR. N88-27562
N88-27563
CAPDEPUY, B. N88-27252
CARDOSI, KIM M. N88-27752
CARLSON, W. F. N88-27895
CARNE, T. G. N88-27632
CARRE, DAVID J. N88-27560
N88-27931
CARRETTA, THOMAS R. N88-27746
CARSTENS, J. C. N88-27666
CASTELOBRANCO, M. SALOME N88-27721
CASTELOBRANCO, NUNO A. A. N88-27721
CAUGHEY, D. A. N88-27485
CAVANNA, F. N88-27891
CERNEY, MICHAEL J. N88-27168
CHAI, B. H.T. N88-27543
CHAN, Y. Y. N88-27168

CHANDER, S. N88-27452
CHANG, B. J. N88-27754
CHANG, HSIU-GUO N88-27585
CHAPMAN, RANDALL A. N88-27919
CHAPMAN, ROBERT M. N88-27692
CHAUNCEY, CAROLE AGATHA N88-27974
CHEKHOV, L. O. N88-27960
CHEN, S. C. N88-27520
CHEN, TSU-YEH N88-27586
CHEN, X. R. N88-27828
N88-27835
CHEN, YUNMEI N88-27962
CHENG, P. N88-27321
CHEYNE, D. N88-27694
N88-27695
CHINN, VICTOR N88-27221
CHU, B. N88-27328
CHU, C. W. N88-27939
CHYLLA, PETER N88-27806
CLARK, E. L. N88-27491
COEN, PETER G. N88-27182
COHEN, NEAL J. N88-27743
COHEN, R. E. N88-27321
COLE, J. K. N88-27189
COLEMAN, P. D. N88-27458
COLLARD, D. N88-27192
COLSON, W. B. N88-27540
COLTRIN, M. E. N88-27275
CONNER, GARY D. N88-27404
CONWAY, TERRY L. N88-27733
COOKE, J. F. N88-27279
N88-27303
COOPER, J. A. N88-27419
COOPER, R. N88-27705
COOPER, T. N88-27486
CORKE, THOMAS C. N88-27476
COSTALES, B. N88-27686
COTTER, DANIEL M. N88-27616
COURY, LAURE N88-27338
COUTANT, R. W. N88-27346
CRANE, E. N88-27750
CRANMER, D. C. N88-27400
CRAWFORD, P. C. N88-27351
CRESPODASILVA, MARCELO R. M. N88-27157
CRIEL, T. M. N88-27189
CRISP, D. N88-27695
CROCKER, S. C. N88-27407
CROSKEY, CHARLES L. N88-27426
N88-27427
CROSLEY, D. R. N88-27271
CROSLIN, MICHAEL EMANUEL N88-27600
CRUTHIRDS, CHARLES N88-27727
CURTIS, H. B. N88-27624
CUTILLO, B. A. N88-27703
N88-27706
CZICHOWSKY, WOLFGANG N88-27169

D

DAHLEN, HELMUT N88-27879
DAINTY, J. C. N88-27655
DALHED, H. E. N88-27547
DARRAH, RODNEY C. N88-27355
DAS-GUPTA, D. K. N88-27237
DAUGHERTY, J. K. N88-27998
DAVID, S. A. N88-27301
DAVIDSON, G. S. N88-27757
DAVIS, CHRISTOPHER C. N88-27736
DAVIS, D. N88-27642
DAVIS, J. A. N88-27786
DAVIS, JAMES V., II N88-27430
DAVOUDZADEH, F. N88-27483
DAWSON, SETH N88-27153
DEALMEIDA, R. C. C. N88-27494
DEALMEIDA, SERGIO FRASCINO MUELLER N88-27229
DEAZCARRAGA, J. A. N88-27862
DEBENHAM, PHILIP H. N88-27538
DEES, D. W. N88-27638
DEFONTAINE, D. N88-27940
DEFREITASMARQUES, MAURO SERGIO N88-27850
DELAURENTIS, J. M. N88-27859
DELHAES, P. N88-27252
DELNICK, FRANK M. N88-27454
DEMISCH, LOTHAR N88-27714
DEMPSEY, J. P. N88-27597
DENOST, J. P. N88-27228
DESAUSSURE, G. N88-27554
DETTMAR, RALF-JUERGEN N88-27965
DEUTSCH, LESLIE J. N88-27220
DEVATY, ROBERT P. N88-27236
DEVLOO, PHILIPPE REMY BERNARD N88-27467
DEVORE, C. E. N88-27950
DEVRIES, F. P. P. N88-27532
DEXTER, R. N. N88-27904
DEY, DIPAK K. N88-27854
DEYOUNG, R. J. N88-27553
DIBBLE, R. W. N88-27269
DICKERMAN, RONALD L. N88-27613
DICKEY, DANIEL W. N88-27559
DIEHL, ROLAND N88-27999
DIETZ, JEAN FREDERIC N88-27309
DIMAGGIO, C. L. N88-27268
DIMAURO, L. F. N88-27884
DIMITRIADES, B. N88-27647
DISSELEN, M. G. N88-27532
DIVER, RICHARD B. N88-27631
DIXON, L. C. N88-27830
DOBRZYNSKI, WERNER N88-27879
DODDS, JAMES N88-27180
DOLLING, D. S. N88-27484
DOLLYHIGH, SAMUEL M. N88-27182
DONAHUE, FRANCIS M. N88-27523
DONALDSON, W. N88-27544
DONCHIN, EMANUEL N88-27696
DONHAM, B. L. N88-27463
DONLEY, SAMUEL W. N88-27434
DORRIS, S. N88-27642
DORRIS, S. E. N88-27638
DOSSANTOS, D. I. N88-27953
DOWNING, R. G. N88-27425
DOYLE, J. C. N88-27706
DRAKE, J. N88-27839
DRAPER, B. L. N88-27926
DREKSLER, SH. L. N88-27924
DRESSELHAUS, M. N88-27238
DREXLER, R. G. N88-27414
DUBETS, M. N88-27964
DUBORAW, I. NEWTON, III N88-27180
DUCK, PETER W. N88-27164
DUFRANE, K. F. N88-27324
DUNCAN, M. G. N88-27528
DUNLOP, J. D. N88-27456
DUPUY, S. L. N88-27814
N88-27815
DURFEE, R. C. N88-27643
DUSEK, J. T. N88-27953
DUSHENKO, T. W. N88-27711
DUTTON, P. L. N88-27724
DUVAL, R. W. N88-27205
DWIGHT, K. N88-27930
DZHELEPOV, V. P. N88-27297

E

EASTMAN, D. E. N88-27713
EBEL, A. N88-27663
ECHENIQUE, P. M. N88-27885
EDDY, DOUGLAS R. N88-27709
EDGECUMBE, T. S. N88-27291
EDGERTON, S. A. N88-27346
EDMUNDS, R. C. N88-27779
EDMUNDS, R. S. N88-27222
EGETH, HOWARD E. N88-27743
EKBOM, L. N88-27292
EKLUND, T. N88-27569
ELIASSON, A. N88-27292
ELLIS, D. E. N88-27888
ELLIS, GRAHAM K. N88-27796
N88-27799
ELMARHOMY, ABD ALLA M. N88-27571
ELORANTA, EDWIN W. N88-27667
ELTGROTH, P. G. N88-27785
ELTON, BRACY N88-27836
EMERSON, J. E. N88-27313
ENRIQUEZ, LEONARDO N88-27248
ENTRUDO, ANTONIO J. N88-27721
ERALP, EMIN N88-27685
ERICKSON, K. L. N88-27274
N88-27276
ERIKSON, JAN N88-27245
ERINGEN, A. C. N88-27582
ERLICH, D. N88-27486
EROR, N. G. N88-27952
ERTEL, PATRICK W. N88-27287
ERWIN, DAVID N. N88-27738
ESCH, HELMUT N88-27171
ESPY, SUSAN K. N88-27355
EVANS, D. S. N88-27656
EVANS, G. H. N88-27275
EVANS, JOANNE N88-27196
EVANS, KARLEYTON C. N88-27729
N88-27735
EVANS, WENZEL G., JR. N88-27906

F

FABIANO, R. H. N88-27810
FAIRHALL, D. M. N88-27870
FAN, Q. S. N88-27580
FANNING, M. L. N88-27644
FAUCETTE, R. N88-27686
FAULKNER, M. A. N88-27594
FEDDER, J. A. N88-27654
FEKETE, A. N88-27802
FELDMAN, LESLIE A. N88-27234
FELLBAUM, CHRISTIANE N88-27970
FENNELL, J. F. N88-27653
FERREL, T. N88-27459
FERREYRA, GUILLERMO N88-27822
N88-27823
FETH, LAWRENCE L. N88-27740
FIELD, J. E. N88-27348
FILIPPOV, YU. P. N88-27495
FINSTERWALDER, REINHARD N88-27794
FISHER, F. H. N88-27872
FISHER, G. B. N88-27268
FLECK, V. N88-27191
FLEER, A. P. N88-27682
FLEETWOOD, D. M. N88-27926
FLEISCHAUER, PAUL D. N88-27931
FLUSS, M. J. N88-27939
FORSTER, ESTRELLA M. N88-27709
FOUKAL, PETER N88-27993
FOWLER-WHITE, R. M. N88-27703
N88-27706
FOWLER, B. N88-27697
FOWLKES, JENNIFER E. N88-27739
FRANCHOIS, P. R. N88-27644
FRANCOIS, GILBERT N88-27208
FRANKEL, J. N88-27280
FRASER, W. D. N88-27713
FRAUENDORF, ALBRECHT N88-27714
N88-27715
FREDERICK, JOHN E. N88-27650
FREEMAN, HERBERT N88-27770
FREESE, J. M. N88-27451
FRENCH, T. R. N88-27322
FREUND, L. B. N88-27597
FRIEDMANN, P. P. N88-27160
FRIEDRICHS, REINHARD N88-27212
FRISCHAT, G. H. N88-27353
FRUEHOLZ, ROBERT P. N88-27868
FRYKMAN, PETER N. N88-27730
FUERSCHBACH, P. W. N88-27564
FUJII, TOSHIFUMI N88-27393
FUJIMURA, K. N88-27973
FUKUYA, KOJI N88-27329
FULLER, CHRIS R. N88-27877
FUTAKAWA, AKEMI N88-27390

G

GAILLARD, A. W. K. N88-27698
GALAMBOS, J. D. N88-27912
GANCARZ, I. N88-27312
GAO, H. W. N88-27322
GARMLAND, SVEN N88-27416
GARNSEY, SUSAN N88-27692
GAUGER, J. R. N88-27414
GEBALLE, T. H. N88-27440
GEE, J. M N88-27624
GEISELHART, KARL N88-27182
GELFAND, ALAN E. N88-27854
GENSHEIMER, V. M. N88-27584
GENT, A. N. N88-27261
GEORGE, THOMAS F. N88-27938
GERLACH, KARL N88-27409
N88-27410
GEROPP, D. N88-27510
GERZ, THOMAS N88-27516
GESSNER, FREDERICK B. N88-27478
GEVINS, A. S. N88-27686
N88-27703
N88-27706
GHOSH, SUBIR N88-27831
GIBALA, R. N88-27941
GILMAN, S. E. N88-27898
GINZBURG, V. L. N88-27925
GIOVANOLA, J. H. N88-27583
GLAESER, A. M. N88-27325
N88-27326
GLAESER, W. A. N88-27324
GLAUSER, MARK NELSON N88-27504
GLYNN, J. L. N88-27172
GLYNN, PETER W. N88-27764
GOEBEL, R. N88-27723
GOLDBERG, ANDREW V. N88-27824
N88-27825
GOLDEN, D. M. N88-27271
GOMEZ, RICHARD B. N88-27613
GOODMAN, D. W. N88-27268
GORDON, R. N88-27694
GORETTA, K. C. N88-27952
N88-27953

GORNEY, D. J. N88-27656
GOUDEY, G. T. N88-27953
GOULIANOS, K. N88-27996
GOWER, DANIEL W., JR. N88-27739
GRADY, D. E. N88-27218
GRAEGER, HELMUT N88-27515
GRAESSLE, D. E. N88-27904
GRAFE, V. G. N88-27757
GRANDT, A. F. N88-27581
GRANOVSKIJ, V. B. N88-27297
GRANT, J. E. N88-27529
GRAS-MARTI, A. N88-27885
GRAY, L. J. N88-27839
GREEN, BERT F., JR. N88-27743
GREEN, R. N. N88-27677
GREENWOOD, J. A. N88-27561
GREER, D. S. N88-27686
N88-27706
GROHMAN, MARK A. N88-27545
GROPP, WILLIAM D. N88-27469
GROSS, G. E. N88-27630
GROSSBERG, STEPHEN N88-27734
N88-27807
N88-27808
GROSZ, CARLA N88-27967
GRUBIN, H. L. N88-27446
GRUESCHOW, GERHARD N88-27573
GRUNER, MARY M. N88-27737
GUBSER, DONALD U. N88-27921
GUENZBURGER, D. N88-27888
GUERIN, M. R. N88-27272
GUILES, R. D. N88-27725
GUSTAFSON, DONALD E. N88-27773
GUTMANN, RONALD J. N88-27445
GUTOWSKI, W. J. N88-27673
GUTZLER, D. S. N88-27673

H

HADA, KAZUHIKO N88-27295
HAGEN, D. E. N88-27666
HAGGERTY, J. S. N88-27623
HAHN, G. T. N88-27286
HAHN, H. T. N88-27597
HAILEY, C. E. N88-27491
HALES, J. M. N88-27674
HALL, PHILIP N88-27164
HALLQUIST, J. O. N88-27604
HAMMAR, T. R. N88-27682
HAMMETTER, W. F. N88-27449
HAMPSTEN, K. L. N88-27895
HAN, K. S. N88-27537
HANNEMANN, KLAUS N88-27518
HANSEN, ULRICH N88-27663
HANSON, R. J. N88-27787
HARA, MASAHORI N88-27394
HARDING, A. K. N88-27998
HARELAND, W. A. N88-27289
HARMAN, EVERETT N88-27765
HARMAN, EVERETT A. N88-27730
HARRIS, C. S. N88-27311
HARRIS, G. W. N88-27641
HARROP, R. N88-27694
N88-27695
HARVEY, D. P., II N88-27584
HASEGAWA, MITSURU N88-27914
HAWKINS, GARY F. N88-27234
HAYASHI, Y. N88-27627
N88-27628
N88-27923
HAYS, A. K. N88-27299
HE, X-C. N88-27930
HEGEDUS, S. S. N88-27944
HEGER, G. N88-27260
HEIBERGER, J. J. N88-27638
HEIKEN, G. N88-27990
HELLER, HANNO N88-27879
HELM, F. H. N88-27351
HELMAN, J. S. N88-27943
HENDERSON, B. N88-27937
HENDRICKSON, CLENDON L. N88-27525
HENDRICKSON, J. J. N88-27772
HENLEY, J. P. N88-27612
HENNEKE, E. G. N88-27575
HENNINGS, WILFRIED N88-27176
HENRIKSEN, P. N. N88-27261
HENSHALL, J. B. N88-27895
HERNANDEZ, R. N88-27254
N88-27255
HERSHEY, A. V. N88-27474
HESLEGRAVE, R. J. N88-27702
HEYERDAHL, E. K. N88-27646
HIBSHOOSH, ELIPHAZ N88-27421
HIGBIE, P. R. N88-27653
HILL, S. L. N88-27273
HILSENRATH, ERNEST N88-27650
HINDMARSH, A. C. N88-27841
HO, KWANG-IL N88-27608
HO, P. N88-27275
HODGES, BILLY R. N88-27803
HODGES, DEWEY H. N88-27157
HODGKISS, W. S. N88-27872
HOFFMANN, R. N88-27701
HOKE, M. N88-27693
HOKENSON, GUSTAVE J. N88-27167
HOLDRIDGE, D. B. N88-27786
HOLMAN, BARRY W. N88-27860
HOMERIN, PIERRE N88-27340
HONDA, MASAO N88-27915
HOPKINS, R. P. N88-27402
HOR, H. P. N88-27939
HORACEK, DOUGLAS N88-27976
HORIUCHI, RITOKU N88-27913
HORNUNG, H. N88-27480
HORST, T. W. N88-27660
HOUDRE, CHRISTIAN N88-27849
HOUSER, R. M. N88-27636
N88-27637
HOWE, M. S. N88-27875
N88-27876
HOWELL, R. H. N88-27939
HREBIEN, LEONID N88-27710
HSU, ANDREW T. N88-27174
HSU, IN-SHEK N88-27220
HSUEH, C. H. N88-27241
HUANG, RONG-FUNG N88-27257
HUBBARD, RICHARD N88-27411
HUBBARD, ROGER W. N88-27731
HULL, J. R. N88-27639
HUNT, EARL N88-27778
HUNTER, JEFFREY J. N88-27855
HUNTLEY, M. S., JR. N88-27752
HURD, A. J. N88-27335
HUSSEY, T. W. N88-27547
HUTH, GAYLORD N88-27180
HUYNH, LOC C. N88-27205
HWANG, DEBORAH J. N88-27801
HWANG, I. H. N88-27230
HWANG, WARREN G. N88-27434
HYVOENEN, T. N88-27610

I

IBRAHIM, RAOUF A. N88-27589
IGLEHART, DONALD L. N88-27764
IKEDA, SADAO N88-27295
IKEDA, YOSHITAKA N88-27915
ILLES, J. N88-27703
N88-27706
IMAI, TSUYOSHI N88-27915
IMHOF, WILLIAM L. N88-27221
IMPROTA, SALVATORE N88-27790
INOUE, YASUO N88-27397
IRENE, E. A. N88-27932
ISHIBASHI, MICHIYASU N88-27393
ISHIHARA, S. N88-27923
ISHII, K. N88-27627
N88-27923
ISTRAIL, SORIN N88-27766
ITIL, KURT Z. N88-27685
ITIL, TURAN M. N88-27685
ITO, J. I. N88-27254
N88-27255
ITOH, TATSUO N88-27437
IWANOW, JERZY N88-27336

J

JACKSON, B. E. N88-27882
JACKSON, S. C. N88-27944
JACOBS, S. D. N88-27898
JACOBSON, M. J. N88-27185
JAEGGY, BERNARD-CHARLES N88-27169
JAJODIA, SUSHIL N88-27804
JANSEN, ROBERT WERNER N88-27945
JASSE, B. N88-27337
JEAN, Y. C. N88-27939
JENNINGS, C. W. N88-27453
JENSEN, J. R. N88-27618
JI, ZHIMING N88-27572
JOCHUM, ANNE M. N88-27669
JOHN, E. R. N88-27687
JOHNSON, B. C. N88-27538
JOHNSON, D. A. N88-27723
JOHNSON, DAVID N88-27714
N88-27715
JOHNSON, W. G. N88-27594
JOHNSTON, J. P. N88-27479
JOLLES, M. I. N88-27584
JOLLES, MITCHELL I. N88-27588
JONES, C. R. N88-27861
JONES, D. P. N88-27568
JONES, E. M. N88-27213
JOOS, HANS-DIETER N88-27793
N88-27795
JOY, K. I. N88-27782
JOYCE, GLENN N88-27411
JU, FREDERICK D. N88-27586
JUDD, R. R. N88-27679
JUHASZ, T. N88-27544

K

KAAE, J. L. N88-27238
KALLENBERG, OLAV N88-27851
KANAKIA, MIKE D. N88-27266
N88-27347
KANG, SANG-WOOK N88-27909
KAO, Y. H. N88-27954
KARASAWA, H. N88-27628
KASCHIEV, M. S. N88-27417
KATO, T. N88-27973
KAUFMAN, LLOYD N88-27684
N88-27747
KAWAHARA, WENDELL A. N88-27591
KAWANAMI, H. N88-27923
KAZAKOS, P. P. N88-27763
KAZMIERCZAK, H. N88-27615
KEE, R. J. N88-27275
KEEFER, K. D. N88-27333
KEGL, JUDY N88-27970
KELBER, J. A. N88-27334
KELLY, SCOTT ROGER N88-27578
KELSO, B. N88-27697
KENNEDY, JOHN M. N88-27593
KENNEDY, ROBERT S. N88-27739
KERN, K. N88-27429
KESKINEN, M. J. N88-27654
KEZERIAN, JEFFREY N88-27217
KHAN, M. A. N88-27927
KHANAKA, G. H. N88-27457
KIDANE, B. N88-27296
KIKUCHI, RYOICHI N88-27935
KILROY, W. P. N88-27441
KIM, CHANGHO N88-27968
KIM, D. N88-27884
KIM, J. K. N88-27290
KIM, KWANG-HO N88-27511
KIM, YIL BONG N88-27901
KINDLER, KNUD N88-27210
KING, R. J. N88-27422
KINGSLEY, L. N88-27544
KIRBY, G. C., III N88-27584
KITTEL, PETER N88-27507
KLARER, P. R. N88-27568
KLAUENBERG, B. J. N88-27738
KLEMETTI, WAYNE I. N88-27405
KLEPPNER, DANIEL N88-27869
KNAPIK, JOSEPH N88-27728
KNAUSS, W. G. N88-27597
KNOBLOCH, BERND J. N88-27789
KNOTT, D. N88-27926
KNUDSEN, JOHN F. N88-27425
KNUTTGEN, HOWARD G. N88-27727
KO, GYM SEK N88-27495
KOBAYASHI, A. S. N88-27597
KOBERSTEIN, J. T. N88-27312
N88-27313
KOERBER, GERMAIN N88-27169
KOGAN, YA. I. N88-27961
KOHL, KAREN B. N88-27266
KOLPAKOV, I. F. N88-27759
KOMHYR, W. D. N88-27644
KONDOH, Y. N88-27911
KONG, JIN A. N88-27617
KORELLIS, JOHN S. N88-27591
KOREZLIOGLU, A. H. N88-27826
KOTELNIKOV, G. A. N88-27988
KOUTNY, M. N88-27402
KOUTSOURAS, DIMITRIS A. N88-27413
KOVALENKO, A. G. N88-27418
KOZUB, J., JR. N88-27197
N88-27198
KRAEMER, WILLIAM J. N88-27727
KRAMER, ARTHUR F. N88-27696
KRAMER, PETER N88-27227
KRAUSE, P. C. N88-27635
KRESIN, V. Z. N88-27951
KRESKOVSKY, J. P. N88-27446
KRISHNAIAH, P. R. N88-27853
KRIVORUCHENKO, M. I. N88-27984
KROGSLUND, K. N88-27681
KRUSINGER, A. E. N88-27685
KUCZKA, DETLEF N88-27211

KUEHNE, UWE N88-27644
KUESTER, S. E. N88-27644
KUHLMAN, JOHN M. N88-27168
KULIKOV, N. I. N88-27927
KUNZ, STEPHANIE C. N88-27352
KURATH, PETER N88-27611
KURY, J. W. N88-27351
KUSANO, KANYA N88-27913
KUSHNER, HAROLD J. N88-27847
KUSSOY, M. I. N88-27519
KYLE, J. N88-27939
KYUMA, KAZUO N88-27389

L

LACOMBE, JEAN FRANCOIS N88-27576
LADOUCEUR, HAROLD D. N88-27319
LAFEMINA, JOHN A. N88-27319
LAGARDE, D. N88-27716
LAGERGREN, ERIC S. N88-27831
LAI, S. T. N88-27543
LALA, ALBERTO N88-27717
LAM, DENNIS KANG-POR N88-27468
LAMALLE N88-27251
LAMPE, MARTIN N88-27411
N88-27887
LANAGAN, M. T. N88-27953
LANDGREBE, A. R. N88-27460
LANDOLT, J. P. N88-27697
N88-27713
LANGNER, A. N88-27938
LANNOM, D. C. N88-27566
LARSSON, FRITZ N88-27245
LAUFFER, J. P. N88-27632
LAUPRETRE, F. N88-27337
LAVIA, A. N88-27246
LAWTON, DARYL T. N88-27404
LEADBETTER, M. R. N88-27848
LEBENS, JOHN ANDREW N88-27946
LEBOCQ, PHILIPPE N88-28000
LEDER, A. N88-27510
LEE, ANNABEL Y. N88-27314
LEE, DING N88-27821
LEE, HO-LUN N88-27429
LEE, J. W. N88-27857
LEE, M. C. N88-27754
LEE, R. L. N88-27838
LEFEBVRE, PAUL J. N88-27481
LEHMAN, DALE A. N88-27616
LEHNERTZ, K. N88-27693
LEHTO, A. N88-27570
LEIBOWITZ, L. N88-27306
LESSI, O. N88-27818
LETAVIC, TED N88-27445
LEUTSCHER, A. J. N88-27532
LEVUSH, B. N88-27534
N88-27536
LEWANDOWSKI, A. N88-27629
LEWIS, NITA L. N88-27709
LIAW, PAUL N88-27168
LILIENTHAL, MICHAEL G. N88-27739
LIM, KAIR CHUAN N88-27224
LIN, HOANG-SHEN N88-27574
LIN, K. Y. N88-27230
LIN, TONG CHING N88-27579
LINCE, JEFFREY R. N88-27931
LINCOLN, JANET E. N88-27749
LINCOLN, K. A. N88-27798
LINS, V. F. C. N88-27330
LINSEY, VONNE N88-27285
LIOU, KUO-NAN N88-27658
LIOU, MENG-SING N88-27174
LITTLE, JAMES J. N88-27819
LIU, N. S. N88-27483
LIU, WING K. N88-27585
LIU, YUNG Y. N88-27300
LOBANOV, YU. YU. N88-27865
LONG, M. N88-27543
LOOMIS, PETER N88-27180
LOUBET, DANIEL N88-27250
LUCHT, R. P. N88-27269
LUCIANI, R. N88-27712
LUEBECK, EGMAR N88-27533
LUETKENHOENER, B. N88-27693
LUKENS, JAMES N88-27435
LUKIERSKI, J. N88-27862
LUTSKO, J. F. N88-27305
LYNCH, N. N88-27802
LYNESS, E. N88-27554

M

MABY, EDWARD W. N88-27445
MACH, H. N88-27259
MACKAY, G. I. N88-27641
MACKENZIE, J. N88-27238
MACKENZIE, J. D. N88-27315
MACKEY, H. E., JR. N88-27618
MADSEN, N. K. N88-27838
MAERKER, R. E. N88-27858
MAGGS, J. E. N88-27905
MAGNITSKAYA, M. V. N88-27927
MAIER, HANS-JUERGEN N88-27204
MAIWALD, INES N88-27243
MALLINAK, E. S. N88-27755
MALOVICHKO, P. P. N88-27995
MAMEDOV, I. S. N88-27495
MAMONOV, V. N. N88-27417
MANCO, A. N88-27685
MANDA, BOSE V. S. N88-27258
MANOJLOVIC, D. N88-27290
MANSON, J. R. N88-27685
MANTEUFFEL, T. A. N88-27817
MANZEY, DIETRICH N88-27748
MANZO, M. A. N88-27267
MARCHITELLI, LOUIS J. N88-27727
MARICI, LIVIO N88-27692
MARR, J. J. N88-27461
MARSH, W. J. N88-27492
MARTIN, GLENN L. N88-27182
MARTIN, LEE U. N88-27412
MARTIN, R. E. N88-27267
MARVAO, JOSE H. N88-27721
MARVIN, D. C. N88-27620
MASON, B. E. N88-27398
MASON, G. N88-27429
MASOOM, ABULKHAIR MOHAMMAD N88-27601
MASSALSKI, T. B. N88-27256
MASTIN, G. A. N88-27787
MASUR, H. N88-27259
MASUTANI, MASAHIRO N88-27239
MATEOS, M. A. N88-27796
MATIC, P. N88-27584
MATIC, PETER N88-27588
MATOBA, TOHRU N88-27897
MATSON, DAVID L. N88-27708
MATSON, R. J. N88-27633
MATSUMOTO, JAMES H. N88-27434
MATYUSHINA, S. A. N88-27493
MATZEN, M. K. N88-27547
MAURICE, A. K. N88-27316
MAYNE, L. K. N88-27641
MAZIASZ, P. J. N88-27293
MCCALLEN, R. E. N88-27909
MCCALLUM, W. C. N88-27705
MCCLANAHAN, E. C. N88-27298
MCCONNELL, CHRISTOPHER C. N88-27404
MCCRARY, JOHN W. N88-27692
MCGOVERN, D. E. N88-27568
MCGOVERN, JENNIFER B. N88-27356
N88-27709
MCGOWN, AMANDA N88-27688
MCGRATH, S. V. N88-27594
MCGUIRE, E. J. N88-27547
MCHARGUE, C. J. N88-27302
N88-27942
MCLARNON, F. R. N88-27460
MCMILLAN, J. C. N88-27179
MCNULTY, MICHAEL J. N88-27148
MCPHEETERS, C. C. N88-27638
MCQUILLAN, B. N88-27238
MCWHORTER, ALAN L. N88-27929
MEDELLIN, ROLAND A. N88-27357
MEHLMAN, G. N88-27907
MEI, H. L. N88-27311
MEKARI, MILAD H. N88-27558
MELISSINOS, A. C. N88-27544
MELKO, OTTO MICHAEL N88-27358
MELLO, ROBERT N88-27728
MELNGAILIS, JOHN N88-27439
MENG, R. L. N88-27939
MENNE, STEFAN N88-27512
MENSING, R. W. N88-27422
MERCATANTE, THERESA A. N88-27746
MERKEL, TH. N88-27191
MERRITT, JAMES H. N88-27738
MERRY, R. T. G. N88-27720
MERTEN, ALFONS N88-27514
MESCALL, J. F. N88-27597
MEYER, ALBERT R. N88-27766
MEYER, PAUL N88-27169
MEYER, RICHARD E. N88-27832
MEYSTEL, A. M. N88-27811
MEYYAPPAN, M. N88-27446
MIANE, J. L. N88-27343
MIANE, JEAN LOUIS N88-27576
MIAO, B. Q. N88-27828
MICHALSKE, T. A. N88-27333
MICHEL, ULF N88-27551
MIDDELMANN, HEINZ-UDO N88-27957
MILES, RICHARD B. N88-27165
MILES, RONALD N. N88-27598
MILGRAM, DAVID L. N88-27404
MILHAUD, C. N88-27716
MILLER, GEORGE A. N88-27970
MILLER, J. C. N88-27703
MILLER, JAMES C. N88-27709
MILLER, KATHERINE N88-27970
MILOVIC, R. N88-27290
MILOVICH, JOSE LUIS N88-27903
MINNIS, P. N88-27677
MIRICK, PAUL H. N88-27154
N88-27155
MISHCHENKO, M. I. N88-27991
N88-27992
MISRA, MOHAN S. N88-27233
MITCHELL, W. F. N88-27840
MITTER, SANJOY K. N88-27773
MOCCI, U. N88-27423
MODENA, IVO N88-27692
MOFFAT, R. J. N88-27479
MOFFITT, A. N88-27701
MOISION, W. K. N88-27408
MOLLEY, P. A. N88-27780
MONNERIE, L. N88-27337
MOODY, LAURA E. N88-27196
MOODY, R. L. N88-27218
MOORE, FRANK W. N88-27359
MORALES, G. J. N88-27905
MORGAN, N. H. N88-27686
N88-27706
MORGAN, STEPHEN T. N88-27360
MORGENS, L. M. N88-27316
MORI, MASAHIRO N88-27914
MOROZOV, YU. I. N88-27982
MORRIS, SHELBY J., JR. N88-27182
MORRISON, B. J. N88-27446
MOSS, STEVEN C. N88-27428
MRAZEK, F. C. N88-27638
MUDAWWAR, I. N88-27492
MUDGE, T. N. N88-27776
MUELLER, IVAN I. N88-27662
MULLEN, STEPHEN P. N88-27730
MULLINS, LARRY N88-27181
MUNFORD, J. W. N88-27590
MUNGER, MICHAEL P. N88-27753
MURRAY, JOHN J. N88-27678
MUSKET, R. G. N88-27332
MUTO, YASUSHI N88-27295
MYLES, K. M. N88-27638

N

NADEL, JEROME I. N88-27361
NAGAI, K. N88-27627
N88-27923
NAGIB, HASSAN M. N88-27476
NAHSTOLL, JUERGEN N88-27517
NAKAGAWA, MASAMI N88-27499
NAKAKURA, TOSHIYUKI N88-27239
NAKANISHI, H. N88-27939
NAKASHIMA, HIROSHI N88-27395
NAKAZAWA, ICHIRO N88-27897
NAKOS, J. T. N88-27496
NANSTAD, R. K. N88-27603
NASH, W. A. N88-27597
NASMAN, VICTORIA TEPE N88-27362
NATARAJ, CHANDRASEKHAR N88-27599
NATESAN, K. N88-27300
NECHAEV, YU. S. N88-27296
NEIL, V. K. N88-27549
NEIMS, D. N88-27718
NELSON, G. C. N88-27299
NELSON, J. G. N88-27928
NELSON, JOHN G. N88-27710
NELSON, KENNETH J. N88-27232
NELSON, R. A. N88-27489
NEUBAUER, F. M. N88-27663
NEWMAN, D. A. N88-27907
NEWMAN, FREDERICK A. N88-27200
NEWNAM, B. E. N88-27541
NG, KING-YUEN N88-27896
NIIYA, K. Y. N88-27254
N88-27255
NISATI, A. N88-27892
NISHIMURA, TADASHI N88-27397
NIU, XUFENG N88-27650
NJOKU, BERNADETTE P. T. N88-27363
NOBLE, DAVID N88-27967
NOERSETT, S. P. N88-27841
NOLTE, D. D. N88-27948
NORBY, R. J. N88-27648
NORDMAN, JAMES E. N88-27436
NORDMARK, H. O. N88-27505
NORFLEET, CHARLES W. N88-27364

NYLUND, N.-O. N88-27569

O

OBRIEN, WALTER F. N88-27877
OBUKHOV, YU. L. N88-27417
OCHAYA, VEN N88-27314
ODAJIMA, KAZUO N88-27914
ODAJIMA, TOSHIKAZU N88-27239
ODORICO, J. N88-27249
N88-27308
N88-27339
N88-27577
OFFENLOCH, KURT N88-27715
OGALLAGHER, J. N88-27629
OGAWA, YUTAKA N88-27295
OGURA, YOSHIAKI N88-27897
OH, SE H. N88-27268
OH, T. S. N88-27325
OHERN, T. J. N88-27497
OHMINE, MEGUMI N88-27391
OHTA, KANJI N88-27914
OHTSUKA, HIDEO N88-27914
OKAMOTO, Y. N88-27311
OLIVER, W. C. N88-27302
OLOUGHLIN, THOMAS E. N88-27282
OLSON, J. G. N88-27668
OPANASENKO, A. N. N88-27493
ORVIS, W. J. N88-27457
OSHIMA, KAZUYOSHI N88-27396
OTTER, MARTIN N88-27793
N88-27794
OU, SZU-CHEN N88-27658
OZAWA, KUNIO N88-27329

P

PADILLA, PETER A. N88-27447
PAIS, MARTIN RABINDRA N88-27500
PALINKAS, LAWRENCE A. N88-27741
PANCAKE, CHERRI M. N88-27809
PANG, J. N88-27452
PANTEW, C. N88-27693
PAPANTONI-KAZAKOS, P. N88-27833
N88-27874
PARKS, SCOTT E. N88-27184
PASAMEHMETOGLU, K. D. N88-27489
PATERAKIS, M. N88-27763
PATTON, JOHN F. N88-27727
PATZ, G. N88-27202
PAUL, HEINRICH N88-27531
PAVLOVICI, ROBERT N88-27976
PEDEN, C. H. F. N88-27268
PEEBLES, D. E. N88-27450
PEEBLES, H. C. N88-27289
PELENC, L. N88-27640
PENADO, FEDERICO ERNESTO N88-27602
PENG, Y. K. M. N88-27912
PENNELL, W. T. N88-27674
PENZES, S. G. N88-27187
PERKINS, A. LOUISE N88-27836
PETERS, DAVID A. N88-27156
PETRAS, KNUT N88-27843
PETRASEK, DONALD W. N88-27310
PETROSIAN, VAHE N88-27986
PETTIT, D. R. N88-27990
PFEIFER, K. B. N88-27899
PHILLIPS, DAVID N88-27320
PHILLIPS, J. N88-27328
PHILLIPS, RICHARD J. N88-27444
PICCIOLO, J. J. N88-27638
PICKERING, HOWARD W. N88-27431
N88-27432
PICO, P. N88-27192
PIDWERBETSKY, ALEXANDER N88-27503
PIERI, ROBERT VICTOR N88-27609
PIERRE, A. C. N88-27342
PIGEAU, R. N88-27701
PIGEAU, R. A. N88-27702
PIHLMAN, M. N88-27462
PILKEV, WALTER D. N88-27587
PIN, F. G. N88-27554
PINEAU, M. D. N88-27651
PIPKIN, F. M. N88-27886
PIZZELLA, VITTORIO N88-27692
PLAKIDA, N. M. N88-27924
POCOCK, P. V. N88-27705
POEPPEL, R. B. N88-27638
N88-27952
N88-27953
POLAK, E. N88-27183
POMYKAL, G. W. N88-27797
POPE, J. E. N88-27581
POPE, L. E. N88-27450
POPE, STEPHEN B. N88-27473
POPPENS, SUSAN A. N88-27365
PORCU, SILVIO N88-27717
PORLIER, G. N88-27697
PORTA, PIERRE N88-27471
N88-27472
PORTA, TIBA N88-27762
PORTMAN, D. N88-27673
POST, D. N88-27575
POSTON, TALMADGE M. N88-27434
POUCHER, D. E. N88-27172
POWELL, RICHARD C. N88-27535
PRACHE, B. N88-27343
PRAGER, S. C. N88-27904
PRECKSHOT, G. G. N88-27781
PRICE, R. N88-27238
PRICHEP, L. S. N88-27687
PROHOFSKY, EARL W. N88-27318
PUCKETT, E. G. N88-27498
PUGH, C. E. N88-27603
PURCELL, S. N88-27701
PURVIS, BRADLEY N88-27704

Q

QUATTLEBAUM, J. C. N88-27530
QUINN, MICHAEL J. N88-27524

R

RABICH, L. N. N88-27918
RABIER, PATRICK J. N88-27845
RAJKOVIC, BORIVOJ N88-27661
RAMAKRISHNAN, R. N88-27606
RAMESH, A. V. N88-27800
RAMSIER, R. D. N88-27261
RAO, C. R. N88-27829
N88-27834
N88-27856
RASCHKE, E. N88-27663
RATCLIFFE, JAIMIE N88-27760
RATINO, D. N88-27712
RAVAIOLI, G. N88-27423
RAVICHANDRAN, M. N88-27501
RAY, S. K. N88-27581
REAVIS, MARK ANDRE N88-27366
RECHESTER, ALEXANDER B. N88-27852
REDA, D. C. N88-27527
REED, IRVING S. N88-27220
REES, DAVID N88-27539
REEVES, ADAM N88-27744
REEVES, D. L. N88-27707
REGAN, D. N88-27690
N88-27718
REGAN, M. P. N88-27690
REIFSNIDER, K. L. N88-27575
REINKE, R. E. N88-27652
REITELBACK, P. J. N88-27644
RENARD, P. N88-27339
RENKER, L. A. N88-27277
RENSCHLER, C. L. N88-27327
RESHETNIKOVA, K. A. N88-27417
RHODE, TORSTEN M. N88-27287
RICH, CHARLES N88-27767
N88-27769
RICHEY, M. W. N88-27301
RICKS, GLEN A. N88-27226
RIDDIFORD, BRYAN P. N88-27367
RIESE, KEITH A. N88-27368
RILEY, M. N88-27750
RIMLINGER, SERGE N88-27278
RITCHIE, B. N88-27420
RITCHIE, R. H. N88-27885
RITCHIE, R. O. N88-27325
RIZZO, H. F. N88-27298
ROBERTS, JOHN P. N88-27664
ROBERTS, RICHARD E. N88-27178
ROBERTSON, A. N88-27695
ROBINS, A. WARNER N88-27182
ROBINSON, A. C. N88-27596
ROBINSON, ERNEST Y. N88-27231
ROBINSON, M. CAROLYN N88-27369
RODEL, J. N88-27325
RODGERS, M. N88-27642
RODRIGUE, GARRY N88-27836
ROEDEL, J. N88-27326
ROHDE, FREDERICK W. N88-27614
ROKHSAR, DANIEL SOLEYMAN N88-27947
ROMANI, GIAN LUCA N88-27691
N88-27692
ROSE, B. H. N88-27349
ROSE, M. E. N88-27508
ROSENAU, TODD J. N88-27804
ROSENBLAT, SIMON N88-27476
ROSENFIELD, A. R. N88-27324
ROSENSTEIN, RICHARD M. N88-27730
ROSENSTOCK, H. N88-27926
ROSLYI, A. A. N88-27863
N88-27884
ROSS, S. P. N88-27783
ROUSSEL, W. T. M. N88-27532
ROUX, J. A. N88-27331
ROY, T. N. N88-27408
RUBIN, C. A. N88-27286
RUBIN, S. B. N88-27417
RUITER, J. P. N88-27619
RYAN, THOMAS W., III N88-27266

S

SACHS, P. L. N88-27682
SAFFER, JEFFERY D. N88-27722
SAHU, D. N88-27938
SAILORS, D. B. N88-27408
SAINTELUCEBANCHELIN, JEAN MARC N88-27344
SAKAI, HIDEO N88-27239
SAKAMOTO, KEISHI N88-27915
SAKULICH, TIMOTHY J. N88-27195
SALAS, F. JIM N88-27352
SALBERT, THOMAS N88-27956
SALO, S. N88-27681
SALUSTRI, CARLO N88-27692
SANCHEZ, J. N88-27246
SANCHEZ, JOSE N88-27248
SANDERS, DAVID W. N88-27177
SANDHOLM, S. N88-27642
SANTAVICCA, D. A. N88-27265
SANTIAGO, FILIBERTO N88-27370
SASAKI, SHINOBU N88-27567
SASUGA, TSUNEO N88-27239
SATO, TETSUYA N88-27913
SAWKA, MICHAEL N. N88-27732
SAYLOR, P. E. N88-27817
SCHAEFER, D. W. N88-27328
SCHARLEMANN, E. T. N88-27540
SCHARPF, RUDOLF N88-27204
SCHIEFFER, JAMES M. N88-27186
SCHIFF, H. I. N88-27641
SCHMALE, D. T. N88-27592
SCHMIDT, W. N88-27675
SCHMIEG, S. J. N88-27268
SCHNABEL, ROBERT B. N88-27812
SCHOLZ, W. N88-27280
SCHROEDER, WOLFGANG N88-27513
SCHUELKE, HELMUT N88-27550
SCHULTZ, E. B. N88-27750
SCHUMMER, G. J. N88-27711
SCHWAGER, L. A. N88-27908
SCHWARTZ, R. J. N88-27621
SCHWARZ, A. S. N88-27863
N88-27864
SCHWEMMER, ROLF N88-27792
SCHWERTL, M. N88-27920
SCOTT, MARION W. N88-27545
SCOTT, R. L., JR. N88-27565
SCOTT, RANDALL E. N88-27406
SEABA, JAMES P. N88-27371
SEAGER, C. H. N88-27299
SEAGER, M. K. N88-27785
SEAMAN, L. N88-27486
SEGUCHI, TADAO N88-27239
SEKIKAWA, KAZUHIKO N88-27396
SEKULER, ROBERT N88-27745
SEMAR, WOLFGANG N88-27244
SEN, R. K. N88-27459
SENNER, A. E. N88-27759
SERBETO, A. N88-27536
SEVIER, N. E. N88-27972
SEXTON, GEORGE A. N88-27196
SHAFER, D. K. N88-27682
SHAH, J. J. N88-27646
SHALTENS, RICHARD K. N88-27980
SHAMROTH, S. J. N88-27483
SHANBHAG, D. N. N88-27834
SHANG, E. C. N88-27821
SHARP, MARILYN N88-27728
SHARPE, DAVID L. N88-27150
SHARPE, WILLIAM N., JR. N88-27522
SHEFI, AMNON N88-27873
SHEN, H-S. N88-27930
SHERMAN, CHRISTOPHER N88-27659
SHESTOPALOV, V. P. N88-27418
SHI, D. N88-27952
SHIDKOV, E. P. N88-27865
SHIELDS, E. W. N88-27182
SHIMIZU, MIKIO N88-27256
SHINN, M. D. N88-27543
SHIONO, SATORU N88-27389
SHIRA, L. N88-27602

SHKLOVSKIJ, V. A. N88-27922
SHOCKEY, D. A. N88-27583
SHOCKLEY, CYNTHIA W. N88-27971
SHOJI, TERUAKI N88-27914
SHORE, B. W. N88-27548
N88-27889
SHULTZ, GERALD A. N88-27812
SHUPE, JON A. N88-27372
SIEM, FREDERICK M. N88-27746
SIERRA, CHRISTOPHER D. N88-27373
SILEVITCH, MICHAEL B. N88-27657
SILS, INGRID V. N88-27729
N88-27735
SIMPSON, R. L. N88-27351
N88-27477
SINES, GEORGE H. N88-27235
SINGH, J. P. N88-27953
SITES, J. R. N88-27622
SKELLY, JUNE J. N88-27704
SKOCYPEC, R. D. N88-27276
SKOLNIK, MERRILL I. N88-27415
SKOTHEIM, T. N88-27311
SLINKER, STEVEN N88-27411
SLOAN, GREGORY N88-27374
SMAGA, J. A. N88-27461
SMALL, RONALD L. N88-27753
SMELA, ELISABETH N88-27375
SMIRNOV, V. A. N88-27759
SMITH, EDWARD B. N88-27489
SMITH, G. L. N88-27677
SMITH, G. P. N88-27271
SMITH, J. C. N88-27711
SMITH, K. N88-27686
SMITH, R. M. N88-27800
SMITH, RITA REX N88-27376
SMITH, S. A. N88-27645
SNELL, S. A. N88-27977
SOCIE, DARRELL F. N88-27611
SOHN, J. E. N88-27313
SONG, JONG CHUL N88-27956
SOSENKO, P. P. N88-27918
SOUDUNSAARI, R. N88-27570
SOULEZELLE, B. N88-27249
SPAIN, EDWARD H. N88-27751
SPANNER, G. E. N88-27546
SPELT, P. F. N88-27554
SPENCER, D. W. N88-27682
SPERLINE, P. D. N88-27546
SPETH, P. N88-27663
SPINDLER, GERHARD N88-27552
SPIROPOULOS, PROCOPIOS T. N88-27281
STACKPOOL, F. M. N88-27455
STAHL, BERNHARD N88-27551
STALKER, K. T. N88-27760
STANNY, R. R. N88-27707
STARK, LOUISE N88-27377
STARKE, EDGAR A., JR. N88-27284
STARRFIELD, S. G. N88-27987
STAUDHAMMER, K. P. N88-27949
STAVROPOULOS, A. N88-27719
STAYLOR, W. F. N88-27677
STEIGER, A. N88-27420
STEINSALTZ, STEVEN J. N88-27378
STEPHENS, J. J. N88-27590
STEPHENS, JOSEPH R. N88-27310
STEPHENS, WENDELL B. N88-27149
STERMAN, M. B. N88-27711
STERN, JOHN A. N88-27699
STEWMAN, JOHN H. N88-27379
STOCK, A. F. N88-27206
STOCKWALD, K. N88-27920
STOLL, JACK K. N88-27616
STONE, C. M. N88-27449
N88-27455
STOWE, L. L. N88-27677
STRICKLER, D. J. N88-27912
STROHMAYER, TOD N88-27380
STUMP, B. W. N88-27652
STURROCK, P. A. N88-27998
SUBIA, S. R. N88-27449
N88-27455
SUDAR, M. N88-27754
SUGAWARA, SAKUO N88-27394
SUGIHARA, MASAYOSHI N88-27914
SUN, C. T. N88-27242
SUTHERLAND, LINDA W. N88-27881
SUTTLES, J. T. N88-27677
SUZUKI, NORIO N88-27914
SWANSON, E. E. N88-27182
SYLWESTER, A. P. N88-27327
SZLYK, PATRICIA C. N88-27729
N88-27735
SZULGA, JERZY N88-27651

T

TAKAHASHI, K. N88-27653
TAKASE, YUICHI N88-27915
TAKSAR, MICHAEL N88-27846
TANIGUCHI, M. N88-27853
TANNEHILL, R. S. N88-27706
TANNER, L. E. N88-27288
N88-27298
TAPSCOTT, R. E. N88-27398
TARIDE, SERGE N88-27219
TARJAN, ROBERT E. N88-27824
N88-27825
TAYLOR, M. J. N88-27625
TAYLOR, V. R. N88-27677
TERASAWA, MITITAKA N88-27329
THEODOROPOULOS, JANNIS N88-27607
THIM, HARTWIG W. N88-27433
THOMAS, G. N88-27290
THOMAS, I. N88-27542
THOMAS, I. M. N88-27332
THOMPSON, CHRIS A. N88-27399
THOMPSON, P. A. N88-27313
THOREN, S. J. N88-27483
THORNTON, EARL A. N88-27606
TIBBING, MIKAEL N88-27245
TIEGS, T. N. N88-27241
TIEN, JOHN K. N88-27264
TISHKOFF, JULIAN N88-27470
TITRAN, ROBERT H. N88-27310
TIWARI, S. N. N88-27490
TOMLINSON, J. J. N88-27625
TONDA, RICHARD DALE N88-27240
TOROK, J. S. N88-27898
TRACY, C. E. N88-27630
TRAN, TIEN N. N88-27381
TRENBERTH, K. E. N88-27668
TRINQUECOSTE, M. N88-27252
TRIVEDI, K. S. N88-27800
TRIZNA, DENNIS B. N88-27412
TROUSSE, BRIGITTE N88-27223
N88-27791
TRUONG, TRIEU-KIE N88-27220
TSAKNAKIS, HARALAMPOS N88-27874
TSUJI, SHUNJI N88-27915
TSVETKOV, D. YU. N88-27962
TURCHI, P. E. A. N88-27939
TURKEL, E. N88-27485
TURTLE, JOHN P. N88-27405
TUTTLE, B. A. N88-27438
TWARDY, HARALD N88-27345

U

UDALOV, SERGEI N88-27180
UEDA, TAKASUMI N88-27395
UEHARA, KAZUYA N88-27915
UESUGI, YOSHIHIKO N88-27914
UHERKA, K. L. N88-27639
UNLU, ISMAIL N88-27775
USENKO, A. S. N88-27916
N88-27917
USHER, JOHN M. N88-27382
USHIGUSA, KENKICHI N88-27915

V

V.D.POL, J. A. N88-27532
VALENTINO, JOHN N88-27314
VANDIBLE, PRETTA L. N88-27383
VANGERPEN, JON N88-27201
VANIMAN, D. T. N88-27990
VANVOORHEES, S. L. N88-27459
VANWIRT, PETER M. N88-27557
VARGA, JOSEPH C. N88-27384
VASKA, L. N88-27262
VEERS, P. S. N88-27595
N88-27671
VEMAGANTI, G. R. N88-27606
VEMURU, C. S. N88-27490
VENKATESAN, C. N88-27160
VENTURINI, E. L. N88-27934
VERMA, T. N88-27270
VERMOREL, JACQUES N88-27878
VICKERS, BRIAN D. N88-27235
VIG, JOHN R. N88-27443
VINCENT, BENOIT N88-27199
VOGEL, GERARD N. N88-27403
VOIGT, J. A. N88-27438
VOLZ, R. A. N88-27776
VORONOV, A. A. N88-27863
N88-27864
VOSS, HENRY D. N88-27221
VOSS, RALPH N88-27880

W

WACHS, A. L. N88-27939
WADE, JAMES W. N88-27385
WAHLSTRAND, KARNA N88-27997
WALKER, I. J. N88-27677
WALL, M. A. N88-27298
WALTON, O. R. N88-27506
WANG, BING N88-27314
WANG, DAUCHUNG N88-27788
WANG, K. C. N88-27522
WANG, W. C. N88-27673
WARMBRODT, WILLIAM N88-27159
WARNECKE, PETER N88-27466
WASYNCZUK, O. N88-27635
WATERS, RICHARD C. N88-27768
N88-27769
WATSON, R. W. N88-27805
WATT, DAVID WILSON N88-27521
WATTS, E. J. N88-27400
WEAVER, D. P. N88-27475
WEBER, ROBERT A. N88-27285
WEFEL, JOHN P. N88-27994
WEI, R. P. N88-27605
WEIKARD, HELMUT N88-27890
WEINBERG, H. N88-27694
N88-27695
WEISBIN, C. R. N88-27554
WEISS, MARC S. N88-27708
WEISSMAN, J. N88-27723
WELCH, MICHAEL N88-27728
WELSH, P. E. N88-27621
WENGER, C. B. N88-27732
WERLE, H. N88-27170
WERNER, U. N88-27259
WERT, JOHN A. N88-27284
WESSEL, JOHN E. N88-27933
WESSENDORF, KURT O. N88-27545
WESTHOFF, RANDALL F. N88-27386
WETJEN, PETER N88-27253
WHARMBY, R. N. N88-27555
WHITE, C. L. N88-27301
WHITE, D. R. N88-27666
WHITEHEAD, R. E. N88-27480
WHITHAM, G. B. N88-27820
WHITTAKER, J. W. N88-27528
N88-27575
WHITTUM, D. H. N88-27549
WICHNER, R. P. N88-27965
WICKENS, CHRISTOPHER D. N88-27696
WIEDEMANN, MARTIN N88-27842
WIELICKI, B. A. N88-27677
WILCOXON, J. P. N88-27328
WILDER, J. N88-27542
WILDIN, M. W. N88-27496
WILKERSON, TERRI N88-27387
WILLE, L. T. N88-27940
WILLIAMS, ELLEN D. N88-27263
WILLIAMS, KENNETH E. N88-27196
WILLIAMS, L. C. N88-27758
WILLIAMS, L. E. N88-27634
WILLIAMS, M. D. N88-27670
WILLIAMS, R. D. N88-27772
WILLIAMSON, DAVID T. N88-27753
WILLIAMSON, R. L. N88-27289
WILLIAMSON, W. N88-27894
WILLIS, B. T. M. N88-27260
WILLSON, V. P. N88-27350
WILSON, D. G. N88-27277
WILSON, G. N88-27712
WILSON, GLENN N88-27704
WILSON, JAMES F. N88-27556
WIMER, WILLIAM W. N88-27347
WINTERSTEIN, S. R. N88-27595
WISE, M. B. N88-27272
WITT, S. N. N88-27934
WITTEN, A. J. N88-27207
WITTUM, GABRIEL N88-27509
WOJCIESZEK, OLGA N88-27336
WOLD, A. N88-27930
WOLF, D. N88-27305
WOLOSHYN, R. M. N88-27963
WOOD, CHARLES D. N88-27559
WOOTEN, LEWIS N88-27181
WRIGHT, BERNARD R. N88-27347
WRIGHT, JAMES N88-27728
WRIGHT, NICOLA A. N88-27668
WU, D. Q. N88-27328
WU, P. N88-27930
WU, STEPHEN N88-27445
WU, Y. N88-27835
WU, Y. H. N88-27828
WYATT, F. V. N88-27189

WYLIE, DONALD P. N88-27667

Y

YAJNIK, S. N88-27331
YAKIMENKO, I. P. N88-27916
N88-27917
YAMANAKA, M. N88-27628
YAMAUCHI, TOSHIHIKO N88-27897
YANAGISAWA, ICHIRO N88-27914
YANG, RU N88-27502
YANG, ZHENG N88-27235
YASUNAGA, SEIJI N88-27391
YATES, E. CARSON, JR. N88-27193
YEE, J. H. N88-27457
YEH, G. T. N88-27816
YEH, KUNG-WEI N88-27649
YEN, JING G. N88-27161
YIN, SHENG K. N88-27161
YOON, K. J. N88-27242
YOSHIHARA, H. N88-27627
YOSHIZAKI, KIYOSHI N88-27392
YOUNG, D. F. N88-27677
YOUNG, L. N88-27318

Z

ZAGORODNIJ, A. G. N88-27916
N88-27917
ZAMAN, AFROZ A. N88-27424
ZANNER, F. J. N88-27289
ZECK, GEORGE N88-27195
ZEITLIN, G. M. N88-27706
ZENCIRCI, NEJAT N88-27959
ZEREGA, A. M. N88-27977
ZHAO, L. C. N88-27835
N88-27853
ZHIDKOV, P. E. N88-27867
ZIELINSKI, ALEX N88-27217
ZILANI, M. N88-27640
ZIRILLI, FRANCESCO N88-27827
ZNOJIL, M. N88-27837
N88-27866

Typical Corporate Source Index Listing

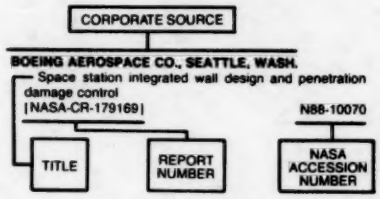

Listings in this index are arranged alphabetically by corporate source. The title of the document provides the user with a brief description of the subject matter. The report number helps to indicate the type of document cited (e.g., NASA report, translation, NASA contractor report). The NASA accession number denotes the number by which the citation is identified. The titles are arranged under each corporate source in ascending accession number order.

A

ACADEMY OF SCIENCES OF THE UKRAINIAN SSR, KHARKOV.
Experimental investigation of simplest inhomogeneities in cylindrical slit line
[DE88-702388] N88-27418
Effect of high-amplitude high-frequency current on non-isothermal equilibrium of NS-boundary in inhomogeneous superconductor
[DE88-701682] N88-27922

ACADEMY OF SCIENCES OF THE UKRAINIAN SSR, KIEV.
Equilibrium distribution functions for limited plasma-molecular systems
[DE88-702412] N88-27916
Electromagnetic wave incoherent reflection by a half-space of weakly-ionized plasma with an absorbing boundary
[DE88-702413] N88-27917
On plasma stability under anisotropic random electric field influence
[DE88-702422] N88-27918
Interpretation of the polarimetric observations of Jupiter
[DE88-702414] N88-27991
Polarization of light reflected by vertically inhomogeneous planetary atmosphere
[DE88-702416] N88-27992
Magnetohydrodynamic wave propagation in the solar wind
[DE88-702411] N88-27995

ADVANCED DECISION SYSTEMS, MOUNTAIN VIEW, CALIF.
Linear feature extraction from radar imagery. Phase 2: Base contract report
[AD-A192828] N88-27404

ADVANCED ROTORCRAFT TECHNOLOGY, INC., MOUNTAIN VIEW, CALIF.
Dynamic modelling and estimation of the error due to asynchronism in a redundant asynchronous multiprocessor system
[NASA-CR-177427] N88-27205

ADVISORY GROUP FOR AEROSPACE RESEARCH AND DEVELOPMENT, NEUILLY-SUR-SEINE (FRANCE).
Aerospace applications studies, 1971-1987
[AGARD-R-759] N88-27147
Design manual for impact damage tolerant aircraft structure, addendum
[AGARD-AG-238-ADD] N88-27185
AGARD standard aeroelastic configurations for dynamic response. 1: Wing 445.6
[AGARD-R-765] N88-27193
Air-to-air radar flight testing
[AGARD-AG-300-VOL-7] N88-27406
Aerodynamics of Hypersonic Lifting Vehicles: Fluid Dynamics Panel AGARD Symposium
[AGARD-AR-246] N88-27480
Flight testing under extreme environmental conditions
[AGARD-AG-300-VOL-8] N88-27525
Atmospheric turbulence research at DFVLR
[AGARD-R-752] N88-27689
Electric and Magnetic Activity of the Central Nervous System: Research and Clinical Applications in Aerospace Medicine
[AGARD-CP-432] N88-27683

AEROJET TECHSYSTEMS CO., SACRAMENTO, CALIF.
Carbon deposition model for oxygen-hydrocarbon combustion, volume 1
[NASA-CR-179375] N88-27254
Carbon deposition model for oxygen-hydrocarbon combustion, volume 2
[NASA-CR-179376] N88-27255

AEROSPACE CORP., EL SEGUNDO, CALIF.
The two isotropic asymptotes of fiber composites
[AD-A192305] N88-27231
Analysis of transverse strength of composites using percolation theory
[AD-A193204] N88-27234
Analysis of debris from accelerated life test of the Hughes five-year Vuilleumier cryocooler
[AD-A193101] N88-27400
NDP (Neutron Depth Profiling) evaluations of boron-implanted compound semiconductors
[AD-A192306] N88-27425
Picosecond optoelectronic sampling of electrical waveforms produced by an optically excited field effect transistor
[AD-A192384] N88-27428
Results from life test in progress on eagle-picher nickel cadmium cells
[AD-A192816] N88-27434
Perfluoropolyalkylether lubricants under boundary conditions: Iron catalysis of lubricant degradation
[AD-A193241] N88-27560
Solar cell modeling and simulation
[AD-A193249] N88-27620
Field-aligned structure of the storm time Pc 5 wave of November 14-15, 1979
[AD-A193022] N88-27653
The low-latitude auroral boundary: Steady-state and time-dependent representations
[AD-A193200] N88-27656
A three-dimensional model of the gas-cell atomic frequency standard
[AD-A193218] N88-27868
Schottky-barrier formation on a covalent semiconductor without Fermi-level pinning: The Metal-MoS2(0001) interface
[AD-A193044] N88-27931
Picosecond transient reflectivity of unpinned gallium arsenide (100) surfaces
[AD-A193242] N88-27933
Paramagnetic point defects in boron-implanted HgO.7CdO.3Te
[AD-A193276] N88-27934

AEROSPACE MEDICAL RESEARCH LABS., WRIGHT-PATTERSON AFB, OHIO.
Fighter pilot performance during airborne and simulator missions: Physiological comparisons N88-27704
Motion evoked vestibular potentials N88-27712
Engineering data compendium. Human perception and performance. User's guide
[LC-87-19580] N88-27749

AIR COMMAND AND STAFF COLL., MAXWELL AFB, ALA.
Ejection situations in the U-2/TR-1: An analysis of emotions and events
[AD-A192872] N88-27175
Pilot report: AFTI (Advanced Fighter Technology Integration) F-111
[AD-A192937] N88-27184
Use of optical disk technology at the Air Command and Staff College
[AD-A192424] N88-27969

AIR FORCE AVIONICS LAB., WRIGHT-PATTERSON AFB, OHIO.
Nozzle lip effects on gas expansion into the plume backflow region
[AD-A192806] N88-27475

AIR FORCE GEOPHYSICS LAB., HANSCOM AFB, MASS.
Scaling laws for geomagnetic tail current sheet acceleration
[AD-A193379] N88-27659

AIR FORCE HUMAN RESOURCES LAB., BROOKS AFB, TEX.
Personality, attitudes, and pilot training performance: Preliminary analysis
[AD-A193102] N88-27746

AIR FORCE INST. OF TECH., WRIGHT-PATTERSON AFB, OHIO.
Three-dimensional scene analysis using stereo based imaging
[AD-A193120] N88-27178
Development of a hybrid simulator for robotic manipulators
[AD-A193119] N88-27557
Image processing using a parallel architecture
[AD-A192833] N88-27803

AIR FORCE LOGISTICS COMMAND, WRIGHT-PATTERSON AFB, OHIO.
Computation of ECM (Electronic Counter-Measures) war reserve materiel spare requirements
[AD-A193301] N88-27195
The assessment of human/computer performance using human productivity measures: MIPS and BIPS are MEGAFLOPS
[DE87-013491] N88-27750

AIR FORCE WEAPONS LAB., KIRTLAND AFB, N. MEX.
Stochastic geologic effects on near-field ground motions in alluvium
[AD-A192315] N88-27652

AIR FORCE WRIGHT AERONAUTICAL LABS., WRIGHT-PATTERSON AFB, OHIO.
Air Force technical objective document, FY89
[AD-A193110] N88-27194
Constant amplitude fatigue life data for notched and unnotched annealed Ti-6Al-4V sheet
[AD-A193420] N88-27267
Calibration of the portable wear metal analyzer
[AD-A192971] N88-27524

AKRON UNIV., OHIO.
An IETS (Inelastic Electron Tunneling Spectroscopy) study of surface reactions applicable to adhesion
[AD-A192274] N88-27261

ALABAMA UNIV., SCOTTSBORO.
Thermal stress and its effects on fine motor skill and decoding tasks N88-27369

ALLIED-SIGNAL CORP., MORRISTOWN, N.J.
A new near-infrared tunable-room temperature solid state laser La3Ga5SiO14:Cr(3+)
[DE88-011341] N88-27543

ARGONNE NATIONAL LAB., ILL.
Oxidation-erosion of metals and alloys: Models, verification, and prediction
[DE88-010016] N88-27300
Computer simulation of elastic properties of grain boundary materials
[DE88-011965] N88-27305
Thermal conductivity and thermal expansion of stainless steels D9 and HT9
[DE88-011973] N88-27306
Post-test observations on CSPL (Chloride Silent Power Limited) cells
[DE88-011975] N88-27461
Monolithic fuel cells
[DE88-012004] N88-27638
Magnetic heat pumps
[DE88-012058] N88-27639
Superconducting properties of LaBa2Cu3O(sub x) and YBa2Cu3O(sub y)
[DE88-012038] N88-27952
Ceramic fabrication technology for high-T(sub)c materials
[DE88-012060] N88-27953

ARIZONA STATE UNIV., TEMPE.
Heat and mass transfer in laminar wavy film absorption with the presence of non-absorbable gases N88-27502
Periodic oscillations in nonlinear mechanical systems N88-27599
Prediction of deep levels and equilibrium concentrations of defects in semiconductors N88-27945
ARMY AEROMECHANICS LAB., MOFFETT FIELD, CALIF.
A comparison of the various helicopter mathematical models used in the methodology assessment N88-27149
Effects of static equilibrium and higher-order nonlinearities on rotor blade stability in hover N88-27157
ARMY AEROMEDICAL RESEARCH LAB., FORT RUCKER, ALA.
Simulator sickness in the AH-64 Apache combat mission simulator
[AD-A193419] N88-27739
ARMY AEROSTRUCTURES DIRECTORATE, HAMPTON, VA.
A comparison of theory and experiment for coupled rotor body stability of a bearingless rotor model in hover and forward flight N88-27154
A comparison of theory and flight test of the BO 105/BMR in hover and forward flight N88-27155
ARMY ARMAMENT RESEARCH AND DEVELOPMENT COMMAND, WATERVLIET, N. Y.
Ultrasonic studies of stresses and plastic deformation in steel during tension and compression
[AD-A192308] N88-27280
ARMY AVIATION RESEARCH AND DEVELOPMENT COMMAND, CLEVELAND, OHIO.
Documentation of the Benson Diesel Engine Simulation Program
[NASA-TM-100940] N88-27201
ARMY AVIATION SYSTEMS COMMAND, MOFFETT FIELD, CALIF.
Integrated Technology Rotor Methodology Assessment Workshop
[NASA-CP-10007] N88-27148
A comparison of theory and experiment for aeroelastic stability of a hingeless rotor model in hover N88-27150
A comparison of theory and experiment for coupled rotor-body stability of a hingeless rotor model in hover under simulated vacuum conditions N88-27151
A comparison of theory and experiment for coupled rotor-body stability of a hingeless rotor model in hover N88-27152
A comparison of theory and experiment for the aeroelastic stability of a bearingless model rotor in hover N88-27153
ARMY AVIATION SYSTEMS COMMAND, ST. LOUIS, MO.
Sources and nature of cost analysis data base reference manual
[AD-A193099] N88-27976
ARMY CONSTRUCTION ENGINEERING RESEARCH LAB., CHAMPAIGN, ILL.
Evaluation of explosive bonding for patching aluminum with aluminum
[AD-A193303] N88-27285
ARMY ENGINEER TOPOGRAPHIC LABS., FORT BELVOIR, VA.
Methods of determining playa surface conditions using remote sensing
[AD-A192663] N88-27612
Army space systems for terrestrial applications
[AD-A192735] N88-27613
Analysis of remotely sensed imagery using digital morphology
[AD-A192736] N88-27614
An empirical surface temperature model
[AD-A192737] N88-27665
ARMY ENGINEER WATERWAYS EXPERIMENT STATION, VICKSBURG, MISS.
IEMIS (Integrated Emergency Management Information System) floodplain mapping based on a LIDAR derived data set
[AD-A193071] N88-27616
ARMY LAB. COMMAND, FORT MONMOUTH, N.J.
Quartz crystal resonators and oscillators for frequency control and timing applications
[AD-A193310] N88-27443
ARMY RESEARCH INST. OF ENVIRONMENTAL MEDICINE, NATICK, MASS.
Hypothalamic-pituitary-adrenal responses to short duration high intensity cycle exercise
[AD-A192597] N88-27727
Metabolic and cardiorespiratory parameters during three consecutive days of exhaustive running
[AD-A192598] N88-27728
Validation of a modified one-step rebreathing technique for measuring exercise cardiac output
[AD-A192600] N88-27729
A resistive-film based force transducer for the study of exercise
[AD-A192601] N88-27730
Hyperthermia: New thoughts on an old problem
[AD-A192602] N88-27731
Physiological responses to acute exercise-heat stress
[AD-A192606] N88-27732
Validation of a modified one-step rebreathing technique for non-invasive measurement of submaximal cardiac output
[AD-A192852] N88-27735
Using IMSL mathematical and statistical computer subroutines in physiological and biomechanical research
[AD-A192594] N88-27765
ARMY TANK-AUTOMOTIVE COMMAND, WARREN, MICH.
The 210-HP diesel engine endurance and performance testing with fire resistant diesel fuel
[AD-A193153] N88-27558
ARMY WAR COLL., CARLISLE BARRACKS, PA.
Future SDI (Strategic Defense Initiative) decision making
[AD-A192794] N88-27860
ATMOSPHERIC AND ENVIRONMENTAL RESEARCH, INC., CAMBRIDGE, MASS.
Surface energy balance of three general circulation models: Current climate and response to increasing atmospheric CO2
[DE88-010967] N88-27673
AUBURN UNIV., ALA.
Improving the performance of AI algorithms
[AD-A192848] N88-27809
AVCO LYCOMING ENGINE GROUP, STRATFORD, CONN.
T55-L-714 engine development and qualification. Engine M11 low cycle fatigue test report. (0213-005-87)
[AD-A192765] N88-27197
T55-l-714 engine development and qualification. Engine M11 low cycle fatigue test report. (0213-005-87), volume 2, part 1
[AD-A192766] N88-27198
AXIOMATIX, LOS ANGELES, CALIF.
Spacecraft applications of advanced global positioning system technology
[NASA-CR-172055] N88-27180

B

BALLISTIC RESEARCH LABS., ABERDEEN PROVING GROUND, MD.
An interferometric measurement technique for railgun structures
[AD-A192851] N88-27217
BATTELLE COLUMBUS LABS., OHIO.
Studies of dynamic contact of ceramics and alloys for advanced heat engines
[DE88-008996] N88-27324
Hydrocarbon fuel spill dispersion on water: Literature review
[AD-A192486] N88-27346
BATTELLE MEMORIAL INST., COLUMBUS, OHIO.
Development of automatic names placement software
[AD-A192786] N88-27770
BEN GURION UNIV. OF THE NEGEV, BEERSHEVA (ISRAEL).
Experimental investigation of the reflection of a planar shock wave over a double wedge
[AD-A193078] N88-27482
BERKELEY RESEARCH ASSOCIATES, INC., CALIF.
Initial electron distributions for free-electron lasers generated by injector and accelerator simulations
[DE88-007022] N88-27540
Research on ocean forecasting and nonlinear wave propagation and numerical hydrodynamics in the ocean
[AD-A193363] N88-27680
BETTIS ATOMIC POWER LAB., WEST MIFFLIN, PA.
TRANSL: A PATRAN translator subroutine library
[DE88-010976] N88-27784
BODENSEEWERK GERAETETECHNIK G.M.B.H., UEBERLINGEN (WEST GERMANY).
Computer system for the primary fly-by-wire control of civil transport aircraft (experimental system)
[FBW-TB-2086/88] N88-27204
BOLT, BERANEK, AND NEWMAN, INC., CAMBRIDGE, MASS.
Theory of sound production by vortex-airfoil interaction
[AD-A193386] N88-27875
The influence of surface rounding on trailing edge noise
[AD-A193387] N88-27876
BONN UNIV. (WEST GERMANY).
FORTRAN programs for computation of time dependent sea levels and trajectory errors from satellite altimeter data
[BONN-MITT-73] N88-27216
Surface photometric investigations for spiral galaxies of large dimension structures in edge-on gemetry
[ETN-88-92126] N88-27985
BORDEAUX 1 UNIV., TALENCE (FRANCE).
Use of microwave measuring systems for the nondestructive control of resins and composites
[SNIAS-881-430-123] N88-27576
BOSTON UNIV., MASS.
The VITE model: A neutral command circuit for a generating arm and articulator trajectories
[AD-A192715] N88-27734
Content-addressable memory storage by neural networks: A general model and global Liapunov method
[AD-A192716] N88-27807
Neural network research: A personal perspective
[AD-A192717] N88-27808
BROOKHAVEN NATIONAL LAB., UPTON, N. Y.
Ionic conductive polymers based on crosslinked elastic siloxane-ethylene oxide copolymers
[DE88-011243] N88-27311
Multiphoton ionization of alkaline earth atoms in an intense laser field
[DE88-008078] N88-27884
BROWN UNIV., PROVIDENCE, R. I.
Methods of quantifying and enhancing reactive oxygen species production N88-27357
Feedback control of a hyperbolic partial-differential equation with viscoelastic damping
[AD-A192896] N88-27810
A Wong-Zakai type theorem for certain discontinuous semimartingales
[AD-A192713] N88-27822
Approximations of stochastic equations driven by predictable processes
[AD-A192714] N88-27823
Approximations and optimal control for the pathwise average cost per unit time and discounted problems for wideband noise driven systems
[AD-A192712] N88-27847
Growth and characterization of CuGaS2, CuAlS2 and CuGa0.9Al0.1S2 single crystals
[AD-A192963] N88-27930
BUNDESMINISTERIUM FUER FORSCHUNG UND TECHNOLOGIE, BONN (WEST GERMANY).
Materials research, superconductor and thin layer technology
[REPT-50/87] N88-27955
BURDEN NEUROLOGICAL INST., BRISTOL (ENGLAND).
Event-related and steady potential changes in the brain related to workload during tracking N88-27705

C

CALIFORNIA INST. OF TECH., PASADENA.
Research in applied mathematics
[AD-A192385] N88-27820
Paramagnetic point defects in boron-implanted HgO.7CdO.3Te
[AD-A193276] N88-27934
CALIFORNIA UNIV., BERKELEY.
Numerical optimization, system theoretic and software tools for the integrated design of flexible structures and their control systems
[AD-A192927] N88-27183
Theoretical predictions of precipitate shapes in cubic alloys
[DE88-010856] N88-27291
Effects of low reflection on the collector and source sheaths of a finite ion temperature plasma
[DE88-008929] N88-27908
CALIFORNIA UNIV., BERKELEY. LAWRENCE BERKELEY LAB.
A method for determining the solubility of hydrogen in molten aluminum-lithium alloys
[DE88-009807] N88-27270
Development of high strength and toughness microcomposite HSLA Fe/Cr/Mn/C steel with and without Nb
[DE88-009813] N88-27290
Theoretical predictions of precipitate shapes in cubic alloys
[DE88-010856] N88-27291
Effects of near interfacial microstructure on toughness and subcritical crack growth in ceramic/metal systems
[DE88-009842] N88-27325
Application of controlled interfacial pore structures to kinetic studies in alumina
[DE88-010884] N88-27326
Improved adhesion for SiO2 particles in silica substrates using helium-ion irradiation
[DE88-008915] N88-27332
Estimation of power-energy plots for secondary batteries
[DE88-011922] N88-27460

Higher order vortex methods with rezoning
[DE88-010777] N88-27505
Transverse resistive wall instability in a high-power, short-wavelength free-electron laser
[DE88-011730] N88-27549
Structure and function of the manganese complex involved in photosynthetic oxygen evolution determined by X-ray adsorption spectroscopy and electron paramagnetic resonance spectroscopy
[DE88-010360] N88-27725
Thermodynamics of oxygen-vacancy ordering in YBa2Cu3O(sub z)
[DE88-009816] N88-27940
Deep level defects in semiconductors: Stress and pressure studies
[DE88-010855] N88-27948
Properties of new low dimensional materials and mechanisms of high T(sub c) superconductivity
[DE88-012026] N88-27951

CALIFORNIA UNIV., DAVIS.
Enhancement of modeling and image generation techniques for high-resolution 3-dimensional imagery
[DE88-008923] N88-27782
Matrix substructuring, domain decomposition and particle methods: Current trends for solving PDEs in parallel
[DE88-009826] N88-27836

CALIFORNIA UNIV., LOS ANGELES.
Comparison of experimental coupled helicopter rotor/body stability results with a simple analytical model N88-27160
Effect of the matrix on the creep-behavior of carbon-carbon composite
[AD-A193211] N88-27235
A study of the interaction of diffusion flames with a vortex pair flowfield N88-27258
Preparation and properties of new inorganic glasses and gel-derived solids
[AD-A192922] N88-27315
The robust tracking control of nonlinear systems with uncertain dynamics N88-27788
Ion Bernstein modes in current-carrying plasmas N88-27903
Heating efficiency of beat wave excitation in a density gradient
[AD-A193066] N88-27905

CALIFORNIA UNIV., RIVERSIDE.
Measuring dispersion effects of factors in factorial experiments
[AD-A193216] N88-27831

CALIFORNIA UNIV., SANTA CRUZ.
Applications of differential geometry to the shape analysis of gray-value images N88-27358

CAMBRIDGE RESEARCH AND INSTRUMENTATION, INC., MASS.
Measurement of macroscopic electric fields in solar plasma structures
[AD-A193291] N88-27993

CAMBRIDGE UNIV. (ENGLAND).
Deformation, fracture and explosive properties of reactive materials
[AD-A193080] N88-27348
Basic mechanisms of diesel lubrication correlation of bench and engine tests
[AD-A193360] N88-27561

CARNEGIE-MELLON UNIV., PITTSBURGH, PA.
Formation of metastable structures and amorphous phases in Cu-W alloys using the triod sputtering technique
[DE88-009051] N88-27296
Size effects in linear elastic fracture mechanics N88-27609

CASE WESTERN RESERVE UNIV., CLEVELAND, OHIO.
An assessment of index term ranking N88-27974

CENTRAL ELECTRICITY GENERATING BOARD, SOUTHAMPTON (ENGLAND).
Distribution of weld quality in thin section stainless steel tube attachment welds
[PB88-109632] N88-27555

CENTRE D'ETUDES ET DE RECHERCHES DE MEDECINE AEROSPATIALE, PARIS (FRANCE).
An approach to studying the effects of psychostimulants on cerebral electrical activity in the non-human primate N88-27716

CENTRE NATIONAL D'ETUDES SPATIALES, TOULOUSE (FRANCE).
History of manned spaceflight
[CNES-NT-121] N88-28000

CENTRO BRASILEIRO DE PESQUISAS FISICAS, RIO DE JANEIRO.
Discrete variational methods and their application to electronic structures
[DE88-702215] N88-27888
Meaning of energy diagrams used to describe hetero-structures
[DE88-702219] N88-27943

CHLORIDE SILENT POWER LTD., RUNCORN (ENGLAND).
Effect of thermal cycling on CSPL (Chloride Silent Power Ltd.) sodium/sulfur cells
[DE88-011205] N88-27455

CHRYSLER CORP., NEW ORLEANS, LA.
Space shuttle phase B wind tunnel model and test information. Volume 2: Orbiter configuration
[NASA-CR-178415-VOL-2-PT-2] N88-27172

CINCINNATI UNIV., OHIO.
Optical interconnections for digital image coding N88-27381

CITY COLL. OF THE CITY UNIV. OF NEW YORK.
Ultrafast physics in semiconductor microstructures
[AD-A193300] N88-27936

CITY UNIV. OF NEW YORK, N.Y.
A study of a meteor burst communication system N88-27421

CLARKSON UNIV., POTSDAM, N.Y.
Catalytic activation of carbon dioxide by metal complexes
[AD-A192310] N88-27262

CLEMSON UNIV., S.C.
An experimental and analytical evaluation of a biaxial test for determining shear properties of composite materials
[NASA-CR-182928] N88-27593
Self-energies and the interactions of particles with surfaces
[DE88-010451] N88-27885

COLOGNE UNIV. (WEST GERMANY).
Time-dependent thermal convection of Earth mantle and double diffusive convection in magma chambers
[MITT-52] N88-27663

COLORADO COLL., COLORADO SPRINGS.
Atmospheric nitrogen oxides: Their detection and chemistry
[PB88-193057] N88-27642

COLORADO STATE UNIV., FORT COLLINS.
Device physics related to the granular nature of CuInSe2 solar cells
[DE88-001159] N88-27622

COLORADO UNIV., BOULDER.
Control and use of unsteady flows: Insect use of various wing kinematics and related pressure measurements using a pitching airfoil N88-27366
ECC (Electrochemical Concentration Cell) ozonesonde observations at South Pole, Antarctica during 1987
[PB88-202015] N88-27644
Parallel quasi-Newton methods for unconstrained optimization
[AD-A193250] N88-27812

COLUMBIA UNIV., NEW YORK, N.Y.
A fundamental understanding of the interfacial compatibility in hybrid material systems
[AD-A192921] N88-27264

COMMISSION OF THE EUROPEAN COMMUNITIES (LUXEMBOURG).
Control, stability and filter for a discrete linear stochastic system with correlated noise
[PB88-109525] N88-27818

COMMUNICATIONS SATELLITE CORP., CLARKSBURG, MD.
Recent developments in nickel hydrogen technology
[DE88-011248] N88-27456

COMPUTER SCIENCES CORP., HUNTSVILLE, ALA.
Space shuttle natural environment analysis
[NASA-CR-179337] N88-27676

CONNECTICUT UNIV., STORRS.
Interfacial tension of immiscible polymer blends: Temperature and molecular weight dependence
[AD-A192463] N88-27312
Rubber-modified epoxies: Interfacial tension and morphology
[AD-A192464] N88-27313

CONSIGLIO NAZIONALE DELLE RICERCHE, ROME (ITALY).
Squid instrumentation for neuromagnetic study of complex brain activity N88-27691
Electric and magnetic brain activity related to cognitive performance N88-27692

CONSTRUCCIONES AERONAUTICAS S.A., MADRID (SPAIN).
Determination of the glass transition temperature of cured composite materials
[DT-87/62-R] N88-27246
Design and implementation of contact ultrasonic sensors to assess internal damage
[I-177/87] N88-27247
Factors affecting strength in composite materials used for aircraft
[DT-212/87] N88-27248
Stress corrosion of C ring specimen in salt spray tests
[I-186/87] N88-27307

CORNELL UNIV., ITHACA, N.Y.
Numerical experiments on turbulent mixing
[AD-A192572] N88-27473
Effects of numerical dissipation on finite-volume solutions of compressible flow problems
[AD-A193173] N88-27485
Kinetic theory for plane flows of rough, inelastic, circular disks N88-27499
Retrieval of temperature and concentration profiles from a limited number of absorption measurements N88-27501
Simulation and analysis of wave propagation through random media N88-27503
A study of tunneling phenomena in gallium arsenide-aluminum gallium arsenide heterostructures N88-27946
Topics in quasicrystallography N88-27947
Some stability criteria in fluid and solid mechanics N88-27966

D

DALHOUSIE UNIV., HALIFAX (NOVA SCOTIA).
Dissecting the visual and auditory pathways by means of the two-input technique N88-27690
Relation between VEP and visual function in lesions of the optic nerve and visual pathway N88-27718

DAYTON UNIV., OHIO.
Aircraft refueling demonstrator using a microbot alpha 2 robot N88-27367

DEFENCE AND CIVIL INST. OF ENVIRONMENTAL MEDICINE, DOWNSVIEW (ONTARIO).
The effect of endogenous alpha on hemispheric asymmetries and the relationship of frontal theta to sustained attention N88-27701
Psychophysiological measures of drowsiness as estimators of mental fatigue and performance degradation during sleep deprivation N88-27702
The effect of mild hypoxia on the vestibular evoked response N88-27713

DEFENCE RESEARCH ESTABLISHMENT, OTTAWA. (ONTARIO).
Automatic omega station and LOP (Line Of Position) selection
[AD-A193302] N88-27179

DEFENCE RESEARCH ESTABLISHMENT SUFFIELD, RALSTON (ALBERTA).
In-flight load measurements of the Robot-X canards
[AD-A193428] N88-27187

DELAWARE UNIV., NEWARK.
NDE performance in predicting failure strength of spherical composite specimens with implanted flaws
[DE88-008223] N88-27575
Low-band-gap, amorphous-silicon-based alloys by photochemical vapor deposition
[DE88-001165] N88-27944

DEPARTMENT OF ENERGY, OAK RIDGE, TENN.
Photovoltaic Energy. Electricity from Sunlight: A current awareness bulletin
[DE88-008289] N88-27634

DEPARTMENT OF ENERGY, WASHINGTON, D. C.
Estimation of power-energy plots for secondary batteries
[DE88-011922] N88-27460
X-ray studies of strain, interface and impurities in semiconductors
[DE88-012460] N88-27954
Technology security, volume 1
[DE88-008612] N88-27978

DEUTSCHE FORSCHUNGS- UND VERSUCHSANSTALT FUER LUFT- UND RAUMFAHRT, BRUNSWICK (WEST GERMANY).
Robust digital model following controller for helicopters
[DFVLR-FB-88-07] N88-27203
Equipment for mass flow measurements in the low-speed wind tunnel at DFVLR in Brunswick, West Germany
[DFVLR-MITT-88-02] N88-27212
Aging of CFRP due to longterm storage in heated air
[DFVLR-FB-88-05] N88-27345
Application of the Single-Axis rate Table (SAT) of the DFVLR for the evaluation of stationary and dynamic gyro properties
[DFVLR-MITT-88-09] N88-27533
Aeroacoustic investigation on the noise from ultralight aircraft
[DFVLR-FB-88-03] N88-27879

DEUTSCHE FORSCHUNGS- UND VERSUCHSANSTALT FUER LUFT- UND RAUMFAHRT, COLOGNE (WEST GERMANY).
Wind tunnel tests of the influence of airfoil-thickness on normal force and pitching moment of two slender wings at transonic and supersonic Mach numbers
[DFVLR-FB-88-17] N88-27171

Cryogenic free jets
[DFVLR-FB-88-16] N88-27210
High technology space flight orientation program: Overview and recommendations
[ETN-88-92332] N88-27979

DEUTSCHE FORSCHUNGS- UND VERSUCHSANSTALT FUER LUFT- UND RAUMFAHRT, GOETTINGEN (WEST GERMANY).
Hybrid procedure for dynamic measurements in transonic wind tunnels: Demonstrated by pitch oscillation
[DFVLR-FB-88-19] N88-27211
Numerical simulation and stability analysis of the absolutely and convectively unstable wake
[DFVLR-FB-88-09] N88-27518
Measurement of pressure fluctuations in a resonant chamber with laser-induced iodine fluorescence
[DFVLR-FB-87-53] N88-27551
Propagation of acoustic disturbances in transonic flow fields of lifting wings
[DFVLR-FB-88-13] N88-27880

DEUTSCHE FORSCHUNGS- UND VERSUCHSANSTALT FUER LUFT- UND RAUMFAHRT, HAMBURG (WEST GERMANY).
Determinants of dual-task interference and resource theories in cognitive psychology
[DFVLR-FB-88-14] N88-27748

DEUTSCHE FORSCHUNGS- UND VERSUCHSANSTALT FUER LUFT- UND RAUMFAHRT, LAMPOLDSHAUSEN (WEST GERMANY).
Investigation of annular flow at high evaporation rates in view of liquid film cooling
[DFVLR-FB-88-08] N88-27517

DEUTSCHE FORSCHUNGS- UND VERSUCHSANSTALT FUER LUFT- UND RAUMFAHRT, OBERPFAFFENHOFEN (WEST GERMANY).
Direct simulation of stable stratified homogeneous turbulent shear flows
[DFVLR-FB-88-04] N88-27516
A hidden-surface removal algorithm for structures defined by triangular and rectangular surface patches
[DFVLR-MITT-88-03] N88-27792
Software engineering guidelines for RASP and ANDECS: Requirements and architectural design
[DFVLR-MITT-88-07] N88-27793
FORTRAN 77 implementation of abstract datatype models
[DFVLR-MITT-88-08] N88-27794
A PRELUDE (analysis and design of control systems-preliminary utilities depository). A data-based interactive system of control software, user's guid e
[DFVLR-MITT-88-12] N88-27795

DEUTSCHE FORSCHUNGS- UND VERSUCHSANSTALT FUER LUFT- UND RAUMFAHRT, STUTTGART (WEST GERMANY).
On the small signal gain of free electron lasers in the low-current regime
[DFVLR-FB-88-10] N88-27552

DREXEL UNIV., PHILADELPHIA, PA.
Intelligent Mobile Autonomous System (IMAS)
[AD-A193181] N88-27811

DU PONT DE NEMOURS (E. I.) AND CO., AIKEN, S.C.
Remote sensing of wetlands: Applications overview
[DE88-010695] N88-27618

DUKE UNIV., DURHAM, N. C.
Compliant robotic structures, part 3
[AD-A192426] N88-27556

DUNDEE UNIV. (SCOTLAND).
Alternate/modified binders for airfield pavements
[AD-A192781] N88-27206

E

ECOLE CENTRALE DE LYON (FRANCE).
Techniques and instrumentation for transient characterization of metal-insulator-semiconductor diodes. Applications to metal-insulator inP system
[ECL-87-17] N88-27959

ECOLE NATIONALE SUPERIEURE DES MINES, SAINTE-ETIENNE (FRANCE).
Preparation and characterization of ceramic materials based on Al2O3 reinforced with a ZrO2 dispersion
[ISAL-87-0041] N88-27340

ECOLE NATIONALE SUPERIEURE DES TELECOMMUNICATIONS, PARIS (FRANCE).
Activities report of the Communications Department
[ENST-88D003] N88-27401

ECOLE SUPERIEURE DE PHYSIQUE ET DE CHIMIE INDUSTRIELLES, PARIS (FRANCE).
Study of crosslinking and nonelastic mechanical properties of epoxy and PSP networks
[ETN-88-92740] N88-27337

EEG SYSTEMS LAB., SAN FRANCISCO, CALIF.
Fourth generation neurocognitive pattern analysis system N88-27686
Neurophysiological patterns of operational fatigue: Preliminary results N88-27703
Neurophysiological precursors of accurate visuomotor performance N88-27706

EIC, INC., NORWOOD, MASS.
Preparation and development of advanced battery catalysts
[AD-A193208] N88-27441

ELECTROTECHNICAL LAB., SAKURA (JAPAN).
Experimental fabrication of thin film single crystalline solar cells
[PB88-131958] N88-27627
Amorphous silicon solar cells using a metal substrate
[PB88-131941] N88-27628
Molecular beam epitaxy of GaP films on Si substrates
[PB88-131974] N88-27923
Pattern information processing and multimedia database system: Current research on multimedia information system
[PB88-131917] N88-27973

ELORET CORP., SUNNYVALE, CALIF.
Synopsis of a computer program designed to interface a personal computer with the fast data acquisition system of a time-of-flight mass spectrometer
[NASA-CR-177474] N88-27798

ENGINEERING RESEARCH ASSOCIATES, INC., VIENNA, VA.
Rules, schema and decision making
[AD-A193389] N88-27967

ENVIRONMENTAL PROTECTION AGENCY, RESEARCH TRIANGLE PARK, N.C.
Photochemical oxidant formation: Overview of current knowledge and emerging issues
[PB88-195235] N88-27647

EUROPEAN NUCLEAR ENERGY AGENCY, PARIS (FRANCE).
Vibration control of large structures
[AD-A193317] N88-27587

F

FLORIDA STATE UNIV., TALLAHASSEE.
Free boundary control of the Markov process
[AD-A192401] N88-27846

FLORIDA UNIV., GAINESVILLE.
Physiological monitoring methodology in the USAFSAM centrifuge N88-27356

FOERENADE FABRIKSVERKEN, LINKOEPING (SWEDEN).
Electromagnetic characterization and acceptance test of the EMP simulator SPERANS
[PB88-203781] N88-27416

FOERSVARETS FORSKINGSANSTALT, STOCKHOLM (SWEDEN).
Hot isostatic pressing of tungsten-nickel-iron composites
[PB88-203070] N88-27292

FONDAZIONE UGO BORDONI, ROME (ITALY).
Utilization of a satellite communication system to protect the national communication network
[FUB-33-1986] N88-27423
Approximation problems of the Hilbert transform to identify minimum phase linear systems
[FUB-42-1986] N88-27790

FOREIGN APPLIED SCIENCES ASSESSMENT CENTER, LA JOLLA, CALIF.
Soviet dynamic fracture mechanics research
[FASAC-TAR-3140] N88-27597

FORSCHUNGSINSTITUT FUER INFORMATIONSVERARBEITUNG, ETTLINGEN (WEST GERMANY).
Automatic line network extraction from aerial imagery of urban areas through knowledge based image analysis
[AD-A193067] N88-27615

G

GENERAL ATOMIC CO., SAN DIEGO, CALIF.
Studies in support of oxidation-resistant composite materials
[AD-A193320] N88-27238

GENERAL ELECTRIC CO., LARGO, FLA.
Coupling of a spark source mass spectrograph and a ND-YAG laser
[DE88-012116] N88-27530

GENERAL MOTORS RESEARCH LABS., WARREN, MICH.
Mechanism of the nitric oxide-carbon monoxide-oxygen reaction over a single crystal rhodium catalyst
[DE88-006274] N88-27268

GEORGIA INST. OF TECH., ATLANTA.
An anisotropic continuum damage model for creep-dominated, multiaxial loading histories N88-27608
Atmospheric nitrogen oxides: Their detection and chemistry
[PB88-193057] N88-27642

GESAMTHOCHSCHULE, SIEGEN (WEST GERMANY).
Laser-Doppler measurements of turbulence structures in free streams behind flat and rotation symmetrical profiles
[ETN-88-92336] N88-27510

GKSS-FORSCHUNGSZENTRUM GEESTHACHT (WEST GERMANY).
Investigations on Mie and Rayleigh scattering as basis for the development of Rayleigh temperature lidars with aid of Michelson interferometry
[GKSS-87/E/62] N88-27675

GOSUDARSTVENNYI KOMITET PO ISPOLZOVANIYU ATOMNOI ENERGII, MOSCOW (USSR).
Geometry of superconformal manifolds, part 1
[DE88-702405] N88-27863
Geometry of superconformal manifolds, part 2
[DE88-702408] N88-27864
Dynamics of a plasma produced under effect of the XeCl-laser radiation on metallic surface
[DE88-701983] N88-27902
Vortices on the world sheet and string's critical dynamics
[DE88-702116] N88-27961
To the opportunities of cluster analysis of light curves of supernovae
[DE88-701642] N88-27982
Strange, quark and metastable neutron stars
[DE88-702404] N88-27984
Is the 3C273 quasar Mach nearer
[DE88-702235] N88-27988

GOSUDARSTVENNYI KOMITET PO ISPOLZOVANIYU ATOMNOI ENERGII, OBNINSK (USSR).
Heat and mass transfer in a transport channel
[DE88-701968] N88-27493

H

HAMPTON INST., VA.
A plasma ultraviolet source for short wavelength lasers
[AD-A192844] N88-27537

HARVARD UNIV., CAMBRIDGE, MASS.
Study of energy levels and decay mechanisms for singlet Rydberg states of molecular nitrogen
[AD-A192505] N88-27886

HATFIELD POLYTECHNIC (ENGLAND).
A review of parallel methods for solving sets of linear equations and their application within optimisation algorithms
[AD-A193137] N88-27830

HELLENIC AIR FORCE GENERAL HOSPITAL, ATHENS (GREECE).
Correlation between EEG abnormal activity and aircraft accidents: A long term observation N88-27719

HIROSHIMA UNIV. (JAPAN).
Global and local magnetohydrodynamic relaxations
[DE88-752602] N88-27913

HOKENSON (GUSTAVE J.), LOS ANGELES, CALIF.
Variable Mach number wall jets for control/propulsion on hypervelocity projectiles/interceptors: Tests with an existing model
[AD-A192845] N88-27167

HORDT RESEARCH, DEVELOPMENT AND THERAPY, RODGAU (WEST GERMANY).
Measurement and classification of the mode of action of antidepressant drugs N88-27714

HOUSTON UNIV., TEX.
The integration of decision support problems into feature modeling based design N88-27372
Probing the electronic and defect structure of perovskite superconductors
[DE88-008349] N88-27939

HUGHES HELICOPTERS, CULVER CITY, CALIF.
Aeroelastic characteristics of the AH-64 bearingless tail rotor N88-27162

I

IIT RESEARCH INST., BARTLESVILLE, OKLA.
Optimal rheological characteristics in dynamic stability of polymer flow through porous media
[DE88-001225] N88-27322

IIT RESEARCH INST., CHICAGO, ILL.
A notch filter instrument for measuring ELF (Extremely Low Frequency) MSK (Minimum Shift Keying) signals
[AD-A193324] N88-27414

ILLINOIS INST. OF TECH., CHICAGO.
Coupled experimental and theoretical investigations of instability, chaos and turbulence in an axisymmetric jet flow
[AD-A192943] N88-27476

ILLINOIS UNIV., CHAMPAIGN.
Event-related brain potentials as indices of mental workload and attentional allocation N88-27696
ILLINOIS UNIV., URBANA.
Processing and additive effects of ZrO2 on microstructure and dielectric porperties of BaTiO3 ceramics
[AD-A193126] N88-27316
Preparation and properties of high Q microwave dielectrics in the (CA, SR, BA) zirconate system
[AD-A193127] N88-27317
Slow-induced deformations in a space-based electromagnetic rail gun N88-27385
Texture perception and shape from texture
[AD-A192923] N88-27771
A taxonomy for conjugate gradient methods
[DE88-008574] N88-27817
Unified multilevel adaptive finite element methods for elliptic problems
[DE88-011938] N88-27840
ILLINOIS UNIV., URBANA-CHAMPAIGN.
A lubrication study of engine bearings N88-27574
The relationship between observed fatigue damage and life estimation models
[NASA-CR-182191] N88-27611
IMPERIAL COLL. OF SCIENCE AND TECHNOLOGY, LONDON (ENGLAND).
Photon limited image processing in the space-time domain
[AD-A193142] N88-27655
INFORMATION SYSTEMS AND TECHNOLOGY CENTER, WRIGHT-PATTERSON AFB, OHIO.
Ada (trade name) compiler validation summary report: Verdix Corporation VAda-010-03315, version 5.5 MicroVAX 2 host ISBC 386/20P Intel target
[AD-A193226] N88-27774
Ada (trade name) compiler validation summary report: Verdix corporation VAda-010-13125, version 5.41 Sun Microsystems Sun-3/160 host microbar GPC68020 target
[AD-A193415] N88-27777
INSTITUT FRANCO-ALLEMAND DE RECHERCHES, ST. LOUIS (FRANCE).
Theoretical and experimental investigations of a vortex drag behind a wing profile with spoiler
[ISL-PU-309/87] N88-27169
A numerical simulation of side force effects by aerodynamic flight trajectory correction
[ISL-CO-211/87] N88-27191
Investigations of aircraft control with jet spoilers
[ISL-R-112/87] N88-27202
Some properties of ignition gases. Review of measuring results in the years 1981-1986)
[PB88-106968] N88-27259
Acoustic propagation in the lower atmosphere
[ISL-R-126/87] N88-27878
Production of intensive electron beam impulsions by setup of pseudoglare discharges
[ISL-CO-210/87] N88-27920
INSTITUT NATIONAL DES SCIENCES APPLIQUEES, LYON (FRANCE).
Prediction of the aeroelastic behavior of tuned blades. Application to aircraft engines
[ISAL-87-0046] N88-27199
Manufacturing of a barium titanate with high dielectric coefficient by decomposition of precipitates of double oxalates
[ISAL-IDI1-88-02] N88-27278
Study of feasibility and optimization conditions of laser treatments: Application of the local recrystallization of aluminum
[ISAL-87-0048] N88-27309
INTERNATIONAL CENTRE FOR THEORETICAL PHYSICS, TRIESTE (ITALY).
Diffusion and solubility of some interstitial impurities in deformed metals
[DE88-701859] N88-27296
Superalgebras with Grassmann algebra-valued structure constants from superfields
[DE88-702239] N88-27862
High-temperature superconductivity: An overview
[DE88-702051] N88-27925
Self energy corrections to the ab initio band structures: Chromium
[DE88-701825] N88-27927
Closed string fields as parameters of extra gauge symmetry of open string field theory
[DE88-702046] N88-27960
Initial boundary value problems of nonlinear wave equations in an exterior domain
[DE88-701883] N88-27962
IOWA UNIV., IOWA CITY.
Experimental research of combustion systems N88-27371
Optimal control of the wing rock phenomenon N88-27373
Database design and menagement in engineering optimization
[AD-A193325] N88-27813
ITALIAN AIR FORCE AEROSPACE MEDICAL CENTER, ROME.
Spontaneous cerebral electrical activity during prolonged hypoglycemia: A quantitative study in humans N88-27717

J

JACKSON LAB., BAR HARBOR, MAINE.
Genetic effects of low level microwave radiation
[AD-A192687] N88-27722
JAPAN ATOMIC ENERGY RESEARCH INST., TOKYO.
Effects of electron beam irradiation on mechanical properties at low and high temperature of fiber reinforced composites using PEEK as matrix material
[DE88-753134] N88-27239
Creep behavior for Hastelloy-XR
[DE88-753428] N88-27295
Data compilation for radiation damage on ceramic insulators. Revised with updated data and reviews
[DE88-753426] N88-27329
General expression of manipulator kinematics
[DE88-753430] N88-27567
Multi-mode optical fibers for simultaneous 13-position measurements Thomson scattering apparatus in the JFT-2M tokamak
[DE88-753133] N88-27897
Design of divertor plate and measurements of double-null open divertor plasma in the JFT-2M tokamak
[DE88-753130] N88-27914
Analysis of lower hybrid current drive and rampup experiments on the JT-60 tokamak
[DE88-753136] N88-27915
JOHANN-WOLFGANG-GOETHE-UNIV., FRANKFURT AM MAIN (WEST GERMANY).
Measurement of electrical activity in the CNS with cortical evoked potentials and EEG: Efficacy profiles of drugs using factor analysis N88-27715
JOHANNES KEPLER UNIV., LINZ (AUSTRIA).
A planar IC-compatible transferred electron device for millimeter-wave operation
[AD-A192692] N88-27433
JOHNS HOPKINS UNIV., BALTIMORE, MD.
Linear programming for Air Force decision aiding N88-27378
Attachable interferometric strain gages
[AD-A192390] N88-27522
Assessing and enhancing human performance: Utility of a workstation network
[AD-A192840] N88-27743
JOHNSON CONTROLS, INC., MILWAUKEE, WIS.
Recent developments in nickel hydrogen technology
[DE88-011248] N88-27456
JOINT INST. FOR NUCLEAR RESEARCH, DUBNA (USSR).
Investigation of hydrogen isotope penetration through stainless steels Kh18N10T and Kh3M2BFR
[DE88-702189] N88-27297
Calculations of high-frequency parameters of disc-loaded waveguides
[DE88-702178] N88-27417
Mass flow rate influence on void fraction of two-phase helium flow
[DE88-702456] N88-27495
Supercomputer for parallel data analysis
[DE88-702148] N88-27759
Structure of bound states in polynomial potentials
[DE88-702437] N88-27837
Evaluation of quantum mechanics path integrals by the approximations exact on a class of polynomial functionals
[DE88-702434] N88-27865
Perturbation expansions generated by an approximate propagator
[DE88-702435] N88-27866
Cauchy problem for the nonlinear Schroedinger equation
[DE88-702454] N88-27867
Anharmonic model for high-Tc superconductors
[DE88-702196] N88-27924
Symmetry problem of energy-momentum tensor and the creation of gravitational field
[DE88-702442] N88-27964

K

KAISERSLAUTERN UNIV. (WEST GERMANY).
Fabrication of SiC fiber reinforced glass matrix by extrusion process and investigation of its mechanical properties
[ETN-88-92367] N88-27244
KANSAS STATE UNIV., MANHATTAN.
A human factors evaluation of the Advanced Visual Technology System (AVTS) eye tracking oculometer N88-27361
KANSAS UNIV., LAWRENCE.
Boundary layer solutions for the free-edge problem in composite laminates N88-27229
Demodulation processes in auditory perception
[AD-A193421] N88-27740
KARLSRUHE UNIV. (WEST GERMANY).
Computation of failure probability of fatigue loaded cracked structures
[ETN-88-92360] N88-27607
KENT STATE UNIV., OHIO.
Numerical calculations of dopent diffusion involving flashlamp heating of silicon N88-27384
KENTUCKY UNIV., LEXINGTON.
Determination of the local heat-transfer characteristics on glaze ice accretions on a cylinder and a NACA 0012 airfoil N88-27500
KERNFORSCHUNGSANLAGE, JUELICH (WEST GERMANY).
Improved procedure for impact probability computation of aircraft crash based on Balfanz model
[JUEL-SPEZ-425] N88-27176
KEURING VAN ELECTROTECHNISCHE MATERIALEN N.V., ARNHEM (NETHERLANDS).
Storage of thermal energy by means of an absorption cycle
[PB88-190814] N88-27619
KIEL UNIV. (WEST GERMANY).
Distributive iteration for indefinite systems as smoothing method in multigrid process on example of Stokes and Navier-Stokes equations with emphasis on incomplete decompositions
[ETN-88-92127] N88-27509
KIENBAUM UNTERNEHMENSBERATUNG, GUMMERSBACH (WEST GERMANY).
Economic impact of space flight activities in West Germany. Influence of allocations of Bundesministerium fuer Forschung und Technologie
[ETN-88-92106] N88-27215
KLINE (NATHAN S.) INST. FOR PSYCHIATRIC RESEARCH, ORANGEBURG, N.Y.
Normative developmental equations for the EEG and their sensitivity to neurological and psychiatric disorders N88-27687

L

LAWRENCE LIVERMORE NATIONAL LAB., CALIF.
Precise rotational alignment of X-ray transmission diffraction gratings
[DE88-010599] N88-27273
On the systematics of phase transformation in metallic alloys
[DE88-008041] N88-27288
Formation of metastable structures and amorphous phases in Cu-W alloys using the triod sputtering technique
[DE88-009051] N88-27298
Shock initiation studies on heterogeneous explosives
[DE88-008681] N88-27351
Nonlinear dynamics of the electron self-field interaction
[DE88-010597] N88-27420
A method for estimating the susceptibility of electronic systems to HPM (High Power Microwave)
[DE88-012246] N88-27422
A GaAs solid state device model for high power applications
[DE88-011320] N88-27457
The design of a digital Eprom oscillator for electrical impedance tomography
[DE88-012243] N88-27462
A fast vortex code for computing 2-D flow in a box
[DE88-011732] N88-27496
Granular flow: Particle-dynamics simulations of steady flow
[DE88-011342] N88-27506
Initial electron distributions for free-electron lasers generated by injector and accelerator simulations
[DE88-007022] N88-27540
Chemical vapor deposition of TiO2 thin films at room temperature
[DE88-008892] N88-27542
A new near-infrared tunable-room temperature solid state laser La3Ga5SiO14:Cr(3+)
[DE88-011341] N88-27543
Target designs for plasma-implosion-driven, photoionization-pumped soft X-ray lasers
[DE88-011278] N88-27547
Wave equations for pulse propagation
[DE88-011760] N88-27548

Transverse resistive wall instability in a high-power, short-wavelength free-electron laser
[DE88-011730] N88-27549
DYNA3D (Nonlinear Dynamic Analysis of Structures in Three Dimensions) user's manual
[DE88-012242] N88-27604
The assessment of human/computer performance using human productivity measures: MIPS and BIPS are MEGAFLOPS
[DE87-013491] N88-27750
A menu-driven menu editor and associated menu system
[DE88-008026] N88-27781
Enhancement of modeling and image generation techniques for high-resolution 3-dimensional imagery
[DE88-008923] N88-27782
The sub-implicit method: New multiprocessor algorithms for old implicit codes
[DE88-011345] N88-27785
Hypervelocity impact analysis with supercomputers
[DE88-008907] N88-27797
Notes on operating system requirements for the next millennium
[DE88-010712] N88-27805
Matrix substructuring, domain decomposition and particle methods: Current trends for solving PDEs in parallel
[DE88-009826] N88-27836
Staggered-grid finite element solution technique for the Maxwell's equations in the time domain
[DE88-011731] N88-27838
KRYSI, an ODE solver combining a semi-implicit Runge-Kutta method and a preconditioned Krylov method
[DE88-012245] N88-27841
Steady-state approximations in Raman excitation equations
[DE88-011759] N88-27889
Plasma behavior in the boundary layer near a railgun surface
[DE88-006889] N88-27909
Optical imaging diagnostics for fusion plasmas
[DE88-997572] N88-27910
Probing the electronic and defect structure of perovskite superconductors
[DE88-008349] N88-27939
Dynamical evolution of cosmic strings
[DE88-011724] N88-27989

LEAR SIEGLER, INC., GRAND RAPIDS, MICH.
Electrical load and power source capacity report for the C-130 aircraft Self Contained Navigation System (SCNS): LSI model 6216A, 6216B, 6216C, revision
[AD-A193079] N88-27186

LEHIGH UNIV., BETHLEHEM, PA.
Corrosion fatigue of small cracks: Mechanics and chemistry
[DE88-012121] N88-27605

LIFE SYSTEMS, INC., CLEVELAND, OHIO.
Advanced EMU electrochemically regenerable CO2 and moisture absorber module breadboard
[NASA-CR-172054] N88-27754
Vapor Compression Distillation Subsystem (VCDS) component enhancement, testing and expert fault diagnostics development, volume 2
[NASA-CR-172076] N88-27755

LOCKHEED AERONAUTICAL SYSTEMS CO., MARIETTA, GA.
An evaluation of flight path formats head-up and head-down
[NASA-CR-4176] N88-27196

LOCKHEED MISSILES AND SPACE CO., PALO ALTO, CALIF.
MAXIE-1 (Magnetospheric Atmospheric X-ray Imaging Experiment)
[AD-A192846] N88-27221

LOGISTICS MANAGEMENT INST., BETHESDA, MD.
Capitalizing on experience with intelligence gateway software
[AD-A193362] N88-27971

LOS ALAMOS NATIONAL LAB., N. MEX.
Steps toward lunar settlement
[DE88-009141] N88-27213
Investigation of the quasi-steady approach used in transient two-phase flow analysis
[DE88-004303] N88-27489
Development of a free-electron laser user facility for the extreme ultraviolet
[DE88-007892] N88-27541
Update on the meso-microscale meteorological hierarchy
[DE88-009133] N88-27670
Overview of the SDI (Strategic Defense Initiative) Program in short wavelength chemical lasers
[DE88-007912] N88-27861
Superconductor consolidation
[DE88-010938] N88-27949
The classical nova outburst
[DE88-009136] N88-27987
Uses of lunar sulfur
[DE88-009119] N88-27990

LOUISIANA STATE DEPT. OF CONSERVATION, BATON ROUGE.
An investigation of performance improvement in knowledge-based control systems N88-27382

LOUISIANA STATE UNIV., BATON ROUGE.
Solar flares and magnetospheric particles: Investigations based upon the ONR-602 and ONR-604 experiments
[AD-A193396] N88-27994

LOWELL UNIV., MASS.
Robust methods for array signal processing
[AD-A192854] N88-27871

M

MANCHESTER UNIV. (ENGLAND).
Nonaxisymmetric viscous lower branch modes in axisymmetric supersonic flows
[NASA-CR-181687] N88-27164

MARTIN CO., DENVER, COLO.
Damping characteristics of metal matrix composites
[AD-A193144] N88-27233

MARYLAND UNIV., COLLEGE PARK.
Scanning tunneling microscopy as a surface chemical probe
[AD-A192710] N88-27263
Optical guiding in the separable beam limit
[AD-A192452] N88-27534
Efficiency optimization for FEL oscillators
[AD-A192541] N88-27536
Effects of pulsed and CW (Continuous Wave) 2450 MHz radiation on transformation and chromosomes of human lymphocytes in vitro
[AD-A193104] N88-27736

MASSACHUSETTS INST. OF TECH., CAMBRIDGE.
Spatial organization of homopolymer chains inside spherical polybutadiene domains of SB diblock copolymers
[AD-A193390] N88-27321
Focused ion beam fabrication of graded channel FETs in GaAs and Si
[AD-A193098] N88-27439
Active and passive remote sensing of ice
[AD-A193307] N88-27617
Bisimulation can't be traced
[AD-A192725] N88-27766
Inspection methods in programming: Cliches and plans
[AD-A192782] N88-27767
Synchronizable series expressions. Part 2: Overview of the theory and implementation
[AD-A192783] N88-27768
The programmer's apprentice project: A research overview
[AD-A192784] N88-27769
Constructing a highly-available location service for a distributed environment
[AD-A192723] N88-27801
A modular proof of correctness for a network synchronizer
[AD-A192726] N88-27802
Parallel solutions to geometric problems on the scan model of computation
[AD-A192321] N88-27819
Finding minimum-cost circulations by successive approximation
[AD-A192724] N88-27824
Finding minimum-cost circulations by canceling negative cycles
[AD-A192727] N88-27825
Statistical description of stochastic dynamics
[AD-A192924] N88-27852
RLE progress report, January 1 to December 31, 1987
[RLE-PR-130] N88-27869

MASSACHUSETTS INST. OF TECH., LEXINGTON.
TDWR (Terminal Doppler Weather Radar) PRF (Pulse Repetition Frequency) selection criteria
[AD-A193089] N88-27407
Forced-convection, liquid-cooled, microchannel heat sinks
[AD-A193337] N88-27444
Solid state research
[AD-A192837] N88-27929

MASSACHUSETTS UNIV., AMHERST.
Soluble metal chelate polymers of coordination numbers six, seven and eight
[AD-A192485] N88-27314
Theory of the dissociation dynamics of small molecules on metal surfaces: Finite temperature studies
[DE88-007763] N88-27882

MAX-PLANCK-INST. FUER PHYSIK UND ASTROPHYSIK, GARCHING (WEST GERMANY).
Activities report of the Werner-Heisenberg Institute of Physics
[ETN-88-92946] N88-27893
Activities report of the Institute for Extraterrestrial Physics
[MPE-206] N88-27981
Gamma radiation from center of the galaxy of the order of MeV values
[MPE-207] N88-27999

MEHARRY MEDICAL COLL., NASHVILLE, TENN.
Microesotropia patients performa well as military jet pilots N88-27363

MICHIGAN STATE UNIV., EAST LANSING.
Energy distribution and transfer in flowing hydrogen microwave plasmas N88-27919

MICHIGAN TECHNOLOGICAL UNIV., HOUGHTON.
Application of Auger electron spectroscopy to the study of trace element effects on weldability
[DE88-010457] N88-27301

MICHIGAN UNIV., ANN ARBOR.
Turbulent flow field visualization with integral interferometric imaging and computed tomography N88-27521
Nuclear magnetic resonance spectrometer
[AD-A192928] N88-27523
Optimal design of viscoelastic structures N88-27579
Research into the architecture of CAD based robot vision systems
[AD-A193330] N88-27776
Investigations on the MBE (Molecular Beam Epitaxy) growth and properties of Al(sub y)Ga(sub y)In(sub 1-x-y)AsInP and InGaAs-InAlAs superlattices
[DE88-009105] N88-27941

MICROBIAL PRODUCTS, INC., FAIRFIELD, CALIF.
An outdoor test facility for the large-scale production of microalgae
[DE88-001146] N88-27723

MIDWEST RESEARCH INST., GOLDEN, COLO.
Laser-heated CVD process for depositing thin films for low-cost solar-cell applications
[DE88-001162] N88-27623
Performance sensitivities for point-focus dish systems with secondary concentrators
[DE88-001152] N88-27629
Specular steel surfaces for solar mirror substrates
[DE88-001153] N88-27630
Photovoltaic Measurements and Performance Branch
[DE88-001142] N88-27633
An outdoor test facility for the large-scale production of microalgae
[DE88-001146] N88-27723
SERI standard broadband format: A solar and meteorological data archival format
[DE88-001145] N88-27975

MIDWEST SYSTEMS RESEARCH, INC., DAYTON, OHIO.
A cockpit natural language study: Vocabulary and grammar analyses
[AD-A193289] N88-27753

MINAS GERAIS UNIV., BELO HORIZONTE (BRAZIL).
Kinetic of oxidation to air of a Fe-Al-Mn alloy system at 600-800(sup 0)C temperature range
[DE88-702309] N88-27330

MISSION RESEARCH CORP., ALEXANDRIA, VA.
Theory and simulation of relaxed plasmoids
[AD-A192884] N88-27997

MISSISSIPPI UNIV., UNIVERSITY.
Determination of radiative properties of fiberglass and foam insulations
[DE88-007845] N88-27331

MISSOURI UNIV., KANSAS CITY.
Probing the electronic and defect structure of perovskite superconductors
[DE88-008349] N88-27939

MISSOURI UNIV., ROLLA.
Investigation of expert system design approaches for electronic design environments N88-27365
Cloud simulation warm cloud experiments: Droplet growth and aerosol scavenging
[AD-A192944] N88-27666

MITSUBISHI ELECTRIC CORP., TOKYO (JAPAN).
Mitsubishi Electric Advance (R and D Edition), Volume 41
[PB88-194162] N88-27388
Basic research on optical neural computers N88-27389
Computer-Aided Engineering (CAE) for engineering design N88-27390
High-speed, precision processing using an electron beam N88-27391
Superconducting oxides with high critical temperatures N88-27392
A 1/2-inch high-definition baseband VCR N88-27393
Thermal-sensation control: A new method of controlling cooled/heated environments N88-27394

The MELCOM PSI 2 AI workstation N88-27395
The MELMUX MX-7100 series high-speed digital multiplexers N88-27396
Polarization selective Raman microspectroscopy N88-27397

MONTCLAIR STATE COLL., UPPER MONTCLAIR, N.J.
A review of workload measurement in relation to verbal comprehension N88-27360

MORTON THIOKOL, BRIGHAM CITY, UTAH.
Assembly Test Article (ATA)
[NASA-CR-179361] N88-27226

MOUND LAB., MIAMISBURG, OHIO.
Relative flow rates of explosive powders
[DE88-010767] N88-27350
Friction, wear and electrical contact resistance of precious metal alloys
[DE88-011244] N88-27450

MUENSTER UNIV. (WEST GERMANY).
Neuromagnetic evidence of place mechanisms for frequency and intensity coding in the human auditory cortex N88-27693

N

NATIONAL ACADEMY OF SCIENCES - NATIONAL RESEARCH COUNCIL, WASHINGTON, D. C.
Geothermal energy technology: Issues, R and D (Research and Development) and cooperative arrangements
[PB88-193107] N88-27626

NATIONAL AERONAUTICAL ESTABLISHMENT, OTTAWA (ONTARIO).
Analysis of experimental data for cast 10-2/DOA2 supercritical airfoil at high Reynolds numbers
[AD-A192827] N88-27166

NATIONAL AERONAUTICS AND SPACE ADMINISTRATION, WASHINGTON, D.C.
Aeronautical engineering: A continuing bibliography with indexes
[NASA-SP-7037(229)] N88-27163
Technology for large space systems: A bibliography with indexes (supplement 18)
[NASA-SP-7046(18)] N88-27214
Unified methods of accelerated laboratory tests of the preparations for temporary protection of cars
[NASA-TT-20298] N88-27336
Aerospace Medicine and Biology: A continuing bibliography with indexes (supplement 314)
[NASA-SP-7011(314)] N88-27742

NATIONAL AERONAUTICS AND SPACE ADMINISTRATION. AMES RESEARCH CENTER, MOFFETT FIELD, CALIF.
Integrated Technology Rotor Methodology Assessment Workshop
[NASA-CP-10007] N88-27148
Comparison of experimental rotor damping data-reduction techniques N88-27159
Temperature rise in superfluid helium pumps
[NASA-TM-100997] N88-27507
A documentation of two- and three-dimensional shock-separated turbulent boundary layers
[NASA-TM-101008] N88-27519

NATIONAL AERONAUTICS AND SPACE ADMINISTRATION. GODDARD SPACE FLIGHT CENTER, GREENBELT, MD.
The detection and interpretation of long-term changes in ozone from space
[NASA-TM-101135] N88-27650
Cascade model of gamma-ray bursts: Power-law and annihilation-line components
[NASA-TM-101176] N88-27998

NATIONAL AERONAUTICS AND SPACE ADMINISTRATION. LANGLEY RESEARCH CENTER, HAMPTON, VA.
Concept development of a Mach 3.0 high-speed civil transport
[NASA-TM-4058] N88-27182
FTMP data acquisition environment
[NASA-TM-100636] N88-27447
Overview and future direction for blackbody solar-pumped lasers
[NASA-TM-100621] N88-27553
Angular radiation models for Earth-atmosphere system. Volume 1: Shortwave radiation
[NASA-RP-1184] N88-27677
Publications on acoustics research at the Langley Research Center during 1980-1986
[NASA-TM-100590] N88-27881

NATIONAL AERONAUTICS AND SPACE ADMINISTRATION. LEWIS RESEARCH CENTER, CLEVELAND, OHIO.
A computational analysis of under-expanded jets in the hypersonic regime
[NASA-TM-101319] N88-27174
Experimental determination of aerodynamic damping in a three-stage transonic axial-flow compressor
[NASA-TM-100953] N88-27200
Documentation of the Benson Diesel Engine Simulation Program
[NASA-TM-100940] N88-27201
Alkaline fuel cell performance investigation
[NASA-TM-100937] N88-27267
Refractory metal alloys and composites for space power systems
[NASA-TM-100946] N88-27310
Analytical approximation of a distorted reflector surface defined by a discrete set of points
[NASA-TM-101323] N88-27424
A comparison of the radiation tolerance characteristics of multijunction solar cells with series and voltage-matched configurations
[NASA-TM-101177] N88-27624
Implementing direct, spatially isolated problems on transputer networks
[NASA-TM-101297] N88-27796
User's manual for the two-dimensional transputer graphics toolkit
[NASA-TM-100974] N88-27799
Phase 1 results from the Stirling-powered vehicle project
[NASA-TM-100978] N88-27980

NATIONAL AERONAUTICS AND SPACE ADMINISTRATION. MARSHALL SPACE FLIGHT CENTER, HUNTSVILLE, ALA.
IPS guidestar selection for stellar mode (ASTRO)
[NASA-TM-100336] N88-27181

NATIONAL AERONAUTICS AND SPACE ADMINISTRATION. PASADENA OFFICE, CALIF.
A VLSI single-chip (225,223) Reed-Solomon encoder with interleaver
[NASA-CASE-NPO-17280-1-CU] N88-27220

NATIONAL BUREAU OF STANDARDS, GAITHERSBURG, MD.
Research opportunities below 300 nm at the NBS Free-Electron Laser Facility
[AD-A193100] N88-27538

NATIONAL CENTER FOR ATMOSPHERIC RESEARCH, BOULDER, COLO.
Intercomparison of NMC (National Meteorological Center) and ECMWF (European Centre for Medium Range Weather Forecasts) global analyses: 1980-1986
[PB88-196548] N88-27668

NATIONAL HOSPITAL, OSLO (NORWAY).
A statistical procedure for the evaluation of presence/non-presence of stimulus-related EEG activity N88-27689

NATIONAL INST. OF HEALTH, BETHESDA, MD.
Vision research. A national plan: 1983-1987, 1987 evaluation and update
[PB88-192604] N88-27726

NATIONAL LAB. FOR HIGH ENERGY PHYSICS, IBARAKI (JAPAN).
Distortion functions
[DE88-752634] N88-27896

NATIONAL OCEANIC AND ATMOSPHERIC ADMINISTRATION, SEATTLE, WASH.
Beaufort sea mesoscale circulation study: Hydrography helicopter operations, April 1987
[PB88-203658] N88-27681

NATIONAL OCEANIC AND ATMOSPHERIC ADMINISTRATION, SILVER SPRING, MD.
ECC (Electrochemical Concentration Cell) ozonesonde observations at South Pole, Antarctica during 1987
[PB88-202015] N88-27644

NAVAL AEROSPACE MEDICAL RESEARCH LAB., PENSACOLA, FLA.
The neuroelectric selection of Naval aviation personnel: An evaluation N88-27707

NAVAL AIR DEVELOPMENT CENTER, WARMINSTER, PA.
Detection of acceleration (+Gz) induced blackout by matched-filtering of visual evoked potentials N88-27710

NAVAL BIODYNAMICS LAB., NEW ORLEANS, LA.
Evoked potential analysis of impact acceleration experiments N88-27708

NAVAL ENVIRONMENTAL PREDICTION RESEARCH FACILITY, MONTEREY, CALIF.
An evaluation of two millimeter wave propagation models for horizontal atmospheric attenuation at 70-115 GHZ
[AD-A192699] N88-27403

NAVAL HEALTH RESEARCH CENTER, SAN DIEGO, CALIF.
Behavioral, psychological and demographic predictors of physical fitness
[AD-A192697] N88-27733
The human element in space: Lessons from Antarctica
[AD-A193440] N88-27741

NAVAL OCEAN SYSTEMS CENTER, SAN DIEGO, CALIF.
Surface-wave model uncertainty assessment
[AD-A193094] N88-27408
MIZPAC (marginal ice zone Pacific) 84-86 CTD (Conductivity, Temperature, Depth) data report
[AD-A192478] N88-27679
Assessments of maneuverability with the TeleOperated Vehicle (TOV)
[AD-A191584] N88-27751

NAVAL POSTGRADUATE SCHOOL, MONTEREY, CALIF.
A feasibility study in path planning using optimization techniques
[AD-A193030] N88-27177
Probabilistic anisotropic failure criteria for composite materials
[AD-A193046] N88-27232
Thermomechanical processing of Al alloy 2090 for grain refinement and superplasticity
[AD-A192333] N88-27281
Determination of Tafel constants in nonlinear polarization curves
[AD-A192335] N88-27282
Analysis of grain refinement and superplasticity in aluminum-magnesium alloys
[AD-A193029] N88-27283
A conceptual design study of a hovering system controller for an autonomous underwater vehicle
[AD-A193423] N88-27399
Performance study of a unipole antenna with conventional and elevated radial wire ground screens
[AD-A193283] N88-27413
The diffusion of vorticity from a plane boundary
[AD-A192706] N88-27474
An analysis of horizontal temperature gradients and heat content in the mixed layer and the surface forcing during PATCHEX
[AD-A192330] N88-27678
Computer aided design for linear control State Variable System (SVS)
[AD-A193282] N88-27775
Passive multipath target tracking in an inhomogeneous acoustic medium
[AD-A193284] N88-27873
The influence of ionization within a plasma opening switch
[AD-A193147] N88-27906

NAVAL RESEARCH LAB., WASHINGTON, D.C.
Radiative heat transfer and selective emission in planar slab coatings on hot emissive substrates
[AD-A193133] N88-27319
Sidelobe level of an adaptive array using the SMI (Sampled Matrix Inversion) algorithm
[AD-A193131] N88-27409
A numerically efficient digital matched filter for periodic and windowed periodic radar waveforms
[AD-A193132] N88-27410
SARLAC: A relativistic electron beam code
[AD-A193134] N88-27411
Definition of long ocean wave slope for radar applications
[AD-A193198] N88-27412
Radar information from the partial derivatives of the echo signal phase from a point scatterer
[AD-A193402] N88-27415
Numerical simulation of fuel droplet interactions and breakup
[AD-A192431] N88-27470
Critical issues and directions for fracture mechanics and structural integrity
[AD-A193050] N88-27584
The influence of weld metal properties, weld geometry and applied load on weld system performance
[AD-A193403] N88-27588
Approximate analytical formulae for electron density and collision frequency in the natural and nuclear-disturbed ionosphere and inner magnetosphere
[AD-A193129] N88-27654
Basic database operations on the butterfly parallel processor: Experiment results
[AD-A193199] N88-27804
Propagation of charged particle beams in the atmosphere
[AD-A193185] N88-27887
Spectral line shapes from highly ionized sodium plasmas
[AD-A193401] N88-27907
Compilation of NRL publications on high temperature superconductivity
[AD-A189137] N88-27921
Dose-enhancement effects in TaSi/Al- and Al-gate MOS devices
[DE88-005483] N88-27926

NAVAL UNDERWATER SYSTEMS CENTER, NEWPORT, R.I.
Characterization of accelerating pipe flow
[AD-A193065] N88-27481
NEBRASKA UNIV., LINCOLN.
Influence of moving visual environment on saccadic eye movements and fixation N88-27368
NERO AND ASSOCIATES, INC., PORTLAND, OREG.
National ambient Volatile Organic Compounds (VOCs) data base update, documentation
[PB88-195631] N88-27646
NEW MEXICO UNIV., ALBUQUERQUE.
Predicting optical degradation of a laser beam through a turbulent shear layer N88-27376
Extinguishing agent for magnesium fire, phases 5 and 6
[AD-A192436] N88-27398
Prediction of velocity and temperature profiles in thermally driven gravity currents applied to stratified thermal storage tanks
[DE88-004452] N88-27496
Thermo-mechanical cracking in coated media with a cavity by a moving asperity friction
[AD-A193311] N88-27586
NEW YORK MEDICAL COLL., H.Y.
CEEG dynamic brain mapping: A new method to evaluate brain function in different psychological and drug conditions N88-27685
NEW YORK UNIV., NEW YORK.
Studies of the intact human brain: Implications for performance N88-27684
Cognitive and neural bases of skilled performance
[AD-A193392] N88-27747
NEW YORK UNIV. MEDICAL CENTER.
Normative developmental equations for the EEG and their sensitivity to neurological and psychiatric disorders N88-27687
NEWCASTLE-UPON-TYNE UNIV. (ENGLAND).
Model for dynamically structured communicating systems
[PB88-105283] N88-27402
NORTH CAROLINA UNIV., CHAPEL HILL.
Computation of filters by sampling and quantization
[AD-A192839] N88-27826
On the exceedance random measures for stationary processes
[AD-A192838] N88-27848
A note on vector bimeasures
[AD-A192841] N88-27849
A study on Lebesgue decomposition of measures induced by stable processes
[AD-A192893] N88-27850
Multiple integration with respect to Poisson and Levy processes
[AD-A192895] N88-27851
The computation of stationary distributions on Markov chains through perturbations
[AD-A193191] N88-27855
Silicon oxidation studies: A review of recent studies on thin film silicon dioxide formation in the physics and chemistry of SiO2 and the Si-SiO2 interface
[AD-A193176] N88-27932
NORTHEASTERN UNIV., BOSTON, MASS.
On the dynamics of the auroral ionosphere during the breakup of a substorm
[AD-A193368] N88-27657
A model for visual attention
[AD-A193061] N88-27744
NORTHWESTERN UNIV., EVANSTON, ILL.
The effects of increased cognitive demands on autonomic self-regulation: An indicator of parallel processing in the brain N88-27362
A study of fluid-structure problems N88-27468
Adaptive finite element methods for shells
[AD-A193221] N88-27585
Perception of motion in statistically-defined displays
[AD-A193076] N88-27745
Effective buffering schemes for performing matrix operations for numerical databases N88-27968

O

OAK RIDGE NATIONAL LAB., TENN.
Vibrational impacts of hush house operation
[DE88-006983] N88-27207
Theoretical and experimental analysis of the toughening behavior of whisker reinforcement in ceramic matrix composites
[DE88-011841] N88-27241
Direct determination of part-per-billion levels of volatile organics in water and soil samples using glow discharge mass spectrometry
[DE88-011389] N88-27272
Survey of the literature on fractals with possible applications to phase change processes
[DE88-012240] N88-27277
Magnetic excitations in transition metal systems
[DE88-011022] N88-27279
Controlling phase formation and stability to improve the high temperature creep resistance of austenitic stainless steels
[DE88-011401] N88-27293
Application of Auger electron spectroscopy to the study of trace element effects on weldability
[DE88-010457] N88-27301
Thin film and near-surface characterization using a mechanical properties microprobe
[DE88-011399] N88-27302
Inelastic electron scattering and electron-hole excitations in iron and nickel
[DE88-011843] N88-27303
Ceramic technology for advanced heat engines project
[DE88-006945] N88-27323
Motor-response learning at a process control panel by an autonomous robot
[DE88-005055] N88-27554
The 000 stage equipment bearing performance with a lower viscosity lubricant
[DE88-011827] N88-27566
Verification of the ADINA finite element code for creep analysis: Problems from the open literature
[DE88-011826] N88-27594
Evaluation of fracture models through pressurized-thermal-shock testing
[DE88-011834] N88-27603
Thermal energy storage
[DE88-010753] N88-27625
Review of geographic processing techniques applicable to regional analysis
[DE88-010759] N88-27643
Foliar nitrate reductase: A marker for assimilation of atmospheric nitrogen oxides
[DE88-010453] N88-27648
Implementation of an OPS5 derivative on the Novix RISC processor
[DE88-011392] N88-27758
A zoomable and adaptable hidden fine-mesh approach to solving advection-dispersion equations
[DE88-006174] N88-27816
Parallel implementation of the boundary element method
[DE88-011846] N88-27839
Comparison of results based on a deterministic versus a statistical uncertainty analysis
[DE88-010751] N88-27858
ITER plasma equilibrium and poloidal field system design
[DE88-011005] N88-27912
Use of Moessbauer spectroscopy to study implanted surfaces
[DE88-010452] N88-27942
Study of the friction and wear-related properties of ceramic superconductors
[DE88-011844] N88-27950
Calculation of the specific and volumetric enthalpies of Ge-Si alloys
[DE88-006949] N88-27965
Technology transfer for DOE's Office of Transportation Systems: Assessment and strategies
[DE88-010760] N88-27977
OAK RIDGE Y-12 PLANT, TENN.
Application of Auger electron spectroscopy to the study of trace element effects on weldability
[DE88-010457] N88-27301
Acoustic emission calibration instrumentation
[DE88-010817] N88-27528
NDE performance in predicting failure strength of spherical composite specimens with implanted flaws
[DE88-008223] N88-27575
OFFICE NATIONAL D'ETUDES ET DE RECHERCHES AEROSPATIALES, PARIS (FRANCE).
Flow around a delta wing with or without a canard control surface (phi BA = 60 deg). Part 1: Hydrodynamic visualization in permanent regime
[ONERA-RT-10/2891-AN-101-A-PT-1] N88-27170
European transonic wind tunnel project: Assistance to the design group
[ONERA-RSF-11/0694-GY-010-G] N88-27208
Studies concerning the European transonic wind tunnel
[ONERA-RSF-10/0694-GY-010-G] N88-27209
OFFICE OF SCIENCE AND TECHNOLOGY, WASHINGTON, D. C.
Federal Council on Science, Engineering and Technology: Committee on Computer Research and Applications, Subcommittee on Science and Engineering Computing: The US Supercomputer Industry
[DE88-011262] N88-27756
OFFICE OF THE UNDER SECRETARY OF DEFENSE (ACQUISITIONS), WASHINGTON, D.C.
Very High Speed Integrated Circuits (VHSIC)
[AD-A193225] N88-27442
OFICINAS GERAIS DE MATERIAL AERONAUTICO, ALVERCA (PORTUGAL).
The auditory evoked response in military pilots N88-27721
OHIO STATE UNIV., COLUMBUS.
An experimental study of the effect of pitch rate on delta wing aerodynamics and stability
[NASA-CR-183159] N88-27173
Basic research for the geodynamics program
[NASA-CR-183149] N88-27662
OKLAHOMA STATE UNIV., STILLWATER.
Laser spectroscopy investigations of materials for solid state laser systems
[AD-A192514] N88-27535
OKLAHOMA UNIV., NORMAN.
The structure and stability of nonpremixed gas jet flames N88-27257
OLD DOMINION UNIV., NORFOLK, VA.
Investigation of viscous/inviscid interaction in transonic flow over airfoils with suction
[NASA-CR-183112] N88-27490
Numerical methods for incompressible viscous flows with engineering applications
[NASA-CR-183143] N88-27508
Finite element methodology for integrated flow-thermal-structural analysis
[NASA-CR-183144] N88-27606
OREGON GRADUATE CENTER FOR STUDY AND RESEARCH, BEAVERTON.
Superconducting properties of LaBa2Cu3O(sub x) and YBa2Cu3O(sub y)
[DE88-012038] N88-27952
ORGANISATIE VOOR TOEGEPAST NATUURWETENSCHAPPELIJK ONDERZOEK, SOESTERBERG (NETHERLANDS).
Using ERPS to study human information processing N88-27698

P

PACIFIC NORTHWEST LABS., RICHLAND, WASH.
Formation of metastable structures and amorphous phases in Cu-W alloys using the triod sputtering technique
[DE88-009051] N88-27298
Metal-air battery assessment
[DE88-011361] N88-27459
Direct measurement of solids: High temperature sensing. Experimental development and testing of high temperature pulsed EMATs
[DE88-009859] N88-27546
Large-eddy simulations of concentration fluctuations
[DE88-009480] N88-27660
The Hanford meteorological data collection system and data base
[DE88-008632] N88-27672
Computer simulation procedure for designing airborne aerometric monitoring programs
[DE88-011896] N88-27674
PAKISTAN INST. OF NUCLEAR SCIENCE AND TECHNOLOGY, RAWALPINDI.
Compilation of temperature factors of cubic elements
[PB88-106170] N88-27260
PARIS VI UNIV. (FRANCE).
Application of sol-gel procedures to ceramic composites
[ETN-88-92741] N88-27338
PENNSYLVANIA STATE UNIV., UNIVERSITY PARK.
Premixed turbulent flame propagation
[AD-A192955] N88-27265
Twin boundaries and heterophase interfaces in ferroelastic martensites
[DE88-011894] N88-27304
Multifilter spectrometer (FEB) for microwave atmospheric sounder
[AD-A192312] N88-27426
FEB (Multifilter Electronics Box) lifting device analysis, revision A
[AD-A192313] N88-27427
A critical review of IR drops and electrode potentials within pits, crevices and cracks
[AD-A192481] N88-27431
Significance of the local electrode potential within pits, crevices and cracks
[AD-A192482] N88-27432
Some equivalent circuit models for AC impedance analysis of pyrite/solution interface
[DE88-010574] N88-27452

PENNSYLVANIA UNIV., PHILADELPHIA.
Thermal conductivity of isotopically pure semiconductors, superlattices, semiconductor alloys and semiconductors as a function of temperature; control of the segregation coefficient in LEC crystal growth; and photo-Hall measurements of GaAs
N88-27375
Factors governing light driven electron and proton translocation in proteins across membranes
[DE88-011120] N88-27724

PHYSICS AND ELECTRONICS LAB. TNO, THE HAGUE (NETHERLANDS).
The FEL CCD-camera: Experimental system for camera and image processing research
[FEL-1987-34] N88-27532

PINNACLE RESEARCH INST., CUPERTINO, CALIF.
High power pulse energy system concept
[AD-A192440] N88-27429

PITTSBURGH UNIV., PA.
Far- and mid-infrared properties of metal-insulator composite materials
[AD-A193227] N88-27236
Microchemical analysis of polycrystalline Ni3Al and other ordered alloys using the field-ion microscope atom probe
[DE88-011519] N88-27294
On solvability of an equation arising in the theory of M-estimates
[AD-A193059] N88-27828
A unified approach to estimation in linear models with fixed and mixed effects
[AD-A193060] N88-27829
Further extensions of the choquet-deny and deny theorems with applications in characterization theory
[AD-A193358] N88-27834
Asymptotic normality of minimum L1-norm estimates in linear models
[AD-A193399] N88-27835
Generalized Jordan chains and two bifurcation theorems of Krasnoselskii
[AD-A192353] N88-27845
Statistical analysis of dyadic stationary processes
[AD-A193057] N88-27853
Joint asymptotic distribution of marginal quantiles and quantile functions in samples from a multivariate population
[AD-A193385] N88-27856

POLYTECHNIC INST. OF NEW YORK, BROOKLYN.
Ionic conductive polymers based on crosslinked elastic siloxane-ethylene oxide copolymers
[DE88-011243] N88-27311

PRAIRIE VIEW AGRICULTURAL AND MECHANICAL COLL., TEX.
Computer modeling for surface properties of carbon fibers
N88-27383

PRINCETON UNIV., N. J.
Velocity measurements and flow visualization in turbulent three-dimensional supersonic flows using oxygen flow tagging
[AD-A192551] N88-27165
Air-sea interaction in the vicinity of a land-sea boundary in the presence of upwelling
N88-27661
WORDNET: An electronic lexical reference system based on theories of lexical memory
[AD-A193086] N88-27970

PUERTO RICO UNIV., MAYAGUEZ.
Design of a mechanism to control wind tunnel turbulence
N88-27370

PURDUE UNIV., WEST LAFAYETTE, IND.
Characterization of elastic-plastic properties of AS4/APC-2 thermoplastic composite
[NASA-CR-183145] N88-27242
Calculation of far infrared absorption in B poly(dA).poly(dT)
[AD-A193128] N88-27318
Effects of surface tension and contact angle on sensible heating and boiling incipience in dielectric falling films
[DE88-007057] N88-27492
Failure analysis of laminated composite angles
N88-27578
Three-dimensional aspects of fatigue crack closure
[AD-A192296] N88-27581
Solar energy conversion through the interaction of plasmons with tunnel junctions. Part A: Solar cell analysis. Part B: Photoconductor analysis
[NASA-CR-183044] N88-27621
Reduced order modeling of grid-connected photovoltaic inverter systems
[DE88-010603] N88-27635

R

RADIAN CORP., AUSTIN, TEX.
National air toxics information clearinghouse: NATICH data base users guide for data viewing, February 1988
[PB88-197470] N88-27645

READING UNIV. (ENGLAND).
Magnetic excitations in transition metal systems
[DE88-011022] N88-27279

RENSSELAER POLYTECHNIC INST., TROY, N.Y.
Silicon-on-insulator pin diodes
[AD-A193359] N88-27445

RESEARCH INST. OF NATIONAL DEFENCE, STOCKHOLM (SWEDEN).
Rocket motor case materials. An evaluation of new fibers for composites
[FOA-C-20696-2.1] N88-27245

ROCHESTER UNIV., N. Y.
Analysis of emission features in IRAS LRS spectra
N88-27380
Radial compression of picosecond electrical pulses
[DE88-008440] N88-27544
Measurement of the thermal conductivity of dielectric thin solid films with a thermal comparator
[DE88-008468] N88-27898

ROCKEFELLER UNIV., NEW YORK.
Are Centaurce diffractive
[DE88-006767] N88-27906

ROCKWELL INTERNATIONAL CORP., THOUSAND OAKS, CALIF.
Atomic layer epitaxy of ZnS and ZnSe
[AD-A192307] N88-27928

ROME AIR DEVELOPMENT CENTER, GRIFFISS AFB, N.Y.
Airborne measurement of low frequency atmospheric noise ALFAN 1
[AD-A193056] N88-27405

ROME UNIV. (ITALY).
Numerical optimization
[AD-A193032] N88-27827
Quark nuclear model: Classification groups and two and three body correlations
[NOTA-INTERNA-896] N88-27891
Study of the production of Ko mesons in proton antiproton interactions at 630 GeV
[NOTA-INTERNA-908] N88-27892

ROYAL AIR FORCE, WROUGHTON (ENGLAND).
Detection of latent epilepsy in aircrew candidates
N88-27720

ROYAL AIR FORCE INST. OF AVIATION MEDICINE, FARNBOROUGH (ENGLAND).
The application of non-stationary data analysis techniques in the identification of changes in the electroencephalogram associated with the onset of drowsiness
N88-27688

ROYAL ARMY MEDICAL COLL., LONDON (ENGLAND).
Can CNV amplitude predict ability to accomplish a demanding task?
N88-27700

ROYAL INSTITUTION OF GREAT BRITAIN, LONDON.
Energy migration, motion and order in synthetic polymers
[AD-A193334] N88-27320

S

SAN DIEGO AIRCRAFT ENGINEERING, INC., CALIF.
Plastic yielding at crack tips
[AD-A192549] N88-27582

SANDIA NATIONAL LABS., ALBUQUERQUE, N. MEX.
Airborne remote operated device
[DE88-010324] N88-27188
A method for reducing the coning of a spinning vehicle
[DE88-010971] N88-27189
An investigation of soft launch and instability breakup with a two-stage light gas gun
[DE88-010371] N88-27218
In-flight motor torque estimates for the second-stage Strypi 9 launch vehicle
[DE88-010833] N88-27222
Mechanism of the nitric oxide-carbon monoxide-oxygen reaction over a single crystal rhodium catalyst
[DE88-006274] N88-27268
Summary of discussions at the Tenth Meeting of the Sandia Cooperative Group on the Aerothermochemistry of Turbulent Combustion
[DE88-008467] N88-27269
Gaseous tracer techniques for pore structure characterization of granular materials
[DE88-011542] N88-27274
Laser probes and numerical modeling as process diagnostics in chemical vapor deposition
[DE88-011622] N88-27275
Development of an experimental system for studying fast transient ignition phenomena
[DE88-011917] N88-27276
Optical diagnostics for metallurgical processes
[DE88-009255] N88-27289
PECVD of amorphous nickel--phosphorus films
[DE88-011088] N88-27299
Refractory films from spin-cast carbon
[DE88-011251] N88-27327
Precursor chemistry and the structure of silica aerogels
[DE88-011253] N88-27328
Adhesion of hydrated silicate films
[DE88-011250] N88-27333
Plasma treatment of polymers for improved adhesion
[DE88-011823] N88-27334
Ellipsometric imaging of drying sol-gel films
[DE88-011785] N88-27335
A concept for an electro-optic explosive device
[DE88-009696] N88-27349
Diode laser ignition of high explosives and pyrotechnics
[DE88-008771] N88-27352
Dependence effects in unique signal transmission
[DE88-010331] N88-27419
The first synthesis of chem-prep varistor LAC (Lightning Arrestor Connector) granules
[DE88-008005] N88-27438
Failure analysis of Chloride Silent Power, Ltd. PB cells
[DE88-010567] N88-27448
Component stress during freeze/thaw cycling
[DE88-011204] N88-27449
Friction, wear and electrical contact resistance of precious metal alloys
[DE88-011244] N88-27450
Sodium/sulfur cell evaluation results
[DE88-011488] N88-27451
Thermal cycling tests on surface-mount assemblies
[DE88-007895] N88-27453
The kinetics of charge-transfer reactions on passive lithium electrodes
[DE88-009256] N88-27454
Effect of thermal cycling on CSPL (Chloride Silent Power Ltd.) sodium/sulfur cells
[DE88-011205] N88-27455
Long-pulse, high-power vircator experiments
[DE88-011787] N88-27458
STAR: Sandia Timing Analyzer Routine
[DE88-012412] N88-27483
Forces and moments on a slender, cavitating body
[DE88-007208] N88-27491
Prediction of velocity and temperature profiles in thermally driven gravity currents applied to stratified thermal storage tanks
[DE88-004452] N88-27496
Cavitation inception in a turbulent shear flow
[DE88-011486] N88-27497
The P delta V fundamental gas leak calibration system qualification report
[DE88-008964] N88-27526
Liquid crystals for unsteady surface shear stress visualization
[DE88-010570] N88-27527
Fiber-optics used to record high-speed photographs inside a pressurized tank during lethality testing
[DE88-011283] N88-27529
Phase comparator for range imaging laser radar
[DE88-008109] N88-27545
Target designs for plasma-implosion-driven, photoionization-pumped soft X-ray lasers
[DE88-011278] N88-27547
Process control improvements in pulsed Nd:YAG laser closure welding of electromechanical relays
[DE88-006275] N88-27564
A demonstration of retro-traverse using a semi-autonomous land vehicle
[DE88-009851] N88-27568
Stress relaxation of a titanium (Ti-6Al-4V) threaded joint
[DE88-010102] N88-27580
Temperature, moisture and strain rate effects on the compressive mechanical behavior of Nylon 6/6
[DE88-010734] N88-27591
Development of a biaxial test system for thin-walled metal tubes using tensile-compressive axial load and internal-external pressure
[DE88-011279] N88-27592
Diffusion models of crack growth due to random overloads
[DE88-008811] N88-27595
A comparison of analytical techniques for modeling the Rayleigh-Taylor response of elastic-plastic solids
[DE88-010372] N88-27596
Reflux heat-pipe solar receivers for dish-electric systems
[DE88-008671] N88-27631
Modal testing in the design evaluation of wind turbines
[DE88-010374] N88-27632
Performance evaluation of large-area glass-mirror heliostats
[DE88-011883] N88-27636

Optical evaluation of prototype stretched-membrane mirror modules for solar central receivers
[DE88-011884] N88-27637
Three-dimensional wind simulation
[DE88-009793] N88-27671
MINIAC: A small embedded computer
[DE88-008142] N88-27757
Verification of flight software written in C using ACSL
[DE88-006100] N88-27779
An optical 2-dimensional correlator for pattern recognition in embedded computing
[DE88-007198] N88-27780
Factorization of large integers on a massively parallel computer
[DE88-011625] N88-27786
Maximum entropy signal restoration with linear programming
[DE88-011740] N88-27787
The SAS System by forms: Putting statistical power into the hands of an end-user
[DE88-010512] N88-27857
A comparison of generators for pseudo-random normal deviates
[DE88-011711] N88-27859
Hypersonic flight testing
[DE88-001655] N88-27894
A fiber optic synchronous detector using sample-and-hold circuits
[DE88-010973] N88-27899
Dose-enhancement effects in TaSi/Al- and Al-gate MOS devices
[DE88-005483] N88-27926
Paramagnetic point defects in boron-implanted HgO.7CdO.3Te
[AD-A193276] N88-27934
Developing a connector selection DBMS (database management system) using NIAM (Nijssen's Information Analysis Methodology)
[DE88-008110] N88-27972

SCHOOL OF AEROSPACE MEDICINE, BROOKS AFB, TEX.
EEG indices of G-induced Loss Of Consciousness (G-LOC) N88-27709
Behavioral effects of exposure to the tempo high-power microwave system
[AD-A193305] N88-27738

SCIENCE RESEARCH COUNCIL, CHILTON (ENGLAND).
Linguistic semantics for parallel computation
[PB88-105960] N88-27761

SCIENTIFIC RESEARCH ASSOCIATES, INC., GLASTONBURY, CONN.
Studying the physics and operation of multi-terminal near-micron and sub-micron length, hot electron semiconductor devices
[AD-A193380] N88-27446
A Navier-Stokes study of cascade flow fields including inlet distortion and rotating stall
[AD-A193109] N88-27483

SCIENTIFIC SYSTEMS, INC., CAMBRIDGE, MASS.
Distributed algorithms for probabilistic solution of computational vision problems
[AD-A193150] N88-27773

SCRIPPS INSTITUTION OF OCEANOGRAPHY, LA JOLLA, CALIF.
Vertical directionality of ambient noise at 32 deg N as a function of longitude: Tape number 86180
[AD-A193226] N88-27872

SIMON FRASER UNIV., BURNABY (BRITISH COLUMBIA).
The interaction of thalamo-cortical systems in the 40 Hz following response N88-27694
A study of sources in the human brain associated with stereopsis N88-27695

SMITHSONIAN ASTROPHYSICAL OBSERVATORY, CAMBRIDGE, MASS.
Application of two-dimensional imaging to very high energy gamma ray astronomy
[DE88-010120] N88-27983

SOCIETE NATIONALE INDUSTRIELLE AEROSPATIALE, CANNES (FRANCE).
Cyrogenic test facilities for an optical cryomechanism qualification
[SNIAS-881-440-116] N88-27219
EXSAT: Expert system to configure telecommunication satellites
[SNIAS-881-440-101] N88-27223
Space photovoltaic generators. State of the art, trends
[SNIAS-881-440-106] N88-27840
Benefits of an object approach in a computer aided design environment
[SNIAS-881-440-102] N88-27791

SOCIETE NATIONALE INDUSTRIELLE AEROSPATIALE, PARIS (FRANCE).
Introduction to artificial intelligence and expert systems
[SNIAS-881-320-101] N88-27814
Expert system contribution to logistics improvement
[SNIAS-881-320-102] N88-27815

SOCIETE NATIONALE INDUSTRIELLE AEROSPATIALE, SAINT-MEDARD-EN-JALLES (FRANCE).
Design of booster wound structures
[SNIAS-881-430-102] N88-27228
Balance of X-ray radioscopy application to nondestructive tests of composite materials
[SNIAS-881-430-110] N88-27250
Programs for preliminary design of composite materials which were developed by the design group of Aerospatiale Aquitaine
[SNIAS-881-430-112] N88-27251
On the electrical properties of carbon/carbon composites densified by chemical deposit in vapor phase
[SNIAS-881-430-117] N88-27252
Reinforced plastics: Winding and weaving technologies for space products
[SNIAS-881-430-103] N88-27341
Comparison of sol-gel procedures for zircon and alumina
[SNIAS-881-430-108] N88-27342
Microwave polymerization of composite structures
[SNIAS-881-430-116] N88-27343
Injection compression for short fiber reinforced plastics
[SNIAS-881-430-118] N88-27344
Experiments in microgravity environment: Protein crystallization
[SNIAS-881-430-101] N88-27354
Use of microwave measuring systems for the nondestructive control of resins and composites
[SNIAS-881-430-123] N88-27576
Waste destruction by plasma
[SNIAS-881-430-113] N88-27651

SOCIETE NATIONALE INDUSTRIELLE AEROSPATIALE, SURESNES (FRANCE).
Relation between the mechanical characteristics of carbon-resin composites and their impact strength
[REPT-48-264/F] N88-27249
Study of surface treatments before adhesive bonding of light alloys
[ETN-88-92743] N88-27308
Refractory fibers surface treatment
[REPT-47-803/F] N88-27339
Interface control using low frequency (3 to 20 MHz) acoustic microscopy
[REPT-48-411/F] N88-27577

SOCIETE NATIONALE INDUSTRIELLE AEROSPATIALE, TOULOUSE (FRANCE).
Supersonic transport/hypersonic transport (SST/HST) development
[SNIAS-881-111-101] N88-27192

SOUTH BANK POLYTECHNIC, LONDON (ENGLAND).
Reflection of sound in open ended ducts
[PB88-103478] N88-27870

SOUTH CAROLINA UNIV., COLUMBIA.
Remote sensing of wetlands: Applications overview
[DE88-010895] N88-27618

SOUTHERN UNIV., BATON ROUGE, LA.
Experimental validation of a zero-dimensional computer model for spark-ignition engines
[DE88-009034] N88-27565

SOUTHWEST RESEARCH INST., SAN ANTONIO, TEX.
Effects of ceramic surfaces on autoignition in a constant volume combustion apparatus
[AD-A193055] N88-27266
A study relating to the fog oil replacement program
[AD-A192536] N88-27347
Analytical and experimental investigation of ringless piston concept
[AD-A193213] N88-27559

SRI INTERNATIONAL CORP., MENLO PARK, CALIF.
Laser probes of natural gas ignition chemistry
[PB88-212568] N88-27271
User's manual for C-HEMP: A two-dimensional wave propagation code. Volume 1: Description and derivations of the code
[AD-A193197] N88-27486
Influence of microstructure and microdamage processes on fracture at high loading rates
[AD-A192957] N88-27583

STANFORD UNIV., CALIF.
Superconducting thin films, composites and junctions
[AD-A193123] N88-27440
The heat transfer and fluid dynamics of concave surface curvature
[AD-A193064] N88-27479
Control of free-flying space robot manipulator systems
[NASA-CR-183017] N88-27562
Control of free-flying space robot manipulator systems
[NASA-CR-183104] N88-27563
Dexterous hands: Optimizing grasp by design and planning N88-27572
Diffusion models of crack growth due to random overloads
[DE88-008811] N88-27595
Simulation methodology
[AD-A192548] N88-27764
On the estimation of a variance ratio
[AD-A193190] N88-27854
Cosmological parameters and evolution of the galaxy luminosity function
[NASA-CR-183081] N88-27986

STATE UNIV. OF NEW YORK, BUFFALO.
Coherent structures in the axisymmetric turbulent jet mixing layer N88-27504
Coupled even-parity superconducting states: Square lattice
[AD-A193432] N88-27938

STATE UNIV. OF NEW YORK, STONY BROOK.
Precursor chemistry and the structure of silica aerogels
[DE88-011253] N88-27328
Equipment for an advanced electron beam lithography system
[AD-A192956] N88-27435

STRATHCLYDE UNIV., GLASGOW (SCOTLAND).
Laser spectroscopy of quantum well and superlattice structures
[AD-A193336] N88-27937

STUTTGART UNIV. (WEST GERMANY).
Contribution to the numerical solution of airplane spin motion
[ETN-88-92368] N88-27190
Propulsion analysis and application potential of air breathing combined propulsion for ballistic space transporter
[ETN-88-92369] N88-27227
Integrated magnetic field sensor using high magnetotransistors
[ETN-88-92356] N88-27465

SVERDRUP TECHNOLOGY, INC., CLEVELAND, OHIO.
Three-dimensional adaptive grid generation for body-fitted coordinate system
[NASA-CR-182192] N88-27520

T

TECHNICAL RESEARCH CENTRE OF FINLAND, ESPOO.
Ethanol as a fuel of a lorry. Use experience from a diesel engine modified to an otto engine
[DE88-752870] N88-27569
Hydraulic pumps and hydraulic equipment at low temperatures
[DE88-752871] N88-27570
Cold worked reinforcing bars in tensile test under high loading rate and low temperatures
[DE88-752993] N88-27610

TECHNISCHE HOCHSCHULE, AACHEN (WEST GERMANY).
Contribution to the development of coated fiber ceramic insolation material
[ETN-88-92351] N88-27243
Numerical computation of three-dimensional turbulent flow in tightly curved ducts and spiral turbine casings
[ETN-88-92362] N88-27511
Rotation symmetric vortex in axiparallel flow
[ETN-88-92364] N88-27512
Numerical integration of Navier-Stokes equations by application of multigrid concept
[ETN-88-92365] N88-27513
Computation of flow and diffusion process in gas centrifuges
[ETN-88-92366] N88-27514
Investigations on beam quality of high frequency excited CO2 high performance lasers
[ETN-88-92363] N88-27550

TECHNISCHE HOGESCHOOL, DELFT (NETHERLANDS).
Nonlinear interaction between overall and local buckling of stiffened panels with symmetric cross-sections
[PB88-104054] N88-27580

TECHNISCHE UNIV., BERLIN (WEST GERMANY).
Contribution to almost realistic picture processing by a computer graphics procedure
[ETN-88-92372] N88-27789
Finite element method for plate structures with inclined angles
[ILR-MITT-182] N88-27842
Investigation of electronic band structure of semiconductors by photoemission
[ETN-88-92370] N88-27957

TECHNISCHE UNIV., BRUNSWICK (WEST GERMANY).
Simulation of moisture diffusion of fiber reinforced components of aircraft for general air transportation
[IFL-IB-87-05] N88-27253

Determination of quantum corrections for electrical conductivity mechanism of three dimensional, perturbed copper coatings. Weak localization and electron-electron interaction
[ETN-88-92378] N88-27466
Investigations on drag reduction in turbulent pipe flows by addition of ionic and nonionic high polymers
[ETN-88-92380] N88-27515
Stability of uncapsulated weight cells with thin film elongation measurement bands under influence of humidity, temperature and operation voltage
[ETN-88-92383] N88-27531
Optimization of planetary gears
[ETN-88-92375] N88-27573
Asymptotic of Peanokerns of finite fixed order
[ETN-88-92381] N88-27843
Flexible valued algebras of four-dimensions
[ETN-88-92382] N88-27844
Measurement of Beta-decay energies of short-lived neutron-rich nuclei in the vicinity of mass number between 101 and 106, and A = 109
[ETN-88-92376] N88-27890
Photodiodes for optical communication in the near infrared
[ETN-88-92379] N88-27900
Interactions between superconductivity and Kondo-grid properties in CeCu2Si2. Measurement results of specific heat under high pressure
[ETN-88-92377] N88-27958

TECHNISCHE UNIV., CLAUSTHAL-ZELLERFELD (WEST GERMANY).
Homogeneity of glasses: Experiment WL-IHF-05 in D1 mission
[ETN-88-92339] N88-27353

TECHNISCHE UNIV., MUNICH (WEST GERMANY).
Conductivity mechanism and operating behavior of electrically conductive adhesives on the example of a power transistor
[ETN-88-92355] N88-27464
Modeling and approximate performance analysis of multiuser computer systems
[ETN-88-92137] N88-27806
Characterization of crystalline silicon by electrochemical and Raman spectroscopy at the frontier semiconductor/electrolyte
[ETN-88-92354] N88-27956

TENNESSEE UNIV., KNOXVILLE.
Evaluation and improvement of liquid propellant rocket chugging analysis techniques. Part 1: A one-dimensional analysis of low frequency combustion instability in the fuel preburner of the space shuttle main engine
[NASA-CR-183106] N88-27224
Evaluation and improvement of liquid propellant rocket chugging analysis techniques. Part 2: A study of low frequency combustion instability in rocket engine preburners using a heterogeneous stirred tank reactor model
[NASA-CR-182724] N88-27225

TEXAS A&M UNIV., COLLEGE STATION.
Techniques for characterizing damage zones in composite materials N88-27240

TEXAS INSTRUMENTS, INC., DALLAS.
The effect of input device on user performance with a menu-based natural language interface
[AD-A193095] N88-27772

TEXAS TECHNOLOGICAL UNIV., LUBBOCK.
Nonlinear stochastic interaction in aeroelastic structures
[AD-A193427] N88-27589

TEXAS UNIV., AUSTIN.
Guided wave interactions in millimeter-wave integrated circuits
[AD-A193017] N88-27437
An h-p adaptive finite element method for steady compressible flow N88-27467
Physical mechanisms in shock-induced turbulent separated flow
[AD-A193165] N88-27484

TEXTRON BELL HELICOPTER, FORT WORTH, TEX.
Aeromechanical stability analysis of COPTER N88-27161

TOKYO UNIV. (JAPAN).
Precise ultraviolet absorbance study of the interaction of amino acids and mononucleosides in aqueous solution
[ISAS-RN-356] N88-27256
A theoretical determination of the density at a traveling source that emitts particles
[ISAS-RN-351] N88-27883

TRANSPORTATION SYSTEMS CENTER, CAMBRIDGE, MASS.
Cockpit and cabin crew coordination
[AD-A192445] N88-27752

TRI-UNIV. MESON FACILITY, VANCOUVER (BRITISH COLUMBIA).
An overview of lattice QCD
[DE88-010867] N88-27963

TRONDHEIM UNIV. (NORWAY).
KRYSI, an ODE solver combining a semi-implicit Runge-Kutta method and a preconditioned Krylov method
[DE88-012245] N88-27841

TRW DEFENSE AND SPACE SYSTEMS GROUP, REDONDO BEACH, CALIF.
Block Oriented Simulation System (BOSS)
[NASA-CR-182947] N88-27760

U

UNION FOR EXPERIMENTING COLL. AND UNIV., YELLOW SPRINGS, OHIO.
An investigation of techniques for determination of optimum/self-optimizing systems N88-27600

UNISEARCH ASSOCIATES, INC., CONCORD (ONTARIO).
Initial testing of the tunable diode laser absorption spectrometer for measuring HNO3 in diesel engine exhaust, stage 2
[PB88-193073] N88-27841

UNITED TECHNOLOGIES RESEARCH CENTER, EAST HARTFORD, CONN.
Aeroelastic modeling of rotor blades with spanwise variable elastic axis offset: Classic issues revisited and new formulations N88-27158
Computational fluid dynamics on parallel processors
[AD-A192397] N88-27469

UNIVERSAL ENERGY SYSTEMS, INC., DAYTON, OHIO.
United States Air Force Graduate Student Summer Support Program, volume 2
[AD-A191122] N88-27355

UNIVERSIDADE DO ESTADO DO RIO DE JANEIRO (BRAZIL).
Stream function-vorticity finite elements and the resolution of the Navier-Stokes equations
[DE88-702318] N88-27494

UNIVERSITY COLL., LONDON (ENGLAND).
Components of an atmospheric lidar system
[AD-A193366] N88-27539
Issues in computer-assisted interpretation of graphs and quantitative information
[PB88-116280] N88-27783

UNIVERSITY COLL. OF NORTH WALES, BANGOR.
Polymer-ceramic composites
[AD-A193244] N88-27237

UNIVERSITY OF EASTERN WASHINGTON, CHENEY.
Hole diameters in plates impacted by projectiles N88-27386

UNIVERSITY OF SOUTH FLORIDA, ST. PETERSBURG.
Creating aspect graphs for use in object recognition N88-27379

UNIVERSITY OF SOUTH FLORIDA, TAMPA.
An aspect graph-based control strategy for 3-D object recognition N88-27377

UNIVERSITY OF SOUTHERN ILLINOIS, CARBONDALE.
Determination of lumped-mass thermal properties associated with autoclave curing of graphite/epoxy composites N88-27364

UTAH UNIV., SALT LAKE CITY.
An investigation of the uses of time domain capable vector network analyzers as a diagnostic for helix traveling-wave circuits
[AD-A192460] N88-27430
The three-dimensional stress field around a cylindrical inclusion in a plate of arbitrary thickness N88-27602
Prediction of regional pollutant dispersion using a nested-grid, three-dimensional numerical model N88-27649
Development of radiation and cloud parameterization programs for AFGL (Air Force Geophysics Laboratory) global models
[AD-A193369] N88-27658

V

VANDERBILT UNIV., NASHVILLE, TENN.
Analysis of crack arrest toughness
[AD-A193340] N88-27286

VETERANS ADMINISTRATION HOSPITAL, SEPULVEDA, CALIF.
Electroencephalographic correlates of pilot performance: Simulation and in-flight studies N88-27711

VIRGINIA POLYTECHNIC INST. AND STATE UNIV., BLACKSBURG.
Experimental study of unsteady separating turbulent boundary layers
[AD-A192997] N88-27477

NDE performance in predicting failure strength of spherical composite specimens with implanted flaws
[DE88-008223] N88-27575
Application of pattern recognition techniques to the identification of aerospace acoustic sources
[NASA-CR-183116] N88-27877

VIRGINIA UNIV., CHARLOTTESVILLE.
Processing and properties of advanced aluminum alloys
[AD-A193224] N88-27264
Full analysis of a powerful window random access algorithm
[AD-A192437] N88-27763
Robust prediction for stationary processes: 2D enriched version
[AD-A193318] N88-27833
Outliner resistant filtering and smoothing: 2D version
[AD-A193319] N88-27874

W

WASHINGTON UNIV., SEATTLE.
Thermo-viscoelastic analysis of composite materials, volume 1
[NASA-CR-183048-VOL-1] N88-27230
Turbulence structure of mixing swirling flows
[AD-A193063] N88-27478
Nonlinear vibrations of periodically stiffened plates N88-27598
Simulation of real time problem solving
[AD-A193436] N88-27778
Migration and stability of HgCdTe lattice defects
[AD-A193293] N88-27935

WASHINGTON UNIV., ST. LOUIS, MO.
The importance of steady and dynamic inflow on the stability of rotor-body systems N88-27156
Cognitive task demands as reflected in physiological measures N88-27699
Assessment of cochlear damage after microwave irradiation
[AD-A193237] N88-27737

WEST VIRGINIA UNIV., MORGANTOWN.
Theoretical-numerical study of feasibility of use of winglets on low aspect ration wings at subsonic and transonic Mach numbers at reduce drag
[NASA-CR-4174] N88-27168

WESTINGHOUSE HANFORD CO., RICHLAND, WASH.
SP-100 Ground Engineering Systems: Test facility control systems
[DE88-009195] N88-27895

WISCONSIN UNIV., MADISON.
Equipment for building and testing superconductive flux flow electronic devices
[AD-A192959] N88-27436
Computational boundary conditions for the incompressible Navier-Stokes equations in channels and pipes
[AD-A193356] N88-27487
Numerical treatment of the pressure singularity at a re-entrant corner
[AD-A193357] N88-27488
Dynamic stability of elastic rotor-bearing systems via Liapunov's direct method N88-27571
Coupled thermal vibrations of beams with temperature-dependent properties N88-27601
Validate algorithms for the determination of rainfall rates from SSM/I microwave satellite imagery
[AD-A192299] N88-27664
The collection of statistics on the frequency of cloud cover over North America
[AD-A193093] N88-27667
A simple explanation of the Stokes phenomenon
[AD-A193253] N88-27832
Moment approach to neoclassical flows, currents and transport in auxiliary heated tokamaks
[DE88-008024] N88-27901
Tokamak magnetic turbulence over the safety factor range 0.6 less than q less than 3
[DE88-008421] N88-27904
Reminimization of energy integral and stability limit for non-ideal MHD (magnetohydrodynamic) plasma
[DE88-008422] N88-27911

WOODS HOLE OCEANOGRAPHIC INSTITUTION, MASS.
The distribution of some chemical elements between dissolved and particulate phases in the ocean
[DE88-010181] N88-27682

WRIGHT STATE UNIV., DAYTON, OHIO.
Investigation of the potential impact of new photonic materials on optical processing systems N88-27359
Human response to prolonged motionless suspension in four types of full body harnesses N88-27387

WYOMING UNIV., LARAMIE.
Calibration and data reduction techniques for the AFGL infrared array spectrometer N88-27374

Y

YALE UNIV., NEW HAVEN, CONN.
Computational fluid dynamics on parallel processors
[AD-A192397] N88-27469
Implicit finite-difference simulation of an internal flow on a hypercube
[AD-A192474] N88-27471
Implicit finite-difference simulation of an internal flow in a nozzle: An example of a physical application on a hypercube
[AD-A192475] N88-27472
A programmable systolic array for factorial analysis. Part 2: The symmetric eigenvalue problem
[AD-A192396] N88-27782
Performability analysis: Measures, an algorithm and a case study
[AD-A192477] N88-27800
A numerical treatment of the fluid/elastic interface under range-dependent environments
[AD-A192476] N88-27821
YORK UNIV., DOWNSVIEW (ONTARIO).
The effects of hypoxia on P300 and reaction time
[DCIEM-87-RR-12] N88-27697

Typical Contract Number Index Listing

Listings in this index are arranged alphanumerically by contract number. Under each contract number the NASA accession numbers denoting documents that have been produced as a result of research done under that contract are arranged in ascending order. The NASA accession number denotes the number by which the citation is identified.

AF AFOSR-0008-85 ..... N88-27589
AF AFOSR-0031-86 ..... N88-27936
AF AFOSR-0048-87 ..... N88-27831
AF AFOSR-0073-86 ..... N88-27479
AF AFOSR-0082-87 ..... N88-27284
AF AFOSR-0083-85 ..... N88-27473
AF AFOSR-0091-87 ..... N88-27740
AF AFOSR-0098-86 ..... N88-27469
N88-27762
AF AFOSR-0112-86 ..... N88-27484
AF AFOSR-0131-84 ..... N88-27845
AF AFOSR-0172-87 ..... N88-27744
AF AFOSR-0194-87 ..... N88-27832
AF AFOSR-0219-86 ..... N88-27165
AF AFOSR-0224-87 ..... N88-27833
N88-27874
AF AFOSR-0235-86 ..... N88-27263
AF AFOSR-0273-85 ..... N88-27476
AF AFOSR-0278-87 ..... N88-27846
AF AFOSR-0315-85 ..... N88-27822
N88-27823
N88-27847
AF AFOSR-0322-82 ..... N88-27813
AF AFOSR-0370-85 ..... N88-27745
AF PROJ. 2308 ..... N88-27470
AF PROJ. 3396 ..... N88-27355
AF-AFOSR-86-0116 ..... N88-27183
AF-AFOSR-0022-84 ..... N88-27315
AF-AFOSR-0061-87 ..... N88-27436
AF-AFOSR-0068-87 ..... N88-27743
AF-AFOSR-0071-85 ..... N88-27666
AF-AFOSR-0097-87 ..... N88-27265
AF-AFOSR-0100-87 ..... N88-27771
AF-AFOSR-0106-85 ..... N88-27581
AF-AFOSR-0134-24 ..... N88-27477
AF-AFOSR-0165-86 ..... N88-27476
AF-AFOSR-0198-85 ..... N88-27539
AF-AFOSR-0231-83 ..... N88-27711
AF-AFOSR-0231-86 ..... N88-27523
AF-AFOSR-0253-86 ..... N88-27435
AF-AFOSR-0254-87 ..... N88-27852
AF-AFOSR-0312-86 ..... N88-27264
AF-AFOSR-0335-82 ..... N88-27711
ARPA ORDER 4395 ..... N88-27411
ARPA ORDER 5092 ..... N88-27556
A80/KL/040 ..... N88-27532
BMFT-FE-LFL-8560-1 ..... N88-27204
BMFT-LFF-8432/9 ..... N88-27253
BMFT-01-QS-233-1 ..... N88-27216
BMFT-01-QV-4832 ..... N88-27353
BMVG-T/R-760/G-0002/G-1702 ..... N88-27202
CNET-86-1B-156-00-780-92-45-PA N88-27959
DA PROJ. IL1-62709-DH-95 ..... N88-27928
DA PROJ. 1L1-61102-AH-45 ..... N88-27201
DA PROJ. 1L1-61102-BH-57 ..... N88-27655
DA PROJ. 1L1-62209-AH-76 ..... N88-27559
DA PROJ. 1L2-63104-D-150 ..... N88-27266
DA PROJ. 1L7-62733-AH-20 ..... N88-27347
DA PROJ. 3E1-62777-A8-79 ..... N88-27739
DAAB07-86-C-F013 ..... N88-27928
DAAG29-81-D-0100 ..... N88-27770
DAAG29-84-K-0030 ..... N88-27764
DAAG29-84-K-0045 ..... N88-27800
DAAG29-84-K-0070 ..... N88-27776
DAAG29-84-K-0076 ..... N88-27437
DAAG29-84-K-0082 ..... N88-27822
N88-27823
DAAG29-84-K-0140 ..... N88-27812
DAAG29-84-K-0293 ..... N88-27935
DAAG29-85-C-0018 ..... N88-27485
DAAG29-85-K-0056 ..... N88-27535
DAAG29-85-K-0167 ..... N88-27935
DAAJ02-86-C-0030 ..... N88-27559
DAAJ09-87-C-A043 ..... N88-27197
N88-27198
DAAK11-83-R-0105 ..... N88-27486
DAAK70-82-C-0001 ..... N88-27266
DAAK70-85-C-0007 ..... N88-27266
N88-27347
N88-27559
DAAK70-87-C-0043 ..... N88-27347
DAAL03-86-G-0003 ..... N88-27537
DAAL03-86-K-0019 ..... N88-27582
DAAL03-86-K-0133 ..... N88-27312
N88-27313
DAAL03-86-K-0171 ..... N88-27847
DAAL03-87-G-0066 ..... N88-27800
DAAL03-87-K-0028 ..... N88-27487
N88-27488
DACA76-85-C-0010 ..... N88-27819
DACW72-86-C-0004 ..... N88-27404
DAII-82-35-178-00-790-75-00-19 ..... N88-27959
DAJA45-85-C-0028 ..... N88-27655
DAJA45-85-C-0052 ..... N88-27348
DAJA45-86-C-0007 ..... N88-27561
DAJA45-86-C-0028 ..... N88-27827
DAJA45-86-C-0034 ..... N88-27237
DAJA45-86-C-0039 ..... N88-27433
DAJA45-86-C-0043 ..... N88-27206
DAJA45-86-C-0049 ..... N88-27615
DAJA45-87-C-0031 ..... N88-27320
DAJA45-87-C-0038 ..... N88-27830
DAJA45-87-C-0042 ..... N88-27482
DAJA45-88-C-0006 ..... N88-27937
DAMD17-85-C-5321 ..... N88-27737
DASG60-87-C-0087 ..... N88-27167
DCIEM-W7711-6-9019 ..... N88-27697
DE-AC02-76CH-00016 ..... N88-27311
N88-27884
DE-AC02-76EV-03566 ..... N88-27682
DE-AC02-80ER-10590 ..... N88-27724
DE-AC02-82ER-40063 ..... N88-27983
DE-AC02-83CH-10093 ..... N88-27622
N88-27623
N88-27629
N88-27630
N88-27633
N88-27723
N88-27944
N88-27975
DE-AC02-87ER-40325 ..... N88-27996
DE-AC03-76SF-00098 ..... N88-27270
N88-27290
N88-27291
N88-27325
N88-27326
N88-27460
N88-27498
N88-27505
N88-27725
N88-27940
N88-27948
N88-27951
DE-AC04-76DP-00053 ..... N88-27350
DE-AC04-76DP-00656 ..... N88-27530
DE-AC04-76DP-00789 ..... N88-27188
N88-27189
N88-27218
N88-27222
N88-27268
N88-27274
N88-27275
N88-27276
N88-27289
N88-27299
N88-27327
N88-27328
N88-27333
N88-27334
N88-27335
N88-27349
N88-27352
N88-27419
N88-27438
N88-27448
N88-27449
N88-27450
N88-27451
N88-27453
N88-27454
N88-27455
N88-27456
N88-27458
N88-27463
N88-27491
N88-27496
N88-27497
N88-27526
N88-27527
N88-27545
N88-27547
N88-27564
N88-27568
N88-27590
N88-27591
N88-27592
N88-27595
N88-27596
N88-27624
N88-27631
N88-27632
N88-27635
N88-27636
N88-27637
N88-27671
N88-27757
N88-27779
N88-27780
N88-27786
N88-27787
N88-27857
N88-27859
N88-27894
N88-27899
N88-27926
N88-27972
DE-AC04-78DR-00789 ..... N88-27269
N88-27529
DE-AC05-84OR-21400 ..... N88-27207
N88-27241
N88-27272
N88-27277
N88-27279
N88-27293
N88-27301
N88-27302
N88-27303
N88-27323
N88-27324
N88-27331
N88-27554
N88-27575
N88-27603
N88-27625
N88-27643
N88-27648
N88-27758
N88-27816
N88-27839
N88-27858
N88-27885
N88-27912
N88-27942
N88-27950
N88-27965
N88-27977
DE-AC05-84OS-21400 ..... N88-27528

DE-AC05-84OT-21400 ..... N88-27568
N88-27594
DE-AC06-76RL-01830 ..... N88-27459
N88-27546
N88-27660
N88-27672
N88-27674
DE-AC06-87RL-10930 ..... N88-27895
DE-AC09-76SR-00001 ..... N88-27618
DE-AC11-76PN-00014 ..... N88-27784
DE-AS04-86AL-38221 ..... N88-27565
DE-FC08-85DP-40200 ..... N88-27544
N88-27896
DE-FC22-83FE-60149 ..... N88-27322
DE-FG01-86CE-31010 ..... N88-27626
DE-FG02-84ER-45136 ..... N88-27605
DE-FG02-85ER-13396 ..... N88-27492
DE-FG02-85ER-45213 ..... N88-27294
DE-FG02-85ER-45214 ..... N88-27304
DE-FG02-85ER-53212 ..... N88-27911
DE-FG02-86ER-45250 ..... N88-27941
DE-FG02-86ER-53218 ..... N88-27901
DE-FG02-86ER-53227 ..... N88-27904
DE-FG02-86ER-60422 ..... N88-27673
DE-FG02-87ER-13744 ..... N88-27882
DE-FG02-87ER-25026 ..... N88-27840
DE-FG02-87ER-45263 ..... N88-27954
DE-FG02-87ER25026 ..... N88-27817
DE-FG03-86ER-53220 ..... N88-27908
DE-FG22-85PC-80523 ..... N88-27452
DFG-EB-56/11-1 ..... N88-27663
DFG-GE-317/4-4 ..... N88-27510
DFG-MI-149/2-1 ..... N88-27551
DFG-149/2-2 ..... N88-27551
DRET-84-34-584-00-470-75-01 ..... N88-27339
DRET-84-166 ..... N88-27337
DRET-85-34-443 ..... N88-27577
DRET-85-34-444 ..... N88-27308
DRET-85-34-489 ..... N88-27249
DRET-85-112 ..... N88-27338
DRET-85/053 ..... N88-27878
DRET-87-820 ..... N88-27208
N88-27209
DTFA01-80-Y-10546 ..... N88-27407
EPA-68-02-4190 ..... N88-27648
EPA-68-02-4330 ..... N88-27645
EY01319 ..... N88-27692
F04701-82-C-0083 ..... N88-27931
F04701-85-C-0086 ..... N88-27231
N88-27234
N88-27400
N88-27425
N88-27428
N88-27434
N88-27560
N88-27620
N88-27653
N88-27656
N88-27668
N88-27933
N88-27934
F08635-85-C-0122 ..... N88-27346
F09603-85-C-1224 ..... N88-27186
F19628-83-K-0014 ..... N88-27657
F19628-83-K-0040 ..... N88-27658
F19628-84-K-0015 ..... N88-27886
F19628-85-C-0002 ..... N88-27444
F19628-85-K-0038 ..... N88-27445
F19628-87-C-0110 ..... N88-27993
F29601-84-C-0060 ..... N88-27398
F30602-81-C-0193 ..... N88-27809
F30602-84-C-0153 ..... N88-27430
F33615-84-C-2479 ..... N88-27483
F33615-85-C-3623 ..... N88-27753
F49620-79-C-0233 ..... N88-27696
F49620-82-C-0014 ..... N88-27440
F49620-83-C-0059 ..... N88-27699
F49620-85-C-0002 ..... N88-27929
F49620-85-C-0006 ..... N88-27828
N88-27829
N88-27834
N88-27835
N88-27853
N88-27856
F49620-85-C-0013 ..... N88-27355
F49620-85-C-0128 ..... N88-27585
F49620-85-C-0144 ..... N88-27826
N88-27848
N88-27849
N88-27850
N88-27851
N88-27855
F49620-86-C-0011 ..... N88-27238
F49620-86-C-0018 ..... N88-27807
N88-27808
F49620-86-C-0037 ..... N88-27734
N88-27807
N88-27808
F49620-86-C-0098 ..... N88-27997
F49620-86-C-0131 ..... N88-27747
F49620-86-K-0009 ..... N88-27587
F49620-86-K-0010 ..... N88-27583
F49620-87-C-0088 ..... N88-27810
F49620-87-C-0110 ..... N88-27810
GRI-5087-260-1444 ..... N88-27271
HD22271 ..... N88-27692
MDA903-84-C-0243 ..... N88-27556
MDA903-85-C-0139 ..... N88-27971
MDA903-85-C-0215 ..... N88-27439
MH40703 ..... N88-27692
MIPR-87-0003 ..... N88-27470
NAG1-363 ..... N88-27490
NAG1-621 ..... N88-27230
NAG1-625 ..... N88-27168
NAG1-641 ..... N88-27173
NAG1-762 ..... N88-27877
NAG1-825 ..... N88-27242
NAG3-433 ..... N88-27621
NAG3-465 ..... N88-27611
NAG5-873 ..... N88-27650
NAG8-542 ..... N88-27224
N88-27225
NASA ORDER A-30146-C N88-27205
NASA ORDER C-99066-G N88-27799
NASW-4307 ..... N88-27336
NAS1-17993 ..... N88-27508
NAS1-18029 ..... N88-27196
NAS1-18107 ..... N88-27164
NAS1-18276 ..... N88-27172
NAS3-24105 ..... N88-27520
NAS7-918 ..... N88-27220
NAS8-30490 ..... N88-27226
NAS8-34715 ..... N88-27254
N88-27255
NAS8-35975 ..... N88-27676
NAS9-16374 ..... N88-27755
NAS9-17307 ..... N88-27754
NAS9-17677 ..... N88-27760
NAS9-17681 ..... N88-27180
NCC1-93 ..... N88-27593
NCC2-322 ..... N88-27986
NCC2-333 ..... N88-27562
N88-27563
NCC2-462 ..... N88-27798
NGR-05-020-668 ..... N88-27996
N88-27998
NSF ATM-87-09659 ..... N88-27668
NSF CCR-87-02403 ..... N88-27812
NSF DCR-85-03662 ..... N88-27801
NSF DCR-85-11190 ..... N88-27766
NSF DMS-85-21687 ..... N88-27832
NSF DMS-87-03804 ..... N88-27851
NSF DMS-87-13103 ..... N88-27851
NSF IRI-84-17756 ..... N88-27734
NSF IRI-86-16644 ..... N88-27767
N88-27768
N88-27769
NSG-1321 ..... N88-27606
NSG-5265 ..... N88-27662
N00014-80-C-0521 ..... N88-27286
N00014-80-C-0622 ..... N88-27824
N88-27825
N00014-81-C-0452 ..... N88-27446
N00014-83-K-0125 ..... N88-27766
N88-27801
N88-27802
N00014-83-K-0258 ..... N88-27617
N00014-83-K-0365 ..... N88-27994
N00014-84-C-0484 ..... N88-27967
N00014-84-K-0097 ..... N88-27872
N00014-84-K-0201 ..... N88-27431
N88-27432
N00014-84-K-0252 ..... N88-27586
N00014-84-K-0583 ..... N88-27905
N00014-84-K-0658 ..... N88-27262
N00014-84-K-5553 ..... N88-27778
N00014-85-C-0680 ..... N88-27680
N00014-85-C-0857 ..... N88-27233
N00014-85-K-0124 ..... N88-27767
N88-27768
N88-27769
N88-27819
N00014-85-K-0168 ..... N88-27802
N00014-85-K-0177 ..... N88-27930
N00014-85-K-0222 ..... N88-27261
N00014-85-K-0292 ..... N88-27828
N88-27829
N88-27835
N88-27853
N00014-85-K-0403 ..... N88-27820
N00014-85-K-0581 ..... N88-27667
N00014-85-K-0667 ..... N88-27235
N00014-85-K-0686 ..... N88-27522
N00014-85-K-0808 ..... N88-27236
N00014-86-K-0043 ..... N88-27938
N00014-86-K-0156 ..... N88-27854
N00014-86-K-0236 ..... N88-27426
N88-27427
N00014-86-K-0252 ..... N88-27318
N00014-86-K-0305 ..... N88-27932
N00014-86-K-0310 ..... N88-27471
N88-27472
N00014-86-K-0345 ..... N88-27314
N00014-86-K-0492 ..... N88-27970
N00014-86-K-0716 ..... N88-27736
N00014-86-K-0742 ..... N88-27763
N00014-86-K-2001 ..... N88-27664
N00014-86-K-2005 ..... N88-27534
N88-27536
N00014-87-C-0050 ..... N88-27221
N00014-87-C-0127 ..... N88-27872
N00014-87-C-0705 ..... N88-27429
N00014-87-C-0763 ..... N88-27773
N00014-87-F-0066 ..... N88-27538
N00014-87-K-0145 ..... N88-27722
N00014-87-K-0394 ..... N88-27671
N00014-87-K-0452 ..... N88-27316
N88-27317
N00014-87-K-0467 ..... N88-27825
N00014-87-K-0517 ..... N88-27321
N00014-87-WX-24234 ..... N88-27821
N00039-84-C-0070 ..... N88-27414
N00167-87-C-0021 ..... N88-27875
N88-27876
N60921-86-C-0209 ..... N88-27441
N66001-87-C-0187 ..... N88-27772
RM3-3-M-20 ..... N88-27970
S40-0021 ..... N88-27722
W-31-109-ENG-38 ..... N88-27305
N88-27306
N88-27461
N88-27638
N88-27639
N88-27952
N88-27953
W-7405-ENG-36 ..... N88-27213
N88-27489
N88-27541
N88-27670
N88-27861
N88-27949
N88-27987
N88-27990
W-7405-ENG-48 ..... N88-27273
N88-27288
N88-27298
N88-27332
N88-27351
N88-27420
N88-27422
N88-27457
N88-27462
N88-27496
N88-27506
N88-27540
N88-27542
N88-27543
N88-27548
N88-27549
N88-27604
N88-27750
N88-27781
N88-27782
N88-27785
N88-27797
N88-27805
N88-27817
N88-27838
N88-27838
N88-27841
N88-27869
N88-27909
N88-27939
N88-27989
W-31109-ENG-38 ..... N88-27300
505-05-11 ..... N88-27200
505-60-11 ..... N88-27519
505-60-21-02 ..... N88-27168
505-61-11-01 ..... N88-27881
505-62-0K N88-27201
505-62-81 ..... N88-27174
505-63-1B N88-27611
N88-27796
N88-27799
505-66-41-06 ..... N88-27196
505-69-61-01 ..... N88-27182
505-90-21-01 ..... N88-27164
506-40-11-08 ..... N88-27172

506-41-21 ..... N88-27267
506-41-41-01 ..... N88-27553
506-43-31 ..... N88-27798
506-46-21-05 ..... N88-27447
582-01-11 ..... N88-27520
584-01-41 ..... N88-27507
586-01-11 ..... N88-27310
650-60-20 ..... N88-27424
665-45-30-01 ..... N88-27677
778-35-13 ..... N88-27980
992-21-01 ..... N88-27148

REPORT/ACCESSION NUMBER INDEX

Typical Report Number Index Listing

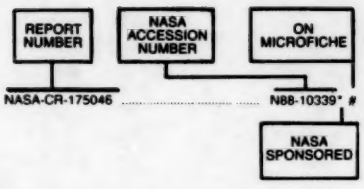

Listings in this index are arranged alphanumerically by report number. The NASA accession number denotes the number by which the citation is identified. An asterisk (*) indicates that the item is a NASA report. A pound sign (#) indicates that the item is available on microfiche.

A-86381 ..... N88-27148* #
A-88172 ..... N88-27507* #
A-88211 ..... N88-27519* #

AAE-88-1 ..... N88-27581 #

ACSC-88-0130 ..... N88-27969 #
ACSC-88-0330 ..... N88-27175 #
ACSC-88-2050 ..... N88-27184 #

AD-A189137 ..... N88-27921 #
AD-A191122 ..... N88-27355 #
AD-A191584 ..... N88-27751 #
AD-A192274 ..... N88-27261 #
AD-A192296 ..... N88-27581 #
AD-A192299 ..... N88-27664 #
AD-A192305 ..... N88-27231 #
AD-A192306 ..... N88-27425 #
AD-A192307 ..... N88-27928 #
AD-A192308 ..... N88-27280 #
AD-A192310 ..... N88-27262 #
AD-A192312 ..... N88-27426 #
AD-A192313 ..... N88-27427 #
AD-A192315 ..... N88-27652 #
AD-A192321 ..... N88-27819 #
AD-A192330 ..... N88-27678 #
AD-A192333 ..... N88-27281 #
AD-A192335 ..... N88-27282 #
AD-A192353 ..... N88-27845 #
AD-A192384 ..... N88-27428 #
AD-A192385 ..... N88-27820 #
AD-A192390 ..... N88-27522 #
AD-A192396 ..... N88-27762 #
AD-A192397 ..... N88-27469 #
AD-A192401 ..... N88-27846 #
AD-A192424 ..... N88-27969 #
AD-A192426 ..... N88-27556 #
AD-A192431 ..... N88-27470 #
AD-A192436 ..... N88-27398 #
AD-A192437 ..... N88-27763 #
AD-A192440 ..... N88-27429 #
AD-A192445 ..... N88-27752 #
AD-A192452 ..... N88-27534 #
AD-A192460 ..... N88-27430 #
AD-A192463 ..... N88-27312 #
AD-A192464 ..... N88-27313 #
AD-A192474 ..... N88-27471 #
AD-A192475 ..... N88-27472 #
AD-A192476 ..... N88-27821 #
AD-A192477 ..... N88-27800 #
AD-A192478 ..... N88-27679 #
AD-A192481 ..... N88-27431 #
AD-A192482 ..... N88-27432 #
AD-A192485 ..... N88-27314 #
AD-A192486 ..... N88-27346 #
AD-A192505 ..... N88-27886 #
AD-A192514 ..... N88-27535 #
AD-A192536 ..... N88-27347 #
AD-A192541 ..... N88-27536 #
AD-A192548 ..... N88-27764 #
AD-A192549 ..... N88-27582 #
AD-A192551 ..... N88-27165 #
AD-A192572 ..... N88-27473 #
AD-A192594 ..... N88-27765 #
AD-A192597 ..... N88-27727 #
AD-A192598 ..... N88-27728 #
AD-A192600 ..... N88-27729 #
AD-A192601 ..... N88-27730 #
AD-A192602 ..... N88-27731 #
AD-A192606 ..... N88-27732 #
AD-A192663 ..... N88-27612 #
AD-A192687 ..... N88-27722 #
AD-A192692 ..... N88-27433 #
AD-A192697 ..... N88-27733 #
AD-A192699 ..... N88-27403 #
AD-A192706 ..... N88-27474 #
AD-A192710 ..... N88-27263 #
AD-A192712 ..... N88-27847 #
AD-A192713 ..... N88-27822 #
AD-A192714 ..... N88-27823 #
AD-A192715 ..... N88-27734 #
AD-A192716 ..... N88-27807 #
AD-A192717 ..... N88-27808 #
AD-A192723 ..... N88-27801 #
AD-A192724 ..... N88-27824 #
AD-A192725 ..... N88-27766 #
AD-A192726 ..... N88-27802 #
AD-A192727 ..... N88-27825 #
AD-A192735 ..... N88-27613 #
AD-A192737 ..... N88-27665 #
AD-A192738 ..... N88-27614 #
AD-A192765 ..... N88-27197 #
AD-A192766 ..... N88-27198 #
AD-A192781 ..... N88-27206 #
AD-A192782 ..... N88-27767 #
AD-A192783 ..... N88-27768 #
AD-A192784 ..... N88-27769 #
AD-A192786 ..... N88-27770 #
AD-A192794 ..... N88-27860 #
AD-A192806 ..... N88-27475 #
AD-A192816 ..... N88-27434 #
AD-A192827 ..... N88-27166 #
AD-A192828 ..... N88-27404 #
AD-A192833 ..... N88-27803 #
AD-A192837 ..... N88-27929 #
AD-A192838 ..... N88-27848 #
AD-A192839 ..... N88-27826 #
AD-A192840 ..... N88-27743 #
AD-A192841 ..... N88-27849 #
AD-A192844 ..... N88-27537 #
AD-A192845 ..... N88-27167 #
AD-A192846 ..... N88-27221 #
AD-A192848 ..... N88-27809 #
AD-A192851 ..... N88-27217 #
AD-A192852 ..... N88-27735 #
AD-A192854 ..... N88-27871 #
AD-A192872 ..... N88-27175 #
AD-A192884 ..... N88-27997 #
AD-A192893 ..... N88-27850 #
AD-A192895 ..... N88-27851 #
AD-A192896 ..... N88-27810 #
AD-A192921 ..... N88-27264 #
AD-A192922 ..... N88-27315 #
AD-A192923 ..... N88-27771 #
AD-A192924 ..... N88-27852 #
AD-A192927 ..... N88-27183 #
AD-A192928 ..... N88-27523 #
AD-A192937 ..... N88-27184 #
AD-A192943 ..... N88-27476 #
AD-A192944 ..... N88-27668 #
AD-A192955 ..... N88-27265 #
AD-A192956 ..... N88-27435 #
AD-A192957 ..... N88-27583 #
AD-A192959 ..... N88-27436 #
AD-A192963 ..... N88-27930 #
AD-A192971 ..... N88-27524 #
AD-A192997 ..... N88-27477 #
AD-A193017 ..... N88-27437 #
AD-A193022 ..... N88-27653 #
AD-A193029 ..... N88-27283 #
AD-A193030 ..... N88-27177 #
AD-A193032 ..... N88-27827 #
AD-A193044 ..... N88-27931 #
AD-A193046 ..... N88-27232 #
AD-A193050 ..... N88-27584 #
AD-A193055 ..... N88-27266 #
AD-A193056 ..... N88-27405 #
AD-A193057 ..... N88-27853 #
AD-A193059 ..... N88-27828 #
AD-A193060 ..... N88-27829 #
AD-A193061 ..... N88-27744 #
AD-A193063 ..... N88-27478 #
AD-A193064 ..... N88-27479 #
AD-A193065 ..... N88-27481 #
AD-A193066 ..... N88-27905 #
AD-A193067 ..... N88-27615 #
AD-A193071 ..... N88-27616 #
AD-A193076 ..... N88-27745 #
AD-A193078 ..... N88-27482 #
AD-A193079 ..... N88-27186 #
AD-A193080 ..... N88-27348 #
AD-A193086 ..... N88-27970 #
AD-A193089 ..... N88-27407 #
AD-A193093 ..... N88-27667 #
AD-A193094 ..... N88-27408 #
AD-A193095 ..... N88-27772 #
AD-A193098 ..... N88-27439 #
AD-A193099 ..... N88-27976 #
AD-A193100 ..... N88-27538 #
AD-A193101 ..... N88-27400 #
AD-A193102 ..... N88-27746 #
AD-A193104 ..... N88-27736 #
AD-A193109 ..... N88-27483 #
AD-A193110 ..... N88-27194 #
AD-A193119 ..... N88-27557 #
AD-A193120 ..... N88-27178 #
AD-A193123 ..... N88-27440 #
AD-A193126 ..... N88-27316 #
AD-A193127 ..... N88-27317 #
AD-A193128 ..... N88-27318 #
AD-A193129 ..... N88-27654 #
AD-A193131 ..... N88-27409 #
AD-A193132 ..... N88-27410 #
AD-A193133 ..... N88-27319 #
AD-A193134 ..... N88-27411 #
AD-A193137 ..... N88-27630 #
AD-A193142 ..... N88-27655 #
AD-A193144 ..... N88-27233 #
AD-A193147 ..... N88-27906 #
AD-A193150 ..... N88-27773 #
AD-A193153 ..... N88-27558 #
AD-A193165 ..... N88-27484 #
AD-A193173 ..... N88-27485 #
AD-A193176 ..... N88-27932 #
AD-A193181 ..... N88-27811 #
AD-A193185 ..... N88-27887 #
AD-A193190 ..... N88-27854 #
AD-A193191 ..... N88-27855 #
AD-A193197 ..... N88-27486 #
AD-A193198 ..... N88-27412 #
AD-A193199 ..... N88-27804 #
AD-A193200 ..... N88-27656 #
AD-A193204 ..... N88-27234 #
AD-A193208 ..... N88-27441 #
AD-A193211 ..... N88-27235 #
AD-A193213 ..... N88-27559 #
AD-A193216 ..... N88-27831 #
AD-A193218 ..... N88-27868 #
AD-A193221 ..... N88-27585 #
AD-A193224 ..... N88-27284 #
AD-A193225 ..... N88-27442 #
AD-A193226 ..... N88-27774 #
AD-A193227 ..... N88-27236 #
AD-A193228 ..... N88-27672 #
AD-A193237 ..... N88-27737 #
AD-A193241 ..... N88-27560 #
AD-A193242 ..... N88-27933 #
AD-A193244 ..... N88-27237 #
AD-A193249 ..... N88-27620 #
AD-A193250 ..... N88-27812 #
AD-A193253 ..... N88-27832 #
AD-A193276 ..... N88-27934 #
AD-A193282 ..... N88-27775 #
AD-A193283 ..... N88-27413 #
AD-A193284 ..... N88-27873 #
AD-A193289 ..... N88-27753 #
AD-A193291 ..... N88-27993 #

AD-A193293 ..... N88-27935 #
AD-A193300 ..... N88-27936 #
AD-A193301 ..... N88-27195 #
AD-A193302 ..... N88-27179 #
AD-A193303 ..... N88-27285 #
AD-A193305 ..... N88-27738 #
AD-A193307 ..... N88-27617 #
AD-A193310 ..... N88-27443 #
AD-A193311 ..... N88-27586 #
AD-A193317 ..... N88-27587 #
AD-A193318 ..... N88-27633 #
AD-A193319 ..... N88-27674 #
AD-A193320 ..... N88-27238 #
AD-A193324 ..... N88-27414 #
AD-A193325 ..... N88-27813 #
AD-A193330 ..... N88-27776 #
AD-A193334 ..... N88-27320 #
AD-A193336 ..... N88-27937 #
AD-A193337 ..... N88-27444 #
AD-A193340 ..... N88-27286 #
AD-A193356 ..... N88-27487 #
AD-A193357 ..... N88-27488 #
AD-A193358 ..... N88-27834 #
AD-A193359 ..... N88-27445 #
AD-A193360 ..... N88-27581 #
AD-A193362 ..... N88-27971 #
AD-A193363 ..... N88-27680 #
AD-A193366 ..... N88-27539 #
AD-A193368 ..... N88-27657 #
AD-A193369 ..... N88-27658 #
AD-A193379 ..... N88-27659 #
AD-A193380 ..... N88-27446 #
AD-A193385 ..... N88-27656 #
AD-A193386 ..... N88-27875 #
AD-A193387 ..... N88-27876 #
AD-A193389 ..... N88-27967 #
AD-A193390 ..... N88-27321 #
AD-A193392 ..... N88-27747 #
AD-A193396 ..... N88-27994 #
AD-A193399 ..... N88-27835 #
AD-A193401 ..... N88-27907 #
AD-A193402 ..... N88-27415 #
AD-A193403 ..... N88-27588 #
AD-A193415 ..... N88-27777 #
AD-A193419 ..... N88-27739 #
AD-A193420 ..... N88-27287 #
AD-A193421 ..... N88-27740 #
AD-A193423 ..... N88-27399 #
AD-A193427 ..... N88-27589 #
AD-A193428 ..... N88-27187 #
AD-A193432 ..... N88-27938 #
AD-A193436 ..... N88-27778 #
AD-A193440 ..... N88-27741 #

AD-E801594 ..... N88-27262 #
AD-E801594 ..... N88-27280 #
AD-E801594 ..... N88-27281 #
AD-E801594 ..... N88-27282 #
AD-E801594 ..... N88-27426 #
AD-E801594 ..... N88-27427 #
AD-E801594 ..... N88-27652 #
AD-E801594 ..... N88-27678 #
AD-E801594 ..... N88-27819 #

AFAL-TR-88-018 ..... N88-27475 #

AFESC/ESL-TR-86-64 ..... N88-27346 #
AFESC/ESL-TR-86-65 ..... N88-27398 #

AFGL-ERP-961 ..... N88-27659 #

AFGL-TR-87-0235 ..... N88-27659 #
AFGL-TR-87-0274 ..... N88-27886 #
AFGL-TR-88-0012 ..... N88-27993 #
AFGL-TR-88-0018 ..... N88-27658 #
AFGL-TR-88-0020 ..... N88-27657 #
AFGL-TR-88-0031 ..... N88-27539 #

AFHRL-TP-87-62 ..... N88-27746 #

AFIT/GE/ENG/87D-25 ..... N88-27803 #
AFIT/GE/ENG/87D-54 ..... N88-27178 #
AFIT/GE/ENG/87D-68 ..... N88-27557 #

AFOSR-87-1710TR ..... N88-27747 #
AFOSR-88-0047TR ..... N88-27846 #
AFOSR-88-0199TR ..... N88-27856 #
AFOSR-88-0202TR ..... N88-27835 #
AFOSR-88-0204TR ..... N88-27834 #
AFOSR-88-0210TR-VOL-2 ..... N88-27355 #
AFOSR-88-0246TR ..... N88-27845 #
AFOSR-88-0247TR ..... N88-27470 #
AFOSR-88-0256TR ..... N88-27473 #
AFOSR-88-0266TR ..... N88-27581 #
AFOSR-88-0267TR ..... N88-27165 #
AFOSR-88-0271TR ..... N88-27477 #
AFOSR-88-0277TR ..... N88-27585 #
AFOSR-88-0284TR ..... N88-27238 #
AFOSR-88-0285TR ..... N88-27284 #
AFOSR-88-0288TR ..... N88-27745 #
AFOSR-88-0291TR ..... N88-27583 #
AFOSR-88-0292TR ..... N88-27484 #
AFOSR-88-0293TR ..... N88-27476 #
AFOSR-88-0296TR ..... N88-27265 #
AFOSR-88-0301TR ..... N88-27936 #
AFOSR-88-0303TR ..... N88-27436 #
AFOSR-88-0306TR ..... N88-27435 #
AFOSR-88-0307TR ..... N88-27440 #
AFOSR-88-0317TR ..... N88-27666 #
AFOSR-88-0325TR ..... N88-27264 #
AFOSR-88-0349TR ..... N88-27849 #
AFOSR-88-0350TR ..... N88-27848 #
AFOSR-88-0356TR ..... N88-27826 #
AFOSR-88-0360TR ..... N88-27850 #
AFOSR-88-0361TR ..... N88-27833 #
AFOSR-88-0362TR ..... N88-27874 #
AFOSR-88-0366TR ..... N88-27813 #
AFOSR-88-0368TR ..... N88-27589 #
AFOSR-88-0369TR ..... N88-27587 #
AFOSR-88-0376TR ..... N88-27740 #
AFOSR-88-0384TR ..... N88-27734 #
AFOSR-88-0387TR ..... N88-27823 #
AFOSR-88-0388TR ..... N88-27822 #
AFOSR-88-0394TR ..... N88-27847 #
AFOSR-88-0396TR ..... N88-27855 #
AFOSR-88-0398TR ..... N88-27853 #
AFOSR-88-0399TR ..... N88-27829 #
AFOSR-88-0400TR ..... N88-27828 #
AFOSR-88-0405TR ..... N88-27183 #
AFOSR-88-0407TR ..... N88-27852 #
AFOSR-88-0409TR ..... N88-27315 #
AFOSR-88-0420TR ..... N88-27851 #
AFOSR-88-0427TR ..... N88-27263 #
AFOSR-88-0431TR ..... N88-27807 #
AFOSR-88-0432TR ..... N88-27808 #
AFOSR-88-0440TR ..... N88-27743 #
AFOSR-88-0485TR ..... N88-27744 #
AFOSR-88-0488TR ..... N88-27478 #
AFOSR-88-0493TR ..... N88-27831 #
AFOSR-88-0503TR ..... N88-27479 #
AFOSR-88-0552TR ..... N88-27997 #
AFOSR-88-0561TR ..... N88-27771 #
AFOSR-88-0573TR ..... N88-27523 #
AFOSR-88-0575TR ..... N88-27810 #

AFWAL-TR-87-2061 ..... N88-27524 #
AFWAL-TR-87-2077 ..... N88-27483 #
AFWAL-TR-87-3108 ..... N88-27753 #
AFWAL-TR-88-1000 ..... N88-27194 #
AFWAL-TR-88-4061 ..... N88-27287 #

AFWL-TR-86-133 ..... N88-27852 #

AGARD-AG-238-ADD ..... N88-27185 #
AGARD-AG-300-VOL-7 ..... N88-27406 #
AGARD-AG-300-VOL-8 ..... N88-27525 #

AGARD-AR-246 ..... N88-27480 #

AGARD-CP-432 ..... N88-27683 #

AGARD-R-752 ..... N88-27669 #
AGARD-R-759 ..... N88-27147 #
AGARD-R-765 ..... N88-27193 #

AI-M-952 ..... N88-27819 #
AI-M-959-PT-2 ..... N88-27768 #
AI-M-1004 ..... N88-27769 #
AI-M-1005 ..... N88-27767 #

AI/DS-TR-3139-01 ..... N88-27404 #

AMSEL-NV-1-21 ..... N88-27928 #

APR-3 ..... N88-27304 #

ARCCB-TR-88005 ..... N88-27280 #

ARO-20244.10-EL ..... N88-27776 #
ARO-20927.22-MA ..... N88-27764 #
ARO-21438.41-EL ..... N88-27437 #
ARO-21453.12-MA ..... N88-27812 #
ARO-22279.25-PH ..... N88-27535 #
ARO-22967.4-EG ..... N88-27582 #
ARO-23187.3-PH ..... N88-27935 #
ARO-23306.156-MA ..... N88-27485 #
ARO-23496.5-PH-H ..... N88-27537 #
ARO-24165.2-MS ..... N88-27313 #
ARO-24165.3-MS ..... N88-27312 #

AVF-VSR-90.0987 ..... N88-27777 #

AVF-87-04-09-VRX ..... N88-27777 #

AVSCOM-TR-88-C-025 ..... N88-27201* #

BBN-6710 ..... N88-27875 #
BBN-6715 ..... N88-27876 #

BFLRF-241 ..... N88-27347 #
BFLRF-248 ..... N88-27266 #

BNL-41103 ..... N88-27884 #
BNL-41200 ..... N88-27311 #

BONN-MITT-73 ..... N88-27216 #

BRA-88-W016R ..... N88-27680 #

BRL-CR-587 ..... N88-27486 #

BRL-MR-5646 ..... N88-27217 #

C-868 ..... N88-27441 #

CBPF-MO-004/87 ..... N88-27888 #

CBPF-NF-055/87 ..... N88-27943 #

CERL-TR-M-88/09 ..... N88-27285 #

CJT4 ..... N88-27539 #

CML-88-3 ..... N88-27242* #

CMS-TSR-88-11 ..... N88-27488 #
CMS-TSR-88-12 ..... N88-27487 #
CMS-TSR-88-18 ..... N88-27832 #

CNES-NT-121 ..... N88-28000 #

CONF-870155 ..... N88-27885 #
CONF-870155-9 ..... N88-27885 #
CONF-870766-1 ..... N88-27951 #
CONF-871060-3 ..... N88-27543 #
CONF-871124-100 ..... N88-27298 #
CONF-871227-1 ..... N88-27894 #
CONF-871254 ..... N88-27541 #
CONF-871254-10 ..... N88-27541 #
CONF-880122-11 ..... N88-27895 #
CONF-880206 ..... N88-27940 #
CONF-880206-8 ..... N88-27940 #
CONF-880210-1 ..... N88-27939 #
CONF-880215-4 ..... N88-27723 #
CONF-880317-1 ..... N88-27450 #
CONF-880317-2 ..... N88-27950 #
CONF-880331-3 ..... N88-27963 #
CONF-880364-16 ..... N88-27781 #
CONF-880383-2 ..... N88-27299 #
CONF-880408-10 ..... N88-27910 #
CONF-880408-14 ..... N88-27332 #
CONF-880408-24 ..... N88-27333 #
CONF-880408-25 ..... N88-27328 #
CONF-880408-26 ..... N88-27275 #
CONF-880408-27 ..... N88-27334 #
CONF-880408-28 ..... N88-27335 #
CONF-880425-1 ..... N88-27528 #
CONF-880434-1 ..... N88-27898 #
CONF-880435-1 ..... N88-27884 #
CONF-880463-3 ..... N88-27660 #
CONF-880466-7 ..... N88-27953 #
CONF-880478-12 ..... N88-27909 #
CONF-880487-1 ..... N88-27575 #
CONF-880488-4 ..... N88-27300 #
CONF-880504-3 ..... N88-27952 #
CONF-880516-1 ..... N88-27750 #
CONF-880547-2 ..... N88-27564 #
CONF-880577-1 ..... N88-27780 #
CONF-880577-5 ..... N88-27797 #
CONF-880579-2 ..... N88-27545 #
CONF-880586-1 ..... N88-27288 #
CONF-880587-1 ..... N88-27595 #
CONF-880594-1 ..... N88-27213 #
CONF-880598-1 ..... N88-27454 #
CONF-880602-4 ..... N88-27268 #
CONF-880606-3 ..... N88-27306 #
CONF-880615-1 ..... N88-27629 #
CONF-880655-3 ..... N88-27636 #
CONF-880655-4 ..... N88-27637 #
CONF-880657-1 ..... N88-27554 #
CONF-880665-2 ..... N88-27456 #
CONF-880665-3 ..... N88-27460 #
CONF-880665-4 ..... N88-27638 #
CONF-880669-1 ..... N88-27327 #
CONF-880671-2 ..... N88-27325 #
CONF-880672-2 ..... N88-27816 #
CONF-880689-2 ..... N88-27188 #
CONF-880693-2 ..... N88-27351 #

CONF-880702-1 ..... N88-27631 #
CONF-880702-13 ..... N88-27639 #
CONF-880705 ..... N88-27279 #
CONF-880705-1 ..... N88-27279 #
CONF-880705-2 ..... N88-27303 #
CONF-880716-2 ..... N88-27496 #
CONF-880716-3 ..... N88-27527 #
CONF-880716-5 ..... N88-27497 #
CONF-880716-6 ..... N88-27498 #
CONF-880719-5 ..... N88-27972 #
CONF-880724-3 ..... N88-27489 #
CONF-880730-2 ..... N88-27926 #
CONF-880733-1 ..... N88-27779 #
CONF-880740-3 ..... N88-27491 #
CONF-880741-2 ..... N88-27207 #
CONF-880744-1 ..... N88-27492 #
CONF-880750-4 ..... N88-27352 #
CONF-880750-6 ..... N88-27349 #
CONF-880750-7 ..... N88-27274 #
CONF-880750-11 ..... N88-27276 #
CONF-880764-1 ..... N88-27222 #
CONF-880766-1 ..... N88-27272 #
CONF-8611154-3 ..... N88-27542 #
CONF-8702142-1 ..... N88-27301 #
CONF-8704229-1 ..... N88-27894 #
CONF-8705282-1 ..... N88-27670 #
CONF-8707109 ..... N88-27925 #
CONF-8708148-4 ..... N88-27785 #
CONF-8708243-1 ..... N88-27987 #
CONF-8709110-21 ..... N88-27540 #
CONF-8709110-24 ..... N88-27549 #
CONF-8709155-2 ..... N88-27506 #
CONF-8710274-7 ..... N88-27996 #
CONF-8710283-5 ..... N88-27311 #
CONF-8710304-SUMM ..... N88-27269 #
CONF-8711172-1 ..... N88-27861 #
CONF-8711180-1 ..... N88-27290 #
CONF-8803113-2 ..... N88-27989 #
CONF-8804104-2 ..... N88-27990 #
CONF-8804112 ..... N88-27326 #
CONF-8804112-4 ..... N88-27326 #
CONF-8804112-5 ..... N88-27293 #
CONF-8804117-3 ..... N88-27305 #
CONF-8804118-1 ..... N88-27836 #
CONF-8804121-1 ..... N88-27289 #
CONF-8804122-1 ..... N88-27624* #
CONF-8804136-1 ..... N88-27805 #
CONF-8804140 ..... N88-27648 #
CONF-8804140-1 ..... N88-27648 #
CONF-8805101-2 ..... N88-27674 #
CONF-8805114-2 ..... N88-27786 #
CONF-8805118-1 ..... N88-27618 #
CONF-8805126 ..... N88-27912 #
CONF-8805126-1 ..... N88-27912 #
CONF-8805132-3 ..... N88-27457 #
CONF-8805132-6 ..... N88-27458 #
CONF-8805134-2 ..... N88-27942 #
CONF-8805134-3 ..... N88-27302 #
CONF-8805139-1 ..... N88-27452 #
CONF-8805141-1 ..... N88-27603 #
CONF-8806118-1 ..... N88-27568 #
CONF-8806127 ..... N88-27448 #
CONF-8806127-2 ..... N88-27455 #
CONF-8806127-3 ..... N88-27449 #
CONF-8806127-4 ..... N88-27448 #
CONF-8806127-5 ..... N88-27451 #
CONF-8806127-7 ..... N88-27461 #
CONF-8806131-1 ..... N88-27949 #
CONF-8806147-1 ..... N88-27838 #
CONF-8806149-1 ..... N88-27758 #
CONF-8806154-1 ..... N88-27839 #
CONF-8806155-1 ..... N88-27241 #

CONTRIB-1029 ..... N88-27681 #

CRC-APRAC-AP-11 ..... N88-27642 #

CRC-APRAC-CAPE-30-81-04A ..... N88-27641 #

CSL-11 ..... N88-27970 #

CSSA-ASTRO-88-13 ..... N88-27998* #

CU-CS-396-88 ..... N88-27812 #

DCIEM-87-RR-12 ..... N88-27697 #

DE87-013491 ..... N88-27750 #
DE88-001142 ..... N88-27633 #
DE88-001145 ..... N88-27975 #
DE88-001146 ..... N88-27723 #
DE88-001152 ..... N88-27629 #
DE88-001153 ..... N88-27630 #
DE88-001159 ..... N88-27622 #
DE88-001162 ..... N88-27623 #
DE88-001165 ..... N88-27944 #
DE88-001225 ..... N88-27322 #
DE88-001655 ..... N88-27694 #
DE88-004303 ..... N88-27489 #
DE88-004452 ..... N88-27496 #
DE88-005055 ..... N88-27554 #
DE88-005483 ..... N88-27926 #
DE88-006100 ..... N88-27779 #
DE88-006174 ..... N88-27816 #
DE88-006274 ..... N88-27268 #
DE88-006275 ..... N88-27564 #
DE88-006963 ..... N88-27207 #
DE88-007022 ..... N88-27540 #
DE88-007057 ..... N88-27492 #
DE88-007198 ..... N88-27780 #
DE88-007208 ..... N88-27491 #
DE88-007695 ..... N88-27453 #
DE88-007763 ..... N88-27882 #
DE88-007845 ..... N88-27331 #
DE88-007892 ..... N88-27541 #
DE88-007912 ..... N88-27861 #
DE88-008005 ..... N88-27438 #
DE88-008024 ..... N88-27901 #
DE88-008026 ..... N88-27781 #
DE88-008041 ..... N88-27288 #
DE88-008078 ..... N88-27884 #
DE88-008109 ..... N88-27545 #
DE88-008110 ..... N88-27972 #
DE88-008142 ..... N88-27757 #
DE88-008223 ..... N88-27575 #
DE88-008289 ..... N88-27634 #
DE88-008349 ..... N88-27939 #
DE88-008421 ..... N88-27904 #
DE88-008422 ..... N88-27911 #
DE88-008440 ..... N88-27544 #
DE88-008467 ..... N88-27269 #
DE88-008468 ..... N88-27898 #
DE88-008574 ..... N88-27817 #
DE88-008612 ..... N88-27978 #
DE88-008632 ..... N88-27672 #
DE88-008671 ..... N88-27631 #
DE88-008681 ..... N88-27351 #
DE88-008767 ..... N88-27996 #
DE88-008771 ..... N88-27352 #
DE88-008811 ..... N88-27595 #
DE88-008889 ..... N88-27909 #
DE88-008892 ..... N88-27542 #
DE88-008907 ..... N88-27797 #
DE88-008915 ..... N88-27332 #
DE88-008923 ..... N88-27782 #
DE88-008929 ..... N88-27908 #
DE88-008945 ..... N88-27323 #
DE88-008949 ..... N88-27965 #
DE88-008964 ..... N88-27526 #
DE88-008996 ..... N88-27324 #
DE88-009034 ..... N88-27565 #
DE88-009051 ..... N88-27298 #
DE88-009105 ..... N88-27941 #
DE88-009119 ..... N88-27990 #
DE88-009133 ..... N88-27670 #
DE88-009138 ..... N88-27987 #
DE88-009141 ..... N88-27213 #
DE88-009195 ..... N88-27895 #
DE88-009255 ..... N88-27289 #
DE88-009256 ..... N88-27454 #
DE88-009468 ..... N88-27624* #
DE88-009480 ..... N88-27660 #
DE88-009696 ..... N88-27349 #
DE88-009793 ..... N88-27671 #
DE88-009807 ..... N88-27270 #
DE88-009813 ..... N88-27290 #
DE88-009816 ..... N88-27940 #
DE88-009826 ..... N88-27836 #
DE88-009842 ..... N88-27325 #
DE88-009851 ..... N88-27568 #
DE88-009859 ..... N88-27546 #
DE88-010016 ..... N88-27300 #
DE88-010102 ..... N88-27590 #
DE88-010120 ..... N88-27963 #
DE88-010181 ..... N88-27682 #
DE88-010324 ..... N88-27188 #
DE88-010331 ..... N88-27419 #
DE88-010360 ..... N88-27725 #
DE88-010371 ..... N88-27218 #
DE88-010372 ..... N88-27596 #
DE88-010374 ..... N88-27632 #
DE88-010451 ..... N88-27885 #
DE88-010452 ..... N88-27942 #
DE88-010453 ..... N88-27648 #
DE88-010457 ..... N88-27301 #
DE88-010512 ..... N88-27857 #
DE88-010567 ..... N88-27448 #
DE88-010570 ..... N88-27527 #
DE88-010574 ..... N88-27452 #
DE88-010597 ..... N88-27420 #
DE88-010599 ..... N88-27273 #
DE88-010603 ..... N88-27635 #
DE88-010712 ..... N88-27805 #
DE88-010734 ..... N88-27591 #
DE88-010751 ..... N88-27658 #
DE88-010753 ..... N88-27625 #
DE88-010759 ..... N88-27643 #
DE88-010780 ..... N88-27977 #
DE88-010787 ..... N88-27350 #
DE88-010777 ..... N88-27505 #
DE88-010817 ..... N88-27528 #
DE88-010833 ..... N88-27222 #
DE88-010855 ..... N88-27948 #
DE88-010856 ..... N88-27291 #
DE88-010867 ..... N88-27963 #
DE88-010884 ..... N88-27326 #
DE88-010895 ..... N88-27618 #
DE88-010938 ..... N88-27949 #
DE88-010967 ..... N88-27673 #
DE88-010971 ..... N88-27189 #
DE88-010973 ..... N88-27899 #
DE88-010976 ..... N88-27784 #
DE88-011005 ..... N88-27912 #
DE88-011022 ..... N88-27279 #
DE88-011088 ..... N88-27299 #
DE88-011120 ..... N88-27724 #
DE88-011204 ..... N88-27449 #
DE88-011205 ..... N88-27455 #
DE88-011243 ..... N88-27311 #
DE88-011244 ..... N88-27450 #
DE88-011248 ..... N88-27456 #
DE88-011250 ..... N88-27333 #
DE88-011251 ..... N88-27327 #
DE88-011253 ..... N88-27326 #
DE88-011262 ..... N88-27756 #
DE88-011278 ..... N88-27547 #
DE88-011279 ..... N88-27592 #
DE88-011283 ..... N88-27529 #
DE88-011320 ..... N88-27457 #
DE88-011341 ..... N88-27543 #
DE88-011342 ..... N88-27506 #
DE88-011345 ..... N88-27785 #
DE88-011361 ..... N88-27459 #
DE88-011369 ..... N88-27272 #
DE88-011392 ..... N88-27758 #
DE88-011399 ..... N88-27302 #
DE88-011401 ..... N88-27293 #
DE88-011486 ..... N88-27497 #
DE88-011488 ..... N88-27451 #
DE88-011519 ..... N88-27294 #
DE88-011542 ..... N88-27274 #
DE88-011622 ..... N88-27275 #
DE88-011623 ..... N88-27334 #
DE88-011625 ..... N88-27786 #
DE88-011711 ..... N88-27859 #
DE88-011724 ..... N88-27989 #
DE88-011730 ..... N88-27549 #
DE88-011731 ..... N88-27836 #
DE88-011732 ..... N88-27496 #
DE88-011740 ..... N88-27787 #
DE88-011759 ..... N88-27869 #
DE88-011760 ..... N88-27548 #
DE88-011785 ..... N88-27335 #
DE88-011787 ..... N88-27458 #
DE88-011826 ..... N88-27594 #
DE88-011827 ..... N88-27566 #
DE88-011834 ..... N88-27603 #
DE88-011841 ..... N88-27241 #
DE88-011843 ..... N88-27303 #
DE88-011844 ..... N88-27950 #
DE88-011846 ..... N88-27839 #
DE88-011883 ..... N88-27636 #
DE88-011884 ..... N88-27637 #
DE88-011894 ..... N88-27304 #
DE88-011896 ..... N88-27674 #
DE88-011917 ..... N88-27276 #
DE88-011922 ..... N88-27460 #
DE88-011938 ..... N88-27840 #
DE88-011965 ..... N88-27305 #
DE88-011973 ..... N88-27306 #
DE88-011975 ..... N88-27461 #
DE88-012004 ..... N88-27838 #
DE88-012026 ..... N88-27951 #
DE88-012038 ..... N88-27952 #
DE88-012058 ..... N88-27639 #
DE88-012060 ..... N88-27953 #
DE88-012116 ..... N88-27530 #
DE88-012121 ..... N88-27605 #
DE88-012240 ..... N88-27277 #
DE88-012242 ..... N88-27604 #
DE88-012243 ..... N88-27462 #
DE88-012245 ..... N88-27841 #
DE88-012248 ..... N88-27422 #
DE88-012412 ..... N88-27463 #
DE88-012460 ..... N88-27954 #
DE88-701642 ..... N88-27962 #
DE88-701682 ..... N88-27922 #
DE88-701825 ..... N88-27927 #

DE88-701859 ..... N88-27296 #
DE88-701883 ..... N88-27962 #
DE88-701960 ..... N88-27493 #
DE88-701983 ..... N88-27902 #
DE88-702048 ..... N88-27960 #
DE88-702051 ..... N88-27925 #
DE88-702116 ..... N88-27961 #
DE88-702148 ..... N88-27759 #
DE88-702178 ..... N88-27417 #
DE88-702189 ..... N88-27297 #
DE88-702190 ..... N88-27924 #
DE88-702215 ..... N88-27888 #
DE88-702219 ..... N88-27943 #
DE88-702235 ..... N88-27986 #
DE88-702239 ..... N88-27862 #
DE88-702309 ..... N88-27330 #
DE88-702318 ..... N88-27494 #
DE88-702386 ..... N88-27418 #
DE88-702404 ..... N88-27984 #
DE88-702405 ..... N88-27863 #
DE88-702406 ..... N88-27864 #
DE88-702411 ..... N88-27995 #
DE88-702412 ..... N88-27916 #
DE88-702413 ..... N88-27917 #
DE88-702414 ..... N88-27991 #
DE88-702416 ..... N88-27992 #
DE88-702422 ..... N88-27918 #
DE88-702434 ..... N88-27865 #
DE88-702435 ..... N88-27866 #
DE88-702437 ..... N88-27837 #
DE88-702442 ..... N88-27964 #
DE88-702454 ..... N88-27867 #
DE88-702456 ..... N88-27495 #
DE88-752602 ..... N88-27913 #
DE88-752634 ..... N88-27896 #
DE88-752670 ..... N88-27569 #
DE88-752671 ..... N88-27570 #
DE88-752993 ..... N88-27610 #
DE88-753130 ..... N88-27914 #
DE88-753133 ..... N88-27897 #
DE88-753134 ..... N88-27239 #
DE88-753136 ..... N88-27915 #
DE88-753426 ..... N88-27329 #
DE88-753428 ..... N88-27295 #
DE88-753430 ..... N88-27567 #
DE88-997572 ..... N88-27910 #

DFVLR-FB-87-53 ..... N88-27551 #
DFVLR-FB-88-03 ..... N88-27879 #
DFVLR-FB-88-04 ..... N88-27516 #
DFVLR-FB-88-05 ..... N88-27345 #
DFVLR-FB-88-07 ..... N88-27203 #
DFVLR-FB-88-08 ..... N88-27517 #
DFVLR-FB-88-09 ..... N88-27518 #
DFVLR-FB-88-10 ..... N88-27552 #
DFVLR-FB-88-13 ..... N88-27880 #
DFVLR-FB-88-14 ..... N88-27748 #
DFVLR-FB-88-16 ..... N88-27210 #
DFVLR-FB-88-17 ..... N88-27171 #
DFVLR-FB-88-19 ..... N88-27211 #

DFVLR-MITT-88-02 ..... N88-27212 #
DFVLR-MITT-88-03 ..... N88-27792 #
DFVLR-MITT-88-07 ..... N88-27793 #
DFVLR-MITT-88-08 ..... N88-27794 #
DFVLR-MITT-88-09 ..... N88-27533 #
DFVLR-MITT-88-12 ..... N88-27795 #

DMS-DB-02-VOL-2 ..... N88-27172* #

DOE/AL-38221/T3 ..... N88-27565 #

DOE/DP-40200/55 ..... N88-27544 #
DOE/DP-40200/70 ..... N88-27898 #
DOE/DP-8005612-VOL-1 ..... N88-27978 #

DOE/ER-0362 ..... N88-27756 #
DOE/ER-10590/2 ..... N88-27724 #
DOE/ER-13396/9 ..... N88-27492 #
DOE/ER-13744/T1 ..... N88-27882 #
DOE/ER-25026/19 ..... N88-27817 #
DOE/ER-25026/21 ..... N88-27840 #
DOE/ER-40063/2 ..... N88-27983 #
DOE/ER-40325/7A ..... N88-27996 #
DOE/ER-45138/T3 ..... N88-27605 #
DOE/ER-45213/3 ..... N88-27294 #
DOE/ER-45214/T1 ..... N88-27304 #
DOE/ER-45250/1 ..... N88-27941 #
DOE/ER-45263/2 ..... N88-27954 #
DOE/ER-53212/121 ..... N88-27911 #
DOE/ER-53227/119 ..... N88-27904 #
DOE/ER-60422/H1 ..... N88-27673 #

DOE/EV-03568/54 ..... N88-27682 #

DOE/NASA/50112-76 ..... N88-27900* #

DOE/PHV-88-1 ..... N88-27634 #

DOT-TSC-FAA-87-4 ..... N88-27752 #

DOT/FAA/PM-87-25 ..... N88-27407 #

DP-MS-88-87 ..... N88-27618 #

DREO-976 ..... N88-27179 #

DRES-SM-1191 ..... N88-27187 #

DT-87/62-R ..... N88-27246 #
DT-212/87 ..... N88-27248 #

DTIC-TR-88/7 ..... N88-27971 #

DUKE-CE-001-87-3 ..... N88-27556 #

E-4217 ..... N88-27267* #
E-4221 ..... N88-27201* #
E-4237 ..... N88-27310* #
E-4266 ..... N88-27799* #
E-4267 ..... N88-27200* #
E-4270 ..... N88-27980* #
E-4278 ..... N88-27796* #
E-4317 ..... N88-27174* #
E-4327 ..... N88-27424* #
E-4331 ..... N88-27520* #

ECL-87-17 ..... N88-27959 #

EMP-MEMO-805 ..... N88-27416 #

ENST-88D003 ..... N88-27401 #

EPA-450/5-88-002 ..... N88-27645 #
EPA-600/D-88-064 ..... N88-27647 #
EPA-600/3-88-010A ..... N88-27646 #

EPA/DF/DK-88/043A ..... N88-27646 #

ESD-TR-87-023 ..... N88-27444 #
ESD-TR-87-073 ..... N88-27929 #

ETL-R-129 ..... N88-27613 #
ETL-R-132 ..... N88-27665 #
ETL-R-135 ..... N88-27612 #
ETL-R-136 ..... N88-27614 #

ETL-0484 ..... N88-27770 #
ETL-0649 ..... N88-27404 #

ETN-88-91453 ..... N88-27999 #
ETN-88-92106 ..... N88-27215 #
ETN-88-92109 ..... N88-27842 #
ETN-88-92126 ..... N88-27985 #
ETN-88-92127 ..... N88-27509 #
ETN-88-92137 ..... N88-27806 #
ETN-88-92332 ..... N88-27979 #
ETN-88-92333 ..... N88-27955 #
ETN-88-92336 ..... N88-27510 #
ETN-88-92339 ..... N88-27353 #
ETN-88-92345 ..... N88-27663 #
ETN-88-92354 ..... N88-27956 #
ETN-88-92355 ..... N88-27464 #
ETN-88-92356 ..... N88-27465 #
ETN-88-92360 ..... N88-27607 #
ETN-88-92361 ..... N88-27243 #
ETN-88-92362 ..... N88-27511 #
ETN-88-92363 ..... N88-27550 #
ETN-88-92364 ..... N88-27512 #
ETN-88-92365 ..... N88-27513 #
ETN-88-92366 ..... N88-27514 #
ETN-88-92367 ..... N88-27244 #
ETN-88-92368 ..... N88-27190 #
ETN-88-92369 ..... N88-27227 #
ETN-88-92370 ..... N88-27957 #
ETN-88-92372 ..... N88-27789 #
ETN-88-92375 ..... N88-27573 #
ETN-88-92376 ..... N88-27890 #
ETN-88-92377 ..... N88-27958 #
ETN-88-92378 ..... N88-27466 #
ETN-88-92379 ..... N88-27900 #
ETN-88-92380 ..... N88-27515 #
ETN-88-92381 ..... N88-27843 #
ETN-88-92382 ..... N88-27844 #
ETN-88-92383 ..... N88-27531 #
ETN-88-92386 ..... N88-27981 #
ETN-88-92569 ..... N88-27532 #
ETN-88-92624 ..... N88-27891 #
ETN-88-92628 ..... N88-27892 #
ETN-88-92646 ..... N88-27423 #
ETN-88-92647 ..... N88-27790 #
ETN-88-92702 ..... N88-27245 #
ETN-88-92712 ..... N88-27246 #

ETN-88-92713 ..... N88-27247 #
ETN-88-92714 ..... N88-27307 #
ETN-88-92715 ..... N88-27248 #
ETN-88-92733 ..... N88-27202 #
ETN-88-92735 ..... N88-27878 #
ETN-88-92736 ..... N88-27169 #
ETN-88-92737 ..... N88-27920 #
ETN-88-92738 ..... N88-27191 #
ETN-88-92740 ..... N88-27337 #
ETN-88-92741 ..... N88-27338 #
ETN-88-92742 ..... N88-27249 #
ETN-88-92743 ..... N88-27308 #
ETN-88-92744 ..... N88-27339 #
ETN-88-92746 ..... N88-27208 #
ETN-88-92748 ..... N88-27209 #
ETN-88-92749 ..... N88-27170 #
ETN-88-92756 ..... N88-27278 #
ETN-88-92757 ..... N88-27199 #
ETN-88-92758 ..... N88-27340 #
ETN-88-92759 ..... N88-27309 #
ETN-88-92760 ..... N88-27401 #
ETN-88-92762 ..... N88-28000 #
ETN-88-92840 ..... N88-27959 #
ETN-88-92842 ..... N88-27192 #
ETN-88-92843 ..... N88-27814 #
ETN-88-92844 ..... N88-27815 #
ETN-88-92849 ..... N88-27354 #
ETN-88-92850 ..... N88-27228 #
ETN-88-92851 ..... N88-27341 #
ETN-88-92856 ..... N88-27342 #
ETN-88-92858 ..... N88-27250 #
ETN-88-92860 ..... N88-27251 #
ETN-88-92861 ..... N88-27651 #
ETN-88-92864 ..... N88-27343 #
ETN-88-92865 ..... N88-27252 #
ETN-88-92866 ..... N88-27344 #
ETN-88-92870 ..... N88-27576 #
ETN-88-92871 ..... N88-27223 #
ETN-88-92872 ..... N88-27791 #
ETN-88-92875 ..... N88-27640 #
ETN-88-92879 ..... N88-27219 #
ETN-88-92882 ..... N88-27577 #
ETN-88-92919 ..... N88-27551 #
ETN-88-92921 ..... N88-27879 #
ETN-88-92922 ..... N88-27516 #
ETN-88-92923 ..... N88-27345 #
ETN-88-92925 ..... N88-27203 #
ETN-88-92926 ..... N88-27517 #
ETN-88-92927 ..... N88-27518 #
ETN-88-92928 ..... N88-27552 #
ETN-88-92931 ..... N88-27880 #
ETN-88-92932 ..... N88-27748 #
ETN-88-92934 ..... N88-27210 #
ETN-88-92935 ..... N88-27171 #
ETN-88-92936 ..... N88-27211 #
ETN-88-92937 ..... N88-27212 #
ETN-88-92938 ..... N88-27792 #
ETN-88-92941 ..... N88-27793 #
ETN-88-92942 ..... N88-27794 #
ETN-88-92943 ..... N88-27533 #
ETN-88-92945 ..... N88-27795 #
ETN-88-92946 ..... N88-27893 #
ETN-88-92961 ..... N88-27176 #
ETN-88-92962 ..... N88-27675 #
ETN-88-92963 ..... N88-27204 #
ETN-88-92964 ..... N88-27253 #
ETN-88-92968 ..... N88-27216 #

EUR-10632-EN ..... N88-27818 #

FAA-FS-88/1 ..... N88-27752 #

FASAC-TAR-3140 ..... N88-27597 #

FBW-TB-2086/88 ..... N88-27204 #

FEI-1828 ..... N88-27493 #

FEL-1987-34 ..... N88-27532 #

FOA-C-20696-2.1 ..... N88-27245 #
FOA-C-20698-2.1 ..... N88-27292 #
FOA-C-30476-4.2 ..... N88-27416 #

FUB-33-1986 ..... N88-27423 #
FUB-42-1986 ..... N88-27790 #

GA-A19195 ..... N88-27238 #

GEPP-TIS-1083 ..... N88-27530 #

GKSS-87/E/62 ..... N88-27675 #

GRI-88/0095 ..... N88-27271 #

GRR-6216-011-REV ..... N88-27186 #

HIFT-137 ..... N88-27913 #

I-177/87 ..... N88-27247 #
I-186/87 ..... N88-27307 #

IAE-4405/1 ..... N88-27988 #
IAE-4443/7 ..... N88-27902 #

IC-86/251 ..... N88-27927 #
IC-87/62 ..... N88-27960 #
IC-87/68 ..... N88-27862 #
IC-87/116 ..... N88-27296 #
IC-87/141 ..... N88-27962 #
IC-87/164 ..... N88-27925 #

ICASE-88-42 ..... N88-27164* #

ICMA-88-115 ..... N88-27845 #

ICOMP-88-13 ..... N88-27799* #
ICOMP-88-14 ..... N88-27796* #

IFL-IB-87-05 ..... N88-27253 #

IITRI-E06549-34 ..... N88-27414 #

ILR-MITT-182 ..... N88-27842 #

INIS-BR-1045 ..... N88-27330 #
INIS-BR-1054 ..... N88-27494 #

INIS-SU-27 ..... N88-27418 #

ISAL-IDI1-88-02 ..... N88-27278 #

ISAL-87-0041 ..... N88-27340 #
ISAL-87-0046 ..... N88-27199 #
ISAL-87-0048 ..... N88-27309 #

ISAS-RN-351 ..... N88-27883 #
ISAS-RN-356 ..... N88-27256 #

ISBN-90-353-0054-8 ..... N88-27619 #
ISBN-92-835-0443-7 ..... N88-27185 #
ISBN-92-835-0447-X ..... N88-27683 #
ISBN-92-835-0453-4 ..... N88-27480 #
ISBN-92-835-0459-3 ..... N88-27525 #
ISBN-92-835-0460-7 ..... N88-27406 #
ISBN-92-835-0462-3 ..... N88-27669 #
ISBN-92-835-0463-1 ..... N88-27193 #

ISL-CO-210/87 ..... N88-27920 #
ISL-CO-211/87 ..... N88-27191 #

ISL-PU-309/87 ..... N88-27169 #

ISL-R-112/87 ..... N88-27202 #
ISL-R-126/87 ..... N88-27878 #
ISL-R-130/86 ..... N88-27259 #

ISSN-0069-5882 ..... N88-27663 #
ISSN-0171-1342 ..... N88-27171 #
ISSN-0171-1342 ..... N88-27203 #
ISSN-0171-1342 ..... N88-27210 #
ISSN-0171-1342 ..... N88-27211 #
ISSN-0171-1342 ..... N88-27345 #
ISSN-0171-1342 ..... N88-27516 #
ISSN-0171-1342 ..... N88-27517 #
ISSN-0171-1342 ..... N88-27518 #
ISSN-0171-1342 ..... N88-27551 #
ISSN-0171-1342 ..... N88-27552 #
ISSN-0171-1342 ..... N88-27748 #
ISSN-0171-1342 ..... N88-27879 #
ISSN-0171-1342 ..... N88-27880 #
ISSN-0173-699X ..... N88-27981 #
ISSN-0176-7739 ..... N88-27212 #
ISSN-0176-7739 ..... N88-27533 #
ISSN-0176-7739 ..... N88-27792 #
ISSN-0176-7739 ..... N88-27793 #
ISSN-0176-7739 ..... N88-27794 #
ISSN-0176-7739 ..... N88-27795 #
ISSN-0178-0719 ..... N88-27999 #
ISSN-0343-7639 ..... N88-27176 #
ISSN-0344-9629 ..... N88-27675 #
ISSN-0347-3694 ..... N88-27245 #
ISSN-0723-4325 ..... N88-27216 #
ISSN-0751-1345 ..... N88-27401 #

ITEF-177(1986) ..... N88-27982 #

ITEP-87(1987) ..... N88-27984 #
ITEP-107(1987)-PT-1 ..... N88-27863 #
ITEP-110(1987) ..... N88-27961 #
ITEP-115(1987)-PT-2 ..... N88-27864 #

ITF-86-137 ..... N88-27995 #

ITF-86-161 ..... N88-27916 #
ITF-87-18 ..... N88-27917 #
ITF-87-22 ..... N88-27991 #
ITF-87-27 ..... N88-27992 #

ITP-87-12 ..... N88-27918 #

JAERI-M-87-192 ..... N88-27914 #
JAERI-M-87-196 ..... N88-27897 #
JAERI-M-87-197 ..... N88-27239 #
JAERI-M-87-200 ..... N88-27915 #
JAERI-M-87-217 ..... N88-27329 #
JAERI-M-88-003 ..... N88-27295 #
JAERI-M-88-018 ..... N88-27567 #

JHU-RR-88-100 ..... N88-27743 #

JINR-E-2-87-507 ..... N88-27865 #
JINR-E-4-87-667 ..... N88-27866 #
JINR-E-5-87-481 ..... N88-27837 #
JINR-E-10-87-378 ..... N88-27759 #

JINR-R-2-87-331 ..... N88-27964 #
JINR-R-5-87-373 ..... N88-27867 #
JINR-R-8-87-505 ..... N88-27495 #
JINR-R-9-87-268 ..... N88-27417 #
JINR-R-13-87-525 ..... N88-27297 #
JINR-R-17-87-498 ..... N88-27924 #

JUEL-SPEZ-425 ..... N88-27176 #

K/ETAC-57 ..... N88-27594 #

K/QT-198 ..... N88-27566 #

KEK-87-11 ..... N88-27896 #

KFTI-87-21 ..... N88-27922 #

L-16414 ..... N88-27677* #
L-16445 ..... N88-27182* #

LA-UR-87-4161 ..... N88-27489 #
LA-UR-88-640 ..... N88-27861 #
LA-UR-88-837 ..... N88-27541 #
LA-UR-88-1192 ..... N88-27213 #
LA-UR-88-1210 ..... N88-27987 #
LA-UR-88-1236 ..... N88-27670 #
LA-UR-88-1345 ..... N88-27990 #
LA-UR-88-1588 ..... N88-27949 #

LBL-23968 ..... N88-27290 #
LBL-24111 ..... N88-27951 #
LBL-24512 ..... N88-27270 #
LBL-24799 ..... N88-27325 #
LBL-24936 ..... N88-27940 #
LBL-25010 ..... N88-27326 #
LBL-25186 ..... N88-27725 #
LBL-25242 ..... N88-27948 #
LBL-25253 ..... N88-27460 #
LBL-25259 ..... N88-27505 #
LBL-25260 ..... N88-27291 #

LC-87-19560 ..... N88-27749 #

LCDS/CCS-87-39 ..... N88-27823 #
LCDS/CCS-88-1 ..... N88-27822 #
LCDS/CCS-88-3 ..... N88-27847 #
LCDS/CCS-88-5 ..... N88-27810 #

LG87ER0154 ..... N88-27196* #

LMI-DL604R1 ..... N88-27971 #

LMSC/F247006 ..... N88-27221 #

LSI-TR-471-26-VOL-2 ..... N88-27755* #
LSI-TR-769-4 ..... N88-27754* #

LYC-87-14 ..... N88-27197 #
LYC-87-14-VOL-2-PT-1 ..... N88-27198 #

MCR-85-721 ..... N88-27233 #

ME-144(88)ONR-233-3 ..... N88-27586 #

MIT/LCS/TM-333 ..... N88-27824 #
MIT/LCS/TM-334 ..... N88-27825 #
MIT/LCS/TM-341 ..... N88-27802 #
MIT/LCS/TM-345 ..... N88-27766 #

MIT/LCS/TR-410 ..... N88-27801 #

MITT-52 ..... N88-27663 #

MLM-3505 ..... N88-27350 #

MPE-206 ..... N88-27981 #
MPE-207 ..... N88-27999 #

MPL-TM-387-E ..... N88-27872 #

MPL-U-32/86 ..... N88-27872 #

MRC/WDC-R-148 ..... N88-27997 #

NAE-AN-49 ..... N88-27166 #

NAS 1.15:4058 ..... N88-27182* #
NAS 1.15:100336 ..... N88-27181* #
NAS 1.15:100590 ..... N88-27881* #
NAS 1.15:100621 ..... N88-27553* #
NAS 1.15:100636 ..... N88-27447* #
NAS 1.15:100937 ..... N88-27267* #
NAS 1.15:100940 ..... N88-27201* #
NAS 1.15:100946 ..... N88-27310* #
NAS 1.15:100953 ..... N88-27200* #
NAS 1.15:100974 ..... N88-27799* #
NAS 1.15:100978 ..... N88-27960* #
NAS 1.15:100997 ..... N88-27507* #
NAS 1.15:101008 ..... N88-27519* #
NAS 1.15:101135 ..... N88-27650* #
NAS 1.15:101176 ..... N88-27998* #
NAS 1.15:101177 ..... N88-27624* #
NAS 1.15:101297 ..... N88-27796* #
NAS 1.15:101319 ..... N88-27174* #
NAS 1.15:101323 ..... N88-27424* #
NAS 1.21:7011(314) N88-27742*
NAS 1.21:7037(229) N88-27183*
NAS 1.21:7046(18) N88-27214*
NAS 1.26:4174 ..... N88-27168* #
NAS 1.26:4176 ..... N88-27196* #
NAS 1.26:172054 ..... N88-27754* #
NAS 1.26:172055 ..... N88-27180* #
NAS 1.26:172076 ..... N88-27755* #
NAS 1.26:177427 ..... N88-27205* #
NAS 1.26:177474 ..... N88-27798* #
NAS 1.26:178415-VOL-2-PT-2 ..... N88-27172* #
NAS 1.26:179337 ..... N88-27676* #
NAS 1.26:179361 ..... N88-27226* #
NAS 1.26:179375 ..... N88-27254* #
NAS 1.26:179376 ..... N88-27255* #
NAS 1.26:181687 ..... N88-27164* #
NAS 1.26:182191 ..... N88-27611* #
NAS 1.26:182192 ..... N88-27520* #
NAS 1.26:182724 ..... N88-27225* #
NAS 1.26:182928 ..... N88-27593* #
NAS 1.26:182947 ..... N88-27760* #
NAS 1.26:183017 ..... N88-27562* #
NAS 1.26:183044 ..... N88-27621* #
NAS 1.26:183048-VOL-1 ..... N88-27230* #
NAS 1.26:183081 ..... N88-27986* #
NAS 1.26:183104 ..... N88-27563* #
NAS 1.26:183106 ..... N88-27224* #
NAS 1.26:183112 ..... N88-27490* #
NAS 1.26:183116 ..... N88-27877* #
NAS 1.26:183143 ..... N88-27508* #
NAS 1.26:183144 ..... N88-27606* #
NAS 1.26:183145 ..... N88-27242* #
NAS 1.26:183149 ..... N88-27662* #
NAS 1.26:183159 ..... N88-27173* #
NAS 1.55:10007 ..... N88-27148* #
NAS 1.61:1184 ..... N88-27677* #
NAS 1.71:NPO-17280-1-CU ..... N88-27220* #
NAS 1.77:20298 ..... N88-27336* #

NASA-CASE-NPO-17280-1-CU ..... N88-27220* #

NASA-CP-10007 ..... N88-27148* #

NASA-CR-4174 ..... N88-27168* #
NASA-CR-4176 ..... N88-27196* #
NASA-CR-172054 ..... N88-27754* #
NASA-CR-172055 ..... N88-27180* #
NASA-CR-172076 ..... N88-27755* #
NASA-CR-177427 ..... N88-27205* #
NASA-CR-177474 ..... N88-27798* #
NASA-CR-178415-VOL-2-PT-2 ..... N88-27172* #
NASA-CR-179337 ..... N88-27676* #
NASA-CR-179361 ..... N88-27226* #
NASA-CR-179375 ..... N88-27254* #
NASA-CR-179376 ..... N88-27255* #
NASA-CR-181687 ..... N88-27164* #
NASA-CR-182191 ..... N88-27611* #
NASA-CR-182192 ..... N88-27520* #
NASA-CR-182724 ..... N88-27225* #
NASA-CR-182928 ..... N88-27593* #
NASA-CR-182947 ..... N88-27760* #
NASA-CR-183017 ..... N88-27562* #
NASA-CR-183044 ..... N88-27621* #
NASA-CR-183048-VOL-1 ..... N88-27230* #
NASA-CR-183081 ..... N88-27986* #
NASA-CR-183104 ..... N88-27563* #

NASA-CR-183106 ..... N88-27224* #
NASA-CR-183112 ..... N88-27490* #
NASA-CR-183116 ..... N88-27677* #
NASA-CR-183143 ..... N88-27508* #
NASA-CR-183144 ..... N88-27606* #
NASA-CR-183145 ..... N88-27242* #
NASA-CR-183149 ..... N88-27662* #
NASA-CR-183159 ..... N88-27173* #

NASA-RP-1184 ..... N88-27677* #

NASA-SP-7011(314) N88-27742*
NASA-SP-7037(229) N88-27163*
NASA-SP-7046(18) N88-27214*

NASA-TM-4058 ..... N88-27182* #
NASA-TM-100336 ..... N88-27181* #
NASA-TM-100590 ..... N88-27681* #
NASA-TM-100621 ..... N88-27553* #
NASA-TM-100636 ..... N88-27447* #
NASA-TM-100937 ..... N88-27267* #
NASA-TM-100940 ..... N88-27201* #
NASA-TM-100946 ..... N88-27310* #
NASA-TM-100953 ..... N88-27200* #
NASA-TM-100974 ..... N88-27799* #
NASA-TM-100978 ..... N88-27980* #
NASA-TM-100997 ..... N88-27507* #
NASA-TM-101008 ..... N88-27519* #
NASA-TM-101135 ..... N88-27650* #
NASA-TM-101176 ..... N88-27998* #
NASA-TM-101177 ..... N88-27624* #
NASA-TM-101297 ..... N88-27796* #
NASA-TM-101319 ..... N88-27174* #
NASA-TM-101323 ..... N88-27424* #

NASA-TT-20296 ..... N88-27336* #

NCAR/TN-310/STR ..... N88-27668 #

NEPRF-TR-88-02 ..... N88-27403 #

NHRC-87-37 ..... N88-27733 #
NHRC-88-8 ..... N88-27741 #

NIH/PUB-87-2755 ..... N88-27726 #

NIPER-303 ..... N88-27322 #

NMERI-WA3-34(3.07) ..... N88-27398 #

NOAA-DR-ERL-ARL-15 ..... N88-27644 #

NOAA-DR-ERL-PMEL-22 ..... N88-27681 #

NOSC-TD-1224 ..... N88-27772 #

NOSC-TR-1199 ..... N88-27408 #

NOTA-INTERNA-896 ..... N88-27891 #
NOTA-INTERNA-908 ..... N88-27892 #

NOTE-E/ES4-20-120 ..... N88-27815 #
NOTE-E/ES4-20-126 ..... N88-27814 #

NPS-62-88-007 ..... N88-27413 #

NPS012-87-006 ..... N88-27474 #

NRC-26595 ..... N88-27166 #

NRL-MR-5987 ..... N88-27588 #
NRL-MR-6035 ..... N88-27584 #
NRL-MR-6096 ..... N88-27412 #
NRL-MR-6134 ..... N88-27654 #
NRL-MR-6140 ..... N88-27411 #
NRL-MR-6148 ..... N88-27415 #
NRL-MR-6159 ..... N88-27887 #
NRL-MR-6173 ..... N88-27804 #
NRL-MR-6186 ..... N88-27907 #

NRL-9055 ..... N88-27410 #
NRL-9073 ..... N88-27319 #
NRL-9079 ..... N88-27409 #

NSWC-TR-87-104 ..... N88-27441 #

NUSC-TD-6666 ..... N88-27481 #

NUSC/TD-1188 ..... N88-27679 #

ODL-88.2 ..... N88-27813 #

ODU/ICAM-88-101 ..... N88-27490* #

ONERA-RSF-10/0694-GY-010-G ..... N88-27209 #
ONERA-RSF-11/0694-GY-010-G ..... N88-27208 #

ONERA-RT-10/2691-AN-101-A-PT-1 ..... N88-27170 #

ORNL/CON-244 ..... N88-27977 #

ORNL/CSD/TM-226 ..... N88-27643 #

ORNL/SUB-84-00216/1 ..... N88-27324 #
ORNL/SUB-86-55930/1 ..... N88-27331 #

ORNL/TM-10548 ..... N88-27965 #
ORNL/TM-10705 ..... N88-27323 #
ORNL/TM-10715 ..... N88-27625 #
ORNL/TM-10773 ..... N88-27658 #
ORNL/TM-10778 ..... N88-27277 #

OTO-1-88 ..... N88-27737 #

PB88-103478 ..... N88-27870 #
PB88-104054 ..... N88-27580 #
PB88-105283 ..... N88-27402 #
PB88-105960 ..... N88-27761 #
PB88-106068 ..... N88-27259 #
PB88-108170 ..... N88-27260 #
PB88-109525 ..... N88-27818 #
PB88-109632 ..... N88-27555 #
PB88-116280 ..... N88-27783 #
PB88-131917 ..... N88-27973 #
PB88-131941 ..... N88-27628 #
PB88-131958 ..... N88-27627 #
PB88-131974 ..... N88-27923 #
PB88-190814 ..... N88-27619 #
PB88-192604 ..... N88-27726 #
PB88-193057 ..... N88-27642 #
PB88-193073 ..... N88-27641 #
PB88-193107 ..... N88-27626 #
PB88-194162 ..... N88-27388 #
PB88-195235 ..... N88-27647 #
PB88-195631 ..... N88-27646 #
PB88-196548 ..... N88-27666 #
PB88-197470 ..... N88-27645 #
PB88-202015 ..... N88-27644 #
PB88-203070 ..... N88-27292 #
PB88-203658 ..... N88-27681 #
PB88-203781 ..... N88-27416 #
PB88-212566 ..... N88-27271 #

PINSTECH/NPD-120 ..... N88-27260 #

PNL-SA-15687 ..... N88-27660 #
PNL-SA-15768 ..... N88-27674 #

PNL-6475 ..... N88-27459 #
PNL-6509 ..... N88-27672 #
PNL-6537 ..... N88-27545 #

PPG-1130 ..... N88-27905 #

R-125-87 ..... N88-27967 #

R/D-5302-EE ..... N88-27433 #
R/D-5499-EN-01 ..... N88-27206 #
R/D-5838-PH-01 ..... N88-27482 #

RADC-TR-87-131 ..... N88-27809 #
RADC-TR-87-170 ..... N88-27405 #
RADC-TR-87-262 ..... N88-27445 #
RADC-TR-88-34 ..... N88-27430 #

RAL-87-023 ..... N88-27761 #

REPT-3 ..... N88-27929 #
REPT-47-803/F ..... N88-27339 #
REPT-48-284/F ..... N88-27249 #
REPT-48-411/F ..... N88-27577 #
REPT-50/87 ..... N88-27955 #
REPT-57 ..... N88-27820 #
REPT-843 ..... N88-27580 #
REPT-1967 ..... N88-27929 #
REPT-2427-IFR-VOL-1 ..... N88-27254* #
REPT-2427-IFR-VOL-2 ..... N88-27255* #

RF-447230 ..... N88-27936 #

RLE-PR-130 ..... N88-27869 #

RM-101 ..... N88-27870 #

RPT/AA0631-A/087-VOL-1 ..... N88-27254* #
RPT/AA0631/087-VOL-2 ..... N88-27255* #

R8805-5 ..... N88-27180* #

SAND-86-2855 ..... N88-27757 #
SAND-87-0873 ..... N88-27453 #
SAND-87-1526C ..... N88-27268 #
SAND-87-1574C ..... N88-27564 #

SAND-87-1818 ..... N88-27590 #
SAND-87-2082C ..... N88-27454 #
SAND-87-2276 ..... N88-27189 #
SAND-87-2356 ..... N88-27857 #
SAND-87-2460C ..... N88-27269 #
SAND-87-2461 ..... N88-27632 #
SAND-87-2508C ..... N88-27334 #
SAND-87-2541C ..... N88-27450 #
SAND-87-2585C ..... N88-27779 #
SAND-87-2570C ..... N88-27894 #
SAND-87-2755C ..... N88-27222 #
SAND-87-2791C ..... N88-27595 #
SAND-87-2866C ..... N88-27637 #
SAND-87-2910C ..... N88-27636 #
SAND-87-2976C ..... N88-27631 #
SAND-87-3007C ..... N88-27458 #
SAND-87-3017C ..... N88-27545 #
SAND-87-3032C ..... N88-27352 #
SAND-87-3061C ..... N88-27496 #
SAND-87-3069C ..... N88-27349 #
SAND-87-3112 ..... N88-27438 #
SAND-87-7017 ..... N88-27635 #
SAND-88-0067C ..... N88-27491 #
SAND-88-0068C ..... N88-27274 #
SAND-88-0108 ..... N88-27596 #
SAND-88-0152 ..... N88-27671 #
SAND-88-0221C ..... N88-27299 #
SAND-88-0249C ..... N88-27926 #
SAND-88-0260 ..... N88-27218 #
SAND-88-0262C ..... N88-27786 #
SAND-88-0272C ..... N88-27972 #
SAND-88-0389 ..... N88-27899 #
SAND-88-0394 ..... N88-27419 #
SAND-88-0451 ..... N88-27787 #
SAND-88-0503 ..... N88-27526 #
SAND-88-0519C ..... N88-27188 #
SAND-88-0553C ..... N88-27276 #
SAND-88-0578C ..... N88-27780 #
SAND-88-0764 ..... N88-27547 #
SAND-88-0825 ..... N88-27592 #
SAND-88-0865C ..... N88-27624* #
SAND-88-0905 ..... N88-27483 #
SAND-88-0952 ..... N88-27859 #
SAND-88-1110C ..... N88-27497 #
SAND-88-1129C ..... N88-27448 #
SAND-88-1131C ..... N88-27333 #
SAND-88-1213C ..... N88-27328 #
SAND-88-1222C ..... N88-27568 #
SAND-88-1313C ..... N88-27275 #
SAND-88-1321C ..... N88-27449 #
SAND-88-1322C ..... N88-27455 #
SAND-88-1330C ..... N88-27335 #
SAND-88-1360C ..... N88-27527 #
SAND-88-1421C ..... N88-27451 #
SAND-88-1453C ..... N88-27327 #
SAND-88-7093C ..... N88-27456 #
SAND-88-8205 ..... N88-27529 #
SAND-88-8217 ..... N88-27269 #
SAND-88-8219 ..... N88-27591 #

SASR-19 ..... N88-27662* #
SASR-20 ..... N88-27662* #

SCEE-PDP/85-48 ..... N88-27809 #

SC5461.FR ..... N88-27928 #

SD-TR-87-62 ..... N88-27933 #
SD-TR-87-63 ..... N88-27428 #
SD-TR-88-03 ..... N88-27934 #
SD-TR-88-05 ..... N88-27653 #
SD-TR-88-11 ..... N88-27234 #
SD-TR-88-19 ..... N88-27931 #
SD-TR-88-20 ..... N88-27620 #
SD-TR-88-27 ..... N88-27560 #
SD-TR-88-41 ..... N88-27868 #
SD-TR-88-43 ..... N88-27231 #
SD-TR-88-44 ..... N88-27425 #
SD-TR-88-47 ..... N88-27656 #
SD-TR-88-52 ..... N88-27434 #

SERI/PR-213-3291 ..... N88-27633 #

SERI/SP-320-3305 ..... N88-27975 #

SERI/STR-211-3214 ..... N88-27944 #
SERI/STR-211-3215 ..... N88-27622 #
SERI/STR-211-3235 ..... N88-27623 #

SERI/TP-231-3325 ..... N88-27723 #
SERI/TP-253-3324 ..... N88-27629 #

SERI/TR-255-3242 ..... N88-27630 #

SLCET-TR-88-1 ..... N88-27443 #

SNIAS-881-111-101 ..... N88-27192 #
SNIAS-881-320-101 ..... N88-27814 #
SNIAS-881-320-102 ..... N88-27815 #
SNIAS-881-430-101 ..... N88-27354 #
SNIAS-881-430-102 ..... N88-27228 #
SNIAS-881-430-103 ..... N88-27341 #
SNIAS-881-430-108 ..... N88-27342 #
SNIAS-881-430-110 ..... N88-27250 #
SNIAS-881-430-112 ..... N88-27251 #
SNIAS-881-430-113 ..... N88-27651 #
SNIAS-881-430-116 ..... N88-27343 #
SNIAS-881-430-117 ..... N88-27252 #
SNIAS-881-430-118 ..... N88-27344 #
SNIAS-881-430-123 ..... N88-27576 #
SNIAS-881-440-101 ..... N88-27223 #
SNIAS-881-440-102 ..... N88-27791 #
SNIAS-881-440-106 ..... N88-27640 #
SNIAS-881-440-116 ..... N88-27219 #

SRA-R88-920010-F ..... N88-27446 #

SRI-MP-88-044 ..... N88-27271 #

SWRI-1362 ..... N88-27559 #

TACOM-TR-13322 ..... N88-27556 #

THC-02GH88031A ..... N88-27167 #

TN-2036-9180-NR/01-REV-A ..... N88-27427 #

TOR-0086A(2057)-1 ..... N88-27400 #

TPRD/M/1622/R87 ..... N88-27555 #

TR-EE-88-37 ..... N88-27621* #

TR-SER-239 ..... N88-27402 #

TR-3 ..... N88-27262 #
TR-3 ..... N88-27321 #
TR-7 ..... N88-27930 #
TR-10 ..... N88-27314 #
TR-12 ..... N88-27261 #
TR-20 ..... N88-27932 #
TR-87-26 ..... N88-27834 #
TR-87-35 ..... N88-27835 #
TR-87-40 ..... N88-27853 #
TR-87-42 ..... N88-27856 #
TR-87-44 ..... N88-27829 #
TR-87-46 ..... N88-27828 #
TR-042 ..... N88-27673 #
TR-159 ..... N88-27831 #
TR-188 ..... N88-27830 #
TR-208 ..... N88-27826 #
TR-214 ..... N88-27849 #
TR-215 ..... N88-27848 #
TR-216 ..... N88-27850 #
TR-224 ..... N88-27851 #
TR-227 ..... N88-27855 #
TR-403 ..... N88-27854 #
TR-787 ..... N88-27444 #
TR-0086(2940-06)-3 ..... N88-27656 #
TR-0086(6935-08)-1 ..... N88-27234 #
TR-0086(6945-06)-4 ..... N88-27933 #
TR-0086(6945-06)-5 ..... N88-27428 #
TR-0086(6945-07)-4 ..... N88-27934 #
TR-0086A(2940-05)-3 ..... N88-27653 #
TR-0086A(2945-01)-6 ..... N88-27620 #
TR-0086A(2945-01)-7 ..... N88-27434 #
TR-0086A(2945-03)-1 ..... N88-27931 #
TR-0086A(2945-03)-6 ..... N88-27560 #
TR-0086A(2945-05)-2 ..... N88-27868 #
TR-0086A(2945-07)-3 ..... N88-27425 #
TR-0088(3533-01)-1 ..... N88-27231 #

TRI-PP-88-9 ..... N88-27963 #

TWR-16829 ..... N88-27226* #

UBUFFALO/DC/88/TR-67 ..... N88-27938 #

UCB/ERL-M-88/25 ..... N88-27908 #

UCID-19592-REV-4 ..... N88-27604 #
UCID-20972 ..... N88-27548 #
UCID-21077 ..... N88-27889 #
UCID-21376 ..... N88-27462 #
UCID-21386 ..... N88-27273 #
UCID-21394 ..... N88-27420 #
UCID-21422 ..... N88-27841 #
UCID-21430 ..... N88-27422 #

UCL-CS-TR-131 ..... N88-27783 #

UCLA-ENG-87-44 ..... N88-27235 #

UCRL-21033 ..... N88-27782 #
UCRL-95282 ..... N88-27542 #
UCRL-96445 ..... N88-27296 #
UCRL-96712 ..... N88-27549 #
UCRL-96744 ..... N88-27785 #
UCRL-96767 ..... N88-27540 #
UCRL-97113 ..... N88-27750 #
UCRL-97431 ..... N88-27909 #
UCRL-97505 ..... N88-27506 #
UCRL-97575 ..... N88-27543 #
UCRL-97598 ..... N88-27332 #
UCRL-97661 ..... N88-27910 #
UCRL-97765 ..... N88-27457 #
UCRL-97787 ..... N88-27351 #
UCRL-97872 ..... N88-27781 #
UCRL-98070 ..... N88-27939 #
UCRL-98232 ..... N88-27286 #
UCRL-98364 ..... N88-27797 #
UCRL-98638 ..... N88-27498 #
UCRL-98663 ..... N88-27836 #
UCRL-98751 ..... N88-27805 #
UCRL-98783 ..... N88-27969 #
UCRL-98822 ..... N88-27838 #

UILU-ENG-88-1719 ..... N88-27817 #
UILU-ENG-88-1741 ..... N88-27840 #

UIUCDCS-R-88-1414 ..... N88-27817 #
UIUCDCS-R-88-1436 ..... N88-27840 #

UMLPF-88-011 ..... N88-27534 #
UMLPF-88-031 ..... N88-27536 #

US-PATENT-APPL-SN-195226 ..... N88-27220* #

USAARL-88-1 ..... N88-27739 #

USAAVSCOM-CP-88-A-001 ..... N88-27148* #

USAAVSCOM-TM-88-F-1 ..... N88-27976 #

USAAVSCOM-TR-88-D-2 ..... N88-27559 #

USAFSAM-TR-87-35 ..... N88-27738 #

USARIEM-M-10/88 ..... N88-27728 #
USARIEM-M-13/88 ..... N88-27731 #
USARIEM-M-14/88 ..... N88-27732 #
USARIEM-M-16/88 ..... N88-27727 #
USARIEM-M-17/88 ..... N88-27730 #
USARIEM-M-19/88 ..... N88-27729 #

USARIEM-T-5/88 ..... N88-27765 #

USARIEM-T8-88 ..... N88-27735 #

UTEC-MD-87-038 ..... N88-27430 #

UVA/525415/EE88/112 ..... N88-27763 #
UVA/525670/MS88/101 ..... N88-27284 #
UVA/525673/MAE88/103 ..... N88-27587 #
UVA/525682/EE88/103 ..... N88-27833 #
UVA/525682/EE88/104 ..... N88-27874 #

UWPR-88-2 ..... N88-27901 #

VTT-TIED-752 ..... N88-27610 #
VTT-TIED-772 ..... N88-27569 #
VTT-TIED-774 ..... N88-27570 #

WAPD-TM-1619 ..... N88-27784 #

WBS-HQ301-10-03 ..... N88-27226* #

WHC-SA-0025-FP ..... N88-27895 #

WHTD-183 ..... N88-27580 #

Y/DW-741 ..... N88-27575 #
Y/DW-781 ..... N88-27528 #

YALEU/DCS/RR-543-PT-2 ..... N88-27762 #
YALEU/DCS/RR-553 ..... N88-27472 #
YALEU/DCS/RR-558 ..... N88-27821 #
YALEU/DCS/RR-570 ..... N88-27469 #
YALEU/DCS/RR-594 ..... N88-27471 #

YALEU/DCS/TR-600 ..... N88-27800 #

☆ U.S. GOVERNMENT PRINTING OFFICE: 1988—241-445/80019

FEDERAL REGIONAL DEPOSITORY LIBRARIES

ALABAMA

AUBURN UNIV. AT MONTGOMERY LIBRARY
Documents Department
Montgomery, AL 36193
(205) 271-9650

UNIV. OF ALABAMA LIBRARY
Documents Dept.-Box S
University, AL 35486
(205) 348-6046

ARIZONA

DEPT. OF LIBRARY, ARCHIVES AND PUBLIC RECORDS
Third Floor—State Cap.
1700 West Washington
Phoenix, AZ 85007
(602) 255-4121

UNIVERSITY OF ARIZONA LIB.
Government Documents Dept.
Tucson, AZ 85721
(602) 621-6433

ARKANSAS

ARKANSAS STATE LIBRARY
One Capitol Mall
Little Rock, AR 72201
(501) 371-2326

CALIFORNIA

CALIFORNIA STATE LIBRARY
Govt. Publications Section
P.O. Box 2037
Sacramento, CA 95809
(916) 324-4863

COLORADO

UNIV OF COLORADO LIB.
Government Pub. Division
Campus Box 184
Boulder, CO 80309
(303) 492-8834

DENVER PUBLIC LIBRARY
Govt. Pub. Department
1357 Broadway
Denver, CO 80203
(303) 571-2131

CONNECTICUT

CONNECTICUT STATE LIBRARY
Government Documents Unit
231 Capitol Avenue
Hartford, CT 06106
(203) 566-7029

FLORIDA

UNIV. OF FLORIDA LIBRARIES
Library West
Documents Department
Gainesville, FL 32611
(904) 392-0367

GEORGIA

UNIV. OF GEORGIA LIBRARIES
Government Reference Dept.
Athens, GA 30602
(404) 542-8949

HAWAII

UNIV. OF HAWAII LIBRARY
Govt. Documents Collection
2550 The Mall
Honolulu, HI 96822
(808) 948-8230

IDAHO

UNIV. OF IDAHO LIBRARY
Documents Section
Moscow, ID 83843
(208) 885-6344

ILLINOIS

ILLINOIS STATE LIBRARY
Information Services Branch
Centennial Building
Springfield, IL 62756
(217) 782-5185

INDIANA

INDIANA STATE LIBRARY
Serials Documents Section
140 North Senate Avenue
Indianapolis, IN 46204
(317) 232-3686

IOWA

UNIV. OF IOWA LIBRARIES
Govt. Documents Department
Iowa City, IA 52242
(319) 353-3318

KANSAS

UNIVERSITY OF KANSAS
Doc. Collect—Spencer Lib.
Lawrence, KS 66045-2800
(913) 864-4662

KENTUCKY

UNIV. OF KENTUCKY LIBRARIES
Govt. Pub. Department
Lexington, KY 40506-0039
(606) 257-3139

LOUISIANA

LOUISIANA STATE UNIVERSITY
Middleton Library
Govt. Docs. Dept.
Baton Rouge, LA 70803
(504) 388-2570

LOUISIANA TECHNICAL UNIV. LIBRARY
Documents Department
Ruston, LA 71272-0046
(318) 257-4962

MAINE

UNIVERSITY OF MAINE
Raymond H. Fogler Library
Tri-State Regional Documents Depository
Orono, ME 04469
(207) 581-1680

MARYLAND

UNIVERSITY OF MARYLAND
McKeldin Lib.—Doc. Div.
College Park, MD 20742
(301) 454-3034

MASSACHUSETTS

BOSTON PUBLIC LIBRARY
Government Docs. Dept.
Boston, MA 02117
(617) 536-5400 ext.226

MICHIGAN

DETROIT PUBLIC LIBRARY
Sociology Department
5201 Woodward Avenue
Detroit, MI 48202-4093
(313) 833-1409

MICHIGAN STATE LIBRARY
P.O. Box 30007
Lansing, MI 48909
(517) 373-1593

MINNESOTA

UNIVERSITY OF MINNESOTA
Government Pubs. Division
409 Wilson Library
309 19th Avenue South
Minneapolis, MN 55455
(612) 373-7870

MISSISSIPPI

UNIV. OF MISSISSIPPI LIB.
Documents Department
University, MS 38677
(601) 232-5857

MONTANA

UNIV. OF MONTANA
Mansfield Library
Documents Division
Missoula, MT 59812
(406) 243-6700

NEBRASKA

UNIVERSITY OF NEBRASKA - LINCOLN
Love Library
Documents Department
Lincoln, NE 68588-0410
(402) 472-2562

NEVADA

UNIVERSITY OF NEVADA LIB.
Govt. Pub. Department
Reno, NV 89557-0044
(702) 784-6579

NEW JERSEY

NEWARK PUBLIC LIBRARY
5 Washington Street
Newark, NJ 07101-0630
(201) 733-7812

NEW MEXICO

UNIVERSITY OF NEW MEXICO
Zimmerman Library
Government Pub. Dept.
Albuquerque, NM 87131
(505) 277-5441

NEW MEXICO STATE LIBRARY
Reference Department
325 Don Gaspar Avenue
Santa Fe, NM 87503
(505) 827-3826

NEW YORK

NEW YORK STATE LIBRARY
Empire State Plaza
Albany, NY 12230
(518) 474-5563

NORTH CAROLINA

UNIVERSITY OF NORTH CAROLINA AT CHAPEL HILL
Davis Library
BA/SS Documents Division
Chapel Hill, NC 27515
(919) 962-1151

NORTH DAKOTA

UNIVERSITY OF NORTH DAKOTA
Chester Fritz Library
Documents Department
Grand Forks, ND 58202
(701) 777-4629
In cooperation with North Dakota State Univ. Library

OHIO

STATE LIBRARY OF OHIO
Documents Department
65 South Front Street
Columbus, OH 43266-0334
(614) 462-7051

OKLAHOMA

OKLAHOMA DEPT. OF LIB.
Government Documents
200 NE 18th Street
Oklahoma City, OK 73105
(405) 521-2502, ext. 252

OKLAHOMA STATE UNIV. LIB.
Documents Department
Stillwater, OK 74078
(405) 624-6546

OREGON

PORTLAND STATE UNIV. LIB.
Documents Department
P.O. Box 1151
Portland, OR 97207
(503) 229-3673

PENNSYLVANIA

STATE LIBRARY OF PENN.
Government Pub. Section
P.O. Box 1601
Harrisburg, PA 17105
(717) 787-3752

TEXAS

TEXAS STATE LIBRARY
Public Services Department
P.O. Box 12927—Cap. Sta.
Austin, TX 78711
(512) 475-2996

TEXAS TECH. UNIV. LIBRARY
Govt. Documents Department
Lubbock, TX 79409
(806) 742-2268

UTAH

UTAH STATE UNIVERSITY
Merrill Library, U.M.C. 30
Logan, UT 84322
(801) 750-2682

VIRGINIA

UNIVERSITY OF VIRGINIA
Alderman Lib.—Public Doc.
Charlottesville, VA 22903-2498
(804) 924-3133

WASHINGTON

WASHINGTON STATE LIBRARY
Documents Section
Olympia, WA 98504
(206) 753-4027

WEST VIRGINIA

WEST VIRGINIA UNIV. LIB.
Documents Department
Morgantown, WV 26506-6069
(304) 293-3640

WISCONSIN

MILWAUKEE PUBLIC LIBRARY
814 West Wisconsin Avenue
Milwaukee, WI 53233
(414) 278-3065

ST. HIST LIB. OF WISCONSIN
Government Pub. Section
816 State Street
Madison, WI 53706
(608) 262-4347

WYOMING

WYOMING STATE LIBRARY
Supreme Ct. & Library Bld.
Cheyenne, WY 82002
(307) 777-5919

National Aeronautics and
Space Administration
Code NTT-4
Washington, D.C.
20546
Official Business
Penalty for Private Use, $300

SPECIAL FOURTH-CLASS RATE
POSTAGE & FEES PAID
NASA
PERMIT No. G 27

POSTMASTER: If Undeliverable (Section 158
Postal Manual) Do Not Return